MATHEUS DAVID INOCENTE DOMINGOS

A Importância dos Tempos de Fluência e Recuperação no Comportamento Reológico e na Suscetibilidade de Ligantes Asfálticos Modificados à Deformação Permanente

A presente tese foi submetida ao Departamento de Engenharia de Transportes da Escola de Engenharia de São Carlos – Universidade de São Paulo (STT/EESC-USP) como parte dos requisitos para a obtenção do título de Doutor em Engenharia Civil.

Área de Concentração: Infraestrutura de Transportes

Orientador: Professor Associado Adalberto Leandro Faxina

São Carlos

2017

Ficha Catalográfica preparada pela Seção de Tratamento da Informação do Serviço de Biblioteca – EESC/USP

DD671c
t

Domingos, Matheus David Inocente
The importance of the creep and recovery times on the rheological behavior and the susceptibility of modified asphalt binders to rutting / Matheus David Inocente Domingos; orientador Adalberto Leandro Faxina. São Carlos, 2017.

Tese (Doutorado) - Programa de Pós-Graduação em Engenharia de Transportes e Área de Concentração em Infraestrutura de Transportes -- Escola de Engenharia de São Carlos da Universidade de São Paulo, 2017.

1. Rutting parameters. 2. Modified asphalt binders. 3. Performance grade. 4. Creep time. 5. Recovery time. 6. Power model. 7. Superpave specification. I. Título.

MATHEUS DAVID INOCENTE DOMINGOS

The Importance of the Creep and Recovery Times on the Rheological Behavior and the Susceptibility of Modified Asphalt Binders to Rutting

This dissertation was submitted to the Department of Transportation Engineering of the São Carlos School of Engineering – University of São Paulo (STT/EESC-USP) in partial fulfillment of the requirements for the degree of Doctor of Civil Engineering.

Subject Area: Transport Infrastructure

Supervisor: Adalberto Leandro Faxina (Associate Professor)

São Carlos

2017

Catalog Card (Prepared by the Department of Information Technology, Library Service – EESC/USP)

DD671ct

Domingos, Matheus David Inocente
The importance of the creep and recovery times on the rheological behavior and the susceptibility of modified asphalt binders to rutting / Matheus David Inocente Domingos; orientador Adalberto Leandro Faxina. São Carlos, 2017.

Tese (Doutorado) - Programa de Pós-Graduação em Engenharia de Transportes e Área de Concentração em Infraestrutura de Transportes -- Escola de Engenharia de São Carlos da Universidade de São Paulo, 2017.

1. Rutting parameters. 2. Modified asphalt binders. 3. Performance grade. 4. Creep time. 5. Recovery time. 6. Power model. 7. Superpave specification. I. Título.

FOLHA DE JULGAMENTO

Candidato: Engenheiro **MATHEUS DAVID INOCENTE DOMINGOS.**

Título da tese: "A importância dos tempos de fluência e recuperação no comportamento reológico e na suscetibilidade de ligantes asfálticos modificados à deformação permanente".

Data da defesa: 24/03/2017.

Comissão Julgadora:	Resultado:
Prof. Titular **José Reynaldo Anselmo Setti** **(Orientador designado)** (Escola de Engenharia de São Carlos/EESC)	aprovado
Prof. Dr. **Jorge Barbosa Soares** (Universidade Federal do Ceará/UFC)	aprovado
Prof. Dr. **Amit Bhasin** (University of Texas at Austin/Texas)	aprovado
Profa. Dra. **Kamilla Vasconcelos Savasini** (Escola Politécnica/EP-USP)	aprovado
Profa. Dra. **Leni Figueiredo Mathias Leite** (Universidade Federal do Rio de Janeiro/UFRJ)	aprovado

Coordenadora do Programa de Pós-Graduação em Engenharia de Transportes:
Profª. Associada **Ana Paula Camargo Larocca**

Presidente da Comissão de Pós-Graduação:
Prof. Associado **Luis Fernando Costa Alberto**

To my lovely grandmother Joana Ferreira Inocente (1919 – 2016) and the grandfather of my current fiancée Arlindo de Souza (1933 – 2017),

in memoriam.

I will miss you forever.

ACKNOWLEDGEMENTS

First of all, I acknowledge God for showing His infinite mercy and giving me life. His existence and generous help made me believe that nothing is impossible.

The scholarships provided by the Research Agency of the São Paulo State (FAPESP) under the Project Numbers 2013/20483-6 and 2014/17584-8 are deeply appreciated, as well as the financial support given by the National Council for Scientific and Technological Development (CNPq, Project Number 141377/2012-7).

My supervisor, Professor Adalberto Leandro Faxina, has been much more than a supervisor throughout these years. His active encouragement, professional assistance, friendship, suggestions of revisions and expert advice were determining factors in the conclusion of this study. He has also enormously contributed to the scientific approaches followed in the experiments and guided me in the definition of the criteria used in the test protocols. I will be eternally grateful to him for everything.

I also acknowledge Professor Hussain U. Bahia (University of Wisconsin-Madison, US) for having received me as a visiting scholar in his research group in the second semester of 2014 and shared valuable ideas and comments. The MARC group – Preeda Chaturabong, Ying Li, Erik Lyngdal, Ryan Sylla, Ann Pahnke, Raquel Moraes, Tirupan Mandal, Cheng Ling, Pouya Teymourpour, Amir Arshadi and Yuming Yang – will forever be in my mind. Thank you!

To my parents Josué David Domingos and Suzana Inocente Domingos, my brother Murilo José Inocente Domingos, my fiancée (future wife) Letícia Eliza Vieira and her family: your positive feelings and daily calls have strengthened my motivation and brought happiness when I was upset. I acknowledge your continued presences in my life, and I know we can always call each other when needed. Big thanks to all of you!

I thank the Bandeirantes quarry (São Carlos, São Paulo, Brazil) and the Lubnor-Petrobras refinery (Fortaleza, Ceará, Brazil) for supplying the aggregates and the base binder used in this research project, respectively.

I give thanks to the laboratory technicians Antonio Carlos Gigante, Paulo Toyama and João Domingos Pereira Filho for their friendship and expert assistance rendered during these years. Their contribution to the development of my study was enormous. Thank you so much!

I show profound gratitude to the Post-Graduate Program in Transportation Engineering from the Polytechnic School of the University of São Paulo (Poli-USP, São Paulo, Brazil), in the name of the Professors Liedi Légi Bariani Bernucci and Kamilla Vasconcelos Savasini and the staff members Robson Costa, Vanderlei Dias and Diomária Rocha Santos. Their contribution to this piece of research was very important.

I could not forget to express my special thanks to the colleagues with whom I have worked in the Department of Transportation Engineering. I recognize their importance and the memorable moments we have enjoyed together. Their names are part of my life story: Andressa Ka Yan Ng, Lucas Lauer Verdade, Thalita Cristina Brito Nascimento, Andrise Buchiewitz Klug, Fernando Hideki Hirose, Aline Colares do Vale, Carolina Kubiaki, Ygor de Mello, Diego Frinhani Nunes, Arthur Piatti Oiticica de Paiva, Anabele Lindner, Javier Yesid Mahecha Nuñez and Bruno Faglioni Rossi. Thanks for sharing a little bit of your lives with me!

Finally, I thank the University of São Paulo at São Carlos (as an academic institution) for the opportunity of doing my post-graduate course in its Department. My acknowledgements are given to the institution in the name of the staff members not mentioned above (especially Elizabeth Ortega, Sabrina Dotta de Brito, Ana Cristina Hildebrand Vita and Antonio Carlos Mariano), the current and past Coordinators – Professors Paulo César Lima Segantine and Ana Paula de Camargo Larocca – and the Faculty members (Transport Infrastructure): Glauco Túlio Pessa Fabbri, Ana Paula Furlan and José Leomar Fernandes Júnior. Thank you.

RESUMO

DOMINGOS, M. D. I. (2017). **A importância dos tempos de fluência e recuperação no comportamento reológico e na suscetibilidade de ligantes asfálticos modificados à deformação permanente**. 559 p. Tese (Doutorado em Engenharia Civil) – Departamento de Engenharia de Transportes, Escola de Engenharia de São Carlos, Universidade de São Paulo, São Carlos.

O ensaio de fluência e recuperação sob tensão múltipla (MSCR) e o parâmetro J_{nr} (compliância não-recuperável) apresentam vantagens em relação ao ensaio em regime oscilatório e ao parâmetro $G^*/sen\delta$, mas as limitações dos tempos padronizados de fluência e recuperação no comportamento dos ligantes asfálticos têm sido um dos motivos de preocupação entre os pesquisadores na literatura científica. Em uma tentativa de superar tais deficiências, o presente estudo foi realizado com o objetivo de quantificar e analisar o comportamento fluência-recuperação de diversos ligantes asfálticos modificados com a mesma classificação PG 76-xx e submetidos aos tempos de 1/9, 2/9, 4/9, 8/9, 1/240 e 1/500 s. Cinco temperaturas (52, 58, 64, 70 e 76°C) foram escolhidas e 12 formulações foram preparadas a partir de um CAP 50/70: CAP+PPA, CAP+Elvaloy+PPA, CAP+borracha, CAP+borracha+PPA, CAP+SBS, CAP+SBS+PPA, CAP+EVA, CAP+EVA+PPA, CAP+PE, CAP+PE+PPA, CAP+SBR e CAP+SBR+PPA. Misturas asfálticas densas também foram preparadas com estes materiais e ensaiadas a 60°C para determinação do valor de F_N (*flow number*). Um modelo de potência com quatro parâmetros (A, B, n e α) foi escolhido para se ajustar aos dados dos CAP's nos tempos escolhidos para o estudo. As correlações entre F_N e os parâmetros do CAP foram altas tanto para J_{nr} quanto G_V (componente viscosa da rigidez de fluência), e os ordenamentos dos ligantes e misturas asfálticas são muito similares para ambos os parâmetros. Tais correlações se tornam ainda melhores quando os tempos de 2/9 e 4/9 s são escolhidos para o MSCR, e se acredita que o fenômeno de *steady state* exerceu influência nos dados dos ligantes asfálticos. Apesar de algumas limitações pontuais, o parâmetro α pode ser utilizado para estimar o percentual de recuperação do CAP (R), especialmente nos tempos de até 8/9 s. O uso do PPA juntamente com um aditivo principal (SBS, EVA, PE e SBR) tende a aumentar a resistência da formulação à deformação permanente quando o tempo de recuperação é de 9 s, mas o CAP+borracha e o CAP+borracha+PPA não se enquadram nestes comentários. Com exceção do CAP+Elvaloy+PPA, do CAP+borracha e do CAP+EVA (reduções em A e B com a temperatura), os aumentos de deformação permanente com o aumento dos tempos de fluência podem ser explicados pela presença de taxas de deformação maiores (parâmetro B); em alguns casos, o parâmetro de não-linearidade (n) também contribui para tais aumentos. Em termos dos materiais com níveis baixos de elasticidade, o tempo de 240 s pode não ser apropriado para todos os tipos de modificadores (especialmente o CAP+borracha, o CAP+SBR e o CAP+SBS). No que diz respeito ao tempo de recuperação de 500 s, o CAP+EVA apresentou recuperações iguais ou tendendo a 100% nas temperaturas de até 64°C e tensão de 100 Pa, e as variáveis internas do DSR podem ter influenciado os resultados de formulações como o CAP+Elvaloy+PPA. Uma proposta de refinamento nos critérios da especificação Superpave® para atribuição do nível de tráfego adequado ao CAP é feita na pesquisa, e se acredita que ela pode auxiliar na escolha da melhor formulação durante uma obra de pavimentação.

Palavras-chave: Parâmetros de deformação permanente, ligantes asfálticos modificados, grau de desempenho, tempo de fluência, tempo de recuperação, modelo de potência, especificação Superpave.

ABSTRACT

DOMINGOS, M. D. I. (2017). **The importance of the creep and recovery times on the rheological behavior and the susceptibility of modified asphalt binders to rutting**. 559 pages. Dissertation (Doctor of Civil Engineering) – Department of Transportation Engineering, São Carlos School of Engineering, University of São Paulo, São Carlos, Brazil.

The performance-related Multiple Stress Creep and Recovery (MSCR) test and its corresponding rutting parameter – nonrecoverable compliance J_{nr} – have advantages over the dynamic oscillatory shear test and the parameter $G^*/sin\delta$, but some limitations such as the limited applicability of the standardized creep-recovery times to modified binders have been a matter of concern in the literature. In an attempt to overcome such deficiencies, this study was conducted to quantify and evaluate the creep-recovery behavior of several modified binders equally graded in the Superpave® high temperature specification (PG 76-xx) with respect to their responses at different loading and unloading times (1/9, 2/9, 4/9, 8/9, 1/240 and 1/500 s). Five temperatures were selected in the study (52, 58, 64, 70 and 76°C) and 12 formulations were prepared from a 50/70 original material: AC+PPA, AC+Elvaloy+PPA, AC+rubber, AC+rubber+PPA, AC+SBS, AC+SBS+PPA, AC+EVA, AC+EVA+PPA, AC+PE, AC+PE+PPA, AC+SBR and AC+SBR+PPA. Dense-graded mixtures were also prepared with these binders and tested at 60°C to obtain the flow number (F_N) values. A modified power model with four parameters (A, B, n and α) was selected to fit the binder data at longer creep and recovery times. The levels of correlation between F_N and the binder data were high either for J_{nr} or G_V (viscous component of the creep stiffness), and the rankings of binders and mixtures are almost the same for both parameters. These correlations became even better when the creep-recovery times of 2/9 s and 4/9 s were used, and it is believed that the steady state phenomenon played a role on the findings of the binder. Despite the identification of specific limitations, the parameter α may be used to have an estimation of the amount of percent recovery (R) in the binder, especially at standardized and longer loading times. The use of PPA together with a major additive in the binder (SBS, EVA, PE and SBR) tends to increase the rutting resistance of the formulation when the unloading time is equal to 9 s, but the AC+rubber and the AC+rubber+PPA are exceptions. With exception of the AC+Elvaloy+PPA, the AC+rubber and the AC+EVA (decreases in A and B with temperature), the increases in the accumulated strain in the binders with increasing creep time may be explained by the presence of higher strain rates (B values) and, in some cases, the nonlinear parameter (n) also gives some contribution to it. In terms of the binders with low levels of elasticity, the recovery time of 240 s may not be appropriate for all types of modifiers (especially the AC+rubber, the AC+SBR and the AC+SBS). With respect to the unloading time of 500 s, the AC+EVA showed recoveries equal to or approaching 100% at 100 Pa and temperatures no greater than 64°C, and the variables of the DSR may have affected the outcomes of materials such as the AC+Elvaloy+PPA. A refinement in the Superpave® specification criteria for assigning a traffic level to the binder is proposed, and these new criteria could help in choosing the best material for a specific paving application.

Keywords: Rutting parameters, modified asphalt binders, performance grade, creep time, recovery time, power model, Superpave specification.

LIST OF TABLES

Table 1 –	Penetration-grade binder specification used in Brazil from July/2005 to the current days [Technical Regulation No. 03/2005, ANP] ………..	43
Table 2 –	Superpave® specification requirements for the PG 58, PG 64 and PG 70 binders [ASTM D6373 standard, Table 1] …..……………………..	44
Table 3 –	Characteristic examples of asphalt binder modifiers (BAHIA et al., 2001a; ISACSSON and LU, 1995; POLACCO et al., 2006; READ and WHITEOAK, 2003; YILDIRIM, 2007) ………………………………	49
Table 4 –	Traffic levels found in the AASHTO M320-09 and M332-14 specifications and corresponding equivalent single-axle loads (ESALs) and/or vehicle speeds (BAHIA, 2014; GIERHART, 2013) …………….	80
Table 5 –	Modifier contents (percentages by weight), PG grades and corresponding true grades of the formulations ………………………...	90
Table 6 –	Processing variables of the modified asphalt binders (mixing temperature, mixing time and rotation speed)…………………………	91
Table 7 –	Some characteristics of the basaltic aggregate from the Bandeirantes quarry (GIGANTE, 2007) ……………………………………………	92
Table 8 –	Binder contents and the corresponding intervals of the mixing and compaction temperatures …………………………………………	93
Table 9 –	Vehicle speeds as based on the equations from Pereira et al. (1998, 2000) and Huang (2004) ………………………………………....	101
Table 10 –	Summary of the results of some mixture and binder tests for analysis of the degrees of correlation ………………………………………………	112
Table 11 –	Rankings of asphalt binders and mixtures from the less (No. 1) to the most susceptible to rutting (No. 7) based on the numerical values of some laboratory tests ………………………………………………....	116
Table 12 –	Degrees of correlation (R^2) between binder and mixture data and corresponding regression equations (power law) ……………………	118
Table 13 –	Constants A, B, C and D from the Francken model (mean values) for the asphalt binders that failed before 10,000 cycles …………………	118
Table 14 –	Coefficients of variation (COV's) for the constants A, B, C and D from the Francken model ……………………………………………	119

Table 15 – Ordering of mixtures from the less (No. 1) to the most susceptible to rutting (No. 7) as based on the flow number F_N, the flow number index FN_I and the constant C (Francken model) …………………………….. 119

Table 16 – Permanent strains of the asphalt mixtures modified with plastomers (EVA and PE) and crumb rubber after 10,000 cycles (γ_{per}) and corresponding asphalt binder parameters ……………………………… 123

Table 17 – Rankings of asphalt binders and mixtures that showed absence of failure from the most (No. 1) to the less rut resistant (No. 5) based on the numerical values of some laboratory tests …………………………... 123

Table 18 – Degrees of correlation (R^2) between some binder and mixture data and corresponding linear equations ……………………………………... 124

Table 19 – Summary of mixture data and recommended traffic levels for the asphalt binders based on the nonrecoverable compliance J_{nr} and the viscous component of the creep stiffness G_V (both at 64°C) and the criteria published by Superpave® and Delgadillo et al. (2006b) ………………... 126

Table 20 – Categories of rutting resistance and corresponding descriptions as based on the laboratory data collected in this study and by Onofre et al. (2013) 128

Table 21 – Classifications of the formulations from the Lubnor-Petrobras refinery according to their mixture and binder data ……………………………. 128

Table 22 – Outcomes of the penetration tests for the unaged and RTFO-aged binders and corresponding retained penetrations ……………………... 134

Table 24 – Outcomes of the softening point ($R\&B$) tests for the unaged and RTFO-aged binders and corresponding increases in softening point …. 136

Table 25 – Rotational viscosities of the unaged and rolling thin-film oven aged asphalt binders (neat and modified ones)…………………………… 140

Table 26 – Viscosity aging indexes (parameter I_A) of the asphalt binders at the temperatures of 135, 143, 150, 163 and 177°C and some statistical parameters …………………………………………………………….. 141

Table 27 – Results of the parameter $G^*/sin\delta$ before accelerated aging in the rolling thin-film oven and constants A and B from the model used by Elseifi et al. (2013) and Laukkanen et al. (2015) ………………………………….. 144

Table 28 – Results of the Shenoy's parameter for the unmodified and modified asphalt binders before accelerated aging (RTFOT) …………………… 146

Table 29 – Percentages of increase in the binder parameter when moving from the original $G^*/sin\delta$ to the Shenoy's parameter $|G^*|/[1-(1/tan\delta sin\delta)]$ – unaged condition ……………………………………………………… 147

Table 30 – Results of the parameter $G^*/sin\delta$ after accelerated aging (RTFOT) and constants A and B from the exponential model used by Elseifi et al. (2013) and Laukkanen et al. (2015) 149

Table 31 – Results of the Shenoy's parameter for the unmodified and modified asphalt binders after aging in the rolling thin-film oven 150

Table 32 – Percentages of increase in the binder parameter when moving from $G^*/sin\delta$ to $|G^*|/[1-(1/tan\delta sin\delta)]$ – short-term aged condition 150

Table 33 – Rankings of binders from the less (No. 1) to the most susceptible to rutting (No. 13) based on the parameters $G^*/sin\delta$ and $|G^*|/[1-(1/tan\delta sin\delta)]$ 151

Table 34 – Elements of the Burgers model based on the strain data of the AC+Elvaloy+PPA and the AC+EVA shown in Figure 47 154

Table 35 – Percent differences in nonrecoverable compliances ($J_{nr,\ diff}$) and recoveries (R_{diff}) of the 50/70 original binder, the AC+PPA and the AC+Elvaloy+PPA 157

Table 36 – Viscous component of the creep stiffness (G_V) and appropriate traffic levels for the 50/70 original binder, the AC+PPA and the AC+Elvaloy+PPA 158

Table 37 – Parameters E_K, E_M, η_K and η_M from the four-element Burgers model at 0.1 kPa and corresponding average absolute errors (AAE) for the 50/70 base binder 159

Table 38 – Parameters E_K, E_M, η_K and η_M from the four-element Burgers model at 0.1 kPa and corresponding average absolute errors (AAE) for the AC+PPA 160

Table 39 – Parameters E_K, E_M, η_K and η_M from the four-element Burgers model at 0.1 kPa and corresponding average absolute errors (AAE) for the AC+Elvaloy+PPA 160

Table 40 – Percent differences in nonrecoverable compliances ($J_{nr,\ diff}$) and recoveries (R_{diff}) of the 50/70 original binder, the AC+PPA, the AC+rubber and the AC+rubber+PPA 162

Table 41 – Viscous component of the creep stiffness (G_V) and appropriate traffic levels for the 50/70 original binder, the AC+PPA, the AC+rubber and the AC+rubber+PPA 164

Table 42 – Parameters E_K, E_M, η_K and η_M from the four-element Burgers model at 0.1 kPa and corresponding average absolute errors (AAE) for the AC+rubber 165

Table 43 – Parameters E_K, E_M, η_K and η_M from the four-element Burgers model at 0.1 kPa and corresponding average absolute errors (AAE) for the AC+rubber+PPA 165

Table 44 – Percent differences in nonrecoverable compliances ($J_{nr,\ diff}$) and recoveries (R_{diff}) of the 50/70 original binder, the AC+PPA, the AC+EVA and the AC+EVA+PPA 167

Table 45 – Viscous component of the creep stiffness (G_V) and appropriate traffic levels for the 50/70 original binder, the AC+PPA, the AC+EVA and the AC+EVA+PPA 169

Table 46 – Parameters E_K, E_M, η_K and η_M from the four-element Burgers model at 0.1 kPa and corresponding average absolute errors (AAE) for the AC+EVA 169

Table 47 – Parameters of the generalized Voigt model with six elements and corresponding average absolute errors (AAE) for the AC+EVA at the temperature of 52°C and the stress level of 0.1 kPa 172

Table 48 – Parameters of the generalized Voigt model with six elements and corresponding average absolute errors (AAE) for the AC+EVA at the temperature of 58°C and the stress level of 0.1 kPa 172

Table 49 – Parameters E_K, E_M, η_K and η_M from the four-element Burgers model at 0.1 kPa and corresponding average absolute errors (AAE) for the AC+EVA+PPA 173

Table 50 – Percent differences in nonrecoverable compliances ($J_{nr,\ diff}$) and recoveries (R_{diff}) of the 50/70 original binder, the AC+PPA, the AC+PE and the AC+PE+PPA 176

Table 51 – Viscous component of the creep stiffness (G_V) and appropriate traffic levels for the 50/70 original binder, the AC+PPA, the AC+PE and the AC+PE+PPA 177

Table 52 – Parameters E_K, E_M, η_K and η_M from the four-element Burgers model at 0.1 kPa and corresponding average absolute errors (AAE) for the AC+PE 178

Table 53 – Parameters E_K, E_M, η_K and η_M from the four-element Burgers model at 0.1 kPa and corresponding average absolute errors (AAE) for the AC+PE+PPA 178

Table 54 – Percent differences in nonrecoverable compliances ($J_{nr,\ diff}$) and recoveries (R_{diff}) of the 50/70 original binder, the AC+PPA, the AC+SBS and the AC+SBS+PPA 182

Table 55 – Viscous component of the creep stiffness (G_V) and appropriate traffic levels for the 50/70 original binder, the AC+PPA, the AC+SBS and the AC+SBS+PPA 183

Table 56 – Parameters E_K, E_M, η_K and η_M from the four-element Burgers model at 0.1 kPa and corresponding average absolute errors (AAE) for the AC+SBS 183

Table 57 – Parameters E_K, E_M, η_K and η_M from the four-element Burgers model at 0.1 kPa and corresponding average absolute errors (AAE) for the AC+SBS+PPA 184

Table 58 – Viscous component of the creep stiffness (G_V) and appropriate traffic levels for the 50/70 original binder, the AC+PPA, the AC+SBR and the AC+SBR+PPA 187

Table 59 – Percent differences in nonrecoverable compliances ($J_{nr,\ diff}$) and recoveries (R_{diff}) of the 50/70 original binder, the AC+PPA, the AC+SBR and the AC+SBR+PPA 188

Table 60 – Parameters E_K, E_M, η_K and η_M from the four-element Burgers model at 0.1 kPa and corresponding average absolute errors (AAE) for the AC+SBR 188

Table 61 – Parameters E_K, E_M, η_K and η_M from the four-element Burgers model at 0.1 kPa and corresponding average absolute errors (AAE) for the AC+SBR+PPA 189

Table 62 – Identification of the traffic levels for each vehicle speed based on the current Superpave® specification criteria 191

Table 63 – Percent recoveries at 100 Pa (*R100*) and 3,200 Pa (*R3200*) for the 50/70 base asphalt binder with increasing loading time and temperature 192

Table 64 – Nonrecoverable compliances at 100 Pa ($J_{nr}100$) and 3,200 Pa ($J_{nr}3200$) for the 50/70 base binder with increasing loading time and temperature 193

Table 65 – Adequate traffic levels for the 50/70 base asphalt binder with increasing creep time and temperature based on the standardized Superpave® criteria 194

Table 66 – Percent differences in nonrecoverable compliances ($J_{nr,\ diff}$) for the 50/70 base asphalt binder with increasing creep time and temperature 194

Table 67 – Comparisons between the actual traffic levels of the 50/70 base asphalt binder and the ones obtained from the equations by Huang (2004) and Pereira et al. (1998) 197

Table 68 – Comparisons between the actual traffic levels of the 50/70 base asphalt binder and the ones obtained from the equations by Huang (2004) and Pereira et al. (2000) 197

Table 69 – Traffic levels of the 50/70 base asphalt binder with increasing loading time and temperature in the current and proposed criteria 198

Table 70 – Numerical values and variations in the parameters/constants *A, B, n* and α from the power law equations by Saboo and Kumar (2015) with increasing temperature and creep time and considering the 50/70 base asphalt binder 200

Table 71 – Degrees of correlation between the parameters *A* and *B* (modified power model) and the creep time t_F for the 50/70 unmodified asphalt binder 204

Table 72 – Degrees of correlation between the parameters *n* and *α* (modified power model) and the creep time t_F for the 50/70 unmodified asphalt binder 204

Table 73 – Rearranged MSCR testing data of the 50/70 base binder to be used in the analysis of variance (ANOVA) – nonrecoverable creep compliance 206

Table 74 – Results from the analysis of variance (ANOVA, *p-value* and *F-value*) as based on the nonrecoverable creep compliances of the 50/70 original binder 206

Table 75 – Percent recoveries at 100 Pa (*R100*) and 3,200 Pa (*R3200*) for the AC+PPA with increasing loading time and temperature 207

Table 76 – Nonrecoverable compliances at 100 Pa ($J_{nr}100$) and 3,200 Pa (J_{nr} *3200*) for the AC+PPA with increasing loading time and temperature 209

Table 77 – Adequate traffic levels for the AC+PPA with increasing creep time and temperature based on the standardized Superpave® criteria 210

Table 78 – Percent differences in nonrecoverable compliances ($J_{nr,\ diff}$) for the AC+PPA with increasing creep time and temperature 211

Table 79 – Regression equations and coefficients of determination between the $J_{nr}3200$ values of the AC+PPA and the corresponding vehicle speeds according to the equations proposed by Pereira et al. (1998, 2000) and Huang (2004) 212

Table 80 – Comparisons between the actual traffic levels of the AC+PPA and the ones obtained from the equations by Huang (2004) and Pereira et al. (1998) 212

Table 81 – Comparisons between the actual traffic levels of the AC+PPA and the ones obtained from the equations by Huang (2004) and Pereira et al. (2000) 213

Table 82 – Traffic levels of the AC+PPA with increasing loading time and temperature in the current and proposed criteria 214

Table 83 – Numerical values and variations in the parameters/constants *A, B, n* and *α* from the power law equations by Saboo and Kumar (2015) with increasing temperature and creep time and considering the AC+PPA .. 216

Table 84 – Degrees of correlation between the parameters *A* and *B* (modified power model) and the creep time t_F for the AC+PPA 220

Table 85 – Degrees of correlation between the parameters *n* and *α* (modified power model) and the creep time t_F for the AC+PPA 221

Table 86 – Rearranged MSCR testing data of the AC+PPA to be used in the analysis of variance (ANOVA) – percent recovery …………………… 223

Table 87 – Rearranged MSCR testing data of the AC+PPA to be used in the analysis of variance (ANOVA) – nonrecoverable creep compliance …... 223

Table 88 – Results from the analysis of variance (ANOVA, *p-value* and *F-value*) as based on the percent recoveries of the AC+PPA …………………….. 224

Table 89 – Results from the analysis of variance (ANOVA, *p-value* and *F-value*) as based on the nonrecoverable compliances of the AC+PPA ………… 225

Table 90 – Percent recoveries at 100 Pa (*R100*) and 3,200 Pa (*R3200*) for the AC+Elvaloy+PPA with increasing loading time and temperature ……... 225

Table 91 – Nonrecoverable compliances at 100 Pa ($J_{nr}100$) and 3,200 Pa (J_{nr} 3200) for the AC+Elvaloy+PPA with increasing loading time and temperature ………………………………………………………... 227

Table 92 – Adequate traffic levels for the AC+Elvaloy+PPA with increasing creep time and temperature based on the standardized Superpave® criteria ….. 228

Table 93 – Percent differences in nonrecoverable compliances ($J_{nr,\ diff}$) for the AC+Elvaloy+PPA with increasing creep time and temperature ……….. 229

Table 94 – Regression equations and coefficients of determination between the $J_{nr}3200$ values of the AC+Elvaloy+PPA and the corresponding vehicle speeds according to the equations by Pereira et al. (1998, 2000) and Huang (2004)……………………………………………………….. 230

Table 95 – Comparisons between the actual traffic levels of the AC+Elvaloy+PPA and the ones obtained from Huang (2004) and Pereira et al. (1998) ………………………………………………… 231

Table 96 – Comparisons between the actual traffic levels of the AC+Elvaloy+PPA and the ones obtained from Huang (2004) and Pereira et al. (2000) ………………………………………………… 231

Table 97 – Traffic levels of the AC+Elvaloy+PPA with increasing loading time and temperature in the current and proposed criteria ……………………….. 232

Table 98 – Numerical values and variations in the parameters/constants A, B, n and α from the power law equations by Saboo and Kumar (2015) with increasing temperature and creep time and considering the AC+Elvaloy+PPA 234

Table 99 – Degrees of correlation between the parameters A and B (modified power model) and the creep time t_F for the AC+Elvaloy+PPA ………………... 238

Table 100 – Degrees of correlation between the parameters n and α (modified power model) and the creep time t_F for the AC+Elvaloy+PPA ………………... 239

Table 101 – Rearranged MSCR testing data of the AC+Elvaloy+PPA to be used in the analysis of variance (ANOVA) – percent recovery ………………… 242

Table 102 – Rearranged MSCR testing data of the AC+Elvaloy+PPA to be used in the analysis of variance (ANOVA) – nonrecoverable creep compliance 242

Table 103 – Results from the analysis of variance (ANOVA, *p-value* and *F-value*) as based on the percent recoveries of the AC+Elvaloy+PPA …………... 243

Table 104 – Results from the analysis of variance (ANOVA, *p-value* and *F-value*) as based on the nonrecoverable compliances of the AC+Elvaloy+PPA .. 243

Table 105 – Percent recoveries at 100 Pa (*R100*) and 3,200 Pa (*R3200*) for the AC+rubber with increasing loading time and temperature …………….. 244

Table 106 – Nonrecoverable compliances at 100 Pa ($J_{nr}100$) and 3,200 Pa ($J_{nr}\ 3200$) for the AC+rubber with increasing loading time and temperature ……... 245

Table 107 – Percent differences in nonrecoverable compliances ($J_{nr,\ diff}$) for the AC+rubber with increasing creep time and temperature ……………….. 246

Table 108 – Adequate traffic levels for the AC+rubber with increasing creep time and temperature based on the standardized Superpave® criteria ……….. 247

Table 109 – Regression equations and coefficients of determination between the $J_{nr}3200$ values of the AC+rubber and the corresponding vehicle speeds according to the equations by Pereira et al. (1998, 2000) and Huang (2004) ……………………………………………………………… 248

Table 110 – Comparisons between the actual traffic levels of the AC+rubber and the ones obtained from the equations by Huang (2004) and Pereira et al. (2000) ………………………………………………………... 248

Table 111 – Comparisons between the actual traffic levels of the AC+rubber and the ones obtained from Huang (2004) and Pereira et al. (1998) ………. 249

Table 112 – Numerical values and variations in the parameters/constants *A, B, n* and *α* from the power law equations by Saboo and Kumar (2015) with increasing temperature and creep time and considering the AC+rubber 250

Table 113 – Degrees of correlation between the parameters *A* and *B* (modified power model) and the creep time t_F for the AC+rubber ……………………….. 254

Table 114 – Degrees of correlation between the parameters *n* and *α* (modified power model) and the creep time t_F for the AC+rubber ……………………….. 255

Table 115 – Rearranged MSCR testing data of the AC+rubber to be used in the analysis of variance (ANOVA) – percent recovery …………………… 257

Table 116 – Rearranged MSCR testing data of the AC+rubber to be used in the analysis of variance (ANOVA) – nonrecoverable creep compliance …... 257

Table 117 – Results from the analysis of variance (ANOVA, *p-value* and *F-value*) as based on the percent recoveries of the AC+rubber 258

Table 118 – Results from the analysis of variance (ANOVA, *p-value* and *F-value*) as based on the nonrecoverable compliances of the AC+rubber 258

Table 119 – Percent recoveries at 100 Pa (*R100*) and 3,200 Pa (*R3200*) for the AC+rubber+PPA with increasing loading time and temperature 260

Table 120 – Nonrecoverable compliances at 100 Pa ($J_{nr}100$) and 3,200 Pa ($J_{nr}\ 3200$) for the AC+rubber+PPA with increasing loading time and temperature 261

Table 121 – Adequate traffic levels for the AC+rubber+PPA with increasing creep time and temperature based on the standardized Superpave® criteria 262

Table 122 – Regression equations and coefficients of determination between the $J_{nr}3200$ values of the AC+rubber+PPA and the corresponding vehicle speeds according to the equations by Pereira et al. (1998, 2000) and Huang (2004) 263

Table 123 – Comparisons between the actual traffic levels of the AC+rubber+PPA and the ones obtained from Huang (2004) and Pereira et al. (1998) 264

Table 124 – Comparisons between the actual traffic levels of the AC+rubber+PPA and the ones obtained from the equations by Huang (2004) and Pereira et al. (2000) 264

Table 125 – Traffic levels of the AC+rubber with increasing loading time and temperature in the current and proposed criteria 265

Table 126 – Traffic levels of the AC+rubber+PPA with increasing loading time and temperature in the current and proposed criteria 265

Table 127 – Percent differences in nonrecoverable compliances ($J_{nr,\ diff}$) for the AC+rubber+PPA with increasing creep time and temperature 266

Table 128 – Numerical values and variations in the parameters/constants *A, B, n* and α from the power law equations by Saboo and Kumar (2015) with increasing temperature and creep time and considering the AC+rubber+PPA 268

Table 129 – Degrees of correlation between the parameters *A* and *B* (modified power model) and the creep time t_F for the AC+rubber+PPA 273

Table 130 – Degrees of correlation between the parameters *n* and α (modified power model) and the creep time t_F for the AC+rubber+PPA 273

Table 131 – Rearranged MSCR testing data of the AC+rubber+PPA to be used in the analysis of variance (ANOVA) – percent recovery 275

Table 132 – Rearranged MSCR testing data of the AC+rubber+PPA to be used in the analysis of variance (ANOVA) – nonrecoverable creep compliance 275

Table 133 – Results from the analysis of variance (ANOVA, *p-value* and *F-value*) as based on the percent recoveries of the AC+rubber+PPA ……………. 276

Table 134 – Results from the analysis of variance (ANOVA, *p-value* and *F-value*) as based on the nonrecoverable compliances of the AC+rubber+PPA …. 276

Table 135 – Percent recoveries at 100 Pa (*R100*) and 3,200 Pa (*R3200*) for the AC+SBS with increasing loading time and temperature ……………….. 278

Table 136 – Nonrecoverable compliances at 100 Pa ($J_{nr}100$) and 3,200 Pa (J_{nr} *3200*) for the AC+SBS with increasing loading time and temperature ………... 279

Table 137 – Percent differences in nonrecoverable compliances ($J_{nr,\ diff}$) for the AC+SBS with increasing creep time and temperature …………………. 280

Table 138 – Adequate traffic levels for the AC+SBS with increasing creep time and temperature based on the standardized Superpave® criteria ……………. 281

Table 139 – Regression equations and coefficients of determination between the $J_{nr}3200$ values of the AC+SBS and the corresponding vehicle speeds according to the equations by Pereira et al. (1998, 2000) and Huang (2004) ……………………………………………………………… 282

Table 140 – Comparisons between the actual traffic levels of the AC+SBS and the ones obtained from Huang (2004) and Pereira et al. (1998) …………... 282

Table 141 – Comparisons between the actual traffic levels of the AC+SBS and the ones obtained from Huang (2004) and Pereira et al. (2000) …………... 283

Table 142 – Traffic levels of the AC+SBS with increasing loading time and temperature in the current and proposed criteria ……………………….. 283

Table 143 – Numerical values and variations in the parameters/constants *A, B, n* and α from the power law equations by Saboo and Kumar (2015) with increasing temperature and creep time and considering the AC+SBS …. 285

Table 144 – Degrees of correlation between the parameters *A* and *B* (modified power model) and the creep time t_F for the AC+SBS …………………………. 289

Table 145 – Degrees of correlation between the parameters *n* and α (modified power model) and the creep time t_F for the AC+SBS …………………………. 289

Table 146 – Rearranged MSCR testing data of the AC+SBS to be used in the analysis of variance (ANOVA) – percent recovery …………………… 291

Table 147 – Rearranged MSCR testing data of the AC+SBS to be used in the analysis of variance (ANOVA) – nonrecoverable creep compliance …... 291

Table 148 – Results from the analysis of variance (ANOVA, *p-value* and *F-value*) as based on the percent recoveries of the AC+SBS 292

Table 149 – Results from the analysis of variance (ANOVA, *p-value* and *F-value*) as based on the nonrecoverable compliances of the AC+SBS 293

Table 150 – Percent recoveries at 100 Pa (*R100*) and 3,200 Pa (*R3200*) for the AC+SBS+PPA with increasing loading time and temperature 294

Table 151 – Nonrecoverable compliances at 100 Pa ($J_{nr}100$) and 3,200 Pa ($J_{nr}3200$) for the AC+SBS+PPA with increasing loading time and temperature 296

Table 152 – Percent differences in nonrecoverable compliances ($J_{nr,\ diff}$) for the AC+SBS+PPA with increasing creep time and temperature 297

Table 153 – Adequate traffic levels for the AC+SBS+PPA with increasing creep time and temperature based on the standardized Superpave® criteria 298

Table 154 – Regression equations and coefficients of determination between the $J_{nr}3200$ values of the AC+SBS+PPA and the corresponding vehicle speeds according to the equations by Pereira et al. (1998, 2000) and Huang (2004) 299

Table 155 – Comparisons between the actual traffic levels of the AC+SBS+PPA and the ones obtained from Huang (2004) and Pereira et al. (1998) 299

Table 156 – Comparisons between the actual traffic levels of the AC+SBS+PPA and the ones obtained from the equations by Huang (2004) and Pereira et al. (2000) 300

Table 157 – Traffic levels of the AC+SBS+PPA with increasing loading time and temperature in the current and proposed criteria 301

Table 158 – Numerical values and variations in the parameters/constants *A, B, n* and *α* from the power law equations by Saboo and Kumar (2015) with increasing temperature and creep time and considering the AC+SBS+PPA 302

Table 159 – Degrees of correlation between the parameters *A* and *B* (modified power model) and the creep time t_F for the AC+SBS+PPA 307

Table 160 – Degrees of correlation between the parameters *n* and *α* (modified power model) and the creep time t_F for the AC+SBS+PPA 308

Table 161 – Rearranged MSCR testing data of the AC+SBS+PPA to be used in the analysis of variance (ANOVA) – percent recovery 310

Table 162 – Rearranged MSCR testing data of the AC+SBS+PPA to be used in the analysis of variance (ANOVA) – nonrecoverable creep compliance 311

Table 163 – Results from the analysis of variance (ANOVA, *p-value* and *F-value*) as based on the percent recoveries of the AC+SBS+PPA 311

Table 164 – Results from the analysis of variance (ANOVA, *p-value* and *F-value*) as based on the nonrecoverable compliances of the AC+SBS+PPA 312

Table 165 – Percent recoveries at 100 Pa (*R100*) and 3,200 Pa (*R3200*) for the AC+SBR with increasing loading time and temperature 313

Table 166 – Nonrecoverable compliances at 100 Pa ($J_{nr}100$) and 3,200 Pa ($J_{nr}3200$) for the AC+SBR with increasing loading time and temperature 314

Table 167 – Percent differences in nonrecoverable compliances ($J_{nr,\ diff}$) for the AC+SBR with increasing creep time and temperature 316

Table 168 – Adequate traffic levels for the AC+SBR with increasing creep time and temperature based on the standardized Superpave® criteria 317

Table 169 – Regression equations and coefficients of determination between the $J_{nr}3200$ values of the AC+SBR and the corresponding vehicle speeds according to the equations by Pereira et al. (1998, 2000) and Huang (2004) 318

Table 170 – Comparisons between the actual traffic levels of the AC+SBR and the ones obtained from Huang (2004) and Pereira et al. (1998) 318

Table 171 – Comparisons between the actual traffic levels of the AC+SBR and the ones obtained from the equations by Huang (2004) and Pereira et al. (2000) 319

Table 172 – Traffic levels of the AC+SBR with increasing loading time and temperature in the current and proposed criteria 320

Table 173 – Numerical values and variations in the parameters/constants *A, B, n* and *α* from the power law equations by Saboo and Kumar (2015) with increasing temperature and creep time and considering the AC+SBR 321

Table 174 – Degrees of correlation between the parameters *A* and *B* (modified power model) and the creep time t_F for the AC+SBR 325

Table 175 – Degrees of correlation between the parameters *n* and *α* (modified power model) and the creep time t_F for the AC+SBR 325

Table 176 – Rearranged MSCR testing data of the AC+SBR to be used in the analysis of variance (ANOVA) – percent recovery 327

Table 177 – Results from the analysis of variance (ANOVA, *p-value* and *F-value*) as based on the percent recoveries of the AC+SBR 328

Table 178 – Rearranged MSCR testing data of the AC+SBR to be used in the analysis of variance (ANOVA) – nonrecoverable creep compliance 328

Table 179 – Results from the analysis of variance (ANOVA, *p-value* and *F-value*) as based on the nonrecoverable compliances of the AC+SBR ………… 329

Table 180 – Percent recoveries at 100 Pa (*R100*) and 3,200 Pa (*R3200*) for the AC+SBR+PPA with increasing loading time and temperature ……….. 329

Table 181 – Nonrecoverable compliances at 100 Pa ($J_{nr}100$) and 3,200 Pa ($J_{nr}\,3200$) for the AC+SBR+PPA with increasing loading time and temperature …. 331

Table 182 – Percent differences in nonrecoverable compliances ($J_{nr,\ diff}$) for the AC+SBR+PPA with increasing creep time and temperature …………... 333

Table 183 – Adequate traffic levels for the AC+SBR+PPA with increasing creep time and temperature based on the standardized Superpave® criteria ….. 334

Table 184 – Regression equations and coefficients of determination between the $J_{nr}3200$ values of the AC+SBR+PPA and the corresponding vehicle speeds according to the equations by Pereira et al. (1998, 2000) and Huang (2004) ………..………...………...………..………...………... 335

Table 185 – Comparisons between the actual traffic levels of the AC+SBR+PPA and the ones obtained from Huang (2004) and Pereira et al. (1998) …... 335

Table 186 – Comparisons between the actual traffic levels of the AC+SBR+PPA and the ones obtained from the equations by Huang (2004) and Pereira et al. (2000) ………..………...………...………..………...……….... 336

Table 187 – Traffic levels of the AC+SBR+PPA with increasing loading time and temperature in the current and proposed criteria ……………………….. 337

Table 188 – Numerical values and variations in the parameters/constants *A, B, n* and *α* from the power law equations by Saboo and Kumar (2015) with increasing temperature and creep time and considering the AC+SBR+PPA ………..………...………...………...………...……… 338

Table 189 – Degrees of correlation between the parameters *A* and *B* (modified power model) and the creep time t_F for the AC+SBR+PPA ………..……….... 343

Table 190 – Degrees of correlation between the parameters *n* and *α* (modified power model) and the creep time t_F for the AC+SBR+PPA ………..……….... 344

Table 191 – Rearranged MSCR testing data of the AC+SBR+PPA to be used in the analysis of variance (ANOVA) – percent recovery …...……….............. 347

Table 192 – Results from the analysis of variance (ANOVA, *p-value* and *F-value*) as based on the percent recoveries of the AC+SBR+PPA ……………… 347

Table 193 – Rearranged MSCR testing data of the AC+SBR+PPA to be used in the analysis of variance (ANOVA) – nonrecoverable creep compliance …... 348

Table 194 – Results from the analysis of variance (ANOVA, *p-value* and *F-value*) as based on the nonrecoverable compliances of the AC+SBR+PPA …... 348

Table 195 – Percent recoveries at 100 Pa (*R100*) and 3,200 Pa (*R3200*) for the AC+EVA with increasing loading time and temperature …..…..…...... 349

Table 196 – Nonrecoverable compliances at 100 Pa ($J_{nr}100$) and 3,200 Pa ($J_{nr}\,3200$) for the AC+EVA with increasing loading time and temperature ……….. 351

Table 197 – Percent differences in nonrecoverable compliances ($J_{nr,\ diff}$) for the AC+EVA with increasing creep time and temperature ………………… 355

Table 198 – Adequate traffic levels for the AC+EVA with increasing creep time and temperature based on the standardized Superpave® criteria ……………. 356

Table 199 – Regression equations and coefficients of determination between the $J_{nr}3200$ values of the AC+EVA and the corresponding vehicle speeds according to the equations by Pereira et al. (1998, 2000) and Huang (2004) ………………………………………………………………. 357

Table 200 – Comparisons between the actual traffic levels of the AC+EVA and the ones obtained from Huang (2004) and Pereira et al. (1998) …………... 357

Table 201 – Comparisons between the actual traffic levels of the AC+EVA and the ones obtained from the equations by Huang (2004) and Pereira et al. (2000) …………..…………..…………...…………...…………...…. 358

Table 202 – Traffic levels of the AC+EVA with increasing loading time and temperature in the current and proposed criteria …………..………….. 358

Table 203 – Numerical values and variations in the parameters/constants *A, B, n* and *α* from the power law equations by Saboo and Kumar (2015) with increasing temperature and creep time and considering the AC+EVA … 360

Table 204 – Degrees of correlation between the parameters *A* and *B* (modified power model) and the creep time t_F for the AC+EVA ………………………… 366

Table 205 – Degrees of correlation between the parameters *n* and *α* (modified power model) and the creep time t_F for the AC+EVA ………………………… 367

Table 206 – Rearranged MSCR testing data of the AC+EVA to be used in the analysis of variance (ANOVA) – percent recovery …………………… 370

Table 207 – Results from the analysis of variance (ANOVA, *p-value* and *F-value*) as based on the percent recoveries of the AC+EVA …………………… 370

Table 208 – Rearranged MSCR testing data of the AC+EVA to be used in the analysis of variance (ANOVA) – nonrecoverable creep compliance …... 371

Table 209 – Results from the analysis of variance (ANOVA, *p-value* and *F-value*) as based on the nonrecoverable compliances of the AC+EVA ……….. 371

Table 210 – Percent recoveries at 100 Pa (*R100*) and 3,200 Pa (*R3200*) for the AC+EVA+PPA with increasing loading time and temperature ……….. 372

Table 211 – Nonrecoverable compliances at 100 Pa ($J_{nr}100$) and 3,200 Pa (J_{nr} *3200*) for the AC+EVA+PPA with increasing loading time and temperature … 377

Table 212 – Percent differences in nonrecoverable compliances ($J_{nr,\ diff}$) for the AC+EVA+PPA with increasing creep time and temperature …………..... 379

Table 213 – Adequate traffic levels for the AC+EVA+PPA with increasing creep time and temperature based on the standardized Superpave® criteria ….. 380

Table 214 – Regression equations and coefficients of determination between the $J_{nr}3200$ values of the AC+EVA+PPA and the corresponding vehicle speeds according to the equations by Pereira et al. (1998, 2000) and Huang (2004) …………...... 381

Table 215 – Comparisons between the actual traffic levels of the AC+EVA+PPA and the ones obtained from Huang (2004) and Pereira et al. (1998) …... 382

Table 216 – Comparisons between the actual traffic levels of the AC+EVA+PPA and the ones obtained from the equations by Huang (2004) and Pereira et al. (2000) 383

Table 217 – Traffic levels of the AC+EVA+PPA with increasing loading time and temperature in the current and proposed criteria …..….......... 383

Table 218 – Numerical values and variations in the parameters/constants *A, B, n* and *α* from the power law equations by Saboo and Kumar (2015) with increasing temperature and creep time and considering the AC+EVA+PPA ……........................ 385

Table 219 – Degrees of correlation between the parameters *A* and *B* (modified power model) and the creep time t_F for the AC+EVA+PPA 391

Table 220 – Degrees of correlation between the parameters *n* and *α* (modified power model) and the creep time t_F for the AC+EVA+PPA 392

Table 221 – Rearranged MSCR testing data of the AC+EVA+PPA to be used in the analysis of variance (ANOVA) – percent recovery 395

Table 222 – Results from the analysis of variance (ANOVA, *p-value* and *F-value*) as based on the percent recoveries of the AC+EVA+PPA ……………... 395

Table 223 – Rearranged MSCR testing data of the AC+EVA+PPA to be used in the analysis of variance (ANOVA) – nonrecoverable creep compliance …... 396

Table 224 – Results from the analysis of variance (ANOVA, *p-value* and *F-value*) as based on the nonrecoverable compliances of the AC+EVA+PPA …... 396

Table 225 – Percent recoveries at 100 Pa (*R100*) and 3,200 Pa (*R3200*) for the AC+PE with increasing loading time and temperature ………………… 397

Table 226 – Nonrecoverable compliances at 100 Pa ($J_{nr}100$) and 3,200 Pa ($J_{nr}\,3200$) for the AC+PE with increasing loading time and temperature ………… 399

Table 227 – Percent differences in nonrecoverable compliances ($J_{nr,\ diff}$) for the AC+PE with increasing creep time and temperature …………………... 400

Table 228 – Adequate traffic levels for the AC+PE with increasing creep time and temperature based on the standardized Superpave® criteria ……………. 400

Table 229 – Regression equations and coefficients of determination between the $J_{nr}3200$ values of the AC+PE and the corresponding vehicle speeds according to the equations by Pereira et al. (1998, 2000) and Huang (2004) …………………...…………………...………………….......... 401

Table 230 – Comparisons between the actual traffic levels of the AC+PE and the ones obtained from Huang (2004) and Pereira et al. (1998) …………... 402

Table 231 – Comparisons between the actual traffic levels of the AC+PE and the ones obtained from the equations by Huang (2004) and Pereira et al. (2000) …………………...…………………...………………….......... 402

Table 232 – Traffic levels of the AC+PE with increasing loading time and temperature in the current and proposed criteria …………...…………... 403

Table 233 – Numerical values and variations in the parameters/constants *A, B, n* and *α* from the power law equations by Saboo and Kumar (2015) with increasing temperature and creep time and considering the AC+PE …… 404

Table 234 – Degrees of correlation between the parameters *A* and *B* (modified power model) and the creep time t_F for the AC+PE …………...……………....... 408

Table 235 – Degrees of correlation between the parameters *n* and *α* (modified power model) and the creep time t_F for the AC+PE …………...……………....... 409

Table 236 – Rearranged MSCR testing data of the AC+PE to be used in the analysis of variance (ANOVA) – percent recovery …………...……………........... 412

Table 237 – Rearranged MSCR testing data of the AC+PE to be used in the analysis of variance (ANOVA) – nonrecoverable creep compliance ………...…. 412

Table 238 – Results from the analysis of variance (ANOVA, *p-value* and *F-value*) as based on the percent recoveries of the AC+PE …………...…………. 413

Table 239 – Results from the analysis of variance (ANOVA, *p-value* and *F-value*) as based on the nonrecoverable compliances of the AC+PE ………...…. 413

Table 240 – Percent recoveries at 100 Pa (*R100*) and 3,200 Pa (*R3200*) for the AC+PE+PPA with increasing loading time and temperature ……….…... 414

Table 241 – Nonrecoverable compliances at 100 Pa ($J_{nr}100$) and 3,200 Pa ($J_{nr}3200$) for the AC+PE+PPA with increasing loading time and temperature …... 416

Table 242 – Percent differences in nonrecoverable compliances ($J_{nr,\ diff}$) for the AC+PE+PPA with increasing creep time and temperature …..…...…..... 420

Table 243 – Adequate traffic levels for the AC+PE+PPA with increasing creep time and temperature based on the standardized Superpave® criteria ……….. 421

Table 244 – Regression equations and coefficients of determination between the $J_{nr}3200$ values of the AC+PE+PPA and the corresponding vehicle speeds according to the equations by Pereira et al. (1998, 2000) and Huang (2004) …..…...…...…...…...…...…...…...…...…...…...…...…..... 422

Table 245 – Comparisons between the actual traffic levels of the AC+PE+PPA and the ones obtained from Huang (2004) and Pereira et al. (1998) ……… 422

Table 246 – Comparisons between the actual traffic levels of the AC+PE+PPA and the ones obtained from the equations by Huang (2004) and Pereira et al. (2000) …..…...…...…...…...…...…...…...…...…...…...…........... 422

Table 247 – Traffic levels of the AC+PE+PPA with increasing loading time and temperature in the current and proposed criteria ……….……….……... 423

Table 248 – Numerical values and variations in the parameters/constants *A, B, n* and *α* from the power law equations by Saboo and Kumar (2015) with increasing temperature and creep time and considering the AC+PE+PPA ……….……….……...……….……….……...………... 425

Table 249 – Degrees of correlation between the parameters *A* and *B* (modified power model) and the creep time t_F for the AC+PE+PPA ……….……….…… 431

Table 250 – Degrees of correlation between the parameters *n* and *α* (modified power model) and the creep time t_F for the AC+PE+PPA ……….……….…… 432

Table 251 – Rearranged MSCR testing data of the AC+PE+PPA to be used in the analysis of variance (ANOVA) – percent recovery ……….……….…... 435

Table 252 – Rearranged MSCR testing data of the AC+PE+PPA to be used in the analysis of variance (ANOVA) – nonrecoverable creep compliance …... 435

Table 253 – Results from the analysis of variance (ANOVA, *p-value* and *F-value*) as based on the percent recoveries of the AC+PE+PPA ………………... 436

Table 254 – Results from the analysis of variance (ANOVA, *p-value* and *F-value*) as based on the nonrecoverable compliances of the AC+PE+PPA …….. 436

Table 255 – Direct comparisons among the effects of the presence of PPA and the addition of Elvaloy® terpolymer on the rheological properties and parameters of the 50/70 unmodified asphalt binder ……………..…….. 444

Table 256 – Direct comparisons among the effects of the presence of PPA and the reduction in the crumb rubber content on the rheological properties and parameters of the AC+rubber+PPA …………….……………..…….. 446

Table 257 – Direct comparisons among the effects of the presence of PPA and the reduction in the SBS content on the rheological properties and parameters of the AC+SBS+PPA …………….……………..……….. 447

Table 258 – Direct comparisons among the effects of the presence of PPA and the reduction in the SBR content on the rheological properties and parameters of the AC+SBR+PPA …………….……………..………. 448

Table 259 – Direct comparisons among the effects of the presence of PPA and the reduction in the EVA content on the rheological properties and parameters of the AC+EVA+PPA ….……………..……………..…… 450

Table 260 – Direct comparisons among the effects of the presence of PPA and the reduction in the PE content on the rheological properties and parameters of the AC+PE+PPA …………….……………..…………………….. 451

Table 261 – Nonrecoverable compliances of the selected asphalt binders at 3.2 kPa ($J_{nr}3200$) and 64°C and three pairs of creep-recovery times (2/9, 4/9 and 8/9 s) to be correlated with their corresponding flow number values (F_N) 452

Table 262 – Rankings of the modified asphalt binders based on $J_{nr}100$ and $J_{nr}3200$ at the temperature of 52°C – individual and corresponding coeffients of variation (CV, in percentage) …………….……………..…………… 456

Table 263 – Rankings of the modified asphalt binders based on $J_{nr}100$ and $J_{nr}3200$ at the temperature of 58°C – individual and corresponding coeffients of variation (CV, in percentage) …………….……………..…………… 458

Table 264 – Rankings of the modified asphalt binders based on $J_{nr}100$ and $J_{nr}3200$ at the temperature of 64°C – individual and corresponding coeffients of variation (CV, in percentage) …………….……………..…………… 459

Table 265 – Rankings of the modified asphalt binders based on $J_{nr}100$ and $J_{nr}3200$ at the temperature of 70°C – individual and corresponding coeffients of variation (CV, in percentage) …………….……………..…………… 461

Table 266 – Rankings of the modified asphalt binders based on $J_{nr}100$ and $J_{nr}3200$ at the temperature of 76°C – individual and corresponding coeffients of variation (CV, in percentage) …………….……………..…………… 463

Table 267 – Rankings of the modified asphalt binders based on $J_{nr,\ diff}$ at the temperatures of 52 and 58°C – individual positions and corresponding mean values …………….……………..…………………………….. 466

Table 268 – Rankings of the modified asphalt binders based on $J_{nr,\ diff}$ at the temperatures of 64 and 70°C – individual positions and corresponding mean values …………….……………..…………………………….. 467

Table 269 – Rankings of the modified asphalt binders based on $J_{nr, diff}$ at the temperature of 76°C (individual positions and corresponding mean values) and average position based on all data from 52 to 76°C ……….. 468

Table 270 – Separation of the formulations according to the groups "A" and "B" and their corresponding degrees of elasticity ………................................ 472

Table 271 – Percent recoveries at 100 Pa (*R100*) and 3,200 Pa (*R3200*) for the AC+Elvaloy+PPA, the AC+EVA and the AC+EVA+PPA at 1/500 s and all the high pavement temperatures ……………………….............. 473

Table 272 – Nonrecoverable compliances at 100 Pa ($J_{nr}100$) and 3,200 Pa ($J_{nr}3200$) and corresponding percent differences ($J_{nr, diff}$) for the AC+Elvaloy+PPA, the AC+EVA and the AC+EVA+PPA at 1/500 s and all temperatures ….. 476

Table 273 – Results of the parameter *α* from the model by Saboo and Kumar (2015) at 100 and 3,200 Pa and the creep-recovery times of 1/500 s ………….. 479

Table 274 – Results of the parameters *A* and *B* from the model by Saboo and Kumar (2015) at 100 and 3,200 Pa and the creep-recovery times of 1/500 s …… 480

Table 275 – Percent recoveries at 100 Pa (*R100*) and 3,200 Pa (*R3200*) for the AC+PPA, the AC+rubber, the AC+rubber+PPA, the AC+SBS and the AC+SBS+PPA at 1/240 s and all the high pavement temperatures …….. 482

Table 276 – Nonrecoverable compliances at 100 Pa ($J_{nr}100$) and 3,200 Pa ($J_{nr}3200$) and corresponding percent differences ($J_{nr, diff}$) for the AC+PPA, the AC+rubber, the AC+rubber+PPA, the AC+SBS and the AC+SBS+PPA at 1/240 s and all the high pavement temperatures ……………………... 485

Table 277 – Results of the parameter *α* from the model by Saboo and Kumar (2015) at 100 and 3,200 Pa and the creep-recovery times of 1/240 s – first group of materials …………………..……………………......................... 487

Table 278 – Results of the parameters *A* and *B* from the model by Saboo and Kumar (2015) at 100 and 3,200 Pa and the creep-recovery times of 1/240 s for the AC+PPA, the AC+rubber and the AC+rubber+PPA ………………. 489

Table 279 – Results of the parameters *A* and *B* from the model by Saboo and Kumar (2015) at 100 and 3,200 Pa and the creep-recovery times of 1/240 s for the AC+SBS and the AC+SBS+PPA ………………………………….. 489

Table 280 – Percent recoveries at 100 Pa (*R100*) and 3,200 Pa (*R3200*) for the AC+PE, the AC+PE+PPA, the AC+SBR and the AC+SBR+PPA at 1/240 s and all the high pavement temperatures ………………………... 491

Table 281 – Nonrecoverable compliances at 100 Pa ($J_{nr}100$) and 3,200 Pa ($J_{nr}3200$) and corresponding percent differences ($J_{nr, diff}$) for the AC+PE, the AC+PE+PPA, the AC+SBR and the AC+SBR+PPA at 1/240 s and all the high pavement temperatures ……………………………………….. 493

Table 282 –	Results of the parameter α from the model by Saboo and Kumar (2015) at 100 and 3,200 Pa and the creep-recovery times of 1/240 s – second group of materials ……..	494
Table 283 –	Results of the parameters *A* and *B* from the model by Saboo and Kumar (2015) at 100 and 3,200 Pa and the creep-recovery times of 1/240 s for the AC+PE, the AC+PE+PPA, the AC+SBR and the AC+SBR+PPA …	496
Table 284 –	Overall and simplified analysis of the creep-recovery data of the asphalt binders from "Group B" with respect to the criteria for reaching full recovery at each creep-recovery cycle …….	498
Table 285 –	Rankings of the modified asphalt binders at longer creep times based on $J_{nr}100$ and $J_{nr}3200$ and for all pavement temperatures …….	500
Table 286 –	Mean values of the rankings of the modified asphalt binders at longer creep times – based on $J_{nr}100$ and $J_{nr}3200$ – and corresponding coefficients of variation (CV) …….	501
Table 287 –	Rankings of the modified asphalt binders at longer creep times based on $J_{nr,\ diff}$ and for all pavement temperatures, together with the corresponding coefficients of variation (CV) ……..	503
Table 288 –	Examples of *R* values from the AC+Elvaloy+PPA at the temperatures of 64 and 70°C and the creep times of 1/9, 2/9, 4/9 and 8/9 s …….	550
Table 289 –	Examples of J_{nr} values from the AC+Elvaloy+PPA at the temperatures of 64 and 70°C and the creep times of 1/9, 2/9, 4/9 and 8/9 s …….	551
Table 290 –	Rearranged MSCR testing data of the AC+Elvaloy+PPA to be used in the analysis of variance (ANOVA) – percent recovery *R* …….	551
Table 291 –	Rearranged MSCR testing data of the AC+Elvaloy+PPA to be used in the analysis of variance (ANOVA) – nonrecoverable compliance J_{nr} …..	551
Table 292 –	Results from ANOVA (*p-value* and *F-value*) as based on the percent recoveries of the AC+Elvaloy+PPA ……..	552
Table 293 –	Results from ANOVA (*p-value* and *F-value*) as based on the nonrecoverable compliances of the AC+Elvaloy+PPA ……...	553
Table 294 –	Preliminary draft of the revised Superpave® specification for RTFO-aged materials with the creep time as a criterion for choosing the adequate traffic level of the binder …….	556
Table 295 –	Technical details of the MSCR tests according to the current and historical versions of the ASTM D7405 standard …….	558
Table 296 –	Technical details of the MSCR tests according to the current and historical versions of the AASHTO TP70/T350 standards ……..	559

LIST OF FIGURES

Figure 1 – Extreme conditions of rutting resistance of the binder based on the following concepts: consistency (*hard* and *soft*), linear viscoelasticity (*elastic* and *viscous*) and damage (*strong* and *weak*) [adapted from Bahia (2014)] 2

Figure 2 – Regions of the creep response of viscoelastic materials (e. g., asphalt binders) for different loading levels [adapted from Lakes (2009)] 4

Figure 3 – Typical illustration of the Newton's experiment for calculating the viscosity (or, more specifically, the *dynamic viscosity*) of a particular fluid (WIKIPEDIA, 2016) 14

Figure 4 – Typical layout of the measurement of the rotational viscosity of a binder sample in a Brookfield viscometer (ROBERTS et al., 1996) 18

Figure 5 – Schematic of the DSR in the oscillatory shear test and identification of the interest points (ROBERTS et al., 1996) 18

Figure 6 – Relationship between the moduli G^*, G'' and G' and the phase angle δ (right triangle) 19

Figure 7 – Representative illustration of the apparatus used in the bending beam rheometer (BBR) tests (ROBERTS et al., 1996) 20

Figure 8 – Variations in viscosity with shear rate for Newtonian, shear-thinning and shear-thickening fluids 26

Figure 9 – Typical responses of perfectly elastic and perfectly viscous bodies in a repeated creep (or creep-recovery) test 26

Figure 10 – Illustration of a typical response of a viscoelastic material subjected to a repeated creep (or creep-recovery) loading mode 27

Figure 11 – Complete descriptions of the strains observed in a viscoelastic material under creep and recovery (repeated creep) loading 28

Figure 12 – Strain responses of viscoelastic and viscous materials under dynamic shear loading and typical values for the phase angle δ 29

Figure 13 – Illustration of a spring element associated with a Young's modulus (E_{spring}) for use in rheological models 32

Figure 14 – Illustration of a dashpot element associated with a Newtonian viscosity ($\eta_{dashpot}$) for use in rheological models 32

Figure 15 – Rheological response of the asphalt binder in a creep-recovery test according to the Maxwell model 34

Figure 16 – Rheological response of the asphalt binder in a creep-recovery test according to the Voigt model 34

Figure 17 – Illustration of a four-element Burgers model with the two springs ($E_{spring,1}$ and $E_{spring,2}$) and two dashpots ($\eta_{dashpot,1}$ and $\eta_{dashpot,2}$) from the Maxwell and Voigt models 35

Figure 18 – Layout of the generalized Burgers model used in this study [adapted from Woldekidan (2011)] 37

Figure 19 – Illustration of the Burgers fractional model with two springs ($E_{spring,\ 1}$ and $E_{spring,\ 2}$) and two springpots (characteristic parameters ψ_1, ψ_∞, α_1 and α_∞) 38

Figure 20 – Typical layout of the 2S2P1D ("2-spring, 2-parabolic, 1-dashpot") model with the identification of the parabolic elements and the fractional constants m_1 and m_2 [adapted from Woldekidan (2011)] 39

Figure 21 – Calculations of the values S_1 and S_2 associated with the parabolic dashpots (angles φ_1 and φ_2 and fractional constants m_1 and m_2) 39

Figure 22 – Current status of the MSCR test in each of the states and districts of the United States (ASPHALT INSTITUTE, 2016) 45

Figure 23 – Three-dimensional structure of the SBS copolymer with the polystyrenic-end blocks (spheres) and the polybutadienic-middle blocks (springs) (READ and WHITEOAK, 2003) 52

Figure 24 – Schematic of the ethylene vinyl acetate (EVA) copolymer [adapted from Read and Whiteoak (2003)] 54

Figure 25 – Typical creep-recovery response of an asphalt binder in the repeated creep and recovery test (RCRT) at 100 Pa [adapted from Anderson (2007)] 68

Figure 26 – Identification of the strains ε_0, ε_c and ε_r in two of the 10 creep-recovery cycles of a standardized MSCR test 73

Figure 27 – Effects of varying creep and recovery times on the permanent strain of an oxidized binder (PG 82-xx) in the RCRT (BAHIA et al., 2001b) 78

Figure 28 – Relationship between R and J_{nr} at 3.2 kPa and identification of the degree of elasticity of the formulation (high or poor) 79

Figure 29 – Mixture sample with the plaster layer on top after the repeated creep (or flow number) test 92

Figure 30 – Aggregate gradation curve (red line) of the mixture samples and upper and lower limits (grey lines) for passing material 94

Figure 31 – Typical strain curve of a mixture subjected to the flow number test (GIBSON et al., 2012) 98

Figure 32 – Comparisons among the average rut depths (in inches) of the pavement sections with and without PPA-modified binders after many years of service life [adapted from Buncher and Von Quintus (2014)] 114

Figure 33 – Number of cycles to achieve 12.5 mm of rut depth in the mixtures designed for 1,000,000 ESALs – temperature of 50°C and the Hamburg wheel tracking device [adapted from Reinke et al. (2012)]…. 114

Figure 34 – Number of cycles to achieve 12.5 mm of rut depth in the mixtures designed for 10,000,000 ESALs – temperature of 50°C and the Hamburg wheel tracking device [adapted from Reinke et al. (2012)] ... 114

Figure 35 – Flow number (F_N) values of each mixture sample for the 50/70 base binder and the AC+PPA 115

Figure 36 – Linear correlations between flow number (F_N) at 60°C and the following binder parameters: (a) nonrecoverable compliance J_{nr} at 3.2 kPa and 64°C; and (b) viscous component of the creep stiffness (G_V) at 64°C... 116

Figure 37 – Linear correlations between flow number (F_N) at 60°C and the following binder parameters: (a) original Superpave® parameter $G^*/sin\delta$ at 64°C; (b) Shenoy's parameter $|G^*|/[1-(1/tan\delta sin\delta)]$ at 64°C; and (c) softening point *R&B* after short-term aging 117

Figure 38 – Linear correlations between flow number (F_N) at 60°C and the following terms: (a) mean value of the low number index FN_I; and (b) the constant *C* from the Francken model 120

Figure 39 – Linear correlations between the accumulated strain after 10,000 cycles (γ_{per}) at 60°C and the following binder parameters: (a) nonrecoverable compliance J_{nr} at 3.2 kPa and 64°C; and (b) viscous component of the creep stiffness (G_V) at 64°C and 0.1 kPa 124

Figure 40 – Accumulated strain versus number of cycles for the base binder (AC), the AC+Elvaloy+PPA, the AC+PPA, the AC+rubber and the AC+rubber+PPA at 60°C (original samples) 129

Figure 41 – Accumulated strain versus number of cycles for the base binder (AC), the AC+EVA, the AC+EVA+PPA, the AC+PE and the AC+PE+PPA at 60°C (original samples) 129

Figure 42 – Accumulated strain versus number of cycles for the base binder (AC), the AC+SBS, the AC+SBS+PPA, the AC+SBR and the AC+SBR+PPA at 60°C (original samples) 129

Figure 43 – Penetration index (P_I) of the 50/70 original binder and the modified materials in terms of their absolute and non-absolute values …………….. 138

Figure 44 – Mass losses of the base binder (AC) and the 12 formulations after short-term aging in the rolling thin-film oven (mean values of at least three replicates) ………………………………………………………… 139

Figure 45 – Decreases in the parameter *G*/sinδ* with temperature for the 50/70 base asphalt binder (continuous line) and the AC+PPA (dotted line) ………… 145

Figure 46 – Decreases in the parameter *G*/sinδ* with temperature for the 50/70 base asphalt binder (continuous line) and the AC+Elvaloy+PPA (dotted line) . 145

Figure 47 – First creep-recovery pulses of two different binders in the MSCR test (AC+EVA and AC+Elvaloy+PPA) at 70°C and 3.2 kPa ……………….. 154

Figure 48 – First creep-recovery pulse of the 50/70 base asphalt binder in the MSCR at 70°C and 3.2 kPa …………………………………………….. 155

Figure 49 – Percent recoveries of the 50/70 base binder, the AC+PPA and the AC+Elvaloy+PPA at 1/9 s …………………………………………… 156

Figure 50 – Nonrecoverable compliances of the 50/70 base binder, the AC+PPA and the AC+Elvaloy+PPA at 1/9 s …………………………………... 157

Figure 51 – Levels of elasticity for the AC+PPA and the AC+Elvaloy+PPA at the creep-recovery times of 1/9 s ………………………………………... 158

Figure 52 – Percent recoveries of the 50/70 base binder, the AC+PPA, the AC+rubber and the AC+rubber+PPA at 1/9 s ……………………….. 161

Figure 53 – Nonrecoverable compliances of the 50/70 base binder, the AC+PPA, the AC+rubber and the AC+rubber+PPA at 1/9 s …………………… 162

Figure 54 – Levels of elasticity for the AC+rubber and the AC+rubber+PPA at the creep-recovery times of 1/9 s …………………………………….. 163

Figure 55 – Percent recoveries of the 50/70 base binder, the AC+PPA, the AC+EVA and the AC+EVA+PPA at 1/9 s …………………………... 166

Figure 56 – Nonrecoverable compliances of the 50/70 base binder, the AC+PPA, the AC+EVA and the AC+EVA+PPA at 1/9 s ……………………… 167

Figure 57 – Levels of elasticity for the AC+EVA and the AC+EVA+PPA at the creep-recovery times of 1/9 s ………………………………………... 168

Figure 58 – Fitting of the four-element Burgers model to the strain data of the AC+EVA at 52°C and 100 Pa (second creep-recovery cycle) ………. 170

Figure 59 – Fitting of the four-element Burgers model and the generalized Voigt model to the strain data of the AC+EVA at 52°C and 100 Pa (third creep-recovery cycle) ………………………………………………….. 173

Figure 60 – Percent recoveries of the 50/70 base binder, the AC+PPA, the AC+PE and the AC+PE+PPA at 1/9 s 174

Figure 61 – Nonrecoverable compliances of the 50/70 base binder, the AC+PPA, the AC+PE and the AC+PE+PPA at 1/9 s 175

Figure 62 – Levels of elasticity for the AC+PE and the AC+PE+PPA at the creep-recovery times of 1/9 s 177

Figure 63 – Percent recoveries of the 50/70 base binder, the AC+PPA, the AC+SBS and the AC+SBS+PPA at 1/9 s 179

Figure 64 – Nonrecoverable compliances of the 50/70 base binder, the AC+PPA, the AC+SBS and the AC+SBS+PPA at 1/9 s 180

Figure 65 – Levels of elasticity for the AC+SBS and the AC+SBS+PPA at the creep-recovery times of 1/9 s 181

Figure 66 – Percent recoveries of the 50/70 base binder, the AC+PPA, the AC+SBR and the AC+SBR+PPA at 1/9 s 185

Figure 67 – Levels of elasticity for the AC+SBR and the AC+SBR+PPA at the creep-recovery times of 1/9 s 185

Figure 68 – Nonrecoverable compliances of the 50/70 base binder, the AC+PPA, the AC+SBR and the AC+SBR+PPA at 1/9 s 186

Figure 69 – Percentages of increase in the nonrecoverable compliances of the 50/70 base asphalt binder with creep time, temperature and stress level 193

Figure 70 – Correlations between the nonrecoverable compliances of the base binder at 3.2 kPa and the vehicle speeds calculated by the equations from Huang (2004) – tire radius of 6 in – and Pereira et al. (1998) at the temperatures of (a) 52°C; (b) 58°C; (c) 64°C; (d) 70°C; and (e) 76°C 195

Figure 71 – Correlations between the nonrecoverable compliances of the base binder at 3.2 kPa and the vehicle speeds calculated by the equations from Huang (2004) – tire radius of 3.68 in – and Pereira et al. (2000) at the temperatures of (a) 52°C; (b) 58°C; (c) 64°C; (d) 70°C; and (e) 76°C 196

Figure 72 – Correlations between the creep time and the constants *A* and *B* from the model by Saboo and Kumar (2015), temperature of 64°C and stress level of 100 Pa – 50/70 base asphalt binder 202

Figure 73 – Correlations between the creep time and the constants *A* and *B* from the model by Saboo and Kumar (2015), temperature of 64°C and stress level of 3,200 Pa – 50/70 base asphalt binder 202

Figure 74 – Correlations between the creep time and the constants *A* and *B* from the model by Saboo and Kumar (2015), temperature of 70°C and stress level of 100 Pa – 50/70 base asphalt binder 203

Figure 75 – Correlations between the creep time and the constants *A* and *B* from the model by Saboo and Kumar (2015), temperature of 70°C and stress level of 3,200 Pa – 50/70 base asphalt binder 203

Figure 76 – Percentages of decrease in the recoveries of the AC+PPA with creep time, temperature and stress level 207

Figure 77 – Percentages of increase in the nonrecoverable compliances of the AC+PPA with creep time, temperature and stress level 209

Figure 78 – Comparison between the *B* values of the 50/70 original binder and the AC+PPA in the modified power model by Saboo and Kumar (2015) ... 217

Figure 79 – Correlations between the creep time and the constants *A* and *B* from the model by Saboo and Kumar (2015), temperature of 64°C and stress level of 100 Pa – AC+PPA 218

Figure 80 – Correlations between the creep time and the constants *A* and *B* from the model by Saboo and Kumar (2015), temperature of 64°C and stress level of 3,200 Pa – AC+PPA 218

Figure 81 – Correlations between the creep time and the constants *A* and *B* from the model by Saboo and Kumar (2015), temperature of 70°C and stress level of 100 Pa – AC+PPA 219

Figure 82 – Correlations between the creep time and the constants *A* and *B* from the model by Saboo and Kumar (2015), temperature of 70°C and stress level of 3,200 Pa – AC+PPA 219

Figure 83 – Degree of correlation between the percent recoveries of the AC+PPA and the corresponding α values from the power law models 222

Figure 84 – Percentages of decrease in the recoveries of the AC+Elvaloy+PPA with creep time, temperature and stress level 226

Figure 85 – Percentages of increase in the nonrecoverable compliances of the AC+Elvaloy+PPA with creep time, temperature and stress level 227

Figure 86 – Degrees of elasticity for the AC+Elvaloy+PPA at increased creep times and temperatures as based on the MSCR testing parameters at 3,200 Pa 229

Figure 87 – Correlations between the creep time and the constants *A* and *B* from the model by Saboo and Kumar (2015), temperature of 64°C and stress level of 100 Pa – AC+Elvaloy+PPA 236

Figure 88 – Correlations between the creep time and the constants *A* and *B* from the model by Saboo and Kumar (2015), temperature of 64°C and stress level of 3,200 Pa – AC+Elvaloy+PPA 236

Figure 89 – Correlations between the creep time and the constants *A* and *B* from the model by Saboo and Kumar (2015), temperature of 70°C and stress level of 100 Pa – AC+Elvaloy+PPA 237

Figure 90 – Correlations between the creep time and the constants *A* and *B* from the model by Saboo and Kumar (2015), temperature of 70°C and stress level of 3,200 Pa – AC+Elvaloy+PPA 237

Figure 91 – Degree of correlation between the percent recoveries of the AC+Elvaloy+PPA and the corresponding α values from the power law models 240

Figure 92 – Individual correlations between the percent recoveries of the AC+Elvaloy+PPA at 100 and 3,200 Pa and the corresponding α values from the power law models 241

Figure 93 – Percentages of decrease in the recoveries of the AC+rubber with creep time, temperature and stress level 244

Figure 94 – Percentages of increase in the nonrecoverable compliances of the AC+rubber with creep time, temperature and stress level 245

Figure 95 – Correlations between the creep time and the constants *A* and *B* from the model by Saboo and Kumar (2015), temperature of 64°C and stress level of 100 Pa – AC+rubber 252

Figure 96 – Correlations between the creep time and the constants *A* and *B* from the model by Saboo and Kumar (2015), temperature of 64°C and stress level of 3,200 Pa – AC+rubber 252

Figure 97 – Correlations between the creep time and the constants *A* and *B* from the model by Saboo and Kumar (2015), temperature of 70°C and stress level of 100 Pa – AC+rubber 253

Figure 98 – Correlations between the creep time and the constants *A* and *B* from the model by Saboo and Kumar (2015), temperature of 70°C and stress level of 3,200 Pa – AC+rubber 253

Figure 99 – Degree of correlation between the nonrecoverable compliances of the AC+rubber at the stress level of 3,200 Pa and the corresponding *n* values from the power law models 256

Figure 100 – Degree of correlation between the percent recoveries of the AC+rubber and the corresponding α values from the power law models 256

Figure 101 – Percentages of decrease in the recoveries of the AC+rubber+PPA with creep time, temperature and stress level 260

Figure 102 – Percentages of increase in the nonrecoverable compliances of the AC+rubber+PPA with creep time, temperature and stress level …….. 261

Figure 103 – Graphical comparison between the values of the constant *A* for the AC+rubber and the AC+rubber+PPA at 100 and 3,200 Pa ………….. 269

Figure 104 – Graphical comparison between the values of the constant *B* for the AC+rubber and the AC+rubber+PPA at 100 and 3,200 Pa ………….. 269

Figure 105 – Correlations between the creep time and the constants *A* and *B* from the model by Saboo and Kumar (2015), temperature of 64°C and stress level of 100 Pa – AC+rubber+PPA …………………………………… 270

Figure 106 – Correlations between the creep time and the constants *A* and *B* from the model by Saboo and Kumar (2015), temperature of 64°C and stress level of 3,200 Pa – AC+rubber+PPA ………………………………… 270

Figure 107 – Correlations between the creep time and the constants *A* and *B* from the model by Saboo and Kumar (2015), temperature of 70°C and stress level of 100 Pa – AC+rubber+PPA …………………………………… 271

Figure 108 – Correlations between the creep time and the constants *A* and *B* from the model by Saboo and Kumar (2015), temperature of 70°C and stress level of 3,200 Pa – AC+rubber+PPA ………………………………… 271

Figure 109 – Degree of correlation between the nonrecoverable compliances of the AC+rubber+PPA at the stress level of 3,200 Pa and the corresponding *n* values from the power law models ………………………………….. 272

Figure 110 – Degree of correlation between the percent recoveries of the AC+rubber+PPA and the corresponding *α* values from the power law models ……………………………………………………………..... 274

Figure 111 – Percentages of decrease in the recoveries of the AC+SBS with creep time, temperature and stress level …………………………………… 278

Figure 112 – Percentages of increase in the nonrecoverable compliances of the AC+SBS with creep time, temperature and stress level ……………... 279

Figure 113 – Correlations between the creep time and the constants *A* and *B* from the model by Saboo and Kumar (2015), temperature of 64°C and stress level of 100 Pa – AC+SBS ……………………………………………. 286

Figure 114 – Correlations between the creep time and the constants *A* and *B* from the model by Saboo and Kumar (2015), temperature of 64°C and stress level of 3,200 Pa – AC+SBS ………………………………………….. 287

Figure 115 – Correlations between the creep time and the constants *A* and *B* from the model by Saboo and Kumar (2015), temperature of 70°C and stress level of 100 Pa – AC+SBS ……………………………………………. 287

Figure 116 – Correlations between the creep time and the constants *A* and *B* from the model by Saboo and Kumar (2015), temperature of 70°C and stress level of 3,200 Pa – AC+SBS 288

Figure 117 – Degree of correlation between the percent recoveries of the AC+SBS and the corresponding α values from the power law models 290

Figure 118 – Individual correlations between the percent recoveries of the AC+SBS at 100 and 3,200 Pa and the corresponding α values from the power law models 290

Figure 119 – Percentages of decrease in the recoveries of the AC+SBS+PPA with creep time, temperature and stress level 295

Figure 120 – Percentages of increase in the nonrecoverable compliances of the AC+SBS+PPA with creep time, temperature and stress level 296

Figure 121 – Plots of the nonrecoverable compliance J_{nr} versus loading time (log-log scale) for the AC+SBS and the AC+SBS+PPA at the temperatures of (a) 58°C; and (b) 64°C 297

Figure 122 – Plots of the data points associated with the ratios of the constants *A* and *B* for the AC+SBS+PPA to the corresponding ones for the AC+SBS (each data point is characterized by one temperature and loading time) 303

Figure 123 – Correlations between the creep time and the constants *A* and *B* from the model by Saboo and Kumar (2015), temperature of 64°C and stress level of 100 Pa – AC+SBS+PPA 305

Figure 124 – Correlations between the creep time and the constants *A* and *B* from the model by Saboo and Kumar (2015), temperature of 64°C and stress level of 3,200 Pa – AC+SBS+PPA 305

Figure 125 – Correlations between the creep time and the constants *A* and *B* from the model by Saboo and Kumar (2015), temperature of 70°C and stress level of 100 Pa – AC+SBS+PPA 306

Figure 126 – Correlations between the creep time and the constants *A* and *B* from the model by Saboo and Kumar (2015), temperature of 70°C and stress level of 3,200 Pa – AC+SBS+PPA 306

Figure 127 – Degree of correlation between the nonrecoverable compliances of the AC+SBS+PPA at 3,200 Pa and the corresponding *n* values from the power law models 308

Figure 128 – Degree of correlation between the percent recoveries of the AC+SBS+PPA and the corresponding α values from the power law models 309

Figure 129 – Individual correlations between the percent recoveries of the AC+SBS+PPA at 100 and 3,200 Pa and the corresponding α values from the power law models 309

Figure 130 – Percentages of decrease in the recoveries of the AC+SBR with creep time, temperature and stress level 313

Figure 131 – Percentages of increase in the nonrecoverable compliances of the AC+SBR with creep time, temperature and stress level 315

Figure 132 – Plots of the data points associated with the ratios of the J_{nr} values for the AC+SBR to the corresponding ones for the AC+SBS (each data point is characterized by one temperature, loading time and stress level), the continuous line is the equality line 315

Figure 133 – Correlations between the creep time and the constants *A* and *B* from the model by Saboo and Kumar (2015), temperature of 64°C and stress level of 100 Pa – AC+SBR 322

Figure 134 – Correlations between the creep time and the constants *A* and *B* from the model by Saboo and Kumar (2015), temperature of 64°C and stress level of 3,200 Pa – AC+SBR 323

Figure 135 – Correlations between the creep time and the constants *A* and *B* from the model by Saboo and Kumar (2015), temperature of 70°C and stress level of 100 Pa – AC+SBR 323

Figure 136 – Correlations between the creep time and the constants *A* and *B* from the model by Saboo and Kumar (2015), temperature of 70°C and stress level of 3,200 Pa – AC+SBR 324

Figure 137 – Degree of correlation between the nonrecoverable compliances of the AC+SBR and the corresponding *n* values from the power law models 326

Figure 138 – Degree of correlation between the percent recoveries of the AC+SBR and the corresponding α values from the power law models 327

Figure 139 – Percentages of decrease in the recoveries of the AC+SBR+PPA with creep time, temperature and stress level 330

Figure 140 – Percentages of increase in the nonrecoverable compliances of the AC+SBR with creep time, temperature and stress level 331

Figure 141 – Plots of the data points associated with the ratios of the J_{nr} values for the AC+SBR+PPA to the corresponding ones for the AC+SBR (each data point is characterized by one temperature, loading time and stress level), the continuous line is the equality line 332

Figure 142 – Plots of the nonrecoverable compliance J_{nr} versus loading time (log-log scale) for the AC+SBR and the AC+SBR+PPA at the temperatures of (a) 70°C; and (b) 76°C 332

Figure 143 – Plots of the data points associated with the *A* values for the AC+SBR+PPA in the X-axes and the corresponding ones for the AC+SBR in the Y-axes at 100 Pa (a) and 3,200 Pa (b), the continuous lines are the equality lines 340

Figure 144 – Correlations between the creep time and the constants *A* and *B* from the model by Saboo and Kumar (2015), temperature of 64°C and stress level of 100 Pa – AC+SBR+PPA 341

Figure 145 – Correlations between the creep time and the constants *A* and *B* from the model by Saboo and Kumar (2015), temperature of 64°C and stress level of 3,200 Pa – AC+SBR+PPA 341

Figure 146 – Correlations between the creep time and the constants *A* and *B* from the model by Saboo and Kumar (2015), temperature of 70°C and stress level of 100 Pa – AC+SBR+PPA 342

Figure 147 – Correlations between the creep time and the constants *A* and *B* from the model by Saboo and Kumar (2015), temperature of 70°C and stress level of 3,200 Pa – AC+SBR+PPA 342

Figure 148 – Degree of correlation between the nonrecoverable compliances of the AC+SBR+PPA and the corresponding *n* values from the power law models 345

Figure 149 – Degree of correlation between the percent recoveries of the AC+SBR+PPA and the corresponding *α* values from the power law models 346

Figure 150 – Percentages of decrease in the recoveries of the AC+EVA with creep time, temperature and stress level 349

Figure 151 – Percentages of increase in the nonrecoverable compliances of the AC+EVA with creep time, temperature and stress level 351

Figure 152 – Plots of the percent recoveries and the nonrecoverable compliances at 3,200 Pa (*R3200* and J_{nr}*3200*) at each cycle for the AC+EVA at 8/9 s and 58°C (original sample) 352

Figure 153 – Plots of the percent recoveries and the nonrecoverable compliances at 3,200 Pa (*R3200* and J_{nr}*3200*) at each cycle for the AC+EVA at 4/9 s and 58°C (original sample) 353

Figure 154 – Degrees of elasticity for the AC+EVA at increased creep times and temperatures as based on the MSCR testing parameters at 3,200 Pa .. 354

Figure 155 – Comparison between the *A* values of the modified power model by Saboo and Kumar (2015) for the AC+EVA and the AC+Elvaloy+PPA under all MSCR testing conditions 362

Figure 156 – Comparison between the B values of the modified power model by Saboo and Kumar (2015) for the AC+EVA and the AC+Elvaloy+PPA under all MSCR testing conditions 363

Figure 157 – Comparison between the α values of the modified power model by Saboo and Kumar (2015) for the AC+EVA and the AC+Elvaloy+PPA under all MSCR testing conditions 363

Figure 158 – Correlations between the creep time and the constants A and B from the model by Saboo and Kumar (2015), temperature of 64°C and stress level of 100 Pa – AC+EVA 364

Figure 159 – Correlations between the creep time and the constants A and B from the model by Saboo and Kumar (2015), temperature of 64°C and stress level of 3,200 Pa – AC+EVA 364

Figure 160 – Correlations between the creep time and the constants A and B from the model by Saboo and Kumar (2015), temperature of 70°C and stress level of 100 Pa – AC+EVA 366

Figure 161 – Correlations between the creep time and the constants A and B from the model by Saboo and Kumar (2015), temperature of 70°C and stress level of 3,200 Pa – AC+EVA 366

Figure 162 – Degree of correlation between the nonrecoverable compliances of the AC+EVA and the corresponding n values from the power law models 368

Figure 163 – Degree of correlation between the percent recoveries of the AC+EVA and the corresponding α values from the power law models 369

Figure 164 – Percentages of variation in the recovery values of the AC+EVA+PPA with creep time, temperature and stress level 372

Figure 165 – Plots of the percent recoveries at 100 Pa (*R100*) at each cycle for the AC+EVA+PPA, temperature of 64°C and creep-recovery times of 1/9 s, 2/9 s and 4/9 s (original samples) 373

Figure 166 – Plots of the percent recoveries at 100 Pa (*R100*) at each cycle for the AC+EVA+PPA, temperature of 70°C and creep-recovery times of 1/9 s, 2/9 s and 4/9 s (original samples) 374

Figure 167 – Plots of the percent recoveries at 100 Pa (*R100*) at each cycle for the AC+EVA+PPA, temperature of 76°C and creep-recovery times of 1/9 s, 2/9 s and 4/9 s (original samples) 375

Figure 168 – Plots of the percent recoveries at 100 Pa (*R100*) at each cycle for the AC+EVA+PPA, temperatures of 52°C (a) and 58°C (b) and creep-recovery times of 1/9 s, 2/9 s and 4/9 s – original samples 375

Figure 169 – Comparison between the percent recoveries of the AC+EVA and the AC+EVA+PPA under all MSCR testing conditions 376

Figure 170 – Comparison between the nonrecoverable compliances (J_{nr}) of the AC+EVA and the AC+EVA+PPA only for the results typically greater than 1.0 kPa^{-1} (temperatures of 64, 70 and 76°C) 377

Figure 171 – Comparison between the nonrecoverable compliances (J_{nr}) of the AC+EVA and the AC+EVA+PPA only for the results lower than 1.0 kPa^{-1} (temperatures of 52 and 58°C) 378

Figure 172 – Comparison between the percent differences in nonrecoverable compliances ($J_{nr,\ diff}$) of the AC+EVA and the AC+EVA+PPA in all of the MSCR testing conditions 379

Figure 173 – Plots of the nonrecoverable compliance J_{nr} versus loading time (log-log scale) for the AC+EVA and the AC+EVA+PPA at the temperatures of (a) 64°C; and (b) 70°C 380

Figure 174 – Percentages of increase in the nonrecoverable compliances of the AC+EVA+PPA with creep time, temperature and stress level 381

Figure 175 – Comparison between the results of the parameter α for the AC+EVA and the AC+EVA+PPA under all MSCR testing conditions 386

Figure 176 – Plots of the data points associated with the ratios of the A and B values for the AC+EVA+PPA to the corresponding ones for the AC+EVA (each data point is characterized by one temperature, loading time and stress level), the continuous line is the equality line and the red circle highlights the results of A and B at 70 and 76°C 387

Figure 177 – Direct comparison between the degrees of nonlinearity (n values) for the AC+EVA and the AC+EVA+PPA at the temperatures of 52, 58 and 64°C 387

Figure 178 – Degrees of elasticity for the AC+EVA+PPA at increased creep times and temperatures as based on the MSCR testing parameters at 3,200 Pa 388

Figure 179 – Correlations between the creep time and the constants A and B from the model by Saboo and Kumar (2015), temperature of 64°C and stress level of 100 Pa – AC+EVA+PPA 389

Figure 180 – Correlations between the creep time and the constants A and B from the model by Saboo and Kumar (2015), temperature of 64°C and stress level of 3,200 Pa – AC+EVA+PPA 389

Figure 181 – Correlations between the creep time and the constants A and B from the model by Saboo and Kumar (2015), temperature of 70°C and stress level of 100 Pa – AC+EVA+PPA 390

Figure 182 – Correlations between the creep time and the constants A and B from the model by Saboo and Kumar (2015), temperature of 70°C and stress level of 3,200 Pa – AC+EVA+PPA 390

Figure 183 – Degree of correlation between the nonrecoverable compliances of the AC+EVA+PPA and the corresponding *n* values from the power law models 393

Figure 184 – Degree of correlation between the percent recoveries of the AC+EVA+PPA and the corresponding *α* values from the power law models 394

Figure 185 – Individual correlations between the percent recoveries of the AC+EVA+PPA at 100 and 3,200 Pa and the corresponding *α* values from the power law models 394

Figure 186 – Percentages of decrease in the recovery values of the AC+PE with creep time, temperature and stress level 397

Figure 187 – Percentages of increase in the nonrecoverable compliances of the AC+PE with creep time, temperature and stress level 399

Figure 188 – Correlations between the creep time and the constants *A* and *B* from the model by Saboo and Kumar (2015), temperature of 64°C and stress level of 100 Pa – AC+PE 406

Figure 189 – Correlations between the creep time and the constants *A* and *B* from the model by Saboo and Kumar (2015), temperature of 64°C and stress level of 3,200 Pa – AC+PE 406

Figure 190 – Correlations between the creep time and the constants *A* and *B* from the model by Saboo and Kumar (2015), temperature of 70°C and stress level of 100 Pa – AC+PE 407

Figure 191 – Correlations between the creep time and the constants *A* and *B* from the model by Saboo and Kumar (2015), temperature of 70°C and stress level of 3,200 Pa – AC+PE 407

Figure 192 – Degrees of correlation between the nonrecoverable compliances of the AC+PE and the corresponding *n* values from the power law models: (a) all data at 100 and 3,200 Pa; (b) only the data at 3,200 Pa 410

Figure 193 – Degrees of correlation between the percent recoveries of the AC+PE and the corresponding *α* values from the power law models: (a) all data at 100 and 3,200 Pa; (b) only the data at 100 Pa 411

Figure 194 – Plots of the percent recoveries at 100 Pa (*R100*) at each cycle for the AC+PE+PPA, temperatures of 70 and 76°C and creep-recovery times of 4/9 s and 8/9 s (original samples) 415

Figure 195 – Percentages of increase in the nonrecoverable compliances of the AC+PE+PPA with creep time, temperature and stress level 417

Figure 196 – Percentages of decrease in the recovery values of the AC+PE+PPA with creep time, temperature and stress level 417

Figure 197 – Plots of the nonrecoverable compliance J_{nr} versus loading time (log-log scale) for the AC+PE and the AC+PE+PPA at the temperatures of (a) 70°C; and (b) 76°C 418

Figure 198 – Comparison between the percent recoveries of the AC+PE and the AC+PE+PPA under all MSCR testing conditions 419

Figure 199 – Comparison between the nonrecoverable compliances (J_{nr}) of the AC+EVA and the AC+EVA+PPA (a) only for the results higher than 2.0 kPa^{-1}; and (b) only for the ones lower than 2.0 kPa^{-1} 419

Figure 200 – Comparison between the percent differences in nonrecoverable compliances ($J_{nr,\ diff}$) of the AC+PE and the AC+PE+PPA in all of the MSCR testing conditions 420

Figure 201 – Plots of the data points associated with the ratios of the *A* and *B* values for the AC+PE+PPA to the corresponding ones for the AC+PE (each data point is characterized by one temperature, loading time and stress level), the continuous line is the equality line 426

Figure 202 – Comparison between the results of the parameter α for the AC+PE and the AC+PE+PPA under all MSCR testing conditions 427

Figure 203 – Direct comparison between the degrees of nonlinearity (*n* values) for the AC+PE and the AC+PE+PPA under all MSCR testing conditions 428

Figure 204 – Correlations between the creep time and the constants *A* and *B* from the model by Saboo and Kumar (2015), temperature of 64°C and stress level of 100 Pa – AC+PE+PPA 428

Figure 205 – Correlations between the creep time and the constants *A* and *B* from the model by Saboo and Kumar (2015), temperature of 64°C and stress level of 3,200 Pa – AC+PE+PPA 429

Figure 206 – Correlations between the creep time and the constants *A* and *B* from the model by Saboo and Kumar (2015), temperature of 70°C and stress level of 100 Pa – AC+PE+PPA 430

Figure 207 – Correlations between the creep time and the constants *A* and *B* from the model by Saboo and Kumar (2015), temperature of 70°C and stress level of 3,200 Pa – AC+PE+PPA 430

Figure 208 – Degree of correlation between the nonrecoverable compliances of the AC+PE+PPA and the corresponding *n* values from the power law models 432

Figure 209 – Degree of correlation between the nonrecoverable compliances of the AC+PE+PPA at 3,200 Pa and the corresponding *n* values from the power law models 433

Figure 210 – Degree of correlation between the percent recoveries of the AC+PE and the corresponding α values from the power law models ………….. 434

Figure 211 – Degree of correlation between the percent recoveries of all modified asphalt binders and their corresponding α values from the power law models ……………………………………………………………… 442

Figure 212 – Degree of correlation between the nonrecoverable compliances of all modified asphalt binders and their corresponding n values from the power law models …………………………………………………….. 443

Figure 213 – Levels of correlation between the nonrecoverable compliances of the selected asphalt binders at 64°C and 3.2 kPa and their corresponding flow number values for the creep-recovery times of (a) 2/9 s; (b) 4/9 s; and (c) 8/9 s …………………………………………………………… 453

Figure 214 – Average positions of the PG 76-xx formulations at the temperature of 52°C and all the creep-recovery times and stress levels ………………... 456

Figure 215 – Average positions of the PG 76-xx formulations at the temperature of 58°C and all the creep-recovery times and stress levels, as based on their J_{nr} values ……………………………………………………………… 458

Figure 216 – Average positions of the PG 76-xx formulations at the temperature of 64°C and all the creep-recovery times and stress levels, as based on their J_{nr} values ……………………………………………………………… 460

Figure 217 – Average positions of the PG 76-xx formulations at the temperature of 70°C and all the creep-recovery times and stress levels, as based on their J_{nr} values ……………………………………………………………… 462

Figure 218 – Average positions of the PG 76-xx formulations at the temperature of 76°C and all the creep-recovery times and stress levels, as based on their J_{nr} values ……………………………………………………………… 463

Figure 219 – Average positions of the PG 76-xx formulations at all temperatures, the creep-recovery times and stress levels, as based on the J_{nr} values of these materials (the grey-shaded boxes with texts highlighted in blue and red refer to the binders with the best and worst positions in the rankings, respectively) …………………………………………………………….. 464

Figure 220 – Plots of the coefficients of variation (CV) at 100 Pa against the corresponding values at 3,200 Pa for all the 12 formulations and the whole ranges of temperatures, loading times and stress levels …………. 465

Figure 221 – Ratios of the average positions of the formulations according to J_{nr} to those according to $J_{nr,\,diff}$ and for the stress levels of 100 and 3,200 Pa … 469

Figure 222 – Final rankings of the studied formulations according to the $J_{nr}100$, $J_{nr}3200$ and $J_{nr,\,diff}$ values from the less (No. 1) to the most susceptible to rutting (No. 12) ……………………………………………………... 471

Figure 223 – Raw strain values of the AC+Elvaloy+PPA at the 12th cycle (R = 36.2%) and the 13th cycle (R = 47.0%) at 100 Pa and the temperature of 76°C ... 475

Figure 224 – Raw strain values of the AC+EVA at the 12th cycle (R = 98.7%) and the 13th cycle (R = 97.5%) at 100 Pa and the temperature of 64°C 475

Figure 225 – Comparisons between the percent recoveries of the AC+Elvaloy+PPA, the AC+EVA and the AC+EVA+PPA at 1/9 s and 1/500 s at all pavement temperatures and stress levels 477

Figure 226 – Ratios of the nonrecoverable compliances of the AC+Elvaloy+PPA, the AC+EVA and the AC+EVA+PPA at 1/9 s to those at 1/500 s for a particular temperature and stress level – each data point corresponds to one temperature (out of five) and one stress level (out of two) 477

Figure 227 – Fitting of the model from Saboo and Kumar (2015) to the raw strain data of the AC+EVA at the temperature of 58°C and the stress level of 100 Pa 478

Figure 228 – Degree of correlation between the parameter α from the modified power model and the percent recoveries of the AC+Elvaloy+PPA, the AC+EVA and the AC+EVA+PPA at the creep-recovery times of 1/500 s 479

Figure 229 – Comparisons between the percent recoveries of the AC+PPA, the AC+rubber, the AC+rubber+PPA, the AC+SBS and the AC+SBS+PPA at 1/9 s and 1/240 s at all pavement temperatures and stress levels 483

Figure 230 – Raw strain values of the AC+rubber+PPA at the 12th cycle (R = 14.5%) and the AC+SBS+PPA at the 11th cycle (R = 9.6%) at 100 Pa and the temperature of 70°C 484

Figure 231 – Fitting of the model from Saboo and Kumar (2015) to the raw strain data of the AC+rubber (11th cycle) at the temperature of 70°C and the stress level of 100 Pa 486

Figure 232 – Degree of correlation between the parameter α from the modified power model and the percent recoveries of the AC+PPA and the formulations with crumb rubber (AC+rubber and AC+rubber+PPA) and SBS (AC+SBS and AC+SBS+PPA) at the creep-recovery times of 1/240 s ... 487

Figure 233 – Ratios of the nonrecoverable compliances of the AC+ PPA, the AC+rubber, the AC+rubber+PPA, the AC+SBS and the AC+SBS+PPA at 1/9 s to those at 1/240 s for a particular temperature and stress level – each data point corresponds to one temperature (out of five) and one stress level (out of two) 488

Figure 234 – Comparisons between the percent recoveries of the AC+PE, the AC+PE+PPA, the AC+SBR and the AC+SBR+PPA at 1/9 s and 1/240 s at all pavement temperatures and stress levels 492

Figure 235 – Raw strain values of the AC+SBR+PPA at the 11th cycle (R = 23.2%), the stress level of 100 Pa and the temperature of 64°C 492

Figure 236 – Ratios of the nonrecoverable compliances of the AC+ PE, the AC+PE+PPA, the AC+SBR and the AC+SBR+PPA at 1/240 s to those at 1/9 s for a particular temperature and stress level – each data point corresponds to one temperature (out of five) and one stress level (out of two) 494

Figure 237 – Degree of correlation between the parameter *α* from the modified power model and the percent recoveries of the AC+PE, the AC+PE+PPA, the AC+SBR and the AC+SBR+PPA the creep-recovery times of 1/240 s .. 495

Figure 238 – Variations in the percent recovery of the AC+rubber and the AC+PE for each creep-recovery cycle at 1/240 s, 100 Pa and 52°C 498

Figure 239 – Raw strain values of the AC+SBS at the 6th cycle (R = 95.2%), stress level of 100 Pa and the temperature of 70°C 499

Figure 240 – Raw strain values of the AC+rubber+PPA at the 10th cycle (R = 58.7%), stress level of 100 Pa and the temperature of 52°C 499

Figure 241 – Plots of the average positions of the 12 formulations in the rankings of $J_{nr}100$ and $J_{nr}3200$ according to the MSCR tests at longer creep and recovery times 502

Figure 242 – Plots of the average positions of the 12 formulations in the rankings of $J_{nr,\ diff}$ according to the MSCR tests at longer creep and recovery times .. 504

Figure 243 – Resulting correlation between the percent difference in compliances ($J_{nr,\ diff}$) at 64°C and 1/9 s and the flow number values of the asphalt mixtures at 60°C 505

Figure 244 – Plot of the percent differences in compliances ($J_{nr,\ diff}$) against the nonrecoverable compliances at 3,200 Pa ($J_{nr}3200$) for the 12 formulations and all the temperatures (52, 58, 64, 70 and 76°C) and values for the creep times (1/9, 2/9, 4/9 and 8/9 s) 505

Figure 245 – Plot of the percent differences in compliances ($J_{nr,\ diff}$) against the nonrecoverable compliances at 3,200 Pa ($J_{nr}3200$) for the 12 formulations and all the temperatures (52, 58, 64, 70 and 76°C) and longer loading times (1/240 s and 1/500 s) 506

LIST OF SYMBOLS

α	Parameter in the modified power law function from Saboo and Kumar (2015), level of significance (ANOVA test)
α_1, α_∞	Real order derivatives of the Burgers fractional model
Γ	Euler Gamma function
$\dot{\gamma}$	Strain rate
γ_c	Maximum strain observed in an oscillatory shear test
γ_{calc}	Strain obtained from the constants of viscoelastic models (in this case, Burgers and generalized Voigt models)
γ_{diff}	Percent difference in strains
$\gamma_{nr,0.1}$	Nonrecoverable strain at the stress level of 0.1 kPa
$\gamma_{nr,3.2}$	Nonrecoverable strain at the stress level of 3.2 kPa
γ_{per}	Permanent strain in the equation by Bouldin et al. (2001), permanent strain in the end of the flow number test after 10,000 cycles (absence of failure)
γ_{raw}	Raw (or measured) strain
δ	Phase angle
δ_e	Phase angle at the temperature of equivalent stiffness (SHENOY, 2004b)
ε_0	Measured strain in the beginning of a creep-recovery cycle in a standardized MSCR test (ASTM or AASHTO)
$\varepsilon_1, \varepsilon_2, \varepsilon_3, \varepsilon_4$	Measured strains during an ordinary creep-recovery cycle
ε_c	Measured strain in the end of the creep portion and the beginning of the recovery portion of a creep-recovery cycle in a standardized MSCR test
ε_i	Initial strain in the binder (CHEN and TSAI, 1999)
ε_{in}	Measured strain in the beginning of an ordinary creep-recovery test
ε_{nr}	Nonrecoverable strain in the end of a creep-recovery cycle in a standardized MSCR test (ASTM or AASHTO)
ε_{pFN}	Permanent strain in the mixture at the flow number cycle
$\varepsilon_p(N)$	Permanent strain in the mixture as a function of the number of the creep-recovery cycle in the uniaxial repeated creep test
$\varepsilon_p(t)$	Permanent strain in the binder as a function of time during an ordinary creep-recovery test
ε_r	Measured strain in the end of a creep-recovery cycle in a standardized MSCR test

ε_{rec}	Recoverable strain observed in a creep-recovery cycle of a standardized MSCR test (ASTM or AASHTO)
$\varepsilon_{rec}(t)$	Strain as a fuction of time in the recovery portion of an ordinary creep-recovery test
$\varepsilon(t)$	Total strain as a function of time during a creep-recovery test
ε_{tot}	Total strain (recoverable + irrecoverable) observed in a creep-recovery cycle of a standardized MSCR test
ζ	Deflection of the asphalt beam in the BBR test
η	Newtonian viscosity (or simply viscosity), dashpot
η'	Real component of the complex viscosity (or storage viscosity)
η^*	Complex viscosity
$\eta_{dashpot,n}$	Newtonian viscosity of the dashpot *n* for use in viscoelastic models with more than one dashpot
η_K	Dashpot element of the four-element Burgers model (equal to $\eta_{dashpot,\,2}$)
η_M	Isolated dashpot element of the four-element Burgers model (equal to $\eta_{dashpot,\,1}$)
η_{per}	Steady state viscosity
θ	Deflection or rotation angle in the dynamic shear rheometer
Λ_i	Retardation time *i* (linear viscoelastic models)
λ_i	Relaxation time *i* (linear viscoelastic models)
λ_T	Characteristic relaxation time (Deborah number)
τ	Shear stress in the Newton's classical experiment for determining the viscosity of any fluid
τ_c	Stress applied in a dynamic oscillatory shear test
τ_t	Stress applied in a creep-recovery (or repeated creep) test
φ_1, φ_2	Angles in the parabolic dashpots of the 2S2P1D model
ψ_1, ψ_∞	Characteristic times of the springpots in the Burgers fractional model
ω	Angular frequency in an oscillatory shear test
a, b, c	Empirical regression parameters (BOULDIN et al., 2001)
a_T	Horizontal shift factor
A	Area of the plates in the Newton's classical experiment (dynamic viscosity), constant/parameter of the modified power law function (SABOO and KUMAR, 2015), constant of the power law equation from Delgadillo et al. (2012), regression parameter (ELSEIFI et al., 2003; LAUKKANEN et al., 2015), regression parameter of the Francken model
b	Width of the asphalt beam in the BBR test

B	Regression parameter (ELSEIFI et al., 2003; LAUKKANEN et al., 2015), regression parameter of the Francken model, constant/parameter of the modified power law function (SABOO and KUMAR, 2015), constant of the power law equation from Delgadillo et al. (2012)
C	Constant of the material (Williams-Landel-Ferry and Arrhenius equations), regression parameter of the Francken model, constant of the power law equation from Delgadillo et al. (2012)
C_1, C_2	Constants of the material (Williams-Landel-Ferry and Arrhenius equations)
D	Regression parameter of the Francken model
De	Deborah number
E	Young's modulus, spring
E_a	Activation energy (Arrhenius equation)
E_K	Spring element of the four-element Burgers model (equal to $E_{spring,\,2}$)
E_M	Isolated spring element of the four-element Burgers model (equal to $E_{spring,\,1}$)
$E_{spring,n}$	Young's modulus of the spring *n* for use in viscoelastic models with more than one spring
$f(\delta)$	Viscoelastic contribution to the accumulated strain rate in the asphalt binder (BOULDIN et al., 2001)
F	Magnitude of the force applied in the upper plate of the Newton's classical experiment (dynamic viscosity)
$F_{critical}$	Critical value of the *F-value* (ANOVA test)
$F\text{-}value$	Parameter from the ANOVA test (statistical analysis)
F_N	Flow number
FN_I	Flow number index
g_2	Parameter of the Schapery's simple integral model (MASAD et al., 2009)
G'	Storage modulus
G''	Loss modulus
G^*	Complex (shear) modulus
G_V	Viscous component of the creep stiffness
H_0	Null hypothesis (ANOVA test)
H_1	Alternative hypothesis (ANOVA test)
h	Specimen height in the dynamic shear rheometer, thickness of the asphalt beam in the BBR test
I_A	Viscosity aging index
I_C	Colloidal instability index

$I_{R\&B}$	Increase in softening point
J''	Loss compliance
$J(t)$	Total creep compliance
$J_D(t)$	Delayed elastic component of the total compliance
J_E	Elastic component of the total compliance
J_{nr}	Nonrecoverable (creep) compliance
$J_{nr}100$	Nonrecoverable compliance at 100 Pa (0.1 kPa)
$J_{nr}3200$	Nonrecoverable compliance at 3,200 Pa (3.2 kPa)
$J_{nr,\ diff}$	Percent difference in nonrecoverable compliances
$J_V(t)$	Viscous component of the total compliance
k	Constant (BOULDIN et al., 2001)
L	Length of the asphalt beam in the BBR test
M_L	Mass loss in the rolling thin-film oven test
m	Relaxation rate in a BBR test
m_1, m_2	Fractional parameters in the 2S2P1D model
N	Number of loading-unloading cycles in repeated creep tests for asphalt binders and mixtures
n	Nonlinear factor in the modified power law function (SABOO and KUMAR, 2015)
N_{10}	Number of load applications to produce a 10-mm rutting level in asphalt mixtures (SYBILSKI, 1996a)
P	Total load on the tire, load applied in the sample during the BBR test
P_{25}	Penetration at 25°C
P_I	Penetration index (Pfeiffer and Van Doormal)
p	Tire inflation pressure
p-$value$	Probability in the ANOVA test (statistical analysis)
r	Tire contact radius (HUANG, 2004), radius of the specimen plate
R	Universal gas constant (Arrhenius equation), percent recovery
R^2	Coefficient of determination
$R100$	Percent recovery at 100 Pa
$R3200$	Percent recovery at 3,200 Pa
$R\&B$	Ring-and-ball softening point value
R_{diff}	Percent difference in recoveries

R_{min}	Minimum percent recovery
R_{PEN}	Retained penetration
S	Stiffness of the asphalt binder in the BBR test
S_1, S_2	Numerical values of the parabolic dashpots in the 2S2P1D model
t	Loading time (stress or strain) in any rheological experiment
t_1, t_2, t_3, t_4	Generic times observed in an ordinary creep-recovery test
t_{in}	Initial time of an ordinary creep-recovery test
t_F	Creep (or loading) time in a repeated creep test (standardized or not)
T	Temperature of any rheological test, torque applied by the dynamic shear rheometer
T_0	Reference temperature (Williams-Landel-Ferry and Arrhenius equations)
T_e	Temperature of equivalent stiffness (SHENOY, 2004b)
T_{HS}	Maximum performance grade temperature of the binder (SHENOY, 2004b)
Tr_{sp}	Truck speed (PEREIRA et al., 1998, 2000)
u	Speed in the Newton's classical experiment for determining the viscosity of an ordinary fluid
W_C	Energy dissipated during a loading cycle
W_D	Delayed elastic component of the energy dissipated during a loading cycle
W_P	Viscous component of the energy dissipated during a loading cycle
X_0, Y_0	Empirical regression parameters (BOULDIN et al., 2001)

l

LIST OF ABBREVIATIONS

2S2P1D	2-spring, 2-parabolic, 1-linear dashpot model
AAE	Average Absolute Error
AASHO	American Association of State Highway Officials
AASHTO	American Association of State Highway and Transportation Officials
AC	Asphalt cement (or asphalt binder)
ALF	Accelerated loading facility
ANOVA	Analysis of variance
ANP	Agência Nacional do Petróleo, Gás Natural e Biocombustíveis [Brazilian National Agency of Petroleum, Natural Gas and Biofuels]
AR	Aged residue
ASTM	American Society for Testing and Materials
BBR	Bending beam rheometer
COV or CV	Coefficient of variation
DER/PR	Departamento de Estradas de Rodagem do Estado do Paraná [The Paraná State Department of Roads]
DER/SP	Departamento de Estradas de Rodagem do Estado de São Paulo [The São Paulo State Department of Roads]
DM	Dynamic modulus
DNER	Departamento National de Estradas de Rodagem [National Department of Roads], Brazil
DNIT	Departamento Nacional de Infraestrutura de Transportes [National Department of Transport Infrastructure], Brazil
DOT	Department of Transportation (commonly used in the US)
DSR	Dynamic shear rheometer
DTT	Direct tension tester
EBA	Ethylene butyl acrylate
ECS	European Committee of Standardization
ESALs	Equivalent single-axle loads
ETG-FHWA	Expert Task Group of the US Federal Highway Administration
EVA	Ethylene vinyl acetate

FHWA	US Federal Highway Administration
GMA	Glycidylmethacrylate
iRLPD	Incremental repeated load permanent deformation
ISI	Internal structure index
MSCR	Multiple stress creep and recovery
MSR	Minimum strain rate (iRLPD test)
PAV	Pressurized aging vessel, long-term aging
PE	Polyethylene, low-density polyethylene
PET	Polyethylene terephthalate
PG	Performance grade
PP	Polypropylene
PPA	Polyphosphoric acid
RCRT	Repeated creep and recovery test
RET	Reactive ethylene terpolymer
RLPDT	Repeated load permanent deformation test
RSST-CH	Repeated simple shear test at constant height
RTFO	Rolling thin-film oven
RTFOT	Rolling thin-film oven test, short-term aging
SARA	Saturates, aromatics, resins and asphaltenes
SBS	Styrene-butadiene-styrene copolymer
SBR	Styrene-butadiene rubber
SEBS	Styrene-ethylene-butadiene-styrene
SGC	Superpave® gyratory compactor
SHRP	Strategic Highway Research Program
SIS	Styrene-isoprene-styrene
SSF	Segundos Saybolt-Furol (SUS, in Portuguese)
SUS	Saybolt Universal Seconds
Superpave®	Superior Performing Asphalt Pavements
TITAN	Commercial designation of a compatibilizing agent (VERDADE, 2015)
TLA	Trinidad Lake Asphalt
URCT	Uniaxial repeated creep test
WLF	Williams-Landel-Ferry

ZSV	Zero-shear viscosity

TABLE OF CONTENTS

ACKNOWLEDGEMENTS ... **i**
RESUMO ... **iii**
ABSTRACT ... **v**
LIST OF TABLES ... **vii**
LIST OF FIGURES ... **xxvii**
LIST OF SYMBOLS ... **xlv**
LIST OF ABBREVIATIONS ... **li**
TABLE OF CONTENTS ... **lv**
CHAPTER 1: Introduction ... **1**
1.1. Gaps in the Literature and Problem-Solving Approaches ... 3
1.2. Supporting Hypotheses and Objectives of the Study ... 5
1.3. Structure of the Dissertation ... 7
1.3.1. Highlights ... 9
CHAPTER 2: Rheology Applied to Asphalt Binders ... **11**
2.1. Highlights ... 11
2.2. Introduction to Rheology and Brief Historical Overview ... 11
2.3. Chemical Composition of Asphalt Binders ... 21
2.4. Fundamentals of the Rheological Behavior of Binders ... 25
2.5. Modeling of the Rheological Behavior of Binders ... 32
2.5.1. Maxwell and Voigt Models ... 33
2.5.2. Burgers Model and its Variants ... 34
2.5.3. Presentation and Discussions on Other Viscoelastic Models ... 37
2.6. Specifications for Asphalt Binders ... 41
2.7. Study and Determination of the Mixing and Compaction Temperatures ... 46
2.8. Comments on the Modifiers for Asphalt Binders ... 48
2.8.1. Introduction ... 48
2.8.2. Interactions between the Binder and the Modifier (s): Chemical Reactions, Consequences and Degrees of Compatibility ... 50
CHAPTER 3: The Multiple Stress Creep and Recovery Test ... **59**
3.1. Highlights ... 59
3.2. Background and Origin of the Test ... 59
3.3. Description of the MSCR Test and Main Outcomes ... 72
3.4. Some Special Advantages of the MSCR Test ... 75

3.5. Current Status of the MSCR Test: Limitations of the Standard Protocols, Repeatability/Reproducibility and a Few Refinements 77
3.6. Examples of Brazilian Studies about the MSCR Test 84
3.6.1. Focuses and Justifications for the Present Study and Literature Gaps 86
CHAPTER 4: Materials, Methods and Analysis of Data 89
4.1. Highlights 89
4.2. Materials and Preparation of the Mixture and Binder Samples 89
4.3. Details about the Protocols of the Mixture and Binder Tests 94
4.3.1. Binder Tests 94
4.3.2. Mixture Tests 97
4.4. Analysis and Implications of the MSCR Data and Rutting Parameters 98
4.4.1. MSCR Tests and Suggesting Refinements in the Superpave® Specification 98
4.4.2. Summary of the Binder Rutting Parameters 102
4.5. Rheological Models for the Binder and Mixture Laboratory Data 103
4.5.1. Binder Data 103
4.5.2. Mixture Data 105
CHAPTER 5: Mixture Rutting Data and Analysis 109
5.1. Highlights 109
5.2. Short Introduction on the Mixture Tests for Rutting: Advantages and Disadvantages 109
5.3. Flow Number Test Results 111
5.3.1. The Role of F_N and Correlations with the Binder Parameters 111
5.3.2. Asphalt Mixtures Modified with Plastomers and Crumb Rubber: Results and Discussion 121
5.4. Categories of Traffic Levels and Direct Comparisons among the Formulations 125
CHAPTER 6: Binder Testing Results and Discussion 133
6.1. Conventional Tests and Aging Parameters 133
6.1.1. Highlights 133
6.1.2. Penetration and Softening Point Protocols and Mass Losses 133
6.1.3. Rotational Viscosity Tests 139
6.2. Oscillatory Shear Tests 143
6.2.1. Highlights 143
6.2.2. Results and Discussion 143
6.3. Multiple Stress Creep and Recovery (MSCR) Tests 152
6.3.1. Highlights 152
6.3.2. Preliminary Comments and MSCR Tests at Standardized Creep-Recovery Times (1/9 s) 153

6.3.3. The Role of Longer Creep Times on the Responses of Asphalt Binders at High Temperatures and Correlations with Speed Values 189

6.3.4. The Role of Longer Recovery Times on the Creep-Recovery Responses of Modified Asphalt Binders and Rheological Modeling 471

6.3.5. Concluding Remarks on the Use of $J_{nr, diff}$ as a Rutting Parameter 504

CHAPTER 7: Conclusions and Recommendations 507

7.1. Preliminary Comments and Leading Questions 507

7.2. The Use of Longer Creep Times in the MSCR Tests and Their Effects on the Binder Parameters, Levels of Elasticity and Rheological Models 508

7.3. The Use of Longer Recovery Times in the MSCR Tests and their Effects on the Creep-Recovery Behavior of the Asphalt Binders 514

7.4. Mixture Rutting Results and Correlations with Binder Data 516

7.5. General Aspects of Binder Modification in the MSCR Tests 518

7.6. Concluding Remarks and Suggestions for Future Studies 520

REFERENCES 523

APPENDIX A: Details and Example of the ANOVA Analysis 547

A.1. Concepts and Brief Overview of the Use of ANOVA in the Literature 547

A.2. Example of the Application of ANOVA in this Dissertation 550

APPENDIX B: Refinement in Superpave® Traffic Criteria 555

APPENDIX C: History of the Standards about the MSCR Test 557

CHAPTER 1: Introduction

Pavements are engineering structures comprised by layers with well-defined thicknesses laid on the top of the natural ground, which is technically named as “subgrade”. With respect to the flexible asphalt pavements (Portland cement concrete pavements are out of the scope of this study), the surface layer is made of aggregates, air voids and a cementitious agent, which is known as *binder* or *asphalt binder* in the US and *bitumen* in Europe[1]. It is important to carry out regular maintenance in the pavement in order to guarantee safety and comfort and offer economic benefits to the users. This is made when a specific section shows one or more distress mechanisms – especially rutting, fatigue cracking or low-temperature cracking – and, in such a case, the state agency (or the private company) that is responsible for the roadway must resolve the problem as soon as possible. If this is not done on time, the drivers will face difficulties in using the road and accidents may occur.

Out of the aforementioned distress mechanisms, rutting (*permanent deformation* in Europe) is the prevailing one in many Brazilian asphalt pavements. It is typically characterized by surface depressions in the wheelpath and, when the condition is more critical, pavement uplift may also be observed along the sides of such depressions. The appearance of this phenomenon can be attributed only to the surface layer or the underneath layers, or even a combination of both factors. Rutting is caused by the progressive accumulation of thousands of small permanent (or viscous) strains in the pavement, and the total amount of strain becomes visible after a period of time. Pavements with very high levels of rutting lead to hazardous driving conditions, since they can pull the vehicle towards the depression path and cause hydroplaning when water accumulates in them. In general, depressions lower than 0.33 in (≈ 0.84 cm) can be left untreated because they are not a matter of great concern (PAVEMENT INTERACTIVE, 2008b).

Several test procedures have been designed to study rutting on binders over the years, from the empirical-based to the performance-related ones. Initially, the idea of “level of rutting resistance” was simply based on the consistency of the binder as measured by the penetration and ring-and-ball softening point tests: *the more consistent the binder is, the more resistant to rutting it will be*. The further updates in the specifications (e. g., Superpave®) brought new insights into the actual performance of the binder in the pavement, and a more sophisticated

[1] Since the study was carried out based on standards (ASTM and AASHTO) and specifications (Superpave®) from the US, the whole document was written in American English.

concept of “level of rutting resistance” was formulated based on the theory of linear viscoelasticity: *a more rut resistant material will be the one that shows less amount of dissipated energy under dynamic oscillatory shear loading*. Currently, the measurements of the rutting resistance of the binder are derived from the concept of damage: *a specific asphalt binder will be more resistant to rutting when the extent of damage in the sample is lower and this is reflected in the improved rheological parameters.* Figure 1 is a chart with the extremes of rutting resistance based on the previously mentioned concepts.

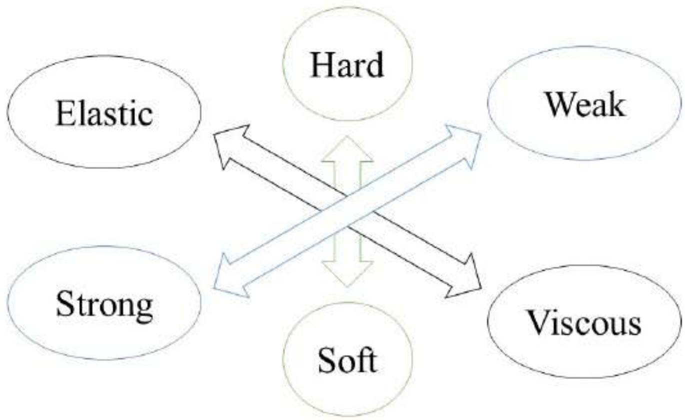

Figure 1 – Extreme conditions of rutting resistance of the binder based on the following concepts: consistency (*hard* and *soft*), linear viscoelasticity (*elastic* and *viscous*) and damage (*strong* and *weak*) [adapted from Bahia (2014)]

The change from an empirical to a more scientific, performance-related approach in the design of test protocols and devices was motivated by three key factors: (a) the seek for higher degrees of correlation between binder and mixture data; (b) the differentiation among the particular rutting characteristics of modified asphalt binders; and (c) a better understanding of the actual rutting phenomenon observed in the pavement. The use of rheological models has also become an effective tool in choosing the binder parameter that would be correlated with rutting measurements on mixtures, even though these models do not seem to have a widespread application in the technical literature before the beginning of the 2000’s.

There is no question that higher temperatures and lower vehicle speeds accelerate the formation of rutting in the pavement. As a consequence, the test protocols must provide alternatives to include such variables in the analysis. This was somewhat taken into consideration during the development of Superpave® in the US, i. e., intervals of pavement temperatures were established based on the climatic conditions and maximum/minimum values for the design parameters were defined. However, the addition of different traffic levels was first made by AASHTO as an amended table to its M320 standard (Table 3) only in 2009.

Nevertheless, the researchers decided to maintain the test conditions unchanged and set maximum values for the rutting parameter as a function of this traffic level. In other words, the identification of a more rut resistant binder is dictated by a stricter specification requirement (upper limits are lower) rather than a more severe testing condition.

1.1. Gaps in the Literature and Problem-Solving Approaches

Researchers have been discussing for some time about the best technique for dealing with more critical loading conditions. With the advent of Superpave®, one practical – but not effective from a scientific point of view – approach was to shift the high PG grade of the binder when the traffic level is too heavy or there is a great percentage of heavy, slow-moving vehicles (intersections or lanes with channelized traffic, e. g., bus lanes). In other words, an asphalt binder graded as PG 76-xx or even PG 82-xx could be used in a pavement with a maximum expected pavement temperature of only 64°C due to the traffic conditions. When this was proved not to be adequate, the next approach was to decrease the maximum allowed value of the binder rutting parameter and keep the test temperature unchanged. For example, if the high pavement temperature is equal to 76°C and the roadway shows a heavier traffic level, the original upper limit of 1.0 (regardless of the unit) should be decreased by 0.5 and the temperature should remain the same. This new approach seems to be quite well accepted in the literature, since it has been used on Superpave® from 2009 onwords.

Although the new technique gets closer to the actual rutting performance of a pavement (i. e., the temperature does not change and the material must comply with stricter requirements to be used in a more extreme condition), it is still not clear that all the issues concerning the rutting behavior of the binder on pavements with varying loading patterns were properly addressed. By assuming that the asphalt binder is a thermo-viscoelastic material, the application of loads for a much longer period of time may lead to a nonlinear increase in strain with time and failure at shorter creep times (see the *tertiary creep* regions in Figure 2). Although the *secondary creep* region appears to indicate that the binder is within the linear viscoelastic range (linear increase in strain with time), this is not exactly the case; in fact, secondary creep almost always portrays a nonlinear viscoelastic behavior as well (LAKES, 2009).

If the accumulated strain falls within the nonlinear range, the material will be much more susceptible to rutting than another one within the linear viscoelastic range for a same stress level. It can be implied here that the artificial correction of “meeting stricter requirements and not modifying the test protocol” does not seem to fully address the issues relating to the actual resistance of the binder at different loading levels and speeds, since the result may be underestimated due to simplifications in the analysis. This becomes even more complex when additives are incorporated into the original material, since it is known that modified binders commonly show nonlinear response at lower stress and strain levels when compared with neat binders. Therefore, it is necessary to try a different (and somewhat more rational) approach in which the degree of nonlinearity of modified asphalt binders is taken into account and the rutting parameter is correlated with the vehicle speed. This has also been identified as a matter of serious concern and recommended by Golalipour (2011) as an important topic for future studies.

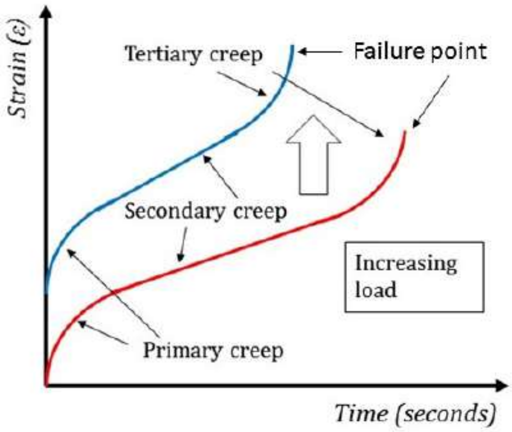

Figure 2 – Regions of the creep response of viscoelastic materials (e. g., asphalt binders) for different loading levels [adapted from Lakes (2009)]

With respect to the recovery time used in creep-recovery test protocols, its value will influence on the amount of recovered strain after the removal of the load. In simple terms, the resulting strain after the application of a creep-recovery cycle may or may not contain a portion of recoverable strain (and not only viscous strain) depending on the testing and modification variables. This means that the analysis of the actual rutting resistance of the binder may be negatively affected by a wrong choice of the recovery time in the test procedure. Such a problem can be solved either by using mathematical models or substantially increasing the unloading time until the binder recovers all the delayed elastic strain. However, one must keep in mind that too long recovery times may be required depending on the modification type (especially highly polymer-modified binders), and this does not seem to be suitable for specification purposes.

By assuming that rutting is a distress phenomenon mainly restricted to the surface layer of the asphalt pavement (BAHIA and ANDERSON, 1995) and that it is characterized by a progressive deterioration of this layer (i. e., accumulation of small permanent strains), one can conclude that the analysis of the rutting susceptibility of the asphalt binder at several temperatures is of great interest. Although the accumulation of permanent strain is much more critical at very high temperatures (typically close to the high PG grade), it is important to investigate the nonlinear relationship between temperature and the rutting susceptibility of the binder. This was somehow considered in the paper by Zhou et al. (2012), who observed that the rutting depth in the asphalt pavement is very low at lower temperatures and increases nonlinearly at temperatures close to the maximum expected one. The authors also concluded that such a nonlinear increase can be recognized regardless of the loading level, with exception of a vertical shift in the curves of accumulated strain with temperature when the load is higher. However, the study from Zhou et al. (2012) was mainly based on data collected from finite-element modeling on the software ABAQUS and assumptions for the pavement structure, increasing temperature and increasing loading levels, and not on standardized creep-recovery tests and pavement temperatures.

1.2. Supporting Hypotheses and Objectives of the Study

To adequately address the limitations of the current practices for evaluating the rutting potential of asphalt binders and propose refinements in it, five major hypotheses were considered in the study. First, it was assumed that the incorporation of one or two modifiers into the base asphalt binder results in a stable and homogeneous formulation, and also that the overall mechanical properties of this formulation are dictated by the ones of its components. Second, the properties of the asphalt binders (modified and unmodified) can be determined from rheological tests that were either designed for one or another category of material, and the current specification requirements can be used in both cases. The first hypothesis makes it possible to study the rutting performance of the modified binder as a whole material (and not a composite one), whereas the second allows the use of all the binder tests currently available in the literature for all types of materials.

While carrying out the analysis of the rutting resistance of the binders at many high pavement temperatures, the other three hypotheses of this group were considered. Firstly, the laboratory tests include temperatures that are fairly representative of the actual ones found in the American and Brazilian pavements (ASPHALT INSTITUTE, 2010; CUNHA et al., 2007; LEITE and TONIAL, 1994) and sufficient to achieve the goals of the present study, even though they do not cover all the environmental conditions observed worldwide. Secondly, the creep times are enough to closely simulate the more severe loading conditions observed in real pavements, since they were based on previously published documents and recommendations for heavier traffic levels in the Superpave® specification. The same can be said for the recovery times, i. e., they are referenced on the literature and are assumed to be enough to accomplish the purposes of this study.

In terms of the third hypothesis, it was assumed that asphalt binders with high degrees of elasticity will show a full recovery after 500 s of unloading, whereas the ones with low degrees of elasticity will depict full recovery after 240 s of unloading time. This was based on some reference values and materials found in the literature (DELGADILLO, 2008; DELGADILLO and BAHIA, 2010; DELGADILLO et al., 2012; MERUSI, 2012), as well as the idea that the amount of recovery in a binder with low degree of elasticity after 1 s of loading time will not be too expressive when compared with the one of a binder with high level of elasticity.

Some complementary hypotheses can be put forward to explain the results obtained in the present dissertation, either in the binder scale or the mixture scale. They can be summarized in the bulleted list shown below:

- the laboratory conditions used in the tests with asphalt mixtures are within the temperature, loading and unloading conditions selected in the binder tests; therefore, correlations between binder and mixture data can be made;
- the maintenance of the loading-unloading ratio of 1/9 in the repeated creep tests with asphalt mixtures and the standardized ones with binders allows comparisons among the data, as it will be highlighted later based on citations from the literature;
- the use of the same high temperature-performance grade in the modified asphalt binders makes it possible to verify the similarities and differences among them, since the classification of the material on Superpave® is enough to identify materials with similar behavior;
- the short-term aging level of the asphalt binder according to the standardized rolling thin-film oven test accurately represents the aging conditions of the material in the field pavement during the occurrence of rutting; and
- the formulations prepared in the study are representative of the ones commonly used in the construction and rehabilitation of pavements, even though they are typically non-commercial.

With respect to the objectives, the following ones were defined:

- to evaluate the susceptibility of asphalt binders modified with polymers, crumb rubber and polyphosphoric acid to rutting at typical high pavement temperatures and based on the concepts of consistency (empirical-based protocols), linear viscoelasticity (oscillatory shear loading mode) and damage (repeated creep tests);
- to compare the numerical values of the mostly used binder rutting parameters with each other and point out the differences among them based on the test temperature, the modifier (s) in the formulation – especially the AC+modifier and the corresponding AC+modifier+PPA ones – and the loading-unloading conditions;

- to identify the formulations with the highest and lowest resistances to rutting at the selected pavement temperatures – i. e., numerical and descendent rankings – and report the changes in such resistances as a function of the rutting parameter and the standardized loading-unloading conditions, similarly to what it was done in the studies from Domingos and Faxina (2016) and Hajikarimi et al. (2015);
- to identify the variations in the percent recovery and the nonrecoverable creep compliances of the asphalt binders with increasing recovery time, study the effects of delayed elasticity on such responses depending on the modifier type and question the validity of the third hypothesis;
- to discuss on the possible effects of the addition of polyphosphoric acid (PPA) to the modified asphalt binders as a function of the other additive found in the composition (polymer or crumb rubber);
- to draw comparisons between the criteria currently used on Superpave® for heavier traffic levels and the one proposed in this dissertation and, if necessary, to propose refinements in the specification based on the J_{nr} values of the binders at different creep times; and
- to correlate the outcomes of the binder rutting tests with data obtained from the flow number tests with dense-graded asphalt mixtures at 60°C and discuss on the numerical values (i. e., R^2) of these correlations.

1.3. Structure of the Dissertation

This dissertation was divided into seven chapters and three appendixes. The present chapter (Chapter 1 – *Introduction*) shows a brief introductory part about rutting in asphalt binders, the changes in the concepts of a more rut resistant material with time, the deficiencies of the current method for dealing with heavier traffic levels and the hypotheses that give support to the study. It finishes with the major objectives and a short description of each chapter.

Chapter 2 – *Rheology Applied to Asphalt Binders* – discusses on the application of the main concepts of rheology in the study of the binder's behavior. Initially, an introduction to rheology and a brief historical review about its use in asphalt binders is provided. Then, the theories about the chemical composition of the base binder and information on the elastic, viscous and viscoelastic responses of the binders are shown. The following part shows a summary of the rheological models that are commonly found in studies with asphalt binders, the methods for calculating the parameters of these models and the advantages/disadvantages of each of them. Next, a summary of the high-temperature properties and parameters of the binders on Superpave® is provided. Finally, the chapter shows a history of the previous and current binder specifications in the US and Brazil, some comments on the determination of the mixing and compaction temperatures and the modifiers for asphalt binders (types and interactions).

Chapter 3 – *The Multiple Stress Creep and Recovery Test* – presents a state-of-the-art report on the multiple stress creep and recovery (MSCR) test. The first part discusses on the contextualization and the origin of the test, as well as the correlations between the outcomes of binder tests and mixture tests in the field and the laboratory. The second part shows the main parameters that can be obtained from this test, which include the percent recovery, the nonrecoverable (creep) compliance and the percent difference in nonrecoverable compliances. The advantages of the MSCR test as a protocol for estimating the susceptibility of asphalt binders to rutting are provided in the third part. The chapter finishes with a literature review on the most recent Brazilian studies and some contributions that this piece of research can bring to the scientific community.

Chapter 4 – *Materials, Methods and Analysis of Data* – shows the materials used in the preparation of the binder and mixture samples, the test protocols followed in the experiments and how the binder and mixture data were analyzed. The first part provides the description of the aggregates, the base binder and the modifiers, as well as the technical details of the preparation of the formulations and the mixture samples. The second part gives the protocols that were adopted in the experiments with mixtures (Uniaxial Repeated Creep Test – URCT) and the binders (especially MSCR and oscillatory shear), the major outcomes of each test and further information about the devices. The third part shows how the MSCR testing results were analyzed and how the Superpave® specification may be refined based on these laboratory data. The fourth (and last) part provides the rheological models used in the mixture and binder data.

Chapter 5 – *Mixture Rutting Data and Analysis* – provides the results of the flow number tests at 60°C and the degrees of correlation between binder and mixture data based on linear and power law equations. An investigation was carried out to see whether the mixture protocol is representative of the actual mixture performance in the field as based on the repeated creep tests for asphalt binders, the discussions in the literature – i. e., if the outcomes of this document match the ones previously drawn by other authors – and the differentiations among the responses of each formulation. The chapter finishes with the determination of the adequate traffic levels for each mixture – as based on the Superpave® criteria and the draft standard published by Delgadillo et al. (2006b) – and some comments on the differences between the AC+modifier and the corresponding AC+modifier+PPA formulations based on the mixture creep curves.

Chapter 6 – *Binder Testing Results and Discussion* – shows the outcomes of the MSCR tests at all the creep and recovery times chosen in this dissertation, either by increasing the creep time (1/9, 2/9, 4/9 and 8/9 s) or increasing the recovery time (1/240 and 1/500 s). Rheological modeling was also conducted in order to make comparisons among the variations in the model parameters with severity of the test conditions, how this can be interpreted in terms of the type of accumulated strain in the binder and how the percent recovery and the level of nonlinearity of the binder change with temperature, creep time and stress level. Finally, some comments on the use of the percent difference in compliances as a performance-related parameter are given, as based on the technical literature and the results collected here.

Chapter 7 – *Conclusions and Recommendations* – summarizes the key findings of the study and gives some recommendations for further investigations. Each subheading of this chapter is referenced on a group of findings (for instance, mixture rutting data, results at longer creep times, results at longer recovery times, etc.), and some general aspects of asphalt binder modification with crumb rubber, plastomeric and elastomeric polymers, reactive terpolymers and polyphosphoric acid are shown. Then, a list of the references used in the development of the dissertation are cited.

With respect to the appendixes, the first one (Appendix A – *Details and Example of the ANOVA Analysis*) gives some essential information about the application of the Analysis of Variance (ANOVA) to binder data in the literature and how this was done in the present study. The second one (Appendix B – *Refinement in Superpave® Traffic Criteria*) shows the details of the proposed method for improving the selection of the most appropriate traffic level for the asphalt binder in the pavement, as well as an early draft of Superpave® with this method. The last one (Appendix C – *Historical Overview of the MSCR Test Standards*) contains two tables with essential details about the current and historical versions of the MSCR protocols according to the ASTM and the AASHTO agencies.

1.3.1. Highlights

The use of highlights in scientific papers has been a common practice in journals published by Elsevier[2]. These highlights aim at presenting the core findings and a quick textural overview of the publication. Other authors decided to summarize the key findings or topics of one or more specific chapters in separate sections (ARSHADI, 2013; WOLDEKIDAN, 2011). To offer readers the possibility of understanding the major findings and fundamentals of this dissertation without referring to the whole written part, highlights were provided in the beginning of each section in Chapter 6 and before Chapters 2-5. They contain no more than 200 characters (including spaces) and are given in bulleted lists before the integral textual part of the chapters.

---

[2] ELSEVIER. (2016). **Highlights**. Elsevier B. V., Amsterdam, The Netherlands. Retrieved from: <https://www.elsevier.com/authors/journal-authors/highlights>. Accessed: 18 Apr. 2016.

CHAPTER 2: Rheology Applied to Asphalt Binders

2.1. Highlights

- The development of Superpave® was a notable advance in binder rheology, and some devices and examination techniques previously used in other areas were adapted for binders.
- The parameters *G*/sinδ* and *G*sinδ* were based on the concept of dissipated energy under oscillatory shear loading, and they were first proposed to control rutting and fatigue cracking, respectively.
- A viscoelastic material has characteristics of either elastic or viscous materials, and this can be studied based on its rheological response under oscillatory shear or repeated creep loading.
- The Burgers model has been commonly used to depict the response of the binder in repeated creep tests, since it can account for the elastic, viscous and delayed elastic strains.
- The specifications for asphalt binders have evolved from penetration to performance-based ones; currently, the implementation of MSCR on Superpave® is still in progress in the US.
- Modifiers for asphalt binders mainly aim at improving pavement performance; polymers (SBS and EVA) and crumb rubber are the prevailing ones on pavements worldwide.

2.2. Introduction to Rheology and Brief Historical Overview

Rheology is a section of Physics that is devoted to the study of flow and deformation of the matter. The word "rheology" comes from the Greek terms *ῥέω* (*rheo*, or "flow") and *λογία* (*logia*, or "study of"). The development of rheology as a science was motivated by a sector of industry (chemical products) in the beginning of the 20th century. These industries of chemical products and the large-scale manufactures of synthetic polymers released several goods with behavior that was classified as non-conventional (or "strange") by the scientific community. In 1920, the study of such goods in the laboratory led Eugene Bingham (professor of Chemistry at the University of Lehigh, Bethlehem, PA, US) to coin the word "rheology" to identify this new area of research. In principle, Bingham would like this new science to be restricted to the flow types that were observed on concentrated suspensions, e. g., paints. The interdisciplinary nature of rheology makes it possible to find it in many subjects that include the study of flow, either in a direct or indirect way: aeronautical engineering, hydraulic engineering, fluid mechanics and so on (MACOSKO, 1994).

Technically speaking, the “strange” goods cited by Bingham and other contemporary scientists are the ones that do not follow the Newton’s and the Hooke’s laws for perfectly viscous and perfectly elastic materials, respectively. Macosko (1994) points out the four most important phenomena in the study of the rheological behavior of ordinary materials: (a) the relationship between a physical property and time; (b) pseudoplasticity and dilatancy, that is, the viscosity as a function of the shear rate; (c) difference between the normal stresses under shear; and (d) elongational viscosity. These phenomena can be explained by using the concepts of rheology and constitutive or fundamental equations, which are able to describe the relationship between the applied force and the response of the material (strain).

The rheological properties are commonly obtained by laboratory tests that take into account the time or the frequency of loading as the key variable that will influence on the output variables. In other words, these tests are conducted in the *time domain* or the *frequency domain* regions, respectively. The choice for one or another protocol will be a function of the material by itself (polymer melt, solid, semi-solid, liquid and so on), the property or parameter that is expected to provide better correlations with performance in the field, and the characteristics of the actual loads experienced by the material. It is possible to adopt mathematical techniques to convert the data from one domain to the other and vice versa, e. g., the Fourier transform, non-linear regression methods and empirical correlations. These and other techniques were discussed and used by some authors in the literature, among which Baumgaertel and Winter (1989) and Haghtalab and Sodeifian (2002) can be mentioned. They proposed methodologies for calculating and plotting the relaxation spectrum of the binder (time domain) based on the oscillatory shear data (frequency domain).

As it can be seen, one remarkable feature of the rheological properties of viscoelastic materials is the interchangeability among them. Another classic example of this interchangeability is the Cox-Merz rule, which was introduced in the 1950’s[3] and states that the viscosity at steady shear mode η_{per} can be correlated with the complex viscosity η^* – see Equation (1).

$$\eta_{per}(\dot{\gamma}) = |\eta^*|(\omega) \rightarrow \dot{\gamma} = \omega \tag{1}$$

With respect to asphalt binders, the use of these materials for paving applications is much earlier than the scientists’ interest in their rheological behavior. The first mention of this type of application dates back to the 7th century B. C., when Nabopolassar ruled Babylon (625 – 604 B. C.) At that time, a binder-cemented mortar was used to cement both the foundation made of at least three burnt

[3] COX, W. P.; MERZ, E. H. (1958). Correlation of dynamic and steady flow viscosities. **Journal of Polymer Science**, Vol. 28, No. 118, pp. 619-622. doi: 10.1002/pol.1958.1202811812.

brick layers and the stone slabs put on top. However, the implementation of the asphalt binder as a cementitious material on pavements demanded many years until the beginning of the 19^{th} century, when the European sources of natural binders were discovered and modern applications for the material were developed. Thanks to the advent of the technique of vacuum distillation in the 1910's, the asphalt binder from natural sources has been gradually replaced by the industrialized one (residue of the distillation of the crude oil). Nowadays, the cementitious agent used in pavements is almost exclusively the one that comes from the distillation of the petroleum (LESUEUR, 2009) and the use of natural asphalts is restricted to binder modification.

By taking into account the rapid increase in the use of the asphalt binder on pavements between the 19^{th} and the early years of the 20^{th} century, the first scientific studies on its rheological behavior were published in the literature. It is believed that the pioneering work on this subject is dated from 1877, when Von Obermayer developed rheometers to measure the absolute viscosity of binders in three different configurations: parallel plates, torsional plates and sliding plates (LESUEUR, 2009; SCHWEYER, 1974). In 1888, H. C. Bowen designed a device that was capable of penetrating a 0.8 mm-thick needle in a binder sample. This device would be the forerunner of the current penetrometers. The inspector of asphalts A. W. Dow refined the Bowen's penetrometer in 1903, and then the penetration test was standardized by ASTM under the designation D5 (HALSTEAD and WELBORN, 1974; LESUEUR, 2009; SCHWEYER, 1974). According to the ASTM website[4], the first version of this standard was published in 1965.

In addition to the penetration test, the softening point (or "ring-and-ball") test was also developed between the 1910's and the 1920's. Initially, the method involved the determination of the temperature at which the bituminous material conditioned in cubic molds changed from the solid to the semi-solid state. The standardization of the test was proposed in 1911 and, five years later (1916), it was replaced by the current softening point test in studies with asphalt binders. The first attempts from ASTM and AASHO (currently, AASHTO) in standardizing the protocol for the determination of the softening point of the binder under the designations D36 and T53 were made in 1916 and 1931, respectively (HALSTEAD and WELBORN, 1974). However, the first standard was published by ASTM only in 1976, as provided by the agency in the historical versions of the document[5].

---

[4] AMERICAN SOCIETY FOR TESTING AND MATERIALS. (1965). **ASTM D5-65:** Standard method of test for penetration of bituminous materials. West Conshohocken, PA. 5 p. Retrieved from: <http://compass.astm.org/Standards/HISTORICAL/D5-65.htm>. Accessed: 05 Aug. 2015.

[5] AMERICAN SOCIETY FOR TESTING AND MATERIALS. (1976). **ASTM D36-76:** Standard test method for softening point of bitumen (ring-and-ball apparatus). West Conshohocken, PA. 4 p. Retrieved from: <http://compass.astm.org/Standards/HISTORICAL/D36-76.htm>. Accessed: 06 Aug. 2015.

Besides the penetration and softening point tests, other devices were designed in the 20th century to evaluate other binder properties. These properties included ductility, the maximum processing temperature of the material (flash point) and the degree of solubility in solvents such as carbon disulfide, carbon tetrachloride and petroleum naphtha. For instance, the first device used in the determination of the flash point was introduced in 1910 and either closed or open cup could be used in it, even though the former provided more accurate results. The ductilometer was designed by A. W. Dow and described in a report dated from 1903, but the test procedure was accepted as a standard only after 1920. The method for analyzing the solubility of the binder has remained essentially the same since it was developed by Dow and described in a report from 1903, together with the details of the ductility test and the straight sided ductility mold (HALSTEAD and WELBORN, 1974; SCHWEYER, 1974).

As cited above, the measurements of the viscosity of the binder date back to the later years of the 19th century. Viscosity can be simply defined as a dimensional measurement (i. e., it demands a unit – typically Pa.s or P and their submultiples – to be fully characterized) of the resistance of a particular fluid to flow, as caused by the application of a shear stress. It can thus be said that, the most viscous the fluid is, the greater the internal friction among its particles will be. When the fluid has no resistance no flow (viscosity is null), it is designated as *inviscid* or *ideal* fluid. The shear stress, the temperature and the molecular structure are the variables that mostly influence on the viscosity of a real material. The classical experiment from Isaac Newton (1642 – 1727) allows the determination of the viscosity (more specifically, the *dynamic viscosity* or *Newtonian viscosity* η), and it is illustrated in Figure 3. The lower plate is stationary, and the upper plate moves at a speed u due to the application of a shear stress τ. The applied force F is proportional to the area of each plate (A) and the speed u, as shown in Equation (2). As it can be seen, the η value is the constant of proportionality in the relationship between F, A and u.

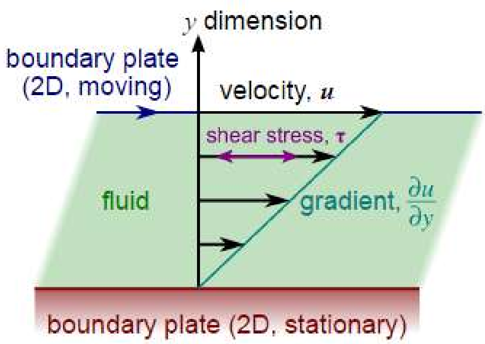

Figure 3 – Typical illustration of the Newton's experiment for calculating the viscosity (or, more specifically, the *dynamic viscosity*) of a particular fluid (WIKIPEDIA, 2016)

$$F = \eta \times A \times \frac{u}{y} \tag{2}$$

To obtain the viscosity of asphalt binders at high temperatures, several viscometers may be used. One of these viscometers is the Saybolt-Furol device, which provides an indirect estimation of the viscosity of the binder by counting the time (in seconds) that 60 cm^3 of the material takes to flow over a standardized tube. In such a case, the unit is designated as *Saybolt Universal Seconds*, or SUS (SSF, in its abbreviation in Portuguese). Another alternative is to determine the viscosity of the binder by rotating a spindle immersed in the sample and at a predefined temperature, and this spindle varies in size depending on the labeled number (No. 21, No. 27 and so on). The amount of binder is dictated by this spindle number, i. e., larger spindles require lower masses of material. The process is carried out in a device commonly known as Brookfield viscometer. Since the rotation speed and the spindle (and thus the shear rate) do not change with time, it can be inferred that the viscosity is obtained in a strain-controlled protocol. The torque and internal constants associated with the spindle and the rotation speed are used to calculate the rotational viscosity, the shear stress and the shear rate. Further details about the Brookfield viscometer are shown later in this chapter.

In the 1980's, the US Congress promoted a massive investment of $ 150 million in a 5-year project that was conducted by researchers from the Strategic Highway Research Program (SHRP). This project started in 1987 and was motivated by the serious limitations of the conventional binder properties, e. g., only one test temperature and the restricted applicability of the results to modified binders (BAHIA and ANDERSON, 1995; ROBERTS et al., 1996). To carry out the studies, three main pavement distress mechanisms were selected: (a) permanent deformation or rutting; (b) fatigue cracking; and (c) low-temperature or thermal cracking. The aging effects on the binder properties after mixing and compaction (short-term aging) and after 5-10 years of service life in the pavement (long-term aging) were also considered. As a result of such efforts, a new specification was released and new devices for studying the properties of the asphalt binders were proposed. This specification is known as Superpave® (acronym of "Superior Performing Asphalt Pavements") and the devices include the following:

- the Brookfield rotational viscometer, to measure the viscosity of the binder at very high temperatures (above 100°C) and ensure that the material has an adequate level of workability during mixing and compaction;
- the pressurized aging vessel (PAV), to simulate the aging process of the asphalt binder within the service life of the pavement;

- the rolling thin-film oven (RTFO), to simulate the aging process of the binder during mixing with the aggregates in the plant and compaction in the field;
- the dynamic shear rheometer (DSR), to characterize the rheological properties of the material (stiffness and elasticity) at intermediate and high pavement temperatures (typically between 4 and 88°C) and all the aging conditions;
- the bending beam rheometer (BBR), which is used to determine the degree of stiffness and the relaxation properties of long-term aged samples at low temperatures (0°C or lower); and
- the direct tension tester (DTT), which is used when the asphalt binder shows a stiffness between 300 and 600 MPa and a sufficiently high relaxation rate (higher than 0.30) after long-term aging and at low temperatures.

Similarly to many areas of research, the publications about asphalt binders were based on devices that had been well-known for many years in other fields of study. As an example, the dynamic shear rheometer had been used for a long time in the industries of plastic materials before the SHRP program was implemented. With respect to the bending beam rheometer, the loading application mode and the characteristics of the sample – layout and dimensions – were based on an ASTM standard (designation D790[6]) for the verification of the flexural properties of plastics and electrical insulating materials (ROBERTS et al., 1996).

The total stiffness (complex modulus G^*) and the relative elasticity (phase angle δ) were selected by the SHRP researchers as the two binder properties that would be able to prevent the formation of rutting and the appearance of fatigue cracking in a road pavement. They chose the oscillatory shear loading mode in the DSR, and then minimum values for $G^*/\sin\delta$ and maximum values for $G^*\sin\delta$ were proposed as the limiting criteria for the resistance of the binder to rutting and fatigue cracking, respectively. To develop the equations of the parameters $G^*/\sin\delta$ and $G^*\sin\delta$, it was assumed that the dissipated energy per loading cycle (W_C) should be minimized in order to obtain materials with higher resistances to rutting and fatigue cracking. Rutting was interpreted as a stress-controlled phenomenon, whereas fatigue cracking was interpreted as a strain-controlled phenomenon. Based on these assumptions, higher $G^*/\sin\delta$ values and lower $G^*\sin\delta$ values would lead to lower W_C values, and thus higher resistances to rutting and fatigue cracking would be achieved (BAHIA and ANDERSON, 1995; ROBERTS et al., 1996).

The calculations of $G^*/\sin\delta$ must be made after short-term aging (rolling thin-film oven test – RTFOT), which simulates the most critical condition for the appearance of rutting in the

---

6 AMERICAN SOCIETY FOR TESTING AND MATERIALS. **ASTM D790:** Standard test methods for flexural properties of unreinforced and reinforced plastics and electrical insulating materials. West Conshohocken, PA.

pavement. They must also be done before aging as a guarantee against the binders whose degree of stiffness after RTFOT do not accurately simulate the actual aging level after mixing and compaction in the field. With respect to the parameter $G^*sin\delta$, it must be obtained after long-term aging (PAV) because this is the most severe aging condition for the occurrence of fatigue cracking in the pavement.

Differently from the fatigue cracking and the rutting phenomena, the SHRP researchers decided to choose a static creep test in the BBR to calculate the stiffness (parameter S) and the relaxation rate (parameter m) of the binder at low pavement temperatures. The binder cannot be too stiff (S is limited to a maximum value) neither to have a very low relaxation rate (m is limited to a minimum value) at such temperatures in order to provide an adequate resistance to thermal cracking. Initially, the correlations between mixture resistance in the field and the binder resistance in the BBR indicated that the test should take between 1.0 and 5.5 h (from 3,600 to 20,000 s), which was too much for a purchase specification such as Superpave®. To decrease this loading time to more rational values, the SHRP researchers applied the time-temperature superposition principle. They concluded that a loading time of 240 s (4 min) and an increase of 10°C in the test temperature would lead to S values equal to the ones obtained in a test with a loading time of 7,200 s (2 h) and a test temperature equal to the minimum pavement temperature (ROBERTS et al., 1996).

The principle of the rotational viscometer on Superpave® is shown in Figure 4. The ASTM D4402 and the AASHTO TP48 standards provide the steps for obtaining the viscosity of the binders at very high temperatures. For specification purposes, the temperature of 135°C and the upper limit of 3.0 Pa.s at 20 rpm are enough to determine the level of workability of the asphalt binder. This is based on the assumption that most neat asphalt binders behave as Newtonian fluids at such temperature, and therefore a single measurement of viscosity is enough to study the workability characteristics of the material. Based on the torque required to maintain the rotation speed unchanged and the constants of the spindle, the viscosity (usually given in cP) is calculated and provided to the user.

Together with the suggestion of the DSR as a new device to study the high-temperature properties of asphalt binders, the Superpave® specification also settled some rheological properties and parameters to describe and quantify its elastic, viscous and viscoelastic components. These properties and parameters are dependent on the loading mode used in the device, i. e., oscillatory shear (reversible) or repeated creep (irreversible). Both loading modes can be used to study the performance of the binder under such temperature conditions, as well as to estimate its contribution to the rutting resistance of the asphalt mixture.

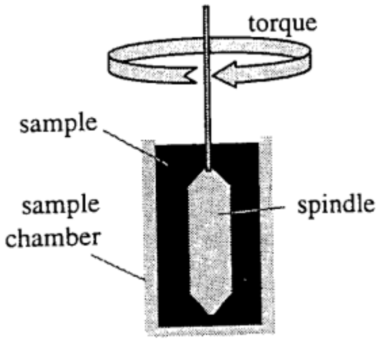

Figure 4 – Typical layout of the measurement of the rotational viscosity of a binder sample in a Brookfield viscometer (ROBERTS et al., 1996)

The Superpave® specification establishes a gap height of 1.0 mm and a sample diameter of 25 mm in the tests at high temperatures (typically between 46 and 82°C), and a gap height of 2.0 mm and diameter of 8.0 mm at intermediate temperatures (typically between 4 and 40°C). Figure 5 illustrates the interest points and the loading scheme of the DSR in the oscillatory shear mode. When torque is applied on the upper plate, it moves from point A to point B. Then, the plate moves back from point B to point A and goes up to point C, thereby returning to point A and finishing one whole loading cycle (A → B → A → C → A). When a stress-controlled rheometer is used, the torque is equal to a constant value and the strain in the sample will vary. For strain-controlled rheometers, the upper plate will move at a fixed distance from point A to point B and measure the corresponding torque value (ROBERTS et al., 1996).

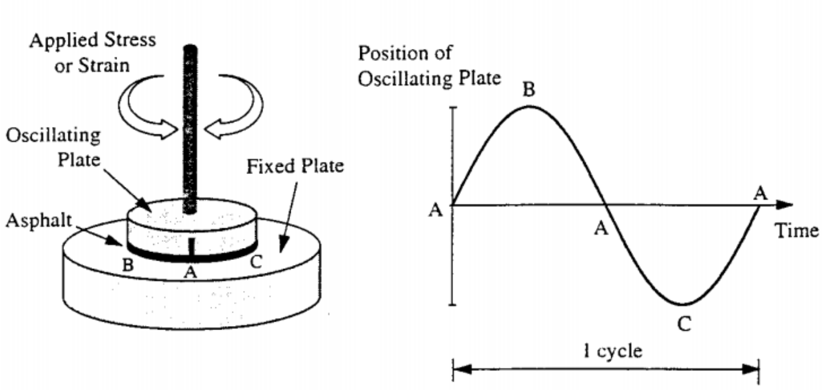

Figure 5 – Schematic of the DSR in the oscillatory shear test and identification of the interest points (ROBERTS et al., 1996)

The DSR determines the stress τ_c and the strain γ_c based on the maximum torque T, the deflection (or rotation) angle θ, the specimen height h and the specimen radius r. Equations (3) and (4) dictate the calculations of τ_c and γ_c, respectively (ROBERTS et al., 1996). As previously shown, the ratio of τ_c to γ_c yields the complex modulus G^* and the time lag between the stress and strain curves is numerically equal to the phase angle δ. The real part of G^* is known as storage modulus *G'* and the imaginary part of G^* is known as loss modulus *G"*. The relationship among these properties is represented by the right triangle in Figure 6. *G"* is directly related to the amount of work dissipated during a loading cycle (viscous part), whereas *G'* is related to the amount of energy stored by the material during this same cycle (elastic part). However, neither *G"* can be labeled as *viscous modulus* nor G' can be labeled as *elastic modulus* because the two moduli contain portions of the delayed elastic response of the binder (BAHIA and ANDERSON, 1995; ROBERTS et al., 1996).

Differently from the oscillatory shear test, the repeated creep test conducted in the DSR does not show reversal in the loading mode and the stress levels can be out of the linear viscoelastic range. In other words, the sample is loaded in only one direction and the strains are measured during the loading and unloading phases of the creep-recovery cycle. The application of several cycles inflicts damage to the binder, and therefore it gets closer to the actual situation of a real pavement. Based on this strain response, some parameters can be calculated and correlated with the expected performance of the material in the field. The revised Superpave® specification establishes two main control parameters to evaluate this performance, namely, the nonrecoverable compliance J_{nr} and the percent difference in compliances $J_{nr,\ diff}$. Both the AASHTO (TP70 and T350) and the ASTM (D7405) standards provide the equations for calculating J_{nr} and $J_{nr,\ diff}$. The precise details about this test and the corresponding parameters are given in Chapter 3.

$$\tau_c = \frac{2 \times T}{\pi \times r^3} \tag{3}$$

$$\gamma_c = \frac{\theta \times r}{h} \tag{4}$$

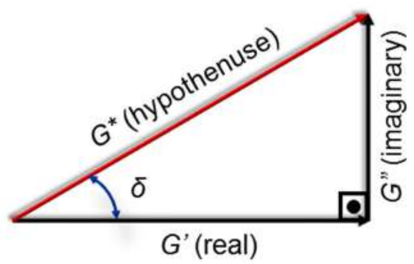

Figure 6 – Relationship between the moduli *G**, *G"* and *G'* and the phase angle δ (right triangle)

The BBR apparatus (Figure 7) was designed to evaluate the low-temperature properties of asphalt binders, and the testing temperatures are expected to simulate the lowest pavement temperatures. At such cold conditions, the elastic properties of the material prevail over the viscous ones and its stress-strain response gets closer to an elastic solid. For the results to be valid, the data gathered in the BBR must fall within the linear viscoelastic region of the asphalt binder. As a consequence, the SHRP researchers set a small standard load of 100 g to be used in the laboratory procedure (ROBERTS et al., 1996). The classic beam analysis theory – Equation (5) – allows the determination of the stiffness of the binder S at 60 s based on its geometric features (length L, width b and thickness h) and the testing variables (load P and deflection ζ). The protocol of the BBR test is established by the ASTM D6648 and the AASHTO T313 standards, and the creep rate m at 60 s (i. e., the derivative of the stiffness of the binder at 60 s with time in a log-log chart) is also obtained.

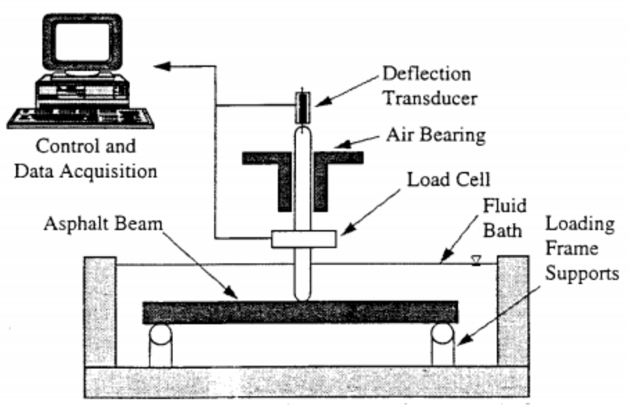

Figure 7 – Representative illustration of the apparatus used in the bending beam rheometer (BBR) tests (ROBERTS et al., 1996)

$$S = \frac{P \times L^3}{4 \times b \times h^3 \times \zeta} \tag{5}$$

As pointed out earlier, the aging mechanisms of asphalt binders on Superpave® are represented by two devices – RTFO and PAV – that are expected to closely simulate actual aging of the material during mixing in the plant and compaction in the pavement (short-term aging, RTFO) and during the service life of 5-10 years (long-term aging, PAV). The ASTM D2872 and the AASHTO T240 standards provide the steps for carrying out the tests in the RTFO, whereas the ASTM D6521 and the AASHTO R28 standards show the sequence for conducting the tests in the PAV. The RTFO device was developed by the California Department of Transportation (US) in 1959 and it was selected because it continually exposes fresh binder to the jets of hot air, it does not allow the formation of surface skins in the sample and the test is not too time-consuming (ROBERTS et al., 1996; SHALABY, 2002). With respect to PAV, the exposure of a short-term aged sample to heat (temperature of 90, 100 or 110°C) and air pressure (around 2.1 MPa) for 20 h was found to accelerate the aging process, develop a more practical protocol and limit the loss of volatiles (ROBERTS et al., 1996).

Finally, the DTT device is used only when the asphalt binder shows a very high stiffness (*S* between 300 and 600 MPa) and a sufficient relaxation rate ($m \geq 0.3$) at the lowest climate temperature. The test is conducted at the same temperature used in the BBR, and a dog-shaped specimen is stretched at a constant rate (1 mm/min) up to failure. If the failure strain (ratio of the change in the length of the sample to its effective gauge length) is of 1.0% or higher, it is assumed that the binder will not show a premature failure by thermal cracking and can thus be used in the field pavement. This phenomenon is particularly visible in some modified asphalt binders, for which the ability of relaxing stresses can avoid the formation of thermal cracks even for considerable degrees of stiffness.

Some years after the implementation of Superpave® as a binder specification in the US, many technical limitations in the failure criteria have been recognized by researchers worldwide. They include the parameters $G^*/sin\delta$ (Chapter 3) and $G^*sin\delta$ (BAHIA et al., 2001a, 2001b; HINTZ, 2012; HINTZ et al., 2011; JOHNSON, 2010; PAMPLONA, 2013; PAMPLONA et al., 2014). Criticisms on the BBR test protocol and its corresponding parameters have also been made in the literature (AFLAKI and HAJIKARIMI, 2012; HESP and SUBRAMANI, 2009; LIU et al., 2010). As a consequence of these studies, further modifications were carried out in the specification such as the incorporation of the nonrecoverable creep compliance J_{nr} in the analysis of the susceptibility of the binder to rutting and the removal of the short-term aging condition in the determination of the high PG grade of the material. Although the specifications are constantly updated due to their inherent characteristics (D'ANGELO and FEE, 2000), it is important to point out that the rheological response of the binder cannot be neglected when seeking for more durable pavements and mixtures with higher resistances to rutting, low-temperature cracking and fatigue cracking.

2.3. Chemical Composition of Asphalt Binders

In a general context, the asphalt binder can be described as a complex chemical system comprised by hydrocarbon molecules associated with small amounts of structurally analogous heterocyclic compounds and functional groups containing oxygen, sulfur and nitrogen atoms. Other atoms such as vanadium, iron, magnesium, calcium and nickel can also be found in trace quantities, e. g., in the form of oxides or inorganic salts. Several chemical analyses suggested that the prevailing chemical elements in the binder are carbon (82 – 88%), hydrogen (8 – 11%), sulfur (0 – 6%), oxygen (0 – 1.5%) and nitrogen (0 – 1%). These contents change not only with the crude oil, but also the refining process and the in-service aging (LESUEUR, 2009; READ and WHITEOAK, 2003).

The separation of the asphalt binder into all its fractions and chemical elements and a detailed analysis of each one would require a very long period of time and would lead to a big amount of data, which is not practical and might not result in good correlations between such data and the rheological properties of the material. To simplify this process, researchers have been employing some techniques for obtaining the components of the binder based on a small number of fractions, e. g., asphaltenes and maltenes. Although Roberts et al. (1996) and the ASTM standard D4124[7] use the terms "petrolene" and "maltene" to designate the fraction that is soluble in *n*-heptane (differently from the asphaltenes, which are not soluble in this diluent) this equivalency may not be correct and only the word "maltene" should be used to designate such fraction (RICHARDSON, 1910[8] *apud* LESUEUR, 2009). In many cases, the maltenes are divided into saturates, aromatics and resins. The combination of these three fractions with the portion of asphaltenes generated the well-known SARA method (LESUEUR, 2009; READ and WHITEOAK, 2003; ROBERTS et al., 1996).

The SARA method, as it is known in the current days, was first proposed by Corbett (1969) and is characterized by liquid chromatography on active alumina with solvents. The components of the maltene fraction are determined according to their elution in *n*-heptane (saturates), benzene (aromatics) and a blend of methanol (50%) and benzene (50%) followed by trichloroethylene (resins). Corbett (1969) and the ASTM D4124 standard refer to the aromatics as "naphthenic aromatics" whereas the resins are the "polar aromatics" (LESUEUR, 2009). Other methods for obtaining the contents of each component of the binder include the extraction of solvents without chromatography and molecular distillation, but they are not recommended due to their scientific and technical limitations (READ and WHITEOAK, 2003). The relationship between the SARA fractions and the physical properties of the asphalt binder can be summarized as follows (CORBETT and PETROSSI, 1978; LEITE, 1999):

- the saturates have a negative influence on the thermal susceptibility and, when found at high percentages, they soften the binder;
- the aromatics contribute to the improvement in the physical properties of the binder by acting as plasticizers;
- although the resins increase the dispersion of asphaltenes in the asphalt binder and its ductility, they exert a negative influence on the thermal susceptibility (as well as the saturates); and
- the asphaltenes increase the viscosity of the binder and improve its thermal susceptibility.

[7] AMERICAN SOCIETY FOR TESTING AND MATERIALS. **ASTM D4124**: Standard test method for separation of asphalt into four fractions. West Conshohocken, PA.
[8] RICHARDSON, C. (1910). **The modern asphalt pavement**. 2nd ed. New York: Wiley.

The saturates may be found in the asphalt binder at contents ranging from 5 to 20% by weight. These components can be described as aliphatic, linear and branch hydrocarbon chains with small percentages of aromatic rings and polar atoms. They are non-polar and colorless (in some cases, straw) oils at room temperatures and the average molecular weight is about 600 g/mol, which is quite similar to the one of aromatics. Their average density at 20°C is equal to 0.9 g/cm^3 (LESUEUR, 2009; READ and WHITEOAK, 2003).

The aromatics, also known as "naphthenic aromatics", are the most abundant constituents of the base asphalt binder together with the resins. Their percentages on the total binder can vary from 30 to 65% depending on the crude source. They are dark brown viscous liquids and the molecular weights can range from 300 to 2,000 g/mol (mean value of 800 g/mol), the lowest values among all the naphthenic aromatic compounds. They are slightly more viscous than the saturates at a same temperature, and their density is very close to 1.0 g/cm^3 at the temperature of 20°C. They are comprised by non-polar carbon chains, in which the unsaturated rings are the dominant system. Due to this chemical structure, the aromatics show a very high dissolving ability on other hydrocarbon systems with high molecular weights (CORBETT, 1969; LESUEUR, 2009; READ and WHITEOAK, 2003).

The resins – polar aromatic fraction of the asphalt binder – are soluble in *n*-heptane and can be responsible for 30-45% of the total weight of the binder. Due to this polar nature, they are strongly adhesive. Differently from the saturates and the aromatics, they form a black solid at room temperature. The resins act like stabilizing agents of the asphaltenes and their density is approximately equal to 1.07 g/cm^3 at 20°C (LESUEUR, 2009). The chains are basically comprised by hydrogen and carbon, as well as small amounts of other elements like oxygen, nitrogen and sulfur. Thanks to the presence of resins, the asphaltenes can disperse widely within the asphalt binder unless the ratio resins/asphaltenes avoids this to happen. Depending on this ratio, the binder will show a more SOL-type behavior or a more GEL-type behavior (READ and WHITEOAK, 2003). The similarities in the structures of the asphaltenes and the resins lead to some controversies among researchers about which are the key differences between them. What is possible to say is that, besides the solubility in *n*-heptane, the ratio hydrogen/carbon is higher for the resins than for the asphaltenes and the molecules of resins commonly show less aromatic rings in the carbon chains – between 2 and 4 – when compared with the asphaltenes (POLACCO et al., 2015).

The asphaltenes constitute from 5 to 25% of the total weight of the binder and, in contrast to the resins, they are not soluble in *n*-heptane. They resemble a dark powder when stored at room temperature, and they are mainly responsible for the dark color of the asphalt binder. In general, the asphaltenes are described as complex aromatic rings with high molecular weight: the values may range from 1,000 to 100,000 g/cm^3 depending on the procedure used in the separation of the fractions. The density is close to 1.15 g/cm^3 at 20°C and, despite the absence of solubility in *n*-heptane, the asphaltenes are soluble in toluene. They have been extensively studied in the literature due to their crucial importance to the rheological characteristics of the asphalt binders. Higher asphaltene contents result in binders with higher viscosities and degrees of stiffness and, thanks to the polar groups and aromatic rings in the molecules, the asphaltenes also contribute to the adhesion between the binder and the aggregates (LESUEUR, 2009; READ and WHITEOAK, 2003). These higher asphaltene contents also lead to an increase in the glass transition temperature of the binder (GAHVARI, 1997).

In addition to the development of test procedures for separating the fractions of the asphalt binders, researchers also suggested a parameter to describe the colloidal state of the material and, as a consequence, its SOL-type and GEL-type behavior. This parameter is known as "colloidal instability index" (I_C) or "Gaestel index" – Equation (6) – and is named after C. Gaestel, who developed it in the 1970's together with some co-workers[9]. The higher the I_C value, the closer to the GEL-type behavior the binder will be. These I_C values typically range from 0.5 to 2.7 for the majority of the asphalt binders used in road pavements, and results higher than 1.2 are commonly observed for GEL-type binders. In general, SOL-type materials show I_C values lower than 0.7 (BRÛLÉ et al., 1994; LESUEUR, 2009; POLACCO et al., 2015).

$$I_C = \frac{Asphaltenes + Saturates}{Aromatics + Resins} \tag{6}$$

While developing the equation of the parameter I_C, Gaestel divided the components of the binder into "surfactants" (aromatic and polar molecules that were adsorbed on alumina) and "flocculants" by means of a pentane elution on alumina. In terms of the SARA fractions, the "surfactants" would be a mix of aromatics and resins and the "flocculants" would be a mix of saturates and aromatics (LESUEUR, 2009). These investigations gave a significant contribution to a better understanding of the relationship between composition and rheological properties of asphalt binders. However, it is important to note that they took into account only the amount of asphaltenes, and not their quality. In fact, later studies published in the literature indicated that asphaltenes from blown asphalt binders are not similar to the ones from straight-run materials (BRÛLÉ et al., 1994).

[9] GAESTEL, C. et al. (1971). Contribution à la connaissance des propiétés des bitumes routiers [Contribution to the knowledge of the properties of road binder]. **Revue Générale des Routes et Aérodromes**, Vol. 466, pp. 85-94.

2.4. Fundamentals of the Rheological Behavior of Binders

The study of the rheological behavior of viscoelastic materials, especially asphalt binders, requires basic knowledge about the following responses: (a) purely elastic, in which the material stores all the work done by the external forces; (b) purely viscous, in which the material dissipates all the work done by these forces; and (c) viscoelastic, in which part of the work is dissipated and the other part is stored. The asphalt binder may depict a more elastic-like or viscous-like behavior, depending on factors such as the temperature and the applied load (type and magnitude).

The most important characteristic of purely elastic materials is that, when subjected to an external force, they recover their original shape after the removal of this force. This is due to the presence of internal forces, which counteract the external load and allow the material to return to its original shape. Many crystalline materials show a linear viscoelastic response at small strain levels, i. e., the relationship between the applied stress and the resulting strain is equal to a constant of proportionality. This concept was first defined by Robert Hooke (1635 – 1703) in 1676 as an anagram (ceiiinosssttuv). The anagram was rearranged by Hooke in 1678 as the Latin phrase *ut tensio sic vis*, or "the power in an elastic body is proportional to the extension". However, the constant of proportionality was recognized as an inherent characteristic of the material only in the 19^{th} century, when Thomas Young (1773 – 1829) announced it in 1807 (SZEKERES, 1999). As a consequence, the modulus of elasticity was named after him – Young's modulus (E).

The most defining characteristic of purely viscous materials is that, when an external force is applied on them, they show an internal resistance to flow. This internal resistance was first announced by Isaac Newton (1642 – 1727) in 1687 as a relationship between the shear rate and the applied stress, and is known in the current days as Newtonian viscosity or simply viscosity (η). Newtonian fluids are the ones in which the shear rate is proportional to the stress, and therefore the viscosity is constant. On the other hand, non-Newtonian fluids do not show a constant viscosity value and other factors may be involved in the calculations, e. g., the shear rate and the loading history. Some typical examples of non-Newtonian fluids include (a) shear-thinning or pseudo-plasticity, for which the viscosity decreases with increasing shear rate; and (b) shear-thickening or dilatancy, for which this viscosity increases with increasing shear rate (Figure 8). A particular modified binder may show a more shear-thinning or shear-thickening behavior, or a combination of both (ZAMAN et al., 1995; NAVARRO et al., 2009; VLACHOVICOVA et al., 2005). Even some unmodified binders may depict non-Newtonian behavior depending on the crude source and the temperature (ZAMAN et al., 1995).

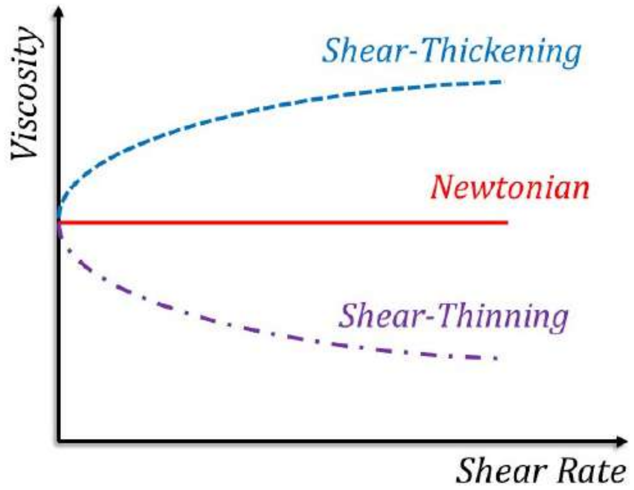

Figure 8 – Variations in viscosity with shear rate for Newtonian, shear-thinning and shear-thickening fluids

The typical responses of purely elastic and purely viscous materials to any applied stress in a repeated creep test can be seen in Figure 9. The variables t_{in}, t_1, t_2, t_3 and t_4 refer to generic times observed in the test and designate the creep (constant stress) and recovery (no applied stress) portions of the cycle. For perfectly elastic materials, the strain response curve follows exactly the pattern behavior observed for the stress curve in the intervals [$(t_1 - t_{in})$ and $(t_3 - t_2)$], and the strains are null in the intervals [$(t_2 - t_1)$ and $(t_4 - t_3)$]. For perfectly viscous bodies, the strain increases at a constant rate until it reaches a maximum value at the time t_1, and then there is no decrease in this accumulated strain within the recovery time $(t_2 - t_1)$. This amount of strain again increases linearly during the loading time $(t_3 - t_2)$, reaches a new maximum value at t_3 and shows no variations within the recovery time $(t_4 - t_3)$. This pattern behavior can be seen throughout the test.

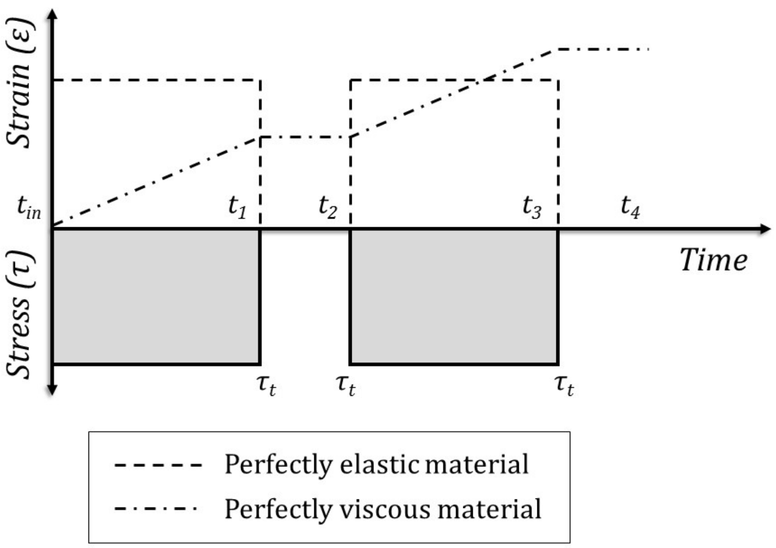

Figure 9 – Typical responses of perfectly elastic and perfectly viscous bodies in a repeated creep (or creep-recovery) test

Differently from the ideal materials (purely elastic and purely viscous ones), several ordinary materials cannot be described only as elastic solids or viscous fluids. This is because their rheological behavior is comprised by both responses, and a portion of the work is dissipated into permanent flow (viscous part) and the other portion is stored by the material (elastic part). This characteristic is inherent to viscoelastic materials such as polymers with high molecular weight (BRETAS and D'ÁVILA, 2000). A viscoelastic material shows a specific degree of stiffness just like a solid body and, at the same time, it flows and dissipates energy like a viscous fluid. This viscoelastic behavior mainly depends upon the time, the temperature and the loading mode, which can be either a force or an extension. Also, the loading story has a crucial influence on the rheological response of a viscoelastic material, and this phenomenon is known in the literature as "memory effect" (CHRISTENSEN, 1982).

The typical creep-recovery response of a viscoelastic material subjected to an applied stress τ_t can be observed in Figure 10. The strains ε_{in}, ε_1, ε_2, ε_3 and ε_4 are associated with the generic times t_{in}, t_1, t_2, t_3 and t_4, respectively. The $\varepsilon_p(t)$ value represents the permanent strain of the material as a function of the loading time. The application of τ_t at the times t_{in} and t_2 generate an instantaneous response in the material and, as this stress remains constant throughout the creep time [$(t_1 - t_{in})$ or $(t_3 - t_2)$], the total strain gradually increases up to a maximum value (ε_1 or ε_3). As soon as the stress becomes null (t_1 or t_3), a portion of the accumulated strain recovers immediately and another portion is recovered with time up to a minimum value (ε_2 or ε_4). For sufficiently long recovery times [$(t_2 - t_1)$ or $(t_4 - t_3)$], this minimum strain value tends to be equal to the permanent strain accumulated in the material (dashed line).

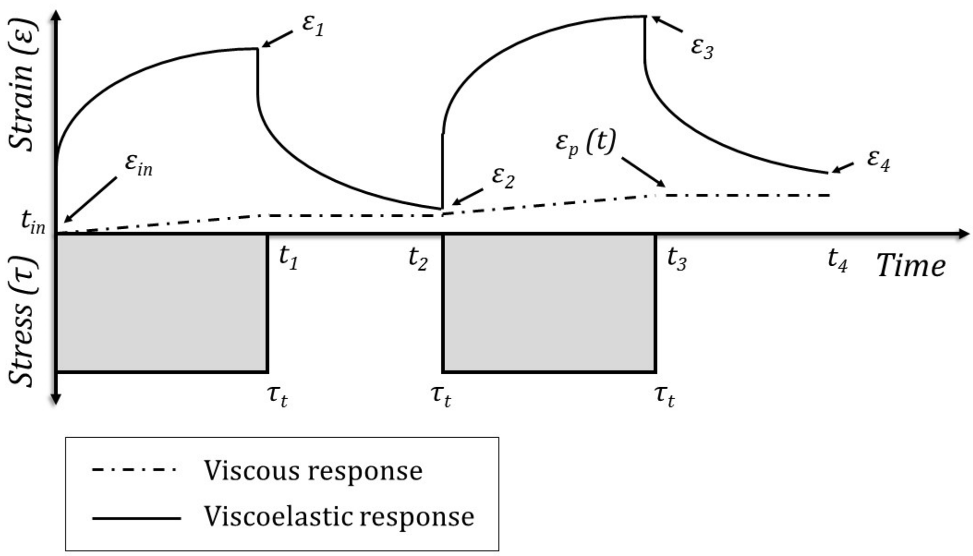

Figure 10 – Illustration of a typical response of a viscoelastic material subjected to a repeated creep (or creep-recovery) loading mode

A more detailed analysis of the components of the strain response of a viscoelastic material under creep and recovery loading can be made based on the descriptions provided in Figure 11. The application of a constant stress during the creep time leads to the appearance of two strain types, i. e., one instantaneous (elastic component) and another that includes the irrecoverable (viscous component) and the delayed elastic (time dependent) components. When the load is removed, the elastic component is recovered immediately and the delayed elastic component can also be fully recovered, provided that the unloading time is long enough. The level of delayed elasticity in a modified binder depends on some factors, among which the type and amount of modifier (s) added to the base material can be cited.

The differentiations among the rheological responses of elastic, viscous and viscoelastic materials can also be made based on the results of dynamic oscillatory shear tests. In these tests (more details were provided in Section 2.2 of this dissertation), a sample is placed between the parallel plates of a dynamic shear rheometer (DSR) and an oscillatory shear stress (τ_c) is applied. The resulting strain (ε_i) is constantly monitored, and the time lag between the curves of τ_c and ε_i dictates the "degree of viscoelasticity" of the material. This time lag is known in the literature as the phase angle or loss angle (δ), and δ values equal to 0° and 90° refer to perfectly elastic and perfectly viscous materials, respectively. Technically speaking, the curves of τ_c and ε_i are coincident when δ = 0°. The phase angle falls between these two extremes (0° < δ < 90°) for viscoelastic materials (see Figure 12).

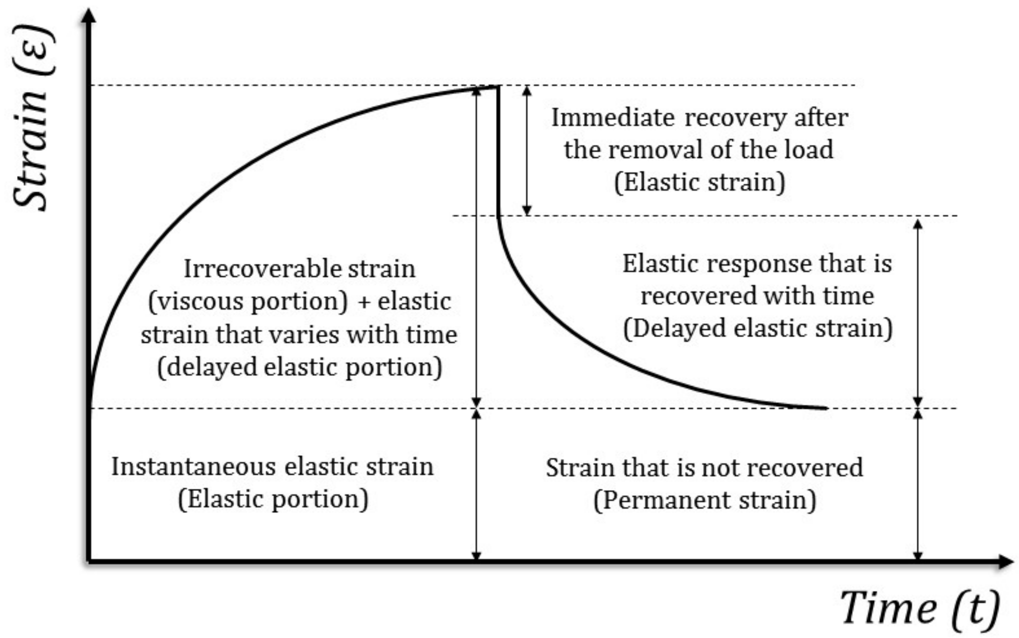

Figure 11 – Complete descriptions of the strains observed in a viscoelastic material under creep and recovery (repeated creep) loading

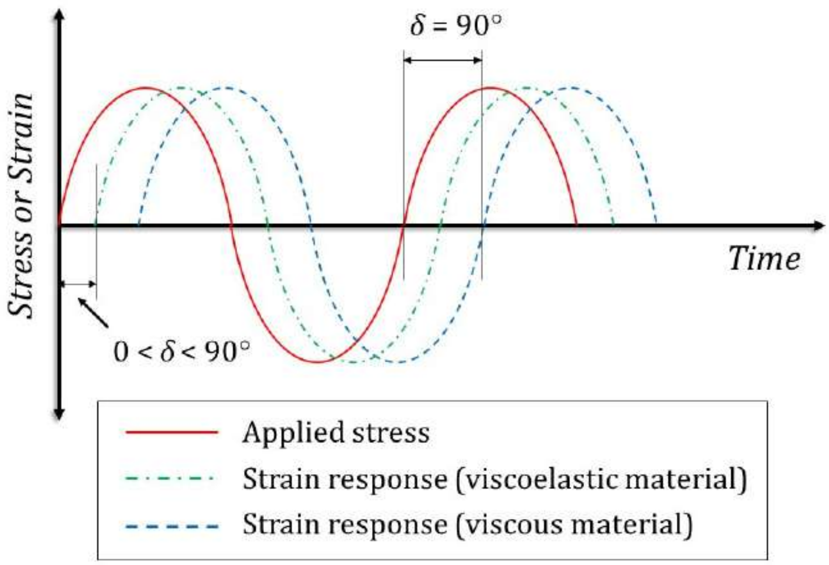

Figure 12 – Strain responses of viscoelastic and viscous materials under dynamic shear loading and typical values for the phase angle δ

Together with the phase angle δ, the oscillatory shear test also provides a rheological property to estimate the degree of stiffness of the binder (i. e., its total resistance to deformation). This property is referred to as complex shear modulus or complex modulus (G^*), and is given by the ratio of the maximum stress to the maximum strain within the oscillatory cycle. The G^* value can be divided into two components, namely, the storage modulus (G') and the loss modulus (G''). The former is related to the elastic response of the binder (real part of G^*), whereas the latter is related to its viscous response (imaginary part of G^*). The relationship between G^*, G' and G'' can be seen in Equation (7), in which the trigonometric functions of δ dictate the contributions of G' and G'' to the total stiffness of the binder. The tangent of δ ($tan\delta = G''/G'$) can be defined as the damping coefficient (BRETAS and D'ÁVILA, 2000).

$$G^* = G' + iG'' = \left[\frac{\tau_c}{\varepsilon_i} \times cos\delta\right] + i\left[\frac{\tau_c}{\varepsilon_i} \times sin\delta\right] \tag{7}$$

In rheology, the difference between the viscous and elastic responses of a viscoelastic material can be illustrated by the ratio of its characteristic relaxation time (λ_T) to the loading time in the rheological test (t). The Deborah number (De), which is the relationship between λ_T and t as shown in Equation (8), was proposed in the 1960's[10] to define the essential concept that everything flows, provided that enough time is given in the test. The De value makes it possible to categorize the materials into three groups: (a) elastic solids, for which De and λ_T approach infinity; (b) viscous

[10] REINER, M. (1964). The Deborah number. **Physics Today**, Vol. 17, No. 1, pp. 62-62. doi: 10.1063/1.3051374.

fluids, for which *De* and λ_T tend to zero; and (c) viscoelastic materials, for which $0 < De < \infty$. The aphorism "everything flows" comes from the Greek words *Πάντα ῥεῖ* (*panta rhei*), and it is believed that was coined by Simplicius of Cilicia (490 – 560) to characterize the line of thought of the Greek philosopher Heraclitus of Ephesus (535 – 475 b. C.)[11].

$$De = \frac{\lambda_T}{t} \tag{8}$$

The Deborah number, as calculated according to Equation (8), indicates that a particular material may depict characteristics of a solid when (a) its relaxation time approaches infinity; or (b) when the loading time is too short, and therefore the material does not have enough time to relax. The opposite trend is also valid, i. e., an ordinary material with very high λ_T value may show a viscoelastic (or even viscous) behavior if the loading time t is also sufficiently high. This is the case of a well-known silicone rubber (*silly putty*), which will flow as a liquid if one stores it in a container for a very long time (t) or will have a solid-like behavior if it is thrown against a wall or the floor because t approaches zero (BRETAS and D'ÁVILA, 2000).

The relaxation time λ_T is associated to the necessary amount of time for the material to make the slowest molecular movements, in an attempt to return to the original condition of equilibrium. With respect to polymer-modified asphalt binders, studies showed that the addition of such modifiers leads to an extension of the relaxation phenomenon; in other words, the relaxation times are higher for the modified binders than for the unmodified ones (ANDERSON et al. 1992; GAHVARI, 1997; RUAN et al., 2003). Measurements carried out by Desmazes et al. (2000) suggested relaxation times of about 15 min for a base asphalt binder, between 1 and 2 h for SBS-modified materials with no more than 4% of SBS by weight and of about 10 h for SBS contents higher than 4% by weight. In graphical terms, these changes are reflected in a flattening of the relaxation spectrum and can be attributed to an increase in both the storage and loss moduli; however, the effects of elasticity are enhanced more than the ones of viscosity (RUAN et al., 2003). Similar patterns can be observed in the relaxation curves of modified binders after an accelerated aging process (GAHVARI, 1997; RUAN et al., 2003).

In terms of the Superpave® specification and the distress mechanisms commonly observed in asphalt pavements, the low-temperature cracking is the only one that takes into account the relaxation mechanism of the binder. An asphalt binder with a higher level of relaxation can deal with higher internal stresses caused by the cooling process of the surface layer without cracking,

---

[11] PETERS, F. E. (1967). **Greek philosophical terms:** a historical lexicon. New York: NYU Press. ISBN 0814765521.

since the tensile stresses are relaxed by means of energy dissipation into permanent flow (BAHIA and ANDERSON, 1995). In the BBR test, the relaxation rate *m* gives an idea of the ability of the binder in relaxing stresses without reaching failure. The λ_T value can be obtained either from rheological tests or mathematical models (subheading 2.4). By considering the fact that both parameters refer to the relaxation phenomenon, it was hypothesized that there is a correlation between them. Liu et al. (2010) tested this hypothesis and correlated the λ_T values from the four-element Burgers model with the *m* values after 60 s of loading in the BBR test. An excellent linear correlation was found in the study ($R^2 > 0.97$) and λ_T was inversely proportional to *m*, i. e., a binder with longer relaxation time tends to show a lower relaxation rate and vice versa.

For linear viscoelastic materials or the ones that are tested within the linear viscoelastic range, it is possible to apply some basic principles to form curves (for instance, master and isochronal curves of G^* and δ) and estimate the effects of temperature (isochronal curve) or loading frequency (master curve) on the rheological response of asphalt binders. One of these principles is the Boltzmann superposition principle, which was named after the German scientist who formulated it in the second half of the 19th century[12]. According to this principle, the effect of a general loading history in a binder sample is equal to the sum of the individual loads and the response of the sample to such loads is linear. The time-temperature superposition principle, which establishes that the effects of loading time and temperature are similar and interchangeable (higher temperatures are equivalent to longer loading times and vice versa), is also commonly found in studies with asphalt binders.

The aforementioned principles are taken as references for the construction of the master/isochronal curves. When the data points of G^* are plotted against the δ values, the resulting curve is known as "black curve". Two equations can be used to shift the data of several curves in the horizontal axis (temperature or frequency), to obtain one smooth curve. One of these equations is referred to as the Williams-Landel-Ferry (WLF) equation, where a_T is the horizontal shift factor, T is the temperature of the curve that is being shifted, T_0 is the reference temperature and C_1 and C_2 are constants that depend on the binder and the T_0 value – see Equation (9). The other option is the Arrhenius equation, where E_a is the energy activation, C is a constant of the material, R is the universal gas constant and the temperatures T and T_0 are given in kelvin – Equation (10). The Arrhenius equation is recommended when

[12] BOLTZMANN, L. (1878). Zur theorie der elastischen nachwirkung [To the theory of elastic after-effect]. **Annalen der Physik**, Vol. 241, No. 11, pp. 430-432. doi: 10.1002/andp.18782411107.

the difference between the temperatures T and T_0 is lower than or equal to 20°C; for differences higher than 20°C, the WLF equation is preferred over the Arrhenius one[13].

$$\log(a_T) = -\frac{C_1 \times (T - T_0)}{C_2 + (T - T_0)} \tag{9}$$

$$\log(a_T) = C \times \left(\frac{1}{T} - \frac{1}{T_0}\right) = \frac{E_a}{2.303 \times R} \times \left(\frac{1}{T} - \frac{1}{T_0}\right) \tag{10}$$

2.5. Modeling of the Rheological Behavior of Binders

The study of the strain response of a binder to the application of an external force requires the observation of laws that dictate the behavior of the material within a predefined period of time. The two simplest laws have been discussed previously, namely, the Hooke's and the Newton's ones. They state that, for a purely elastic material, the resulting strain is proportional to the external force and the constant of proportionality is the Young's modulus E (Hooke's law); for a purely viscous material, the applied stress is proportional to the shear rate and the constant of proportionality is the Newtonian viscosity η (Newton's law). The former is represented by a spring in rheological models (Figure 13), whereas the latter is represented by a dashpot (Figure 14).

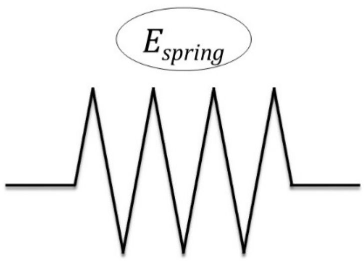

Figure 13 – Illustration of a spring element associated with a Young's modulus (E_{spring}) for use in rheological models

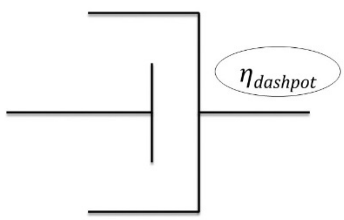

Figure 14 – Illustration of a dashpot element associated with a Newtonian viscosity ($\eta_{dashpot}$) for use in rheological models

---

[13] GHEUNG, C. Y. (1995). **Mechanical behaviour of bitumens and bituminous mixtures**. Dissertation (Doctor of Philosophy) – University of Cambridge, Cambridge, UK.

Since the asphalt binder does not show a perfectly elastic neither a perfectly viscous response at the typical pavement service temperatures (but a combination of both, i. e, viscoelastic), the use of only a spring or a dashpot to describe its response is not sufficient. Consequently, it is necessary to associate one or more of these elements to better represent the rheological behavior of the binder. In rheology, two of the most basic linear viscoelastic models are the Maxwell model, which is comprised by a spring and a dashpot in series, and the Voigt model, which is comprised by a spring and a dashpot associated in parallel. Other models such as Burgers and Maxwell-Wiechert – or generalized Maxwell model – can also be found in scientific documents published worldwide (e.g., DIVYA et al., 2013; DONGRÉ and D'ANGELO, 2003; KRISHNAN and RAJAGOPAL, 2005; LIU and YOU, 2009; MERUSI, 2012; PARTAL et al., 1999; WOLDEKIDAN, 2011). More precise details on these models are given in the next two sections. The last one (Section 2.5.3) is devoted to some additional models used in the linear and nonlinear viscoelastic range of asphalt binders.

2.5.1. Maxwell and Voigt Models

In simple terms, the Maxwell model can describe the response of the asphalt binder under constant strain (relaxation) and the Voigt model can describe this response under constant stress (creep). Figure 15 depicts the behavior of the binder under a constant stress τ_t according to the Maxwell model: an instantaneous strain is observed in the material due to the spring, followed by a linear increase in the amount of permanent strain because of the dashpot. When the stress is removed, the elastic strain is recovered immediately and the permanent strain remains.

Similarly, Figure 16 shows the pattern behavior of the asphalt binder according to the Voigt model for a constant τ_t value: the resulting strain increases asymptotically to the total strain in the spring (τ_t/E_{spring}). As soon as the stress is removed, the material starts the recovery process and the resulting strain decreases asymptotically to zero. The elastic and viscous strains can be observed in the Maxwell model, but not in the Voigt model. Conversely, the Voigt model is the only one that includes the delayed elastic strain in the creep-recovery curve. In summary, both models are too simple to give a complete description of the major components of the total strain in the binder.

Equation (11) is used to calculate the total strain in the Maxwell model under a constant stress, whereas Equation (12) makes it possible to calculate the total strain in the Voigt model and at the same stress (VAN DER VEGT, 2006). The first term in the right hand side of Equation (11) represents the instantaneous elastic strain of the binder, and the second term represents its permanent strain. The exponential term in Equation (12) reflects the asymptotic character of the increase in the accumulated strain with increasing loading time *t*. The ratio of the dashpot η to the spring E in this equation yields the retardation time Λ_1, which represents the time-dependent behavior (or delayed) response of the material under an applied shear stress.

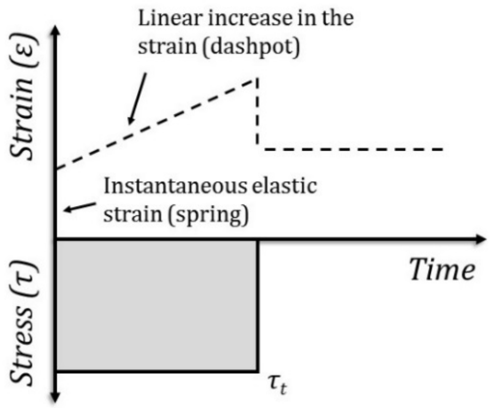

Figure 15 – Rheological response of the asphalt binder in a creep-recovery test according to the Maxwell model

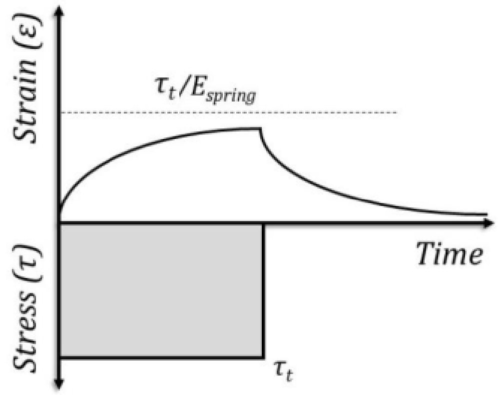

Figure 16 – Rheological response of the asphalt binder in a creep-recovery test according to the Voigt model

$$\varepsilon(t) = \tau_t \times \left(\frac{1}{E} + \frac{t}{\eta}\right) \tag{11}$$

$$\varepsilon(t) = \frac{\tau_t}{E} \times \left(1 - e^{\frac{(-t)\times E}{\eta}}\right) \tag{12}$$

2.5.2. Burgers Model and its Variants

As previously discussed, one must take into account the fact that the measured strains are comprised by the viscous, delayed elastic and instantaneous elastic components (Figure 11) when conducting a creep-recovery test. The Burgers model – which was proposed in the 1930's[14] and is comprised by an association of the Maxwell and Voigt models in series, Figure 17 – is a more acceptable alternative for modeling the response of the binder because these three strain components can be found in it. Many researchers have utilized the Burgers model in their analyses with varying purposes, for instance, to further validate the conclusions drawn in the studies (BAHIA, 2014; BAHIA et al., 2001a, 2001b; DELGADILLO et al., 2006b; DOMINGOS and FAXINA, 2015b; GOLALIPOUR, 2011; LIU and YOU, 2009). This was the case of Golalipour (2011), who observed the reductions in the percent differences among the parameters of the model with the application of more loading-unloading cycles in the multiple stress creep and recovery (MSCR) test. Bahia et al. (2001a) and Delgadillo et al. (2006b) utilized the model to isolate the permanent strain of the binder in the repeated creep and recovery test (RCRT) and suggest a new binder rutting parameter, i. e., the viscous component of the creep stiffness (G_V).

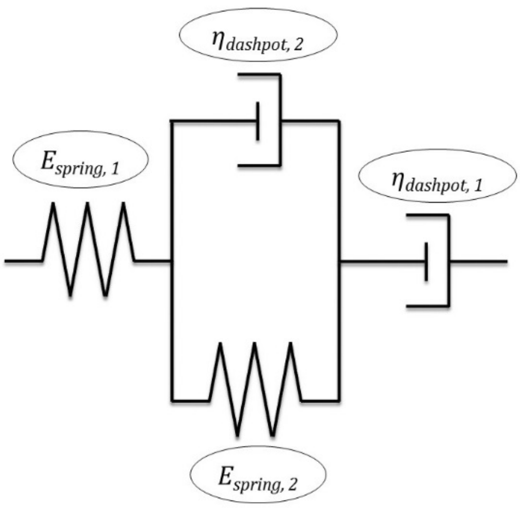

Figure 17 – Illustration of a four-element Burgers model with the two springs ($E_{spring,1}$ and $E_{spring,2}$) and two dashpots ($\eta_{dashpot,1}$ and $\eta_{dashpot,2}$) from the Maxwell and Voigt models

In order to determine the numerical values of the parameters of the Burgers model, Liu and You (2009) developed an easy-to-use, seven-step procedure. This procedure was followed by the author in a previous paper (DOMINGOS and FAXINA, 2015b), and the resulting parameters fitted the binder data quite well. Equation (13) depicts the strain $\varepsilon(t)$ during the creep portion of the cycle, whereas Equation (14) shows this permanent strain during the recovery portion of the cycle. It can be inferred from these equations that there is only one retardation time Λ_1 in the

[14] BURGERS, J. M.; JEFFERY, G. B. (1939). Mechanical considerations – model systems – phenomenological theories of relaxation and of viscosity. **First Report on Viscosity and Plasticity**: Prepared by the Committee for the Study of Viscosity of the Academy of Sciences at Amsterdam. 2nd ed. New York: Nordemann Publishing Company Inc., pp. 161-179.

model, namely, the ratio of $\eta_{dashpot,2}$ to $E_{spring,2}$. This seems to be quite simple and, as previously indicated by other authors in the literature (KRISHNAN and RAJAGOPAL, 2005; VAN DER VEGT, 2006; WOLDEKIDAN, 2011), it does not account for the complex rheological behavior of real viscoelastic materials. However, the continued use of the model in the literature – from the NCHRP Report 459 (BAHIA et al., 2001a) to the current days (e. g., BAHIA, 2014; DOMINGOS and FAXINA, 2015b; HAJIKARIMI et al., 2015) – makes it possible to imply that such limitations did not discourage researchers from applying it in their studies.

$$\varepsilon(t) = \frac{\sigma_0}{E_{spring,1}} + \frac{\sigma_0 \times t}{\eta_{dashpot,1}} + \frac{\sigma_0}{E_{spring,2}} \times \left(1 - e^{\frac{-E_{spring,2} \times t}{\eta_{dashpot,2}}}\right) \tag{13}$$

$$\varepsilon(t) = \frac{\sigma_0 \times t}{\eta_{dashpot,1}} + \frac{\sigma_0}{E_{spring,2}} \times \left(1 - e^{\frac{-E_{spring,2} \times t_F}{\eta_{dashpot,2}}}\right) \times e^{\frac{-E_{spring,2} \times (t - t_F)}{\eta_{dashpot,2}}} \tag{14}$$

In a different mathematical approach, Divya et al. (2013) modeled the response of the binder in the MSCR tests according to a generalized Voigt model with two Voigt elements and one isolated spring. The presence of these two Voigt models in series provides two different retardation times (Λ_1 and Λ_2), and it was assumed that one of these retardation times is associated with the binder and the other is associated with the modifier (in this case, crumb rubber). It was also suggested that a third variable (interaction between the modifier and the binder) could be included in the study, even though this hypothesis was not further investigated.

By attaching one more Voigt element to the original Burgers model, both Equations (13) and (14) will depict a summation of the strains in each of these elements, as it can be observed in Equations (15) and (16). Figure 18 shows a layout of this modified model. The ratios of $\eta_{dashpot,2}$ to $E_{spring,2}$ and $\eta_{dashpot,3}$ to $E_{spring,3}$ yield the retardation times Λ_1 and Λ_2, respectively. Strictly speaking, there is no maximum limit for the number of Voigt models associated with the isolated spring and dashpot elements. For example, Woldekidan (2011) studied the responses of asphalt binders, mastics and mortars in time domain tests based on generalized Burgers models with at least 10 Voigt elements in series, which resulted in 22 parameters (or more) to be calculated. In another paper, Merusi (2012) took into account an association of three Voigt elements with one isolated spring and one isolated dashpot to model the response of binders in the RCRT.

Up to the development of the present study, it is believed that Burgers models with no more than two Voigt models have been used in research reports about the MSCR testing of binders. Probably the restricted conditions of the standardized MSCR protocol and the great degrees of fitting with one and two Voigt elements do not justify the need to increase the number of elements in the analysis.

$$\varepsilon(t) = \frac{\sigma_0}{E_{spring,1}} + \frac{\sigma_0 \times t}{\eta_{dashpot,1}} + \left[\sum_{i=2}^{3} \frac{\sigma_0}{E_{spring,i}} \times \left(1 - e^{\frac{-E_{spring,i} \times t}{\eta_{dashpot,i}}}\right)\right] \tag{15}$$

$$\varepsilon(t) = \frac{\sigma_0 \times t}{\eta_{dashpot,1}} + \left[\sum_{i=2}^{3} \frac{\sigma_0}{E_{spring,i}} \times \left(1 - e^{\frac{-E_{spring,i} \times t_F}{\eta_{dashpot,i}}}\right) \times e^{\frac{-E_{spring,i} \times (t - t_F)}{\eta_{dashpot,i}}}\right] \tag{16}$$

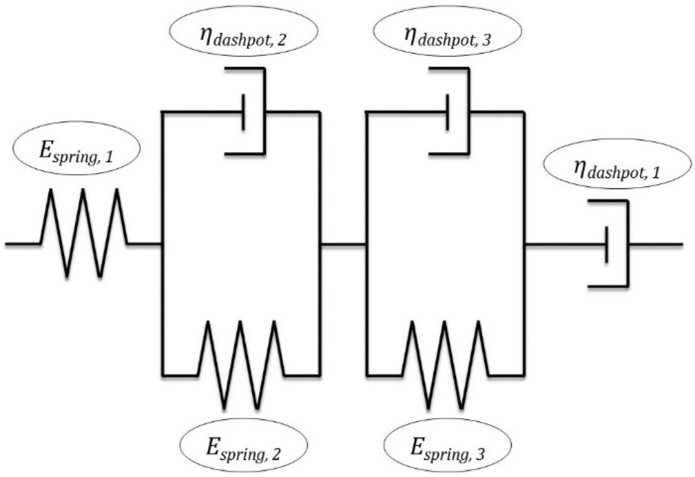

Figure 18 – Layout of the generalized Burgers model used in this study [adapted from Woldekidan (2011)]

In summary, the four-element Burgers model and a variation of this model with one more Voigt element are the ones that have been mostly used in the investigations into the rutting potential of modified asphalt binders. The use of more than two Voigt elements in the model is possibly restricted to testing conditions and repeated creep protocols that are devoted only to academic purposes (MERUSI, 2012; WOLDEKIDAN, 2011), which is not the case of the performance-related tests used on Superpave®. It may be important to note that the number of relaxation times is the same either for the original Burgers model (Figure 17) or the modified one (Figure 18) and, as a consequence, both models provide only one parameter G_V.

2.5.3. Presentation and Discussions on Other Viscoelastic Models

The springs and dashpots used in the aforementioned models are associated with an integer order, that is, the real order derivatives of the constitutive equations of the elements – parameters α_1 and α_∞ in Figure 19 and Equation (17) in the case of the Burgers model – are assumed as invariable numbers. When either α_1 or α_∞ may vary from 0 to 1, then fractional models are obtained. The designation *fractional* comes from the fact that the springpot element (i. e., the rhombus in Figure 19) may indicate a more elastic behavior (α_1 and α_∞ approach zero) or a more viscous behavior (α_1 and α_∞ approach one). The terms ψ_1 and ψ_∞ are the characteristic times of the springpots and Γ is the Euler Gamma function. The use of a fractional model may considerably reduce the number of elements in the constitutive relationship of a real viscoelastic material when high degrees of precision are required. If this option is not chosen, a huge number of parameters – from 20 to 30 in some cases – may be needed to yield satisfactory results (WOLDEKIDAN, 2011). Such fractional models can also avoid the occurrence of physically meaningless negative values for the springs in the traditional associations between springs and dashpots, depending on the experimental data (CELAURO et al., 2012).

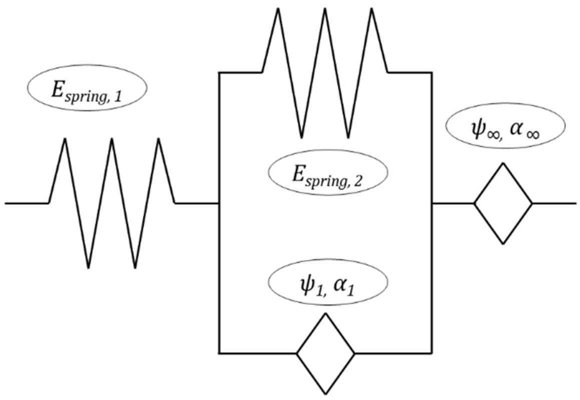

Figure 19 – Illustration of the Burgers fractional model with two springs ($E_{spring,\,1}$ and $E_{spring,\,2}$) and two springpots (characteristic parameters ψ_1, ψ_∞, α_1 and α_∞)

$$\varepsilon(t) = \frac{1}{E_{spring,2}} \times \left\{1 - E_{spring,2} \times \left[\left(\frac{-t}{\psi_1}\right)^{\alpha_1}\right]\right\} \times \sigma_0 + \frac{1}{E_{spring,1}} \times \left[1 + \frac{1}{\Gamma \times (1+\alpha_\infty)} \times \left(\frac{t}{\psi_\infty}\right)^{\alpha_\infty}\right] \times \sigma_0 \tag{17}$$

Another type of fractional model is known in the literature as 2S2P1D (abbreviation for "2-spring, 2-parabolic, 1-dashpot") model, Figure 20. The parabolic dashpot is the fractional element that shows a stress-strain response between the linear spring and the linear dashpot, and the degree of viscous response will depend on the numerical values of the constants m_1 and m_2, see Figure 21. Researchers have been using this model to fit laboratory data collected in frequency domain tests with a great degree of success, and some examples include the studies from Sauzeat and Di Benedetto (2015), Woldekidan (2011) and Yusoff et al. (2013). On the other hand, the applicability of the 2S2P1D model to data obtained in time domain tests is extremely difficult from the point of view of Woldekidan (2011) and not possible in the publication from Anderson and Marasteanu (2010). Even some artificial techniques when moving from the frequency domain to the time domain regime in the 2S2P1D model – e. g., the Fourier transform and truncations in the loading story – have a limited range of use, and the data may not accurately represent the actual response of the material precisely due to these simplifications (WOLDEKIDAN, 2011).

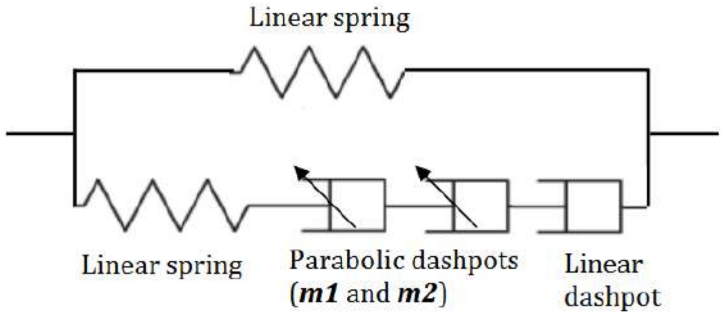

Figure 20 – Typical layout of the 2S2P1D ("2-spring, 2-parabolic, 1-dashpot") model with the identification of the parabolic elements and the fractional constants m_1 and m_2 [adapted from Woldekidan (2011)]

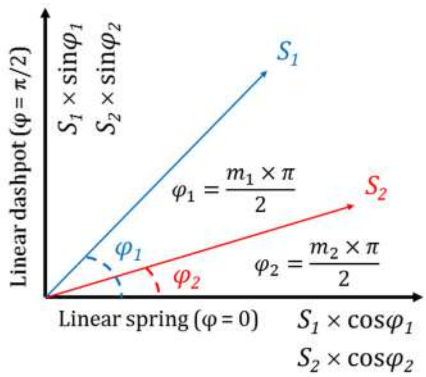

Figure 21 – Calculations of the values S_1 and S_2 associated with the parabolic dashpots (angles φ_1 and φ_2 and fractional constants m_1 and m_2)

Among the nonlinear viscoelastic models currently available in the literature, the Schapery's theory is the most widely used one in modeling nonlinear time-dependent materials. This may be attributed to several factors such as the simplicity of the laboratory tests on which the theory can be used, the rigorous theoretical foundation behind it and the successful implementations of other nonlinear variables in the analysis, among which moisture damage and aging can be cited (WOLDEKIDAN, 2011). Masad et al. (2009) followed this approach and applied the theory for asphalt binders tested according to the original MSCR protocol and the temperatures of 58, 64, 70 and 76°C. The authors assumed that all the recoverable strain was time-dependent (i. e., delayed elastic), and the J_{nr} values calculated according to a new method proposed by them (averaged nonrecoverable strain at all cycles divided by the stress level at which the nonlinear parameter g_2 drops off by more than 20%). They also suggested that linear viscoelastic models may lead to major errors in the identification of the actual rutting performance of modified binders.

Delgadillo et al. (2012) chose another method for studying the creep-recovery response of asphalt binders within the nonlinear viscoelastic range. These authors assumed that the creep portion of the strain response of the asphalt binders at very long loading and unloading times (in this case, from 1/2,000 s to 10/10,000 s and then 100/20,000 and 1,000/40,000 s) may be represented by a power law equation with two arguments, namely, one associated with the linear component (power of the stress τ_t is equal to one) and the other associated with the nonlinear component (power of the stress τ_t is higher than one), Equation (18). The recovery portion of the cycles was modeled by subtracting the permanent strain from the total strain in the binder, and the recoverable strains were found to be reasonably represented by a linear viscoelastic function. According to the authors, the average errors in the predictions of the data were of about 16 to 20% for the two studied binders (unmodified and Elvaloy-modified one), and this was attributed to the testing variability.

$$\varepsilon(t) = \sum_{i=1}^{2} A_i \times t^{B_i} \times (\tau_t)^{C_i} \tag{18}$$

Differently from these previously mentioned studies, Saboo and Kumar (2015) decided to use a modified power law function to fit the MSCR testing data within the nonlinear viscoelastic range of response. These authors modified the equation of the original power function by adding a factor that accounts for the nonlinearity of the binder in the recovery portion of the cycle (factor n), as it can be seen in Equation (19). The constants A and B are associated with the characteristics of the material, whereas the multiplication of B by n (factor α) is supposed to be well correlated with the percent recovery. The authors proposed the use of such power equation because either the original one (without the constant n) or the four-element Burgers model were unable to describe the pattern of behavior observed for highly-modified asphalt binders (in this case, SBS- and EVA-modified ones). According to their paper, the α value may indicate not only the level of delayed elasticity in the asphalt binder, but also the most appropriate traffic level for it.

$$\varepsilon_{rec}(t) = A \times t^{B} - A \times (t - t_F)^{B \times n} \tag{19}$$

It can be concluded from these studies that the description of the creep-recovery behavior of asphalt binders may be based on several linear and nonlinear models, even though simplifications must be made in order to fit these models to actual binder data. Some of them are more commonly used in the literature (four-element Burgers, Schapery's and generalized Maxwell models are characteristic examples), whereas others have a more local application. As a consequence, the choice for one or another equation will essentially be dependent on factors such as the theoretical foundation behind the model, its validation with experimental results and (in some cases) its simplicity. The present document also took into account these factors in the choice for the linear and nonlinear viscoelastic models to be used with the MSCR binder data, as it will be shown in the forthcoming chapters.

2.6. Specifications for Asphalt Binders

Prior to the development of the penetration machine by H. C. Bowen in 1888, the method – if it can be designated as such – for evaluating the degree of consistency of the asphalt binder was by chewing. Even after the release of this machine, the chewing method still served as a valuable check. By the beginning of the 1900's, successive refinements in the Bowen's penetrometer and the continued efforts from the Bureau of Public Roads (now the Federal Highway Administration – FHWA) and ASTM have led to the development of the first penetration-grade specifications. The Bureau of Public Roads introduced the penetration-grade system in 1918, and the American Association of the State Highway Officials (AASHO, currently AASHTO) published the standard specifications in 1931 (HALSTEAD and WELBORN, 1974; ROBERTS et al., 1996). The testing temperature was settled at 25°C.

The next great change in the binder specifications started in the early 1960's with a cooperation among FHWA, ASTM, AASHTO, industries and several state highway departments. These public organizations and industries aimed at developing a specification based on the viscosity of the binder at 60°C and defining intervals of acceptable values for each climatic condition and application. The primary purpose of these changes in the test protocol and the corresponding specification was to measure a fundamental (and not empirical-based) property of the binder at a temperature that is much closer to the actual one observed in the pavement. In parallel, the California Department of Highways prepared a viscosity specification based on the aged residue (AR) of the binder, i. e., the material aged in the rolling thin-film oven. The staff members of this department decided to choose the aged binder rather than the unaged one, since they observed that some binders did not undergo great increases in their viscosity during the mixing phase when compared to others (ROBERTS et al., 1996).

The ASTM standard D946[15] establishes five intervals of penetration values, i. e., 40-50, 60-70, 85-100, 120-150 and 200-300. Minimum limits for the flash point, solubility in trichloroethylene, ductility at 25°C before and after aging and retained penetration are also defined. Similarly, ASTM D3381[16] classifies the unaged asphalt binders in six categories (AC-2.5, AC-5, AC-10, AC-20, AC-30 and AC-40) and the aged ones in five categories (AR-1000, AR-2000, AR-4000, AR-8000 and AR-16000). The numbers in the viscosity-graded systems

[15] AMERICAN SOCIETY FOR TESTING AND MATERIALS. **ASTM D946**: Standard specification for penetration-graded asphalt binder for use in pavement construction. West Conshohocken, PA.
[16] AMERICAN SOCIETY FOR TESTING AND MATERIALS. **ASTM D3381**: Standard specification for viscosity-graded asphalt cement for use in pavement construction. American Society for Testing and Materials, West Conshohocken, PA.

indicate the target viscosity divided by 100 (unit of poise, unaged condition) or divided by 10 (unit of Pa.s, aged condition), e. g., 250 P for the AC-2.5 asphalt binder and 1,600 Pa.s for the AR-16000 binder. As with the penetration-grade system, minimum requirements for other tests such as ductility, flash point and solubility in trichloroethylene can also be found in the AC and AR specifications.

In Brazil, the viscosity- and the penetration-grade systems were the two prevailing criteria for classifying asphalt binders from 1992 up to the middle of 2005. There were three intervals in the viscosity-based specification (AC-7, AC-20 and AC-40) and four intervals in the penetration-based one (30-45, 50-60, 85-100 and 150-200). The numbers in the viscosity-based system indicate the minimum value for each interval: from 700 to 1,500 P (AC-7), from 2,000 to 3,500 P (AC-20) and from 4,000 to 8,000 P (AC-40). In July/2005, the Brazilian National Agency of Petroleum, Natural Gas and Biofuels (ANP, in Portuguese) introduced a new specification for asphalt binders based only on the penetration at 25°C and comprised by four intervals of penetration values: 30-45, 50-70, 85-100 and 150-200 (BERNUCCI et al., 2006). Table 1 shows all the details of this specification.

The penetration- and viscosity-based specifications have several advantages and disadvantages, many of which were placed by Roberts et al. (1996). The relatively short period of time and the low equipment costs are pointed out as some of the advantages of the penetration-grade system, whereas the disadvantages include the degree of empiricism behind the measurements and the absence of viscosity values for calculating the mixing and compaction temperatures. The fundamental property used in the classification of the asphalt binders, the suitability to a wide range of environmental temperatures and the presence of several test instruments (e. g., ductilometer, Cleveland open cup, thin-film oven and penetrometer) are suggested as some of the advantages of the viscosity-grade specification, whereas the time duration of the test, the limitations in evaluating the low-temperature performance of the binder and the high cost of the testing system are pointed out as its disadvantages.

Despite the important advances in the classification of the asphalt binders according to their rheological properties and parameters, an extensive literature review conducted by researchers from SHRP concluded that there was significant confusion about the binder properties and which of them could reliably be related to pavement performance. This was mainly caused by underestimation of the complex rheological behavior of the binder and the empirical nature of the methods used in the determination of the properties of interest (BAHIA and ANDERSON, 1995). Also, neither the penetration-grade nor the viscosity-grade specifications account for all the climatic and aging conditions of the binder, as it can be inferred from the absence of tests at low pavement temperatures and no long-term aging protocols (ROBERTS et al., 1996). In other words, a new specification should be developed in order to consider and address these issues.

Table 1 – Penetration-grade binder specification used in Brazil from July/2005 to the current days [Technical Regulation No. 03/2005, ANP]

property or parameter		unit	requirements for each classification			
			AC 30-45	AC 50-70	AC 85-100	AC 150-200
penetration (25°C, 5 s, 100 g)		dmm	30 to 45	50 to 70	85 to 100	150 to 200
softening point (R&B)		°C	> 52	> 46	> 43	> 37
Saybolt-Furol viscosity	135°C	s	> 192	> 141	> 110	> 80
	150°C	s	> 90	> 50	> 43	> 36
	177°C	s	40 to 150	30 to 150	15 to 60	15 to 60
Brookfield viscosity, spindle 21	135°C (20 rpm)	cP	> 374	> 274	> 214	> 155
	150°C	cP	> 203	> 112	> 97	> 81
	177°C	cP	76 to 285	57 to 285	28 to 114	28 to 114
penetration index		-	(-1.5) to (+0.7)			
flash point		°C	> 235			
solubility in trichloroethylene		%	> 99.5			
ductility (25°C)		cm	> 60	> 60	> 100	> 100
after RTFOT (163°C, 85 min)	mass change	%	< 0.5			
	ductility (25°C)	cm	> 10	> 20	> 50	> 50
	increase in R&B	°C	8.0			
	retained penetration	%	> 60	> 55	> 55	> 50

The so-called Superpave® specification (ASTM D6373 and AASHTO M320 standards) was designed to guide researchers and members from industry and highway agencies on how to classify and select the best binder for a predefined climatic condition. This specification grades the binders (either modified or unmodified ones) according to the notation "PG X-Y", where "X" is the average seven-day maximum expected pavement temperature and "-Y" is the minimum expected temperature. The "X" values vary from 46 to 82°C with intervals of 6°C in between (46, 52, 58, 64, 70, 76 and 82°C) and the "-Y" values range from -10 to -46°C with 6°C in between the classifications (-10, -16, -22, -28, -34, -40 and -46°C). Critical temperatures for the occurrence of fatigue cracking are also defined (from 4 to 40°C with regular spacing of 3°C between one and the next), even though they are not shown in the official notation. Table 2 depicts part of this specification with the requirements for the PG 64, PG 70 and PG 76 binders.

Table 2 – Superpave® specification requirements for the PG 64, PG 70 and PG 76 binders [ASTM D6373 standard, Table 1]

description		unit	PG 64	PG 70	PG 76
average 7-day maximum pavement temperature		°C	64	70	76
minimum design temperature of the pavement		°C	-10, -16, -22, -28, -34, -40	-10, -16, -22, -28, -34, -40	-10, -16, -22, -28, -34
unaged condition	flash point	°C	> 230		
	Brookfield viscosity at 135°C (spindle 21, 20 rpm)	Pa.s	< 3.0		
	G/sinδ* at 10 rad/s, 25 mm geometry and 1.0 mm gap	kPa	> 1.0 (maximum pavement temperature)		
after RTFOT (163°C, 85 min)	mass change	%	≤ 1.0		
	G/sinδ* at 10 rad/s, 25 mm geometry and 1.0 mm gap	kPa	> 2.2 (maximum pavement temperature)		
after PAV (2.1 MPa and 20 h)	PAV temperature	°C	100	100 or 110	100 or 110
	*G*sinδ* < 5000 kPa at 10 rad/s, 8 mm geometry and 2.0 mm gap, temp.	°C	31, 28, 25, 22, 19, 16	34, 31, 28, 25, 22, 19	37, 34, 31, 28, 25
	creep stiffness *S* < 300 MPa and *m* > 0.3, after 60 s, temp.	°C	0, -6, -12, -18, -24, -30	0, -6, -12, -18, -24, -30	0, -6, -12, -18, -24
	direct tension (300 ≤ *S* < 600 MPa and *m* > 0.3), failure strain > 1.0% at 1.0 mm/min, temp.	°C	0, -6, -12, -18, -24, -30	0, -6, -12, -18, -24, -30	0, -6, -12, -18, -24

Some years after the release of Superpave® as a binder specification, many changes were incorporated into the criteria for short-term aged asphalt binders in an attempt to solve the deficiencies of the parameter *G*/sinδ* and the oscillatory shear test. Prior to the publication of the first studies about the MSCR test, approximately half of the states of the US had been adopted the "PG Plus" tests (e. g., toughness and tenacity, force ductility and elastic recovery) in their specifications (DuBOIS et al., 2014). As a consequence of the release of the MSCR test, the minimum value of 2.2 kPa for *G*/sinδ* after short-term aging was no longer a mandatory requirement and the determination of the high PG grade of the binder became dependent only on the unaged condition (*G*/sinδ* no lower than 1.0 kPa). These new criteria were first approved and published by AASHTO in 2009 as an amended table (Table 3) to its M320 specification.

The implementation guidance published by D'Angelo (2010c) indicated that Table 1 in the AASHTO M320 standard should be replaced by Table 3, and this should start in 2011. According to Harder (2012), the MSCR test should be fully implemented in the US by 2014 and the provisional AASHTO standard TP70 should become a full standard up to the same year. However, a comparison between the implementation goals published by D'Angelo (2010c) and Harder (2012) and the current status of the MSCR test and the corresponding AASHTO standards reveals that some goals were fully achieved, whereas others were not. For instance, AASHTO published the first full standard of the MSCR test under the designation T350 exactly in 2014. Conversely, Figure 22 suggests that the MSCR protocol has not yet been implemented in all the states of the US, since some states are currently under partial or planned implementation within a year and others are still considering the possibility of implementation or evaluating the test. Only a few states in the east side of the country have already reached the goal of full implementation. The database created by the Asphalt Institute (ASPHALT INSTITUTE, 2016) is updated periodically, which makes it possible to track the changes in the implementation of the MSCR test with time.

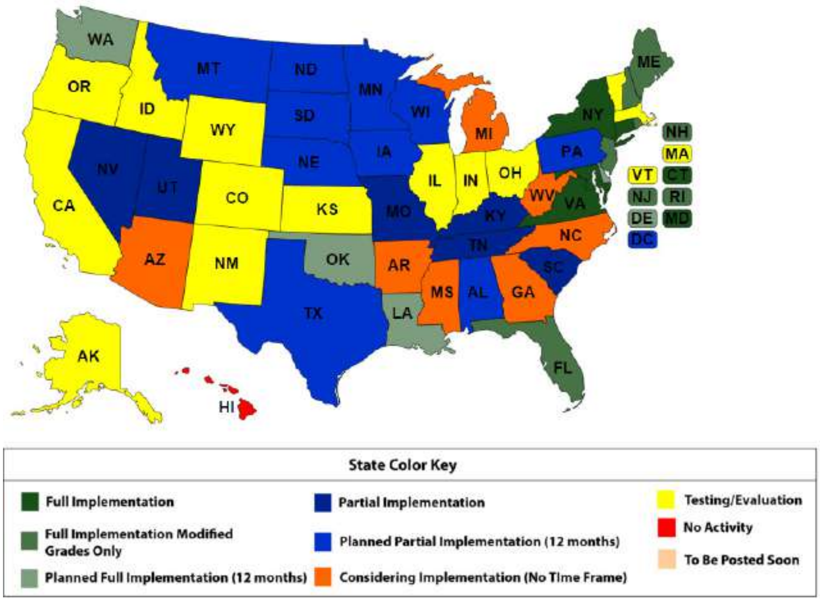

Figure 22 – Current status of the MSCR test in each of the states and districts of the United States (ASPHALT INSTITUTE, 2016)

As it will be discussed in detail later (Chapter 3), the development of the repeated creep tests for asphalt binders also introduced the concept of traffic level in the Superpave® specification. In simple terms, this traffic level is associated with an appropriate number of equivalent single-axle loads (ESALs) and the average vehicle speed that the binder may deal with in the pavement without showing significant levels of rutting. This started with the suggestion of a preliminary draft based on the parameter G_V (DELGADILLO et al., 2006b) and, some years later, an early specification based on J_{nr} and a maximum limit of 75% for the parameter $J_{nr,\, diff}$ was proposed by D'Angelo (2010a, 2010b). Rather than changing the test temperature, the researchers from FHWA decided to decrease the maximum allowed J_{nr} value with increasing traffic level. More recently, average traffic speeds were associated with each of the four available traffic levels – i. e., standard (S), heavy (H), very heavy (V) and extremely heavy (E). These traffic speeds are given by the following intervals and designations: (a) standing traffic, for which the average vehicle speeds are lower than 20 km/h; (b) slow moving traffic, for average vehicle speeds between 20 and 70 km/h; and (c) standard traffic, for average speeds higher than 70 km/h.

2.7. Study and Determination of the Mixing and Compaction Temperatures

For the asphalt binder to be mixed with the aggregates in the plant and compacted in the field, the engineers must ensure that the viscosity is within an acceptable range of values. This is because the binder must be fluid enough during mixing to uniformly cover the surface of the aggregate particles. At the same time, the viscosity range of values during compaction must allow the movement of the particles within the mixture such that the optimum air void content can be reached. If the binder temperatures fall outside of these predefined intervals, either the mixing process will be affected by an unequal distribution of the binder in the mixture (some aggregate particles will not be properly covered by the binder, whereas others will) or the compaction procedure will become extremely difficult due to the high viscosity of the bituminous material.

Historically, the viscosity values have been used to calculate the mixing and compaction temperatures. In the Marshall mix design protocol (which was developed in the 1940's), capillary viscometers were used to obtain the temperature ranges at which the binder shows viscosities of 170 ± 20 cSt for mixing and 280 ± 30 cSt for compaction. Despite the changes in the device (from the capillary viscometer to the Brookfield rotational viscometer) and the compaction method (from impact to shearing in the gyratory compactor), both viscosity intervals remained the same in the Superpave® specification. This is not a great problem for unmodified binders, since these materials typically depict a Newtonian behavior at high temperatures (i. e., the viscosity does not change with shear rate). However, the non-Newtonian characteristics observed for many modified binders (especially shear-thinning) create some difficulties in calculating the appropriate mixing and compaction temperatures for such materials.

In Brazil, some service specifications adopt different approaches for the calculation of the mixing and compaction temperatures of modified asphalt binders. For example, the Specification

No. 112/2009[17] states that the crumb rubber-modified binder must be heated at temperatures ranging from 170 to 180°C and that the compaction temperature cannot be lower than 145°C. In another approach, the Specification No. 385/1999[18] states that the mixing temperature of the SBS-modified asphalt binder starts at 150°C, and 3°C is summed to the original value for each 1% of SBS added to the binder up to a maximum limit of 180°C. Similarly, the compaction temperature starts at 140°C and 3°C is summed to this value for each 1% of SBS in the formulation.

By taking into account this intrinsic characteristic of the modified binders, some researchers devoted attention and efforts to the development of alternatives to the conventional methods and intervals of mixing and compaction temperatures. This was the case of Yildirim et al. (2000) and Yildirim et al. (2006), who suggested the use of higher shear rates in the tests to measure viscosity, in order to simulate the actual values found in the Superpave® gyratory compactor. As a result of the proposal of shear rates as higher as 490 and 500 s^{-1} and the observation of the shear-thinning behavior of many of the studied formulations, the authors concluded that the appropriate mixing and compaction temperatures can be reduced by 10 to more than 50°C depending on the modification type. Yildirim et al. (2006) also indicated that such temperatures can be determined based on higher viscosity values for mixing (0.275 ± 0.03 Pa.s) and compaction (0.550 ± 0.06 Pa.s). In other words, modified asphalt binders could be mixed with the aggregates and compacted in the field at higher viscosities without affecting the quality of the asphalt pavement.

Notwithstanding the evidences that the viscosity ranges of 0.17 ± 0.02 Pa.s for mixing and 0.28 ± 0.03 Pa.s for compaction – as well as the shear rates typically used in the viscosity measurements – may not be adequate for several modified asphalt binders, the Superpave® specification still sets rotation speeds and spindle numbers that result in very low shear rates. This is the case of the upper limit of 3.0 Pa.s at the temperature of 135°C, speed of 20 rpm and with the spindles 21 and 27, which result in shear rates of about 6.8 s^{-1} (spindle 27) and 18.6 s^{-1} (spindle 21). As it can be inferred from the laboratory data collected by Yildirim et al. (2000), the actual shear rates observed in the gyratory compactor can easily overcome 400 s^{-1}. Since many modified binders show a shear-thinning behavior, it is possible to say that the viscosity of the material will be much lower than the ones measured in the viscometer, and maybe the mixing and compaction temperatures do not need to be so high to achieve such viscosities.

---

[17] DEPARTAMENTO NACIONAL DE INFRAESTRUTURA DE TRANSPORTES. (2009). **DNIT 112/2009-ES:** Pavimentos flexíveis – Concreto asfáltico com asfalto-borracha, via úmida, do tipo “Terminal Blending” – Especificação de serviço [Flexible asphalt pavements – Preparation of crumb rubber-modified asphalt concrete according to the wet process – Service specification]. Norma Técnica, Especificação de Serviço. Rio de Janeiro, RJ. In Portuguese.

[18] DEPARTAMENTO NACIONAL DE ESTRADAS DE RODAGEM. (1999). **DNER-ES 385/1999:** Pavimentação – concreto asfáltico com asfalto polímero [Paving services – asphalt concrete prepared with polymer-modified binder]. Norma Rodoviária, Especificação de Serviço. Rio de Janeiro, RJ. In Portuguese.

A discussion on the aforementioned studies and the application of two viscosity ranges of values – i. e., the conventional and the one proposed by Khatri et al. (2001)[19] – for the determination of the mixing and compaction temperatures of several modified asphalt binders were made in the paper by Domingos et al. (2012). These authors took into account 12 formulations with the same high PG grade (76-xx) and one base binder from the Replan-Petrobras refinery to calculate the appropriate temperatures for mixing and compaction operations based on the two criteria. They concluded that the simplified criterion developed by Khatri et al. (2001) – intervals of 1.4 ± 0.1 Pa.s and 0.75 ± 0.1 Pa.s for the compaction and mixing procedures, respectively – can reduce the processing temperatures by 20 to 45°C for several formulations when compared with the conventional one. It was also observed that, despite the reductions in the temperature values obtained from the conventional method (from 10 to 20°C) during the preparation of mixture samples, all of these samples achieved the target air voids of 4%. This is a clear indication that the conventional criterion has some serious limitations and that the calculation of the processing temperatures requires the input of other variables (especially shear rate) to provide more accurate results.

2.8. Comments on the Modifiers for Asphalt Binders

2.8.1. Introduction

The use of modifiers (or additives) in the asphalt industry has emerged as a practical solution for the increasing traffic levels and axle loads on the roads and highways, as well as the severe climatic conditions during the summer (distress mechanism is rutting) and winter (distress mechanism is thermal cracking) and the damaging effects of aging and load application on the service life of the pavement (distress mechanism is fatigue cracking). The improved pavement performance and the lower maintenance costs compensate for the higher production costs of modified asphalt binders. Depending on factors such as the traffic level, the importance of the road and the climatic conditions, the use of modified binders is almost a mandatory requirement in the current days. Some additives are well-known in the paving industry and their use is widespread among the countries, whereas others have a more local application or are restricted to academic publications.

[19] In the study from Khatri et al. (2001), asphalt mixtures prepared with modified binders showed higher contents of air voids than those with unmodified materials. The authors suggested that this difference can be mainly explained by the measurements of viscosity at low shear rates. Such shear rates are believed to be applied by the Superpave® compactor during the critical phase of the compaction. If only the viscosity data from the Brookfield viscometer are available to the user, the intervals of 1.4 ± 0.1 Pa.s for compaction and 0.75 ± 0.1 Pa.s for mixing are proposed as a simplified and promising approach for modified binders.

The binder additives can be classified in several ways, e. g., the mechanism by which the properties of the original material are changed, the composition and the physical nature of the additive or the property that needs to be improved. Table 3 contains some representative examples of additives that were taken from the studies by Bahia et al. (2001a), Isacsson and Lu (1995), Polacco et al. (2006), Read and Whiteoak (2003) and Yildirim (2007). Globally, at least 90% of all modifiers used in paving applications are classified as polymers: 75% are within the group of elastomeric and 15% are plastomeric. The remaining 10% include the binders modified either with crumb rubber or more than one additive (AIREY, 2003; POLACCO et al., 2015).

Table 3 – Characteristic examples of asphalt binder modifiers (BAHIA et al., 2001a; ISACSSON and LU, 1995; POLACCO et al., 2006; READ and WHITEOAK, 2003; YILDIRIM, 2007)

<table>
<tr><th>modifier</th><th colspan="2">classes and examples</th></tr>
<tr><td rowspan="3">fillers</td><td colspan="2">carbon black</td></tr>
<tr><td colspan="2">mineral (hydrated lime, fly ash and Portland cement)</td></tr>
<tr><td colspan="2">baghouse fines</td></tr>
<tr><td rowspan="2">rubber</td><td colspan="2">natural rubber</td></tr>
<tr><td colspan="2">crumb tire rubber (different sizes, treatments and processes)</td></tr>
<tr><td rowspan="10">polymers</td><td rowspan="4">thermoplastic elastomers (or elastomers)</td><td>styrene-butadiene-styrene (SBS)</td></tr>
<tr><td>styrene-ethylene-butadiene-styrene (SEBS)</td></tr>
<tr><td>styrene-isoprene-styrene (SIS)</td></tr>
<tr><td>styrene-butadiene rubber (SBR)</td></tr>
<tr><td rowspan="4">thermoplastic polymers (or plastomers)</td><td>polyethylene (PE)</td></tr>
<tr><td>ethylene vinyl acetate (EVA)</td></tr>
<tr><td>ethylene butyl acrylate (EBA)</td></tr>
<tr><td>polypropylene (PP)</td></tr>
<tr><td rowspan="2">reactive ethylene terpolymers (RET)</td><td>ethylene butyl acrylate glycidylmethacrylate (Elvaloy®)</td></tr>
<tr><td>ethylene-glycidyl methacrylate (Lotader®)</td></tr>
<tr><td rowspan="4">process-based and others</td><td colspan="2">air-blowing</td></tr>
<tr><td colspan="2">steam distillation</td></tr>
<tr><td colspan="2">polyphosphoric acid (PPA)</td></tr>
<tr><td colspan="2">natural asphalt (TLA – Trinidad Lake Asphalt)</td></tr>
</table>

Some of the early uses of modified asphalt binders in Brazil were made in the 1990's, when a pavement section of the Leopoldo Bulhões Street (city of Rio de Janeiro, extension of 300 m) was modified with SBS copolymer. Another section of this same street (extension of 300 m) was prepared with asphalt binder modified with EVA copolymer. The Ipiranga Company has been selling SBS-modified asphalt binders since 1997, whereas the commercialization of SBS- and SBR-modified binders by Petrobras started in 1998 (LEITE, 1999).

The evolution of the science of asphalt binder modification has taken place for more than 150 years. The first patents for modifying binders with polymers are dated from the 19th century and, in the middle of the past century, the European countries began to carry out test projects with modified asphalt binders and the neoprene latex was introduced in North America, especially in Canada and the western portion of the US. In the late 1970's, Europe was ahead of the US with respect to the use of modified binders due to the different points of view in each case: while the European contractors would like to decrease the life cycle costs regardless of the initial costs, the American ones were not motivated to choose the modified materials in their projects due to the higher initial cost. A more optimistic scenario was constructed among the American engineers in the 1980's because a better understanding of the economic benefits of modified asphalt binders was broadened, the European technologies were introduced and new types of asphalt modifiers were developed (KING et al., 1999; YILDIRIM, 2007).

2.8.2. Interactions between the Binder and the Modifier (s): Chemical Reactions, Consequences and Degrees of Compatibility

Since there is a huge variety of modifiers for asphalt binders and each one has its own composition or manufacturing process, it is quite natural that different reactions between them and the original binder will be observed. In a general context, the level of reaction is a function of the chemical structure of the modifier (e. g., elements and polarity of the polymer chain), the crude source and the distillation process in the refinery (both are related to the percentages of the SARA fractions). As a consequence, the original properties of the binder will be improved at different levels and some problems may occur after the modification process. These problems mainly lie in the modifier content, the processing conditions and the degree of compatibility between the base material and the modifier (s), either from the point of view of absence of compatibility between them or the formation of an insoluble asphalt-gel. The former case can be illustrated by the non-polar nature of some thermoplastic polymers, whereas the latter can be exemplified by the reactive ethylene terpolymers. These and other examples will be discussed later.

For the properties of a particular polymer-modified binder to be considerably improved after the modification process, several requirements must be met. Firstly, a *phase inversion* – i. e., the polymer-rich phase becomes the continuous phase and the asphalt-rich phase becomes the dispersed phase – must take place in the asphalt-polymer system. Secondly, the processing variables – e. g., temperature, mixing time and shear level – must allow the modifier to be adequately sheared and completely mixed with the binder without causing degradation and aging to them. This means that the modifier should be blended with the original binder at sufficient time and shear level such that neither the aging nor the degrading phenomena will be induced in the system. Lastly but not less important, the degrees of swelling and dissolution of the polymer in the formulation should achieve a balance between conservation of the original properties of the material (which will be reflected into a remarkable improvement in the ones of the binder) and storage stability (POLACCO et al., 2015; ZHU et al., 2014).

To facilitate the understanding of the different types of reactions between the additive and the binder, the forthcoming paragraphs were divided into introductory words highlighted in bold. If no words are provided in the paragraph, the subject will refer to the last introductory word cited in the text. Since the present piece of work included the three types of polymers mentioned in Table 3, polyphosphoric acid (PPA) and crumb rubber (see Chapter 4), these will be the modifiers covered by the discussion.

Thermoplastic Elastomers (or simply Elastomers): This category of polymers, also known as *thermoplastic block copolymers* or *thermoplastic rubbers* (ISACSSON and LU, 1995), has been the mostly used one for modifying asphalt binders. Thanks to their molecular structure and composition, they are able to impart strength and elasticity to the binder. These polymers are formed by joining several polymer blocks into linear series of identical monomers, thereby resulting in *linear copolymers*. Another possibility is to conduct successive polymerization of monomers into a precursor di-block structure, and then start a chemical reaction with a coupling agent. As a result of this process, *radial* (or *star-shaped*) *copolymers* can be obtained (POLACCO et al., 2006; READ and WHITEOAK, 2003).

The most well-known additive of this group is the styrene-butadiene-styrene (or SBS) copolymer, which is comprised by a tri-block and three-dimensional association of spherical polystyrene blocks within a matrix of polybutadiene (Figure 23). The polystyrene end-blocks are responsible for the strength of the polymer, whereas the polybutadienic middle blocks give an exceptional elasticity to the material (AIREY, 2003; ISACSSON and LU, 1995; READ and WHITEOAK, 2003). The disadvantages of SBS include its high cost and, similarly to all the other unsaturated rubbers, the low resistances to heat, atmospheric agents and oxidation (POLACCO et al., 2006). Phase separation may also occur if the molecular weight of the additive is at least similar to the one of the asphaltenes and there is no enough maltenes to dissolve both the asphaltenes and the polymer (AIREY, 2003; READ and WHITEOAK, 2003). This problem of phase separation may be solved by adding aromatic oils to the formulation, but the oil content must be carefully chosen in order to avoid the dissolution of the polystyrene blocks (AIREY, 2003).

Despite the presence of the same monomers – polystyrene and polybutadiene – in the chemical structure when compared with SBS, the random distribution of them in the polymer chain of the styrene-butadiene rubber (SBR) copolymer provides different physical properties to the material. SBR is commonly used as a binder modifier when dispersed in water, i. e., in the latex form. One great advantage of this modification type is the uniformity and the small size of the rubber particles, which makes it possible to thoroughly mix the additive with the binder and obtain a formulation with greater degrees of improvement in its properties (KING et al., 1999; YILDIRIM, 2007). Some disadvantages of SBR include the loss of ductility at low temperatures after short-term aging and phase separation, as observed by Zhang and Yu (2010). These authors also concluded that SBR-modified asphalt binders may become more stable if PPA or PPA+sulfur are added to the original formulation.

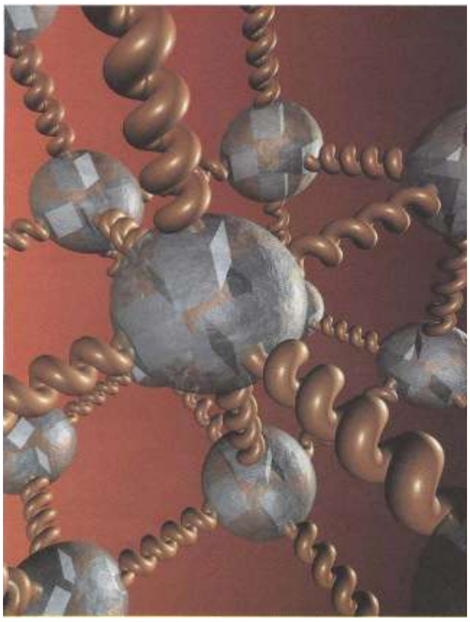

Figure 23 – Three-dimensional structure of the SBS copolymer with the polystyrenic-end blocks (spheres) and the polybutadienic-middle blocks (springs) (READ and WHITEOAK, 2003)

Thermoplastic Polymers (or Plastomers): Differently from the thermoplastic elastomers, the rigid and three-dimensional network of plastomers are able to substantially increase the rigidity of the binder, much like a hard plastic. Plastomers are also cheaper than elastomers because they are available at larger quantities and with a wider range of technical grades and characteristics. However, this marked increase in the stiffness of the binder may also lead to the formation of a material with low strain tolerance (i. e., very brittle) and too much susceptible to failure by fatigue cracking or low-temperature cracking (AIREY, 2002; BECKER et al., 2001; ISACSSON and LU, 1995; KING et al., 1999; POLACCO et al., 2006). As a prime example, the ethylene vinyl acetate (EVA) copolymer has a history of more than 20 years in binder modification in order to increase the overall resistance to deformation and improve the workability during construction (AIREY, 2003). Nowadays, EVA "is probably the second in order of importance after SBS for asphalt modification" (POLACCO et al., 2015, pp. 89).

In addition to EVA, the polyethylene (PE) and the polypropylene (PE) also belong to the group of the main representatives of plastomers. Conversely, both the polymer chains of PE and PP have a non-polar nature and usually high degrees of crystallinity, and this can be translated into an almost null compatibility with the binder. In practical terms, phase separation will be observed in the formulation within a very short period of time if it is stored at high temperatures and without a constant stirring (POLACCO et al., 2006, 2015; READ and WHITEOAK, 2003). As a consequence, the main application of PE and PP is in asphaltic roofing membranes: the blending process at high temperatures and shear levels is followed by a rapid cooling that freezes the asphalt-polymer system and makes it stable during room-temperature storage (BECKER et al., 2001; POLACCO et al., 2015).

As a practical alternative to minimize the phase separation problems and maintain the major advantages of the plastomers, polar functional groups have been attached to the original, non-polar chains. This led to the release of several copolymers for the paving industry, among which EVA deserves a close attention. This copolymer is formed by polymerization of ethylene with vinyl acetate (an ester group) as shown in Figure 24, which in turn decreases the crystallization ability of the polymer chain and increases its polarity. The higher this vinyl acetate content is, the higher the compatibility of EVA with the asphalt binder is expected to be. On the other hand, this does not mean that EVA-modified binders will never show phase separation because EVA is a semi-crystalline polymer and the degree of asphalt-modifier interaction is quite limited (POLACCO et al., 2006, 2015; READ and WHITEOAK, 2003; ZHU et al., 2014). This was also highlighted in the article prepared by Airey (2002), who observed that some base binders did not depict a polymer-rich phase (i. e., *phase inversion*) even for higher polymer contents (around 5-7% by weight).

A literature review carried out by Becker et al. (2001) lists more advantages and disadvantages of the aforementioned plastomers. These authors cite the high temperature and aging resistances among the advantages of PE, as well as the disadvantages of the need for high polymer contents to achieve good properties and the serious difficulty in mixing the modifier with the binder. PP has the advantages of improving the rutting resistance of the binder and the ease of handling, whereas the low-temperature cracking resistance and absence of improvement in elasticity are among its main disadvantages. Finally, the advantages of EVA include a good compatibility with the asphalt binder in some cases (higher vinyl acetate contents), great thermal stability at common mixing and compaction temperatures and lower costs when compared with the block copolymers. These authors also indicated that EVA may not increase the elastic recovery of the binder, which is a major disadvantage.

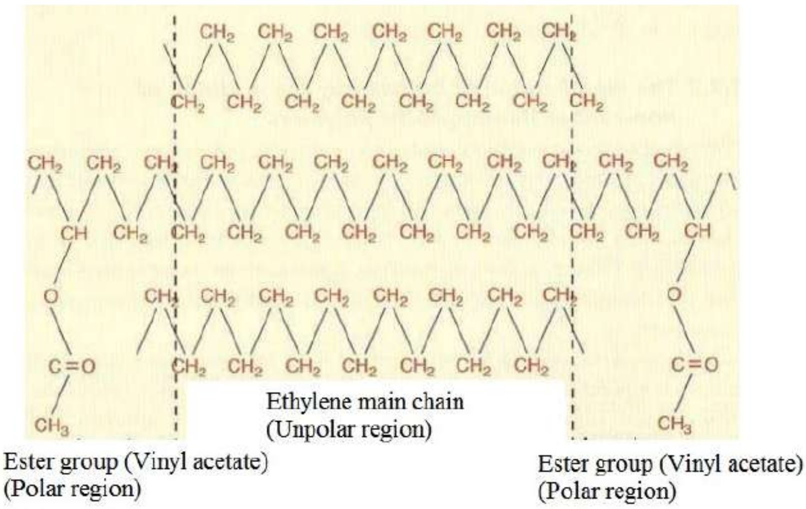

Figure 24 – Schematic of the ethylene vinyl acetate (EVA) copolymer [adapted from Read and Whiteoak (2003)]

Reactive Ethylene Terpolymers (or RETs): By taking into account the complex chemical composition of the binder, another attempt to improve the compatibility between the original material and the modifier can be made by utilizing RETs. The term "ethylene" comes from the fact that ethylene is the main component of the polymer chain. The designation "terpolymer" comes from the composition of such modifiers, i. e., three monomers: (a) ethylene; (b) glycidylmethacrylate (GMA); and (c) an ester group, usually ethyl, butyl acrylate or methyl. The improved polarity of the chain is due to the acrylic functionalization in the ester group. The oxiranic ring found in the GMA group can react with some functional groups of the binder, which justifies the use of the term "reactive" in the designation of the RETs (POLACCO et al., 2006, 2015). The major representatives of this category are Lotader® and Elvaloy® from Arkema™ and DuPont™, respectively.

Although the RETs can react with the binder and greatly minimize the phase separation problems, there are some important issues that need to be considered. The first is the high cost, whereas the second is the risk of formation of a useless asphalt-gel system. The high costs are an intrinsic characteristic of RETs, since they are artificially manufactured by the polymer industry. The second issue is somewhat related to the high number of GMA groups in a single RET macromolecule, i. e., the very high level of reactivity of the modifier. To avoid this risk, the additive content is usually limited to small upper limits (between 1.5 and 2.5% by weight). This limitation in the use of RETs reduces their effects on the properties of the binder, since the phase inversion may not be recognized at such upper limits and other modifiers may be required to achieve better properties (POLACCO et al., 2006, 2015). One classic example among these additional modifiers is PPA, as it can be seen in the publications by Domingos and Faxina (2015a), Fee et al. (2010), Kodrat et al. (2007) and Shell Oil Company (1996).

Crumb Rubber (or Recycled Tire Rubber): The use of virgin polymers in the paving industry has been taken as a quite expensive option, which led researchers to seek for cheaper modifiers. In this manner, the recycling activity has emerged as an interesting alternative not only to supply the market with new additives and at lower costs, but also to combat an environmental problem. Two of these recycled modifiers are the polyethylene terephthalate (PET)[20] and the *crumb rubber*, also known as *recycled tire rubber* (KING et al., 1999).

Crumb rubber-modified asphalt binders were first used in the US more than 40 years ago. In these first applications, several state agencies conducted limited experiments and projects with a wide variety of rubber gradations and preparation processes. Since the results of these and other experiments were promising, crumb rubber has remained as a viable option to improve binder properties. In 1991, a law related to the use of crumb-rubber modified binders on investments with federal funds passed in the US. According to this law, 5% of the roads built with federal funds after 1994 should include crumb rubber as a binder additive. Such a percentage was then increased by 20% in 1997 (FONTES et al., 2010; YILDIRIM, 2007).

There are two different possibilities for obtaining crumb rubber particles, and two more to prepare asphalt-rubber mixtures. In the first production method, rubber is grinded to the required sizes at temperatures at least equal to the room one. In the second method, rubber is first frozen to temperatures as lower as -120°C by using liquid nitrogen, and then shattered to the desired sizes with the use of an impact device. The first method yields the *ambient crumb rubber modifier*, whereas the second yields the *cryogenic crumb rubber modifier*. While the ambient rubber particles show porous surface and high surface area, the cryogenic particles have smooth and cracked surfaces and resemble shattered glass (DIVYA et al., 2013; FONTES et al., 2010). With respect to the blending procedures, the rubber particles can be mixed with the binder prior to the addition of

[20] KALANTAR, Z. N. et al. (2010). Properties of bituminous binder modified with waste polyethylene terephthalate. In: MALAYSIAN UNIVERSITIES TRANSPORTATION RESEARCH FORUM AND CONFERENCES, Selangor. **Green Transportation for Future Generation: Proceeding of the International Conference and Building Technology**. Selangor: Universiti Tenaga Nasional, 2010. pp. 333-344.

the aggregates (*wet process*) or they can be mixed with the aggregates prior to the addition of the binder (*dry process*). The modifier acts as part of the binder in the former and mainly like an inert filler in the latter (DIVYA et al., 2013; FONTES et al., 2010; KING et al., 1999).

The reaction mechanisms between the rubber particles and the binder in the *wet process* depend upon a number of factors: nature of the rubber (natural or synthetic), particle size (coarse or fine), production method (ambient or cryogenic), tire type (e. g., car tire or truck tire) and structure (radial or bias), chemical composition of the original asphalt binder (percentage of light fractions) and so on. Once the rubber modifier is mixed with the binder at temperatures greater than 160°C, the particles are believed to swell from 3-5 times their original volume and soften due to the absorption of the aromatic fractions. As a result, a gel-like structure is created in the formulation and the viscosity can increase up to 10 times the initial value (DIVYA et al., 2013; KING et al., 1999). The mixing temperature and the blending time also exercise influence on the formation of this gel-like structure. Longer blending times and higher mixing temperatures and shear levels lead to depolymerization of the modifier into the binder, as well as a reduction in the curing time to an acceptable value (BILLITER et al., 1996; DIVYA et al., 2013).

In addition to the ecological appeal, Becker et al. (2001) also pointed out that asphalt-rubber has other advantages such as potential improvement of fatigue resistance, reduction in the formation of reflective cracks and longer durability. On the other hand, the processing conditions – especially the need for higher mixing temperatures and longer blending time – are highlighted as disadvantages of the asphalt-rubber. According to the authors, the rubber particles mainly act like a filler if these processing conditions do not lead to an adequate dispersion of the modifier within the formulation and its partial devulcanization.

Polyphosphoric Acid: Initially, asphalt binder modification with PPA did not attract an assiduous attention from researchers and the industry mainly because of concerns about safety (generation of dangerous by-products), corrosion issues and the complicated modification process. The effects of acid modification on the properties of the asphalt binder are somehow comparable to those of air-blowing; however, PPA does not generate a fragile modified binder as it is expected in the air-blowing modification type (LESUEUR, 2009; POLACCO et al., 2015). The first use of PPA in the modification of the base binder dates back to 1972, and the early uses of PPA in conjunction with polymers are from 1997 (BAUMGARDNER, 2012; BENNERT and MARTIN, 2012). More recently, a national survey undertaken in the US reported that from 3.5 to 14% of the asphalt mixtures placed on pavements from 2005 to 2010 contained PPA, which represented up to 400 million tons of hot mix (FEE et al., 2010; LESUEUR, 2009).

PPA is an oligomer of H_3PO_4 (phosphoric acid) or, in other words, the association of several phosphoric acid units in a same chain. The length of the chain essentially depends on the production method, i. e., dehydration of phosphoric acid at high temperatures or heating of P_2O_5 (phosphorus pentoxide) dispersed in phosphoric acid (MASSON, 2008). PPA contains no free water and is a viscous liquid at 25°C: the viscosity can range from 0.84 to 60 Pa.s depending on the concentration. It is highly soluble in organic compounds and slowly reverts to orthophosphoric acid when diluted in water. This tendency may also be recognized when PPA is blended with asphalt, as reported by some authors in the literature (BAUMGARDNER, 2012; POLACCO et al., 2015).

In general, the addition of 1% of PPA can shift the high PG grade of the asphalt binder by one grade (LESUEUR, 2009; PAMPLONA, 2013). However, some base materials may show much higher increases in the PG classification system after modification with about 1.0% of PPA, which was the case of the asphalt binder from the Replan-Petrobras refinery (increase by two grades, from PG 64-xx to 76-xx, with 1.2% of PPA by weight, according to Domingos et al. (2012)), and the one from the Reduc-Petrobras refinery (almost two grades, from PG 64-xx to a continuous grade very close to 76°C, with 1.0% of PPA by weight, according to Pamplona (2013)). These results indicate that the effects of PPA on the high-temperature properties of the original binder are strongly dependent on its chemical composition. This can be applied to the low-temperature properties as well, since the idea that "PPA barely affects the low PG grade of the material" is not a consensus among researchers (BALDINO et al., 2012; FEE et al., 2010; YADOLLAHI and MOLLAHOSSEINI, 2011).

The interaction mechanisms between PPA and the base asphalt binder are ill-understood. In addition to the reverse to orthophosphoric acid, many authors referred to scientific theories to explain this interaction in detail. One of these theories is about a reaction between PPA and the functional groups of the binder, in which the original stacked asphaltene molecules are dispersed and the solid fraction – as well as the viscosity and the effective volume of asphaltenes – is thus increased. This dispersion takes place after a neutralization of the polar interactions among such molecules, which is probably caused by esterification or protonation of basic sites (FEE et al., 2010; LESUEUR, 2009; POLACCO et al., 2015; YADOLLAHI and MOLLAHOSSEINI, 2011). Irrespective of the mechanism, the result of this modification process is a change in the gel characteristics of the asphalt binder: sol-like binders may become more gel-like binders and vice versa upon PPA modification, depending on the aging condition (THOMAS and TURNER, 2008; ZHANG and YU, 2010). PPA can also improve the storage stability of modified asphalt binders, as shown in the papers by Polacco et al. (2015) and Zhang and Yu (2010).

It is important to emphasize that the amount of PPA should be carefully chosen, since very high contents may negatively affect the properties of the formulation and very low contents may not be enough to yield the desired PG grades (YADOLLAHI and MOLLAHOSSEINI, 2011). Also, the SARA fractions are among the key factors that will dictate the amount and degree of interaction between PPA and the base asphalt binder. For instance, Pamplona (2013) observed that a more GEL-type binder (Lubnor-Petrobras refinery) showed decreases in the parameter I_C after the addition of PPA and another binder with a colloidal structure between SOL and GEL (Reduc-Petrobras refinery) showed increases in the I_C values after such modification type. From a chemical point of view, intermolecular associations may have grouped the asphaltene molecules into stacked units in the binder from Reduc-Petrobras, and dispersion of the asphaltenes may have prevailed over other mechanisms in the one from Lubnor-Petrobras. In either case, the author recommended the determination of the average molecular weights and the glass transition temperatures to give more support to the findings.

CHAPTER 3: The Multiple Stress Creep and Recovery Test

3.1. Highlights

- The Superpave® specification was designed in order to overcome the deficiencies of the conventional tests (penetration and softening point) and provide a more performance-related rutting parameter.
- The original parameter $G^*/sin\delta$ works well for unmodified binders and shows serious limitations when used on modified ones: loading mode, viscoelastic range, elasticity and "grade-bumping" practice.
- Some of the candidate parameters to replace $G^*/sin\delta$ were the Shenoy's parameter, G_V, a hyperbolic function, η' and ZSV; however, none of them were universally accepted.
- The MSCR test was designed by FHWA and its major outcomes – R and J_{nr} – have been extensively studied worldwide; the compliance J_{nr} replaced $G^*/sin\delta$ as the official rutting parameter on Superpave®.
- This study is intended to address two of the mostly known limitations of the standardized MSCR test (creep and recovery times) and propose changes in the consideration of heavier traffic levels.

3.2. Background and Origin of the Test[21]

From the point of view of conventional tests, the susceptibility of asphalt binders to rutting has been estimated based on the results of some empirical measurements such as penetration and softening point. The European specifications, which are published by the European Committee of Standardization (ECS), mainly rely on the softening point to address rutting on binders (DREESSEN et al., 2009). However, studies indicated that the high degrees of empiricism and the very simple protocols reduce the reliability of the measurements, in such a way that the industries cannot use them. Also, these measurements cannot properly characterize the viscoelastic nature of asphalt binders because they underestimate the level of complexity of the rheological properties of the materials (BAHIA and ANDERSON, 1995).

[21] For a summary of this section of the chapter, the reader is referred to the literature review paper published by Domingos and Faxina (2016).

Studies were carried out in order to test the validity of the conventional rheological properties of the binder in the characterization of the resistance of asphalt mixtures to rutting. Sybilski (1996a) determined the penetration and the ring-and-ball softening points ($T_{R\&B}$ values) of unmodified binders and formulations prepared with several contents of a polyolefin plastomer and styrene-butadiene-styrene (SBS) copolymer. The author correlated such results with the number of load applications to generate a 10-mm rutting level in asphalt mixtures (N_{10}). The tire had a contact pressure of 600 kPa and applied a load of 0.5 kN on the mixture samples. A weak correlation between $T_{R\&B}$ and N_{10} was obtained ($R^2 \approx 0.56$), which indicated that the softening point cannot be taken as a reliable parameter to estimate the rutting resistance of the mixture. The validity of $T_{R\&B}$ and penetration tests was found to be restricted to formulations with relatively low polymer contents.

In the paper published by Dreessen et al. (2009), the results of the penetration tests at 25°C (P_{25}) and the softening point tests of several unmodified and modified binders were correlated with the rutting measurements observed on test sections. These measurements were made at the temperature of 60°C and at the frequency of 1.0 Hz after many loading cycles (from 100 to 30,000 cycles). The tire applied a load of 5.0 kN on the mixture samples. The asphalt binders selected in the study were graded as 20/30, 35/50 and 70/100 in the penetration tests, and some of them were modified with SBS and EVA copolymers. The correlations between the mixture and binder data were better for the softening point values than for the penetration ones; however, none of them proved to be satisfactory in the estimation of the resistance of the mixture to rutting. These authors also observed that asphalt binders with similar P_{25} and $T_{R\&B}$ values may have very different J_{nr} values, which is a clear indication that the conventional binder properties are too limited in characterizing the rheological behavior of asphalt binders.

Based on the severe restrictions imposed by the empirical binder properties, e. g., the use of only one temperature in the tests and their limited applicability to modified binders (ROBERTS et al., 1996), researchers have sought for other tests and performance-related properties that could adequately capture the contribution of the binder to the resistance of the mixture to failure. From 1987 to 1994, the US Congress invested $ 150 million on a research program – the SHRP program – that was intended to identify the rheological properties of the binder that could predict pavement performance, as well as to suggest devices that could reliably determine such properties (ROBERTS et al., 1996).

One of the most important outcomes of the SHRP program was the development of a new binder specification and the suggestion of new devices for measuring the rheological properties of asphalt binders. This specification is known as Superpave®, and it has markedly contributed to the scientific knowledge of rheology of binders and the proposal of parameters that correlate these properties with pavement performance. Devices such as DSR, DTT, BBR, Brookfield rotational viscometer, RTFO and PAV were introduced in order to obtain the performance-related properties of the material at low (BBR and DTT), intermediate (DSR) and high (DSR) pavement temperatures, to quantify its degree of workability during mixing and compaction (Brookfield viscometer) and to simulate the short-term and long-term aging processes (RTFO and PAV) (ROBERTS et al., 1996).

In the original Superpave® binder specification (ASTM D6373 and AASHTO M320[22] standards), the resistance of the asphalt binder to rutting is quantified by means of a ratio of the magnitude of the complex modulus (or simply "complex modulus") G^* to the sine of the phase angle δ ($G^*/sin\delta$) under oscillatory shear loading. The numerical value of this parameter is equal to the inverse of the loss compliance J''; however, $G^*/sin\delta$ was preferred over J'' to avoid the insertion of one more parameter in the specification. According to Aroon Shenoy (discussion in DONGRÉ et al., 2004), G^* was multiplied by $1/sin\delta$ to enhance the effects of elasticity in the asphalt binder. The technical background outlined by Bahia and Anderson (1995) and Roberts et al. (1996) indicates that an increase in $G^*/sin\delta$ results in a lower amount of dissipated energy at each loading cycle, which is responsible for the appearance of rutting in the pavement. This can be obtained either by increasing the stiffness of the binder (higher G^* value) or by increasing its relative elasticity (lower δ value).

Other details in the original Superpave® specification must be pointed out with respect to the binder rutting test. It is conducted at the frequency of 10 rad/s ($\omega \approx 1.59$ Hz), which is believed to simulate the average frequency of a stress wave in the pavement surface layer as caused by a vehicle at 50-60 mph or 80.5-96.6 km/h (BAHIA and ANDERSON, 1995). These tests are performed at the high PG grade of the asphalt binder and, to limit the amount of permanent strain in the pavement and determine this high PG grade, the parameter $G^*/sin\delta$ must be no greater than 1.0 kPa in the unaged condition and no greater than 2.2 kPa in the short-term aged one.

The choice for the limiting values of 1.0 kPa and 2.2 kPa was made based on a common consensus among the researchers of the Expert Task Group of the US Federal Highway Administration (ETG-FHWA). This task group included members from the industry, the specifying agencies and academia. The limiting criterion of 1.0 kPa was established as a reference value for

[22] The most recent versions of the AASHTO M320 specification provide two criteria for determining the high PG grade of the asphalt binder. The original criterion – minimum $G^*/sin\delta$ values of 1.0 and 2.2 kPa for the unaged and short-term aged binders, respectively – can be found in Tables 1 and 2. Table 3 contains the new binder rutting criteria based on the MSCR test and the parameter J_{nr}.

AC-10 viscosity-graded asphalt binders tested in the DSR at the frequency of 10 rad/s and the temperature of 60°C. The test temperature is referenced on a moderate climatic condition in which the AC-10 binder would be more commonly used. In addition, the results collected by ETG-FHWA indicated that the viscosity aging indexes varied from 2.0 to 2.5 for the tested binders. Therefore, the mean value of the interval (2.2) was adopted as the minimum required value for the parameter $G^*/sin\delta$ after short term aging of binders (ROBERTS et al., 1996).

Although the Superpave® specification has markedly contributed to a better understanding of the rheological behavior of asphalt binders at a wide range of temperatures and frequencies of loading, some concerns regarding its applicability to modified materials have been shown by many researchers worldwide. This is because the Superpave® test protocols and technical requirements were primarily based on the results of unmodified asphalts (ANDERSON et al., 2010; BAHIA et al., 1997). As a consequence, many issues relating to the modified asphalts – e. g., shear rate dependency of viscosity, the target viscosities of 0.17 and 0.28 Pa.s for mixing and compaction (respectively), stability of the system, strain dependency and time-temperature equivalency – were not fully explored in the specification and may lead to underestimation or overestimation of the actual performance of the materials (BAHIA et al., 1997). These limitations were also highlighted by D'Angelo and Fee (2000), according to whom the test results were not able to capture all the contribution of the modified binders to the increase in pavement performance because Superpave® is not truly blind to modification type.

As a consequence of the above-mentioned deficiencies, the determination of the mixing and compaction viscosities according to the ASTM D2493 standard[23] has also become a matter of concern among researchers. The original procedure and the adequate viscosity values for mixing (0.17 ± 0.02 Pa.s) and compaction (0.28 ± 0.03 Pa.s) may result in very high temperatures for some modified asphalt binders, in such a way that the binder can be damaged and the operators face a safety risk. Modifications in the shear rate and/or the ranges of viscosity values were proposed in many reports (BAHIA et al., 2001b; KHATRI et al., 2001; YILDIRIM et al., 2000, 2006) as an option to take into account the non-Newtonian behavior of the modified binders, some of which were studied in the paper published by Domingos et al. (2012). The authors observed that a change in the criterion for calculating the processing temperatures – from the conventional method to the simplified one proposed by Khatri et al. (2001) – can decrease the mixing and compaction temperatures of several modified binders by 20-45°C without affecting the Superpave® mixture design procedures, and it included EVA-, PE-, Elvaloy- and SBR-

[23] AMERICAN SOCIETY FOR TESTING AND MATERIALS. **ASTM D2493**: Standard viscosity-temperature chart for asphalts. West Conshohocken, PA.

modified materials. This enhances the efficiency of the new methods in safeguarding the characteristics of modified binders and obtaining more reasonable temperature values.

Since the use of modified binders for paving applications has been gradually increasing in several countries and these modifiers prevent the pavement from an early failure by rutting, fatigue cracking or low-temperature cracking (AIREY, 2002; BECKER et al., 2001; ISACSSON and LU, 1995), the seek for new parameters and further refinements in the Superpave specification has become a crucial component of many later studies. With respect to the parameter *G*/sinδ*, the multiplication of *G** by the term *1/sinδ* is too oversimplified to fully capture the effects of elasticity on modified binders, even though its applicability to unmodified materials was found to be adequate (BOULDIN et al., 2001; SHERWOOD et al., 1998). Due to this limitation, various researchers have highlighted the disadvantages of the parameter *G*/sinδ* in predicting rutting performance and debated on its problems and possible solutions (ANDERSON et al., 2010; BAHIA et al., 2001a, 2001b; BOULDIN et al., 2001; CHEN and TSAI, 1999; D'ANGELO, 2008, 2009, 2010b; D'ANGELO et al., 2007; DELGADILLO et al., 2006a, 2006b; DONGRÉ and D'ANGELO, 2003; DONGRÉ et al., 2004; DREESSEN et al., 2009; HICKS et al., 1993; SHENOY, 2001, 2004a, 2004b; STUART and MOGAWER, 1997). On the other hand, some researchers claimed that *G*/sinδ* still has some merits as a rutting parameter (GIBSON et al., 2012). More specifically, the following subjects were covered with respect to the parameter *G*/sinδ* and the test procedure:

- the correlations between the *G*/sinδ* values and the rutting measurements on asphalt mixtures (BAHIA et al. 2001a, 2001b; CHEN and TSAI, 1999; D'ANGELO, 2008, 2009; D'ANGELO et al., 2007; DREESSEN et al., 2009; HICKS et al., 1993; STUART and MOGAWER, 1997); and
- the mode of loading (oscillatory shear), the effects of damage (no damage is caused in the sample after only a few loading-unloading cycles) and the low strain levels used in the oscillatory shear tests, as cited in the studies by Anderson et al. (2010), Bahia et al. (2001a, 2001b), D'Angelo (2010b) and Delgadillo et al. (2006a, 2006b).

In addition to the limitations of the parameter *G*/sinδ*, other problems of the original Superpave® specification were also encountered and debated in the literature (BAHIA et al. 1997, 2001b), as previously discussed. Such problems have grown in importance insofar as modified asphalt binders with similar high PG grades can produce mixtures with very different rutting performances at typical pavement temperatures. This was observed for several PG 76-22 binders selected by Jones et al. (1998) and mixtures prepared with such binders and tested at the temperatures of 52 and 58°C, which is a clear indication that the premise of the Superpave®

specification – i. e., asphalt binders with the same high PG grade will perform similarly with respect to rutting – is not valid for all binders. In other words, refinements in the specification criteria were urgently required and led researchers to find alternatives for them.

Another severe criticism over the original Superpave® specification was on the practice for considering heavy traffic levels and/or low vehicle speeds on roads and highways. This practice is known as "grade-bumping" in the literature, and it basically consists of shifting the high PG grade of the asphalt binder to one grade – or even two grades – higher than the original value to account for these traffic/loading conditions. For example, asphalt binders graded as 70-xx or 76-xx may be used on pavements with a 7-day maximum expected pavement temperature of 64°C. The basic assumption was that the temperature susceptibility of all binders (including the modified ones) is very similar, and therefore a shift of 6°C in the high PG grade of the material would be equal to the double of its original stiffness (D'ANGELO, 2010; discussion in D'ANGELO et al., 2007). However, this assumption was proved to be incorrect because modified materials can show considerably different susceptibilities to loading time and temperature, even if their high PG grade are the same (BAHIA et al., 2001a; D'ANGELO, 2010; D'ANGELO et al., 2007; DELGADILLO et al., 2006b).

As a consequence of the deficiencies of the parameter $G^*/sin\delta$ and the original Superpave® binder specification, many researchers and highway agencies looked for alternatives and additional tests to be incorporated into this specification. Some of the state highway agencies in the US adopted modified versions of Superpave® – also known as "PG+" (PG Plus) or "SHRP+" (SHRP Plus) – in an attempt to ensure that modifiers were really added to the asphalt binder (ANDERSON et al., 2010; D'ANGELO et al., 2007; DELGADILLO et al., 2006b). Specific requirements for the phase angle or the direct tension test and empirical tests such as ductility and elastic recovery are among the differences that exist between the "PG Plus" and the Superpave® specifications (DELGADILLO et al., 2006b). Such amendments were introduced into Superpave® as a guarantee against the industries that had been selling asphalt binders with similar high PG grades and costs, but different elastic properties. The problem is that these additional tests are not specifically related to performance; rather, they can only indicate the presence or absence of a modifier in the asphalt binder (D'ANGELO et al. 2007).

One of the possible alternatives to the parameter $G^*/sin\delta$ was suggested by Aroon Shenoy in the beginning of the 2000's (SHENOY, 2001, 2004a, 2004b). Although the repeated creep and recovery test (RCRT) had been announced at approximately the same time as a viable option to estimate the susceptibility of the binder to rutting (BAHIA et al., 2001a, 2001b), Shenoy claimed that his parameter did not demand a stress-controlled DSR to be determined and could prevent some agencies from buying new devices, which would be the case of the RCRT (SHENOY, 2004b). The Shenoy's parameter is shown in Equation (20) and comes from theoretical derivations based on fundamental concepts. The higher its numerical value, the lower the amount of permanent strain in the binder. To determine the equation of this parameter, Shenoy calculated the total strain in the binder and subtracted the elastic and the delayed elastic portions from it, thereby remaining the viscous portion.

$$\frac{|G^*|}{1 - \frac{1}{tan\delta \times sin\delta}} \tag{20}$$

As stated by Shenoy (2001), the high PG grade of the asphalt binder is the one at which the parameter from Equation (20) shows the minimum values of 1.0 and 2.2 kPa for the unaged and short-term aged conditions, respectively. These limiting values were not changed in order to assure that not only modified asphalts would be correctly graded according to the new parameter, but also the unmodified ones. Even though the Shenoy's parameter maximizes the effects of elasticity (δ) when compared to the original $G^*/sin\delta$, it is not possible to say that the new parameter addressed all the issues concerning the susceptibility of asphalt binders to rutting. This is because the parameter has a singularity at $\delta = 52°$, i. e., negative values are obtained when $\delta < 52°$ and positive values are obtained for δ values higher than 52°. For mathematical purposes, Shenoy (2001, 2004a) proposes the use of the term $(sin\delta)^9$ as a close approximation to the term $[1\text{-}(1/tan\delta sin\delta)]$ when $\delta <$ 52°, and the results are similar for both terms at $\delta = 55°$. However, this artificial solution is not recommended to be used in a binder specification because it does not contain any fundamental basis (SHENOY, 2004a). In summary, the following parameters should be used in the Superpave® specification to address the issues about the rutting resistance of asphalt binders (discussion in DONGRÉ et al., 2004; SHENOY, 2004a):

- the Shenoy's parameter – Equation (20) – for δ values higher than 55°; and
- the original Superpave® rutting parameter $G^*/sin\delta$ for δ values lower than 55°.

Some years after the publication of his parameter as an alternative to the rutting parameter $G^*/sin\delta$, Aroon Shenoy made a refinement of the original criterion for determining the high PG grade of the asphalt binders (discussion in DONGRÉ et al., 2004; SHENOY, 2004b). This original criterion establishes that the unaged and RTFO-aged binders have minimum values of 1.0 and 2.2 kPa (respectively) for the Shenoy's parameter – Equation (20) – and at their high

PG grades. This was done because an odd case occurred among the I-80 binders[24] that were graded according to such criterion. As stated in the refined criteria, the maximum PG grade temperature of the binder (T_{HS}) is the one at which the Shenoy's parameter is equal to 50 Pa at ω = 0.25 rad/s. Another suggestion is to determine the T_{HS} value based on the temperature of equivalent stiffness when G^* = 50 Pa and ω = 0.25 rad/s (T_e) and the corresponding phase angle at T_e (δ_e), as shown in Equation (21)[25]. The former is known as "Criterion No. 1", and the latter is known as "Criterion No. 2". Shenoy (2004b) emphasized that the "Criterion No. 2" provided a good correlation between the performance grade temperatures of two of the binders from the I-80 project (one unmodified and one modified) and their performances in the field, even though the criterion must be validated for other binders and formulations.

$$T_{HS} = \frac{T_e}{1 - \frac{1}{tan\delta_e \times sin\delta_e}} \tag{21}$$

In broader studies with many types of modified asphalt binders, Bahia et al. (2001a, 2001b) formulated two hypotheses for choosing a test procedure and a specification parameter that would be closer to the performance of the pavement. First, the strain levels experienced by the binder in the pavement are much higher than the ones used in the Superpave® oscillatory shear tests. Second, the application of sinusoidal loads with reversals in the stress or strain does not seem to be the best procedure for estimating the rutting resistance of the binder, since rutting is caused by irreversible cyclic loading. The discussions on both hypotheses led to the conclusion that either the oscillatory shear protocol or the parameter $G^*/sin\delta$ do not provide researchers and highway agencies with good indications as to what is the actual rutting resistance of asphalt binders. Thus, Bahia et al. (2001a, 2001b) sought for new parameters and test procedures that had not yet been published in the literature and evaluated their applicability to asphalt binders and the Superpave® specification.

Researchers have debated on the loading type used in the oscillatory shear tests, and the subjects of these debates involved the concept of dissipated energy and its delayed elastic (W_D) and viscous

---

[24] **I-80 Project:** This project was carried out in the I-80 highway (State of Nevada). In September 1998, the Nevada Department of Transportation (NDOT) built four test sections at I-80 with the purpose of evaluating the applicability of the Superpave® mix design method to the local climate and traffic conditions. Two of the test sections were built according to the Hveem method from NDOT, whereas the other two followed the Superpave® method (HAND et al., 2004).

[25] More simply, Aroon Shenoy proposed the determination of the high PG grade of the asphalt binder based on the temperature at which G^* = 50 Pa for a frequency of 0.25 rad/s (T_e value) and the corresponding phase angle δ (δ_e value). This high PG grade – i. e., T_{HS} value – and the corresponding test protocol would therefore replace the current procedure for calculating the high PG grade temperature.

components (W_P). According to Bahia et al. (2001a) and Delgadillo et al. (2006b), the reversal in the stress/strain during the oscillatory shear test makes it difficult to easily distinguish among the W_D and the W_P values. This is because both can be found in the total dissipated energy per cycle W_C, as shown in Equation (22). The W_C value is taken into account in the calculation of the parameter $G^*/sin\delta$, see Equation (23) (BAHIA and ANDERSON, 1995; ROBERTS et al., 1996). However, W_P is the only portion of W_C that really contributes to the appearance of rutting in the pavement, and W_D may be very high for some modified asphalt binders. This explains why the parameter $G^*/sin\delta$ is not able to accurately predict the rutting performance of modified asphalt binders. The presence of very low levels of delayed elasticity in the unmodified materials indicates that W_C is approximately equal to W_P, and this accounts for the fact that $G^*/sin\delta$ works relatively well for such materials (DELGADILLO et al., 2006b).

$$W_C = W_D + W_P \tag{22}$$

$$W_C = \pi \times \tau_c^2 \times \frac{1}{G^*/_{sin\delta}} \tag{23}$$

The issues concerning the dissipated energy per loading cycle were also considered in the paper published by Chen and Tsai (1999). The authors believe that the interpretation of rutting as a stress-controlled phenomenon and the loading frequency of 10 rad/s in the DSR may not be associated with the actual loading conditions in the pavement. Based on fundamental concepts, they made a theoretical derivation to calculate the W_C value from the loss modulus G'' and the initial strain observed in the binder ε_i – see Equation (24). The permanent strain values in asphalt mixtures were correlated with the W_C values of the asphalt binders at $\omega = 5$ rad/s and 0.6 rad/s, and the results were better than the ones obtained for the parameter $G^*/sin\delta$ at these same frequencies. In conclusion, the authors suggested the use of W_C as a new binder rutting parameter and lower frequencies of loading in the DSR tests to get closer to the rutting performance of the mixture.

$$W_C = \pi \times G'' \times \varepsilon_i^2 \tag{24}$$

By recognizing the limitations of the oscillatory shear test and the loading type that better simulates the passage of vehicles in a real pavement, a repeated creep test (RCRT) was proposed by some researchers (BAHIA et al., 2001a, 2001b) together with an initial protocol (BAHIA et al., 2001a). Based on this protocol, a creep stress between 30 and 300 Pa is applied on the binder sample during 1 s and the material is allowed to rest for 9 s. The cycle is repeated 100 times such that the binder can reach the steady state condition. The viscous component of the creep stiffness G_V – i. e., the inverse of the viscous compliance J_V – was taken by Bahia et al. (2001a, 2001b) as an indicator of the resistance of asphalt binders to rutting. According to these authors, G_V was preferred over J_V in order to be compatible with the concept of stiffness and keep the unit of stress unchanged. A typical plot of the strain response of the binder in the RCRT can be seen in Figure 25.

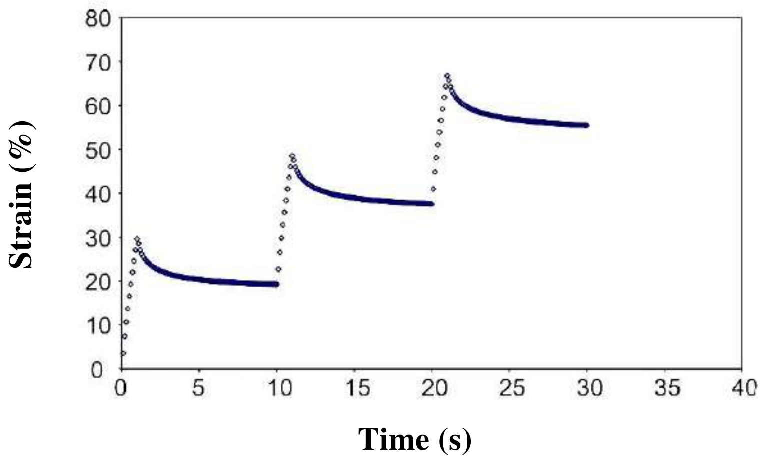

Figure 25 – Typical creep-recovery response of an asphalt binder in the repeated creep and recovery test (RCRT) at 100 Pa [adapted from Anderson (2007)]

The RCRT is based on a test procedure for evaluating the susceptibility of asphalt mixtures to rutting. This mixture test is known as "Repeated Simple Shear Test at Constant Height" (RSST-CH) and was proposed by researchers from the University of California (Berkeley, CA) during the SHRP program. The RSST-CH protocol basically consists of applying subsequent creep-recovery cycles with 0.1-s loading and 0.6-s unloading in a mixture sample, thereby resulting in a 0.7-s creep-recovery cycle (ANDERSON et al., 2010; PEREIRA et al., 2000). The magnitude of the load is equal to 68 kPa and the test is finished when 5,000 loading-unloading cycles are applied, or when a 5% strain is achieved. The permanent strain in the sample is plotted against the number of cycles (JONES et al., 1998).

According to Bahia et al. (2001b), the use of the RCRT in studies about the rutting potential of asphalt binders can deal with two crucial problems of the Superpave® parameter $G^*/sin\delta$: (a) this parameter is derived from linear viscoelastic responses measured after only a few loading cycles, and therefore it does not take into account the effects of damage on the performance of the material; and (b) the equation is obtained from reversible cyclic loads, which are not able to properly characterize the accumulation of permanent strain in the binder under creep-recovery loading and impede direct measurements of this accumulated strain during the test. The RCRT was selected by Bahia et al. (2001a, 2001b) and Delgadillo et al. (2006a) in studies with modified asphalt binders and, in a general context, good correlations with permanent strains in asphalt mixtures were found.

In another study, Bouldin et al. (2001) used laboratory data from asphalt binders tested according to the RCRT protocol as a reference for the development of a semi-empiric model. This model was intended to replace the original parameter $G^*/sin\delta$ and, in the authors' opinion, it is a better option to take into account the impact of δ on the permanent strain in the binder (γ_{per}). By considering appropriate shear rates and temperatures, it was assumed that the rate of accumulation of irrecoverable strain depends upon the stiffness of the asphalt binder and the viscoelastic contribution $f(\delta)$, and also that both factors are independent of each other. The hyperbolic function obtained in the paper – Equation (25) – includes five empirical regression parameters (a, b, c, X_0 and Y_0) and one constant (k); however, its applicability to other binder data was called into question by scientists such as Shenoy (2001). This researcher claimed that the empirical parameters would probably not be the same if a different set of data were used in the experiments or if more binder data were considered in the analysis, which constitutes a serious limitation of the proposed parameter.

$$\left(\gamma_{per}\right)^{-1} = k \times G^* \times \left\{ Y_0 + a \times \left[1 - \frac{1}{e^{\left[\left|\left(\delta - X_0 + b \times ln(2)^{\frac{1}{c}}\right)\right|\right]^c}} \right] \right\} \tag{25}$$

In addition to these suggestions, Dongré et al. (2004) proposed the use of the storage viscosity (η') – also known as "Low Shear Viscosity" – as an alternative to the parameter $G^*/sin\delta$ in the characterization of the resistance of asphalt binders to rutting. By definition, η' is the ratio of the loss modulus G'' to the angular frequency ω, or $\eta' = G''/\omega$. The authors made an attempt to see whether the η' values at $\omega = 0.01$ rad/s would correlate well with mixture data or not. It was found out that these correlations are reasonable and that η' could be taken as a promising candidate to replace $G^*/sin\delta$. Further studies carried out by Morea et al. (2011, 2014) have drawn quite similar conclusions for η' values at approximately the same frequency and mixture data from accelerated loading facilities, and empirical equations were also developed by Morea et al. (2014) to estimate the rutting level in the wheel tracking device based on η', the magnitude of the load and the test temperature. According to Dongré et al. (2004), the high PG grade temperature of the binder based on η' would be the one at which the parameter is equal to 220 Pa.s – ratio of the limiting value of $G^*/sin\delta$ for short-term aged binders (2,200 Pa) to the angular frequency of 10 rad/s.

Although the study from Dongré et al. (2004) published reasonable results, the idea of replacing *G*/sinδ* by *η'* was heavily criticized by Aroon Shenoy (discussion in DONGRÉ et al., 2004). Shenoy put the concepts used by Dongré et al. (2004) into question and asked as to why the authors were moving to an opposite direction (when compared to the SHRP researchers) when proposing *η'* as a new binder rutting parameter in the Superpave® specification. One of the key problems posed by Shenoy in the discussion was that polymer-modified asphalt binders are much more elastic than unmodified ones, and therefore a specification parameter (*G*/sinδ* or a future one) must be able to highlight this difference. Shenoy also believed that the shear rates and loading frequencies used by Dongré et al. (2004) were very low and would not match the actual loading conditions observed in real pavements.

To counter the arguments that were put forward by Shenoy, Dongré et al. (2004) asserted that *η'* was chosen among many other parameters – including Shenoy's parameter – because it could reasonably identify the presence of polymers in the formulation and measure their impact on the rheological response of the binder without changing instrumentation and/or software. According to the authors, there was not too much information about the capability of *G*/senδ* in accurately estimating the susceptibility of polymer-modified asphalt binders or other materials with $\delta < 80°$ to rutting when the SHRP program was concluded. Dongré et al. (2004) also emphasized that lower *δ* values is not the only key issue that must be taken into account while developing a new binder specification, since this could lead to a specification that overestimates the actual performance and focuses on the production of very elastic (but weak) materials.

Another property that was studied in the literature and suggested by some authors as a prospective candidate to replace the parameter *G*/sinδ* is the zero-shear viscosity, or simply ZSV (ANDERSON et al., 2002; DESMAZES et al., 2000; DONGRÉ and D'ANGELO, 2003; ROWE et al., 2002; SYBILSKI, 1996b). ZSV is defined as the viscosity at a constant strain rate when the stress approaches zero. Either *η'* or ZSV are rheological properties with high sensitivity to the molecular weight of the modifiers added to the binder, such that formulations prepared with modifiers with higher molecular weights will depict higher ZSV values (D'ANGELO et al., 2007). However, the use of ZSV as a specification criterion shows some major limitations:

- this high sensitivity to the molecular weight may overestimate the performance of some polymer-modified asphalt binders (DONGRÉ et al., 2004);
- an exact measurement of the ZSV value requires sophisticated computer software and complex procedures (DONGRÉ et al., 2004), even though measurements like this became much easier to be done in newer rheometers;
- the laboratory test for determining ZSV is time-consuming (SHENOY, 2004b); and

- highly-modified asphalt binders behave as solids and never reach a steady state rate, which makes it difficult to obtain a numerical value for ZSV (D'ANGELO et al., 2007).

Many of the aforementioned parameters and rheological properties were selected by Dongré and D'Angelo (2003) in a detailed study to see which one would show the highest correlations with rutting measurements on mixtures tested in the Accelerated Loading Facility (ALF) from FHWA. The following parameters were considered in the paper: (a) the parameter from Shenoy (2001, 2004a, 2004b); (b) the G_V value as suggested by Bahia et al. (2001a, 2001b); (c) ZSV as obtained from the fitting of the Carreau model to the creep-recovery binder data; (d) ZSV as obtained from master curves and computational software; and (e) ZSV as calculated from a frequency sweep test in the DSR. It was observed that the two highest correlations between binder and mixture rutting data were obtained for the ZSV values derived from the master curves and the Carreau model. However, both procedures are time-consuming and could not be accepted in a binder specification such as Superpave®. In conclusion, the authors suggested that ZSV as derived from a frequency sweep test may be taken as a possible replacement to the original parameter ($G^*/sin\delta$) because the parameters can be obtained from a simple oscillatory shear test, they reasonably correlate with mixture data and the test durations are quite short.

More recently, there have been several discussions in the literature about the development of a test procedure and/or a parameter to replace the existing Superpave® parameter and oscillatory shear test. These forums have raised some key issues that should be considered by researchers before proposing refinements in the Superpave® specification. First, the new rheological property/parameter must correlate well with mixture rutting data in the laboratory and the real pavement and show higher R^2 values than $G^*/sin\delta$. Second, the test protocol must be able to adequately characterize unmodified and modified binders and clearly show their differences at high pavement temperatures (D'ANGELO et al., 2007). Third, the highway agencies should not be forced to buy new instrumentation and software to carry out the proposed laboratory test and calculate the resulting parameters. Lastly (but not less important), this proposed test cannot be time-consuming and extremely complex because of its use in the Superpave® specification (D'ANGELO et al., 2007; DONGRÉ et al., 2004).

Based on the creep and recovery concepts introduced by Bahia et al. (2001a, 2001b) in the binder tests and the publication of a test protocol in the NCHRP Report 459 (BAHIA et al. 2001a), the US Federal Highway Administration conducted several internal studies and made some modifications in the original protocol to improve the RCRT procedure and develop an easy-to-use, performance-related test. The choice for the RCRT was due to its ability to reasonably simulate the actual loading condition in a real pavement, i. e., repetitive load pulses (creep) followed by resting periods (recovery) in between. The addition of increasing stress levels in a same test and the application of 10 creep-recovery cycles at each stress level can be listed as some of the modifications carried out by FHWA. Then, FHWA renamed the RCRT as “Multiple Stress Creep and Recovery” (MSCR) test, also known as “massacre” in the US (GIERHART, 2013). It may be important to note that the use of different stress levels in the RCRT was not restricted to the studies from FHWA, e. g., Delgadillo et al. (2006a) took into account six increasing values from 25 to 10,000 Pa in their laboratory tests.

Nowadays, the MSCR test can be interpreted as a major innovation in the characterization of asphalt binders with respect to their resistance to rutting. Together with the advent of the parameters R (percent recovery), J_{nr} (nonrecoverable creep compliance) and $J_{nr,\ diff}$ (percent difference in nonrecoverable compliances), some marked changes in the Superpave® specification occurred and MSCR was adopted as the high-temperature specification criterion of performance-graded binders in 2009 (D’ANGELO, 2010b; WHITE, 2016). These changes aimed at overcoming deficiencies of the specification in grading modified binders from the most to the less resistant to rutting according to their rheological parameters (see Chapter 2), as well as to adequately identify and measure the elastic response of the materials. Consequently, J_{nr} replaced $G^*/sin\delta$ as the Superpave® binder rutting parameter in the revised versions of Superpave® and new criteria for grading asphalt binders according to their acceptable traffic level were added to the specification. More details about the outcomes of the MSCR test are provided in the next section.

3.3. Description of the MSCR Test and Main Outcomes

The original protocol of the MSCR test includes the application of 11 increasing stress levels (0.025, 0.05, 0.1, 0.2, 0.4, 0.8, 1.6, 3.2, 6.4, 12.8 and 25.6 kPa) and the sample is loaded with 10 creep-recovery cycles at each of these levels. The primary reasons for choosing increasing stress levels in one binder sample are to save material and test time. The MSCR test is started at the lowest stress level and, as soon as the 10 loading-unloading cycles are applied, the stress is doubled and there are no time lags between one load magnitude and the other (D’ANGELO, 2010a; D’ANGELO et al., 2007). The creep and recovery times remained respectively as 1 and 9 s, and this was done in order to avoid the standardization of a time-consuming test. However, it is known that some modified binders do not show full recovery before 9 s of recovery in the DSR. Even with these limitations, the MSCR test criteria satisfy the expectations of one who wants a more accurate characterization of the susceptibility of asphalt binders to rutting (John D'Angelo, from the discussion in D'ANGELO et al., 2007).

Although the original MSCR protocol recommended the use of 11 different stress levels, the standardization of the test by AASHTO (TP70 and T350) and ASTM (D7405) took into account only two of the original values: 0.1 and 3.2 kPa. The developers of the MSCR test intended its use for J_{nr} values between 0.1 and 5.0 kPa^{-1} at both stress levels, which means that results falling outside of this interval may not yield meaningful analyses on the stress sensitivity of the binders (WHITE, 2016). Appendix C provides a brief historical overview of these standards. From all the strain data collected by the DSR, the following ones are selected to calculate R and J_{nr}: (a) the strain in the beginning of the creep-recovery cycle ε_0; (b) the strain in the end of the creep portion of the cycle ε_c; and (c) the strain in the end of the recovery portion of the cycle ε_r. The locations of such strains in the MSCR data are illustrated in Figure 26. The R value is given by the ratio of the strain labeled as recoverable (ε_{rec}) to the total strain observed in a creep-recovery cycle (ε_{tot}), as shown in Equation (26). The J_{nr} value is calculated as the ratio of the strain labeled as irrecoverable (ε_{nr}) to the applied stress (τ_t), as shown in Equation (27).

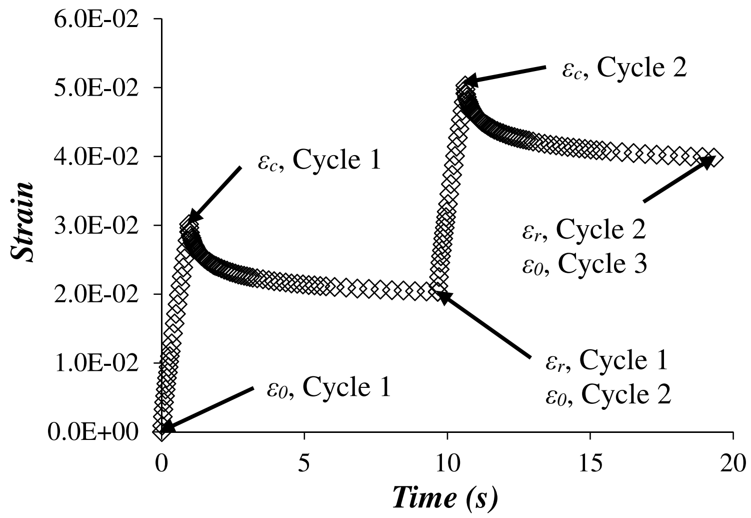

Figure 26 – Identification of the strains ε_0, ε_c and ε_r in two of the 10 creep-recovery cycles of a standardized MSCR test

$$R(\%) = \frac{\varepsilon_{rec} \times 100}{\varepsilon_{tot}} = \frac{[(\varepsilon_c - \varepsilon_0) - (\varepsilon_r - \varepsilon_0)]}{\varepsilon_c - \varepsilon_0} \times 100 \tag{26}$$

$$J_{nr}[Pa^{-1}, kPa^{-1}] = \frac{\varepsilon_{nr}}{\tau_t} = \frac{\varepsilon_r - \varepsilon_0}{\tau_t} \tag{27}$$

Since the MSCR test was mainly based on the RCRT to be developed, many of the technical details of the RCRT protocol remained the same in the new test. These ones included the creep and recovery times (1 and 9 s, respectively) and the application of a stress level between 30 and 300 Pa in the binder sample (in this case, 100 Pa). With respect to the highest stress level, there was a concern among researchers about the magnitude of the stress that should be considered in order to draw direct comparisons between the previous and the new rutting criteria. This concern was caused by the fact that the parameter $G^*/sin\delta$ had been working well for unmodified binders, and thus a new Superpave® criterion should be able to accurately predict the rutting resistance of modified materials without affecting the forecasts for base binders (D'ANGELO, 2010a; D'ANGELO et al., 2007). This means that the MSCR testing conditions should estimate quite similar rutting resistances for the original materials when compared with the parameter $G^*/sin\delta$ and, at the same time, to provide researchers and highway agencies with more accurate estimations of the susceptibility of modified binders to rutting.

Several tests indicated that the majority of the neat binders show repeated creep responses within the linear viscoelastic range up to stress levels of about 3.2 kPa, after which a nonlinear fashion – in general, shear-thinning behavior – is typically observed (D'ANGELO, 2010a; D'ANGELO et al., 2007). It was also realized that the J_{nr} values are all close to 4.0 kPa^{-1} for these materials at their continuous grades, which means that they depict approximately the same resistance either in the original or the new criteria (D'ANGELO, 2010a). Other publications suggested that many polymer-modified binders show slippage of the polymer chains at stresses higher than 3.2 kPa (D'ANGELO et al., 2007), and some field studies give support to the use of 3.2 kPa as a good representation of the real loading conditions (D'ANGELO, 2009). Due to these and other reasons, the upper limit of 3.2 kPa for the standardized MSCR test was chosen.

In some cases when J_{nr} is very close to 4.0 kPa^{-1}, a negative value for the percent recovery ($R < 0$) may be obtained. These R values indicate that the difference between the strains in the beginning and the end of the creep-recovery cycle – term ε_{rec} in Equation (26) – is negative, i. e., the strain in the end of the creep-recovery cycle is lower than the one in the beginning of the cycle. This occurs because, for some types of DSR, the inertia of the upper plate causes it to continue to rotate and load the sample as soon as the load is cut off. When the binder shows very little or no recovery, this can appear as a negative R value. In such a case, the ASTM D7405-15 standard states that the strain in the end of the creep portion (ε_c) – rather than the original ε_{nr} – should be used to determine J_{nr}.

After calculating the nonrecoverable creep compliances at 0.1 and 3.2 kPa, the percent difference between them ($J_{nr,\,diff}$) can be determined. This percent difference is given by the ratio of the difference between the J_{nr} values at 3.2 kPa ($J_{nr}3200$) and 0.1 kPa ($J_{nr}100$) to the compliance at 0.1 kPa, see Equation (28). Higher $J_{nr,\,diff}$ values are associated with a higher sensitivity of the asphalt binder to an increase in the stress level, which is harmful to its resistance to rutting. This occurs because, in such loading conditions, a particular material with a high percent difference will be more prone to rutting (J_{nr} value will increase at a higher rate) than another one with lower $J_{nr,\,diff}$ values, even if their compliances at 0.1 kPa are similar. In other words, the parameter $J_{nr,\,diff}$ constitutes an attempt to address the issues concerning the stress sensitivity and the degree of nonlinearity in the rheological response of modified asphalt binders.

$$J_{nr,diff}(\%) = \frac{J_{nr}3200 - J_{nr}100}{J_{nr}100} \times 100 \tag{28}$$

To account for the stress sensitivity of asphalt binders and their degree of nonlinearity, the Superpave® specification sets a maximum limit of 75% for the parameter $J_{nr,\,diff}$ at the high PG grade temperature (ANDERSON et al., 2010; ASPHALT INSTITUTE, 2010). This means that the increase in the stress level from 0.1 to 3.2 kPa can lead to a maximum increase of 75% in the initial J_{nr} value. Anderson et al. (2010) stated that the observation of this requirement is important because overly stress sensitive binders may be potentially susceptible to rutting in the field, regardless of the other Superpave® criteria. With respect to polymer-modified materials, the parameter $J_{nr,\,diff}$ gives an idea of the degree of rearrangement of the polymer chains with increasing stress level (ANDERSON, 2011). In practical terms, asphalt binders with lower $J_{nr,\,diff}$ values tend to show lower susceptibility to rutting when unexpected loads and/or unpredicted pavement temperatures are observed in the field.

3.4. Some Special Advantages of the MSCR Test

Together with the MSCR test, the FHWA researchers have chosen the nonrecoverable compliance J_{nr} as the new rheological parameter that should be used by academia and highway agencies in the characterization of the rutting behavior of asphalt binders. Several studies have been conducted later in order to further demonstrate the ability of this parameter in correlating well with mixture rutting data (ADORJÁNYI and FÜLEKI, 2013; ANDERSON, 2011; D'ANGELO, 2008, 2009, 2010a, 2010b; D'ANGELO et al., 2007; DREESSEN et al., 2009; GIERHART, 2013; HAFEEZ and KAMAL, 2014; LAUKKANEN et al., 2015; REINKE, 2010), even though one or more characteristics of the standardized protocol were changed in some of them. Among other conclusions, these authors underlined the facts that J_{nr} provided much better correlations with mixture data than $G^*/sin\delta$ and that the MSCR test represents a considerable improvement over the oscillatory shear method and the resulting properties.

The deficiencies of the parameter *G*/sinδ* in estimating the rutting resistance of the binder can be explained by a series of factors (as previously discussed), many of which were corrected during the development of the MSCR test. These factors include the low stress levels applied in the binder during the oscillatory shear test, which are not enough to activate the polymer network in the material. The modifier is interpreted only as a filler that stiffens the binder under such testing conditions, and thus the elastic effects are not observed (ANDERSON et al., 2010; D'ANGELO, 2010b). The application of high stress levels in the specimen and the use of the concept of creep-recovery in the studies with asphalt binders at high temperatures made it possible to address these issues and, as a consequence, one can easily recognize the elastic (R) and stiffening effects (J_{nr}) of binder modification on the results of the MSCR test.

The benefits of the MSCR test as a procedure for evaluating the rutting performance of binders are not restricted to the correlations between mixture and binder data (higher R^2 values) and the study of the stress sensitivity of modified materials. The new criteria derived from the parameters of this test also provided a more suitable alternative to deal with extreme, heavy traffic conditions on roads and highways. More specifically, the grade-bumping practice (see page 62 for more details) – which was used by some highway agencies as a fairly simple criterion to account for these traffic issues – was not necessary anymore and could be left aside. The test temperatures should be based only on the climatic conditions and, for heavy traffic levels and volumes, the specification criterion should be changed. Therefore, D'Angelo (2010a) and D'Angelo et al. (2007) suggested a reduction in the J_{nr} value in order to obtain more rut resistant binders. Generally speaking, a decrease in J_{nr} by half will decrease the amount of permanent strain in the mixture by half as well (ANDERSON, 2011; D'ANGELO, 2009, 2010a).

The interpretation of MSCR as a "blind to modification type" protocol and a clear observation of the elastic response of the modified binders are also pointed out as great advantages of this test. Differently from the empirical tests such as elastic recovery and forced ductility, the *R* value can somewhat be correlated with the presence and the extent of the polymer network in the formulation. This was observed by D'Angelo (2010a) and D'Angelo and Dongré (2009) in their studies with asphalt binders modified with styrene-butadiene-styrene copolymer, either with or without PPA. In other words, the percent recovery obtained in the MSCR test is an essential step towards a better understanding of the effects of polymer modification on the response of the binder and how it can be more precisely measured.

Based on the topics discussed above, it may be inferred that the MSCR test is a remarkable improvement in the study of the rutting performance of asphalt binders when compared to the previous Superpave® tests and suggesting refinements. These degrees of improvement can be partly explained by the determination of the binder parameters within the nonlinear viscoelastic range, which corresponds to the actual field conditions. Measurements obtained by Kose et al. (2000) suggest that the stress values in the pavement can be as high as 10^6 Pa. Also, a more realistic representation of the actual loads applied by the vehicles (creep-recovery pulses) and the evaluation of the stress sensitivity of the binder (parameter $J_{nr,\ diff}$) can be pointed out as advantages of the MSCR test. Finally, two of the main effects of modification on the response of the base binder – elastic (R) and stiffening ones (J_{nr}) – can be studied in this test.

3.5. Current Status of the MSCR Test: Limitations of the Standard Protocols, Repeatability/Reproducibility and a Few Refinements

Despite the substantial advances provided by the MSCR test in binder characterization and evaluation, it was later realized that not all the issues concerning the rutting potential of asphalt binders were thoroughly explored. As an example, it is questionable as to whether the two stress levels used in the standardized MSCR tests closely simulate the field loading conditions, since they have an arbitrary nature (DELGADILLO et al., 2012; GOLALIPOUR, 2011). Several researchers have concluded that high correlations between the rutting data from binder tests and mixture tests can be obtained when the stress levels are much greater than 3.2 kPa: (a) 10 kPa in the studies from Delgadillo et al. (2006a), Golalipour (2011) and Saboo and Kumar (2015); (b) 12.8 kPa in the papers from Anderson (2011), D'Angelo (2009) and Wasage et al. (2011); and (c) 25.6 kPa in the publications from Anderson (2011), D'Angelo (2009) and D'Angelo et al. (2007). The same can be said for the number of creep-recovery cycles at each stress level, i. e., they are not enough to characterize long-term rutting performance of the binder and the steady state phenomenon exerts a significant impact on the results of the parameters R and J_{nr} (DELGADILLO et al., 2012; GOLALIPOUR, 2011).

In addition to the number of creep-recovery cycles and the stress levels, the unloading time has also become a matter of great concern. This is because the current time of 9 s is not enough to capture all the delayed elastic portion of the total strain in some modified binders, especially the polymer-modified ones. Typically, loading-unloading ratios of 1:10 or lower are not appropriate to be used in creep-recovery tests with these modified materials (DELGADILLO et al., 2006b, 2012; MERUSI, 2012). Therefore, mathematical techniques and different loading-unloading ratios have been suggested in the literature in order to overcome this problem. For instance, Masad et al. (2009) proposed the use of the Schapery's single integral model and a nonlinear viscoelasticity theory to isolate the actual nonrecoverable strain from the delayed elastic one, and then to recalculate J_{nr} based on such actual value. Others suggested marked increases in the recovery time, but the exact values differ from a study to the other as follows:

- proportions between 1:20 and 1:30 in the discussion from D'Angelo et al. (2007);
- values as high as 1,000 s in the paper from Delgadillo et al. (2012); and
- 240 s in the publication from Merusi (2012).

It may be important to emphasize that the creep and recovery times of 1 and 9 s were not randomly chosen; rather, they were based on studies conducted by Bahia et al. (2001b) and involving many pairs of creep and recovery times. These authors observed that, for creep times greater than 1 s and recovery times greater than 9 s, the normalized viscous component of the asphalt binder (G_V value) did not significantly change from one loading-unloading condition to the other. On the other hand, an opposite trend was observed when the creep and recovery times were shorter (see Figure 27). Thus, the authors justified their choice for the values of 1 and 9 s based on the small variations in the normalized strain response of the asphalt binder at longer loading times, the possible inability of the DSR in applying a perfect loading-unloading cycle, the reasonable interpretation of viscosity as a decreasing function of time and the total test time required in the rheometer.

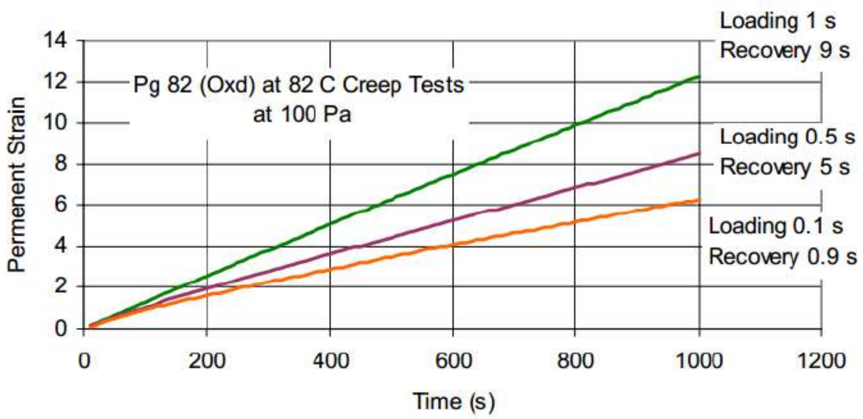

Figure 27 – Effects of varying creep and recovery times on the permanent strain of an oxidized binder (PG 82-xx) in the RCRT (BAHIA et al., 2001b)

As a consequence of aforementioned deficiencies, AASHTO and ASTM have recently modified their MSCR standards (TP70 was last updated in 2013, T350 was launched in 2014 and D7405 was last updated in 2015) to account for the steady state behavior of the binder. The main differences between the current and the previous protocols rely on the number of creep-recovery cycles at 0.1 kPa, the method for calculating R and J_{nr} at such stress level and the determination of the degree of elasticity of the formulation. The latest standards take into account 20 creep-recovery cycles at 0.1 kPa (10 in the previous ones) and the last 10 cycles in the calculation of R

and J_{nr} at this same loading level (all the cycles in the previous ones). Finally, the TP70-13 protocol and the AASHTO M332-14 standard provide a chart to analyze the degree of elasticity of the modified binder when $J_{nr} \leq 2.0$ kPa^{-1} at 3.2 kPa (Figure 28). The combination of both parameters was proposed as a useful tool to conclude that the binder was really modified by a polymer (ANDERSON, 2011; ASPHALT INSTITUTE, 2010; GIERHART, 2013).

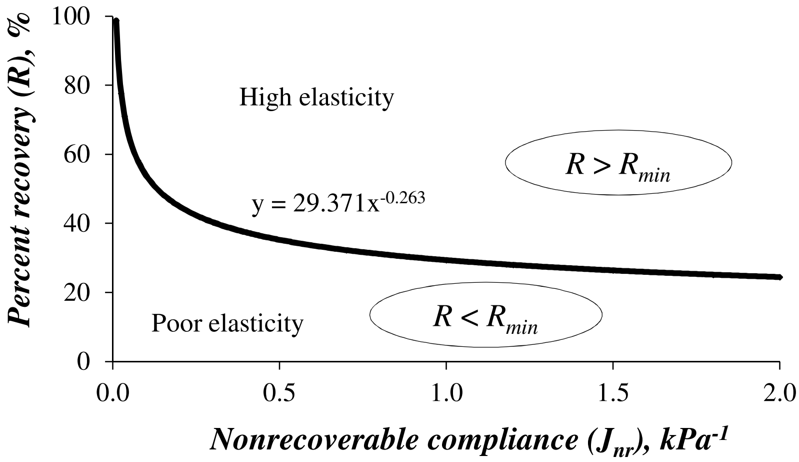

Figure 28 – Relationship between R and J_{nr} at 3.2 kPa and identification of the degree of elasticity of the formulation (high or poor)

As it can be seen, the percent recovery of the polymer-modified binder must be higher than a minimum value (R_{min}) in order to be considered "acceptable". It can be implied here that the term "acceptable" means "an extensive polymer network was formed in the material, and it imparts significant levels of elastic response at high pavement temperatures". One can also perform such analysis based on tables with intervals of J_{nr} values and one corresponding fixed value for R_{min} (ANDERSON, 2011; D'ANGELO, 2008, 2010b). Obviously, the relationship between R and J_{nr} will depend upon variables such as the crude source, the temperature, the modifier type and the modifier content.

In terms of the Superpave® specification (Chapter 2), one example of the refined criterion based on J_{nr} can be seen in Table 3 of the AASHTO M320-09 standard. Each traffic level is associated with a maximum J_{nr} value and, more recently, corresponding traffic speeds have also been incorporated into the analysis (BAHIA, 2014; GIERHART, 2013). Table 4 gives the four traffic levels used in the AASHTO specifications M320-09 and M332-14, together with their corresponding design ESALs (equivalent single-axle loads) and vehicle speeds, according to the technical literature. The ESALs increase and the vehicle speed decreases with increasing traffic level, and the maximum J_{nr} value is reduced. This approach is much closer to the actual loading conditions experienced by the pavement when compared to the previous Superpave® parameter $G^*/\sin\delta$ and grade-bumping criterion.

Table 4 – Traffic levels found in the AASHTO M320-09 and M332-14 specifications and corresponding equivalent single-axle loads (ESALs) and/or vehicle speeds (BAHIA, 2014; GIERHART, 2013)

traffic level	maximum J_{nr} value (kPa^{-1})[a]	design ESALs and/or traffic loading
S (standard)	4.0[b]	ESALs < 10 million **and** standard traffic loading (average speed > 70 km/h)
H (heavy)	2.0	ESALs between 10 and 30 million **or** slow moving traffic loading (average speed between 20 and 70 km/h)
V (very heavy)	1.0	ESALs > 30 million **or** standing traffic loading (average speed < 20 km/h)
E (extremely heavy)	0.5	ESALs > 30 million **and** standing traffic loading (average speed < 20 km/h)

[a] the J_{nr} value is obtained at the high PG grade and the stress level of 3,200 Pa.
[b] the maximum J_{nr} value according to AASHTO M332-14 is 4.5 kPa^{-1}. The other values are similar for both standards.

Rather than making small modifications in the standard MSCR protocol and/or correlating binder data with mixture data, Santagata et al. (2013) decided to apply long and single creep-recovery cycles (900-s creep and 900-s recovery) on SBS- and EVA-modified binders. Later, these authors added a subsequent step in which two stress levels (20 and 500 Pa) are applied on the sample without recovery, and the creep times are a function of the temperature and the modification type. The same approach was followed in the creep-recovery portion of the proposed test, i. e., the loading and unloading times were determined based on the formulation and the temperature (SANTAGATA et al., 2015). The shear stress used in the creep-recovery cycle was fixed at 100 Pa in both studies. The chief purpose of these procedures was to achieve both steady state flow under loading and a full recovery of the delayed elastic component after the removal of this load. Despite the apparent simplicity, it seems that the proposed protocol has some limitations:

- the times used in the creep-recovery portion of the test may be extremely long (time-consuming procedure) and will be dependent upon the modifier type/content and the temperature; therefore, they must be determined empirically or be referenced on previous studies prior to their use in the protocol;
- as pointed out by Santagata et al. (2015), some modified materials may not reach a steady-state condition even after several hours of loading and unloading; in other words, the protocol may not work well for the modified binders who fall into this category (for example, the ones with very high dosages of elastomeric SBS copolymer); and
- none of the studies showed any mixture data and/or correlations between binder and mixture rutting performances.

A just-released paper by White (2016) devoted a special attention to the applicability of the MSCR test and corresponding parameters R, J_{nr} and $J_{nr,\ diff}$ to highly-modified asphalt binders typically used in Australia, as well as their degrees of correlation with mixture data collected according to the flow number, Marshall and wheel tracking tests. In addition to the lack of enough time for these binders to fully recover the delayed elastic strain, the author also mentioned the following issues concerning the standardized MSCR tests:

- the high stress sensitivity of such binders are better explained by $J_{nr}100$ than by $J_{nr}3200$ (higher correlations between $J_{nr}100$ and $J_{nr,\ diff}$ in a log-log chart), and he suggested that the upper limit of 75% for $J_{nr,\ diff}$ may be waived when $J_{nr}3200$ is lower than 0.5 kPa^{-1};
- the parameter $J_{nr}3200$ did not provide a good correlation with flow number and rut depth in the mixture, which points to a diametrically opposite direction with respect to the feasibility of J_{nr} as a binder rutting parameter; and
- the inadequacy of the MSCR testing protocol is given as the main reason why the findings of the paper were not as promising as the ones reported in other studies; however, it should be noted that the author did not follow all the necessary steps for determining the parameters of the flow number test, neither he considered other stress levels and recovery times in an attempt to improve the R^2 values (which was done in other publications from the literature).

The change from the old to the new binder specification has generated concerns among researchers about some major problems that could raise by making such a modification in the classification system. These problems included the material specifications, the engineering properties of the binders, the merits of the MSCR test, the correlations between one grading system and the other and the adaptations that many Departments of Transportation (DOT's) would have to make in the classifications of the binders typically used for paving applications (BEHNOOD et al., 2016; STEVENS et al., 2015). To conduct the investigations, these researchers selected databases from some states in the US such as Arizona (STEVENS et al., 2015) and Indiana (BEHNOOD et al., 2016). They concluded that, despite the need for grading the binders in a different way and possibly extending the interval of allowable materials for the local temperature and climate conditions (from 8 to 14 in the paper from Stevens et al. (2015)), the benefits of MSCR – such as the elimination of the grade-bumping practice, the separation of the traffic issues from the ones of temperature, the improved correlations with mixture data and a better characterization of the responses of polymer-modified materials – compensated for these adaptations.

Another point of great concern about MSCR was the levels of repeatability (i. e., the variability among the results obtained by a particular person in the laboratory, also called "intralaboratory variability") and reproducibility (i. e., the variability among the data points collected by different laboratories, also labeled as "interlaboratory variability") of the standardized protocols. These two statistical features were investigated by Soenen et al. (2013) and, basically, five laboratories were selected to conduct MSCR experiments on nine types of asphalt binders (three unmodified, five polymer-modified, one modified only with wax and the other modified with polymer and wax). The authors concluded that MSCR is a simple and quick laboratory test, but the variations exceeded the maximum limits of the ASTM 7405-10a protocol. It is believed that the sample preparation procedures, the absence of RTFO aging, the responses among the different DSR's and the inherent variations of the materials – among other reasons – led to such high variations. In other words, it seems that the MSCR test deserves further studies with respect to the statistical variations among its results in order to be further accepted among researchers.

This great variability of the MSCR testing results was also emphasized in the paper by Mohseni and Azari (2014), who proposed a new binder test – the incremental repeated load permanent deformation (iRLPD) test – to replace MSCR and better describe the repeated creep response of highly-modified asphalt binders. According to these authors, the loading time of 1.0 s in the MSCR test is very high, and thus the actual recovery of such modified binders is underestimated and negative recoveries may be observed for the neat materials. This is especially critical when the nonlinear relationship between permanent strain and loading time for the modified binders is considered in the analysis (this relationship is approximately linear for the unmodified binders). They also suggested that shorter loading times in the DSR are more representative of the actual creep times experienced by the binder in a real pavement when the traffic speeds are of about 89 km/h. As a consequence, the authors proposed the following protocol for the iRLPD test: 20 creep-recovery cycles at each of the stress levels of 1.0, 3.2 and 5.0 kPa, in which every cycle is comprised by a creep time of 0.1 s and a recovery time of 0.9 s (total duration of the test is 60 s). Other findings were also highlighted in the paper:

- the levels of variability within the binder data may be decreased by more than 10 times with the change in the test protocol (from MSCR to iRLPD), depending on the degree of modification of the binder;
- the minimum strain rate (MSR), which is proposed as the new binder parameter in the iRLPD test, showed good correlations with the numbers of ESAL's obtained from mixture tests; and
- the negative percent recoveries found in the MSCR tests are not observed in the iRLPD tests, since the amount of strain accumulated in the binders is much lower for iRLPD than for MSCR.

More recently, the method for estimating the stress sensitivity of the asphalt binder – based on the parameter $J_{nr,\ diff}$ – has raised several concerns among researchers and agencies. The aforementioned study from White (2016) is one of the examples that show these concerns, but there are others in the literature as well (STEMPIHAR et al., 2017; ZHOU et al., 2014). The problems pointed out by these authors include high variability within the laboratory data and poor correlation with mixture performance. As a consequence, alternative parameters and methods have been developed such as the following: (a) the possibility of disconsidering $J_{nr,\ diff}$ when J_{nr} is lower than 0.5 kPa^{-1}; and (b) the use of the parameter γ_{diff} instead of the original one.

According to Stempihar et al. (2017), γ_{diff} is labeled as "percent difference in strains" and is calculated as the ratio of the difference between the nonrecoverable strain values at 3.2 kPa ($\gamma_{nr,3.2}$) and 0.1 kPa ($\gamma_{nr,0.1}$) to 3.1, Equation (29). This new parameter can also be calculated from *$J_{nr}100$ and $J_{nr}3200$*, as shown in the same equation. The correlations reported by these authors suggest the existence of a trendline between the results of accelerated loading facilities and γ_{diff}; however, the fact that the authors are currently working on the proposed parameter[26] indicates that more studies are required before γ_{diff} is taken as a viable option to replace $J_{nr,\ diff}$ on Superpave® or not. Currently, the AASHTO M332-14 specification still utilizes $J_{nr,\ diff}$ as the official parameter to evaluate stress sensitivity in asphalt binders.

$$\gamma_{diff} = \frac{\gamma_{nr,3.2} - \gamma_{nr,0.1}}{3.1} \times 100 = 3.2258 \times [32 \times J_{nr}3200 - J_{nr}100] \tag{29}$$

As these and other previously published studies suggest, the deficiencies of the MSCR test have been investigated and alternatives have been proposed to solve or, at least, minimize them. These deficiencies mainly rely on the great variabilities among the laboratory data and the limitations of the estimation of the stress sensitivity and the rutting performance of highly-modified asphalt binders (i. e., elastic response and accumulation of permanent strain). With respect to the latter, the studies took into account the nonlinear variations in the accumulated strain with creep time and the occurrence of negative R values for the unmodified binders to decrease the original creep time by 10 (from 1.0 to 0.1 s). However, it must be pointed out that the actual loading times and rutting resistance of binders are a function of the number of axles and the axle type (single or tandem), the truck speed, the stress level and the delayed elastic response of the materials, among other variables (e. g., DELGADILLO et al., 2012; MERUSI, 2012; PEREIRA et al., 1998, 2000; SARKAR, 2016).

[26] DONGRÉ, R. **[Matheus, PhD. Candidate, Brazil] Proposals for Replacing the Parameter Jnr, diff on Superpave** [private message]. Message received by <matheusdavid@sc.usp.br> on Mar. 18, 2017.

3.6. Examples of Brazilian Studies about the MSCR Test

Differently from its practical application in the US, the MSCR test is restricted to the academic studies in Brazil up to the present moment. This can be attributed to the fact that the Brazilian specification for asphalt binders is based on the penetration value at 25 °C[27], whereas Superpave® is the prevailing specification in the US (Chapter 2). Even with these limitations, it is noteworthy that many Brazilian studies have covered interesting aspects of MSCR. For instance, Martins et al. (2011) showed that not only the rut depth in the wheel tracking device has a good correlation with J_{nr} at 3.2 kPa, but also the flow number (F_N) value at the stress level of 204 kPa. On the other hand, the parameter calculated from the dynamic modulus test at the temperature of 60°C (AASHTO TP62-05 standard) showed a poor correlation with the compliance J_{nr} from the MSCR test.

More recently, papers from Domingos and Faxina (2014, 2015b) have focused on the rheological behavior of modified binders after changing both the creep and recovery times in the MSCR test. The creep and recovery times were doubled in these studies, and the rheological parameters were monitored before and after such changes. Many of the binders studied by the authors became more susceptible to rutting at longer creep and recovery times (R decreased and J_{nr} increased), and they include formulations with ethylene vinyl acetate copolymer, low-density polyethylene and PPA. Two possible explanations can be put forward here: (a) the presence of longer unloading times was not enough to recover greater portions of the accumulated strain after 2 s of loading; or (b) the effects of elasticity are not as pronounced as the effects of viscous behavior on the response of the binder, especially at very high temperatures.

Pamplona (2013) studied the changes in the creep-recovery parameters of asphalt binders from the Lubnor-Petrobras and the Reduc-Petrobras refineries and modified with several contents of PPA (from 0.0 to 2.0% by weight with intervals of 0.5% in between), considering the high temperatures of 52, 58, 64, 70 and 76°C. The type of PPA used by Pamplona (2013) was similar to the one selected in this dissertation. Higher percent recoveries and lower nonrecoverable compliances could be seen for the PPA-modified materials when compared with the corresponding original ones, and these benefits were more visible for higher additive contents. However, the author identified contents in which the improved parameters seemed to reach optimum values – i. e., 1.5% for the asphalt binder from Reduc-Petrobras and 1.0% for the one

[27] AGÊNCIA NACIONAL DO PETRÓLEO, GÁS NATURAL E BIOCOMBUSTÍVEIS. (2005). Resolução ANP No. 19, de 11 de julho de 2005 [Resolution No. 19, from July 11, 2005]. **Diário Oficial da União**, Brasília, DF, Brazil. Retrieved from: <http://nxt.anp.gov.br/NXT/gateway.dll/leg/resolucoes_anp/2005/julho/ranp%2019%20-%202005.xml>. Accessed: 21 Jan. 2016. In Portuguese.

from Lubnor-Petrobras. In other words, it was recommended not to choose contents higher than these optimum values because no marked improvements in the rutting performance of the binders will be noticed. Also, the formulations with PPA were not found to be overly stress sensitive (i. e., $J_{nr,\,diff} < 75\%$), even for the PPA contents of 1.5 and 2.0% by weight.

The M.Sc. thesis from Verdade (2015) considered nine types of modified asphalt binders with 4% of an aromatic oil (AC+oil) and prepared with the same SBS copolymer used in the present study and varying contents of a compatibilizing agent labeled as “TITAN 9686”. The SBS contents were equal to 0.0, 2.5 and 5.0% by weight and the TITAN contents ranged from 0.0 up to 1.0 and 2.0% by weight. In other words, the three TITAN contents were used in each of the asphalt binders modified with 0.0, 2.5 and 5.0% of SBS. The main objective of his thesis was to see if the addition of TITAN could improve the rheological characteristics of the AC+SBS, and one of the tests selected in the experiments was MSCR (ASTM D7405-10a protocol). In general, the author observed that the addition of SBS was beneficial to the rutting resistance of the formulation because the percent recoveries increased and the nonrecoverable compliances decreased at the testing temperatures of 52, 58, 64 and 70°C, either at 100 or at 3,200 Pa.

With respect to the TITAN agent, Verdade (2015) observed that it further contributed to the degrees of improvement in the MSCR test because the R values increased and the J_{nr} decreased when compared with the original AC+SBS+oil formulations. The major disadvantage of TITAN was to increase the stress sensitivity of the modified binders (parameter $J_{nr,\,diff}$) and, in some cases (especially for TITAN contents higher than 1%), the maximum allowed value of 75% was exceeded. In other words, the contents that could be used for paving applications would be restrited to lower percentages in the AC+SBS+oil modifications. In a general context, percentages of TITAN higher than 1% by weight would not be recommended in the AC+oil formulations (regardless of the SBS content), since $J_{nr,\,diff}$ values much higher than 100% were typically observed in the asphalt binders with such modifier contents and prepared by the author.

The study carried out by Feitosa (2015) showed the outcomes of the MSCR tests for a 50/70-penteration grade asphalt binder modified with 3 and 5% by weight of a dark green carnauba wax (labeled as “Carnauba Wax Type 4”) with no more than 2% of moisture content and less than 2% of impurities. It was observed that the addition of such percentages of carnauba wax could improve the adequate traffic levels for the binder on pavements with the high PG grade of 64°C; however, the benefits in the percent recovery and the nonrecoverable compliance values were not clearly visible at the PG grade of 70°C. In terms of the traffic levels by themselves, the author concluded that binder modification with carnauba wax may allow its use on pavements with at least heavy levels, provided that the pavement temperature was equal to 64°C.

3.6.1. Focuses and Justifications for the Present Study and Literature Gaps

The discussions on possible refinements in the MSCR test – especially the creep and recovery times – led to the development of the present study. As pointed out earlier, the creep and recovery times used in the test have been recognized as limited and not able to cover all the aspects concerning the complex rheological behavior of modified binders, neither the wide loading and temperature spectra found in real pavements. However, these previous studies did not include one or more of the variables selected in this document, e. g., the test temperatures, the number of binder samples, the correlations with other rutting parameters and rheological modeling of the creep-recovery behavior of the binder. The paper from Delgadillo et al. (2012) showed the repeated creep response of the binder at many pairs of creep-recovery times (for instance, 1/2000, 10/10000 and 100/20000), but only one test temperature (46 °C) and one modified material (a PG 70-22 binder modified with Elvaloy® terpolymer) were considered. The study from Merusi (2012) took into account six modified asphalt binders and a much longer recovery time (240 s) in the tests, but only one modifier type (SBS copolymer) and one temperature (60 °C) were used by the author.

As it can be seen, the reports about the repeated creep tests – MSCR and RCRT – seem to be more focused on the nonlinear behavior of the binder at higher stress levels (ADORJÁNYI and FÜLEKI, 2011; D'ANGELO, 2009, 2010a; D'ANGELO et al., 2007; DELGADILLO et al., 2006a; HAFEEZ and KAMAL, 2014; LAUKKANEN et al., 2015), the effects of steady state on the response of the material (BAHIA et al., 2001a; DELGADILLO et al., 2006b; GOLALIPOUR, 2011; GOLALIPOUR et al., 2016) and the use of rheological models to determine the fitting/rutting parameters (BAHIA et al., 2001a, 2001b; DELGADILLO et al., 2006b, 2012; GOLALIPOUR, 2011; HAJIKARIMI et al., 2015; MASAD et al., 2009). There is no doubt that such issues are crucial and must be carefully examined. However, the creep and recovery times in the MSCR test are also very important and deserve a close attention from researchers, since they are somehow related to traffic (loading mode, vehicle speed and spacing between vehicles on the roadway) and the axle configuration and distribution (SARKAR, 2016).

The creep time is expected to represent the time duration of a load in a pavement surface, and this may be directly related to the vehicle speed. The existence/absence of a correlation between the loading time t_F and the vehicle speed Tr_{sp} was examined in the papers by Pereira et al. (1998, 2000), in which increasing creep times (0.1, 0.2 and 0.3 s) were used in the RSST-CH protocols and the mixture data were correlated with the measured rut depths on the pavement sections of a road in a mountainous region. These speeds were obtained by following five different trucks as they climbed up the hills in the roadway. Based on preliminary data gathered by Pereira et al.

(1998), Equation (30) was proposed to demonstrate the aforementioned correlation. However, this equation was not suitable to interpret the data collected by the authors in a later study (PEREIRA et al., 2000), and Equation (31) was suggested to replace the original one. In either case, the authors claimed that truck speed and loading time can be studied together by means of a mathematical problem, even though several external factors – e. g., compaction problems and shear deformation caused by increasing torque on the rear wheels of the truck when the gear is changed – may create difficulties in the determination of such equations.

$$t_F[s] = \frac{8}{Tr_{sp}[\frac{km}{h}]} \tag{30}$$

$$Tr_{sp}\left[\frac{km}{h}\right] = -94.9 \times t_F[s] + 73.4 \tag{31}$$

It is believed that the present study is able to bring some contribution to the asphalt community, in that a further understanding of the impact of the creep-recovery times on the rutting potential of modified binders at high testing temperatures is acquired. More specifically, the study investigates the effects of delayed elasticity on the repeated creep responses of several modified binders at more than one high pavement temperature – which was not fully addressed by other authors in previous papers (e. g., D'ANGELO et al., 2007; DELGADILLO et al., 2012; MASAD et al., 2009; MERUSI, 2012) – and what is the relationship between longer creep times and the susceptibility to rutting, similarly to what was done by Golalipour (2011) and Pereira et al. (1998, 2000). Kataware and Singh (2015) have taken this direction and studied the effect of longer creep and recovery times on the responses of SBS- and crumb rubber-modified materials, but their study was limited to only three temperatures (52, 64 and 76°C), one additional creep time (2 s), two quite short recovery times (18 and 27 s) and binders not equally graded in the Superpave® specification (PG 70-xx, PG 82-xx and PG 88-xx). In addition, these authors did not take into account the Burgers model in their investigation of the susceptibility of the binder to rutting.

Although the researchers have endeavored to overcome the deficiencies of the Superpave® specification over the years (e. g., to replace $G^*/sin\delta$ by J_{nr} and to establish traffic levels and vehicle speeds as a function of J_{nr} at 3.2 kPa) and that the idea of decreasing the maximum J_{nr} value to account for higher traffic levels is closer to the actual condition of real pavements, this seems to be not enough to account for the very complex rheological response of modified binders. This is because the truck speeds may decrease to very low values – as lower as 20-30 km/h – when they are climbing up mountains and hills (PEREIRA et al., 1998, 2000) and, since the accumulated strain is related to the vehicle speed by means of a nonlinear relationship (GOLALIPOUR, 2011), the susceptibility of the material to rutting will probably increase dramatically if the speed slightly decreases. Therefore, a careful investigation into the nonlinear response of the modified binders at longer creep times may yield valuable insights about its actual resistance to rutting and help engineers and highway agencies in choosing the best material for a specific paving application.

CHAPTER 4: Materials, Methods and Analysis of Data

4.1. Highlights

- A 50/70 base binder from Lubnor-Petrobras, one reactive terpolymer (Elvaloy®), three copolymers (SBS, SBR and EVA), linear low-density PE, crumb rubber and PPA were used in the formulations.
- With exception of the Elvaloy® terpolymer, all the other formulations were prepared with one modifier only (AC+modifier) and the same one with PPA as well (AC+modifier+PPA).
- A dense-graded gradation curve – Gradation "III" – from a technical document published by the São Paulo State Department of Roads (DER/SP) was used in the mixture samples.
- Binder tests included penetration, softening point, rotational viscosity, oscillatory shear and MSCR, whereas mixtures were subjected only to the flow number protocol.
- Four creep times (1, 2, 4 and 8 s) and three recovery times (9, 240 and 500 s) were used in the MSCR tests, and small amendments on Superpave® were proposed.
- Five rutting parameters (softening point, Shenoy's parameter, $G^*/sin\delta$, G_V and J_{nr}) and four rheological models (Burgers, generalized Burgers, Francken and modified power law) were fitted to the data.

4.2. Materials and Preparation of the Mixture and Binder Samples

The base binder used in the present study was supplied by the Lubnor-Petrobras refinery (Fortaleza, Ceará, Brazil), and is graded as 50/70 in the Brazilian specification. This base binder is graded as PG 64-xx in the Superpave® specification and its true (or continuous) grade is equal to 66.3°C in the unaged condition. The modifiers were added to the binder such that the high PG grade in the revised Superpave® specification (Table 3 from the AASHTO M320-09 standard) is the same for all materials (76-xx) and the true grades fall between 76.0 and 78.0°C. This was made in order to control the degree of stiffness of the formulations, since it is known that the PG grade of 76-xx can include binders with continuous grades between 76.01 and 81.99°C from a strict point of view. Table 5 reports the modifier contents and the corresponding true grades of the materials.

The technical details of the modifiers can be given as follows. Crumb rubber was prepared by chopping tread layers of passenger vehicle tires, and 100% of the particles passed through a

#30 sieve size (0.6 mm). The D1101 linear triblock styrene-butadiene-styrene (SBS) copolymer was provided by Kraton Performance Polymers Inc. and has a polystyrene content of 31%. The Solprene® 1205 linear random-block styrene butadiene rubber (SBR) copolymer was supplied by Dynasol Elastomers and has a total styrene content of 25%. The HM 728 ethylene vinyl acetate (EVA) copolymer was provided by Braskem (Brazil) and has a vinyl acetate content of 28%. The UB-160C low-density polyethylene (PE) was supplied by Quattor-Braskem (Brazil) and has a Vicat softening temperature of 85°C and density of 0.918 g/cm^3. The 4170 ethylene butyl acrylate glycidylmethacrylate (Elvaloy®) terpolymer was supplied by DuPont™, contains 8% of GMA by weight and shows a maximum processing temperature of 280°C, density of 0.94 g/cm^3 and a melting point of 72°C. Finally, the Innovalt® E200 PPA was provided by Innophos Inc. (US).

Table 5 – Modifier contents (percentages by weight), PG grades and corresponding true grades of the formulations

asphalt binder	contents (% by weight)			AASHTO M320-09, Table 3	
	binder	modifier[a]	PPA	PG grade	true grade (°C)
base binder (AC)	100.0	-	-	64-xx	66.3
AC+PPA	98.0	-	2.0	76-xx	77.8
AC+Elvaloy+PPA	97.9	1.6	0.5	76-xx	76.6
AC+rubber	85.0	15.0	-	76-xx	77.8
AC+rubber+PPA	87.4	12.0	0.6	76-xx	77.8
AC+SBS	95.3	4.7	-	76-xx	78.0
AC+SBS+PPA	96.0	3.4	0.6	76-xx	76.9
AC+EVA	91.3	8.7	-	76-xx	77.0
AC+EVA+PPA	95.3	4.0	0.7	76-xx	77.0
AC+PE	93.0	7.0	-	76-xx	78.0
AC+PE+PPA	94.7	4.5	0.8	76-xx	77.8
AC+SBR	92.5	7.5	-	76-xx	77.4
AC+SBR+PPA	94.8	4.5	0.7	76-xx	76.6

[a] the column "modifier" does not include PPA in the list of modifiers, but only the other six ones (SBS, SBR, EVA, PE, Elvaloy® and crumb rubber).

As pointed out in Chapter 1, the formulations prepared in this study are taken as representatives of those commonly used in pavement construction and rehabilitation, even though they typically have a non-commercial nature. One of the facts that illustrate such a difference is the limited use of compatibilizing agents here, which in turn is very common in the asphalt industry and other publications – e. g., sulfur, PPA, TITAN, Vestenamer and others (VERDADE, 2015; YADOLLAHI and MOLLAHOSSEINI, 2011; ZHANG and HU, 2013; ZHANG and YU, 2010). By keeping the base binder and the high PG grade unchanged, it is hypothesized that the resulting formulations will not necessarily be the best ones for all types of modifiers. In other words, caution must be taken when claiming that one binder is better than the other, since one or more formulations obtained in the study may not be the most adequate ones for a specific modifier.

Two mixers were used in the preparation of the aforementioned formulations, i. e., a Fisatom 722D low-shear mixer and a Silverson L5M-A high shear mixer. With exception of the SBS- and the crumb-rubber modified binders (AC+SBS, AC+SBS+PPA, AC+rubber and AC+rubber+PPA), all the other materials were prepared in the Fisatom mixer. The processing variables used in the production of each formulation can be seen in Table 6. It may be important to note that the AC+Elvaloy – asphalt binder modified with Elvaloy® terpolymer only – is not included in the list of formulations, since it was not possible to produce a formulation with a PG grade of 76-xx and, at the same time, a reasonable amount of Elvaloy® and a sufficient level of workability (especially after aging). It is known that PPA can increase the workability of the binder by decreasing the total amount of polymer in the formulation, which decreases the rotational viscosity and consequently the mixing and compaction temperatures (DOMINGOS et al., 2012). By assuming that the binder has a colloidal structure, it can also be said that the pair PPA-polymer can act in a synergetic way and be more efficient in the modification of the asphalt binder when compared to the polymer alone, provided that the effects of PPA and polymer modification on the properties of the binder are summed up (LESUEUR, 2009).

Table 6 – Processing variables of the modified asphalt binders (mixing temperature, mixing time and rotation speed)

formulation	shear level	variables		
		temperature (°C)	time (min)	rotation speed (rpm)
AC+PPA	low	130	30	300
AC+Elvaloy+PPA	low	190	120[a]	300
AC+rubber	high	190	90	4,000
AC+rubber+PPA	high	190	120[b]	4,000
AC+SBS	high	180	120	4,000
AC+SBS+PPA	high	180	120[a]	4,000
AC+EVA	low	180	120	300
AC+EVA+PPA	low	180	120[b]	300
AC+PE	low	150	120	440
AC+PE+PPA	low	150	120[a]	400
AC+SBR	low	180	120	400
AC+SBR+PPA	low	180	120[b]	300

[a] PPA was added to the formulation after 60 min of mixing time.
[b] PPA was added to the formulation after 90 min of mixing time.

The aggregate used in the mixture samples came from the Bandeirantes quarry (São Carlos, São Paulo, Brazil), and some of its characteristics are provided in Table 7. Three replicates were prepared for each binder and the target air voids was equal to 7.0 ± 0.5%, as recommended by Witczak et al. (2002) in their protocol for repeated load tests in uniaxial compression. Prior to the beginning of the tests, the upper surfaces of the samples were regularized with a plaster layer (Figure 29) in order to ensure a uniform distribution of the load within the material. These samples were kept in the environmental chamber of a MTS 651 device at 60°C for 10-15 min, and then subjected to load pulses of 204 kPa (≈ 29.6 psi) for 0.1 s followed by a 0.9-s rest period with a contact load of 5.2 kPa (0.73 psi). This test temperature is expected to represent the worst climate conditions during a pavement rehabilitation in the southern portion of Brazil (FONTES et al., 2010), and is also the highest value recommended by Witczak et al. (2002) in the protocol for repeated creep tests in uniaxial compression. The test was interrupted when 10,000 loading-unloading cycles were applied on the sample or the tertiary creep region was achieved, whichever came first.

Table 7 – Some characteristics of the basaltic aggregate from the Bandeirantes quarry (GIGANTE, 2007)

property	standard	result
adhesion (Riedel Weber)	DNER-ME 78/94	bad
adhesion (Modified RRL)	DNER-ME 79/94	not satisfactory
Los Angeles abrasion	DNER-ME 35/98	25%
actual specific gravity	ASTM C-128	2.872
bulk specific gravity	ASTM C-127	2.808

Figure 29 – Mixture sample with the plaster layer on top after the repeated creep (or flow number) test

A Servopac Superpave® gyratory compactor (SGC) was selected for preparing the 39 mixture samples (three replicates with 100-mm diameter and 150-mm height for each of the 13 binders). The mixing and compaction temperatures were obtained from the viscosity-temperature charts of the asphalt binders at the temperatures of 135, 143, 150, 163 and 177°C, according to the procedures outlined in the ASTM D2493-09 standard. In the cases that the mixing and/or the compaction temperatures were higher than 177°C, they were limited to 177°C to prevent damage from heating at such very high temperatures. This maximum temperature is also established as a limiting criterion in some Brazilian specifications about pavement rehabilitation with hot-mix asphalt concrete (e. g., DER/PR ES-P 21/05, from the Paraná State Department of Roads[28]). Table 8 gives the full details of the binder contents, the corresponding intervals of air voids for the 3 replicates, the ranges of values for the mixing and compaction temperatures and the ones effectively used in the preparation of the samples.

Table 8 – Binder contents and the corresponding intervals of the mixing and compaction temperatures

asphalt binder	control variables (%)		temperature intervals (°C)[b]	
	binder content[a]	air voids	mixing	compaction
base binder (AC)	4.4	6.9 – 7.1	151 – 156 (154)	140 – 144 (142)
AC+PPA	4.7	6.9 – 7.1	165 – 171 (168)	154 – 159 (157)
AC+Elvaloy+PPA	4.8	6.8 – 6.9	179 – 184 (177)	166 – 173 (170)
AC+rubber	5.5	6.9 – 7.1	196 – 199 (177)	190 – 193 (177)
AC+rubber+PPA	5.5	6.9 – 7.0	184 – 188 (177)	170 – 177 (174)
AC+SBS	5.0	6.9 – 7.1	180 – 183 (177)	167 – 173 (170)
AC+SBS+PPA	5.0	6.9 – 7.1	179 – 183 (177)	166 – 172 (169)
AC+EVA	4.9	6.9 – 7.1	191 – 193 (177)	186 – 189 (177)
AC+EVA+PPA	5.0	6.9 – 7.0	187 – 190 (177)	179 – 183 (177)
AC+PE	4.9	6.9 – 7.0	180 – 184 (177)	167 – 174 (171)
AC+PE+PPA	4.9	7.0 – 7.1	183 – 187 (177)	172 – 177 (175)
AC+SBR	5.0	6.9 – 7.1	182 – 186 (177)	171 – 177 (174)
AC+SBR+PPA	4.9	7.0 – 7.1	186 – 190 (177)	177 – 181 (177)

[a] the binder contents were taken from a previous study by Onofre et al. (2013), in which the high PG grades of 76-xx for the modified binders and 64-xx for the unmodified one remained unchanged.

[b] the numbers in parentheses (i. e., the ones effectively used in the preparation of the samples) are the mean values of each temperature interval. For results higher than 177°C, the limiting value of 177°C was selected.

[28] DEPARTAMENTO DE ESTRADAS DE RODAGEM DO ESTADO DO PARANÁ. (2005). **DER/PR ES-P 21/05:** Pavimentação: concreto asfáltico usinado a quente [Paving with hot-mix asphalt concrete]. Norma Técnica, Especificação de Serviço. Curitiba, PR. Retrieved from: <http://www.dtt.ufpr.br/Pavimentacao/Notas/ES-P21-05CAUQ.pdf>. Accessed: 26 Jan. 2016. In Portuguese.

A dense-graded gradation curve (red line in Figure 30) comprised by the center points of the Gradation "III" of the São Paulo State Department of Roads (DER/SP, ET-DE-P00/027[29]) was chosen as reference to produce the asphalt mixtures. The corresponding upper and lower limits in the percentages of passing material (grey lines) can also be seen in the figure. Dense-graded curves have been used in several road construction and maintenance programmes around Brazil, and it was selected in other Brazilian academic studies as well – see Onofre et al. (2013) and Pilati (2008) as some representative examples.

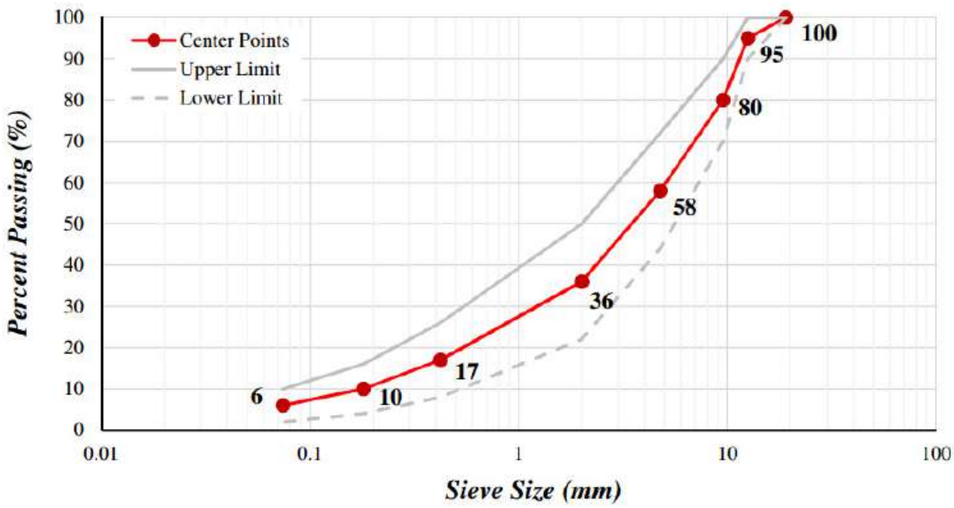

Figure 30 – Aggregate gradation curve (red line) of the mixture samples and upper and lower limits (grey lines) for passing material

4.3. Details about the Protocols of the Mixture and Binder Tests

4.3.1. Binder Tests

The following binder tests were carried out in this study: (a) penetration at 25°C; (b) ring-and-ball softening point; (c) rotational viscosity at 135, 143, 150, 163 and 177°C; (d) short-term aging; (e) dynamic oscillatory shear at the temperatures of 52, 58, 64, 70, 76 and 82°C and ω = 10 rad/s; and (f) MSCR tests at the same temperatures used in the oscillatory shear tests, with exception of 82°C. The latter was the only test that was not performed on the unaged materials, since the analysis of the rutting resistance of binders must be made on short-term aged samples. This aging condition is expected to simulate the most critical condition under which the asphalt mixture shows rutting, i. e., the highest pavement temperatures and right after construction of the

[29] DEPARTAMENTO DE ESTRADAS DE RODAGEM DO ESTADO DE SÃO PAULO. (2005). **ET-DE-P00/027:** Concreto asfáltico [Asphalt concrete]. Especificação Técnica. São Paulo, SP. Retrieved from: <ftp://ftp.sp.gov.br/ftpder/normas/ET-DE-P00-027_A.pdf>. Accessed: 26 Jan. 2016. In Portuguese.

surface layer. The temperature of 64°C was selected in the MSCR tests to make direct comparisons with the mixture data (see Chapter 5), similarly to what was done in another study conducted by researchers from Petrobras (MARTINS et al., 2011). This temperature can also be found in many Brazilian asphalt pavements (CUNHA et al., 2007; LEITE and TONIAL, 1994), and is recommended by Asphalt Institute (2010) to be used in several MSCR tests, even when the high PG grade of the pavement is equal to 70, 76 or 82°C.

The penetration and softening point tests followed the steps shown in the ASTM D5-06 and the ASTM D36-06 standards, respectively. The former was performed on a Solotest universal penetrometer, whereas the latter was carried out on a RB 36-5G automatic ring-and-ball apparatus. In both cases, four replicates were determined for each binder type and aging condition and the results were averaged to yield the final values. The retained penetrations (R_{PEN}), the increases in softening point ($I_{R\&B}$) and the penetration indexes (P_I) were also calculated, and the numerical values were analyzed with respect to the sensitivity of the binder to short-term aging and temperature. The literature suggests that indexes such as R_{PEN} and $I_{R\&B}$ are a powerful tool to examine the changes in the properties and/or the chemical composition of the binder after aging in the laboratory (ROBERTS et al., 1996; SIDDIQUI and ALI, 1999; TAREFDER and YOUSEFI, 2015), and this can be applied either to unmodified or modified materials.

The rotational viscosity tests were conducted according to the ASTM D4402-06 standard using a Brookfield DV-II+ Pro viscometer equipped with a Thermosel temperature controller. Two replicates were tested, and the final values were calculated by averaging these replicates. The rotation speeds were chosen such that the percentage of torque was always within the interval between 10 and 98% of the maximum capacity of the device, as established by the ASTM standard. The aforementioned temperatures were based on a previous study published by the author and some co-workers (DOMINGOS et al., 2012). Then, the viscosity aging index (I_A) – ratio of the viscosity after RTFO-aging to the one before aging – was determined for each binder type and test temperature.

The short-term aging tests were conducted on a Matest rolling thin-film oven according to the ASTM protocol (D2872-04). In summary, 35 g ± 0.5 g of binder was poured into a standardized cylindrical bottle and later placed in the rolling oven at 163°C for 85 min. The weights before and after short-term aging were determined and used in the calculation of the mass loss (M_L), which is an aging parameter that shows the difference between loss of volatiles and oxidation. The M_L value must be no greater than 0.5% for the 50/70 unmodified binder to meet the Brazilian specification requirements. This maximum value is equal to 1.0% in the Superpave® specification.

An AR-2000ex dynamic shear rheometer (DSR) from TA Instruments was used to carry out the dynamic oscillatory shear and the MSCR tests. With respect to the oscillatory shear protocol, it was performed on the 25-mm parallel plate geometries and the 1-mm gap height to determine the high-temperature performance grade (AASHTO M320-09, Table 3) and to calculate two of the rutting parameters of the binder between 52 and 82°C: (a) the original Superpave® parameter $G^*/sin\delta$; and (b) the Shenoy's parameter $|G^*|/[1-(1/tan\delta sin\delta)]$. Although these and other parameters have a more limited application in the current binder specifications when compared to the nonrecoverable compliance J_{nr} from the MSCR test, very recent studies have indicated that they still call the researchers' attention in the academic area and some of them have merits as indicators of the rutting potential of the binder (DOMINGOS and FAXINA, 2016; GIBSON et al., 2012; HAJIKARIMI et al., 2015; SABOO and KUMAR, 2016). Thus, the addition of such parameters to the scope of the present study may further contribute to the literature with respect to their use in the choice of binders with the highest and lowest susceptibilities to rutting.

The MSCR tests were conducted according to the procedures established by the latest AASHTO and ASTM standards (T350-14 and D7405-15, respectively). A 25-mm binder sample with a 1-mm gap height was placed between the parallel steel plates of the DSR, and then subjected to repeated creep pulses at a particular stress level and temperature (20 cycles at 100 Pa and 10 more cycles at 3,200 Pa). The rheological parameters R and J_{nr} were calculated at each creep-recovery cycle, and their final results were reported together with the corresponding percent differences in nonrecoverable compliances ($J_{nr,\ diff}$). Although the chart for the determination of the level of elasticity of the binder cannot be found in the T350-14 and the D7405-15 standards (only in the TP70-13 one), it was also used in the analysis of the repeated creep response of the binder.

The MSCR test protocol included the temperatures of 52, 58, 64, 70 and 76°C and the standardized stress levels of 0.1 and 3.2 kPa. MSCR testing at different temperatures appears to be a very common practice among researchers (DIVYA et al., 2013; DOMINGOS and FAXINA, 2014, 2015a, 2015b; GOLALIPOUR, 2011; HAFEEZ and KAMAL, 2014; KATAWARE and SINGH, 2015; SABOO and KUMAR, 2015; WASAGE et al., 2011; ZHANG et al., 2015), and the temperature values from 52 to 76°C were based on an early paper published by the author (DOMINGOS and FAXINA, 2015b) and climatic conditions typically observed in the US (ASPHALT INSTITUTE, 2010) and Brazil (LEITE and TONIAL, 1994; CUNHA et al., 2007). Although the Superpave® specification also takes into account the temperatures of 46 and 82°C, they were not selected in this study. The PG grade of 46-xx is limited to very cold regions in countries such as the US (ASPHALT INSTITUTE, 2010) and the PG 82-xx one can be found in the grade-bumping cases of some countries such as Thailand (JITSANGIAM et al., 2013). In other words, the PG grade temperature of 82°C represents a possible grade for the binder, but it is perhaps not able to be achieved in any real pavement.

Different pairs of creep and recovery times were considered in this dissertation for the MSCR tests with asphalt binders. With respect to creep, it was decided to choose three longer loading times (2/9, 4/9 and 8/9 s) as representative values of the more severe loading conditions found in the pavement. The twofold increases in the original creep time (1 s) were chosen based on the reductions in the J_{nr} value by half in the AASHTO M320-09 specification for heavier traffic levels (from 4.0 to 2.0, 1.0 and then 0.5 kPa^{-1}) – which is also related to the average vehicle speed on the roadway – and the constant increments made by other authors (DELGADILLO et al., 2012; KATAWARE and SINGH, 2015). It was shown that the relationship between accumulated strain and loading time is nonlinear (GOLALIPOUR, 2011), and therefore no linear correlations between J_{nr} and longer loading times are expected. Finally, analyses of variance (ANOVA, see Appendix A) were conducted in order to see whether creep time or temperature is the most influential factor in the changes in the MSCR parameters with increasing severity of the tests.

Similarly, three recovery times (1/9, 1/240 and 1/500 s) were chosen with reference to the technical literature (DELGADILLO and BAHIA, 2010; DELGADILLO et al., 2012; MERUSI, 2012). It was assumed that the level of elasticity of the binder can be studied in test conditions other than the standardized one, and thus the same chart was used to all the other test conditions.

4.3.2. Mixture Tests

The flow number (FN) tests with asphalt mixtures were based on the repeated creep tests in uniaxial compression (WITCZAK et al., 2002). As described earlier, these tests were run at 60°C and loading-unloading pulses of 0.1/0.9 s were selected. Cyclic loading was interrupted as soon as 10,000 cycles were applied or the mixture achieved the tertiary creep region, whichever came first. It is believed that the creep time of 0.1 s represents the time duration of a load applied by a vehicle traveling at 80-90 km/h (MOHSENI and AZARI, 2014; PEREIRA et al., 1998), which is quite close to the vehicle speeds that were considered by the SHRP researchers during the development of the Superpave® specification (80.5 – 96.6 km/h) (BAHIA and ANDERSON, 1995). Figure 31 shows a typical layout of the mixture creep curve and the three regions that are commonly observed in it, i. e., primary (Region 1), secondary (Region 2) and tertiary (Region 3). The boundary between Regions 2 and 3 is the flow number (F_N) value, which is also the minimum value of the curve given by the rate of change in the axial strain *versus* the number of cycles.

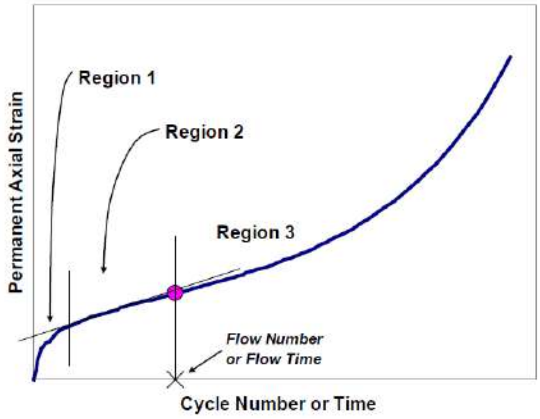

Figure 31 – Typical strain curve of a mixture subjected to the flow number test (GIBSON et al., 2012)

The confined tests were not considered in the study, although it is believed that they better represent the actual conditions of the mixture in the pavement (ARSHADI, 2013; BORGES, 2014). Some reasons can be pointed out here to give support to this decision. First, the unconfined tests have a wide application in the academic studies conducted in Brazil (e. g., MARTINS et al., 2011; NASCIMENTO, 2008; ONOFRE et al., 2013), even though other authors took a different approach and carried out confined tests (FONTES et al., 2010). Second, there was an expectation about the publication of a Brazilian standard test method for the uniaxial repeated creep test and the determination of F_N (BORGES, 2014). This test is currently standardized in Brazil under the designation ABNT NBR 16505[30]. Third, there seems to be a consensus among researchers that the results of the FN tests can be well correlated with mixture rutting in the wheel tracking devices, even in the unconfined condition (GIBSON et al., 2012; MOHAMMAD et al., 2006; NASCIMENTO, 2008; ZHANG et al., 2015). One last reason is that dense-graded asphalt mixtures are typically used at the top of the surface layer, even when the thickness of this layer is very large. In such a case, they are not subjected to confinement in the pavement.

4.4. Analysis and Implications of the MSCR Data and Rutting Parameters

4.4.1. MSCR Tests and Suggesting Refinements in the Superpave® Specification

As described earlier, the MSCR tests with asphalt binders provide the results of the parameters R, J_{nr} and $J_{nr,\,diff}$. The percent recovery is able to indicate the amount of elastic response in the

[30] ASSOCIAÇÃO BRASILEIRA DE NORMAS TÉCNICAS. (2016). **ABNT NBR 16505:** Misturas asfálticas – Resistência à deformação permanente utilizando o ensaio uniaxial de carga repetida [Hot mixtures asphalt – Resistance to permanent deformation by uniaxial repeated load test]. 9 p. São Paulo, SP. In Portuguese.

binder and, to some extent, the strength and distribution of polymer networks within the formulation. The nonrecoverable compliance provides an indication of the susceptibility of the material to rutting and the most suitable traffic level at the maximum expected pavement temperature. The percent difference in nonrecoverable compliances shows the level of stress sensitivity of the binder and its degree of nonlinear response, and it must be no greater than 75% for the material to be used for paving applications (Table 3 from the AASHTO M320-09 standard). The percent difference in recoveries at 0.1 kPa (*R100*) and 3.2 kPa (*R3200*) – parameter R_{diff}, see Equation (32) – can be currently found only in the ASTM D7405-15 standard, but it was also included in the analysis of data in an attempt to evaluate the effect of higher stress levels on the elastic response of the binder, but only at 1/9 s. Differently from the parameter $J_{nr,\,diff}$, the current Superpave® specifications do not set any minimum or maximum value for R_{diff}.

$$R_{diff}(\%) = \frac{R100 - R3200}{R100} \times 100 \tag{32}$$

The rutting data in the MSCR tests and at longer creep times were examined with focus on the following topics: (a) the level of increase in the rutting potential of the material as the loading conditions become more severe; (b) the degree of nonlinearity between J_{nr} and loading time; (c) calculations of the corresponding vehicle speeds as based on the Equations (30), (31) and (33) where r is the tire contact radius (HUANG, 2004); (d) the variations in the adequate traffic level of the binder with increasing creep time and changes in the criteria for assigning it (see Appendix B); and (e) the reduction in the amount of elastic response. While developing Equation (33), Huang (2004) assumed that the magnitude of the load changes with time according to a haversine function, and also that this load has practically no effect at a distance of (6×r) from the point of its application. In conclusion, two empirically-based equations proposed by Pereira et al. (1998, 2000) and one theoretically-derived equation suggested by Huang (2004) were used here in order to observe the correlations between Tr_{sp} and J_{nr}. Such correlations may indicate whether the creep time can or cannot be used as a complementary analysis of the current Superpave® criteria for choosing the traffic level, which is assumed here to be the one established by AASHTO M320-09.

$$t_F = \frac{12 \times r}{Tr_{sp}} \tag{33}$$

It is known that the contact area between the tire and the surface of the pavement is not exactly circular, but it is assumed to have this shape for simplification purposes. Another conservative approach made in the calculations is that the tire pressure is equal to the contact pressure, which is not exactly true because it will depend on the type of tire, i. e., low-pressure or high-pressure one (HUANG, 2004; PAVEMENT INTERACTIVE, 2008a). The relationship between the contact radius *r* and the tire inflation pressure *p* is given by Equation (34), where *P* is the total load on the tire. Typical values for *P* and *p* are 18.9 kN (4,250 lb) and 689 kPa (100 psi), respectively (PAVEMENT INTERACTIVE, 2008a). Based on these values, it can be concluded that the contact radius is approximately equal to 3.68 in (≈ 9.34 cm). Huang (2004) proposed an *r* value of 6 in (≈ 15.24 cm) in pavement problems, which was closely followed by Golalipour (2011). The present study took into account the two numerical values and identified the one that provided the best correlations with the MSCR laboratory data.

$$r = \sqrt{\frac{P}{p \times \pi}} \tag{34}$$

The four creep times selected in this study were used in the equations above and the corresponding speeds were determined. Table 9 shows a summary of the data and, as it can be seen, the equation proposed by Huang (2004) was applied to the tire contact radii of 6 and 3.68 in. As can be inferred from this table, the creep times in the MSCR tests (binder tests) were divided by 10 in order to yield the creep times in the mixture. This is because the three equations are referenced on the pavement (mixtures), either in a theoretical or field-based way. It seems that the proportion of 1:10 between the loading times in the mixture and the binder tests is appropriate, since it has been extensively used in the literature to identify correlations from both laboratory tests with a great degree of success (BAHIA et al., 2001a, 2001b; DELGADILLO and BAHIA, 2010; GIBSON et al., 2012; GOLALIPOUR, 2011; MARTINS et al., 2011). It may also be important to remind that the MSCR and the RCRT tests – creep time of 1.0 s – were both derived from the RSST-CH test, which takes into account a creep time of 0.1 s (ANDERSON et al., 2010).

Initially, linear regression trendlines between J_{nr} and Tr_{sp} were explored because this was the method adopted by Pereira et al. (2000) to establish a correlation between the vehicle speed and loading time (which is indirectly related to J_{nr}). Since this study was conducted at the pavement temperature of 50°C, the linear correlations between J_{nr} and Tr_{sp} were investigated only at 52°C. On the other hand, the one found in the publication by Huang (2004) was used at all MSCR testing temperatures due to its theoretical derivation, i. e., not associated with any pavement temperature. By assuming that the asphalt binder can be represented by a four-element Burgers model as shown in Equations (13) and (14), it is possible to describe the response of the material in terms of the total creep compliance *J(t)* rather than the total strain *ε(t)*. In such a case, the resulting equation will be the following – Equation (35):

Table 9 – Vehicle speeds as based on the equations from Pereira et al. (1998, 2000) and Huang (2004)

equation and source[c]	creep time (s)[a]	truck speed (km/h)
$Tr_{sp}\left[\frac{km}{h}\right] = -94.9 \times t_F[s] + 73.4$ (PEREIRA et al., 2000)	0.1	63.9
	0.2	54.4
	0.4	35.4
	0.8	N/A[b]
$t_F[s] = \frac{8}{Tr_{sp}\left[\frac{km}{h}\right]}$ (PEREIRA et al., 1998)	0.1	80.0
	0.2	40.0
	0.4	20.0
	0.8	10.0
$t_F[s] = \frac{1.8288}{Tr_{sp}\left[\frac{m}{s}\right]}$ (HUANG, 2004) → r = 6 in	0.1	65.8
	0.2	32.9
	0.4	16.5
	0.8	8.2
$t_F[s] = \frac{1.1217}{Tr_{sp}\left[\frac{m}{s}\right]}$ (HUANG, 2004) → r = 3.68 in	0.1	40.4
	0.2	20.2
	0.4	10.1
	0.8	5.0

[a] the creep times in the MSCR tests were divided by 10 in order to obtain the corresponding times in the mixture and calculate the vehicle speeds.
[b] N/A: not applicable (vehicle speed < 0).
[c] t_F = creep or loading time, Tr_{sp} = truck speed, r = tire contact radius.

$$J(t) = J_E + J_V(t) + J_D(t) = \frac{1}{E_{spring,1}} + \frac{t}{\eta_{dashpot,1}} + \frac{1}{E_{spring,2}} \times \left(1 - e^{\frac{-t}{\Lambda_1}}\right) \qquad (35)$$

where J_E is the elastic component, $J_D(t)$ is the delayed elastic component and $J_V(t)$ is the viscous component. It is implicit in this equation that $J_V(t)$ is related to J_{nr} because both are associated with the unrecoverable portion of the total strain, and $J_V(t)$ is linearly related to the creep time. Since this loading time increases by following a nonlinear function ($t_F = 2^x$ where $0 \leq x \leq 3$), nonlinear regression trendlines will be used. It is anticipated that the delayed elastic portion of the response of the binder will have some effect on the degrees of correlation between J_{nr} and creep time.

The two longer recovery times used in this dissertation – 240 and 500 s – aimed at evaluating the effects of delayed elasticity on the response of the binder, as previously described. It was hypothesized that the asphalt binders with high degrees of elasticity would demand much longer recovery times than those with low levels of elasticity, as based on the responses of these materials at standardized and longer creep times. As a consequence, the 12 formulations were separated according to their degrees of elasticity – two groups, “Group A” and “Group B” – and their creep-recovery behavior at such longer creep times was investigated and correlated with the technical literature. Excel spreadsheets were used in the calculations to determine the model parameters. These experiments are in accordance with other studies, even though some authors decided to study the time-dependent elastic response of the material based on mathematical approaches (MASAD et al., 2009).

4.4.2. Summary of the Binder Rutting Parameters

The binder rutting parameters selected in this study covered all the mostly used tests for the characterization of the rheological behavior of the material: (a) empirical-based softening point *R&B*; (b) original Superpave® parameter $G^*/sin\delta$ and the Shenoy’s parameter $|G^*|/[1-(1/tan\delta sin\delta)]$ under dynamic oscillatory shear loading; (c) the nonrecoverable creep compliance J_{nr} under repeated creep loading in the MSCR test and at 3.2 kPa; and (d) the viscous component of the creep stiffness G_V from the four-element Burgers model. Some authors have made attempts to evaluate the high- and low-temperature resistances of asphalt binders by means of only one single parameter (LI et al., 2015; YI-QIU et al., 2014), e. g., Equation (36) from Li et al. (2015). However, such parameters were not considered in the present study because the low-temperature properties (i. e., creep stiffness and relaxation rate after 60 s of loading) were not determined in the experimental part.

$$\frac{G^*}{sin\delta \times (1 - cos\delta)} \tag{36}$$

It may be important to note that the determination of G_V in the present piece of research did not follow exactly the same procedure described in the report by Bahia et al. (2001a). In the original NCHRP Report 459, it was suggested to calculate G_V based on the fitting parameters at the 50th and the 51th cycles in order to account for the steady state phenomenon of the binder. Since the number of cycles remained unchanged in the MSCR protocols, G_V was determined by fitting the Burgers model to the last two cycles at 0.1 kPa (19th and 20th ones) and averaging the results for the original and replicate samples. Even with this limitation, it is believed that the choice for the last two creep-recovery cycles in the calculations of G_V will maximize the effects of steady state on the analysis of data.

4.5. Rheological Models for the Binder and Mixture Laboratory Data

4.5.1. Binder Data

Basically, four models were used in this study to evaluate the rheological response of the asphalt binders at high pavement temperatures. The first model is an exponential equation to fit binder data under oscillatory shear loading and observe the reduction in $G^*/sin\delta$ with increasing temperature (LAUKKANEN et al., 2015). This model is comprised by two regression parameters (A and B), as shown in Equation (37). Elseifi et al. (2003) used a quite similar model in their paper to study the rutting performance of styrene-butadiene-styrene and styrene-ethylene/butylene-styrene-modified binders, but the parameter was $G^*/tan\delta$ rather than $G^*/sin\delta$[31]. Since the numerical value of $G^*/sin\delta$ will always decrease with temperature, the constant B will be negative for all binders. If a specific material shows a lower sensitivity to temperature than another one, the B value will be lower for the former than the latter.

$$\frac{G^*}{sin\delta} = A \times e^{B \times T} \tag{37}$$

The binder data in the repeated creep tests at 100 Pa were modeled by using two linear viscoelastic models. The first is the well-known four-element Burgers model, which has been considerably used in the literature to determine the rutting parameter G_V. The second is the generalized Voigt model with two retardation times (Λ_1 and Λ_2), which resembles the one considered in the piece of research by Divya et al. (2013). The main difference between the model used by Divya et al. (2013) and the one applied here is the presence of one isolated dashpot element in the latter (Figure 18). In many cases, the literature makes reference to this model as a traditional association of Voigt models in series without any isolated spring or dashpot element. However, the format used here is also alternatively used (MERUSI, 2012; WOLDEKIDAN, 2011).

From the data obtained in the MSCR test, the model parameters $E_{spring,\,1}$ (E_M), $E_{spring,\,2}$ (E_K), $E_{spring,\,3}$, $\eta_{dashpot,\,1}$ (η_M), $\eta_{dashpot,\,2}$ (η_K) and $\eta_{dashpot,\,3}$ were determined. The subscript "1" refers to the isolated elements, whereas the subscripts "2" and "3" refer to the elements associated in parallel. As it can be implied from these explanations, the elements $E_{spring,\,3}$ and $\eta_{dashpot,\,3}$ are restricted to the generalized Voigt model – three springs and three dashpots – and the other four elements can be found either in the Burgers or the generalized Voigt model. The differences between the

[31] Elseifi et al. (2013) preferred the parameter $G^*/tan\delta$ over the conventional $G^*/sin\delta$ because, according to their literature review, the term $tan\delta$ is more sensitive to variations in the phase angle than $sin\delta$. As a consequence, $G^*/tan\delta$ would reflect the changes in the rutting resistance of the binder more accurately than $G^*/sin\delta$.

calculated strains γ_{calc} and the raw strains γ_{raw} at all cycles were used to obtain the average absolute error (AAE), see Equation (38) (LIU and YOU, 2009). The AAE value conveys the idea of how well the model describes the response of the asphalt binder under repeated creep loading. Due to the successful application of this parameter in a previous paper by Domingos and Faxina (2015b), it was used in the present study as well. It may be important to emphasize that the generalized Voigt model was fitted to the raw data at 1/9 s and 100 Pa only when AAE > 5%.

$$AAE(\%) = \sum_{i=1}^{N} \left(\frac{\gamma_{calc,i} - \gamma_{raw,i}}{\gamma_{raw,i}} \right) \times 100 \tag{38}$$

With respect to the responses of the asphalt binders in the remaining test conditions (2/9, 4/9, 8/9, 1/240 and 1/500 s, as well as 3,200 Pa at 1/9 s), the Equations (19) and (39) were used (SABOO and KUMAR, 2015). For the reader's convenience, Equation (19) is shown again below and the material parameters are characterized by the constants A, B, n and α (multiplication of B by n). Some reasons can be cited to justify the choice for these models: (a) they are comprised by simple equations with a few parameters and the power law increment during creep is based on typical representations of the creep compliance function; (b) the parameter n accounts for the nonlinearity of the binder, and also corrects the deficiencies of the original power equation and the Boltzmann superposition principle in describing the response of the material during recovery; (c) the parameter α correlated very well with the percent recovery from MSCR, which reinforces the idea that elasticity has some impact on the rutting resistance of asphalt binders; and (d) the α value may be used as a complementary criterion to estimate the traffic level of the binder. In other words, power law equations seem to be appropriate to cover either the linear or the nonlinear regions of the creep-recovery curves (CELAURO et al., 2012; SABOO and KUMAR, 2015).

$$\varepsilon_{rec}(t) = A \times t^{B} - A \times (t - t_F)^{B \times n} \tag{19}$$

$$\varepsilon(t) = A \times t^{B} \tag{39}$$

The constants of the two reported equations were determined with the use of Excel spreadsheets, and the highest possible R^2 value (i. e., the best fitted curve) was targeted in the analysis. It is anticipated here that all the R^2 values were higher than 0.85, which indicates that the modified power model could represent the response of the binders in the MSCR tests fairly well. The variations in the α values with t_F were compared with the ones in R at 100 and 3,200 Pa for the same creep times, similarly to what was one in the paper by Saboo and Kumar (2015). Comments about the decreases in the level of elasticity of the asphalt binder with increasing t_F

values were also made, but only for the materials that showed a high degree of elasticity at the standardized creep-recovery times.

The steps followed in the analysis of the degree of nonlinearity of modified asphalt binders with increasing t_F values are similar to the ones reported in a recently published paper by Domingos and Faxina (2017). Basically, these steps can be defined as follows: (a) correlations between the n values and the parameters R and J_{nr} from the MSCR test; (b) percentages of increase and decrease in the parameters A, B and n with increasing t_F (SABOO and KUMAR, 2015); and (c) degrees of correlation between J_{nr} and t_F in a log-log chart (DELGADILLO and BAHIA, 2010; DELGADILLO et al., 2012). With respect to the latter, deviations from a straight line can be interpreted as a nonlinear response of the material, and they were associated with the n values from the power models. In other words, two different approaches (variations in n and graphical analyses of the correlations between J_{nr} and t_F) were adopted to determine if the MSCR testing conditions were enough to place the binders within the nonlinear viscoelastic range.

4.5.2. Mixture Data

The repeated creep data of the asphalt mixtures were studied with respect to the parameters of the Francken model, Equation (40). The permanent strain $\varepsilon_p(N)$ is calculated at each creep-recovery cycle (N) based on the numerical values of the fitting parameters A, B, C and D. The first part of the equation describes the response of the mixture in the primary and secondary regions of the creep curve (i. e., before the F_N value is reached), whereas the second and exponential part can describe this response within the tertiary region (i. e., after the F_N value). This model was proposed by researchers from the Arizona State University, US (BILIGIRI et al., 2007), among many other models as the one that better explains the data and characterizes all the three regions of the mixture's creep curve. The second derivative of the model – Equation (41) – is the gradient of the strain slope, and the cycle at which this gradient changes from negative to positive (i. e., the inflection point) corresponds to the F_N value. It is also possible to estimate F_N as the cycle that shows the minimum strain slope (i. e., the first derivative of the model reaches a minimum value), but this task requires a harder effort from researchers.

$$\varepsilon_p(N) = A \times N^B + C \times (e^{D \times N} - 1) \tag{40}$$

$$\frac{\partial^2 \varepsilon_p}{\partial N^2} = A \times B \times (B - 1) \times N^{B-2} + (C \times D^2 \times e^{D \times N}) \tag{41}$$

In addition to the determination of F_N, there are some fair indications that the constant C is representative of the plastic failure of the sample: the higher the numerical value of this constant is, the higher the resistance of the mixture to rutting might be. The promising outcomes of the Francken model have also been identified by another study from Ameri et al. (2014), whose experimental plan and analysis closely approached the ones from Biligiri et al. (2007). In addition to the technical advantages over other models (e. g., some models could not identify the occurrence of the tertiary stage in the creep curve), Ameri et al. (2014) pointed out that the Francken model showed the lowest variability among the replicates of the mixtures prepared with the unmodified and EVA-modified mixtures. However, some authors (PAPAGIANNAKIS et al., 2015) claimed that the model can mask the minimum strain rate of some mixture curves when compared with the corresponding original curves. In other words, there seems to be no consensus about the applicability of the model to all types of mixtures and gradation curves.

Differently from the F_N value (which is the number of a specific cycle), Zhang et al. (2013) have recommended the FN index (FN_I) as a better indicator of the susceptibility of asphalt mixtures to permanent deformation. As can be seen in Equation (42), this index is obtained by the ratio of the accumulated strain at the FN point (ε_{pFN}) to the corresponding cycle number. In other words, FN_I is a normalized strain value and mixtures with lower values for this index are expected to show higher rutting resistances. The authors concluded that FN_I may replace the current F_N value in the analysis of the rutting potential of mixtures, since this parameter was able to provide better correlations with the rankings of mixtures in other laboratory tests (e.g., the repeated load permanent deformation test – RLPDT) than the FN cycle by itself. Promising results were also obtained by Li et al. (2014) and Walubita et al. (2013), who concluded that the parameter FN_I is able to differentiate among the repeated creep responses of hot-mix asphalt mixtures and can be used to add important information to the accelerated loading protocols for routine mix design projects.

$$FN_I = \frac{\varepsilon_{pFN}}{F_N} \tag{42}$$

In summary, the Francken model was selected to fit the mixture data and the constant C was evaluated with respect to its numerical value and the susceptibility of the mixture to rutting (i. e., F_N). Then, the permanent strain at F_N was used to determine the parameter FN_I and comparisons between the two were drawn to identify differences and similarities among the rankings of mixtures. In the cases that the mixture sample did not fail by excessive tertiary deformation before 10,000 cycles (i. e., F_N is not observed up to the end of the test), FN_I was not determined and the analysis was focused on the accumulated strain in the end of the test (γ_{per}). It may be important to note that the mixtures were separated into two different groups – the ones which failed before 10,000 cycles and the ones which did not fail before this number of cycles – and the aforementioned comparisons were made among the mixtures that belong to the same group.

CHAPTER 5: Mixture Rutting Data and Analysis

5.1. Highlights

- Differently from other tests such as DM, the FN protocol does not seem to cause many controversies among researchers about its applicability as an appropriate mixture rutting test.
- The very low degrees of improvement in the F_N values of the AC+PPA suggest that the modifier content (2.0% by weight) may not be the optimum one for the binder from the Lubnor refinery.
- Good to excellent correlations ($R^2 > 0.70$) between the parameters from the repeated creep tests (J_{nr} and G_V) at 64°C and F_N at 60°C were obtained for the mixtures that failed in the FN tests.
- The rankings of binders based on the parameters from oscillatory shear and empirical tests hardly showed any degree of correlation with the ones referenced on F_N and γ_{per} (mixtures).
- The parameter FN_I and the constant C from the Francken model did not correlate well with F_N, which indicates that their applicability as mixture rutting parameters is fairly limited.
- The criteria found on Superpave® and Delgadillo et al. (2006b) did a good job in proposing the intervals of ESAL's and traffic levels that each mixture is expected to deal with in the pavement.
- Despite the advances of MSCR and its parameters in the study of rutting on binders, the intervals of traffic levels contain a certain degree of subjectivity and cannot be taken literally.

5.2. Short Introduction on the Mixture Tests for Rutting: Advantages and Disadvantages

The resistance of the asphalt mixture to rutting has been a matter of serious concern for a long time, especially because heavier traffic loads, lower vehicle speeds and higher climatic temperatures accelerate the formation of rutting and lead to hazardous driving conditions. This phenomenon can be attributed to a combination of densification (change in the volume of the mixture) and shear deformation. Shear deformation is the primary rutting mechanism and plays a major role after the initial densification phase (BROVELLI et al., 2015; WASAGE et al., 2009). Rutting typically takes place at very high stress and strain levels, i. e., the nonlinear viscoelastic range of the asphalt binder (D'ANGELO, 2010a). Literature reviews made by Tapkin et al. (2009) and Wasage et al. (2009) indicated that rutting commonly occurs within a depth of 50-100 mm of the pavement. Since the binder properties have a crucial role in the response of the mixture, the characterization of these properties and parameters and the ability of the test in estimating the performance of the material are extremely important.

In order to accurately estimate the susceptibility of asphalt mixtures to rutting, the test protocol must simulate the actual loading, climate and confining conditions of the pavement as close as possible. In this manner, researchers have been studying the applicability of some laboratory tests in providing reasonable results and good estimations of the rutting potential of mixtures. These include dynamic modulus – DM (GIBSON et al., 2012; LI et al., 2011; MOHAMMAD et al., 2006; WALUBITA et al., 2012; WITCZAK et al., 2002; ZHANG et al., 2013), accelerated loading facilities – ALF's (D'ANGELO et al., 2007; GIBSON et al., 2012; HICKS et al., 1993) and repeated creep/FN tests (APEAGYEI, 2014; BORGES, 2014; FONTES et al., 2010; GIBSON et al., 2012; MOHAMMAD et al., 2006; ONOFRE et al., 2013; TAPKIN et al., 2009; WALUBITA et al., 2012; WASAGE et al., 2009; ZHANG et al., 2013). As it can be seen, the repeated creep tests have a widespread application in the characterization of the asphalt mixtures with the highest and the lowest susceptibilities to rutting, including the Brazilian studies. Their advantages over other procedures such as DM have been outweighed in the literature (APEAGYEI, 2014; GIBSON et al., 2012; MOHAMMAD et al., 2006; WALUBITA et al., 2012; ZHANG et al., 2013), which justifies the selection of FN as the mixture test in the study. These advantages include the following:

- good correlations with the rut depths measured on ALF's and field pavement sections;
- fairly good representation of the loading and confining conditions of the pavement; and
- reasonable test time (less than three hours).

Although many researchers have explored the possibility of utilizing the DM test in the characterization of the rutting performance of asphalt mixtures, the results seemed to be not very conclusive. This is because the rankings of mixtures based on the DM value – with or without the incorporation of the phase angle δ in the analysis – did not correlate well with the ones of the permanent deformation tests (APEAGYEI, 2014; GIBSON et al., 2012; MOHAMMAD et al., 2006), even though other publications indicated an opposite trend (WALUBITA et al., 2012; WITCZAK et al., 2002). Zhang et al. (2013) did not recommend the DM test for routine hot-mix asphalt design projects, since it is a time-consuming procedure (more than three days). However, Gibson et al. (2012) claimed that the DM test still has its own merits and must be taken into account in the mechanistic-empirical performance prediction of a pavement and the viscoelastic continuum damage analysis. Due to the opposite points of view about the DM test, there seems to be no consensus in the literature about the applicability of the DM test in predicting the rutting resistance of mixtures (APEAGYEI, 2014).

The flow number test, which is also labeled as *repeated load testing in uniaxial compression* in the NCHRP Report 465 (WITCZAK et al., 2002), is basically comprised by the application of haversine axial loads on an asphalt mixture sample – diameter of 100 mm and height of 150 mm – until failure by excessive tertiary deformation or the absence of failure after 10,000 creep-recovery cycles. The stress levels can vary from 69 to 207 kPa in the unconfined tests and from 483 to 966 kPa in the confined ones. The confining pressures may range from 35 to 207 kPa. As previously discussed, the confined tests are expected to better represent the actual conditions of the mixture in the pavement, but they were not considered in this piece of research. It is also possible to reduce the confining pressure and obtain similar results in less-confined tests by controlling the deviator stress (GIBSON et al., 2012).

Based on the aforementioned paragraphs, it can be implied that the technical literature highlights the benefits of utilizing the unconfined repeated creep test (FN test) in the study of the rutting potential of asphalt mixtures, and also that similar results can be obtained in other laboratory tests by choosing the appropriate temperature, loading and confining conditions. There are some concerns regarding the performances of permeable friction course mixtures and the ones with very high percentages of air voids (as higher as 20%) in the FN tests, as pointed out in the papers by Walubita et al. (2013) and Zhang et al. (2013). However, this does not seem to affect the outcomes of the tests carried out in the present study, since the mixtures were prepared by following a dense-graded gradation curve and the percentages of air voids are much lower than 20% (about 7%).

5.3. Flow Number Test Results

5.3.1. The Role of F_N and Correlations with the Binder Parameters

Table 10 shows a summary of the results of the flow number tests (mean values) for all the eight mixtures that failed before 10,000 cycles: 50/70 original asphalt binder, AC+PPA, AC+Elvaloy+PPA, AC+rubber+PPA, AC+SBS, AC+SBS+PPA, AC+SBR+PPA and AC+SBR. The corresponding coefficients of variation (COV's) and the binder parameters after short-term aging (Shenoy's parameter $|G^*|/[1-(1/\tan\delta\sin\delta)]$, Superpave® parameter $G^*/\sin\delta$, G_V, *R&B* and J_{nr} at 3.2 kPa and 1/9 s) are also reported for comparison purposes. The COV's ranged from 4.5 to 24.8% for all the studied formulations, with exception of the AC+rubber+PPA (COV ≈ 33.9%). These variations are in close agreement with the ones reported by other authors, see the experimental results published by Ameri et al. (2014), Apeagyei (2014), Bhasin et al. (2005), Li et al. (2014), Walubita et al. (2013), Zhang et al. (2013) and Rodezno et al. (2010) as some representative examples.

Table 10 – Summary of the results of some mixture and binder tests for analysis of the degrees of correlation

asphalt binder	mixture (60°C)		binder data at 64°C and after RTFO-aging				
	F_N (mean)	COV (%)[a]	G_V (kPa)[b]	*R&B* (°C)	Shenoy's parameter (kPa)	$G^*/\sin\delta$ (kPa)	J_{nr} (kPa^{-1})[b]
base binder (AC)	2,167	4.49	0.31	53.3	3.30	2.98	3.352
AC+PPA	2,533	8.22	2.66	65.5	22.16	6.42	0.416
AC+Elvaloy+PPA	7,050	24.82	2.24	65.3	11.49	6.47	0.367
AC+rubber+PPA	4,191	33.87	1.27	61.0	9.73	6.96	1.069
AC+SBS	4,991	8.21	1.43	68.1	9.00	6.77	0.997
AC+SBS+PPA	6,110	21.11	2.17	63.1	14.46	10.31	0.634
AC+SBR	3,312	11.27	1.23	64.6	8.35	6.42	1.055
AC+SBR+PPA	5,875	12.90	1.80	66.8	12.69	9.29	0.662

[a] COV: coefficient of variation.
[b] the parameters G_V and J_{nr} were determined at 1/9 s and the stress levels of 0.1 and 3.2 kPa, respectively.

The asphalt mixtures prepared with modified binders typically showed much higher F_N values at 60°C than the ones prepared with the original material, and this can be translated into higher resistances to rutting. Surprisingly, the AC+PPA was the only formulation that did not follow this trend (mean F_N values of 2,167 for the unmodified asphalt binder and only 2,533 for the AC+PPA). Since all the binder data of the AC+PPA point to a very low rutting potential of the modified material, one may be inclined to think that there is something wrong with the analysis or the laboratory testing results. However, an extensive investigation into the technical literature reveals that some odd cases with PPA-modified asphalt binders were also reported by other researchers, including field-performance cases. This will be discussed in the forthcoming paragraphs before a thorough evaluation of the other binder and mixture data and the correlations among them is made.

Similarly to any other modifier, the incorporation of PPA into the binder is intended to improve the service life of the pavement. Many studies indicated that the use of PPA in conjunction with another modifier can increase the rutting and the fatigue resistances of the mixture at higher rates than the corresponding ones with PPA alone. For instance, Fee et al. (2010) observed that a PG 64-22 binder modified with 0.75% of PPA and 1.0% of hydrated lime yielded an excellent rutting response in the Hamburg wheel tracking test, as well as the combination of this same binder with 1.1% of Elvaloy® and 0.3% of PPA. Clyne et al. (2012) reached similar conclusions with respect to the behavior of mixtures prepared with PPA, SBS, SBS+PPA and Elvaloy+PPA, i. e., the binders modified with PPA and another additive typically performed better than the ones with PPA alone. Finally, Li et al. (2011) found out that mixtures prepared with PPA alone are statistically less resistant to fatigue cracking than the ones with SBS, SBS+PPA and Elvaloy+PPA in the DM tests.

In a detailed investigation about the long-term field performance of asphalt mixtures with and without PPA in the composition, Buncher and Von Quintus (2014) concluded that the average rut depths of pavement sections with PPA-modified asphalt binders are approximately equal to the ones with non-PPA-modified materials. This can be inferred from the data plotted in Figure 32, which indicates that the differences among the depths of the wheel paths are not significant and can be null – or even lower – for the sections without PPA in some cases (red circle in the figure). In another study with granite and limestone aggregates, Reinke et al. (2012) found out that the rutting response of the control binder (PG 58-28) in the Hamburg wheel tracking test and at 50°C may be quite similar to the one of the PPA-modified binder (PG 64-28) for some aggregate types, see the yellow boxes in Figure 33 and Figure 34 for the mixtures designed for 1 and 10 million ESAL's (respectively). Based on these results, it can be implied that binder modification with PPA does not always ensure a better rut performance of the asphalt mixture in the field or the laboratory.

The combination of these findings with the strong dependency of PPA on the chemical composition of the base binder (BAUMGARDNER et al., 2012; BUNCHER, 2016; FEE et al., 2010) and the issues regarding the effect of aggregate type on mixture performance make it possible to infer that the determination of the real benefits of PPA modification is a challenging task (BUNCHER, 2016). In other words, it might be said that some AC+PPA formulations will result in mixtures with very high degrees of improvement in their mechanical properties and others will not, and also that the chemical composition of the original binder is one of the variables that will profoundly influence on this amount of improvement. As it can be seen in Figure 35, all the replicates of the AC+PPA showed higher F_N values when compared with the original binder; however, these values do not markedly differ from one material to the other. In summary, it is not clear that the addition of 2.0% of PPA to the binder from the Lubnor-Petrobras refinery will result in mixtures with much higher resistances to rutting, as based on the outcomes of the FN tests.

Due to the particular characteristics of the asphalt mixtures prepared with the AC+PPA, they were excluded from the next steps of the analysis of the correlations between mixture and binder rutting data. Initially, these correlations were based on the binder parameters summarized in Table 10 and the mean F_N values by themselves. Later, an attempt to discover the presence or absence of correlations between the constant C from the Francken model and F_N was made. This last subject of investigation is quite interesting, since it has not been deeply studied by other authors who used the model in their papers (AMERI et al., 2014; BILIGIRI et al., 2007; PAPAGIANNAKIS. et al., 2015). The same approach was adopted for the flow number index FN_I, that is, the rankings of asphalt mixtures based on F_N and FN_I were compared with each other in order to show similarities and differences among them.

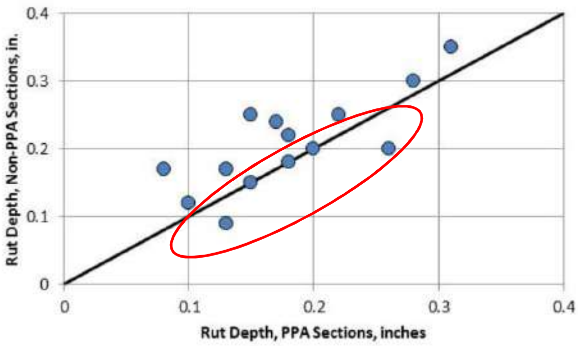

Figure 32 – Comparisons among the average rut depths (in inches) of the pavement sections with and without PPA-modified binders after many years of service life [adapted from Buncher and Von Quintus (2014)]

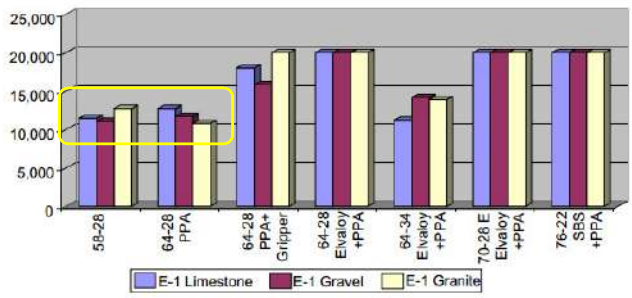

Figure 33 – Number of cycles to achieve 12.5 mm of rut depth in the mixtures designed for 1,000,000 ESALs – temperature of 50°C and the Hamburg wheel tracking device [adapted from Reinke et al. (2012)]

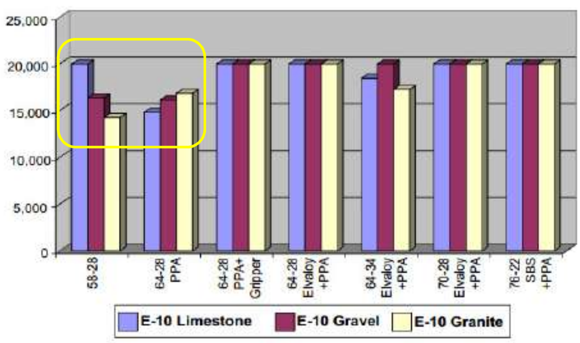

Figure 34 – Number of cycles to achieve 12.5 mm of rut depth in the mixtures designed for 10,000,000 ESALs – temperature of 50°C and the Hamburg wheel tracking device [adapted from Reinke et al. (2012)]

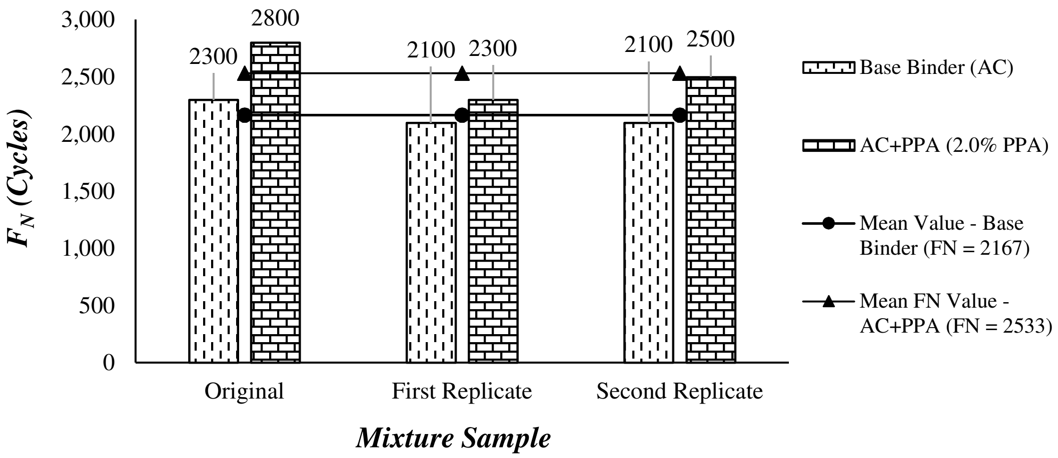

Figure 35 – Flow number (F_N) values of each mixture sample for the 50/70 base binder and the AC+PPA

The outputs of the binder and mixture tests reported above were ranked from the less to the most susceptible to rutting (numbers from 1 to 7), and the data are presented in Table 11. The rankings based on the two parameters derived from repeated creep tests – G_V and J_{nr} – clearly show a pattern of behavior, i. e., there are many similarities across the numerical values. On the other hand, the other three binder parameters based on empirical and oscillatory shear protocols (*R&B*, $G^*/sin\delta$ and the Shenoy's parameter $|G^*|/[1-(1/tan\delta sin\delta)]$) show totally different rankings and the similarities between them and the reference one are weak. Other than underlining the superiority of J_{nr} and G_V over *R&B*, $G^*/sin\delta$ and $|G^*|/[1-(1/tan\delta sin\delta)]$, this is in accordance with the conclusions drawn by others worldwide (ADORJÁNYI and FÜLEKI, 2013; ANDERSON, 2011; BAHIA et al., 2001a; BEHNOOD et al., 2016; D'ANGELO, 2008; 2009, 2010b; D'ANGELO et al., 2007; DELGADILLO et al., 2006a; DREESSEN et al., 2009; DuBOIS et al., 2014; GIERHART, 2013; GOLALIPOUR, 2011; HICKS et al., 1993; JONES et al., 1998; LAUKKANEN et al., 2015; MARTINS et al., 2011; SYBILSKI, 1996a; WASAGE et al., 2011; ZHANG et al., 2015).

With respect to the degrees of correlation between the outcomes of binder and mixture tests, it has been usual among authors to determine these R^2 values by means of linear regression trendlines (ANDERSON, 2011; BAHIA et al., 2001a, 2001b; D'ANGELO, 2008; 2009, 2010b; D'ANGELO et al., 2007; DELGADILLO et al., 2006a; GOLALIPOUR, 2011; HICKS et al., 1993; LAUKKANEN et al., 2015; SYBILSKI, 1996a; WASAGE et al., 2011). However, logarithmic and power law equations were also used in some publications (D'ANGELO, 2009; DREESSEN et al., 2009; MARTINS et al., 2011; MOHAMMAD et al., 2006; SHERWOOD et al., 1998). As a consequence, linear and power trendlines were selected and fitted to the data in an attempt to identify the existence of correlations between them. The choice for the power law equations is mainly referenced on a previous study conducted by Martins et al. (2011).

Table 11 – Rankings of asphalt binders and mixtures from the less (No. 1) to the most susceptible to rutting (No. 7) based on the numerical values of some laboratory tests

asphalt binder[b]	F_N at 60°C (reference ranking)[a]	rankings of asphalt binders at 64°C[a, c]				
		G_V at 0.1 kPa	J_{nr} at 3.2 kPa	*R&B*, aged	*G*/sinδ*, aged	Shenoy's parameter
AC+Elvaloy+PPA	1	1	1	3	5	3
AC+SBS+PPA	2	2	2	5	1	1
AC+SBR+PPA	3	3	3	2	2	2
AC+SBS	4	4	4	1	4	5
AC+rubber+PPA	5	5	6	6	3	4
AC+SBR	6	6	5	4	6	6
base binder (AC)	7	7	7	7	7	7

[a] the gray-shaded boxes indicate agreement between rankings of mixtures and binders.
[b] with exception of the base binder (PG 64-xx), all the other materials are graded as PG 76-xx in the AASHTO M320-09 specification, Table 3.
[c] the parameters G_V and J_{nr} were determined at 1/9 s (1-s creep time and 9-s recovery time).

The next two figures show the R^2 values and the corresponding linear regression equations for all the above-mentioned binder rutting parameters, i. e., the repeated creep parameters J_{nr} and G_V (Figure 36) and the oscillatory shear-based parameters *G*/sinδ* and *|G*|/[1-(1/tanδsinδ)]* and the softening point *R&B* (Figure 37). The two parameters derived from repeated creep protocols yielded good to excellent correlations with mixture data (0.705 for J_{nr} and 0.926 for G_V). Even though the Shenoy's parameter provided a good correlation with F_N as well ($R^2 \approx 0.76$), the marked differences between the rankings of binders and mixtures reported in Table 11 clearly indicate that this correlation is only a coincidence. The same can be said for *R&B* and *G*/sinδ*, that is, the R^2 values of 0.472 and 0.502 (respectively) cannot be interpreted as positive findings because the binders and mixtures are not ranked in a similar way.

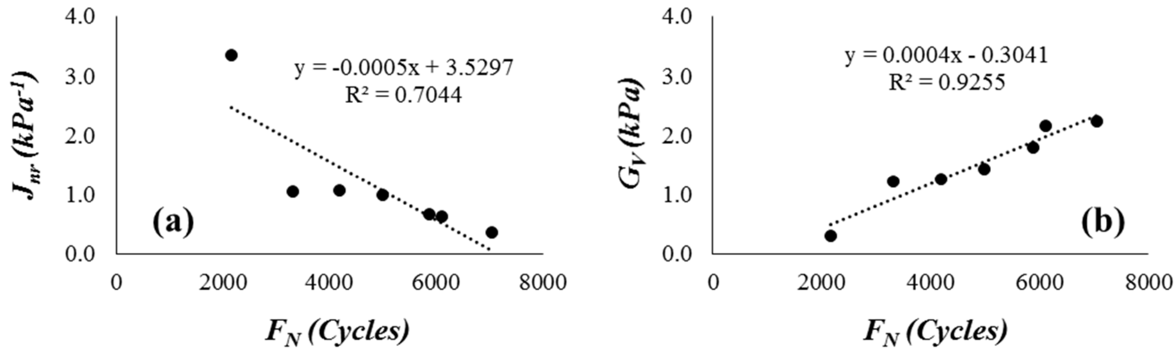

Figure 36 – Linear correlations between flow number (F_N) at 60°C and the following binder parameters: (a) nonrecoverable compliance J_{nr} at 3.2 kPa and 64°C; and (b) viscous component of the creep stiffness (G_V) at 64°C

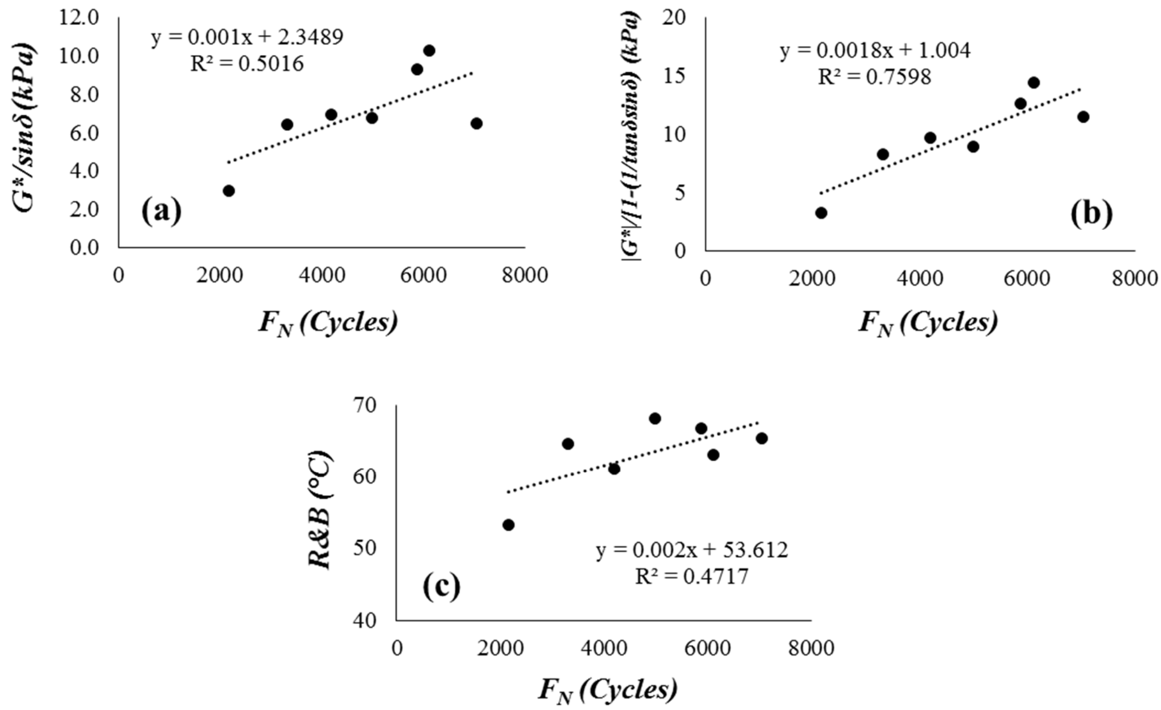

Figure 37 – Linear correlations between flow number (F_N) at 60°C and the following binder parameters: (a) original Superpave® parameter *G*/sinδ* at 64°C; (b) Shenoy's parameter *|G*|/[1-(1/tanδsinδ)]* at 64°C; and (c) softening point *R&B* after short-term aging

Table 12 is a summary of the degrees of correlation between F_N and the binder parameters, as based on power equations. The pattern of behavior observed for the linear regression analysis remained the same here, i. e., the parameters J_{nr} and G_V resulted in good to excellent correlations and the other parameters displayed a tendency of blurring the distinctions among the rankings of binders and mixtures. It is interesting to note that, differently from the linear regression, the R^2 value of the correlation between J_{nr} and F_N (almost 0.91) is higher than the one between G_V and F_N (almost 0.89). It is known that high stresses and strains are able to reach the nonlinear viscoelastic domain of binders and mixtures, which is where rutting typically occurs. Moreover, it is quite difficult to correlate numerical values obtained within this domain (in this case, F_N, G_V and J_{nr}) because the rutting phenomenon in the mixture is fairly complicated when compared with the one in the corresponding binder (D'ANGELO, 2010a; WASAGE et al., 2011). Thus, what can be pointed out is that the repeated creep tests for asphalt binders and their corresponding parameters – J_{nr} and G_V – are among the current alternatives that provide researchers and highway agencies with good estimates of the rutting potential of mixtures.

The average values of the constants *A*, *B*, *C* and *D* from the Francken model are provided in Table 13. These constants were determined by using spreadsheets from Microsoft Excel™ 2013, and then averaged to yield the final values. Several attempts were made in order to ensure that the F_N value calculated by the model (i. e., the cycle in which the second derivative changes from negative to positive, Equation (41) in Section 4.4.2) was as close to the real F_N value as possible. As it can be observed, the model was able to fit the numerical data with very small deviations from the raw values (R^2 is always higher than 0.92), and only minor errors in the prediction of F_N were detected as well (≤ 0.1%). With respect to the variations in the results of the constants *A*, *B*, *C* and *D*, the data in Table 14 suggest that they followed the same pattern of the actual F_N in the mixture samples and the data published by Ameri et al. (2014): most of the COV's ranging from 2.0 to 26.0% and only a few exceptions in the constant *D* falling outside of this interval.

Table 12 – Degrees of correlation (R^2) between binder and mixture data and corresponding regression equations (power law)

variable (X-axis)	variable (Y-axis)	equation	R^2
flow number at 60°C (F_N, number of cycles)	nonrecoverable compliance at 64°C and 3.2 kPa (J_{nr}, kPa^{-1})	$y = 587203x^{-1.588}$	0.9058
	viscous component of the creep stiffness at 64°C and 0.1 kPa (G_V, kPa)	$y = 3E\text{-}06x^{1.5487}$	0.8865
	original Superpave® parameter at 64°C ($G^*/\sin\delta$, kPa)	$y = 0.0081x^{0.7976}$	0.6763
	softening point after short-term aging (*R&B*, °C)	$y = 17.022x^{0.1555}$	0.6045
	Shenoy's parameter at 64°C ($\lvert G^*\rvert/[1-(1/\tan\delta\sin\delta)]$, kPa)	$y = 0.001x^{1.0861}$	0.8386

Table 13 – Constants *A*, *B*, *C* and *D* from the Francken model (mean values) for the asphalt binders that failed before 10,000 cycles

asphalt binder	constants of the Francken model				R^2	error (%)[a]
	A	*B*	*C*	*D*		
base binder (AC)	1.775E-01	5.213E-02	34.33	8.468E-06	> 0.9814	≤ 0.10
AC+Elvaloy+PPA	1.153E-01	1.009E-01	77.18	2.785E-06	> 0.9204	≤ 0.09
AC+rubber+PPA	5.227E-01	2.954E-02	78.02	4.069E-06	> 0.9591	≤ 0.07
AC+SBS	9.426E-02	1.029E-01	91.31	3.031E-06	> 0.9840	≤ 0.07
AC+SBS+PPA	1.835E-01	5.057E-02	130.53	1.881E-06	> 0.9551	≤ 0.03
AC+SBR	3.250E-01	3.000E-02	63.00	3.972E-06	> 0.9569	≤ 0.09
AC+SBR+PPA	3.010E-01	2.600E-02	113.72	1.548E-06	> 0.9521	≤ 0.02

[a] error: difference (in percentage) between the predicted and the actual F_N values. These differences are given as absolute numbers (i. e., regardless of the signal).

Table 14 – Coefficients of variation (COV's) for the constants *A*, *B*, *C* and *D* from the Francken model

asphalt binder	COV's for each constant of the Francken model (%)			
	A	*B*	*C*	*D*
base binder (AC)	17.46	13.26	5.08	2.23
AC+Elvaloy+PPA	11.50	0.09	7.93	32.47
AC+rubber+PPA	5.25	12.71	6.22	26.03
AC+SBS	25.73	2.08	3.83	20.63
AC+SBS+PPA	9.00	18.93	15.69	43.33
AC+SBR	10.68	20.34	14.89	3.60
AC+SBR+PPA	3.82	21.15	1.86	2.84

As pointed out above, the constant *C* and the parameter FN_I were both correlated with the actual F_N value to see if there is any relationship among them. Some authors reported that FN_I worked better in the determination of the less and most rut resistant mixtures in the laboratory than F_N, even though many of them recognized that more tests are needed to give support to this suggestion (LI et al., 2014; WALUBITA et al., 2013; ZHANG et al., 2013). The rankings of asphalt mixtures based on *C* and FN_I are shown in Table 15 and, for the reader's convenience, the one based on F_N is provided again. It can be seen that no agreement exists among them, and therefore neither *C* nor FN_I can be taken as reliable parameters to replace F_N.

Table 15 – Ordering of mixtures from the less (No. 1) to the most susceptible to rutting (No. 7) as based on the flow number F_N, the flow number index FN_I and the constant *C* (Francken model)

asphalt binder	F_N (reference ranking)	FN_I (values and ranking)		*C* (ranking)[a]
		mean value	ranking[a]	
AC+Elvaloy+PPA	1	2.37E-04	2	5
AC+SBS+PPA	2	2.72E-04	3	1
AC+SBR+PPA	3	2.32E-04	1	2
AC+SBS	4	3.14E-04	4	3
AC+rubber+PPA	5	4.92E-04	7	4
AC+SBR	6	3.80E-04	5	6
base binder (AC)	7	3.95E-04	6	7

[a] the gray-shaded boxes indicate agreement between rankings of mixtures and binders.

Some comments may be drawn here to explain the results summarized in Table 15. Walubita et al. (2013) emphasized that outliers may create distortions in the rankings of mixtures as based on the parameter FN_I. However, it is not clear as to whether the differences between the orderings of F_N and FN_I in this study can be attributed only to such distortions or they are inherent limitations of FN_I. This is pointed out as a relevant issue because the parameters F_N and FN_I tended to order the mixtures in a quite similar way in the papers by Walubita et al. (2013) and Zhang et al. (2013), with only a few exceptions. The only common characteristic in the rankings of F_N and FN_I is that both gave higher positions to the formulations with PPA and a polymer (AC+Elvaloy+PPA, AC+SBS+PPA and AC+SBR+PPA) and lower ones to the remaining materials (base binder, AC+SBS, AC+rubber+PPA and AC+SBR). This can also be somewhat seen in the ordering based on the constant from the Francken model and, as a consequence, the R^2 values are approximately the same either for FN_I or C (Figure 38).

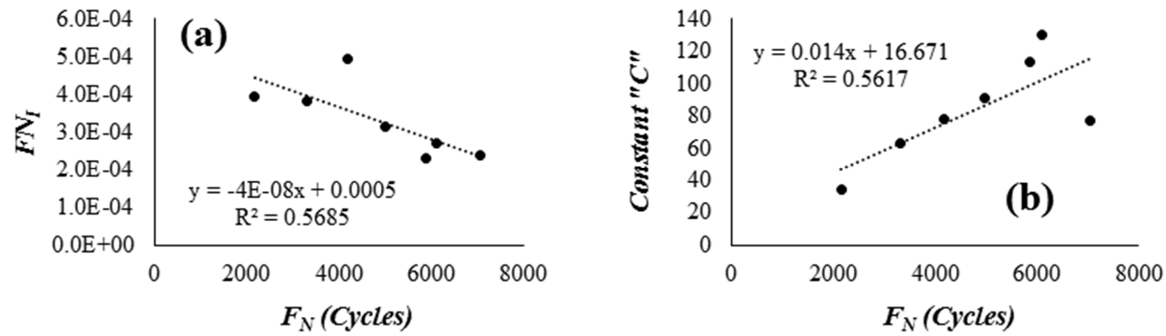

Figure 38 – Linear correlations between flow number (F_N) at 60°C and the following terms: (a) mean value of the low number index FN_I; and (b) the constant C from the Francken model

Brief Summary of the Findings of this Section: Other than being in agreement with several previously published documents, the outcomes of this section indicate that there is no satisfactory substitute for F_N in the characterization of the susceptibility of asphalt mixtures to rutting in the FN test. Moreover, the performance-related MSCR test worked better in the evaluation of the susceptibilities of polymer- and crumb rubber-modified asphalt binders to rutting, as based on the parameters G_V at 0.1 kPa and J_{nr} at 3.2 kPa (both at 64°C). The odd case among the studied binders was the AC+PPA, for which F_N was only about 16.9% higher than the corresponding F_N of the base material. There is some evidence that PPA should be added to the binder at an optimum content, since modifier contents higher or lower than this optimum value may lead to increases in the rut depth of the mixture and its premature failure (KHADER et al., 2015). This gives even more support to the idea that the actual benefits of PPA must be interpreted with caution, since they are strongly dependent on the crude source and demand a careful investigation before being used in the preparation of asphalt mixtures.

Differently from the PPA-modified binders, the formulations with polymers and crumb rubber showed much higher rutting resistances and the ones with Elvaloy+PPA and SBR+PPA provided the best results. On the other hand, the absence of PPA in the SBS- and SBR-modified materials markedly decreased the F_N values of the mixtures. Several authors pointed out that PPA acts in a synergetic way with SBS, Elvaloy® and other polymers (BENNERT and MARTIN, 2012; BUNCHER, 2016; ORANGE et al., 2004; LESUEUR, 2009), which means that the network connections are improved and thus the overall properties of the formulation (CLYNE et al., 2012; D'ANGELO, 2010a; D'ANGELO and DONGRÉ, 2009; FEE et al., 2010; ONOFRE et al., 2013; ORANGE et al., 2004; REINKE et al., 2012; ZHANG and YU, 2010). To some extent, this reveals that the combination of PPA with a polymer may bring more benefits to the properties of binders and mixtures than the ones with polymer alone, even though a few authors reported quite similar rutting performances for mixtures prepared with polymer-modified binders with and without PPA – see the paper from Bennert and Martin (2012) as an example with SBS-modified binders.

5.3.2. Asphalt Mixtures Modified with Plastomers and Crumb Rubber: Results and Discussion

As stated in the literature review, the most particular characteristic of plastomers is to significantly stiffen the original binder when compared with other additives such as elastomers and reactive terpolymers. In practical terms, this can be translated into asphalt mixtures with very high degrees of stiffness and low levels of accumulated strain. In a direct comparison among mixtures prepared with PG 76-xx binders modified with 3.2% of SBS, 4.7% of oxidized PE and 7.1% of crumb rubber, Golalipour (2011) observed that binder modification with PE yielded much higher F_N values at 46°C than with SBS and crumb rubber and for the two stress levels used in the tests (345 and 1,034 kPa), and these differences were more marked for the fine aggregate gradation. These higher resistances to rutting for plastomer-modified binders when compared with elastomer-modified binders were also noted in the study by Orange et al. (2004), in which a PG 76-22 binder modified with EVA+PPA showed much lower rut depths in the Hamburg wheel tracking test at 50°C and after 20,000 cycles when compared with another PG 76-22 binder, but modified with SBS+PPA.

As a consequence of this substantial increase in the overall stiffness of the binder, none of the asphalt mixtures prepared with EVA and PE (AC+EVA, AC+EVA+PPA, AC+PE and AC+PE+PPA) showed failure after 10,000 loading-unloading cycles. The AC+rubber did not fail in the test either and, since the AC+rubber+PPA followed another pattern (i. e., it failed in this test), it is possible to say that the stiffness of the asphalt binder was directly governed by the presence of crumb rubber in the formulation and that PPA does not interact with the rubber particles (or this degree of interaction is very small). In such a case, the PPA content of 0.6% was not able to account for the difference of 3.0% between the rubber contents of the AC+rubber and the AC+rubber+PPA. The relationship between higher rubber contents in a PPA-modified binder and better mechanical properties was also highlighted by Yadollahi and Mollahosseini (2011), since they concluded that the properties of an original material modified with 1.0% of PPA and Vestenamer® (semicrystalline rubber that acts as a plasticizer of rubber compounds) continuously improved as the rubber content increased from 5% to 8, 10, 12 and then 15%.

Table 16 summarizes the permanent strain values (γ_{per}) of the above-mentioned mixtures together with their corresponding binder parameters *R&B*, J_{nr}, $G^*/sin\delta$ and $|G^*|/[1-(1/tan\delta sin\delta)$, all of them obtained at 64°C. The COV's of γ_{per} ranged within the same intervals observed for F_N (Table 10) and in the papers by Li et al. (2014) and Rodezno et al. (2010), among others. Differently from the samples that showed an F_N value in the test, the absence of failure makes it difficult to associate the mixture parameters with the binder parameters. In other words, no accurate forecasts of the mixtures with the highest and lowest susceptibilities to rutting can be made when F_N is not observed. For instance, G_V is precisely the same for three asphalt binders (AC+rubber, AC+PE and AC+PE+PPA) and not even the parameter J_{nr} can be easily correlated with γ_{per}. What can be said is that these mixtures belong to the group of materials that can deal with very high traffic levels in the pavement, but it is not possible to state which of them will fail first based only on these experimental data. The considerable differences in the orderings of binders and mixtures (Table 17) take readers to this direction as well.

This notable absence of correlations between G_V, J_{nr} and γ_{per} can be attributed to the idea that the output parameters were not determined in the same "condition". More simply, this means that either the binder or the mixture samples must experience a very critical testing condition (failure or great amount of accumulated strain) before the data are interpreted and correlated. It has been observed over the years that the promising results of the binder tests – MSCR and RCRT – were due to the fact that the mixtures were severely loaded on accelerated loading facilities, pavement sections or in the FN test up to failure and, similarly, the binders were subjected to very high stress levels in the MSCR protocol or many loading-unloading cycles in the RCRT before G_V or J_{nr} were determined (BAHIA et al., 2001a; D'ANGELO, 2009; D'ANGELO et al., 2007; DELGADILLO et al., 2006a; DREESSEN et al., 2009; GOLALIPOUR, 2011; LAUKKANEN et al., 2015; MARTINS et al., 2011; WASAGE et al., 2011). Therefore, it can be hypothesized that the γ_{per} values obtained here did not correlate well with J_{nr} and G_V because the mixtures did not show failure after 10,000 creep-recovery cycles, and also that γ_{per} is not closely associated with the status of the binder in the MSCR test.

Table 16 – Permanent strains of the asphalt mixtures modified with plastomers (EVA and PE) and crumb rubber after 10,000 cycles (γ_{per}) and corresponding asphalt binder parameters

formulation	mixture data		binder data at 64°C and after RTFO-aging				
	γ_{per}, mm (mean)	COV (%)[a]	G_V (kPa)[b]	$R\&B$ (°C)	Shenoy's parameter (kPa)	$G^*/sin\delta$ (kPa)	J_{nr} (kPa^{-1})[b]
AC+rubber	0.583	27.80	2.08	60.8	12.56	7.79	0.948
AC+EVA	0.665	14.61	1.91	64.9	11.88	7.19	0.856
AC+EVA+PPA	0.899	27.14	1.47	67.4	16.48	10.62	1.214
AC+PE	0.768	9.42	2.08	79.5	13.64	10.38	0.648
AC+PE+PPA	0.694	29.04	2.08	72.6	15.02	11.34	0.572

[a] COV: coefficient of variation.
[b] the parameters G_V and J_{nr} were determined at 1/9 s and the stress levels of 0.1 and 3.2 kPa, respectively.

Table 17 – Rankings of asphalt binders and mixtures that showed absence of failure from the most (No. 1) to the less rut resistant (No. 5) based on the numerical values of some laboratory tests

formulation	γ_{per} at 60°C, mm (reference ranking)[a]	rankings of asphalt binders at 64°C[a, b]				
		G_V at 0.1 kPa	J_{nr} at 3.2 kPa	$R\&B$, aged	$G^*/sin\delta$, aged	Shenoy's parameter
AC+rubber	1	1	4	5	4	4
AC+EVA	2	2	3	4	5	5
AC+PE+PPA	3	1	1	2	1	2
AC+PE	4	1	2	1	3	3
AC+EVA+PPA	5	3	5	3	2	1

[a] the gray-shaded boxes indicate agreement between rankings of mixtures and binders.
[b] the parameters G_V and J_{nr} were determined at 1/9 s (1-s creep time and 9-s recovery time).

Figure 39 and Table 18 give the equations and the corresponding R^2 values of the linear correlations between the mixture and asphalt binder data shown in Table 16. The choice for a figure to represent the degrees of correlation between γ_{per} and the repeated creep parameters (J_{nr} and G_V) was due to the promising findings obtained for the previously reported mixture data (Figure 36), whereas the same cannot be said for $G^*/sin\delta$, the Shenoy's parameter and $R\&B$ (Figure 37). Although R^2 is of about 0.61 and 0.65 for G_V and $|G^*|/[1-(1/tan\delta sin\delta)]$, respectively, one cannot take these correlations as reliable because they do not express the important limitations of the two parameters, i. e., the opposite rankings of binders and mixtures (Table 17). In other words, these equations are only statistical fits and cannot be used in the prediction of the less and most rut resistant materials in the pavement.

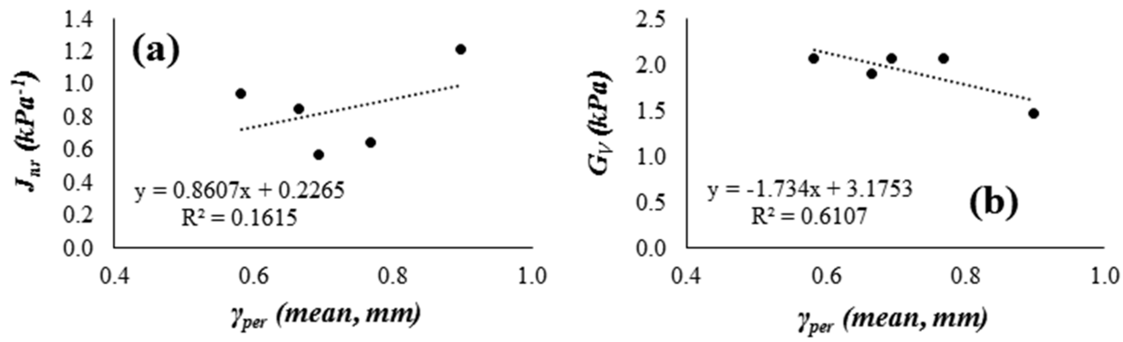

Figure 39 – Linear correlations between the accumulated strain after 10,000 cycles (γ_{per}) at 60°C and the following binder parameters: (a) nonrecoverable compliance J_{nr} at 3.2 kPa and 64°C; and (b) viscous component of the creep stiffness (G_V) at 64°C and 0.1 kPa

Table 18 – Degrees of correlation (R^2) between some binder and mixture data and corresponding linear equations

variable (X-axis)	variable (Y-axis)	equation	R^2
mean accumulated strain value in the mixture after 10,000 cycles and at 60°C (γ_{per})	original Superpave® parameter at 64°C (*G*/sinδ*, kPa)	y = 9.7994x + 2.3924	0.3986
	softening point after short-term aging (*R&B*, °C)	y = 25.967x + 50.302	0.1823
	Shenoy's parameter at 64°C (|*G**|*/[1-(1/tanδsinδ)*, kPa)	y = 12.583x + 4.8357	0.6484

Brief Summary of the Findings of this Section: The most important characteristic of the EVA-, PE- and crumb rubber-modified mixtures (AC+rubber, AC+EVA, AC+EVA+PPA, AC+PE and AC+PE+PPA) is that their susceptibility to rutting cannot be estimated by any of the binder parameters selected in this study, namely, *R&B*, G_V, J_{nr}, *G*/sinδ* and |*G**|*/[1-(1/tanδsinδ)]*. The literature indicates that researchers have loaded mixture samples for several times up to the failure point or when a great rut depth was achieved, and then the correlations were studied and found to be good. This does not match with the γ_{per} values presented above and, in addition, F_N could not be recognized in the tests. It is believed that the lack of correlation between γ_{per} and the binder rutting parameters may be explained by the absence of failure in the mixtures (the load applications were interrupted before F_N), since this is not in agreement with the severe loading conditions and the amount of strain to which the binders are subjected in the MSCR tests.

The rankings based on γ_{per}, *R&B*, G_V, J_{nr}, *G*/sinδ* and |*G**|*/[1-(1/tanδsinδ)]* form totally different groups of less and most rut resistant materials. While the binder parameters tend to give higher positions for the formulations with PE (AC+PE and AC+PE+PPA), the γ_{per} values rank the AC+rubber and the AC+EVA as the most resistant ones to rutting. As a consequence, it is hard to accurately forecast the rutting potential of the materials based only on the data available in the present study. What can be implied here is that these mixtures belong to the group of materials with sufficient resistances to deal with heavier traffic levels. Even though the idea of categorizing the formulations into one or more groups appears to be a practical solution, it is not necessarily the best option because the mixtures may have different failure points (i. e., F_N or accumulated strains) after thousands of loading applications in the pavement. This will be discussed in detail in the next section.

5.4. Categories of Traffic Levels and Direct Comparisons among the Formulations

The concept of clustering the materials into one or more groups is certainly not new in the subject area of asphalt binders, since it started with the penetration and viscosity grades in the 1910's and the 1960's (respectively) and has been continuously used in the past and current versions of the Superpave® specification. However, one great concern that arises from the use of these groups is that the intervals between one grade and the other (e. g., 20 dmm in the 50/70 Brazilian penetration grade system) may be wide enough to cause distortions in the interpretation of the actual performance of the materials. This is the case of Superpave®, in which the difference of 6°C between one PG grade and the other does not have a full agreement among researchers. For example, Chen and Tsai (1999) graded one of their asphalt binders as PG 67-xx (an intermediate classification between the PG 64-xx and the PG 70-xx ones) rather than PG 64-xx because the parameter $G^*/sin\delta$ was equal to 1.47 and 1.02 kPa at 64 and 67°C, respectively. Similar classifications were made by Baumgardner (2012), D'Angelo and Dongré (2009), Dongré and D'Angelo (2003) and Orange et al. (2004) among others, which suggest that the original interval of 6°C between the PG grades may be revised to address such limitations.

Table 19 provides the adequate traffic levels of the binders and the ranges of equivalent single-axle loads (ESAL's) at 64°C as based on J_{nr} at 3.2 kPa and G_V at 0.1 kPa, both at the creep-recovery times of 1/9 s. To facilitate the comparisons between the results of binder and mixture tests, the F_N and the γ_{per} values after 10,000 cycles are shown as well. These traffic levels and intervals of ESAL's can be found in Table 3 of the AASHTO M320-09 specification (parameter J_{nr}) and in the draft specification published by Delgadillo et al. (2006b) (parameter G_V). It may be important to note that, differently from the final draft published by Delgadillo et al. (2006b), only the data from the short-term aged asphalt binders were used in the determination of the ESAL's and the minimum G_V values were assumed to be in Pa, rather than kPa in the original paper.

Table 19 – Summary of mixture data and recommended traffic levels for the asphalt binders based on the nonrecoverable compliance J_{nr} and the viscous component of the creep stiffness G_V (both at 64°C) and the criteria published by Superpave® and Delgadillo et al. (2006b)

asphalt binder	mixture data at 60°C[a]		traffic level (J_{nr}, 3.2 kPa and 1/9 s)[b]	traffic (G_V, 0.1 kPa, and 1/9 s)	
	F_N (mean)	γ_{per} (mean)		ESAL's fast[c]	ESAL's slow[d]
base binder (AC)	2,167	-	S	1 – 3	0 – 0.3
AC+PPA	2,533	-	E	> 30	1 – 3
AC+Elvaloy+PPA	7,050	-	E	10 – 30	0.3 – 1
AC+rubber	-	0.583	V	10 – 30	0.3 – 1
AC+rubber+PPA	4,191	-	H	3 – 10	0.3 – 1
AC+SBS	4,991	-	V	3 – 10	0.3 – 1
AC+SBS+PPA	6,110	-	V	10 – 30	0.3 – 1
AC+EVA	-	0.665	V	10 – 30	0.3 – 1
AC+EVA+PPA	-	0.899	H	3 – 10	0.3 – 1
AC+PE	-	0.768	V	10 – 30	0.3 – 1
AC+PE+PPA	-	0.694	V	10 – 30	0.3 – 1
AC+SBR	3,312	-	H	3 – 10	0.3 – 1
AC+SBR+PPA	5,875	-	V	10 – 30	0.3 – 1

[a] if the mixture failed before 10,000 cycles, then F_N is presented; otherwise, γ_{per} at 10,000 cycles is presented.
[b] S = standard; H = heavy; V = very heavy; E = extremely heavy (AASHTO M320-09 standard, Table 3).
[c] numbers in millions. The term "fast" refers to an average traffic speed of 60 mph, or 96.5 km/h (DELGADILLO et al., 2006b).
[d] numbers in millions. The term "slow" refers to an average traffic speed of 15 mph, or 24.2 km/h (DELGADILLO et al., 2006b).

Due to the somewhat conflicting findings of the PPA-modified asphalt binder, it can be clearly seen that this material is an outlier within the data set. Even the PPA-modified material studied by Domingos and Faxina (2014, 2015a, 2015b) and Onofre et al. (2013)[32] and graded as PG 76-xx showed an unexpected repeated creep behavior because the binder response in the MSCR test is not compatible with the relatively low F_N value in the mixture test: while the other PG 76-xx formulations prepared with polymers and crumb rubber did not fail in the FN tests (ONOFRE et al., 2013), the AC+PPA failed in this same test and depicted J_{nr} values very close to the ones of the modifications with EVA (DOMINGOS and FAXINA, 2014), Elvaloy® terpolymer (DOMINGOS and FAXINA, 2015a) and low-density PE (DOMINGOS and FAXINA, 2015b). PPA modification

[32] To place the reader a little bit in the context of these Brazilian studies (DOMINGOS and FAXINA, 2014, 2015a, 2015b; ONOFRE et al., 2013), the same groups of modifiers used in this dissertation (SBS, SBR, EVA, Elvaloy®, PPA, PE and crumb rubber) were used in the preparation of another set of modified materials graded as PG 76-xx, either with or without PPA. The designations are similar to the ones used here, but the base binder was different (Replan-Petrobras refinery, rather than Lubnor-Petrobras). The aggregates and aggregate gradations did not change either in the paper by Onofre et al. (2013), but the testing device was the UTM-25 rather than the MTS 651).

may also lead to mixture data comparable to the ones of some neat binders, as it can be inferred from the results published by Martins et al. (2011) and Tabatabaee and Teymourpour (2010). It appears that the expected outcomes of PPA-modified binders cannot be automatically interpreted when compared with the ones observed for polymer and crumb rubber modification types.

From the data shown in Table 19, one can see that the traffic levels set by the Superpave® specification and Delgadillo et al. (2006b) have some major limitations. The groups of heavy (H) and very heavy (V) levels may include formulations that range from failure (F_N) to absence of failure (γ_{per}) in the mixture tests and from 3 to 30 million ESAL's at fast traffic speeds. A classic example of this limitation is the AC+EVA+PPA, which did not fail in the mixture tests (γ_{per} = 0.899) and its traffic level is similar to the ones of the AC+rubber+PPA (F_N = 4,191) and the AC+SBR (F_N = 3,312). The same can be said for the AC+SBR+PPA (F_N = 5,875), the AC+SBS (F_N = 4,991) and the AC+SBS+PPA (F_N = 6,110), whose traffic levels are equal to the ones of several mixtures that did not fail in the FN tests (AC+rubber, AC+EVA, AC+PE and AC+PE+PPA). The only exception was the 50/70 base binder, for which the F_N value of 2,167 is rather compatible with the standard traffic level and the low numbers of ESAL's at fast and slow traffic speeds.

An attempt was made to separate the formulations into four groups and adequately describe each of them as based on both specifications. This preliminary system of classification is provided in Table 20 and, although all the mixtures within the group of extremely heavy traffic level failed in the FN tests here, some of the materials tested by Onofre et al. (2013) and that belong to this same traffic level – e. g., the AC+EVA and the AC+EVA+PPA (DOMINGOS and FAXINA, 2014) as well as the AC+Elvaloy+PPA (DOMINGOS and FAXINA, 2015a) – showed very low γ_{per} values (lower than 0.800). Similarly, it was also observed in the paper by Onofre et al. (2013) that some binders that can deal with very heavy traffic levels as based on J_{nr} at 64°C – e. g., the AC+SBS and the AC+rubber (DOMINGOS and FAXINA, 2016) – may present a little bit higher γ_{per} values than the ones reported in this study.

The separation of the above-mentioned formulations within the corresponding groups is given in Table 21. One of the surprising findings was the AC+SBS, for which the G_V values yielded a lower number of ESAL's at fast traffic speeds (3 – 10 million) when compared with the other materials that belong to the same category. The other one was the AC+PPA, which was ranked as a material with intermediate resistance to rutting due to its mixture data (F_N between 2,200 and 4,500 cycles), even though its J_{nr} value is compatible with extremely heavy traffic levels. It appears that the proposed classification did a good job in ranking the binders based not only on their MSCR testing data, but also their mixture data. The formulations with plastomers (EVA and PE) and elastomers (SBS and SBR) reached approximately the same levels in the categories of rutting resistance, and the ones with PPA in the composition (except for the AC+PPA) typically occupied higher positions in the ranking. This means that such materials can be used on pavements where at least heavy traffic levels are expected to occur during the service life.

Table 20 – Categories of rutting resistance and corresponding descriptions as based on the laboratory data collected in this study and by Onofre et al. (2013)

category (rutting resistance)	traffic level at 64°C (M320-09)	minimum ESAL's (millions)[b]		intervals of acceptable F_N and γ_{per} values (60°C and 204 kPa)[a]
		fast (96.5 km/h)	slow (24.2 km/h)	
low	standard	1 – 3	0 – 0.3	$F_N < 2{,}200$
intermediate	heavy	3 – 10	0.3 – 1	$2{,}200 < F_N < 4{,}500$ or $\gamma_{per} > 0.800$
high	very heavy	3 – 10	0.3 – 1	$4{,}500 < F_N < 7{,}000$ or $0.500 < \gamma_{per} < 1.500$
very high	extremely heavy	10 – 30	0.3 – 1	$F_N > 7{,}000$ or $\gamma_{per} < 0.800$

[a] if the mixture fails in the flow number test before 10,000 cycles, then F_N will be considered in the classification; otherwise, γ_{per} will be taken into account.

[b] the intervals of ESAL's correspond to the minimum range of values to which the short-term aged binder will possibly be subjected in the field pavement during the service life. See Delgadillo et al. (2006b) for more details.

Table 21 – Classifications of the formulations from the Lubnor-Petrobras refinery according to their mixture and binder data

category (rutting resistance)	traffic level at 64°C (M320-09, Table 3)	formulations
low	standard	base binder (AC)
intermediate	heavy	AC+PPA, AC+SBR, AC+EVA+PPA and AC+rubber+PPA
high	very heavy	AC+rubber, AC+SBS, AC+SBS+PPA, AC+EVA, AC+PE, AC+PE+PPA and AC+SBR+PPA
very high	extremely heavy	AC+Elvaloy+PPA

The following three figures depict the repeated creep curves of the asphalt mixtures as referenced on the modification type: terpolymers, PPA and crumb rubber (Figure 40), plastomers (Figure 41) and elastomers (Figure 42). Overall these figures indicate that binder modification and the aggregate variables increased the F_N values or avoided failure by markedly decreasing the accumulated strain values at each creep-recovery cycle, flattening the secondary creep region and extending it. The AC+rubber+PPA in Figure 40 and the AC+SBR in Figure 42 are two of the typical representative materials, since they showed much higher F_N values due to the extension and flattening of the secondary creep part regardless of the higher accumulated strain values in the first cycles (AC+SBR) or throughout the test (AC+rubber+PPA).

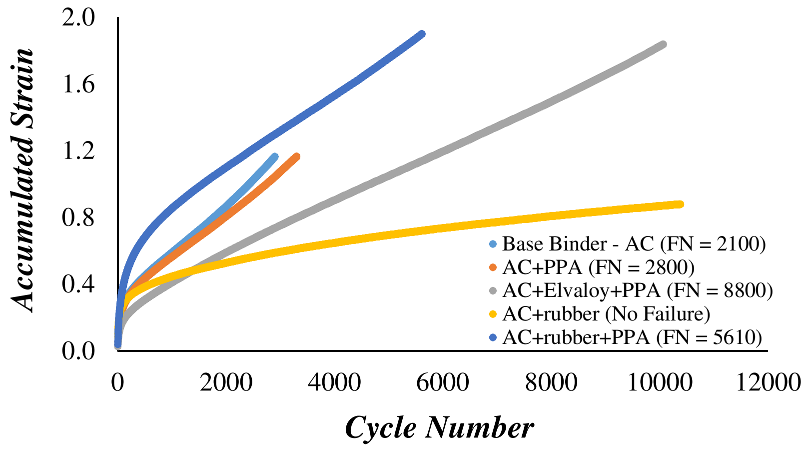

Figure 40 – Accumulated strain versus number of cycles for the base binder (AC), the AC+Elvaloy+PPA, the AC+PPA, the AC+rubber and the AC+rubber+PPA at 60°C (original samples)

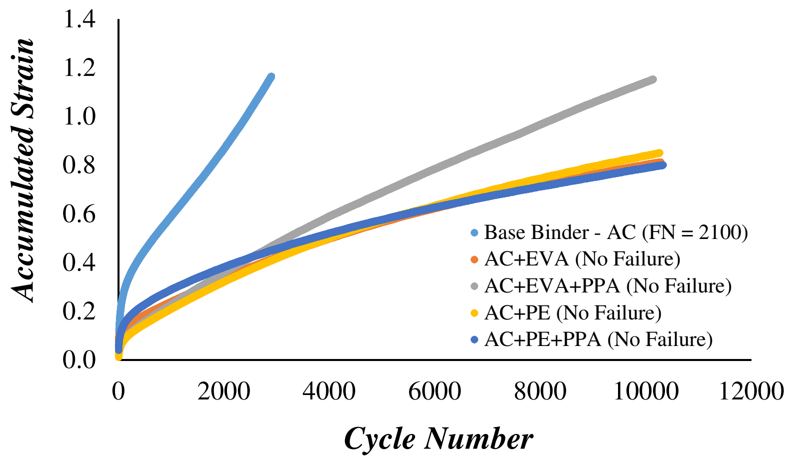

Figure 41 – Accumulated strain versus number of cycles for the base binder (AC), the AC+EVA, the AC+EVA+PPA, the AC+PE and the AC+PE+PPA at 60°C (original samples)

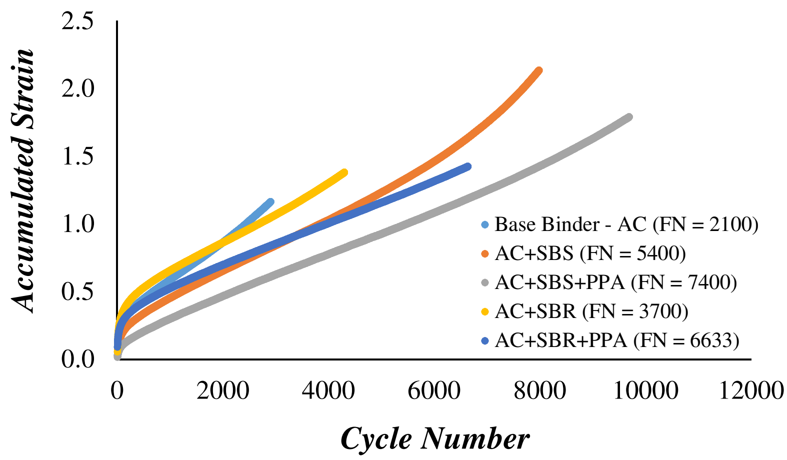

Figure 42 – Accumulated strain versus number of cycles for the base binder (AC), the AC+SBS, the AC+SBS+PPA, the AC+SBR and the AC+SBR+PPA at 60°C (original samples)

In terms of binder modification with one additive only (AC+rubber, AC+SBS, AC+EVA and AC+PE) and this same additive combined with PPA (AC+rubber+PPA, AC+SBS+PPA, AC+EVA+PPA, AC+PE+PPA and AC+SBR+PPA), the noticeable differences between the curves of the AC+rubber and the AC+rubber+PPA deserve a close attention. This suggests that PPA did not markedly contribute to the rutting resistance of the mixture compounded with AC+rubber and that the internal microstructures of such mixture samples are very different. These occurrences can be graphically described by a reverse effect in the curves of the materials (i. e., shortening and steepening of the secondary region when PPA is added and the crumb rubber content is reduced) when compared with the other curves. In practical terms, the AC+rubber+PPA accumulates permanent strain at much higher rates than the AC+rubber throughout the test and for all the regions of the creep curve (primary and secondary), and this goes up to the failure point (F_N). Both effects can be somehow identified in the creep curve of the AC+EVA+PPA as well when compared with the AC+EVA, even though the two materials dealt with 10,000 cycles in the FN test (no failure).

From a technical point of view, Bahia et al. (2001a) explained that the asphalt binder properties play a key role in the first (primary) region of the repeated creep curve and the aggregates play a key role in the second (secondary) region of the curve. A detailed investigation on the internal structure of the mixture was carried out by Sefidmazgi et al. (2012), who concluded that the most statistically significant variables associated with this structure – number of contact points, contact length and absolute angle of the plane-to-plane contact (i. e., the angle that is formed by the contact between one aggregate particle and the other) – can be combined within one single index (in this case, the internal structure index – ISI) and this index has a strong correlation with F_N. These authors also emphasized that the rheological properties of the modified binders have a profound influence on the structure of the mixture, thereby increasing ISI and F_N. It may be implied from this comment that binder modification can somehow improve aggregate interlocking and increase the number of contacts among adjacent aggregate particles, which consequently affects the overall performance of the mixture.

Short Summary of the Conclusions of this Section: The modification of the original binder with additives led to improvement in its rheological properties, and this modification process in some way affected the internal structure of the asphalt mixture (higher F_N values or no failure in the FN test). With exception of the AC+EVA, the AC+EVA+PPA, the AC+rubber and the AC+rubber+PPA, the combined effects of lower polymer content (SBS, SBR and PE) and the addition of PPA resulted in binders and mixtures with lower susceptibilities to rutting. Despite the higher γ_{per} values when compared with the AC+EVA, the AC+EVA+PPA may be included in this list as well because the mixture samples did not fail in the flow number tests. It is believed that the synergy and interaction between PPA and the polymers compensated for the lower polymer contents in the formulations, and also that this may not have happened to the AC+rubber. Since the mechanical properties of the PPA-modified mixture did not markedly vary from the ones of the base binder, this supports the following theories:

- the binder tests do not necessarily predict mixture performance with a great degree of accuracy for all the categories of modifiers, similarly to what was highlighted by Tabatabaee and Teymourpour (2010);
- in some cases, the effects of PPA modification on the resistance of the original binder to rutting can be more restricted to the binder alone; or
- binder modification must be cautiously interpreted with respect to the inherent characteristics of each additive and its interaction with the base material.

The MSCR test and the parameters J_{nr} and G_V are a great advance towards the understanding of the actual resistance of modified binders to rutting and its correlation with mixture performance, as it can be implied from the very high R^2 values for the SBS-, SBR- and crumb rubber-modified materials. The idea of ranking the asphalt binders according to their acceptable traffic levels relies on more performance-related approaches, and this could be verified by the FN tests on dense-graded mixtures. However, there are large gaps in these classifications because one single category of traffic level cover a wide span of F_N values or levels of accumulated strain after 10,000 cycles (γ_{per}). For example, it may be possible to address rutting on a pavement with very heavy traffic level either by substantially increasing F_N to an acceptable range of values (e. g., from 4,500 to 7,000 cycles) or by choosing a mixture with very low levels of permanent strain (e. g., γ_{per} between 0.800 and 1.500). Therefore, one must keep in mind that such classifications contain a certain degree of subjectivity and only provide general instructions about the choice of the best asphalt mixture for a specific paving application.

CHAPTER 6: Binder Testing Results and Discussion

This chapter presents the results of all the binder tests together with some comparisons among the responses of the formulations. Since the tests can be classified into conventional (penetration, softening point and viscosity), oscillatory shear (original Superpave® rutting protocol) and repeated creep procedures (MSCR), this was the simplest structure on which the chapter was based. Each heading also has its own highlights. To conduct the analysis of the MSCR test parameters, the formulations were then separated into different groups according to the modifier type: (a) terpolymers and PPA alone; (b) crumb rubber; (c) plastomers; and (d) elastomers. Some charts of the creep-recovery pulses of the asphalt binders are given here to help in explaining the findings. Then, some general guidelines for the use of one or another formulation based on the current and proposed MSCR criteria are set out.

6.1. Conventional Tests and Aging Parameters

6.1.1. Highlights

- Binder modification with one or two additives increased viscosity and softening point and decreased penetration, which indicates an increased hardness of the material.
- The use of plastomers generally provided higher degrees of stiffness to the binder than elastomers and crumb rubber, even though the binder data did not correlate well with mixture data (F_N and γ_{per}).
- The formulations with PPA (AC+modifier+PPA) typically depicted a higher sensitivity to aging than the ones without PPA (AC+modifier), as based on the results of the parameters R_{PEN}, $I_{R\&B}$, M_L and I_A.
- The penetration indexes (P_I) experienced decreases after binder modification, and they are typically lower for the formulations with PPA than the corresponding binders without PPA.

6.1.2. Penetration and Softening Point Protocols and Mass Losses

Table 22 shows the outcomes of the penetration tests for the unaged and short-term aged asphalt binders, together with their retained penetrations (parameter R_{PEN}). The modified materials typically depict lower penetration values than the base binder, especially for the ones with PE, PE+PPA, PPA, EVA+PPA and rubber+PPA. Also, the presence of PPA somehow highlighted the stiffnening effects of the asphalt binder after short-term aging, as can be inferred from the negative variations in R_{PEN} when moving from the AC+modifier formulations to the AC+modifier+PPA ones. In other words, the sensitivity of the penetrations of several asphalt binders with PPA in the composition to aging (AC+rubber+PPA, AC+SBS+PPA, AC+EVA+PPA and AC+SBR+PPA) is higher than the ones of the corresponding formulations without PPA (AC+rubber, AC+SBS, AC+EVA and AC+SBR). These conclusions are in accordance with other publications in the literature that also studied AC+modifier and AC+modifier+PPA formulations, e. g., Domingos and Faxina (2015b).

Table 22 – Outcomes of the penetration tests for the unaged and RTFO-aged binders and corresponding retained penetrations

asphalt binder	penetration values (dmm)[b]		retained penetration (%)	variation (%)[a]
	unaged	RTFO-aged		
base binder (AC)	52.0 (9)	30.0 (7)	57.7	N/A[c]
AC+PPA	24.0 (1)	22.0 (3)	91.7	58.9
AC+Elvaloy+PPA	39.0 (8)	31.0 (8)	79.5	37.8
AC+rubber	38.0 (7)	33.0 (9)	86.8	N/A
AC+rubber+PPA	35.5 (5)	26.0 (5)	73.2	-15.7
AC+SBS	31.0 (3)	29.0 (6)	93.5	N/A
AC+SBS+PPA	31.0 (3)	26.0 (5)	83.9	-10.3
AC+EVA	35.0 (4)	34.0 (10)	97.1	N/A
AC+EVA+PPA	37.0 (6)	22.5 (4)	60.8	-37.4
AC+PE	31.0 (3)	21.0 (2)	67.7	N/A
AC+PE+PPA	27.0 (2)	20.0 (1)	74.1	9.5
AC+SBR	37.0 (6)	36.0 (11)	97.3	N/A
AC+SBR+PPA	39.0 (8)	29.0 (6)	74.4	-23.5

[a] the column "variation" shows the percentages of increase or decrease in R_{PEN} for a specific binder when compared to its reference one. The base binder was used as reference for the AC+PPA and the AC+Elvaloy+PPA, whereas the AC+modifier binders were the references for their corresponding AC+modifier+PPA ones.
[b] the numbers in parentheses refer to the positions of the binders in a ranking from the lowest to the highest penetration values, either before or after RTFO-aging. Similar values received similar positions in the rankings.
[c] N/A: not applicable.

In a general context, it can be said that binder modification with plastomers (EVA and PE) depicted lower penetrations than the ones with elastomers (SBS and SBR) and Elvaloy® terpolymer. Although this is in agreement with the mixture data, it cannot be taken as a positive conclusion because penetration is an empirical measurement of the consistency of the asphalt binder, and therefore the differences among the responses of binders and mixtures will not be the same as based on penetration values. For instance, the penetrations of the AC+rubber, the

AC+EVA and the base material (33, 34 and 30 dmm, respectively) suggest that the two modified binders have poorer performance (higher penetrations) than the original one. However, it was shown that a completely opposite trend is observed in the repeated creep tests, i. e., the AC+EVA and the AC+rubber showed much better performances than the original binder. The R_{PEN} value of the base binder (57.7%) also complies with the requirement of the Brazilian specification for 50/70-penetration grade materials ($R_{PEN} \geq 55\%$).

Table 23 draws the comparisons among the rankings of binders (as based on their penetrations before and after RTFO aging) and mixtures (F_N or γ_{per}, depending on the formulation). Similarly to any other empirical-based property, the penetration data do not have strong correlations with mixture data in the flow number tests. This is not restricted to the present study, since other authors (DREESSEN et al., 2009; SYBILSKI, 1996a) had already pointed out similar conclusions. In addition, many formulations showed similar penetrations either before or after aging; as a consequence, they received similar positions in the rankings. This was the case of the AC+SBS and the AC+SBS+PPA (unaged), the AC+Elvaloy+PPA and the AC+SBR+PPA (unaged), the AC+SBS+PPA and the AC+rubber+PPA (short-term aged) and the AC+SBS and the AC+SBR+PPA (short-term aged). Again, it is clear that the penetration tests are too limited and cannot be used in the analysis of the actual rutting performance of the binder and the mixture in the pavement, especially because rutting is not typically observed in a real pavement at 25°C. In fact, this test only provides an estimation of the increased hardness – or stiffness – of the binder after the incorporation of modifiers and accelerated aging (AIREY, 2002, 2003, 2004).

Table 24 is a summary of the ring-and-ball softening point values of the studied formulations, as well as the associated aging parameters ($I_{R\&B}$). The Brazilian asphalt binder specification states that $I_{R\&B}$ cannot be higher than 8°C for the 50/70 base binders, which is the case of the one used in this dissertation (equal to 3.0°C). By assuming that such limit can be extended to the modified binders as well, only the AC+PE+PPA would not meet the requirement of maximum $I_{R\&B}$ value (10.8°C). With exception of the AC+rubber and the AC+SBS, the addition of PPA and the reduction in the content of the other modifier increased the differences between the softening point values after and before aging. It is also interesting to observe that the AC+EVA+PPA and the AC+PE+PPA are the materials with the highest increases in $I_{R\&B}$, and they did not fail in the flow number tests. Differently from the AC+rubber, the AC+rubber+PPA showed a profound decrease in $I_{R\&B}$ (more than 60%) and failed in this same test. Despite the empirical nature of the softening point protocol, this might indicate that some binders with higher degrees of stiffness after short-term aging may depict better performances in the asphalt mixture than the ones with lower increases in the overall stiffness after aging.

Table 23 – Similarities and differences among the rankings of asphalt binders (penetrations before and after RTFO aging) and asphalt mixtures (F_N and γ_{per})

asphalt binder	failure in the FN test	rankings of penetrations[a, b]		rankings of mixtures[a, b]	
		unaged	RTFO-aged	F_N	γ_{per}
base binder (AC)	Yes	6	4	8	-
AC+PPA	Yes	1	1	7	-
AC+Elvaloy+PPA	Yes	5	5	1	-
AC+rubber+PPA	Yes	3	2	5	-
AC+SBS	Yes	2	3	4	-
AC+SBS+PPA	Yes	2	2	2	-
AC+SBR	Yes	4	6	6	-
AC+SBR+PPA	Yes	5	3	3	-
AC+rubber	No	5	4	-	1
AC+EVA	No	3	5	-	2
AC+EVA+PPA	No	4	3	-	5
AC+PE	No	2	2	-	3
AC+PE+PPA	No	1	1	-	4

[a] these rankings of asphalt binders and mixtures were made separately, as a function of the presence or absence of failure in the FN tests (F_N and γ_{per}, respectively). Similar penetration values received the same positions in the rankings.
[b] the gray-shaded boxes indicate agreement between the rankings of binders and mixtures.

Table 24 – Outcomes of the softening point (*R&B*) tests for the unaged and RTFO-aged binders and corresponding increases in softening point

asphalt binder	*R&B* values (°C)[b]		increase in *R&B* (°C)	variation (%)[a]
	unaged	RTFO-aged		
base binder (AC)	50.3 (11)	53.3 (13)	3.0	N/A[c]
AC+PPA	60.1 (5)	65.5 (6)	5.4	80.0
AC+Elvaloy+PPA	61.0 (3)	65.3 (7)	4.3	43.3
AC+rubber	57.0 (10)	60.8 (12)	3.8	N/A
AC+rubber+PPA	59.5 (8)	61.0 (11)	1.5	-60.5
AC+SBS	60.4 (4)	68.1 (3)	7.7	N/A
AC+SBS+PPA	59.3 (9)	63.1 (10)	3.8	-50.6
AC+EVA	61.8 (2)	64.9 (8)	3.1	N/A
AC+EVA+PPA	59.8 (6)	67.4 (4)	7.6	145.2
AC+PE	73.6 (1)	79.5 (1)	5.9	N/A
AC+PE+PPA	61.8 (2)	72.6 (2)	10.8	83.1
AC+SBR	59.6 (7)	64.6 (9)	5.0	N/A
AC+SBR+PPA	59.8 (6)	66.8 (5)	7.0	40.0

[a] the column "variation" shows the percentages of increase or decrease in $I_{R\&B}$ for a specific binder when compared to its reference one. The base binder was used as reference for the AC+PPA and the AC+Elvaloy+PPA, whereas the AC+modifier binders were the references for their corresponding AC+modifier+PPA ones.
[b] the numbers in parentheses refer to the positions of the binders in a ranking from the highest to the lowest *R&B* values, either before or after RTFO-aging. Binders with similar softening points received similar positions in the ranking.
[c] N/A: not applicable.

As can be inferred from the rankings, the AC+PE is the formulation with the highest softening points in the two aging conditions, and it is typically followed by other formulations prepared with plastomers or with PPA in the composition (AC+PE+PPA, AC+EVA, AC+EVA+PPA or AC+Elvaloy+PPA). At the other extreme of the rankings, the asphalt-rubber binders and the modifications with SBS+PPA and SBR generally showed much lower *R&B* values. In addition, the presence of PPA somehow tends to shift the positions of the asphalt binder to higher levels, especially for the AC+PE+PPA, the AC+EVA+PPA and the AC+SBS+PPA. This is an indication that PPA may contribute to the sensitivity of the asphalt binder to aging, even though its interaction with the other components and the individual resistances of the additives to aging play a major role in the extent and degree of stiffness of the material. The RTFO-aging procedure also underlined the differences between the *R&B* values of the AC+EVA and the AC+PE+PPA in the unaged condition (61.8°C for both), as well as the ones of the AC+EVA+PPA and the AC+SBR+PPA (59.8°C for both).

The results of the empirical-based tests indicate that plastomeric modification of asphalt binder (i. e., PE and EVA with or without PPA) tends to increase the consistency of the original material at higher rates than the modifications with elastomeric polymers (SBS and SBR) and crumb rubber. PPA-modified binders also depicted a high degree of stiffness in the penetration tests, even tough their mixture data did not show the same trend. In addition, the presence of PPA in the formulations with crumb rubber, SBS, EVA, PE and SBR typically enhances the stiffness of the asphalt binder (lower penetrations and higher softening points), especially after RTFO aging. These observations are supported by other publications from the literature as well, see the one from Domingos and Faxina (2015b) as an example. In any case, either the penetration or the softening point tests are too empirical and do not reflect the actual performance of the materials in the pavement. This can be concluded not only from the absence of correlations between such data, but also the similar penetration values for some formulations in the unaged and short-term aged conditions (Table 23).

In the middle of the 1930's, Pfeiffer and Van Doormaal[33] early developed an equation to estimate the penetration index (P_I) of the asphalt binder based on the penetration and softening point values. This index is supposed to show the changes in penetration with increasing temperature, and therefore to estimate the temperature susceptibility of the material. As can be seen in Equation (43), it is necessary to determine the penetration at 25°C (P_{25} value) and the corresponding softening point *R&B* to obtain P_I. The assumption is that the binder has a

[33] PFEIFFER, J. P.; VAN DOORMAAL, P. M. (1936). The rheological properties of asphaltic bitumens. **Journal of the Institute of Petroleum**, Vol. 22, No. 4, pp. 414-440.

penetration of about 800 dmm when tested at its softening point (LESUEUR, 2009; READ and WHITEOAK, 2003), and this is taken into account in the Brazilian specification for asphalt binders (BERNUCCI et al., 2006). The lower the absolute P_I value, the lower the temperature susceptibility of the material will be.

$$P_I = \frac{1952 - 500 \times \log(P_{25}) - 20 \times R\&B}{50 \times \log(P_{25}) - R\&B - 120} \tag{43}$$

The penetration indexes of all binders are shown in Figure 43. The absolute values of P_I are also provided because some results are positive and others are negative, which may create difficulties in their correct interpretation. Asphalt binder modification decreased the P_I values except for the AC+PE (2.23). Lower P_I values suggest that the temperature susceptibility was reduced after the incorporation of modifiers, which is in accordance with other publications from the literature (AIREY, 2002, 2003, 2004). The results are all between -2 and 8, and this is the interval within which the P_I values of several binders fall (LESUEUR, 2009). Although P_I can be used as a good estimation of the behavior of the asphalt binder, the simplifications made in the analysis – e. g., a hypothetical penetration of 800 dmm at the softening point temperature and a small range of temperatures considered in the material characterization – may require additional stiffness and viscosity tests to confirm the results (LESUEUR, 2009; READ and WHITEOAK, 2003).

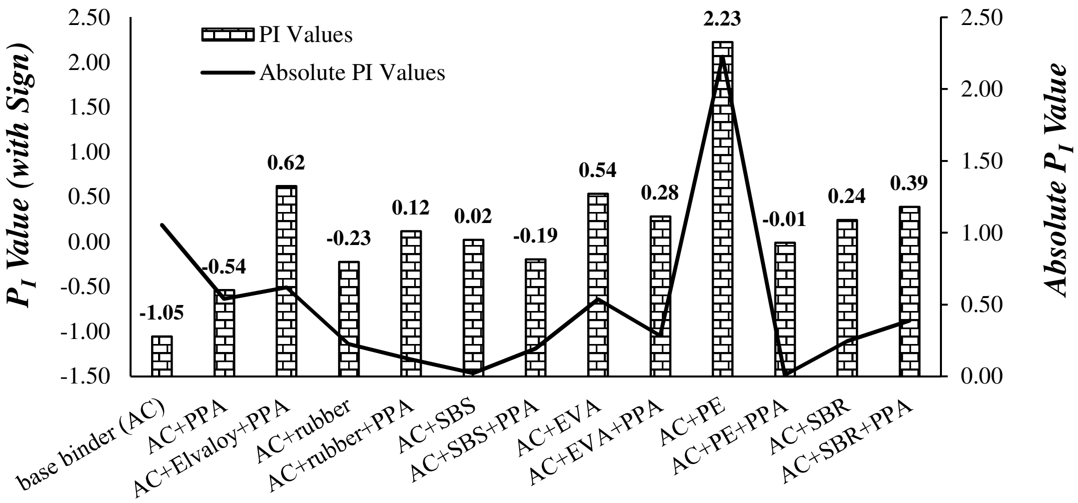

Figure 43 – Penetration index (P_I) of the 50/70 original binder and the modified materials in terms of their absolute and non-absolute values

The Brazilian asphalt binder specification establishes that the P_I values of all penetration-graded materials must be between -1.5 and 0.7, which is the case of the 50/70 original material from the Lubnor-Petrobras refinery (-1.05). The results for the other binders ranged from 0.01

to 2.23 (absolute values), and they are typically lower than 1. In general, the presence of PPA contributed to a decrease in the temperature susceptibility of the formulations (lower absolute P_I values). These include the AC+rubber and the AC+rubber+PPA (from 0.23 to 0.12), the AC+EVA and the AC+EVA+PPA (from 0.54 to 0.28), the AC+PE and the AC+PE+PPA (from 2.23 to only 0.01) and the group comprised by the base material, the AC+PPA and the AC+Elvaloy+PPA (from -1.05 to -0.54 and 0.62, respectively).

With respect to the mass losses after RTFOT, the results shown in Figure 44 indicate that binder modification with one or two additives reduces the M_L values, with only a few exceptions. Positive numbers suggest that the effects of oxidation are more pronounced than the ones of volatilization, whereas negative numbers indicate an opposite trend. None of the results exceeded the maximum allowed values of 1.0 and 0.5% set by Superpave® and the Brazilian specification, respectively. The presence of one or two additives decreased M_L by 42% (AC+EVA) up to 284% (AC+rubber+PPA) and, in general, these reductions were more pronounced for the ones with PPA. It is also interesting to note that M_L is higher for the AC+modifier+PPA binders than for the corresponding AC+modifier ones and, in some cases, they are higher than the mass loss of the base material as well. As previously observed for the softening point data (Table 24), this suggests that PPA contributed to the preparation of a more sensitive binder to aging. Thus, the resulting binder will probably have a higher concentration of asphaltenes than the ones without PPA because either the modifier or PPA will contribute to this increase in the amount of asphaltenes (LESUEUR, 2009).

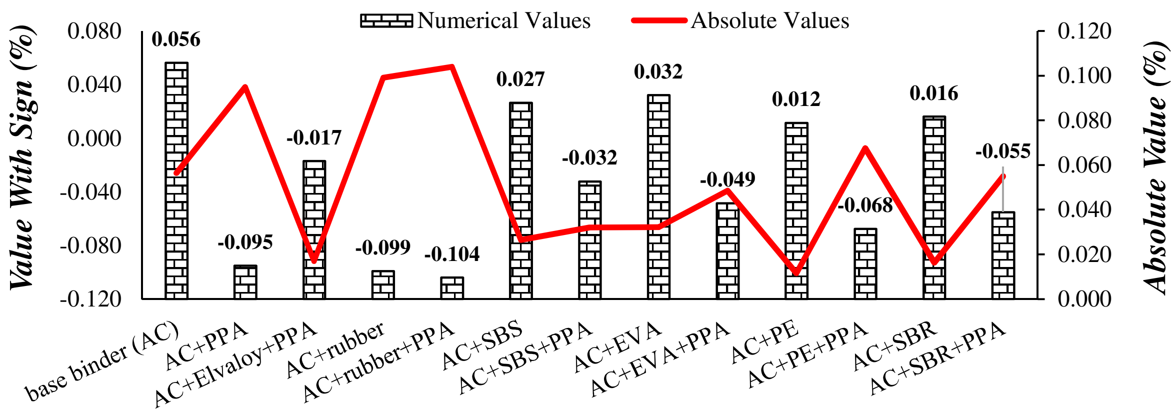

Figure 44 – Mass losses of the base binder (AC) and the 12 formulations after short-term aging in the rolling thin-film oven (mean values of at least three replicates)

6.1.3. Rotational Viscosity Tests

Table 25 shows the results of the rotational viscosity tests, either in the unaged or the short-term aged condition. With respect to the unaged materials, three different groups of binders can be identified here: (a) the AC+PPA and the base binder, which depict viscosities no greater than 0.9 and 0.6 Pa.s at 135°C and the other temperatures, respectively; (b) the AC+Elvaloy+PPA, the AC+rubber+PPA, the AC+EVA+PPA and all the formulations prepared with SBS, PE and SBR, for which the viscosities do not overcome 1.6 and 1.1 Pa.s at 135°C and the other four temperatures, respectively; and (c) the AC+rubber and the AC+EVA, the two modified binders with the highest viscosity values under all testing and aging conditions. In terms of the mixing and compaction temperatures (Table 8, Chapter 4), these three groups have some particular characteristics as follows:

- the processing temperatures of the members of the first group (i. e., the original binder and the AC+PPA) were directly obtained from the viscosity-temperature charts, which means that the upper limit of 177°C did not need to be considered;
- the temperatures of the members of the second group (i. e., the AC+rubber and the AC+EVA) were both limited to 177°C because the calculated temperatures were much higher than this maximum allowed value; and
- at least one of the temperatures of the members of the third group (all the remaining binders) was restricted to 177°C because the mean and individual temperatures were beyond this boundary of acceptable values.

Table 25 – Rotational viscosities of the unaged and rolling thin-film oven aged asphalt binders (neat and modified ones)

asphalt binder	viscosities, in Pa.s → unaged (RTFO-aged)				
	135°C	143°C	150°C	163°C	177°C
base binder (AC)	0.39 (0.50)	0.27 (0.33)	0.19 (0.24)	0.12 (0.14)	0.07 (0.08)
AC+PPA	0.81 (1.62)	0.53 (0.99)	0.37 (0.67)	0.21 (0.36)	0.12 (0.20)
AC+Elvaloy+PPA	1.42 (2.93)	0.91 (1.52)	0.64 (1.03)	0.36 (0.54)	0.21 (0.29)
AC+rubber	2.58 (4.74)	1.74 (3.00)	1.28 (2.10)	0.83 (1.22)	0.55 (0.72)
AC+rubber+PPA	1.37 (1.93)	0.89 (1.12)	0.64 (0.78)	0.39 (0.47)	0.26 (0.29)
AC+SBS	1.41 (1.51)	0.81 (0.97)	0.57 (0.71)	0.36 (0.43)	0.22 (0.26)
AC+SBS+PPA	1.17 (1.73)	0.74 (1.05)	0.55 (0.76)	0.34 (0.45)	0.20 (0.27)
AC+EVA	2.73 (3.42)	1.86 (2.10)	1.36 (1.52)	0.82 (0.88)	0.50 (0.53)
AC+EVA+PPA	1.29 (2.05)	0.85 (1.33)	0.61 (0.94)	0.36 (0.52)	0.22 (0.30)
AC+PE	1.39 (2.15)	0.94 (1.39)	0.69 (1.00)	0.42 (0.58)	0.26 (0.34)
AC+PE+PPA	1.38 (2.23)	0.88 (1.43)	0.65 (1.00)	0.41 (0.55)	0.25 (0.32)
AC+SBR	1.58 (1.86)	1.05 (1.23)	0.77 (0.90)	0.47 (0.55)	0.30 (0.34)
AC+SBR+PPA	1.27 (2.10)	0.85 (1.38)	0.62 (0.98)	0.37 (0.56)	0.22 (0.33)

It has been pointed out in the literature that the increase in viscosity is closely related to the asphaltene content in the aged and original materials, but this trend was not found to be valid for unaged materials. This may be due to the fact that, during accelerated aging in the laboratory and the exposition of the binder to heat and air, chemical reactions take place and they are actually responsible for the degree of stiffness of the binder (SIDDIQUI and ALI, 1999). Each material and formulation has its own relative increases in viscosity, and they are also dependent on the crude source and the modification type. As can be inferred from the data summarized in Table 26, the viscosities of all binders increased from 5 to about 84% with short-term aging except for the AC+Elvaloy+PPA and the AC+PPA. The mean values and the differences among the results decrease with increasing temperature, and the formulations with PPA show higher I_A values than the corresponding ones without PPA for several materials (an exception is made for the crumb rubber-modified binders).

Table 26 – Viscosity aging indexes (parameter I_A) of the asphalt binders at the temperatures of 135, 143, 150, 163 and 177°C and some statistical parameters

asphalt binder or parameter	I_A values at each temperature (η after aging / η before aging)				
	135°C	143°C	150°C	163°C	177°C
base binder (AC)	1.28	1.26	1.24	1.20	1.17
AC+PPA	1.99	1.89	1.82	1.74	1.68
AC+Elvaloy+PPA	2.06	1.66	1.60	1.50	1.36
AC+rubber	1.84	1.73	1.63	1.46	1.30
AC+rubber+PPA	1.41	1.26	1.22	1.21	1.13
AC+SBS	1.07	1.20	1.26	1.20	1.19
AC+SBS+PPA	1.48	1.42	1.39	1.33	1.34
AC+EVA	1.25	1.13	1.11	1.08	1.05
AC+EVA+PPA	1.59	1.56	1.53	1.45	1.36
AC+PE	1.55	1.47	1.45	1.39	1.34
AC+PE+PPA	1.62	1.63	1.54	1.37	1.28
AC+SBR	1.18	1.17	1.16	1.17	1.14
AC+SBR+PPA	1.65	1.62	1.58	1.51	1.47
Mean Value	1.55	1.47	1.45	1.37	1.30
Standard Deviation	0.29	0.23	0.21	0.17	0.16

As previously discussed, the major effect of asphaltenes on viscosity is to increase it with increasing asphaltene content. Lesueur (2009) emphasized in the literature review part of his paper that, in general, an increase of 1-4% by weight in the asphaltene content after RTFOT will probably multiply the viscosity by a factor of 1.5-4.0 (parameter I_A). It was also pointed out above in the present document that one of the theories to explain the reaction between PPA and the binder refers to the dispersion of the stacked asphaltene molecules, which in turn increases the viscosity. In other words, PPA may speed up the aging process of the pavement and contribute to a higher rate of increase in the asphaltene content of the binder when compared with the materials without PPA. As a result, this may lead to a premature failure of the pavement by cracking (TAM, 2012). Due to these and other concerns over PPA, many state highway agencies restricted or banned the use of this acid in pavement design projects and rehabilitations. In a quite recent survey conducted by Maurer and D'Angelo (2012), it was concluded that 29 of the states of the US banned or imposed restrictions to the use of PPA in their pavements.

Interestingly, the AC+rubber followed a different pattern of behavior after aging when PPA was added and the rubber content was reduced, even though the tendency was not changed in the unaged condition (i. e., the AC+rubber+PPA has lower viscosities than the AC+rubber before aging). Some odd cases with the results of aged rubber-modified asphalt binders can also be found elsewhere, e. g., longer durations of exposition to heat and air do not necessarily lead to higher rotational viscosities for such materials (LEE et al., 2008). It is not clear as to whether PPA reacts with crumb rubber or any of its components during short-term aging or not, but it seems that such combination somehow decreased the extent of oxidative age hardening in the binder. This also happens when other additives – e. g., hydrated lime – are blended with AC+PPA or the original material (HUANG et al., 2011; PETERSEN, 2009). Another possibility is that the degree of oxidative aging in crumb rubber-modified binders is directly governed by the rubber particles, and the presence of less particles diminishes the intensity of the aging phenomena in the AC+rubber+PPA. This can also be implied by analyzing the increases in softening point after aging for the AC+rubber (3.8°C) and the AC+rubber+PPA (only 1.5°C) – see Table 24.

It is known that crumb rubber may be comprised by a number of components other than rubber – for instance, sulfur, ash and extract contents (BIRO and FAZEKAS, 2005; NAVARRO et al., 2005; YADOLLAHI and MOLLAHOSSEINI, 2011) – and that the interactions between the particles and the binder are dictated by their chemical compositions and sizes and result in an asphalt-rubber system with a very complex nature (DIVYA et al., 2013; KING et al., 1999). Thus, it is rather difficult to cite only one reason for the marked increases in I_A after the addition of crumb rubber to the base binder. Ruan et al. (2003) mentioned that, when crumb rubber-modified binders are subjected to heat and air for a long time, this process might break down the rubber particles into smaller units and increase their concentration in the formulation. In summary, it seems that the combined effects of degradation of the rubber particles – and hence their expansion in the formulation – and the oxidation of the fractions of the binder led to this substantial increase in the rotational viscosity after aging.

Modified asphalt binders commonly show lower aging indexes than their corresponding original ones, and this may be due to the degradation of the polymers during RTFOT (RUAN et al., 2003). This was observed for the great majority of the polymer-modified materials studied here and without PPA, e. g., the AC+SBS, the AC+EVA and the AC+SBR. As one may have realized, the AC+PE is an exception within the group of the polymer-modified materials. In this manner, Ruan et al. (2003) highlighted the fact that the oxidation rate may not always be lower for the modified binders when compared with the unmodified ones. This is possibly the case of the AC+PE, which is the only formulation among the ones with polymers and no PPA that presented higher I_A values than the original binder.

6.2. Oscillatory Shear Tests

6.2.1. Highlights

- Some modifications have a greater effect on the stiffness of the binder as measured by $G^*/sin\delta$, whereas others – especially elastomers and without PPA – markedly change its temperature susceptibility.
- The differences between the parameters $G^*/sin\delta$ and $|G^*|/[1-(1/tan\delta sin\delta)]$ before aging decrease with the addition of PPA and the reduction in the polymer content for the polymer-modified materials.
- The stiffening effects of PPA are more pronounced after aging, and the high δ values may have contributed to the higher increases in the Shenoy's parameter for AC+Elvaloy+PPA, AC+EVA and AC+EVA+PPA.
- The rankings based on $G^*/sin\delta$ and $|G^*|/[1-(1/tan\delta sin\delta)]$ tend to be the same at higher temperatures, which indicates that the Shenoy's parameter did not solve all the issues about rutting characterization.

6.2.2. Results and Discussion

Table 27 depicts the results of the parameter $G^*/sin\delta$ in the unaged condition, together with the constants A and B from the model used by Elseifi et al. (2013) and Laukkanen et al. (2015) – Equation (37), Chapter 4. As known, this condition is used to determine the high PG grade of the binder in the selected version of the Superpave® specification (Table 3 from AASHTO M320-09 standard). The constant A indicates the value of the parameter $G^*/sin\delta$ when the temperature drops to the hypothetical value of 0°C, whereas the constant B is representative of the rate of decrease in *G*/sinδ* with increasing temperature. In other words, higher *A* values are associated with a more marked vertical shift of the curve and lower |*B*| values are associated with a lower susceptibility of the stiffness of the binder to temperature. The model was able to almost perfectly fit the data and, although the R^2 values are not reported here, they were all higher than 0.994.

The data suggest that two main phenomena occurred after binder modification: (a) marked increases in the numerical values of the parameter *G*/sinδ* and no great changes in the thermal susceptibility of the stiffness of the material; and (b) smaller increases in *G*/sinδ* and significant reductions in this temperature susceptibility. The first phenomenon includes the AC+PPA, the AC+SBS+PPA, the AC+PE, the AC+PE+PPA and the AC+SBR+PPA, and is characterized by sharp increases in the constant *A* and almost no variations in the constant *B*. In practical terms, the curves of these materials were considerably shifted in the vertical axis and their slopes do not differ from the one of the original binder (example in Figure 45). The second phenomenon includes all the remaining materials (AC+Elvaloy+PPA, AC+rubber, AC+rubber+PPA, AC+SBS, AC+EVA+PPA, AC+EVA and AC+SBR) and is mainly characterized by big reductions in |*B*|; as a consequence, the slopes of their curves are less steep than the curve of the original binder (example in Figure 46).

Table 27 – Results of the parameter *G*/sinδ* before accelerated aging in the rolling thin-film oven and constants *A* and *B* from the model used by Elseifi et al. (2013) and Laukkanen et al. (2015)

asphalt binder	*G*/sinδ* (in kPa) at each temperature						constants of the model	
	52°C	58°C	64°C	70°C	76°C	82°C	*A*	*B*
base binder (AC)	7.74	3.14	1.36	0.63	0.31	-	7711.8	-0.134
AC+PPA	31.50	13.42	5.88	2.64	1.23	0.61	28335	-0.132
AC+Elvaloy+PPA	14.17	6.82	3.50	1.87	1.04	0.60	3104	-0.105
AC+rubber	18.04	8.75	4.39	2.25	1.18	0.66	5387.3	-0.111
AC+rubber+PPA	20.58	9.62	4.69	2.35	1.21	0.67	7439.5	-0.114
AC+SBS	19.85	9.44	4.62	2.33	1.22	0.68	6608	-0.113
AC+SBS+PPA	23.91	10.62	4.81	2.24	1.10	0.58	14632	-0.125
AC+EVA	15.75	7.26	3.54	1.93	1.10	0.65	3425.4	-0.106
AC+EVA+PPA	20.82	9.43	4.75	2.43	1.24	0.65	7612.8	-0.115
AC+PE	28.91	11.97	5.32	2.52	1.23	0.65	18768	-0.126
AC+PE+PPA	30.71	12.63	5.48	2.52	1.21	0.62	24380	-0.130
AC+SBR	15.95	7.80	3.90	2.04	1.15	0.69	3498.1	-0.105
AC+SBR+PPA	22.14	9.80	4.49	2.15	1.09	0.58	11443	-0.122

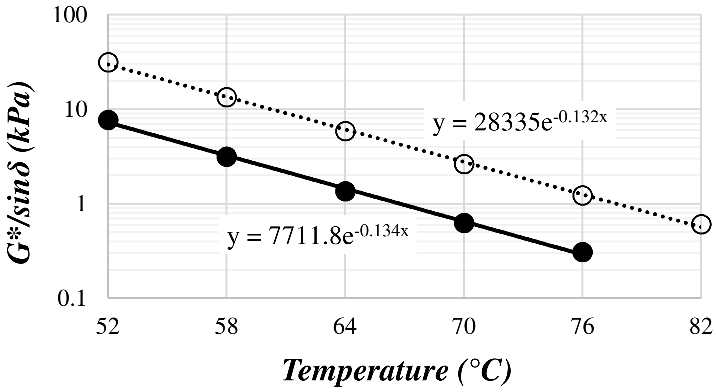

Figure 45 – Decreases in the parameter *G*/sinδ* with temperature for the 50/70 base asphalt binder (continuous line) and the AC+PPA (dotted line)

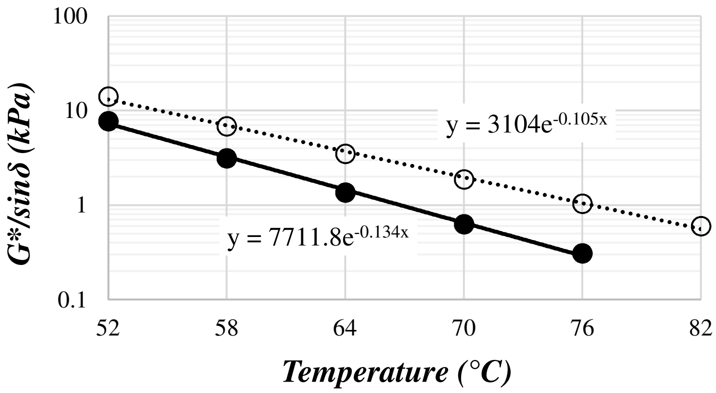

Figure 46 – Decreases in the parameter *G*/sinδ* with temperature for the 50/70 base asphalt binder (continuous line) and the AC+Elvaloy+PPA (dotted line)

It may be important to note that some binders show *A* values close to the one of the base material (AC+rubber+PPA, AC+SBS and AC+EVA+PPA), whereas others show much lower *A* values (AC+Elvaloy+PPA, AC+rubber, AC+EVA and AC+SBR). This essentially means that some modification types had a stronger effect on the stiffness of the binder (*A* value) than on its susceptibility to temperature (*B* value), whereas others depicted a different trend. Interestingly, the addition of PPA and the reduction in the content of the other modifier (crumb rubber, SBS, EVA, PE and SBR) led to simultaneous increases in *A* and |*B*|. The same can be said for the AC+PPA when compared with the original binder. This indicates that the presence of PPA contributed – at least at some extent – to the increase in the overall stiffness of the modified binder, and also that it increased the temperature susceptibility of the material.

With respect to the modifiers, it can be seen that the elastomers (SBS and SBR) mainly acted by decreasing the temperature susceptibility of the binder and their effects on stiffness are not as significant as the ones observed for other modification types. These findings were also observed by other authors who worked with elastomeric-modified asphalt binders (AIREY, 2003, 2004), and they are in agreement with the softening points (Table 24) and the rotational viscosities (Table

25) as well. On the other hand, the use of PE and PE+PPA (a plastomer) markedly increased the stiffness of the binder and showed a marginal effect on its susceptibility to temperature. Although the EVA copolymer is also a plastomer, its effects on $G^*/sin\delta$ – either with or without PPA – resemble the ones of the elastomers and the Elvaloy® terpolymer, i. e., substantial decreases in the parameter B and small to great reductions in the parameter A. Finally, the AC+rubber and the AC+rubber+PPA depict lower temperature susceptibilities than the original binder (lower $|B|$ values) and similar effects on A when compared with the AC+EVA and the AC+EVA+PPA.

Table 28 provides the values of the Shenoy's parameter $|G^*|/[1-(1/tan\delta sin\delta)]$ for the unaged asphalt binders. As previously discussed, the weight of the phase angle δ is heavier in this parameter than in the original $G^*/sin\delta$, and this means that binders with higher levels of elasticity will show greater increases from $G^*/sin\delta$ to $|G^*|/[1-(1/tan\delta sin\delta)]$ than the materials with lower levels of elasticity. This is the case of the modifiers that have significant degrees of reactivity with the neat asphalt binder, e. g., Elvaloy®, SBS, PPA and EVA. It may be important to remind that the vinyl acetate content in the HM 728 EVA copolymer used here is 28%, which is very close to the upper limits typically used for asphalt modification – 28 to 29%, according to Polacco et al. (2006, 2015). The results in Table 29 clearly indicate that the AC+Elvaloy+PPA, the AC+SBS, the AC+EVA and the AC+PPA are among the binders with the highest increases from one parameter to the other, whereas the AC+PE, the AC+PE+PPA, the AC+SBR and the AC+SBR+PPA showed much lower percentages (no greater than 36% and 28% for the materials with SBR and PE, respectively).

Table 28 – Results of the Shenoy's parameter for the unmodified and modified asphalt binders before accelerated aging (RTFOT)

asphalt binder	$\lvert G^*\rvert/[1-(1/tan\delta sin\delta)]$ (in kPa) at each temperature					
	52°C	58°C	64°C	70°C	76°C	82°C
base binder (AC)	8.20	3.27	1.39	0.64	0.31	-
AC+PPA	45.93	18.31	7.50	3.17	1.40	0.66
AC+Elvaloy+PPA	20.69	10.28	5.34	2.80	1.49	0.82
AC+rubber	28.22	12.34	5.70	2.73	1.34	0.73
AC+rubber+PPA	31.82	13.64	6.19	2.90	1.40	0.75
AC+SBS	30.64	13.93	6.34	2.99	1.49	0.81
AC+SBS+PPA	34.59	14.22	5.96	2.61	1.23	0.62
AC+EVA	30.05	12.60	5.15	2.52	1.34	0.76
AC+EVA+PPA	30.35	12.99	6.08	2.94	1.43	0.73
AC+PE	35.87	14.60	6.37	2.96	1.44	0.77
AC+PE+PPA	39.17	15.41	6.44	2.88	1.35	0.69
AC+SBR	21.64	10.06	4.83	2.47	1.38	0.85
AC+SBR+PPA	29.02	12.28	5.36	2.47	1.21	0.64

Table 29 – Percentages of increase in the binder parameter when moving from the original *G*/sinδ* to the Shenoy's parameter *|G*|/[1-(1/tanδsinδ)]* – unaged condition

asphalt binder	percentages of increase (%)[a]					
	52°C	58°C	64°C	70°C	76°C	82°C
base binder (AC)	5.9	4.1	2.6	1.7	1.2	-
AC+PPA	45.8	36.4	27.6	20.2	14.1	9.6
AC+Elvaloy+PPA	46.0	50.6	52.5	49.6	43.5	36.8
AC+rubber	56.4	41.0	29.8	21.3	14.3	11.5
AC+rubber+PPA	54.6	41.8	32.1	23.5	15.7	13.3
AC+SBS	54.4	47.5	37.4	28.6	22.3	19.7
AC+SBS+PPA	44.7	33.8	23.9	16.4	11.3	8.2
AC+EVA	90.8	73.6	45.6	30.9	22.2	16.3
AC+EVA+PPA	45.7	37.8	27.9	21.2	15.4	11.3
AC+PE	24.1	22.0	19.8	17.6	16.5	19.2
AC+PE+PPA	27.6	22.1	17.6	14.2	11.4	10.9
AC+SBR	35.6	28.9	23.8	20.8	20.4	23.2
AC+SBR+PPA	31.1	25.3	19.4	14.9	11.5	9.6

[a] percent difference between the numerical values of *G*/sinδ* and *|G*|/[1-(1/tanδsinδ)]*.

The formulations with crumb rubber (AC+rubber and AC+rubber+PPA) followed the pattern observed for the materials with high degrees of reactivity with the base binder (high percentages of increase) and their results are very close to the ones of the AC+EVA+PPA, especially at 64, 70 and 76°C. It is believed that the grinding process of crumb rubber until relatively fine particle sizes are obtained – in this case, less than 0.6 mm – and the use of intermediate rubber concentrations in the formulations (14% in the AC+rubber and 11% in the AC+rubber+PPA) contributed to this marked increase in the binder parameter. It was observed elsewhere that higher rubber contents further enhance the elasticity of the binder when only rubber is used in the modification process (NAVARRO et al., 2005), and other authors pointed out that complementary additives such as PPA and Vestenamer® may enhance the performance of crumb rubber-modified materials (YADOLLAHI and MOLLAHOSSEINI, 2011). This seems to be the case of the AC+rubber and the AC+rubber+PPA, in which the presence of PPA contributed to the slight increases in the percent difference between *G*/sinδ* and *|G*|/[1-(1/tanδsinδ)]* for the AC+rubber+PPA when compared with the AC+rubber.

By analyzing the data for the other formulations without PPA (AC+SBS, AC+EVA, AC+PE and AC+SBR) and their corresponding ones with PPA (AC+SBS+PPA, AC+EVA+PPA, AC+PE+PPA and AC+SBR+PPA), it is possible to infer that the differences among the parameters decrease in all cases except for the temperatures of 58 and 64°C and the PE-modified binders. This is an indication that, for such modifiers, the contribution of PPA to the results of the parameters $G^*/sin\delta$ and $|G^*|/[1-(1/tan\delta sin\delta)]$ was mainly restricted to the stiffness of the formulation, and also that the elastic properties within the linear viscoelastic region are more influenced by the amount of polymer. In other words, PPA acted by considerably increasing G^* (overall stiffness) and slightly increasing δ (a small decrease in the elastic response), and the fact that both parameters are higher for the AC+polymer+PPA materials than for the AC+polymer ones is due to the effects of PPA on the G^* values of the asphalt binders.

Table 30 shows a summary of the $G^*/sin\delta$ values for the RTFO-aged binders at the temperatures of 52, 58, 64, 70 and 76°C. The constants A and B (ELSEIFI et al., 2013; LAUKKANEN et al., 2015) are also provided. Again, the model showed excellent fits to the binder data (R^2 all higher than 0.993) and two different modification effects can be seen in the formulations. The first type of effect is the increase in the constant A and minor reductions in $|B|$, which means that the temperature susceptibility of the material is only slightly changed and its stiffness is markedly improved. Similarly to the unaged asphalt binders, this first group includes the AC+PPA, the AC+SBS+PPA, the AC+PE, the AC+PE+PPA and the AC+SBR+PPA. The second type is typically characterized by reductions in A and $|B|$ at the same time – temperature susceptibility is much lower – and it includes all the remaining formulations (AC+Elvaloy+PPA, AC+rubber, AC+rubber+PPA, AC+SBS, AC+EVA, AC+EVA+PPA and AC+SBR). In other words, the pattern of behavior was not radically modified from one aging condition to the other and the key differences between these binders rely on the numerical values of $G^*/sin\delta$.

The effects of PPA and lower modifier contents on the stiffness and the temperature susceptibility of the AC+rubber, the AC+SBS, the AC+PE and the AC+SBR remained essentially the same in the short-term aged condition, i. e., simultaneous increases in A and $|B|$. This can be translated into higher temperature susceptibilities, marked improvements in G^* (stiffness) and small increases in δ (less elastic responses) for the AC+modifier+PPA formulations than for the AC+modifier ones. Similarly, the differences between the behaviors of the formulations with EVA and PE – both are plastomers – may be explained by the high degree of reactivity of EVA with the base asphalt binder. According to the literature review made by Polacco et al. (2015), this reaction is too complex because the polar groups in the EVA chain may associate either with themselves or with the asphaltenes in the binder phase, and this process leads to crosslinking when the modifier is used at appropriate contents. Finally, the SBS and the SBR copolymers (elastomers) caused expressive reductions in A and B when they are not used in conjunction with PPA, which is in agreement with the main features of these materials (ISACSSON and LU, 1995).

Table 30 – Results of the parameter $G^*/sin\delta$ after accelerated aging (RTFOT) and constants A and B from the exponential model used by Elseifi et al. (2013) and Laukkanen et al. (2015)

asphalt binder	$G^*/sin\delta$ (in kPa) at each temperature					constants	
	52°C	58°C	64°C	70°C	76°C	*A*	*B*
base binder (AC)	17.69	7.07	2.98	1.33	0.62	23778	-0.140
AC+PPA	65.76	29.51	13.55	6.42	3.13	47027	-0.127
AC+Elvaloy+PPA	25.55	12.50	6.47	3.53	2.01	5951.1	-0.106
AC+rubber	30.12	15.14	7.79	4.14	2.25	8094.2	-0.108
AC+rubber+PPA	31.49	14.54	6.96	3.47	1.78	15290	-0.120
AC+SBS	31.14	14.36	6.77	3.26	1.63	18249	-0.123
AC+SBS+PPA	48.87	22.38	10.31	4.82	2.36	34724	-0.127
AC+EVA	31.42	14.65	7.19	4.00	2.38	7793.3	-0.108
AC+EVA+PPA	36.95	19.34	10.62	6.12	3.47	5834.7	-0.098
AC+PE	56.23	23.36	10.38	4.83	2.29	53884	-0.133
AC+PE+PPA	61.90	26.07	11.34	5.18	2.46	64628	-0.134
AC+SBR	28.00	13.25	6.42	3.24	1.71	11661	-0.117
AC+SBR+PPA	43.35	19.81	9.29	4.55	2.34	23543	-0.122

The values of the Shenoy's parameter for the RTFO-aged binders are reported in Table 31. It can be inferred from these laboratory data that the stiffening effects of PPA on the response of the asphalt binder are much more pronounced than in the unaged condition, i. e., the complex modulus increases at higher rates after RTFO aging than before aging. The only exceptions were the AC+rubber+PPA and the AC+EVA+PPA, for which the percentages of increase from one parameter to the other ($G^*/sin\delta$ to $|G^*|/[1-(1/tan\delta sin\delta)]$) are lower than for the AC+rubber and the AC+EVA, see Table 32. In practical terms, the levels of interaction between PPA and the other modifier are not the same for all of them and are expected to be higher for SBS, SBR and Elvaloy® than for EVA and crumb rubber. This could somewhat be seen in the outcomes of the mixture tests reported in Chapter 5 as well, in which the AC+Elvaloy+PPA, the AC+SBS+PPA and the AC+SBR+PPA had a better rutting performance than the AC+PPA, the AC+SBS and the AC+SBR, respectively.

One interesting finding reported in Table 32 is the increasing percentages for the AC+Elvaloy+PPA with increasing temperature, which was not observed for the other materials. It is believed that the low phase angles played a major role in the increasing values of the Shenoy's parameter for such material, since AC+Elvaloy+PPA binders are known as formulations with very high levels of elastic response (CLYNE et al., 2012; DELGADILLO et al., 2012;

DOMINGOS and FAXINA, 2015a; FEE et al., 2010) and they may retain such high elastic responses even with increasing temperature (DOMINGOS and FAXINA, 2015a).

Table 31 – Results of the Shenoy's parameter for the unmodified and modified asphalt binders after aging in the rolling thin-film oven

asphalt binder	$\lvert G^*\rvert/[1-(1/\tan\delta\sin\delta)]$ (in kPa) at each temperature				
	52°C	58°C	64°C	70°C	76°C
base binder (AC)	21.23	8.10	3.30	1.42	0.65
AC+PPA	128.06	53.31	22.16	9.59	4.29
AC+Elvaloy+PPA	41.40	21.29	11.49	6.35	3.51
AC+rubber	62.26	27.33	12.56	6.06	3.01
AC+rubber+PPA	51.44	21.97	9.73	4.52	2.18
AC+SBS	48.74	21.02	9.00	4.03	1.93
AC+SBS+PPA	85.05	35.34	14.46	6.23	2.88
AC+EVA	85.92	31.66	11.88	5.69	3.14
AC+EVA+PPA	65.70	32.09	16.48	8.92	4.74
AC+PE	78.38	31.19	13.64	6.08	2.76
AC+PE+PPA	92.85	36.60	15.02	6.54	2.98
AC+SBR	40.49	18.00	8.35	4.08	2.11
AC+SBR+PPA	66.28	28.70	12.69	5.89	2.90

Table 32 – Percentages of increase in the binder parameter when moving from $G^*/\sin\delta$ to $\lvert G^*\rvert/[1-(1/\tan\delta\sin\delta)]$ – short-term aged condition

asphalt binder	percentages of increase (%)[a]				
	52°C	58°C	64°C	70°C	76°C
base binder (AC)	20.1	14.6	10.5	7.4	5.1
AC+PPA	94.7	80.6	63.6	49.5	37.3
AC+Elvaloy+PPA	62.0	70.3	77.6	79.7	74.7
AC+rubber	106.7	80.5	61.3	46.4	34.0
AC+rubber+PPA	63.4	51.1	39.7	30.2	21.9
AC+SBS	56.5	46.3	33.0	23.6	18.3
AC+SBS+PPA	74.0	57.9	40.3	29.1	22.4
AC+EVA	173.5	116.2	65.4	42.2	31.7
AC+EVA+PPA	77.8	65.9	55.2	45.7	36.5
AC+PE	39.4	33.5	31.4	25.9	20.2
AC+PE+PPA	50.0	40.4	32.5	26.4	21.2
AC+SBR	44.6	35.8	29.9	25.8	23.0
AC+SBR+PPA	52.9	44.9	36.6	29.4	23.9

[a] percent difference between the numerical values of $G^*/\sin\delta$ and $\lvert G^*\rvert/[1-(1/\tan\delta\sin\delta)]$.

Table 33 draws a comparison between the orderings of binders from the less to the most susceptible to rutting based on $G^*/sin\delta$ and $|G^*|/[1-(1/tan\delta sin\delta)]$. The substantially high values of $G^*/sin\delta$ and $|G^*|/[1-(1/tan\delta sin\delta)]$ for the AC+PPA resulted in the first positions for this material, and the same procedure can be applied to the 50/70 original binder (lowest results in both cases). The impact of δ on the numerical values of the Shenoy's parameter is reflected in the higher positions of the formulations that show great degrees of elasticity and lower δ values under oscillatory shear loading, e. g., the AC+Elvaloy+PPA (all temperatures), the AC+EVA and the AC+EVA+PPA (temperatures up to 64°C). The similarities among the rankings of the parameters increase with increasing test temperature, and this may be explained by the fact that δ has much lower influence on the results of $G^*/sin\delta$ and $|G^*|/[1-(1/tan\delta sin\delta)]$ when the temperature is higher and the binder shows a more viscous behavior.

Table 33 – Rankings of binders from the less (No. 1) to the most susceptible to rutting (No. 13) based on the parameters $G^*/sin\delta$ and $|G^*|/[1-(1/tan\delta sin\delta)]$

asphalt binder	rankings ($G^*/sin\delta$) – reference[a, b]					rankings ($|G^*|/[1-(1/tan\delta sin\delta)]$)[a, b]				
	52°C	58°C	64°C	70°C	76°C	52°C	58°C	64°C	70°C	76°C
base binder (AC)	13	13	13	13	13	13	13	13	13	13
AC+PPA	1	1	1	1	2	1	1	1	1	2
AC+Elvaloy+PPA	12	12	11	9	9	11	10	9	4	3
AC+rubber	10	7	7	7	8	8	8	7	7	5
AC+rubber+PPA	7	9	9	10	10	9	9	10	10	10
AC+SBS	9	10	10	11	12	10	11	11	12	12
AC+SBS+PPA	4	4	5	5	5	4	3	4	5	8
AC+EVA	8	8	8	8	4	3	5	8	9	4
AC+EVA+PPA	6	6	3	2	1	7	4	2	2	1
AC+PE	3	3	4	4	7	5	6	5	6	9
AC+PE+PPA	2	2	2	3	3	2	2	3	3	6
AC+SBR	11	11	12	12	11	12	12	12	11	11
AC+SBR+PPA	5	5	6	6	6	6	7	6	8	7

[a] the gray-shaded boxes indicate agreement between the rankings of $G^*/sin\delta$ and $|G^*|/[1-(1/tan\delta sin\delta)]$.
[b] the numbers show the position of the binder in a ranking from the less (No. 1) to the most susceptible to rutting (No. 13).

Although the Shenoy's parameter constitutes an attempt to better rank the binders according to their actual mixture performance, it can be seen that not all the limitations concerning this characterization were solved by any of the parameters, especially at higher temperatures (the rankings tend to be the same). This is because elasticity is an important factor in the resistance of the binder to rutting, but its actual effect on the mixture is not directly identified due to the influence of other variables such as the aggregate (GOLALIPOUR, 2011). As a consequence, the degrees of correlation tend to be higher for the Shenoy's parameter than for $G^*/sin\delta$ (Figure 37 and Table 18, Chapter 5), but the results were not satisfactory in any case. This is one of the reasons why both parameters were replaced by the nonrecoverable compliance J_{nr} from the MSCR test, and the percent recovery R was proposed as a better indicator of the elasticity of the binder. Either R or J_{nr} were used in the study of the responses of the binders in this document, as it will be shown later in the chapter.

6.3. Multiple Stress Creep and Recovery (MSCR) Tests

6.3.1. Highlights

- Binder modification with Elvaloy+PPA, EVA and EVA+PPA typically yields formulations with high degrees of elasticity regardless of the loading time, differently from the other modification types.
- The Burgers model was able to fit the strain data of the asphalt binders at the standardized creep-recovery times (1/9 s), and the only exception was the AC+EVA at the pavement temperature of 52°C.
- The use of PPA in the modification of the asphalt binder with SBS, EVA, PE and SBR tends to increase its rutting resistance at standardized and longer creep times (2/9, 4/9 and 8/9 s), except for the AC+rubber.
- The formulations with crumb rubber and EVA are typically overly stress sensitive (parameter $J_{nr,\ diff}$ is higher than 75%), and this does not necessarily depend on the loading-unloading times used in the tests.
- The equations from Huang (2004) and Pereira et al. (1998, 2000) showed good correlations with $J_{nr}3200$ at longer creep times, but the predicted traffic levels barely correlated with the actual ones.
- The parameter α from the model by Saboo and Kumar (2015) commonly shows good to excellent correlations with the percent recoveries of the binders, despite the identification of some intrinsic limitations.
- The binders commonly show higher levels of accumulated strain with increasing severity in the tests due to increases in the strain rate (parameter B) and, in some cases, increases in nonlinearity (parameter n) as well.

- The tendency of decrease in the initial strain (*A* values) and increase in the strain rate (*B* values) is reversed when very long loading times are used, which may be associated with the delayed elasticity of the binder.
- Binders with very high levels of stiffness show decreases either in the *A* or the *B* values and, in such cases, the nonlinear response (*n* values) is the main responsible factor for the increases in the permanent strain.
- The MSCR tests at very long loading times showed that, for the binders with high levels of elasticity, the unloading time of 500 s looks enough to reach full recovery in several materials at each creep-recovery cycle.
- In terms of the binders with low levels of elasticity, the unloading time of 240 s may not be appropriate for all modification types, especially the AC+rubber, the AC+SBR and the AC+SBS.
- The correlations between the F_N values and the corresponding $J_{nr}3200$ values of the binders improved up to the loading-unloading times of 4/9 s, which suggests that these binders approached steady state faster.
- The parameter associated with nonlinearity (*n*) barely correlates with the nonrecoverable compliances of the asphalt binders at longer creep times, but the results tend to be better at the stress level of 3,200 Pa.
- The steady state phenomenon can help in explaining some particular creep-recovery responses of formulations such as the AC+EVA, which could not be clearly seen for several binders.
- According to ANOVA, the variances within the *R* and J_{nr} values of the binders with increasing temperature and loading time may not be considered as statistically significant in all cases, except for the AC+SBS.
- The proposed Superpave® specification criteria highlighted the stress sensitivity of some formulations such as the AC+PPA, the AC+EVA and the AC+Elvaloy+PPA.

6.3.2. Preliminary Comments and MSCR Tests at Standardized Creep-Recovery Times (1/9 s)

Before the MSCR test data are presented and discussed in this dissertation, some comments must be made with respect to the analysis of the Burgers model parameters. As previously shown, the model has some limitations in the characterization of the creep-recovery response of the asphalt binder at high temperatures, since it is devoted to the linear viscoelastic range of this response. As a consequence, some adaptations and considerations had to be made in order to overcome the intrinsic limitations of this model. Figure 47 shows an example of two different responses of binders in the MSCR tests at the same temperature and stress level, together with their corresponding percent recoveries. The data suggest that the relationships among the elements of the AC+Elvaloy+PPA point to the existence of higher recoveries (approximately 57%), and the opposite trend is observed for the AC+EVA (less than 5%). In other words, the components of the model indicate the presence of higher amounts of elastic and delayed elastic strains in the AC+Elvaloy+PPA than the AC+EVA, see Table 34.

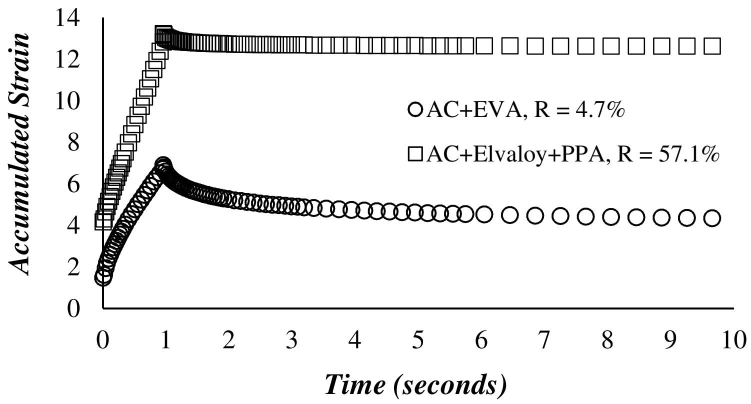

Figure 47 – First creep-recovery pulses of two different binders in the MSCR test (AC+EVA and AC+Elvaloy+PPA) at 70°C and 3.2 kPa

Table 34 – Elements of the Burgers model based on the strain data of the AC+Elvaloy+PPA and the AC+EVA shown in Figure 47

formulation	E_M (Pa)	η_M (Pa.s)	E_K (Pa)	η_K (Pa.s)	Λ (s)	λ (s)
AC+Elvaloy+PPA	7,007.62	867.08	807.54	1,642.08	2.03	0.12
AC+EVA	17,139.19	363.74	11,291.08	20,081.96	1.78	0.02

As can be seen in the table, the elements of the model indicate that the amount of elastic strain is higher for the AC+Elvaloy+PPA (lower E_M values) than for the AC+EVA. At the same time, the amount of viscous strain is higher for the AC+EVA (lower η_M values) than for the AC+Elvaloy+PPA. The ratio of η_K to E_K (retardation time Λ) and the ratio of η_M to E_M (relaxation time λ) are also higher for the AC+Elvaloy+PPA than for the AC+EVA, which suggest that the amount of delayed elastic strain is higher for the formulation with Elvaloy+PPA than for the one with EVA. Due to the higher η_M values for the AC+Elvaloy+PPA, this material is less prone to rutting than the AC+EVA in such testing conditions (higher G_V values), as previously discussed in Chapter 5.

With respect to a material with no recovery (for instance, at 70°C and 3.2 kPa), one representative example is the 50/70 base binder (Figure 48). In such a case, it can be assumed that all the strain accumulated by the binder during the creep phase is equal to the viscous strain. In other words, only the η_M value of the Burgers model is non-null and all the other parameters (E_M, E_K and η_K) will be equal to zero. It is possible to obtain non-null values for E_M, E_K and η_K from a mathematical point of view, but they will not be representative of the response of the asphalt binder (AKYILDIZ et al., 1990; CELAURO et al., 2012). Therefore, only the η_M values were determined for the binders that showed absence of recovery at a specific temperature and stress level.

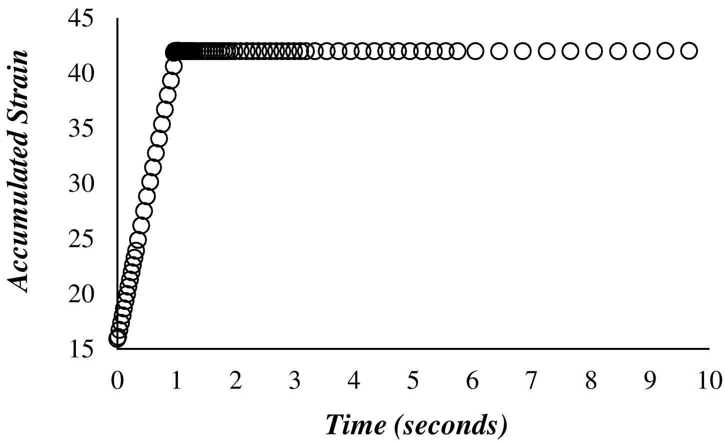

Figure 48 – First creep-recovery pulse of the 50/70 base asphalt binder in the MSCR at 70°C and 3.2 kPa

One last comment on the data collected in this study refers to the inertia of the upper plate of the DSR. As shown above, the upper plate continues to rotate and load the binder sample due to its inertia when the load is cut off in the end of the creep portion of the cycle. In simple terms, this means that the loading is not immediately removed from the sample as soon as the creep phase is finished. This may explain why a portion of the recovery of the binder right after the removal of the load is not immediate (Figure 47), and the strain after 10.0 s seems to be higher than the one after 1.0 s in some cases (Figure 48). When the binder approaches the Newtonian behavior and has little to no recovery, this can lead to a negative *R* value in the calculations (JAFARI and BABAZADEH, 2016; NEJAD et al., 2015). In this manner, the ASTM D7405-15 standard recommends the use of the strain in the end of the creep portion of the cycle – rather than the one in the end of the recovery portion – to calculate J_{nr}. The *R* value shall be reported as zero.

Reactive Terpolymers (Elvaloy®) and PPA Alone. Figure 49 reports the *R* values of the 50/70 base binder, the AC+PPA and the AC+Elvaloy+PPA. Binder modification with PPA and Elvaloy+PPA considerably increased the percent recoveries at several pavement temperatures, especially for the one with Elvaloy®. The values range from 31 to 77% for the AC+Elvaloy+PPA within the whole temperature range and at both stress levels, even at very high temperatures. On the other hand, the AC+PPA shows much lower recoveries (no greater than 59%) and can be null or very low at 70 and 76°C. The base binder has practically no recovery at all temperatures and stress levels. These promising findings of the AC+Elvaloy+PPA were also obtained elsewhere (DOMINGOS and FAXINA, 2015a), and they may be attributed to the reaction between Elvaloy® and the binder with PPA acting as a catalyst. It has also been pointed out that PPA does not provide significant elasticity to the binder (BENNERT and MARTIN, 2012).

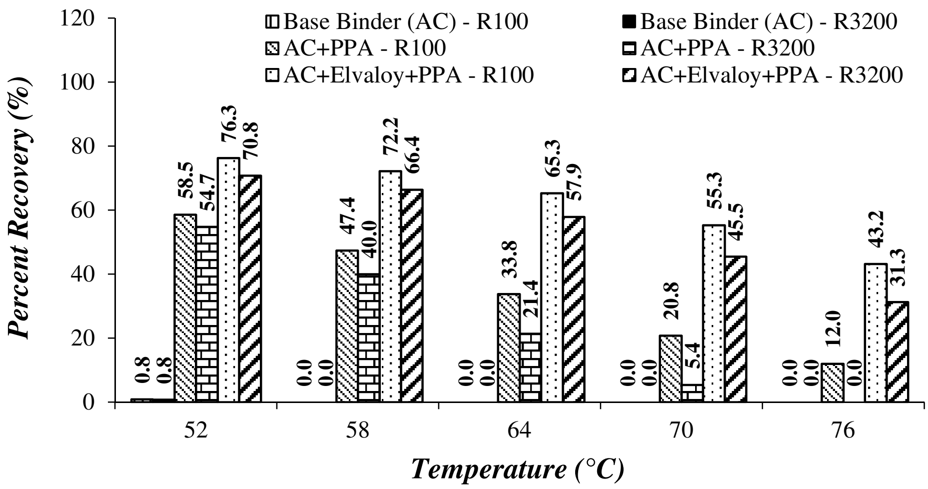

Figure 49 – Percent recoveries of the 50/70 base binder, the AC+PPA and the AC+Elvaloy+PPA at 1/9 s

The nonrecoverable compliances of the base material, the AC+PPA and the AC+Elvaloy+PPA are plotted in Figure 50. The effect of binder modification with PPA and Elvaloy+PPA on the J_{nr} value shows an opposite trend when compared with the recovery, i. e., the two formulations are more stiff than the 50/70 unmodified binder. Although the AC+PPA has J_{nr} values comparable to the ones of the AC+Elvaloy+PPA at the temperatures of 52 and 58°C, the differences among the results become more marked at 64, 70 and 76°C; in these cases, it can be seen that the AC+Elvaloy+PPA is less susceptible to rutting than the AC+PPA. The compliances range from 0.03 to 3.15 kPa^{-1} and from 0.05 to 2.09 kPa^{-1} for the AC+PPA and the AC+Elvaloy+PPA, respectively. These compliances can overcome 3.0 kPa^{-1} for the base binder at temperatures higher than 58°C. Similar conclusions can be found elsewhere in the literature for another Brazilian crude source (DOMINGOS and FAXINA, 2015a).

The $J_{nr,\ diff}$ and the R_{diff} values of the PPA- and Elvaloy-modified asphalt binders are summarized in Table 35. The data suggest that none of the binders are too stress sensitive at any of the selected pavement temperatures, since the $J_{nr,\ diff}$ values are lower than 75%. The results of the base binder (no greater than 5.0%) are inevitably attributed to the absence of modifiers in the material, since modified binders – especially the polymer-modified ones – are known by their nonlinear responses at much lower stress levels (D'ANGELO et al., 2007). The stress sensitivity of the AC+Elvaloy+PPA does not considerably change with temperature ($J_{nr,\ diff}$ between 20 and 24%), whereas the AC+PPA is more sensitive to an increase in the stress level at higher temperatures ($J_{nr,\ diff}$ is almost multiplied by 5 with an increase from 52 to 76°C in the temperature). With respect to the parameter R_{diff}, the data indicate that the differences between the recoveries at 100 and 3,200 Pa become more significant with increasing temperature. This is explained by a major increase in the amount of unrecovered strain in the binder at 3,200 Pa than at 100 Pa when the temperature is more critical.

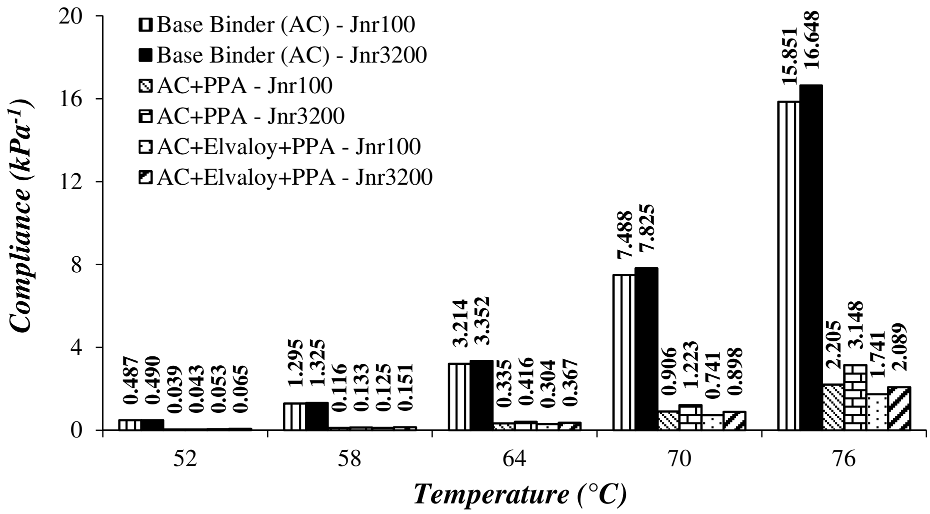

Figure 50 – Nonrecoverable compliances of the 50/70 base binder, the AC+PPA and the AC+Elvaloy+PPA at 1/9 s

Table 35 – Percent differences in nonrecoverable compliances ($J_{nr,\ diff}$) and recoveries (R_{diff}) of the 50/70 original binder, the AC+PPA and the AC+Elvaloy+PPA

asphalt binder	$J_{nr,\ diff}$ values (%)					R_{diff} values (%)				
	52°C	58°C	64°C	70°C	76°C	52°C	58°C	64°C	70°C	76°C
base binder (AC)	0.6	2.3	4.3	4.5	5.0	4.6	-	-	-	-
AC+PPA	9.2	14.9	24.4	35.1	42.8	6.5	15.6	36.8	74.0	100.0
AC+Elvaloy+PPA	23.5	20.7	20.9	21.2	20.0	7.2	8.1	11.3	17.8	27.5

The combination of high percent recoveries with low nonrecoverable compliances results in high degrees of elasticity for the AC+Elvaloy+PPA, as can be observed in Figure 51. This is an indication that the modification with Elvaloy+PPA was enough to impart high elasticity to the material (points above the boundary line). On the other hand, the acid-modification type did not provide enough elasticity to the asphalt binder (points below the boundary line). This was quite expected because high elastic responses are commonly observed for binders modified with polymers, especially the elastomers and reactive terpolymers (BULATOVIĆ et al., 2014; DOMINGOS and FAXINA, 2015a; ISACSSON and LU, 1995).

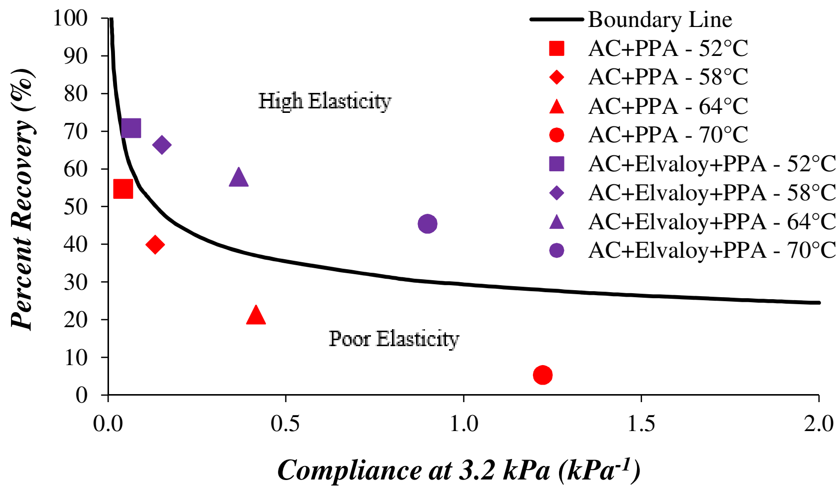

Figure 51 – Levels of elasticity for the AC+PPA and the AC+Elvaloy+PPA at the creep-recovery times of 1/9 s

The adequate traffic levels and the G_V values for each asphalt binder are provided in Table 36. Either the AC+PPA or the AC+Elvaloy+PPA are able to deal with extremely heavy traffic levels at temperatures up to 64°C, and the main difference between them lies on the traffic level at 70°C (heavy for the AC+PPA and very heavy for the AC+Elvaloy+PPA). On the other hand, the base binder cannot be used not even on pavements with standard traffic levels at the temperatures of 70 and 76°C, and this is naturally related to its high PG grade (only 64-xx). With respect to the G_V values, the data suggest that the AC+PPA is less susceptible to rutting than the AC+Elvaloy+PPA at temperatures up to 64°C, and an opposite trend is observed at 70 and 76°C. More simply, the AC+Elvaloy+PPA and the AC+PPA show quite similar rut resistances within the temperature interval from 64 to 76°C, and the results tend to be slightly better for the material modified with Elvaloy+PPA.

Table 36 – Viscous component of the creep stiffness (G_V) and appropriate traffic levels for the 50/70 original binder, the AC+PPA and the AC+Elvaloy+PPA

asphalt binder	G_V values (kPa)					adequate traffic levels[a]				
	52°C	58°C	64°C	70°C	76°C	52°C	58°C	64°C	70°C	76°C
base binder (AC)	2.05	0.77	0.31	0.13	0.06	E	H	S	-	-
AC+PPA	19.43	7.13	2.66	0.99	0.43	E	E	E	H	S
AC+Elvaloy+PPA	10.40	4.84	2.24	1.03	0.48	E	E	E	V	S

[a] S = standard; H = heavy; V = very heavy; E = extremely heavy (AASHTO M320-09 standard, Table 3).

The parameters of the four-element Burgers model for the unmodified asphalt binder are summarized in Table 37. Only minor deviations from the raw data (|AAE| < 0.9%) were observed at all temperatures and stress levels. The very low R values for this material – i. e., absence of elastic response – clearly indicate that the elastic strain is almost null (E_M is very high), the delayed elastic strain is also very small (ratio of E_K to η_K is lower than one) and the viscous strain prevails over the other two (η_M is much lower than the other three elements). Since the amount of dissipated energy is inversely related to the η_M value (HAJIKARIMI et al., 2015) and the E_K, η_K and E_M values could not be determined at the temperatures of 58, 64, 70 and 76°C, it can be concluded that all of the energy transferred to the binder during the MSCR test was dissipated into permanent flow (i. e., rutting).

Table 37 – Parameters E_K, E_M, η_K and η_M from the four-element Burgers model at 0.1 kPa and corresponding average absolute errors (AAE) for the 50/70 base binder

T (°C)	parameters of the model				decrease E_M (%)[a]	decrease η_M (%)[a]	AAE (%)
	E_K (Pa)	η_K (Pa.s)	E_M (Pa)	η_M (Pa.s)			
52	3,451,890.53	1,253,559.14	135,181.23	1,949.69	-	-	-0.15
58	-	-	-	737.05	-	-95.7	-0.35
64	-	-	-	297.70	-	-98.3	-0.54
70	-	-	-	128.01	-	-99.3	-0.54
76	-	-	-	60.32	-	-99.6	-0.53

[a] percent difference between the value at the test temperature under consideration and the one at 52°C.

With respect to the AC+PPA, Table 38 indicates that the Burgers model could also fit the data quite well (|AAE| < 2.2% in all cases). The rate of decrease in η_M with temperature is higher than the one in E_M, especially at the stress level of 3,200 Pa. This is an indication that the unrecovered strain increases at a higher rate, and the reductions in E_M are not enough to compensate for the ones in η_M. The ratio of η_K to E_K also decreases with temperature, which means that the viscoelastic strain goes to a more viscous behavior (η_K always decreases and E_K starts to increase at the temperatures of 70 and 76°C) as the temperature conditions become more severe. In other words, the percentage of viscous strain in the total strain of the binder gets higher with increasing temperature. As will be discussed throughout the dissertation, this pattern of behavior tends to show some similarities within the binders, and the key differences among them may be identified in the variations from one parameter to the other.

The data reported in Table 39 refers to the Burgers model parameters for the AC+Elvaloy+PPA. It can be observed that the |AAE| values are much higher than the ones of the 50/70 base material and the AC+PPA, and this may be explained by the limitations of the model (e. g., only one retardation time Λ) and the high elastic response of the material. The maximum allowed value of 5% was not overcome at any test temperature, which means that the generalized Burgers model may be used to fit the laboratory data and reasonably explain the response of the AC+Elvaloy+PPA. Differently from the 50/70 unmodified binder and the AC+PPA, the decreases in η_M and E_M with temperature are approximately the same and tend to be higher for η_M at the highest temperatures. This means that the viscous strain starts to play a major role in the response of the formulation only under the most critical testing conditions (T values of 70 and 76°C) and, in turn, the decreases in R for $T \leq 64$°C are mainly attributed to the increase in the viscous portion of the viscoelastic strain of the binder (ratio of η_K to E_K).

Table 38 – Parameters E_K, E_M, η_K and η_M from the four-element Burgers model at 0.1 kPa and corresponding average absolute errors (AAE) for the AC+PPA

T (°C)	parameters of the model				decrease	decrease	AAE
	E_K (Pa)	η_K (Pa.s)	E_M (Pa)	η_M (Pa.s)	E_M (%)[a]	η_M (%)[a]	(%)
52	9,835.27	22,182.49	116,903.13	17,224.31	-	-	2.16
58	5,130.44	11,557.77	57,842.95	6,556.67	-50.5	-61.9	1.57
64	3,394.51	7,099.48	30,150.63	2,456.14	-74.2	-85.7	1.00
70	11,735.04	7,960.25	17,165.74	945.79	-85.3	-94.5	0.38
76	35,151.01	13,215.60	10,596.22	403.15	-90.9	-97.7	0.17

[a] percent difference between the value at the test temperature under consideration and the one at 52°C.

Table 39 – Parameters E_K, E_M, η_K and η_M from the four-element Burgers model at 0.1 kPa and corresponding average absolute errors (AAE) for the AC+Elvaloy+PPA

T (°C)	parameters of the model				decrease	decrease	AAE
	E_K (Pa)	η_K (Pa.s)	E_M (Pa)	η_M (Pa.s)	E_M (%)[a]	η_M (%)[a]	(%)
52	2,918.96	7,142.96	57,536.50	9,388.19	-	-	3.59
58	1,542.58	3,720.84	26,598.94	4,403.21	-77.2	-74.4	3.43
64	900.68	2,120.92	13,414.80	2,057.62	-88.5	-88.1	2.90
70	578.20	1,318.37	7,484.77	963.28	-93.6	-94.4	2.32
76	428.30	917.69	4,571.02	454.69	-96.1	-97.4	1.80

[a] percent difference between the value at the test temperature under consideration and the one at 52°C.

It can be implied from the MSCR testing data at 1/9 s that the AC+Elvaloy+PPA is the best formulation within the group comprised by the base binder, the AC+PPA and the AC+Elvaloy+PPA. The promising findings – very high R values, low J_{nr} values, high degrees of elasticity and relatively small stress sensitivity – are supported by another study about formulations prepared with Elvaloy+PPA and PPA and graded as PG 76-xx, but a different crude source for the original binder (DOMINGOS and FAXINA, 2015a). The addition of PPA alone also leads to a lower rutting potential and increases in the percent recovery of the binder, as well as to fairly low stress sensitivity (parameter $J_{nr,\ diff}$) at typical high pavement temperatures. In terms of the Burgers model parameters, it can be concluded that the viscoelastic portion of the total strain in the binder typically plays a key role in the creep-recovery response of the AC+Elvaloy+PPA, and also that the decreases in the *R* values of the AC+PPA are explained by the major decreases in the isolated dashpot element of the model (η_M).

Crumb Rubber-Modified Asphalt Binders. Figure 52 displays the *R* values of the two reference materials (unmodified binder and AC+PPA), the AC+rubber and the AC+rubber+PPA. The results of the AC+rubber are much better than the ones of the AC+rubber+PPA, especially at 100 Pa. In terms of the numerical values, the AC+rubber shows recoveries between 41 and 76% at 100 Pa and they do not exceed 44% at 3,200 Pa. As a matter of comparison, the *R* values of the AC+rubber+PPA are between 13 and 47% at 100 Pa and do not exceed 36% at 3,200 Pa. The AC+PPA also shows higher recoveries than the AC+rubber+PPA, even though the differences between the results at 100 Pa are not significant. This is an indication that the crumb rubber particles are mainly responsible for the elasticity of the formulation, i. e., higher rubber contents leads to formulations with higher elastic responses (NAVARRO et al., 2005).

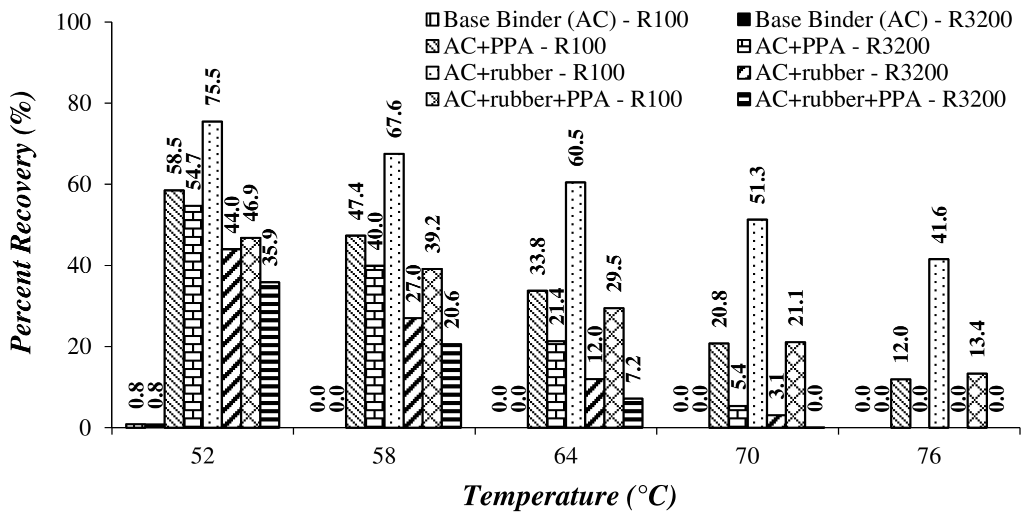

Figure 52 – Percent recoveries of the 50/70 base binder, the AC+PPA, the AC+rubber and the AC+rubber+PPA at 1/9 s

Figure 53 shows the nonrecoverable compliances of the two reference materials and the two crumb rubber-modified samples. The AC+rubber+PPA shows higher compliances than the AC+rubber and the AC+PPA within the whole temperature spectrum, which suggests that this formulation is more prone to rutting at pavement temperatures from 52 to 76°C. The data range from 0.03 to 3.15 kPa^{-1} for the AC+PPA, from 0.05 to 4.70 kPa^{-1} for the AC+rubber and from 0.11 to 5.65 kPa^{-1} for the AC+rubber+PPA. From the point of view of susceptibility to rutting, it is not recommended to replace part of the rubber content by PPA because this option may result in a formulation with much higher J_{nr} values. This was also observed in the mixture data as well (see Chapter 5).

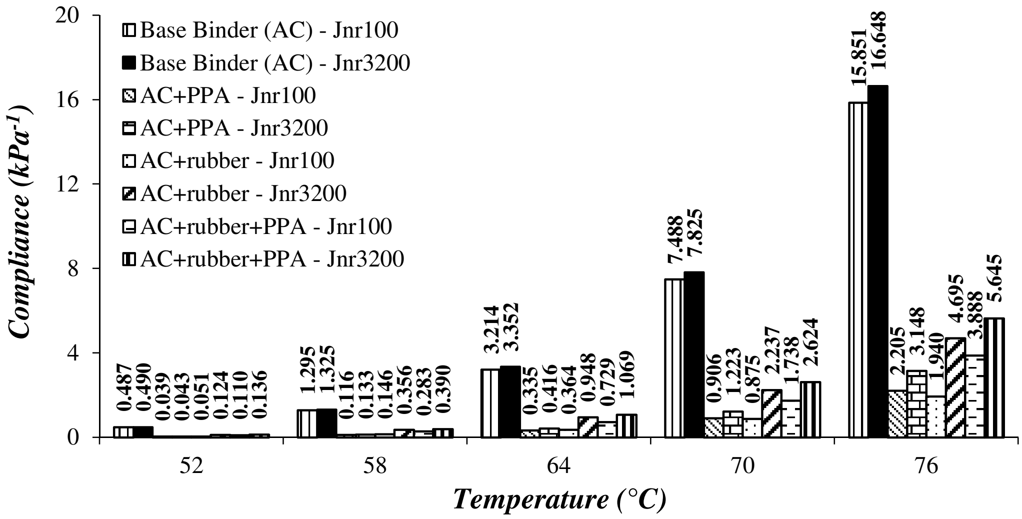

Figure 53 – Nonrecoverable compliances of the 50/70 base binder, the AC+PPA, the AC+rubber and the AC+rubber+PPA at 1/9 s

The two stress sensitivity parameters – $J_{nr,\ diff}$ and R_{diff} – of the reference materials, the AC+rubber and the AC+rubber+PPA are provided in Table 40. The pattern of behavior previously observed for the parameter R_{diff} – progressive increase with increasing temperature – remained the same here, that is, the differences between the recoveries at 100 and 3,200 Pa become greater for all binders as the temperature increases. With respect to $J_{nr,\ diff}$, it can be seen that the AC+rubber is too stress sensitive (values higher than 142%) and the AC+rubber+PPA meets the Superpave® specification requirements (values lower than 75%). Strictly speaking, the AC+rubber cannot be used for paving applications because it does not comply with all the requirements of the specification. However, the excellent rutting performance of the formulation in the mixture (see Chapter 5) suggests that the high stress sensitivity may not necessarily affect its performance in the real pavement.

Table 40 – Percent differences in nonrecoverable compliances ($J_{nr,\ diff}$) and recoveries (R_{diff}) of the 50/70 original binder, the AC+PPA, the AC+rubber and the AC+rubber+PPA

asphalt binder	$J_{nr,\ diff}$ values (%)					R_{diff} values (%)				
	52°C	58°C	64°C	70°C	76°C	52°C	58°C	64°C	70°C	76°C
base binder (AC)	0.6	2.3	4.3	4.5	5.0	4.6	-	-	-	-
AC+PPA	9.2	14.9	24.4	35.1	42.8	6.5	15.6	36.8	74.0	100.0
AC+rubber	143.1	143.8	160.4	155.7	142.0	41.8	60.0	80.1	93.9	100.0
AC+rubber+PPA	23.5	38.1	46.7	51.0	45.2	23.4	47.5	75.5	99.9	100.0

The chart plotted in Figure 54 shows the degrees of elasticity of the AC+rubber and the AC+rubber+PPA. The formulation with crumb rubber alone has a higher degree of elasticity than the one with rubber and PPA, but both of them fall within the region of "materials with poor elasticity". This means that their *R* values at 3,200 Pa are very low when compared with their corresponding J_{nr} values, which is in agreement with other publications that also studied crumb rubber-modified binders (TEYMOURPOUR et al., 2016). It is possible that higher rubber contents could increase the level of elasticity of the formulations and place them within the region of "materials with higher elasticity"; however, this may also lead to increases in the high PG grades for one or another material (namely, PG 82-xx) and create difficulties in the comparisons between the AC+rubber and the AC+rubber+PPA.

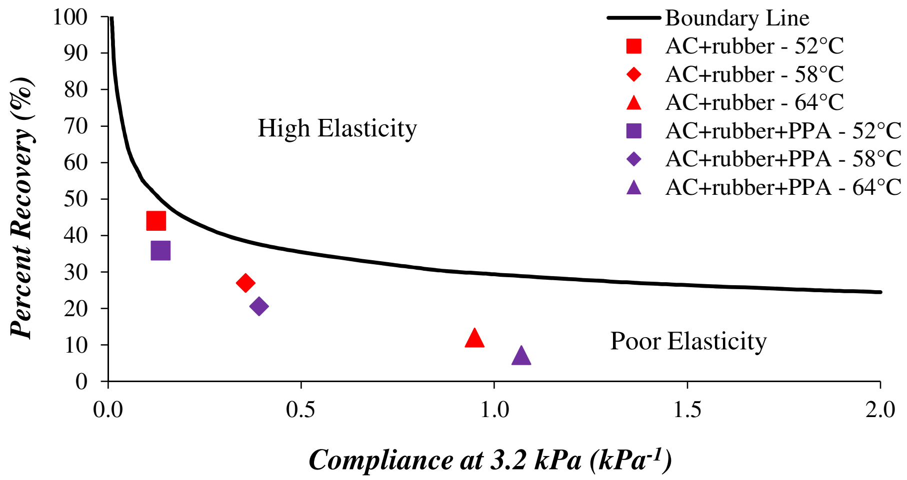

Figure 54 – Levels of elasticity for the AC+rubber and the AC+rubber+PPA at the creep-recovery times of 1/9 s

The traffic levels and the G_V values of the AC+rubber and the AC+rubber+PPA – as well as the two reference materials – are shown in Table 41. In addition to the higher *R* values and lower J_{nr} values, the AC+rubber also has higher G_V values than the AC+rubber+PPA: in average, these parameters are from 57 to 79% higher for the AC+rubber than for the AC+rubber+PPA. On the other hand, no substantial differences among their traffic levels can be identified at any MSCR test temperature except for 70°C (very heavy for the AC+rubber and heavy for the AC+rubber+PPA). None of these crumb rubber-modified binders can be used at any traffic level when the maximum expected pavement temperature reaches 76°C, since their J_{nr} values are about 4.6 kPa^{-1} (AC+rubber) and 5.6 kPa^{-1} (AC+rubber+PPA) in such climate conditions.

It may be important to remind that, although the results of the AC+PPA are better than the ones of the AC+rubber and the AC+rubber+PPA in some cases, this cannot be observed in the asphalt mixture. In other words, PPA-modified asphalt binders do not necessarily increase the rutting resistance from the point of view of the mixture, even though they may increase the rut resistance in a binder scale. This can be implied from the data reported in this study (MSCR and oscillatory shear tests) and the ones published by Tabatabaee and Teymourpour (2010) (oscillatory shear tests) as well. Such a conclusion is quite surprising, since the AC+PPA is the only formulation that can deal with standardized traffic levels at 76°C (Table 41).

Table 41 – Viscous component of the creep stiffness (G_V) and appropriate traffic levels for the 50/70 original binder, the AC+PPA, the AC+rubber and the AC+rubber+PPA

asphalt binder	G_V values (kPa)					adequate traffic levels[a]				
	52°C	58°C	64°C	70°C	76°C	52°C	58°C	64°C	70°C	76°C
base binder (AC)	2.05	0.77	0.31	0.13	0.06	E	H	S	-	-
AC+PPA	19.43	7.13	2.66	0.99	0.43	E	E	E	H	S
AC+rubber	12.09	4.89	2.08	0.93	0.44	E	E	V	S	-
AC+rubber+PPA	7.67	3.13	1.27	0.55	0.25	E	E	H	S	-

[a] S = standard; H = heavy; V = very heavy; E = extremely heavy (AASHTO M320-09 standard, Table 3).

The parameters of the four-element Burgers model for the AC+rubber are given in Table 42, whereas the ones of the AC+rubber+PPA are given in Table 43. It can be said that the lower η_M values (higher viscous strain) and higher E_M values (lower elastic strain) for the AC+rubber+PPA are among the reasons why this material shows lower percent recoveries and higher nonrecoverable compliances than the AC+rubber. The differences between the rates of decrease in E_M and η_M with temperature also suggest that the decreases in R are due to the accumulation of viscous strain for both materials and, since these rates are quite similar for a specific pavement temperature (e. g., around 89 and 95% at 70°C and for E_M and η_M, respectively), it can be implied that the two binders show almost equivalent rates of decrease in their recoveries with temperature (Figure 52). With respect to the viscoelastic strain, it can be said that the elastic portion of this total strain is high either for the AC+rubber or the AC+rubber+PPA (ratios η_K / E_K are higher than 2 for the asphalt binders).

In summary, the MSCR data at 1/9 s indicate that the AC+rubber has a lower rutting potential (J_{nr} values are lower) and a more elastic response (R values are higher) than the AC+rubber+PPA within the temperature interval from 52 to 76°C, even though none of these formulations can be classified as "materials with high elasticity". The AC+PPA shows better J_{nr} results than the two crumb rubber-modified binders, but a correlation with the mixture data (Chapter 5) indicate that this cannot necessarily be translated into mixtures with good rutting performance. In terms of the appropriate traffic levels, the AC+rubber and the AC+rubber+PPA can deal with similar traffic levels at all pavement temperatures except for 70°C – very heavy (V) for the AC+rubber and heavy (H) for the AC+rubber+PPA. The four-element Burgers model was enough to model the creep-recovery responses of the AC+rubber and the AC+rubber+PPA with a great degree of success (|AAE| < 1.8%), and the decreases in R may be explained by the higher rates of decrease in η_M than in E_M for the two formulations. The presence of higher η_M values and lower E_M values justifies the better results (higher percent recoveries and lower nonrecoverable compliances) for the AC+rubber than for the AC+rubber+PPA.

Table 42 – Parameters E_K, E_M, η_K and η_M from the four-element Burgers model at 0.1 kPa and corresponding average absolute errors (AAE) for the AC+rubber

T (°C)	parameters of the model				decrease	decrease	AAE
	E_K (Pa)	η_K (Pa.s)	E_M (Pa)	η_M (Pa.s)	E_M (%)[a]	η_M (%)[a]	(%)
52	2,869.93	7,858.67	54,251.90	10,453.37	-	-	1.74
58	1,417.69	4,015.52	31,636.48	4,291.87	-72.9	-75.1	0.95
64	775.12	2,162.13	18,946.25	1,877.43	-83.8	-89.1	0.84
70	489.41	1,312.25	11,789.18	834.09	-89.9	-95.2	0.81
76	345.19	881.78	7,421.76	401.10	-93.7	-97.7	0.53

[a] percent difference between the value at the test temperature under consideration and the one at 52°C.

Table 43 – Parameters E_K, E_M, η_K and η_M from the four-element Burgers model at 0.1 kPa and corresponding average absolute errors (AAE) for the AC+rubber+PPA

T (°C)	parameters of the model				decrease	decrease	AAE
	E_K (Pa)	η_K (Pa.s)	E_M (Pa)	η_M (Pa.s)	E_M (%)[a]	η_M (%)[a]	(%)
52	5,091.89	12,608.16	71,476.86	7,152.67	-	-	1.12
58	2,575.46	6,641.24	38,265.10	2,938.22	-67.3	-82.9	0.59
64	1,581.78	4,063.83	22,531.20	1,192.15	-80.7	-93.1	0.27
70	1,038.97	2,630.77	14,203.75	522.92	-87.8	-97.0	0.04
76	812.04	1,972.66	10,281.00	241.26	-91.2	-98.6	0.00

[a] percent difference between the value at the test temperature under consideration and the one at 52°C.

Asphalt Binders Modified with Plastomers (EVA and PE). Figure 55 summarizes the percent recoveries of the 50/70 base asphalt binder, the AC+PPA, the AC+EVA and the AC+EVA+PPA. The considerable decreases in R with temperature are visible for the AC+EVA and the AC+EVA+PPA, which indicates that both formulations are very sensitive to an increase in the pavement temperature. The values range from 4 to more than 95% for the AC+EVA and from 12 to 90% for the AC+EVA+PPA, both at 100 Pa. When the stress level of 3,200 Pa is taken into consideration, the R values can exceed 49 and 90% for the AC+EVA+PPA and the AC+EVA, respectively, at the lowest test temperatures (52 and 58°C). These findings were also reached by Domingos and Faxina (2014) for another crude source – Replan-Petrobras refinery –

and the same modifiers and PG grades used in the present study. It seems that the very complex nature of the crosslinking formed by binder modification with EVA (POLACCO et al., 2015) is somewhat affected by the increases in pavement temperature and loading level. Other papers in the literature also highlighted these great dependences of the effects of EVA modification on the load magnitude and temperature based on oscillatory shear tests (AIREY, 2002) and MSCR tests (SABOO and KUMAR, 2015).

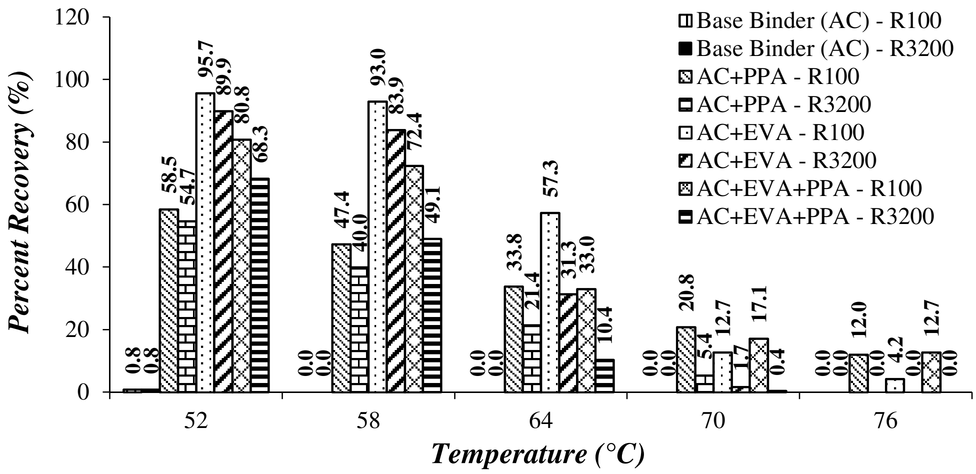

Figure 55 – Percent recoveries of the 50/70 base binder, the AC+PPA, the AC+EVA and the AC+EVA+PPA at 1/9 s

The nonrecoverable compliances of the base material, the AC+PPA, the AC+EVA and the AC+EVA+PPA are plotted in Figure 56. Similarly to the percent recoveries, the EVA-modified binders depict substantial increases in the J_{nr} values with temperature, especially for the AC+EVA+PPA. This pattern of behavior was observed for the formulations from the Replan-Petrobras refinery as well (DOMINGOS and FAXINA, 2014), and suggest that such binders may not be used at all the high pavement temperatures selected in the study. For instance, the compliances of the AC+EVA at 3.2 kPa almost doubled (from 2.7 to 5.2 kPa^{-1}) when moving from 70 to 76°C, and the same could be observed for the AC+EVA+PPA (from 3.1 to 6.0 kPa^{-1}). The differences among their responses at the temperatures of 52 to 58°C is not easily recognized, and this may be explained by the very low strain levels found in such materials. As the temperature and the stress level increase, the polymer network is activated and the creep-recovery responses of asphalt binders become a function of the modification type.

Table 44 provides the parameters $J_{nr,\ diff}$ and R_{diff} for the two EVA-modified binders and the reference materials (base binder and AC+PPA). The results of R_{diff} indicate that the percent recoveries of the AC+EVA+PPA are susceptible to larger decreases in their magnitudes with increasing stress level and temperature, but the ones of the AC+EVA show the sharpest increases when temperatures higher than 64°C are reached. The AC+EVA is overly stress sensitive at temperatures from 52 to 64°C ($J_{nr,\ diff}$ is higher than 75%), and the same can be said for the AC+EVA+PPA at 58 and 64°C ($J_{nr,\ diff}$ values between 94 and 100%). The AC+PPA becomes more stress sensitive than these formulations at 70 and 76°C, even though its results are all lower than 43%. Similarly to what it was observed for the AC+rubber, the very high $J_{nr,\ diff}$ values at 64°C did not seem to affect the rutting performance of the AC+EVA and the AC+EVA+PPA in the FN tests (Chapter 5). This contributes even more to the idea that, depending on the testing conditions, the presence of $J_{nr,\ diff}$ values higher than 75% may not lead to a premature failure by rutting.

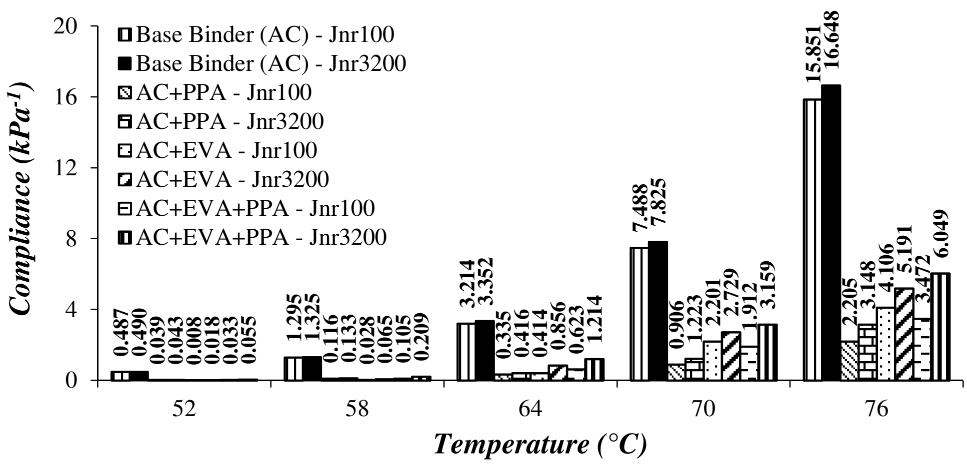

Figure 56 – Nonrecoverable compliances of the 50/70 base binder, the AC+PPA, the AC+EVA and the AC+EVA+PPA at 1/9 s

Table 44 – Percent differences in nonrecoverable compliances ($J_{nr,\ diff}$) and recoveries (R_{diff}) of the 50/70 original binder, the AC+PPA, the AC+EVA and the AC+EVA+PPA

asphalt binder	$J_{nr,\ diff}$ values (%)					R_{diff} values (%)				
	52°C	58°C	64°C	70°C	76°C	52°C	58°C	64°C	70°C	76°C
base binder (AC)	0.6	2.3	4.3	4.5	5.0	4.6	-	-	-	-
AC+PPA	9.2	14.9	24.4	35.1	42.8	6.5	15.6	36.8	74.0	100.0
AC+EVA	135.7	132.7	106.7	24.0	26.4	6.0	9.8	45.3	86.5	100.0
AC+EVA+PPA	66.8	100.0	94.9	65.2	74.2	15.5	32.2	68.6	97.6	100.0

In terms of the degrees of elasticity, Figure 57 clearly indicates that either the AC+EVA or the AC+EVA+PPA showed high elasticity at 52 and 58°C. This suggests that the level of modification of the asphalt binder with EVA and EVA+PPA was very high, and maybe the vinyl acetate content in the EVA copolymer contributed to these results. When moving from 58 to 64°C, the AC+EVA+PPA falls within the region of "materials with poor elasticity" and the AC+EVA is approximately in the boundary line. It can be inferred from the data that the combination of a lower EVA content with PPA yielded a formulation with high elastic responses as well, but the levels of elasticity are not as high as the ones of the modification with EVA alone. One of the possible reasons is that the EVA copolymer already has a high degree of reactivity with the asphalt binder and, in such a case, PPA mainly acted by improving the workability of the formulation in the unaged condition (see Table 25) without significantly decreasing the levels of elasticity. It must be important to note that, similarly to the reactive terpolymers (e. g., Elvaloy®), innapropriate uses and operating conditions of EVA may lead to the formation of an insoluble asphalt gel (POLACCO et al., 2015).

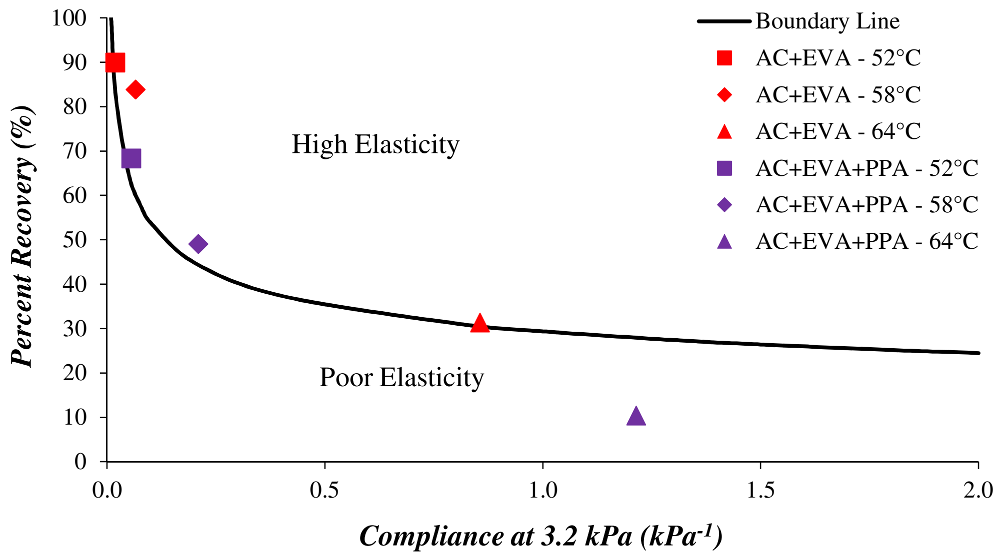

Figure 57 – Levels of elasticity for the AC+EVA and the AC+EVA+PPA at the creep-recovery times of 1/9 s

The numerical values of the parameter G_V and the adequate traffic levels of the EVA-modified asphalt binders and the reference materials are shown in Table 45. According to the G_V data, the AC+EVA is less susceptible to rutting than the AC+EVA+PPA at temperatures no greater than 64°C, and the opposite is observed at 70 and 76°C. However, the adequate traffic levels are exactly the same for both formulations at temperatures from 52 to 70°C except for 64°C (very heavy for the AC+EVA and heavy for the AC+EVA+PPA). By taking into account the promising findings of these formulations in the mixture (Chapter 5) and the ones for a difference crude source for the base asphalt binder (DOMINGOS and FAXINA, 2014), it can be concluded that binder modification with EVA yields asphalt binders and mixtures with much lower susceptibility to the accumulation of permanent strain in the field pavement. The papers from Tabatabaee and Teymourpour (2010) and Saboo and Kumar (2015, 2016) also emphasized these very good results of EVA-modified materials in the mixture and the binder scales.

Table 45 – Viscous component of the creep stiffness (G_V) and appropriate traffic levels for the 50/70 original binder, the AC+PPA, the AC+EVA and the AC+EVA+PPA

asphalt binder	G_V values (kPa)					adequate traffic levels[a]				
	52°C	58°C	64°C	70°C	76°C	52°C	58°C	64°C	70°C	76°C
base binder (AC)	2.05	0.77	0.31	0.13	0.06	E	H	S	-	-
AC+PPA	19.43	7.13	2.66	0.99	0.43	E	E	E	H	S
AC+EVA	21.16	8.84	1.91	0.45	0.24	E	E	V	S	-
AC+EVA+PPA	15.32	6.15	1.47	0.50	0.27	E	E	H	S	-

[a] S = standard; H = heavy; V = very heavy; E = extremely heavy (AASHTO M320-09 standard, Table 3).

The parameters of the four-element Burgers model for the AC+EVA are given in Table 46. It is clear that this model could not fit the binder data very well at the temperatures of 52 and 58°C, since the |AAE| values are greater than 5%. This is due to the very high levels of elasticity of the formulation and the inability of the model in describing the recovery response after the creep portion of the cycle. Technically speaking, the presence of only one retardation time in the Burgers model overestimated the actual strain throughout the recovery phase of the cycle, as illustrated in Figure 58. This is related to the fact that very simple linear viscoelastic models may not be enough to properly simulate the creep-recovery behavior of materials with high levels of delayed elasticity, which is the case of the AC+EVA. Saboo and Kumar (2015) also identified and debated on the problems in modeling the creep-recovery response of EVA-modified binders in the MSCR test with the Burgers model. As an alternative to address these limitations, the authors proposed the use of a power law model with some adaptations to account for the recovery phase of the cycles. Differently from these authors, a generalized Voigt model with six parameters was considered in the present study, as discussed below.

Table 46 – Parameters E_K, E_M, η_K and η_M from the four-element Burgers model at 0.1 kPa and corresponding average absolute errors (AAE) for the AC+EVA

T (°C)	parameters of the model				decrease E_M (%)[a]	decrease η_M (%)[a]	AAE (%)
	E_K (Pa)	η_K (Pa.s)	E_M (Pa)	η_M (Pa.s)			
52	2,991.96	7,185.05	46,684.35	18,235.74	-	-	10.58
58	1,258.56	3,253.03	25,369.99	7,518.48	-78.3	-56.3	5.71
64	804.86	2,207.21	16,645.19	1,689.66	-85.8	-90.2	0.74
70	1,612.02	3,764.87	11,266.70	419.39	-90.4	-97.6	0.02
76	10,095.12	9,510.76	10,202.34	230.97	-91.3	-98.7	0.19

[a] percent difference between the value at the test temperature under consideration and the one at 52°C.

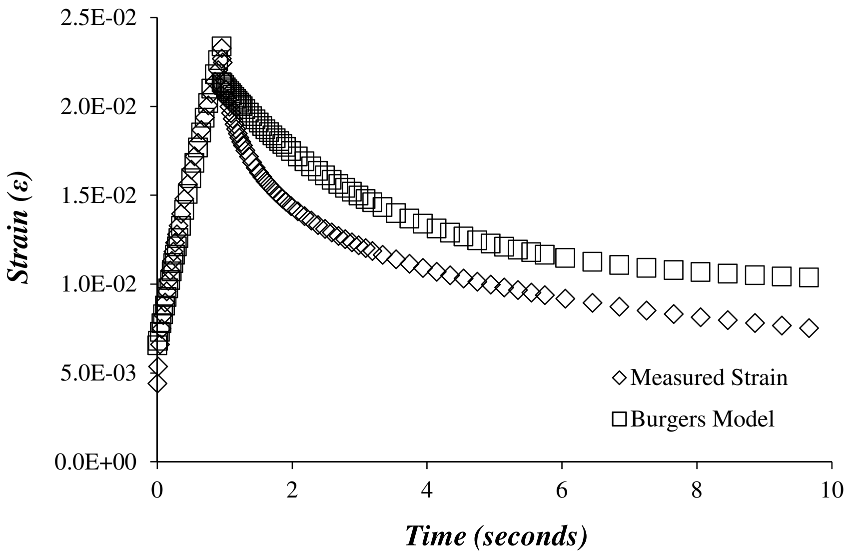

Figure 58 – Fitting of the four-element Burgers model to the strain data of the AC+EVA at 52°C and 100 Pa (second creep-recovery cycle)

The limitations of the Burgers model in fitting data from polymer-modified binders with high amounts of recoverable strain are not restricted to the present study, since De Visscher et al. (2004) among others reported problems in applying the model to such materials as well. They observed that not only the high level of recovery of the sample is poorly represented by the equations of the Burgers model, but also the steady state phenomenon. According to the authors, the model is better fitted to the data when the binder approaches steady state (the rate of increase in the permanent strain gets closer to a constant value, which is actually simulated by the model) and the percentage of elastic response in the total strain is lower. Further investigations also reported quite similar conclusions, and this is why the use of the Burgers model after a certain number of creep-recovery cycles is proposed. Some examples include at least 50 cycles in the final report by Bahia et al. (2001a), a minimum of 30 cycles in the publications by Delgadillo et al. (2006b), Golalipour (2011) and Golalipour et al. (2016) and at least 100 cycles in the paper by Marasteanu et al. (2005).

The complexity of the natural configuration of the unmodified asphalt binder is due to the diversity of its components – some of which are amorphous and others are crystalline in nature – and the external factors that may influence on its behavior (e. g., aging and incorporation of modifiers). This becomes even more complex when one assumes that the relaxation/retardation mechanisms may be associated with several time values, each of which representing one portion of the total response of the material. For instance, one of these values could be associated with the amorphous phase, one associated with the crystalline phase and a third value simulating the changes in the internal structure with time (KRISHNAN and RAJAGOPAL, 2005). In addition, the presence of modifiers further increases the difficulty in modeling and understanding the rheological behavior of asphalt binders. In other words, the generalized Voigt model with two retardation times is closer to the actual response of the asphalt binder in the MSCR test, but it cannot account for all of the variables of the complex phenomena involved in this response.

Even with the aforementioned limitations, it must be said that this study is not focused on an accurate modeling of all the possible relaxation/retardation mechanisms; rather, the idea is to analyze the feasibility of a more detailed model in representing this response without deviating from a practical application of it in the literature (DIVYA et al., 2013; WOLDEKIDAN, 2011). In this manner, it can be implied from the Burgers model parameters that the decreases in R and increases in J_{nr} – especially at temperatures greater than 58°C – are due to the significant decreases in η_M and the increase in the amount of viscous strain in the viscoelastic response of the material (parameters E_K and η_K). It is not surprising at all that this viscous strain prevails over the other strains (elastic and delayed elastic) at the temperatures of 70 and 76°C, when η_M is much smaller than E_K, E_M and η_K. The rates of decrease in η_M are also higher than the ones in E_M at 64, 70 and 76°C.

As previously shown, the generalized Voigt model with six elements was used to address the limitations of the conventional, four-element Burgers model. These elements were calculated by targeting a |AAE| value of 0.5% and keeping the values of the isolated spring and dashpot unchanged, and the results are reported in Table 47 (temperature of 52°C) and Table 48 (temperature of 58°C). As the data suggest, two distinct retardation mechanisms can be observed in the material: (a) one with retardation times lower than 1.0 s (Λ_1) and that can be attributed to the base asphalt binder; and (b) another with retardation times higher than 1.0 s (Λ_2) and that can be attributed to the modifier. This is in accordance with the analysis carried out by Divya et al. (2013) and can be considered as the simplest mechanical model, as based on the distribution of springs and dashpots within the generalized Voigt model. The increase in the differences between Λ_1 and Λ_2 with increasing temperature may be explained by the fact that, at higher temperatures, the modifier starts to play a major role in the elastic response of the material than at lower temperatures, and thus the binder has a minor contribution to this response.

The differences between the creep-recovery curves of the AC+EVA according to the four-element and the generalized Voigt models can be seen in Figure 59. The overestimated strains from the Burgers model are considerably reduced by using the generalized Voigt model and, as the curves suggest, two different recovery regions can be observed in the recovery portion of the curve from the generalized model – one between 1 and 6 s of total time and the other from 6 to 10 s, when the curve reaches an asymptote at a total strain between 1.0 and 1.5E-02. This seems to be a limitation of the model, as the actual data suggest that the material did not recover all of its elastic strain after 10 s. In other words, the generalized Voigt model was able to better describe the data of the AC+EVA in the standardized MSCR testing conditions than the four-element Burgers model, but it appears that not all the problems about the actual repeated creep behavior of the material were properly solved.

Table 47 – Parameters of the generalized Voigt model with six elements and corresponding average absolute errors (AAE) for the AC+EVA at the temperature of 52°C and the stress level of 0.1 kPa

parameter	description	unit	numerical value
$E_{spring,\,1}$	isolated spring (Maxwell model)	Pa	46,684.35
$\eta_{dashpot,\,1}$	isolated dashpot (Maxwell model)	Pa.s	18,235.74
$E_{spring,\,2}$	spring of the first Voigt model	Pa	16,145.12
$\eta_{dashpot,\,2}$	dashpot of the first Voigt model	Pa.s	6,817.77
$E_{spring,\,3}$	spring of the second Voigt model	Pa	26,070.78
$\eta_{dashpot,\,3}$	dashpot of the second Voigt model	Pa.s	29,375.52
R^2	coefficient of determination	-	0.888
AAE	average absolute error	-	0.50
Λ_1	retardation time (first Voigt model)	s	0.42
Λ_2	retardation time (second Voigt model)	s	1.13

Table 48 – Parameters of the generalized Voigt model with six elements and corresponding average absolute errors (AAE) for the AC+EVA at the temperature of 58°C and the stress level of 0.1 kPa

parameter	description	unit	numerical value
$E_{spring,\,1}$	isolated spring (Maxwell model)	Pa	25,369.99
$\eta_{dashpot,\,1}$	isolated dashpot (Maxwell model)	Pa.s	7,518.48
$E_{spring,\,2}$	spring of the first Voigt model	Pa	7,876.21
$\eta_{dashpot,\,2}$	dashpot of the first Voigt model	Pa.s	6,512.90
$E_{spring,\,3}$	spring of the second Voigt model	Pa	3,278.43
$\eta_{dashpot,\,3}$	dashpot of the second Voigt model	Pa.s	8,567.45
R^2	coefficient of determination	-	0.956
AAE	average absolute error	-	0.50
Λ_1	retardation time (first Voigt model)	s	0.83
Λ_2	retardation time (second Voigt model)	s	2.61

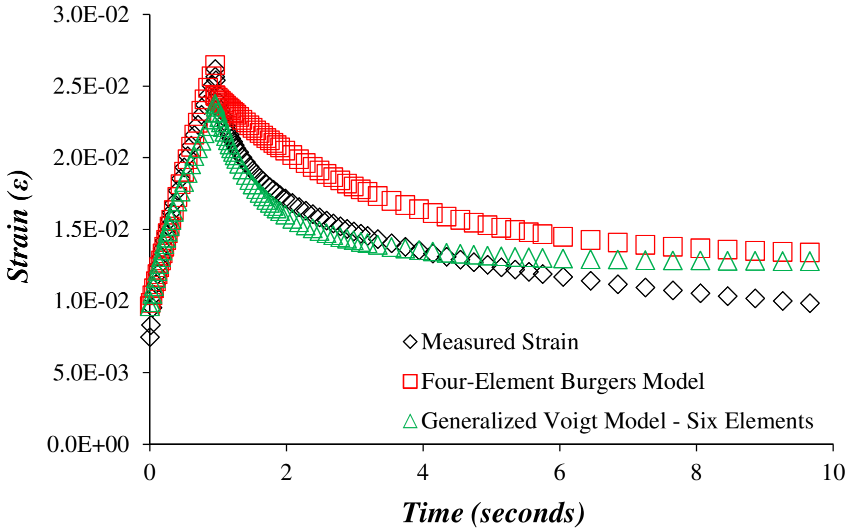

Figure 59 – Fitting of the four-element Burgers model and the generalized Voigt model to the strain data of the AC+EVA at 52°C and 100 Pa (third creep-recovery cycle)

With respect to the AC+EVA+PPA, Table 49 shows the parameters of the four-element Burgers model for this binder. Differently from the AC+EVA, the conventional Burgers model was able to fit the data at 52 and 58°C with smaller deviations from the raw values. In addition, the considerable decreases in the parameter η_M (much higher than the ones of the parameter E_M) suggest that the increases in the viscous strain are mainly responsible for the reductions in the percent recovery of the material. A direct comparison between these data and the ones from the AC+EVA (Table 46) indicate that the AC+EVA+PPA has lower elastic strains (higher E_M values) and higher viscous strains (lower η_M values) than the AC+EVA at temperatures no greater than 64°C, and the variations among these parameters are very small at 70 and 76°C. This matches the results of the R values (Figure 55) and the J_{nr} values (Figure 56).

Table 49 – Parameters E_K, E_M, η_K and η_M from the four-element Burgers model at 0.1 kPa and corresponding average absolute errors (AAE) for the AC+EVA+PPA

T (°C)	parameters of the model				decrease E_M (%)[a]	decrease η_M (%)[a]	AAE (%)
	E_K (Pa)	η_K (Pa.s)	E_M (Pa)	η_M (Pa.s)			
52	3,390.14	8,711.47	67,065.76	13,453.25	-	-	3.17
58	1,652.50	4,434.39	35,972.47	5,295.09	-69.2	-69.3	1.69
64	1,565.92	3,968.90	21,762.36	1,369.53	-81.4	-92.0	0.51
70	1,249.41	3,100.13	13,348.99	480.17	-88.6	-97.2	0.14
76	884.33	2,320.42	10,965.23	274.17	-90.6	-98.4	0.36

[a] percent difference between the value at the test temperature under consideration and the one at 52°C.

Some final comments on the findings of the AC+EVA and the AC+EVA+PPA can be made as follows. The presence of PPA and the reduction in the EVA content slightly increased the rutting potential of the EVA-modified asphalt binder at high pavement temperatures, as based on the J_{nr} and G_V values. However, this was not quite damaging to the performance of the material because the adequate traffic levels were not changed at any temperature except for 70°C (very heavy for the AC+EVA and heavy for the AC+EVA+PPA) and the mixture data are very good for both of them (Chapter 5). In terms of the stress sensitivity, the AC+EVA is much more sensitive to an increase in the stress level in the pavement (parameter $J_{nr,\ diff}$) than the AC+EVA+PPA, even though this higher stress sensitivity is not observed for the percent recovery (parameter R_{diff}). Either the AC+EVA or the AC+EVA+PPA are graded as “materials with high elasticity” at 52 and 58°C, but the AC+EVA is the only one that maintains this classification at 64°C. Finally, the four-element Burgers model was able to represent the creep-recovery response of the AC+EVA+PPA at all testing temperatures, but the same cannot be said for the AC+EVA at 52 and 58°C.

Figure 60 depicts the percent recoveries of the two PE-modified asphalt binders, as well as the ones of the unmodified material and the AC+PPA. The modifications with PE and PE+PPA did not provide good elastic responses to the asphalt binder when compared with others such as PPA alone, Elvaloy+PPA, EVA and EVA+PPA, even though the recoveries of the AC+PE+PPA are higher than the ones of the AC+PE. The results at 100 Pa are between 12 and 38% for the AC+PE and are between 6 to 44% for the AC+PE+PPA. When moving to the highest stress level (3,200 Pa), these results become no greater than 22 and 36% for the AC+PE and the AC+PE+PPA, respectively. Both materials show much lower *R* values when compared with the AC+PPA, especially at temperatures lower than 70°C. This was somewhat expected because PE does not react with the asphalt binder and, when mixed with the base material, it resembles spheres surrounded by an asphalt-rich phase and with no linkages in between (POLACCO et al., 2006, 2015; VARGAS et al., 2013).

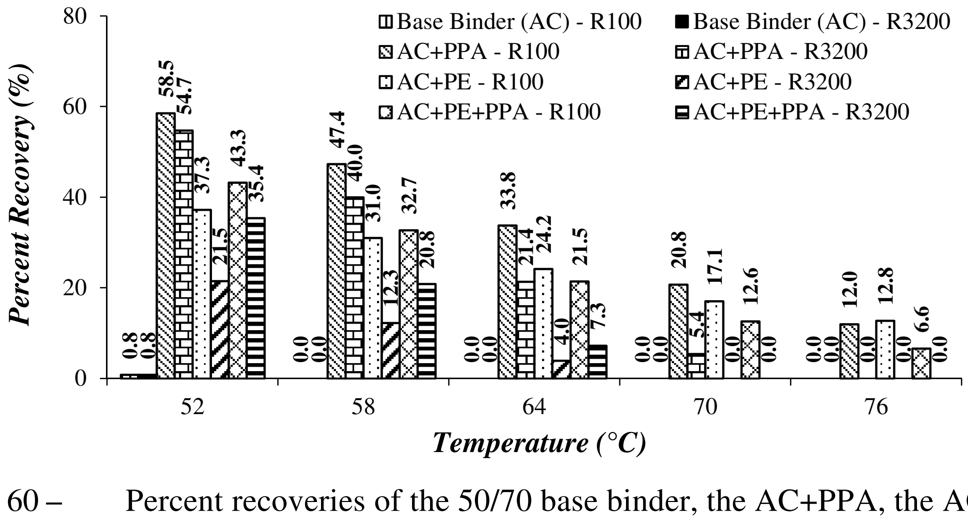

Figure 60 – Percent recoveries of the 50/70 base binder, the AC+PPA, the AC+PE and the AC+PE+PPA at 1/9 s

The nonrecoverable compliances shown in Figure 61 precisely emphasize the stiffening nature of binder modification with PE. The data also indicate that the addition of PPA and the reduction in the PE content had a minimal effect on the J_{nr} values of the formulation: the results are slightly lower for the AC+PE+PPA than for the AC+PE at 3,200 Pa and the opposite is observed at 100 Pa. The results vary from 0.05 to 2.92 kPa^{-1} for both materials at 100 Pa and vary from 0.05 to 3.96 kPa^{-1} at 3,200 Pa. From the point of view of the resistance to rutting and the Superpave® criteria, the two formulations are expected to have similar performances in the pavement at temperatures ranging from 52 to 76°C. This was somewhat confirmed by the mixture data shown in Chapter 5, since none of the mixtures samples prepared with AC+PE and AC+PE+PPA failed in the FN tests.

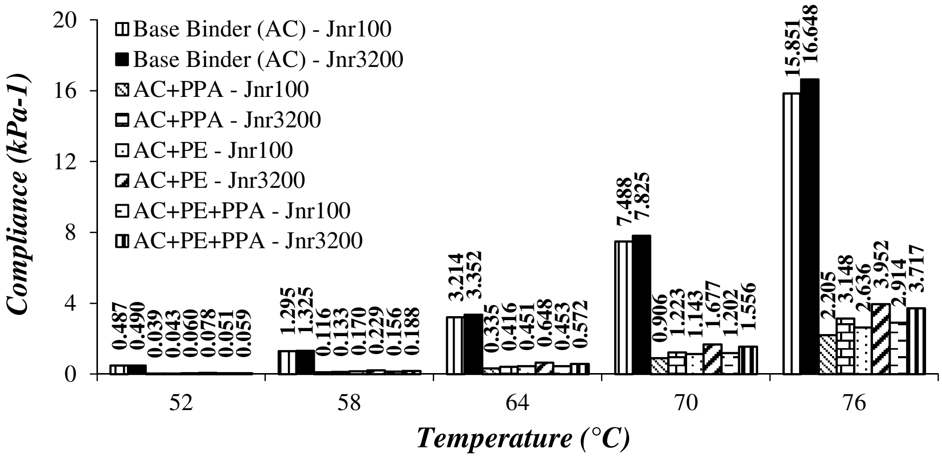

Figure 61 – Nonrecoverable compliances of the 50/70 base binder, the AC+PPA, the AC+PE and the AC+PE+PPA at 1/9 s

Similarly to what it was observed for other comparisons, the good results of the AC+PPA are restricted to the binder scale, even though the numerical values of J_{nr} do not markedly differ from the ones of the AC+PE and the AC+PE+PPA. A similar trend can be seen for another Brazilian crude source and the same modifiers used in this study, i. e., the AC+PPA shows much higher percent recoveries and nonrecoverable compliances comparable to the ones of the AC+PE and the AC+PE+PPA (DOMINGOS and FAXINA, 2015b). More simply, the substantial increase in the degree of stiffness can be observed in this research study either in the asphalt binder or the asphalt mixture after the addition of PE, which is in agreement with other publications from the technical literature (AWWAD and SHBEEB, 2007; GHUZLAN et al., 2015; ONOFRE et al., 2013; VARGAS et al., 2013).

The stress sensitivity parameters of the MSCR tests ($J_{nr,\,diff}$ and R_{diff}) for the AC+PE and the AC+PE+PPA are provided in Table 50. It is clear that the Superpave® specification requirements ($J_{nr,\,diff} \leq 75\%$) are all met for the modifications with PE, since the values are lower than 50 and 30% for the AC+PE and the AC+PE+PPA, respectively. This means that, from the point of view of degree of nonlinearity and stress sensitivity, either the formulation with PE or the one with PE+PPA can be used for paving applications. It can also be seen that the variations in R and J_{nr} with increasing stress level are lower for the AC+PE+PPA than for the AC+PE, but the AC+PPA shows the lowest results at temperatures lower than or equal to 64°C. Domingos and Faxina (2015b) reported that such promising $J_{nr,\ diff}$ values can be seen in other PE and PE+PPA formulations prepared with a base binder from the Replan-Petrobras refinery as well, which indicates that this type of modifier does not have a negative effect on the sensitivity of the binder to an increase in the stress level.

Table 50 – Percent differences in nonrecoverable compliances ($J_{nr,\ diff}$) and recoveries (R_{diff}) of the 50/70 original binder, the AC+PPA, the AC+PE and the AC+PE+PPA

asphalt binder	$J_{nr,\ diff}$ values (%)					R_{diff} values (%)				
	52°C	58°C	64°C	70°C	76°C	52°C	58°C	64°C	70°C	76°C
base (AC)	0.6	2.3	4.3	4.5	5.0	4.6	-	-	-	-
AC+PPA	9.2	14.9	24.4	35.1	42.8	6.5	15.6	36.8	74.0	100.0
AC+PE	31.2	34.3	43.8	46.7	49.9	42.3	60.4	83.6	100.0	100.0
AC+PE+PPA	16.2	21.1	26.3	29.4	27.6	18.2	36.3	66.0	100.0	100.0

As a consequence of the low R values, the two formulations with PE show poor elasticity at temperatures ranging from 52 to 70°C (Figure 62). Although the degree of elasticity was slightly increased when PPA was added and the PE content was reduced, this was not enough to place the asphalt binder above the boundary line. These outcomes suggest that PPA did not react with the low-density PE to produce a formulation with much higher levels of elasticity or, in other words, the combined effects of PE and PPA on the repeated creep response of the asphalt binder are restricted to the stiffness of the formulation. It is interesting to note that the mixtures prepared with AC+PE and AC+PE+PPA perform quite similarly in the FN tests, see Figure 41 in Chapter 5. This again suggests that elasticity does not play a major role in the resistance of the asphalt mixture to rutting, as previously shown by other authors in the literature (ARSHADI, 2013; GOLALIPOUR, 2011).

Table 51 shows the outcomes of the parameter G_V (viscous component of the creep stiffness) and the adequate traffic levels for each of the formulations studied in this section, namely, the base material, the AC+PPA, the AC+PE and AC+PE+PPA. In addition to the equivalent traffic levels for the AC+PE and the AC+PE+PPA at all testing temperatures, the G_V values are also very similar among these formulations with PE, especially at temperatures higher than 64°C. This reinforces the idea that the degrees of stiffness are approximately the same for the AC+PE and the AC+PE+PPA and, as a consequence, both materials can be used on pavements with higher traffic levels with no marked distinctions between them. Since the modification costs are usually higher when virgin polymers are used in the asphalt binder, the use of PPA may be an interesting option to decrease this total cost and, at the same time, to retain the high performance level (MASSON, 2008; ORANGE et al., 2004).

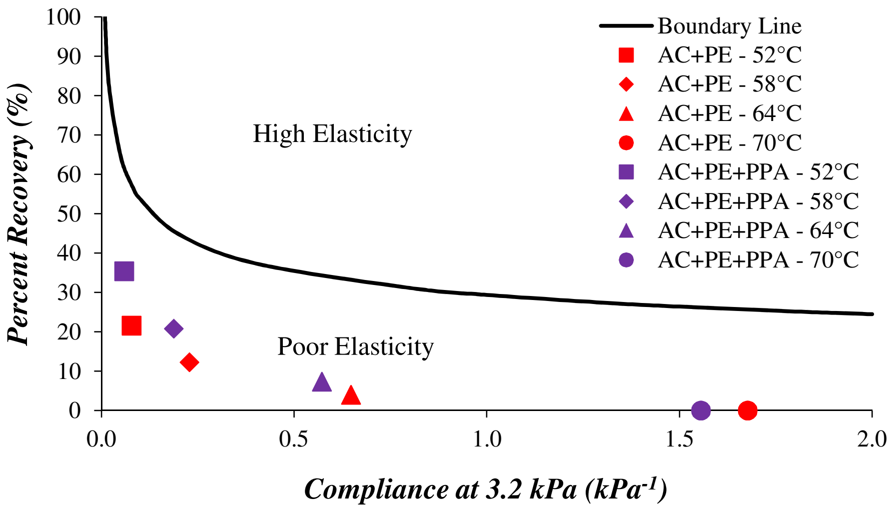

Figure 62 – Levels of elasticity for the AC+PE and the AC+PE+PPA at the creep-recovery times of 1/9 s

Table 51 – Viscous component of the creep stiffness (G_V) and appropriate traffic levels for the 50/70 original binder, the AC+PPA, the AC+PE and the AC+PE+PPA

asphalt binder	G_V values (kPa)					adequate traffic levels[a]				
	52°C	58°C	64°C	70°C	76°C	52°C	58°C	64°C	70°C	76°C
base binder (AC)	2.05	0.77	0.31	0.13	0.06	E	H	S	-	-
AC+PPA	19.43	7.13	2.66	0.99	0.43	E	E	E	H	S
AC+PE	15.18	5.38	2.08	0.84	0.37	E	E	V	H	S
AC+PE+PPA	16.88	5.84	2.08	0.81	0.34	E	E	V	H	S

[a] S = standard; H = heavy; V = very heavy; E = extremely heavy (AASHTO M320-09 standard, Table 3).

The parameters E_K, η_K, E_M and η_M from the four-element Burgers model are given in Table 52 for the AC+PE and in Table 53 for the AC+PE+PPA. It is noteworthy that the AC+PE+PPA shows slightly higher η_M values and a little bit lower E_M values than the AC+PE within the whole temperature spectrum, which is confirmed by their almost similar percent recoveries in the MSCR tests. These E_M values are also much higher than the ones obtained for other formulations such as the AC+Elvaloy+PPA (Table 39), the AC+EVA (Table 46) and the AC+EVA+PPA (Table 49), which suggests that the amount of elastic response in the binder considerably decreases after the addition of PE and PE+PPA. It is also interesting to note that the |AAE| values are lower than 1.0% at all test temperatures, which means that the Burgers model fitted the data quite well. The ratios of η_K to E_K do not markedly differ from one material to the other, and the reductions in η_M with increasing temperature are at least 15% higher than the ones in E_M. This indicates that the delayed elastic responses of the AC+PE and the AC+PE+PPA are very similar, and also that the decreases in R are due to the increases in the viscous portion of the total strain in the binder.

Table 52 – Parameters E_K, E_M, η_K and η_M from the four-element Burgers model at 0.1 kPa and corresponding average absolute errors (AAE) for the AC+PE

T (°C)	parameters of the model				decrease	decrease	AAE
	E_K (Pa)	η_K (Pa.s)	E_M (Pa)	η_M (Pa.s)	E_M (%)[a]	η_M (%)[a]	(%)
52	13,066.66	34,279.32	228,472.07	13,924.71	-	-	0.48
58	5,734.05	15,710.43	113,947.32	5,020.28	-2.5	-70.9	0.32
64	3,118.87	8,445.57	58,530.23	1,956.95	-49.9	-88.6	0.22
70	1,974.30	5,147.01	33,619.24	792.66	-71.2	-95.4	0.12
76	1,269.36	3,215.70	21,812.71	345.47	-81.3	-98.0	0.04

[a] percent difference between the value at the test temperature under consideration and the one at 52°C.

Table 53 – Parameters E_K, E_M, η_K and η_M from the four-element Burgers model at 0.1 kPa and corresponding average absolute errors (AAE) for the AC+PE+PPA

T (°C)	parameters of the model				decrease	decrease	AAE
	E_K (Pa)	η_K (Pa.s)	E_M (Pa)	η_M (Pa.s)	E_M (%)[a]	η_M (%)[a]	(%)
52	12,849.49	31,361.57	186,378.94	15,631.98	-	-	0.93
58	6,506.93	16,043.18	90,773.52	5,445.38	-22.4	-68.4	0.58
64	4,062.68	9,727.87	47,869.06	1,970.99	-59.1	-88.6	0.33
70	3,008.66	6,971.22	27,683.16	767.27	-76.3	-95.5	0.13
76	2,566.00	5,989.44	18,726.98	322.19	-84.0	-98.1	0.01

[a] percent difference between the value at the test temperature under consideration and the one at 52°C.

Based on the discussions on the MSCR testing results of the AC+PE and the AC+PE+PPA, it can be concluded that binder modification with low-density PE had a marked effect on the stiffness of the material and no great changes in its elastic response. This was observed elsewhere as well (DOMINGOS and FAXINA, 2015b) and is in agreement with the technical characteristics of the modifier published in the literature (ISACSSON and LU, 1995; KING et al., 1999). Consequently, poor degrees of elasticity were observed for the AC+PE and the AC+PE+PPA, even though they were a little bit higher for the AC+PE+PPA. The traffic levels are exactly the same and the stress sensitivity criteria ($J_{nr,\,diff} \leq 75\%$) are all met for the testing conditions selected in the study. With respect to the parameters of the Burgers model, the similarities among the R

and J_{nr} values of these formulations can be seen by comparing their elastic (E_M) and viscous (η_M) portions of the total strain: the differences between the numerical values are all lower than 23%.

Asphalt Binders Modified with Elastomers (SBS and SBR). Figure 63 reports the percent recovery values of the two control binders (50/70 unmodified material and AC+PPA) and the ones of the AC+SBS and AC+SBS+PPA. A preliminary analysis indicates that the modification with SBS copolymer imparts high elasticity to the asphalt binder at the test temperatures used in this study, especially at the stress level of 100 Pa. When PPA is added to the formulation and the SBS content is reduced, slightly increases in the R values can be observed at lower temperatures and decreases are seen at higher temperatures. In other words, the benefits of the interaction between PPA and SBS on the percent recoveries of the asphalt binder are more restricted to the lower temperatures. In terms of the numerical values, the results vary from 40 to 53% for the AC+SBS and vary from 30 to 49% for the AC+SBS+PPA, both at 100 Pa. They range from 8 to 33% and from 6 to 41% for the AC+SBS and the AC+SBS+PPA, respectively, at 3,200 Pa.

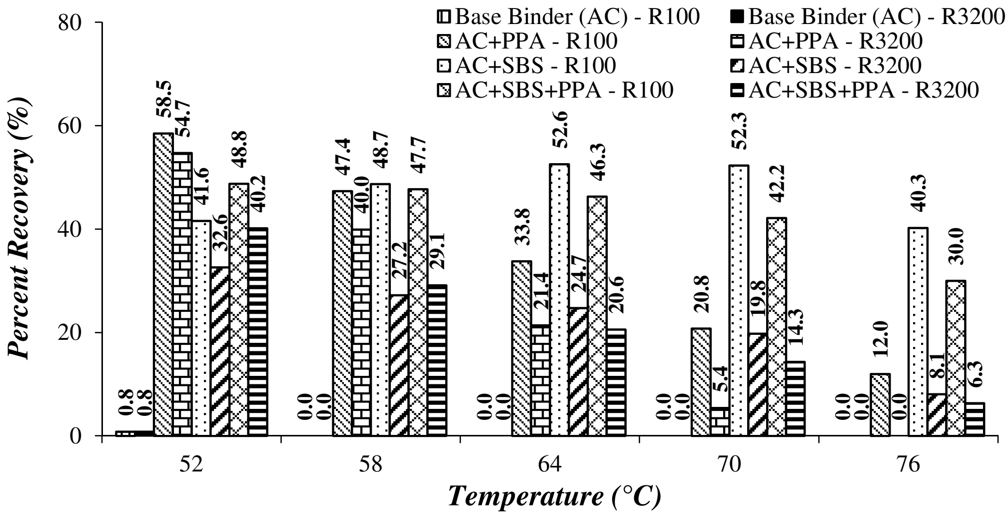

Figure 63 – Percent recoveries of the 50/70 base binder, the AC+PPA, the AC+SBS and the AC+SBS+PPA at 1/9 s

By comparing the data of the SBS-modified asphalt binders with the ones of the PE-modified binders (Figure 60), it is clear that SBS modification had a greater influence on the elastic response of the binder than PE modification. This is explained by the formation of a physical elastomeric network in the formulation after mixing with the base material at high temperatures, which is responsible for the rubber band-like behavior (BECKER et al., 2001; POLACCO et al., 2006). Typically, the compatibility between SBS and the asphalt binder tends to be higher when polystyrene content in the modifier is equally higher, provided that the mixing conditions are adequately met (POLACCO et al., 2015). The modifier also has to be rich in butadiene (around

60 – 70%) to be compatible with the binder (BECKER et al., 2001). As will be discussed in detail later, the *R3200* values reported in the study and by other authors who also utilized a Kraton D1101 linear SBS copolymer in the modification of a PG 64-xx binder (D'ANGELO, 2010a; D'ANGELO and DONGRÉ, 2009) suggest that this compatibility is limited.

Together with the increases in the *R* values, the J_{nr} values of the two SBS-modified binders also showed considerable decreases when compared with the base material (Figure 64). Differently from the percent recoveries, the benefits of the addition of PPA are more visible when the binder parameter under consideration is the nonrecoverable compliance: the results of the AC+SBS+PPA are from 19 to 48% lower than the corresponding ones of the AC+SBS for a specific temperature and stress level. In other words, the AC+SBS+PPA is stiffer at high pavement temperatures than the AC+SBS, especially at 3,200 Pa. This is in accordance with the improvement in the overall stiffness of the formulation caused by the addition of PPA, and maybe the synergetic and cooperated action of PPA with SBS (BUNCHER, 2016; ORANGE et al., 2004) contributed to these findings as well.

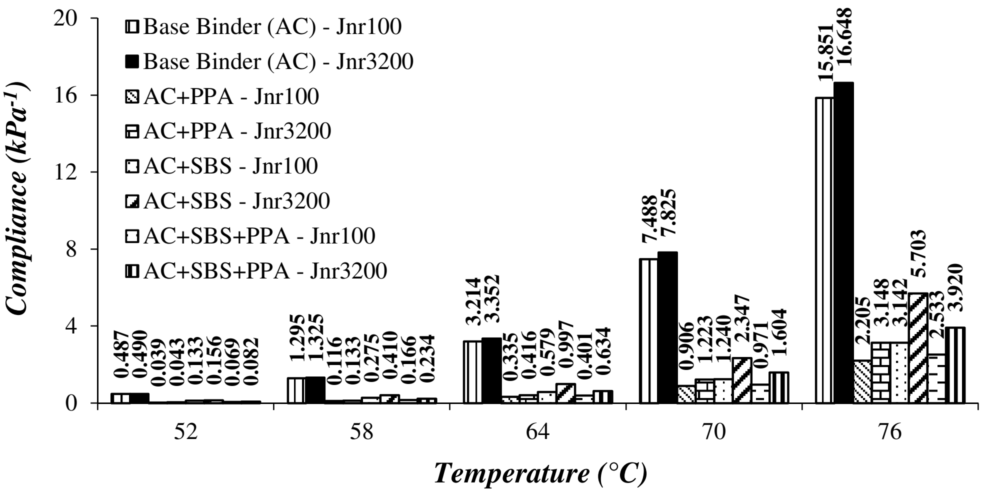

Figure 64 – Nonrecoverable compliances of the 50/70 base binder, the AC+PPA, the AC+SBS and the AC+SBS+PPA at 1/9 s

As a consequence of the decreases in the J_{nr} values and the interaction between SBS and PPA, it is expected that the AC+SBS+PPA formulations will show a lower susceptibility to rutting in the field pavement (i. e., higher FN values or lower γ_{per} values when failure is not reached) than the corresponding AC+SBS ones. This was observed not only for the binders tested in the present study, but also in other papers from the literature (D'ANGELO, 2010a; D'ANGELO and DONGRÉ, 2009). However, some odd cases can be found with respect to the performance of SBS-modified materials with PPA in the composition – e. g., the publication from Biro and Fazekas (2005). More simply, PPA tends to improve the compatibility between SBS and the base asphalt binder due to its synergetic action with the other components of the formulation, but the extent of such improvement will be a function of the crude source.

Although fluorescent micrographs are not shown in this study, the plots of the $J_{nr}3200$ values versus the corresponding *R3200* values (Figure 65) indicate that the compatibility between SBS and the base binder is really limited, and also that the reductions in J_{nr} were not enough to place the AC+SBS+PPA in the region of high elasticity. This again confirms that SBS modification of the Lubnor-Petrobras binder improves elasticity and stiffness, but the asphalt-polymer compatibility is rather limited. Airey (2003) also discussed on the degree of compatibility between SBS and the base asphalt binder, and the author concluded that one of the factors that influence on this compatibility is the percentage of aromatics (i. e., the binder with a larger amount of aromatics was more compatible with the SBS copolymer).

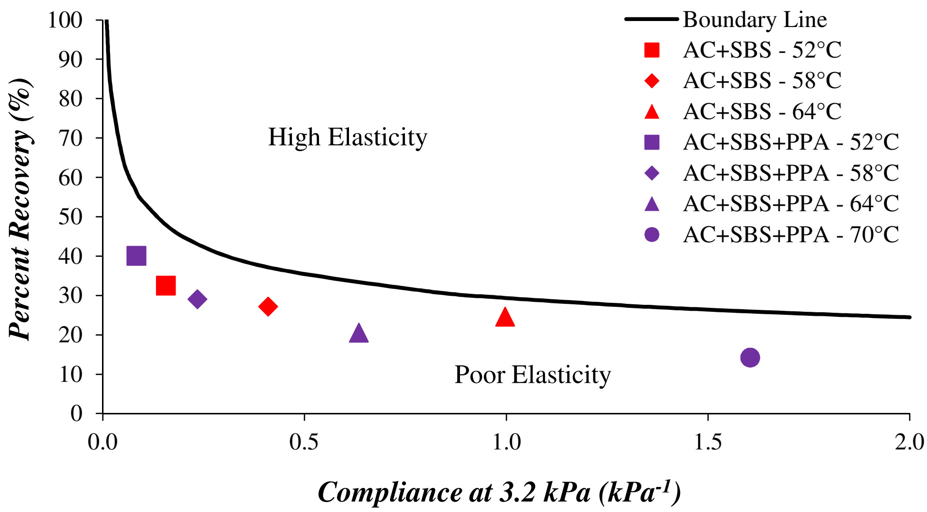

Figure 65 – Levels of elasticity for the AC+SBS and the AC+SBS+PPA at the creep-recovery times of 1/9 s

The percent differences in compliances and recoveries ($J_{nr,\,diff}$ and R_{diff}, respectively) for the original binder, the AC+PPA, the AC+SBS and the AC+SBS+PPA are given in Table 54. The AC+SBS is the only formulation that shows a high stress sensitivity ($J_{nr,\,diff} > 75\%$) at some testing temperatures, i. e., 70 and 76°C. This means that the combination of a small amount of PPA with a lower SBS content had a positive effect on the stress sensitivity and degree of nonlinearity of the formulation, since the $J_{nr,\,diff}$ values decreased and the R_{diff} values showed minor variations from the AC+SBS to the AC+SBS+PPA. Strictly speaking, the AC+SBS cannot be used on pavements with maximum expected temperatures of 70 and 76°C due to its high susceptibility to rutting in unusual loading and/or temperature conditions. On the other hand, the AC+SBS+PPA and the AC+PPA met all the requirements for the parameter $J_{nr,\,diff}$ at the temperatures used in the MSCR tests. The numerical values of $J_{nr,\ diff}$ vary from 17 to 90% for the AC+SBS and from 18 to 66% for the AC+SBS+PPA.

Table 54 – Percent differences in nonrecoverable compliances ($J_{nr,\ diff}$) and recoveries (R_{diff}) of the 50/70 original binder, the AC+PPA, the AC+SBS and the AC+SBS+PPA

asphalt binder	$J_{nr,\ diff}$ values (%)					R_{diff} values (%)				
	52°C	58°C	64°C	70°C	76°C	52°C	58°C	64°C	70°C	76°C
base (AC)	0.6	2.3	4.3	4.5	5.0	4.6	-	-	-	-
AC+PPA	9.2	14.9	24.4	35.1	42.8	6.5	15.6	36.8	74.0	100.0
AC+SBS	17.5	48.7	72.0	89.2	81.5	21.6	44.1	53.0	62.1	80.0
AC+SBS+PPA	18.4	40.6	58.2	65.2	54.7	17.6	39.0	55.5	66.1	78.9

The results of the parameter G_V and the appropriate traffic levels of the AC+SBS and the AC+SBS+PPA are provided in Table 55. The higher traffic levels and G_V values for the AC+SBS+PPA when compared with the AC+SBS were quite expected, once the J_{nr} values are lower for the former than for the latter. However, the parameter G_V gives even more focus on the differences between the rut resistances of the AC+SBS and the AC+SBS+PPA than the Superpave® parameter J_{nr} – the results of the formulation with SBS+PPA (between 0.3 and 12.3 kPa) are from 32 to 84% higher than the ones of the formulation with SBS alone (between 0.2 and 6.7 kPa). In terms of the traffic levels, it can be observed that the AC+SBS+PPA is able to deal with standard and heavy traffics on pavements with maximum temperatures of 76°C and 70°C, respectively; on the other hand, these traffic levels are one grade lower for the AC+SBS at the same pavement temperatures (no traffic at 76°C and standard traffic at 70°C). The results of the AC+SBS+PPA are also similar to the ones of the AC+PPA except for the temperature of 64°C – extremely heavy for the AC+PPA and very heavy for the AC+SBS+PPA.

The Burgers model parameters of the AC+SBS are shown in Table 56. The |AAE| values are all lower than 0.35%, which suggest that the use of only four parameters in the rheological model was enough to describe the repeated creep response of the formulation. As previously observed for other modified asphalt binders, the decreases in the percent recovery R may be attributed to the higher reductions in η_M when compared with E_M. Interestingly, the E_K values are much lower than the η_K values for a specific temperature in the MSCR test, and this is typically found in modified binders with very high levels of elastic response such as the AC+Elvaloy+PPA (Table 39) and the AC+EVA (Table 46). In other words, the elastic portion of the viscoelastic strain in the binder is higher than the viscous portion under the temperature and stress level conditions selected in the study.

Table 55 – Viscous component of the creep stiffness (G_V) and appropriate traffic levels for the 50/70 original binder, the AC+PPA, the AC+SBS and the AC+SBS+PPA

asphalt binder	G_V values (kPa)					adequate traffic levels[a]				
	52°C	58°C	64°C	70°C	76°C	52°C	58°C	64°C	70°C	76°C
base binder (AC)	2.05	0.77	0.31	0.13	0.06	E	H	S	-	-
AC+PPA	19.43	7.13	2.66	0.99	0.43	E	E	E	H	S
AC+SBS	6.69	3.11	1.43	0.66	0.27	E	E	V	S	-
AC+SBS+PPA	12.27	5.18	2.17	0.91	0.36	E	E	V	H	S

[a] S = standard; H = heavy; V = very heavy; E = extremely heavy (AASHTO M320-09 standard, Table 3).

Table 56 – Parameters E_K, E_M, η_K and η_M from the four-element Burgers model at 0.1 kPa and corresponding average absolute errors (AAE) for the AC+SBS

T (°C)	parameters of the model				decrease E_M (%)[a]	decrease η_M (%)[a]	AAE (%)
	E_K (Pa)	η_K (Pa.s)	E_M (Pa)	η_M (Pa.s)			
52	5,044.92	13,443.02	86,187.42	5,993.02	-	-	0.31
58	1,520.42	4,746.11	47,779.84	2,747.00	-59.1	-84.1	0.02
64	592.05	1,930.49	30,257.51	1,251.47	-74.1	-92.7	0.27
70	280.99	911.72	19,920.13	580.97	-83.0	-96.6	0.27
76	187.90	578.25	14,139.62	252.44	-87.9	-98.5	0.03

[a] percent difference between the value at the test temperature under consideration and the one at 52°C.

With respect to the AC+SBS+PPA, the data shown in Table 57 point out that all the parameters are higher than the corresponding ones of the AC+SBS, and also that the increase in the amount of viscous strain with increasing temperature is due to the marked reductions in η_M. It is also interesting to note that the |AAE| values vary within a larger interval when compared with the one observed for the AC+SBS (from 0.08 to 1.11%), even though they did not exceed the maximum allowed value of 5%. The presence of higher η_M values for this formulation leads to the higher G_V values reported above and, at the same time, a lower susceptibility to rutting. The ratios of η_K to E_K are equally higher within the temperature interval used in the MSCR tests, which suggest that the viscoelastic strain is mainly comprised by elastic response than viscous response.

The MSCR testing data obtained for the SBS-modified asphalt binders reveal that the percent recoveries of the AC+SBS and the AC+SBS+PPA are much higher than the ones of the corresponding formulations with PE (AC+PE and AC+PE+PPA), which is associated with the essential nature of the elastomeric modification – increase in the stiffness and elasticity of the bituminous material. The presence of PPA in the formulation did not have as many positive effects in the R values as in the J_{nr} values, that is, the benefits of the addition of PPA were mainly restricted to the stiffness of the binder. Consequently, the mixtures prepared with the AC+SBS+PPA were expected to show better rut performances than the ones prepared with the AC+SBS, and this was confirmed by the mixture data reported in Chapter 5. The AC+SBS also showed high stress sensitivity at some pavement temperatures (i. e., 70 and 76°C), which was not the case of the AC+SBS+PPA. In terms of the parameter G_V and the adequate traffic levels, it can be said that this parameter gave even more focus to the superior rutting resistance of the AC+SBS+PPA and the traffic levels are one grade higher for this formulation with SBS+PPA at 70 and 76°C than for the one with SBS alone.

Table 57 – Parameters E_K, E_M, η_K and η_M from the four-element Burgers model at 0.1 kPa and corresponding average absolute errors (AAE) for the AC+SBS+PPA

T (°C)	parameters of the model				decrease	decrease	AAE
	E_K (Pa)	η_K (Pa.s)	E_M (Pa)	η_M (Pa.s)	E_M (%)[a]	η_M (%)[a]	(%)
52	7,335.60	18,544.08	100,345.95	11,057.47	-	-	1.11
58	2,727.70	7,948.59	54,915.46	4,682.32	-53.0	-72.8	0.52
64	1,135.30	3,540.97	33,275.39	1,943.31	-71.5	-88.7	0.08
70	536.81	1,731.20	21,712.82	818.81	-81.4	-95.2	0.12
76	368.22	1,144.60	15,065.48	335.06	-87.1	-98.1	0.09

[a] percent difference between the value at the test temperature under consideration and the one at 52°C.

The percent recovery data of the AC+SBR and the AC+SBR+PPA are given in Figure 66. The SBR-modified binders followed the same pattern of behavior identified in the SBS-modified materials, that is: (a) the benefits of the addition of PPA to the elastic response of the formulation are restricted to the lower test temperatures; (b) the R values are much higher than the ones observed for the formulations with low-density PE; and (c) the results of the asphalt binder modified with SBR alone are better than the ones of the material modified with SBR+PPA at temperatures greater than 58°C and for both stress levels. The major difference between the responses of the SBS- and SBR-modified binders lies on the numerical values of the percent recoveries, i. e., the results are typically higher after modification with SBS than with SBR. Based on this, it can be implied that a similar trend will also be noticed in the levels of elasticity of the AC+SBR and the AC+SBR+PPA. The answer to this comment is shown in Figure 67.

From Figure 67, it can be clearly seen that none of the formulations with SBR are labeled as "materials with high elasticity". Similarly to what was observed for the SBS-modified binders, this indicates that the degree of compatibility between the SBR copolymer and the base binder is fairly limited. These problems may be overcome by the incorporation of other additives such as sulfur and PPA; however, in some cases, these additives must be used together to achieve better results (ZHANG and HU, 2013; ZHANG and YU, 2010). This seems to be the case of the AC+SBS+PPA and the AC+SBR+PPA, in that the reductions in J_{nr} were not enough to place the formulations in the region of "materials with high elasticity". Compatibility problems may also result in poor pavement performance, as pointed out in the literature review paper by Yildirim (2007). Although elasticity is not the main factor involved in pavements with lower susceptibility to rutting, it certainly has some contribution in the construction of pavements with improved rutting performance.

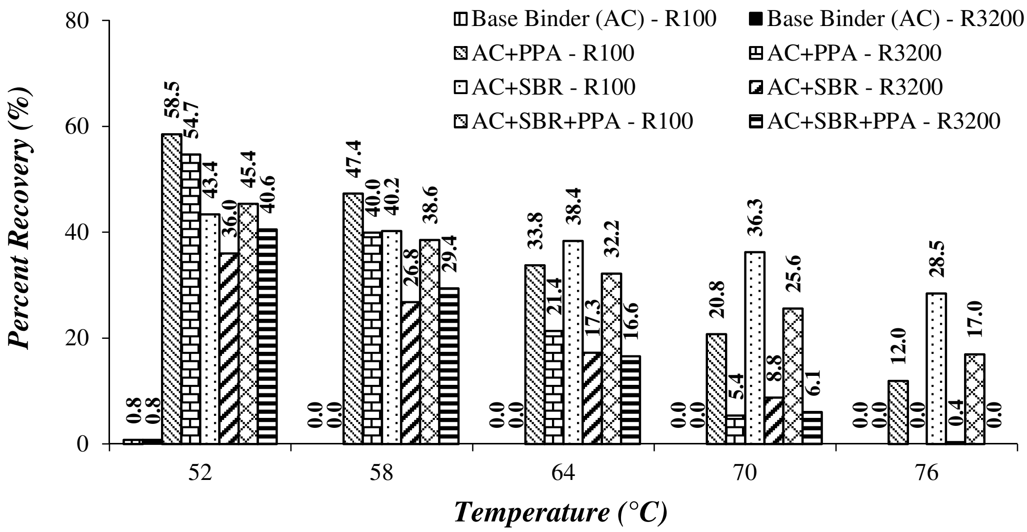

Figure 66 – Percent recoveries of the 50/70 base binder, the AC+PPA, the AC+SBR and the AC+SBR+PPA at 1/9 s

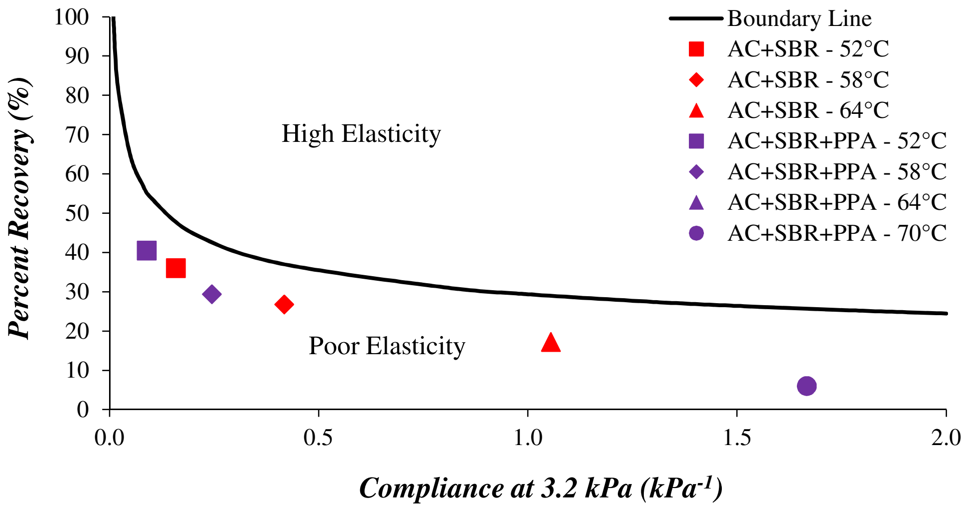

Figure 67 – Levels of elasticity for the AC+SBR and the AC+SBR+PPA at the creep-recovery times of 1/9 s

One last comment regarding asphalt binder modification with SBS and SBR is that the differences between the responses of the formulations with and without PPA increase with increasing pavement temperature. This cannot be seen for other formulations studied here (e. g. the PE-modified materials in Figure 60), and it may be considered as dependent on the modification type. It is believed that the great interactions between PPA and the two aforementioned elastomers contributed to these results, which was probably not the case of the AC+PE and the AC+PE+PPA. With respect to the AC+EVA and the AC+EVA+PPA (Figure 55), the *R* values show marked differences from one formulation to the other at temperatures lower than 64°C and they are quite similar at 70 and 76°C. For crumb rubber-modified materials (Figure 52), the great differences between the AC+rubber and the AC+rubber+PPA are restricted to the data at 100 Pa.

The nonrecoverable compliances of the reference binders, the AC+SBR and the AC+SBR+PPA are shown in Figure 68. As the data suggest, the benefits of the addition of PPA are particularly visible from the point of view of susceptibility to rutting: the J_{nr} values of the AC+SBR+PPA are from 19 to 44% lower than the corresponding ones of the AC+SBR. Again, this highlights the main characteristic of PPA (increase the stiffness of the binder) and is associated with a synergetic action of the additive with the SBR copolymer. It has been discussed in the literature that, due to the elastomeric properties of SBR, it may negatively affect the high temperature properties of the asphalt binder up to some extent (ZHANG and YU, 2010). This is probably the case of the AC+SBR and the AC+SBR+PPA formulations studied in the present dissertation, in which the incorporation of a small amount of PPA was enough to enhance the rut resistance of the binder and the mixture as well (Chapter 5). The numerical values range from 0.13 to 5.74 kPa^{-1} for the AC+SBR and range from 0.08 to 3.84 kPa^{-1} for the AC+SBR+PPA.

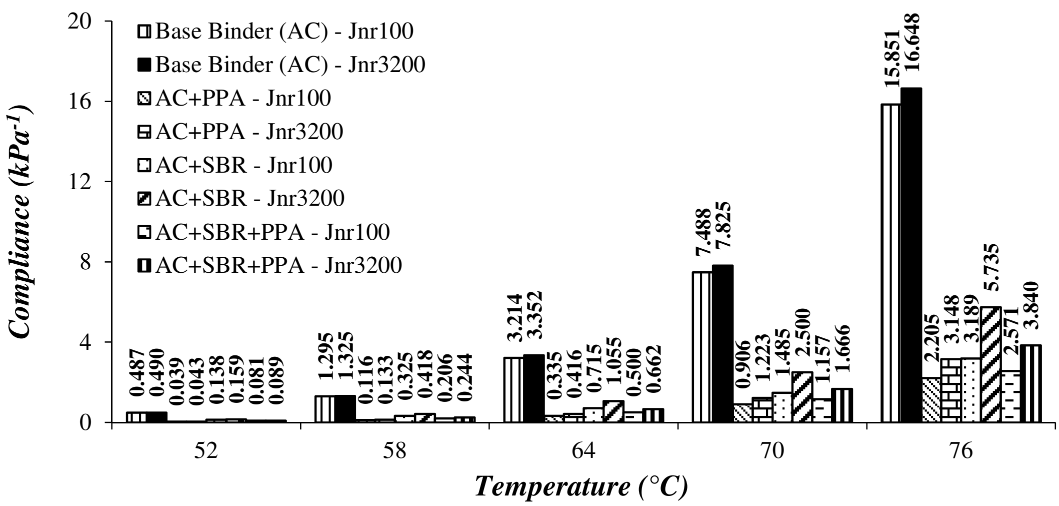

Figure 68 – Nonrecoverable compliances of the 50/70 base binder, the AC+PPA, the AC+SBR and the AC+SBR+PPA at 1/9 s

The G_V values and the corresponding traffic levels of the AC+SBR, the AC+SBR+PPA and the two control binders are provided in Table 58. Similarly to the formulations prepared with SBS copolymer, the increased stiffness provided by PPA is reflected on the higher G_V values (percentages of increase from 32 to 69%) for the AC+SBR+PPA than for the AC+SBR, especially at temperatures no greater than 64°C. In terms of the appropriate traffic levels, the AC+SBR+PPA is able to deal with heavier traffic than the AC+SBR at 64°C (one grade higher, from heavy to very heavy), 70°C (also one grade higher, from standard to heavy) and 76°C (standard traffic level). These findings were somehow confirmed by the mixture data shown and discussed in Chapter 5, in which the AC+SBR+PPA has a much higher F_N value than the AC+SBR at a high pavement temperature of 60°C.

Table 58 – Viscous component of the creep stiffness (G_V) and appropriate traffic levels for the 50/70 original binder, the AC+PPA, the AC+SBR and the AC+SBR+PPA

asphalt binder	G_V values (kPa)					adequate traffic levels[a]				
	52°C	58°C	64°C	70°C	76°C	52°C	58°C	64°C	70°C	76°C
base binder (AC)	2.05	0.77	0.31	0.13	0.06	E	H	S	-	-
AC+PPA	19.43	7.13	2.66	0.99	0.43	E	E	E	H	S
AC+SBR	6.21	2.69	1.23	0.59	0.28	E	E	H	S	-
AC+SBR+PPA	10.45	4.23	1.80	0.80	0.37	E	E	V	H	S

[a] S = standard; H = heavy; V = very heavy; E = extremely heavy (AASHTO M320-09 standard, Table 3).

Table 59 shows the two stress sensitivity parameters ($J_{nr,\,diff}$ and R_{diff}) for the base material, the AC+PPA, the AC+SBR and the AC+SBR+PPA. Similarly to the SBS-modified binders, the addition of PPA and the use of a lower polymer content in the AC+SBR+PPA decreased the Superpave® parameter $J_{nr,\,diff}$ by 30 to 40% within the whole temperature range. The same can be said for the parameter R_{diff}, i. e., the data do not considerably differ from one formulation to the other and are typically lower for the AC+SBR+PPA than for the AC+PPA. The numerical values of $J_{nr,\,diff}$ are between 10 and 50% for the AC+SBR+PPA and between 15 to 80% for the AC+SBR. As can be inferred from these values, the AC+SBR shows a high degree of nonlinearity at 76°C, even though it is very close to the upper limit of 75%. Even with these reductions in $J_{nr,\,diff}$ and R_{diff} when compared with the AC+SBR, the AC+SBR+PPA is still more sensitive to an increase in the stress level than the AC+PPA.

The Burgers model parameters of the AC+SBR – E_K, E_M, η_K and η_M – are shown in Table 60. It is clear that this model can adequately describe the repeated creep response of the formulation in the MSCR test, since the |AAE| values are all lower than 1%. The reductions in

η_M are from 7 to 42% higher than the ones in E_M, and this strongly suggests that the increases in the viscous portion of the total strain in the binder are mostly due to the parameter η_M. The viscoelastic response of the material is quite significant, as can be inferred from the η_K and E_K values (ratios always higher than 2).

Table 59 – Percent differences in nonrecoverable compliances ($J_{nr,\ diff}$) and recoveries (R_{diff}) of the 50/70 original binder, the AC+PPA, the AC+SBR and the AC+SBR+PPA

asphalt binder	$J_{nr,\ diff}$ values (%)					R_{diff} values (%)				
	52°C	58°C	64°C	70°C	76°C	52°C	58°C	64°C	70°C	76°C
base (AC)	0.6	2.3	4.3	4.5	5.0	4.6	-	-	-	-
AC+PPA	9.2	14.9	24.4	35.1	42.8	6.5	15.6	36.8	74.0	100.0
AC+SBR	15.5	28.4	47.6	68.4	79.8	17.0	33.4	55.0	75.7	98.6
AC+SBR+PPA	10.0	18.5	32.4	44.0	49.4	10.6	23.8	48.5	76.2	100.0

Table 60 – Parameters E_K, E_M, η_K and η_M from the four-element Burgers model at 0.1 kPa and corresponding average absolute errors (AAE) for the AC+SBR

T (°C)	parameters of the model				decrease	decrease	AAE
	E_K (Pa)	η_K (Pa.s)	E_M (Pa)	η_M (Pa.s)	E_M (%)[a]	η_M (%)[a]	(%)
52	4,511.67	11,501.01	86,736.60	5,716.17	-	-	0.70
58	2,073.73	5,519.31	46,070.61	2,470.80	-60.6	-85.7	0.56
64	987.88	2,720.98	25,933.05	1,133.42	-77.8	-93.4	0.40
70	527.68	1,425.65	15,446.97	549.60	-86.8	-96.8	0.37
76	382.57	932.39	9,414.19	266.53	-91.9	-98.5	0.52

[a] percent difference between the value at the test temperature under consideration and the one at 52°C.

When moving from the AC+SBR to the AC+SBR+PPA (Table 61), it can be seen that all the parameters of the Burgers model show considerable increases and the |AAE| values are a little bit higher for the AC+SBR+PPA at the temperatures of 52, 58 and 64°C. However, the increases in η_M are more marked than the ones in E_M for a specific temperature, and this indicates that the amount of viscous strain in the binder modified with SBR+PPA is lower than in the binder with SBR only. In other words, the AC+SBR+PPA is expected to be less prone to rutting than the AC+SBR because this binder shows less accumulation of permanent strain according to the parameters of the four-element Burgers model. The ratios of η_K to E_K are also higher than 2 for this formulation with SBR+PPA, which suggest that the viscoelastic response of the two binders is mainly comprised by elastic strain.

The MSCR data of the AC+SBR and the AC+SBR+PPA point out that, similarly to the AC+SBS and the AC+SBS+PPA, the presence of PPA in the formulation with SBR only –

together with a lower SBR content – yielded a superior degree of stiffness at high pavement temperatures, as evaluated by the parameters J_{nr} and G_V. The AC+SBR+PPA is also less stress sensitive than the AC+SBR, either from the point of view of compliance ($J_{nr,\ diff}$) or percent recovery (R_{diff}). On the other hand, the effects of this acid on the elasticity of the formulation are not profound and either the AC+SBR or the AC+SBR+PPA are labeled as "materials with poor elasticity". In simple terms, this indicates that the degree of compatibility between the SBR copolymer and the base binder was not considerably improved after the incorporation of PPA, and complementary additives (e. g., sulfur) may be used to achieve higher recoveries. Finally, the increases in the elastic response of the AC+SBR+PPA when compared with the AC+SBR can be explained by the much higher η_M values in the Burgers model, which consequently influences on the rutting performances of both materials in the mixture (Chapter 5).

Table 61 – Parameters E_K, E_M, η_K and η_M from the four-element Burgers model at 0.1 kPa and corresponding average absolute errors (AAE) for the AC+SBR+PPA

T (°C)	parameters of the model				decrease	decrease	AAE
	E_K (Pa)	η_K (Pa.s)	E_M (Pa)	η_M (Pa.s)	E_M (%)[a]	η_M (%)[a]	(%)
52	7,345.19	17,891.09	113,355.48	9,612.19	-	-	1.07
58	3,814.07	9,306.99	59,120.12	3,953.50	-49.4	-77.0	0.80
64	2,054.52	5,067.15	32,309.76	1,688.14	-72.4	-90.2	0.59
70	1,239.06	3,035.08	18,900.00	751.89	-83.8	-95.6	0.41
76	1,080.79	2,350.28	12,113.66	348.68	-89.6	-98.0	0.32

[a] percent difference between the value at the test temperature under consideration and the one at 52°C.

6.3.3. The Role of Longer Creep Times on the Responses of Asphalt Binders at High Temperatures and Correlations with Speed Values

As discussed previously, the equations proposed by Pereira et al. (1998, 2000) and Huang (2004) were chosen to generate traffic speed data and correlate them with the J_{nr} values in the MSCR tests. The chief purpose of these correlations was to identify patterns of behavior among the responses of the modified binders and, if so, to choose one or more traffic speed values that can reasonably be correlated with actual binder data. Based on the values calculated by these equations and the plots of binder data versus traffic speed on a semi-log chart (GOLALIPOUR, 2011), exponential trendlines were used in the dissertation together with linear correlations (PEREIRA et al., 2000). Only the J_{nr} data at 3,200 Pa were involved in the analysis, as this is the stress level used by Superpave® to establish an adequate traffic level for the binder.

With respect to the rheological models, the linear four-element Burgers model is not appropriate to adequately describe the repeated creep behavior of modified asphalt binders at longer creep times. One of the reasons is that the nonlinear increase in the permanent strain with time is poorly represented by a single isolated dashpot, whose concept reflects the asymptotic behavior of the binder for infinite t_F values. By assuming that the linear viscoelastic response of a rheological material can be represented by a mechanical association of springs and dashpots, each of these elements would have corresponding positive viscosities and moduli (AKYILDIZ et al., 1990). However, the need for modeling complex rheological responses may demand associations of several springs and dashpots to obtain acceptable degrees of fitting, which in turn could lead to unrealistic negative viscosities and moduli in some cases (AKYILDIZ et al., 1990; CELAURO et al., 2012). In other words, it is not clear that the description of viscoelasticity by means of mechanical models is universally applicable. Thus, fractional models and power law equations may work better in the characterization of these and other complex responses (CELAURO et al., 2012; SABOO and KUMAR, 2015).

Table 62 places each of the calculated vehicle speeds in a specific category of traffic level. It is believed that a twofold increase in the creep time t_F increases the J_{nr} value in such a way that the traffic level will decrease by one grade in the most critical temperature conditions. As can be seen, the equation from Pereira et al. (1998) generated traffic levels that are very close to the relationships between average traffic speeds and traffic levels currently found on Superpave®. The use of a tire contact radius of 6.0 inches in the equation by Huang (2004) also resulted in traffic levels close to the standardized (and expected) designations with increasing creep time, and the reduction in the *r* value (3.68 in) did not change any of the designations but only the numerical values of the speeds. It may be important to remind that the equations from Pereira et al. (1998, 2000) were restricted to the temperatures around the one actually used by the authors (in this case, 50°C), and the equation from Huang (2004) was applied to all of the testing temperatures due to its theoretical derivation.

The variations in the percent recoveries at 100 and 3,200 Pa were monitored with increasing creep-recovery times, and the same can be said for the nonrecoverable compliances. Since $J_{nr,\ diff}$ is the official stress sensitivity parameter in the Superpave® specification, its magnitudes with increasing loading times were also studied. All of the collected data were summarized in tables and compared with each other, similarly to what was done in the paper by Kataware and Singh (2015). In some cases, charts were used to describe the degree of linearity or nonlinearity in such decreases. The formulations were separated according to the type of the main modifier, namely:

(a) original material and formulations with terpolymers and PPA alone; (b) crumb tire rubber; (c) plastomers; and (d) elastomers.

Table 62 – Identification of the traffic levels for each vehicle speed based on the current Superpave® specification criteria

source and technical data[a]	calculated speed (km/h)	Superpave® traffic level[c]	selected temperatures
Pereira et al. (2000)	63.9	H	only 52°C
	54.4	H	
	35.4	H	
	N/A[b]	-	
Pereira et al. (1998)	80.0	S	only 52°C
	40.0	H	
	20.0	V or E[d]	
	10.0	V or E	
Huang (2004), r = 6 in	65.8	H	all the test temperatures from 52 to 76°C
	32.9	H	
	16.5	V or E	
	8.2	V or E	
Huang (2004), r = 3.68 in	40.4	H	all the test temperatures from 52 to 76°C
	20.2	H	
	10.1	V or E	
	5.0	V or E	

[a] r = tire contact radius.
[b] N/A: not applicable (vehicle speed lower than zero).
[c] S = standard; H = heavy; V = very heavy; E = extremely heavy.
[d] in such a case, the choice for one or another traffic level will be a function of J_{nr} at 3,200 Pa.

Base Material and Formulations Prepared with Terpolymers and PPA Alone. The percent recoveries *R100* and *R3200* of the 50/70 base asphaltic material at increasing creep times are summarized in Table 63. This binder shows non-null recoveries only at 1/9 s and the lowest MSCR testing temperature (52°C), which is even worse than the data obtained for a base binder from the Replan-Petrobras Brazilian refinery (DOMINGOS and FAXINA, 2014, 2015a, 2015b, 2016). Unmodified binders are typically not used on pavements with heavier traffic levels, since the production methods have a limited extent in their final properties and there are only a few crude sources recommended for obtaining very good materials (BECKER et al., 2001). More simply, the absence of recovery for the unmodified material at longer creep times and higher temperatures only suggests that the R values are not able to contribute to the rut resistance of the mixture in the pavement.

Table 63 – Percent recoveries at 100 Pa (*R100*) and 3,200 Pa (*R3200*) for the 50/70 base asphalt binder with increasing loading time and temperature

parameter	creep time (s)	results (%) at each pavement temperature				
		52°C	58°C	64°C	70°C	76°C
R100	1.0	0.8	0.0	0.0	0.0	0.0
	2.0	0.0	0.0	0.0	0.0	0.0
	4.0	0.0	0.0	0.0	0.0	0.0
	8.0	0.0	0.0	0.0	0.0	0.0
R3200	1.0	0.8	0.0	0.0	0.0	0.0
	2.0	0.0	0.0	0.0	0.0	0.0
	4.0	0.0	0.0	0.0	0.0	0.0
	8.0	0.0	0.0	0.0	0.0	0.0

The nonrecoverable compliances at 100 Pa ($J_{nr}100$) and 3,200 Pa ($J_{nr}3200$) of the 50/70 original material are provided in Table 64, whereas the percentages of increase in J_{nr} with t_F and temperature are shown in Figure 69. It can be inferred from the data that the percentages of increase in $J_{nr}100$ with creep time are approximately the same at all temperatures, and this suggests that the degree of nonlinearity is small under such testing conditions. These percentages are also very similar to the ones at the stress level of 3,200 Pa and creep times up to 4.0 s and, when moving to the longest time (8.0 s) and the highest temperatures, the nonlinear response starts to play some role in the J_{nr} values (i. e., the differences between the numerical values at 100 and 3,200 Pa become greater). This is consistent with the repeated creep data of the unmodified asphalt binders in varying test conditions, i. e., this type of material commonly shows nonlinear response only at stress levels higher than 3,200 Pa (D'ANGELO, 2010a). Despite the low degree of nonlinearity, the substantially high $J_{nr}3200$ values at creep times longer than 2.0 s – even at the temperatures of 52 and 58°C – clearly indicate that the use of this binder on pavements with a great percentage of slow-moving vehicles is not recommended due to the great probability of failure by rutting.

Table 65 summarizes the traffic levels of the original asphalt binder for each creep time. It can be said that this material is not suggested for use on pavements with loading applications longer than 2.0 s and temperature values higher than 52°C, since the adequate traffic levels are typically restricted to such creep times and temperatures. In other words, the upper value of 4.0 kPa^{-1} for $J_{nr}3200$ recommended by the AASHTO M320-09 standard is easily overcome when T > 52°C and t_F > 2.0 s. As previously recommended, the original binder has a limited application on pavements with heavier traffics due to its high J_{nr} value at standardized loading times. This becomes even worse when the loading time is increased and, similarly to the comments made by Kataware and Singh (2015), it is not possible to assign any traffic level to the binder in the most critical temperature and loading conditions. These authors created a separate category labeled as "S-" (material not suitable for paving purposes) to group the binders with J_{nr} values higher than 4.0 kPa^{-1}, but this approach was not followed in the present study because it is not official. In such cases, modified asphalt binders are urgently required due to the inability of the original material in showing acceptable resistances to rutting (low nonrecoverable compliance values).

Table 64 – Nonrecoverable compliances at 100 Pa ($J_{nr}100$) and 3,200 Pa ($J_{nr}\ 3200$) for the 50/70 base binder with increasing loading time and temperature

parameter	creep time (s)	results at each temperature (kPa^{-1}), J_{nr} > 4.0 kPa^{-1} is in bold				
		52°C	58°C	64°C	70°C	76°C
$J_{nr}100$	1.0	0.487	1.295	3.214	**7.488**	**15.851**
	2.0	0.955	2.538	**6.380**	**14.959**	**32.072**
	4.0	1.814	**4.875**	**12.348**	**29.086**	**62.744**
	8.0	3.573	**9.742**	**24.724**	**58.552**	**128.000**
$J_{nr}3200$	1.0	0.490	1.325	3.352	**7.825**	**16.648**
	2.0	0.969	2.630	**6.694**	**15.781**	**33.933**
	4.0	1.873	**5.136**	**13.153**	**31.320**	**68.025**
	8.0	3.929	**10.923**	**28.397**	**67.878**	**149.834**

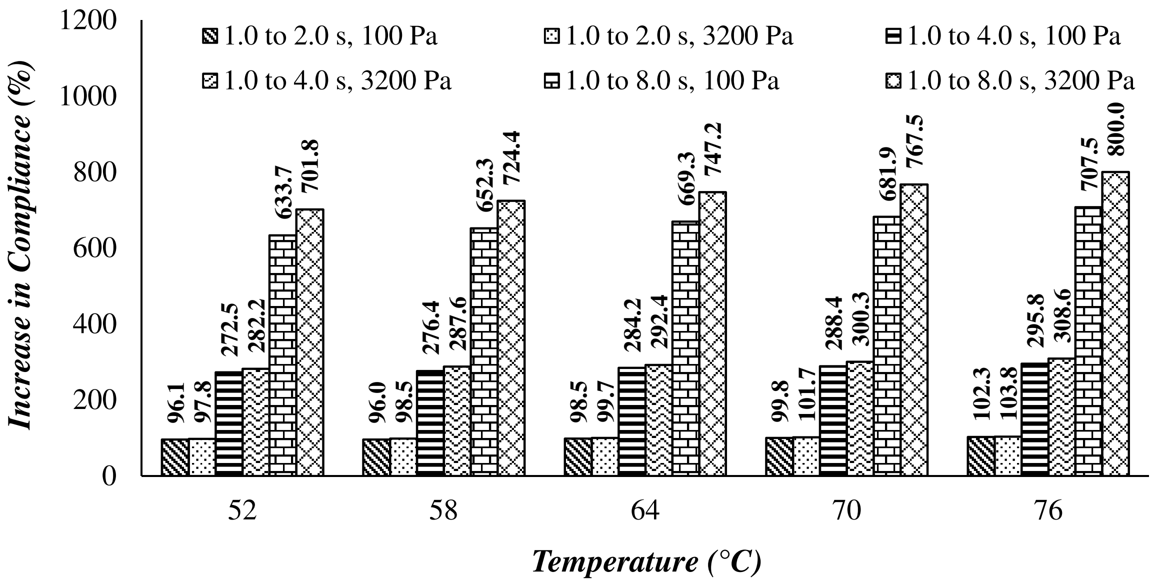

Figure 69 – Percentages of increase in the nonrecoverable compliances of the 50/70 base asphalt binder with creep time, temperature and stress level

Table 65 – Adequate traffic levels for the 50/70 base asphalt binder with increasing creep time and temperature based on the standardized Superpave® criteria

creep time (s)	traffic levels for each temperature[a]				
	52°C	58°C	64°C	70°C	76°C
1.0	E	H	S	-	-
2.0	V	S	-	-	-
4.0	H	-	-	-	-
8.0	S	-	-	-	-

[a] S = standard; H = heavy; V = very heavy; E = extremely heavy.

With respect to the stress sensitivity of the binder (parameter $J_{nr,\ diff}$), the values reported in Table 66 indicate that the degree of nonlinearity does not markedly change with increasing temperature, even for higher t_F values. The same can be said for the $J_{nr,\ diff}$ values at loading times up to 4.0 s and a specific pavement temperature, after which they show substantial increases from one testing condition to the other. The boundary between linear and nonlinear response of the 50/70 base binder may be equal to a creep time between 4.0 and 8.0 s, similarly to what it can be implied by analyzing the percentages of increase in $J_{nr}3200$ when the loading conditions become more critical (Figure 69). However, none of the $J_{nr,\ diff}$ values exceeded 75% at any testing condition (i. e., the stress sensitivity is not a deciding factor in the use of the original binder for paving applications).

Table 66 – Percent differences in nonrecoverable compliances ($J_{nr,\ diff}$) for the 50/70 base asphalt binder with increasing creep time and temperature

creep time (s)	$J_{nr,\ diff}$ values (%) at each creep time and temperature				
	52°C	58°C	64°C	70°C	76°C
1.0	0.6	2.3	4.3	4.5	5.0
2.0	1.4	3.6	4.9	5.5	5.8
4.0	3.2	5.4	6.5	7.7	8.4
8.0	10.0	12.1	14.9	15.9	17.1

The plots of the correlations between traffic speed and $J_{nr}3200$ values for each MSCR testing temperature and the equations by Huang (2004) – tire contact radius of 6 in – and Pereira et al. (1998) are shown in Figure 70. The R^2 values are all higher than 0.90, which suggest that the equations can reasonably predict the numerical decrease in J_{nr} with increasing creep time. The correlations did not greatly change from one temperature to the other, and the R^2 values of the equations are almost identical within the whole temperature range. This may be caused by the degree of nonlinearity in the original asphalt binder, which is typically lower than the ones found in modified asphalt binders. As a consequence, either the equation from Huang (2004) or the one from Pereira et al. (1998) can be used to estimate the susceptibility of the unmodified binder to rutting as based on the creep time.

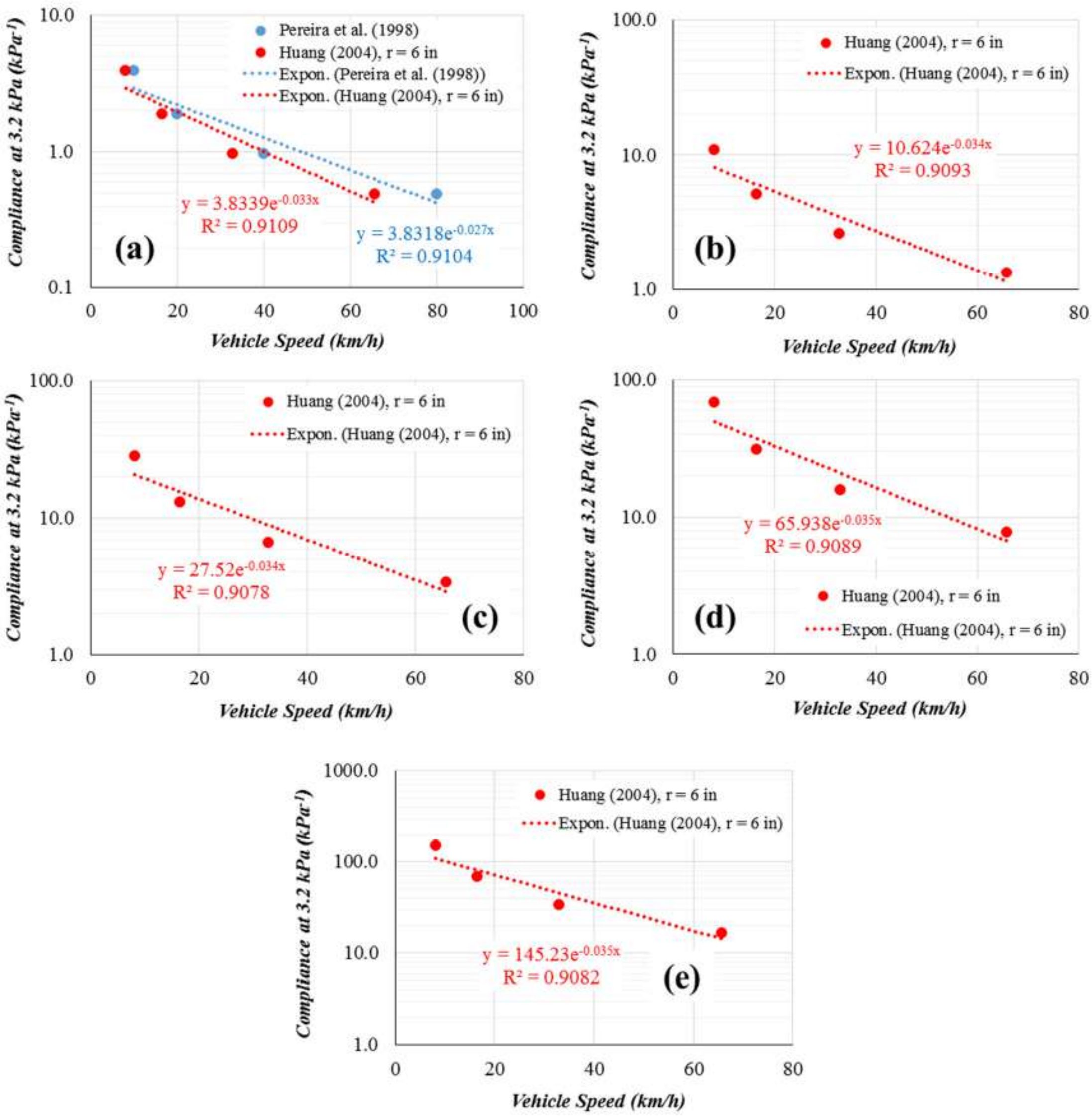

Figure 70 – Correlations between the nonrecoverable compliances of the base binder at 3.2 kPa and the vehicle speeds calculated by the equations from Huang (2004) – tire radius of 6 in – and Pereira et al. (1998) at the temperatures of (a) 52°C; (b) 58°C; (c) 64°C; (d) 70°C; and (e) 76°C

The charts plotted in Figure 71 were derived from the equations by Huang (2004) – tire radius of 3.68 in – and Pereira et al. (2000). As can be seen, the degree of correlation for the equation from Pereira et al. (2000) is excellent at the temperature of 52°C, even though the decreases in the traffic speed are assumed to be linear (rather than exponential). With respect to the other equation, the R^2 values are very close to the ones of the equations shown in Figure 70 (between 0.90 and 0.92). The data indicate that the decreases in $J_{nr}3200$ with increasing creep time can be described by several equations, depending on the criteria used in the calculations of these speeds. However, it must be important to note that the simulations of the actual truck speeds are not as simple and intuitive as the equations may suppose, and therefore the Tr_{sp} values reported here can only be taken as reference values in the study about the effect of vehicle speed on the nonrecoverable compliances of the asphalt binder. Also, a preliminary analysis indicated that the fitting processes of the speeds calculated according to Pereira et al. (1998, 2000) and Huang (2004) to the J_{nr} data of the other binders yielded similar charts with modifications restricted to the constants of the equations and the R^2 values. Therefore, the next charts were replaced by tables in order to reduce the number of pages in the dissertation.

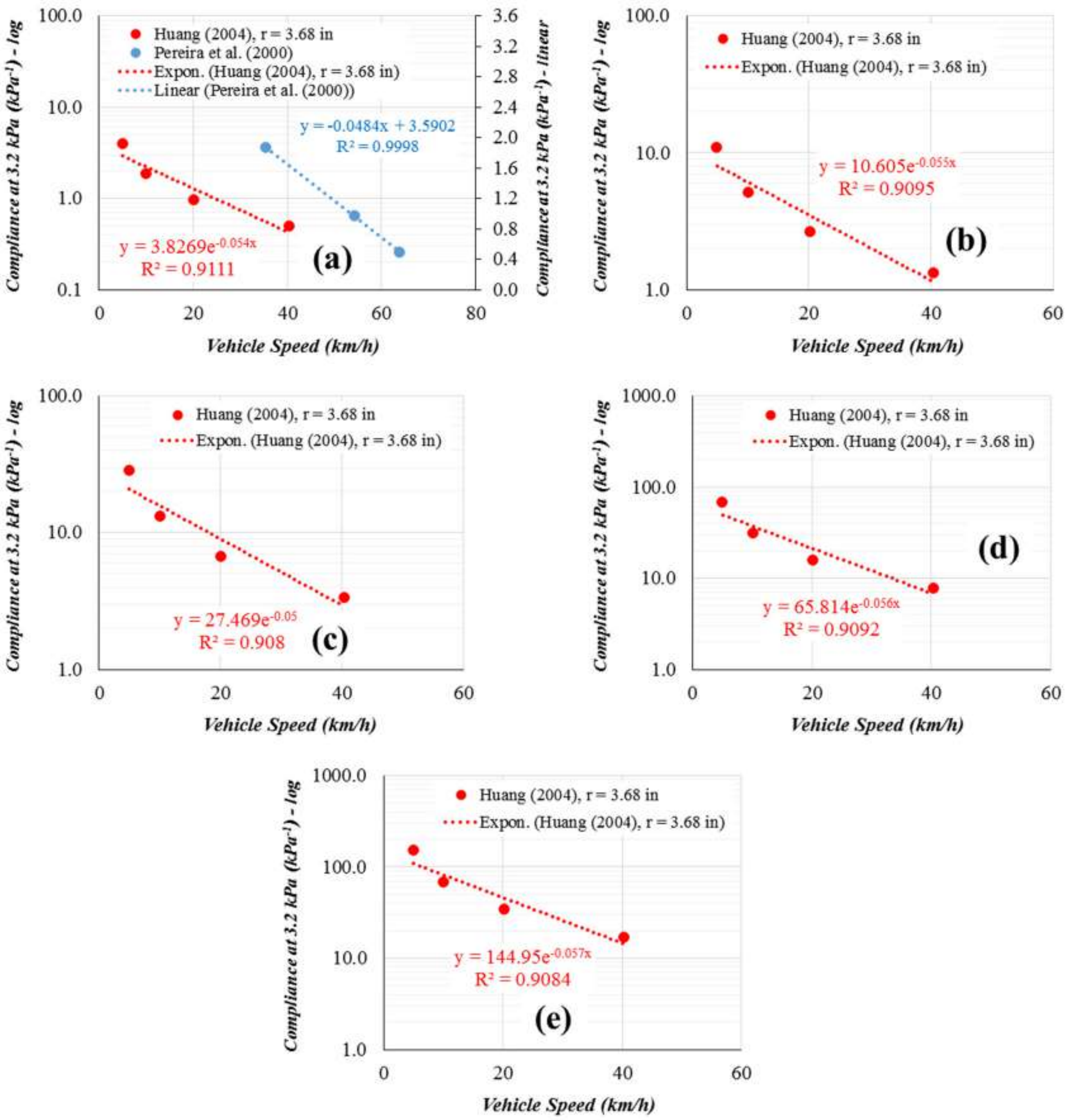

Figure 71 – Correlations between the nonrecoverable compliances of the base binder at 3.2 kPa and the vehicle speeds calculated by the equations from Huang (2004) – tire radius of 3.68 in – and Pereira et al. (2000) at the temperatures of (a) 52°C; (b) 58°C; (c) 64°C; (d) 70°C; and (e) 76°C

To make one step further into the choice of the best equation to simulate the average traffic speed based on J_{nr}, each of the traffic levels calculated by the aforementioned equations (Table 62) was compared with the actual levels obtained from the data of the original binder, and then Table 67 and Table 68 were constructed. Since the criteria used by Superpave® and the equations to establish a traffic level are inversely related to each other (the former is based on **lower** J_{nr} values and the latter is based on **higher** traffic speeds), the traffic levels obtained from the equations were inverted to make direct comparisons among the data, and this was observed throughout the study.

Table 67 – Comparisons between the actual traffic levels of the 50/70 base asphalt binder and the ones obtained from the equations by Huang (2004) and Pereira et al. (1998)

t_F (s)[d]	actual[a] and estimated[b, c] traffic levels at each temperature[d]				
	52°C	58°C	64°C	70°C	76°C
1.0	**E (V/E) [V/E]**	H [V/E]	S [V/E]	-	-
2.0	**V (V/E) [V/E**]	S [V/E]	-	-	-
4.0	**H (H) [H]**	-	-	-	-
8.0	**S (S)** [H]	-	-	-	-

[a] S = standard; H = heavy; V = very heavy; E = extremely heavy (AASHTO M320-09 standard, Table 3).
[b] (parentheses) = traffic levels from Pereira et al. (1998).
[c] [brackets] = traffic levels from Huang (2004), r = 6 in.
[d] similarities among the rankings are highlighted in bold, t_F = creep time.

Table 68 – Comparisons between the actual traffic levels of the 50/70 base asphalt binder and the ones obtained from the equations by Huang (2004) and Pereira et al. (2000)

t_F (s)[d]	actual[a] and estimated[b, c] traffic levels at each temperature[d]				
	52°C	58°C	64°C	70°C	76°C
1.0	**E** (H) **[V/E]**	H [V/E]	S [V/E]	-	-
2.0	**V** (H) **[V/E**]	S [V/E]	-	-	-
4.0	**H (H) [H]**	-	-	-	-
8.0	S (H) [H]	-	-	-	-

[a] S = standard; H = heavy; V = very heavy; E = extremely heavy (AASHTO M320-09 standard, Table 3).
[b] (parentheses) = traffic levels from Pereira et al. (2000).
[c] [brackets] = traffic levels from Huang (2004), r = 3.68 in.
[d] similarities among the rankings are highlighted in bold, t_F = creep time.

As can be seen in Table 67, the equation proposed by Pereira et al. (1998) precisely matched the actual traffic levels for all creep times at 52°C, and the one from Huang (2004) provided similar traffic levels only at creep times up to 4.0 s and this same test temperature. However, none of the equations matched the actual levels at the temperatures of 58 and 64°C, which may be a serious limitation to their use on asphalt binder data. This becomes even more serious when the similarities and differences within the traffic levels summarized in Table 68 are shown and, among other conclusions, they suggest that the empirical equation from Pereira et al. (2000) has a more restricted application to actual binder data than the ones from Huang (2004) and Pereira et al. (1998). These problems may be attributed to the fact that the equation from Pereira et al. (2000) is linear and, as previously discussed, the relationship between J_{nr} and traffic speed is expected to have a nonlinear nature.

Table 69 shows the similarities and differences within the traffic levels of the 50/70 base binder in the current and proposed classifications. These adequate levels are exactly the same at 58 and 64°C and, when the MSCR test temperature is equal to 52°C, the new classification decreases the traffic level of the binder by one degree (from extremely heavy to very heavy). This is possibly due to the presence of one more requirement in the determination of the appropriate traffic level, i. e., the binder must comply with an additional requirement to be designated as "appropriate for use on roadways with a particular traffic condition". None of these criteria could assign a traffic level to the binder at the temperatures of 70 and 76°C, since the J_{nr} values are higher than the maximum allowed value of 4.0 kPa^{-1}.

Table 69 – Traffic levels of the 50/70 base asphalt binder with increasing loading time and temperature in the current and proposed criteria

temperature (in °C)	No. of required MSCR tests[b]	Superpave® designations (current and new criteria)[a, c]	
		current criterion	new criterion
52	4	52E-xx	52V-xx
58	3	**58H-xx**	**58H-xx**
64	2	**64S-xx**	**64S-xx**
70	1	-	-
76	1	-	-

[a] S = standard; H = heavy; V = very heavy; E = extremely heavy (AASHTO M320-09 standard, Table 3).
[b] minimum number of MSCR tests to determine the adequate traffic level in the proposed classification.
[c] similarities among the classifications are highlighted in bold.

In a general context, it can be said that the 50/70 original binder shows a consistent increase in the nonrecoverable compliance values at creep times up to 4.0 s, after which the nonlinear response starts to play some role in its rheological response. This can be implied by evaluating the rates of increase in J_{nr} and the numerical values of $J_{nr,\ diff}$ with increasing creep time, i. e., quite similar percentages among the MSCR testing temperatures up to t_F = 4.0 s and much higher values when t_F is equal to 8.0 s. No traffic levels may be assigned to the base material at temperatures higher than 52°C and loading times longer than 2.0 s, which means that its use on field pavements with great percentages of slow-moving vehicles and/or high numbers of ESAL's is very limited. The empirical- and theoretical-based equations proposed in the literature and studied in the present document could adequately be fitted to the binder data ($R^2 > 0.90$) and, at a first glance, one could imply that any of them may be used to evaluate the relationship between Tr_{sp} and J_{nr}. However, it was shown that their application is fairly limited to the binder data and must be used with caution, since the points of similarity with the current traffic level criterion are scarce.

Table 70 shows the numerical values of A, B, n and α for the base asphalt binder at all stress levels and creep and recovery times, together with the corresponding variations when compared with the standardized loading-unloading conditions (1/9 s). With exception of the constant A, the elements of the power models do not greatly differ from the lowest to the highest stress level (0.1 kPa to 3.2 kPa), and the percentages of variation are all lower than 6.2% for such parameters. In other words, there is a vertical shift in the total strain accumulated by the binder with no marked changes in its degree of nonlinearity (parameter n) when the magnitude of the load is increased. In addition, α values very close to one are associated with the absence of recovery in the formulation during the MSCR test at 1/9 s and, as the data provided in the table may suggest, such a behavior can be observed for the other creep and recovery times as well. In graphical terms, the accumulated strain curves of the 50/70 base asphalt binder have a staircase shape similar to the one shown in the paper by De Visscher et al. (2004), and the major difference among them will be a vertical shift caused by an increase in the total strain accumulated by the material.

More simply, the unmodified asphalt binder accumulates strain at rates that show approximately linear shifts with increasing pavement temperature (decreasing A values) and severity of loading and no recoveries are observed in the creep-recovery cycles (α values around one). However, the nonlinear response of the material is not greatly affected by the higher pavement temperatures and a particular creep-recovery time (n values around one), and some slight modifications in this response can be observed when $t_F = 8.0$ s (n between 1.01 and 1.02). In any case, this does not seem to be as significant as expected for asphalt binders that show much higher levels of nonlinearity in the MSCR tests, which is the case of the modified ones.

From the point of view of the asphalt pavement, A values higher than unity suggest the existence of premature rutting and low values point to low initial rutting (SARKAR, 2016). This first stage of rutting takes place in the first years of the pavement life and is characterized by densification (i. e., increase in density), which is when the major portion of rutting occurs. The air voids are expelled and the mixture is stiffened and load-compacted due to a rearrangement of the aggregate particles (WASAGE et al., 2009). Since the rutting rate (B) does not considerably differ from unity and the A value increases by more than 32 times at 3.2 kPa when t_F is multiplied by 8, it can be said that the base material is extremely susceptible to the accumulation of permanent strain at the highest stress level and these accumulated strains are mainly restricted to the initial stages of rutting.

Table 70 – Numerical values and variations in the parameters/constants *A, B, n* and *α* from the power law equations by Saboo and Kumar (2015) with increasing temperature and creep time and considering the 50/70 base asphalt binder

temperature	test times	parameter A^a		parameter B^a		parameter n^a		parameter α^a	
		0.1 kPa	3.2 kPa	0.1 kPa	3.2 kPa	0.1 kPa	3.2 kPa	0.1 kPa	3.2 kPa
52°C	1/9 s	0.0527	1.6974	0.9835	0.9872	0.9989	0.9996	0.9825	0.9867
	2/9 s	0.0517 (-1.9)	1.6672 (-1.8)	0.9931 (1.0)	1.0016 (1.5)	1.0002 (0.1)	1.0012 (0.2)	0.9932 (1.1)	1.0028 (1.6)
	4/9 s	0.0486 (-7.8)	1.5747 (-7.2)	1.0051 (2.2)	1.0174 (3.1)	1.0040 (0.5)	1.0058 (0.6)	1.0091 (2.7)	1.0233 (3.7)
	8/9 s	0.0464 (-12.0)	1.5164 (-10.7)	1.0203 (3.7)	1.0326 (4.6)	1.0104 (1.2)	1.0142 (1.5)	1.0308 (4.9)	1.0473 (6.1)
58°C	1/9 s	0.1391	4.5729	1.0007	1.0032	0.9999	1.0006	1.0006	1.0038
	2/9 s	0.1362 (-2.1)	4.4902 (-1.8)	1.0082 (0.7)	1.0148 (1.2)	1.0009 (0.1)	1.0029 (0.2)	1.0091 (0.8)	1.0178 (1.4)
	4/9 s	0.1283 (-7.8)	4.2641 (-6.8)	1.0183 (1.8)	1.0266 (2.3)	1.0062 (0.6)	1.0079 (0.7)	1.0246 (2.4)	1.0347 (3.1)
	8/9 s	0.1235 (-11.2)	4.1334 (-9.6)	1.0313 (3.1)	1.0390 (3.6)	1.0136 (1.4)	1.0166 (1.6)	1.0454 (4.5)	1.0562 (5.2)
64°C	1/9 s	0.3464	11.5674	1.0083	1.0125	1.0008	1.0015	1.0092	1.0141
	2/9 s	0.3400 (-1.8)	11.3967 (-1.5)	1.0163 (0.8)	1.0200 (0.7)	1.0025 (0.2)	1.0038 (0.2)	1.0189 (1.0)	1.0239 (1.0)
	4/9 s	0.3213 (-7.2)	10.8438 (-6.3)	1.0259 (1.7)	1.0306 (1.8)	1.0079 (0.7)	1.0091 (0.8)	1.0340 (2.5)	1.0400 (2.6)
	8/9 s	0.3092 (-10.7)	10.5861 (-8.5)	1.0372 (2.9)	1.0429 (3.0)	1.0159 (1.5)	1.0183 (1.7)	1.0537 (4.4)	1.0619 (4.7)
70°C	1/9 s	0.8070	27.0589	1.0156	1.0173	1.0014	1.0021	1.0170	1.0195
	2/9 s	0.7951 (-1.5)	26.8149 (-0.9)	1.0214 (0.6)	1.0237 (0.6)	1.0037 (0.2)	1.0045 (0.2)	1.0251 (0.8)	1.0283 (0.9)
	4/9 s	0.7515 (-6.9)	25.6583 (-5.2)	1.0303 (1.4)	1.0338 (1.6)	1.0090 (0.8)	1.0100 (0.8)	1.0396 (2.2)	1.0442 (2.4)
	8/9 s	0.7267 (-10.0)	25.0361 (-7.5)	1.0409 (2.5)	1.0462 (2.8)	1.0173 (1.6)	1.0199 (1.8)	1.0590 (4.1)	1.0671 (4.7)
76°C	1/9 s	1.7157	57.7214	1.0220	1.0235	1.0024	1.0028	1.0245	1.0264
	2/9 s	1.6989 (-1.0)	57.5185 (-0.4)	1.0268 (0.5)	1.0286 (0.5)	1.0045 (0.2)	1.0054 (0.3)	1.0315 (0.7)	1.0341 (0.8)
	4/9 s	1.6138 (-5.9)	55.2641 (-4.3)	1.0344 (1.2)	1.0384 (1.5)	1.0101 (0.8)	1.0114 (0.9)	1.0449 (2.0)	1.0502 (2.3)
	8/9 s	1.5832 (-7.7)	54.5387 (-5.5)	1.0441 (2.2)	1.0504 (2.6)	1.0187 (1.6)	1.0219 (1.9)	1.0636 (3.8)	1.0734 (4.6)

[a] the percentages of variation reported in parenthesis refer to the changes in the parameter when moving from 1.0 s to the creep time into question (2.0, 4.0 or 8.0 s).

Overall, the data reported in Table 70 point out that the rutting phenomenon in the base material is essentially comprised by accumulation of permanent strain in the initial stages of rutting, and this is explained by the considerably high magnitudes of the parameter *A* when compared with the other parameters. In terms of the correlations with the vehicle speeds (creep time), the applied loads (stress level) and the temperature, it can be said that decreases in the *A* values with increasing severity of loading are associated with increases in the *B* values and vice versa. These results are in agreement with the analyses conducted by Sarkar (2016), that is, asphalt mixtures with higher initial strains will show rutting over a shorter period of time. In other words, the application of loads for longer periods of time will extend the rutting phenomenon (increase in *B*) and diminish the contribution of densification to the total strain accumulated in the material (decrease in *A*). This can be seen for both stress levels, even though some considerably high loading levels (e. g., 276 kPa in the asphalt mixture) may reverse the relationship beween the variations in *A* and *B* (SARKAR, 2016).

The percentages of variation are no greater than 12% from a numerical point of view, which is an indication that the increases in the creep time, temperature and stress level were probably not enough to place the binder within the nonlinear viscoelastic range of response. Decreases in the *A* values and increases in the numerical values of the other parameters can be observed for longer creep times and higher stress levels, regardless of the testing condition. This suggests that, although the vertical shifs in the accumulated strain in the binder during the MSCR tests prevail over the other nonlinear phenomena (*A* values are much higher than the *B*, *n* and α values), its importance on the rheological response of the material tends to decrease as the temperature and loading conditions become more critical. More simply, the effects of nonlinearity on the creep-recovery response of the asphalt binder start to increase with increasing severity in the tests, even though its relative importance is still minor for the temperature, loading time and stress level spectra selected in the study. These data are in agreement with other publications that studied the degrees of nonlinearity in original asphalt binders in the MSCR tests, see the ones from D'Angelo et al. (2007) and D'Angelo (2010a) as typical representative examples.

Figure 72 to Figure 75 show the degrees of linear correlation between t_F and the parameters *A* and *B* at 64 and 70°C. These temperatures were selected because, as previously shown, they are representative of the temperatures mostly found in Brazilian flexible asphalt pavements (CUNHA et al., 2007; LEITE and TONIAL, 1994). It can be seen that the degrees of correlation are high in all cases ($R^2 > 0.89$), and they tend to be slightly higher for the constant *A* at 100 Pa than at 3,200 Pa (the opposite is observed for the constant *B*). Another finding is that, with increasing stress level, the rate of decrease in *A* – i. e., the slope of the regression trendline –

increases at a faster rate than the corresponding rates of increases in *B*. In other words, the role of initial densification on the appearance of rutting in the asphalt binder diminishes much faster than the increase in the contribution of the rutting rate to the rutting phenomenon. In addition, the numerical value of *A* at $t_F = 4.0$ s is the odd case in all regression trendlines – i. e., the data point does not fall close to the regression trendline when compared with the other data points. This may be explained by the complex interaction between stress level, creep time and number/type of axles in the vehicle to describe the repeated creep response of the binder (SARKAR, 2016).

Table 71 (page 204) reports all the remaining correlations between the power model constants *A* and *B* and the creep times for the 50/70 unmodified asphalt binder. The data were grouped as a function of the parameter and the stress level, and the results at 64 and 70°C are shown again for the reader's convenience.

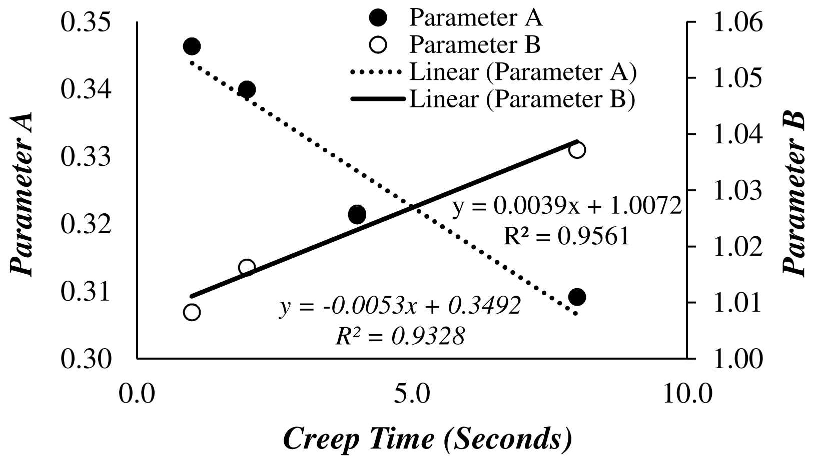

Figure 72 – Correlations between the creep time and the constants *A* and *B* from the model by Saboo and Kumar (2015), temperature of 64°C and stress level of 100 Pa – 50/70 base asphalt binder

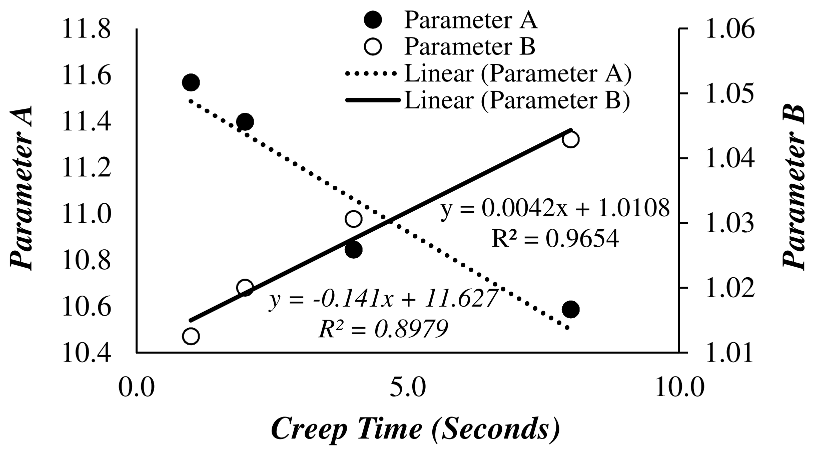

Figure 73 – Correlations between the creep time and the constants *A* and *B* from the model by Saboo and Kumar (2015), temperature of 64°C and stress level of 3,200 Pa – 50/70 base asphalt binder

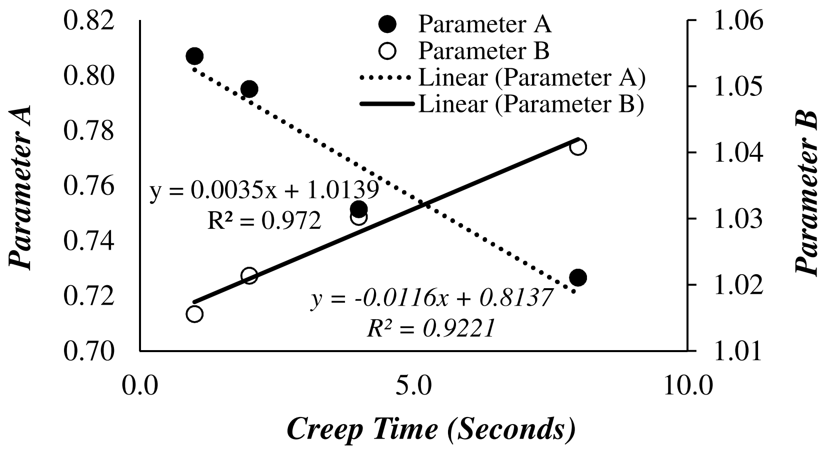

Figure 74 – Correlations between the creep time and the constants *A* and *B* from the model by Saboo and Kumar (2015), temperature of 70°C and stress level of 100 Pa – 50/70 base asphalt binder

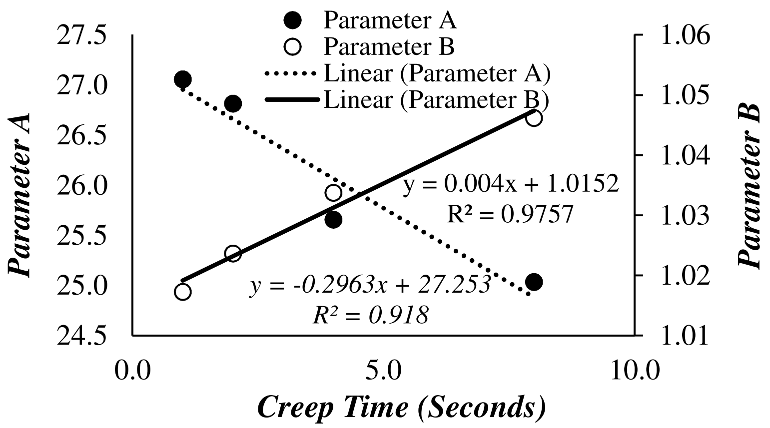

Figure 75 – Correlations between the creep time and the constants *A* and *B* from the model by Saboo and Kumar (2015), temperature of 70°C and stress level of 3,200 Pa – 50/70 base asphalt binder

Very interesting findings can be collected from the results and equations shown in Table 71. For example, the constant *A* – initial rutting – is very sensitive to an increase in the stress level and/or the temperature because the elements of the regression equations considerably differ from one testing condition to the other. At the same time, the R^2 values decrease with increasing temperature and stress level in the MSCR tests (from about 0.94 at 52°C to less than 0.88 at 76°C). On the other hand, the equations for the constant *B* show small variations in their coefficients and the R^2 values are all around 0.92-0.99. In other words, the rutting mechanism of the 50/70 original binder that is greatly affected by the pavement conditions is the initial densification phase, and the fact that the rates of decrease in *A* and R^2 become greater at higher temperatures and longer creep times suggests the presence of a more visible nonlinear response of the material (as pointed out earlier as well). In addition, the small changes in the regression coefficients and the R^2 values of the constant *B* indicate that the rutting rates are approximately the same regardless of the pavement conditions. In practical terms, it is better to control the amount of initial rutting in the base asphalt binder to minimize the formation of wheelpaths in the asphalt mixture.

Table 71 – Degrees of correlation between the parameters *A* and *B* (modified power model) and the creep time t_F for the 50/70 unmodified asphalt binder

T (°C)	stress (kPa)	linear regression equations and R^2 values (in parenthesis)[a]	
		parameter *A*	parameter *B*
52	0.1	y = -0.0009x + 0.0532 (0.9438)	y = 0.005x + 0.9816 (0.9661)
	3.2	y = -0.026x + 1.7114 (0.9308)	y = 0.0061x + 0.9868 (0.9250)
58	0.1	y = -0.0022x + 0.1401 (0.9242)	y = 0.0042x + 0.9988 (0.9720)
	3.2	y = -0.0626x + 4.6000 (0.9187)	y = 0.0048x + 1.0029 (0.9281)
64	0.1	y = -0.0053x + 0.3492 (0.9328)	y = 0.0039x + 1.0072 (0.9561)
	3.2	y = -0.1410x + 11.6270 (0.8979)	y = 0.0042x + 1.0108 (0.9654)
70	0.1	y = -0.0116x + 0.8137 (0.9221)	y = 0.0035x + 1.0139 (0.9720)
	3.2	y = -0.2963x + 27.2530 (0.9180)	y = 0.0040x + 1.0152 (0.9757)
76	0.1	y = -0.0195x + 1.7258 (0.8739)	y = 0.0031x + 1.0203 (0.9789)
	3.2	y = -0.4795x + 58.0590 (0.8614)	y = 0.0038x + 1.0210 (0.9822)

[a] the Y-axis is associated with the parameter (*A* or *B*), whereas the X-axis is associated with t_F.

With respect to the other components of the equations (exponents n and α), the regression analysis shown in Table 72 suggests that stress level and pavement temperature do not have a marked influence on the degree of nonlinearity of the material. In numerical terms, the regression coefficients are quite similar within the whole temperature range and for both stress levels, especially for the parameter n.

Table 72 – Degrees of correlation between the parameters n and α (modified power model) and the creep time t_F for the 50/70 unmodified asphalt binder

T (°C)	stress (kPa)	linear regression equations and R^2 values (in parenthesis)[a]	
		parameter n	parameter α
52	0.1	y = 0.0017x + 0.9971 (0.9984)	y = 0.0067x + 0.9787 (0.9813)
	3.2	y = 0.0021x + 0.9973 (0.9989)	y = 0.0083x + 0.9839 (0.9598)
58	0.1	y = 0.0020x + 0.9976 (0.9922)	y = 0.0063x + 0.9962 (0.9868)
	3.2	y = 0.0023x + 0.9984 (0.9990)	y = 0.0072x + 1.0013 (0.9642)
64	0.1	y = 0.0022x + 0.9986 (0.9959)	y = 0.0062x + 1.0057 (0.9799)
	3.2	y = 0.0024x + 0.9991 (0.9991)	y = 0.0067x + 1.0099 (0.9847)
70	0.1	y = 0.0023x + 0.9993 (0.9970)	y = 0.0059x + 1.0130 (0.9861)
	3.2	y = 0.0026x + 0.9995 (0.9995)	y = 0.0067x + 1.0146 (0.9906)
76	0.1	y = 0.0023x + 1.0001 (0.9969)	y = 0.0055x + 1.0204 (0.9901)
	3.2	y = 0.0027x + 1.0001 (0.9992)	y = 0.0067x + 1.0210 (0.9931)

[a] the Y-axis is associated with the parameter (n or α), whereas the X-axis is associated with t_F.

Slight increases in the coefficients of the linear regression equations can be seen for the parameter *n*, and a twofold conclusion can be reached: (a) the contribution of nonlinearity to the rutting behavior of the unmodified material is a little bit greater at higher temperatures and stress levels; and (b) both parameters barely deviate from unity in all testing conditions. The *α* values become greater with increasing stress level, but this increase is not consistent with temperature. This is probably because the *R* values are null, and therefore the parameter *α* cannot distinguish among the responses of the binder when no recovery exists. As a consequence, what can be said is that nonlinearity starts to play some role on the repeated creep behavior of the asphalt binder when the longest creep time (8.0 s) is used. Since almost no differences exist between the coefficients for the parameter *n* at 0.1 and 3.2 kPa, it can also be pointed out that the boundary between the linear and nonlinear ranges of response is probably not located between these two stresses. In fact, some base materials may show a nonlinear fashion only at stress levels of about 6.4 kPa or higher (D'ANGELO, 2010a).

It can be inferred from the aforementioned discussions about rheological modeling of the 50/70 base asphalt binder in the MSCR tests that, in general, the increases in the accumulated strain in this material at longer creep times and higher temperatures and stress levels are mainly attributed to vertical shifts in the curves of strain versus time, and such curves resemble a staircase shape (DE VISSCHER et al., 2004). This is reflected into the relative importance of each of the parameters of the models proposed by Saboo and Kumar (2015), i. e., the constant *A* typically plays a major role in the repeated creep response when compared with the constant *B* and the factors *n* and *α*, even when the degrees of severity in the MSCR tests increase (lower *A* values and higher values for the other elements at longer creep times and higher stress levels). These findings for *A* and *B* are in accordance with the ones reported elsewhere by Sarkar (2016), in that *A* seems to be more sensitive to stress level and loading time than *B* for some pavement materials. The results of *n* and *α* (all around one) at creep times up to 4.0 s can be translated into a minor influence of nonlinearity and null or very small recoveries, and the *n* values slightly deviate from unity when t_F = 8.0 s.

Once the percent recoveries of the 50/70 original binder are all equal to zero, the ANOVA analysis was carried out only on its nonrecoverable creep compliances. The data reported in Table 64 (see page 193) were rearranged according to the steps outlined in Appendix A, and then the *p-value* and the *F-value* were calculated and compared with the the level of significance (5%, or 0.05) and the $F_{critical}$ value, respectively. The organized $J_{nr}100$ and $J_{nr}3200$ values are provided in Table 73. The statistical parameters and the final recommendations for the null hypothesis H_0 are shown in Table 74 for the two studied stress levels.

Table 73 – Rearranged MSCR testing data of the 50/70 base binder to be used in the analysis of variance (ANOVA) – nonrecoverable creep compliance

stress level of 0.1 kPa ($J_{nr}100$, kPa^{-1})[a]		stress level of 3.2 kPa ($J_{nr}3200$, kPa^{-1})[a]	
increasing creep time	increasing temperature	increasing creep time	increasing temperature
0.487	0.487	0.490	0.490
0.955	1.295	0.969	1.325
1.814	3.214	1.873	3.352
3.573	7.488	3.929	7.825
N/A[b]	15.851	N/A[b]	16.648

[a] the starting point in both cases was the temperature of 52°C.
[b] N/A: Not applicable.

Table 74 – Results from the analysis of variance (ANOVA, *p-value* and *F-value*) as based on the nonrecoverable creep compliances of the 50/70 original binder

null hypothesis H_0	statistical parameters (ANOVA)				recommendation
	$F_{critical}$	*F-value*	α	*p-value*	
equivalency between J_{nr} values with increasing creep time and temperature, 0.1 kPa	5.5914	1.4823	0.05	0.2629	H_0 is not rejected
equivalency between J_{nr} values with increasing creep time and temperature, 3.2 kPa	5.5914	1.4389	0.05	0.2693	H_0 is not rejected

As the data suggest, the recommendation is not to reject the null hypothesis either at 0.1 or at 3.2 kPa. This is because the *F-value* is much lower than $F_{critical}$ (about 26%) for both stress levels and the *p-value* is more than 5 times higher than α. In other words, the effects of temperature and loading time on the J_{nr} values of the base material are quite similar from the point of view of statistics, and they can be considered as derived from a common group of experimental values. More simply, either progressive increases in temperature by 6°C or loading time (multiplication by 2) generate approximately the same effect on the rutting susceptibility of the 50/70 original binder. It is hypothesized that such conclusions may be attributed to the possibility that the asphalt binder did not reach the nonlinear viscoelastic range within the testing conditions. In such a range, the binder could show much higher increases in J_{nr} when compared with the ones in temperatures and H_0 would perhaps be rejected.

The percent recovery values of the AC+PPA at all creep times and MSCR testing temperatures are provided in Table 75. The variations in these same recoveries are shown in Figure 76. The recoveries decrease by 12 to 73% with increasing loading time at the lowest pavement temperatures (52, 58 and 64°C) and 0.1 kPa and, when the temperature goes to 70°C and higher values, the decreases are considerably higher as well (no lower than 23%). It is also interesting to observe that, when the stress level is increased from 0.1 to 3.2 kPa, the *R* values decrease much faster and are typically null at temperatures higher than 64°C and loading times longer than 2.0 s. As can be implied from the data, the AC+PPA is highly susceptible to rutting in the most critical temperature and loading conditions, especially 70 and 76°C and stress level of 3.2 kPa. This is probably because PPA is not a polymer and, as a consequence, no networks may be formed in the formulation. Baumgardner et al. (2005) among others suggested that, upon PPA modification of some asphalt binders, cross-linking of reactive segments may be developed to create a matrix of unreacted or long chains of PPA; however, this matrix of covalently linked matter may be too weak to provide high degrees of elasticity to the AC+PPA. In numerical terms, the non-null *R100* values vary from 2 to 59% and the *R3200* values are all lower than 55%.

Table 75 – Percent recoveries at 100 Pa (*R100*) and 3,200 Pa (*R3200*) for the AC+PPA with increasing loading time and temperature

parameter	creep time (s)	results at each temperature (%)[a]				
		52°C	58°C	64°C	70°C	76°C
R100	1.0	58.5	47.4	33.8	20.8	12.0
	2.0	51.0	38.5	26.4	15.8	7.7
	4.0	40.9	28.7	17.2	8.3	2.2
	8.0	29.0	18.0	9.1	2.9	0.0
R3200	1.0	54.7	40.0	21.4	5.4	0.0
	2.0	43.8	26.5	9.5	0.0	0.0
	4.0	28.5	11.2	0.6	0.0	0.0
	8.0	14.3	2.7	0.0	0.0	0.0

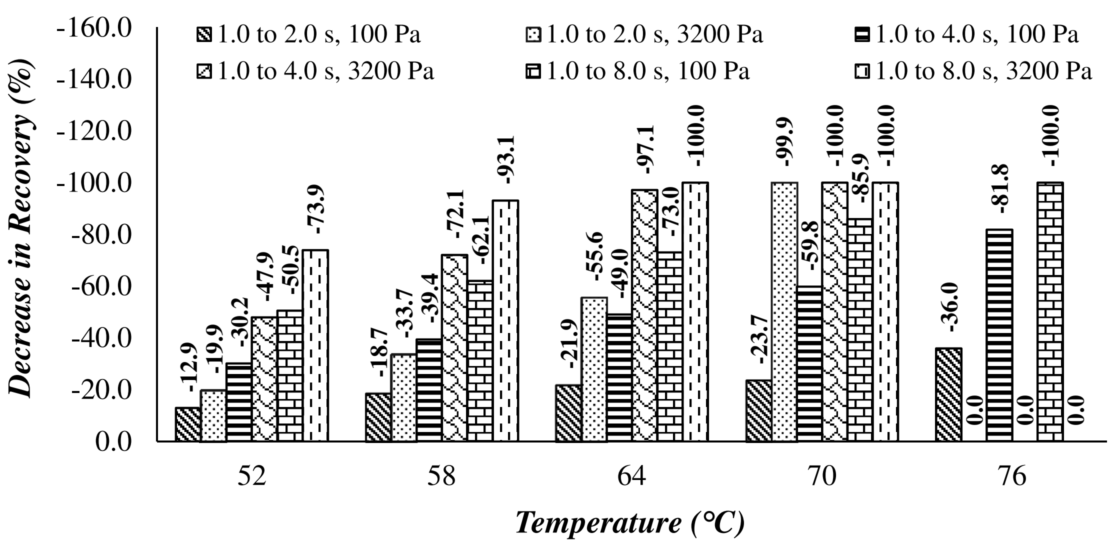

Figure 76 – Percentages of decrease in the recoveries of the AC+PPA with creep time, temperature and stress level

The above discussions on the recoveries of the AC+PPA lead to the idea that the absence of elastic response (or the presence of small *R* values) may occur on PPA-modified binders, even at temperatures lower than their high PG grades on Superpave®. This is not restricted to the present dissertation, since other publications from the literature reported similar findings. For example, Jafari and Babazadeh (2016) observed that a PG 64-xx binder modified with 1.0% of PPA by weight showed recoveries no greater than 17% at 55°C and stress levels of 3.2 and 12.8 kPa. Such recoveries were all equal to zero at the high PG grade of the material and the same stress levels. Pamplona (2013) investigated the recovery values of asphalt binders from the Lubnor-Petrobras refinery and modified with PPA contents varying from 0.5% to 2.0% by weight. It was noticed that, for the formulations with 1.0% and 1.5% by weight (PG 70-xx for both) at 64°C and 3.2 kPa in the MSCR tests, the *R* values were of 3.2% for the former and 30.7% for the latter. By increasing the temperature to 70°C, the binder with 1.0% of PPA showed no recoveries and the one with 1.5% of PPA recovered only 12.7% of the total amount of strain. In summary, PPA modification of asphalt binders does not ensure very high *R* values in all pavement conditions, especially when relatively high temperatures and stress levels are involved in the analysis.

The nonrecoverable compliances of the AC+PPA are summarized in Table 76, whereas Figure 77 depicts the variations in these same compliances with time and temperature. The effect of loading time on the J_{nr} values at a particular pavement temperature is not significant at the stress level of 0.1 kPa, i. e., the percentages of increase do not considerably differ from one temperature to the other. This can somehow be seen when the loading time is increased from 1.0 to 2.0 s at the highest stress level as well (3.2 kPa) – the percentages are all around 87-100%. It is also interesting to point out that the compliances easily overcome 4.0 kPa^{-1} at the longest loading times (4.0 and 8.0 s) and the stress level used on Superpave® (3.2 kPa), which indicates that the AC+PPA is not suitable for pavement sections with trucks traveling at very low speeds. The numerical values of $J_{nr}100$ are typically between 0.03 and 6.92 kPa^{-1}, with only a few exceptions at 76°C. With respect to the $J_{nr}3200$ values, they are mainly between 0.04 and 15.54 kPa^{-1} with exceptions at 76°C as well.

A few more comments can be made with respect to the J_{nr} values of the AC+PPA. The percentages of increase in J_{nr} are typically higher for the PPA-modified material when compared with the original one (Figure 69), especially when higher temperatures and longer creep times are considered. This means that, although binder modification with PPA decreases the nonrecoverable compliance at high pavement temperatures (i. e., lower susceptibility to rutting), the effects of loading time and temperature on the J_{nr} values of the binder become greater. In such a case, the maximum allowed value of 4.0 kPa^{-1} for J_{nr} may be exceeded when t_F is slightly increased or the maximum temperature in the pavement is higher than or equal to 64°C, even though the results at

52 and 58°C and shorter creep times are promising. In other words, the benefits of PPA addition on the rutting performance of the asphalt binder are more limited to the less severe testing conditions. This is not restricted to the creep time and temperature, since PPA-modified binders may also be innapropriate for paving applications when the stress level is increased to values beyond the ones used in the standardized MSCR protocols (JAFARI and BABAZADEH, 2016).

Table 76 – Nonrecoverable compliances at 100 Pa ($J_{nr}100$) and 3,200 Pa ($J_{nr}\ 3200$) for the AC+PPA with increasing loading time and temperature

parameter	creep time (s)	results at each temperature (kPa^{-1}), J_{nr} > 4.0 kPa^{-1} is in bold				
		52°C	58°C	64°C	70°C	76°C
$J_{nr}100$	1.0	0.039	0.116	0.335	0.906	2.205
	2.0	0.072	0.216	0.609	1.608	3.974
	4.0	0.151	0.454	1.308	3.476	**8.603**
	8.0	0.298	0.906	2.601	**6.916**	**17.537**
$J_{nr}3200$	1.0	0.043	0.133	0.416	1.223	3.148
	2.0	0.083	0.267	0.830	2.359	**5.906**
	4.0	0.191	0.655	2.004	**5.581**	**15.539**
	8.0	0.404	1.342	**4.287**	**15.413**	**69.433**

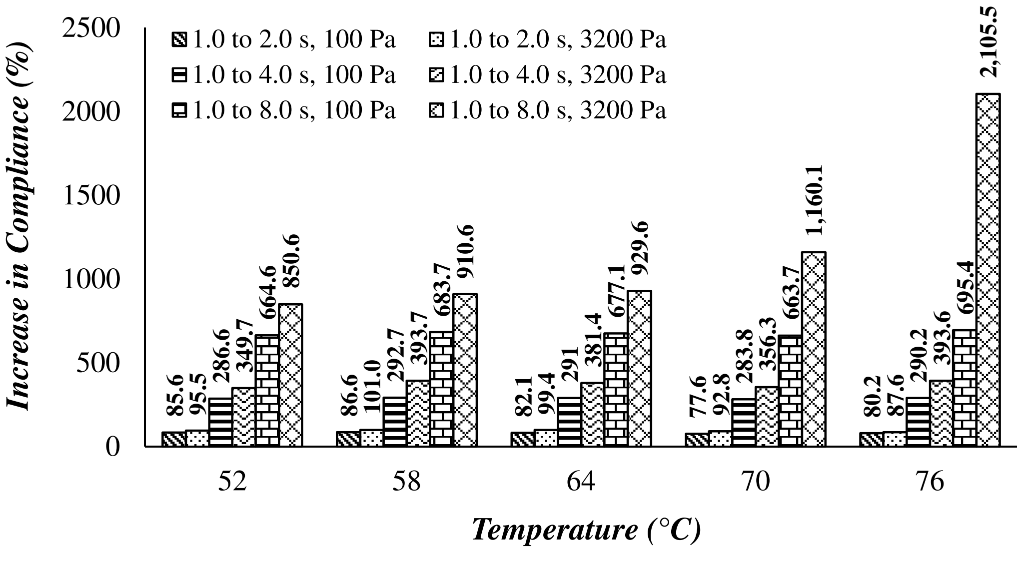

Figure 77 – Percentages of increase in the nonrecoverable compliances of the AC+PPA with creep time, temperature and stress level

Table 77 reports the adequate traffic levels of the AC+PPA based on the criteria currently found on Superpave®. Marked decreases in the traffic levels can be observed at the loading times of 4.0 and 8.0 s, and no appropriate levels may be assigned to the binder at 70 and 76°C and such loading times. The temperatures of 52 and 58°C were the only ones that provided at least one traffic level in all loading conditions, i. e., heavy or another one. By increasing the pavement temperature to 70 and 76°C, it can be seen that the AC+PPA has a limited application due to its inadequate J_{nr} values: in some cases, the compliances can overcome 15.0 kPa^{-1}. These conclusions match the particular creep-recovery responses of the AC+PPA found in the literature, i. e., the presence of the modifier and the increases by 6°C or 12°C in the high PG grade may not be enough to avoid the occurrence of quite high compliances when the temperature is close or equal to this PG grade (JAFARI and BABAZADEH, 2016; PAMPLONA, 2013). Other than showing the limitations of the requirements on Superpave® with respect to the susceptibility to rutting, these findings also indicate that further MSCR tests may be necessary to evaluate the actual resistance of the material to rutting in more severe loading and temperature conditions.

Table 77 – Adequate traffic levels for the AC+PPA with increasing creep time and temperature based on the standardized Superpave® criteria

creep time (s)	traffic levels for each temperature[a]				
	52°C	58°C	64°C	70°C	76°C
1.0	E	E	E	H	S
2.0	E	E	V	S	-
4.0	E	V	S	-	-
8.0	E	H	-	-	-

[a] S = standard; H = heavy; V = very heavy; E = extremely heavy.

Once the nonrecoverable compliances of the AC+PPA at 3.2 kPa considerably increase with increasing loading time and stress level (Table 76), it is quite natural to say that the stress sensitivity parameter ($J_{nr,diff}$) will depict marked increases as well. This can be seen in Table 78, in which a multiplication of the creep time t_F by 8 multiplies the results of $J_{nr,diff}$ by 3 to 7 depending on the temperature. As a consequence, the material becomes overly stress sensitive ($J_{nr,diff}$ > 75%) at t_F = 8.0 s and the temperature of 70°C (122.9%) and the creep times of 4.0 and 8.0 s at the temperature of 76°C (80.6 and 295.9%, respectively). The results range from 9 to 65% in the other testing temperatures and loading times. In other words, the $J_{nr,\ diff}$ value may be one more justifiable reason to avoid the use of the AC+PPA on pavements with too severe loading and climate conditions.

PPA-modified asphalt binders typically depict very high stress sensitivity when tested in the standardized or a modified MSCR protocol. For instance, Jafari et al. (2015) reported considerable increases in J_{nr} for the PPA-modified binders with 0.5, 1.0 and 1.5% of modifier by weight when increasing the stress level from 3.2 to 12.8 kPa, and the same was not observed for the SBS-modified materials (2.0, 4.0 and 6.0% of modifier by weight) at the temperatures of 55 and 70°C. One possible explanation given by the authors is that such high stress level caused irreversible and considerable damage to the formulations with PPA, which was not the case of the ones with SBS. Therefore, it may be implied that the AC+PPA studied here showed a great amount of damage when loaded at creep times longer than 2.0 s and the stress level of 3.2 kPa, which led to the substantial increases in J_{nr} and $J_{nr,\ diff}$ (some values are even higher than the upper limit of 75% set by Superpave®).

Table 78 – Percent differences in nonrecoverable compliances ($J_{nr,\ diff}$) for the AC+PPA with increasing creep time and temperature

creep time (s)	$J_{nr,\ diff}$ values (%) at each creep time and temperature[a]				
	52°C	58°C	64°C	70°C	76°C
1.0	9.2	14.9	24.4	35.1	42.8
2.0	15.1	23.7	36.3	46.7	48.6
4.0	27.1	44.4	53.2	60.6	**80.6**
8.0	35.8	48.1	64.9	**122.9**	**295.9**

[a] the numbers in bold are the ones that exceeded the maximum $J_{nr,\ diff}$ (75%) according to Superpave®.

The data summarized in Table 79 show the degrees of correlation and the corresponding regression equations between $J_{nr}3200$ and the vehicle speeds, as calculated according to the equations from Pereira et al. (1998, 2000) and Huang (2004) – tire contact radii of 3.68 and 6 in. The R^2 values are all higher than 0.90 for pavement temperatures up to 64°C and, when these temperatures are equal to 70 and 76°C, the correlations are a little bit weaker ($R^2 < 0.87$). It is believed that the nonlinear response of the material had some influence on the estimations of the vehicle speeds, since no marked differences in the results of the base binder could be seen from one temperature to the other (Figure 70 and Figure 71). The correlations are also very similar for the equations from Pereira et al (1998) and Huang (2004), and the only difference between them is the slightly higher exponent (0.037 instead of 0.030) in the one from Pereira et al. (1998).

When the tire contact radius in the equation from Huang (2004) is reduced and the equation from Pereira et al. (2000) is used rather than the one from Pereira et al. (1998), it can be observed that the differences between the R^2 values are more significant, especially at the temperatures of 70 and 76°C. In addition, the changes in the equation from Huang (2004) did not have any adverse effect on the correlations with actual binder data because the R^2 values are almost the same for the two tire contact radii (6.0 and 3.68 in). Again, it is rather difficult to say that the empirical equation from Pereira et al. (2000) is better than the theoretical-based one from Huang (2004) because several variables are involved in the determination of the average vehicle speeds in the pavement. Thus, more in-depth analyses must be conducted to identify similarities and differences among the predicted and actual traffic levels as per the results of $J_{nr}3200$.

Table 79 – Regression equations and coefficients of determination between the $J_{nr}3200$ values of the AC+PPA and the corresponding vehicle speeds according to the equations proposed by Pereira et al. (1998, 2000) and Huang (2004)

source and data	temperature (in °C)	equation	R^2
Pereira et al. (1998)	52	$y = 0.3977e^{-0.03x}$	0.9037
Pereira et al. (2000)	52	$y = -0.0053x + 0.3764$	0.9956
Huang (2004) $r = 6$ in	52	$y = 0.3979e^{-0.037x}$	0.9041
	58	$y = 1.3563e^{-0.038x}$	0.9114
	64	$y = 4.2437e^{-0.038x}$	0.9048
	70	$y = 13.642e^{-0.04x}$	0.8620
	76	$y = 50.968e^{-0.047x}$	0.7945
Huang (2004) $r = 3.68$ in	52	$y = 0.3971e^{-0.06x}$	0.9043
	58	$y = 1.3536e^{-0.062x}$	0.9117
	64	$y = 4.2351e^{-0.062x}$	0.9051
	70	$y = 13.613e^{-0.065x}$	0.8624
	76	$y = 50.843e^{-0.077x}$	0.7948

Table 80 is a summary of the comparisons between the actual and predicted traffic levels from the equations by Huang (2004) and Pereira et al. (1998). The actual levels precisely match the predicted ones only at the loading times of 1.0 and 2.0 s and the lowest pavement temperatures (i. e., 52 and 58°C). An odd case can also be found at $t_F = 8.0$ s and $T = 58$°C. When the loading and temperature conditions are more critical, there are no points of similarity between the levels assigned by the equations and the parameter $J_{nr}3200$. In other words, the approaches considered by Huang (2004) and Pereira et al. (1998) should be used only at temperatures lower than 64°C because the traffic levels determined by the MSCR tests can also be estimated by the vehicle speeds calculated from their equations.

Table 80 – Comparisons between the actual traffic levels of the AC+PPA and the ones obtained from the equations by Huang (2004) and Pereira et al. (1998)

t_F (s)[d]	actual[a] and estimated[b, c] traffic levels at each temperature[d]				
	52°C	58°C	64°C	70°C	76°C
1.0	**E (V/E) [V/E]**	**E [V/E]**	**E [V/E]**	H [V/E]	S [V/E]
2.0	**E (V/E) [V/E]**	**E [V/E]**	**V [V/E]**	S [V/E]	-
4.0	E (H) [H]	V [H]	S [H]	-	-
8.0	E (S) [H]	**H [H]**	-	-	-

[a] S = standard; H = heavy; V = very heavy; E = extremely heavy (AASHTO M320-09 standard, Table 3).
[b] (parentheses) = traffic levels from Pereira et al. (1998).
[c] [brackets] = traffic levels from Huang (2004), $r = 6$ in.
[d] similarities among the rankings are highlighted in bold, t_F = creep time.

The comparisons in Table 81 reveal that the traffic levels estimated by Huang (2004) showed reasonable correlations with the actual levels obtained by the MSCR tests, but only at 52, 58 and 64°C: there are at least two loading times at which the calculated and actual traffic levels are exactly the same. On the other hand, the levels estimated by Pereira et al. (2000) showed no correlations with the real ones from MSCR. The same trend was identified for the 50/70 original binder as well (Table 68). In other words, the results suggest that the proposed equation by Pereira et al. (2000) has serious and inherent limitations that may restrict its use on actual laboratory data, and also that the equation from Huang (2004) may yield Tr_{sp} values that are somewhat closer to the real values in the pavement. This seems to be quite logical, since Huang (2004) followed a more theoretical-based approach to propose a correlation between speed and loading time and the equation from Pereira et al. (2000) is based on limited mixture data.

Table 81 – Comparisons between the actual traffic levels of the AC+PPA and the ones obtained from the equations by Huang (2004) and Pereira et al. (2000)

t_F (s)[d]	actual[a] and estimated[b, c] traffic levels at each temperature[d]				
	52°C	58°C	64°C	70°C	76°C
1.0	**E** (H) **[V/E]**	**E [V/E]**	**E [V/E]**	H [V/E]	S [V/E]
2.0	**E** (H) **[V/E]**	**E [V/E]**	**V [V/E]**	S [V/E]	-
4.0	E (H) [H]	V [H]	S [H]	-	-
8.0	E (H) [H]	**H [H]**	-	-	-

[a] S = standard; H = heavy; V = very heavy; E = extremely heavy (AASHTO M320-09 standard, Table 3).
[b] (parentheses) = traffic levels from Pereira et al. (2000).
[c] [brackets] = traffic levels from Huang (2004), r = 3.68 in.
[d] similarities among the rankings are highlighted in bold, t_F = creep time.

As shown in Table 82, the current and proposed criteria assigned the same traffic levels for the AC+PPA at typical high pavement temperatures from 52 to 76°C, except for 64°C – extremely heavy according to the current methodology and very heavy according to the new one, see Domingos and Faxina (2017) as well. In other words, the proposed criterion would state that the AC+PPA can deal with a less severe traffic level at the temperature of 64°C. Based on the mixture data at 60°C and the discussions on the actual rutting performance of this material in the literature (Chapter 5), it can be said that the proposed traffic level criterion is an important step towards a better understanding of the rut resistance of the asphalt binder (i. e., the binder is probably not able to resist to extremely heavy traffic at 64°C, differently from what the current Superpave® method suggests). In other words, PPA-modified asphalt mixtures may be used with caution on pavements with several slow-moving vehicles, since the high degrees of nonlinearity and the substantial increases in J_{nr} at longer creep times may cause premature failure by rutting.

Table 82 – Traffic levels of the AC+PPA with increasing loading time and temperature in the current and proposed criteria

temperature (in °C)	No. of required MSCR tests[b]	Superpave® designations (current and new criteria)[a, c]	
		current criterion	new criterion
52	4	**52E-xx**	**52E-xx**
58	4	**58E-xx**	**58E-xx**
64	4	64E-xx	64V-xx
70	3	**70H-xx**	**70H-xx**
76	2	**76S-xx**	**76S-xx**

[a] S = standard; H = heavy; V = very heavy; E = extremely heavy (AASHTO M320-09 standard, Table 3).
[b] minimum number of MSCR tests to determine the adequate traffic level in the proposed classification.
[c] similarities among the classifications are highlighted in bold.

Based on the MSCR testing data of the AC+PPA at longer creep times and several high temperatures, it can be concluded that the AC+PPA shows a greater degree of nonlinearity at 3,200 Pa and very long loading times (that is, 4.0 and 8.0 s). The percent recoveries of this material depict very high percentages of decrease at 70 and 76°C and the lowest stress level (0.1 kPa), as well as all temperatures at 3.2 kPa. The percent differences in compliances may increase from 3 to 7 times their original values with increasing creep time, in such a way that the formulation becomes too stress sensitive in the most critical temperature and loading conditions (t_F of 4.0 and 8.0 s and temperatures of 70 and 76°C). The differences between the traffic levels predicted by the equation from Huang (2004) and the actual data become more significant with increasing temperature, especially at 70 and 76°C. This may be attributed to the influence of the nonlinear response of the AC+PPA at longer creep times and higher temperatures, since the cited phenomenon could not be seen for the 50/70 base binder. With respect to the comparisons between the current and proposed methods for assigning a traffic level, it can be observed that these levels are similar at all temperatures except for 64°C.

Table 83 (page 216) gives the values of the constants *A* and *B* and the factors *n* and *α* for the AC+PPA at all stress levels and creep-recovery times. It can be seen at 100 Pa and 1/9 s that, differently from the data obtained for the 50/70 base material (Table 70), the results of *B* and *n* showed greater modifications from one temperature to the other and the constant *A* depicted substantial increases with increasing test temperature (from 0.01 to more than 0.26). Another difference relies on the *α* values, i. e., the presence of higher recoveries in the AC+PPA are associated with lower numerical values for this constant (lower than 0.93 in all cases). These *α* values are much lower at temperatures up to 64°C and approach unity when the temperature is equal to 70 and 76°C. The *n* values typically close to one suggest that nonlinearity does not exert great influence on the repeated creep response of the material at such stress level and loading time. Similarly to what was reported by Saboo and Kumar (2015), the association of "higher R values" with "lower α values" seems to be valid for the MSCR data of the AC+PPA in this dissertation as well, as will be evaluated later.

By increasing the creep time to 2.0 s, 4.0 s and then 8.0 s, one may see that the α values constantly increase (i. e., R gradually decreases), the n values were all around 0.99 – 1.02, the A values decrease and the B values increase. The variations in these last two variables point to a more exponential increase in the permanent strain of the AC+PPA with loading time and temperature when compared with the conventional pair of creep-recovery times (1/9 s). In other words, the PPA-modified material accumulates strain at much higher rates when the loading conditions are more severe, differently to what was observed for the 50/70 original binder (vertical shifts in the permanent strain curves). This may be associated with the presence of the modifier, even though the stress level of 100 Pa may be too small to assess nonlinearity in some modified asphalt binders.

With respect to the constants A, B, n and α at 3,200 Pa, it may be concluded that the numerical values of A increase at much higher rates than the ones of the other elements of the power law model. The factor n is always around one, and the factor α and the constant B go from about 0.75 to 1.00 with an increase of 24°C in temperature. These data lead to the conclusion that the pattern of behavior observed for the AC+PPA at 100 Pa remained the same at 3,200 Pa, i. e., the nonlinear range of response does not seem to be achieved at the highest stress level used in the MSCR tests. Other authors have recently pointed out such a conclusion about PPA-modified materials (JAFARI et al., 2015; JAFARI and BABAZADEH, 2016), and this indicates that the current MSCR protocol should be refined to identify and address nonlinearity in modified binders.

When moving to longer creep times – i. e., 2.0 s, 4.0 s and 8.0 s – in the MSCR protocol, what can be seen is that the relative impact of the constant A with increasing creep time decreases for temperatures up to 64°C and typically increases at 70 and 76°C. On the other hand, the B and n values always increase when the testing conditions are more critical. The constant increments in the factor α (higher than or equal to 1.0 at 70 and 76°C) are associated with the null or very small recoveries of the formulation at such temperatures. Although the permanent strains in the AC+PPA are lower than the corresponding ones in the original binder, the rates of increase in these strains are much higher for the PPA-modified binder within the temperature and loading time intervals considered in the study when compared with the data at 1/9 s. In addition, the influence of nonlinearity on the response of the material tends to be somehow expressive when $t_F \geq 4.0$ s and $T \geq 70$°C ($n \approx 1.01$ or greater).

Table 83 – Numerical values and variations in the parameters/constants *A, B, n* and *α* from the power law equations by Saboo and Kumar (2015) with increasing temperature and creep time and considering the AC+PPA

temperature	test times	parameter A^a		parameter B^a		parameter n^a		parameter α^a	
		0.1 kPa	3.2 kPa	0.1 kPa	3.2 kPa	0.1 kPa	3.2 kPa	0.1 kPa	3.2 kPa
52°C	1/9 s	0.0099	0.3171	0.7467	0.7527	0.9995	0.9979	0.7463	0.7511
	2/9 s	0.0092 (-7.1)	0.2945 (-7.1)	0.7550 (1.1)	0.7688 (2.1)	1.0016 (0.2)	0.9951 (-0.3)	0.7562 (1.3)	0.7651 (1.9)
	4/9 s	0.0094 (-5.1)	0.2986 (-5.8)	0.7656 (2.5)	0.7991 (6.2)	1.0028 (0.3)	0.9853 (-1.3)	0.7677 (2.9)	0.7874 (4.8)
	8/9 s	0.0087 (-12.1)	0.2741 (-13.6)	0.7864 (5.3)	0.8453 (12.3)	1.0037 (0.4)	0.9740 (-2.4)	0.7893 (5.8)	0.8234 (9.6)
58°C	1/9 s	0.0232	0.7510	0.7913	0.8117	0.9956	0.9933	0.7879	0.8062
	2/9 s	0.0213 (-8.2)	0.6914 (-7.9)	0.8046 (1.7)	0.8431 (3.9)	0.9944 (-0.1)	0.9985 (0.5)	0.8001 (1.5)	0.8334 (3.4)
	4/9 s	0.0217 (-6.5)	0.7157 (-4.7)	0.8223 (3.9)	0.8961 (10.4)	0.9936 (-0.2)	0.9839 (-0.9)	0.8170 (3.7)	0.8817 (9.4)
	8/9 s	0.0201 (-13.4)	0.6482 (-13.7)	0.8500 (7.4)	0.9476 (16.7)	0.9929 (-0.3)	0.9875 (-0.6)	0.8440 (7.1)	0.9357 (16.1)
64°C	1/9 s	0.0538	1.8073	0.8428	0.8902	0.9934	0.9933	0.8372	0.8842
	2/9 s	0.0488 (-9.3)	1.6503 (-8.7)	0.8567 (1.6)	0.9301 (4.5)	0.9921 (-0.1)	0.9922 (-0.1)	0.8500 (1.5)	0.9229 (4.4)
	4/9 s	0.0500 (-7.1)	1.7445 (-3.5)	0.8794 (4.3)	0.9822 (10.3)	0.9903 (-0.3)	0.9980 (0.5)	0.8709 (4.0)	0.9802 (10.9)
	8/9 s	0.0464 (-13.8)	1.6549 (-8.4)	0.9084 (7.8)	1.0188 (14.4)	0.9910 (-0.2)	1.0114 (1.8)	0.9002 (7.5)	1.0305 (16.5)
70°C	1/9 s	0.1215	4.4158	0.8904	0.9641	0.9931	0.9972	0.8843	0.9614
	2/9 s	0.1092 (-10.1)	4.0547 (-8.2)	0.9047 (1.6)	0.9924 (2.9)	0.9927 (0.0)	0.9997 (0.3)	0.8980 (1.5)	0.9920 (3.2)
	4/9 s	0.1125 (-7.4)	4.4844 (1.6)	0.9283 (4.3)	1.0222 (6.0)	0.9919 (-0.1)	1.0077 (1.1)	0.9207 (4.1)	1.0301 (7.1)
	8/9 s	0.1053 (-13.3)	4.8754 (10.4)	0.9550 (7.3)	1.0589 (9.8)	0.9945 (0.1)	1.0273 (3.0)	0.9498 (7.4)	1.0878 (13.1)
76°C	1/9 s	0.2673	10.7582	0.9299	1.0015	0.9949	1.0005	0.9252	1.0020
	2/9 s	0.2399 (-10.3)	10.0069 (-7.0)	0.9438 (1.5)	1.0154 (1.4)	0.9946 (0.0)	1.0033 (0.3)	0.9387 (1.5)	1.0187 (1.7)
	4/9 s	0.2483 (-7.1)	11.6464 (8.3)	0.9665 (3.9)	1.0446 (4.3)	0.9956 (0.1)	1.0137 (1.3)	0.9623 (4.0)	1.0589 (5.7)
	8/9 s	0.2415 (-9.7)	17.5011 (62.7)	0.9906 (6.5)	1.0872 (8.6)	1.0004 (0.6)	1.0391 (3.9)	0.9910 (7.1)	1.1297 (12.7)

[a] the percentages of variation reported in parenthesis refer to the changes in the parameter when moving from 1.0 s to the creep time into question (2.0, 4.0 or 8.0 s).

The fact that the *A* values of the AC+PPA are lower than 1.0 at temperatures up to 64°C are directly related to the reduced susceptibility of the binder to rutting in these temperature conditions, and the J_{nr} values lower than 2.0 kPa^{-1} (see Table 76) point to this direction as well. The reduced *B* values indicate that this formulation accumulates viscous strain at lower rates than the original binder; however, the differences between the results tend to be small at 3,200 Pa and the AC+PPA may even show similar or higher rates than the base material at the temperatures of 70 and 76°C. This is graphically illustrated in Figure 78, in that such data points are placed above or very close to the equality line. In practical terms, the stiffening properties of PPA in the asphalt binder are easily visible when the temperature does not exceed 64°C and the creep time is lower than 4.0 s. When the pavement is subjected to extreme temperature and loading conditions, PPA modification is not able to impart high rutting resistances to the original material. This can be also be confirmed by the *A* values at 3,200 Pa and the temperatures of 64°C (between 1.65 and 1.81), 70°C (between 4.0 and 5.0) and 76°C (no lower than 10).

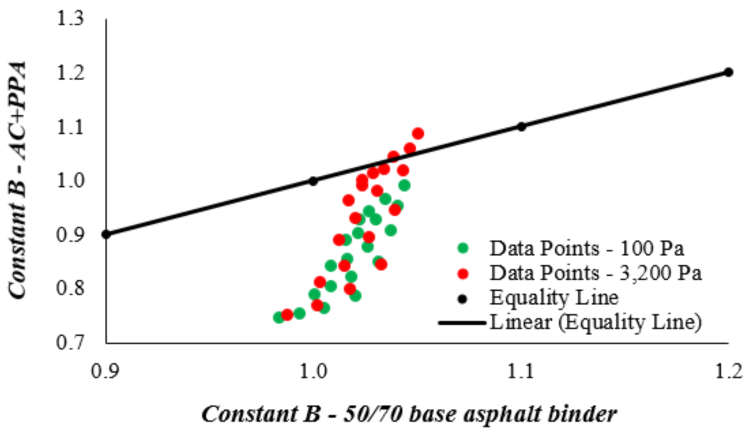

Figure 78 – Comparison between the *B* values of the 50/70 original binder and the AC+PPA in the modified power model by Saboo and Kumar (2015)

The percentages of variation in the constants of the modified power model for the AC+PPA show some similarities with the pattern of behavior observed for the original binder, i. e., decreases in *A* and increases in many of the other constants with increasing severity in the MSCR tests. The main differences between the two materials rely on the sharp increases in *A* at 70 and 76°C (from 1 to 63%) and slight decreases in *n* at the stress level of 0.1 kPa, as well as the percent differences between the variations in *A*, *B* and α from one material to the other (typically higher for the AC+PPA than for the base material). In other words, the parameters of the AC+PPA are more sensitive to the effects of loading time, temperature and stress level than the corresponding ones of the original binder. As shown above, this high sensitivity is also reflected into the considerable drops in *R* at 3,200 Pa (from around 54% to zero), the wide intervals of J_{nr} at this same stress level (from about 0.1 kPa^{-1} to more than 15.0 kPa^{-1}) and the inability of the material in always complying with the Superpave® requirements for $J_{nr,\,diff}$ (< 75%).

Figure 79 and Figure 80 portray the correlations between the constants *A* and *B* and the creep time t_F for the AC+PPA and the pavement temperature of 64°C. It is clear that the R^2 values for *A* are much lower than the corresponding ones for *B* especially at 3,200 Pa, even though the tendencies of decreasing *A* and increasing *B* with increasing t_F remained the same. Interestingly, t_F = 2.0 s is the data point that seems to be an outlier within the group of *A* values, whereas t_F = 4.0 s seems to be an outlier for the 50/70 base material (see Figure 72 to Figure 75). This may be explained by the nonlinear characteristics of the rutting phenomenon and the intrinsic properties of the asphalt binder and the modifier. In other words, each asphalt binder will show a particular response when tested under creep-recovery loading, and some peculiar details may be observed in the data.

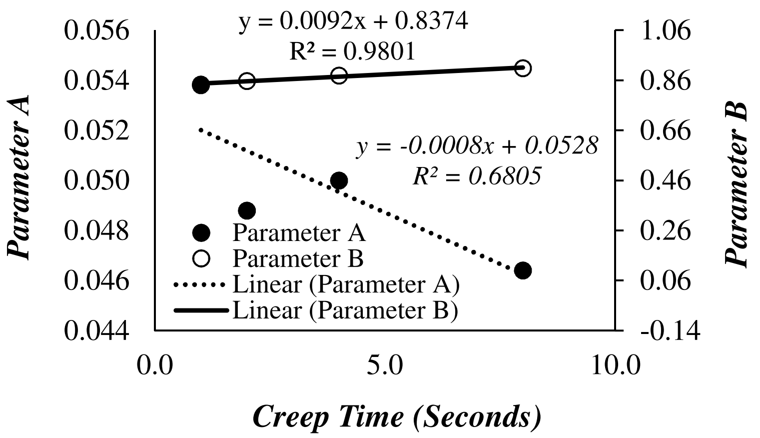

Figure 79 – Correlations between the creep time and the constants *A* and *B* from the model by Saboo and Kumar (2015), temperature of 64°C and stress level of 100 Pa – AC+PPA

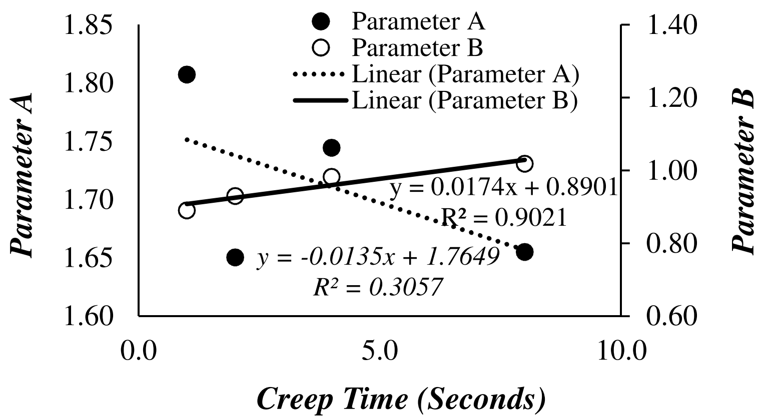

Figure 80 – Correlations between the creep time and the constants *A* and *B* from the model by Saboo and Kumar (2015), temperature of 64°C and stress level of 3,200 Pa – AC+PPA

The charts for the AC+PPA and the unmodified binder resemble the ones reported by Sarkar (2016), i. e., inflection and maximum/minimum points can be found in the intercept (constant *A*) and/or the slope (constant *B*) with increasing creep times depending on the characteristics of the creep-recovery tests and the material. However, the general trendline is what should be taken into account in the analysis, and this was done in the present study and by Sarkar (2016) as well. Similar conclusions can also be drawn by analyzing the data and regression trendlines plotted in the two figures below (Figure 81 and Figure 82), which refer to the correlations between the *A* and *B* values and the creep time for the temperature of 70°C and the AC+PPA. Other than emphasizing the presence of an outlier for *A* at t_F = 2.0 s and stress level of 100 Pa, these figures also depict a reverse in the general behavior of the constant *A* with increasing severity in the MSCR tests (i. e., decreases rather than increases).

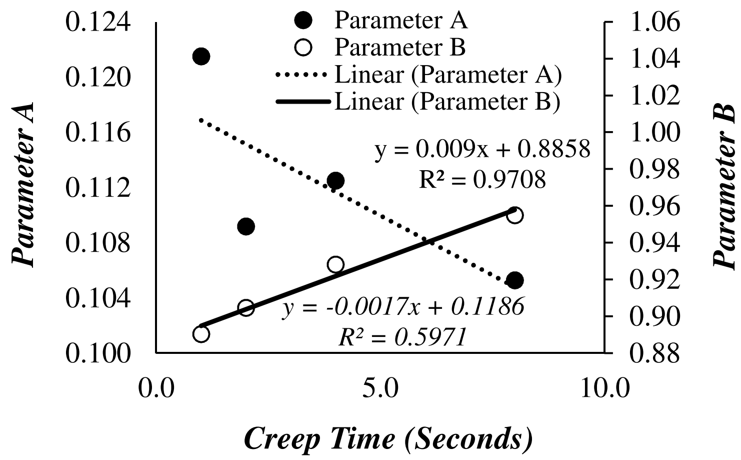

Figure 81 – Correlations between the creep time and the constants *A* and *B* from the model by Saboo and Kumar (2015), temperature of 70°C and stress level of 100 Pa – AC+PPA

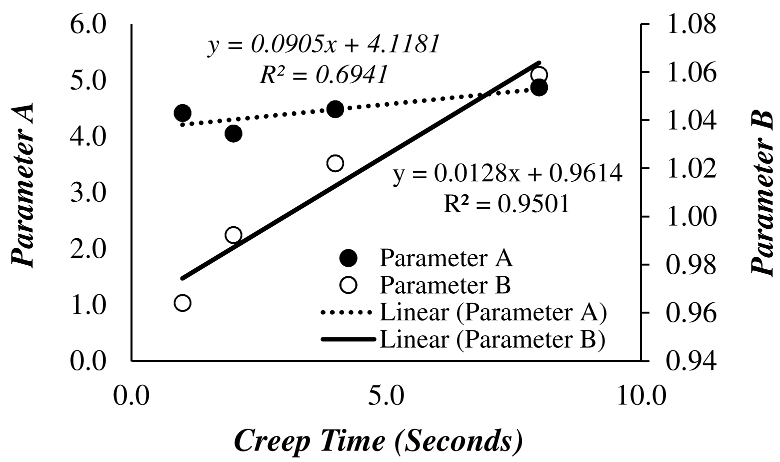

Figure 82 – Correlations between the creep time and the constants *A* and *B* from the model by Saboo and Kumar (2015), temperature of 70°C and stress level of 3,200 Pa – AC+PPA

The change in the pattern of response of the intercept *A* for the AC+PPA might be associated not only with the degree of nonlinearity in the MSCR test, but also the inability of the material in dealing with extreme loading and temperature conditions. In other words, there seems to exist a boundary line after which the rutting resistance of the PPA-modified binder decreases considerably and even the initial strains (constant *A*) contribute to such higher rutting potential. This was further investigated from the regression equations and corresponding R^2 values shown in Table 84. As can be seen, the signal of the gradient of the regression equation changes from negative to positive at 70°C and the stress level of 3,200 Pa, and this positive signal is retained at 76°C and 3,200 Pa. Such test conditions correspond to the ones under which $J_{nr}3200$ typically overcomes 5.0 kPa^{-1} (see Table 76), regardless of the loading time. Although this signal was not changed in the regression trendlines for the stress level of 100 Pa, it is clear that the intercept and the slope increases significantly and the correlations are only regular (R^2 < 0.60) when moving to the temperatures of 70 and 76°C.

Table 84 – Degrees of correlation between the parameters *A* and *B* (modified power model) and the creep time t_F for the AC+PPA

T (°C)	stress (kPa)	linear regression equations and R^2 values (in parenthesis)[a, b]	
		parameter *A*	parameter *B*
52	0.1	y = -0.0001x + 0.0098 (0.7521)	y = 0.0055x + 0.7427 (0.9946)
	3.2	y = -0.0051x + 0.3154 (0.8140)	y = 0.0131x + 0.7423 (0.9940)
58	0.1	y = -0.0004x + 0.0229 (0.7410)	y = 0.0081x + 0.7865 (0.9857)
	3.2	y = -0.0119x + 0.7461 (0.7247)	y = 0.0189x + 0.8037 (0.9575)
64	0.1	y = -0.0008x + 0.0528 (0.6805)	y = 0.0092x + 0.8374 (0.9801)
	3.2	y = -0.0135x + 1.7649 (0.3057)	y = 0.0174x + 0.8901 (0.9021)
70	0.1	y = -0.0017x + 0.1186 (0.5971)	y = 0.0090x + 0.8858 (0.9708)
	3.2	y = 0.0905x + 4.1181 (0.6941)	y = 0.0128x + 0.9614 (0.9501)
76	0.1	y = -0.0023x + 0.2579 (0.3239)	y = 0.0084x + 0.9260 (0.9645)
	3.2	y = 1.0502x + 8.5398 (0.9064)	y = 0.0122x + 0.9914 (0.9937)

[a] the Y-axis is associated with the parameter (*A* or *B*), whereas the X-axis is associated with t_F.
[b] changes in the signal of the slope of the regression trendlines are highlighted with a grey-shaded box.

It can be implied from the aforementioned discussion that the amount of damage accumulated in the binder – either at 70 or at 76°C – may have contributed to the reverse in the trend of decreases in *A* when the temperature is close or equal to the high PG grade of the material. In practical terms, the two components (i. e., initial strain and rutting rate) contributed to the substantial increases in the amount of viscous strain in the binder at both critical temperatures, which led to such great levels of rutting. As a consequence, the limiting temperature for the use of the AC+PPA could be equal to 64°C, even though its high PG grade is equal to 76-xx. Finally, the consistent and progressive increases in *B* with increasing temperature and stress level only indicate that the asphalt binder accumulates viscous strain at higher rates (i. e., higher values for the regression constants) as the severity of loading and temperature becomes greater.

Table 85 shows the regression trendlines for the parameters *n* and *α* and the PPA-modified asphalt binder. While these trendlines point to a consistent increase in *α* with increasing temperature and stress level (the gradients are all positive and the R^2 values are greater than 0.93 in all cases), the same cannot be said for the parameter *n*. It can be observed that the resulting equations at temperatures up to 64°C do not reveal any marked tendency in increasing or decreasing nonlinearity in the formulation (positive and negative signals are found in the gradients), which is also reinforced by the wide variations in R^2 – from about 0.37 to more than 0.98 – within the same group of data. The nonlinear portion of the total response of the asphalt binder becomes more noticeable at 70 and 76°C, when *n* deviates a little bit more from unity (Table 83) and all the regression equations point to increases in this parameter at longer loading times and with excellent correlations (typically higher than 0.99). This can also be implied by evaluating the magnitudes of the gradients and intercepts at such temperatures and 3.2 kPa, i. e., they are at least 25% higher than the ones observed at lower pavement temperatures.

Table 85 – Degrees of correlation between the parameters *n* and *α* (modified power model) and the creep time t_F for the AC+PPA

T (°C)	stress (kPa)	linear regression equations and R^2 values (in parenthesis)[a, b]	
		parameter *n*	parameter *α*
52	0.1	y = 0.0005x + 0.9999 (0.7905)	y = 0.0059x + 0.7426 (0.9898)
	3.2	y = -0.0035x + 1.0011 (0.9856)	y = 0.0102x + 0.7437 (0.9931)
58	0.1	y = -0.0003x + 0.9954 (0.8422)	y = 0.0078x + 0.7830 (0.9884)
	3.2	y = -0.0013x + 0.9955 (0.3654)	y = 0.0181x + 0.7962 (0.9727)
64	0.1	y = -0.0003x + 0.9928 (0.4787)	y = 0.0088x + 0.8315 (0.9864)
	3.2	y = 0.0028x + 0.9883 (0.9552)	y = 0.0201x + 0.8791 (0.9390)
70	0.1	y = 0.0002x + 0.9922 (0.3951)	y = 0.0092x + 0.8788 (0.9809)
	3.2	y = 0.0044x + 0.9915 (0.9922)	y = 0.0174x + 0.9525 (0.9805)
76	0.1	y = 0.0008x + 0.9932 (0.9911)	y = 0.0092x + 0.9197 (0.9788)
	3.2	y = 0.0057x + 0.9930 (0.9905)	y = 0.0184x + 0.9835 (0.9993)

[a] the Y-axis is associated with the parameter (*n* or *α*), whereas the X-axis is associated with t_F.
[b] changes in the signal of the slope of the regression trendlines are highlighted with a grey-shaded box.

One remarkable feature of the results of the AC+PPA is that, as the loading and temperature conditions in the MSCR tests become more critical, the *A* values tend to decrease at higher rates and the *B* and *n* values increase faster. The results of *B* and *n* for the 50/70 base binder point to the existence of such pattern of behavior as well, but not the ones of *A*. Again, it can be implied from these comments that nonlinearity has a greater impact on the stress-strain response of the AC+PPA than the original binder and that such impact increases when the pavement is subjected to higher temperatures and stress levels and longer creep times, even though the degrees of nonlinearity are still quite small for both formulations as based on the outcomes of the power law models proposed by Saboo and Kumar (2015).

Figure 83 gives the correlation between α and the percent recoveries *R100* and *R3200* for the AC+PPA. A quite good degree of correlation is obtained ($R^2 \approx 0.81$), which means that α may be used to estimate the level of elastic response in the asphalt binder. When only the non-null *R* values are considered, this correlation is increased to about 0.87 (chart not shown here). Lower α values suggest that the material has higher recoveries and vice versa (i. e., one parameter is inversely related to the other). Once a binder has higher *R* values, there is an expectation for this material of showing lower J_{nr} values as well because the amount of unrecovered strain tends to be reduced. The establishment of a limiting value for α as a complementary criterion for the traffic levels currently used on Superpave® was proposed by Saboo and Kumar (2015), but they will not be included here due to the limitations imposed by the scope of the present study.

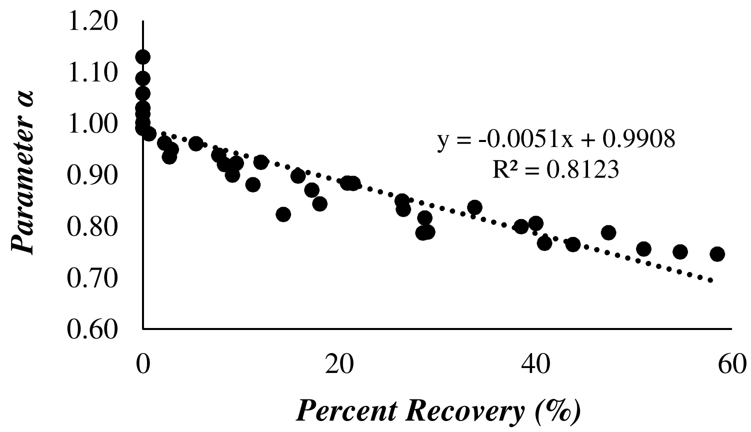

Figure 83 – Degree of correlation between the percent recoveries of the AC+PPA and the corresponding α values from the power law models

It can be inferred from the data of the rheological models of the AC+PPA that, differently from the 50/70 original material, the increases in the permanent strain probably do not follow a linear increase with increasing loading time. The presence of greater decreases in the parameter *A* and more expressive increases in the parameter *B* for the PPA-modified binder are an indication of this phenomenon. On the other hand, nonlinearity (parameter *n*) seems to exert some influence on the rheological data of the AC+PPA only when the creep time is too long (4.0 and 8.0 s), the temperature is very high (70 and 76°C) and the stress level of 3,200 Pa is considered in the analyses. With respect to the parameter α, the numerical values are lower for the AC+PPA than for the base binder, but the variations are more significant. The increases in α with increasing severity in the MSCR tests are followed by reductions in the percent recovery and, as a consequence, a good correlation between them is expected. This was confirmed by the results plotted in Figure 83, and they will be compared with the ones collected from the other binders.

Since there is only one null *R3200* value for the AC+PPA with increasing temperature and all the *R100* values are different from zero (see Table 75), it can be concluded that the ANOVA analysis may be carried out either for the *R* values or the J_{nr} values. By following the same approach used in the 50/70 original binder, four data sets were prepared in order to test the null hypothesis H_0 – i. e., the effects of temperature and creep time on the results of the MSCR tests are statistically similar. The tables with the rearranged *R* and J_{nr} values can be seen below, namely, Table 86 for the percent recoveries and Table 87 for the nonrecoverable compliances. Obviously, the null *R3200* value at 76°C is not reported in these tables.

Table 86 – Rearranged MSCR testing data of the AC+PPA to be used in the analysis of variance (ANOVA) – percent recovery

stress level of 0.1 kPa (*R100*, %)[a]		stress level of 3.2 kPa (*R3200*, %)[a]	
increasing creep time	increasing temperature	increasing creep time	increasing temperature
58.5	58.5	54.7	54.7
51.0	47.4	43.8	40.0
40.9	33.8	28.5	21.4
29.0	20.8	14.3	5.4
N/A[b]	12.0	N/A[b]	N/A[b]

[a] the starting point in both cases was the temperature of 52°C.
[b] N/A: Not applicable.

Table 87 – Rearranged MSCR testing data of the AC+PPA to be used in the analysis of variance (ANOVA) – nonrecoverable creep compliance

stress level of 0.1 kPa ($J_{nr}100$, kPa^{-1})[a]		stress level of 3.2 kPa ($J_{nr}3200$, kPa^{-1})[a]	
increasing creep time	increasing temperature	increasing creep time	increasing temperature
0.039	0.039	0.043	0.043
0.072	0.116	0.083	0.133
0.151	0.335	0.191	0.416
0.298	0.906	0.404	1.223
N/A[b]	2.205	N/A[b]	3.148

[a] the starting point in both cases was the temperature of 52°C.
[b] N/A: Not applicable.

Table 88 summarizes the key findings of the ANOVA analysis for the percent recoveries of the AC+PPA. The results do not suggest the rejection of the null hypothesis, once the *F-value* is much lower than $F_{critical}$ (ratio of one to the other is no greater than 22%) and the *p-value* is far higher than α (from 7 to 15 times). More simply, ANOVA indicates that both groups of *R100* values are derived from a common group of original data, and the same can be said for the *R3200* values. In other words, the temperature and the creep time have approximately the same impact on the elastic response of the AC+PPA in the MSCR tests from the point of view of statistics. It is believed that the nonlinear viscoelastic range of response was not fully achieved in order to allow a clear distinction between the variations in the responses of the binder, as a function of temperature and loading time.

Table 88 – Results from the analysis of variance (ANOVA, *p-value* and *F-value*) as based on the percent recoveries of the AC+PPA

null hypothesis H_0	statistical parameters (ANOVA)				recommendation
	$F_{critical}$	*F-value*	α	*p-value*	
equivalency between *R* values with increasing creep time and temperature, 0.1 kPa	5.5914	0.8644	0.05	0.3835	H_0 is not rejected
equivalency between *R* values with increasing creep time and temperature, 3.2 kPa	5.9874	0.1265	0.05	0.7343	H_0 is not rejected

When moving to the nonrecoverable creep compliances, Table 89 indicates that the same conclusions may also be applied to them because the *F-value* is still lower than $F_{critical}$ and the *p-value* barely exceeds 0.240 (about half of α). However, it is clear that the variances in J_{nr} are much higher than the corresponding ones in *R* because the *F-value* was almost doubled from one parameter to the other and the *p-value* was reduced by more than 36%. In other words, the compliance is able to better distinguish between the time and temperature dependencies of the creep-recovery responses of the AC+PPA when compared with the percent recovery, even though this is not enough to say that the two dependencies are statistically different. By comparing these results with the ones for the 50/70 unmodified binder (Table 74), one may observe that the variations in J_{nr} are slightly higher – from 5 to 9% in the case of the *F-value* – for the AC+PPA than for the original material. Also, temperature seems to play a major role in the outcomes of the MSCR tests for the AC+PPA when compared with creep time (see Table 86 and Table 87 for further details) because the decreases in *R* and increases in J_{nr} are higher for the former than for the latter.

Table 89 – Results from the analysis of variance (ANOVA, *p-value* and *F-value*) as based on the nonrecoverable compliances of the AC+PPA

null hypothesis H_0	statistical parameters (ANOVA)				recommendation
	$F_{critical}$	*F-value*	α	*p-value*	
equivalency between J_{nr} values with increasing creep time and temperature, 0.1 kPa	5.5914	1.6080	0.05	0.2453	H_0 is not rejected
equivalency between J_{nr} values with increasing creep time and temperature, 3.2 kPa	5.5914	1.5207	0.05	0.2573	H_0 is not rejected

The percent recoveries of the AC+Elvaloy+PPA at all creep times and temperatures are shown in Table 90, and the percentages of decrease in these same recoveries are summarized in Figure 84. Although the decreases in recovery are much lower than the ones found in the AC+PPA, it can be observed that these percentages considerably increase with increasing creep time, stress level and temperature – e .g., from 16 to 49% at t_F = 4.0 s and stress of 100 Pa and from 35 to 97% at t_F = 8.0 s and stress of 3,200 Pa. The *R100* values range from 12 to 77% within the whole temperature range, whereas the *R3200* values range from 1 to 71% at these same temperatures. Interestingly, the binder did not show any null *R* value not even when t_F = 8.0 s, *T* = 76°C and the stress level is the highest one (3.2 kPa). The paper from Hafeez et al. (2013) also indicated that formulations prepared with Elvaloy® terpolymer may depict high levels of elastic response within a wide interval of temperatures, including the PG grade one. The one from Domingos and Faxina (2015a) points to the same direction, and also emphasizes that the AC+Elvaloy+PPA may depict *R* values higher than 50% even when the formulation is tested at creep times longer than the one standardized by ASTM and AASHTO.

Table 90 – Percent recoveries at 100 Pa (*R100*) and 3,200 Pa (*R3200*) for the AC+Elvaloy+PPA with increasing loading time and temperature

parameter	creep time (s)	results at each temperature and increases (%)[a]				
		52°C	58°C	64°C	70°C	76°C
R100	1.0	76.3	72.2	65.3	55.3	43.2
	2.0	71.1	66.3	57.4	46.1	33.3
	4.0	63.8	57.8	47.3	34.6	22.3
	8.0	53.5	45.7	34.4	22.7	12.8
R3200	1.0	70.8	66.4	57.9	45.5	31.3
	2.0	64.4	58.5	47.2	32.7	17.3
	4.0	59.0	48.9	33.1	18.8	6.4
	8.0	45.7	34.5	20.6	8.8	1.2

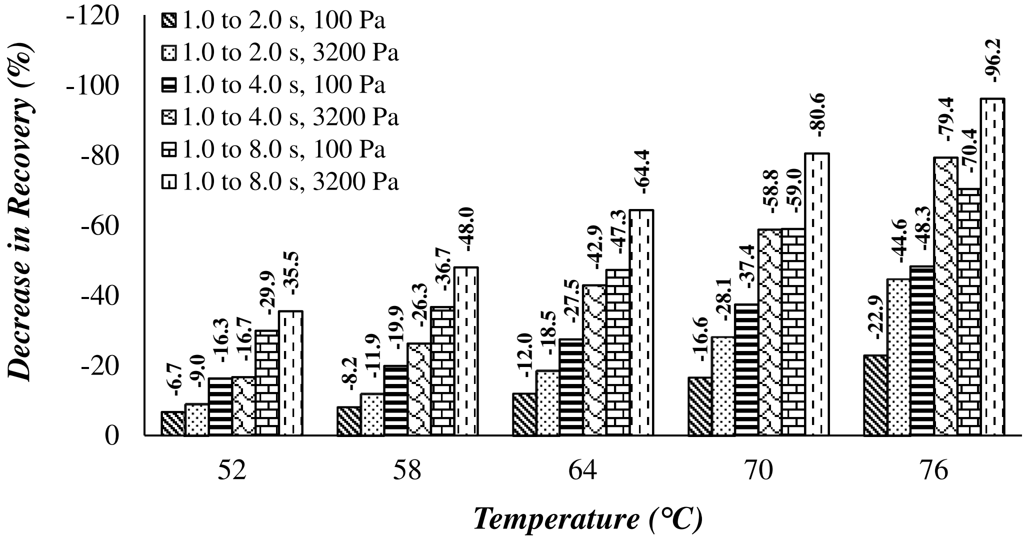

Figure 84 – Percentages of decrease in the recoveries of the AC+Elvaloy+PPA with creep time, temperature and stress level

The data shown in this study give support to the idea that the AC+Elvaloy+PPA can deal with heavier traffic levels and/or slow-moving vehicles than the AC+PPA, since higher *R* values are associated with a higher amount of recoverable strain in the MSCR test and lower amounts of viscous strain after each cycle. The fact that Elvaloy-modified binders may depict very high recoveries under severe MSCR testing conditions has been underlined by others in the literature as well (DOMINGOS and FAXINA, 2015a, 2017). However, it is not clear that the t_F value of 8.0 s is long enough to reach the nonlinear region of response for the Elvaloy-modified asphalt binder at 3.2 kPa, especially when the test temperature is far lower than the high PG grade of the material. In such a case, loading times as longer as 100 s may be used to observe this nonlinear region in Elvaloy-modified binders (DELGADILLO and BAHIA, 2010; DELGADILLO et al., 2012).

The J_{nr} values of the Elvaloy-modified asphalt binder are provided in Table 91, whereas the corresponding variations with time, temperature and stress level are given in Figure 85. It is quite surprising to say that the percentages of increase in compliance resemble the ones of the base material, e. g., an increase in the loading time from 1.0 to 4.0 s at 100 Pa (increase of 300%) yields an increase in the J_{nr} value of approximately 300% as well (from 275 to 306%). In addition, the susceptibility of the AC+Elvaloy+PPA to rutting at longer creep times is not as affected by the temperature and the creep time as the one of the AC+PPA. This means that the AC+Elvaloy+PPA has a great possibility of being used on pavements with chanellized traffic or high percentages of slow-moving vehicles, since the nonrecoverable compliances increase at approximately the same proportions observed for the t_F values. The J_{nr} values are typically lower than 5.0 kPa^{-1} at 100 Pa and lower than 6.0 kPa^{-1} at 3,200 Pa except for a few temperature and loading times.

Table 91 – Nonrecoverable compliances at 100 Pa ($J_{nr}100$) and 3,200 Pa (J_{nr} *3200*) for the AC+Elvaloy+PPA with increasing loading time and temperature

parameter	creep time (s)	results at each temperature (kPa^{-1}), J_{nr} > 4.0 kPa^{-1} is in bold				
		52°C	58°C	64°C	70°C	76°C
$J_{nr}100$	1.0	0.053	0.125	0.304	0.741	1.741
	2.0	0.104	0.248	0.619	1.520	3.593
	4.0	0.198	0.473	1.205	3.005	**7.068**
	8.0	0.360	0.876	2.218	**5.473**	**12.760**
$J_{nr}3200$	1.0	0.065	0.151	0.367	0.898	2.089
	2.0	0.130	0.304	0.761	1.877	**4.527**
	4.0	0.221	0.562	1.520	3.776	**9.273**
	8.0	0.420	1.049	2.706	**6.811**	**16.653**

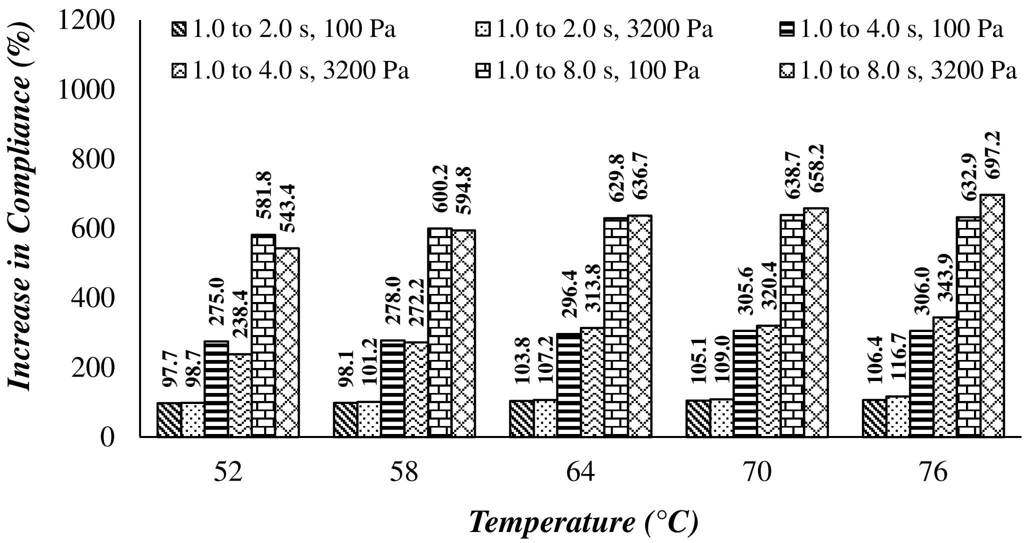

Figure 85 – Percentages of increase in the nonrecoverable compliances of the AC+Elvaloy+PPA with creep time, temperature and stress level

One interesting aspect about the rutting potential of the AC+Elvaloy+PPA at different stress levels is that the increase in such stress from 100 to 3,200 Pa did not considerably affect the percentages of increase in J_{nr} with loading time. These observations indicate that the stress sensitivity of the asphalt binder tends to decrease after the addition of Elvaloy® terpolymer, even at very high temperatures. This tendency was also pointed out by Hafeez and Kamal (2014) in their investigation about the variations in J_{nr} with increasing Elvaloy® content in the formulation. All the differences between the percentages of increase at 100 and 3,200 Pa vary from 0.9 to 13.3% and indicate that, for the range of stress levels considered in the MSCR tests, the loading time and the temperature will cause greater impacts in the rut resistance of the AC+Elvaloy+PPA than the magnitude of the applied stress by itself.

Table 92 displays the adequate traffic levels for the AC+Elvaloy+PPA at all MSCR testing temperatures and loading times. Differently from the AC+PPA, the AC+Elvaloy+PPA can deal with at least standard traffics at longer creep times and intermediate temperatures (e. g., heavy traffic for the AC+Elvaloy+PPA at t_F = 4.0 s and 64°C and only standard traffic for the AC+PPA in these test conditions). This means that the addition of Elvaloy® to the binder modified with PPA had a greater impact on the rut resistance of the material at pavement temperatures typically found in Brazil – 64 and 70°C, according to the papers by Cunha et al. (2007) and Leite and Tonial (1994). On the other hand, no marked improvements in the traffic levels of the AC+Elvaloy+PPA could be seen at the temperatures of 52, 58 and 76°C when compared with the AC+PPA, even though the J_{nr} values were considerably reduced. No traffic levels were assigned to the material at 70°C (t_F = 8.0 s) and 76°C (t_F values of 2.0 s and longer).

Table 92 – Adequate traffic levels for the AC+Elvaloy+PPA with increasing creep time and temperature based on the standardized Superpave® criteria

creep time (s)	traffic levels for each temperature[a]				
	52°C	58°C	64°C	70°C	76°C
1.0	E	E	E	V	S
2.0	E	E	V	H	-
4.0	E	V	H	S	-
8.0	E	H	S	-	-

[a] S = standard; H = heavy; V = very heavy; E = extremely heavy.

Since the AC+Elvaloy+PPA is one of the binders that showed a high degree of elasticity in the Superpave® tests, a more detailed investigation was carried out to see if the formulation holds this classification at the three longer creep times used in the tests. The data plotted in Figure 86 allow the comparisons among the classifications of the formulation at each creep time. As can be seen, there are four data points at t_F = 1.0 s, four data points at t_F = 2.0 s, three points at t_F = 4.0 s and two more at t_F = 8.0 s. The reductions in the number of points were due to the increases in J_{nr} with increasing pavement temperature and loading time, and such increases placed some J_{nr} values beyond the maximum allowed value of 2.0 kPa^{-1}, especially at higher temperatures (see Table 91). On the other hand, none of the plotted data is designated as "poor elasticity". This means that the AC+Elvaloy+PPA can hold its classification as a "formulation with high elasticity", provided that J_{nr} is lower than 2.0 kPa^{-1}. It is also in alignment with the promising findings for this type of modification in ALF's when subjected to very high stress levels (D'ANGELO, 2009; D'ANGELO et al., 2007).

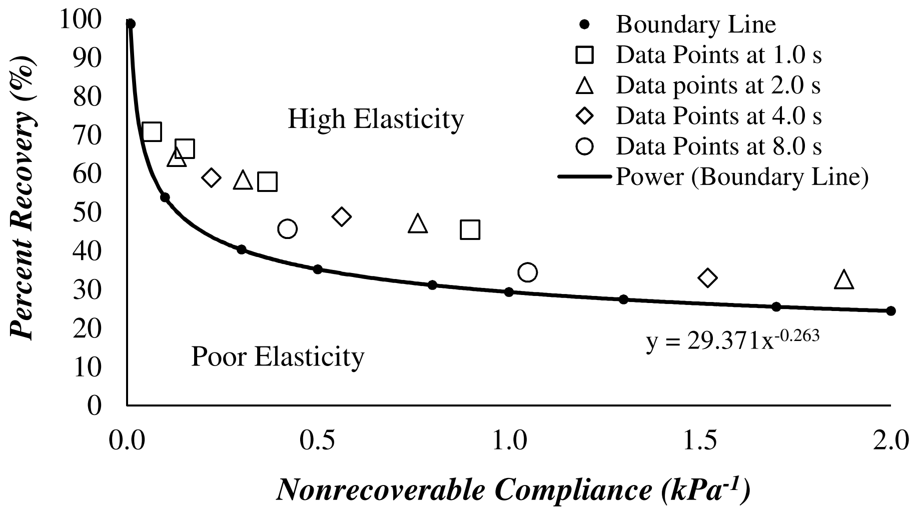

Figure 86 – Degrees of elasticity for the AC+Elvaloy+PPA at increased creep times and temperatures as based on the MSCR testing parameters at 3,200 Pa

The Superpave® stress sensitivity parameter values ($J_{nr,\ diff}$) for the AC+Elvaloy+PPA are given in Table 93. These values are all lower than 32% and do not seem to be markedly affected by the longer creep times t_F. In other words, the presence of slow-moving vehicles in the asphalt pavement will probably not cause a substantial increase in the rutting potential of the AC+Elvaloy+PPA. This is in agreement with the results obtained for another crude source of the base binder (Replan-Petrobras refinery), and it is believed that the formation of a stable asphalt-polymer system contributed – at least at some extent – to the reduction in the stress sensitivity of the material (DOMINGOS and FAXINA, 2015a). As an immediate consequence of these findings, the AC+Elvaloy+PPA does not show a high degree of stress sensitivity at any pavement temperature and loading time ($J_{nr,\ diff}$ is always far lower than 75%) and its use on paving applications – regardless of the severity of the loading condition – is possible. The values typically range from 16 to 27%, with only a few exceptions at the highest temperature (76°C).

Table 93 – Percent differences in nonrecoverable compliances ($J_{nr,\ diff}$) for the AC+Elvaloy+PPA with increasing creep time and temperature

creep time (s)	$J_{nr,\ diff}$ values (%) at each creep time and temperature				
	52°C	58°C	64°C	70°C	76°C
1.0	23.5	20.7	20.9	21.2	20.0
2.0	24.1	22.6	22.9	23.5	26.0
4.0	11.4	18.9	26.2	25.7	31.2
8.0	16.5	19.8	22.0	24.4	30.5

By correlating the $J_{nr}3200$ values of the AC+Elvaloy+PPA with the vehicle speeds derived from Huang (2004) and Pereira et al. (1998), the equations given in Table 94 may be obtained.

Differently from the AC+PPA, the degrees of correlation do not decrease with increasing pavement temperature; rather, they are all around 0.93-0.95 and are very similar from one equation to the other. Since the $J_{nr,\ diff}$ values of the AC+Elvaloy+PPA are much lower than the ones of the AC+PPA, it is believed that the degree of nonlinearity was reduced with the addition of Elvaloy® and its combination with PPA. In other words, it seems that both equations better fitted the experimental data when nonlinearity does not play a substantial role in the response of the material. Also, the main difference between the results from Huang (2004) and Pereira et al. (1998) is the higher slope (rate of decrease in speed in a semi-log scale) for the former.

Table 94 – Regression equations and coefficients of determination between the $J_{nr}3200$ values of the AC+Elvaloy+PPA and the corresponding vehicle speeds according to the equations by Pereira et al. (1998, 2000) and Huang (2004)

source and data	temperature (in °C)	equation	R^2
Pereira et al. (1998)	52	$y = 0.4213e^{-0.025x}$	0.9302
Pereira et al. (2000)	52	$y = -0.0054x + 0.4133$	0.9918
Huang (2004) *r* = 6 in	52	$y = 0.4215e^{-0.03x}$	0.9306
	58	$y = 1.0731e^{-0.032x}$	0.9348
	64	$y = 2.8640e^{-0.033x}$	0.9442
	70	$y = 7.1946e^{-0.033x}$	0.9434
	76	$y = 17.844e^{-0.034x}$	0.9486
Huang (2004) *r* = 3.68 in	52	$y = 0.4208e^{-0.049x}$	0.9308
	58	$y = 1.0712e^{-0.051x}$	0.9350
	64	$y = 2.8588e^{-0.054x}$	0.9444
	70	$y = 7.1815e^{-0.054x}$	0.9436
	76	$y = 17.811e^{-0.056x}$	0.9488

With respect to the R^2 values for the other two equations (HUANG, 2004; PEREIRA et al., 2000), Table 94 reveals that they are also high within the whole temperature range (no lower than 0.93). Again, the reduction in the tire contact radius – equation from Huang (2004) – did not cause any impact on the correlations with binder data except for slight increases in the slopes of the curves. Although these correlations are almost perfect for the equation suggested by Pereira et al. (2000) ($R^2 \approx 1$), the absence of data at the other creep times makes it difficult to evaluate its real effect on the prediction of the average vehicle speeds. This can be applied to the other correlations and analyses reported above as well.

The predicted traffic levels – as based on the equations from Huang (2004) and Pereira et al. (1998) – are equal to the actual ones at many pavement temperatures. This is the major conclusion that can be reached from the comparisons in Table 95, in which the similarities are particularly apparent at 58 and 64°C (extremely heavy at loading times up to 2.0 s, heavy at 4.0 s and standard/heavy at 8.0 s). Conversely, the same cannot be said for the two highest MSCR testing temperatures (70 and 76°C): there is only one point of similarity between the Superpave® traffic levels and the ones predicted by Huang (2004). In simple terms, it seems that the use of empirical or theoretical-based equations to estimate the traffic speeds on the roadways has a restricted application, and they may be used only at intermediate temperatures (e. g., 52 to 64°C).

Table 95 – Comparisons between the actual traffic levels of the AC+Elvaloy+PPA and the ones obtained from Huang (2004) and Pereira et al. (1998)

t_F (s)[d]	actual[a] and estimated[b, c] traffic levels at each temperature[d]				
	52°C	58°C	64°C	70°C	76°C
1.0	**E (V/E) [V/E]**	**E [V/E]**	**E [V/E]**	**V [V/E]**	S [V/E]
2.0	**E (V/E) [V/E]**	**E [V/E]**	**V [V/E]**	H [V/E]	-
4.0	E (H) [H]	V [H]	**H [H]**	S [H]	-
8.0	E (S) [H]	**H [H]**	S [H]	-	-

[a] S = standard; H = heavy; V = very heavy; E = extremely heavy (AASHTO M320-09 standard, Table 3).
[b] (parentheses) = traffic levels from Pereira et al. (1998).
[c] [brackets] = traffic levels from Huang (2004), r = 6 in.
[d] similarities among the rankings are highlighted in bold, t_F = creep time.

By replacing the original r value of 6.0 inches by 3.68 incles in the equation from Huang (2004) and utilizing the most recent equation from Pereira et al. (2000) to compare the predicted data with the actual data (Table 96), some interesting conclusions can be drawn. First, the points of similarity are scattered within the matrix of temperatures and loading times selected in the study, in such a way that there are at least two similar traffic levels at each of the temperatures of 52, 58, 64 and 70°C. Second, the presence of only heavy traffic levels in the equation from Pereira et al. (2000) creates difficulties to its use on the asphalt binder data. Due to this last reason, the estimated and real traffic levels are not similar in any of the testing conditions.

Table 96 – Comparisons between the actual traffic levels of the AC+Elvaloy+PPA and the ones obtained from Huang (2004) and Pereira et al. (2000)

t_F (s)[d]	actual[a] and estimated[b, c] traffic levels at each temperature[d]				
	52°C	58°C	64°C	70°C	76°C
1.0	**E** (H) **[V/E]**	**E [V/E]**	**E [V/E]**	**V [V/E]**	S [V/E]
2.0	**E** (H) **[V/E]**	**E [V/E]**	**V [V/E]**	**H** [V/E]	-
4.0	E (H) [H]	V [H]	**H [H]**	S [H]	-
8.0	E (H) [H]	**H [H]**	S [H]	-	-

[a] S = standard; H = heavy; V = very heavy; E = extremely heavy (AASHTO M320-09 standard, Table 3).
[b] (parentheses) = traffic levels from Pereira et al. (2000).
[c] [brackets] = traffic levels from Huang (2004), r = 3.68 in.
[d] similarities among the rankings are highlighted in bold, t_F = creep time.

Table 97 shows the classifications of the AC+Elvaloy+PPA according to each high PG grade and appropriate traffic level, either in the current or the proposed methodology. The traffic levels are the same at 52, 58 and 64°C (extremely heavy), as well as 76°C (standard). On the other hand, this level was decreased by one grade at the temperature of 70°C, see Domingos and Faxina (2017) as well. According to the suggesting criteria, the AC+Elvaloy+PPA is not as resistant to very heavy traffic levels at 70°C as the original criteria may imply, and this is due to the substantial increases in J_{nr} when the original loading time is multiplied by 4. Similar observations were also made for the AC+PPA (Table 82) and, based on such cases, it can be said that the suggesting refinements may identify some particular characteristics of the creep-recovery behavior of binders that might contribute to an increase in the amount of rutting on pavements.

Table 97 – Traffic levels of the AC+Elvaloy+PPA with increasing loading time and temperature in the current and proposed criteria

temperature (in °C)	No. of required MSCR tests[b]	Superpave® designations (current and new criteria)[a, c]	
		current criterion	new criterion
52	4	**52E-xx**	**52E-xx**
58	4	**58E-xx**	**58E-xx**
64	4	**64E-xx**	**64E-xx**
70	3	70V-xx	70H-xx
76	2	**76S-xx**	**76S-xx**

[a] S = standard; H = heavy; V = very heavy; E = extremely heavy (AASHTO M320-09 standard, Table 3).
[b] minimum number of MSCR tests to determine the adequate traffic level in the proposed classification.
[c] similarities among the classifications are highlighted in bold.

The repeated creep behavior of the AC+Elvaloy+PPA with increasing creep time and testing temperature was studied. The MSCR data suggest that this material showed quite significant decreases in the percent recovery with increasing severity of the loading and temperature conditions, even though no null R values were found. The percentages of increase in J_{nr} at 100 Pa were very close to the ones at 3,200 Pa within the whole temperature and loading time intervals, and they indicate that the susceptibility of the binder to rutting is not as stress-dependent as the results obtained for the AC+PPA. The stress sensitivity is also low ($J_{nr,\,diff} < 75\%$), even at high temperatures and long loading times. The correlations between the actual and predicted traffic levels are more concentrated at intermediate pavement temperatures (especially 58 and 64°C), and this suggests that a limited extent to the use of such equations must be considered in academic and field-based studies.

The parameters of the power law equations (A, B, n and α) for the AC+Elvaloy+PPA at the stress level of 100 Pa and the standardized creep-recovery times of 1/9 s are all shown in Table 98 (page 234). The very high recoveries for this material are reflected on its α values, which are much lower than the corresponding ones for the AC+PPA (Table 83) and the base binder (Table 70). In addition, nonlinearity seems to play some role in the response of the binder only when the temperature is lower than 64°C (n between 1.01 and 1.07). For temperatures higher than or equal to 64°C, it is clear that the amount of viscous strain in the formulation increases due to the presence of higher strain rates (higher B values). In other words, the increases in the susceptibility of the AC+Elvaloy+PPA to rutting at higher temperatures and longer loading times are mainly dictated by increases in the nonlinear portion of the total strain (parameter n) for $T < 64°C$ and by higher strain rates (parameter B) when $T \geq 64°C$. In both cases, the contribution of the initial strain (parameter A) to this lower rutting resistance is reduced when the loading time becomes longer.

In general, the constant B is slightly higher for the AC+PPA (from 0.74 to 1.09) than for the AC+Elvaloy+PPA (between 0.66 and 0.97), and an opposite trend is observed for the constant A: between 0.008 and 17.502 for the AC+PPA and between 0.020 and 10.407 for the AC+Elvaloy+PPA. In other words, the increases in the permanent strain values with increasing temperature and creep time are mainly caused by two different rutting accumulation mechanisms in the materials (higher initial strains for the AC+Elvaloy+PPA and higher strain rates for the AC+PPA). The data also suggest that the influence of nonlinearity on the response of the Elvaloy-modified material becomes a little bit more visible at t_F values up to 2.0 s ($n > 1.02$ in many cases) and $t_F = 8.0$ s ($n < 0.99$ in many cases). This was typically observed for the AC+PPA only at 70 and 76°C, which is an indication that nonlinearity has a greater contribution to the response of the AC+Elvaloy+PPA at shorter creep times when compared with the AC+PPA. The changes in α with creep time and temperature are marginal at temperatures up to 64°C, and this may be associated with the relatively small variations in R at such temperatures. The rates of increase in B are much higher at 70 and 76°C than at the other pavement temperatures, and the decreases in A show approximately the same pattern of response within the whole temperature interval.

These discussions about the variations in the constants of the power model at 100 Pa suggest that the rate of accumulation of permanent strain in the AC+Elvaloy+PPA (constant B) is not greatly influenced by the temperature when $T \leq 64°C$. On the other hand, the degree of nonlinearity increases at faster rates for this material than for the AC+PPA, especially at temperatures up to 64°C. By comparing these data with the ones collected by Delgadillo and Bahia (2010) and Delgadillo et al. (2012) on Elvaloy-modified binders, it can be said that higher temperatures and stress levels tend to decrease the boundary t_F value between linear and nonlinear responses. The effect of temperature (T values higher than 50°C) is possibly one of the reasons why nonlinearity could be somehow seen at shorter creep times in the present study

Table 98 – Numerical values and variations in the parameters/constants *A, B, n* and *α* from the power law equations by Saboo and Kumar (2015) with increasing temperature and creep time and considering the AC+Elvaloy+PPA

temperature	test times	parameter A^a		parameter B^a		parameter n^a		parameter α^a	
		0.1 kPa	3.2 kPa	0.1 kPa	3.2 kPa	0.1 kPa	3.2 kPa	0.1 kPa	3.2 kPa
52°C	1/9 s	0.0233	0.7473	0.7162	0.7194	1.0184	1.0151	0.7293	0.7302
	2/9 s	0.0233 (0.0)	0.7439 (-0.5)	0.7074 (-1.2)	0.7108 (-1.2)	1.0309 (1.2)	1.0238 (0.9)	0.7293 (0.0)	0.7278 (-0.3)
	4/9 s	0.0221 (-5.2)	0.7004 (-6.3)	0.6952 (-2.9)	0.6969 (-3.1)	1.0498 (3.1)	1.0339 (1.9)	0.7298 (0.1)	0.7206 (-1.3)
	8/9 s	0.0202 (-13.3)	0.6372 (-14.7)	0.6719 (-6.2)	0.6694 (-7.0)	1.0704 (5.1)	1.0378 (2.2)	0.7191 (-1.4)	0.6947 (-4.9)
58°C	1/9 s	0.0472	1.5085	0.7168	0.7206	1.0131	1.0087	0.7261	0.7268
	2/9 s	0.0471 (-0.2)	1.4991 (-0.6)	0.7126 (-0.6)	0.7167 (-0.5)	1.0218 (0.9)	1.0114 (0.3)	0.7282 (0.3)	0.7249 (-0.3)
	4/9 s	0.0445 (-5.7)	1.402 (-7.1)	0.7063 (-1.5)	0.7105 (-1.4)	1.0345 (2.1)	1.0091 (0.0)	0.7306 (0.6)	0.7169 (-1.4)
	8/9 s	0.04 (-15.3)	1.2411 (-17.7)	0.6969 (-2.8)	0.7065 (-2.0)	1.0423 (2.9)	0.9900 (-1.9)	0.7264 (0.0)	0.6994 (-3.8)
64°C	1/9 s	0.0922	2.9501	0.7311	0.7399	1.0058	1.0001	0.7354	0.7399
	2/9 s	0.0923 (0.1)	2.9189 (-1.1)	0.7344 (0.5)	0.7464 (0.9)	1.0092 (0.3)	0.9953 (-0.5)	0.7411 (0.8)	0.7429 (0.4)
	4/9 s	0.0869 (-5.7)	2.7012 (-8.4)	0.7378 (0.9)	0.7601 (2.7)	1.0131 (0.7)	0.9813 (-1.9)	0.7474 (1.6)	0.7459 (0.8)
	8/9 s	0.0760 (-17.6)	2.2899 (-22.4)	0.7439 (1.8)	0.7803 (5.5)	1.0097 (0.4)	0.9580 (-4.2)	0.7511 (2.1)	0.7476 (1.0)
70°C	1/9 s	0.1751	5.6199	0.7599	0.7786	0.9988	0.9919	0.7590	0.7723
	2/9 s	0.1752 (0.1)	5.4974 (-2.2)	0.7700 (1.3)	0.7987 (2.6)	0.9981 (-0.1)	0.9843 (-0.8)	0.7685 (1.3)	0.7861 (1.8)
	4/9 s	0.1644 (-6.1)	5.0225 (-10.6)	0.7833 (3.1)	0.8367 (7.5)	0.9954 (-0.3)	0.9733 (-1.9)	0.7796 (2.7)	0.8144 (5.5)
	8/9 s	0.1413 (-19.3)	4.1235 (-26.6)	0.8017 (5.5)	0.8770 (12.6)	0.9866 (-1.2)	0.9649 (-2.7)	0.7909 (4.2)	0.8463 (9.6)
76°C	1/9 s	0.3246	10.4069	0.7997	0.8327	0.9938	0.9894	0.7948	0.8239
	2/9 s	0.3250 (0.1)	10.2701 (-1.3)	0.8162 (2.1)	0.8751 (5.1)	0.9905 (-0.3)	0.9852 (-0.4)	0.8085 (1.7)	0.8621 (4.6)
	4/9 s	0.3031 (-6.6)	9.3836 (-9.8)	0.8379 (4.8)	0.9288 (11.5)	0.9851 (-0.9)	0.9860 (-0.3)	0.8254 (3.9)	0.9158 (11.2)
	8/9 s	0.2587 (-20.3)	7.7369 (-25.7)	0.8630 (7.9)	0.9665 (16.1)	0.9771 (-1.7)	0.9916 (0.2)	0.8432 (6.1)	0.9584 (16.3)

[a] the percentages of variation reported in parenthesis refer to the changes in the parameter when moving from 1.0 s to the creep time into question (2.0, 4.0 or 8.0 s).

when compared with the strain values analyzed by Delgadillo and Bahia (2010) and Delgadillo et al. (2012) – not even 100 s for t_F was enough at 100 Pa and 46°C to see nonlinearity in the Elvaloy-modified binder studied by those authors. In addition, the presence of lower *A* and *B* values and *n* values less than one – especially at 70 and 76°C – further contribute to the understanding that the AC+Elvaloy+PPA accumulates strain at lower rates than the AC+PPA and the base binder.

Similarly to the data at 100 Pa, the parameter *n* shows small variations from one temperature to the other at 3,200 Pa and the parameter α is much lower than one within the whole temperature range. The main differences between the two set of data lay on the greater increases in *A* and *B* at 3,200 Pa (from 0.74 to more than 10.0 and from 0.71 to 0.84, respectively), as well as in the parameter α at temperatures higher than 64°C. This is consistent with the rates of decrease in *R* with temperature at 100 and 3,200 Pa (see Table 90), that is, the recoveries at 3,200 Pa more clearly differentiate from the ones at 100 Pa when the temperature is of 64°C or higher.

By increasing the creep time from 1.0 to 2.0 s and then 4.0 s at temperatures no lower than 64°C, it can be observed that the constant *A* slightly decreases and the constant *B* slightly increases with the twofold increases in t_F. However, the variations in both parameters are considerably higher when the loading time is doubled from 4.0 to 8.0 s. At the same time, the parameter α increases more rapidly with loading time at such pavement temperatures. This is not exactly the same pattern of behavior observed for the AC+PPA (see Table 83), and it is believed that the polymer network was damaged at t_F = 8.0 s due to the nonlinear response of polymers at high strain (D'ANGELO et al., 2007). Such a network can not only confer high elasticity and low stress sensitivity to the binder, but also contribute to a further increase in the rutting resistance of the material. Domingos and Faxina (2015a, 2017) showed quite similar trends for the Elvaloy-modified binders, i. e., the MSCR parameters of the formulations with Elvaloy+PPA were not as sensitive to changes in the creep-recovery times as the ones with PPA alone.

The above conclusions are in agreement with the changes in the MSCR parameters *R* and J_{nr} (Table 90 and Table 91), i. e., the decreases in *R* and increases in J_{nr} tend to be greater when the temperature is equal to 70 and 76°C. In other words, the presence of longer creep times in the repeated creep tests do not seem to cause as much impact in the elastic response (*R*) and the susceptibility of the AC+Elvaloy+PPA to rutting (J_{nr}) at 52, 58 and 64°C as in the pavement temperatures of 70 and 76°C. Also, the degree of nonlinearity – factor *n* – is perhaps the parameter that is less affected by such changes in the test conditions (percentages of variation are all lower than 5%), even when the temperature is greater than 64°C and the creep times are very long. Thus, the considerable increases in *B* and α and decreases in *A* for temperature values higher than 64°C are complementary criteria for identifying the testing conditions under which the rutting resistance of the AC+Elvaloy+PPA decreases significantly, and the material may become inappropriate for some paving applications.

Figure 87 shows the levels of correlation between the *A* and *B* values and the creep time for the pavement temperature of 64°C and the stress level of 100 Pa. Figure 88 provides the correlations for the same constants, but considering the stress level of 3,200 Pa. The excellent correlations ($R^2 > 0.97$) give support to the aforementioned discussions on the decreases in *A* and increases in *B* with increasing loading time, as well as the consistency of the stress-strain response in the MSCR tests due to the presence of the polymeric system in the formulation. Differently from the base material and the AC+PPA, there does not seem to exist any outlier among the data sets of the AC+Elvaloy+PPA. In other words, the relationships between the constants *A* and *B* and the creep time are closer to a straight line than the ones observed for the other two previously cited binders.

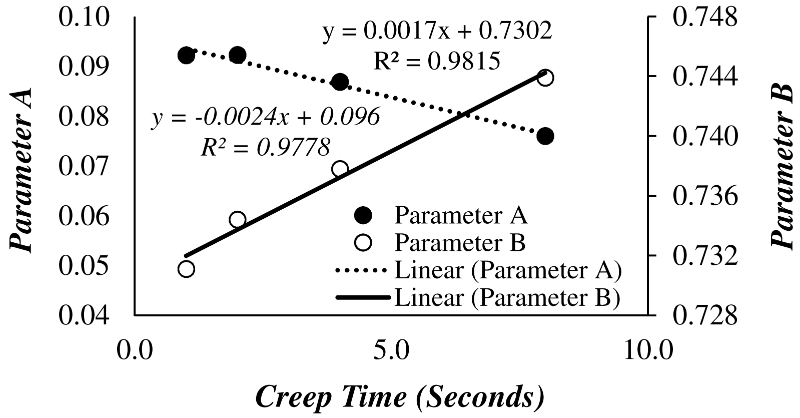

Figure 87 – Correlations between the creep time and the constants *A* and *B* from the model by Saboo and Kumar (2015), temperature of 64°C and stress level of 100 Pa – AC+Elvaloy+PPA

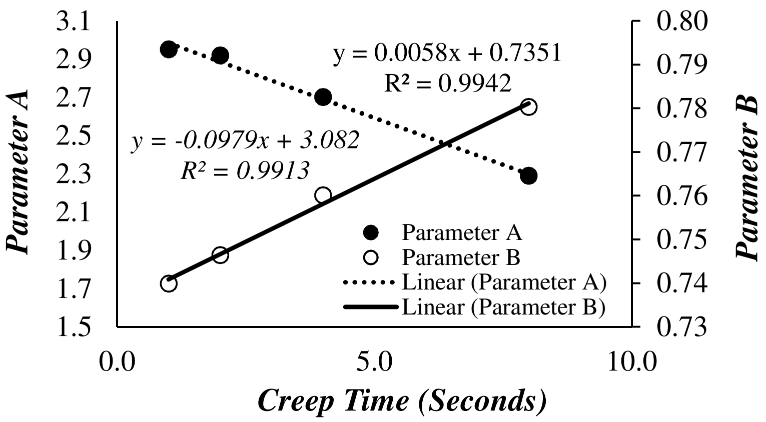

Figure 88 – Correlations between the creep time and the constants *A* and *B* from the model by Saboo and Kumar (2015), temperature of 64°C and stress level of 3,200 Pa – AC+Elvaloy+PPA

The above correlations also indicate that the degrees of nonlinearity are so small that the four selected creep times are not enough to highlight the nonlinear stress-strain relationship of the response of the binder. This is reinforced by the n values approximately equal to unity at 64°C, namely, between 0.95 and 1.02 at all creep times and stress levels. By moving to the temperature of 70°C (Figure 89 and Figure 90 below), it can be observed that the trendlines and the behaviors of the constants A and B remain essentially the same except for slight reductions in R^2. These reductions may be attributed to marginal changes in the nonlinear response of the formulation (parameter n) under creep-recovery loading. In other words, the AC+Elvaloy+PPA does not show any significant change in its pattern of response after the increase in the pavement temperature from 64 to 70°C.

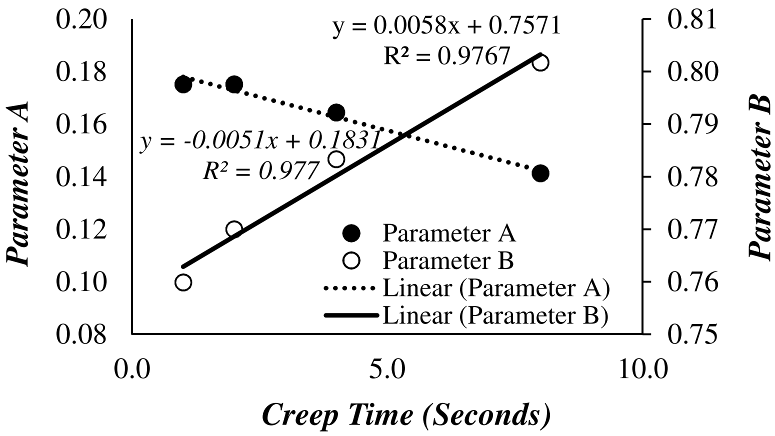

Figure 89 – Correlations between the creep time and the constants A and B from the model by Saboo and Kumar (2015), temperature of 70°C and stress level of 100 Pa – AC+Elvaloy+PPA

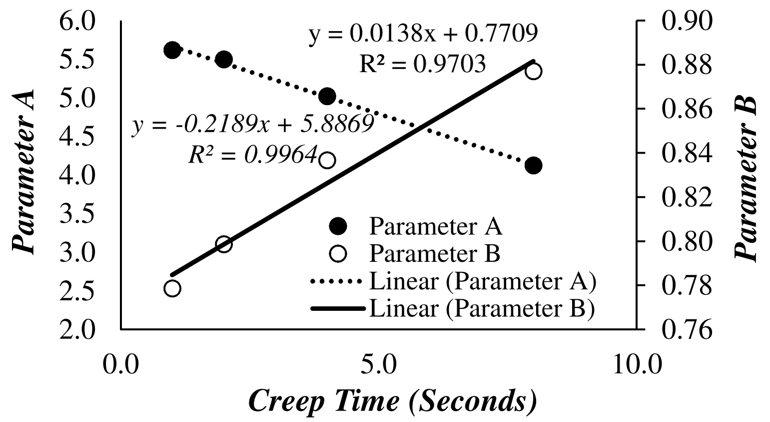

Figure 90 – Correlations between the creep time and the constants A and B from the model by Saboo and Kumar (2015), temperature of 70°C and stress level of 3,200 Pa – AC+Elvaloy+PPA

A more detailed investigation was conducted to see whether these consistent responses of the AC+Elvaloy+PPA may be observed for the other temperatures and parameters as well. In this manner, Table 99 was constructed to show the regression equations and the corresponding R^2 values for the whole group of parameters from the modified power model. As previously discussed, the role of the strain rate *B* on the total accumulated strain in the binder starts to play a major role only at higher pavement temperatures (in this case, 64°C or higher). From a mathematical point of view, this occurs when the signal of the gradient of the regression trendline changes from negative to positive, i. e., the *B* values increase with increasing loading time.

Table 99 – Degrees of correlation between the parameters *A* and *B* (modified power model) and the creep time t_F for the AC+Elvaloy+PPA

T (°C)	stress (kPa)	linear regression equations and R^2 values (in parenthesis)[a, b]	
		parameter *A*	parameter *B*
52	0.1	y = -0.0005x + 0.0240 (0.9826)	y = -0.0062x + 0.7209 (0.9958)
	3.2	y = -0.0165x + 0.7690 (0.9878)	y = -0.0071x + 0.7256 (0.9990)
58	0.1	y = -0.0011x + 0.0488 (0.9854)	y = -0.0028x + 0.7186 (0.9874)
	3.2	y = -0.0399x + 1.5622 (0.9898)	y = -0.0019x + 0.7208 (0.9072)
64	0.1	y = -0.0024x + 0.0960 (0.9778)	y = 0.0017x + 0.7302 (0.9815)
	3.2	y = -0.0979x + 3.0820 (0.9913)	y = 0.0058x + 0.7351 (0.9942)
70	0.1	y = -0.0051x + 0.1831 (0.9770)	y = 0.0058x + 0.7571 (0.9767)
	3.2	y = -0.2189x + 5.8869 (0.9964)	y = 0.0138x + 0.7709 (0.9703)
76	0.1	y = -0.0100x + 0.3402 (0.9777)	y = 0.0087x + 0.7966 (0.9607)
	3.2	y = -0.3953x + 10.9320 (0.9921)	y = 0.0180x + 0.8331 (0.8992)

[a] the Y-axis is associated with the parameter (*A* or *B*), whereas the X-axis is associated with t_F.
[b] changes in the signal of the slope of the regression trendlines are highlighted with a grey-shaded box.

With respect to the parameter *A*, the constants of the trendlines at 3,200 Pa are far higher than the corresponding ones at 100 Pa within the whole temperature range, which means that the initial strain (densification in the asphalt mixture) greatly increases with increasing stress level. The temperature of 64°C is also the limiting value beyond which these constants increase at faster rates than the ones observed at temperatures lower than 64°C. Just to give an example, the moduli of the slopes observed at 58 and 64°C (0.0011 and 0.0024, respectively) and at 100 Pa did not increase by more than 380% when compared with the corresponding slope at 52°C (0.0005). However, these moduli are more than 900% higher when the temperatures of 70°C (0.0051) and 76°C (0.0100) are considered. Similar approaches can be taken when studying the changes in the independent term of the regression trendlines at 100 Pa: percentages of increase lower than or equal to 300% for the temperatures of 58°C (from 0.0240 to 0.0488) and 64°C (from 0.0240 to 0.0960) and much higher percentages – as higher as 1,300% – at the temperatures of 70°C (from 0.0240 to 0.1831) and 76°C (from 0.0240 to 0.3402). The conclusions and analyses for the constants at 3,200 Pa are equivalent.

Table 100 shows the correlations between n and α and the four creep times for the AC+Elvaloy+PPA. The identification of positive and negative slopes in the linear regression trendlines is noteworthy, as well as the presence of some poor levels of correlation ($R^2 < 0.40$) in both parameters. This may be associated with a quite low degree of nonlinearity in the formulation at temperatures up to 64°C, which is where the majority of these uncommon results can be found. More simply, such obtained trendlines are only mathematical fits and their interpretations one by one may lead to misleading conclusions about the actual degree of nonlinearity in the AC+Elvaloy+PPA. What can be said is that nonlinearity typically increases with increasing loading time in the MSCR test when $T \leq 64$°C (positive slopes in many of the regression equations) and it generally decreases with increasing t_F when $T > 64$°C (negative slopes in almost all the regression equations), as pointed out above. However, none of these findings may be considered as relevant because the n values barely exceed 1.07 and the gradients are all lower than 7.0×10^{-3}.

Table 100 – Degrees of correlation between the parameters n and α (modified power model) and the creep time t_F for the AC+Elvaloy+PPA

T (°C)	stress (kPa)	linear regression equations and R^2 values (in parenthesis)[a, b]	
		parameter n	parameter α
52	0.1	y = 0.0072x + 1.0154 (0.9632)	y = -0.0015x + 0.7325 (0.8046)
	3.2	y = 0.0030x + 1.0164 (0.8173)	y = -0.0052x + 0.7378 (0.9734)
58	0.1	y = 0.0040x + 1.0130 (0.8948)	y = -4E-05x + 0.7280 (0.0044)
	3.2	y = -0.0029x + 1.0158 (0.8303)	y = -0.0040x + 0.7321 (0.9927)
64	0.1	y = 0.0004x + 1.0078 (0.2014)	y = 0.0021x + 0.7360 (0.8618)
	3.2	y = -0.0061x + 1.0065 (0.9983)	y = 0.0010x + 0.7403 (0.8448)
70	0.1	y = -0.0018x + 1.0014 (0.9756)	y = 0.0043x + 0.7583 (0.9378)
	3.2	y = -0.0037x + 0.9924 (0.9210)	y = 0.0105x + 0.7655 (0.9778)
76	0.1	y = -0.0023x + 0.9954 (0.9896)	y = 0.0066x + 0.7933 (0.9462)
	3.2	y = 0.0006x + 0.9860 (0.3267)	y = 0.0184x + 0.8212 (0.9234)

[a] the Y-axis is associated with the parameter (n or α), whereas the X-axis is associated with t_F.
[b] changes in the signal of the slope of the regression trendlines are highlighted with a grey-shaded box.

With respect to the parameter α, a little bit better picture of the actual response of the material may be found in the data. The α values generally increase with increasing temperature and stress level, and the degrees of correlation range from good to excellent (R^2 between 0.84 and 0.98) at higher temperatures, i. e., 64°C and more. The odd case identified at 58°C and 100 Pa (R^2 almost equal to zero) and the reductions in α with increasing t_F at lower temperatures have a reasonable explanation. As the data in Table 90 may suggest, the presence of relatively high *R100* and *R3200* values at longer loading times indicates that the proper identification of the role of nonlinearity on the response of the formulation is a rather difficult task, especially when high stress levels are used and the binder has a high degree of elasticity. The role of nonlinearity may be minimized when steady state is achieved (BAHIA et al., 2001a), and this is probably one additional factor – together with the small range of creep times – that contributed to the difficulties in correctly observing nonlinearity in the results of the MSCR tests. Finally, the strange correlations obtained for α in some test conditions may be attributed to the test variability, since all the other equations and correlations are consistent with the behavior reported by Saboo and Kumar (2015).

Figure 91 shows the relationship between α and the percent recoveries as a unique group, i. e., by considering either the results at 100 Pa or the ones at 3,200 Pa. The R^2 value is of about 0.65, which is reasonably good. However, this result is approximately 26.4% lower than the one obtained for the AC+PPA (0.87, see Figure 83). Even though the tendency of decreasing α with increasing recovery remains essentially the same for the AC+Elvaloy+PPA in a general context, it seems that the deviations observed at 52 and 58°C (lower α values for lower recoveries, Table 100) affected the overall correlation. In other words, the approach followed by Saboo and Kumar (2015) is acceptable when one is looking for a relationship between percent recovery and constants derived from mathematical models, even though it contains some limitations when applied to materials with high levels of elastic response.

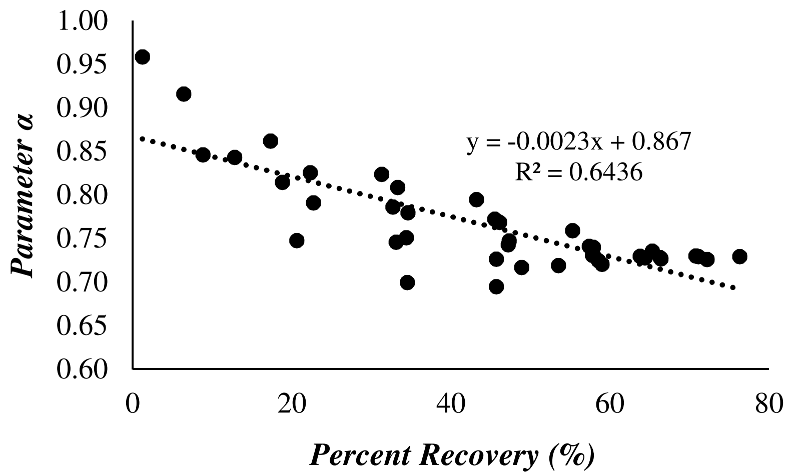

Figure 91 – Degree of correlation between the percent recoveries of the AC+Elvaloy+PPA and the corresponding α values from the power law models

According to the data plotted in Figure 92, the *R100* values depict a higher correlation with α (about 0.74) than the *R3200* values (around 0.65). Since the two coefficients of determination are very close to each other, it can be implied that the stress level was not a relevant factor in the reduction in R^2 for the AC+Elvaloy+PPA when compared with the AC+PPA. As a consequence, it is suggested that the natural variability of the laboratory data and the inadequacies of the modified power model are the most fundamental components in the determination of such lower R^2 values.

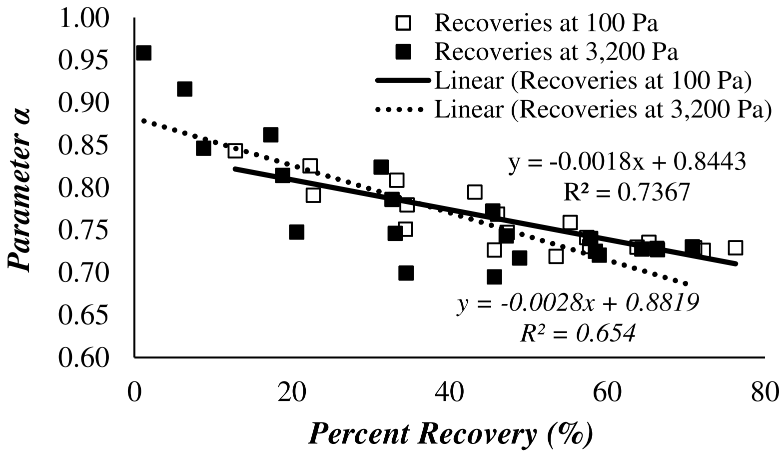

Figure 92 – Individual correlations between the percent recoveries of the AC+Elvaloy+PPA at 100 and 3,200 Pa and the corresponding α values from the power law models

It can be inferred from the rheological modeling of the creep-recovery curves of the AC+Elvaloy+PPA that, due to the presence of comparatively high recoveries within the whole temperature range, the α values are much lower than the corresponding ones of the AC+PPA. At the same time, two prevailing phenomena seem to dictate the increases in the rutting susceptibility of the material in the MSCR tests, namely: (a) increases in the nonlinear portion of the total strain at pavement temperatures up to 64°C; and (b) increases in the strain rate at the temperatures of 70 and 76°C. The changes in the degree of nonlinearity (parameter n) with creep time are marginal, either at lower or higher temperatures. As a consequence, it is not possible to clearly evaluate the role of nonlinearity on the behavior of the binder with increasing loading time (regression equations with positive and negative gradients). Finally, the limitations of the constants of the modified power model and the natural variability of the data possibly affected the level of correlation between α and percent recovery ($R^2 \approx 0.65$, which is about 26.4% lower than the one obtained for the AC+PPA).

The statistical analysis (ANOVA) was carried out on the R and J_{nr} values of the AC+Elvaloy+PPA, as shown in the rearranged data in Table 101 (percent recovery) and Table 108 (nonrecoverable compliance). It is possible to conduct such analyses for both parameters because none of the recoveries are equal to zero. In other words, the data sets are comprised by four numerical values under the influence of the creep time and five numerical values under the influence of the test temperature.

Table 101 – Rearranged MSCR testing data of the AC+Elvaloy+PPA to be used in the analysis of variance (ANOVA) – percent recovery

stress level of 0.1 kPa (*R100*, %)[a]		stress level of 3.2 kPa (*R3200*, %)[a]	
increasing creep time	increasing temperature	increasing creep time	increasing temperature
76.3	76.3	70.8	70.8
71.1	72.2	64.4	66.4
63.8	65.3	59.0	57.9
53.5	55.3	45.7	45.5
N/A[b]	43.2	N/A[b]	31.3

[a] the starting point in both cases was the temperature of 52°C.
[b] N/A: Not applicable.

Table 102 – Rearranged MSCR testing data of the AC+Elvaloy+PPA to be used in the analysis of variance (ANOVA) – nonrecoverable creep compliance

stress level of 0.1 kPa ($J_{nr}100$, kPa^{-1})[a]		stress level of 3.2 kPa ($J_{nr}3200$, kPa^{-1})[a]	
increasing creep time	increasing temperature	increasing creep time	increasing temperature
0.053	0.053	0.065	0.065
0.104	0.125	0.130	0.151
0.198	0.304	0.221	0.367
0.360	0.741	0.420	0.898
N/A[b]	1.741	N/A[b]	2.089

[a] the starting point in both cases was the temperature of 52°C.
[b] N/A: Not applicable.

Table 103 reports the results of ANOVA for the recovery values of the AC+Elvaloy+PPA and the stress levels of 100 and 3,200 Pa. The determination of a very small *F-value* at both stresses – as well as a *p-value* at least 10 times higher than α – indicates that the selected loading times and temperatures have quite similar influences on the recoveries of the formulation under a level of significance of 5%. By comparing these results with the ones of the AC+PPA (Table 88), it can be observed that the *R* values of the AC+Elvaloy+PPA are much less sensitive to the effects of loading and temperature than the corresponding values of the AC+PPA. It is quite natural to say that the polymeric network formed in the Elvaloy-modified binder has a major contribution to these promising findings.

By moving from the percent recoveries to the nonrecoverable compliances (Table 104), one may notice that the variations (*F-value*) increase by 3 to 6 times, even though this is not enough to say that the effects of temperature and loading time on the parameter J_{nr} are different (i. e., the *p-value* is higher than α and the *F-value* is lower than $F_{critical}$). Despite the marked increases in these variations when compared with the parameter *R*, the ANOVA analyses indicate that the compliances of the AC+PPA (Table 89) are still more sensitive to changes in both parameters than the corresponding compliances of the AC+Elvaloy+PPA. This again may be explained by the stability caused by the polymeric network in the polymer-modified material, which was also highlighted in previous papers from the literature (DOMINGOS and FAXINA, 2015a, 2017).

Table 103 – Results from the analysis of variance (ANOVA, *p-value* and *F-value*) as based on the percent recoveries of the AC+Elvaloy+PPA

null hypothesis H_0	statistical parameters (ANOVA)				recommendation
	$F_{critical}$	*F-value*	α	*p-value*	
equivalency between *R* values with increasing creep time and temperature, 0.1 kPa	5.5914	0.2126	0.05	0.6587	H_0 is not rejected
equivalency between *R* values with increasing creep time and temperature, 3.2 kPa	5.5914	0.3530	0.05	0.5711	H_0 is not rejected

Table 104 – Results from the analysis of variance (ANOVA, *p-value* and *F-value*) as based on the nonrecoverable compliances of the AC+Elvaloy+PPA

null hypothesis H_0	statistical parameters (ANOVA)				recommendation
	$F_{critical}$	*F-value*	α	*p-value*	
equivalency between J_{nr} values with increasing creep time and temperature, 0.1 kPa	5.5914	1.3412	0.05	0.2848	H_0 is not rejected
equivalency between J_{nr} values with increasing creep time and temperature, 3.2 kPa	5.5914	1.3897	0.05	0.2770	H_0 is not rejected

Asphalt Binders Modified with Crumb Rubber and Rubber+PPA. Table 105 summarizes the *R* values of the AC+rubber at all pavement temperatures and loading times. When tested at 100 Pa, the percentages of decrease in *R100* are considerably lower than the corresponding ones in *R3200* – see Figure 93 – and the material does not show any null *R* value at the lowest stress level. These results suggest that the parameter *R* is quite sensitive to stress level and loading time. The percentages of decrease for the AC+rubber are comparable to the ones of the AC+PPA (Table 75), even though the numerical values of *R100* are higher for the formulation with crumb rubber – between 5 and 76% – than for the one with PPA alone and an opposite trend is observed for *R3200* (no greater than 44% for the AC+rubber). It is interesting to note that this high sensitivity of the recovery values of the crumb rubber-modified binder when compared with polymeric modification types (e. g., Table 90 for the AC+Elvaloy+PPA) may also be found elsewhere in the literature (KATAWARE and SINGH, 2015).

Table 105 – Percent recoveries at 100 Pa (*R100*) and 3,200 Pa (*R3200*) for the AC+rubber with increasing loading time and temperature

parameter	creep time (s)	results at each temperature (%)				
		52°C	58°C	64°C	70°C	76°C
R100	1.0	75.5	67.6	60.5	51.3	41.6
	2.0	62.5	56.7	48.9	37.9	27.3
	4.0	55.1	47.9	39.8	29.3	19.1
	8.0	36.6	29.2	19.7	11.2	5.0
R3200	1.0	44.0	27.0	12.0	3.1	0.0
	2.0	29.4	13.7	3.8	0.0	0.0
	4.0	19.1	6.8	0.4	0.0	0.0
	8.0	4.9	0.0	0.0	0.0	0.0

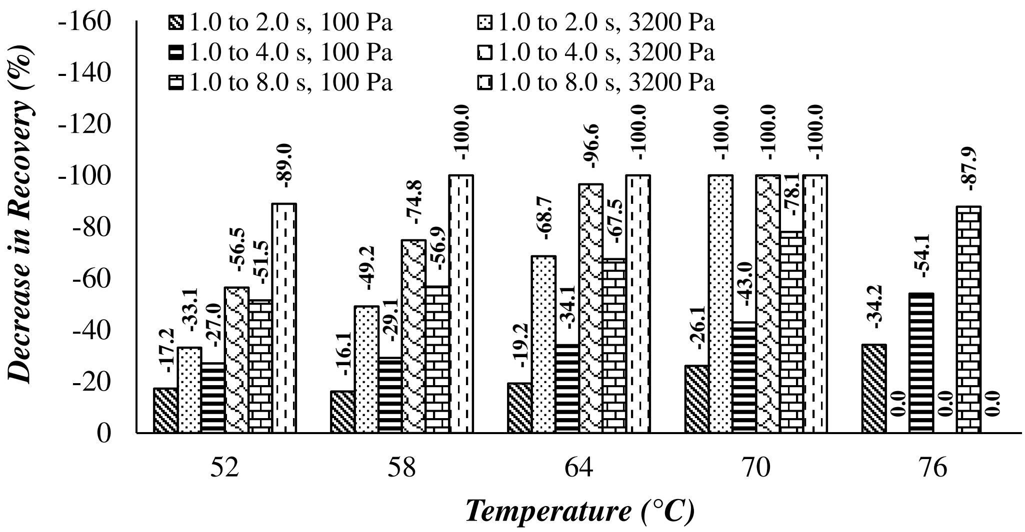

Figure 93 – Percentages of decrease in the recoveries of the AC+rubber with creep time, temperature and stress level

The nonrecoverable compliances of the AC+rubber in all MSCR test conditions are shown in Table 106, whereas the variations in the J_{nr} values with loading time and temperature are reported in Figure 94. This formulation has a special characteristic that has not been clearly seen for the AC+PPA and the AC+Elvaloy+PPA, i. e., the percentages of increase in J_{nr} are generally lower than the corresponding ones in the creep time up to t_F = 4.0 s (either at 100 or at 3,200 Pa) and the opposite is observed for t_F = 8.0 s. In other words, the material becomes highly susceptible to rutting and its nonlinear response is probably more visible for loading times longer than 4.0 s. This can also be implied by evaluating the percent recovery data (Table 105), i. e., the decreases in recovery at the stress level of 100 Pa are much more pronounced for t_F = 8.0 s and the recoveries are null at temperatures higher than 52°C, loading time of 8.0 s, and stress level of 3,200 Pa. In numerical terms, the J_{nr} values vary from 0.05 to 15.33 kPa^{-1} at 100 Pa and from 0.12 to 41.98 kPa^{-1} at 3,200 Pa. The limiting J_{nr} value of 4.0 kPa^{-1} for assigning a traffic level is easily overcome at the temperatures of 70 and 76°C, either at practically all the creep times at 3,200 Pa or the very long creep times (4.0 and 8.0 s) at 100 Pa.

Table 106 – Nonrecoverable compliances at 100 Pa ($J_{nr}100$) and 3,200 Pa (J_{nr} *3200*) for the AC+rubber with increasing loading time and temperature

parameter	creep time (s)	results at each temperature (kPa^{-1}) , J_{nr} > 4.0 kPa^{-1} is in bold				
		52°C	58°C	64°C	70°C	76°C
$J_{nr}100$	1.0	0.051	0.146	0.364	0.875	1.940
	2.0	0.125	0.317	0.782	1.874	**4.179**
	4.0	0.207	0.530	1.268	2.983	**6.591**
	8.0	0.596	1.497	3.685	**8.641**	**19.127**
$J_{nr}3200$	1.0	0.124	0.356	0.948	2.237	**4.695**
	2.0	0.261	0.750	1.934	**4.418**	**9.161**
	4.0	0.452	1.276	3.202	**7.228**	**15.325**
	8.0	1.279	3.435	**8.429**	**19.354**	**41.972**

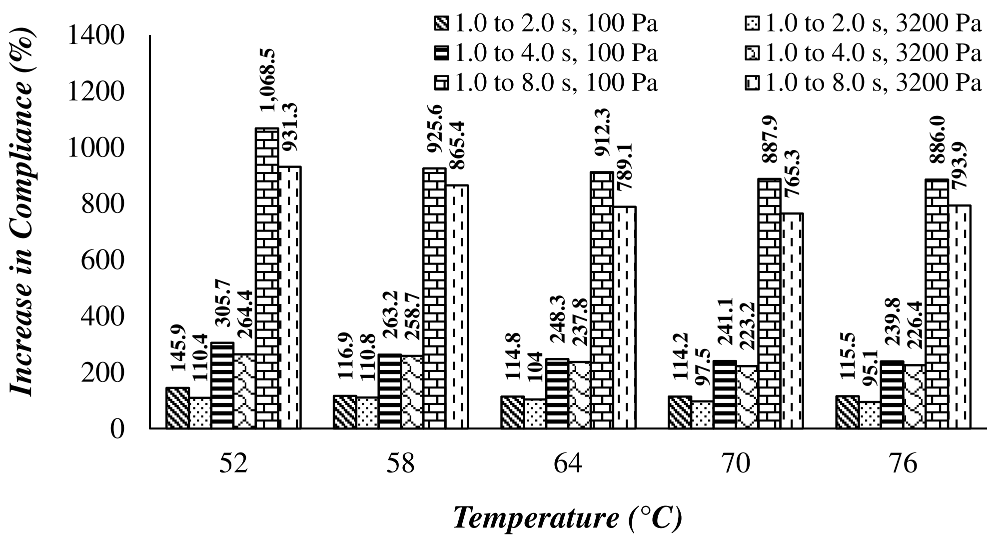

Figure 94 – Percentages of increase in the nonrecoverable compliances of the AC+rubber with creep time, temperature and stress level

A careful analysis of the percentages of increase in J_{nr} from one stress level to the other and a particular creep time (Figure 94 – for instance, from 263.2% at t_F = 4.0 s, 100 Pa and 58°C to 258.7% at the same temperature and loading time, but the applied stress of 3,200 Pa) may lead to the conclusion that, for some pavement temperatures, this is not a key factor in the increase in the stress sensitivity of the binder. This can also be observed by evaluating the $J_{nr,\ diff}$ values in Table 107, i. e., they do not greatly change from one loading time to the other when the temperature is equal to 58 and 64°C. In addition, the presence of $J_{nr,\ diff}$ values always higher than 100% clearly demonstrates that the AC+rubber is an overly stress sensitive material, similarly to what was pointed out elsewhere (DOMINGOS and FAXINA, 2016; KATAWARE and SINGH, 2015; TEYMOURPOUR et al., 2016).

Table 107 – Percent differences in nonrecoverable compliances ($J_{nr,\ diff}$) for the AC+rubber with increasing creep time and temperature

creep time	$J_{nr,\ diff}$ values (%) at each creep time and temperature[a]				
(s)	52°C	58°C	64°C	70°C	76°C
1.0	**143.1**	**143.8**	**160.4**	**155.7**	**142.0**
2.0	**107.9**	**136.9**	**147.3**	**135.8**	**119.2**
4.0	**118.3**	**140.7**	**152.5**	**142.3**	**132.5**
8.0	**114.5**	**129.5**	**128.7**	**124.0**	**119.4**

[a] the numbers in bold are the ones that exceeded the maximum $J_{nr,\ diff}$ (75%) according to Superpave®.

One favorable comment on the stress sensitivity of the AC+rubber is that it typically decreases with increasing loading time, that is, the differences between the J_{nr} values at 100 and 3,200 Pa get smaller at longer loading times. This pattern of behavior could also be observed for the AC+Elvaloy+PPA at 52 and 58°C (Table 93) and the crumb rubber-modified binder studied by Kataware and Singh (2015). However, such decreases were not enough to rank the material as with acceptable stress sensitivity ($J_{nr,\ diff} < 75\%$), and this may imply that potentially great rut depths may be observed in the field pavement if the loading conditions fall outside of the designed values. The mixture data reported in Chapter 5 specifically indicate that the crumb rubber-modified asphalt binder may have an excellent rut performance, provided that the pavement/test conditions do not lead to J_{nr} values that cause premature failure. There are some conflicting opinions about the actual stress level applied in the binder under loading of a mixture sample (ARSHADI, 2013; DELGADILLO et al., 2006a, 2006b; KOSE et al., 2000). Therefore, it can be said that $J_{nr,\ diff}$ is an essential requirement for preventing the formation of rutting in the asphalt mixture, but it cannot be analyzed separately.

Table 108 summarizes the appropriate traffic levels for each loading time and temperature. The marked increases in $J_{nr}3200$ shown above indicate that the ability of the AC+rubber in dealing with heavier levels is seriously compromised. As an example, the adequate traffic level at 52°C decreases by two grades – from extremely heavy to heavy – when the loading time is doubled from 4.0 to 8.0 s. The decrease is equal to one level at 58°C (from heavy to standard) and 64°C (from standard to no appropriate level) in these same loading conditions. The binder cannot be used not even on pavements with standard levels when the temperature is equal to

76°C and, by decreasing this temperature to 70°C, the binder may be placed only on pavements with standardized traffic levels and loading-unloading times. The same can be said for the longest creep time (8.0 s) at 58°C and the loading-unloading times of 4/9 s at 64°C. This table resembles the one of the AC+PPA (Table 77) except for a little bit lower traffic levels for the AC+rubber at 64 and 70°C.

Table 108 – Adequate traffic levels for the AC+rubber with increasing creep time and temperature based on the standardized Superpave® criteria

creep time (s)	traffic levels for each temperature[a]				
	52°C	58°C	64°C	70°C	76°C
1.0	E	E	V	S	-
2.0	E	V	H	-	-
4.0	E	H	S	-	-
8.0	H	S	-	-	-

[a] S = standard; H = heavy; V = very heavy; E = extremely heavy.

Table 109 shows the correlations between the calculated $J_{nr}3200$ values for the AC+rubber and the estimated traffic speeds from Huang (2004) and Pereira et al. (1998, 2000). One more time, the R^2 values are very similar between the two equations and for a particular test temperature, with exception of the slope of the curve – higher for the equation from Pereira et al. (1998). This is caused by the higher differences in the calculated speeds at shorter creep times (1.0 and 2.0 s), and such differences become smaller at 4.0 and 8.0 s (the points are almost coincident). The coefficients R^2 range from 0.85 to 0.90 for all the MSCR testing temperatures and, similarly to what was identified in the charts from the AC+ PPA, the nonlinear response of the material at longer creep times may have contributed to the decreases in R^2 when compared with the AC+Elvaloy+PPA. The correlations are better at the temperatures of 58 and 64°C and a little bit worse at the remaining ones (52, 70 and 76°C).

Other than highlighting the similar R^2 values for the modified equation from Huang (2004) when compared with the original values (r = 6 in), Table 109 also indicates that the use of the suggesting expression from Pereira et al. (2000) may yield higher correlations with binder data (almost equal to 1.00). On the other hand, it should be noted that such linear equation may not be the best alternative to simulate the changes in the actual traffic speeds, as will be shown later in this dissertation.

The comparisons between the actual and predicted levels for the AC+rubber are summarized in Table 110 for the equations by Huang (2004) – tire contact radius of 6 in – and Pereira et al. (2000), as well as in Table 111 for the ones from Huang (2004) – tire contact radius of 3.68 in – and Pereira et al. (1998). The linear equation suggested by Pereira et al. (2000) did not yield promising results in the estimation of the actual traffic that the AC+rubber can deal with in the pavement. On the contrary, the ones from Huang (2004) and Pereira et al. (1998) were able to match these actual traffic levels for several loading times and temperatures up to 64°C. The results are slightly better for Pereira et al. (1998) (total of 8 points of similarity), followed by Huang (2004) and regardless of the tire contact radius used in the calculations (total of 7 points of similarity). This gives support to the idea that, as previously observed for the AC+PPA and the AC+Elvaloy+PPA, the selected equations cannot be used in all testing conditions because their ability to estimate the traffic level are restricted to some pavement temperatures (in these cases, no greater than 64°C).

Table 109 – Regression equations and coefficients of determination between the $J_{nr}3200$ values of the AC+rubber and the corresponding vehicle speeds according to the equations by Pereira et al. (1998, 2000) and Huang (2004)

source and data	temperature (in °C)	equation	R^2
Pereira et al. (1998)	52	$y = 1.1198e^{-0.030x}$	0.8667
Pereira et al. (2000)	52	$y = -0.0113x + 0.8579$	0.991
Huang (2004) $r = 6$ in	52	$y = 1.1206e^{-0.036x}$	0.8674
	58	$y = 3.0662e^{-0.035x}$	0.8761
	64	$y = 7.4967e^{-0.034x}$	0.8717
	70	$y = 16.914e^{-0.033x}$	0.8602
	76	$y = 36.293e^{-0.034x}$	0.8543
Huang (2004) $r = 3.68$ in	52	$y = 1.1184e^{-0.058x}$	0.8676
	58	$y = 3.0603e^{-0.057x}$	0.8763
	64	$y = 7.4829e^{-0.055x}$	0.8719
	70	$y = 16.884e^{-0.054x}$	0.8604
	76	$y = 36.227e^{-0.055x}$	0.8546

Table 110 – Comparisons between the actual traffic levels of the AC+rubber and the ones obtained from the equations by Huang (2004) and Pereira et al. (2000)

t_F (s)[d]	actual[a] and estimated[b, c] traffic levels at each temperature[d]				
	52°C	58°C	64°C	70°C	76°C
1.0	**E** (H) **[V/E]**	**E [V/E]**	**V [V/E]**	S [V/E]	-
2.0	**E** (H) **[V/E]**	**V [V/E]**	H [V/E]	-	-
4.0	E (H) [H]	**H [H]**	S [H]	-	-
8.0	**H (H) [H]**	S [H]	-	-	-

[a] S = standard; H = heavy; V = very heavy; E = extremely heavy (AASHTO M320-09 standard, Table 3).
[b] (parentheses) = traffic levels from Pereira et al. (2000).
[c] [brackets] = traffic levels from Huang (2004), $r = 3.68$ in.
[d] similarities among the rankings are highlighted in bold, t_F = creep time.

Table 111 – Comparisons between the actual traffic levels of the AC+rubber and the ones obtained from Huang (2004) and Pereira et al. (1998)

t_F (s)[d]	actual[a] and estimated[b, c] traffic levels at each temperature[d]				
	52°C	58°C	64°C	70°C	76°C
1.0	**E (V/E) [V/E]**	**E [V/E]**	**V [V/E]**	S [V/E]	-
2.0	**E (V/E) [V/E]**	**V [V/E]**	H [V/E]	-	-
4.0	E (H) [H]	**H [H]**	S [H]	-	-
8.0	**H** (S) **[H]**	S [H]	-	-	-

[a] S = standard; H = heavy; V = very heavy; E = extremely heavy (AASHTO M320-09 standard, Table 3).
[b] (parentheses) = traffic levels from Pereira et al. (1998).
[c] [brackets] = traffic levels from Huang (2004), $r = 6$ in.
[d] similarities among the rankings are highlighted in bold, t_F = creep time.

It can be inferred from the MSCR testing data of the AC+rubber that its degree of nonlinearity is more pronounced when t_F is higher than 4.0 s, and this is particularly visible in the results of the parameter J_{nr}. In terms of $J_{nr,\ diff}$, the material can be interpreted as an overly stress sensitive formulation because the results are higher than 100% regardless of the loading and temperature conditions. On the other hand, decreases in $J_{nr,\ diff}$ can be identified at several temperatures (especially at 58 and 64°C) and this is in accordance with other papers from the technical literature – see the one from Kataware and Singh (2015) as an example. With respect to the appropriate traffic levels, the use of the AC+rubber is not recommended on asphalt pavements with maximum expected temperatures of 76°C because not even the standard traffic can be assigned to the material. Finally, the equations from Huang (2004) and Pereira et al. (1998) were the ones that could more closely predict the actual traffic levels of the asphalt binder.

Table 112 provides the numerical values of the parameters/constants of the modified power equation by Saboo and Kumar (2015) within the whole temperature and loading time spectra, and considering the AC+rubber. Initially, it can be said that the high stress sensitivity ($J_{nr,\ diff}$ much higher than 75%) plays a role on the variations in the model parameters and imparts a special characteristic in the response of the material. More specifically, the contribution of nonlinearity (parameter n) to the repeated creep behavior of the AC+rubber when subjected to longer loading times seems to be greater than for the previously reported binders – base binder, AC+PPA and AC+Elvaloy+PPA. This can be implied by analyzing the progressive increases in n with increasing creep time t_F for both stress levels, namely, 100 Pa (temperatures of 52 and 58°C) and 3,200 Pa (temperatures of 64, 70 and 76°C). In other words, the effects of nonlinearity on the drops in R and the increases in J_{nr} must be considered when studying the rutting resistance of the AC+rubber on pavements with relevant percentages of slow-moving vehicles.

Table 112 – Numerical values and variations in the parameters/constants *A, B, n* and *α* from the power law equations by Saboo and Kumar (2015) with increasing temperature and creep time and considering the AC+rubber

temperature	test times	parameter A^a		parameter B^a		parameter n^a		parameter α^a	
		0.1 kPa	3.2 kPa	0.1 kPa	3.2 kPa	0.1 kPa	3.2 kPa	0.1 kPa	3.2 kPa
52°C	1/9 s	0.0219	0.7419	0.7447	0.7902	1.0164	0.9936	0.7569	0.7851
	2/9 s	0.0208 (-4.9)	0.7048 (-5.0)	0.7641 (2.6)	0.8345 (5.6)	1.0215 (0.5)	0.9898 (-0.4)	0.7806 (3.1)	0.8260 (5.2)
	4/9 s	0.0173 (-20.9)	0.5815 (-21.6)	0.7447 (0.0)	0.8547 (8.2)	1.0365 (2.0)	0.9832 (-1.0)	0.7719 (2.0)	0.8404 (7.0)
	8/9 s	0.0195 (-10.8)	0.6468 (-12.8)	0.7923 (6.4)	0.9379 (18.7)	1.0374 (2.1)	0.9896 (-0.4)	0.8219 (8.6)	0.9281 (18.2)
58°C	1/9 s	0.0475	1.6355	0.7931	0.8640	1.0143	0.9929	0.8044	0.8579
	2/9 s	0.0445 (-6.4)	1.5713 (-3.9)	0.8018 (1.1)	0.9157 (6.0)	1.0205 (0.6)	0.9928 (0.0)	0.8183 (1.7)	0.9091 (6.0)
	4/9 s	0.0363 (-23.5)	1.2726 (-22.2)	0.7879 (-0.7)	0.9392 (8.7)	1.0308 (1.6)	0.9919 (-0.1)	0.8122 (1.0)	0.9317 (8.6)
	8/9 s	0.0412 (-13.3)	1.4740 (-9.9)	0.8305 (4.7)	0.9947 (15.1)	1.0266 (1.2)	1.0036 (1.1)	0.8525 (6.0)	0.9982 (16.4)
64°C	1/9 s	0.0977	3.6184	0.8213	0.9317	1.0125	0.9955	0.8316	0.9275
	2/9 s	0.0921 (-5.7)	3.5049 (-3.1)	0.8308 (1.2)	0.9710 (4.2)	1.0158 (0.3)	0.9977 (0.2)	0.8439 (1.5)	0.9688 (4.4)
	4/9 s	0.0730 (-25.3)	2.8013 (-22.6)	0.8197 (-0.2)	0.9881 (6.0)	1.0205 (0.8)	1.0002 (0.5)	0.8365 (0.6)	0.9883 (6.5)
	8/9 s	0.0827 (-15.3)	3.3575 (-7.2)	0.8699 (5.9)	1.0206 (9.5)	1.0112 (-0.1)	1.0111 (1.6)	0.8797 (5.8)	1.0319 (11.2)
70°C	1/9 s	0.1913	7.7706	0.8434	0.9716	1.0088	0.9980	0.8508	0.9696
	2/9 s	0.1802 (-5.8)	7.5826 (-2.4)	0.8581 (1.7)	0.9981 (2.7)	1.0079 (-0.1)	1.0009 (0.3)	0.8649 (1.7)	0.9990 (3.0)
	4/9 s	0.1404 (-26.6)	6.1185 (-21.3)	0.8534 (1.2)	1.0112 (4.1)	1.0082 (-0.1)	1.0048 (0.7)	0.8603 (1.1)	1.0161 (4.8)
	8/9 s	0.1596 (-16.6)	7.3986 (-4.8)	0.9064 (7.5)	1.0324 (6.3)	1.0005 (-0.8)	1.0146 (1.7)	0.9069 (6.6)	1.0475 (8.0)
76°C	1/9 s	0.3563	11.8726	0.8658	0.9813	1.0045	0.9988	0.8697	0.9801
	2/9 s	0.3375 (-5.3)	15.6319 (31.7)	0.8847 (2.2)	1.0109 (3.0)	1.0019 (-0.3)	1.0026 (0.4)	0.8864 (1.9)	1.0136 (3.4)
	4/9 s	0.2591 (-27.3)	12.8081 (7.9)	0.8872 (2.5)	1.0223 (4.2)	0.9988 (-0.6)	1.0072 (0.8)	0.8862 (1.9)	1.0296 (5.1)
	8/9 s	0.3084 (-13.4)	15.6769 (32.0)	0.9424 (8.9)	1.0389 (5.9)	0.9962 (-0.8)	1.0169 (1.8)	0.9388 (7.9)	1.0565 (7.8)

[a] the percentages of variation reported in parenthesis refer to the changes in the parameter when moving from 1.0 s to the creep time into question (2.0, 4.0 or 8.0 s).

Another interesting aspect of the results of the AC+rubber is the presence of a “maximum point” in the *A* values at t_F = 4.0 s and for all the pavement temperatures, which has not been observed for any other parameter so far but may be found in publications from elsewhere (e. g., SARKAR, 2016). However, the parameters *B, n* and α typically show a sharp increase in their numerical values when t_F is changed from 4.0 to 8.0 s. In practical terms, this suggests that the initial strain further contributes to the increases in the total strain in the binder when the creep time is very long, which was not the case of the AC+Elvaloy+PPA (Table 98), the AC+PPA (Table 83) and the original material (Table 70). This is probably one of the reasons why the J_{nr} values of the AC+rubber show a kind of exponential increase when moving from t_F = 4.0 s to t_F = 8.0 s (see Table 106), especially at 3,200 Pa, and the absence of recovery is not an uncommon situation: not only the binder accumulates strain at higher rates (higher *B* values) in such critical loading conditions; rather, the initial strains also increase (the rates of decrease in *A* are reduced) and nonlinearity has a more notable contribution to the strain response in the MSCR test (much higher *n* values).

In a more in-depth discussion about the *A* and α values, a comparison between the data reported in Table 105 and Table 112 reveals that null recoveries are commonly associated with results higher than one for α. This has been noticed for the 50/70 original binder as well, and it may be linked to the paper from Saboo and Kumar (2015) in that very small or total absence of recovery can be translated into α values approaching unity. The consistent increases in this parameter with loading time, temperature and stress level were expected, and the presence of values no greater than 0.94 at 100 Pa are reflected on the positive results for *R* in all cases (all between 5.0 and 76%). Finally, the identification of *A* values much greater than 1.0 at temperatures at least equal to 64°C and the stress level of 3,200 Pa points to the existence of a high susceptibility to rutting, which may also be inferred from the J_{nr} values of the binder (typically higher than 3.0 kPa^{-1}).

Figure 95 and Figure 96 show the levels of linear correlation between the *A* and *B* values and the creep time t_F at 64°C and the stress levels of 100 and 3,200 Pa, respectively. The quite poor correlations for the constant *A* (R^2 no greater than 0.36) indicate that nonlinearity somehow affected the responses of the asphalt binder, as previously seen in the AC+PPA. The reductions in R^2 with increasing stress level also point to the role of nonlinearity on these results for *A* and *B*. The data points for t_F = 4.0 s and the constant *A* are precisely the ones located far from the regression trendlines, i. e., they look like outliers in the data sets. Although the correlations for the parameter *B* are much higher than the corresponding ones for *A*, they still depict some effects of nonlinearity on the behavior of the binder (for instance, they are lower than the correlations obtained for the AC+Elvaloy+PPA). However, the overall behavior for both parameters is similar to the one reported by the previously studied binders, i. e., decreases in *A* and increases in *B* when the inputs of the MSCR tests (temperature, loading time and stress level) are more critical.

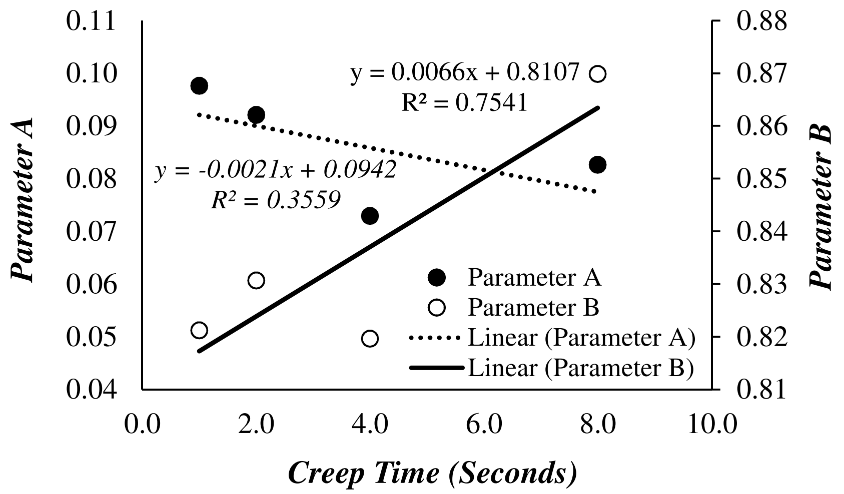

Figure 95 – Correlations between the creep time and the constants *A* and *B* from the model by Saboo and Kumar (2015), temperature of 64°C and stress level of 100 Pa – AC+rubber

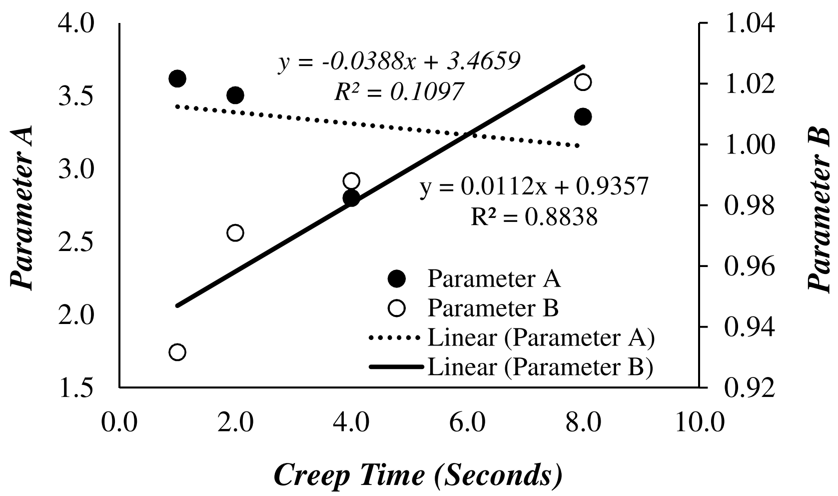

Figure 96 – Correlations between the creep time and the constants *A* and *B* from the model by Saboo and Kumar (2015), temperature of 64°C and stress level of 3,200 Pa – AC+rubber

By moving to a higher pavement temperature (70°C, Figure 97 and Figure 98), one may see that the coefficient of determination is very small for the parameter *A* and the stress level of 3,200 Pa (R^2 lower than 0.1) and the one at 100 Pa showed almost no change (from 0.36 to 0.37). With respect to the constant *B*, the correlation is better at 100 Pa (from 0.75 to almost 0.88) and the ones at 3,200 Pa are identical (0.884 and 0.882). In terms of the variations in both parameters from one temperature to the other, the *B* values decrease at a faster rate at 70°C and 100 Pa –

higher slope of the regression trendline – than at 64°C and 100 Pa, and the opposite is observed at 3,200 Pa. Differently from the constant *B*, the *A* values show a faster decrease with loading time from 64 to 70°C either at the highest stress level (from about 0.039 to 0.058) or the lowest one (from 0.0021 to 0.0044). It is believed that the higher percentages of increase for *n* at 70°C and 3,200 Pa than at 64°C compensated for the reductions in such percentages for *B*. Since the parameter J_{nr} considerably increases when t_F is equal to 4.0 and 8.0 s (and this is also reflected on the variations in the parameters/constants of the model), it can be implied that the loading time of 4.0 s is a boundary value for the use of the AC+rubber on pavements.

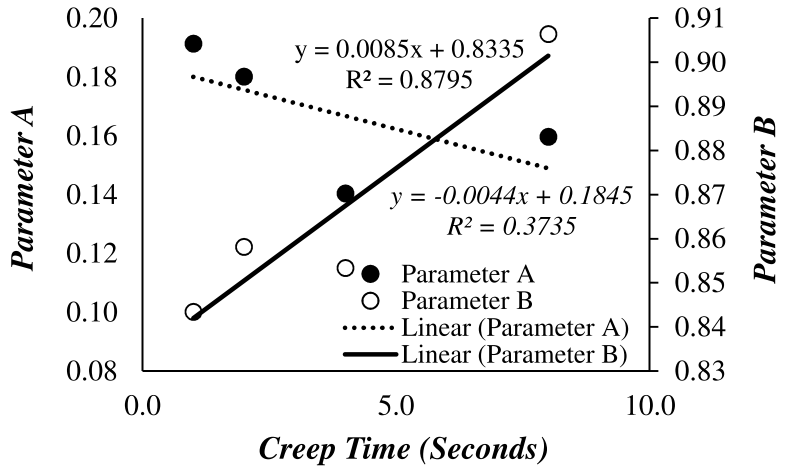

Figure 97 – Correlations between the creep time and the constants *A* and *B* from the model by Saboo and Kumar (2015), temperature of 70°C and stress level of 100 Pa – AC+rubber

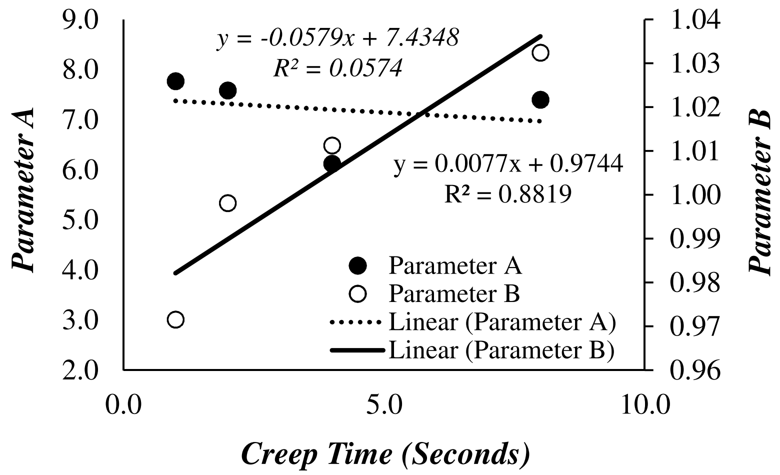

Figure 98 – Correlations between the creep time and the constants *A* and *B* from the model by Saboo and Kumar (2015), temperature of 70°C and stress level of 3,200 Pa – AC+rubber

In order to investigate whether the degrees of correlation reported above would remain consistent throughout the selected pavement temperatures, Table 113 was prepared to depict the regression equations, the corresponding slopes and intercepts and the R^2 values for *A* and *B*. It can be observed that the resulting equations for *A* show poor correlations with the loading time (R^2 is no greater than 0.38) throughout the MSCR temperature and stress conditions. There is even a reverse in the signal of the gradient of the trendline (from negative to positive) at 76°C and 3,200 Pa, and this may be attributed to the above-mentioned exponential increase in the rutting potential of the AC+rubber when t_F goes from 4.0 to 8.0 s. On the other hand, the equations for *B* show reasonable to excellent correlations (R^2 between 0.65 and 0.98) and this parameter seems to be less sensitive to changes in the creep-recovery response of the material than the other one (e. g., there are no reverses in the signal of the slope of the regression equation). The increases in the numerical values of the constants of these equations – especially for *A* – are somehow masked by the decreases in R^2, which makes it difficult to interpret the exact role of the initial strain and the strain rate on the rutting resistance of the binder.

Table 113 – Degrees of correlation between the parameters *A* and *B* (modified power model) and the creep time t_F for the AC+rubber

T (°C)	stress (kPa)	linear regression equations and R^2 values (in parenthesis)[a, b]	
		parameter *A*	parameter *B*
52	0.1	y = -0.0003x + 0.0211 (0.2594)	y = 0.0058x + 0.7395 (0.6478)
	3.2	y = -0.0132x + 0.7182 (0.3394)	y = 0.0197x + 0.7805 (0.9710)
58	0.1	y = -0.0008x + 0.0456 (0.2977)	y = 0.0049x + 0.7848 (0.6518)
	3.2	y = -0.0231x + 1.5751 (0.2042)	y = 0.0168x + 0.8653 (0.9230)
64	0.1	y = -0.0021x + 0.0942 (0.3559)	y = 0.0066x + 0.8107 (0.7541)
	3.2	y = -0.0388x + 3.4659 (0.1097)	y = 0.0112x + 0.9357 (0.8838)
70	0.1	y = -0.0044x + 0.1845 (0.3735)	y = 0.0085x + 0.8335 (0.8795)
	3.2	y = 0.0579x + 7.4348 (0.0574)	y = 0.0077x + 0.9744 (0.8819)
76	0.1	y = -0.0068x + 0.3408 (0.2459)	y = 0.0104x + 0.8562 (0.9446)
	3.2	y = 0.3417x + 12.716 (0.2939)	y = 0.0071x + 0.9869 (0.8142)

[a] the Y-axis is associated with the parameter (*A* or *B*), whereas the X-axis is associated with t_F.
[b] changes in the signal of the slope of the regression trendlines are highlighted with a grey-shaded box.

Table 114 provides the correlations between *n* and *α* and the creep time for the AC+rubber. Positive and negative signals for the slopes of the regression equations of the parameter *n* are alternated as the temperature and the stress level increase. This could lead to the idea that nonlinearity does not follow an overall pattern of response under more critical MSCR testing conditions, as pointed out earlier. However, a careful analysis of the data reveals some essential details as follows: (a) the R^2 values are usually very low (< 0.15) for the equations that show negative slopes in their trendlines, especially at the stress level of 100 Pa, whereas the ones with positive slopes are all higher than 0.40; (b) the gradients of these equations with negative values are smaller than 0.0015, which suggests that the reductions in *n* with creep time are merely associated with a mathematical fit and not with an actual phenomenon; and (c) there is not a clear relationship between higher temperatures and higher values for the constants of such equations. In other words, one cannot state that the *n* values really decrease when the pavement temperature and the stress level are higher due to the great variations in the constants and the poor degrees of correlation with actual binder data.

Table 114 – Degrees of correlation between the parameters *n* and *α* (modified power model) and the creep time t_F for the AC+rubber

T (°C)	stress (kPa)	linear regression equations and R^2 values (in parenthesis)[a, b]	
		parameter *n*	parameter *α*
52	0.1	y = 0.0030x + 1.0168 (0.7528)	y = 0.0083x + 0.7517 (0.8520)
	3.2	y = -0.0005x + 0.9907 (0.1053)	y = 0.0191x + 0.7731 (0.9675)
58	0.1	y = 0.0016x + 1.0171 (0.4600)	y = 0.0063x + 0.7981 (0.8542)
	3.2	y = 0.0016x + 0.9894 (0.7780)	y = 0.0183x + 0.8557 (0.9446)
64	0.1	y = -0.0003x + 1.0162 (0.0588)	y = 0.0064x + 0.8239 (0.8289)
	3.2	y = 0.0022x + 0.9929 (0.9793)	y = 0.0134x + 0.9287 (0.9219)
70	0.1	y = -0.0012x + 1.0107 (0.8657)	y = 0.0075x + 0.8426 (0.8791)
	3.2	y = 0.0023x + 0.9958 (0.9979)	y = 0.0101x + 0.9701 (0.9273)
76	0.1	y = -0.0011x + 1.0045 (0.9156)	y = 0.0093x + 0.8602 (0.9259)
	3.2	y = 0.0025x + 0.9969 (0.9947)	y = 0.0097x + 0.9836 (0.8825)

[a] the Y-axis is associated with the parameter (*n* or *α*), whereas the X-axis is associated with t_F.
[b] changes in the signal of the slope of the regression trendlines are highlighted with a grey-shaded box.

Although the equations of *n* with positive constants do not show a clear relationship between the numerical values of these constants and the increasing severity in the MSCR tests either, the presence of only regular to excellent correlations (no lower than 0.46) point to a more reasonable certainty about the effect of nonlinearity on the repeated creep behavior of the binder at 3,200 Pa. However, it must be important to remind that the levels of nonlinearity observed in the AC+rubber are probably small when compared with other studies that considered much higher stresses and creep times in the binder tests (e. g., DELGADILLO and BAHIA, 2010; DELGADILLO et al., 2012; JAFARI and BABAZADEH, 2016; JAFARI et al., 2015; SABOO and KUMAR, 2015). Hence, it can be postulated that the nonlinear behavior has a more visible role on the outputs of the MSCR tests at 3,200 Pa, and also that this influence seems to be higher for the AC+rubber than for the 50/70 base binder, the AC+PPA and the AC+Elvaloy+PPA. This may be confirmed by the good correlation ($R^2 \approx 0.78$) between *n* and the nonrecoverable compliance at 3,200 Pa (i. e., $J_{nr}3200$) in a semi-log scale, Figure 99.

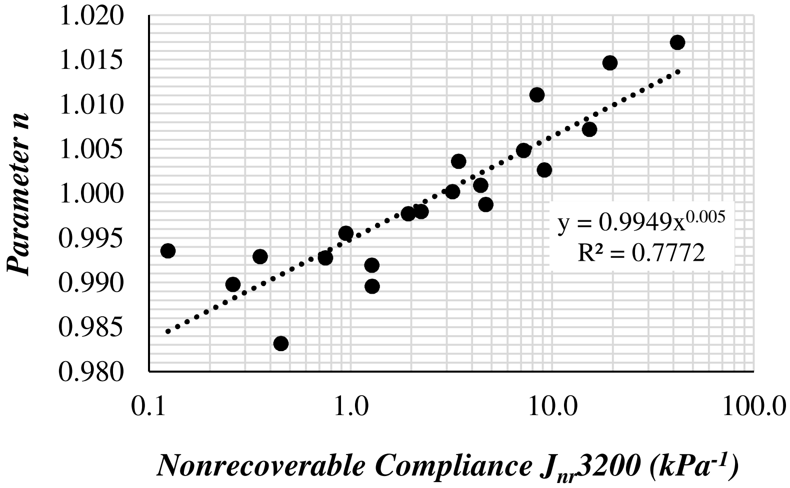

Figure 99 – Degree of correlation between the nonrecoverable compliances of the AC+rubber at the stress level of 3,200 Pa and the corresponding *n* values from the power law models

With respect to the parameter *α*, the equations shown in Table 114 point to a tendency of increasing values for this parameter with increasing temperature and magnitude of the stress level, as previously observed for other formulations. This is even more highlighted by an evaluation of the results of the intercepts of the regression equations – i. e., they constantly increase with increasing severity of the tests – and the promising values for R^2 (always greater than 0.82). Therefore, one may expect that the plot of *α* values against *R100* and *R3200* values will yield a high correlation as well. As shown in Figure 100, this expectation is met because the R^2 value is approximately equal to 0.82 – which is very close to the correlation found in the AC+PPA – and the inverse relationship between *α* and percent recovery (i. e., higher *α* values lead to lower *R* values and vice versa) is also observed.

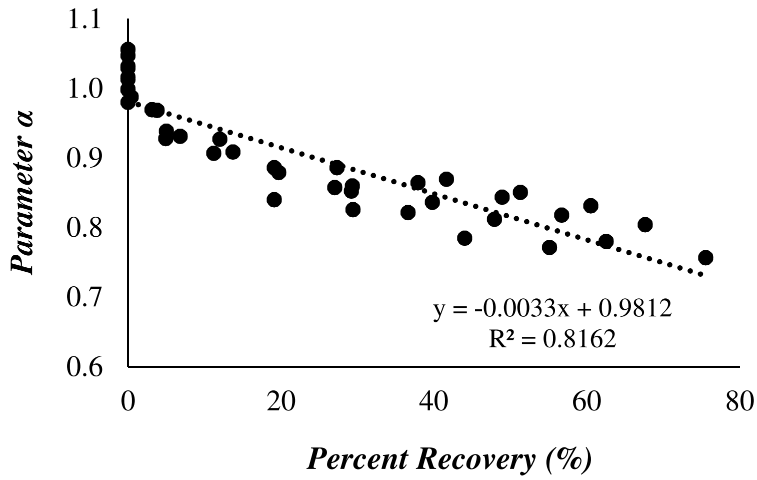

Figure 100 – Degree of correlation between the percent recoveries of the AC+rubber and the corresponding *α* values from the power law models

By taking the starting point of 52°C and 1/9 s and the percent recovery values as a reference, it can be seen that only one null *R3200* value is found in the data set (76°C and 1/9 s, Table 105). When the *R100* values are taken into account, one may observe that none of these values are equal to zero (the lowest one at 76°C and 1/9 s is equal to 41.6%). Therefore, the ANOVA analysis may be conducted either for the percent recovery or the nonrecoverable compliance data. Table 115 provides the organized *R100* and *R3200* values, and Table 116 shows the organized $J_{nr}100$ and $J_{nr}3200$ values.

Table 115 – Rearranged MSCR testing data of the AC+rubber to be used in the analysis of variance (ANOVA) – percent recovery

stress level of 0.1 kPa (*R100*, %)[a]		stress level of 3.2 kPa (*R3200*, %)[a]	
increasing creep time	increasing temperature	increasing creep time	increasing temperature
75.5	75.5	44.0	44.0
62.5	67.6	29.4	27.0
55.1	60.5	19.1	12.0
36.6	51.3	4.9	3.1
N/A[b]	41.6	N/A[b]	N/A[b]

[a] the starting point in both cases was the temperature of 52°C.
[b] N/A: Not applicable.

Table 116 – Rearranged MSCR testing data of the AC+rubber to be used in the analysis of variance (ANOVA) – nonrecoverable creep compliance

stress level of 0.1 kPa ($J_{nr}100$, kPa^{-1})[a]		stress level of 3.2 kPa ($J_{nr}3200$, kPa^{-1})[a]	
increasing creep time	increasing temperature	increasing creep time	increasing temperature
0.051	0.051	0.124	0.124
0.125	0.146	0.261	0.356
0.207	0.364	0.452	0.948
0.596	0.875	1.279	2.237
N/A[b]	1.940	N/A[b]	4.695

[a] the starting point in both cases was the temperature of 52°C.
[b] N/A: Not applicable.

Table 117 reports the outcomes of the ANOVA analysis on the percent recoveries of the AC+rubber. There is a strong possibility of both groups of *R100* values to belong to the same original group, since the *p-value* is about 17 times higher than α and the *F-value* is less than 1% of $F_{critical}$. In other words, the differences between the effects of temperature and creep time on the elastic response of the binder at 100 Pa are not clear as based on the statistical data collected by ANOVA. The same can be applied to the *R3200* values, that is, the *p-value* is only 3.6% lower than the one obtained at 100 Pa and the *F-value* is approximately 33% higher than the one obtained at the lowest stress level. In other words, the *R3200* values collected after variations in the creep time and the test temperature can also be considered as derived from a common group of data values, which are supposed to be representative of the elastic behavior of the AC+rubber. What can be pointed out is that temperature has a greater influence on the elastic response of the asphalt binder than the creep time at 3,200 Pa (*R3200* values vary at faster rates with increasing temperature than with increasing loading time) and that the tendency is reversed at 100 Pa; however, this is not enough to say that the data values are statistically different.

Table 117 – Results from the analysis of variance (ANOVA, *p-value* and *F-value*) as based on the percent recoveries of the AC+rubber

null hypothesis H_0	statistical parameters (ANOVA)				recommendation
	$F_{critical}$	*F-value*	α	*p-value*	
equivalency between *R* values with increasing creep time and temperature, 0.1 kPa	5.5914	0.036	0.05	0.8540	H_0 is not rejected
equivalency between *R* values with increasing creep time and temperature, 3.2 kPa	5.9874	0.054	0.05	0.8244	H_0 is not rejected

When moving from the percent recovery to the nonrecoverable compliance (Table 118), one may see that the variations in the J_{nr} values are much higher than the corresponding ones in *R*, either at 100 or at 3,200 Pa. This can be translated into *F-values* approaching 1.40 and *p-values* around 0.30, whereas the corresponding values for the percent recovery barely exceed 0.05 and are all higher than 0.80, respectively. Even with such greater variabilities, the null hypothesis is not rejected in any case because the limiting requirements ($F_{critical}$ and α) are complied. Again, temperature has a higher impact on the results of the AC+rubber in the MSCR tests because the J_{nr} values increase at faster rates with increasing temperature than with increasing loading time, see Table 116 for further details.

Table 118 – Results from the analysis of variance (ANOVA, *p-value* and *F-value*) as based on the nonrecoverable compliances of the AC+rubber

null hypothesis H_0	statistical parameters (ANOVA)				recommendation
	$F_{critical}$	*F-value*	α	*p-value*	
equivalency between J_{nr} values with increasing creep time and temperature, 0.1 kPa	5.5914	1.1159	0.05	0.3258	H_0 is not rejected
equivalency between J_{nr} values with increasing creep time and temperature, 3.2 kPa	5.5914	1.3626	0.05	0.2813	H_0 is not rejected

In summary, it can be suggested that nonlinearity plays a more significant role on the creep-recovery behavior of the AC+rubber when compared with the previously studied binders, especially at 3,200 Pa. In practical terms, this can be translated into a good correlation between the parameter *n* from the model by Saboo and Kumar (2015) and the $J_{nr}3200$ values at all pavement temperatures and loading times. On the other hand, it is not clear that more severe loading conditions will reduce the contribution of the initial strain (constant *A*) to the formation of rutting in the binder, since the R^2 values are all lower than 0.38 (correlations are poor). This particular behavior of the constant *A* may be due to a kind of exponential increase in the susceptibility of the AC+rubber when t_F goes from 4.0 to 8.0 s (t_F = 4.0 s seems to be an outlier within the data sets of *A*). However, the results indicate that the *B* values (i. e., strain rates) increase when the temperature and the creep time are higher in the MSCR tests. Finally, the statistical investigations (ANOVA) indicated that the effects of temperature and creep time on the *R* and J_{nr} can be considered as similar under a level of significance of 5%, even though temperature has a more prominent influence on the outcomes of J_{nr} than the creep time.

The percent recovery values of the AC+rubber+PPA are summarized in Table 119, and the percentages of decrease in this parameter with creep time and temperature are provided in Figure 101. It is clear that higher temperatures and longer loading times have a greater impact on the *R100* and *R3200* values of this material when compared with the original formulation without PPA (AC+rubber, Table 105). In other words, the presence of PPA and the addition of a smaller percentage of crumb rubber produced a formulation that shows lower percent recoveries and greater susceptibility to temperature and loading time, which is not desirable for paving applications. From these comments, it may be inferred that elasticity is mainly provided by the crumb rubber particle sizes, and also that the replacement of part of the rubber content by PPA did not yield similar recoveries for the modified asphalt binder. Other authors (BAUMGARDNER and D'ANGELO, 2012) also reported increases in the percent recovery of the binder with increasing rubber content.

As some representative examples of the results of the AC+rubber+PPA, the *R3200* values are typically null at temperatures of 64°C and higher despite the PG grade of 76-xx. The same can be said for the temperature of 76°C and the lowest stress level (parameter *R100*), i. e., the values are null for loading times of 4.0 and 8.0 s. The magnitudes of *R100* and *R3200* are no greater than 47 and 36% for the two stress levels, respectively. It can also be seen that an increase in the stress level from 100 to 3,200 Pa may lead to a reduction in the recovery values from 30% to more than 100% depending on the temperature. For example, the recoveries at 100 Pa and 64°C decrease by 28.6% when the loading time is changed from 1.0 to 2.0 s. By increasing the stress level to 3,200 Pa and keeping the other input parameters unchanged, this reduction boosts to nearly 91% (an increase by more than 2,000%). Although the percent recovery is not a criterion for the selection of binders on Superpave®, it may be anticipated here that the rutting performances of the AC+rubber+PPA are not as satisfactory as the ones of the AC+rubber. This will be further discussed later in the current section.

Table 119 – Percent recoveries at 100 Pa (*R100*) and 3,200 Pa (*R3200*) for the AC+rubber+PPA with increasing loading time and temperature

parameter	creep time (s)	results at each temperature (%)				
		52°C	58°C	64°C	70°C	76°C
R100	1.0	46.9	39.2	29.5	21.1	13.4
	2.0	37.4	29.4	21.0	12.9	6.6
	4.0	24.9	16.6	8.7	3.0	0.0
	8.0	15.5	8.2	3.0	0.0	0.0
R3200	1.0	35.9	20.6	7.2	0.0	0.0
	2.0	22.9	9.0	0.7	0.0	0.0
	4.0	9.7	1.1	0.0	0.0	0.0
	8.0	2.3	0.0	0.0	0.0	0.0

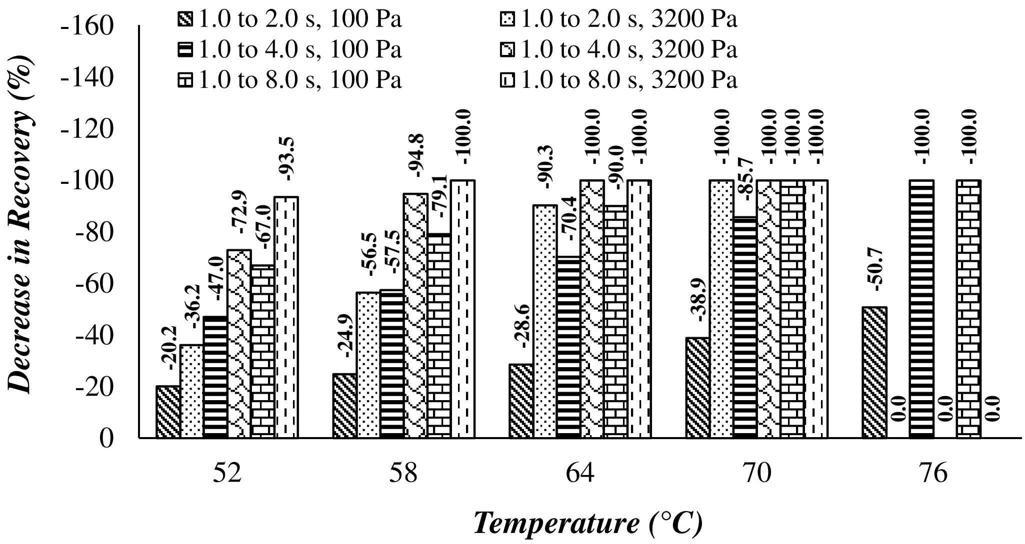

Figure 101 – Percentages of decrease in the recoveries of the AC+rubber+PPA with creep time, temperature and stress level

The nonrecoverable compliance values of the AC+rubber+PPA are all provided in Table 120, whereas Figure 102 depicts the percentages of increase in this parameter as the input variables become more severe. In numerical terms, the compliances range from 0.11 to 34.46 kPa^{-1} at 100 Pa and from 0.13 to 50.65 kPa^{-1} at 3,200 Pa. As a consequence of the marked decreases in *R*, the J_{nr} values of this formulation are higher than the ones of the AC+rubber (Table 106). As previously highlighted in the results of the *R* values, this contributes even more to the idea that the rutting response of the AC+rubber+PPA is not as favorable as the one of the AC+rubber. In addition, the percentages of increase in J_{nr} are typically higher for the AC+rubber+PPA than for the AC+rubber when moving from 1.0 to 4.0 s, either at 100 or at 3,200 Pa and for all the selected temperatures. However, the tendency is reversed for the other creep times (from 1.0 to 2.0 s and from 1.0 to 8.0 s) and the AC+rubber shows higher rates of increase in J_{nr} than the AC+rubber+PPA. These observations can be made by comparing the data shown in Figure 102 with the ones shown in Figure 94 (page 245).

Table 120 – Nonrecoverable compliances at 100 Pa ($J_{nr}100$) and 3,200 Pa (J_{nr} *3200*) for the AC+rubber+PPA with increasing loading time and temperature

parameter	creep time (s)	results at each temperature (kPa^{-1}), J_{nr} > 4.0 kPa^{-1} is in bold				
		52°C	58°C	64°C	70°C	76°C
$J_{nr}100$	1.0	0.110	0.283	0.729	1.738	3.888
	2.0	0.220	0.576	1.464	3.519	**7.799**
	4.0	0.503	1.358	3.544	**8.541**	**18.791**
	8.0	0.981	2.665	**6.804**	**16.079**	**34.454**
$J_{nr}3200$	1.0	0.136	0.390	1.069	2.624	**5.645**
	2.0	0.285	0.832	2.209	**5.154**	**11.146**
	4.0	0.672	1.924	**4.883**	**11.510**	**25.359**
	8.0	1.352	3.755	**9.680**	**23.216**	**50.648**

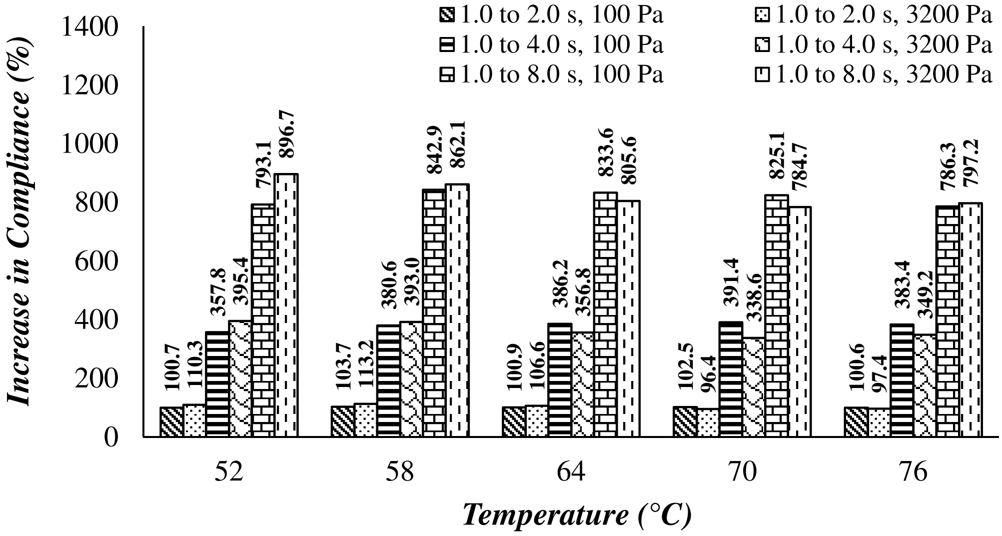

Figure 102 – Percentages of increase in the nonrecoverable compliances of the AC+rubber+PPA with creep time, temperature and stress level

The apparent discrepancy between the patterns of behavior of the AC+rubber and the AC+rubber+PPA may be explained by examining other papers from the literature and considering the nonlinearity and stress sensitivity phenomena. The first reason may be associated with the level of interaction between the rubber particles and the surfaces of the parallel plates of the DSR, whereas the second one is related to the nonlinear response of these particles. Baumgardner and D'Angelo (2012) reported problems while using the parallel plates on binders modified with 10 and 15% of crumb rubber passing through the 20, 30 and 60 mesh sieves. Based on previous versions of standardized testing procedures, Teymourpour et al. (2016) claimed that the parallel plate geometry and the 1-mm gap height should not be used on crumb rubber-modified binders with particle sizes greater than 250 μm. Since the geometry used in this study is the parallel plate one, it is hypothesized that the rubber particles had some influence on the deviations in the responses of the formulations. This hypothesis is somehow corroborated by the smaller deviations in the percentages of the AC+rubber+PPA from one stress level to the other, since the rubber content is smaller in this formulation.

The appropriate traffic levels for the AC+rubber+PPA at all loading times and temperatures are shown in Table 121. As can be seen, these levels are extremely heavy only at 52 and 58°C and the shortest creep times (1.0 and 2.0 s) and the binder is not suitable for any paving application at 76°C and loading times longer than 1.0 s at the temperature of 70°C (i. e., no traffic levels can be assigned). The traffic levels decrease by one grade for each increase in the loading time when the temperature is equal to 58°C: from extremely heavy to very heavy (t_F is doubled from 1.0 to 2.0 s), from very heavy to heavy when t_F goes from 2.0 to 4.0 s, and then from heavy to standard when t_F is again doubled. By comparing these data with the ones of the AC+rubber (Table 108, page 247), it can be observed that the greatest reductions are restricted to the temperatures of 52°C (one grade lower for the AC+rubber+PPA at t_F = 4.0 s) and 64°C (also one grade lower at each of the loading times of 1.0, 2.0 and 4.0 s).

Table 121 – Adequate traffic levels for the AC+rubber+PPA with increasing creep time and temperature based on the standardized Superpave® criteria

creep time (s)	traffic levels for each temperature[a]				
	52°C	58°C	64°C	70°C	76°C
1.0	E	E	H	S	-
2.0	E	V	S	-	-
4.0	V	H	-	-	-
8.0	H	S	-	-	-

[a] S = standard; H = heavy; V = very heavy; E = extremely heavy.

From a practical point of view, the reductions in the traffic levels for the AC+rubber+PPA at 52 and 64°C indicate that the applicability of this formulation on pavements with more slow-moving vehicles or higher numbers of ESAL's is limited. It may be important to note that, depending on the recovery time used in the MSCR tests, the decreases in the traffic level after a twofold increase in the creep time may be of two grades rather than only one. This was seen in the crumb rubber-modified binder studied by Kataware and Singh (2015), in that the material experienced a reduction from "extremely heavy" (E) to "heavy" at 64°C after a change in the loading-unloading times from 1/27 s to 2/27 s. The same was observed for the SBS-modified binder when moving from 1/27 s to 2/27 s at 52 and 64°C in the MSCR tests.

The correlations between $J_{nr}3200$ and traffic speed for each of the selected equations and technical data are depicted in Table 122 (HUANG, 2004; PEREIRA et al., 1998, 2000). These correlations are higher than 0.91 for all the equations and tire contat radii used in the study, as previously observed for the other materials. However, this does not necessarily mean that they will accurately identify the traffic level of the binder based on a given $J_{nr}3200$ value, since many problems could be found in their use for other formulations. The higher gradients in the power equations referring to the radius of 3.68 in (HUANG, 2004) when compared with the radius of 6.0 in simply mean that a shorter range of speed values must be allocated within the interval of $J_{nr}3200$ values, thus leading to a higher slope for the trendline. At the same time, the almost identical regression constants for the equations from Huang (2004) and Pereira et al. (1998) may be attributed to their quite similar structures, i. e., a number in the numerator and the vehicle speed in the denominator. Both observations can be extended to the previously reported asphalt binders as well.

Table 122 – Regression equations and coefficients of determination between the $J_{nr}3200$ values of the AC+rubber+PPA and the corresponding vehicle speeds according to the equations by Pereira et al. (1998, 2000) and Huang (2004)

source and data	temperature (in °C)	equation	R^2
Pereira et al. (1998)	52	$y = 1.3888e^{-0.031x}$	0.9228
Pereira et al. (2000)	52	$y = -0.019x + 1.3394$	0.9964
Huang (2004) *r* = 6 in	52	$y = 1.3896e^{-0.038x}$	0.9231
	58	$y = 3.9167e^{-0.037x}$	0.9299
	64	$y = 9.9012e^{-0.036x}$	0.9245
	70	$y = 23.245e^{-0.036x}$	0.9125
	76	$y = 51.073e^{-0.036x}$	0.9143
Huang (2004) *r* = 3.68 in	52	$y = 1.3867e^{-0.062x}$	0.9233
	58	$y = 3.9088e^{-0.061x}$	0.9302
	64	$y = 9.8819e^{-0.059x}$	0.9247
	70	$y = 23.201e^{-0.058x}$	0.9128
	76	$y = 50.975e^{-0.058x}$	0.9146

A more detailed analysis of these limitations is shown in Table 123, referring to Pereira et al. (1998) and the contact radius of 6.0 in, and Table 124, referring to Pereira et al. (2000) and the contact radius of 3.68 in. Comparisons between the actual and predicted traffic levels are provided in both cases. The results point out to the fact that, similarly to the other studied formulations, the equations have a limited applicability and cannot be used at all pavement temperatures. More specifically, the theoretical-based equation from Huang (2004) and the empirical-based one from Pereira et al. (1998) should be considered only when the maximum expected temperature is no greater than 64°C. This is because the correlations between the predicted and calculated traffic levels are similar for two or more loading times in such temperature conditions, and therefore the equations can predict the average traffic speed and estimate the traffic level in the pavement. With respect to the equation from Pereira et al. (2000), its use is not recommended because the correlations between the actual and estimated traffic levels are very weak.

Table 123 – Comparisons between the actual traffic levels of the AC+rubber+PPA and the ones obtained from Huang (2004) and Pereira et al. (1998)

t_F (s)[d]	actual[a] and estimated[b, c] traffic levels at each temperature[d]				
	52°C	58°C	64°C	70°C	76°C
1.0	**E (V/E) [V/E]**	**E [V/E]**	H [V/E]	S [V/E]	-
2.0	**E (V/E) [V/E]**	**V [V/E]**	S [V/E]	-	-
4.0	V (H) [H]	**H [H]**	-	-	-
8.0	**H** (S) **[H]**	S [H]	-	-	-

[a] S = standard; H = heavy; V = very heavy; E = extremely heavy (AASHTO M320-09 standard, Table 3).
[b] (parentheses) = traffic levels from Pereira et al. (1998).
[c] [brackets] = traffic levels from Huang (2004), $r = 6$ in.
[d] similarities among the rankings are highlighted in bold, t_F = creep time.

Table 124 – Comparisons between the actual traffic levels of the AC+rubber+PPA and the ones obtained from the equations by Huang (2004) and Pereira et al. (2000)

t_F (s)[d]	actual[a] and estimated[b, c] traffic levels at each temperature[d]				
	52°C	58°C	64°C	70°C	76°C
1.0	**E** (H) **[V/E]**	**E [V/E]**	H [V/E]	S [V/E]	-
2.0	**E** (H) **[V/E]**	**V [V/E]**	S [V/E]	-	-
4.0	V (H) [H]	**H [H]**	-	-	-
8.0	**H (H) [H]**	S [H]	-	-	-

[a] S = standard; H = heavy; V = very heavy; E = extremely heavy (AASHTO M320-09 standard, Table 3).
[b] (parentheses) = traffic levels from Pereira et al. (2000).
[c] [brackets] = traffic levels from Huang (2004), $r = 3.68$ in.
[d] similarities among the rankings are highlighted in bold, t_F = creep time.

The classifications of the crumb rubber-modified asphalt binders according to the current and proposed criteria are shown in Table 125 (AC+rubber) and Table 126 (AC+rubber+PPA). There are no differences between these classifications for the AC+rubber, but the current Superpave® criteria give a higher traffic level for the AC+rubber+PPA at 58°C (extremely heavy) when compared with the proposed one (very heavy). This in an indication that, depending on the severity of the loading conditions in the pavement, the formulation with rubber+PPA may depict a higher susceptibility to rutting at 58°C than the Superpave® parameters may suggest. The AC+PPA also depicted a decrease in its traffic grade at 64°C (Table 82, page 214) as shown above, and binders modified with SBS and EVA may have this peculiarity as well (DOMINGOS and FAXINA, 2017). In addition, no traffic levels can be designated for the AC+rubber+PPA at 76°C – neither in the current nor the proposed criteria – due to the very high J_{nr} values in all loading conditions (> 5.0 kPa^{-1}).

Table 125 – Traffic levels of the AC+rubber with increasing loading time and temperature in the current and proposed criteria

temperature (in °C)	No. of required MSCR tests[b]	Superpave® designations (current and new criteria)[a, c]	
		current criterion	new criterion
52	4	**52E-xx**	**52E-xx**
58	4	**58E-xx**	**58E-xx**
64	4	**64V-xx**	**64V-xx**
70	2	**70S-xx**	**70S-xx**
76	1	**76-xx**	**76-xx**

[a] S = standard; H = heavy; V = very heavy; E = extremely heavy (AASHTO M320-09 standard, Table 3).
[b] minimum number of MSCR tests to determine the adequate traffic level in the proposed classification.
[c] similarities among the classifications are highlighted in bold.

Table 126 – Traffic levels of the AC+rubber+PPA with increasing loading time and temperature in the current and proposed criteria

temperature (in °C)	No. of required MSCR tests[b]	Superpave® designations (current and new criteria)[a, c]	
		current criterion	new criterion
52	4	**52E-xx**	**52E-xx**
58	4	58E-xx	58V-xx
64	3	**64H-xx**	**64H-xx**
70	2	**70S-xx**	**70S-xx**
76	1	**76-xx**	**76-xx**

[a] S = standard; H = heavy; V = very heavy; E = extremely heavy (AASHTO M320-09 standard, Table 3).
[b] minimum number of MSCR tests to determine the adequate traffic level in the proposed classification.
[c] similarities among the classifications are highlighted in bold.

The MSCR testing parameters suggest that the AC+rubber+PPA is more susceptible to rutting than the AC+rubber at all loading times and temperatures. The decreases in R are also more pronounced for the AC+rubber+PPA than for the AC+rubber, which indicates that the negative effects of longer loading times on the elastic response of the binder are more apparent for the formulation with rubber+PPA. With respect to the rates of increase in J_{nr} with increasing creep time, they are typically higher for the AC+rubber+PPA only in the transition from 2.0 s to 4.0 s in the loading time (this tendency is reversed under other test conditions). However, the interaction between the parallel plates of the DSR and the rubber particles may adversely affect the study of the creep-recovery response of the crumb rubber-modified binders. This issue has been debated in the literature and, among the possible solutions, some authors have recommended the use of alternative geometries such as cup and bob (BAUMGARDNER and D'ANGELO, 2012) or an increase in the original gap from 1 to 3 mm (TEYMOURPOUR et al., 2016). No differences among the traffic levels obtained from the original and proposed methodologies could be seen in the AC+rubber, but there was a decrease of one grade in the traffic level assigned to the AC+rubber+PPA at 58°C (from extremely heavy to very heavy).

Despite the lower rut resistance of the AC+rubber+PPA, this formulation was able to meet the stress sensitivity requirements of the Superpave® specification in all testing conditions ($J_{nr,\ diff}$ no greater than 75%, see Table 127). These positive findings for $J_{nr,\ diff}$ reinforce the association of the rubber particles with a high stress sensitivity in the binder, since the AC+rubber+PPA utilizes a lower amount of rubber in its composition and the rubber particles show a nonlinear response to shear stress in the DSR due to their complex overall composition. There are no great differences within the $J_{nr,\ diff}$ values for a particular temperature with increasing creep time, and they all range from 23 to 51%. In practical terms, the formulation with crumb rubber and PPA is not expected to show a high rutting potential in the field when unpredicted loading and/or temperature conditions are observed.

Table 127 – Percent differences in nonrecoverable compliances ($J_{nr,\ diff}$) for the AC+rubber+PPA with increasing creep time and temperature

creep time	$J_{nr,\ diff}$ values (%) at each creep time and temperature				
(s)	52°C	58°C	64°C	70°C	76°C
1.0	23.5	38.1	46.7	51.0	45.2
2.0	29.4	44.5	50.9	46.5	42.9
4.0	33.6	41.7	37.8	34.8	35.0
8.0	37.8	40.9	42.3	44.4	47.0

By comparing the $J_{nr,\ diff}$ data of the AC+rubber+PPA with the ones for the AC+PPA (Table 78, page 211), it can be seen that the AC+rubber+PPA shows lower values at temperatures and loading times in which the AC+PPA is typically overly stress sensitive (70 and 76°C and very long loading times). It is not clear as to whether this was caused by any kind of interaction between the rubber particles and PPA, or even if there was a reaction between some components of the crumb rubber and the ones of PPA and the base binder. What can be implied is that the presence of crumb rubber imparts strength and elasticity to the asphalt binder (reduction in J_{nr} and increase in R), but it has the disadvantage of bringing a high stress sensitivity to the formulation. The use of PPA in replacement to a portion of the rubber content may address this issue of stress sensitivity and minimize the negative effects of loading time in the MSCR test; however, it cannot account for all the original stiffness and elasticity properties of the bituminous material without PPA.

Table 128 provides the results of rheological modeling (constants A, B, n and α) of the AC+rubber+PPA in all MSCR testing conditions and according to the model proposed by Saboo and Kumar (2015). The general pattern of behavior is that A decreases and either B or n increase with increasing loading time for a particular pavement temperature. This means that the increase in the susceptibility of the formulation to rutting is derived from a higher strain rate and a higher contribution of nonlinearity to the creep-recovery response of the material. The presence of a kind of "maximum point" for the A values at t_F = 4.0 s are somehow compensated by greater increases in the B and n values at this same creep time when compared with the results at 2.0 s. As discussed earlier, these "maximum points" are not exclusive to the present study because they may be found elsewhere as well (SARKAR, 2016). In addition, the null percent recoveries at 3,200 Pa and temperatures at least equal to 64°C may be associated with α values higher than or equal to one (up to 1.07).

By comparing the n values – i. e., the level of nonlinearity – of the AC+rubber+PPA with the corresponding ones of the AC+rubber, it can be seen that the formulation with crumb rubber alone has a more nonlinear response (higher n values) at 100 Pa and an approximately equivalent degree of nonlinearity at 3,200 Pa. Although it is not very clear that n becomes greater with increasing temperature at 100 Pa, the data at 70 and 76°C and the creep times of 4.0 and 8.0 s suggest that there is threshold at t_F = 4.0 s for identifying a more relevant contribution of nonlinearity to the response of the binder. In terms of the nonrecoverable compliance (Table 120), these are the test conditions under which J_{nr} easily exceeds 16.0 kPa^{-1} and 23.0 kPa^{-1} at 100 and 3,200 Pa, respectively, which makes it innapropriate for paving applications. As a matter of comparison, the nonrecoverable compliances of the AC+rubber at these same temperatures and creep-recovery times barely overcome 8.0 kPa^{-1} (100 Pa) and 19.0 kPa^{-1} (3,200 Pa).

The numerical values of the constants A and B for the AC+rubber and the AC+rubber+PPA are approximately the same at 52 and 58°C and for both stress levels (typically lower than 15%), with only a few exceptions and generally higher for the formulation with rubber+PPA. This was

Table 128 – Numerical values and variations in the parameters/constants *A, B, n* and *α* from the power law equations by Saboo and Kumar (2015) with increasing temperature and creep time and considering the AC+rubber+PPA

temperature	test times	parameter A^a		parameter B^a		parameter n^a		parameter α^a	
		0.1 kPa	3.2 kPa	0.1 kPa	3.2 kPa	0.1 kPa	3.2 kPa	0.1 kPa	3.2 kPa
52°C	1/9 s	0.0219	0.7173	0.8173	0.8366	0.9995	0.9945	0.8169	0.8321
	2/9 s	0.0210 (-3.9)	0.6907 (-3.7)	0.8334 (2.0)	0.8682 (3.8)	1.0003 (0.1)	0.991 (-0.4)	0.8337 (2.1)	0.8604 (3.4)
	4/9 s	0.0216 (-1.3)	0.7109 (-0.9)	0.8643 (5.7)	0.9176 (9.7)	1.001 (0.2)	0.9901 (-0.4)	0.8652 (5.9)	0.9086 (9.2)
	8/9 s	0.0197 (-9.8)	0.6416 (-10.6)	0.8867 (8.5)	0.9595 (14.7)	1.0033 (0.4)	0.9939 (-0.1)	0.8896 (8.9)	0.9537 (14.6)
58°C	1/9 s	0.0494	1.6731	0.8564	0.8993	0.9997	0.9945	0.8561	0.8944
	2/9 s	0.0476 (-3.8)	1.6318 (-2.5)	0.8734 (2.0)	0.9384 (4.3)	1.0000 (0.0)	0.9941 (0.0)	0.8734 (2.0)	0.9329 (4.3)
	4/9 s	0.0499 (0.8)	1.7083 (2.1)	0.9059 (5.8)	0.9798 (8.9)	1.0001 (0.0)	0.9983 (0.4)	0.9060 (5.8)	0.9782 (9.4)
	8/9 s	0.0451 (8.9)	1.5449 (-7.7)	0.9310 (8.7)	1.0086 (12.2)	1.0016 (0.2)	1.0071 (1.3)	0.9325 (8.9)	1.0158 (13.6)
64°C	1/9 s	0.1102	3.9327	0.8959	0.9590	0.9995	0.9974	0.8954	0.9565
	2/9 s	0.1059 (-3.9)	3.8466 (-2.2)	0.9114 (1.7)	0.9867 (2.9)	1.0000 (0.1)	0.9992 (0.2)	0.9114 (1.8)	0.9860 (3.1)
	4/9 s	0.1127 (2.3)	4.1119 (4.6)	0.9447 (5.5)	1.0114 (5.5)	1.0000 (0.1)	1.0047 (0.7)	0.9447 (5.5)	1.0162 (6.2)
	8/9 s	0.1010 (-8.4)	3.7480 (-4.7)	0.9689 (8.2)	1.0296 (7.4)	1.0035 (0.4)	1.0138 (1.6)	0.9723 (8.6)	1.0437 (9.1)
70°C	1/9 s	0.2361	8.9864	0.9257	0.9929	0.9997	0.9999	0.9254	0.9927
	2/9 s	0.2267 (-4.0)	8.8015 (-2.1)	0.9428 (1.8)	1.0081 (1.5)	1.0000 (0.0)	1.0022 (0.2)	0.9428 (1.9)	1.0102 (1.8)
	4/9 s	0.2455 (3.9)	9.5230 (6.0)	0.9751 (5.3)	1.0242 (3.2)	1.0015 (0.2)	1.0076 (0.8)	0.9766 (5.5)	1.0320 (4.0)
	8/9 s	0.2188 (-7.3)	8.7649 (-2.5)	0.9965 (7.7)	1.0383 (4.6)	1.0070 (0.7)	1.0167 (1.7)	1.0035 (8.4)	1.0556 (6.3)
76°C	1/9 s	0.4822	19.3979	0.9501	1.0075	1.0000	1.0012	0.9501	1.0087
	2/9 s	0.4611 (-4.4)	18.9579 (-2.3)	0.9668 (1.8)	1.0173 (1.0)	1.0006 (0.1)	1.0036 (0.2)	0.9674 (1.8)	1.0210 (1.2)
	4/9 s	0.5104 (5.9)	20.8175 (7.3)	0.9973 (5.0)	1.0304 (2.3)	1.0037 (0.4)	1.0092 (0.8)	1.001 (5.4)	1.0398 (3.1)
	8/9 s	0.4517 (-6.3)	18.9057 (-2.5)	1.0156 (6.9)	1.0430 (3.5)	1.0105 (1.1)	1.0186 (1.7)	1.0262 (8.0)	1.0624 (5.3)

[a] the percentages of variation reported in parenthesis refer to the changes in the parameter when moving from 1.0 s to the creep time into question (2.0, 4.0 or 8.0 s).

somehow expected because the AC+rubber+PPA has higher compliances and lower recoveries than the AC+rubber. As the temperature becomes higher in the MSCR tests, the differences between the *A* and *B* values of both formulations also increase and the variations are even more significant for the constant *A* (from 8 to 97%) than for the constant *B* (no greater than 16%). In other words, the great susceptibility of the AC+rubber+PPA to rutting at higher temperatures can be mainly described by higher amounts of initial strain accumulated in the pavement (i. e., phenomenon of densification) followed by higher rates of accumulated strain at each loading cycle.

The above discussion about the variations in the constants of the power model for the AC+rubber and the AC+rubber+PPA can be graphically illustrated by the plots in Figure 103 (constant *A*) and Figure 104 (constant *B*). It is clear that the differences between the constants of the formulations with and without PPA are much greater for *A* than for *B* (higher deviations from the equality line when the constant *A* is evaluated). Again, the initial strain accumulated in the sample is the major factor in the differentiation between the rutting resistances of the AC+rubber and the AC+rubber+PPA.

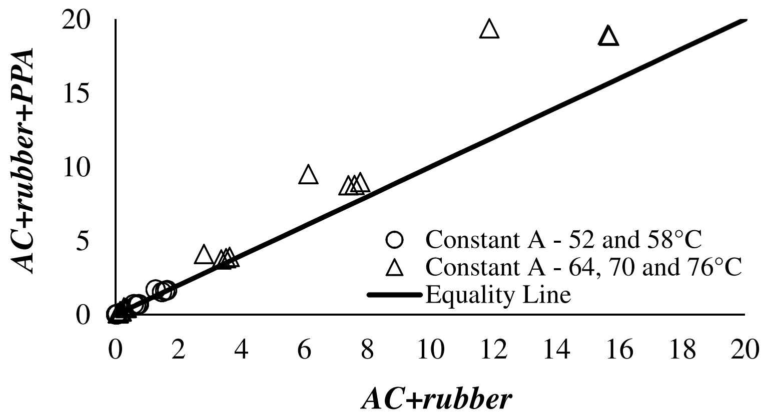

Figure 103 – Graphical comparison between the values of the constant *A* for the AC+rubber and the AC+rubber+PPA at 100 and 3,200 Pa

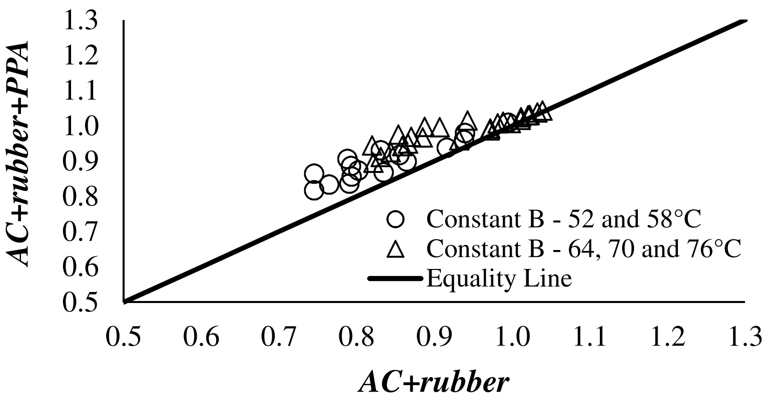

Figure 104 – Graphical comparison between the values of the constant *B* for the AC+rubber and the AC+rubber+PPA at 100 and 3,200 Pa

The variations in the *A* and *B* values of the AC+rubber+PPA with loading time were studied, similarly to what was done for the AC+rubber and the other previously reported materials. Figure 105 shows the levels of correlation between the constants *A* and *B* and the creep time t_F, by considering a stress level of 100 Pa and a pavement temperature of 64°C. Figure 106 shows the same correlations for the same pavement temperature, but considering a stress level of 3,200 Pa. It can be observed that these correlations are similar or better for 100 Pa than for 3,200 Pa, and also that the rate of increase in *B* is about 10 times higher than the rate of decrease in *A* (gradients of the regression equations) at 100 Pa. As previously identified in Table 128, the data points at t_F = 4.0 s seem to be outliers within the groups of values for the constant *A* because they fall quite far from the regression trendlines. Although the corresponding values for *B* also look like an outlier, the tendency of continuously increasing *B* with increasing creep time is maintained in both cases and the resulting correlations are thus better.

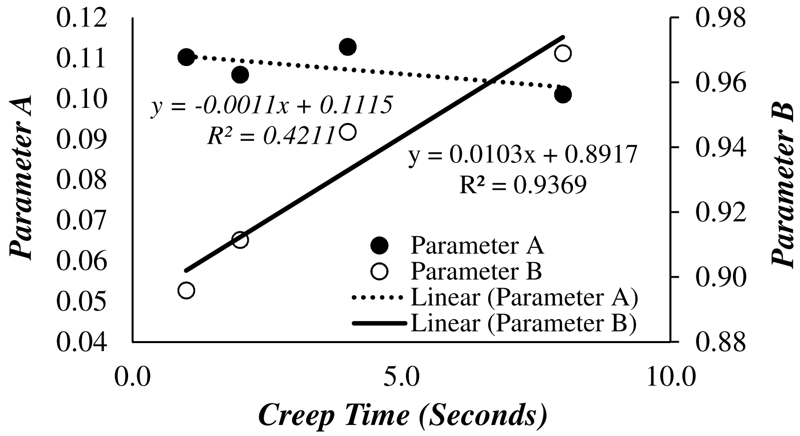

Figure 105 – Correlations between the creep time and the constants *A* and *B* from the model by Saboo and Kumar (2015), temperature of 64°C and stress level of 100 Pa – AC+rubber+PPA

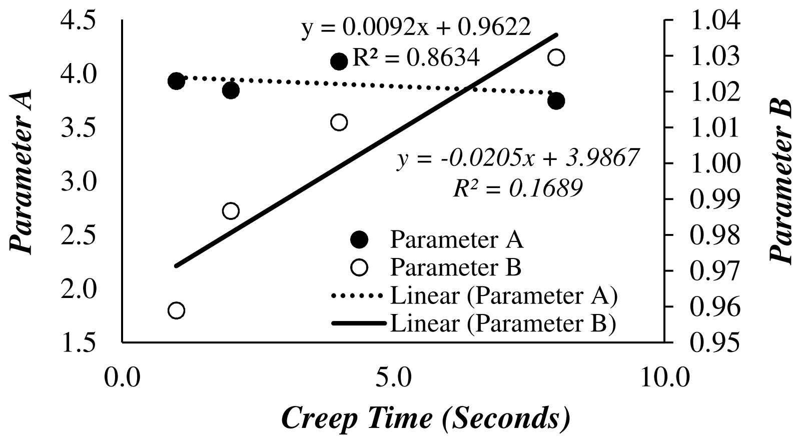

Figure 106 – Correlations between the creep time and the constants *A* and *B* from the model by Saboo and Kumar (2015), temperature of 64°C and stress level of 3,200 Pa – AC+rubber+PPA

When moving to the temperature of 70°C (Figure 107 and Figure 108), one may see that the correlations for the *A* values became much worse at both stress levels (from 0.42 to 0.26 at 100 Pa and from 0.17 to less than 0.1 at 3,200 Pa). The correlations for the *B* values at 70°C are improved at 3,200 Pa and become a little bit worse at 100 Pa. However, the general pattern of behavior remained the same at both temperatures, i. e., the *A* values decrease and the *B* values increase at longer loading times. The gradients of the regression trendlines are generally greater in modulus at 70°C than at 64°C at the lowest stress level (100 Pa), and the opposite is observed at the highest stress level (3,200 Pa). It is believed that the increased percentages of the parameter *n* at 3,200 Pa (see the numerical values at 64°C and 70°C in Table 128) compensated for the reductions in the gradients of variation of *A* and *B* with creep time.

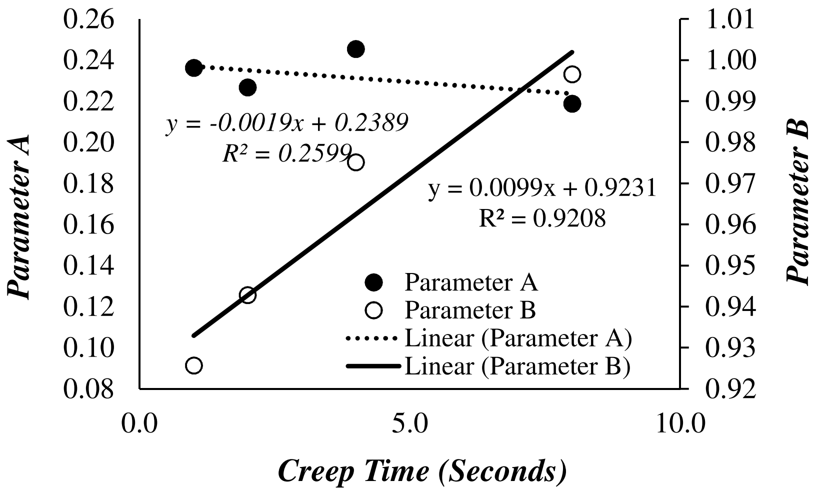

Figure 107 – Correlations between the creep time and the constants *A* and *B* from the model by Saboo and Kumar (2015), temperature of 70°C and stress level of 100 Pa – AC+rubber+PPA

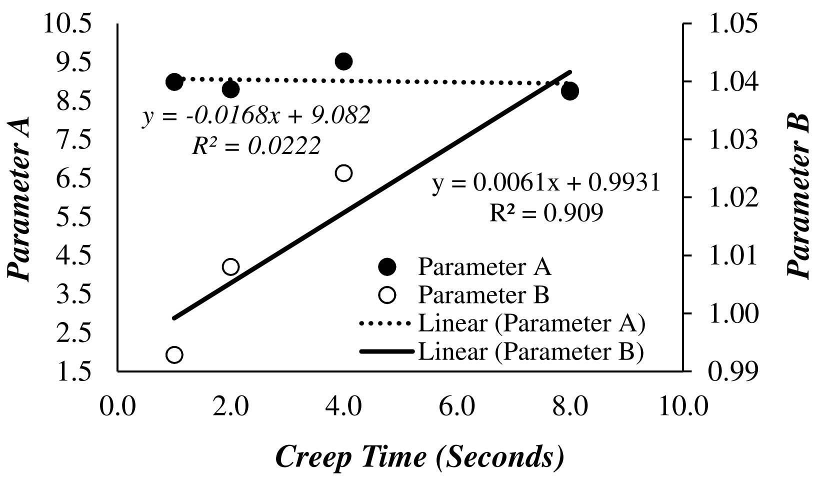

Figure 108 – Correlations between the creep time and the constants *A* and *B* from the model by Saboo and Kumar (2015), temperature of 70°C and stress level of 3,200 Pa – AC+rubber+PPA

As pointed out earlier, it is believed that there is a correlation between the *n* values and the nonrecoverable compliance $J_{nr}3200$ – similarly to what was found for the AC+rubber – due to the consistent increases in this parameter with creep time within the whole temperature range. Figure 109 precisely indicates that this assumption is true, since the coefficient of determination R^2 is higher than 0.80 (which is a quite good correlation). In a complementary analysis conducted with the numerical values of *n* at 100 Pa and $J_{nr}100$, the resulting correlation is much worse ($R^2 \approx 0.458$, chart not shown here for brevity). Other than indicating that the stress level of 3,200 Pa is closer to the actual loads applied in the pavement than 100 Pa, these results give support to the idea that the compliances around 10-100 kPa^{-1} and the *n* values around 1.01-1.03 are – at least to some extent – representative of a creep-recovery behavior approaching the nonlinear viscoelastic range.

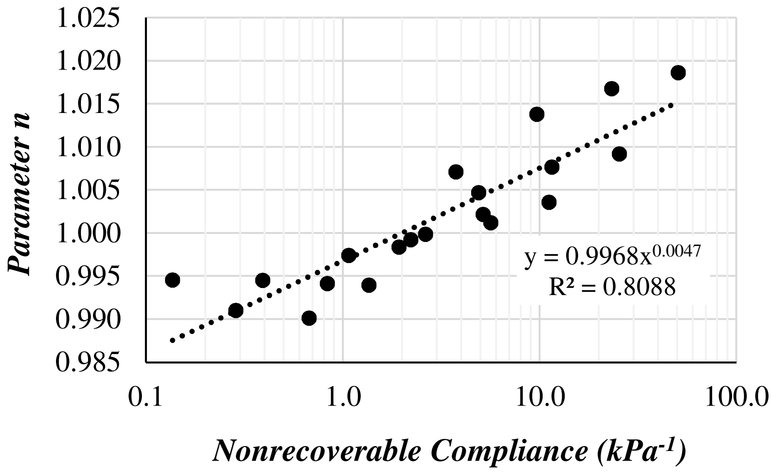

Figure 109 – Degree of correlation between the nonrecoverable compliances of the AC+rubber+PPA at the stress level of 3,200 Pa and the corresponding *n* values from the power law models

The correlations involving all parameters and pavement temperatures are summarized in Table 129 with respect to the constants *A* and *B*. The levels of correlation typically decrease with increasing temperature and stress level and for both constants, which suggests that nonlinearity had some influence on the increase in the susceptibility of the formulation to rutting. One interesting aspect of the regression equations of the AC+rubber+PPA is that no reverses in the signals of the gradients can be found, which is a different pattern of response when compared with other materials such as the AC+rubber (Table 113, page 254). In a general context, a precise estimation of the effect of the initial strain with increasing temperature and stress level cannot be made. This is because the correlations do not point to a clear tendency of decreasing *A* at longer loading times, as the negative signals of the gradients may suggest.

Therefore, it can be implied that higher temperatures cause increases in the initial strains accumulated by the binder; however, an exact measurement of these increases is not possible.

Table 129 – Degrees of correlation between the parameters *A* and *B* (modified power model) and the creep time t_F for the AC+rubber+PPA

T (°C)	stress (kPa)	linear regression equations and R^2 values (in parenthesis)[a]	
		parameter *A*	parameter *B*
52	0.1	y = -0.0003x + 0.0221 (0.7590)	y = 0.0097x + 0.8141 (0.9317)
	3.2	y = -0.0096x + 0.7263 (0.7565)	y = 0.0169x + 0.8320 (0.9385)
58	0.1	y = -0.0005x + 0.0500 (0.5618)	y = 0.0104x + 0.8526 (0.9387)
	3.2	y = -0.0161x + 1.7000 (0.5030)	y = 0.0145x + 0.9022 (0.8790)
64	0.1	y = -0.0011x + 0.1115 (0.4211)	y = 0.0103x + 0.8917 (0.9369)
	3.2	y = -0.0205x + 3.9867 (0.1689)	y = 0.0092x + 0.9622 (0.8634)
70	0.1	y = -0.0019x + 0.2389 (0.2599)	y = 0.0099x + 0.9231 (0.9208)
	3.2	y = -0.0168x + 9.0820 (0.0222)	y = 0.0061x + 0.9931 (0.9090)
76	0.1	y = -0.0030x + 0.4875 (0.1252)	y = 0.0091x + 0.9484 (0.9073)
	3.2	y = -0.0336x + 19.6460 (0.0136)	y = 0.0048x + 1.0064 (0.9422)

[a] the Y-axis is associated with the parameter (*A* or *B*), whereas the X-axis is associated with t_F.

With respect to the parameter *B*, it is clear that higher temperatures and longer creep times increase the rate of accumulation of permanent strain in the formulation (no reverses in the signals of the gradients occur and the R^2 values are always good to excellent). In other words, the influence of the strain rate on the increase in the rutting potential of the binder is easily recognized. The same can somehow be applied to the degree of nonlinearity (parameter *n*) and the indicator of the elastic response of the material (parameter α), as may be inferred from the quite good correlations reported in Table 130.

Table 130 – Degrees of correlation between the parameters *n* and *α* (modified power model) and the creep time t_F for the AC+rubber+PPA

T (°C)	stress (kPa)	linear regression equations and R^2 values (in parenthesis)[a]	
		parameter *n*	parameter *α*
52	0.1	y = 0.0005x + 0.9990 (0.9923)	y = 0.0101x + 0.8133 (0.9384)
	3.2	y = 9E-05x + 0.9921 (0.0157)	y = 0.0169x + 0.8252 (0.9540)
58	0.1	y = 0.0003x + 0.9994 (0.9254)	y = 0.0107x + 0.8520 (0.9440)
	3.2	y = 0.0019x + 0.9913 (0.9697)	y = 0.0163x + 0.8941 (0.9134)
64	0.1	y = 0.0006x + 0.9987 (0.8950)	y = 0.0108x + 0.8904 (0.9498)
	3.2	y = 0.0024x + 0.9949 (0.9981)	y = 0.0116x + 0.9570 (0.9109)
70	0.1	y = 0.0011x + 0.9980 (0.9628)	y = 0.0109x + 0.9211 (0.9434)
	3.2	y = 0.0024x + 0.9975 (0.9985)	y = 0.0086x + 0.9905 (0.9502)
76	0.1	y = 0.0015x + 0.9979 (0.9913)	y = 0.0106x + 0.9463 (0.9365)
	3.2	y = 0.0025x + 0.9987 (0.9987)	y = 0.0075x + 1.0050 (0.9726)

[a] the Y-axis is associated with the parameter (*n* or *α*), whereas the X-axis is associated with t_F.

With expection of an odd case for the parameter *n* at 52°C and 3.2 kPa, all the other correlations are at least equal to 0.96 (which is excellent). On the other hand, the constants of the individual regression trendlines do not always indicate a consistent behavior of the binder in the MSCR tests. For instance, the individual terms of the equations for *n* at 100 Pa show an alternate response with increasing loading time (from 0.9990 to 0.9994, and then 0.9987, 0.9980 and 0.9979), and this does not match the constant increases in the gradients at temperatures higher than 52°C (from 0.0003 at 58°C to 0.0006, 0.0011 and 0.0015 at 64, 70 and 76°C, respectively). This may explain why the overall correlation between *n* and $J_{nr}100$ is not as good as the one between *n* and $J_{nr}3200$, as shown above. This kind of response also has some similarities with the one of the parameter α at 3,200 Pa, in that the gradients do not always increase for more critical loading conditions.

In a general context, there is a pretty good correlation between the α values and the percent recoveries *R100* and *R3200* for the AC+rubber+PPA, see Figure 110. This result (≈ 0.85) is slightly better than the one obtained for the AC+rubber (≈ 0.82, Figure 100). The expected relationship between both parameters – decrease in α with increase in recovery – is also observed, i. e., the gradient of the regression trendline is negative. Either the consistent increases in the intercepts of the regression equations or the increases (but not consistent) in the gradients of these same equations for α – see Table 136 – contributed to the good results reported here.

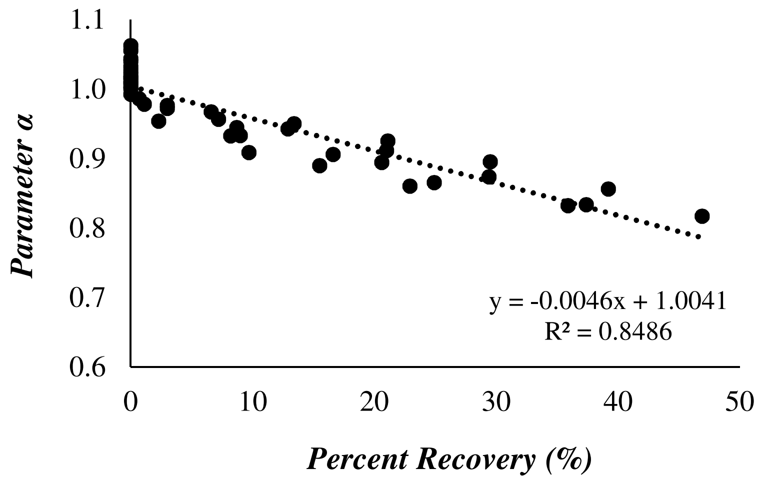

Figure 110 – Degree of correlation between the percent recoveries of the AC+rubber+PPA and the corresponding α values from the power law models

By taking a look at the percent recoveries of the AC+rubber+PPA (Table 119, page 260), one may see that there are two null values at the stress level of 3,200 Pa and the creep-recovery times of 1/9 s. As a consequence, the ANOVA analysis was restricted to the percent recoveries at 100 Pa to avoid misleading interpretations about the effect of temperature on the recoveries of the asphalt binder. The two tables shown below provide the organized *R100* values (Table 131) and the organized $J_{nr}100$ and $J_{nr}3200$ values (Table 132).

Table 131 – Rearranged MSCR testing data of the AC+rubber+PPA to be used in the analysis of variance (ANOVA) – percent recovery

stress level of 0.1 kPa (*R100*, %)[a]		stress level of 3.2 kPa (*R3200*, %)[a]	
increasing creep time	increasing temperature	increasing creep time	increasing temperature
46.9	46.9	These calculations were not made due to the lack of enough data points at higher temperatures.	These calculations were not made due to the lack of enough data points at higher temperatures.
37.4	39.2		
24.9	29.5		
15.5	21.1		
N/A[b]	13.4		

[a] the starting point in both cases was the temperature of 52°C.
[b] N/A: Not applicable.

Table 132 – Rearranged MSCR testing data of the AC+rubber+PPA to be used in the analysis of variance (ANOVA) – nonrecoverable creep compliance

stress level of 0.1 kPa ($J_{nr}100$, kPa^{-1})[a]		stress level of 3.2 kPa ($J_{nr}3200$, kPa^{-1})[a]	
increasing creep time	increasing temperature	increasing creep time	increasing temperature
0.110	0.110	0.136	0.136
0.220	0.283	0.285	0.390
0.503	0.729	0.672	1.069
0.981	1.738	1.352	2.624
N/A[b]	3.888	N/A[b]	5.645

[a] the starting point in both cases was the temperature of 52°C.
[b] N/A: Not applicable.

Table 133 shows the results of ANOVA for the percent recoveries of the AC+rubber+PPA at 100 Pa. The *F-value* is too low (less than 0.3% of $F_{critical}$) and the *p-value* is about 18 times higher than α. As a consequence of these findings, the null hypothesis should not be rejected and the influences of temperature and loading time on the *R100* values of the formulation should be considered as "statistically similar". In a direct comparison between the results of the AC+rubber+PPA and the AC+rubber (Table 117, page 258), one may conclude that the formulation with PPA in the composition shows a more uniform variation in the percent recovery – i. e., more similar decreases in this parameter with creep time and temperature – than the corresponding formulation without PPA.

When moving from the percent recovery to the nonrecoverable compliance (Table 134), the first conclusion that can be drawn is that the compliances are much more sensitive to changes in the loading time and temperature. From a pratical point of view, the *F-value* always higher than 1.23 and the *p-value* always lower than 0.31 suggest that one of the variables (in this case, the temperature) has a much stronger effect on the stiffness and the susceptibility of the AC+rubber+PPA to failure by rutting in the pavement than the other. The AC+rubber showed *F-values* and *p-values* quite close to the ones obtained for the AC+rubber+PPA (see Table 118, page 258), which means that the changes in the composition did not affect the statistical significance of temperature on the results of the nonrecoverable compliances of the two crumb rubber-modified binders.

Table 133 – Results from the analysis of variance (ANOVA, *p-value* and *F-value*) as based on the percent recoveries of the AC+rubber+PPA

null hypothesis H_0	statistical parameters (ANOVA)				recommendation
	$F_{critical}$	*F-value*	α	*p-value*	
equivalency between R values with increasing creep time and temperature, 0.1 kPa	5.5914	0.016	0.05	0.9029	H_0 is not rejected
equivalency between R values with increasing creep time and temperature, 3.2 kPa	Not calculated due to the lack of enough data points.				

Table 134 – Results from the analysis of variance (ANOVA, *p-value* and *F-value*) as based on the nonrecoverable compliances of the AC+rubber+PPA

null hypothesis H_0	statistical parameters (ANOVA)				recommendation
	$F_{critical}$	*F-value*	α	*p-value*	
equivalency between J_{nr} values with increasing creep time and temperature, 0.1 kPa	5.5914	1.2359	0.05	0.3030	H_0 is not rejected
equivalency between J_{nr} values with increasing creep time and temperature, 3.2 kPa	5.5914	1.3419	0.05	0.2847	H_0 is not rejected

The rheological modeling of the AC+rubber+PPA according to the modified power model and its comparison with the AC+rubber yielded some interesting findings. The degree of nonlinearity (parameter n) is higher for the AC+rubber at 100 Pa, but these degrees seem to be equivalent for both materials (approximately similar values) at 3,200 Pa. On the other hand, the AC+rubber+PPA depicts much higher accumulations of initial strain than the AC+rubber (higher A values), as well as slightly higher strain rates (B values) within the test conditions considered in the present study. Based on this, it can be implied that the rubber particles are mainly responsible for imparting strength and elasticity to the asphalt binder, and also that the presence of PPA was not enough to return to the original values of the parameters of the crumb rubber-modified asphalt binder. There is a strong correlation between *n* and the $J_{nr}3200$ values of the AC+rubber+PPA, but the same cannot be said for $J_{nr}100$ – similar conclusions were reached based on the data of the AC+rubber. Higher temperatures and stress levels clearly lead to increases in the strain rates (*B* values) accumulated by the AC+rubber+PPA; however, the quite poor correlations for the initial strains (*A* values) make it difficult to quantify the rate of increase in such strain with temperature and stress level.

The levels of correlation between α and percent recovery for the AC+rubber+PPA and the AC+rubber are very close to each other, but they are slightly better for the AC+rubber+PPA. The absence of two numerical values for *R3200* avoided the implementation of ANOVA to such data. It could be observed that the percent recoveries are not too sensitive to the variable that is affecting them (creep time or temperature), since the statistical parameters are far from the critical values. However, the nonrecoverable compliances are much more sensitive to variations in the temperature than in the creep time, and this is reflected into the *F-value* higher than 1.3 and the *p-value* lower than 0.31 for the two formulations with crumb rubber.

Asphalt Binder Modification with Elastomers (SBS and SBR). Table 135 provides the percent recovery values of the AC+SBS for all the testing variables used in this study. The percent recoveries are very sensitive to an increase in the stress level, as the percentages of decrease are considerably higher at 3,200 Pa than at 100 Pa, see Figure 111. Also, these percentages follow different patterns of behavior as a function of the temperature: for instance, the parameter *R100* tends to stabilize at values around 30-40% or 20-30% when the material is tested at the intermediate temperatures of 58, 64 and 70°C. This phenomenon is possibly attributed to the differences in the arrangement and orientation of the structural units of the polymer (polystyrene and polybutadiene blocks) within the binder sample and, as a consequence, some regions may have given more contribution to the elastic response of the binder than others at a specific temperature and loading time. It is also possible that, at high strain levels, some polystyrene blocks move to a different polymer-rich domain of the sample; as a consequence of this process, the physical network is rearranged (POLACCO et al., 2006; ZOOROB et al., 2012).

Another discussion on this issue is pointed out by D'Angelo et al. (2007). Although the MSCR test is carried out according to a stress-controlled protocol, it was not clear to the authors as to whether the presence of lower *R* values was caused by the high applied stresses or the high strain experienced by the polymer-modified binder sample. The MSCR tests carried out at a variety of stresses, loading times and temperatures suggested that, for a particular strain level, the results at higher stresses may yield higher *R* values than the ones at lower stresses depending on the response of the modifier. In such a case, these authors pointed out that the responses at high strain rates can be interpreted as a more overall elastic behavior and the ones at lower strain rates can be interpreted as a more yield behavior. This phenomenon may also lead to reductions in J_{nr} at higher stress levels, which makes the interpretation of the outcomes of the MSCR tests even more complicated.

Table 135 – Percent recoveries at 100 Pa (*R100*) and 3,200 Pa (*R3200*) for the AC+SBS with increasing loading time and temperature

parameter	creep time (s)	results at each temperature (%)				
		52°C	58°C	64°C	70°C	76°C
R100	1.0	41.6	48.7	52.6	52.3	40.3
	2.0	39.7	46.0	45.9	35.6	14.4
	4.0	28.4	30.4	22.6	7.0	0.0
	8.0	22.5	36.2	22.5	4.9	0.0
R3200	1.0	32.6	27.2	24.7	19.8	8.1
	2.0	24.9	18.6	15.0	7.0	0.2
	4.0	17.4	10.8	3.2	0.0	0.0
	8.0	9.8	6.0	0.0	0.0	0.0

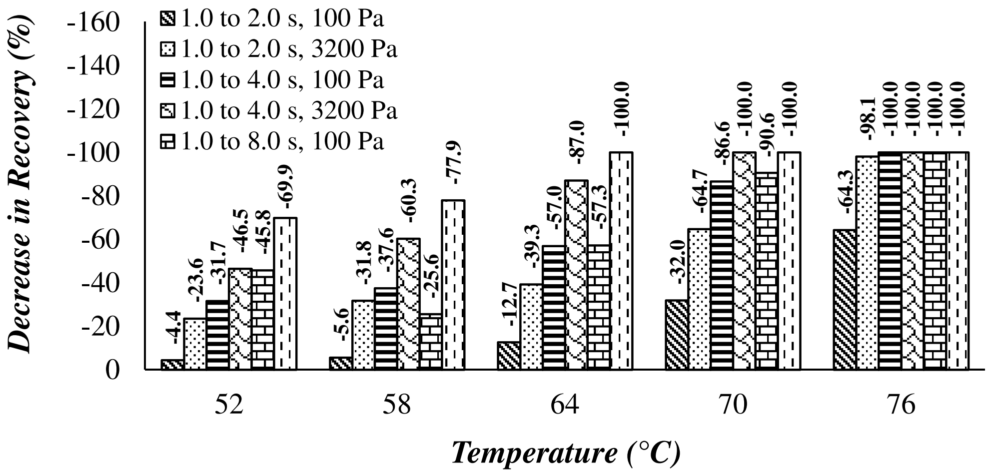

Figure 111 – Percentages of decrease in the recoveries of the AC+SBS with creep time, temperature and stress level

The *R3200* values of the AC+SBS are all equal to zero at very high temperatures (70 and 76°C) and long loading times (4.0 and 8.0 s). It is believed that the polymer network was considerably damaged under such test conditions, and also that the extremely large strains experienced by the material caused it to enter the tertiary flow region and become unstable (JAFARI et al., 2015). Negative *R* values may be observed in these cases as shown elsewhere (e. g., JAFARI and BABAZADEH, 2016; JAFARI et al., 2015), but they were assumed as zero in the present study for calculation purposes. As a general conclusion of these findings, the SBS-modified asphalt binder would be recommended only on pavements with a maximum high

PG grade of 64-xx and with creep times no longer than 4.0 s. Finally, the increases in *R100* with temperature at 1/9 s and 2/9 s may be primarily explained by softening of the base binder and activation of the polymer network at higher strain levels (ANDERSON et al., 2010).

The nonrecoverable compliances shown in Table 136 and the corresponding percentages of increase depicted in Figure 112 refer to the asphalt binder modified with SBS copolymer and without the presence of PPA (AC+SBS). As these data suggest, the rates of increase in J_{nr} are substantially higher for the two longest creep times (4.0 and 8.0 s), regardless of the applied stress level. This nonlinear response was somehow expected because, when polymers are extended, there is a distortion in the morphology of the material and a change in the original properties due to chain entanglements and the appearance of glassy regions (D'ANGELO et al., 2007). With respect to SBS, these glassy regions are formed by the fragmentation of the long polystyrene blocks (ZOOROB et al., 2012).

Table 136 – Nonrecoverable compliances at 100 Pa ($J_{nr}100$) and 3,200 Pa (J_{nr} 3200) for the AC+SBS with increasing loading time and temperature

parameter	creep time (s)	results at each temperature (kPa^{-1}), J_{nr} > 4.0 kPa^{-1} is in bold				
		52°C	58°C	64°C	70°C	76°C
$J_{nr}100$	1.0	0.133	0.275	0.579	1.240	3.142
	2.0	0.221	0.470	1.093	2.928	**8.482**
	4.0	0.453	1.050	2.806	**8.039**	**19.609**
	8.0	0.927	1.704	**5.236**	**16.376**	**39.764**
$J_{nr}3200$	1.0	0.156	0.410	0.997	2.347	**5.703**
	2.0	0.289	0.777	1.949	**4.906**	**11.753**
	4.0	0.555	1.518	**4.114**	**10.330**	**23.868**
	8.0	1.219	3.230	**9.202**	**24.121**	**57.634**

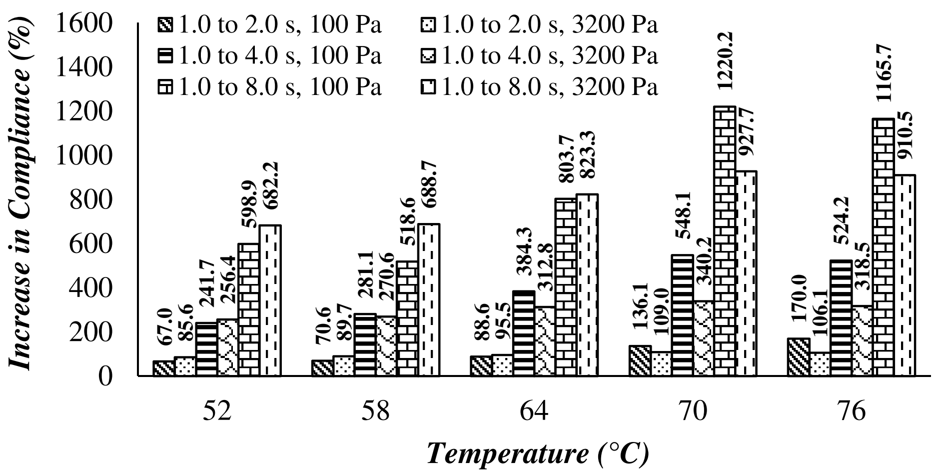

Figure 112 – Percentages of increase in the nonrecoverable compliances of the AC+SBS with creep time, temperature and stress level

As a matter of comparison, the $J_{nr}100$ and $J_{nr}3200$ values can range from 0.13 to only 9.20 kPa^{-1} at temperatures no greater than 64°C, irrespective of the loading time or stress level. However, the results can easily overcome 20.0 kPa^{-1} when very high temperatures (70 and 76°C) and long creep times are considered in the MSCR tests. Based on the recommendation made for the percent recoveries ($T \leq 64$°C and $t_F \leq 4.0$ s), it can be concluded that J_{nr} would be limited to the upper value of 4.114 kPa^{-1}. This result is very close to the maximum allowed compliance that can be used on pavements with standard traffic levels, i. e., 4.0 kPa^{-1}.

Surprisingly, the stress sensitivity of the AC+SBS – as measured by the Superpave® parameter $J_{nr,\,diff}$ – markedly decreased at the temperatures of 70 and 76°C and for t_F values longer than the standardized one (1.0 s), as summarized in Table 137. For instance, the $J_{nr,\,diff}$ value is reduced by almost 90% at 70°C (from 89.2 to 47.3%) and 76°C (from 81.5 to 44.9%) when moving the original creep time from 1.0 to 8.0 s. It is hypothesized that, as the loading time and the temperature increase, the degradation of the polymer network in the formulation already takes place at 100 Pa and not only at 3,200 Pa; thus, the repeated creep response of the formulation at lower stresses (i. e., relationships between permanent and elastic strains and numerical values of R and J_{nr}) tends to be closer to the one at higher stresses. Some odd cases of extremely high stress sensitivity may be seen when the temperature or the creep time is more severe in the MSCR test, especially at 70 and 76°C. This is in accordance with the technical literature, as reported in the papers by Domingos and Faxina (2017) and Kataware and Singh (2015) among others.

Table 137 – Percent differences in nonrecoverable compliances ($J_{nr,\,diff}$) for the AC+SBS with increasing creep time and temperature

creep time (s)	$J_{nr,\,diff}$ values (%) at each creep time and temperature[a]				
	52°C	58°C	64°C	70°C	76°C
1.0	17.5	48.7	72.0	**89.2**	**81.5**
2.0	30.5	65.3	78.3	67.5	38.6
4.0	22.5	44.6	46.6	28.5	21.7
8.0	31.5	**89.6**	75.7	47.3	44.9

[a] the numbers in bold are the ones that exceeded the maximum $J_{nr,\,diff}$ (75%) according to Superpave®.

With respect to the traffic levels according to the procedure from Superpave®, the data shown in Table 138 reveal that the AC+SBS cannot be placed on asphalt pavements subjected to the maximum pavement temperature of 76°C, as well as pavements with PG grades of 70-xx and traffic levels heavier than the standardized one. This binder also has a fairly limited applicability on highways with a high PG grade of 64-xx, since no traffic levels could be assigned when t_F is longer than 2.0 s. Similarly to what was reported in the studies from Domingos and Faxina (2017) and Kataware and Singh (2015), at least two temperatures showed decreases in the traffic level by one grade or more when the loading time was doubled. For instance, the appropriate level decrased from "heavy" to "no traffic" at 64°C (two grades) and this level decreased from "very heavy" to "heavy" (one grade) at 58°C with a change in t_F from 2.0 to 4.0 s. It is hypothesized that the lack of appropriate compatibility between the polymer and the binder – the AC+SBS is never graded as with "high elasticity", see Figure 65 on page 181 – contributed to these relatively poor results of the formulation in the MSCR test.

Table 138 – Adequate traffic levels for the AC+SBS with increasing creep time and temperature based on the standardized Superpave® criteria

creep time (s)	traffic levels for each temperature[a]				
	52°C	58°C	64°C	70°C	76°C
1.0	E	E	V	S	-
2.0	E	V	H	-	-
4.0	V	H	-	-	-
8.0	H	S	-	-	-

[a] S = standard; H = heavy; V = very heavy; E = extremely heavy.

The equations with the correlations between the $J_{nr}3200$ values and the traffic speeds based on the equations from Huang (2004) and Pereira et al. (1998, 2000) can be seen in Table 139. It may be noted that the degrees of correlation slightly increase with increasing pavement temperature for the equation from Huang (2004), either for the tire contact radius of 6.0 in or 3.68 in. This may be explained by the fact that, as the temperature gets higher, the percentages of increase in $J_{nr}3200$ approach the ones observed for the loading time t_F. In addition, no great differences can be seen among the R^2 values of the equations from Huang (2004) and Pereira et al. (1998) except for the slopes of the curves. In other words, one of the possible criteria for choosing a specific equation and tire contact radius may be the desired rate of decrease in the J_{nr} value with increasing traffic speed. Again, the major difference between the regression equations based on one or another contact radius (HUANG, 2004) is the slope of the exponential trendline, since the gradient and the R^2 values are almost equivalent in both cases.

Table 140 summarizes the comparisons between the predicted and actual traffic levels of the AC+SBS for the equations from Huang (2004) and Pereira et al. (1998), whereas Table 141 shows these same comparisons for the equations from Huang (2004) and Pereira et al. (2000). It can be implied from the data that, as the temperature increases, the ability of the equations in estimating the actual traffic level is seriously compromised. This is not something restricted to the AC+SBS, since other formulations also showed similar patterns of behavior. As representative examples, the use of the equation from Pereira et al. (1998) at 52°C would correctly estimate three out of four traffic levels for the AC+SBS and the one from Huang (2004) – regardless of the tire contact radius – would also predict three out of four levels at the temperature of 52°C. Again, the empirical-based equation from Pereira et al. (2000) was unable to accurately estimate more than three traffic levels within the group of temperatures and loading times used in the dissertation. The present discussion endorses the idea that such equations have a limited applicability to actual nonrecoverable compliance values and the current traffic level criteria, even though the results were promising at 52 and 58°C.

Table 139 – Regression equations and coefficients of determination between the $J_{nr}3200$ values of the AC+SBS and the corresponding vehicle speeds according to the equations by Pereira et al. (1998, 2000) and Huang (2004)

source and data	temperature (in °C)	equation	R^2
Pereira et al. (1998)	52	$y = 1.1445e^{-0.027x}$	0.8890
Pereira et al. (2000)	52	$y = -0.014x + 1.0513$	1.0000
Huang (2004) $r = 6$ in	52	$y = 1.1451e^{-0.033x}$	0.8895
	58	$y = 3.0973e^{-0.033x}$	0.8997
	64	$y = 8.7931e^{-0.036x}$	0.8971
	70	$y = 23.127e^{-0.037x}$	0.9033
	76	$y = 54.132e^{-0.037x}$	0.8953
Huang (2004) $r = 3.68$ in	52	$y = 1.1431e^{-0.053x}$	0.8898
	58	$y = 3.0918e^{-0.054x}$	0.9000
	64	$y = 8.7764e^{-0.058x}$	0.8974
	70	$y = 23.0800e^{-0.061x}$	0.9035
	76	$y = 54.0250e^{-0.060x}$	0.8955

Table 140 – Comparisons between the actual traffic levels of the AC+SBS and the ones obtained from Huang (2004) and Pereira et al. (1998)

t_F (s)[d]	actual[a] and estimated[b, c] traffic levels at each temperature[d]				
	52°C	58°C	64°C	70°C	76°C
1.0	**E (V/E) [V/E]**	**E [V/E]**	**V [V/E]**	S [V/E]	-
2.0	**E (V/E) [V/E]**	**V [V/E]**	H [V/E]	-	-
4.0	V **(H) [H]**	**H [H]**	-	-	-
8.0	**H** (S) **[H]**	S [H]	-	-	-

[a] S = standard; H = heavy; V = very heavy; E = extremely heavy (AASHTO M320-09 standard, Table 3).
[b] (parentheses) = traffic levels from Pereira et al. (1998).
[c] [brackets] = traffic levels from Huang (2004), $r = 6$ in.
[d] similarities among the rankings are highlighted in bold, t_F = creep time.

Table 141 – Comparisons between the actual traffic levels of the AC+SBS and the ones obtained from Huang (2004) and Pereira et al. (2000)

t_F (s)[d]	actual[a] and estimated[b, c] traffic levels at each temperature[d]				
	52°C	58°C	64°C	70°C	76°C
1.0	**E** (H) **[V/E]**	**E [V/E]**	**V [V/E]**	S [V/E]	-
2.0	**E** (H) **[V/E]**	**V [V/E]**	H [V/E]	-	-
4.0	V (H) [H]	**H [H]**	-	-	-
8.0	**H (H) [H]**	S [H]	-	-	-

[a] S = standard; H = heavy; V = very heavy; E = extremely heavy (AASHTO M320-09 standard, Table 3).
[b] (parentheses) = traffic levels from Pereira et al. (2000).
[c] [brackets] = traffic levels from Huang (2004), r = 3.68 in.
[d] similarities among the rankings are highlighted in bold, t_F = creep time.

Similarly to other formulations, the traffic levels based on the criteria proposed here were compared with the ones from the Superpave® methodology (Table 142). The results point out that a decrease by one grade in this appropriate traffic level can be seen at 64°C (from very heavy to heavy), and this was also published in an earlier paper by Domingos and Faxina (2017). The other levels were not changed, neither the fact that the AC+SBS is unable to deal with any traffic level at 76°C. It can be implied that the addition of one more requirement in the establishment of the most adequate traffic level for the binder goes to a more conservative side and, at the same time, it does not considerably differ from the outcomes of the procedures available in the current versions of the specification. In other words, the slight changes in the current protocol mainly aim at avoiding the use of modified binders with very high degrees of nonlinearity on pavements with at least heavy traffic levels. This seems to be the case of the AC+SBS, as well as the majority of the formulations reported earlier (i. e., AC+rubber+PPA at 58°C, AC+Elvaloy+PPA at 70°C and AC+PPA at 64°C).

Table 142 – Traffic levels of the AC+SBS with increasing loading time and temperature in the current and proposed criteria

temperature (in °C)	No. of required MSCR tests[b]	Superpave® designations (current and new criteria)[a, c]	
		current criterion	new criterion
52	4	**52E-xx**	**52E-xx**
58	4	**58E-xx**	**58E-xx**
64	3	64V-xx	64H-xx
70	2	**70S-xx**	**70S-xx**
76	1	**76-xx**	**76-xx**

[a] S = standard; H = heavy; V = very heavy; E = extremely heavy (AASHTO M320-09 standard, Table 3).
[b] minimum number of MSCR tests to determine the adequate traffic level in the proposed classification.
[c] similarities among the classifications are highlighted in bold.

In general, it may be said that the AC+SBS showed a tendency of stabilization of the percent recovery at intermediate pavement temperatures (58, 64 and 70°C) and the lowest stress level (100 Pa). This may be attributed to a rearrangement and reorientation of the polymeric blocks within the binder phase, or even a movement of these blocks from one location of the sample to the other and a rearrangement of the polymer network. With respect to the marked increases in J_{nr} with increasing temperature and loading time, they can be explained by the nonlinear response of the SBS copolymer under high shear – i. e., distortion in the morphology and changes in its original properties – and the fragmentation of the polystyrene blocks. The stress sensitivity parameter $J_{nr,\ diff}$ tends to decrease with increasing severity of the MSCR test for a particular temperature, and this is possibly caused by the rearrangement of the polymer network at lower stress levels. Finally, the traffic levels estimated by the new criterion are quite similar to the ones based on the current Superpave® criterion, except for the temperature of 64°C.

Table 143 is a summary of the results of the model parameters *A*, *B*, *n* and *α* for the AC+SBS, as recommended in the equation by Saboo and Kumar (2015). In a general context, the importance of the initial strain (*A*) on the increase in the accumulated strain at higher temperatures and longer loading times is reduced and the one of the strain rate (*B*) is increased, as previously observed for other formulations. However, the percentages of variation with loading time are considerably higher for *A* than for *B* (typically between 1 and 15 times higher), and the role of nonlinearity on this creep-recovery response becomes more expressive when t_F is equal to 4.0 and 8.0 s, especially at temperatures between 52 and 64°C. The rates of increase in *α* with creep time and temperature are comparable to the ones observed for the constant *B*, which means that nonlinearity acts together with the increases in the strain rate to compensate for the reductions in the role of initial strain on the behavior of the binder in the MSCR test.

Interestingly, the rates of decrease in *A* with creep time tend to be smaller at the temperatures of 70 and 76°C than for the lower ones (52 to 64°C). At the same time, the variations with *B* tend to be higher at 70 and 76°C and the increases in *n* are reduced when compared with the temperatures up to 64°C. In practical terms, the initial strain starts to have a greater importance on the total accumulated strain – together with the strain rate – when the pavement temperature approaches the high PG grade of the formulation or is equal to this PG grade. Consequently, nonlinearity has a minor importance in this response: the maximum variation in *n* is 1.6% at 70 and 76°C when compared with a maximum value of 7.5% at temperatures no greater than 64°C. In addition, *n* increases at faster rates when the creep time goes from 4.0 to 8.0 s, regardless of the pavement temperature. This suggests that the t_F value of 4.0 s can be taken as a limiting point for seeing nonlinearity a little bit more clearer in the response of the AC+SBS.

Table 143 – Numerical values and variations in the parameters/constants *A, B, n* and *α* from the power law equations by Saboo and Kumar (2015) with increasing temperature and creep time and considering the AC+SBS

temperature	test times	parameter A^a		parameter B^a		parameter n^a		parameter α^a	
		0.1 kPa	3.2 kPa	0.1 kPa	3.2 kPa	0.1 kPa	3.2 kPa	0.1 kPa	3.2 kPa
52°C	1/9 s	0.0241	0.7844	0.8653	0.8762	1.0020	0.9995	0.8670	0.8758
	2/9 s	0.0217 (-10.0)	0.7144 (-8.9)	0.8506 (-1.7)	0.8754 (-0.1)	1.0056 (0.4)	0.9960 (-0.4)	0.8554 (-1.3)	0.8719 (-0.4)
	4/9 s	0.0205 (-14.9)	0.6689 (-14.7)	0.8644 (-0.1)	0.8970 (2.4)	1.0057 (0.4)	0.9952 (-0.4)	0.8693 (0.3)	0.8927 (1.9)
	8/9 s	0.0204 (-15.4)	0.6640 (-15.3)	0.8927 (3.2)	0.9421 (7.5)	1.0296 (2.8)	1.0100 (1.1)	0.9192 (6.0)	0.9515 (8.6)
58°C	1/9 s	0.0571	1.9148	0.8849	0.9164	1.0105	1.0030	0.8942	0.9191
	2/9 s	0.0505 (-11.6)	1.7122 (-10.6)	0.8774 (-0.8)	0.9265 (1.1)	1.0206 (1.0)	1.0027 (0.0)	0.8955 (0.1)	0.9291 (1.1)
	4/9 s	0.0469 (-17.9)	1.5857 (-17.2)	0.8922 (0.8)	0.9446 (3.1)	1.0236 (1.3)	1.0031 (0.0)	0.9133 (2.1)	0.9475 (3.1)
	8/9 s	0.0463 (-18.9)	1.5920 (-16.9)	0.8740 (-1.2)	0.9699 (5.8)	1.0860 (7.5)	1.0180 (1.5)	0.9491 (6.1)	0.9874 (7.4)
64°C	1/9 s	0.1301	4.5130	0.8981	0.9432	1.0152	1.0062	0.9117	0.9490
	2/9 s	0.1155 (-11.2)	4.0439 (-10.4)	0.8986 (0.1)	0.9545 (1.2)	1.0260 (1.1)	1.0066 (0.0)	0.9219 (1.1)	0.9609 (1.3)
	4/9 s	0.1074 (-17.4)	3.7585 (-16.7)	0.9265 (3.2)	0.9775 (3.6)	1.0212 (0.6)	1.0038 (-0.2)	0.9462 (3.8)	0.9813 (3.4)
	8/9 s	0.1068 (-17.9)	3.8402 (-14.9)	0.9174 (2.1)	1.0058 (6.6)	1.0555 (4.0)	1.0141 (0.8)	0.9683 (6.2)	1.0200 (7.5)
70°C	1/9 s	0.2772	10.0460	0.9053	0.9573	1.0164	1.0058	0.9201	0.9628
	2/9 s	0.2562 (-7.6)	9.1987 (-8.4)	0.9227 (1.9)	0.9779 (2.2)	1.0202 (0.4)	1.0044 (-0.1)	0.9413 (2.3)	0.9822 (2.0)
	4/9 s	0.2412 (-13.0)	8.7675 (-12.7)	0.9700 (7.1)	1.0041 (4.9)	1.0077 (-0.9)	1.0044 (-0.1)	0.9775 (6.2)	1.0085 (4.7)
	8/9 s	0.2406 (-13.2)	9.1655 (-8.8)	0.9767 (7.9)	1.0314 (7.7)	1.0195 (0.3)	1.0157 (1.0)	0.9957 (8.2)	1.0476 (8.8)
76°C	1/9 s	0.5611	21.3248	0.9198	0.9834	1.0116	1.0034	0.9305	0.9867
	2/9 s	0.5426 (-3.3)	20.2602 (-5.0)	0.9587 (4.2)	1.0021 (1.9)	1.0072 (-0.4)	1.0031 (0.0)	0.9656 (3.8)	1.0052 (1.9)
	4/9 s	0.5250 (-6.4)	19.6865 (-7.7)	1.0019 (8.9)	1.0223 (4.0)	1.0056 (-0.6)	1.0071 (0.4)	1.0075 (8.3)	1.0296 (4.3)
	8/9 s	0.5186 (-7.6)	21.0284 (-1.4)	1.0121 (10.0)	1.0438 (6.1)	1.0142 (0.3)	1.0191 (1.6)	1.0264 (10.3)	1.0638 (7.8)

[a] the percentages of variation reported in parenthesis refer to the changes in the parameter when moving from 1.0 s to the creep time into question (2.0, 4.0 or 8.0 s).

From the point of view of rutting resistance, the limiting conditions observed for the creep time (4.0 s) and the pavement temperature (64°C) can be applied to the model constants as well. The *A* values at such temperature and loading time are equal to 0.1074 (100 Pa) and 3.7585 (3,200 Pa), whereas the *α* values are equal to 0.9462 (100 Pa) and 0.9813 (3,200 Pa). The *B* values easily overcome unity when higher temperatures and longer creep times are used in the MSCR tests. This indicates that *A* values greater than 4.0 and *α* values greater than 0.94 point to a very high susceptibility to rutting, that is, compliances exceeding 4.0 kPa^{-1} and recoveries generally lower than 20%, even at 100 Pa. The boundary value of *B* = 1.00 can also be added to the requirements with which the AC+SBS may comply for recommending its application on a pavement. In other words, the model constants provide important analyses about the rutting potential of the AC+SBS and can be used together with the standardized MSCR parameters to identify critical conditions for the use of the asphalt binder in the pavement. Some kinds of "inflection points" may be found in the constants *A*, *B* and *n* at specific temperatures, but they seem to be associated with a natural variability of the data.

By plotting the *A* and *B* values with loading time at the temperature of 64°C, Figure 113 and Figure 114 may be obtained for the stresses of 100 and 3,200 Pa, respectively. Surprisingly, the R^2 value for the constant *B* at 100 Pa is lower than the one for the constant *A* (0.45 for the former and 0.62 for the latter). However, the tendency is reversed at 3,200 Pa: the R^2 value for *B* is almost equal to one (0.98) and the corresponding value for *A* is approximately equal to 0.50. As pointed out above, this is perhaps associated with a natural variability of the data values because the expected patterns of response for both constants is the same at 100 and 3,200 Pa, namely, decreases in *A* and increases in *B* with increasing values for the loading time t_F.

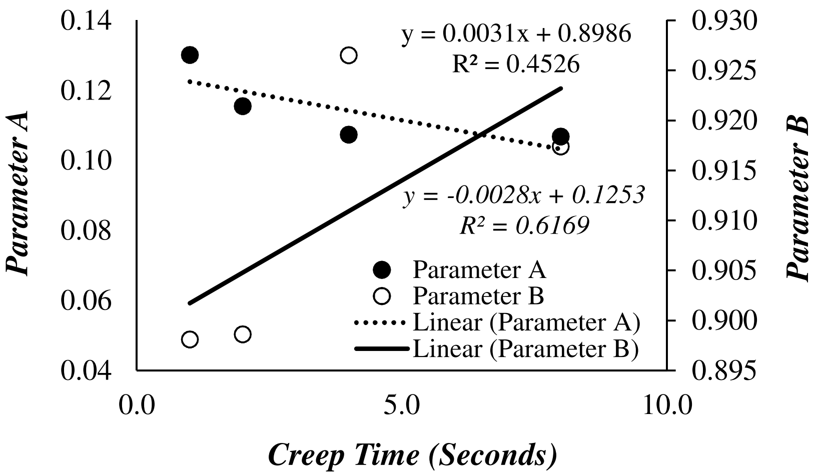

Figure 113 – Correlations between the creep time and the constants *A* and *B* from the model by Saboo and Kumar (2015), temperature of 64°C and stress level of 100 Pa – AC+SBS

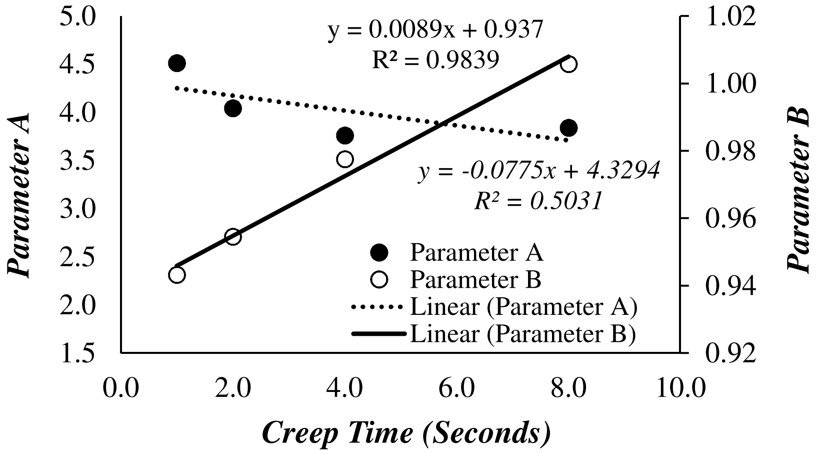

Figure 114 – Correlations between the creep time and the constants *A* and *B* from the model by Saboo and Kumar (2015), temperature of 64°C and stress level of 3,200 Pa – AC+SBS

With an increase in the pavement temperature by 6°C, the resulting correlations for *A* and *B* at the stress levels of 100 and 3,200 Pa are shown in Figure 115 and Figure 116, respectively. No marked changes in the R^2 values of the constant *A* can be seen at 3,200 Pa, whereas the correlation at 70°C and 100 Pa (≈ 0.641) is slightly better than the corresponding one at 64°C and the same stress level (≈ 0.617). With respect to the constant *B*, the levels of correlation at 70°C are about two times higher at 100 Pa (0.787 against 0.453) and slightly lower (0.947 against 0.984) at 3,200 Pa when compared with the corresponding levels at 64°C. The absolute values of the slopes of the regression trendlines for *A* and *B* are higher at 70°C than at 64°C, which means that the rates of decrease in the constant *A* and increase in the constant *B* are greater when the test temperature is higher. The pattern of response observed for the results at 64°C also remains the same at 70°C, namely, the *A* values decrease and the *B* values increase with increasing creep time.

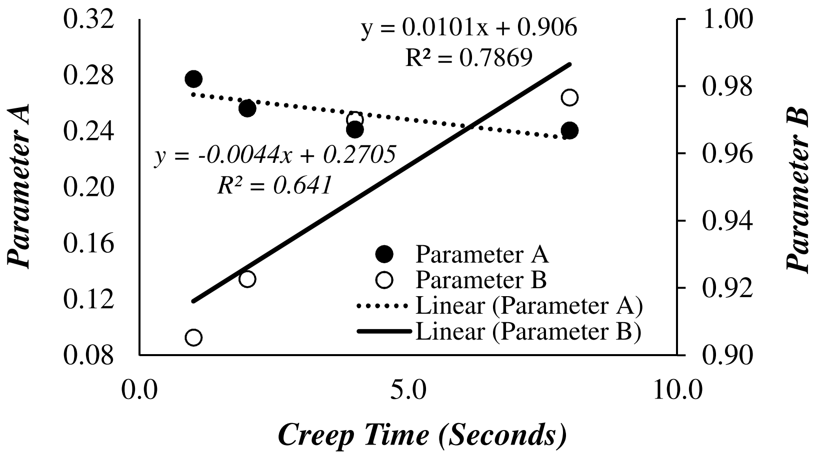

Figure 115 – Correlations between the creep time and the constants *A* and *B* from the model by Saboo and Kumar (2015), temperature of 70°C and stress level of 100 Pa – AC+SBS

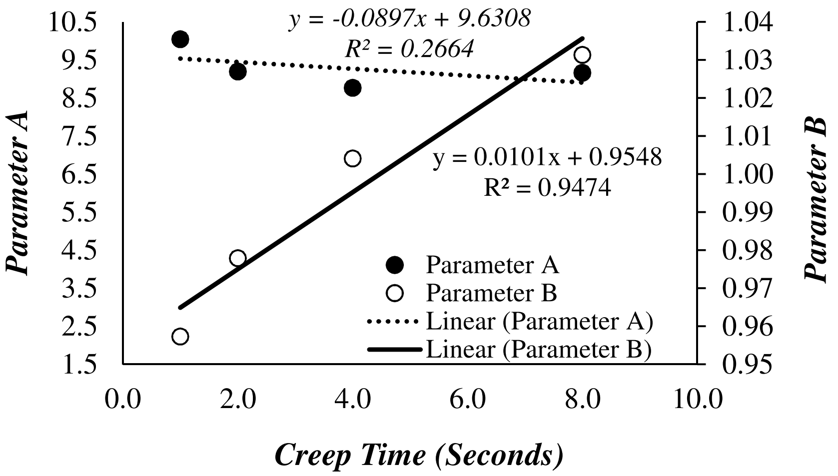

Figure 116 – Correlations between the creep time and the constants *A* and *B* from the model by Saboo and Kumar (2015), temperature of 70°C and stress level of 3,200 Pa – AC+SBS

The remaining correlations between the constants *A* and *B* of the modified power model and the t_F values are given in Table 144. The levels of correlation are much better for the strain rates (*B* values) than for the initial strains (*A* values) in a general context, and some odd cases of reverse in the signal of the gradient of the regression trendline occurred. However, this is probably not a matter of concern because the R^2 values are very small (no greater than 0.18) for the equations with positive gradients in *A* and negative gradients in *B*. In other words, such "strange" equations simply refer to mathematical fits and are not necessarily related to a profound change in the response of the material. Increases in the slopes and intercepts with increasing temperature and stress level can be seen for the two constants, and R^2 decreases with increasing temperature values only for the *A* values at 3,200 Pa. This suggests that, differently from other formulations such as the the AC+rubber and the AC+rubber+PPA, nonlinearity did not seem to have a strong impact on the response of the AC+SBS at higher temperatures. The presence of lower *n* values at 70 and 76°C than at 52, 58 and 64°C (see Table 150) also goes to the same direction.

Table 145 reports the regression equations and the corresponding R^2 values for the exponents/constants *n* and *α* at all pavement temperatures and stress levels. The levels of correlation for *n* were poorer than the corresponding ones for *α*, which was quite expected because the variations in *n* with loading time in Table 143 were sometimes positive, sometimes negative (especially at 3,200 Pa). Conversely, the changes in *α* with creep time were always positive and the results increased with increasing t_F, thus leading to regression equations with only good to excellent correlations ($R^2 > 0.78$). As a consequence, no overall correlations between J_{nr} and *n* must be expected: in fact, a complementary analysis – chart not reported here – indicated that the R^2 value is of only 0.016, which is in agreement with the aforementioned discussion.

Table 144 – Degrees of correlation between the parameters A and B (modified power model) and the creep time t_F for the AC+SBS

T (°C)	stress (kPa)	linear regression equations and R^2 values (in parenthesis)[a, b]	
		parameter A	parameter B
52	0.1	y = -0.0004x + 0.0233 (0.6042)	y = 0.0049x + 0.8497 (0.7513)
	3.2	y = -0.0145x + 0.7625 (0.6507)	y = 0.0100x + 0.8603 (0.9751)
58	0.1	y = -0.0013x + 0.0550 (0.6417)	y = -0.0011x + 0.8862 (0.1733)
	3.2	y = -0.0382x + 1.8446 (0.5923)	y = 0.0075x + 0.9111 (0.9888)
64	0.1	y = -0.0028x + 0.1253 (0.6169)	y = 0.0031x + 0.8986 (0.4526)
	3.2	y = -0.0775x + 4.3294 (0.5031)	y = 0.0089x + 0.9370 (0.9839)
70	0.1	y = -0.0044x + 0.2705 (0.6410)	y = 0.0101x + 0.9060 (0.7869)
	3.2	y = -0.0897x + 9.6308 (0.2664)	y = 0.0101x + 0.9548 (0.9474)
76	0.1	y = -0.0055x + 0.5573 (0.7860)	y = 0.0120x + 0.9282 (0.7656)
	3.2	y = 0.0067x + 20.550 (0.0008)	y = 0.0081x + 0.9824 (0.9358)

[a] the Y-axis is associated with the parameter (A or B), whereas the X-axis is associated with t_F.
[b] changes in the signal of the slope of the regression trendlines are highlighted with a grey-shaded box.

Table 145 – Degrees of correlation between the parameters n and α (modified power model) and the creep time t_F for the AC+SBS

T (°C)	stress (kPa)	linear regression equations and R^2 values (in parenthesis)[a]	
		parameter n	parameter α
52	0.1	y = 0.0039x + 0.9961 (0.9004)	y = 0.0084x + 0.8461 (0.8522)
	3.2	y = 0.0017x + 0.9937 (0.6167)	y = 0.0116x + 0.8546 (0.9477)
58	0.1	y = 0.0107x + 0.9952 (0.9233)	y = 0.0082x + 0.8823 (0.9854)
	3.2	y = 0.0022x + 0.9983 (0.8442)	y = 0.0097x + 0.9093 (0.9997)
64	0.1	y = 0.0054x + 1.0094 (0.8564)	y = 0.0080x + 0.9069 (0.9632)
	3.2	y = 0.0011x + 1.0035 (0.6076)	y = 0.0101x + 0.9401 (0.9989)
70	0.1	y = 0.0002x + 1.0154 (0.0067)	y = 0.0104x + 0.9197 (0.8820)
	3.2	y = 0.0015x + 1.0018 (0.7599)	y = 0.0118x + 0.9562 (0.9833)
76	0.1	y = 0.0006x + 1.0074 (0.2206)	y = 0.0127x + 0.9348 (0.8380)
	3.2	y = 0.0024x + 0.9993 (0.9562)	y = 0.0106x + 0.9814 (0.9778)

[a] the Y-axis is associated with the parameter (n or α), whereas the X-axis is associated with t_F.

Differently from the exponent n, the promising results and correlations for the parameter α are expected to result in a reasonable or good correlation between this parameter and the percent recovery of the asphalt binder. This may be confirmed by the linear equation and the R^2 value in Figure 117 and, in fact, there is a reasonable correlation between n and the recoveries (*R100* and *R3200* values) of the AC+SBS: the coefficient of determination is approximately equal to 0.65. Although this value is comparable to the ones found in the previously reported formulations (especially the AC+Elvaloy+PPA), complementary investigations were carried out to see which of the percent recoveries – *R100* or *R3200* – provides better correlations than the other, or even if the results are approximately the same for both of them. As shown in Figure 118, the percent recoveries at 3,200 Pa yield better correlations than the ones at 100 Pa (0.78 against 0.61), which is the opposite of what was found in the AC+Elvaloy+PPA – see Figure 92, page 241.

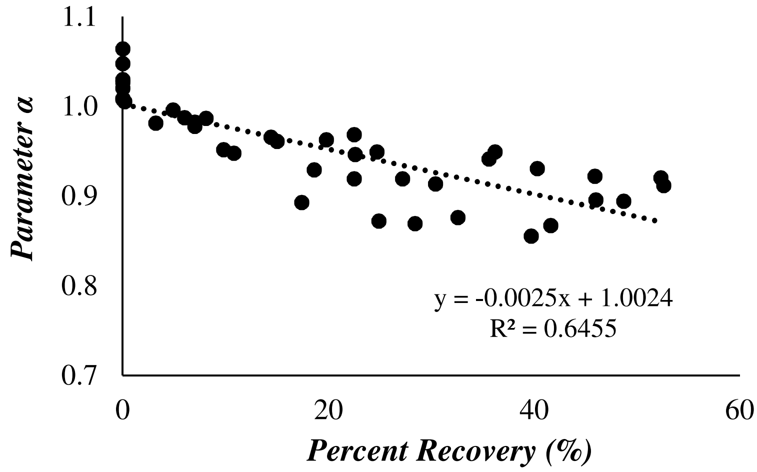

Figure 117 – Degree of correlation between the percent recoveries of the AC+SBS and the corresponding α values from the power law models

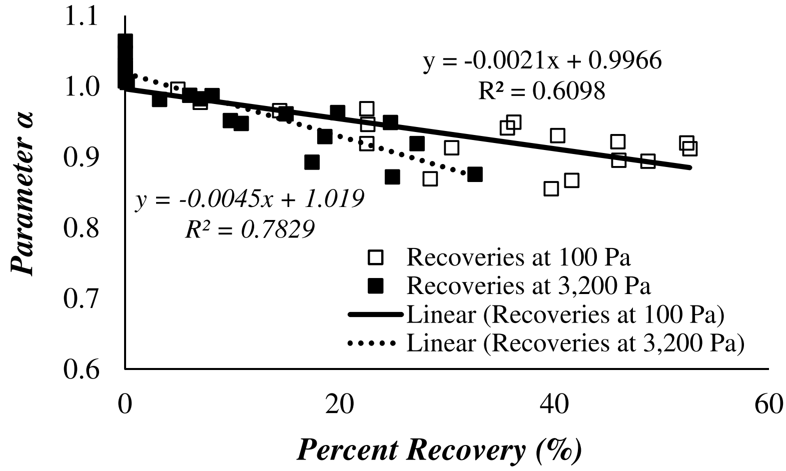

Figure 118 – Individual correlations between the percent recoveries of the AC+SBS at 100 and 3,200 Pa and the corresponding α values from the power law models

Since the R^2 values in Figure 118 differ from each other by more than 27% (and not only 12%, which was the case of the AC+Elvaloy+PPA), there must be another key element acting together with the natural variability of the data. It is hypothesized that the above-mentioned rearrangement of the components of the SBS copolymer and reorganization of the polymer networks during loading in the DSR (POLACCO et al., 2006; ZOOROB et al., 2012) may have contributed to such variations in the *R100* values. This phenomenon may not have occurred with the same intensity at the stress level of 3,200 Pa, since this magnitude of loading is supposed to cause more damage in the binder sample and diminish the effects of the nonlinear response of the polymer on the *R* values after several loading-unloading cycles.

By following the procedures adopted for the previously studied formulations, the analysis of variance was also conducted on the percent recovery and the nonrecoverable compliance values of the AC+SBS. This was made in order to see which variable (temperature or loading time) more greatly affects the elastic response and the rutting potential of the material in the MSCR tests, as well as to conclude if the groups of data – as based on one variable and the other – may be considered as "derived from a common universal group of values" under a level of significance of 5% or not. In this manner, Table 146 shows the reorganized *R100* and *R3200* values to be tested in ANOVA and Table 147 shows the reorganized nonrecoverable compliances ($J_{nr}100$ and $J_{nr}3200$).

Table 146 – Rearranged MSCR testing data of the AC+SBS to be used in the analysis of variance (ANOVA) – percent recovery

stress level of 0.1 kPa (*R100*, %)[a]		stress level of 3.2 kPa (*R3200*, %)[a]	
increasing creep time	increasing temperature	increasing creep time	increasing temperature
41.6	41.6	32.6	32.6
39.7	48.7	24.9	27.2
28.4	52.6	17.4	24.7
22.5	52.3	9.8	19.8
N/A[b]	40.3	N/A[b]	8.1

[a] the starting point in both cases was the temperature of 52°C.
[b] N/A: Not applicable.

Table 147 – Rearranged MSCR testing data of the AC+SBS to be used in the analysis of variance (ANOVA) – nonrecoverable creep compliance

stress level of 0.1 kPa ($J_{nr}100$, kPa^{-1})[a]		stress level of 3.2 kPa ($J_{nr}3200$, kPa^{-1})[a]	
increasing creep time	increasing temperature	increasing creep time	increasing temperature
0.133	0.133	0.156	0.156
0.221	0.275	0.289	0.410
0.453	0.579	0.555	0.997
0.927	1.240	1.219	2.347
N/A[b]	3.142	N/A[b]	5.703

[a] the starting point in both cases was the temperature of 52°C.
[b] N/A: Not applicable.

The ANOVA results for the percent recoveries of the AC+SBS are summarized in Table 148 below. Two very different pictures can be developed from these data, i. e., one at 100 Pa and another at 3,200 Pa. With respect to the lowest stress level, the variations among the data according to temperature and loading time were great enough to exceed the limiting values of $F_{critical}$ and α and recommend the rejection of the null hypothesis H_0 (as a consequence, the alternative hypothesis H_1 is not rejected). In other words, the effects of temperature and loading time on the recoveries at 100 Pa are not similar from the point of view of statistics, and modifications in each variable will lead to a particular creep-recovery response in the AC+SBS during the MSCR test. More simply, the groups of *R100* values as based on creep time and temperature may be taken as derived from different sets of data and one of the variables (in this case, the temperature) will affect the recoveries of the AC+SBS in a much greater way than the other (creep time).

Table 148 – Results from the analysis of variance (ANOVA, *p-value* and *F-value*) as based on the percent recoveries of the AC+SBS

null hypothesis H_0	statistical parameters (ANOVA)				recommendation
	$F_{critical}$	*F-value*	α	*p-value*	
equivalency between *R* values with increasing creep time and temperature, 0.1 kPa	5.5914	7.9430	0.05	0.0258	H_0 is rejected
equivalency between *R* values with increasing creep time and temperature, 3.2 kPa	5.5914	0.0419	0.05	0.8436	H_0 is not rejected

As discussed above, the use of higher temperatures in the MSCR tests at 1/9 s and 100 Pa may have activated the polymeric network and thus improved the elastic response of the AC+SBS. On the other hand, longer loading times perhaps caused irreversible damage in this polymer network during the tests; as a consequence, the formulation was not able to recover greater portions of the total strain during the unloading phase. The occurrence of damage also took place at the stress level of 3,200 Pa, but for both cases (higher temperatures and loading times longer than 1.0 s). This may be the reason why the variations between the two sets of data (*p-value* higher than 0.84 and *F-value* lower than 0.05) were small enough to say that the *R3200* values generated from different temperatures and creep times are derived from a common group of data. In terms of the impacts of each variable on the *R* values, it can be seen that the creep time mostly affected the *R100* values of the formulation than the temperature and the opposite is observed for the *R3200* values.

With respect to the nonrecoverable compliances (Table 149), one may observe that the critical parameters $F_{critical}$ (5.5914) and α (0.05) are not exceeded by the *F-value* and the *p-value* at any stress level, even though the variations in J_{nr} are greater at 3,200 Pa than at 100 Pa. In other words, the compliances of the AC+SBS as a function of creep time and temperature may be taken as similar from a statistical point of view, since the effects of each of these variables on the responses of the material were not enough to place them into different groups of data and the variances are acceptable under the selected level of significance. It is clear that the statistical parameters point to a much greater variation in the $J_{nr}3200$ values than in the $J_{nr}100$ ones, and this is because the accumulated strains generated from higher temperatures and longer creep times can show the differences between the effects of each variable more clearly. However, such differences are acceptable according to the statistical criteria used in this study.

Table 149 – Results from the analysis of variance (ANOVA, *p-value* and *F-value*) as based on the nonrecoverable compliances of the AC+SBS

null hypothesis H_0	statistical parameters (ANOVA)				recommendation
	$F_{critical}$	*F-value*	α	*p-value*	
equivalency between J_{nr} values with increasing creep time and temperature, 0.1 kPa	5.5914	0.9884	0.05	0.3532	H_0 is not rejected
equivalency between J_{nr} values with increasing creep time and temperature, 3.2 kPa	5.5914	1.3595	0.05	0.2818	H_0 is not rejected

It can be concluded from the rheological modeling of the creep-recovery responses of the AC+SBS that, in general, the importance of the initial strain on the reduction in the rut resistance of the formulation decreases with increasing temperature and stress level. At the same time, nonlinearity plays a more visible role on the creep-recovery behavior of the material when t_F is doubled from 4.0 to 8.0 s and when the test temperature is no greater than 64°C. In terms of limiting values for the binder to be recommended for paving applications, the upper limits of 4.0 for the constant *A* and 1.0 for the constant *B* may be used because they match the minimum requirements for J_{nr} and the binder shows a non-null recovery. Some odd cases may be found in the patterns of variation in the constants *A* and *B* with creep time depending on the temperature, but they may be simply interpreted as mathematical fits.

Due to the small changes in the nonlinear term *n* with creep time, no good correlations between this term and the compliance J_{nr} were obtained. However, the parameter α showed a reasonable correlation with the percent recovery *R* (about 0.65) and the variabilities among the individual data were higher at 100 Pa than at 3,200 Pa. In terms of the ANOVA analysis, the effects of loading time and temperature on the *R100* values are not statistically similar because the limiting requirements ($F_{critical}$ and α) were not met. This happened because the polymeric network was activated with increasing temperature, and thus the recoveries increased a little bit with increasing temperature up to the value of 64°C; then, these recoveries constantly decreased with increasing creep time. The *R3200*, $J_{nr}100$ and $J_{nr}3200$ values of the AC+SBS at longer creep times and higher temperatures were found to be statistically similar in the ANOVA analysis, by considering a level of significance of 5%.

The percent recoveries of the AC+SBS+PPA are provided in Table 150, whereas the corresponding rates of decrease with creep time are summarized in Figure 119. These values are typically more sensitive to temperature and loading time than the ones observed for the AC+SBS (Table 135, page 278), especially at 100 Pa, creep times shorter than 4.0 s and temperatures no greater than 64°C. This phenomenon resembles the marked decreases in the recoveries of the AC+PPA (Figure 76, page 207), i. e., the presence of PPA has a negative effect on the sensivitity of the binder properties to variations in the temperature and loading conditions. Other authors have also highlighted the fact that the parameters of the formulations with PPA – either with or without a main modifier – typically show higher sensitivities to an increase in temperature, and this is directly related to the amount of PPA in the composition as well (DOMINGOS and FAXINA, 2015b; JAFARI et al., 2015; JAFARI and BABAZADEH, 2016). Since the recoveries of the AC+SBS+PPA are generally equal to zero at temperatures higher than 64°C and loading times longer than 4.0 s, these conditions may be taken as a critical threshold for the use of the formulation on asphalt pavements.

Table 150 – Percent recoveries at 100 Pa (*R100*) and 3,200 Pa (*R3200*) for the AC+SBS+PPA with increasing loading time and temperature

parameter	creep time (s)	results at each temperature (%)				
		52°C	58°C	64°C	70°C	76°C
R100	1.0	48.8	47.7	46.3	42.2	30.0
	2.0	32.3	21.9	13.2	5.2	0.2
	4.0	29.5	28.1	23.7	10.4	0.7
	8.0	16.0	11.9	4.0	0.0	0.0
R3200	1.0	40.2	29.1	20.6	14.3	6.3
	2.0	26.2	12.3	2.7	0.0	0.0
	4.0	18.0	10.0	3.6	0.0	0.0
	8.0	7.4	0.9	0.0	0.0	0.0

The combination of PPA with SBS increases some *R* values of the binder at t_F = 4.0 s and stress level of 100 Pa, as well as the temperatures of 52 and 58°C and the stress level of 3,200 Pa (creep times up to 4.0 s). The non-null results do not exceed 49% at 100 Pa and 41% at 3,200 Pa. One interesting aspect of binder modification with SBS+PPA – as well as with SBS only, as shown earlier – is that the percent recoveries at 100 Pa and 3,200 Pa approximately reach asymptote values at intermediate creep times (from 2.0 to 4.0 s) and temperatures (typically from 58 to 64°C), and they continue to decrease at t_F = 8.0 s. This can be observed even at the highest temperature (76°C), i. e., the *R100* values decrese from 30 to 0.2% at 2.0 s, slightly increase to 0.7% at 4.0 s and become null at 8.0 s of loading time. As previously discussed and observed in documents from elsewhere in the literature, this reveals that PPA and SBS worked in a synergetic way to modify the asphalt binder and the combination of both yielded a formulation with some improved elastic properties. The above-mentioned rearrangement of the polymer particles and reorganization of the polymeric networks in the SBS copolymer also played a role in the response of the AC+SBS+PPA between 2/9 s and 4/9 s, similarly to what could be seen in the responses of the AC+SBS between 4/9 s and 8/9 s.

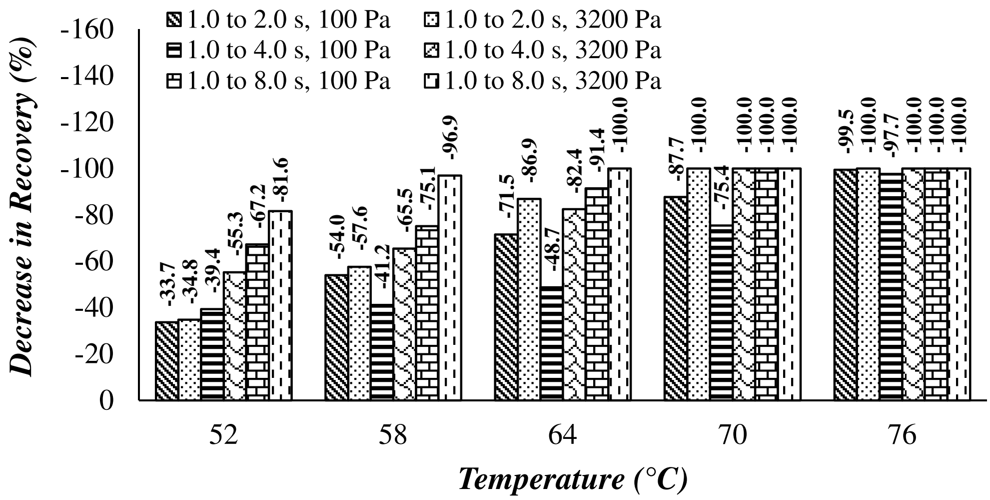

Figure 119 – Percentages of decrease in the recoveries of the AC+SBS+PPA with creep time, temperature and stress level

The nonrecoverable compliances of the formulation with SBS+PPA can be seen in Table 151. The J_{nr} values are lower than the corresponding ones for the AC+SBS (i. e., a higher degree of stiffness) and, at the same time, the percentages of increase in J_{nr} are comparable for the two formulations, Figure 120. The presence of a plateau in the results of *R* can be typically translated as a marked change in the slopes of the log-log curves of J_{nr} at t_F values from 2.0 to 4.0 s, especially at and the stress level of 100 Pa (see examples in Figure 121 for more details and the two binders modified with SBS). Differently from the AC+SBS, the results of the AC+SBS+PPA at 3,200 Pa also indicated the presence of a very small reduction in the slope of the curve of J_{nr} at creep times between 4.0 ans 8.0 s. It is hypothesized that the amount of damage inflicted in the polymer network during the load applications at 3,200 Pa diminished the range of reorganization of this network, which also led to the determination of very small or null recoveries for the loading times of 4.0 and 8.0 s. This gains even more relevance when one observes that the *R* values at 3,200 Pa and t_F = 8.0 s are generally equal to zero not only for the AC+SBS+PPA (Table 150), but also for the AC+SBS (Table 135).

In terms of the numerical values of J_{nr} for the AC+SBS+PPA, the data indicate that the critical threshold observed for the *R* values (*T* = 64°C and t_F = 4.0 s for a stress level of 3,200 Pa) can also be taken in the determination of the limiting conditions for the use of this material on pavements as based on its rut resistance. This is because the susceptibility to rutting increases at much higher rates when *T* or t_F goes beyond the maximum selected values (i. e., 70-76°C and 8.0 s). In other words, the use of the AC+SBS+PPA under more severe climate and loading conditions may cause early premature failure of the mixture because the compliances can easily overcome 5.0 kPa^{-1} at 100 Pa and 7.0 kPa^{-1} at 3,200 Pa. The other results commonly range between 0.06 and 3.0 kPa^{-1} at 100 Pa and between 0.08 and 4.0 kPa^{-1} at 3,200 Pa.

Table 151 – Nonrecoverable compliances at 100 Pa (*J_{nr}100*) and 3,200 Pa (*J_{nr} 3200*) for the AC+SBS+PPA with increasing loading time and temperature

parameter	creep time (s)	results at each temperature (kPa^{-1}), J_{nr} > 4.0 kPa^{-1} is in bold				
		52°C	58°C	64°C	70°C	76°C
J_{nr}100	1.0	0.069	0.166	0.401	0.971	2.533
	2.0	0.145	0.409	1.110	2.896	**6.889**
	4.0	0.261	0.657	1.718	**4.960**	**12.800**
	8.0	0.542	1.472	**4.250**	**11.236**	**26.497**
J_{nr}3200	1.0	0.082	0.234	0.634	1.604	3.920
	2.0	0.161	0.482	1.367	3.505	**8.141**
	4.0	0.322	0.920	2.541	**6.727**	**16.381**
	8.0	0.651	1.932	**5.521**	**14.890**	**36.260**

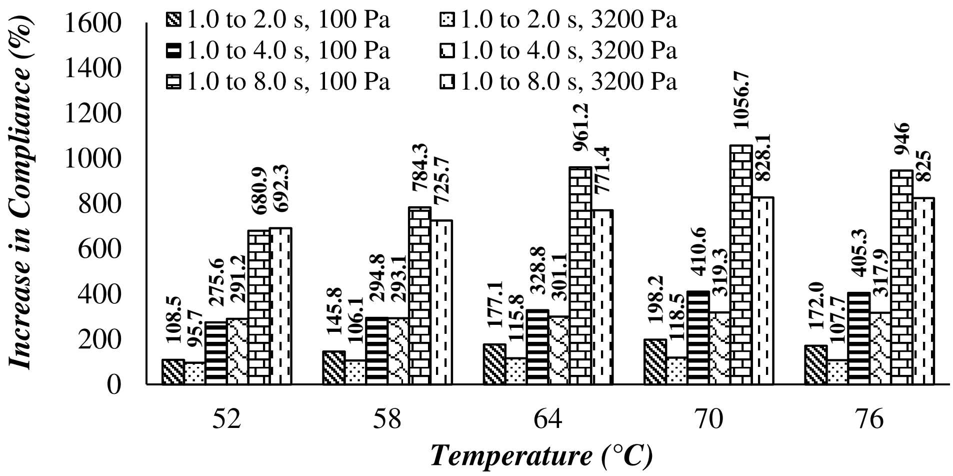

Figure 120 – Percentages of increase in the nonrecoverable compliances of the AC+SBS+PPA with creep time, temperature and stress level

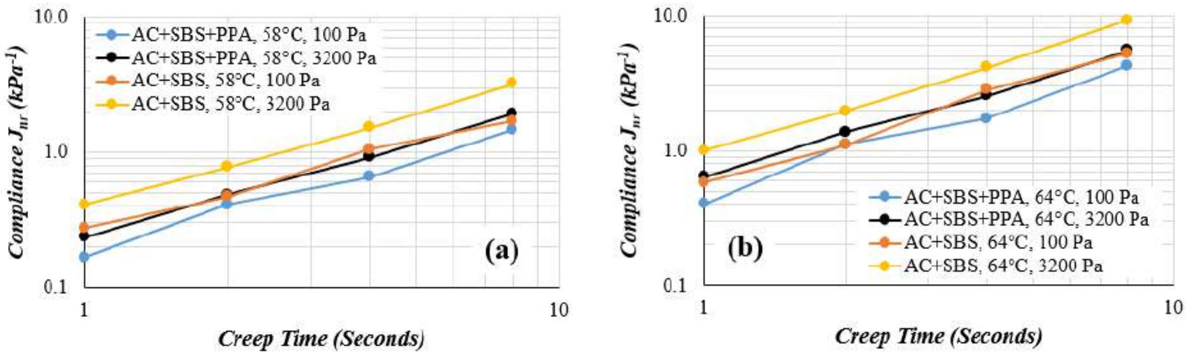

Figure 121 – Plots of the nonrecoverable compliance J_{nr} versus loading time (log-log scale) for the AC+SBS and the AC+SBS+PPA at the temperatures of (a) 58°C; and (b) 64°C

The stress sensitivity data of the AC+SBS+PPA (that is, the parameter $J_{nr,\ diff}$) are shown in Table 152. Other than indicating that the formulation is not overly sensitive to stress level at any temperature and creep time, these results are also considerably lower than the corresponding ones of the AC+SBS (Table 137). As emphasized above, the combination of PPA with SBS copolymer was able to yield better results in the MSCR test and give one step further into the compatibility of the polymer with the binder, even though this improved compatibility was not enough to reach the zone of high elasticity (Figure 65, page 181). The minimum $J_{nr,\ diff}$ values are all located at the creep time of 2.0 s, which is exactly the time after which the J_{nr} curves at 100 Pa deviate from the original trendlines and get as close as possible to the ones at 3,200 Pa (see Figure 121). As a consequence, the compliances at 100 Pa and loading time of 4.0 s increase at lower rates than the corresponding values at 3,200 Pa, and this rate increases a little bit when the loading time is equal to 8.0 s. This pattern of response could be seen within the whole temperature range used in the MSCR tests.

Table 152 – Percent differences in nonrecoverable compliances ($J_{nr,\ diff}$) for the AC+SBS+PPA with increasing creep time and temperature

creep time	$J_{nr,\ diff}$ values (%) at each creep time and temperature				
(s)	52°C	58°C	64°C	70°C	76°C
1.0	18.4	40.6	58.2	65.2	54.7
2.0	11.1	17.9	23.1	21.0	18.2
4.0	23.3	40.0	48.0	35.6	28.0
8.0	20.1	31.3	29.9	32.5	36.8

It is interesting to note that the aforementioned phenomenon can be seen in the AC+SBS as well, i. e., there is an inflection point at $t_F = 4.0$ s in which the J_{nr} values at 100 Pa get as close to the values at 3,200 Pa as possible ($J_{nr,\ diff}$ reaches a minimum numerical result, see Table 137, page 280). In graphical terms, the curve of the parameter $J_{nr}100$ approaches the one of $J_{nr}3200$ at t_F values up to 4.0 s, and then deviates from it (Figure 121). Such loading time also refers to the testing condition in which the *R100* values of the AC+SBS enter at the plateau zone, i. e., the results of *R100* approach asymptote values at t_F = 4.0 s and 8.0 s and the percentages of decrease in recovery tend not to increase anymore or increase with a much lower rate (Figure 111, page 278). The same discussion can be applied to the AC+SBS+PPA as well (Figure 119). The reasons for these results are similar for the two SBS-modified binders, i. e., rearrangement of the polymer network, nonlinear response of the polymer chains and a more overall elastic behavior of the formulation. The difference in the inflection point (t_F = 4.0 s for the AC+SBS and t_F = 2.0 s for the AC+SBS+PPA) may be explained by the interaction between PPA and SBS and the changes in the structure of the binder phase after the addition of PPA to the formulation.

The traffic levels of the AC+SBS+PPA at each temperature and loading condition are summarized in Table 153. The degrees of improvement in the $J_{nr}3200$ values when compared with the AC+SBS are reflected in these levels as follows: (a) acceptance of standard traffic levels at 76°C and 1/9 s (no traffic levels in the AC+SBS); (b) increases by one grade in these levels at 70°C and the creep-recovery times of 1/9 s (from standard to heavy) and 2/9 s (from "no traffic" to standard); (c) the possibility of use of the AC+SBS+PPA on pavements with standard levels, a maximum temperature of 64°C and loading times of 4.0 s ("no traffic" in the AC+SBS); and (d) increases by one grade at 52°C and the longest creep times (from very heavy to extremely heavy at t_F = 4.0 s and from heavy to very heavy at t_F = 8.0 s). No changes were identified in the other temperature and loading conditions, even though the J_{nr} values are numerically lower for the AC+SBS+PPA as discussed above. In other words, the higher levels of stiffness provided by the addition of PPA could extend the range of climate and loading conditions under which the formulation may be used in the asphalt pavement.

Table 153 – Adequate traffic levels for the AC+SBS+PPA with increasing creep time and temperature based on the standardized Superpave® criteria

creep time	traffic levels for each temperature[a]				
(s)	52°C	58°C	64°C	70°C	76°C
1.0	E	E	V	H	S
2.0	E	E	H	S	-
4.0	E	V	S	-	-
8.0	V	H	-	-	-

[a] S = standard; H = heavy; V = very heavy; E = extremely heavy.

The equations from Huang (2004) and Pereira et al. (1998, 2000) were used in the analysis of the degrees of correlation between J_{nr} and loading time, similarly to what was done for the other formulations. The results for the first set of equations – tire contact radius of 6.0 inches in the equation from Huang (2004) and the one from Pereira et al. (1998) – are shown in Table 154, whereas the correlations between the actual and predicted traffic levels are provided in Table 155. It can be seen that, although the correlations are at least excellent in both cases ($R^2 > 0.91$), the predictions of the actual traffic levels in the binder are far from promising. There are no more than three points of similarity within the whole temperature interval, and this becomes even worse when the material is tested at 70 and 76°C. As previously noticed for other materials, the data suggest that the applicability of such equations is restricted to lower pavement temperatures ($T <$ 64°C) and some loading times (no longer than 4.0 s).

Table 154 – Regression equations and coefficients of determination between the $J_{nr}3200$ values of the AC+SBS+PPA and the corresponding vehicle speeds according to the equations by Pereira et al. (1998, 2000) and Huang (2004)

source and data	temperature (in °C)	equation	R^2
Pereira et al. (1998)	52	$y = 0.6440e^{-0.028x}$	0.9138
Pereira et al. (2000)	52	$y = -0.0084x + 0.6192$	1.0000
Huang (2004) $r = 6$ in	52	$y = 0.6443e^{-0.033x}$	0.9142
	58	$y = 1.9057e^{-0.034x}$	0.9185
	64	$y = 5.4381e^{-0.035x}$	0.9210
	70	$y = 14.6560e^{-0.036x}$	0.9200
	76	$y = 35.2910e^{-0.036x}$	0.9109
Huang (2004) $r = 3.68$ in	52	$y = 0.6432e^{-0.054x}$	0.9145
	58	$y = 1.9022e^{-0.055x}$	0.9188
	64	$y = 5.4277e^{-0.056x}$	0.9212
	70	$y = 14.6280e^{-0.058x}$	0.9202
	76	$y = 35.2220e^{-0.058x}$	0.9111

Table 155 – Comparisons between the actual traffic levels of the AC+SBS+PPA and the ones obtained from Huang (2004) and Pereira et al. (1998)

t_F (s)[d]	actual[a] and estimated[b, c] traffic levels at each temperature[d]				
	52°C	58°C	64°C	70°C	76°C
1.0	**E (V/E) [V/E]**	**E [V/E]**	**V [V/E]**	H [V/E]	S [V/E]
2.0	**E (V/E) [V/E]**	**E [V/E]**	H [V/E]	S [V/E]	-
4.0	E (H) [H]	V [H]	S [H]	-	-
8.0	V (S) [H]	**H [H]**	-	-	-

[a] S = standard; H = heavy; V = very heavy; E = extremely heavy (AASHTO M320-09 standard, Table 3).
[b] (parentheses) = traffic levels from Pereira et al. (1998).
[c] [brackets] = traffic levels from Huang (2004), $r = 6$ in.
[d] similarities among the rankings are highlighted in bold, t_F = creep time.

With respect to the equations from Huang (2004) – tire contact radius of 3.68 in – and Pereira et al. (2000) in Table 154, their corresponding degrees of correlation and the points of similarity with the actual traffic levels of the AC+SBS+PPA (Table 156), one may observe that such correlations are also very high ($R^2 > 0.91$). However, the deficiencies in the predictions of the actual traffic levels are a little bit worse for these equations. For example, the equation from Pereira et al. (2000) could not accurately estimate any traffic level of the AC+SBS+PPA at the temperature of 52°C, which was possible for the other two equations by Huang (2004) and Pereira et al. (1998) at 1/9 s and 2/9 s. However, the scattering of the data at all temperatures clearly indicate that the use of one or another equation in the estimation of the appropriate traffic level of the binder is rather limited.

Table 156 – Comparisons between the actual traffic levels of the AC+SBS+PPA and the ones obtained from the equations by Huang (2004) and Pereira et al. (2000)

t_F (s)[d]	actual[a] and estimated[b, c] traffic levels at each temperature[d]				
	52°C	58°C	64°C	70°C	76°C
1.0	**E** (H) **[V/E]**	**E [V/E]**	**V [V/E]**	H [V/E]	S [V/E]
2.0	**E** (H) **[V/E]**	**E [V/E]**	H [V/E]	S [V/E]	-
4.0	E (H) [H]	V [H]	S [H]	-	-
8.0	V (H) [H]	**H [H]**	-	-	-

[a] S = standard; H = heavy; V = very heavy; E = extremely heavy (AASHTO M320-09 standard, Table 3).
[b] (parentheses) = traffic levels from Pereira et al. (2000).
[c] [brackets] = traffic levels from Huang (2004), r = 3.68 in.
[d] similarities among the rankings are highlighted in bold, t_F = creep time.

Table 157 draws comparisons amongst the traffic levels of the AC+SBS+PPA as based on the current Superpave® criteria and the one proposed in this dissertation. No differences in the estimated traffic levels could be identified at any MSCR testing temperature, which suggests that the degree of nonlinearity of the AC+SBS+PPA at very long creep times is acceptable and justifies its use on pavements with high percentages of slow-moving vehicles. Since the AC+SBS showed a decrease of one grade in this level at 64°C when moving to the new criterion (Table 142, page 283), the data also indicate that the rut resistance of the AC+SBS+PPA was markedly improved after the addition of PPA and its combination with SBS. The fact that the AC+SBS+PPA is not an overly stress sensitive material at any of the five selected temperatures (Table 152) may also have contributed to a smaller degree of nonlinearity; as a consequence, the material was able to retain its original traffic levels at longer creep times. Hence, the formulation with SBS+PPA has a broader range of uses for paving applications when compared with the formulation with SBS only, including the high PG grade temperature (76°C).

Table 157 – Traffic levels of the AC+SBS+PPA with increasing loading time and temperature in the current and proposed criteria

temperature (in °C)	No. of required MSCR tests[b]	Superpave® designations (current and new criteria)[a, c]	
		current criterion	new criterion
52	4	**52E-xx**	**52E-xx**
58	4	**58E-xx**	**58E-xx**
64	4	**64V-xx**	**64V-xx**
70	3	**70H-xx**	**70H-xx**
76	2	**76S-xx**	**76S-xx**

[a] S = standard; H = heavy; V = very heavy; E = extremely heavy (AASHTO M320-09 standard, Table 3).
[b] minimum number of MSCR tests to determine the adequate traffic level in the proposed classification.
[c] similarities among the classifications are highlighted in bold.

The creep-recovery responses of the AC+SBS+PPA at several creep times and temperatures and their comparisons with the ones from the AC+SBS indicate that, by adding PPA and decreasing the SBS content, the percent recoveries showed higher sensitivity to loading time and temperature and the nonrecoverable compliances were decreased. As a beneficial consequence of these lower J_{nr} values, the AC+SBS+PPA can deal with heavier traffic levels than the AC+SBS at some pavement temperatures and loading times, e. g., 76°C and 1/9 s (from "no traffic" to standard) and 70°C and 1/9 s (from standard to heavy). Differently from the AC+SBS, the AC+SBS+PPA is not too sensitive to an increase in the stress level from 100 to 3,200 Pa at any pavement temperature: in numerical terms, the parameter $J_{nr,\ diff}$ is always lower than the upper limit of 75% for the AC+SBS+PPA and exceeds this limiting value at the temperatures of 58°C (8/9 s), 64°C (1/9 s) and 76°C (1/9 s) for the AC+SBS. The current and proposed classifications for determining the adequate traffic levels yielded similar results for the AC+SBS+PPA, and this suggests that the binder has an acceptable degree of nonlinearity at longer creep times.

Table 158 is a summary of the model parameters A, B, n and α of the modified power model for the AC+SBS+PPA. Again, increases in the loading time, temperature and stress level may be interpreted as a lower importance of the initial strain (A values) and increases in the roles of the strain rate (B values) and nonlinearity (n values) on the lower rutting resistances of the binder in the MSCR tests. In other words, the material becomes more susceptible to rutting primarily due to the higher strain rates, followed by a slight increase in its nonlinear response during the application of loading-unloading cycles. The presence of much higher percentages of decrease in A with loading time (3-23%) when compared with the relatively small percentages for B (2-11%) and n (< 2%) suggest that both elements act together in compensating for the reductions in the initial strain of the material with increasing severity in the tests.

Table 158 – Numerical values and variations in the parameters/constants *A, B, n* and *α* from the power law equations by Saboo and Kumar (2015) with increasing temperature and creep time and considering the AC+SBS+PPA

temperature	test times	parameter A^a		parameter B^a		parameter n^a		parameter α^a	
		0.1 kPa	3.2 kPa	0.1 kPa	3.2 kPa	0.1 kPa	3.2 kPa	0.1 kPa	3.2 kPa
52°C	1/9 s	0.0143	0.4654	0.8097	0.8217	0.9988	0.9951	0.8087	0.8117
	2/9 s	0.0128 (-10.5)	0.4138 (-11.1)	0.8294 (2.4)	0.8441 (2.7)	0.9912 (-0.8)	0.9877 (-0.7)	0.8221 (1.7)	0.8337 (2.7)
	4/9 s	0.0124 (-13.3)	0.3996 (-14.1)	0.8414 (3.9)	0.8743 (6.4)	0.9998 (0.1)	0.9881 (-0.7)	0.8412 (4.0)	0.8639 (6.4)
	8/9 s	0.0113 (-21.0)	0.3606 (-22.5)	0.8719 (7.7)	0.9148 (11.3)	0.9946 (-0.4)	0.9842 (-1.1)	0.8671 (7.2)	0.9003 (10.9)
58°C	1/9 s	0.0337	1.1213	0.8527	0.8829	1.0054	0.9978	0.8572	0.8809
	2/9 s	0.0302 (-10.4)	0.9945 (-11.3)	0.8873 (4.1)	0.9198 (4.2)	0.9946 (-1.1)	0.9925 (-0.5)	0.8825 (3.0)	0.9129 (3.6)
	4/9 s	0.0287 (-14.8)	0.9569 (-14.7)	0.8814 (3.4)	0.9407 (6.5)	1.0150 (1.0)	0.9985 (0.1)	0.8947 (4.4)	0.9394 (6.6)
	8/9 s	0.0264 (-21.7)	0.8751 (-22.0)	0.9192 (7.8)	0.9797 (11.0)	1.0095 (0.4)	1.0005 (0.3)	0.9280 (8.3)	0.9801 (11.3)
64°C	1/9 s	0.0792	2.7189	0.8861	0.9332	1.0093	1.0014	0.8944	0.9345
	2/9 s	0.0717 (-9.5)	2.4503 (-9.9)	0.9326 (5.2)	0.9754 (4.5)	0.9975 (-1.2)	0.9981 (-0.3)	0.9303 (4.0)	0.9735 (4.2)
	4/9 s	0.0675 (-14.8)	2.3327 (-14.2)	0.9174 (3.5)	0.9816 (5.2)	1.0200 (1.1)	1.0050 (0.4)	0.9357 (4.6)	0.9864 (5.6)
	8/9 s	0.0638 (-19.4)	2.2280 (-18.1)	0.9668 (9.1)	1.0152 (8.8)	1.0064 (-0.3)	1.0096 (0.8)	0.9730 (8.8)	1.0250 (9.7)
70°C	1/9 s	0.1788	6.3960	0.9113	0.9656	1.0105	1.0031	0.9208	0.9685
	2/9 s	0.1678 (-6.2)	6.0162 (-5.9)	0.9671 (6.1)	1.0021 (3.8)	0.9987 (-1.2)	1.0014 (-0.2)	0.9658 (4.9)	1.0035 (3.6)
	4/9 s	0.1569 (-12.2)	5.6941 (-11.0)	0.9595 (5.3)	1.0073 (4.3)	1.0095 (-0.1)	1.0062 (0.3)	0.9686 (5.2)	1.0136 (4.7)
	8/9 s	0.1507 (-15.7)	5.6317 (-11.9)	1.0019 (9.9)	1.0336 (7.0)	1.0063 (-0.4)	1.0149 (1.2)	1.0083 (9.5)	1.0491 (8.3)
76°C	1/9 s	0.3864	14.3691	0.9359	0.9842	1.0070	1.0024	0.9424	0.9866
	2/9 s	0.3735 (-3.3)	13.8901 (-3.3)	0.9901 (5.8)	1.0144 (3.1)	1.0002 (-0.7)	1.0030 (0.1)	0.9903 (5.1)	1.0174 (3.1)
	4/9 s	0.3479 (-10.0)	13.4176 (-6.6)	0.9939 (6.2)	1.0247 (4.1)	1.0049 (-0.2)	1.0082 (0.6)	0.9987 (6.0)	1.0331 (4.7)
	8/9 s	0.3413 (-11.7)	13.3405 (-7.2)	1.0222 (9.2)	1.0434 (6.0)	1.0108 (0.4)	1.0188 (1.6)	1.0332 (9.6)	1.0630 (7.7)

[a] the percentages of variation reported in parenthesis refer to the changes in the parameter when moving from 1.0 s to the creep time into question (2.0, 4.0 or 8.0 s).

By comparing the results of the AC+SBS+PPA with those of the AC+SBS (Table 143, page 285), it is possible to say that the formulation with SBS+PPA shows a higher rutting resistance due to the less accumulated strain in the first few cycles. In mathematical terms, this may be translated into lower *A* values for the AC+SBS+PPA than for the AC+SBS. In average, the percentages of reduction from the AC+SBS to the AC+SBS+PPA range from 31 to 46% depending on the temperature, stress level and creep time, and they tend to be higher at 3,200 Pa than at 100 Pa. On the other hand, the variations in *B* and *n* from one formulation to the other do not overcome 7.0% in any test condition, and the numerical values are typically higher for the AC+SBS+PPA than for the AC+SBS when the temperature ranges from 52 to 64°C.

The comparisons within the model parameters *A* and *B* for the AC+SBS and the AC+SBS+PPA are graphically illustrated in Figure 122. Each data point is characterized by one temperature and one t_F value and, since five temperatures and four loading times were used in the tests, a total of 20 data points (4 × 5) is obtained. The ratio "AC+SBS+PPA / AC+SBS" means that the result of the AC+SBS+PPA was divided by the corresponding one of the AC+SBS and, if the ratio is higher than unity, the parameter into question is higher for the formulation with SBS+PPA than for the formulation with SBS alone and vice versa. As it can be seen, all the data points associated with the ratios of the *A* values are far below the equality line and the ones of the *B* values are right above or below this equality line. These conclusions are in agreement with the ones drawn for the formulations with crumb rubber and rubber+PPA, in that the major difference between the rutting resistances of the formulations with and without PPA is due to the initial strain accumulated by the asphalt binder.

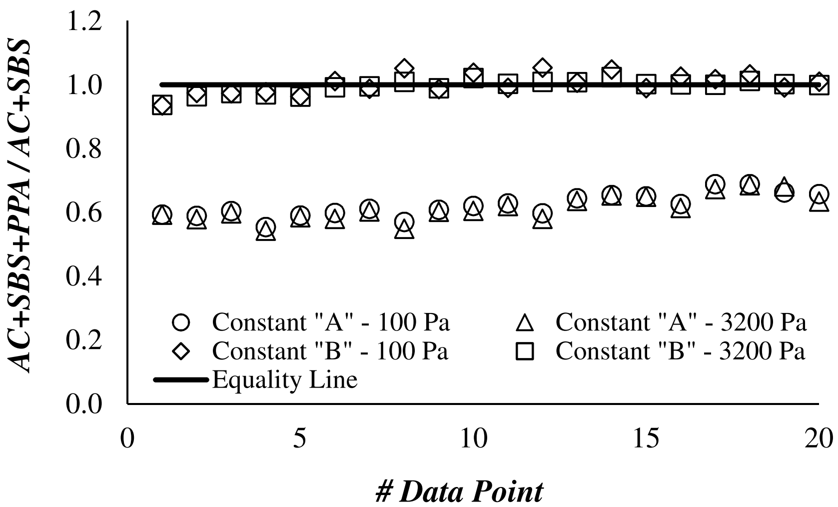

Figure 122 – Plots of the data points associated with the ratios of the constants *A* and *B* for the AC+SBS+PPA to the corresponding ones for the AC+SBS (each data point is characterized by one temperature and loading time)

One interesting aspect about the variations in the parameters of the power model for the AC+SBS+PPA is worth to be mentioned. Due to the effects of the rearrangement and reorganization of the polymer networks in the formulation on the percent recoveries at creep times between 2.0 and 4.0 s and the lowest stress level (100 Pa), the percentages of increase or reduction in the parameters of the power model show some kinds of "inflection points" with increasing loading time. Similar findings may be identified in the data values for the AC+SBS at the creep times of 4.0 s and 8.0 s as well, see Table 143 (page 285). More simply, the particular characteristics of the polymeric modification type may be associated with "breaks" in the percentages of variation of the model parameters from one loading time to the other. These points may be described by one of the following characteristics:

- percentages of increase/decrease from 4.0 to 8.0 s considerably higher than the corresponding values from 1.0 to 2.0 s, which is commonly observed for the constant *B* at all temperatures and stress levels, the parameter *n* at 70 and 76°C and the constant *A* at 52 and 58°C;
- rates of variation in these percentages of increase/decrease are reduced when moving from 4.0 to 8.0 s, which is the case of the constant *A* at 70 and 76°C; and
- the presence of a "vertex" when plotting the percentages of variation in the *n* and *B* values with increasing creep time at some temperatures and stress levels, e. g., 52°C and 100 Pa.

In terms of the limiting properties and parameters for the use of the AC+SBS+PPA on pavements according to the results from MSCR, the data in Table 158 indicate that the *A* value is around 2.33 and the *B* value is approximately equal to unity (0.9816) at the high pavement temperature of 64°C, stress level of 3,200 Pa and creep time of 4.0 s. The α value is also very close to one (0.9864), whereas the *n* value is equal to 1.0050. These numerical results are in accordance with the recommendations from the literature (SARKAR, 2016; SABOO and KUMAR, 2015), in that *A* values much greater than unity and *B* and α values higher than one suggest the existence of a high rutting potential in the binder. Once these limiting conditions are similar to the ones of the AC+SBS, it can be said that the degrees of improvement in the formulation after the addition of PPA and the use of a lower SBS content are somehow limited from the point of view of the binder properties.

The levels of correlation between the *A* and *B* values and the creep time t_F at the pavement temperatures of 64 and 70°C are given in Figure 123 and Figure 124, respectively. It can be observed that the correlations for *B* are more affected by the typical polymeric-type behavior during the MSCR tests as described above, especially at 100 Pa (R^2 value is lower than the corresponding one for *A*). As the stress level increases, the *B* values tend to show higher correlatiosn with creep time than the *A* values (0.8413 for *B* and 0.7608 for *A*). The data point for *B* at t_F = 2.0 s and 100 Pa looks like an outlier within the data set, which is in accordance with the slight increases in the *R* values when moving from 2/9 s to 4/9 s (see Table 150, page 294) and the minimum $J_{nr,\,diff}$ values at this same creep time (see Table 152, page 297). In terms of the *A* values, it can be seen that the slopes of the regression equations are lower for the AC+SBS+PPA than for the AC+SBS at both stress levels. This points out that the AC+SBS+PPA shows a smaller variation in the accumulation of the initial strain in the sample with increasing loading time than the AC+SBS.

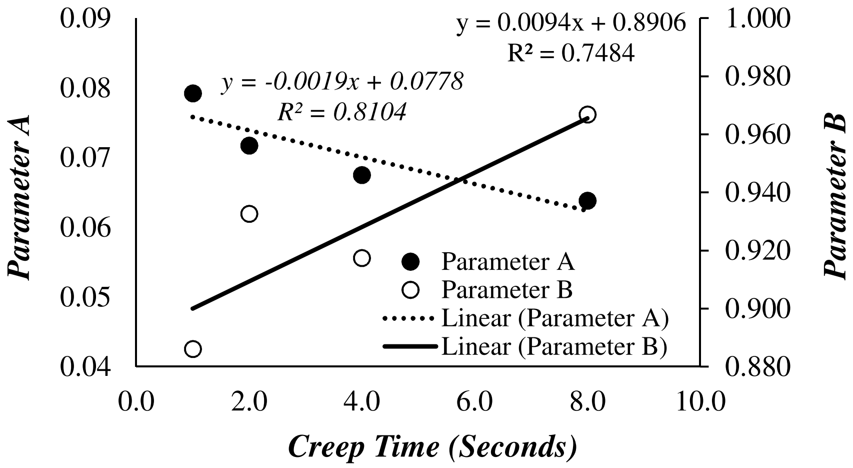

Figure 123 – Correlations between the creep time and the constants *A* and *B* from the model by Saboo and Kumar (2015), temperature of 64°C and stress level of 100 Pa – AC+SBS+PPA

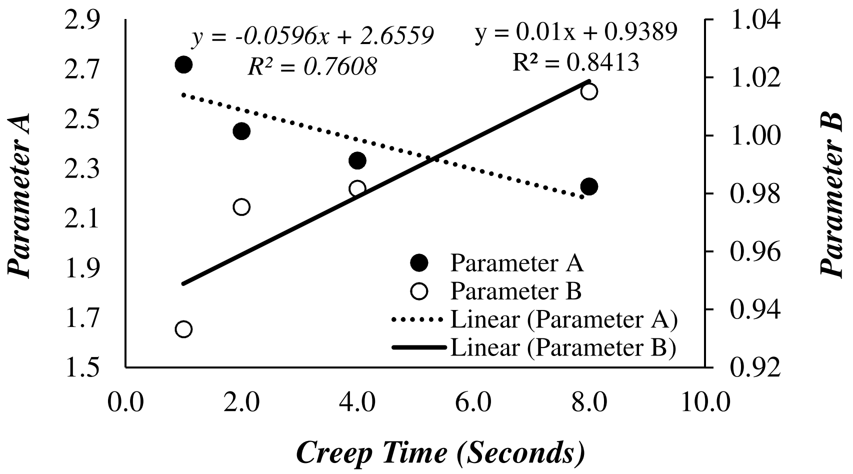

Figure 124 – Correlations between the creep time and the constants *A* and *B* from the model by Saboo and Kumar (2015), temperature of 64°C and stress level of 3,200 Pa – AC+SBS+PPA

Figure 125 (stress level of 100 Pa) and Figure 126 (stress level of 3,200 Pa) depict the same correlations for the AC+SBS+PPA, but considering the pavement temperature of 70°C. Again, the data values for the constant *B* at 2/9 s and 100 Pa look like outliers within the results of rheological modeling, which is why the coefficient of determination R^2 is lower for *B* than for *A* at such stress level. This effect is minimized at 3,200 Pa and, as a consequence, the *B* values have a higher correlation than the *A* values. The gradients of the regression trendlines of the constant *A* are lower for the AC+SBS+PPA than for the AC+SBS at 100 Pa, and the results are approximately the same at 3,200 Pa. With respect to the constant *B*, these gradients are quite similar for the two formulations at 100 Pa and smaller for the AC+SBS+PPA at 3,200 Pa. One more time, the parameters of the AC+SBS+PPA show a lower sensitivity to modifications in the creep time than the corresponding ones of the AC+SBS.

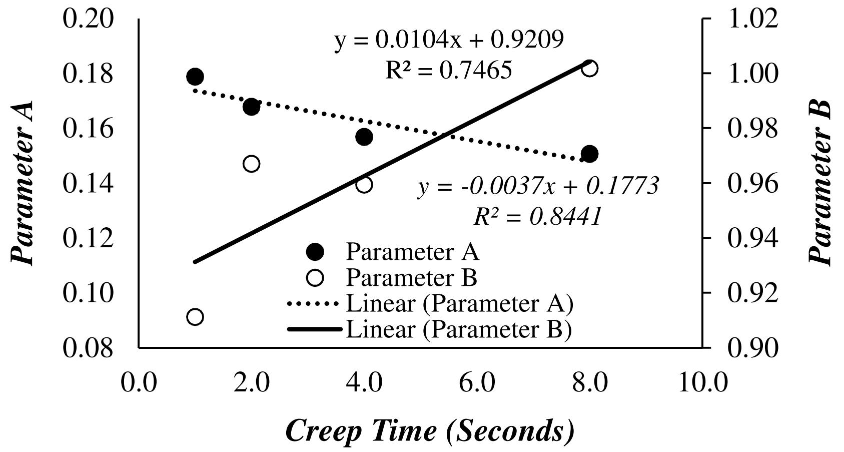

Figure 125 – Correlations between the creep time and the constants *A* and *B* from the model by Saboo and Kumar (2015), temperature of 70°C and stress level of 100 Pa – AC+SBS+PPA

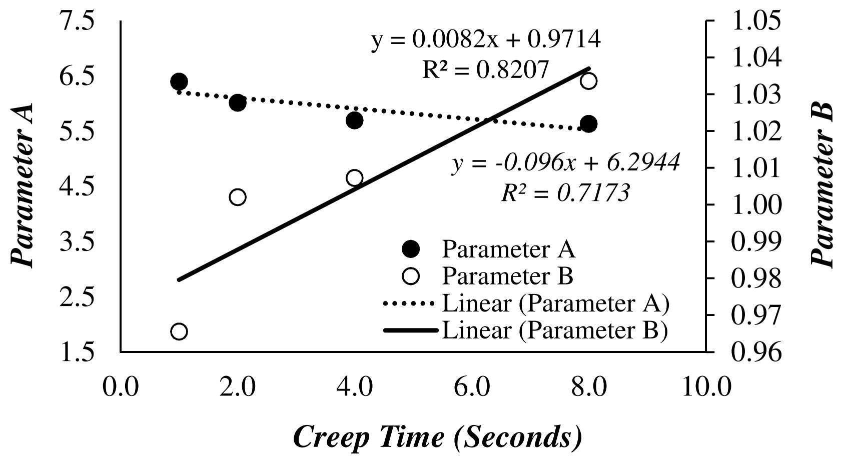

Figure 126 – Correlations between the creep time and the constants *A* and *B* from the model by Saboo and Kumar (2015), temperature of 70°C and stress level of 3,200 Pa – AC+SBS+PPA

The correlations and regression equations reported in Table 159 refer to the parameters *A* and *B* of the modified power model, as applied to the AC+SBS+PPA at all the pavement temperatures. No reverses in the signals of the gradients of the regression equations may be seen, and the R^2 values vary from 0.71 to 0.97 in all cases (i. e., the correlations are from good to excellent). These correlations are better for the *B* values than for the *A* values at 3,200 Pa in a general context, and the opposite is observed at 100 Pa. This may be explained by the influence of the polymer networks on the elastic behavior of the material in the MSCR tests and the appearance of outliers within the groups of values for *A*, as discussed above. It may also be observed for the AC+SBS at several test temperatures, especially the ones lower than 70°C – see Table 144 (page 289) for further details. However, the overall pattern of behavior (i. e., decreases in *A* and increases in *B* with increasing creep time) remains unchanged within the whole temperature range and for the two selected stress levels.

Table 159 – Degrees of correlation between the parameters *A* and *B* (modified power model) and the creep time t_F for the AC+SBS+PPA

T (°C)	stress (kPa)	linear regression equations and R^2 values (in parenthesis)[a]	
		parameter *A*	parameter *B*
52	0.1	y = -0.0004x + 0.0141 (0.8459)	y = 0.0083x + 0.8071 (0.9663)
	3.2	y = -0.0129x + 0.4583 (0.8526)	y = 0.0129x + 0.8155 (0.9754)
58	0.1	y = -0.0009x + 0.0332 (0.8455)	y = 0.0080x + 0.8522 (0.8193)
	3.2	y = -0.0301x + 1.0998 (0.8267)	y = 0.0126x + 0.8837 (0.9256)
64	0.1	y = -0.0019x + 0.0778 (0.8104)	y = 0.0094x + 0.8906 (0.7484)
	3.2	y = -0.0596x + 2.6559 (0.7608)	y = 0.0100x + 0.9389 (0.8413)
70	0.1	y = -0.0037x + 0.1773 (0.8441)	y = 0.0104x + 0.9209 (0.7465)
	3.2	y = -0.0960x + 6.2944 (0.7173)	y = 0.0082x + 0.9714 (0.8207)
76	0.1	y = -0.0062x + 0.3856 (0.8202)	y = 0.0100x + 0.9482 (0.7319)
	3.2	y = -0.1312x + 14.2460 (0.7264)	y = 0.0073x + 0.9894 (0.8254)

[a] the Y-axis is associated with the parameter (*A* or *B*), whereas the X-axis is associated with t_F.

With respect to the correlations between the parameters *n* and *α* and the t_F values (Table 160), one may realize that the parameter associated with nonlinearity (*n*) typically depicts good to excellent correlations with the loading time at 3,200 Pa and the temperatures of 64, 70 and 76°C. On the other hand, these correlations are poor (< 0.45) at the stress level of 100 Pa and there is almost total absence of correlation (< 0.02) at 52 and 64°C. Therefore, no good overall correlations between *n* and J_{nr} must be expected for the AC+SBS+PPA. In fact, a complementary analysis indicated that the R^2 value is of about 0.346 when all the *n* and J_{nr} values are plotted in a semi-log chart. However, the promising R^2 values obtained at 3,200 Pa suggest that there may exist a reasonable correlation between *n* and $J_{nr}3200$: according to Figure 127, the coefficient of determination is approximately equal to 0.706 and one parameter is directly related to the other (gradient is positive). Thus, it may be possible to suppose that there is a common pattern of behavior for the *n* and $J_{nr}3200$ values, i. e., *n* and $J_{nr}3200$ increase with increasing creep time at a fixed relationship between the two proportions, at least within the same temperature.

Table 160 – Degrees of correlation between the parameters *n* and *α* (modified power model) and the creep time t_F for the AC+SBS+PPA

T (°C)	stress (kPa)	linear regression equations and R^2 values (in parenthesis)[a, b]	
		parameter *n*	parameter *α*
52	0.1	y = -0.0001x + 0.9967 (0.0136)	y = 0.0081x + 0.8044 (0.9790)
	3.2	y = -0.0012x + 0.9934 (0.6861)	y = 0.0122x + 0.8066 (0.9673)
58	0.1	y = 0.0013x + 1.0011 (0.2334)	y = 0.0093x + 0.8559 (0.9478)
	3.2	y = 0.0007x + 0.9946 (0.4335)	y = 0.0132x + 0.8787 (0.9505)
64	0.1	y = 0.0004x + 1.0069 (0.0163)	y = 0.0098x + 0.8966 (0.8883)
	3.2	y = 0.0014x + 0.9981 (0.8213)	y = 0.0115x + 0.9369 (0.9030)
70	0.1	y = 9E-05x + 1.0059 (0.0026)	y = 0.0106x + 0.9261 (0.8432)
	3.2	y = 0.0019x + 0.9994 (0.9341)	y = 0.0102x + 0.9705 (0.9024)
76	0.1	y = 0.0010x + 1.0021 (0.4498)	y = 0.0011x + 0.9499 (0.8273)
	3.2	y = 0.0024x + 0.9990 (0.988)	y = 0.0098x + 0.9882 (0.9121)

[a] the Y-axis is associated with the parameter (*n* or *α*), whereas the X-axis is associated with t_F.
[b] changes in the signal of the slope of the regression trendlines are highlighted with a grey-shaded box.

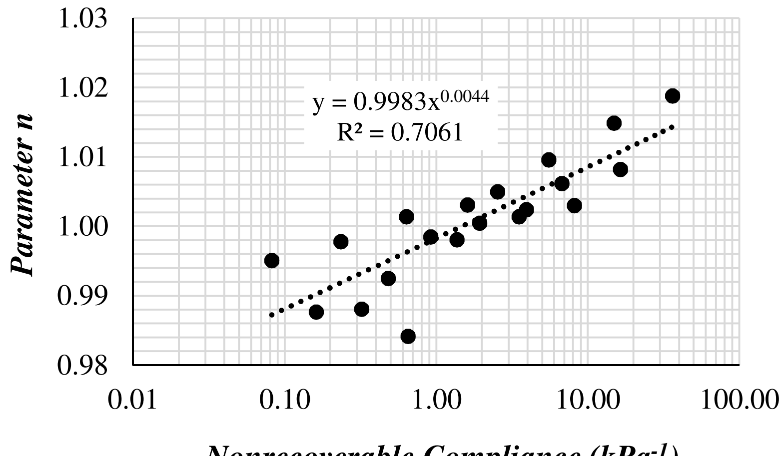

Figure 127 – Degree of correlation between the nonrecoverable compliances of the AC+SBS+PPA at 3,200 Pa and the corresponding *n* values from the power law models

Figure 128 shows the overall degree correlation between the *α* values and the corresponding percent recoveries of the AC+SBS+PPA. The gradient of the regression equation is negative, which means that *α* decreases with increasing recovery. However, the overall correlation (≈ 0.69) indicates that either the *R100* or the *R3200* values may depict a much worse correlation with α than the others, as previously observed for the AC+SBS. This was further investigated in the study and, as shown in Figure 129, the R^2 value is about 23.5% higher for the *R3200* values than for the *R100* values. A similar trend was obtained for the AC+SBS as well, refer to Figure 118 (page 290) for more details. Since the major modifier and the phenomena associated with polymer modification of asphalt binder – together with their effects on the percent recoveries in the MSCR tests – are the same, the reasons for such a difference in the results remain unchanged as well.

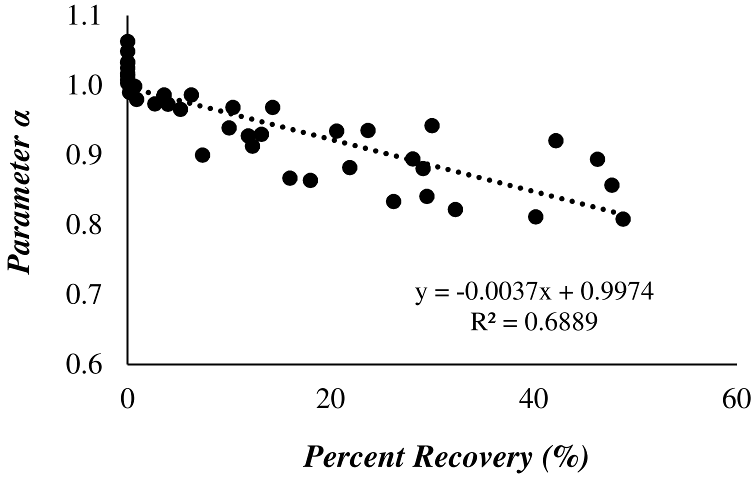

Figure 128 – Degree of correlation between the percent recoveries of the AC+SBS+PPA and the corresponding α values from the power law models

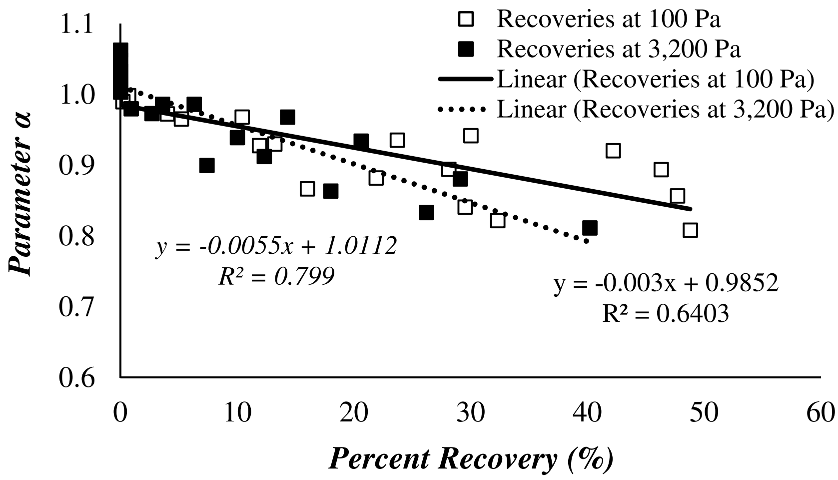

Figure 129 – Individual correlations between the percent recoveries of the AC+SBS+PPA at 100 and 3,200 Pa and the corresponding α values from the power law models

In a general context, the formulation with SBS+PPA depicts a higher rutting potential at longer creep times and higher temperatures and stress levels primarily due to the increases in the strain rates (higher *B* values) and slightly greater role of nonlinearity (*n* values) on its repeated creep response. By comparing the parameters of the AC+SBS+PPA with the ones of the

AC+SBS, it can be concluded that the higher rutting resistance of the material with SBS+PPA is directly related to the presence of less initial strain under creep-recovery loading than the material with SBS alone (the *B* and *n* values are approximately the same for both). The effects of polymeric modification type on the variations of such parameters are more visible at the creep times of 4.0 and 8.0 s, when some kinds of "inflection points" may be seen and the percentages of increase/decrease deviate from the original trendline. Such a modification type also had a significant influence on the levels of correlation between the *B* values and the creep time at 100 Pa, which was not found in the *A* values and the stress level of 3,200 Pa.

The overall correlation between the parameter *n* and the nonrecoverable compliances of the AC+SBS+PPA was found to be very weak (≈ 0.35), so individual correlations were investigated. It was observed that a good correlation between $J_{nr}3200$ and the corresponding *n* values (about 0.71) exists, even though the data are quite scattered around the regression trendline. With respect to the α values and the percent recoveries associated to it, a global correlation of around 0.69 was obtained. Similarly to the AC+SBS, the *R3200* values correlated much better with the α values than the *R100* values. Again, the effects associated with the polymeric modification type of the percent recoveries of the AC+SBS+PPA may explain the divergences of correlation between one stress level and the other.

According to the numerical values shown in Table 150 (see page 294), none of the percent recoveries of the AC+SBS+PPA at 1/9 s are equal to zero. Thus, either the *R100* or the *R3200* values may be used in the analysis of variance to identify the variable – temperature or creep time – that mostly affects the responses of the formulation. Table 161 provides the organized recoveries and the corresponding groups with all the values, as a function of the stress level. The same was made for the nonrecoverable compliances $J_{nr}100$ and $J_{nr}3200$, as depicted in Table 162 (organized groups as a function of the applied stress).

Table 161 – Rearranged MSCR testing data of the AC+SBS+PPA to be used in the analysis of variance (ANOVA) – percent recovery

stress level of 0.1 kPa (*R100*, %)[a]		stress level of 3.2 kPa (*R3200*, %)[a]	
increasing creep time	increasing temperature	increasing creep time	increasing temperature
48.8	48.8	40.2	40.2
32.3	47.7	26.2	29.1
29.5	46.3	18.0	20.6
16.0	42.2	7.4	14.3
N/A[b]	30.0	N/A[b]	6.3

[a] the starting point in both cases was the temperature of 52°C.
[b] N/A: Not applicable.

Table 162 – Rearranged MSCR testing data of the AC+SBS+PPA to be used in the analysis of variance (ANOVA) – nonrecoverable creep compliance

stress level of 0.1 kPa ($J_{nr}100$, kPa^{-1})[a]		stress level of 3.2 kPa ($J_{nr}3200$, kPa^{-1})[a]	
increasing creep time	increasing temperature	increasing creep time	increasing temperature
0.069	0.069	0.082	0.082
0.145	0.166	0.161	0.234
0.261	0.401	0.322	0.634
0.542	0.971	0.651	1.604
N/A[b]	2.533	N/A[b]	3.920

[a] the starting point in both cases was the temperature of 52°C.
[b] N/A: Not applicable.

A summary of the results of ANOVA for the percent recoveries is provided in Table 163. As may be implied from the data, either the *R100* values of the *R3200* ones do not markedly differ from each other within a particular group of results because the *F-value* is always lower than $F_{critical}$ and the *p-value* is lower than α. In other words, the effects of temperature and creep time on the recoveries of the AC+SBS+PPA may be considered as statistically similar under a level of significance of 5%. However, it is clear that the variances in the *R100* values are considerably higher than the ones in *R3200* (the *F-value* is about 288 times higher for *R100* than for *R3200*). Although the null hypothesis H_0 was not rejected in any case, the degree of homogeneity in the data points at 3,200 Pa is much higher than at 100 Pa. Furthermore, temperature plays a major role in the reductions in recovery when compared with creep time, and this can be seen either at 100 Pa or at 3,200 Pa.

Table 163 – Results from the analysis of variance (ANOVA, *p-value* and *F-value*) as based on the percent recoveries of the AC+SBS+PPA

null hypothesis H_0	statistical parameters (ANOVA)				recommendation
	$F_{critical}$	*F-value*	α	*p-value*	
equivalency between *R* values with increasing creep time and temperature, 0.1 kPa	5.5914	2.5679	0.05	0.1531	H_0 is not rejected
equivalency between *R* values with increasing creep time and temperature, 3.2 kPa	5.5914	0.0089	0.05	0.9275	H_0 is not rejected

By comparing these results with the ones of the AC+SBS (Table 148, page 292), it can be observed that the presence of PPA somehow contributed to a greater homogeneity of data at 100 Pa (H_0 at 100 Pa was rejected in the case of the AC+SBS and not rejected in the case of the AC+SBS+PPA). In terms of the data at 3,200 Pa, the comparisons among the results of ANOVA point to a reduction in the *F-value* by 79%, i. e., from 0.0419 to 0.0089. In other words, the recovery data of the AC+SBS+PPA at 3,200 Pa also became more homogeneous than the corresponding data of the AC+SBS. It is hypothesized that the above-mentioned synergy between PPA and the main modifier contributed to a greater degree of stability in the formulation and a more regular pattern of behavior in the MSCR with increasing temperature and loading time.

Table 164 summarizes the results of ANOVA for the nonrecoverable compliances of the AC+SBS+PPA at 100 and 3,200 Pa. A direct comparison between these data and the ones of the AC+SBS (Table 149, page 293) reveals that the statistical parameters *F-value* and *p-value* are from 10 to 22% higher and from 7 to 13% lower (respectively) for the AC+SBS+PPA than for the AC+SBS. More simply, the variances in the J_{nr} values of the formulation of the SBS+PPA are more sensitive to the particular effects of creep time and temperature than the ones of the formulation with SBS alone. However, these higher variances were not enough to say that both effects are considerably different under a level of significance of 5%; thus, the null hypothesis was not rejected for any of the stress levels. Again, the pavement temperature plays a major role in the increases in compliance when compared with the loading time.

Table 164 – Results from the analysis of variance (ANOVA, *p-value* and *F-value*) as based on the nonrecoverable compliances of the AC+SBS+PPA

null hypothesis H_0	statistical parameters (ANOVA)				recommendation
	$F_{critical}$	*F-value*	α	*p-value*	
equivalency between J_{nr} values with increasing creep time and temperature, 0.1 kPa	5.5914	1.2040	0.05	0.3088	H_0 is not rejected
equivalency between J_{nr} values with increasing creep time and temperature, 3.2 kPa	5.5914	1.4956	0.05	0.2609	H_0 is not rejected

The percent recoveries of the AC+SBR can be seen in Table 165. Either the temperature or the loading time have a profound impact on the recoveries of the formulation, especially at t_F values longer than 2.0 s and T values higher than 64°C. These effects are enhanced when the binder is loaded at 3,200 Pa rather than at 100 Pa, that is, the elastic response of the AC+SBR is seriously affected by an increase in the stress level at all creep times (see Figure 130). The results are no greater than 44% at 100 Pa and are no greater than 36% at 3,200 Pa. Differently from the SBS-modified binders, no plateau regions can be seen in the recoveries of the material. Zhang and Yu (2010) reported in a literature review that the SBR molecules typically have more butadiene units than the SBS ones and, as a consequence, these molecules can be more easily oxidized and decomposed after RTFO aging. This may help in explaining why the *R* values of the AC+SBR at longer creep times are not as good as the ones of the AC+SBS, especially at 3,200 Pa.

Table 165 – Percent recoveries at 100 Pa (*R100*) and 3,200 Pa (*R3200*) for the AC+SBR with increasing loading time and temperature

parameter	creep time (s)	results at each temperature and increases (both in %)[a]				
		52°C	58°C	64°C	70°C	76°C
R100	1.0	43.4	40.2	38.4	36.3	28.5
	2.0	41.8	42.1	33.1	25.6	12.6
	4.0	37.3	36.1	24.9	15.0	3.9
	8.0	20.9	23.8	15.9	5.4	0.0
R3200	1.0	36.0	26.8	17.3	8.8	0.4
	2.0	29.9	20.0	9.6	1.3	0.0
	4.0	22.1	11.8	2.1	0.0	0.0
	8.0	10.2	2.7	0.0	0.0	0.0

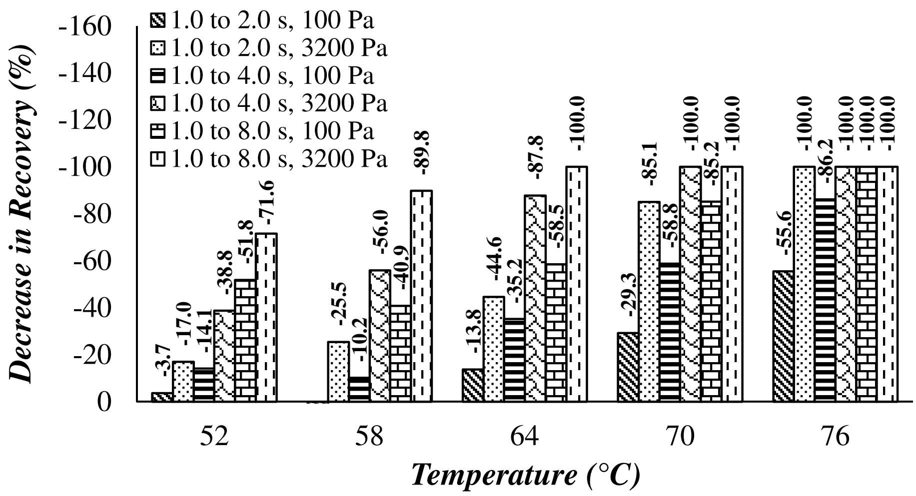

Figure 130 – Percentages of decrease in the recoveries of the AC+SBR with creep time, temperature and stress level

Together with the significant loss of recovery of the AC+SBR at 3,200 Pa when compared with 100 Pa, it can be noticed that the *R* values used to be lower than 10% when the temperature exceeds 64°C and/or the creep time becomes longer than 2.0 s. These may be taken as limiting conditions for the use of the formulation on pavements, which are slightly less severe than the ones chosen for the AC+SBS (64°C and 4.0 s of loading time). The AC+SBR barely shows any recovery response when the temperature reaches 70 and 76°C and, based on the low degree of elasticity in the MSCR tests (see Figure 67, page 185), it may be concluded that the degree of compatibility between the polymer and the binder also contributed to the relatively smaller amounts of recovery when compared with other polymeric modification types such as Elvaloy®. In this case, the incorporation of compatibilizing agents such as sulfur and PPA may be used to improve the elastic responses, as discussed earlier in the present dissertation. Finally, the recovery values of the AC+SBS tend to be higher than the corresponding values of the AC+SBR, especially at temperatures between 64 and 76°C and creep times no longer than 2.0 s.

The nonrecoverable compliances of the AC+SBR are shown in Table 166. The great sensitivity of the rheological parameters of the formulation to loading times longer than 2.0 s can also be seen in J_{nr} as well, i. e., the percentages of increase in J_{nr} are more than doubled when the binder is loaded for 4.0 s in the MSCR test rather than 2.0 s. Again, the t_F value of 2.0 s seems to be a critical threshold in the use of the AC+SBR on pavements. With respect to temperature, it can be observed that the percentages of increase in compliance are typically lower than the corresponding ones in the loading time at temperatures up to 64°C and the opposite is observed at 70 and 76°C. In practical terms, the binder has a reasonable resistance to rutting when $T \leq 64$°C and $t_F \leq 2.0$ s (J_{nr} values are lower than 1.50 and 2.5 kPa^{-1} at 0.1 and 3.2 kPa, respectively) and higher temperatures and longer loading times have a seriously damaging effect on its rutting potential, even though the high PG grade is 76-xx.

Table 166 – Nonrecoverable compliances at 100 Pa (J_{nr}*100*) and 3,200 Pa (J_{nr} *3200*) for the AC+SBR with increasing loading time and temperature

parameter	creep time (s)	results at each temperature (kPa^{-1}), $J_{nr} > 4.0$ kPa^{-1} is in bold				
		52°C	58°C	64°C	70°C	76°C
J_{nr}*100*	1.0	0.138	0.325	0.715	1.485	3.189
	2.0	0.254	0.563	1.430	3.243	**7.688**
	4.0	0.471	1.079	2.867	**6.835**	**16.494**
	8.0	1.060	2.267	**5.684**	**14.657**	**34.614**
J_{nr}*3200*	1.0	0.159	0.418	1.055	2.500	**5.735**
	2.0	0.325	0.884	2.318	**5.684**	**12.333**
	4.0	0.664	1.838	**4.941**	**11.861**	**26.379**
	8.0	1.383	3.820	**10.189**	**25.775**	**61.774**

As a representative example of the above-mentioned discussion, the J_{nr} values at 64°C and 2/9 s are equal to 1.43 and 2.32 kPa^{-1} at 100 and 3,200 Pa, respectively, and an increase of 6°C in the temperature and 2.0 s in the loading time multiply the original J_{nr} values by 4-5 times – approximately 6.84 kPa^{-1} at 100 Pa and 11.86 kPa^{-1} at 3,200 Pa. The influence of the stress level on the percentages of increase in J_{nr} with loading time is quite expressive when the temperature does not overcome 64°C, according to the data summarized in Figure 131. Other than showing the nonlinear response of SBR with increasing stress and temperatures up to 64°C, it is suggested that the polymer network was extensively damaged during the loading-unloading cycles at 70 and 76°C and the prevailing creep-recovery response in such climate conditions is dictated by the base material. This may be inferred by comparing the data of the AC+SBR at 70 and 76°C with the ones of the base binder (Figure 69, page 193) and plotting the ratios of the J_{nr} values of the AC+SBR to the corresponding values of the AC+SBS, Figure 132.

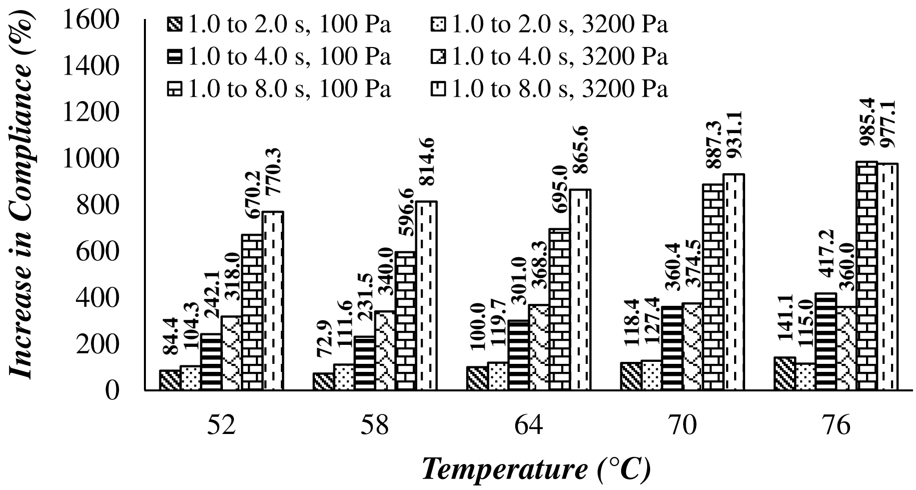

Figure 131 – Percentages of increase in the nonrecoverable compliances of the AC+SBR with creep time, temperature and stress level

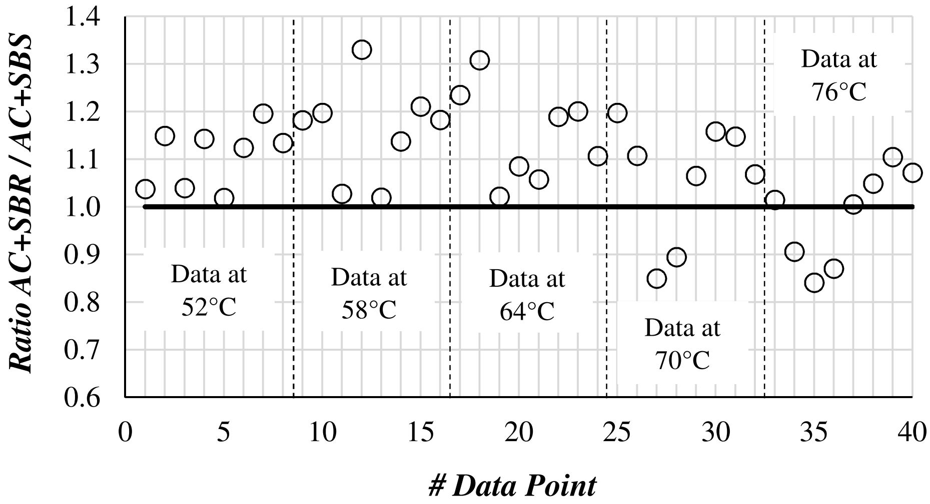

Figure 132 – Plots of the data points associated with the ratios of the J_{nr} values for the AC+SBR to the corresponding ones for the AC+SBS (each data point is characterized by one temperature, loading time and stress level), the continuous line is the equality line

As can be observed in Figure 132, only five out of 40 data points (less than 15%) are placed below the equality line – i. e., the compliance of the AC+SBR is lower than the one of the AC+SBS. It may be important to note that each data point is associated with one temperature, one loading time and one stress level, and therefore the multiplication of five temperatures by four loading times and two stress levels yields the 40 groups of data reported above (5 × 4 × 2 = 40). Since more than 85% of the data points are placed above the equality line (including many of the results associated with the temperatures of 70 and 76°C – from #25 to #40), it may be implied that the polymer network generated by asphalt binder modification with SBS is stronger than the network generated after modification with SBR. The mixture data in Chapter 5 also give support to this conclusion, as well as the fact that the variations in the compliances of the AC+SBS considerably change from one stress level to the other, even at 70 and 76°C (see Figure 112, page 279).

The values of the Superpave® stress sensitivity parameter $J_{nr,\ diff}$ are provided in Table 167. It can be observed that longer creep times typically increase the stress sensitivity of the AC+SBR, especially at temperatures up to 70°C. By considering that the compatibility of the SBR copolymer with the binder is rather limited and the above-mentioned discussion on the effects of short-term aging on the SBR polymer chains, one probable explanation for these higher $J_{nr,\ diff}$ values is the nonlinear response of the polymer blocks within the binder sample. This can also be found in the AC+SBS formulation, but only at pavement temperatures no greater than 64°C (Table 137, page 280). In other words, the increases in the test temperature softened the polymer blocks in the AC+SBR and highlighted its nonlinear response while testing at very long creep times, especially 4.0 and 8.0 s (the level of nonlinearity is higher for the AC+SBR than for the AC+SBS). The formulation does not comply with the Superpave® requirements ($J_{nr,\ diff} < 75\%$) at 64°C and t_F = 8.0 s, 70°C and t_F values of 2.0 and 8.0 s and the two extreme loading times (1.0 and 8.0 s) at 76°C.

Table 167 – Percent differences in nonrecoverable compliances ($J_{nr,\ diff}$) for the AC+SBR with increasing creep time and temperature

creep time (s)	$J_{nr,\ diff}$ values (%) at each creep time and temperature[a]				
	52°C	58°C	64°C	70°C	76°C
1.0	15.5	28.4	47.6	68.4	**79.8**
2.0	27.9	57.0	62.1	**75.3**	60.4
4.0	41.1	70.3	72.3	73.5	59.9
8.0	30.5	68.5	**79.3**	**75.9**	**78.5**

[a] the numbers in bold are the ones that exceeded the maximum $J_{nr,\ diff}$ (75%) according to Superpave®.

Table 168 provides the appropriate traffic levels of the AC+SBR at each loading time and pavement temperature. The data clearly indicate that this material is not suitable for paving applications at its high PG grade (76°C), and its applicability on roads and highways with maximum expected temperatures of 64 and 70°C is very limited. These levels are similar to the ones of the AC+SBS (Table 138, page 281) except for the results at 64°C (decreases by one grade at 1/9 s and 2/9 s for the AC+SBR). It is believed that the compatibility between the SBR copolymer and the base binder was not sufficient to improve the elastic behavior and the degree of stiffness of the formulation, either because of the characteristics of the modifier or the chemical composition of the asphalt binder. Another attempt to improve the stiffening properties is the use of a stabilizing agents such as PPA and sulfur, as will be evaluated later (formulation with SBR+PPA).

Table 168 – Adequate traffic levels for the AC+SBR with increasing creep time and temperature based on the standardized Superpave® criteria

creep time (s)	traffic levels for each temperature[a]				
	52°C	58°C	64°C	70°C	76°C
1.0	E	E	H	S	-
2.0	E	V	S	-	-
4.0	V	H	-	-	-
8.0	H	S	-	-	-

[a] S = standard; H = heavy; V = very heavy; E = extremely heavy.

The outcomes of the equations from Huang (2004) – highest tire contact radius (6.0 in) – and Pereira et al. (1998, 2000) were correlated with the $J_{nr}3200$ values of the AC+SBR, and the corresponding equations and coefficients of determination are provided in Table 169. The excellent correlations (R^2 > 0.90) reported for the previously studied formulations can also be found here and for the whole temperature interval, as well as the lower slopes for the speeds calculated by Pereira et al. (1998). However, it is necessary to investigate the ability of the equations in accurately predicting the traffic levels of the binder at such test temperatures. This can be made with the help of the data summarized in Table 170 for the predicted levels according to Huang (2004) and Pereira et al. (1998).

As the results in Table 170 suggest, the equations from Huang (2004) and Pereira et al. (1998) can reasonably predict the traffic levels of the AC+SBR only at the temperatures of 52 and 58°C: at least three points of similarity may be identified for each equation at such temperatures. More simply, the use of one or another equation can provide vehicle speeds that are expected to correlate well with the J_{nr} values of the binder at longer creep times and its actual traffic levels, provided that the maximum pavement temperature is equal to 52 or 58°C. Similar trends can be observed for other formulations shown above, which reinforces the idea that the two equations have a limited applicability on real binders tested in the MSCR protocol.

Table 169 – Regression equations and coefficients of determination between the $J_{nr}3200$ values of the AC+SBR and the corresponding vehicle speeds according to the equations by Pereira et al. (1998, 2000) and Huang (2004)

source and data	temperature (in °C)	equation	R^2
Pereira et al. (1998)	52	$y = 1.3726e^{-0.029x}$	0.9170
Pereira et al. (2000)	52	$y = -0.0177x + 1.2916$	1.0000
Huang (2004) $r = 6$ in	52	$y = 1.3733e^{-0.035x}$	0.9174
	58	$y = 3.8428e^{-0.036x}$	0.9234
	64	$y = 10.4230e^{-0.037x}$	0.9301
	70	$y = 26.0550e^{-0.038x}$	0.9283
	76	$y= 59.7570e^{-0.038x}$	0.9078
Huang (2004) $r = 3.68$ in	52	$y = 1.3707e^{-0.057x}$	0.9176
	58	$y = 3.8353e^{-0.058x}$	0.9236
	64	$y = 10.4020e^{-0.060x}$	0.9303
	70	$y = 26.0020e^{-0.062x}$	0.9286
	76	$y = 59.6340e^{-0.062x}$	0.9081

Table 170 – Comparisons between the actual traffic levels of the AC+SBR and the ones obtained from Huang (2004) and Pereira et al. (1998)

t_F (s)[d]	actual[a] and estimated[b, c] traffic levels at each temperature[d]				
	52°C	58°C	64°C	70°C	76°C
1.0	**E (V/E) [V/E]**	**E [V/E]**	H [V/E]	S [V/E]	-
2.0	**E (V/E) [V/E]**	**V [V/E]**	S [V/E]	-	-
4.0	V **(H) [H]**	**H [H]**	-	-	-
8.0	**H** (S) **[H]**	S [H]	-	-	-

[a] S = standard; H = heavy; V = very heavy; E = extremely heavy (AASHTO M320-09 standard, Table 3).
[b] (parentheses) = traffic levels from Pereira et al. (1998).
[c] [brackets] = traffic levels from Huang (2004), $r = 6$ in.
[d] similarities among the rankings are highlighted in bold, t_F = creep time.

By utilizing the equations from Huang (2004) – lower tire contact radius – and Pereira et al. (2000), it can be concluded that the patterns of behavior (correlations with the J_{nr} values and points of similarity between the predicted and actual traffic levels) remained essentially the same for the AC+SBR, see Table 171. However, the ability of the equation from Pereira et al. (2000) in predicting such traffic levels is much worse than the one from Huang (2004), as can be implied by the scattered data for the former. This is because the correlation between traffic speed and loading time proposed by Pereira et al. (2000) suggests that the asphalt pavement will be always subjected to heavy traffic levels, regardless of the loading time. However, it is clear that this cannot be always seen in the results of the asphalt binder; as a consequence, the predictions are not necessarily reliable from the point of view of different laboratory data.

Table 171 – Comparisons between the actual traffic levels of the AC+SBR and the ones obtained from the equations by Huang (2004) and Pereira et al. (2000)

t_F (s)[d]	actual[a] and estimated[b, c] traffic levels at each temperature[d]				
	52°C	58°C	64°C	70°C	76°C
1.0	**E** (H) **[V/E]**	**E [V/E]**	H [V/E]	S [V/E]	-
2.0	**E** (H) **[V/E]**	**V [V/E]**	S [V/E]	-	-
4.0	V (H) [H]	**H [H]**	-	-	-
8.0	**H (H) [H]**	S [H]	-	-	-

[a] S = standard; H = heavy; V = very heavy; E = extremely heavy (AASHTO M320-09 standard, Table 3).
[b] (parentheses) = traffic levels from Pereira et al. (2000).
[c] [brackets] = traffic levels from Huang (2004), r = 3.68 in.
[d] similarities among the rankings are highlighted in bold, t_F = creep time.

The comparisons between the current and suggesting Superpave® criteria for defining the appropriate traffic levels of the asphalt binder are shown in Table 172. As these data indicate, the binder received a lower grade at the temperature of 58°C: very heavy in the proposed criterion and extremely heavy in the current one. Similar case may be observed for the AC+SBS, but at the high pavement temperature of 64°C (see Table 142, page 283). This may be explained by the nonlinear response of the AC+SBR at longer creep times, which leads to a marked increase in its susceptibility to rutting. In other words, the actual resistance of the AC+SBR to rutting when used on traffic lanes with great percentages of slow-moving vehicles may not correspond to the one estimated by the current Superpave® procedures. Therefore, the creep-recovery behavior of the asphalt binder in a more critical loading condition must be taken into account in order to yield a more realistic estimate of the resistance to rutting.

The MSCR tests carried out at longer loading times (up to 8.0 s) and several pavement temperatures (from 52 to 76°C) reveal that the AC+SBR is a very sensitive material to loading time and temperature. This is because the results of the percent recoveries and the nonrecoverable compliances are much worse when T > 64°C and t_F > 2.0 s, i. e., loading and temperature conditions more severe than these reported ones will lead to a considerable increase in the rutting potential of the formulation. As a consequence of this repeated creep behavior, the binder shows increasing $J_{nr,\,diff}$ values with increasing temperature (typically up to 70°C) and loading time; when the most critical testing conditions are reached (T = 70 and 76°C or t_F = 8.0 s), the AC+SBR becomes overly stress sensitive ($J_{nr,\,diff}$ > 75%). Also, the binder cannot be placed on roads and highways with maximum pavement temperatures of 76°C and its use on locations with a high PG grade of 70-xx is very limited. When this degree of nonlinearity is considered in the Superpave® criteria for traffic levels, it can be observed that the appropriate level at 58°C is reduced by one grade (from extremely heavy to very heavy).

Table 172 – Traffic levels of the AC+SBR with increasing loading time and temperature in the current and proposed criteria

temperature (in °C)	No. of required MSCR tests[b]	Superpave® designations (current and new criteria)[a, c]	
		current criterion	new criterion
52	4	**52E-xx**	**52E-xx**
58	4	58E-xx	58V-xx
64	3	**64H-xx**	**64H-xx**
70	2	**70S-xx**	**70S-xx**
76	1	**76-xx**	**76-xx**

[a] S = standard; H = heavy; V = very heavy; E = extremely heavy (AASHTO M320-09 standard, Table 3).
[b] minimum number of MSCR tests to determine the adequate traffic level in the proposed classification.
[c] similarities among the classifications are highlighted in bold.

Table 173 shows all the numerical values of the parameters A, B, n and α of the modified power model, as applied to the creep-recovery data of the AC+SBR in the MSCR tests. Overall, the pattern of behavior of this formulation at temperatures up to 64°C is similar to the one observed for the previous formulations: the A values decrease and the B values increase with increasing loading time in the DSR. In practical terms, this means that the presence of higher levels of accumulated strain in the binder after the passage of slow-moving vehicles is due primarily to the presence of higher strain rates, by considering pavements with high PG grades of 64-xx or lower. At the same time, the level of nonlinearity in the asphalt binder typically increases with the application of longer loading times in the MSCR test (n increases no more than 3.5% from 1.0 to 8.0 s), regardless of the pavement temperature. Other formulations such as the AC+rubber+PPA also showed this pattern of response, see Table 128 in page 268. As a consequence, it is possible to suppose that there is a quite good correlation between the parameter n and the compliance J_{nr}. This will be investigated later in the next paragraphs.

By taking into account the limiting paving conditions for the AC+SBR imposed by the recovery and compliance data (64°C and loading time of 2.0 s), one may observe that the A value is of about 4.50, the B and α values are almost equivalent to one (about 0.962 and 0.964, respectively) and the n value is approximately equal to one (1.0025). These results are not promising, since the constant A is much greater than one and the parameters B and n approach unity. Therefore, it may be inferred that the AC+SBR has a relatively high rutting potential – especially in the first few loading-unloading cycles – and the amount of recovered strain is null or very small. As previously observed in the MSCR testing data, these assumptions may be accepted because the compliance at 3,200 Pa is of about 2.32 kPa^{-1}, the percent recovery is lower than 10% (9.6%) and $J_{nr,\ diff} \approx 62\%$ at such temperature and loading time.

Table 173 – Numerical values and variations in the parameters/constants *A, B, n* and *α* from the power law equations by Saboo and Kumar (2015) with increasing temperature and creep time and considering the AC+SBR

temperature	test times	parameter A^a		parameter B^a		parameter n^a		parameter α^a	
		0.1 kPa	3.2 kPa	0.1 kPa	3.2 kPa	0.1 kPa	3.2 kPa	0.1 kPa	3.2 kPa
52°C	1/9 s	0.0259	0.8433	0.8551	0.8679	1.0040	1.0016	0.8586	0.8693
	2/9 s	0.0259 (0.0)	0.8560 (1.5)	0.8474 (-0.9)	0.8784 (1.2)	1.0115 (0.7)	1.0054 (0.4)	0.8572 (-0.2)	0.8832 (1.6)
	4/9 s	0.0250 (-3.5)	0.8356 (-0.9)	0.8428 (-1.4)	0.8982 (3.5)	1.0239 (2.0)	1.0094 (0.8)	0.863 (0.5)	0.9066 (4.3)
	8/9 s	0.0233 (-10.0)	0.7620 (-9.6)	0.8779 (2.7)	0.9363 (7.9)	1.0222 (1.8)	1.0109 (0.9)	0.8974 (4.5)	0.9465 (8.9)
58°C	1/9 s	0.0579	1.9426	0.8736	0.9031	1.0045	1.0008	0.8776	0.9038
	2/9 s	0.0572 (-1.2)	1.9864 (2.3)	0.8555 (-2.1)	0.9219 (2.1)	1.0145 (1.0)	1.0039 (0.3)	0.8679 (-1.1)	0.9255 (2.4)
	4/9 s	0.0551 (-4.8)	1.9261 (-0.8)	0.8517 (-2.5)	0.9433 (4.5)	1.0275 (2.3)	1.0072 (0.6)	0.8752 (-0.3)	0.9501 (5.1)
	8/9 s	0.0513 (-11.4)	1.7640 (-9.2)	0.8770 (0.4)	0.9780 (8.3)	1.0385 (3.4)	1.0109 (1.0)	0.9107 (3.8)	0.9886 (9.4)
64°C	1/9 s	0.1236	4.3526	0.8880	0.9415	1.0054	1.0011	0.8927	0.9426
	2/9 s	0.1237 (0.1)	4.5016 (3.4)	0.8806 (-0.8)	0.9616 (2.1)	1.0089 (0.3)	1.0025 (0.1)	0.8884 (-0.5)	0.9640 (2.3)
	4/9 s	0.1195 (-3.3)	4.3978 (1.0)	0.8841 (-0.4)	0.9861 (4.7)	1.0134 (0.8)	1.0052 (0.4)	0.8959 (0.4)	0.9911 (5.1)
	8/9 s	0.1105 (-10.6)	4.1040 (-5.7)	0.8998 (1.3)	1.0153 (7.8)	1.0219 (1.6)	1.0131 (1.2)	0.9195 (3.0)	1.0286 (9.1)
70°C	1/9 s	0.2488	9.3821	0.8950	0.9702	1.0055	1.0011	0.8999	0.9713
	2/9 s	0.2506 (0.7)	9.9336 (5.9)	0.8956 (0.1)	0.9929 (2.3)	1.0041 (-0.1)	1.0022 (0.1)	0.8992 (-0.1)	0.9950 (2.4)
	4/9 s	0.2417 (-2.9)	9.8433 (4.9)	0.9105 (1.7)	1.0159 (4.7)	1.0044 (-0.1)	1.0069 (0.6)	0.9145 (1.6)	1.0230 (5.3)
	8/9 s	0.2285 (-8.2)	9.5231 (1.5)	0.9466 (5.8)	1.0382 (7.0)	1.0072 (0.2)	1.0178 (1.7)	0.9534 (5.9)	1.0567 (8.8)
76°C	1/9 s	0.4770	19.7771	0.9042	0.9967	1.0025	1.0011	0.9065	0.9977
	2/9 s	0.4928 (3.3)	21.0263 (6.3)	0.9324 (3.1)	1.0139 (1.7)	0.9990 (-0.3)	1.0033 (0.2)	0.9315 (2.8)	1.0172 (2.0)
	4/9 s	0.4828 (1.2)	21.3053 (7.7)	0.9630 (6.5)	1.0297 (3.3)	1.0000 (-0.2)	1.0092 (0.8)	0.9629 (6.2)	1.0392 (4.2)
	8/9 s	0.4685 (-1.8)	21.2726 (7.6)	0.9937 (9.9)	1.0572 (6.1)	1.0070 (0.4)	1.0255 (2.4)	1.0007 (10.4)	1.0841 (8.7)

[a] the percentages of variation reported in parenthesis refer to the changes in the parameter when moving from 1.0 s to the creep time into question (2.0, 4.0 or 8.0 s).

One interesting feature of the AC+SBR is that the contribution of nonlinearity to the total response of the material (increases in n) are greater when the test temperature varies from 52 to 64°C at 100 Pa (especially from 4.0 to 8.0 s), and the same can be said for the temperatures of 70 and 76°C and the stress level of 3,200 Pa. Furthermore, both constants A and B increase in magnitude with increasing creep time at these two temperatures and the highest stress level. These observations raise the possibility that the formulation shows a great loss of resistance to rutting on pavements with high PG grades of 70-xx or greater, which is confirmed by the compliance values as well. As reported in Table 166 (page 314), the $J_{nr}3200$ values easily overcome 10.0 kPa^{-1} when $T > 64$°C and $t_F > 2.0$ s, whereas the results barely exceed 2.0 kPa^{-1} in less severe testing conditions. It is not a great surprise at all if one concludes that the stress sensitivity of the material also becomes a serious issue at 70 and 76°C, which is where the formulation is not in agreement with the Superpave® requirements at several loading times (see Table 167, page 316).

The results of A and B were correlated with the creep times in order to analyze the overall levels of correlation between them, similarly to what was done for the previously reported materials. Some problems with these correlations are expected, since negative and positive percentages of increase at the same temperature may be found for some parameters such as A, B and n. Figure 133 and Figure 134 refer to the correlations at the temperature of 64°C and the stress levels of 100 and 3,200 Pa, respectively. The general pattern of behavior is the same for both constants either at 100 or at 3,200 Pa, i. e., the A values decrease and the B values increase with increasing stress. In addition, the role of one and another constant on the total strain in the binder becomes more visible at higher stress levels, in that the rates of decrease in A and increase in B with increasing loading time (i. e., the gradients) are higher at 3,200 Pa than at 100 Pa.

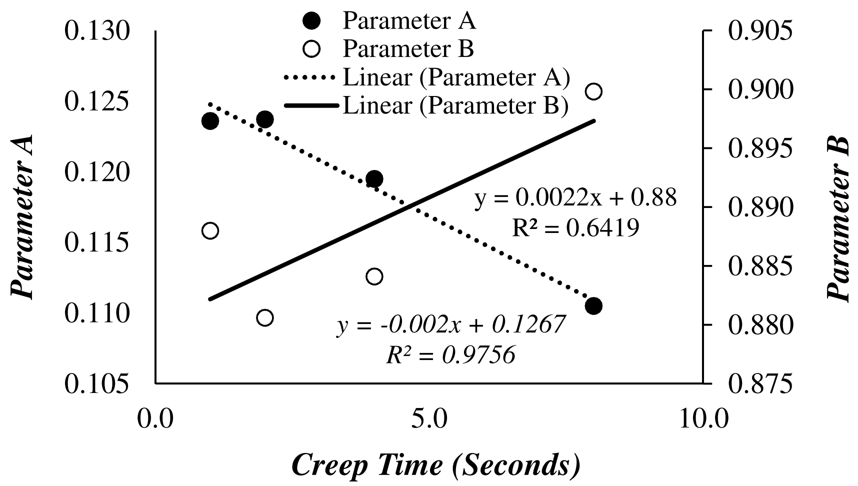

Figure 133 – Correlations between the creep time and the constants A and B from the model by Saboo and Kumar (2015), temperature of 64°C and stress level of 100 Pa – AC+SBR

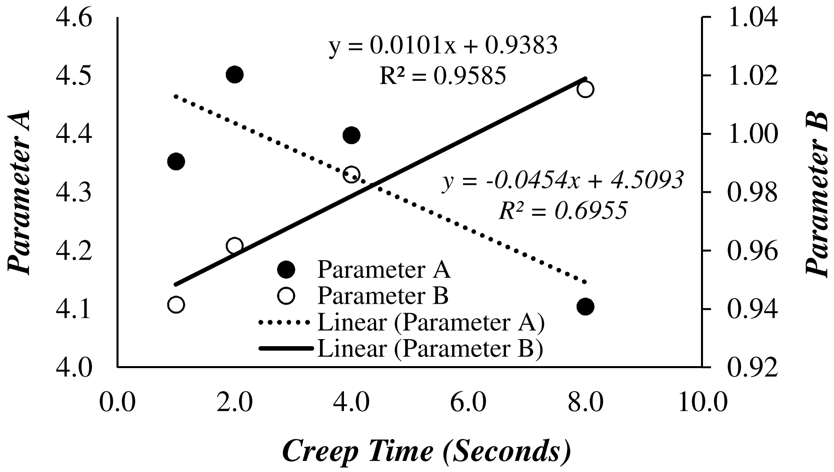

Figure 134 – Correlations between the creep time and the constants *A* and *B* from the model by Saboo and Kumar (2015), temperature of 64°C and stress level of 3,200 Pa – AC+SBR

By moving to the pavement temperature of 70°C (Figure 135 and Figure 136), what can be seen is that the trend of increasing slopes of the regression equations with increasing stress level remains the same here and for both parameters. In addition, the tendency of increasing *B* and decreasing *A* with increasing t_F values (especially at 100 Pa) is also unchanged. The major difference between the data points and correlations at 64 and 70°C is located at the *A* values at 70°C and 3,200 Pa – namely, almost complete absence of correlation ($R^2 \approx 0.01$). As discussed above, the AC+SBR depicts a great loss of rutting resistance at the pavement temperatures of 70 and 76°C and this is reflected into the model parameters. In other words, the reverse in the tendency of the *A* values with increasing loading time (from negative to positive percentages of variation from one creep time to the other) may explain why the correlation is so poor in the test conditions reported in Figure 136.

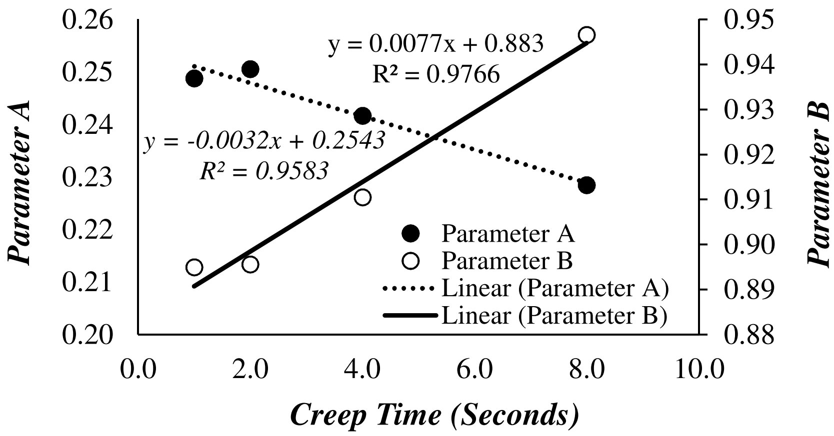

Figure 135 – Correlations between the creep time and the constants *A* and *B* from the model by Saboo and Kumar (2015), temperature of 70°C and stress level of 100 Pa – AC+SBR

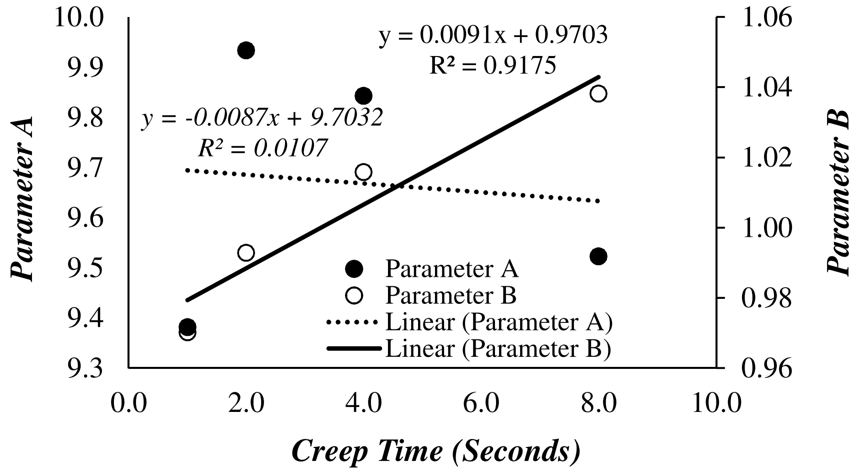

Figure 136 – Correlations between the creep time and the constants *A* and *B* from the model by Saboo and Kumar (2015), temperature of 70°C and stress level of 3,200 Pa – AC+SBR

The full list of regression equations and levels of correlation between the results of *A* and *B* and the creep time is summarized in Table 174. In general, higher temperatures and stress levels lead to increases in the slopes and intercepts of the regression trendlines, especially at 100 Pa. This may be translated as a greater susceptibility of the formulation to the accumulation of permanent strain either in the first few cycles (*A*) or during the application of loading-unloading cycles (*B*). The levels of correlation commonly range from regular to excellent (between 0.50 and 1.00) for both parameters, with only a few exceptions. It is interesting to observe that, as the pavement temperature increases, the R^2 values for the parameter *A* tend to decrease and the signal of the slope of the regression equation becomes positive at 76°C and 3,200 Pa. This is in alignment with the substantial increases in the rutting potential of the AC+SBR under more severe testing conditions, in that either the initial strain or the strain rate perform an important role in this susceptibility to rutting.

With respect to the exponents n and α (Table 175), what can be seen is that the tendency of increasing n and α with increasing creep time remains the same within the whole temperature range and for both stress levels. The coefficients of determination are always higher than 0.52, and they are typically better for α. Furthermore, the exponent α is equal to unity or slightly higher than one at 70 and 76°C when compared with lower temperatures, and these are the climate conditions under which the AC+SBR practically shows no recovery (see Table 173). These discussions suggest that an overall correlation between α and R – as well as between n and J_{nr} – may be expected at a first glance, differently from several previously reported formulations such as the AC+rubber+PPA and the AC+SBS+PPA (good correlations between n and J_{nr} were obtained only at 3,200 Pa). However, a more detailed analysis shows that the n

values do not necessarily become greater at higher temperatures and stress levels, which is not in agreement with the J_{nr} values. On the other hand, α generally increases with increasing severity of temperature and stress levels in the MSCR tests, especially at 3,200 Pa.

Table 174 – Degrees of correlation between the parameters *A* and *B* (modified power model) and the creep time t_F for the AC+SBR

T (°C)	stress (kPa)	linear regression equations and R^2 values (in parenthesis)[a, b]	
		parameter *A*	parameter *B*
52	0.1	y = -0.0004x + 0.0265 (0.9810)	y = 0.0037x + 0.8418 (0.5497)
	3.2	y = -0.0129x + 0.8724 (0.8844)	y = 0.0097x + 0.8587 (0.9997)
58	0.1	y = -0.0010x + 0.0590 (0.9987)	y = 0.0014x + 0.8591 (0.1188)
	3.2	y = -0.0292x + 2.0143 (0.8649)	y = 0.0103x + 0.8980 (0.9805)
64	0.1	y = -0.0020x + 0.1267 (0.9756)	y = 0.0022x + 0.8800 (0.6419)
	3.2	y = -0.0454x + 4.5093 (0.6955)	y = 0.0101x + 0.9383 (0.9585)
70	0.1	y = -0.0032x + 0.2543 (0.9583)	y = 0.0077x + 0.8830 (0.9766)
	3.2	y = -0.0087x + 9.7032 (0.0107)	y = 0.0091x + 0.9703 (0.9175)
76	0.1	y = -0.0022x + 0.4884 (0.4322)	y = 0.0120x + 0.9032 (0.9291)
	3.2	y = 0.1583x + 20.2520 (0.4596)	y = 0.0082x + 0.9937 (0.9717)

[a] the Y-axis is associated with the parameter (*A* or *B*), whereas the X-axis is associated with t_F.
[b] changes in the signal of the slope of the regression trendlines are highlighted with a grey-shaded box.

Table 175 – Degrees of correlation between the parameters *n* and α (modified power model) and the creep time t_F for the AC+SBR

T (°C)	stress (kPa)	linear regression equations and R^2 values (in parenthesis)[a]	
		parameter *n*	parameter α
52	0.1	y = 0.0024x + 1.0064 (0.6317)	y = 0.0059x + 0.8471 (0.9055)
	3.2	y = 0.0012x + 1.0023 (0.8025)	y = 0.0109x + 0.8606 (0.9962)
58	0.1	y = 0.0046x + 1.0039 (0.9249)	y = 0.0055x + 0.8624 (0.7905)
	3.2	y = 0.0014x + 1.0006 (0.9405)	y = 0.0116x + 0.8984 (0.9777)
64	0.1	y = 0.0023x + 1.0038 (0.9935)	y = 0.0043x + 0.8832 (0.8930)
	3.2	y = 0.0017x + 0.9990 (0.9916)	y = 0.0118x + 0.9372 (0.9746)
70	0.1	y = 0.0003x + 1.0041 (0.5209)	y = 0.0081x + 0.8865 (0.9670)
	3.2	y = 0.0025x + 0.9978 (0.9907)	y = 0.0116x + 0.9679 (0.9572)
76	0.1	y = 0.0009x + 0.9989 (0.5523)	y = 0.0129x + 0.9020 (0.9616)
	3.2	y = 0.0035x + 0.9965 (0.9896)	y = 0.0119x + 0.9898 (0.9920)

[a] the Y-axis is associated with the parameter (*n* or α), whereas the X-axis is associated with t_F.

Figure 137 depicts the level of correlation between *n* and the nonrecoverable compliance J_{nr} for all of the test temperatures, loading times and stress levels. It is clear that the correlation is very weak ($R^2 < 0.01$), even though the tendency of increasing *n* with increasing J_{nr} is unchanged (slope of the trendline is positive). The simplest explanation for such a finding is that, as pointed out above, the parameter *n* does not have a proportional relationship with the increasing J_{nr} values as the test conditions become more critical. In other words, one particular *n* value is not necessarily associated with only one corresponding J_{nr} value, and the data are scattered around the regression trendline. Similar tendencies were observed for the individual groups of *n* and J_{nr} values at each stress level (charts not reported here), and the corresponding coefficients of determination are approximately equal to 0.043 and 0.359 at 100 and 3,200 Pa, respectively. More simply, the *n* values may indicate that some degree of nonlinearity exists in the creep-recovery responses of the AC+SBR, but it is not possible to estimate such degree based on the nonrecoverable compliance data.

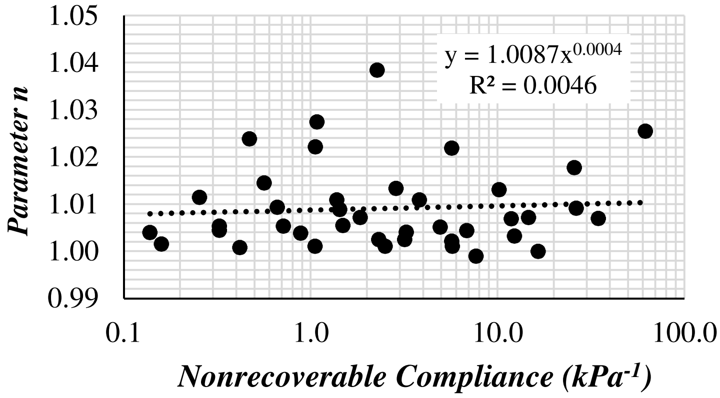

Figure 137 – Degree of correlation between the nonrecoverable compliances of the AC+SBR and the corresponding *n* values from the power law models

The quite good correlation that exists between α and the percent recovery of the AC+SBR (see Figure 138, $R^2 \approx 0.85$) is in aligment with the discussions and results reported for the previously studied binders. In a few words, the decreases in α may be associated with the increases in the percent recovery derived from the MSCR tests, and one parameter may be reasonably estimated from the results of the other and the regression equation. Since the overall correlation is higher than 0.8, it may be concluded that the individual correlations at 100 and 3,200 Pa do not considerably differ from each other. In fact, additional investigations revealed that the R^2 values are approximately equal to 0.874 at 100 Pa and 0.863 at 3,200 Pa, a difference of only 1.27%. In other words, there is no risk of obtaining a more reliable estimation of the recovery of the asphalt binder in the MSCR test at one stress level than the other, which is different from the conclusions drawn for other formulations such as the AC+SBS+PPA and the AC+SBS.

Lastly, an investigation was carried out to see whether the effects of temperature or the loading time are more pronounced in the outcomes of *R* and J_{nr} for the AC+SBR. Thus, the ANOVA analysis was conducted on the recoveries and the nonrecoverable compliances of the formulation and the same level of significance used in the previously reported formulation (5%)

was selected. Once all of the *R3200* values at 3,200 Pa and 1/9 s are non-null (see Table 165, page 313), ANOVA may be carried out either for the recovery or the compliance data. Table 176 provides the rearranged *R100* and *R3200* values for the AC+SBR, as they were submitted to ANOVA in the present dissertation.

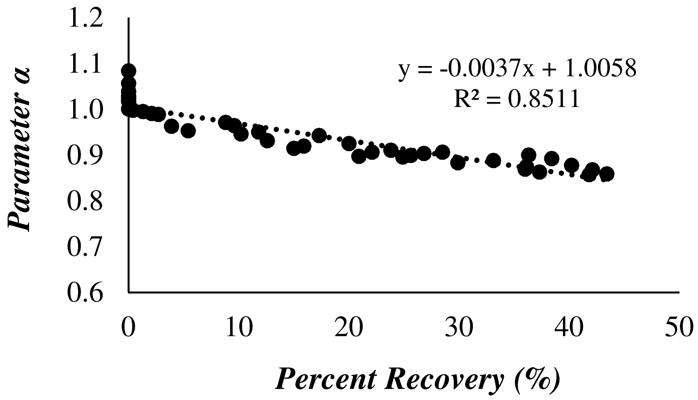

Figure 138 – Degree of correlation between the percent recoveries of the AC+SBR and the corresponding α values from the power law models

Table 176 – Rearranged MSCR testing data of the AC+SBR to be used in the analysis of variance (ANOVA) – percent recovery

stress level of 0.1 kPa (*R100*, %)[a]		stress level of 3.2 kPa (*R3200*, %)[a]	
increasing creep time	increasing temperature	increasing creep time	increasing temperature
43.4	43.4	36.0	36.0
41.8	40.2	29.9	26.8
37.3	38.4	22.1	17.3
20.9	36.3	10.2	8.8
N/A[b]	28.5	N/A[b]	0.4

[a] the starting point in both cases was the temperature of 52°C.
[b] N/A: Not applicable.

Table 177 shows the resulting parameters *F-value* and *p-value* for the percent recoveries of the AC+SBR according to ANOVA and the aforementioned level of significance. It is quite natural to say that the null hypothesis should not be rejected neither at 100 nor at 3,200 Pa, since the *p-value* easily overcomes 0.40 and the *F-value* is no greater than 0.60 in any case. In proportional terms, the *F-value* ranges from 1.4 to 10.6% of $F_{critical}$ (≈ 5.591) and the *p-value* is from 9 to 16 times the level of significance α = 5%. From the point of view of statistics, this means that the pavement temperature and the loading time yields elastic responses that do not significantly differ from each other, and therefore they may be taken as derived from a common universal set of numerical values. The statistical results are lower for 100 Pa than for 3,200 Pa, which means that the degree of homogeneity within these data is higher for the former stress level than for the latter one. Temperature also has a slightly higher impact on the *R* values of the asphalt binder than the creep time at 3,200 Pa, and the opposite is typically observed at 100 Pa.

Table 177 – Results from the analysis of variance (ANOVA, *p-value* and *F-value*) as based on the percent recoveries of the AC+SBR

null hypothesis H_0	statistical parameters (ANOVA)				recommendation
	$F_{critical}$	*F-value*	α	*p-value*	
equivalency between *R* values with increasing creep time and temperature, 0.1 kPa	5.5914	0.0800	0.05	0.7854	H_0 is not rejected
equivalency between *R* values with increasing creep time and temperature, 3.2 kPa	5.5914	0.5961	0.05	0.4653	H_0 is not rejected

Similarly to the recoveries, the nonrecoverable compliance values of the AC+SBR were also rearranged in order to be tested under ANOVA (Table 178). Table 179 supplies the final *F-values* and *p-values* for the J_{nr} values of the formulation according to ANOVA. One more time, the null hypothesis – i. e., the variances in the results of MSCR with increasing temperature and creep time may be considered as statistically similar – is not rejected because the critical limiting requirements (*F-value* < $F_{critical}$ and *p-value* > α) are not exceeded. Even though *F-value* is at least 100% higher and *p-value* is at least 36% lower for the compliances than for the corresponding percent recoveries, this was not enough to say that the null hypothesis should be rejected. What can be inferred from these comments is that J_{nr} is more sensitive to changes in the loading time and the temperature than *R*, and also that temperature and the stress level of 3,200 Pa exert a greater impact on the rutting potential of the formulation (i. e., higher J_{nr} values) than the creep time.

Table 178 – Rearranged MSCR testing data of the AC+SBR to be used in the analysis of variance (ANOVA) – nonrecoverable creep compliance

stress level of 0.1 kPa ($J_{nr}100$, kPa^{-1})[a]		stress level of 3.2 kPa ($J_{nr}3200$, kPa^{-1})[a]	
increasing creep time	increasing temperature	increasing creep time	increasing temperature
0.138	0.138	0.159	0.159
0.254	0.325	0.325	0.418
0.471	0.715	0.664	1.055
1.060	1.485	1.383	2.500
N/A[b]	3.189	N/A[b]	5.735

[a] the starting point in both cases was the temperature of 52°C.
[b] N/A: Not applicable.

Table 179 – Results from the analysis of variance (ANOVA, *p-value* and *F-value*) as based on the nonrecoverable compliances of the AC+SBR

null hypothesis H_0	statistical parameters (ANOVA)				recommendation
	$F_{critical}$	*F-value*	α	*p-value*	
equivalency between J_{nr} values with increasing creep time and temperature, 0.1 kPa	5.5914	1.1099	0.05	0.3271	H_0 is not rejected
equivalency between J_{nr} values with increasing creep time and temperature, 3.2 kPa	5.5914	1.2787	0.05	0.2954	H_0 is not rejected

The percent recovery data of the AC+SBR+PPA at all loading and temperature conditions selected in the MSCR tests are provided in Table 180, whereas the percentages of decrease in recovery at each temperature and pair of creep-recovery times are given in Figure 139. It is clear that this formulation has a much higher sensitivity to increases in the loading time when compared with the AC+SBR (Figure 130, page 313), especially at t_F values up to 4.0 s. At the same time, the *R* values of the AC+SBR+PPA are higher than the corresponding values of the AC+SBR (Table 166, page 314) only at 52 and 58°C and the creep times of 1.0 and 2.0 s, and the opposite is seen in the remaining test conditions. As previously noticed in the SBS-modified binders and early published studies, the presence of PPA in the composition of the formulation is somehow associated with these higher degrees of sensitivity. This can be observed not only when the loading conditions in the MSCR tests are modified (DOMINGOS and FAXINA, 2015b), but also when higher stress levels are used in the tests (JAFARI et al., 2015; JAFARI and BABAZADEH, 2016). The *R100* values commonly range from 1.5 to 45.5%, whereas the non-null *R3200* values typically vary from 6.0 to 41.0%.

Table 180 – Percent recoveries at 100 Pa (*R100*) and 3,200 Pa (*R3200*) for the AC+SBR+PPA with increasing loading time and temperature

parameter	creep time (s)	results at each temperature and increases (both in %)				
		52°C	58°C	64°C	70°C	76°C
R100	1.0	45.4	38.6	32.2	25.6	17.0
	2.0	38.3	32.3	25.0	17.4	7.9
	4.0	28.1	22.3	15.1	7.2	0.5
	8.0	18.7	14.4	8.4	1.6	0.0
R3200	1.0	40.6	29.4	16.6	6.1	0.0
	2.0	30.1	17.8	6.7	0.2	0.0
	4.0	16.5	6.3	0.0	0.0	0.0
	8.0	6.9	0.7	0.0	0.0	0.0

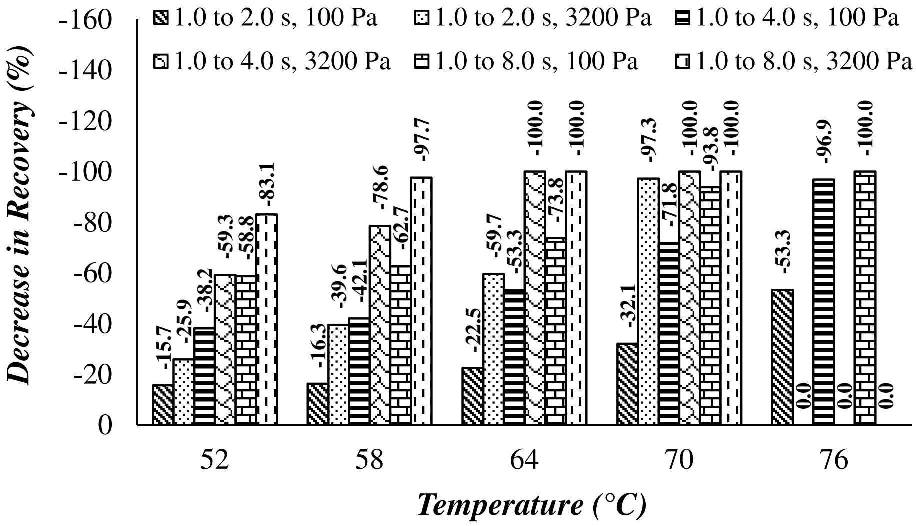

Figure 139 – Percentages of decrease in the recoveries of the AC+SBR+PPA with creep time, temperature and stress level

Another issue relating to the percent recoveries of the AC+SBR+PPA is the presence of many null or extremely low values (< 1.0%) at the temperatures of 70 and 76°C. This is quite surprising, since greater degrees of improvement in the elasticity of the binder were expected after the addition of PPA. It seems that, depending on the compositions of the original material and the average molecular weight of the SBR copolymer, PPA may not be enough to further improve the stability and the properties of the binder by means of the creation of a cross-linked network in it (ZHANG and YU, 2010). This is possibly the case of the components used in the AC+SBR, in that sulfur or other cross-linking agent may be required to obtain formulations with high degrees of elasticity and better results at the MSCR temperatures of 70 and 76°C. Zhang and Hu (2013) reported in a literature review that, from the point of view of chemistry, sulfur acts by developing cross-linking among the polymer molecules and coupling the polymer particles with the asphalt molecules by means of sulfide and/or polysulfide bonds. However, one serious limitation of this modification type is the sensitivity to aging, either when SBS or SBR are used as major modifiers.

The nonrecoverable compliances of the AC+SBR+PPA are shown in Table 181, and the corresponding percentages of increase in J_{nr} are given in Figure 140. Although the compliances of the formulation with SBR+PPA show a high sensitivity to increases in the loading time than the corresponding ones of the material with SBR alone (Figure 131, page 315), the presence of PPA contributed to the decreases in the J_{nr} values of the AC+SBR either at 100 Pa or 3,200 Pa. In other words, PPA increased the high-temperature stiffness of the asphalt binder modified with SBR and resulted in mixtures with lower susceptibility to rutting (see data in Chapter 5). It is interesting to note that the increases in $J_{nr}100$ with creep time do not markedly differ from the ones for *J_{nr}3200* at creep times up to 4.0 s, and this may be somewhat seen either for the AC+SBR or the AC+SBR+PPA. However, the greatest differences between the values at 100 and 3,200 Pa can be identified at t_F = 8.0 s and for the formulation with SBR+PPA, especially at the temperatures of 70 and 76°C. In summary, PPA mainly acts by increasing the sensitivity of the formulation to longer loading times (higher percentages) and highlighting the stress sensitivity of the SBR-modified binder when t_F is equal to 8.0 s.

Table 181 – Nonrecoverable compliances at 100 Pa (*J_{nr}100*) and 3,200 Pa (*J_{nr} 3200*) for the AC+SBR+PPA with increasing loading time and temperature

parameter	creep time (s)	results at each temperature (kPa^{-1}), J_{nr} > 4.0 kPa^{-1} is in bold				
		52°C	58°C	64°C	70°C	76°C
J_{nr}100	1.0	0.081	0.206	0.500	1.157	2.571
	2.0	0.159	0.405	1.011	2.394	**5.529**
	4.0	0.351	0.905	2.299	**5.636**	**13.110**
	8.0	0.732	1.878	**4.775**	**12.077**	**27.878**
J_{nr}3200	1.0	0.089	0.244	0.662	1.666	3.840
	2.0	0.185	0.526	1.434	3.572	**7.914**
	4.0	0.440	1.264	3.408	**8.319**	**19.144**
	8.0	0.979	2.768	**7.592**	**20.838**	**51.525**

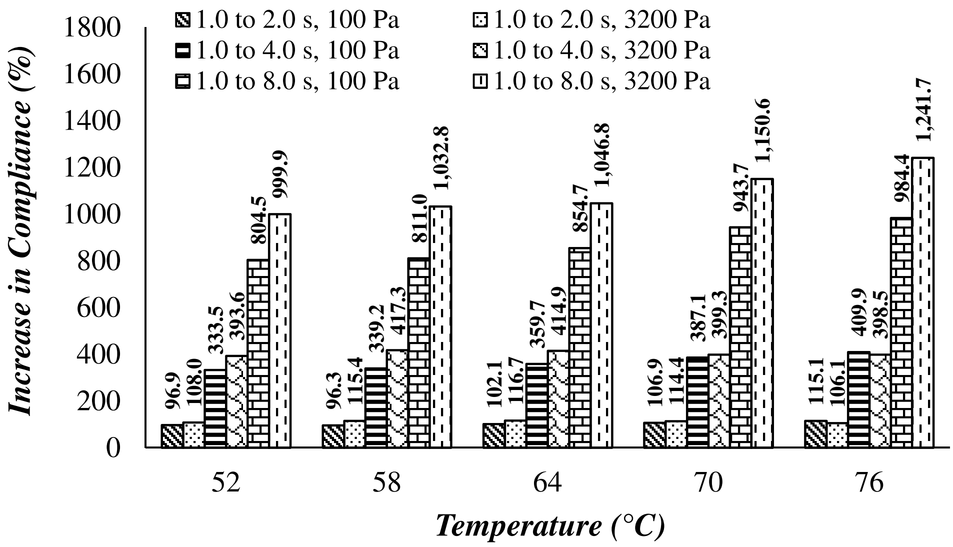

Figure 140 – Percentages of increase in the nonrecoverable compliances of the AC+SBR with creep time, temperature and stress level

The results of the AC+SBR+PPA range from 0.08 to 27.88 kPa^{-1} at 100 Pa and from 0.08 to 51.53 kPa^{-1} at 3,200 Pa. As a matter of comparison, the minimum compliances of the AC+SBR approach 0.15 kPa^{-1} and the maximum ones approach 60.0 kPa^{-1} at both stress levels. As portrayed in Figure 141 (each data point is comprised by one stress level, one pair of creep-recovery times and one pavement temperature), the J_{nr} values of the AC+SBR are from 20% to 80% higher than the corresponding values of the AC+SBR+PPA – the ratios of one compliance to the other are all ranging from 1.2 to 1.8. In a general context, the AC+SBR+PPA is stiffer and more sensitive to changes in the loading time than the AC+SBR. From a graphical point of view, this high sensitivity can be interpreted as greater slopes for the curves of the AC+SBR+PPA and their approach to the curves of the AC+SBR, as shown in Figure 142 (examples at 70 and 76°C).

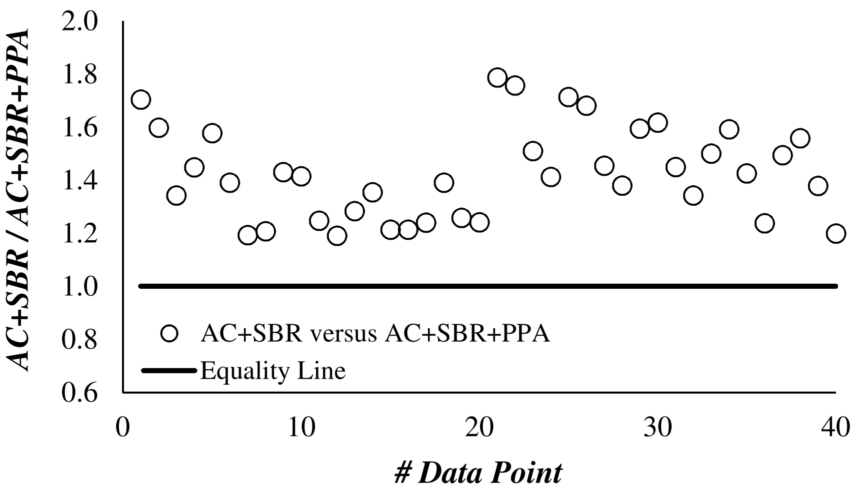

Figure 141 – Plots of the data points associated with the ratios of the J_{nr} values for the AC+SBR+PPA to the corresponding ones for the AC+SBR (each data point is characterized by one temperature, loading time and stress level), the continuous line is the equality line

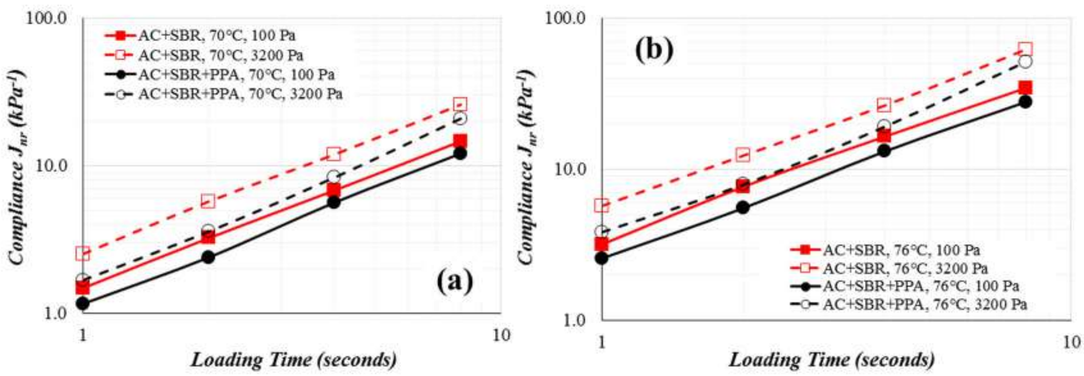

Figure 142 – Plots of the nonrecoverable compliance J_{nr} versus loading time (log-log scale) for the AC+SBR and the AC+SBR+PPA at the temperatures of (a) 70°C; and (b) 76°C

Differently from the SBS-modified asphalt binders, no plateau regions could be identified in the creep-recovery responses of the SBR-modified ones. This reinforces the idea that no effective cross-linking occurred in the AC+SBR and the AC+SBR+PPA, and thus the benefits of PPA addition were restricted to the overall stiffness of the binder. Even though stiffness is the target property for obtaining binders and mixtures with higher resistances to rutting, elasticity is essential for dealing with other distress mechanisms such as fatigue cracking and low-temperature cracking. It may also give some contribution to the preparation of more rut resistant materials, as discussed above. Therefore, it is not desirable for polymer-modified binders to show a poor degree of compatibility between their components and lower levels of elastic response, especially at PG grades as higher as 76-xx.

Table 182 provides the results of the Superpave® parameter $J_{nr,\ diff}$ for the asphalt binder modified with SBR and PPA. As a consequence of the increases in the sensitivity of the AC+SBR+PPA to loading time and temperature, there are marked and consistent increases in the $J_{nr,\ diff}$ values of this material with increasing temperature and loading time up to the extreme testing condition (t_F = 8.0 s and temperature of 76°C) in which the maximum value of 75% is exceeded. This is especially attributed to an increasing role of the nonlinear response of the SBR copolymer in the repeated creep behavior of the modified asphalt binder and, since the amount of polymer is lower for the AC+SBR+PPA than for the AC+SBR, this may be one of the reasons why the $J_{nr,\ diff}$ values typically decrease when moving from the formulation without PPA to the one with PPA (see Table 167, page 316). Similar conclusions were drawn for the two SBS-modified asphalt binders, as discussed earlier.

Table 182 – Percent differences in nonrecoverable compliances ($J_{nr,\ diff}$) for the AC+SBR+PPA with increasing creep time and temperature

creep time (s)	$J_{nr,\ diff}$ values (%) at each creep time and temperature[a]				
	52°C	58°C	64°C	70°C	76°C
1.0	10.0	18.5	32.4	44.0	49.4
2.0	16.2	30.0	41.9	49.2	43.1
4.0	25.3	39.6	48.2	47.6	46.0
8.0	33.8	47.4	59.0	72.5	**84.8**

[a] the numbers in bold are the ones that exceeded the maximum $J_{nr,\ diff}$ (75%) according to Superpave®.

From a more practical point of view, the stress sensitivity of the AC+SBR+PPA does not seem to be a key issue concerning its use on road pavements, provided that the pavement temperature is not very high and the loading conditions are not too severe. The numerical results range from 10 to 60% at temperatures up to 64°C, and they can easily overcome 45% at temperatures higher than 64°C. However, the percent recovery and nonrecoverable compliance data (see Table 180 and Table 181) indicate that the use of the material for paving applications may be particularly restricted to PG grades lower than or equal to 64-xx and creep times no longer than 2.0 s. In such a cases, the parameter $J_{nr,\ diff}$ would not overcome 50% at any pavement temperature and loading-unloading pattern adopted in the study.

Table 183 shows the appropriate traffic levels for the AC+SBR+PPA at the temperatures and loading times studied in the dissertation. By comparing these levels with those for the AC+SBR (Table 168, page 317), it can be inferred that the degrees of improvement were much greater at 64, 70 and 76°C than at any other pavement temperature. The traffic levels were increased by one grade at the creep times of 1.0, 2.0 and 4.0 s at 64°C (very heavy, heavy and standard *versus* heavy, standard and "no traffic", respectively), creep times of 1.0 and 2.0 s at 70°C (heavy and standard *versus* standard and "no traffic", respectively), t_F of 8.0 s and temperature of 52°C (very heavy *versus* heavy) and temperature of 76°C and the standardized creep time of 1.0 s (standard *versus* "no traffic"). As a consequence, the AC+SBR+PPA tends to be more resistant to the accumulation of permanent strain in the field pavement than the AC+SBR. However, it is still not possible to utilize neither the AC+SBR nor the AC+SBR+PPA on pavements with high PG grades of 70-xx and 76-xx and creep times of 4.0 s or longer, since no traffic levels may be assigned under such test conditions.

Table 183 – Adequate traffic levels for the AC+SBR+PPA with increasing creep time and temperature based on the standardized Superpave® criteria

creep time	traffic levels for each temperature[a]				
(s)	52°C	58°C	64°C	70°C	76°C
1.0	E	E	V	H	S
2.0	E	V	H	S	-
4.0	E	H	S	-	-
8.0	V	S	-	-	-

[a] S = standard; H = heavy; V = very heavy; E = extremely heavy.

The ability of the equations from Huang (2004) – suggesting tire contact radii of 3.68 and 6.0 in – and Pereira et al. (1998, 2000) in correlating with $J_{nr}3200$ data of the AC+SBR+PPA was investigated in the study, as well as the comparisons between the traffic levels estimated by such equations and the actual ones provided by Superpave®. As a result, Table 184 was constructed. All the R^2 values range from 0.87 to 0.92, which are a little bit lower than the corresponding ones obtained for the AC+SBR. This may be explained by the increased sensitivity of the formulation with SBR+PPA to loading time and temperature, as pointed out above. Based on the previously reported data, it is not clear as to whether the predicted traffic levels are similar to the ones obtained for the binder according to the $J_{nr}3200$ values. This is discussed on the basis of the comparisons made in Table 185.

As the results in Table 185 indicate, the correlations are excellent at the temperature of 58°C, reasonable at 52°C and poor at 64 and 70°C. These conclusions are quite similar to the ones obtained for other formulations, and they are in agreement with the tendency of both equations in predicting the appropriate traffic levels of the binder only at temperatures lower than 64°C. It can be implied here that the equations have a limited applicability to actual MSCR testing data, even though the calculated traffic speeds can adequately fit the J_{nr} values at 3,200 Pa.

Table 184 – Regression equations and coefficients of determination between the $J_{nr}3200$ values of the AC+SBR+PPA and the corresponding vehicle speeds according to the equations by Pereira et al. (1998, 2000) and Huang (2004)

source and data	temperature (in °C)	equation	R^2
Pereira et al. (1998)	52	$y = 0.9643e^{-0.032x}$	0.9070
Pereira et al. (2000)	52	$y = -0.0125x + 0.8759$	0.9958
Huang (2004) $r = 6$ in	52	$y = 0.9649e^{-0.039x}$	0.9074
	58	$y = 2.7774e^{-0.040x}$	0.9153
	64	$y = 7.5749e^{-0.040x}$	0.9144
	70	$y = 19.762e^{-0.040x}$	0.8968
	76	$y = 47.0980e^{-0.041x}$	0.8792
Huang (2004) $r = 3.68$ in	52	$y = 0.9629e^{-0.063x}$	0.9076
	58	$y = 2.7715e^{-0.064x}$	0.9156
	64	$y = 7.5588e^{-0.065x}$	0.9147
	70	$y = 19.7190e^{-0.066x}$	0.8970
	76	$y = 46.9950e^{-0.067x}$	0.8795

Table 185 – Comparisons between the actual traffic levels of the AC+SBR+PPA and the ones obtained from Huang (2004) and Pereira et al. (1998)

t_F (s)[d]	actual[a] and estimated[b, c] traffic levels at each temperature[d]				
	52°C	58°C	64°C	70°C	76°C
1.0	**E (V/E) [V/E]**	**E [V/E]**	**V [V/E]**	H [V/E]	-
2.0	**E (V/E) [V/E]**	**V [V/E]**	H [V/E]	S [V/E]	-
4.0	E (H) [H]	**H [H]**	S [H]	-	-
8.0	V (S) [H]	S [H]	-	-	-

[a] S = standard; H = heavy; V = very heavy; E = extremely heavy (AASHTO M320-09 standard, Table 3).
[b] (parentheses) = traffic levels from Pereira et al. (1998).
[c] [brackets] = traffic levels from Huang (2004), $r = 6$ in.
[d] similarities among the rankings are highlighted in bold, t_F = creep time.

The fitting of binder data to the traffic speeds calculated from the equations by Huang (2004) – tire contact radius of 3.68 in – and Pereira et al. (2000) is analyzed in Table 186. One more time, the equation from Huang (2004) was able to provide good to excellent correlations ($R^2 > 0.87$) for all the selected temperatures according to Table 184. However, it is clear that the prediction of the actual traffic levels of the binder is restricted to only a few temperatures and loading times, and the points of similarity (texts highlighted in bold in Table 186) are no more than three at the temperatures of 52, 58, 64 and 70°C. In addition, the empirical-based equation from Pereira et al. (2000) could not match any traffic level of the binder at the temperature of 52°C, which is quite close to the one actually used by the authors in their mixture tests. Similarly to what was observed for other binders with and without PPA, such equations have a restricted application to a few high PG grade temperatures and creep times because the estimates of the appropriate traffic levels have major deficiencies.

Table 186 – Comparisons between the actual traffic levels of the AC+SBR+PPA and the ones obtained from the equations by Huang (2004) and Pereira et al. (2000)

t_F (s)[d]	actual[a] and estimated[b, c] traffic levels at each temperature[d]				
	52°C	58°C	64°C	70°C	76°C
1.0	**E** (H) **[V/E]**	**E [V/E]**	**V [V/E]**	H [V/E]	S [V/E]
2.0	**E** (H) **[V/E]**	**V [V/E]**	H [V/E]	S [V/E]	-
4.0	E (H) [H]	**H [H]**	S [H]	-	-
8.0	V (H) [H]	S [H]	-	-	-

[a] S = standard; H = heavy; V = very heavy; E = extremely heavy (AASHTO M320-09 standard, Table 3).
[b] (parentheses) = traffic levels from Pereira et al. (2000).
[c] [brackets] = traffic levels from Huang (2004), r = 3.68 in.
[d] similarities among the rankings are highlighted in bold, t_F = creep time.

The differences among the traffic levels of the AC+SBR+PPA estimated by the current and proposed criteria are highlighted in Table 187. The results point to the absence of differences between the Superpave® and the proposed criteria, i. e., the traffic levels are exactly the same within the whole temperature interval. They also indicate that the level of nonlinear response of the AC+SBR+PPA at longer creep times is acceptable, and thus the formulation can deal with the traffic of several slow-moving vehicles on highways without the risk of developing great amounts of rutting under the selected traffic level. As previously reported, this was not observed for the AC+SBR at all pavement temperatures (see Table 172, page 320). Also, these conclusions are in agreement with the improved rutting resistance of the AC+SBR+PPA when compared with the original AC+SBR formulation (Table 181, page 331), even though the improvements were limited to the stiffness parameter J_{nr}.

In summary, the analysis of the high-temperature performance of the AC+SBR+PPA at typical pavement temperatures and longer loading times – as well as the comparisons of its data with the ones from the original AC+SBR – points out to the fact that the addition of PPA and the reduction in the SBR content were beneficial to the rutting resistance of the binder modified with SBR, but these benefits were essentially limited to stiffness (parameter J_{nr}). Although the variations in R and J_{nr} are greater for the AC+SBR+PPA than for the AC+SBR with increasing loading time, this did not change the appropriate traffic levels assigned to the AC+SBR+PPA in a new proposed classification. More simply, the degrees of nonlinearity in the creep-recovery response at high temperatures and creep times from 1.0 to 8.0 s are lower for the AC+SBR+PPA than for the AC+SBR, which is desirable for pavements with chanellized traffic or high percentages of slow-moving trucks and buses. One minor disadvantage of the AC+SBR+PPA is the higher stress sensitivity (parameter $J_{nr,\,diff}$) at 8.0 s and 76°C, even though the maximum value of 75% was not exceeded in almost all test conditions.

Table 187 – Traffic levels of the AC+SBR+PPA with increasing loading time and temperature in the current and proposed criteria

temperature (in °C)	No. of required MSCR tests[b]	Superpave® designations (current and new criteria)[a, c]	
		current criterion	new criterion
52	4	**52E-xx**	**52E-xx**
58	4	**58E-xx**	**58E-xx**
64	4	**64V-xx**	**64V-xx**
70	3	**70H-xx**	**70H-xx**
76	2	**76S-xx**	**76S-xx**

[a] S = standard; H = heavy; V = very heavy; E = extremely heavy (AASHTO M320-09 standard, Table 3).
[b] minimum number of MSCR tests to determine the adequate traffic level in the proposed classification.
[c] similarities among the classifications are highlighted in bold.

Table 188 summarizes all the results of the constants A, B, n and α of the modified power model for the AC+SBR+PPA. Depending on the temperature, there are two different patterns of response for the formulation with respect to the constant A as follows: (a) only marginal variations with increasing creep time when this temperature does not exceed 58°C; and (b) relatively high percentages of increase with loading time at 64, 70 and 76°C, especially when the t_F value is equal to 4.0 or 8.0 s (very long creep times) and the stress level is of 3,200 Pa. In other words, the initial strain plays a relevant role on the increases in the susceptibility of the material to rutting when the temperature exceeds 58°C and the loading time is longer than 2.0 s. By achieving the high PG grades of 70-xx and 76-xx in the MSCR test, these rates of increase in A may be as higher as 10-30% and suggest that the formulation shows a great loss of resistance to rutting. For comparison purposes, one may see that the A values do not exceed 1.5 at 52 and 58°C and can easily overcome 7.0 at 64, 70 and 76°C.

Differently from the initial strain, the strain rates (B values) always increase with increasing loading time, regardless of the test condition. This means that the strain rate is mainly responsible for the higher J_{nr} values in the AC+SBR+PPA when tested at 52 and 58°C. For higher pavement temperatures, either the strain rate or the initial accumulated strain are the reasons why the binder

Table 188 – Numerical values and variations in the parameters/constants *A, B, n* and *α* from the power law equations by Saboo and Kumar (2015) with increasing temperature and creep time and considering the AC+SBR+PPA

temperature	test times	parameter A^a		parameter B^a		parameter n^a		parameter α^a	
		0.1 kPa	3.2 kPa	0.1 kPa	3.2 kPa	0.1 kPa	3.2 kPa	0.1 kPa	3.2 kPa
52°C	1/9 s	0.0157	0.5081	0.8300	0.8381	1.0015	0.9998	0.8313	0.8379
	2/9 s	0.0154 (-1.9)	0.4976 (-2.1)	0.8382 (1.0)	0.8571 (2.3)	1.0041 (0.3)	0.9992 (-0.1)	0.8417 (1.3)	0.8563 (2.2)
	4/9 s	0.0160 (1.9)	0.5189 (2.1)	0.8535 (2.8)	0.8944 (6.7)	1.0065 (0.5)	0.9966 (-0.3)	0.8590 (3.3)	0.8914 (6.4)
	8/9 s	0.0158 (0.6)	0.5127 (0.9)	0.8717 (5.0)	0.9353 (11.6)	1.0114 (1.0)	0.9984 (-0.1)	0.8816 (6.1)	0.9338 (11.4)
58°C	1/9 s	0.0357	1.1776	0.8573	0.8794	1.0006	0.9981	0.8579	0.8777
	2/9 s	0.0350 (-2.0)	1.1637 (-1.2)	0.8642 (0.8)	0.9094 (3.4)	1.0031 (0.2)	0.9972 (-0.1)	0.8668 (1.0)	0.9069 (3.3)
	4/9 s	0.0367 (2.8)	1.2282 (4.3)	0.8813 (2.8)	0.9543 (8.5)	1.0047 (0.4)	0.9987 (0.1)	0.8855 (3.2)	0.953 (8.6)
	8/9 s	0.0362 (1.4)	1.2184 (3.5)	0.8990 (4.9)	0.9887 (12.4)	1.0101 (0.9)	1.0067 (0.9)	0.9080 (5.8)	0.9953 (13.4)
64°C	1/9 s	0.0786	2.7085	0.8827	0.9298	1.0002	0.9982	0.8829	0.9282
	2/9 s	0.0776 (-1.3)	2.7005 (-0.3)	0.8924 (1.1)	0.9624 (3.5)	1.0011 (0.1)	0.9990 (0.1)	0.8934 (1.2)	0.9615 (3.6)
	4/9 s	0.0821 (4.5)	2.9181 (7.7)	0.9129 (3.4)	0.9968 (7.2)	1.0003 (0.0)	1.0036 (0.5)	0.9131 (3.4)	1.0004 (7.8)
	8/9 s	0.0809 (2.9)	2.9622 (9.4)	0.9312 (5.5)	1.0232 (10.0)	1.0041 (0.4)	1.0138 (1.6)	0.9350 (5.9)	1.0373 (11.8)
70°C	1/9 s	0.1660	6.0600	0.9062	0.9729	0.9997	0.9998	0.9059	0.9727
	2/9 s	0.1644 (-1.0)	6.1511 (1.5)	0.9182 (1.3)	0.9962 (2.4)	0.9988 (-0.1)	1.0014 (0.2)	0.9171 (1.2)	0.9976 (2.6)
	4/9 s	0.1760 (6.0)	6.8536 (13.1)	0.9462 (4.4)	1.0197 (4.8)	0.9973 (-0.2)	1.0070 (0.7)	0.9436 (4.2)	1.0269 (5.6)
	8/9 s	0.1752 (5.5)	7.3145 (20.7)	0.9715 (7.2)	1.0474 (7.7)	1.0009 (0.1)	1.0217 (2.2)	0.9724 (7.3)	1.0701 (10.0)
76°C	1/9 s	0.3316	13.1669	0.9293	0.9997	0.9982	1.0008	0.9277	1.0005
	2/9 s	0.3342 (0.8)	13.4802 (2.4)	0.9509 (2.3)	1.0136 (1.4)	0.9971 (-0.1)	1.0030 (0.2)	0.9482 (2.2)	1.0166 (1.6)
	4/9 s	0.3652 (10.1)	15.3728 (16.8)	0.9810 (5.6)	1.0319 (3.2)	0.9990 (0.1)	1.0097 (0.9)	0.9801 (5.6)	1.0419 (4.1)
	8/9 s	0.3724 (12.3)	16.8867 (28.3)	1.0051 (8.2)	1.0691 (6.9)	1.0055 (0.7)	1.0309 (3.0)	1.0106 (8.9)	1.1022 (10.2)

[a] the percentages of variation reported in parenthesis refer to the changes in the parameter when moving from 1.0 s to the creep time into question (2.0, 4.0 or 8.0 s).

shows a higher rutting potential when loaded for longer periods of time in the DSR. The variations in the percentages of increase in *B* are approximately the same from one loading time to the other, and results higher than one may be commonly found at 70 and 76°C. These features and patterns of response in *A* and *B* resemble the ones observed for the AC+SBR (see Table 173, page 321), especially at the stress level of 3,200 Pa.

With respect to the degree of nonlinearity (parameter *n*), it is clear that its effect on the higher susceptibility of the AC+SBR+PPA to rutting is minimal when the temperature is no greater than 64°C, especially at 100 Pa. This can be translated into percentages of increase or decrease lower than 1.6% in modulus, regardless of the applied stress. When the test conditions are more critical (temperatures greater than 64°C and stress level of 3,200 Pa), this effect is a little bit more visible and percentages achieving 2-3% may be seen in some cases. The *n* values are slightly higher for the AC+SBR than for the AC+SBR+PPA, but the results do not differ by more than 3% from one material to the other.

By comparing the percent recovery data of the AC+SBR+PPA (Table 180, page 329) with its corresponding α values, it can be observed that the null recoveries – especially at the temperatures of 64, 70 and 76°C and the loading-unloading times of 4/9 s and 8/9 s – are associated with α values between 0.91 and 1.10 (i. e., all approaching unity). These α values are a little bit lower for the AC+SBR+PPA than for the AC+SBR at 52 and 58°C (differences between the results are no greater than 3.6%), and the opposite is found at 64, 70 and 76°C (differences between the numerical values are no greater than 3.2%). This discussion is compatible with the higher recoveries for the AC+SBR+PPA when compared with the AC+SBR at lower pavement temperatures (T < 64°C) and the opposite trend at higher temperatures ($T \geq$ 64°C), refer to page 329 for more details. Again, the parameter α may be used as an indicator of the level of recovery in the asphalt binder during the MSCR tests.

By taking into account the limiting criteria for the use of the AC+SBR+PPA on pavements as suggested by the R and J_{nr} data (64°C, 3,200 Pa and t_F = 2.0 s), one may see that the constant *A* is equal to 2.7, the constant *B* is almost equal to unity (0.9624) and the parameter α approaches one as well (0.9615). As recommended in the literature, such conditions indicate that the asphalt binder may depict a reasonable potential for accumulating permanent strain. Therefore, the critical values for the parameters/constants of the power model provide additional information on the possible uses of the asphalt binder on field pavements. Since the *n* values do not overcome 1.04 neither for the AC+SBR nor for the AC+SBR+PPA, it can be said that nonlinearity should not be a great concern in the study of the rutting potential of the SBR-modified asphalt binders according to the previously selected test conditions.

Direct comparisons between the *A* values of the AC+SBR+PPA and the AC+SBR were made, and the results are plotted in Figure 143. A total of 20 data points were collected in these comparisons at each stress level, and every data point is associated with one temperature (out of five) and one loading time (out of four) – the multiplication 5 × 4 yields the 20 aforementioned data points. As may be observed, all the data points are placed above the equality lines and suggest that the *A* values of the AC+SBR are higher than the ones of the AC+SBR+PPA. This gives support to the previously cited arguments, according to which the AC+SBR+PPA is less prone to rutting than the AC+SBR mainly because of the less initial strain accumulated in the material. The numerical values are from 25 to 75% higher for the AC+SBR than for the AC+SBR+PPA and, in average, they are 50% greater for the formulation with SBR alone.

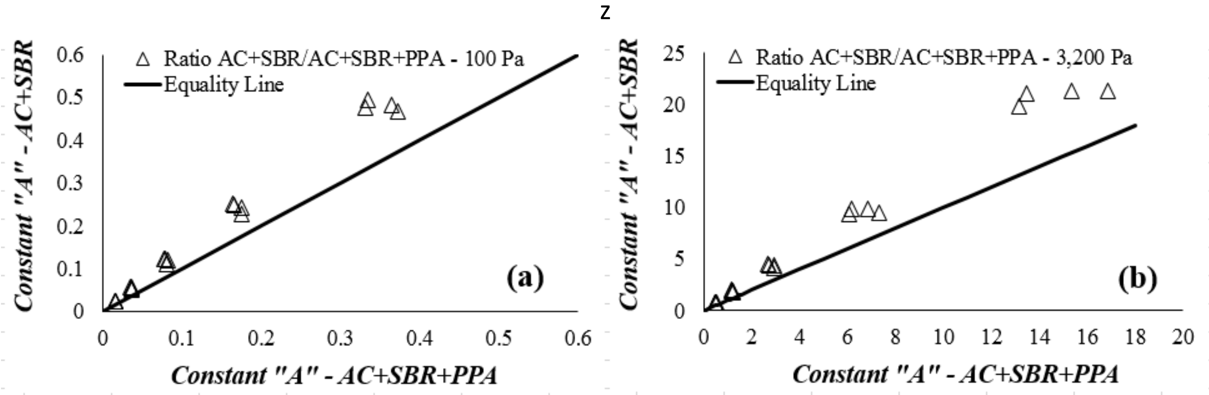

Figure 143 – Plots of the data points associated with the *A* values for the AC+SBR+PPA in the X-axes and the corresponding ones for the AC+SBR in the Y-axes at 100 Pa (a) and 3,200 Pa (b), the continuous lines are the equality lines

The analyses of the variations in the constants *A* and *B* with loading time for the AC+SBR+PPA were conducted similarly to what was made for the other reported formulations. Figure 144 shows the resulting linear correlations for *A* and *B* at 64°C and 100 Pa, whereas Figure 145 reports these same correlations for the same temperature, but considering the stress level of 3,200 Pa. As discussed above, the initial strain (*A* values) has a relevant influence in the loss of rutting resistance of the formulation at temperatures of 64°C and greater. This can be seen not only in the positive gradients of the regression equations, but also the increasing values of the constants of these equations (0.0004 and 0.0782 at 100 Pa, *versus* 0.0398 and 2.6730 at 3,200 Pa). More specifically, the rate of increase in the initial strain with creep time is considerably higher when the applied stress is equal to 3,200 Pa (almost 100 times, from 0.0004 to 0.0398). In addition, one may see that the *A* values at 2/9 s seem to be a kind of outliers within the group of data points at both stress levels; however, this feature tends to disappear with increasing stress level since R^2 is much higher at 3,200 Pa than at 100 Pa.

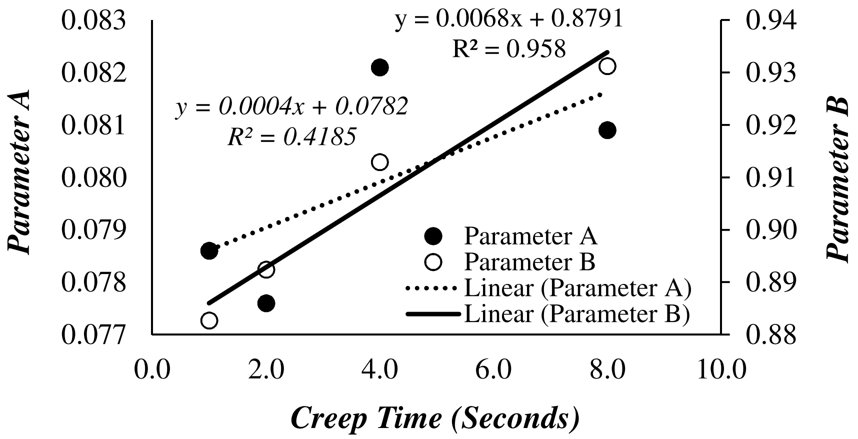

Figure 144 – Correlations between the creep time and the constants *A* and *B* from the model by Saboo and Kumar (2015), temperature of 64°C and stress level of 100 Pa – AC+SBR+PPA

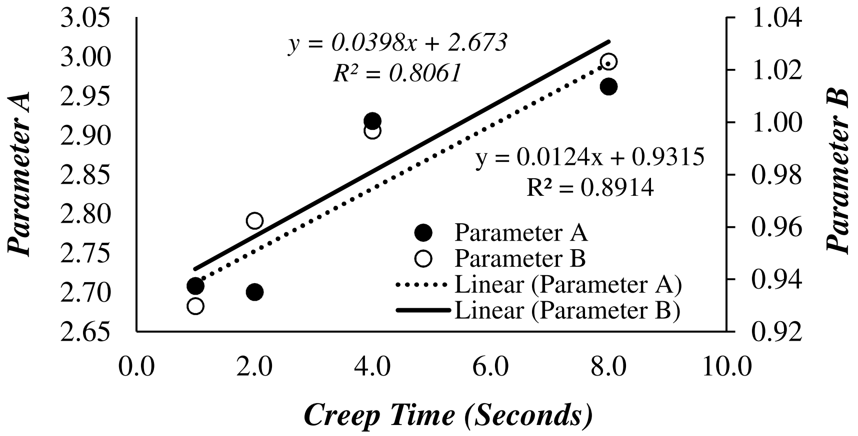

Figure 145 – Correlations between the creep time and the constants *A* and *B* from the model by Saboo and Kumar (2015), temperature of 64°C and stress level of 3,200 Pa – AC+SBR+PPA

By carefully analyzing all the data reported in Table 188, it can be observed that the constant *A* slightly decreases when moving from 1/9 s to 2/9 s and the temperature is no greater than 64°C. This is a typical characteristic of formulations that showed a great resistance to rutting, e. g., AC+SBS+PPA (Table 158, page 302), AC+SBS (Table 143, page 285) and AC+Elvaloy+PPA (Table 98, page 234). The AC+SBR also showed this pattern of response, but only at 100 Pa (see Table 173, page 321). Up to the present moment, it has been observed that formulations with higher resistances to rutting generally depict decreasing *A* values with increasing temperature and loading time in the MSCR tests; however, this is not a universal rule because each modifier behaves differently when subjected to creep-recovery loading. The "outliers" for the AC+SBR+PPA at 2/9 s may be explained by a transitional phase between this type of response at temperatures lower than 64°C (see Table 188) and a consistent increase in the *A* values with creep time at 70 and 76°C.

By increasing the temperature to 70°C (Figure 146 and Figure 147 for the data at 100 and 3,200 Pa, respectively), it can be observed that the pattern of response for the constant *B* is essentially the same at both temperatures, namely, progressive increases with loading time and rates of increase that almost perfectly fit a straight line when plotted against the t_F values (R^2 always higher than 0.89). The slope of the regression equation for *B* at 70°C and 100 Pa (0.0093) is higher than the corresponding value at 64°C and 100 Pa (0.0068); however, the same cannot be said for the results at 3,200 Pa (0.0124 at 64°C and 0.0100 at 70°C). This is an indication that the importance of the strain rate on the increases in the susceptibility of the AC+SBR+PPA to rutting becomes a little bit smaller at 70°C when compared with the initial strain. As a matter of comparison, the slopes of the linear regression equations of *A* increase by 3.75 times (from 0.0004 to 0.0015) at 100 Pa and by 4.7 times (from 0.0398 to 0.1868) at 3,200 Pa after the shift in the pavement temperature by 6°C.

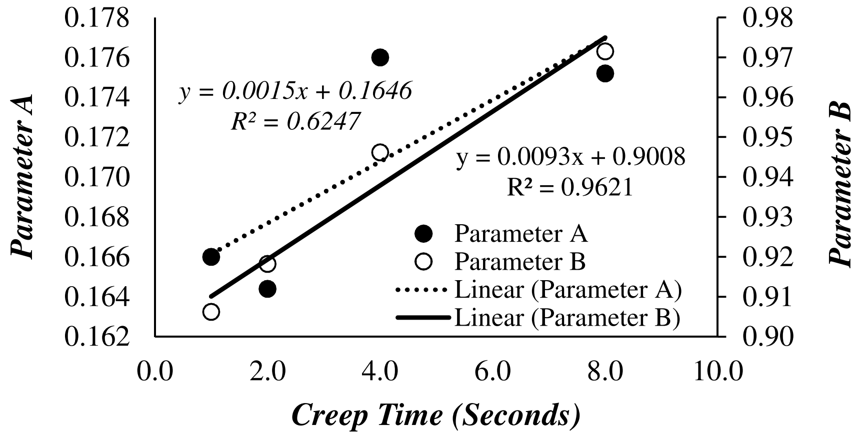

Figure 146 – Correlations between the creep time and the constants *A* and *B* from the model by Saboo and Kumar (2015), temperature of 70°C and stress level of 100 Pa – AC+SBR+PPA

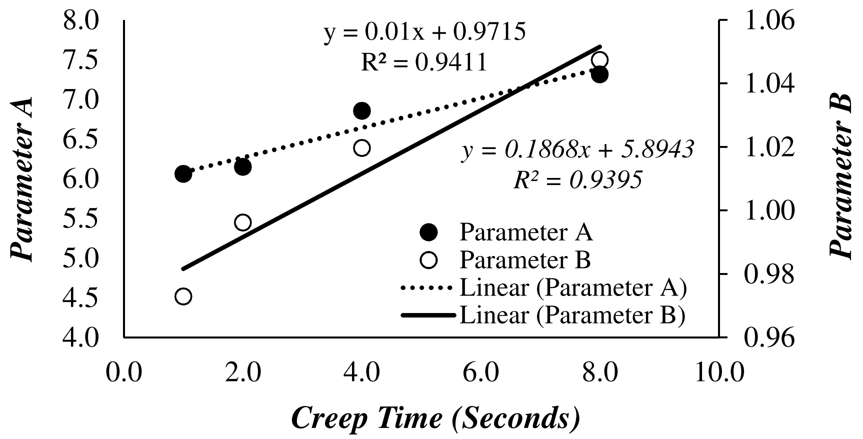

Figure 147 – Correlations between the creep time and the constants *A* and *B* from the model by Saboo and Kumar (2015), temperature of 70°C and stress level of 3,200 Pa – AC+SBR+PPA

Table 189 shows all the resulting correlations for *A* and *B* with loading time at the selected pavement temperatures and stress levels. Due to the particular characteristic of the behavior observed for the *A* values of the AC+SBR+PPA reported above (i. e., small decreases in *A* when moving from 1.0 to 2.0 s of creep time, especially at 100 Pa), the coefficients of determination R^2 at temperatures no greater than 64°C are substantially lower than the corresponding values at 70 and 76°C. Overall, it can be seen that the *A* values become higher with increasing severity in the loading conditions during the MSCR tests. However, this phenomenon is not clear at 52 and 58°C in a general context because the correlations are from poor to regular (< 0.54) in all cases. What can be mentioned is that, as the temperature becomes higher and the vehicle speed decreases (i. e., t_F increases), the role of the initial strain on the increase in the susceptibility of the AC+SBR+PPA to rutting is more visible (R^2 is higher) and greater (slopes and intercepts of the equations are higher as well).

Table 189 – Degrees of correlation between the parameters *A* and *B* (modified power model) and the creep time t_F for the AC+SBR+PPA

T (°C)	stress (kPa)	linear regression equations and R^2 values (in parenthesis)[a]	
		parameter *A*	parameter *B*
52	0.1	y = 4E-05 + 0.0156 (0.1949)	y = 0.0059x + 0.8263 (0.9792)
	3.2	y = 0.0014x + 0.5040 (0.2372)	y = 0.0137x + 0.8298 (0.9744)
58	0.1	y = 0.0001x + 0.0354 (0.2853)	y = 0.0060x + 0.8531 (0.9752)
	3.2	y = 0.0073x + 1.1695 (0.5278)	y = 0.0150x + 0.8768 (0.9238)
64	0.1	y = 0.0004x + 0.0782 (0.4185)	y = 0.0068x + 0.8791 (0.9580)
	3.2	y = 0.0398x + 2.6730 (0.8061)	y = 0.0124x + 0.9315 (0.8914)
70	0.1	y = 0.0015x + 0.1646 (0.6247)	y = 0.0093x + 0.9008 (0.9621)
	3.2	y = 0.1868x + 5.8943 (0.9395)	y = 0.0100x + 0.9715 (0.9411)
76	0.1	y = 0.0062x + 0.3277 (0.8291)	y = 0.0103x + 0.9278 (0.9238)
	3.2	y = 0.5500x + 12.6640 (0.9589)	y = 0.0097x + 0.9922 (0.9963)

[a] the Y-axis is associated with the parameter (*A* or *B*), whereas the X-axis is associated with t_F.

With respect to the correlations for the parameter *B*, two distinctive pictures can be drawn: one at 100 Pa and another at 3,200 Pa. The values of this parameter consistently increase with increasing loading time at 100 Pa, and higher temperatures simply contribute to the determination of higher *B* values as well. In other words, the role of the strain rate on the higher rutting potential of the AC+SBR+PPA at 100 Pa is proportionally associated with the temperature. By moving to the stress level of 3,200 Pa, this proportion can be observed only at 52 and 58°C – i. e., either the slope or the intercept increase with increasing temperature. For higher temperatures (64, 70 and 76°C), one may see that the slopes continuously decrease and the intercepts increase as the climate conditions become more severe. This is associated with the lower importance of the strain rate on the presence of a higher rutting potential in the formulation and, at the same time, the *A* values increase much faster at such temperatures. In a few words, the AC+SBR+PPA becomes more prone to rutting at very high PG grades (64-xx and greater) especially because of the increasing contribution of the initial strain on this condition of the binder, even though the strain rate also plays some role on it.

Table 190 summarizes all the correlations between the parameters n and α and the loading times for the AC+SBR+PPA. While the parameter n does not seem to depict a clear relationship with increasing temperature neither the constants of its regression equations, it is reasonable to say that the correlations for the parameter α point to a consistent increase in the numerical values with loading time and temperature, either at 100 Pa or at 3,200 Pa. In addition, reverses in the signal of the gradients of the equations for n may be found at 52 and 58°C, but not in the equations for α. Finally, the levels of correlation are not necessarily good for n within the whole temperature interval, especially at 100 Pa (some poor correlations can be found at 52 and 70°C). As a consequence of these findings, good correlations between n and J_{nr} may not be expected and (at least) regular correlations between α and R can be obtained.

Table 190 – Degrees of correlation between the parameters n and α (modified power model) and the creep time t_F for the AC+SBR+PPA

T (°C)	stress (kPa)	linear regression equations and R^2 values (in parenthesis)[a, b]	
		parameter n	parameter α
52	0.1	y = 0.0013x + 1.0008 (0.9829)	y = 0.0070x + 0.8270 (0.9824)
	3.2	y = -0.0002x + 0.9992 (0.1948)	y = 0.0135x + 0.8291 (0.9810)
58	0.1	y = 0.0013x + 0.9998 (0.9830)	y = 0.0071x + 0.8529 (0.9830)
	3.2	y = 0.0013x + 0.9952 (0.8799)	y = 0.0163x + 0.8722 (0.9479)
64	0.1	y = 0.0005x + 0.9995 (0.7831)	y = 0.0073x + 0.8786 (0.9741)
	3.2	y = 0.0023x + 0.9950 (0.9891)	y = 0.0147x + 0.9266 (0.9293)
70	0.1	y = 0.0002x + 0.9984 (0.1858)	y = 0.0095x + 0.8992 (0.9781)
	3.2	y = 0.0032x + 0.9955 (0.9882)	y = 0.0134x + 0.9667 (0.9754)
76	0.1	y = 0.0012x + 0.9956 (0.8912)	y = 0.0115x + 0.9237 (0.9515)
	3.2	y = 0.0044x + 0.9946 (0.9808)	y = 0.0144x + 0.9862 (0.9989)

[a] the Y-axis is associated with the parameter (n or α), whereas the X-axis is associated with t_F.
[b] changes in the signal of the slope of the regression trendlines are highlighted with a grey-shaded box.

Figure 148 is in aligment with the above-mentioned discussions, in that no clear correlations between n and J_{nr} exist (R^2 is of only 0.23) and a particular n value may refer to several J_{nr} values. Even though this correlation is better than the one obtained for the AC+SBR (see Figure 137, page 326), it is still not enough to say that n is directly related to J_{nr}. The most appropriate explaination for such a finding is that the level of nonlinearity in the binder is not high enough to be clearly detected by the modified power model and, in this case, much longer creep times could yield better results. What may be inferred from the chart is that, similarly to the AC+SBR, there is really a portion of nonlinear response in the results of the AC+SBR+PPA, but it is quite small to be observed and correlated with other rheological data in a general context. If the data values of n and J_{nr} at 100 Pa and 3,200 Pa are plotted on separate charts, the resulting R^2 values will be very small at 100 Pa (only 0.044) and regular at 3,200 Pa (0.6351). These results resemble the ones determined for other formulations, e. g., the AC+rubber+PPA.

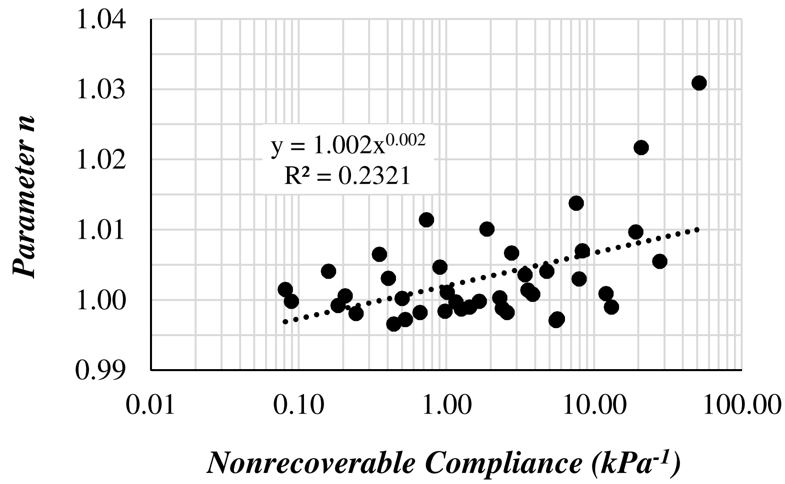

Figure 148 – Degree of correlation between the nonrecoverable compliances of the AC+SBR+PPA and the corresponding n values from the power law models

In addition to confirming that the parameter α is a quite good indicator of the percent recovery of the AC+SBR+PPA in the MSCR test, the regression equation and the R^2 value of almost 0.825 – as shown in Figure 149 – are also very close to the results of the AC+SBR (Figure 138, page 327). In numerical terms, the gradient of the equation is about 21% higher for the material with SBR+PPA and the intercept is almost equivalent for the two materials (percent difference of only 0.25%). The level of correlation is about 3.1% higher for the AC+SBR when compared with the AC+SBR+PPA, but this cannot be considered as significant because the two R^2 values are from good to excellent (i. e., between 0.8 and 0.9). The presence of a higher slope for the AC+SBR+PPA is in agreement with the faster decreases in R for this formulation in comparison to the AC+SBR, as pointed out earlier.

The rheological modeling of the creep-recovery data of the AC+SBR+PPA reveals that the initial strain (constant A) plays a less important role in the increase in the susceptibility of the material to rutting at the temperatures of 52 and 58°C, but this role increases significantly at the temperatures of 64°C and higher. This can also be inferred by studying the regression constants of the strain rate B at the same temperatures, that is, the slopes of the equations decrease with increasing pavement temperature. In addition, nonlinearity (parameter n) does not seem to considerably affect the response of the AC+SBR+PPA in the MSCR tests because the variations in the corresponding parameter are typically lower than 3%. The AC+SBR is more prone to rutting than the AC+SBR+PPA mainly because of the higher initial strains for the former than the latter, and this is valid throughout the test conditions used in the study. Due to the difficulties in correctly estimating the contribution of nonlinearity to the creep-recovery behavior of the formulation, the degrees of correlation between n and J_{nr} are generally poor (R^2 lower than 0.64). However, good to excellent correlations ($R^2 > 0.80$) can be found when plotting the parameter α against the percent recoveries of the material.

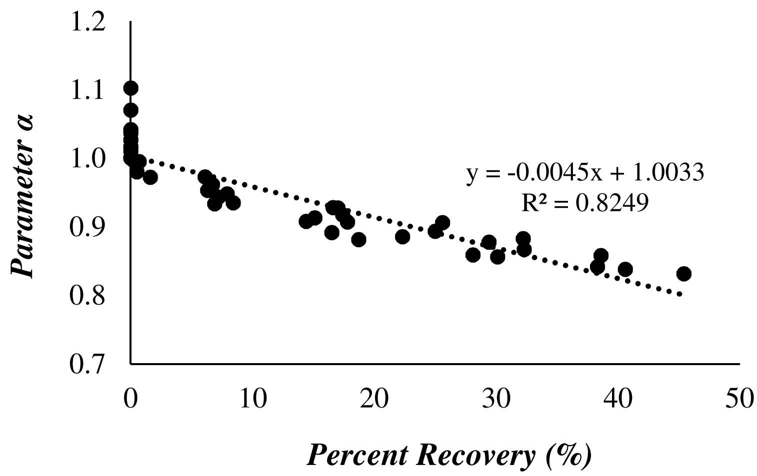

Figure 149 – Degree of correlation between the percent recoveries of the AC+SBR+PPA and the corresponding α values from the power law models

The study of the analysis of variance (ANOVA) may be carried out either in the percent recoveries or the nonrecoverable compliances of the AC+SBR+PPA, since there is only one null value among the data points at 1/9 s and 3,200 Pa (refer to Table 180, page 329). Again, the level of significance of 5% remained unchanged and the rearranged R values are provided in Table 191. The outcomes of ANOVA for these recoveries are given in Table 192.

As can be seen, the *F-value* and the *p-value* in Table 192 reveal the existence of a great similarity among the R values of the AC+SBR+PPA as a function of temperature and loading time. In other words, both variables seem to cause approximately the same effect on the elastic responses of the formulation under the test conditions studied here. This degree of similarity is much higher at 3.2 kPa than at 0.1 kPa, since the *F-value* was decreased by more than 90% and the *p-value* was increased by 6.8% after such a change in the stress level. The *p-value* is never lower than 0.90 (against a level of significance of 0.05), and the *F-value* is always lower than

0.014 (against $F_{critical}$ values between 5 and 6). Thus, the null hypothesis should not be rejected at any stress level. The AC+SBR yielded quite similar findings, but there is a reverse in the stress level that shows a higher level of homogeneity within the groups of data points: 100 Pa for the AC+SBR and 3,200 Pa for the AC+SBR+PPA (see Table 177 in page 328 for further details).

Table 191 – Rearranged MSCR testing data of the AC+SBR+PPA to be used in the analysis of variance (ANOVA) – percent recovery

stress level of 0.1 kPa (*R100*, *%*)[a]		stress level of 3.2 kPa (*R3200*, *%*)[a]	
increasing creep time	increasing temperature	increasing creep time	increasing temperature
45.4	45.4	40.6	40.6
38.3	38.6	30.1	29.4
28.1	32.2	16.5	16.6
18.7	25.6	6.9	6.1
N/A[b]	17.0	N/A[b]	N/A[b]

[a] the starting point in both cases was the temperature of 52°C.
[b] N/A: Not applicable.

Table 192 – Results from the analysis of variance (ANOVA, *p-value* and *F-value*) as based on the percent recoveries of the AC+SBR+PPA

null hypothesis H_0	statistical parameters (ANOVA)				recommendation
	$F_{critical}$	*F-value*	α	*p-value*	
equivalency between R values with increasing creep time and temperature, 0.1 kPa	5.5914	0.0130	0.05	0.9126	H_0 is not rejected
equivalency between R values with increasing creep time and temperature, 3.2 kPa	5.9874	0.0011	0.05	0.9746	H_0 is not rejected

The same approach was followed for the nonrecoverable compliances of the AC+SBR+PPA, and the organized J_{nr} values to be tested in ANOVA can be found in Table 193. Table 194 shows the results of ANOVA according to the input J_{nr} data. As can be observed, the variances within the J_{nr} values are considerably higher than the corresponding variances within the R values, especially at 3,200 Pa. Similar conclusions were drawn for the AC+SBR, refer to Table 179 (page 329). This indicates that the compliances can distinguish among the effects of temperature and loading time on the creep-recovery behavior of the material more clearly, and the stiffness of the AC+SBR+PPA is affected by increases in the temperature in a higher proportion than in the creep time. However, the results cannot be interpreted as derived from different sets of data from a statistical point of view. This is because the critical parameters α and $F_{critical}$ were not exceeded by the *F-value* and the *p-value*, respectively. As a consequence, the null hypothesis should not be rejected with respect to the nonrecoverable compliance values.

Table 193 – Rearranged MSCR testing data of the AC+SBR+PPA to be used in the analysis of variance (ANOVA) – nonrecoverable creep compliance

stress level of 0.1 kPa ($J_{nr}100$, kPa^{-1})[a]		stress level of 3.2 kPa ($J_{nr}3200$, kPa^{-1})[a]	
increasing creep time	increasing temperature	increasing creep time	increasing temperature
0.081	0.081	0.089	0.089
0.159	0.206	0.185	0.244
0.351	0.500	0.440	0.662
0.732	1.157	0.979	1.666
N/A[b]	2.571	N/A[b]	3.840

[a] the starting point in both cases was the temperature of 52°C.
[b] N/A: Not applicable.

Table 194 – Results from the analysis of variance (ANOVA, *p-value* and *F-value*) as based on the nonrecoverable compliances of the AC+SBR+PPA

null hypothesis H_0	statistical parameters (ANOVA)				recommendation
	$F_{critical}$	*F-value*	α	*p-value*	
equivalency between J_{nr} values with increasing creep time and temperature, 0.1 kPa	5.5914	1.1515	0.05	0.3188	H_0 is not rejected
equivalency between J_{nr} values with increasing creep time and temperature, 3.2 kPa	5.5914	1.1901	0.05	0.3114	H_0 is not rejected

Asphalt Binder Modification with Plastomers (EVA and PE). Table 195 is a summary of the percent recovery values of the AC+EVA under all the MSCR testing conditions. Surprisingly, the results of *R100* showed almost no variations at the temperatures of 52 and 58°C (reductions of only 4.1% at 52°C and 8.6% at 58°C with loading times increasing from 1.0 to 8.0 s at 100 Pa, see Figure 150). This can somehow be observed at 52°C and the stress level of 3,200 Pa as well, i. e., the *R3200* value decreased by only 26% when the creep time was boosted from 1.0 to 8.0 s. On the other hand, these promising findings were apparently restricted to temperatures no greater than 64°C, since the recoveries sharply dropped to values no greater than 13% at 70 and 76°C and the application of longer creep times have a more damaging effect on the elasticity of the binder. Similar patterns of behavior were also observed for another crude source of the base asphalt binder and EVA-modified materials graded as 76-xx, i. e., different loading conditions in the MSCR tests caused more damage in the formulation when the temperatures were higher than 64°C (DOMINGOS and FAXINA, 2014).

Table 195 – Percent recoveries at 100 Pa (*R100*) and 3,200 Pa (*R3200*) for the AC+EVA with increasing loading time and temperature

parameter	creep time (s)	results at each temperature and increases (both in %)[a]				
		52°C	58°C	64°C	70°C	76°C
R100	1.0	95.7	93.0	57.3	12.7	4.2
	2.0	94.6	90.7	53.5	12.4	3.1
	4.0	93.8	88.1	46.7	3.3	0.0
	8.0	91.8	85.0	37.8	0.0	0.0
R3200	1.0	89.9	83.9	31.3	1.7	0.0
	2.0	85.6	72.0	17.5	0.0	0.0
	4.0	82.5	43.0	3.7	0.0	0.0
	8.0	66.5	17.7	0.0	0.0	0.0

[a] the percentages refer to the decreases in *R* at longer creep times when compared with the data at 1.0 second.

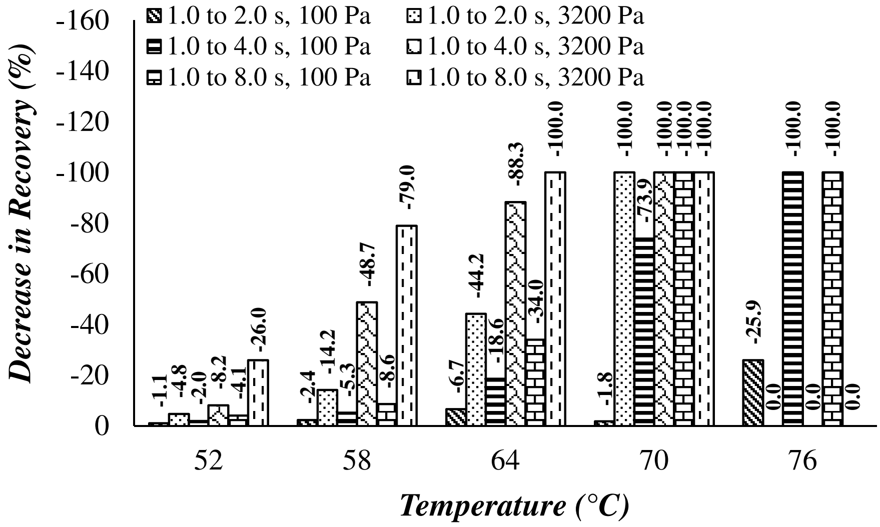

Figure 150 – Percentages of decrease in the recoveries of the AC+EVA with creep time, temperature and stress level

This characteristic of the AC+EVA makes it possible to infer that its response resembles a brittle and elastic material with a "failure point" in the MSCR test. More specifically, this "failure point" could be defined as the test conditions (temperature and loading time) under which the formulation cannot depict reasonable percent recoveries anymore – arbitrarily defined here as recoveries of 10% or higher – due to a possible melting of the polymer network (SABOO and KUMAR, 2016). It may also be explained by the higher susceptibility of the EVA-modified binders to temperature and stress level when compared with other modification types such as SBS (DOMINGOS and FAXINA, 2017; SABOO and KUMAR, 2015, 2016). By carefully analyzing the *R* values in Table 195, it can be seen that the "failure point" at 100 Pa is located at T = 70°C and t_F = 2.0 s and the one at 3,200 Pa is located at T = 64°C and t_F = 2.0 s. In other words, the

AC+EVA will have a great probability of failure if the temperature and the loading time increase beyond the values established by the "failure points". In practical terms, the use of the AC+EVA on pavements with field conditions more severe than the ones of the "failure points" does not ensure a good rutting performance of the material, even though its PG grade is 76-xx.

This discussion about the presence of "failure points" is intrinsically related to the nature of the EVA copolymer. Since this modifier is a plastomer and the vinyl acetate content used in the study is very high (28%), the tough and rigid network formed in the binder is able to resist deformation and impart high degrees of stiffness to the original material. In other words, the great levels of elasticity – R values approaching 100% in some cases – were caused by the reaction of the polar acetate groups in the polymer chain with the components of the binder and the use of quite high modifier contents (POLACCO et al., 2006, 2015; ZHU et al., 2014). However, the consequence of the formation of a too stiff material is that the amount of strain must be kept below a "yield" level, otherwise failure may occur. This is considered in the study of the low-temperature resistance of asphalt binders on Superpave® and the evaluation of the failure properties of brittle materials, and it seems to be found here as well.

The nonrecoverable compliances of the AC+EVA in all testing conditions are summarized in Table 196. By transferring the previously defined "failure points" to the J_{nr} values, it can be seen that the limiting values are equal to 3.444 and 1.785 kPa^{-1} at 100 and 3,200 Pa, respectively. When the testing conditions defined by the "failure points" are increased (temperature and loading time), it can be seen that the compliances easily overcome 7.0 kPa^{-1} at 100 Pa and 4.0 kPa^{-1} at 3,200 Pa. These values are certainly very high and not suitable at all for paving applications. The percentages of variation are also considerably increased above the "failure points", namely, 150% or more at 100 Pa and 190% or more at 3,200 Pa (see Figure 151). The excellent rutting performance of asphalt mixtures prepared with the AC+EVA (Chapter 5) may be inserted into the aforementioned analysis as well, i. e., the temperature (60°C) and the loading-unloading times (0.1-0.9 s) are less severe than the ones found in the "failure points".

Surprisingly, the J_{nr} values of the AC+EVA increased by more than 2,500% when moving from 1.0 to 8.0 s at the temperature of 58°C and the stress level of 3,200 Pa. This result is much greater than any other one found in the nonrecoverable compliance data of the formulation. It is believed that such a percentage of increase may be attributed to the effects of steady state and nonlinearity on the response of the material, i. e., the compliances in the beginning of the first cycles at 8/9 s considerably differ from the ones in the last few cycles. As a consequence, the differences between the values in the two extremes of the 10 cycles (1st and 10th cycle) at 8/9 s may have contributed to the determination of a mean value that does not necessarily reflect the great variations in J_{nr} during the application of loading-unloading cycles. A third possibility is that, due to the use of very long creep times in the MSCR tests, the polymer network accumulated a considerable amount of damage during the test and the percentages of recovery dropped to very small results from the beginning to the end of the group of cycles at 3,200 Pa.

Table 196 – Nonrecoverable compliances at 100 Pa ($J_{nr}100$) and 3,200 Pa (J_{nr} *3200*) for the AC+EVA with increasing loading time and temperature

parameter	creep time (s)	results at each temperature (kPa^{-1}), J_{nr} > 4.0 kPa^{-1} is in bold				
		52°C	58°C	64°C	70°C	76°C
$J_{nr}100$	1.0	0.008	0.028	0.414	2.201	**4.106**
	2.0	0.012	0.051	0.612	3.444	**7.113**
	4.0	0.019	0.096	1.425	**7.841**	**14.741**
	8.0	0.034	0.171	2.814	**15.482**	**30.201**
$J_{nr}3200$	1.0	0.018	0.065	0.856	2.729	**5.191**
	2.0	0.034	0.161	1.785	**4.933**	**9.341**
	4.0	0.053	0.577	**4.321**	**9.744**	**19.666**
	8.0	0.146	1.715	**8.931**	**21.640**	**45.630**

[a] the percentages refer to the increases in J_{nr} and the creep time when compared with the data at 1.0 second.

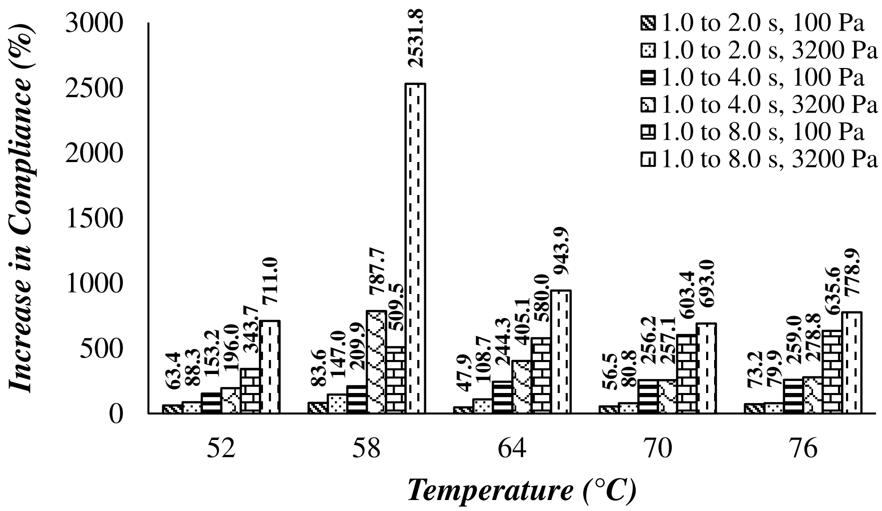

Figure 151 – Percentages of increase in the nonrecoverable compliances of the AC+EVA with creep time, temperature and stress level

To give one step further into the aforementioned discussion on the steady state and damage phenomena of the AC+EVA at 58°C, 8/9 s and 3,200 Pa, Figure 152 (original sample) was prepared to illustrate the differences within the *R3200* and the $J_{nr}3200$ values from the first to the last creep-recovery cycle. As one can see, the *R3200* values dropped from about 33% to 10% after the application of the 10 standardized cycles – a decrease of 68.4%. At the same time, the $J_{nr}3200$ values increased from 1.0 kPa^{-1} to about 2.2 kPa^{-1} – a percentage of increase approximately equal to 116.8%. This is an indication that the material suffered a considerable loss of elasticity (*R*) and stiffness (J_{nr}) during the test, and also that the polymeric network was extensively damaged. Loading times longer than 3.0 s may cause great amounts of damage in the binder sample and reach the tertiary flow during the creep portion of the cycle, as pointed out in a literature review by Mturi et al. (2012). This gives even more support to the assumption that the benefits of EVA addition to the base binder are particularly limited to creep times lower than 4.0 s and temperatures no greater than 64°C.

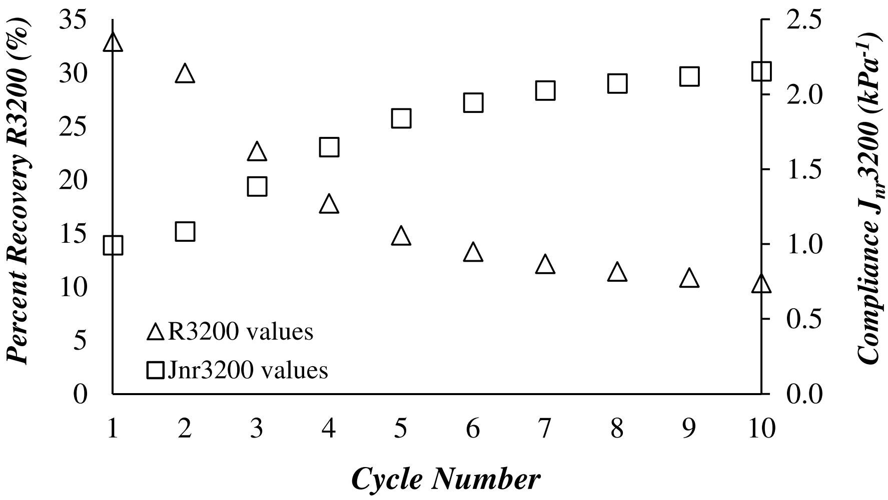

Figure 152 – Plots of the percent recoveries and the nonrecoverable compliances at 3,200 Pa (*R3200* and $J_{nr}3200$) at each cycle for the AC+EVA at 8/9 s and 58°C (original sample)

For comparison purposes, Figure 153 (original sample) refers to the *R3200* and $J_{nr}3200$ data of the AC+EVA at the same temperature and the same stress level, but considering the creep-recovery times of 4/9 s. The recoveries decrease from approximately 48% to results around 30-40% (more specifically, 35%) – a decrease of only 27.2%. In turn, the compliances increase from results around 0.50 kPa^{-1} (more specifically, 0.475 kPa^{-1}) to numerical values approximately equal to 0.72 kPa^{-1} – an increase of 51.2%. The slight increases in *R3200* and decreases in $J_{nr}3200$ in the first five cycles may be explained by the role of delayed elasticity on the creep-recovery response of the material in the DSR. In this manner, the delayed elastic response of the cycle will continue after its end and may be confounded with the subsequent cycle results. With the application of more loading-unloading cycles, the relative effect of the delayed elasticity from each additional cycle decreases and the binder tends to approach the steady state behavior (GOLALIPOUR et al., 2016; SOENEN et al., 2013). Perhaps the delayed elastic portion of the response of the AC+EVA at 8/9 s – previous figure – could not be seen due to damage inflicted to the polymer network, as discussed above.

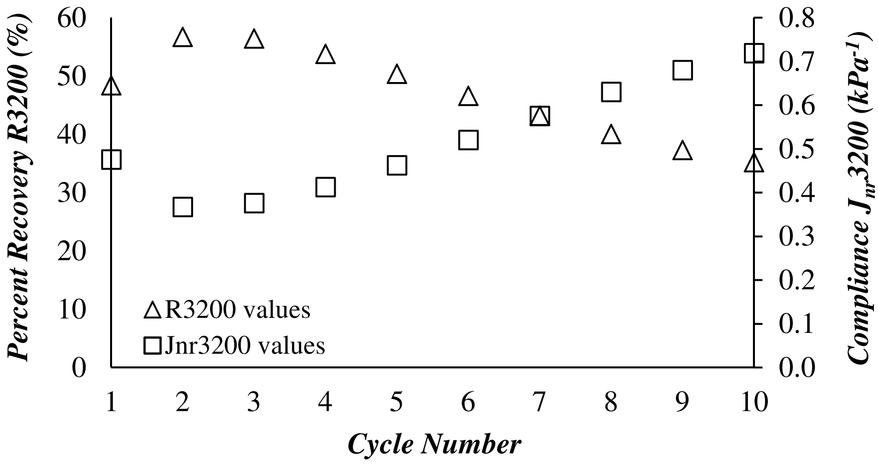

Figure 153 – Plots of the percent recoveries and the nonrecoverable compliances at 3,200 Pa (*R3200* and J_{nr}*3200*) at each cycle for the AC+EVA at 4/9 s and 58°C (original sample)

The limitations of temperature and loading time imposed by the *R* and J_{nr} values of the AC+EVA have justifications in other studies. Very high temperatures may negatively affect the rutting resistance of the EVA-modified binders in much greater proportions when compared with other modification types such as PPA, and this was also observed in a previous study conducted by Domingos and Faxina (2014) with a different base binder and the same type of EVA used here. In addition, it might be important to remind that the AC+EVA practically shows no recovery when the temperature is greater than 58°C and the material is subjected to the loading times of 4.0 and 8.0 s and the stress level of 3,200 Pa (see Table 195). Based on these findings and observations, the following conclusions may be reached:

- the loading time of 4.0 s does not inflict as much damage in the polymeric network of the AC+EVA as 8.0 s in the MSCR tests, which is in accordance with the literature;
- temperatures higher than 64°C lead to much smaller recoveries for the formulation at 3,200 Pa, which may be linked to a combination of melting of the polymer network and high degrees of damage in the sample during the test;
- the delayed elasticity has a key role in the study of the creep-recovery behavior of the AC+EVA for t_F values no greater than 4.0 s; and
- similarly to what was highlighted by Golalipour et al. (2016), the consideration of all cycles in the determination of the *R* and J_{nr} values at 3,200 Pa may cause problems to the correct interpretation of the actual rutting resistance of some modified asphalt binders, especially the highly-modified ones and with significant levels of delayed elasticity.

Since the AC+EVA is graded as a binder with "high elasticity" at the standardized loading-unloading times of 1/9 s and temperatures no greater than 64°C (refer to Figure 57, page 168), further analyses were conducted to see whether the material still retains this classification at longer creep times in the MSCR tests. Figure 154 precisely indicates that this is true for the all the acceptable $J_{nr}3200$ values (that is, results no greater than 2.0 kPa^{-1}) at 1/9 s and 4/9 s, as well as two out of three data points at 2/9 s and one out of two data points at 8/9 s. In other words, the grading of the AC+EVA as a binder with high elasticity will depend upon the selected test conditions. This formulation shows a low level of elasticity – i. e., "poor elasticity" – at some temperatures at 8/9 s (58°C) and 2/9 s (64°C). In a few words, it is not possible to say that the AC+EVA will hold the classification of "material with high elasticity" under all the MSCR testing conditions, even the ones in which $J_{nr}3200 \leq 2.0$ kPa^{-1}. In contrast, the AC+Elvaloy+PPA does not show any decay in its classification (Figure 86, page 229), and this is associated with the much higher sensitivity of the AC+EVA to increases in the pavement temperature.

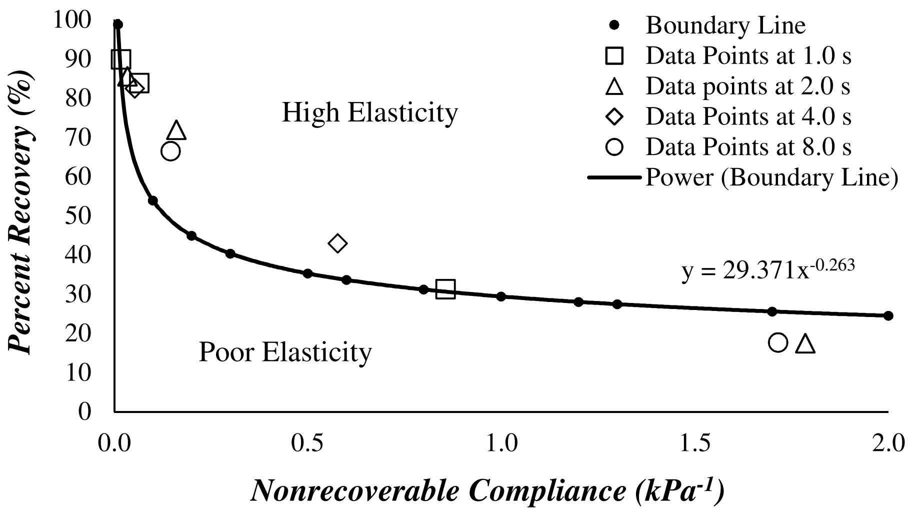

Figure 154 – Degrees of elasticity for the AC+EVA at increased creep times and temperatures as based on the MSCR testing parameters at 3,200 Pa

The percent differences in nonrecoverable compliances of the AC+EVA are shown in Table 197. Two very distinctive responses can be seen here; i. e., one at temperatures up to 64°C (the binder is overly stress sensitive, $J_{nr,\ diff}$ is no lower than 106%) and the other at the temperatures of 70 and 76°C (the binder is not overly stress sensitive, $J_{nr,\ diff}$ is always lower than 45%). By drawing comparisons between these results with the ones from R and J_{nr}, one may conclude that the $J_{nr,\ diff}$ data are consistent with the concept of "failure point" described above. More specifically, the two conditions specified by the "failure points" at 100 Pa (T = 70°C and t_F = 2.0 s) and 3,200 Pa (T = 64°C and t_F = 2.0 s) are closely related to the change in the stress sensitivity of the AC+EVA. The material is very sensitive to an increase in the stress level for $T \leq 64$°C possibly due to a direct influence of the nonlinear response of the polymer network on the creep-recovery data. On the other hand, the binder is not too stress sensitive at 70 and 76°C probably because the sample is extremely damaged and the role of the polymer on the repeated creep behavior of the material is minimized.

Table 197 – Percent differences in nonrecoverable compliances ($J_{nr,\ diff}$) for the AC+EVA with increasing creep time and temperature

creep time (s)	$J_{nr,\ diff}$ values (%) at each creep time and temperature[a]				
	52°C	58°C	64°C	70°C	76°C
1.0	**135.7**	**132.7**	**106.7**	24.0	26.4
2.0	**171.7**	**213.1**	**191.6**	43.2	31.3
4.0	**175.6**	**563.2**	**203.3**	24.3	33.4
8.0	**330.8**	**904.7**	**217.4**	39.8	51.1

[a] the numbers in bold are the ones that exceeded the maximum $J_{nr,\ diff}$ (75%) according to Superpave®.

With respect to the complex polymer network that is formed after binder modification with EVA (POLACCO et al., 2015), one may imply that this network played a major role in the substantially high *R* values at 100 Pa and temperatures no greater than 64°C. On the other hand, its contribution to the elasticity of the formulation is reduced when the critical testing conditions dictated by the "failure points" are not observed. Based on the mixture testing data reported in Chapter 5 and the very high $J_{nr,\ diff}$ values for the AC+EVA at 58 and 64°C, it may be implied that the flow number testing results were not seriously affected by the stress sensitivity of the EVA-modified binder. With respect to the criterion of $J_{nr,\ diff}$ no greater than 75%, there are some concerns about its applicability to all types of modified binders as pointed out by Teymourpour et al. (2016) and Zhou et al. (2014). Thus, it is believed that some refinements in the specification may be needed to take into account the rheological behavior of modified materials.

Some final comments regarding the melting of the polymer network on EVA-modified asphalt binders and their great temperature susceptibility can be made based on information published elsewhere. As shown and discussed above, the presence of very high *R* values at temperatures up to 64°C is compatible with the temperature at which the ethylene-rich segments of EVA usually melt – about 55°C, according to Airey (2002) and Zhu et al. (2014). The considerable decreases in the benefits of EVA modification at temperatures greater than 55°C were also noticed by other authors such as Saboo and Kumar (2015), for which the elastic response of an EVA-modified binder at 10,000 Pa became worse than the one of an SBS-modified binder at the temperatures of 50 and 60°C in the MSCR tests. Saboo and Kumar (2016) reported that an EVA-modified asphalt binder showed a higher temperature susceptibility than an SBS-modified binder when the materials were tested at 40, 50 and 60°C and in the oscillatory shear mode. Finally, Domingos and Faxina (2014) reported considerable variations in the R and J_{nr} values of a pure EVA-modified material at 52, 58, 64, 70 and 76°C when compared with a pure PPA-modified one.

The appropriate traffic levels of the AC+EVA are summarized in Table 198. As a consequence of the substantially high J_{nr} values above the "failure point" at 3,200 Pa (64°C and 2.0 s), the binder is not able to deal with any traffic level under more severe testing conditions except for the standard traffic at 70°C and 1/9 s. On the other hand, these traffic levels are very high (especially very heavy and extremely heavy) at 52 and 58°C and point to the existence of a high degree of stiffness in the binder at such pavement temperatures. Again, the definition of a "failure point" for the AC+EVA seems to be a good alternative to establish the range of temperatures and loading times under which the binder can be used for paving applications.

Table 198 – Adequate traffic levels for the AC+EVA with increasing creep time and temperature based on the standardized Superpave® criteria

creep time (s)	traffic levels for each temperature[a]				
	52°C	58°C	64°C	70°C	76°C
1.0	E	E	V	S	-
2.0	E	E	H	-	-
4.0	E	V	-	-	-
8.0	E	H	-	-	-

[a] S = standard; H = heavy; V = very heavy; E = extremely heavy.

As done for the other formulations, the equations from Huang (2004) – tire radii of 3.68 and 6.0 in – and Pereira et al. (1998, 2000) were used to calculate the traffic speeds for each vehicle as a function of the loading time. Then, such speeds were correlated with the $J_{nr}3200$ values at the temperatures of 52, 58, 64, 70 and 76°C. Table 199 provides all the data for these aforementioned equations. The effects of nonlinearity, a very high degree of stiffness at temperatures up to 64°C and a poor rutting performance at 70 and 76°C are reflected into the coefficients of determination for the material, i. e., they may vary from values as lower as 0.84 to others higher than 0.90. Although these coefficients are still good, the great disparities among the responses of the binder at high pavement temperatures indicate that such equations may not be suitable for estimating the actual traffic levels of the AC+EVA. A further clarification to this doubt can be obtained based on the comparisons in Table 200.

The comparisons made in Table 200 suggest that, as previously obtained for other modified materials, the predictions of the actual traffic levels for the AC+EVA are mainly restricted to the temperatures of 52 and 58°C. When the temperature is increased to 64 and 70°C, these estimations are not acceptable due to the poor correlations with the actual traffic levels, and also because the binder cannot deal with any type of traffic at 70 and 76°C in a general context. More simply, the equations and levels of correlation shown in Table 199 are only mathematical fits and cannot be used to study the relationship between J_{nr} and average traffic speed in all cases.

Table 199 – Regression equations and coefficients of determination between the $J_{nr}3200$ values of the AC+EVA and the corresponding vehicle speeds according to the equations by Pereira et al. (1998, 2000) and Huang (2004)

source and data	temperature (in °C)	equation	R^2
Pereira et al. (1998)	52	$y = 0.1241e^{-0.026x}$	0.8398
Pereira et al. (2000)	52	$y = -0.0012x + 0.0969$	0.9824
Huang (2004) $r = 6$ in	52	$y = 0.1242e^{-0.032x}$	0.8405
	58	$y = 1.8109e^{-0.055x}$	0.9039
	64	$y = 9.0858e^{-0.038x}$	0.9173
	70	$y = 20.1320e^{-0.033x}$	0.8814
	76	$y = 41.9020e^{-0.035x}$	0.8729
Huang (2004) $r = 3.68$ in	52	$y = 0.1240e^{-0.052x}$	0.8407
	58	$y = 1.8057e^{-0.089x}$	0.9042
	64	$y = 9.0671e^{-0.063x}$	0.9176
	70	$y = 20.0970e^{-0.054x}$	0.8817
	76	$y = 41.8260e^{-0.056x}$	0.8732

Table 200 – Comparisons between the actual traffic levels of the AC+EVA and the ones obtained from Huang (2004) and Pereira et al. (1998)

t_F (s)[d]	actual[a] and estimated[b, c] traffic levels at each temperature[d]				
	52°C	58°C	64°C	70°C	76°C
1.0	**E (V/E) [V/E]**	**E [V/E]**	**V [V/E]**	S [V/E]	-
2.0	**E (V/E) [V/E]**	**E [V/E]**	H [V/E]	-	-
4.0	E **(H) [H]**	V [H]	-	-	-
8.0	E (S) [H]	**H [H]**	-	-	-

[a] S = standard; H = heavy; V = very heavy; E = extremely heavy (AASHTO M320-09 standard, Table 3).
[b] (parentheses) = traffic levels from Pereira et al. (1998).
[c] [brackets] = traffic levels from Huang (2004), $r = 6$ in.
[d] similarities among the rankings are highlighted in bold, t_F = creep time.

By changing the equations and the tire contact radius, the comparisons between actual and predicted traffic levels shown in Table 201 can be obtained. The pattern of behavior seen in the previous equations remained the same here, that is, great differences among the R^2 values and the inability of both equations in reasonably predicting the maximum traffic levels that the binder can experience in the field pavement without a premature failure by rutting. In addition, the correct estimations of the traffic levels according to the equation from Pereira et al. (2000) could be achieved only at very long creep times (4/9 and 8/9 s) and the temperature of 52°C. Therefore, none of these equations are recommended on general studies about the estimates of the traffic levels of the AC+EVA and the corresponding average vehicle speeds.

Table 201 – Comparisons between the actual traffic levels of the AC+EVA and the ones obtained from the equations by Huang (2004) and Pereira et al. (2000)

t_F (s)[d]	actual[a] and estimated[b, c] traffic levels at each temperature[d]				
	52°C	58°C	64°C	70°C	76°C
1.0	**E** (H) **[V/E]**	**E [V/E]**	**V [V/E]**	S [V/E]	-
2.0	**E** (H) **[V/E]**	**E [V/E]**	H [V/E]	-	-
4.0	E **(H) [H]**	V [H]	-	-	-
8.0	E **(H) [H]**	**H [H]**	-	-	-

[a] S = standard; H = heavy; V = very heavy; E = extremely heavy (AASHTO M320-09 standard, Table 3).
[b] (parentheses) = traffic levels from Pereira et al. (2000).
[c] [brackets] = traffic levels from Huang (2004), r = 3.68 in.
[d] similarities among the rankings are highlighted in bold, t_F = creep time.

Table 202 shows the comparisons between the current and proposed criteria for establishing the appropriate traffic levels of the AC+EVA at pavement temperatures from 52 to 76°C. The high degree of nonlinearity of the formulation at longer creep times affected its designation at the pavement temperature of 64°C: the traffic level decreased by one grade (from very heavy to heavy). Other binders also showed this one-grade reduction at one or more pavement temperatures, e. g., the AC+Elvaloy+PPA and the AC+PPA as presented earlier and in the paper by Domingos and Faxina (2017). The other levels were not changed, which means that the nonlinear response of the AC+EVA at longer creep times was not enough to substantially increase the amount of unrecovered strain and affect its rutting performance, as referenced on the newly proposed Superpave® traffic criteria.

Table 202 – Traffic levels of the AC+EVA with increasing loading time and temperature in the current and proposed criteria

temperature (in °C)	No. of required MSCR tests[b]	Superpave® designations (current and new criteria)[a, c]	
		current criterion	new criterion
52	4	**52E-xx**	**52E-xx**
58	4	**58E-xx**	**58E-xx**
64	3	64V-xx	64H-xx
70	2	**70S-xx**	**70S-xx**
76	1	**76-xx**	**76-xx**

[a] S = standard; H = heavy; V = very heavy; E = extremely heavy (AASHTO M320-09 standard, Table 3).
[b] minimum number of MSCR tests to determine the adequate traffic level in the proposed classification.
[c] similarities among the classifications are highlighted in bold.

The MSCR testing results of the AC+EVA indicate that two distinctive responses can be identified in the asphalt binder, that is, one at temperatures no greater than 64°C and the other at temperatures higher than this upper limit. Based on the inherent characteristics of plastomeric modification of asphalt binders with EVA copolymer (i. e., very high degrees of stiffness and reactivity with the base material), the melting of the polymeric network at temperatures typically higher than 55°C, the temperature susceptibility and the amount of accumulated damage during the MSCR test, the concept of "failure point" was introduced to explain the marked differences in the creep-recovery behavior of the formulation as a function of temperature, stress level and loading time. This "failure point" is approximately located at T = 70°C and t_F = 2.0 s for the lowest stress level and at T = 64°C and t_F = 2.0 s for the highest one. In addition, the delayed elasticity plays a relevant role in the response of the AC+EVA at each creep-recovery cycle at 3,200 Pa and for loading times no greater than 4.0 s. As a consequence, refinements in the MSCR protocol and methods of calculation of R and J_{nr} at 3,200 Pa are recommended to account for these singularities of the AC+EVA.

The stress sensitivity can also be studied based on these observations, in that the AC+EVA is too sensitive to increases in the stress level before the "failure point" and not overly stress sensitive after it. The binder cannot deal with almost any traffic level when the test conditions are more severe than the ones established by the "failure point" at 3,200 Pa, whereas the levels are much higher when the testing conditions do not exceed the limits imposed by the "failure point". This excessive level of nonlinear response also influenced on the maximum traffic level allowable for the binder at 64°C, i. e., there was a decrease by one grade (from very heavy according to the standardized criteria and heavy according to the proposed one). In other words, it may not be enough to accurately evaluate the repeated creep behavior of the AC+EVA in the real pavement without varying the loading patterns in the MSCR test.

Table 203 provides all the values of the parameters/constants A, B, n and α for the AC+EVA, according to the modified power model from Saboo and Kumar (2015). The particular creep-recovery responses of this formulation as a function of temperature, stress level and loading time are visible and, in each case, the parameters of the model vary differently from the shortest to the longest creep times. Only the constant A shows a uniform pattern of behavior with creep time at all temperatures and stress levels, i. e., it consistently decreases as the loading conditions become more severe. This is especially observed for the formulations with very high degrees of stiffness in the MSCR tests, e. g., the AC+Elvaloy+PPA (Table 98, page 234), the AC+rubber (Table 112, page 250) and the AC+SBS+PPA (Table 158, page 302). In these cases, the decreases in R and increases in J_{nr} are explained by increases in one or more of the remaining parameters of the model, i. e., B and/or n. With respect to the AC+rubber and the AC+SBS+PPA, it was observed that the reductions in A were compensated by increases in either B or n with loading time. For the

Table 203 – Numerical values and variations in the parameters/constants *A, B, n* and *α* from the power law equations by Saboo and Kumar (2015) with increasing temperature and creep time and considering the AC+EVA

temperature	test times	parameter A^a		parameter B^a		parameter n^a		parameter α^a	
		0.1 kPa	3.2 kPa	0.1 kPa	3.2 kPa	0.1 kPa	3.2 kPa	0.1 kPa	3.2 kPa
52°C	1/9 s	0.0181	0.5850	0.6107	0.6135	1.0424	1.0366	0.6366	0.6360
	2/9 s	0.0159 (-12.2)	0.5118 (-12.5)	0.5929 (-2.9)	0.5946 (-3.1)	1.0738 (3.0)	1.0573 (2.0)	0.6367 (0.0)	0.6287 (-1.1)
	4/9 s	0.0154 (-14.9)	0.4904 (-16.2)	0.5337 (-12.6)	0.5382 (-12.3)	1.1385 (9.2)	1.0824 (4.4)	0.6076 (-4.6)	0.5826 (-8.4)
	8/9 s	0.0163 (-9.9)	0.5040 (-13.8)	0.4666 (-23.6)	0.5069 (-17.4)	1.2484 (19.8)	1.0860 (4.8)	0.5825 (-8.5)	0.5504 (-13.5)
58°C	1/9 s	0.0414	1.3438	0.6688	0.6682	1.0370	1.0288	0.6935	0.6874
	2/9 s	0.0367 (-11.4)	1.2091 (-10.0)	0.6567 (-1.8)	0.6704 (0.3)	1.0644 (2.6)	1.0317 (0.3)	0.6990 (0.8)	0.6916 (0.6)
	4/9 s	0.0357 (-13.8)	1.2176 (-9.4)	0.6141 (-8.2)	0.7328 (9.7)	1.119 (7.9)	0.9986 (-2.9)	0.6871 (-0.9)	0.7318 (6.5)
	8/9 s	0.0371 (-10.4)	1.1988 (-10.8)	0.5648 (-15.6)	0.8445 (26.4)	1.2091 (16.6)	0.9813 (-4.6)	0.6829 (-1.5)	0.8287 (20.6)
64°C	1/9 s	0.1028	4.2160	0.8195	0.8763	1.0085	0.9986	0.8265	0.8750
	2/9 s	0.0794 (-22.8)	3.8934 (-7.7)	0.8183 (-0.1)	0.9143 (4.3)	1.0184 (1.0)	0.9974 (-0.1)	0.8334 (0.8)	0.9119 (4.2)
	4/9 s	0.0895 (-12.9)	3.9710 (-5.8)	0.8155 (-0.5)	0.9647 (10.1)	1.0334 (2.5)	0.9990 (0.0)	0.8427 (2.0)	0.9637 (10.1)
	8/9 s	0.0863 (-16.1)	3.7408 (-11.3)	0.8116 (-1.0)	1.0066 (14.9)	1.0585 (5.0)	1.0099 (1.1)	0.8591 (3.9)	1.0165 (16.2)
70°C	1/9 s	0.2708	9.4980	0.9416	0.9822	0.9974	0.9987	0.9392	0.9809
	2/9 s	0.2167 (-20.0)	8.4743 (-10.8)	0.9405 (-0.1)	0.9986 (1.7)	0.9995 (0.2)	1.0005 (0.2)	0.9400 (0.1)	0.9991 (1.9)
	4/9 s	0.2277 (-15.9)	8.2897 (-12.7)	0.9705 (3.1)	1.0161 (3.5)	1.0006 (0.3)	1.0054 (0.7)	0.9710 (3.4)	1.0216 (4.1)
	8/9 s	0.2133 (-21.2)	8.2799 (-12.8)	0.9914 (5.3)	1.0372 (5.6)	1.0060 (0.9)	1.0166 (1.8)	0.9973 (6.2)	1.0544 (7.5)
76°C	1/9 s	0.4597	17.7972	0.9718	1.0046	0.9983	1.0008	0.9702	1.0054
	2/9 s	0.3978 (-13.5)	15.9180 (-10.6)	0.9783 (0.7)	1.0129 (0.8)	1.0002 (0.2)	1.0027 (0.2)	0.9785 (0.9)	1.0156 (1.0)
	4/9 s	0.3974 (-13.6)	16.0145 (-10.0)	0.9994 (2.8)	1.0277 (2.3)	1.0034 (0.5)	1.0084 (0.8)	1.0028 (3.4)	1.0364 (3.1)
	8/9 s	0.3949 (-14.1)	16.8606 (-5.3)	1.0179 (4.7)	1.0508 (4.6)	1.0106 (1.2)	1.0225 (2.2)	1.0287 (6.0)	1.0744 (6.9)

[a] the percentages of variation reported in parenthesis refer to the changes in the parameter when moving from 1.0 s to the creep time into question (2.0, 4.0 or 8.0 s).

AC+Elvaloy+PPA, it could be seen that only the parameter *n* typically increased with t_F at temperatures no greater than 64°C and both parameters *B* and *n* experienced increases with t_F at 70 and 76°C.

From the results reported in Table 203, one may observe that the pattern of behavior of the AC+EVA at 52 and 58°C shows similarities with the one of the AC+Elvaloy+PPA at the same temperatures (only *n* generally increases with loading time). In other words, the presence of lower recoveries and higher nonrecoverable compliances at longer creep times are dictated by the increase in the role of nonlinearity on the response of the binder. As described above, these temperatures are smaller or very close to the one at which the EVA copolymer is expected to melt, and thus it is believed that the polymer network was the main responsible for providing high percentages of recovery during the test and a nonlinear fashion with increasing t_F. This is particularly noticeable at 52°C (both stress levels) and 58°C (only at 100 Pa), in which *n* can boost to results 16-19% higher than the initial values and the constants *A* and *B* show percentages of reduction as higher as 15-26% when moving from 1/9 s to 8/9 s. Lastly, the reductions in α reflect the presence of high recoveries in the material (~ 66-96%), even at very long loading times.

By moving to test conditions more severe than – or equal to – the temperature of 58°C and the stress level of 3,200 Pa, a completely different pattern of response may be seen in the AC+EVA. The importance of nonlinearity on this response becomes particularly minor (*n* does not vary by more than 5% in modulus) and the strain rate starts to play a key role on the increase in the susceptibility of the formulation to rutting (i. e., *B* increases at longer loading times). At the same time, the α values show higher percentages of increase from one loading time to the other at 3,200 Pa (~ 16-20% in some cases) than at 100 Pa (< 4%), both at 58 and 64°C. These differences might be attributed to great accumulation of damage in the polymer network when loaded at 3,200 Pa and very long creep times and temperatures, which did not occurred with the same proportion at 100 Pa. Since the EVA copolymer is expected to be fully melted at 70 and 76°C and the amount of damage is higher even at 100 Pa, the percentages of variation within the parameters *B*, *n* and α tend to be similar at 100 and 3,200 Pa and nonlinearity is rather difficult to be seen in the results (*n* always lower than 1.06).

The percent recoveries of the AC+EVA are practically null at 70 and 76°C and the highest stress level (3,200 Pa), and this may be translated into α values between 0.98 and 1.08 – in accordance with other previously studied binders. The above-mentioned "failure points" of the material at 100 Pa (70°C and 2/9 s) and 3,200 Pa (64°C and 2/9 s) are associated with *A* values of 0.22 and 3.89, *B* values of 0.94 and 0.91, *n* values almost equal to unity and α values always greater than 0.90. The results at 3,200 Pa are associated with a formulation with a rather high susceptibility to failure by rutting, particularly because the propensity to the accumulation of initial strains is very high ($A >> 1.0$), the strain rate is relatively high as well ($B \approx 1.0$) and the amount of recovery at each cycle is very small ($\alpha \approx 0.92$).

A complementary investigation was carried out to determine which formulation – AC+Elvaloy+PPA or AC+EVA – depicts the best results of the parameters A, B and α in a general context. This was made because both materials showed high levels of elasticity and very promising findings in the MSCR test, and thus a direct comparison between the formulations would allow a further understanding of the advantages and disadvantages of each modification type as a whole. In this manner, Figure 155 was prepared to provide comparisons between the A values for the two materials. The majority of the data points are placed above the equality line, which means that the AC+Elvaloy+PPA typically depicts lower initial strains than the AC+EVA under creep-recovery loading. This may be explained by the stability and high elastic response provided by the asphalt-polymer system developed in the formulation, which can reduce the amount of strain accumulated in the sample even under very critical test conditions.

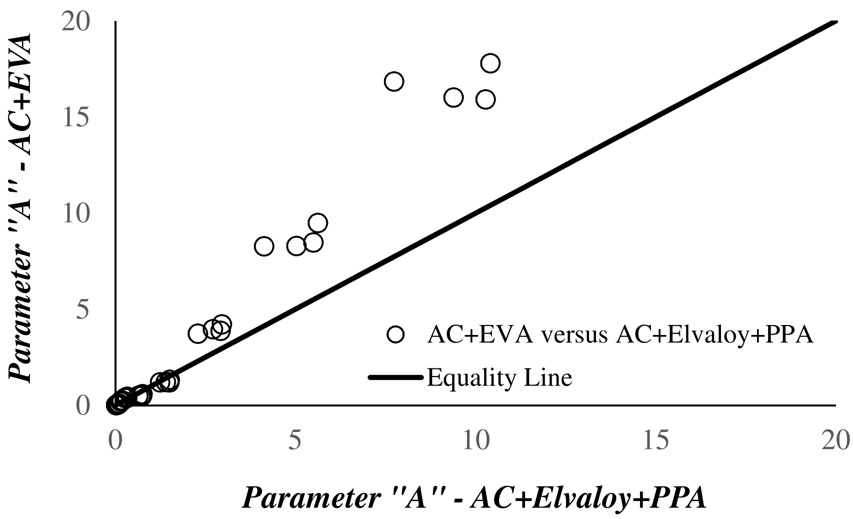

Figure 155 – Comparison between the A values of the modified power model by Saboo and Kumar (2015) for the AC+EVA and the AC+Elvaloy+PPA under all MSCR testing conditions

With respect to the B and α values, Figure 156 and Figure 157 reveal that the boundary test condition is given by the temperature of 58°C, the stress level of 3,200 Pa and the creep-recovery times of 4/9 s. These limiting conditions are precisely the ones under which the polymeric network in the AC+EVA may suffer considerable damage if one or more input data values become more severe, as shown earlier. Higher temperatures and stress levels and/or longer creep times emphasize the benefits of binder modification with Elvaloy® and PPA when compared with

EVA alone (points above the equality lines), and the opposite is observed for less critical conditions in the tests (points below the equality lines).

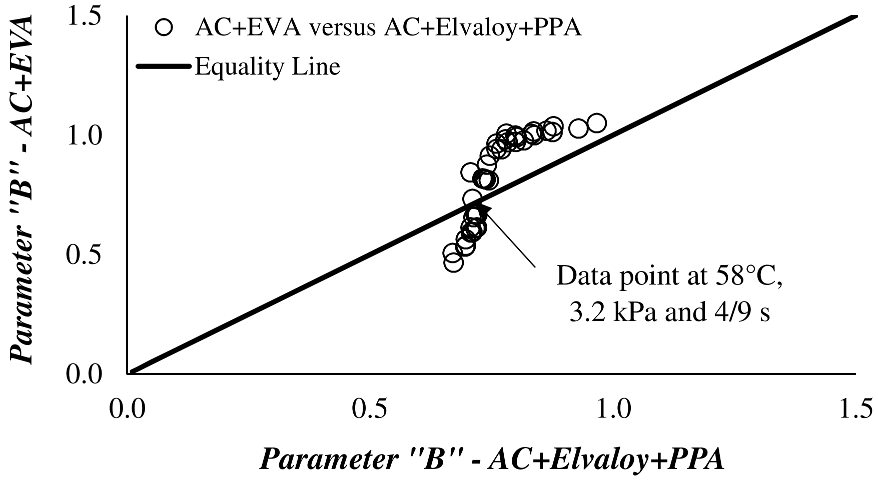

Figure 156 – Comparison between the *B* values of the modified power model by Saboo and Kumar (2015) for the AC+EVA and the AC+Elvaloy+PPA under all MSCR testing conditions

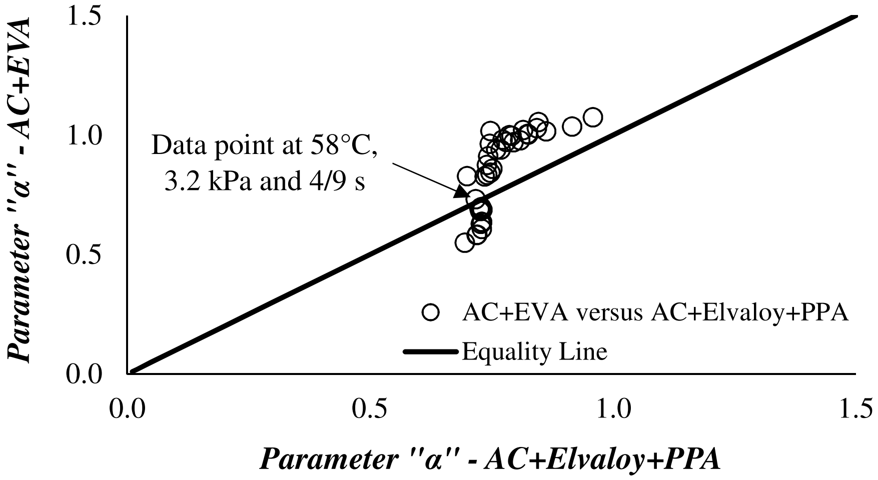

Figure 157 – Comparison between the *α* values of the modified power model by Saboo and Kumar (2015) for the AC+EVA and the AC+Elvaloy+PPA under all MSCR testing conditions

More simply, the AC+EVA depicts lower strain rates and higher elastic responses than the AC+Elvaloy+PPA when the stress level is equal to 100 Pa – regardless of the other variables – or equal to 58°C, provided that the loading time is shorter than 4.0 s. If the the stress level is of 3,200 Pa, the temperature is greater than 58°C and/or the loading time is longer than 4.0 s, the AC+Elvaloy+PPA will show the best results for *B* and *α*. This again confirms that the AC+Elvaloy+PPA has more stability and less variability within the responses in the MSCR test, and also that the AC+EVA has better results for the model parameters than the AC+Elvaloy+PPA, unless the polymer network is melted or seriously damaged.

Figure 158 and Figure 159 are graphical representations of the variations in the constants *A* and *B* with creep time for the pavement temperature of 64°C and the stress levels of 100 and 3,200 Pa, respectively. As the full data in Table 203 suggest, the *A* values always decrease with increasing t_F and the *B* values show a reverse in their pattern of response at 70°C (stress of 100 Pa) and 58°C (stress of 3,200 Pa). This reverse is associated with an increasing role of the strain rate on the presence of higher susceptibilities of the AC+EVA to rutting in the MSCR test, which takes place when the structure of the polymer network in the formulation becomes seriously compromised (as pointed out earlier). The decreases in *A* at 100 Pa do not precisely follow a straight line, whereas the data at 3,200 Pa are more closely associated with a linear relationship with the t_F values.

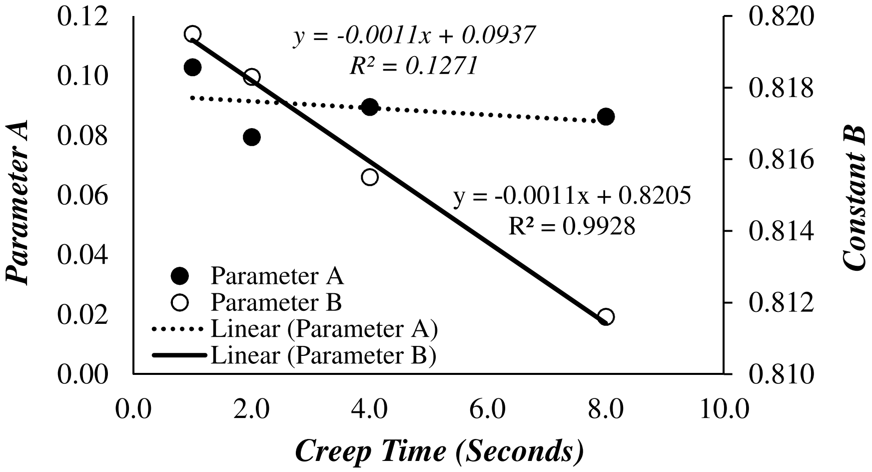

Figure 158 – Correlations between the creep time and the constants *A* and *B* from the model by Saboo and Kumar (2015), temperature of 64°C and stress level of 100 Pa – AC+EVA

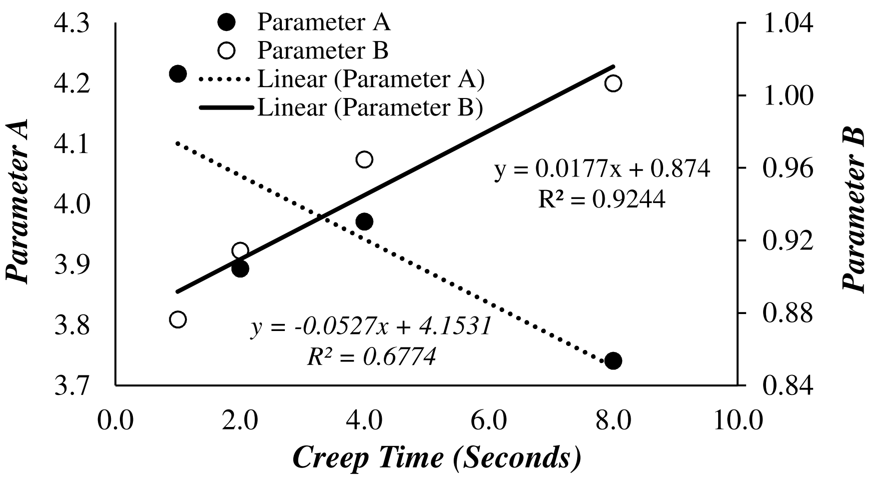

Figure 159 – Correlations between the creep time and the constants *A* and *B* from the model by Saboo and Kumar (2015), temperature of 64°C and stress level of 3,200 Pa – AC+EVA

The differences between the R^2 values of the linear regression trendlines of *A* are possibly due to the influence of nonlinearity on the final results of the AC+EVA. The *n* values may reach 1.05 at very long creep times and 100 Pa, whereas the results do not overcome 1.01 at 3,200 Pa (see Table 203). On the other hand, the *B* values show progressive increases with t_F and the results have excellent correlations with loading time ($R^2 > 0.92$ in both cases). In other words, the *A* values are more sensitive to effects of nonlinearity on the creep-recovery responses of the asphalt binder than the *B* values. Other binders with relevant levels of nonlinearity such as the AC+rubber also depicted these particular features, refer to Table 112 and Figure 95 to Figure 98 for more details (pages from 250 to 253). The great differences among the numerical values of the constants of the equations at 100 and 3,200 Pa are in agreement with the stress sensitivity of the formulation at 64°C (Table 197) and the amount of damage accumulated in the sample when higher stress levels are used.

Figure 160 and Figure 161 may be obtained by increasing the pavement temperature to 70°C and keeping the other variables unchanged. The correlations for the *A* values are better than the corresponding ones at 64°C and 100 Pa, but an opposite trend is seen at 3,200 Pa. Again, this may be linked to the *n* values varying slightly around unity (~ 0.99-1.02) in such test conditions. Similar findings were reported for the AC+rubber as well, i. e., the degree of nonlinearity affected – at least at some extent – the response of the AC+EVA under longer loading times. However, the magnitudes of the constants of the regression equations typically increase from 64 to 70°C, especially for the *A* values: the percentages of increase vary from 110 to more than 400% from one temperature to the other. The rate of variation in *B* decreases from 64 to 70°C at 3,200 Pa, but the intercept of the regression equation experiences an increase of about 12% (from 0.874 to 0.932). These smaller variations in *B* are somewhat compensated by increases in *n* at very high temperatures, especially 70 and 76°C. Since the polymeric network is considerably damaged and melted at such temperatures, it is hypothesized that the slight increases in nonlinearity are mainly dictated by the base asphalt binder (see Table 70, page 200).

Table 204 indicates that the correlations for the *A* values are affected by nonlinearity within the whole temperature range, either from the EVA copolymer or the original binder (or maybe a combination of both). The R^2 values for this constant barely exceed 0.47, whereas the ones for the constant *B* are always greater than 0.91. The reverses in the signals of the gradients for *B* were already explained in detail in the previous paragraphs, that is, the contribution of the copolymer to the reductions in the strain rate is minimized when the physical network is damaged and melted at very high temperatures and stress levels and longer loading times. In these cases, the strain rate plays a major role in the susceptibility of the binder to rutting.

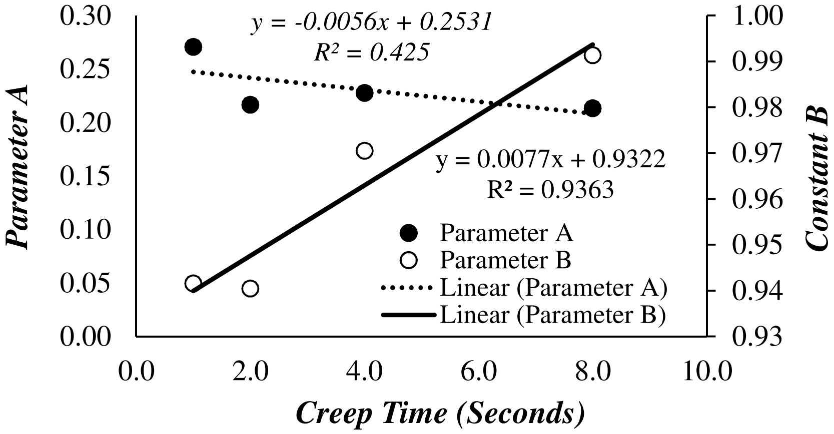

Figure 160 – Correlations between the creep time and the constants *A* and *B* from the model by Saboo and Kumar (2015), temperature of 70°C and stress level of 100 Pa – AC+EVA

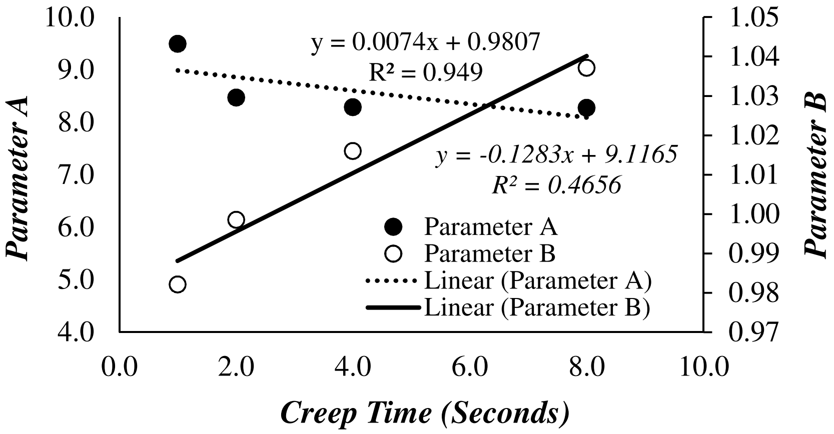

Figure 161 – Correlations between the creep time and the constants *A* and *B* from the model by Saboo and Kumar (2015), temperature of 70°C and stress level of 3,200 Pa – AC+EVA

Table 204 – Degrees of correlation between the parameters *A* and *B* (modified power model) and the creep time t_F for the AC+EVA

T (°C)	stress (kPa)	linear regression equations and R^2 values (in parenthesis)[a, b]	
		parameter *A*	parameter *B*
52	0.1	y = -0.0002x + 0.0170 (0.1679)	y = -0.0209x + 0.6293 (0.9844)
	3.2	y = -0.0083x + 0.5541 (0.3709)	y = -0.0153x + 0.6205 (0.9161)
58	0.1	y = -0.0004x + 0.0392 (0.2405)	y = -0.0151x + 0.6828 (0.9858)
	3.2	y = -0.0143x + 1.2961 (0.4247)	y = 0.0265x + 0.6296 (0.9848)
64	0.1	y = -0.0011x + 0.0937 (0.1271)	y = -0.0011x + 0.8205 (0.9928)
	3.2	y = -0.0527x + 4.1531 (0.6774)	y = 0.0177x + 0.8740 (0.9244)
70	0.1	y = -0.0056x + 0.2531 (0.4250)	y = 0.0077x + 0.9322 (0.9363)
	3.2	y = -0.1283x + 9.1165 (0.4656)	y = 0.0074x + 0.9807 (0.9490)
76	0.1	y = -0.0064x + 0.4363 (0.3892)	y = 0.0067x + 0.9669 (0.9649)
	3.2	y = -0.0396x + 16.7960 (0.0196)	y = 0.0065x + 0.9995 (0.9940)

[a] the Y-axis is associated with the parameter (*A* or *B*), whereas the X-axis is associated with t_F.
[b] changes in the signal of the slope of the regression trendlines are highlighted with a grey-shaded box.

Table 205 is a summary of the levels of correlation between the parameters *n* and *α* of the AC+EVA and the creep time t_F for all the test temperatures and stress levels. As previously noticed in other tables and figures, the temperature of 58°C and the stress level of 3,200 Pa are limiting conditions that distinguish two remarkable features of the rheological behavior of the formulation: (a) one dictated by a great contribution of nonlinearity to the increase in the propensity of the material to rutting, in which the percent recoveries are very high and either the initial strain or the strain rate decrease with increasing loading time; and (b) another dictated by increases in the strain rate at longer loading times, extensive amounts of damage and/or melting of the polymer network and a lower contribution of nonlinearity to the response of the formulation. The features described in (a) can be seen at the temperature of 52°C and the stress level of 100 Pa at 58°C, whereas the ones described in (b) can be observed for the temperatures of 64, 70 and 76°C. The transition from one type of response to the other is given by reverses in the signals of the slopes of the regression equations, i. e., from positive to negative with respect to *n* and from negative to positive with respect to *α*.

Table 205 – Degrees of correlation between the parameters *n* and *α* (modified power model) and the creep time t_F for the AC+EVA

T (°C)	stress (kPa)	linear regression equations and R^2 values (in parenthesis)[a, b]	
		parameter *n*	parameter *α*
52	0.1	y = 0.0294x + 1.0156 (0.9984)	y = -0.0083x + 0.6468 (0.9570)
	3.2	y = 0.0064x + 1.0414 (0.7416)	y = -0.0127x + 0.6470 (0.9461)
58	0.1	y = 0.0245x + 1.0156 (0.9974)	y = -0.0020x + 0.6980 (0.7319)
	3.2	y = -0.0075x + 1.0381 (0.9001)	y = 0.0210x + 0.6561 (0.9816)
64	0.1	y = 0.0070x + 1.0034 (0.9934)	y = 0.0045x + 0.8234 (0.9923)
	3.2	y = 0.0017x + 0.9947 (0.8625)	y = 0.0194x + 0.8689 (0.9520)
70	0.1	y = 0.0012x + 0.9965 (0.9786)	y = 0.0088x + 0.9288 (0.9588)
	3.2	y = 0.0026x + 0.9956 (0.9962)	y = 0.0101x + 0.9761 (0.9773)
76	0.1	y = 0.0017x + 0.9966 (0.9995)	y = 0.0084x + 0.9635 (0.9796)
	3.2	y = 0.0032x + 0.9968 (0.9926)	y = 0.0098x + 0.9960 (0.9995)

[a] the Y-axis is associated with the parameter (*n* or *α*), whereas the X-axis is associated with t_F.
[b] changes in the signal of the slope of the regression trendlines are highlighted with a grey-shaded box.

Other characteristics of the two distinctive types of response of the binder may be seen in Table 205. Firstly, the rates of increase in *n* are relatively high and the intercepts of the regression equations are greater than unity at 52 and 58°C (i. e., nonlinearity has a relevant contribution to the response of the AC+EVA), whereas much lower rates and intercepts very close to one can be found at 64, 70 and 76°C. Secondly, the parameter *α* shows a consistent and progressive increase with increasing t_F at the temperatures of 64, 70 and 76°C and the intercepts approach one with increasing temperature. The reductions in this parameter with increasing loading time at 52 and 58°C may indicate that the model is not able to precisely capture all the elastic behavior of the formulations in the MSCR tests in all cases. This may be associated with the assumption that the Boltzmann superposition principle is valid for both creep and recovery phenomena, as highlighted by Saboo and Kumar (2015) during the development of the modified power model.

The degrees of correlation between n and J_{nr} were investigated, even though it was anticipated that good correlations would not be obtained due to the lack of uniformity in the increases in this parameter with temperature and stress level. Further analyses concluded that the fitting of power regression equations would yield poor correlations ($R^2 \approx 0.36$) due to the presence of several scaterred data points and a very wide interval of variation in the J_{nr} values (from about 0.008 kPa^{-1} to more than 30 kPa^{-1}), as shown in Figure 162. These analyses also indicated that the correlations for the individual data at 100 and 3,200 Pa did not show great degrees of improvement in the levels of correlation, since the R^2 values ranged from 0.35 to 0.40 in both cases (charts not shown here). Furthermore, the tendency of decreasing n with increasing J_{nr} is not in agreement with the results found in other modified asphalt binders. Thus, it was not possible to establish a clear pattern of response for the variations in n for the AC+EVA with increasing J_{nr}.

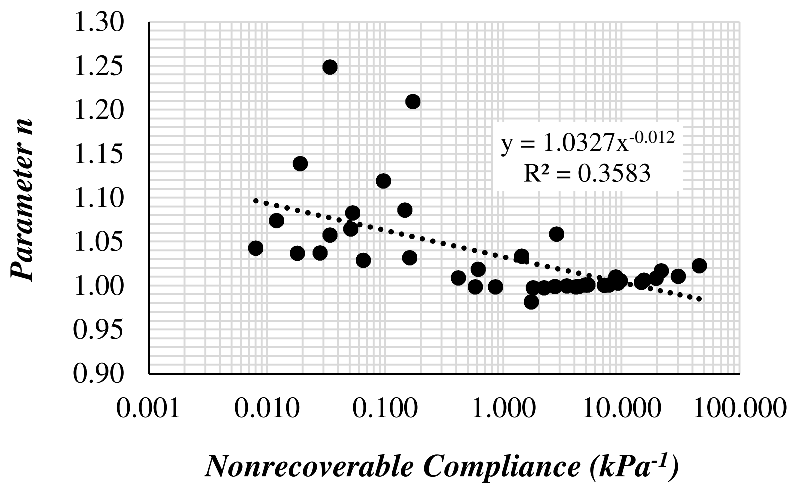

Figure 162 – Degree of correlation between the nonrecoverable compliances of the AC+EVA and the corresponding n values from the power law models

Similar investigations were carried out for the α values and the corresponding percent recoveries, and the results are plotted in Figure 163. An excellent correlation ($R^2 > 0.90$) can be seen, and the tendency of decreasing α with increasing R remains unchanged as well. However, the presence of a high number of data points associated with null recoveries ($R = 0$) and very high recoveries (R between 80 and 100%) suggests that the parameter α has some limitations when applied to extreme recovery conditions in the asphalt binder. The chart plotted by Saboo and Kumar

(2015) does not report such limitations for the SBS- and EVA-modified materials studied by the authors, even though the interval of α values shown by them (from 0.6 to 1.0) is very close to the one found in the present study (from 0.5 to 1.1). In either case, the parameter α may be used when one is seeking for an estimate of the amount of recovery in the AC+EVA during the MSCR test.

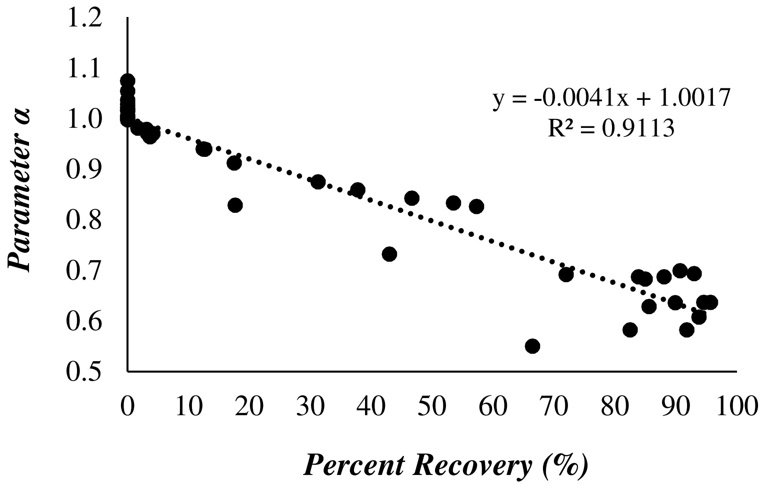

Figure 163 – Degree of correlation between the percent recoveries of the AC+EVA and the corresponding α values from the power law models

The rheological modeling of the AC+EVA at the creep-recovery times of 1/9 s, 2/9 s, 4/9 s and 8/9 s reveals the existence of a particular testing condition under which the polymer network is considerably damaged at 3,200 Pa (58°C and 4/9 s). A quite similar picture may be observed at the stress level of 100 Pa as well, by considering the temperature of 70°C and the creep-recovery times of 2/9 s. For temperatures and loading times more critical than the ones established by such conditions, the elastic benefits imparted by polymer modification are not visible anymore and the strain rate exerts a significant influence on the increases in the rutting potential of the formulation. On the other hand, the recovery responses and the strain rates of the AC+EVA are even better than those of the AC+Elvaloy+PPA when the limits defined by the previously mentioned test conditions are not exceeded. As previously observed for other modified asphalt binders, the initial strain (A values) is more affected by the nonlinear portion of the total strain in the formulation than the strain rate (B values), either at 100 or at 3,200 Pa.

With respect to the correlations between the model parameters and the MSCR testing results, it could be seen that n barely correlates with J_{nr} when all or a portion of the whole set of data are considered in the analysis. The parameter α shows an excellent correlation with the percent recovery of the AC+EVA ($\approx$ 0.91), which is in accordance with the literature and other previously reported binders. However, the presence of several data points when R is null or very high (~ 80-100%) suggests that α has some limitations when used in extreme recovery conditions of the formulations. In either case, this parameter can be used when an estimate of the amount of recovery in the asphalt binder during the MSCR test must be made.

Finally, the ANOVA analysis was conducted to identify which variable – loading time t_F or temperature T – mostly affects the percent recoveries and the nonrecoverable compliances of the AC+EVA, as well as if the variations in the results may be considered as statistically significant (H_0 is rejected) or not (H_0 is accepted). Table 206 depicts the organized *R100* and *R3200* values and, as can be seen, both parameters could be used because there is only one null *R* value within the data sets. The results of ANOVA – i. e., *p-value*, *F-value* and acceptance/rejection of H_0 – can be found in Table 207.

Table 206 – Rearranged MSCR testing data of the AC+EVA to be used in the analysis of variance (ANOVA) – percent recovery

stress level of 0.1 kPa (*R100*, %)[a]		stress level of 3.2 kPa (*R3200*, %)[a]	
increasing creep time	increasing temperature	increasing creep time	increasing temperature
95.7	95.7	89.9	89.9
94.6	93.0	85.6	83.9
93.8	57.3	82.5	31.3
91.8	12.7	66.5	1.7
N/A[b]	4.2	N/A[b]	N/A[b]

[a] the starting point in both cases was the temperature of 52°C.
[b] N/A: Not applicable.

Table 207 – Results from the analysis of variance (ANOVA, *p-value* and *F-value*) as based on the percent recoveries of the AC+EVA

null hypothesis H_0	statistical parameters (ANOVA)				recommendation
	$F_{critical}$	*F-value*	α	*p-value*	
equivalency between *R* values with increasing creep time and temperature, 0.1 kPa	5.5914	3.5757	0.05	0.1005	H_0 is not rejected
equivalency between *R* values with increasing creep time and temperature, 3.2 kPa	5.9874	1.8148	0.05	0.2266	H_0 is not rejected

As the statistical parameters suggest, the null hypothesis was not rejected and the variations within the data values with incrasing temperature and creep time cannot be considered as statistically significant. In other words, it is hypothesized that both are part of a particular set of data with a configuration of a normal distribution. However, the *F-value* and the *p-value* at 100 Pa are close to the limits $F_{critical}$ and α such that the differences among the results approach the boundary of acceptable variances. Temperature has a greater impact on the percent recoveries of the AC+EVA at 100 Pa (that is, higher rates of decrease in *R100*) than the loading times. These differences are much smaller for 3,200 Pa, since the *F-value* was decreased by half (from 3.58 to 1.82) and the *p-value* was more than doubled (from 0.100 to 0.227) with such increase in the applied stress. Again, the null hypothesis was not rejected and the effects of temperature on the recovery values of the binder are greater than those of the loading times.

Similarly to the percent recoveries, Table 208 provides the organized J_{nr} values of the AC+EVA to be tested in ANOVA and Table 209 shows the results of this statistical analysis. One more time, temperature has a greater influence on the susceptibility of the binder to rutting (higher increases in J_{nr}) than t_F, either at the lowest or the highest stress level. However, this was not enough to say that the variances within the data points of each group are statistically significant because H_0 was not rejected in any case. In addition, the *F-value* and the *p-value* vary by only 7-8% when moving from 100 to 3,200 Pa and the results are slightly greater at this last stress level. The variances in J_{nr} are higher than those observed for *R3200*, but lower than those found in *R100*.

Table 208 – Rearranged MSCR testing data of the AC+EVA to be used in the analysis of variance (ANOVA) – nonrecoverable creep compliance

stress level of 0.1 kPa ($J_{nr}100$, kPa^{-1})[a]		stress level of 3.2 kPa ($J_{nr}3200$, kPa^{-1})[a]	
increasing creep time	increasing temperature	increasing creep time	increasing temperature
0.008	0.008	0.018	0.018
0.012	0.028	0.034	0.065
0.019	0.414	0.053	0.856
0.034	2.201	0.146	2.729
N/A[b]	4.106	N/A[b]	5.191

[a] the starting point in both cases was the temperature of 52°C.
[b] N/A: Not applicable.

Table 209 – Results from the analysis of variance (ANOVA, *p-value* and *F-value*) as based on the nonrecoverable compliances of the AC+EVA

null hypothesis H_0	statistical parameters (ANOVA)				recommendation
	$F_{critical}$	*F-value*	α	*p-value*	
equivalency between J_{nr} values with increasing creep time and temperature, 0.1 kPa	5.5914	2.1692	0.05	0.1843	H_0 is not rejected
equivalency between J_{nr} values with increasing creep time and temperature, 3.2 kPa	5.5914	2.3367	0.05	0.1702	H_0 is not rejected

Table 210 provides the percent recoveries of the AC+EVA+PPA at all loading times, stress levels and temperatures, whereas Figure 164 reports the variations in *R100* and *R3200* with increasing loading time and at each pavement temperature. Interestingly, the combination of EVA and PPA increased the *R* values of the binder at 100 Pa when moving from 1/9 s to 2/9 s and for the temperatures of 64, 70 and 76°C (i. e., positive variations in recovery). As previously noticed for the AC+EVA, it is hypothesized that such increases may be explained by the delayed elastic effects on the amount of recovered strain in the asphalt binder at each creep-recovery cycle. In other words, the portion of the delayed elastic response of the material that could not be recovered during 9 s of unloading time is carried to the next cycle. This will be further analyzed in the next few paragraphs.

Table 210 – Percent recoveries at 100 Pa (*R100*) and 3,200 Pa (*R3200*) for the AC+EVA+PPA with increasing loading time and temperature

parameter	creep time (s)	results at each temperature and increases (both in %)[a]				
		52°C	58°C	64°C	70°C	76°C
R100	1.0	80.8	72.4	33.0	17.1	12.7
	2.0	69.6	64.4	35.7	22.9	14.0
	4.0	61.5	55.5	28.5	15.8	6.0
	8.0	52.3	44.0	18.2	5.8	0.0
R3200	1.0	68.3	49.1	10.4	0.4	0.0
	2.0	50.3	31.8	5.3	0.0	0.0
	4.0	33.8	14.5	0.0	0.0	0.0
	8.0	15.6	3.9	0.0	0.0	0.0

[a] increases in the percent recovery from one creep time to the other are highlighted with a grey-shaded box.

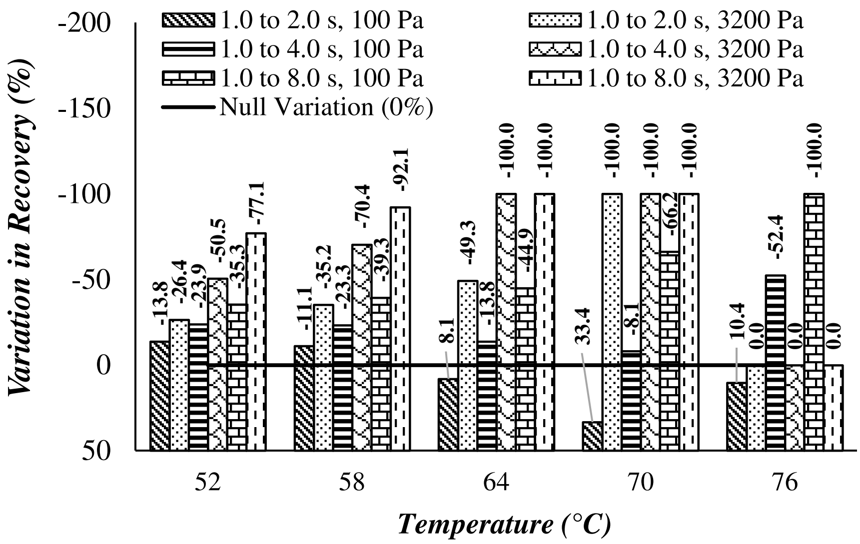

Figure 164 – Percentages of variation in the recovery values of the AC+EVA+PPA with creep time, temperature and stress level

Figure 165 shows plots of the *R100* values of the AC+EVA+PPA at the temperature of 64°C and the creep-recovery times of 1/9 s, 2/9 s and 4/9 s. As can be seen, the recoveries at 1/9 s and 4/9 s show progressive increases with the application of the loading-unloading cycles due to delayed elasticity up to Cycle #11, which is where the results tend to stabilize around 35% and 27%, respectively. On the other hand, the recoveries at 2/9 s increase at faster rates than those at 1/9 s in the first 10 cycles and continue to increase up to Cycle #15, then stabilizing around 37% in the last five cycles. In other words, it is not possible to ensure that all binders will be as close as possible to the steady state behavior in the last 10 cycles of the MSCR test, since the variances tend to decrease with the application of more cycles and the results in Cycles #16-20 are even more homogeneous than in Cycles #11-20. These findings are in alignment with the conclusions drawn by Golalipour et al. (2016), according to whom the MSCR test should have more cycles at each stress level (30, rather than 20 and 10) and the consideration of the last five cycles in the determination of *R* and J_{nr}.

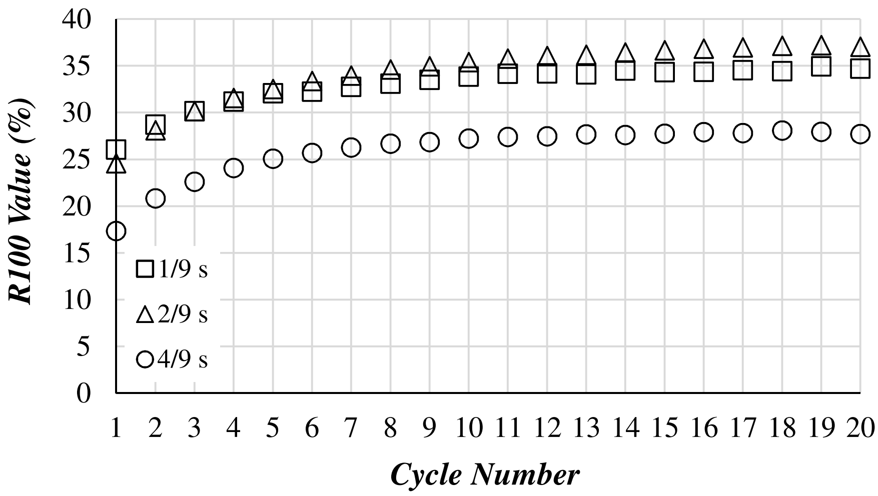

Figure 165 – Plots of the percent recoveries at 100 Pa (*R100*) at each cycle for the AC+EVA+PPA, temperature of 64°C and creep-recovery times of 1/9 s, 2/9 s and 4/9 s (original samples)

Figure 166 further highlights the need for evaluating the steady state response of highly-modified asphalt binders more carefully, since not all the recoveries of the AC+EVA+PPA show a tendency of stabilization after 10 cycles of creep and recovery. Again, the increases in *R100* in the first few cycles are due to the role of delayed elasticity on the total strain observed in the binder. The results at 1/9 s approach 20% from Cycle #10 on and the ones at 2/9 s increase much faster in the first eight cycles, then showing small decreases and more consistency in the numerical values (around 22%) after Cycle #12. Finally, the percent recoveries at 4/9 s reach a peak value in Cycles #6-8 (approximately 17%) and continuously decrease with the application of more loading-unloading cycles. This is a clear indication that the polymeric network is being progressively damaged during the test and, as a consequence, the material is unable to maintain their original recoveries in the last cycles of loading and unloading. More simply, the effects of damage should also be considered when studying the steady state behavior of asphalt binders.

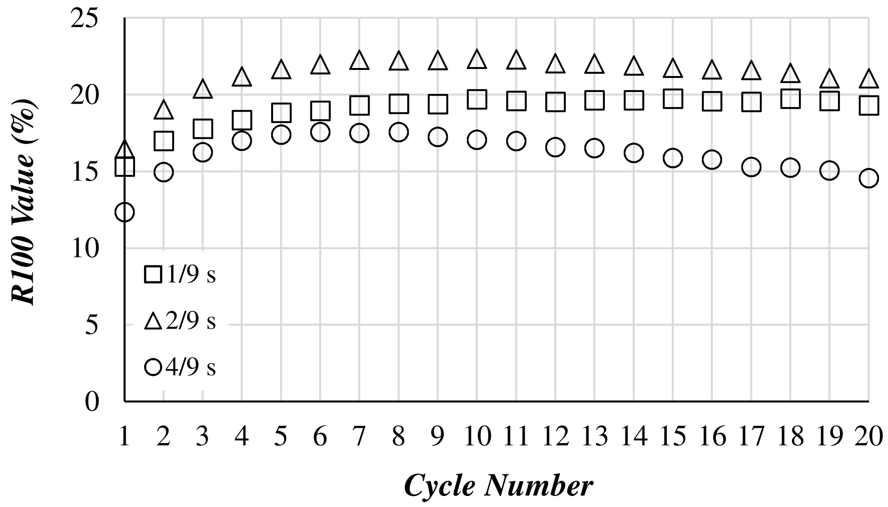

Figure 166 – Plots of the percent recoveries at 100 Pa (*R100*) at each cycle for the AC+EVA+PPA, temperature of 70°C and creep-recovery times of 1/9 s, 2/9 s and 4/9 s (original samples)

With respect to the temperature of 76°C, Figure 167 indicates that quite similar patterns of response may be observed for the results at 1/9 s and 2/9 s, as follows: (a) slightly higher rates of increase in *R100* for 2/9 s than at 1/9 s in the first five cycles and a tendency of stabilization of the results at 1/9 s from Cycle #10 on; (b) decreases in *R100* after the first five cycles at 4/9 s due to the accumulation of damage in the polymer network; and (c) a similar phenomenon in the results at 2/9 s after 5-8 cycles of creep and recovery. The irregularities in the *R100* values in Cycles #15-20 at 1/9 s can also be attributed to damage in the sample. Again, the effects of damage cannot be neglected while studying the repeated creep behavior of the modified asphalt binders in the MSCR tests and their corresponding parameters.

As a complementary analysis of the discussions about the effects of steady state on the results of the AC+EVA+PPA in the MSCR test, Figure 168 reports the *R100* values of this material at each cycle and the temperatures of 52 and 58°C. One more time, it is not clear that the formulation reaches a more steady state type of response after 10 cycles of creep and recovery, especially at 58°C. In fact, the stabilizations in the *R100* values tend to be more visible after Cycle #15 for both temperatures, even though the binder seems to need more creep-recovery cycles at 58°C to clearly depict steady state. This again is in agreement with the literature, since not even 20 creep-recovery cycles may be enough to show steady state for some modified asphalt binders (BAHIA et al., 2001a; DELGADILLO et al., 2006b; GOLALIPOUR, 2011; GOLALIPOUR et al., 2016; MARASTEANU et al., 2005).

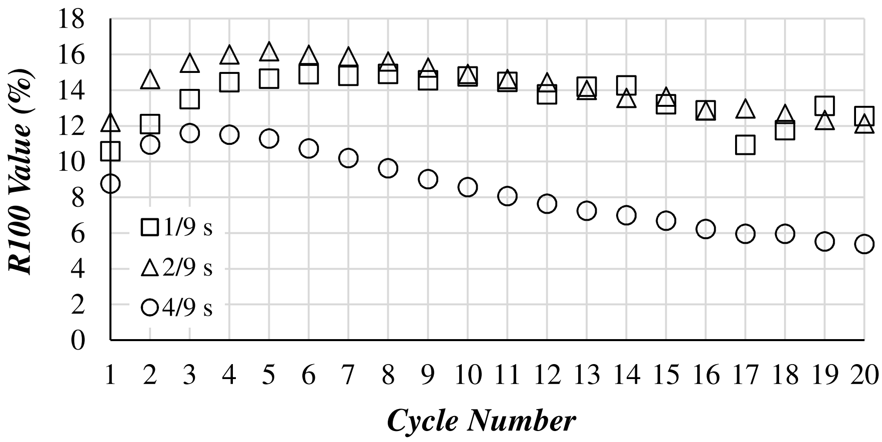

Figure 167 – Plots of the percent recoveries at 100 Pa (*R100*) at each cycle for the AC+EVA+PPA, temperature of 76°C and creep-recovery times of 1/9 s, 2/9 s and 4/9 s (original samples)

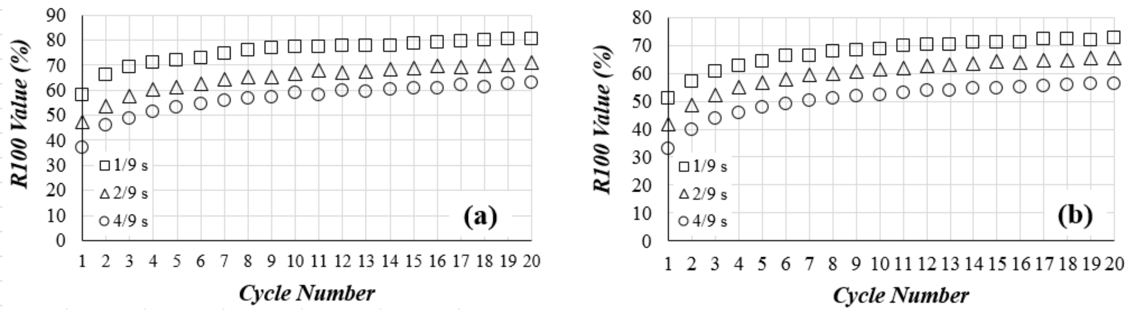

Figure 168 – Plots of the percent recoveries at 100 Pa (*R100*) at each cycle for the AC+EVA+PPA, temperatures of 52°C (a) and 58°C (b) and creep-recovery times of 1/9 s, 2/9 s and 4/9 s – original samples

Although no improvements in the *R3200* values at 70 and 76°C were observed, the results at temperatures up to 64°C were decreased by at least 20% when compared with the original ones for the AC+EVA. The decreases in the percent recoveries at 100 Pa varied by 15 to 53% with the addition of PPA and the reduction in the EVA content. Figure 169 graphically illustrates these comments, in that the percent recoveries are higher for the AC+EVA+PPA at 70 and 76°C (points above the equality line) and higher for the AC+EVA at the remaining temperatures (points below the equality line). Such effects in turn decreased the temperature susceptibility of the material, either at 100 or 3,200 Pa. Similar effects were observed for another crude source for the base asphalt binder and simultaneous increases in the creep and recovery times in the MSCR test (from 1/9 s to 2/18 s), see the paper from Domingos and Faxina (2014) for further details. In terms of the numerical values of *R* for the AC+EVA+PPA, it can be seen that the non-null results range from 5 to 81% at 100 Pa and from 0.4 to almost 70% at 3,200 Pa.

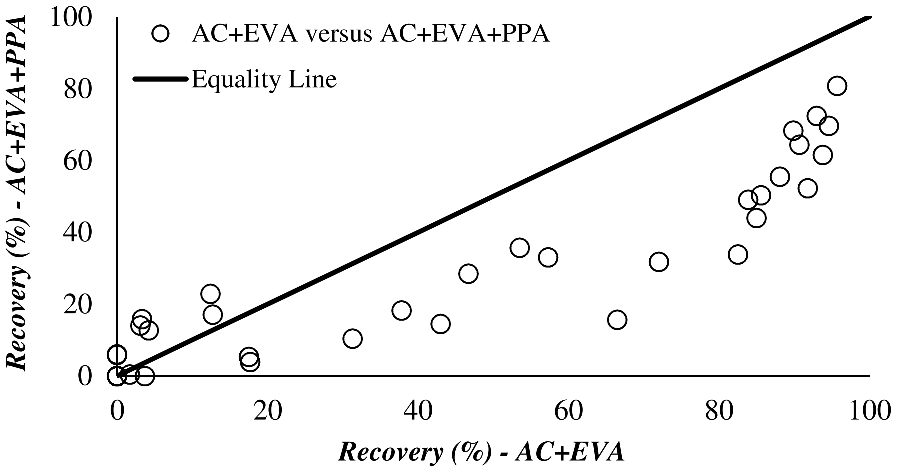

Figure 169 – Comparison between the percent recoveries of the AC+EVA and the AC+EVA+PPA under all MSCR testing conditions

The decreases in the percent recovery of the EVA-modified binder after the addition of PPA suggest that the percentages of asphaltenes and maltenes and the changes in the gel characteristics of the binder influenced on the degree of modification. Fawcett and McNally (2001) and Polacco et al. (2015) mentioned in their papers that the polar groups in the EVA copolymer may react with themselves or the asphaltenes and the polymers may compete with the resins in the dispersion of the asphaltenes. If EVA has a very high vinyl acetate content, these polar groups can directly bind to the asphaltenes to further improve the rheological properties. Since the effects of PPA are dependent on the crude source, some base materials may not show increase in their asphaltene content upon the addition of PPA, which is commonly observed in the literature. For such binders, it is possible that part of the asphaltene fraction be converted to maltenes (THOMAS and TURNER, 2008). This may be the reason why PPA modification of the base material from the Lubnor-Petrobras refinery decreased either the percentages of asphaltenes or the resins, as reported in the thesis by Pamplona (2013). Thus, it can be pointed out that the mechanisms of action of EVA were limited by the decreases in either the amounts of asphaltenes and resins in the original material with the incorporation of PPA and its gel-like characteristics.

The nonrecoverable compliances of the AC+EVA+PPA are summarized in Table 211, whereas direct comparisons among the J_{nr} values of the two formulations with EVA can be made based on the plots in Figure 170 and Figure 171. These data suggest that the formulation with EVA+PPA is more susceptible to rutting ($J_{nr}3200$ values are higher) than the one with EVA alone for pavement temperatures no greater than 64°C. This is consistent with the smaller percent recoveries reported above, i. e., the AC+EVA+PPA is typically less elastic and more prone to the accumulation of permanent strain than the AC+EVA at such temperatures. Although slight decreases in $J_{nr}100$ and $J_{nr}3200$ can be seen for the AC+EVA+PPA, they are restricted to few pavement temperatures (typically 70 and 76°C). In terms of the numerical results of J_{nr}, they vary from 0.03 up to 27.16 kPa^{-1} at 100 Pa and vary from 0.05 up to to 48.99 kPa^{-1} at 3,200 Pa.

Overall, it can be concluded that the main MSCR testing parameters of the two formulations with EVA in the DSR show similarities among them, especially in the degree of stiffness (J_{nr}). However, the presence of smaller recoveries and higher compliances for the AC+EVA+PPA than for the AC+EVA at the majority of the pavement temperatures studied here (three out of five) indicate that the replacement of part of the EVA content by PPA was not able to fully recover the original properties of the material. Based only on the *R* and J_{nr} values, the AC+EVA can be taken as a better formulation to deal with the traffic loads in the pavement due to the slightly higher levels of stiffness and higher amounts of recoverable strain after the passage of each load. These conclusions are similar to those obtained with the same modifiers and a different crude source for the base asphalt binder (DOMINGOS and FAXINA, 2014).

Table 211 – Nonrecoverable compliances at 100 Pa ($J_{nr}100$) and 3,200 Pa (J_{nr} 3200) for the AC+EVA+PPA with increasing loading time and temperature

parameter	creep time (s)	results at each temperature (kPa^{-1}), J_{nr} > 4.0 kPa^{-1} is in bold				
		52°C	58°C	64°C	70°C	76°C
$J_{nr}100$	1.0	0.033	0.105	0.623	1.912	3.472
	2.0	0.073	0.190	0.749	2.125	**5.074**
	4.0	0.130	0.340	1.283	3.771	**10.972**
	8.0	0.241	0.684	2.863	**9.393**	**27.155**
$J_{nr}3200$	1.0	0.055	0.209	1.214	3.159	**6.049**
	2.0	0.127	0.429	1.924	**4.847**	**10.437**
	4.0	0.257	0.912	3.691	**8.906**	**20.096**
	8.0	0.601	1.958	**7.425**	**19.418**	**48.982**

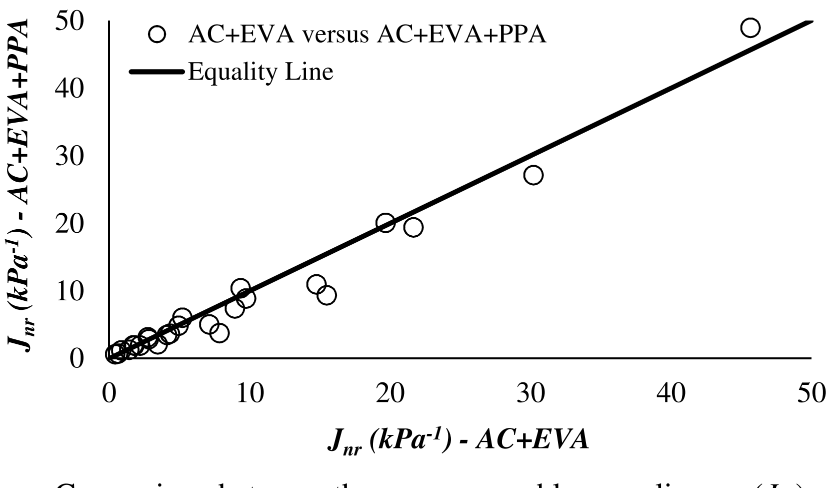

Figure 170 – Comparison between the nonrecoverable compliances (J_{nr}) of the AC+EVA and the AC+EVA+PPA only for the results typically greater than 1.0 kPa^{-1} (temperatures of 64, 70 and 76°C)

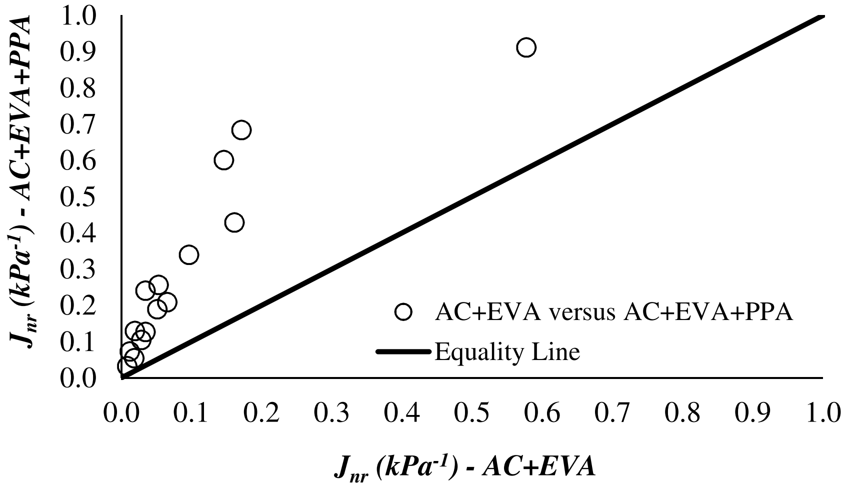

Figure 171 – Comparison between the nonrecoverable compliances (J_{nr}) of the AC+EVA and the AC+EVA+PPA only for the results lower than 1.0 kPa^{-1} (temperatures of 52 and 58°C)

One interesting aspect about binder modification with EVA+PPA is that the concept of "failure point" used in the formulation with EVA alone can somehow be applied here as well. These "failure points" of the AC+EVA+PPA could be seen at the temperature of 70°C and the loading time of 4.0 s (stress level of 100 Pa) and the temperature of 64°C associated with a loading time of 2.0 s (stress level of 3,200 Pa), which are quite close to the ones found in the AC+EVA. If the testing conditions become more severe, it can be implied that the AC+EVA+PPA will probably show a premature failure by rutting. Since the flow number testing variables – 60°C and creep-recovery times of 0.1/0.9 s – did not exceed the ones imposed by the "failure points", the mixtures prepared with the AC+EVA+PPA did not fail in the FN tests (very good rutting performance, see Chapter 5). On the other hand, the presence of higher $J_{nr}3200$ values led to increases in the amount of permanent strain accumulated by the samples.

The results of the parameter $J_{nr,\ diff}$ are shown in Table 212. Similarly to the AC+EVA, the AC+EVA+PPA is very sensitive to an increase in the stress level from 0.1 to 3.2 kPa ($J_{nr,\ diff}$ > 75%) with only a few exceptions. These exceptions are located at the temperatures of 52°C (66.8 and 72.9%), 70°C (65.2%) and 76°C (74.2%), almost all of them at 1/9 s. It can be hypothesized that the presence of PPA contributed to the "intensification" of the high stress sensitivity of the formulation at 70 and 76°C, since these are the temperatures at which the AC+PPA is overly stress sensitive (see Table 78, page 211) and similar findings were reported by Domingos and Faxina (2014) as well. The $J_{nr,\ diff}$ values are lower for the AC+EVA+PPA than for the AC+EVA at the temperatures of 52, 58 and 64°C, and the opposite is found at 70 and 76°C – see Figure 172 for graphical comparisons. The numerical results are within the interval comprised by the minimum of 65.2% and the maximum of 187.6%, and the increases in $J_{nr,\ diff}$ with loading time may be explained by the nonlinear response of polymers at high strain levels (D'ANGELO et al., 2007; DOMINGOS and FAXINA, 2017).

Table 212 – Percent differences in nonrecoverable compliances ($J_{nr,\ diff}$) for the AC+EVA+PPA with increasing creep time and temperature

creep time (s)	$J_{nr,\ diff}$ values (%) at each creep time and temperature[a]				
	52°C	58°C	64°C	70°C	76°C
1.0	66.8	**100.0**	**94.9**	65.2	74.2
2.0	72.9	**126.1**	**156.9**	**128.0**	**105.7**
4.0	**98.0**	**168.1**	**187.6**	**136.2**	**83.2**
8.0	**149.6**	**186.4**	**159.3**	**106.7**	**80.4**

[a] the numbers in bold are the ones that exceeded the maximum $J_{nr,\ diff}$ (75%) according to Superpave®.

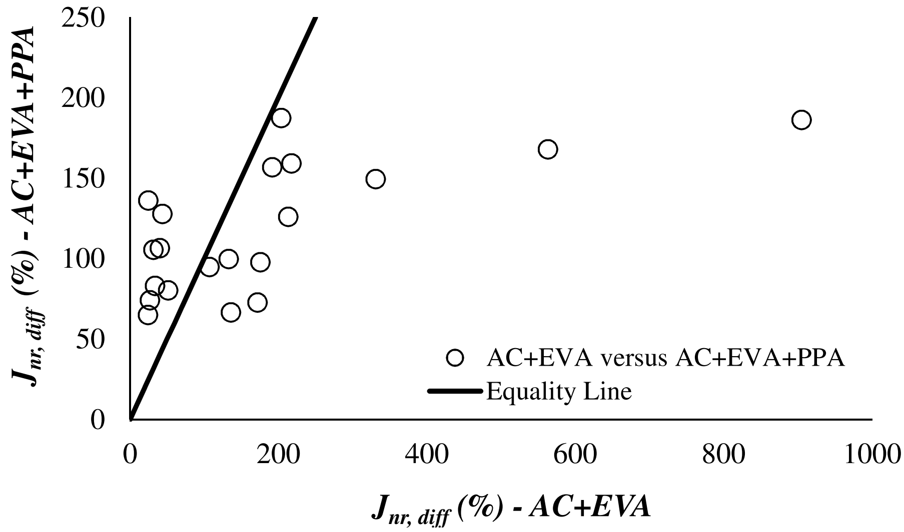

Figure 172 – Comparison between the percent differences in nonrecoverable compliances ($J_{nr,\ diff}$) of the AC+EVA and the AC+EVA+PPA in all of the MSCR testing conditions

The nonlinear responses of the AC+EVA and the AC+EVA+PPA at some pavement temperatures – in terms of their J_{nr} values and longer creep times – can be studied based on the charts shown in Figure 173 (in this case, 64 and 70°C). It may be implied that the formulation with EVA+PPA shows a higher level of nonlinear response at 100 Pa with increasing loading time, either at 64 or 70°C. The delayed elastic portion of the total strain in the binder may also have contributed to the decreases in the rates of variation in J_{nr} at smaller t_F values, as discussed earlier. The results of the two formulations tend to be similar at very long creep times and all the plotted temperatures and stress levels, except for 70°C and 100 Pa. However, the combination of EVA with PPA in the asphalt binder acts by decreasing the rates of increase in J_{nr} with creep time when $t_F \leq 4.0$ s, and a complementary analysis indicated that this could be seen at the other temperatures as well. This might be associated either with the presence of lower amounts of EVA in the AC+EVA+PPA or the high levels of accumulated damage in the binder sample when subjected to very long loading times.

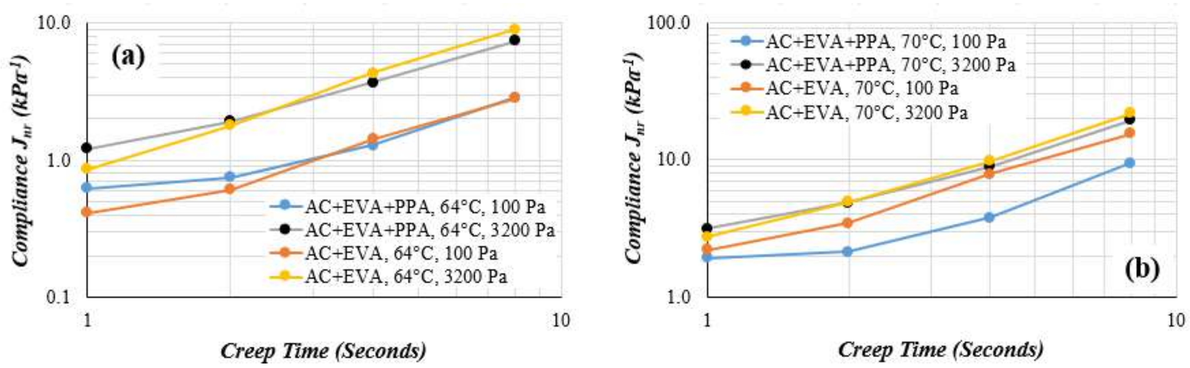

Figure 173 – Plots of the nonrecoverable compliance J_{nr} versus loading time (log-log scale) for the AC+EVA and the AC+EVA+PPA at the temperatures of (a) 64°C; and (b) 70°C

The adequate traffic levels for the AC+EVA+PPA at each temperature and creep time are shown in Table 213. By comparing these results with those obtained for the AC+EVA (Table 198, page 356), one may see that there was a decrease by one grade at 52°C and t_F = 8.0 s (from extremely heavy to very heavy) and one grade at 64°C and t_F = 1.0 s (from very heavy to heavy) after the addition of PPA and the reduction in the EVA content. However, the AC+EVA+PPA can be used on pavements with standard traffic at 64°C and t_F = 4.0 s, which is not the case of the AC+EVA. This is possibly due to the lower rates of increase in J_{nr} for the AC+EVA+PPA than for the AC+EVA at such temperature with increasing creep time, and is also somehow correlated with the fact that the parameter $J_{nr,\ diff}$ is higher for the material with EVA alone than for the one with EVA+PPA when T = 64°C. None of the EVA-modified asphalt binders can be used on pavements with high PG grades of 76-xx, nor those with PG grade of 70-xx and t_F > 1.0 s.

Table 213 – Adequate traffic levels for the AC+EVA+PPA with increasing creep time and temperature based on the standardized Superpave® criteria

creep time (s)	traffic levels for each temperature[a]				
	52°C	58°C	64°C	70°C	76°C
1.0	E	E	H	S	-
2.0	E	E	H	-	-
4.0	E	V	S	-	-
8.0	V	H	-	-	-

[a] S = standard; H = heavy; V = very heavy; E = extremely heavy.

The correlations between traffic speed – as calculated by the aforementioned equations from Huang (2004) and Pereira et al. (1998, 2000) – were also investigated for the AC+EVA+PPA, and the resulting equations and R^2 values are given in Table 214. It can be seen that the degrees of correlation slightly decrease with increasing temperature up to 70°C, and then it starts to increase again. This is associated with the percentages of increase in J_{nr} shown in Figure 174, i. e., decreases in such percentages at temperatures up to 70°C and increases from 70 to 76°C for all the selected creep times. This particular characteristic of the AC+EVA+PPA cannot be seen in the AC+EVA (Figure 151, page 351), for which there is no clear pattern of response in the percentages of increase in J_{nr} with loading time. The equation from Huang (2004) shows the same type of behavior for both tire contact radii, except for the minor increases in R^2 for the lowest value of radius.

Table 214 – Regression equations and coefficients of determination between the $J_{nr}3200$ values of the AC+EVA+PPA and the corresponding vehicle speeds according to the equations by Pereira et al. (1998, 2000) and Huang (2004)

source and data	temperature (in °C)	equation	R^2
Pereira et al. (1998)	52	$y = 0.5917e^{-0.032x}$	0.9201
Pereira et al. (2000)	52	$y = -0.0007x+0.5070$	0.9992
Huang (2004) $r = 6$ in	52	$y = 0.5921e^{-0.038x}$	0.9206
	58	$y = 1.9295e^{-0.036x}$	0.9123
	64	$y = 6.8790e^{-0.029x}$	0.8650
	70	$y = 17.1990e^{-0.028x}$	0.8380
	76	$y = 43.2260e^{-0.033x}$	0.8523
Huang (2004) $r = 3.68$ in	52	$y = 0.5909e^{-0.063x}$	0.9208
	58	$y = 1.9258e^{-0.059x}$	0.9126
	64	$y = 6.8686e^{-0.047x}$	0.8653
	70	$y = 17.1740e^{-0.046x}$	0.8383
	76	$y = 43.1510e^{-0.053x}$	0.8526

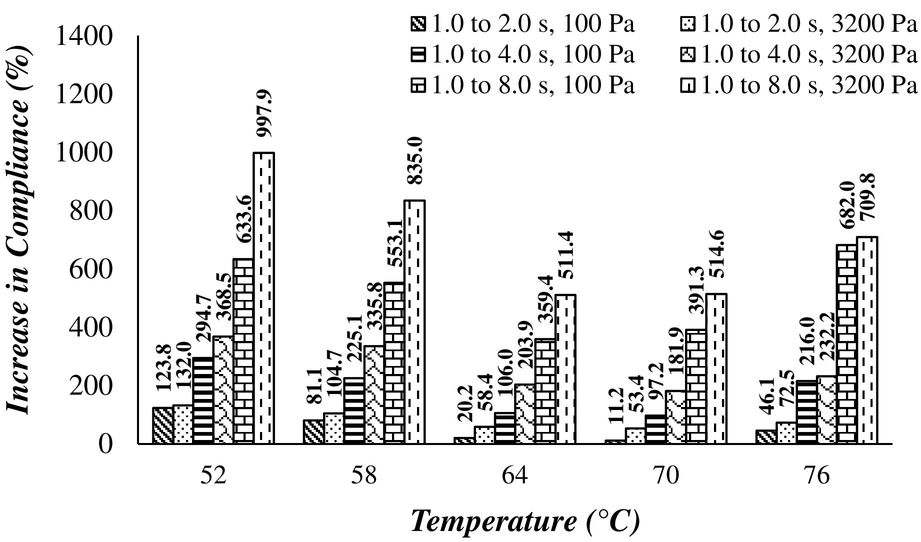

Figure 174 – Percentages of increase in the nonrecoverable compliances of the AC+EVA+PPA with creep time, temperature and stress level

Based on the conclusions reached for the other modified asphalt binders, it is not clear as to whether the traffic levels of the AC+EVA+PPA can be reasonably predicted by one or more of these equations. The first part of the answer to this doubt is given in Table 215, in which the estimated traffic levels – as based on the speeds calculated from the equations by Huang (2004) and Pereira et al. (1998) – are compared with the actual ones provided by the binder (Table 213). As can be observed, the use of these equations has a restricted applicability to high pavement temperatures and actual J_{nr} data. There are only three points of similarity (i. e., the same traffic level as estimated by J_{nr} and the equations) at 52°C and three points at 58°C. No equivalencies between the predicted and real traffic levels may be seen at 64 and 70°C and quite similar findings were obtained for the AC+EVA (Table 200, page 357). As previously concluded for the other asphalt binders, it is not recommended to estimate the actual traffic level of the AC+EVA+PPA from the above-mentioned vehicle speeds and equations.

Table 215 – Comparisons between the actual traffic levels of the AC+EVA+PPA and the ones obtained from Huang (2004) and Pereira et al. (1998)

t_F (s)[d]	actual[a] and estimated[b, c] traffic levels at each temperature[d]				
	52°C	58°C	64°C	70°C	76°C
1.0	**E (V/E) [V/E]**	**E [V/E]**	H [V/E]	S [V/E]	-
2.0	**E (V/E) [V/E]**	**E [V/E]**	H [V/E]	-	-
4.0	E **(H) [H]**	V [H]	S [H]	-	-
8.0	V (S) [H]	**H [H]**	-	-	-

[a] S = standard; H = heavy; V = very heavy; E = extremely heavy (AASHTO M320-09 standard, Table 3).
[b] (parentheses) = traffic levels from Pereira et al. (1998).
[c] [brackets] = traffic levels from Huang (2004), r = 6 in.
[d] similarities among the rankings are highlighted in bold, t_F = creep time.

When the equation found in the paper by Pereira et al. (1998) is replaced by the one from Pereira et al. (2000) and the tire contact radius is reduced in the equation by Huang (2004), the results summarized in Table 216 can be obtained. The R^2 values of the AC+EVA+PPA in the equation from Huang (2004) followed the same pattern observed above, i. e., decreases with increasing temperature up to 70°C and small increases when moving from 70 to 76°C. The ability of the empirical equation from Pereira et al. (2000) in fitting the binder data is great, that is, the coefficient of determination is higher than 0.99. However, this does not mean that the traffic levels estimated by such equation and the $J_{nr}3200$ values are the same because just a few points of similarity can be identified. This gives even more support to the hypothesis that the applicability of the equations to actual binder data is fairly limited. Therefore, it is not possible to draw comparisons among the responses of binders at all pavement temperatures based only on empirical or theroterical-based equations.

Table 216 – Comparisons between the actual traffic levels of the AC+EVA+PPA and the ones obtained from the equations by Huang (2004) and Pereira et al. (2000)

t_F (s)[d]	actual[a] and estimated[b, c] traffic levels at each temperature[d]				
	52°C	58°C	64°C	70°C	76°C
1.0	**E** (H) **[V/E]**	**E [V/E]**	H [V/E]	S [V/E]	-
2.0	**E** (H) **[V/E]**	**E [V/E]**	H [V/E]	-	-
4.0	E **(H) [H]**	V [H]	S [H]	-	-
8.0	V **(H) [H]**	**H [H]**	-	-	-

[a] S = standard; H = heavy; V = very heavy; E = extremely heavy (AASHTO M320-09 standard, Table 3).
[b] (parentheses) = traffic levels from Pereira et al. (2000).
[c] [brackets] = traffic levels from Huang (2004), $r = 3.68$ in.
[d] similarities among the rankings are highlighted in bold, t_F = creep time.

The use of the new criterion to evaluate the most suitable traffic levels for the AC+EVA+PPA at some high pavement temperatures yielded the results shown in Table 217. By comparing these levels with the ones provided by the current Superpave® criterion, one may imply that there are no differences in the classifications of the binder at any temperature. In other words, the degree of nonlinearity of the AC+EVA+PPA at loading times from 1.0 to 8.0 s was not high enough to decrease the appropriate traffic levels of the material. This is in aggrement with the observation that the AC+EVA+PPA has a lower level of nonlinear response with increasing loading time than the AC+EVA, as can be inferred from the curves in Figure 173 and the data of the AC+EVA in Table 202 (page 358). More simply, the increases in t_F do not seem to affect the rutting resistance of the AC+EVA+PPA as much as the AC+EVA at temperatures ranging from 52 to 76°C.

Table 217 – Traffic levels of the AC+EVA+PPA with increasing loading time and temperature in the current and proposed criteria

temperature (in °C)	No. of required MSCR tests[b]	Superpave® designations (current and new criteria)[a, c]	
		current criterion	new criterion
52	4	**52E-xx**	**52E-xx**
58	4	**58E-xx**	**58E-xx**
64	3	**64H-xx**	**64H-xx**
70	3	**70S-xx**	**70S-xx**
76	1	**76-xx**	**76-xx**

[a] S = standard; H = heavy; V = very heavy; E = extremely heavy (AASHTO M320-09 standard, Table 3).
[b] minimum number of MSCR tests to determine the adequate traffic level in the proposed classification.
[c] similarities among the classifications are highlighted in bold.

Based on the aforementioned discussions and results, it can be said that the AC+EVA+PPA is less elastic and rut resistant than the AC+EVA at the highest stress level in the MSCR tests (3.2

kPa), even though small degrees of improvement can be seen in *R100* and $J_{nr}100$ for some pavement temperatures (especially 70 and 76°C). This may possibly be explained by the decreases in the percentages of asphaltenes and resins after the addition of PPA to the original binder from the Lubnor-Petrobras refinery, which limited the extent of modification by the EVA copolymer. Although the the AC+EVA+PPA is less sensitive to increases in the stress levels than the AC+EVA at temperatures lower than or equal to 64°C (lower $J_{nr,\ diff}$ values), the compliances of the formulation with EVA+PPA are more sensitive to increases in the loading time than the ones of the formulation with EVA alone, either at 100 or at 3,200 Pa. This somehow affected the appropriate traffic levels of the material for some temperatures and loading times, e. g., 52°C and 8.0 s (decrease by one grade, from extremely heavy to very heavy). However, the designations of these traffic levels were not changed with the addition of one more requirement ($J_{nr}3200$ lower than a maximum allowed value for highr t_F values) in the current Superpave® specification.

Table 218 provides all the numerical values of the parameters of the modified power models for the AC+EVA+PPA. It can be seen that the responses of this formulation according to the model parameters have some similarities with those of the AC+EVA. First, the A values continuously decrease with loading time at all pavement temperatures and for both materials, and these rates of decrease are much higher for the formulation with EVA+PPA. Second, the importance of nonlinearity (n values) on the increase in the susceptibility to rutting becomes typically greater with loading time either for the AC+EVA+PPA or the AC+EVA, especially at the temperatures of 64, 70 and 76°C. The rates of increase in n are approximately the same for the two EVA-modified asphalt binders at these temperatures, but they are greater for the AC+EVA at 52 and 58°C. In other words, the replacement of part of the EVA content by PPA in the AC+EVA+PPA diminished the role of nonlinearity on the creep-recovery response of the formulation at temperatures up to 58°C, as well as the importance of the strain rate on the increase in the susceptibility of the material to rutting.

While some variables lost part of their importance on the increases in the rutting potential of the AC+EVA+PPA when compared with the AC+EVA, others gained more importance with such changes in the composition of the formulation. One of these variables is the strain rate (B values), which typically increases with t_F for the AC+EVA+PPA regardless of the test temperature. This means that the AC+EVA+PPA becomes more prone to rutting at longer creep times mainly because of higher strain rates and, as a consequence, nonlinearity has a lower contribution to this rutting potential. At the same time, the α values never decrease with increasing creep time in the MSCR test for the AC+EVA+PPA, which could be seen for the AC+EVA at 52 and 58°C (see Table 203, page 360). This may be explained by the presence of smaller amounts

Table 218 – Numerical values and variations in the parameters/constants *A, B, n* and *α* from the power law equations by Saboo and Kumar (2015) with increasing temperature and creep time and considering the AC+EVA+PPA

temperature	test times	parameter A^a		parameter B^a		parameter n^a		parameter α^a	
		0.1 kPa	3.2 kPa	0.1 kPa	3.2 kPa	0.1 kPa	3.2 kPa	0.1 kPa	3.2 kPa
52°C	1/9 s	0.0180	0.5782	0.7124	0.7190	1.0222	1.0121	0.7282	0.7278
	2/9 s	0.0154 (-14.4)	0.5102 (-11.8)	0.7287 (2.3)	0.7612 (5.9)	1.0285 (0.6)	1.0059 (-0.6)	0.7494 (2.9)	0.7657 (5.2)
	4/9 s	0.0131 (-27.2)	0.4365 (-24.5)	0.7251 (1.8)	0.7864 (9.4)	1.0455 (2.3)	0.9983 (-1.4)	0.7580 (4.1)	0.7850 (7.9)
	8/9 s	0.0123 (-31.7)	0.4033 (-30.2)	0.7167 (0.6)	0.8434 (17.3)	1.0728 (5.0)	0.9854 (-2.6)	0.7689 (5.6)	0.8311 (14.2)
58°C	1/9 s	0.0418	1.3784	0.7179	0.7949	1.0265	1.0012	0.7369	0.7959
	2/9 s	0.0331 (-20.8)	1.1900 (-13.7)	0.7669 (6.8)	0.8421 (5.9)	1.0259 (-0.1)	0.9967 (-0.4)	0.7868 (6.8)	0.8393 (5.5)
	4/9 s	0.0282 (-32.5)	1.0240 (-25.7)	0.7659 (6.7)	0.8887 (11.8)	1.0415 (1.5)	0.9922 (-0.9)	0.7977 (8.3)	0.8817 (10.8)
	8/9 s	0.0267 (-36.1)	0.9413 (-31.7)	0.7660 (6.7)	0.9488 (19.4)	1.0612 (3.4)	0.9961 (-0.5)	0.8129 (10.3)	0.9451 (18.7)
64°C	1/9 s	0.0987	4.5276	0.8780	0.9402	0.9992	0.9964	0.8773	0.9369
	2/9 s	0.0678 (-31.3)	3.5364 (-21.9)	0.8598 (-2.1)	0.9681 (3.0)	1.0046 (0.5)	0.9984 (0.2)	0.8638 (-1.5)	0.9666 (3.2)
	4/9 s	0.0555 (-43.8)	3.0813 (-31.9)	0.8668 (-1.3)	0.9993 (6.3)	1.0110 (1.2)	1.0038 (0.7)	0.8763 (-0.1)	1.0031 (7.1)
	8/9 s	0.0530 (-46.3)	2.8801 (-36.4)	0.8851 (0.8)	1.0282 (9.4)	1.0200 (2.1)	1.0157 (1.9)	0.9028 (2.9)	1.0444 (11.5)
70°C	1/9 s	0.2455	10.6237	0.9342	0.9806	0.9990	0.9986	0.9332	0.9791
	2/9 s	0.1521 (-38.0)	8.2648 (-22.2)	0.9065 (-3.0)	1.0057 (2.6)	1.0024 (0.3)	1.0022 (0.4)	0.9087 (-2.6)	1.0078 (2.9)
	4/9 s	0.1222 (-50.2)	7.2545 (-31.7)	0.9154 (-2.0)	1.0251 (4.5)	1.0068 (0.8)	1.0084 (1.0)	0.9216 (-1.2)	1.0337 (5.6)
	8/9 s	0.1267 (-48.4)	7.1345 (-32.8)	0.9489 (1.6)	1.0439 (6.5)	1.0126 (1.4)	1.0201 (2.2)	0.9609 (3.0)	1.0649 (8.8)
76°C	1/9 s	0.4158	20.3546	0.9523	0.9978	1.0001	1.0001	0.9524	0.9979
	2/9 s	0.3078 (-26.0)	17.7054 (-13.0)	0.9405 (-1.2)	1.0178 (2.0)	1.0025 (0.2)	1.0038 (0.4)	0.9428 (-1.0)	1.0217 (2.4)
	4/9 s	0.2788 (-32.9)	16.3320 (-19.8)	0.9604 (0.9)	1.0325 (3.5)	1.0070 (0.7)	1.0101 (1.0)	0.9672 (1.6)	1.0430 (4.5)
	8/9 s	0.3070 (-26.2)	16.6404 (-18.2)	0.9964 (4.6)	1.0608 (6.3)	1.0150 (1.5)	1.0273 (2.7)	1.0114 (6.2)	1.0898 (9.2)

[a] the percentages of variation reported in parenthesis refer to the changes in the parameter when moving from 1.0 s to the creep time into question (2.0, 4.0 or 8.0 s).

of polymer in the formulation, which in turn minimized the ability of the polymer network in recovering greater portions of the total strain during the creep-recovery cycles. This is also reinforced by the fact that the α values are commonly greater for the AC+EVA+PPA than for the AC+EVA, as given by the positions of the data points above or very close to the equality line in Figure 175. Only a few data points are placed below this equality line (i. e., the α values are greater for the AC+EVA than for the AC+EVA+PPA), but the differences between the results in such cases are very small.

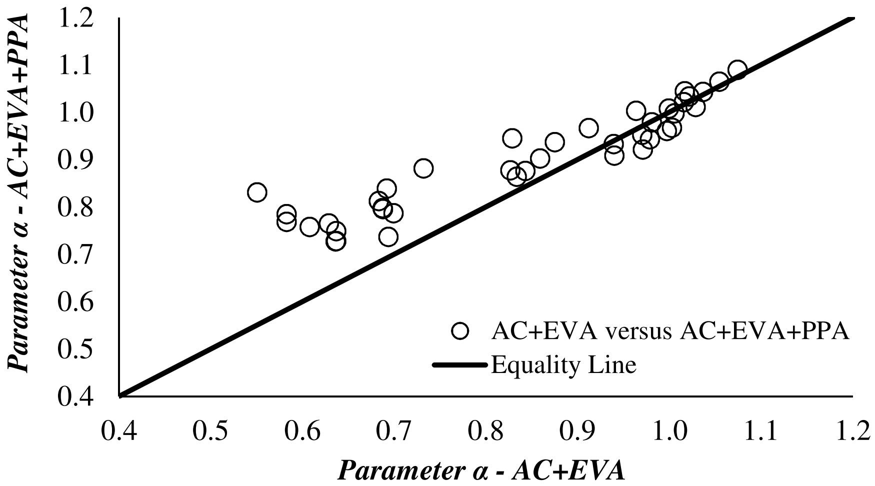

Figure 175 – Comparison between the results of the parameter α for the AC+EVA and the AC+EVA+PPA under all MSCR testing conditions

As emphasized earlier, the A values tend to decrease faster for the AC+EVA+PPA with loading time than for the AC+EVA, and this can be seen at all the test temperatures. In addition, the B values always increase with creep time for the AC+EVA+PPA and are typically greater for this formulation than for the AC+EVA. This suggests that the presence of higher strain rates is one of the reasons why the AC+EVA+PPA depicts higher nonrecoverable compliances – and thus a greater susceptibility to rutting – than the AC+EVA, as previously discussed and plotted in Figure 170 and Figure 171. With respect to the initial strain (parameter A), direct comparisons among the values of this parameter indicate that the use of PPA and less EVA content in the preparation of the AC+EVA+PPA lead to decreases in this type of strain, as shown graphically in Figure 176 (points below the equality line, each data point is comprised by one temperature, one creep time and one stress level in the MSCR test). This phenomenon tends to be reversed at the temperatures of 70 and 76°C and the creep-recovery times of 1/9 s and 2/9 s, as can be inferred from the points above the equality line and inside the red circle in Figure 176.

As a direct consequence of these smaller amounts of polymer in the AC+EVA+PPA and the nonlinear response of polymers when subjected to high strain levels, one may imply that the level of nonlinearity is smaller for the AC+EVA+PPA than for the AC+EVA as soon as the polymeric network does not suffer extensive damage and/or is melted at very high temperatures (i. e., temperatures no greater than 64°C). This may be confirmed by comparing the *n* values of the AC+EVA+PPA with those of the AC+EVA, see Figure 177. In summary, the AC+EVA commonly depicts a higher level of nonlinearity than the AC+EVA+PPA at temperatures up to 64°C due to the influence of the EVA copolymer, and the differences between the *n* values for both formulations are no greater than 1% in modulus at 70 and 76°C because the role of EVA on the response of the asphalt binder is greatly minimized.

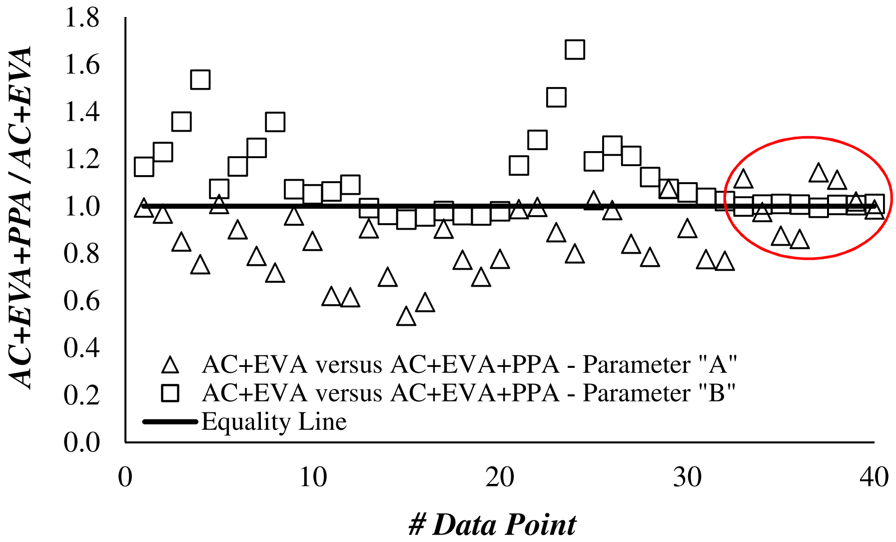

Figure 176 – Plots of the data points associated with the ratios of the *A* and *B* values for the AC+EVA+PPA to the corresponding ones for the AC+EVA (each data point is characterized by one temperature, loading time and stress level), the continuous line is the equality line and the red circle highlights the results of *A* and *B* at 70 and 76°C

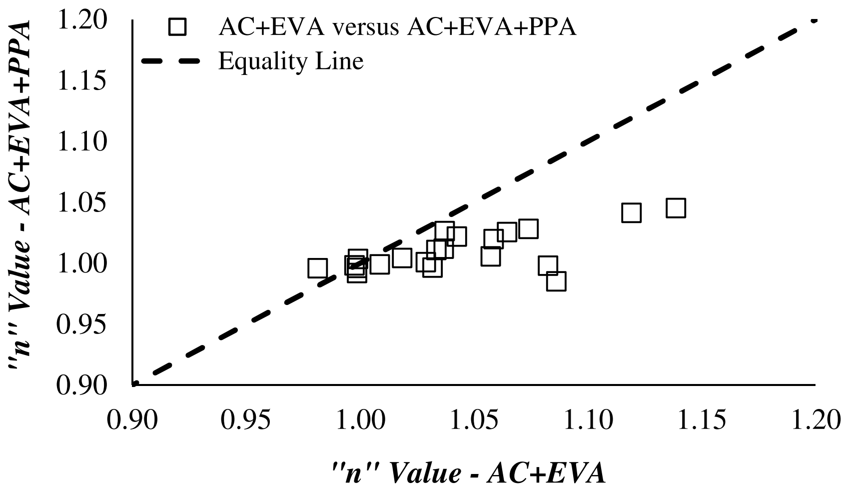

Figure 177 – Direct comparison between the degrees of nonlinearity (*n* values) for the AC+EVA and the AC+EVA+PPA at the temperatures of 52, 58 and 64°C

Similarly to the AC+EVA, the AC+EVA+PPA also depicts a high level of elasticity at some temperatures, more specifically, 52 and 58°C (refer to Figure 57, page 168). Therefore, further analyses were conducted to see if this classification still remains the same at longer creep times in the MSCR tests. The final results are given in Figure 178 and, as may be observed, the binder is not able to keep its classification as a formulation with "high elasticity" when the creep time is longer than the standardized one (1.0 s) and the testing temperature is higher than 58°C. As a consequence, the process of binder modification with EVA+PPA cannot provide sufficiently high levels of elasticity to the material when compared with other modification types such as Elvaloy+PPA and EVA alone, probably because of the use of a lower polymer content and the limitations involving the use of PPA together with EVA, as discussed above.

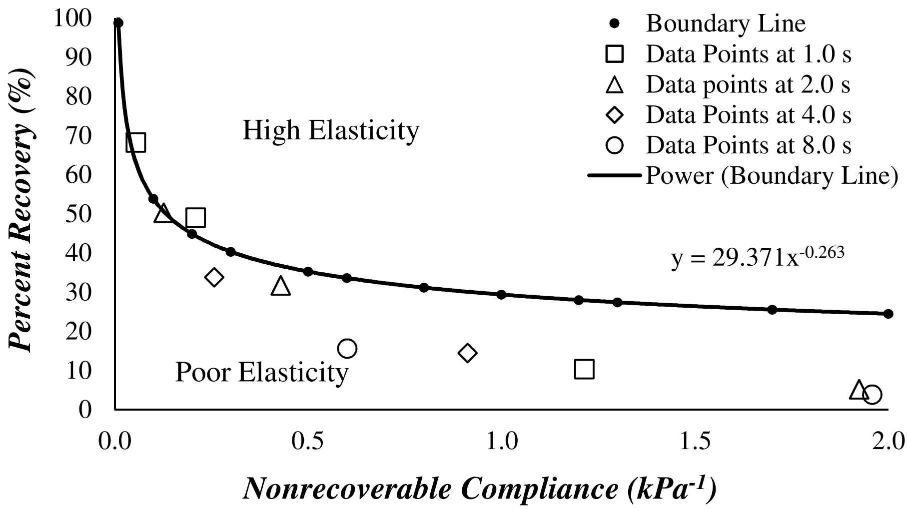

Figure 178 – Degrees of elasticity for the AC+EVA+PPA at increased creep times and temperatures as based on the MSCR testing parameters at 3,200 Pa

The studies about the changes in the parameters *A* and *B* with creep time for the AC+EVA+PPA were also made, and the procedure followed in the previously studied formulations was applied here as well. Figure 179 and Figure 180 depict the variations in *A* and *B* with creep time at 64°C and the stress levels of 100 and 3,200 Pa (respectively), together with the levels of linear correlation for each set of data. It is not clear that the increases in *B* with creep time may be sufficiently described by a straight line at 100 Pa, which is in the opposite direction of the findings for the AC+EVA (see Figure 158 and Figure 159, page 364, for more details). Much better correlations for *B* may be obtained at 3,200 Pa, whereas the R^2 values for *A* differ by only 13.7% when moving from 100 to 3,200 Pa. It is suggested that the polymer is playing an important role in the response of the binder at 100 Pa, that is, the *n* values continuously increase with t_F according to the data shown in Table 218. Although these increases can be seen at 3,200

Pa as well, it is suggested that the high amounts of damage accumulated by the sample during the test diminished the influence of the polymer network on the response of the formulation.

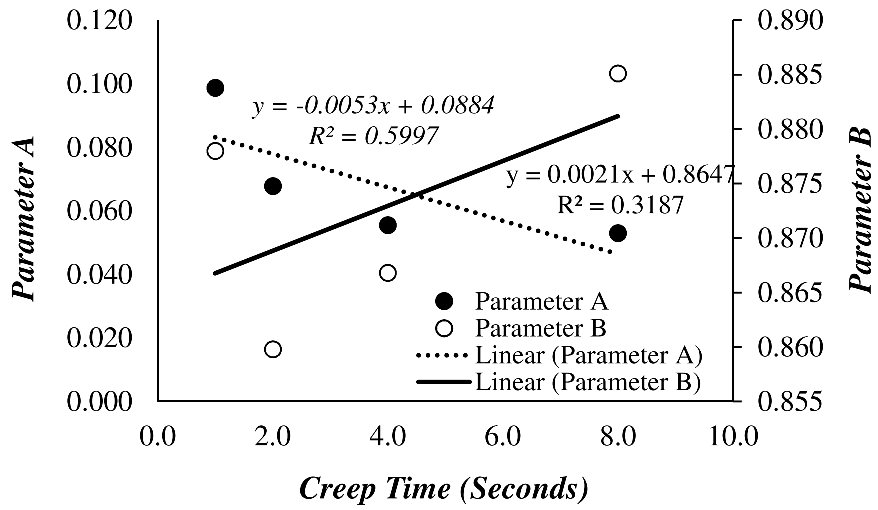

Figure 179 – Correlations between the creep time and the constants *A* and *B* from the model by Saboo and Kumar (2015), temperature of 64°C and stress level of 100 Pa – AC+EVA+PPA

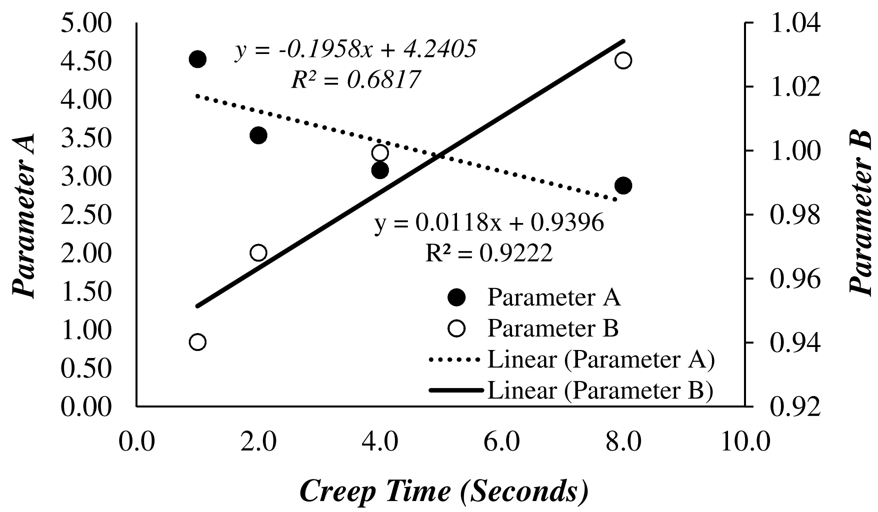

Figure 180 – Correlations between the creep time and the constants *A* and *B* from the model by Saboo and Kumar (2015), temperature of 64°C and stress level of 3,200 Pa – AC+EVA+PPA

Figure 181 and Figure 182 show the same charts and correlations for *A* and *B* and the AC+EVA+PPA, but considering the temperature of 70°C. It can be seen that slight increases in the correlations for *B* and decreases in the ones for *A* may be seen at 100 Pa, whereas both R^2 values for *A* and *B* decreased when moving from 64 to 70°C at 3,200 Pa. Despite such decreases, the levels of correlation for *A* in the AC+EVA+PPA are still better than those found in the AC+EVA, see Figure 160 and Figure 161 (page 366) for comparisons. As with other formulations with comparatively high degrees of nonlinearity, the increasing values for *n* at both stress levels – refer to Table 218 – may have contributed to the limitations in the correlations for both parameters. Again, it is not clear that the variations in *A* and *B* with creep time may be represented by a straight line, even though no reverses in the signals of the gradients of regression equations for *B* were found (which was observed for the AC+EVA).

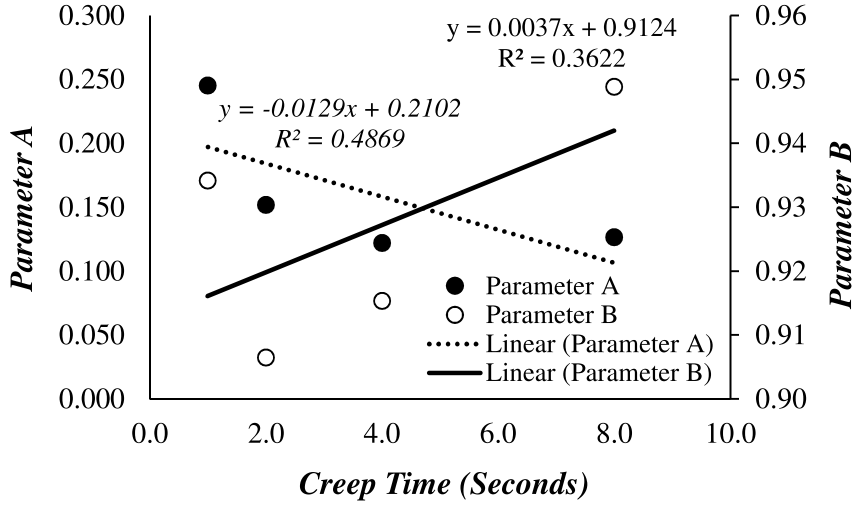

Figure 181 – Correlations between the creep time and the constants *A* and *B* from the model by Saboo and Kumar (2015), temperature of 70°C and stress level of 100 Pa – AC+EVA+PPA

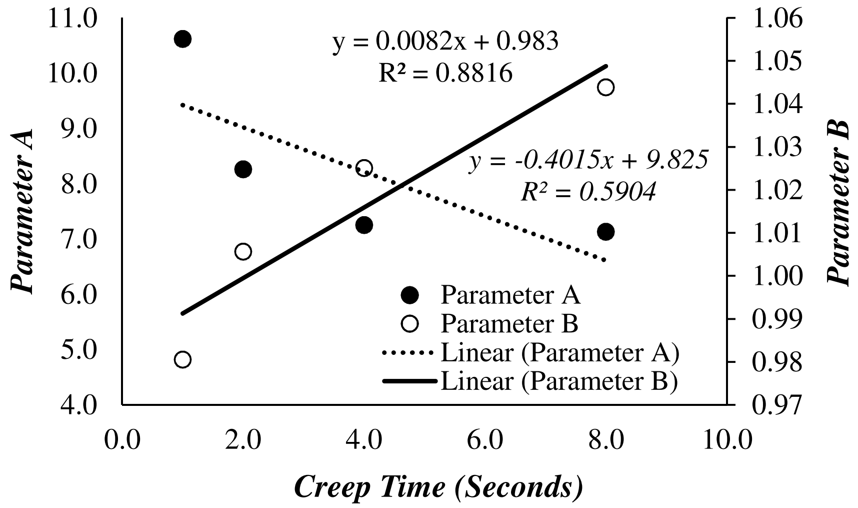

Figure 182 – Correlations between the creep time and the constants *A* and *B* from the model by Saboo and Kumar (2015), temperature of 70°C and stress level of 3,200 Pa – AC+EVA+PPA

Table 219 shows all the linear correlations between the parameters *A* and *B* for the AC+EVA+PPA and the creep times used in the MSCR tests, including the ones reported in Figure 179 to Figure 182 for the reader's convenience. By comparing these data with the ones observed for the AC+EVA (Table 204, page 366), it can be seen that the correlations for *A* and the AC+EVA+PPA are much better at the temperatures of 52, 58 and 64°C (which is specifically associated with the lower degrees of nonlinearity for the formulation with EVA+PPA, Figure 177) and that the reverse in the signal of the slopes of the trendlines for *B* takes place at 52°C, and not 64°C as found in the AC+EVA. These observations indicate that the initial strain is less affected by nonlinearity in the AC+EVA+PPA than in the AC+EVA, and also that the strain rate further contributes to the rutting performance of the AC+EVA+PPA than for the AC+EVA at temperatures up to 64°C. However, it is not possible to say that this greater contribution of the strain rate in the performance of the AC+EVA+PPA may be always described by linear relationships due to the effects of nonlinearity. As a consequence, the correlations of *B* are poorer for the AC+EVA+PPA than for the AC+EVA within the whole temperature range at 100 Pa.

Table 219 – Degrees of correlation between the parameters *A* and *B* (modified power model) and the creep time t_F for the AC+EVA+PPA

T (°C)	stress (kPa)	linear regression equations and R^2 values (in parenthesis)[a, b]	
		parameter *A*	parameter *B*
52	0.1	y = -0.0007x +0.0174 (0.7712)	y = -0.0002x + 0.7216 (0.0103)
	3.2	y = -0.0229x +0.5681 (0.8267)	y = 0.0164x + 0.7160 (0.9543)
58	0.1	y = -0.0018x + 0.0393 (0.6859)	y = 0.0045x + 0.7371 (0.3384)
	3.2	y = -0.0562x + 1.3443 (0.8109)	y = 0.0207x + 0.7910 (0.9492)
64	0.1	y = -0.0053x + 0.0884 (0.5997)	y = 0.0021x + 0.8647 (0.3187)
	3.2	y = -0.1958x + 4.2405 (0.6817)	y = 0.0118x + 0.9396 (0.9222)
70	0.1	y = -0.0129x + 0.2102 (0.4869)	y = 0.0037x + 0.9124 (0.3622)
	3.2	y = -0.4015x + 9.8250 (0.5904)	y = 0.0082x + 0.9830 (0.8816)
76	0.1	y = -0.0107x + 0.3675 (0.2999)	y = 0.0073x + 0.9350 (0.8816)
	3.2	y = -0.4228x + 19.3440 (0.5125)	y = 0.0084x + 0.9957 (0.9609)

[a] the Y-axis is associated with the parameter (*A* or *B*), whereas the X-axis is associated with t_F.
[b] changes in the signal of the slope of the regression trendlines are highlighted with a grey-shaded box.

Table 220 provides the regression equations and the corresponding R^2 values for the parameters *n* and *α* and the AC+EVA+PPA. The constant variations in the signals of the slopes of the equations for *n* at 52 and 58°C – as well as the *n* values around 0.99-1.02 – indicate that nonlinearity exerts some influence in the response of the binder during the MSCR test; however, it cannot be stated whether this influence mainly increases or decreases with loading time. This could also be seen in the results of the AC+EVA (Table 205, page 367), but only at the temperatures of 58 and 64°C. In addition, the presence of only positive slopes and *n* values approaching unity at 64, 70 and 76°C point to a reduction in the role of the polymer network on the nonlinear response of the formulation, which is quite similar to the conclusions drawn for the AC+EVA. With respect to the *α* values, a more homogeneous behavior with temperature and creep time may be seen for the AC+EVA+PPA when compared with the AC+EVA because no changes in the signals of the gradients of the trendlines are found. The correlations are not as good as those reported for the AC+EVA, but the equations point to a consistent increase in α with increasing severity in the MSCR tests (especially the intercepts).

Table 220 – Degrees of correlation between the parameters n and α (modified power model) and the creep time t_F for the AC+EVA+PPA

T (°C)	stress (kPa)	linear regression equations and R^2 values (in parenthesis)[a, b]	
		parameter n	parameter α
52	0.1	y = 0.0073x + 1.0149 (0.9979)	y = 0.0050x + 0.7324 (0.8012)
	3.2	y = -0.0037x + 1.0143 (0.9869)	y = 0.0135x + 0.7269 (0.9406)
58	0.1	y = 0.0053x + 1.0189 (0.9755)	y = 0.0087x + 0.7509 (0.6739)
	3.2	y = -0.0006x + 0.9986 (0.2198)	y = 0.0202x + 0.7899 (0.9634)
64	0.1	y = 0.0028x + 0.9980 (0.9720)	y = 0.0046x + 0.8629 (0.7516)
	3.2	y = 0.0028x + 0.9931 (0.9972)	y = 0.0147x + 0.9328 (0.9537)
70	0.1	y = 0.0019x + 0.9982 (0.9718)	y = 0.0055x + 0.9105 (0.5827)
	3.2	y = 0.0030x + 0.9959 (0.9989)	y = 0.0114x + 0.9786 (0.9318)
76	0.1	y = 0.0021x + 0.9982 (0.9986)	y = 0.0094x + 0.9331 (0.9266)
	3.2	y = 0.0039x + 0.9958 (0.9956)	y = 0.0125x + 0.9911 (0.9849)

[a] the Y-axis is associated with the parameter (n or α), whereas the X-axis is associated with t_F.
[b] changes in the signal of the slope of the regression trendlines are highlighted with a grey-shaded box.

It can be inferred from the comparisons between the values of the parameters for the AC+EVA and the AC+EVA+PPA that, differently from the AC+EVA, the strain rate is more affected by the nonlinear response of the polymer network in the AC+EVA+PPA. In addition, the levels of nonlinearity and elastic response seem to be lower for the formulation with EVA+PPA than for the one with EVA alone. This is because the n values were reduced when moving from the AC+EVA to the AC+EVA+PPA and the α values only increase for the AC+EVA+PPA with increasing time, temperature and stress level in the MSCR test. The presence of higher strain rates may be pointed out as one of the reasons why the AC+EVA+PPA is a little bit more prone to rutting (slightly higher J_{nr} values) than the AC+EVA, and the smaller amounts of recovered strain for the AC+EVA+PPA in the creep-recovery cycles might also have contributed to these conclusions. Finally, none of the EVA-modified binders can hold the classification of "material with high elasticity" in the *R3200*-J_{nr}*3200* chart from the AASHTO standard at all creep times and temperatures, even though the results are worse for the AC+EVA+PPA.

By plotting all the J_{nr} values of the AC+EVA+PPA against the n values (Figure 183), it can be seen that the overall correlation is very poor (R^2 < 0.1). This conclusion is similar to the one obtained for the data of the AC+EVA, see Figure 162 (page 368) for more details. The major difference between both materials is that the correlation is better for the AC+EVA, but still poor enough to say that there is no clear relationship between the increases in J_{nr} and the variations in the parameter n. The J_{nr} values of the AC+EVA+PPA also range within a wide interval – from about 0.03 kPa^{-1} to 50 kPa^{-1} – and the n values do not necessarily follow the same pattern of increase with loading time and stress level at all test temperatures. When only the data points at 100 Pa and 3,200 Pa are considered separately, it could be seen that the R^2 values are almost the same for the two stress levels (approximately equal to 0.26 at 100 Pa and 0.24 at 3,200 Pa) and the slopes of the regression trendlines are reversed (i. e., negative at 100 Pa and positive at 3,200 Pa). As previously reported for the AC+EVA, it is not possible to ensure that the variations in n for the AC+EVA+PPA may be described by the ones in J_{nr} during the MSCR test.

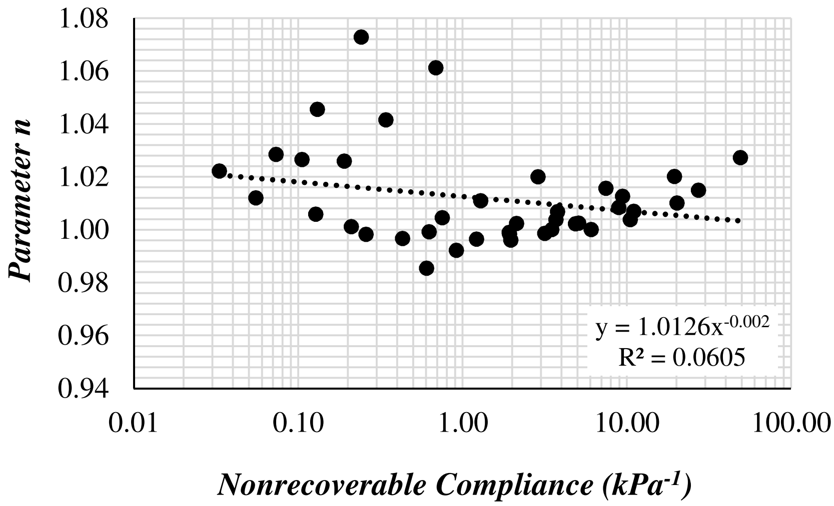

Figure 183 – Degree of correlation between the nonrecoverable compliances of the AC+EVA+PPA and the corresponding n values from the power law models

With respect to the α values and their correlations with the percent recoveries of the AC+EVA+PPA (Figure 184), it can be said that a pretty good correlation exists between the two parameters ($R^2 \approx 0.88$). This is in aligment with the data reported for the other modified asphalt binders, including the AC+EVA (see Figure 163, page 369). The fact that α continuously decreases with increasing R is also in accordance with the literature and the analyses carried out for other formulations in this dissertation. Altough the overall correlation is of about 0.88, complementary analyses showed that the individual correlation for the data at 100 Pa is much better ($R^2 \approx 0.97$) than the one obtained for the data at 3,200 Pa ($R^2 \approx 0.84$), refer to Figure 185 for a graphical representation of such a conclusion. This could be found in other formulations as well, e. g., the AC+Elvaloy+PPA (Figure 92, page 241), the AC+SBS (Figure 118, page 290) and the AC+SBS+PPA (Figure 129, page 309). It can be hypothesized that the rapid degradation of the polymer network of the AC+EVA+PPA at 3,200 Pa due to accumulated damage and the presence of several α values for one particular R value (0%) – which is also a limitation of the modified power model – may explain such a great difference in the correlations at each stress level.

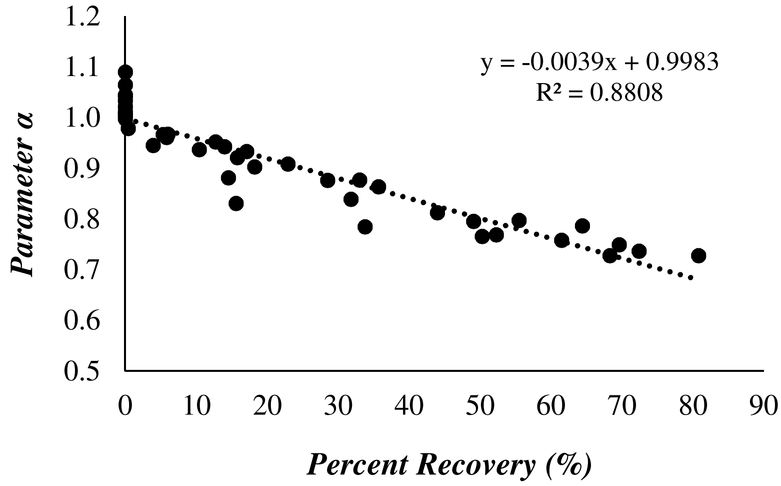

Figure 184 – Degree of correlation between the percent recoveries of the AC+EVA+PPA and the corresponding α values from the power law models

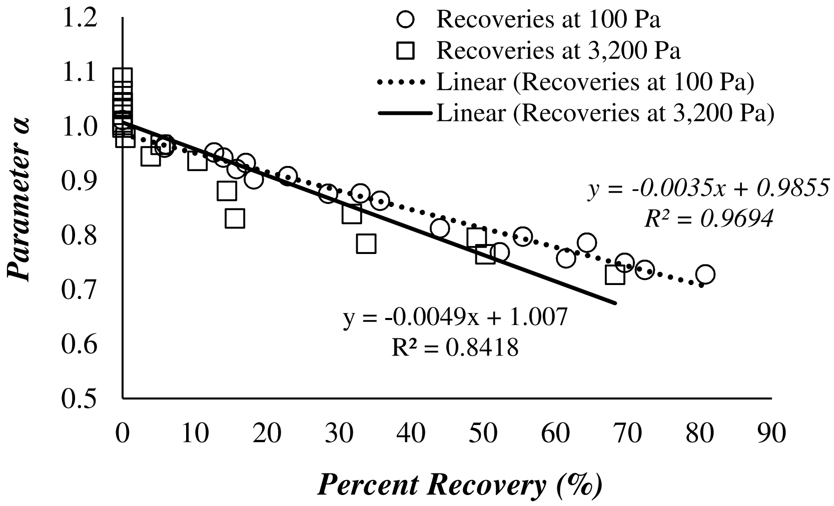

Figure 185 – Individual correlations between the percent recoveries of the AC+EVA+PPA at 100 and 3,200 Pa and the corresponding α values from the power law models

Finally, the statistical analysis of variance (ANOVA) was carried out on the R and J_{nr} values of the AC+EVA+PPA starting from the temperature of 52°C and the creep-recovery times of 1/9 s. The objective was to identify the variable that mostly influences on the results of the MSCR testing parameters, as well as if these effects may be considered as statistically significant and the results vary significantly from one variable to the other (*F-value* > $F_{critical}$ and *p-value* < α) or not. To do this, the *R100* and *R3200* values were rearranged according to the layout provided in Table 221. As can be seen, there is only one *R3200* value equal to zero among the data collected with increasing temperature. This is acceptable according to the requirements established in the present study for conducting ANOVA in the recovery data.

Table 221 – Rearranged MSCR testing data of the AC+EVA+PPA to be used in the analysis of variance (ANOVA) – percent recovery

stress level of 0.1 kPa (*R100*, %)[a]		stress level of 3.2 kPa (*R3200*, %)[a]	
increasing creep time	increasing temperature	increasing creep time	increasing temperature
80.8	80.8	68.3	68.3
69.3	72.4	50.3	49.1
61.5	33.0	33.8	10.4
52.3	17.1	15.6	0.4
N/A[b]	12.7	N/A[b]	N/A[b]

[a] the starting point in both cases was the temperature of 52°C.
[b] N/A: Not applicable.

Table 222 shows the results of ANOVA for the percent recoveries of the AC+EVA+PPA. It can be seen that the null hypothesis H_0 may not be rejected in any case, that is, the effects of temperature and loading time on the percent recoveries of the AC+EVA+PPA cannot be considered as statistically different under a level of significance of 5%. The *F-value* does not exceed 1.84 (about 30-32% of $F_{critical}$) and the *p-value* is higher than 0.20 (from 4 to 13 times higher than α) either at 100 or at 3,200 Pa, even though the variances at 100 Pa are greater than those at 3,200 Pa. The same general conclusions were reported for the AC+EVA (Table 207, page 370), but the *F-value* is from 90 to 600% higher and the *p-value* is from 50 to 70% lower for the AC+EVA than for the AC+EVA+PPA at both stress levels. More simply, the presence of PPA and the use of lower EVA contents diminished the variabilities within the results of the *R100* and *R3200* values when compared with the use of EVA alone.

Table 222 – Results from the analysis of variance (ANOVA, *p-value* and *F-value*) as based on the percent recoveries of the AC+EVA+PPA

null hypothesis H_0	statistical parameters (ANOVA)				recommendation
	$F_{critical}$	*F-value*	α	*p-value*	
equivalency between *R* values with increasing creep time and temperature, 0.1 kPa	5.5914	1.8368	0.05	0.2174	H_0 is not rejected
equivalency between *R* values with increasing creep time and temperature, 3.2 kPa	5.9874	0.2583	0.05	0.6294	H_0 is not rejected

Table 223 shows the organized $J_{nr}100$ and $J_{nr}3200$ values of the AC+EVA+PPA to be tested under ANOVA, whereas Table 224 provides the results of this statistical analysis for both MSCR parameters. Again, the variations in these parameters cannot be considered as relevant according to a level of significance of 5% (F-$value$ < $F_{critical}$ and p-$value$ > α) and are similar to the conclusions reported for the AC+EVA, see Table 209 (page 371) for comparisons. The differences among the ANOVA parameters of the AC+EVA and the AC+EVA+PPA are not great, since they do not vary by more than 10% at the two studied stress levels. In other words, the parameter J_{nr} is less sensitive to the effects of temperature and creep time on the results of the two EVA-modified asphalt binders in the MSCR tests when compared with the parameter *R*.

Table 223 – Rearranged MSCR testing data of the AC+EVA+PPA to be used in the analysis of variance (ANOVA) – nonrecoverable creep compliance

stress level of 0.1 kPa ($J_{nr}100$, kPa^{-1})[a]		stress level of 3.2 kPa ($J_{nr}3200$, kPa^{-1})[a]	
increasing creep time	increasing temperature	increasing creep time	increasing temperature
0.033	0.033	0.055	0.055
0.073	0.105	0.127	0.209
0.130	0.623	0.257	1.214
0.241	1.912	0.601	3.159
N/A[b]	3.472	N/A[b]	6.049

[a] the starting point in both cases was the temperature of 52°C.
[b] N/A: Not applicable.

Table 224 – Results from the analysis of variance (ANOVA, *p-value* and *F-value*) as based on the nonrecoverable compliances of the AC+EVA+PPA

null hypothesis H_0	statistical parameters (ANOVA)				recommendation
	$F_{critical}$	*F-value*	α	*p-value*	
equivalency between J_{nr} values with increasing creep time and temperature, 0.1 kPa	5.5914	2.2319	0.05	0.1788	H_0 is not rejected
equivalency between J_{nr} values with increasing creep time and temperature, 3.2 kPa	5.5914	2.1557	0.05	0.1855	H_0 is not rejected

The *R100* and *R3200* values of the AC+PE are reported in Table 225 for all temperatures and loading times selected in the study. PE-modified asphalt binders typically do not depict very high percent recoveries in the MSCR tests, and this was observed in other papers as well (DOMINGOS and FAXINA, 2015b; NEJAD et al., 2015). The results are all lower than 38% at 100 Pa and do not overcome 22% at 3,200 Pa. The lack of elasticity is also reflected on the great number of null *R3200* values, especially when $T \geq 64$°C. As a consequence, it can be implied that the influence of elasticity on the rutting resistance of the AC+PE is very small, and also that the application of loads for creep times longer than 2.0 s has a substantial impact on the results of *R100* and *R3200*. More specifically, this can be translated into considerable reductions in the recoveries when the creep time is longer than 2.0 s – the decreases are of at least 44% when compared with the much smaller percentages from 1.0 to 2.0 s, see Figure 186 – and almost complete absence of recovery at the stress level of 3,200 Pa and for creep times of 4.0 s and longer.

Table 225 – Percent recoveries at 100 Pa (*R100*) and 3,200 Pa (*R3200*) for the AC+PE with increasing loading time and temperature

parameter	creep time (s)	results at each temperature and increases (both in %)[a]				
		52°C	58°C	64°C	70°C	76°C
R100	1.0	37.3	31.0	24.2	17.1	12.8
	2.0	33.3	28.3	19.6	12.6	7.8
	4.0	20.9	16.9	10.4	6.0	2.4
	8.0	13.6	8.1	3.5	0.6	0.0
R3200	1.0	21.5	12.3	4.0	0.0	0.0
	2.0	16.5	7.2	0.4	0.0	0.0
	4.0	5.5	0.0	0.0	0.0	0.0
	8.0	0.1	0.0	0.0	0.0	0.0

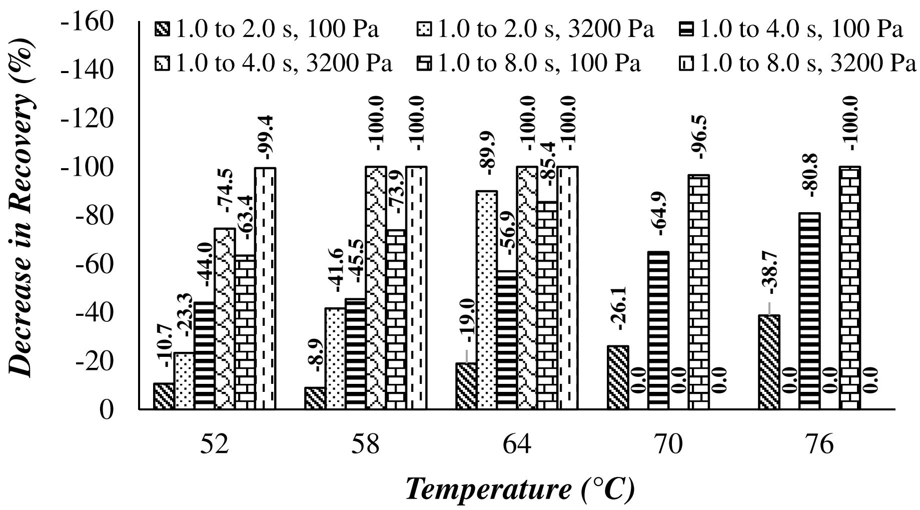

Figure 186 – Percentages of decrease in the recovery values of the AC+PE with creep time, temperature and stress level

It can be implied here that the “elastic” response of the AC+PE under load in the MSCR test is mainly due to the stiffness of the formulation, and not specifically the response of the polymer chain. In other words, the crystalline structure of the low-density PE avoids its interaction with the components of the asphalt binder, and the apparent "mixing" of the polymer with the base material takes place because of shearing during the preparation of the formulation (POLACCO et al., 2006). Also, very high PE contents are usually required to achieve phase inversion and a more effective modification of the binder. Despite the observation of a certain degree of interdiffusion after mixing the modifier with the original binder at high temperatures and shear levels, phase separation may occur at quite short periods of time in such cases (POLACCO et al., 2015). As a consequence, the softening of the base asphalt binder at temperatures of 64°C and greater reveals that the polymeric chain has practically no effect on the elastic response of the AC+PE. Probably the most visible contribution of PE to the results of the MSCR tests is linked to the great differences between the percentages of decrease in R at 100 and 3,200 Pa and for each pair of t_F values.

The nonrecoverable compliances of the AC+PE in the MSCR testing conditions are shown in Table 226. The major increases in $J_{nr}100$ and $J_{nr}3200$ when t_F > 2.0 s suggest that the susceptibility of the material to rutting is much greater at 4.0 and 8.0 s, which may lead to a premature failure of the mixture on pavements with high percentages of vehicles traveling at low speeds. As a matter of comparison, these percentages of increase in $J_{nr}100$ and $J_{nr}3200$ are no greater than 85% when the creep time is doubled for the first time – from 1.0 to 2.0 s, see Figure 187. However, the percentages are boosted to values no lower than 400% and 900% when the creep time is doubled one and two more times (from 2.0 to 4.0 s, and then to 8.0 s), respectively. Similarly to the EVA-modified binders, the loading time of t_F = 2.0 s can be interpreted as a limiting criterion for the use the AC+PE on pavements. By combining such creep time with the high PG grade temperature of 70°C, one may assume that this test condition is the "failure point" for the AC+PE used in the study.

In terms of the numerical results of $J_{nr}100$ and $J_{nr}3200$, it can be seen that they are all between 0.06 and 28.60 kPa^{-1} at 100 Pa and between 0.07 and 46.55 kPa^{-1} at 3,200 Pa. Since the differences between the percentages of increase in J_{nr} at 100 and 3,200 Pa become greater with increasing creep time, it can be inferred that the stress sensitivity of the binder is also higher at longer creep times, as will be discussed later. One interesting aspect of the outcomes of the AC+PE is that these percentages at 100 and 3,200 Pa do not differ too much from each other at a particular test temperature, e. g., 410.5 and 430.8% at 70°C and with the creep time increasing from 2.0 to 4.0 s. Other formulations such as the AC+SBS+PPA (Figure 120, page 296), the AC+rubber+PPA (Figure 102, page 261), the AC+Elvaloy+PPA (Figure 85, page 227) and the 50/70 base binder (Figure 69, page 193) also showed this pattern of response and, in all cases, the stress sensitivity was below the maximum value of 75% allowed by Superpave®. This may be explained by the relatively great stability provided by the modifier (s) in the formulation, as exemplified earlier for the AC+Elvaloy+PPA. Therefore, it may be implied from these comments that the stress sensitivity of the AC+PE is not very high when compared with other formulations such as the AC+rubber and the AC+EVA.

Table 226 – Nonrecoverable compliances at 100 Pa (*$J_{nr}100$*) and 3,200 Pa (*J_{nr} 3200*) for the AC+PE with increasing loading time and temperature

parameter	creep time (s)	results at each temperature (kPa^{-1}), J_{nr} > 4.0 kPa^{-1} is in bold				
		52°C	58°C	64°C	70°C	76°C
$J_{nr}100$	1.0	0.060	0.170	0.451	1.143	2.636
	2.0	0.102	0.284	0.786	2.013	**4.827**
	4.0	0.323	0.871	2.349	**5.834**	**13.618**
	8.0	0.664	1.862	**5.052**	**12.477**	**28.594**
$J_{nr}3200$	1.0	0.078	0.229	0.648	1.677	3.952
	2.0	0.135	0.407	1.176	3.015	**7.282**
	4.0	0.421	1.304	3.566	**9.020**	**21.251**
	8.0	0.920	2.829	**7.823**	**19.699**	**46.542**

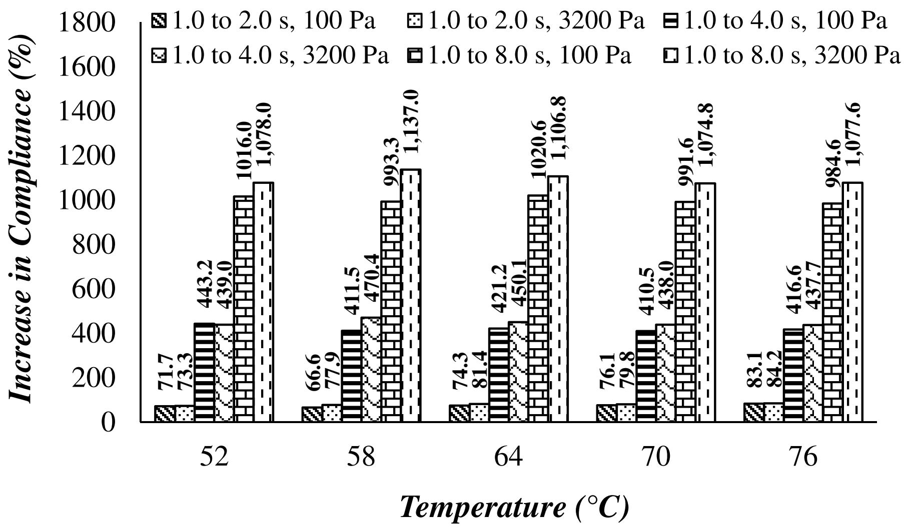

Figure 187 – Percentages of increase in the nonrecoverable compliances of the AC+PE with creep time, temperature and stress level

The laboratory results shown in Table 227 precisely indicate that the AC+PE is not an overly stress sensitive formulation, once that all the $J_{nr,\ diff}$ values are placed below the maximum value of 75% (the results range from 30 to 63% for all temperatures and loading times). As the data also suggest, the temperature has some influence in the sensitivity of the binder to increases in the stress level. In other words, higher temperatures result in a formulation more sensitive to the applications of higher stresses in the pavement, as hypothesized earlier. These increases are especially associated with the presence of the polyethylene chains in the AC+PE, since the 50/70 base material contributes with a very small percentage to the increases in $J_{nr,\ diff}$ (see Table 66, page 194). In addition, the continuous increases in $J_{nr,\ diff}$ with temperature and creep time suggest that the polymer network may not have suffered considerable damage in the test when compared with other polymeric modification types, e. g., the AC+EVA (Table 197, page 355) and the AC+EVA+PPA (Table 212, page 379).

Table 227 – Percent differences in nonrecoverable compliances ($J_{nr,\ diff}$) for the AC+PE with increasing creep time and temperature

creep time (s)	$J_{nr,\ diff}$ values (%) at each creep time and temperature				
	52°C	58°C	64°C	70°C	76°C
1.0	31.2	34.3	43.8	46.7	49.9
2.0	32.4	43.4	49.7	49.7	50.9
4.0	30.2	49.7	51.8	54.6	56.1
8.0	38.5	51.9	54.9	57.9	62.8

The adequate traffic levels for the AC+PE are shown in Table 228. Due to the considerable increases in $J_{nr}3200$ after the application of creep times longer than 2.0 s, the AC+PE cannot deal with almost any traffic level at temperatures of 64°C and higher. The impact of such longer creep times is also reflected on the decrease in the traffic level by two grades at 58°C (from extremely heavy at $t_F = 2.0$ s to heavy at $t_F = 4.0$ s). Again, these results indicate that the AC+PE may not be appropriate for pavements with many trucks and buses traveling at very low speeds, since they can negatively affect the rutting performance of the material. Quite similar findings were obtained in a previously published study with a different crude source for the original binder, in that doubling either the creep or the recovery times in the MSCR tests considerably decreased the traffic levels assigned to the AC+PE at the same pavement temperatures studied here (DOMINGOS and FAXINA, 2015b).

Table 228 – Adequate traffic levels for the AC+PE with increasing creep time and temperature based on the standardized Superpave® criteria

creep time (s)	traffic levels for each temperature[a]				
	52°C	58°C	64°C	70°C	76°C
1.0	E	E	V	H	S
2.0	E	E	H	S	-
4.0	E	H	S	-	-
8.0	V	S	-	-	-

[a] S = standard; H = heavy; V = very heavy; E = extremely heavy.

The correlations between the traffic speeds calculated from the equations by Huang (2004) and Pereira et al. (1998, 2000) and the $J_{nr}3200$ values were determined, and the resulting equations and corresponding R^2 values are summarized in Table 229. Because of the high degree of nonlinearity of the AC+PE at the loading times of 4.0 and 8.0 s, the correlations are not as excellent as the ones obtained for the other studied binders (R^2 is between 0.86 and 0.89). In graphical terms, it can be seen that the $J_{nr}3200$ values increase at lower rates for speeds around 30-80 km/h (shorter creep times) and there are sharp increases in this parameter for speeds around 10-30 km/h (longer creep times). Since the equations did not work well for the previously studied binders at temperatures higher than 64°C, it is believed that they will not accurately characterize the traffic speeds of the AC+PE either.

Table 229 – Regression equations and coefficients of determination between the $J_{nr}3200$ values of the AC+PE and the corresponding vehicle speeds according to the equations by Pereira et al. (1998, 2000) and Huang (2004)

source and data	temperature (in °C)	equation	R^2
Pereira et al. (1998)	52	$y = 0.8836e^{-0.033x}$	0.8654
Pereira et al. (2000)	52	$y = -0.0125x + 0.8493$	0.969
Huang (2004) $r = 6$ in	52	$y = 0.8841e^{-0.041x}$	0.8657
	58	$y = 2.7566e^{-0.042x}$	0.8711
	64	$y = 7.5983e^{-0.041x}$	0.8758
	70	$y = 19.0930e^{-0.040x}$	0.8748
	76	$y = 45.2980e^{-0.040x}$	0.8803
Huang (2004) $r = 3.68$ in	52	$y = 0.8822e^{-0.066x}$	0.8661
	58	$y = 2.7507e^{-0.068x}$	0.8715
	64	$y = 7.5822e^{-0.067x}$	0.8761
	70	$y = 19.0530e^{-0.066x}$	0.8752
	76	$y = 45.2030e^{-0.066x}$	0.8807

To clarify the doubts about the differences and similarities among the traffic levels determined by the equations from Huang (2004) and Pereira et al. (1998) and the ones provided by the Superpave® specification, Table 230 was prepared. One more time, the predictions of the actual traffic levels of the binder are from reasonable to good only at 52 and 58°C (at least two corrected predictions for each equation), and no correlations exist between the predicted and actual levels for $T > 64$°C. The results are not acceptable at all either when the equations from Huang (2004) – lower tire contact radius – and Pereira et al. (2000) are used in the analysis, see Table 231 for more details. As a consequence, the selected equations must be used with caution because the mathematical fits are not enough to obtain good estimations of the actual traffic levels of the binder and the corresponding average vehicle speeds on road pavements. This gives support to the hypothesis that the selected equations have some difficulties in estimating the actual speed and traffic level that the binder may experience in the field pavement, as it will be further analyzed later.

Table 230 – Comparisons between the actual traffic levels of the AC+PE and the ones obtained from Huang (2004) and Pereira et al. (1998)

t_F (s)[d]	actual[a] and estimated[b, c] traffic levels at each temperature[d]				
	52°C	58°C	64°C	70°C	76°C
1.0	**E (V/E) [V/E]**	**E [V/E]**	**V [V/E]**	H [V/E]	S [V/E]
2.0	**E (V/E) [V/E]**	**E [V/E]**	H [V/E]	S [V/E]	-
4.0	E **(H) [H]**	**H [H]**	S [H]	-	-
8.0	V (S) [H]	S [H]	-	-	-

[a] S = standard; H = heavy; V = very heavy; E = extremely heavy (AASHTO M320-09 standard, Table 3).
[b] (parentheses) = traffic levels from Pereira et al. (1998).
[c] [brackets] = traffic levels from Huang (2004), $r = 6$ in.
[d] similarities among the rankings are highlighted in bold, t_F = creep time.

Table 231 – Comparisons between the actual traffic levels of the AC+PE and the ones obtained from the equations by Huang (2004) and Pereira et al. (2000)

t_F (s)[d]	actual[a] and estimated[b, c] traffic levels at each temperature[d]				
	52°C	58°C	64°C	70°C	76°C
1.0	**E** (H) **[V/E]**	**E [V/E]**	**V [V/E]**	H [V/E]	S [V/E]
2.0	**E** (H) **[V/E]**	**E [V/E]**	H [V/E]	S [V/E]	-
4.0	E **(H) [H]**	**H [H]**	S [H]	-	-
8.0	V **(H) [H]**	S [H]	-	-	-

[a] S = standard; H = heavy; V = very heavy; E = extremely heavy (AASHTO M320-09 standard, Table 3).
[b] (parentheses) = traffic levels from Pereira et al. (2000).
[c] [brackets] = traffic levels from Huang (2004), $r = 3.68$ in.
[d] similarities among the rankings are highlighted in bold, t_F = creep time.

Table 232 provides the classifications of the AC+PE according to the current and suggested Superpave® criteria for the traffic levels. As can be observed, there is a decrease by one grade (from very heavy to heavy) at the temperature of 64°C and the other traffic levels remain unchanged. This is one more indication of the high degree of nonlinear response of the material at creep times at least equal to 4.0 s, and it may restrict its use on some pavements with too severe loading conditions (e. g., lanes with chanellized traffic or roads with very high slopes). It is hypothesized that the excellent mixture performance of the AC+PE (Chapter 5) was due to the testing conditions (creep-recovery times of 0.1/0.9 s), even though the mixture variables and the differences between the actual stresses and speeds experienced by the binder during the flow number test and the MSCR test are equally important. In other words, the very critical conditions under which the binder is subjected in the rheological tests in the laboratory must be applied with caution in the real pavement.

Table 232 – Traffic levels of the AC+PE with increasing loading time and temperature in the current and proposed criteria

temperature (in °C)	No. of required MSCR tests[b]	Superpave® designations (current and new criteria)[a, c]	
		current criterion	new criterion
52	4	**52E-xx**	**52E-xx**
58	4	**58E-xx**	**58E-xx**
64	4	64V-xx	64H-xx
70	3	**70H-xx**	**70H-xx**
76	2	**76S-xx**	**76S-xx**

[a] S = standard; H = heavy; V = very heavy; E = extremely heavy (AASHTO M320-09 standard, Table 3).
[b] minimum number of MSCR tests to determine the adequate traffic level in the proposed classification.
[c] similarities among the classifications are highlighted in bold.

The outcomes of the MSCR tests at high temperatures and long loading times suggest that, as for any other binder modification with non-reactive modifiers, the percent recoveries are not high ($R < 38\%$) for the AC+PE and become much lower at the creep times of 4.0 and 8.0 s. The nonrecoverable compliances show considerably high percentages of increase at the creep times of 4.0 s (> 400%) and 8.0 s (> 900%), which is an indication of the role of the nonlinear response of the material in such repeated creep responses. Due to these nonlinear responses, the *R3200* values of the AC+PE are typically null when $T \geq 64$°C and the $J_{nr,\,diff}$ values also increase, even though the binder is not graded as overly stress sensitive in any test condition ($J_{nr,\,diff} < 75\%$). Finally, the effect of nonlinearity on the traffic level of the binder according to the proposed criterion is reflected on the decrease in its level by one grade at the temperature of 64°C (from very heavy to heavy).

Table 233 provides the results of the parameters A, B, n and α for the AC+PE and all the MSCR testing conditions studied in this dissertation. There is a limiting creep time at $t_F = 2.0$ s, after which the rutting resistance of the formulation considerably decreases and either the initial strain or the strain rate (A and B) contribute to the substantial increases in the accumulated strains in the binder. The level of nonlinearity (n) also increases at faster rates when moving from 2.0 to 4.0 s and from 4.0 to 8.0 s. In other words, loading times longer than 2.0 s result in a great loss of resistance of the AC+PE to rutting and a more nonlinear creep-recovery response of the material, regardless of the temperature. The very promising findings associated with the mixture rutting performance of the AC+PE (Chapter 5) may be explained by the proportion and numerical values of the loading and unloading times used in the flow number tests.

Table 233 – Numerical values and variations in the parameters/constants *A, B, n* and *α* from the power law equations by Saboo and Kumar (2015) with increasing temperature and creep time and considering the AC+PE

temperature	test times	parameter A^a		parameter B^a		parameter n^a		parameter α	
		0.1 kPa	3.2 kPa	0.1 kPa	3.2 kPa	0.1 kPa	3.2 kPa	0.1 kPa	3.2 kPa
52°C	1/9 s	0.0101	0.3388	0.8752	0.9091	1.0022	0.9975	0.8771	0.9068
	2/9 s	0.0088 (-12.9)	0.2934 (-13.4)	0.8781 (0.3)	0.9163 (0.8)	1.0066 (0.4)	0.9974 (0.0)	0.8839 (0.8)	0.9140 (0.8)
	4/9 s	0.0123 (21.8)	0.4071 (20.2)	0.9121 (4.2)	0.9607 (5.7)	1.0110 (0.9)	1.0000 (0.3)	0.9221 (5.1)	0.9607 (5.9)
	8/9 s	0.0121 (19.8)	0.4037 (19.2)	0.9273 (6.0)	0.9894 (8.8)	1.0189 (1.7)	1.0057 (0.8)	0.9449 (7.7)	0.9951 (9.7)
58°C	1/9 s	0.0263	0.8909	0.9040	0.9462	1.0028	0.9984	0.9065	0.9447
	2/9 s	0.0226 (-14.1)	0.7729 (-13.2)	0.9038 (0.0)	0.9591 (1.4)	1.0072 (0.4)	0.9987 (0.0)	0.9103 (0.4)	0.9579 (1.4)
	4/9 s	0.0309 (17.5)	1.1167 (25.3)	0.9295 (2.8)	0.9985 (5.5)	1.0116 (0.9)	1.0040 (0.6)	0.9403 (3.7)	1.0026 (6.1)
	8/9 s	0.0302 (14.8)	1.1221 (26.0)	0.9520 (5.3)	1.0218 (8.0)	1.0148 (1.2)	1.0130 (1.5)	0.9661 (6.6)	1.0351 (9.6)
64°C	1/9 s	0.0634	2.3133	0.9260	0.9795	1.0022	0.9998	0.9281	0.9792
	2/9 s	0.0548 (-13.6)	2.0377 (-11.9)	0.9304 (0.5)	0.9933 (1.4)	1.0044 (0.2)	1.0012 (0.1)	0.9346 (0.7)	0.9945 (1.6)
	4/9 s	0.0751 (18.5)	2.9618 (28.0)	0.9552 (3.2)	1.0202 (4.2)	1.0085 (0.6)	1.0077 (0.8)	0.9633 (3.8)	1.0281 (5.0)
	8/9 s	0.0737 (16.2)	2.9669 (28.3)	0.9772 (5.5)	1.0380 (6.0)	1.0128 (1.1)	1.0179 (1.8)	0.9897 (6.6)	1.0565 (7.9)
70°C	1/9 s	0.1473	5.7615	0.9461	1.0002	1.0015	1.0009	0.9475	1.0011
	2/9 s	0.1279 (-13.2)	5.1454 (-10.7)	0.9533 (0.8)	1.0113 (1.1)	1.0031 (0.2)	1.0031 (0.2)	0.9563 (0.9)	1.0144 (1.3)
	4/9 s	0.1731 (17.5)	7.3803 (28.1)	0.9725 (2.8)	1.0306 (3.0)	1.0069 (0.5)	1.0098 (0.9)	0.9793 (3.4)	1.0406 (3.9)
	8/9 s	0.1709 (16.0)	7.3257 (27.1)	0.9944 (5.1)	1.0440 (4.4)	1.0117 (1.0)	1.0196 (1.9)	1.0060 (6.2)	1.0645 (6.3)
76°C	1/9 s	0.3251	13.6093	0.9599	1.0113	1.0014	1.0017	0.9613	1.0130
	2/9 s	0.2886 (-11.2)	12.3634 (-9.2)	0.9698 (1.0)	1.0203 (0.9)	1.0028 (0.1)	1.0042 (0.2)	0.9726 (1.2)	1.0245 (1.1)
	4/9 s	0.3839 (18.1)	17.2962 (27.1)	0.9879 (2.9)	1.0342 (2.3)	1.0060 (0.5)	1.0104 (0.9)	0.9938 (3.4)	1.0450 (3.2)
	8/9 s	0.3796 (16.8)	17.1079 (25.7)	1.0096 (5.2)	1.0469 (3.5)	1.0123 (1.1)	1.0205 (1.9)	1.0221 (6.3)	1.0684 (5.5)

[a] the percentages of variation reported in parenthesis refer to the changes in the parameter when moving from 1.0 s to the creep time into question (2.0, 4.0 or 8.0 s).

More detailed explanations about the findings reported in Table 233 can be given as follows. After doubling t_F from the standardized value (1.0 s) to 2.0 s, the increases in J_{nr} are explained by a combined effect of strain rate (B) and nonlinearity (n) on the response of the formulation during the MSCR test. This type of behavior may be compared with the one of a brittle material, in which stress and strain values below a maximum level (yield point, failure point, etc.) does not lead to failure. By applying this concept to the data of the AC+PE, it seems that the creep time of 2.0 s is associated with the "failure point" of the formulation not only because the compliances hardly exceed 4.0 kPa^{-1} (the maximum value for assigning a traffic level according to AASHTO M320-09) for $t_F \leq 2.0$ s, but also due to the decreases in the role of the initial strain on the greater susceptibilities of the binder to rutting. However, t_F values of 4.0 s and longer seem to be harmful to the modifier and the rut resistance of the AC+PE because J_{nr} increases by at least 400% (see Figure 187), the strain rate gives its contribution to the loss of resistance of the AC+PE in the MSCR test (percentages of variation in A become positive), and the nonlinear response of the material is more visible (rates of increase in n are much greater when $t_F \geq 4.0$ s).

By comparing the results of the model parameters with those of the MSCR parameters (Table 225 and Table 226), one may conclude that the most critical levels of traffic, loading time, and temperature under which the AC+PE can be subjected in a real pavement are given by the temperature of 64°C and the creep time of 2.0 s (stress level of 3,200 Pa). The A value is equal to 2.04 and the B value is almost equivalent to one (0.9933) in such test conditions. The α value is also very close to unity (0.9945), which is in agreement with the recovery value of 0.4% as well (Table 225). From a practical point of view, the AC+PE cannot be used on road pavements subjected to the application of loads for too long periods of time – even at lower climate temperatures – because the fragility of the material may quickly lead to the accumulation of great amounts of unrecovered strain, and therefore failure.

Even though a creep time of 8.0 s seems to be exaggerated in the representation of actual loads applied by trucks on the roadway, it is able to show the limitations of the use of the AC+PE for paving applications and how this can influence on the rutting performance of the binder. In other words, it is quite easy to see the stiffening characteristics of the AC+PE when the loading time is not too long; however, the benefits of a very high level of stiffness to the rutting resistance of the binder are minimized when $t_F > 2.0$ s. In addition, the nonlinear portion of the total strain in the binder increases significantly for t_F values of 4.0 and 8.0 s, together with the strain rate. Again, the AC+PE is not recommended on pavements or traffic lanes with high percentages of slow-moving vehicles because this may lead to strain levels far beyond the ones dictated by the fragility characteristics of the material, as well as to accelerate the process of failure by rutting.

Figure 188 and Figure 189 are graphical representations of the levels of correlation between the *A* and *B* values and the creep times from 1.0 to 8.0 s at 100 and 3,200 Pa, respectively. As a consequence of the decreases in *A* when moving from 1.0 to 2.0 s of loading time in the MSCR tests, the degrees of correlation are lower for the initial strain than for the strain rate at both stress levels. On the other hand, the R^2 values for *A* increase with increasing stress level because the accumulated strain in the binder is greater at 3,200 Pa than at 100 Pa. As a consequence, the formulation gets closer to the "failure point" and the ability of the polymer in resisting to rutting – which is probably one of the reasons why the constant *A* decreased when moving from 1.0 to 2.0 s – is minimized as well.

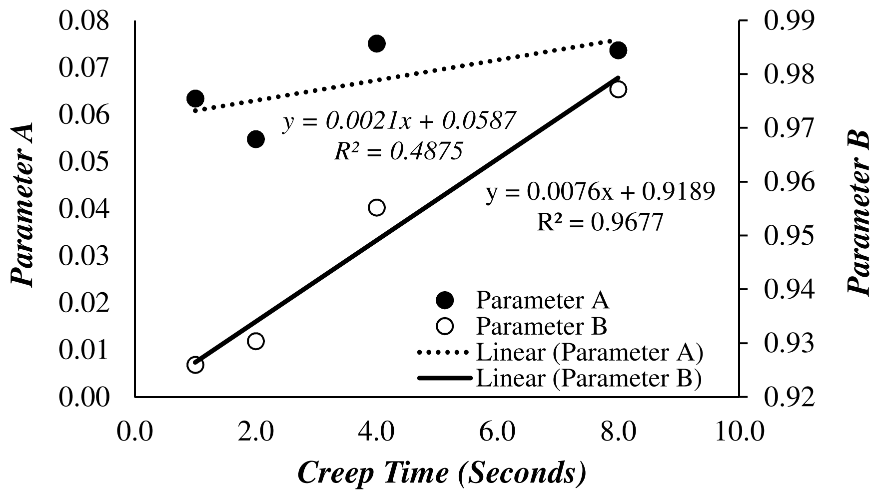

Figure 188 – Correlations between the creep time and the constants *A* and *B* from the model by Saboo and Kumar (2015), temperature of 64°C and stress level of 100 Pa – AC+PE

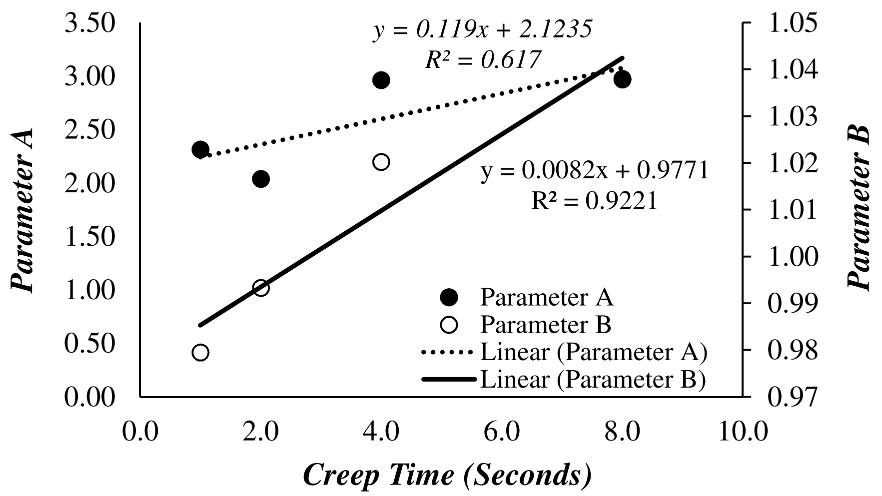

Figure 189 – Correlations between the creep time and the constants *A* and *B* from the model by Saboo and Kumar (2015), temperature of 64°C and stress level of 3,200 Pa – AC+PE

Together with the levels of correlation between the *A* values and the creep time when moving from 100 to 3,200 Pa at 64°C, it is also possible to observe that these levels are not greatly affected by increasing the pavement temperature from 64 to 70°C, see Figure 190 and Figure 191. For instance, R^2 increased by 2.8% at 100 Pa (from 0.4875 to 0.5012) and decreased by 1.9% at 3,200 Pa (from 0.617 to 0.6052). The same can be said for the *B* values, i. e., increase of only 1.6% at 100 Pa (0.9677 to 0.9832) and almost null variation at 3,200 Pa (0.9221- to 0.9217). This suggests that the inherent characteristics of the material were not changed with the increase in the pavement temperature (as well as the fact that either *A* or *B* become greater at longer creep times), and also that the variable that mostly affected its response was the stress level.

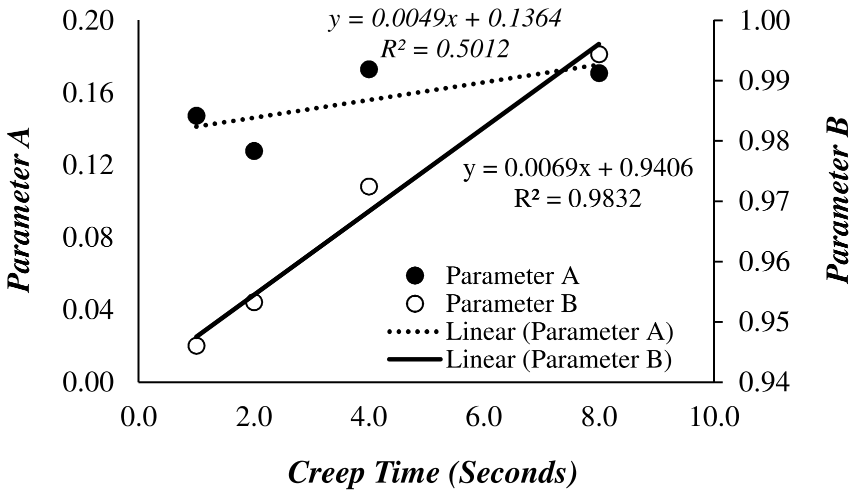

Figure 190 – Correlations between the creep time and the constants *A* and *B* from the model by Saboo and Kumar (2015), temperature of 70°C and stress level of 100 Pa – AC+PE

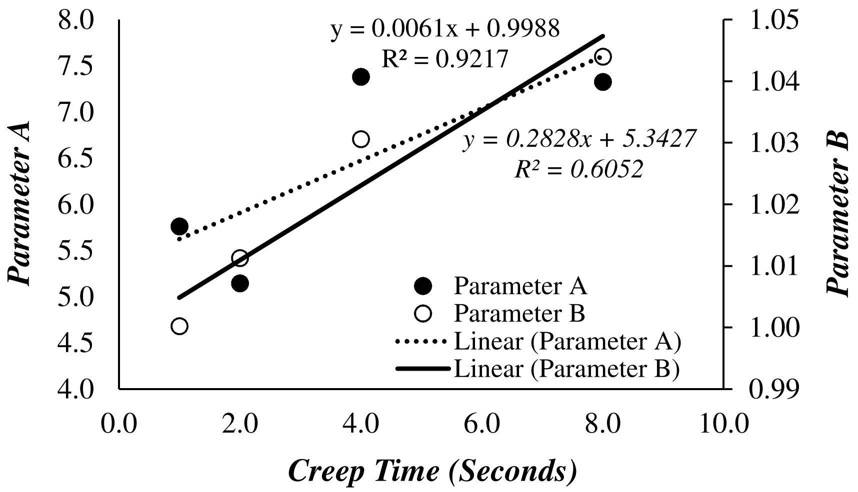

Figure 191 – Correlations between the creep time and the constants *A* and *B* from the model by Saboo and Kumar (2015), temperature of 70°C and stress level of 3,200 Pa – AC+PE

It can be pointed out that nonlinearity plays some role in the decreases in the correlations for the *B* values of the AC+PE when moving from 100 to 3,200 Pa. Other binders with much lower rutting resistances in the mixture scale such as the AC+SBR+PPA (Figure 144 to Figure 147, page 341) show the same pattern of response found in the AC+PE, which emphasizes the need for more loading times in the MSCR tests to investigate the actual creep-recovery behavior of the asphalt binder in more severe loading conditions. In addition, the continuous and progressive increases in the intercepts and slopes of the regression equations for *A* with temperature and stress level (see Table 234) indicate that this parameter is more sensitive to the test condition than the other (*B* values). The absence of reverses in the signals of the slopes of the trendlines suggests that the pattern of response of the formulation is the same throughout the test, whereas the increases in the accumulated strain may have contributed to the slight degrees of improvement for R^2 in the equations of *A* at higher temperatures.

Table 234 – Degrees of correlation between the parameters *A* and *B* (modified power model) and the creep time t_F for the AC+PE

T (°C)	stress (kPa)	linear regression equations and R^2 values (in parenthesis)[a]	
		parameter *A*	parameter *B*
52	0.1	y = 0.0004x + 0.0093 (0.5293)	y = 0.0078x + 0.8688 (0.8970)
	3.2	y = 0.0130x + 0.3122 (0.5352)	y = 0.0119x + 0.8993 (0.9383)
58	0.1	y = 0.0008x + 0.0243 (0.4598)	y = 0.0073x + 0.8498 (0.9587)
	3.2	y = 0.0433x + 0.8132 (0.6020)	y = 0.0108x + 0.9407 (0.9237)
64	0.1	y = 0.0021x + 0.0587 (0.4875)	y = 0.0076x + 0.9189 (0.9677)
	3.2	y = 0.1190x + 2.1235 (0.6170)	y = 0.0082x + 0.9771 (0.9221)
70	0.1	y = 0.0049x + 0.1364 (0.5012)	y = 0.0069x + 0.9406 (0.9832)
	3.2	y = 0.2828x + 5.3427 (0.6052)	y = 0.0061x + 0.9988 (0.9217)
76	0.1	y = 0.0108x + 0.3038 (0.5325)	y = 0.0070x + 0.9556 (0.9792)
	3.2	y = 0.6251x + 12.750 (0.6051)	y = 0.0049x + 1.0097 (0.9462)

[a] the Y-axis is associated with the parameter (*A* or *B*), whereas the X-axis is associated with t_F.

These progressive variations in the *A* values – as well as the presence of quite similar correlations for *A* and *B* at 100 and 3,200 Pa within the whole temperature interval – are indications that the delayed elasticity and the amount of damage accumulated in the modifier did not affect the creep-recovery behavior of the AC+PE when compared with other modified asphalt binders such as the EVA-, the SBS- and the SBR-modified ones. This kind of response resembles those observed for the 50/70 unmodified binder (refer to Table 71, page 204) and the AC+Elvaloy+PPA (Table 99, page 238), i. e., one neat material and the other with a very stable polymeric network system in the formulation. As a matter of comparison, the AC+EVA and the AC+SBR+PPA depict substantial differences among the R^2 values of the parameter *A* (Table 189 and Table 204, refer to page 343 and 366, respectively) and the AC+EVA+PPA shows these great differences for *A* and *B*, regardless of the temperature (Table 219, page 391) and, in all these cases, at least one of the aforementioned findings – delayed elasticity and/or damage in the polymer network – may be found in the formulation.

As may be implied from the data in Table 235, the parameter associated with nonlinearity (n) shows increases with increasing values for t_F (i. e., longer creep times) regardless of the test temperature and stress level, and this may be described by straight regression trendlines because the R^2 values are from good to excellent in all cases. On the other hand, this increase is not associated with temperature because the n values for the intercepts always range between 0.995 and 1.010 and the slopes of the trendlines are very similar within the same stress level. Hence, it is hypothesized that a general correlation between n and J_{nr} does not exist or is very poor, as will be shown later. With respect to the α values, it is believed that the correlations with the percent recovery R are better because the intercepts of the equations continuously increase with temperature and the results approach – or are equal to – unity at 70 and 76°C. Again, linear regression trendlines do a good job in characterizing the variations in α with loading time and temperature, as previously observed for the other formulations.

Table 235 – Degrees of correlation between the parameters n and α (modified power model) and the creep time t_F for the AC+PE

T (°C)	stress (kPa)	linear regression equations and R^2 values (in parenthesis)[a]	
		parameter n	parameter α
52	0.1	y = 0.0023x + 1.0011 (0.9798)	y = 0.0100x + 0.8695 (0.9298)
	3.2	y = 0.0012x + 0.9955 (0.9735)	y = 0.0131x + 0.8951 (0.9512)
58	0.1	y = 0.0016x + 1.0032 (0.8777)	y = 0.0089x + 0.8975 (0.9644)
	3.2	y = 0.0022x + 0.9953 (0.9869)	y = 0.0131x + 0.9361 (0.9475)
64	0.1	y = 0.0015x + 1.0014 (0.9689)	y = 0.0090x + 0.9201 (0.9706)
	3.2	y = 0.0027x + 0.9967 (0.9951)	y = 0.0109x + 0.9736 (0.9538)
70	0.1	y = 0.0015x + 1.0003 (0.9881)	y = 0.0084x + 0.9408 (0.9841)
	3.2	y = 0.0027x + 0.9982 (0.9956)	y = 0.0089x + 0.9968 (0.9577)
76	0.1	y = 0.0016x + 0.9998 (0.9998)	y = 0.0086x + 0.9553 (0.9872)
	3.2	y = 0.0027x + 0.9991 (0.9982)	y = 0.0078x + 1.0086 (0.9745)

[a] the Y-axis is associated with the parameter (n or α), whereas the X-axis is associated with t_F.

After plotting the nonrecoverable compliances against the n values in a semi-log chart, Figure 192(a) is obtained as the final result. As can be seen, the R^2 value is poor (approximately equal to 0.33) and indicates that n barely correlates with J_{nr} in a general context. One of the possible explanations is that one single value for n may be associated with two or more J_{nr} values, which can also be found in other parameters from the literature such as *G*/sinδ* (GOLALIPOUR, 2011). Even though the tendency of increasing *n* with increasing J_{nr} is shown in the regression equation, this cannot be taken as enough to study the relationship between nonlinearity according to *n* and nonlinearity according to J_{nr}. The individual correlations – i. e., the ones between *n* and J_{nr} – showed the same tendencies, and the one at 100 Pa yielded an R^2 value of only 0.063 (chart not shown in this study). However, the individual relationship between *R* and J_{nr} at 3,200 Pa yielded a good correlation, with an R^2 value almost equal to 0.72 – see Figure 192(b). This suggests that the data at 3,200 Pa leads the binder more close to the nonlinear range, which is something quite naturally expected. However, the lack of good correlations for several modified binders leads to the conclusion that nonlinearity cannot be always described by the *n* values, since it will depend upon the input variables in the MSCR test.

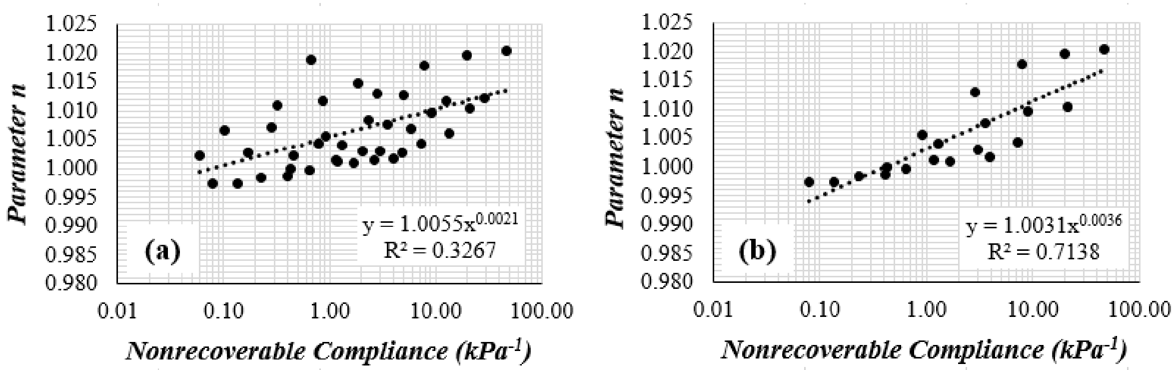

Figure 192 – Degrees of correlation between the nonrecoverable compliances of the AC+PE and the corresponding *n* values from the power law models: (a) all data at 100 and 3,200 Pa; (b) only the data at 3,200 Pa

With respect to the parameter *α*, the consideration of all the data values for *R* and *α* yields the correlation depicted in Figure 193(a). The resulting R^2 value is quite high, approximately equal to 0.83. The *R* and *α* values are inversely related with each other and there are several results for *α* associated with only one *R* value (0%, or absence of recovery). This is one more supporting finding that points to the use of *α* as a complementary indicator of the level of elastic response in the asphalt binder. Since the null recoveries are typically observed at the stress level of 3,200 Pa, it is hypothesized that the correlations are better for 100 Pa than for 3,200 Pa. The resulting correlation for the data at 3,200 Pa is approximately equal to 0.754 (chart not shown here), whereas the one for the data at 100 Pa is almost equal to 0.967, see Figure 193(b). In any case, the results of the AC+PE follow the same tendency observed for the previously reported formulations and the good correlations for *α* are in agreement with the literature as well (SABOO and KUMAR, 2015).

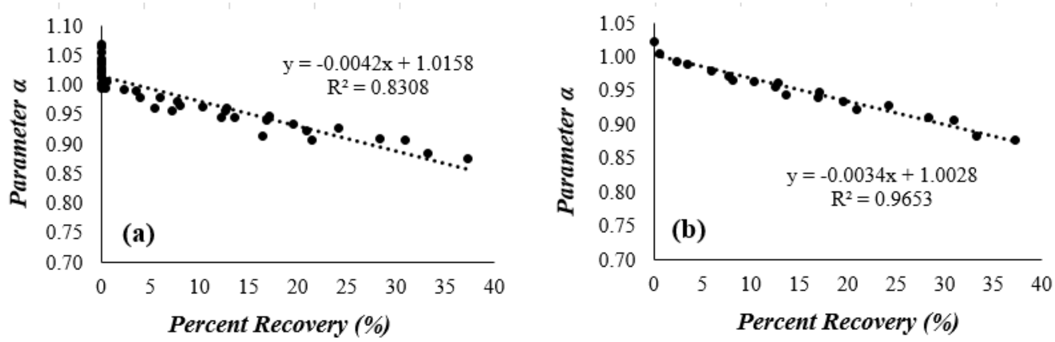

Figure 193 – Degrees of correlation between the percent recoveries of the AC+PE and the corresponding α values from the power law models: (a) all data at 100 and 3,200 Pa; (b) only the data at 100 Pa

In summary, the rheological modeling of the creep-recovery data of the AC+PE points to the existence of a critical creep time (in this case, t_F = 2.0 s) at which the material suffers a considerable loss of rutting resistance, and this can be observed at all pavement temperatures. The fragility characteristics of the formulation – or its very high degree of stiffness due to the plastomeric modification type – are proposed as reasonable explanations for such findings. When the material is subjected to very long loading times in the MSCR tests (4.0 and 8.0 s), the level of accumulated strain is equally high and the substantial increases in J_{nr} can be attributed to increases in the initial strain and the strain rate (parameters A and B). The degree of nonlinearity in the response of the binder also increases faster with loading time when the creep portion of the cycles lasts 4.0 s or more. In addition, the AC+PE typically does not show any recovery during MSCR when the temperature is of 64°C or more and the creep time is longer than 1.0 s. As a consequence, the AC+PE is not recommended on pavements subjected to very high climate temperatures (at least equal to 64°C) and several slow-moving vehicles in the traffic lanes.

The degrees of linear correlation between the parameters A and B and the corresponding creep times tend to be higher as the temperature increases, since the stiffening effects of the formulation at 2.0 s of loading time are minimized by the accumulation of higher levels of permanent strain. The increases in A and B with creep time follow the tendencies observed for other modified asphalt binders, and the presence of progressive increases in A with temperature and stress level suggest that the delayed elasticity does not play an important role in the response of the formulation, which was the case of the AC+EVA and the AC+EVA+PPA (as some examples). The level of nonlinearity in the AC+PE – as measured by the parameter n – does not have a good correlation with J_{nr} when all the data values are considered, but the same cannot be said for the individual results at 3,200 Pa. It can be said that n has some relationship with the increasing nonlinearity in the binder according to the J_{nr} values, but this cannot be taken as a universal rule because the same was not observed for other formulations. With respect to the parameter α, the results show similarities with those collected by Saboo and Kumar (2015) and the previously reported asphalt binders: decreasing α with increasing R and good correlations between them.

The ANOVA analysis was conducted on the R and J_{nr} values in order to conclude whether the creep time or the temperature has more influence in the MSCR parameters of the binder, as well as to observe if their effects can be considered as statistically significant or not. The organized values of the percent recovery may be seen in Table 236, whereas the organized ones of the nonrecoverable creep compliance are provided in Table 237. It is clear that the recoveries at 3,200 Pa were not studied because there are two null values at 70 and 76°C (see Table 225, page 397), which results in an insufficient number of data points for analysis. A level of significance of 5% was used in both cases, in accordance with the previously studied binders.

Table 236 – Rearranged MSCR testing data of the AC+PE to be used in the analysis of variance (ANOVA) – percent recovery

stress level of 0.1 kPa (*R100*, *%*)[a]		stress level of 3.2 kPa (*R3200*, *%*)[a]	
increasing creep time	increasing temperature	increasing creep time	increasing temperature
37.3	37.3	These calculations were not made due to the lack of enough data points at higher temperatures.	These calculations were not made due to the lack of enough data points at higher temperatures.
33.3	31.0		
20.9	24.2		
13.6	17.1		
N/A[b]	12.8		

[a] the starting point in both cases was the temperature of 52°C.
[b] N/A: Not applicable.

Table 237 – Rearranged MSCR testing data of the AC+PE to be used in the analysis of variance (ANOVA) – nonrecoverable creep compliance

stress level of 0.1 kPa ($J_{nr}100$, kPa^{-1})[a]		stress level of 3.2 kPa ($J_{nr}3200$, kPa^{-1})[a]	
increasing creep time	increasing temperature	increasing creep time	increasing temperature
0.060	0.060	0.078	0.078
0.102	0.170	0.135	0.229
0.323	0.451	0.421	0.648
0.664	1.143	0.920	1.677
N/A[b]	2.636	N/A[b]	3.952

[a] the starting point in both cases was the temperature of 52°C.
[b] N/A: Not applicable.

Table 238 reports the final results of ANOVA for the percent recoveries of the AC+PE at 100 Pa. The *F-value* is of about 0.066 and the *p-value* is approximately equal to 0.805, which leads to the recommendation of not rejecting H_0 under α = 5%. In other words, the variances within the *R100* values with increasing creep time and temperature – and both departuring from the same reference point, i. e., 52°C and 1/9 s – are not great enough to say that the their effects on the recovery values of the AC+PE are statistically different. On the other hand, the recoveries decrease at faster rates when the creep times are longer, especially at 4/9 and 8/9 s (last two values in Table 236). As a consequence, t_F has a more damaging effect on the elastic response of the AC+PE under creep and recovery loading in the DSR.

Table 238 – Results from the analysis of variance (ANOVA, *p-value* and *F-value*) as based on the percent recoveries of the AC+PE

null hypothesis H_0	statistical parameters (ANOVA)				recommendation
	$F_{critical}$	*F-value*	α	*p-value*	
equivalency between *R* values with increasing creep time and temperature, 0.1 kPa	5.5914	0.066	0.05	0.8045	H_0 is not rejected
equivalency between *R* values with increasing creep time and temperature, 3.2 kPa	Not calculated due to the lack of enough data points.				

Table 239 is a summary of the final results of ANOVA for the nonrecoverable creep compliances of the AC+PE at 100 and 3,200 Pa. Similarly to the percent recoveries, the recommendation is not to reject H_0 at both stress levels because the control parameters *F-value* and *p-value* do not exceed the critical values assigned to $F_{critical}$ and α, respectively. The *F-values* are all lower than 1.26 ($F_{critical} \approx 5.592$) and the *p-values* are approximately equal to 0.30 (α = 0.05). The variances within the J_{nr} values are slightly higher at 3,200 Pa than at 100 Pa or, in numerical terms, the *F-value* increases by 4.57% and the *p-value* decreases by 3.23% when moving from the lowest to the highest stress level. Differently from the recovery values, the temperature is the most influential variable in the increases in J_{nr} for the AC+PE either at 100 or at 3,200 Pa. This means that the compliances increase faster with increasing pavement temperature, and not due to longer loading times.

Table 239 – Results from the analysis of variance (ANOVA, *p-value* and *F-value*) as based on the nonrecoverable compliances of the AC+PE

null hypothesis H_0	statistical parameters (ANOVA)				recommendation
	$F_{critical}$	*F-value*	α	*p-value*	
equivalency between J_{nr} values with increasing creep time and temperature, 0.1 kPa	5.5914	1.1998	0.05	0.3096	H_0 is not rejected
equivalency between J_{nr} values with increasing creep time and temperature, 3.2 kPa	5.5914	1.2547	0.05	0.2996	H_0 is not rejected

Table 240 provides the percent recoveries at 100 and 3,200 Pa for the AC+PE+PPA. The addition of PPA somehow contributed to the presence of higher *R100* and *R3200* values in this formulation when compared with the original AC+PE (Table 225, page 397), especially at 3,200 Pa. Such increase in recovery may be explained by the improved compatibility of the asphalt binder modified with PE after the addition of PPA (GAMA et al., 2016), and this can be seen for other plastomers as well such as polypropylene (GIAVARINI et al., 1996). Due to the non-reactive nature of the low-density PE, it is hypothesized that the better results of the AC+PE+PPA and its higher compatibility with the base binder were mainly caused by the changes in the gel characteristics of the original material (PAMPLONA, 2013). While the increases in *R100* are mainly restricted to 52 and 58°C, the ones in *R3200* include all the non-null values of the original AC+PE (temperatures up to 64°C). In other words, the AC+PE+PPA is able to recover a higher portion of the total strain when loaded in the pavement and further contribute to enhancement in the resistance of the asphalt mixture to rutting. This topic will be discussed in detail later.

Table 240 – Percent recoveries at 100 Pa (*R100*) and 3,200 Pa (*R3200*) for the AC+PE+PPA with increasing loading time and temperature

parameter	creep time (s)	results at each temperature and increases (both in %)[a]				
		52°C	58°C	64°C	70°C	76°C
R100	1.0	43.3	32.7	21.5	12.6	6.6
	2.0	35.2	23.1	13.6	6.5	2.0
	4.0	27.6	17.1	8.9	3.5	0.1
	8.0	19.0	14.1	9.4	6.0	3.1
R3200	1.0	35.4	20.8	7.3	0.0	0.0
	2.0	24.5	10.4	0.7	0.0	0.0
	4.0	15.1	3.7	0.0	0.0	0.0
	8.0	5.8	0.0	0.0	0.0	0.0

[a] the percentages refer to the decreases in *R* at longer creep times when compared with the data at 1.0 second.

With respect to the numerical values of *R* at 100 and 3,200 Pa (non-null values), they vary from 2.0 to more than 43% at 100 Pa and from about 3.7 to more than 35% at 3,200 Pa. Surprisingly, some *R100* results at 64, 70 and 76°C depict slight increases after increasing the loading time from 4.0 to 8.0 s, which was not observed for the AC+PE. It is known from the literature that, when LDPE's without chemical modification of the polymer chains – i. e., non-grafted PE's – are used for binder modification, the modifier is dispersed into the binder phase as spherical particles with no linkages between them. The size of these spheres will essentially depend on the molecular weight of the modifier (POLACCO et al., 2015; VARGAS et al., 2013).

As a consequence, it is believed that *R100* increased with increasing creep time due to a rearrangement of the polymer spheres during the application of the loading cycles, and the dispersed asphaltenes within the binder phase caused by the presence of PPA might have restricted the movements of such particles. Since the modifier particles are not cross-linked in a network, very high stress levels and long creep times will probably keep them apart from each other (*R3200* values do not increase with increasing t_F values).

The results of *R100* for the AC+PE+PPA at each creep-recovery cycle, the temperatures of 70 and 76°C, and the creep-recovery times of 4/9 s and 8/9 s are given in Figure 194. It can be seen that the delayed elasticity does not play a significant role in the recoveries of the formulation when compared with other asphalt binders such as the AC+EVA and the AC+EVA+PPA, since these recoveries tend to stabilize after only a few cycles (no more than eight). The irregularities in the results in the last 5-7 cycles may be attributed to small levels of damage in the polymer particles, especially at 8/9 s. By taking these results and comments into account, it is possible that the presence of higher *R100* values at 8/9 s than at 4/9 s be associated with a rearrangement of the modifier particles during the test, and not with the delayed elasticity as observed for the EVA-modified asphalt binders.

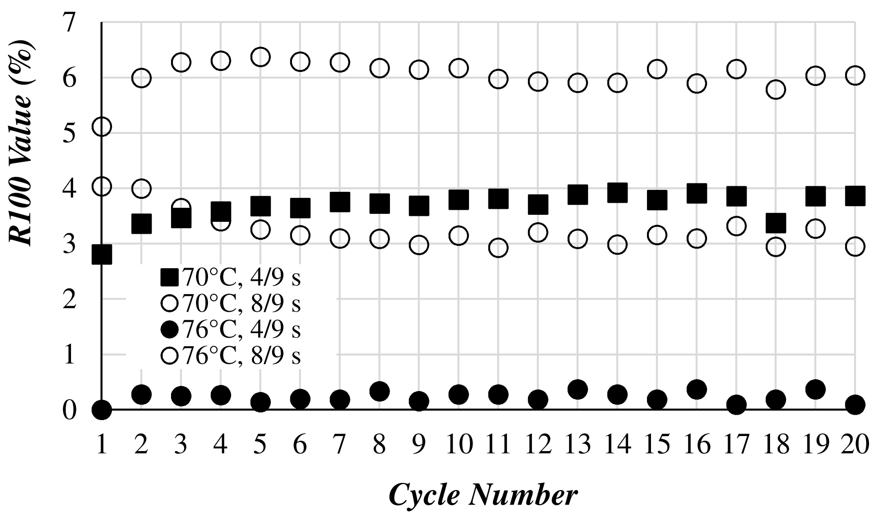

Figure 194 – Plots of the percent recoveries at 100 Pa (*R100*) at each cycle for the AC+PE+PPA, temperatures of 70 and 76°C and creep-recovery times of 4/9 s and 8/9 s (original samples)

The nonrecoverable compliances of the AC+PE+PPA at all MSCR temperatures and loading times are shown in Table 241. By comparing these data with the ones for the AC+PE (Table 226, page 399), it is possible to say that the compliances are typically lower for the formulation with PE+PPA than for the one with PE only. As known, lower J_{nr} values may be interpreted as lower susceptibility to rutting in the field pavement, especially when the stress level is high and the vehicle applies the load for a very long time (longer creep times). While the compliances of the AC+PE may exceed 12.0 kPa^{-1} and 19.0 kPa^{-1} at 100 and 3,200 Pa (respectively), the ones of the AC+PE+PPA are typically lower than 11.0 kPa^{-1} and 15.0 kPa^{-1} at these same stress levels. However, the values higher than 4.0 kPa^{-1} and commonly found at 70 and 76°C suggest that this binder cannot be used on field pavements with high PG grades and several vehicles traveling at slow speeds, despite the fact that the PG grade of the material is 76-xx.

Table 241 – Nonrecoverable compliances at 100 Pa ($J_{nr}100$) and 3,200 Pa (J_{nr} *3200*) for the AC+PE+PPA with increasing loading time and temperature

parameter	creep time (s)	results at each temperature (kPa^{-1}), J_{nr} > 4.0 kPa^{-1} is in bold				
		52°C	58°C	64°C	70°C	76°C
$J_{nr}100$	1.0	0.051	0.156	0.453	1.202	2.914
	2.0	0.101	0.324	0.937	2.491	**6.047**
	4.0	0.181	0.574	1.688	**4.462**	**10.879**
	8.0	0.445	1.246	3.313	**7.798**	**18.094**
$J_{nr}3200$	1.0	0.059	0.188	0.572	1.556	3.717
	2.0	0.123	0.401	1.217	3.188	**7.751**
	4.0	0.228	0.753	2.229	**5.908**	**14.582**
	8.0	0.602	1.994	**5.631**	**14.845**	**37.783**

[a] the percentages refer to the increases in J_{nr} and the creep time when compared with the data at 1.0 second.

The most appropriate temperatures for the use of the AC+PE+PPA on pavements can also be implied from the J_{nr} values of AC+PE, as well as the fact that the creep time of 2.0 s seems to be the limiting condition for the use of the AC+PE+PPA under creep and recovery loading. This is because the compliances of the material increase very fast for creep times longer than 2.0 s (percentages no lower than 250%), and the results from 1.0 to 2.0 s hardly exceed 108% according to the values plotted in Figure 195. In addition, the differences between the percentages at 100 and 3,200 Pa are greater for the t_F value of 8.0 s, which could not be clearly seen for the AC+PE (see Figure 187, page 399). This is an evidence of the increased stress sensitivity after modification with PE+PPA rather than PE alone, as will be evaluated later in this section. With respect to the percentages of decrease in recovery shown in Figure 196, they are typically greater for the AC+PE+PPA than for the AC+PE (Figure 186, page 397) at the creep times of 1.0 and 2.0 s regardless of the selected test temperature, and the opposite is seen at 4.0 and 8.0 s.

Since the trends observed for the variations in the percent recoveries of the two PE-modified asphalt binders remain the same for their nonrecoverable compliances, it can be said that the parameters of the AC+PE+PPA are more sensitive to shorter creep times and the ones of the

AC+PE are more sensitive to longer creep times. In other words, small variations in the t_F values will probably cause greater impact on the MSCR parameters of the AC+PE+PPA than those of the AC+PE, provided that they do not exceed 4.0 s of duration. This is in accordance with the charts of J_{nr} against t_F plotted in Figure 197 for the two formulations with PE, according to which the compliances of the AC+PE+PPA increase at much higher percentages and become greater than those of the AC+PE when t_F is equal to 4.0 and 8.0 s. Small deviations from the original straight lines can also be seen for the AC+PE+PPA at such creep times and the stress level of 3,200 Pa, but they are not enough to overcome the values found in the AC+PE. Hence, it can be inferred that the smaller amount of polymer used in the AC+PE+PPA contributed to a reduction in its level of nonlinearity at very long loading times.

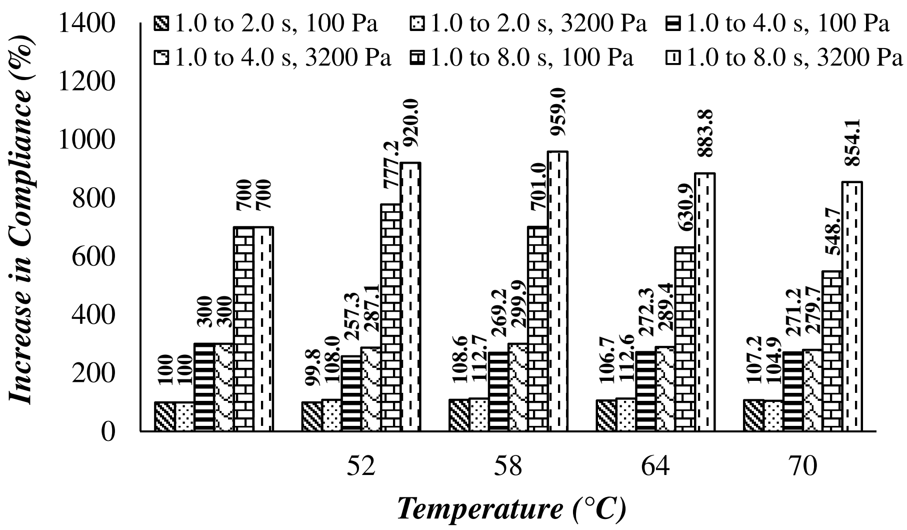

Figure 195 – Percentages of increase in the nonrecoverable compliances of the AC+PE+PPA with creep time, temperature and stress level

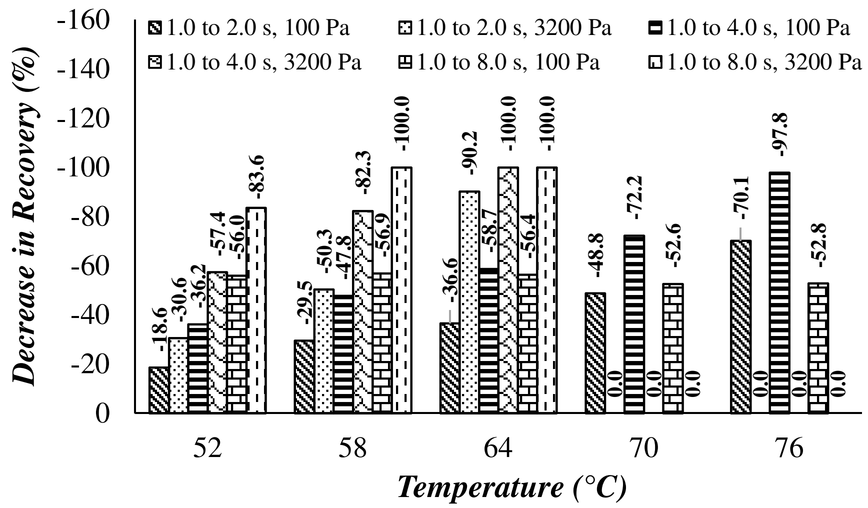

Figure 196 – Percentages of decrease in the recovery values of the AC+PE+PPA with creep time, temperature and stress level

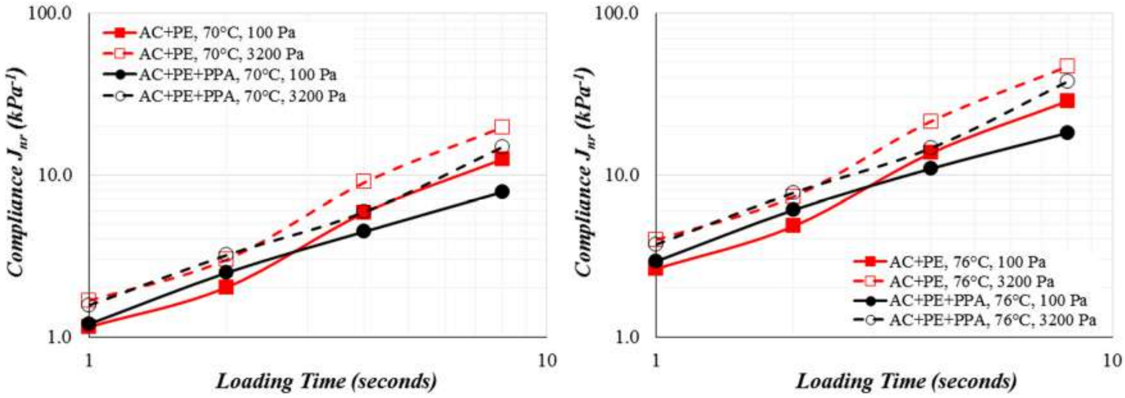

Figure 197 – Plots of the nonrecoverable compliance J_{nr} versus loading time (log-log scale) for the AC+PE and the AC+PE+PPA at the temperatures of (a) 70°C; and (b) 76°C

As a general conclusion, the charts in Figure 197 suggest that the AC+PE+PPA tends to accumulate lower levels of permanent strain at very long creep times (especially 4.0 and 8.0 s) than the AC+PE. These differences can also be seen when the stress level – rather than the loading time – is increased in the MSCR tests, and then a particular binder that is less prone to rutting in a predefined test condition becomes the most susceptible one in more critical conditions (D'ANGELO, 2009; D'ANGELO et al., 2007; LAUKKANEN et al., 2015). It again indicates that a complete study of the repeated creep behavior of modified asphalt binders at longer loading times is necessary, since this will give a complete picture of the responses of the asphalt binders for different loading patterns (the results are approximately the same for the two binders at t_F = 1.0 and 2.0 s).

As previously discussed, asphalt binder modification with PE+PPA leads to increases in the sensitivity of the MSCR parameters to creep time when these t_F values are relatively short. In a general context, the AC+PE+PPA shows a lower rutting potential and a higher elastic response in the binder scale when compared with the AC+PE, as can be implied from the positions of the data points in Figure 198 (percent recoveries) and Figure 199 (nonrecoverable compliances). The majority of these data points are placed above the equality line for R and below for J_{nr} or, more specifically, 70% out of the 27 non-null values for the recoveries and 75% out of the 40 numerical values for the compliances. Although J_{nr} seems not to considerably differ from one binder to the other when the values are lower than 0.3 kPa^{-1} (i. e., the degree of stiffness is very high for both of them) according to Figure 199(b), the results are still better for the AC+PE+PPA than for the AC+PE. The points above the equality lines in the two figures specifically refer to the test conditions in which the AC+PE shows more promising findings than the AC+PE+PPA, that is, very long creep times (8/9 s).

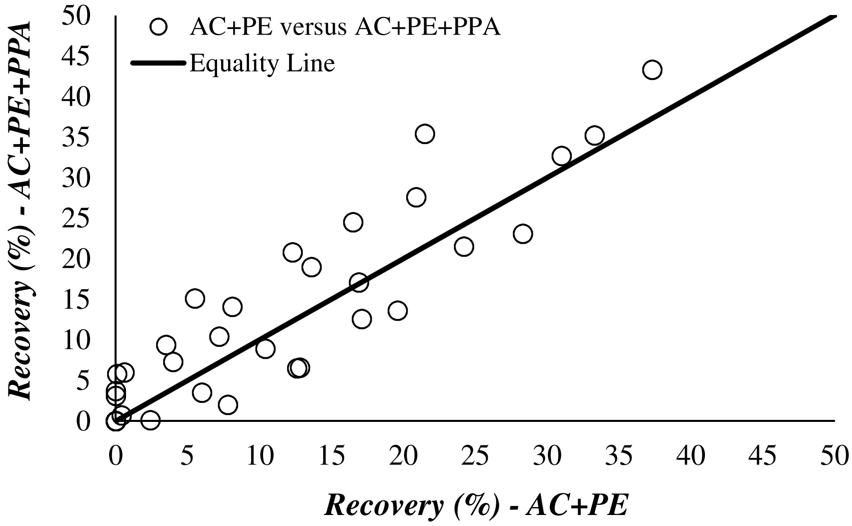

Figure 198 – Comparison between the percent recoveries of the AC+PE and the AC+PE+PPA under all MSCR testing conditions

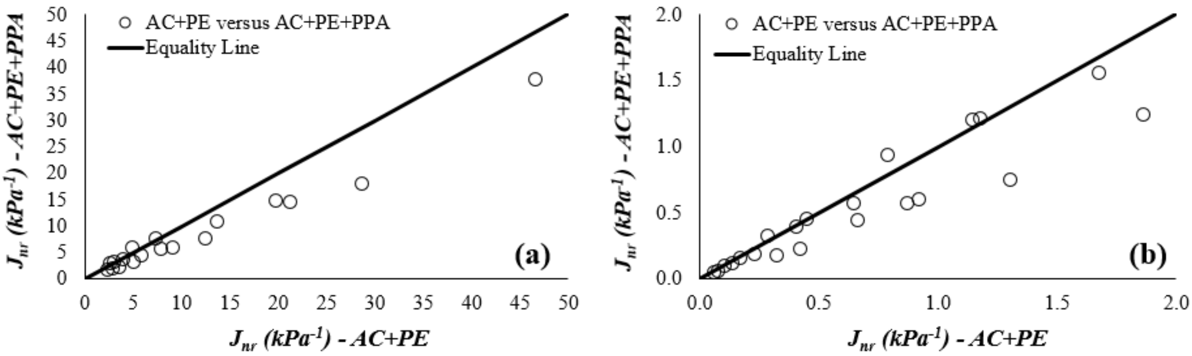

Figure 199 – Comparison between the nonrecoverable compliances (J_{nr}) of the AC+EVA and the AC+EVA+PPA (a) only for the results higher than 2.0 kPa^{-1}; and (b) only for the ones lower than 2.0 kPa^{-1}

The percent differences in compliances for the AC+PE+PPA – parameter $J_{nr,\ diff}$ – are shown in Table 242. This formulation is less stress sensitive than the AC+PE for creep times up to 4.0 s (see Table 227, page 400), and then it becomes the most sensitive material when t_F = 8.0 s. The chart provided in Figure 200 precisely shows these comparisons in a clearer way, since the four data points above the equality line are the ones collected at 8/9 s and temperatures higher than 52°C. In other words, the nonlinear response of the AC+PE+PPA at higher stress levels is more pronounced only at very long loading times, which is when the maximum value of 75% is exceeded. This can be translated into a deviation in the $J_{nr}3200$ curve of the AC+PE+PPA when t_F goes from 4.0 to 8.0 s (refer to Figure 197). With exception of such odd cases, the $J_{nr,\ diff}$ values are all between 16 and 70% – and thus below the maximum value of 75% according to Superpave®. Based on these findings, one may infer that the AC+PE+PPA is better not only because the elastic response and the level of stiffness are higher than those of the AC+PE (*R* and J_{nr}), but also due to the lower stress sensitivity in the test conditions typically considered in the standardized protocols.

Table 242 – Percent differences in nonrecoverable compliances ($J_{nr,\ diff}$) for the AC+PE+PPA with increasing creep time and temperature

creep time (s)	$J_{nr,\ diff}$ values (%) at each creep time and temperature[a]				
	52°C	58°C	64°C	70°C	76°C
1.0	16.2	21.1	26.3	29.4	27.6
2.0	21.0	23.5	29.9	28.0	28.2
4.0	25.9	31.1	32.1	32.4	34.0
8.0	35.1	60.1	70.0	**90.4**	**108.8**

[a] the numbers in bold are the ones that exceeded the maximum $J_{nr,\ diff}$ (75%) according to Superpave®.

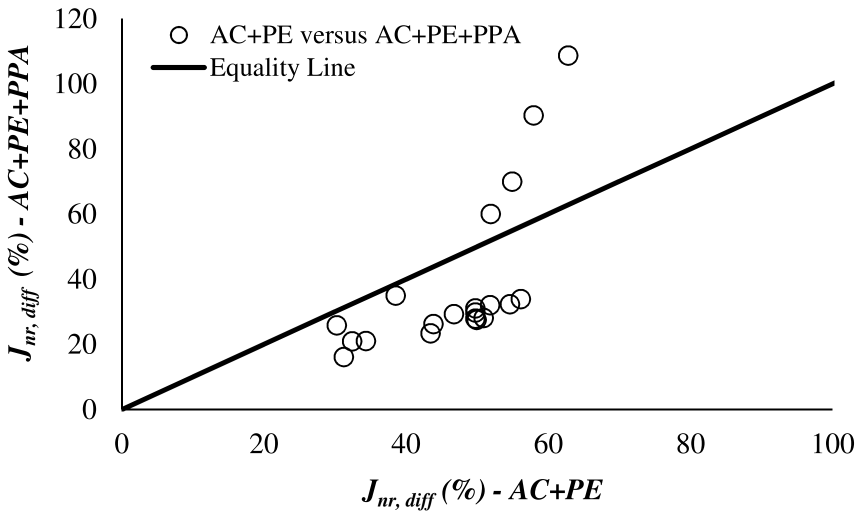

Figure 200 – Comparison between the percent differences in nonrecoverable compliances ($J_{nr,\ diff}$) of the AC+PE and the AC+PE+PPA in all of the MSCR testing conditions

As a consequence of the reductions in J_{nr} after the addition of PPA and the reduction in the PE content, one may imply that the traffic levels assigned to the AC+PE+PPA are higher than the corresponding levels of the AC+PE. The data summarized in Table 243 and its comparison with Table 228 (page 400) reveal that this conclusion is partially true, since the traffic level increased by one grade at the temperature of 58°C and two loading times – t_F = 4.0 s (from heavy to very heavy) and t_F = 8.0 s (from standard to heavy). No further modifications were observed at the other temperatures and stress levels, which means that the AC+PE+PPA is not recommended on pavements with high PG grades of 70 and 76°C and loading conditions more severe than the ones standardized by the current MSCR test protocol (1/9 s). The same can be said for the temperature of 64°C and the longest loading time used in the study (8.0 s).

Therefore, it may be concluded that the reductions in J_{nr} from the AC+PE to the AC+PE+PPA (higher levels of stiffness) were not enough to allow a general use of the AC+PE+PPA on pavements with heavier traffic levels than those assigned to the AC+PE.

Table 243 – Adequate traffic levels for the AC+PE+PPA with increasing creep time and temperature based on the standardized Superpave® criteria

creep time (s)	traffic levels for each temperature[a]				
	52°C	58°C	64°C	70°C	76°C
1.0	E	E	V	H	S
2.0	E	E	H	S	-
4.0	E	V	S	-	-
8.0	V	H	-	-	-

[a] S = standard; H = heavy; V = very heavy; E = extremely heavy.

The trendlines and corresponding R^2 values shown in Table 244 refer to the equations from Huang (2004) – tire contact radii of 3.68 and 6.00 in – and Pereira et al. (1998, 2000) and the corresponding correlations between the traffic speeds and the $J_{nr}3200$ values of the AC+PE+PPA. Overall the data indicate that the regressions yield good correlations for all pavement temperatures ($R^2 \approx 0.88$-0.89), and the variations from one temperature to the other are very small. Similarly to the previously studied binders, these results may suggest that the equations from Huang (2004) and Pereira et al. (1998) could provide good estimations of the actual traffic level experienced by the asphalt binder in the real pavement. However, the comparisons made in Table 245 reveal that this is not the case for the AC+PE+PPA at all pavement temperatures, and the reasonable to accurate fits of the data are restricted to only a few temperatures (52 and 58°C). Again, the use of one or another equation in the study of the adequate traffic levels of the binder is limited to test temperatures up to 64°C.

By replacing the equation from Pereira et al. (1998) by the one from Pereira et al. (2000) and reducing the tire contact radius in the equation from Huang (2004), the resulting expressions and R^2 values in Table 246 can be obtained. One more time, these individual comparisons point to the existence of a correlation that is typically restricted to the mathematical approach. In other words, the R^2 values do not mean that the adequate traffic levels of the binder can be well explained by the mathematical representation of such decrease; rather, they only indicate that the decreases in J_{nr} with loading time may be approximately described by an exponential fit. Since this is a tendency identified for all the formulations studied in the present dissertation (not only the AC+PE+PPA), there seems to exist some external factors that were not considered in the correlations and that are playing a major role in the determination of the traffic speed and their association with binder data. They will be discussed in detail later in the present study.

Table 244 – Regression equations and coefficients of determination between the $J_{nr}3200$ values of the AC+PE+PPA and the corresponding vehicle speeds according to the equations by Pereira et al. (1998, 2000) and Huang (2004)

source and data	temperature (in °C)	equation	R^2
Pereira et al. (1998)	52	$y = 0.5431e^{-0.030x}$	0.8802
Pereira et al. (2000)	52	$y = -0.0059x + 0.4382$	0.9977
Huang (2004) $r = 6$ in	52	$y = 0.5435e^{-0.036x}$	0.8808
	58	$y = 1.8120e^{-0.037x}$	0.8847
	64	$y = 5.1995e^{-0.036x}$	0.8921
	70	$y = 13.5960e^{-0.035x}$	0.8860
	76	$y = 34.4180e^{-0.036x}$	0.8846
Huang (2004) $r = 3.68$ in	52	$y = 0.5424e^{-0.059x}$	0.8810
	58	$y = 1.8084e^{-0.060x}$	0.8849
	64	$y = 5.1893e^{-0.058x}$	0.8923
	70	$y = 13.5700e^{-0.058x}$	0.8862
	76	$y = 34.3510e^{-0.059x}$	0.8848

Table 245 – Comparisons between the actual traffic levels of the AC+PE+PPA and the ones obtained from Huang (2004) and Pereira et al. (1998)

t_F (s)[d]	actual[a] and estimated[b, c] traffic levels at each temperature[d]				
	52°C	58°C	64°C	70°C	76°C
1.0	**E (V/E) [V/E]**	**E [V/E]**	**V [V/E]**	H [V/E]	S [V/E]
2.0	**E (V/E) [V/E]**	**E [V/E]**	H [V/E]	S [V/E]	-
4.0	E **(H) [H]**	V [H]	S [H]	-	-
8.0	V (S) [H]	**H [H]**	-	-	-

[a] S = standard; H = heavy; V = very heavy; E = extremely heavy (AASHTO M320-09 standard, Table 3).
[b] (parentheses) = traffic levels from Pereira et al. (1998).
[c] [brackets] = traffic levels from Huang (2004), $r = 6$ in.
[d] similarities among the rankings are highlighted in bold, t_F = creep time.

Table 246 – Comparisons between the actual traffic levels of the AC+PE+PPA and the ones obtained from the equations by Huang (2004) and Pereira et al. (2000)

t_F (s)[d]	actual[a] and estimated[b, c] traffic levels at each temperature[d]				
	52°C	58°C	64°C	70°C	76°C
1.0	**E** (H) **[V/E]**	**E [V/E]**	**V [V/E]**	H [V/E]	S [V/E]
2.0	**E** (H) **[V/E]**	**E [V/E]**	H [V/E]	S [V/E]	-
4.0	E **(H) [H]**	V [H]	S [H]	-	-
8.0	V **(H) [H]**	**H [H]**	-	-	-

[a] S = standard; H = heavy; V = very heavy; E = extremely heavy (AASHTO M320-09 standard, Table 3).
[b] (parentheses) = traffic levels from Pereira et al. (2000).
[c] [brackets] = traffic levels from Huang (2004), $r = 3.68$ in.
[d] similarities among the rankings are highlighted in bold, t_F = creep time.

The points of similarity between the actual and the predicted traffic levels – as based on the equations by Huang (2004) and Pereira et al. (2000) in Table 246 – are quite scarce and scattered within the MSCR test matrix. It is interesting to note that these points of similarity are more concentrated at the temperatures of 52 and 58°C when the equations from Huang (2004) – higher tire contact radius – and Pereira et al. (1998) are used in the analysis, see Table 245. However, this does not necessarily mean that one type of equation is better or worse than the other, since none of them can provide a reasonable picture of the decrease in the traffic speed assigned to the binder and its association with the actual values found in the Superpave® specification.

The estimates of the traffic levels according to the current and proposed methodologies are given in Table 247. It can be seen that the AC+PE+PPA does not show reductions in any appropriate traffic level, which was not the case of the AC+PE at 64°C (Table 232, page 403). This is one more confirmation of the reduction in the degree of nonlinear response of the formulation with PE+PPA and, depending on the paving application and the average vehicle speed, it may help in preventing the formation of premature rut depths in the surface layer, especially on pavements with very high percentages of buses and trucks traveling at very low speeds. In other words, the new criterion distinguishes among the ability of one formulation in showing a higher resistance to rutting and lower levels of nonlinearity (AC+PE+PPA) and the inability of the other in keeping the degree of nonlinearity below a maximum allowed level (AC+PE), even though the rut resistances according to the current criteria and laboratory tests are equally high for both of them.

Table 247 – Traffic levels of the AC+PE+PPA with increasing loading time and temperature in the current and proposed criteria

temperature (in °C)	No. of required MSCR tests[b]	Superpave® designations (current and new criteria)[a, c]	
		current criterion	new criterion
52	4	**52E-xx**	**52E-xx**
58	4	**58E-xx**	**58E-xx**
64	4	**64V-xx**	**64V-xx**
70	3	**70H-xx**	**70H-xx**
76	2	**76S-xx**	**76S-xx**

[a] S = standard; H = heavy; V = very heavy; E = extremely heavy (AASHTO M320-09 standard, Table 3).
[b] minimum number of MSCR tests to determine the adequate traffic level in the proposed classification.
[c] similarities among the classifications are highlighted in bold.

The MSCR testing data of the AC+PE+PPA show that, differently from the AC+PE, the formulation is stiffer and more elastic, especially at higher stress levels and longer loading times. The addition of PPA and the reduction in the PE content also decrease the stress sensitivity of the material, with exception of the longest creep time (t_F = 8.0 s). The "failure point" for the AC+PE+PPA could be set at the temperature of 70°C and the creep time of 2.0 s (similarly to the AC+PE), and there is a great risk of premature failure of pavements prepared with such formulation if the field conditions are more critical than those established by this point. Differently from the AC+PE, the AC+PE+PPA does not show any decrease in the adequate traffic level when the new criterion was applied to the collected data. This finding may be attributed to the aforementioned reductions in the stress sensitivity of the AC+PE+PPA, even though this is not a universal rule and the opposite may be seen in the MSCR tests for different crude sources and pairs of loading-unloading times (DOMINGOS and FAXINA, 2015b).

Table 248 shows all the model parameters A, B, n and α for the AC+PE+PPA and the testing conditions used in this study. There seems to exist a limiting value for the creep time t_F (more specifically, 4.0 s) after which the patterns of response for A, B and n change significantly. This can be observed at all test temperatures and may be associated with the increase in the level of nonlinearity of the binder, as discussed above. The AC+PE+PPA tends to show a rutting behavior more typically observed in formulations with a relatively high rutting resistance when t_F < 4.0 s: the initial strain (A values) decreases, the strain rate (B values) increases and nonlinearity (n values) shows marginal variations with increasing loading time. This is the case of the AC+EVA+PPA (Table 218, page 385), the AC+SBS+PPA (Table 158, page 302) and the AC+rubber (Table 112, page 250), among others. It can be taken as a great advance in the rutting performance of the AC+PE+PPA when compared with the AC+PE, for which either A or B increase when t_F becomes higher (Table 233, page 404). More simply, the AC+PE+PPA is more rut resistant because the initial accumulated strain increases at lower rates and the strain rates are reduced.

By doubling the creep time from 4/9 s to 8/9 s in the MSCR tests, the creep-recovery behavior of the AC+PE+PPA changes radically. As shown above in Figure 197 (page 418), Figure 199 (page 419) and Table 242 (page 420), the stress sensitivity of the formulation becomes much greater at t_F = 8.0 s and its resulting nonrecoverable compliances are higher than those of the AC+PE. As a consequence, there is a kind of loss of resistance to rutting in the AC+PE+PPA when the MSCR tests are carried out at 8/9 s and either A or B increases with loading time. This means that the asphalt binder not only depicts higher strain rates in the creep-recovery curves, but also higher initial strains in the first cycles. In addition, nonlinearity plays a more important role in these curves of the AC+PE+PPA at 8/9 s because the percentages increase very fast when compared with the data at 4/9 s. It is believed that creep times longer than 4.0 s do great amounts of damage in the polymer particles of the AC+PE+PPA, and this is reflected into a higher susceptibility to failure by rutting from the point of view of the binder data.

Table 248 – Numerical values and variations in the parameters/constants *A, B, n* and *α* from the power law equations by Saboo and Kumar (2015) with increasing temperature and creep time and considering the AC+PE+PPA

temperature	test times	parameter A^a		parameter B^a		parameter n^a		parameter α^a	
		0.1 kPa	3.2 kPa	0.1 kPa	3.2 kPa	0.1 kPa	3.2 kPa	0.1 kPa	3.2 kPa
52°C	1/9 s	0.0095	0.3100	0.8349	0.8494	0.9999	0.9970	0.8348	0.8468
	2/9 s	0.0093 (-2.1)	0.3032 (-2.2)	0.8469 (1.4)	0.8712 (2.6)	1.0014 (0.2)	0.9949 (-0.2)	0.8480 (1.6)	0.8667 (2.4)
	4/9 s	0.0082 (-13.7)	0.2671 (-13.8)	0.8520 (2.0)	0.8916 (5.0)	1.0041 (0.4)	0.9917 (-0.5)	0.8556 (2.5)	0.8843 (4.4)
	8/9 s	0.0096 (1.1)	0.3128 (0.9)	0.8704 (4.3)	0.9329 (9.8)	1.0106 (1.1)	0.9921 (-0.5)	0.8796 (5.4)	0.9255 (9.3)
58°C	1/9 s	0.0246	0.8116	0.8766	0.9048	0.9990	0.9962	0.8758	0.9014
	2/9 s	0.0242 (-1.6)	0.8016 (-1.2)	0.8941 (2.0)	0.9346 (3.3)	0.9988 (0.0)	0.9952 (-0.1)	0.8929 (2.0)	0.9301 (3.2)
	4/9 s	0.0212 (-13.8)	0.7096 (-12.6)	0.9018 (2.9)	0.9607 (6.2)	1.0005 (0.2)	0.9959 (0.0)	0.9022 (3.0)	0.9568 (6.1)
	8/9 s	0.0238 (-3.3)	0.8384 (3.3)	0.9040 (3.1)	0.9973 (10.2)	1.011 (1.2)	1.0059 (1.0)	0.9140 (4.4)	1.0032 (11.3)
64°C	1/9 s	0.0615	2.1139	0.9153	0.9594	0.9984	0.9978	0.9138	0.9572
	2/9 s	0.0609 (-1.0)	2.1267 (0.6)	0.9324 (1.9)	0.9857 (2.7)	0.9982 (0.0)	0.9992 (0.1)	0.9308 (1.9)	0.9849 (2.9)
	4/9 s	0.0537 (-12.7)	1.9038 (-9.9)	0.9433 (3.1)	1.0053 (4.8)	1.0000 (0.2)	1.0035 (0.6)	0.9433 (3.2)	1.0089 (5.4)
	8/9 s	0.0562 (-8.6)	2.1903 (3.6)	0.9368 (2.3)	1.0296 (7.3)	1.0111 (1.3)	1.0154 (1.8)	0.9472 (3.7)	1.0455 (9.2)
70°C	1/9 s	0.1473	5.7615	0.9461	1.0002	1.0015	1.0009	0.9475	1.0011
	2/9 s	0.1467 (-0.4)	5.4471 (-5.5)	0.9626 (1.7)	1.0094 (0.9)	0.9991 (-0.2)	1.0023 (0.1)	0.9618 (1.5)	1.0117 (1.1)
	4/9 s	0.1290 (-12.4)	4.9263 (-14.5)	0.9947 (5.1)	1.0236 (2.3)	1.0040 (0.2)	1.0076 (0.7)	0.9987 (5.4)	1.0314 (3.0)
	8/9 s	0.1210 (-17.9)	5.5065 (-4.4)	0.9579 (1.2)	1.0458 (4.6)	1.0121 (1.1)	1.0213 (2.0)	0.9695 (2.3)	1.0681 (6.7)
76°C	1/9 s	0.1471	12.7899	0.9466	1.0090	0.9987	1.0013	0.9454	1.0103
	2/9 s	0.3353 (127.9)	13.1784 (3.0)	0.9843 (4.0)	1.0188 (1.0)	1.0005 (0.2)	1.0037 (0.2)	0.9847 (4.2)	1.0226 (1.2)
	4/9 s	0.2954 (100.8)	12.0418 (-5.8)	0.9947 (5.1)	1.0314 (2.2)	1.004 (0.5)	1.0095 (0.8)	0.9987 (5.6)	1.0412 (3.1)
	8/9 s	0.2603 (77.0)	13.4761 (5.4)	0.9787 (3.4)	1.0540 (4.5)	1.0129 (1.4)	1.0245 (2.3)	0.9913 (4.9)	1.0798 (6.9)

[a] the percentages of variation reported in parenthesis refer to the changes in the parameter when moving from 1.0 s to the creep time into question (2.0, 4.0 or 8.0 s).

It is noticeable that the pattern of response of the strain rate strongly depends upon the stress level and, to some extent, the one of the initial strain as well. When the lowest stress level (100 Pa) is used, a change in the loading time from 4.0 to 8.0 s leads to lower rates of decrease in *A* and increase in *B* and, at the same time, increases from 0.6 to 1.2% in the parameter *n* (which is significant if compared with the percentages no greater than 0.5% at creep times up to 4.0 s). This role of nonlinearity can be seen again at 3,200 Pa, but the difference between the two stress levels is that the negative variations in *A* typically become positive (i. e., the initial strain increases in comparison to the initial values) and the results for *B* at 8/9 s boost to values at least 4.0% higher than the original ones at 1/9 s. In addition, the *n* values may exceed 1.02 at the temperatures of 70 and 76°C and the *α* values quickly overcome 1.00 at the temperatures of 64°C and higher.

In summary, it can be pointed out that the combination of a smaller amount of low-density PE with PPA in the AC+PE+PPA yields a formulation with lower tendencies of accumulation of initial strain (*A* values) and slightly higher levels of elastic response (*α* values) in some test conditions when compared with the original formulation AC+PE. As depicted in Figure 201, the majority of the ratios of the *A* values (AC+PE+PPA / AC+PE) are placed below the equality line and confirm that the initial strains in the AC+PE+PPA are lower than those of the AC+PE for the same temperature, creep time and stress level in the MSCR test. The ratios of the *B* values are approximately equal to one in all cases, even though some of the data points are slightly below the equality line (i. e., lower results for the AC+PE+PPA). Again, the major benefits of asphalt binder modification with PE+PPA in comparison to PE alone are associated with the presence of lower strain levels accumulated in the AC+PE+PPA after the first creep-recovery cycles.

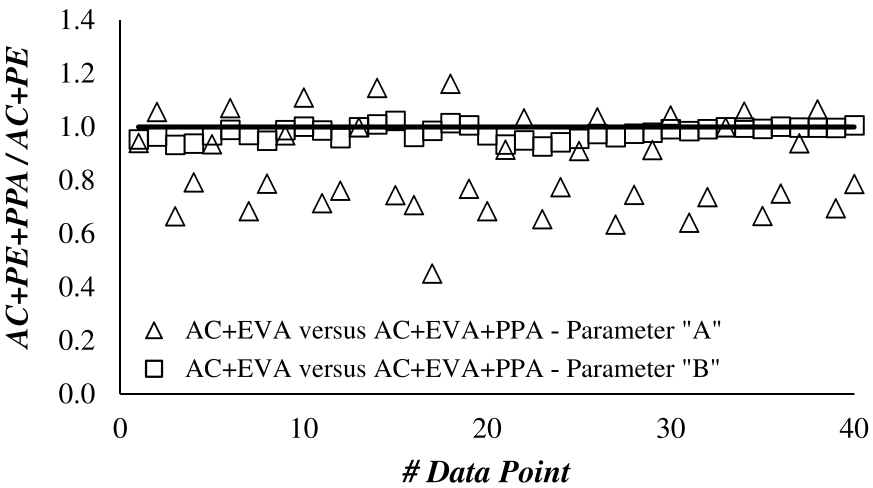

Figure 201 – Plots of the data points associated with the ratios of the *A* and *B* values for the AC+PE+PPA to the corresponding ones for the AC+PE (each data point is characterized by one temperature, loading time and stress level), the continuous line is the equality line

With respect to the levels of elastic response (which is indirectly measured in the modified power model by the parameter α), the comparisons in Figure 202 suggest that the AC+PE+PPA is a little bit more elastic than the AC+PE once that the majority of the data points are located below the equality line. In such a case, the α values are lower for the AC+PE+PPA and the percent recoveries tend to be higher for this material than for the AC+PE. As could be seen earlier (Figure 198, page 419), the comments on the results of α match those raised from the *R100* and *R3200* values with respect to the more promising findings obtained for the AC+PE+PPA in terms of its elastic response. Other authors also highlighted these benefits of the addition of PPA to the amount of recovered strain in conventional PE-modified asphalt binders, i. e., formulations with non-grafted modifiers (DOMINGOS and FAXINA, 2015b; GAMA et al., 2016).

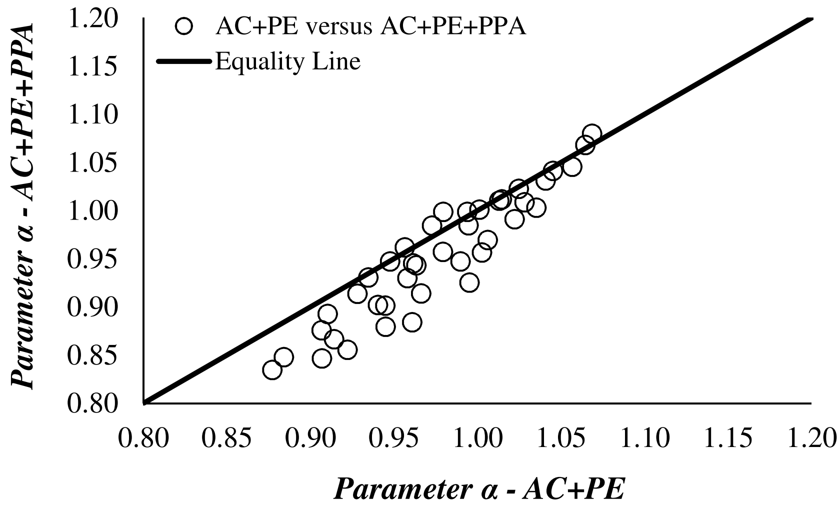

Figure 202 – Comparison between the results of the parameter α for the AC+PE and the AC+PE+PPA under all MSCR testing conditions

The positions of the data points in Figure 203 and the scales of the X- and Y-axes show that the differences among the levels of nonlinearity of the AC+PE and the AC+PE+PPA (i. e., *n* values) are quite small within the whole temperature and loading conditions used in the tests. The results tend to be slightly higher for the AC+PE, with only a few exceptions. This is in accordance with the $J_{nr,\ diff}$ values of the two formulations (see Figure 200, page 420), in that the stress sensitivity is higher for the AC+PE than for the AC+PE+PPA, except for the data values at 8/9 s. In other words, the contribution of nonlinearity to the increase in the amount of permanent strain at longer creep times is greater for the AC+PE than for the AC+PE+PPA in several test conditions, but the differences from one formulation to the other are marginal.

Figure 204 depicts the degrees of linear correlation between the *A* and *B* values of the AC+PE+PPA and the creep times for the temperature of 64°C and the stress level of 100 Pa. Due to the peculiar characteristic of the response of the formulation at 8/9 s, the correlation for *A* is quite poor ($R^2 \approx 0.45$) and the data point at 8/9 s (last one from the left to the right) behaves like as an outlier in the data set. The same can be said for the correlation obtained for the *B* values ($R^2 \approx 0.38$), that is, the straight line does not accurately reflect the actual behavior of the material throughout the loading times used in the tests. What can be said is that the overall tendency of decreasing *A* and increasing *B* with increasing t_F can be seen in the two sets of data points, which represents an advance towards a further resistance of the asphalt binder to rutting when compared with the AC+PE (increases in *A* and *B* at longer creep times, see Figure 190, page 407).

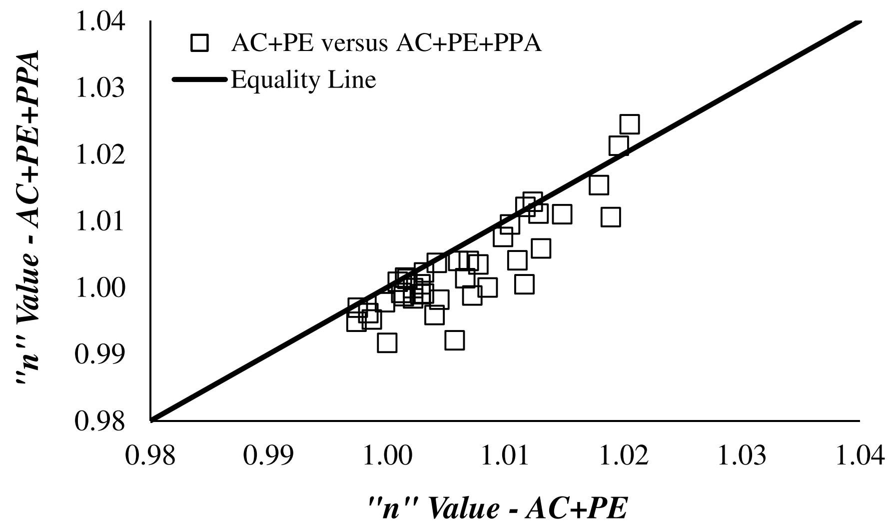

Figure 203 – Direct comparison between the degrees of nonlinearity (*n* values) for the AC+PE and the AC+PE+PPA under all MSCR testing conditions

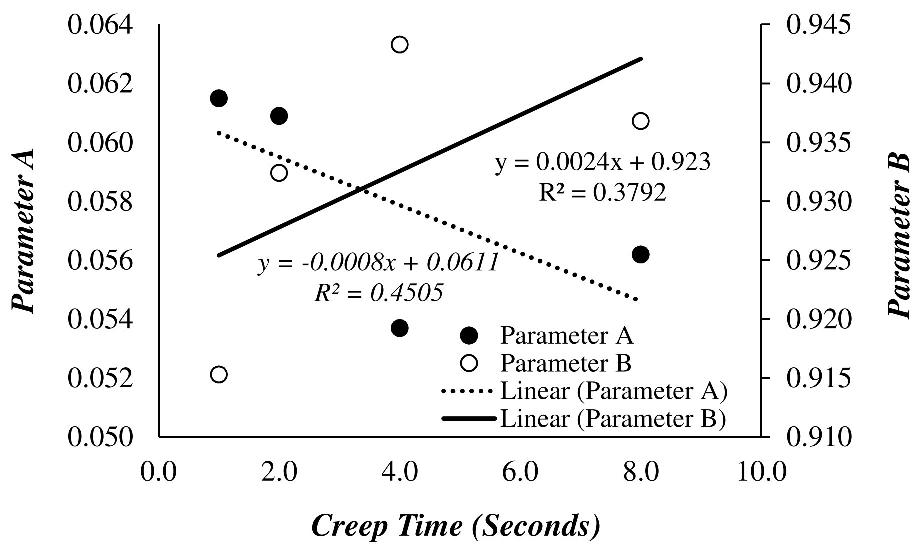

Figure 204 – Correlations between the creep time and the constants *A* and *B* from the model by Saboo and Kumar (2015), temperature of 64°C and stress level of 100 Pa – AC+PE+PPA

By moving to the highest stress level in the MSCR test (3.2 kPa, Figure 205), one may observe that there is a tendency of reverse in the pattern of response of the *A* values with increasing t_F (from decrease to increase) and the increases in the *B* values with t_F are more closely associated with a straight line ($R^2 \approx 0.91$). These degrees of improvement in the correlations for *B* may be associated with a considerable increase in *B* at the creep-recovery times of 4/9 and 8/9 s, and also to the fact that the characteristic of the AC+PE+PPA in suffering a great loss of rutting resistance after moving from 4/9 to 8/9 s (see Table 248) does not lead to any reverse in the signals of the percentages of variation for *B*. As a consequence, the final correlation for *A* is very low ($R^2 \approx 0.05$). In addition, the rate of increase in *B* with creep time is much higher at 3,200 Pa than at 100 Pa (almost four times higher) and the intercept shows a slight increase from one stress level to the other – from 0.92 to about 0.96.

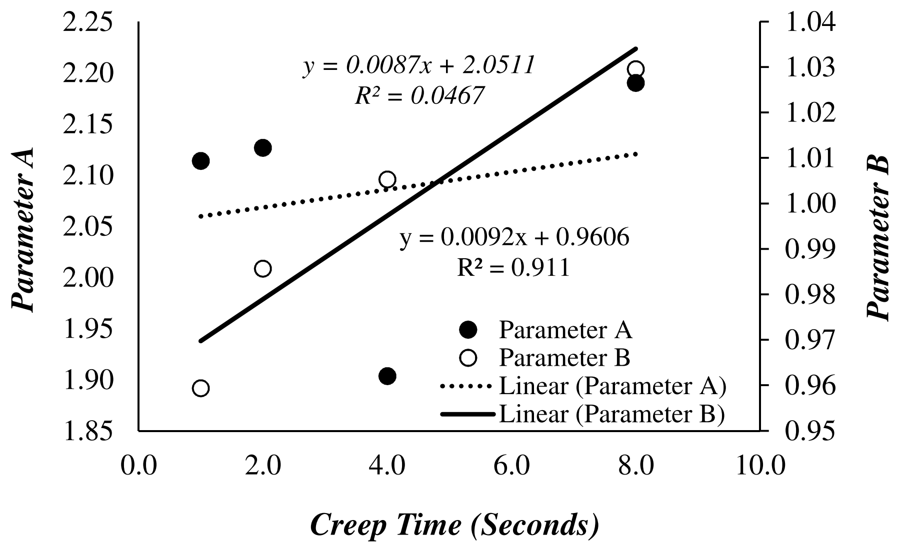

Figure 205 – Correlations between the creep time and the constants *A* and *B* from the model by Saboo and Kumar (2015), temperature of 64°C and stress level of 3,200 Pa – AC+PE+PPA

When the pavement temperature of 70°C is considered in the MSCR tests (Figure 206 for the data at 100 Pa and Figure 207 for the ones at 3,200 Pa), it can be observed that some marked changes between the observations made for the data at 64°C and the charts at 70°C exist. First, the correlations for the constant *A* increase and the ones for *B* considerably decrease at 100 Pa. By utilizing the stress level of 3,200 Pa in the MSCR test, it can be concluded that the tendency is reversed – i. e., the R^2 values are much lower for *A* than for *B*. The high levels of correlation for *A* at 100 Pa and 70°C may be taken as an exception, since all the other temperatures in Table 248 point to a deviation in the response of the binder at 8/9 s (and thus, poorer correlations). The overall pattern of decreasing *A* and increasing *B* with increasing t_F at 100 Pa remains unchanged, and the very small R^2 values for *A* at 3,200 Pa indicate that the binder is experiencing a tendency of increasing initial strains at 8/9 s when compared with the shorter creep times.

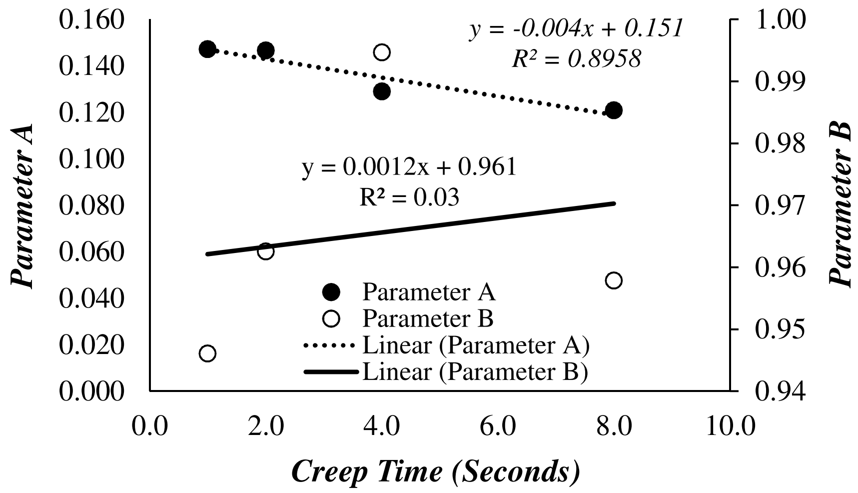

Figure 206 – Correlations between the creep time and the constants *A* and *B* from the model by Saboo and Kumar (2015), temperature of 70°C and stress level of 100 Pa – AC+PE+PPA

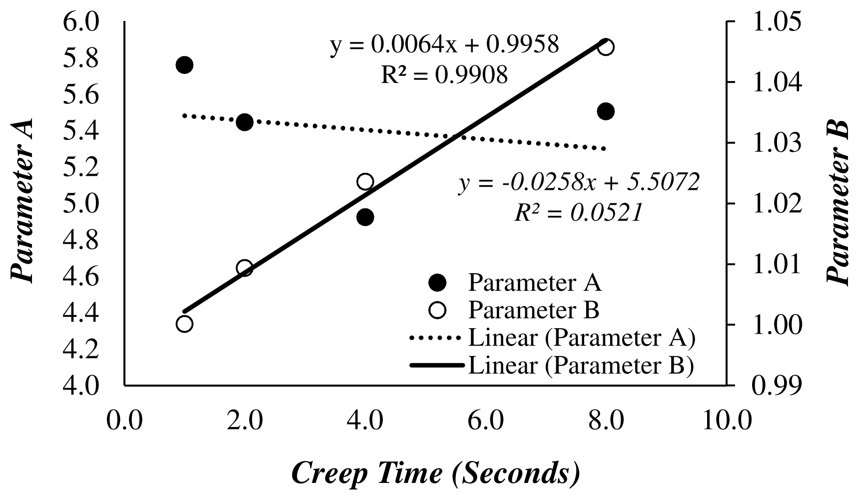

Figure 207 – Correlations between the creep time and the constants *A* and *B* from the model by Saboo and Kumar (2015), temperature of 70°C and stress level of 3,200 Pa – AC+PE+PPA

Table 249 contains all the linear regression equations and corresponding degrees of correlation for the parameters *A* and *B* and the AC+PE+PPA. The equation and correlation obtained at 70°C and 100 Pa for *A* may be considered as outliers within the data sets, since they do not follow the linear model observed for the other equations and R^2 values. In addition, the signals of the slopes of the trendlines for *A* constantly change from negative to positive and vice versa with increasing temperature and stress level in the tests, which could not be seen in the AC+PE (Table 234, page 408). This may be interpreted as a more complex pattern of response of the AC+PE+PPA under creep and recovery loading in comparison to the AC+PE, which, for instance, does not show any reverse in the signals of the slopes of the linear trendlines (see Table 234, page 408). The correlations are also typically higher for the AC+PE than for the AC+PE+PPA, especially in the trendlines associated with the *A* values.

Table 249 – Degrees of correlation between the parameters *A* and *B* (modified power model) and the creep time t_F for the AC+PE+PPA

T (°C)	stress (kPa)	linear regression equations and R^2 values (in parenthesis)[a, b]	
		parameter *A*	parameter *B*
52	0.1	y = 2E-05x + 0.0091 (0.0056)	y = 0.0047x + 0.8336 (0.9580)
	3.2	y = 0.0005x + 0.2966 (0.0044)	y = 0.0114x + 0.8436 (0.9832)
58	0.1	y = -0.0001x + 0.0239 (0.0620)	y = 0.0032x + 0.8821 (0.6368)
	3.2	y = 0.0037x + 0.7765 (0.0415)	y = 0.0123x + 0.9031 (0.9464)
64	0.1	y = -0.0008x + 0.0611 (0.4505)	y = 0.0024x + 0.9230 (0.3792)
	3.2	y = 0.0087x + 2.0511 (0.0467)	y = 0.0092x + 0.9606 (0.9110)
70	0.1	y = -0.0040x + 0.1510 (0.8958)	y = 0.0012x + 0.9610 (0.0300)
	3.2	y = -0.0258x + 5.5072 (0.0521)	y = 0.0064x + 0.9958 (0.9908)
76	0.1	y = 0.0066x + 0.2349 (0.0631)	y = 0.0029x + 0.9653 (0.1834)
	3.2	y = 0.0713x + 12.6040 (0.1265)	y = 0.0063x + 1.0049 (0.9915)

[a] the Y-axis is associated with the parameter (*A* or *B*), whereas the X-axis is associated with t_F.
[b] changes in the signal of the slope of the regression trendlines are highlighted with a grey-shaded box.

The equations and R^2 values summarized in Table 250 refer to the *n* and *α* values of the AC+PE+PPA under all testing conditions. There are some odd cases within the groups of equations and levels of correlation, e. g., reverses in the signals of the equations for *n* at 52 and 58°C – from positive to negative and vice versa – and very poor correlations in the equations for *α* at 70 and 76°C (R^2 < 0.40), both at 100 Pa. However, the general patterns of response of the material with increasing stress level and temperature are not markedly changed, i. e., either the level of nonlinearity (*n*) increases or the amount of elastic response (*α*) decreases at longer loading times during the application of the loading-unloading cycles. By comparing these data with those of the AC+PE (Table 235, page 409), one may see that the formulation with PE alone shows a more homogeneous response during MSCR because the aforementioned exceptions cannot be found in the equations and R^2 values of the AC+PE. The degrees of correlation also depict several points of similarity between the two PE-modified asphalt binders, which is in accordance with the comparisons among their results of *n* and *α* made above – i. e., not great differences within the groups of data, see Figure 202 (page 427) and Figure 203 (page 428) for further details.

By conducting a more detailed analysis on the *n* values of the AC+PE+PPA, it can be seen that the increases in *n* are consistent with creep time only for a particular stress level and temperature, and the same cannot be said in an overall context. In other words, the *n* values for a particular stress level and temperature are not necessarily greater than those obtained at a lower stress level and/or temperature. More simply, one single n value may refer to two or more MSCR testing conditions used in the AC+PE+PPA (e. g., 64°C/100 Pa and 76°C/100 Pa). From the point of view of degree of correlation and special distribution of the data points in a chart, this results in a poor overall correlation between the n and J_{nr} values as depicted in Figure 208 ($R^2 \approx 0.46$). Although this correlation is better than the one obtained for the AC+PE ($R^2 \approx 0.33$ according to Figure 192(a), page 410) and the tendency of increasing n with increasing J_{nr} is found in the data points, these arguments are still not sufficient to claim that n may be associated with J_{nr} in the study of nonlinearity in modified asphalt binders during the MSCR tests.

Table 250 – Degrees of correlation between the parameters n and α (modified power model) and the creep time t_F for the AC+PE+PPA

T (°C)	stress (kPa)	linear regression equations and R^2 values (in parenthesis)[a, b]	
		parameter n	parameter α
52	0.1	y = 0.0015x + 0.9983 (0.9984)	y = 0.0060x + 0.8320 (0.9750)
	3.2	y = -0.0006x + 0.9963 (0.6353)	y = 0.0107x + 0.8405 (0.9871)
58	0.1	y = 0.0018x + 0.9956 (0.9117)	y = 0.0048x + 0.8781 (0.8620)
	3.2	y = 0.0015x + 0.9927 (0.8256)	y = 0.0138x + 0.8962 (0.9725)
64	0.1	y = 0.0019x + 0.9948 (0.9123)	y = 0.0042x + 0.9182 (0.7326)
	3.2	y = 0.0026x + 0.9944 (0.9876)	y = 0.0118x + 0.9548 (0.9544)
70	0.1	y = 0.0017x + 0.9977 (0.9037)	y = 0.0028x + 0.9588 (0.1646)
	3.2	y = 0.0030x + 0.9968 (0.9879)	y = 0.0095x + 0.9924 (0.9993)
76	0.1	y = 0.0020x + 0.9964 (0.9966)	y = 0.0049x + 0.9618 (0.3997)
	3.2	y = 0.0034x + 0.9972 (0.9937)	y = 0.0098x + 1.0017 (0.9988)

[a] the Y-axis is associated with the parameter (n or α), whereas the X-axis is associated with t_F.
[b] changes in the signal of the slope of the regression trendlines are highlighted with a grey-shaded box.

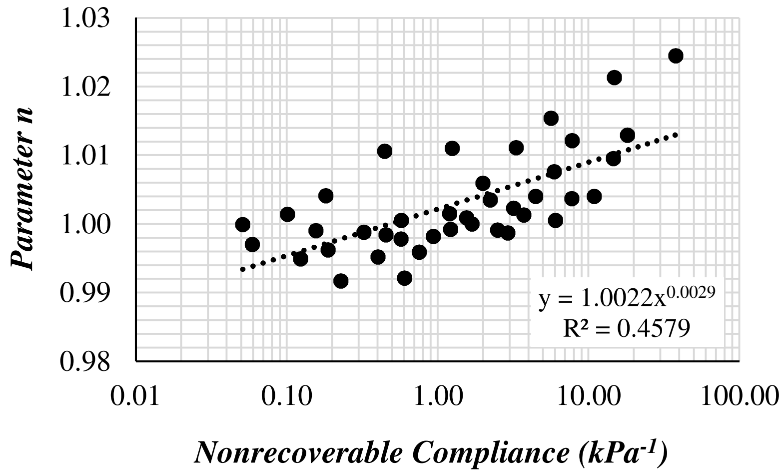

Figure 208 – Degree of correlation between the nonrecoverable compliances of the AC+PE+PPA and the corresponding n values from the power law models

Similarly to the AC+PE, the *n* values of the AC+PE+PPA at 3,200 Pa also depict a good correlation with the $J_{nr}3200$ values – R^2 is equal to 0.72, Figure 209. On the other hand, the correlation between $J_{nr}100$ and its corresponding *n* values was found to be very poor ($R^2 \approx 0.19$, chart not shown here). One more time, testing the binder at 3,200 Pa naturally tends to place it closer to the nonlinear viscoelastic range than at 100 Pa, and this may explain why the correlations are much better at 3,200 Pa for several formulations (not only the AC+PE and the AC+PE+PPA, but also others such as the AC+rubber, the AC+rubber+PPA and the AC+SBR+PPA). It can be implied from these comments that the association of nonlinearity from the model (*n*) with nonlinearity as evaluated by compliance (J_{nr}) has a greater probability of success when higher stress levels are used, even though this cannot be taken as a universal rule because not all binders show good correlations at 3,200 Pa and the results at 100 Pa are not consistent in a general context.

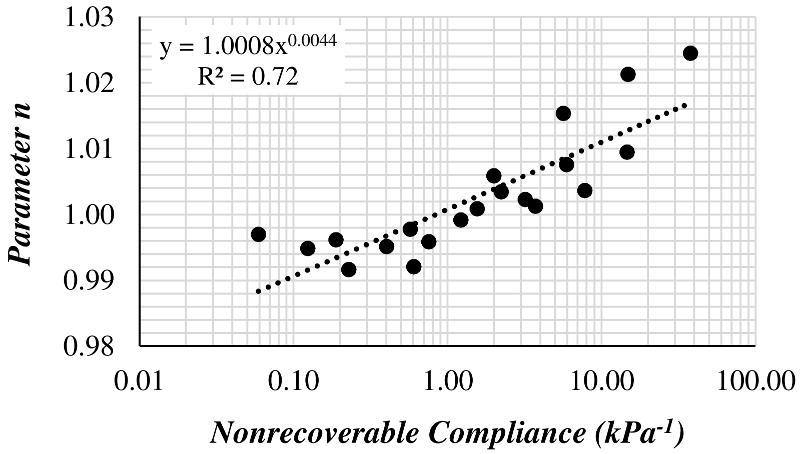

Figure 209 – Degree of correlation between the nonrecoverable compliances of the AC+PE+PPA at 3,200 Pa and the corresponding *n* values from the power law models

The resulting correlation between all the α and *R* values is shown in Figure 210. One more time, the parameter α does a good job in estimating the percent recovery of the material despite the presence of several results for one particular *R* value (in this case, 0%). The overall correlation of 0.829 is very promising, and is almost equivalent to the one reported for the AC+PE (Figure 193, page 411). When only the outcomes at 100 Pa are considered, the correlation is considerably improved (R^2 is equal to 0.9076, chart not shown here). In turn, the restriction of the data points to the results at 3,200 Pa yields a final correlation of 0.784 (chart not shown either). The α value decreases with increasing recovery in the binder sample in all cases, and this points to a possible use of α as a complementary analysis of the level of elasticity in the material. These individual results of the AC+PE+PPA are very close to the ones of the AC+PE, either at 100 Pa (0.908 and 0.967, respectively) or at 3,200 Pa (0.784 and 0.754, respectively).

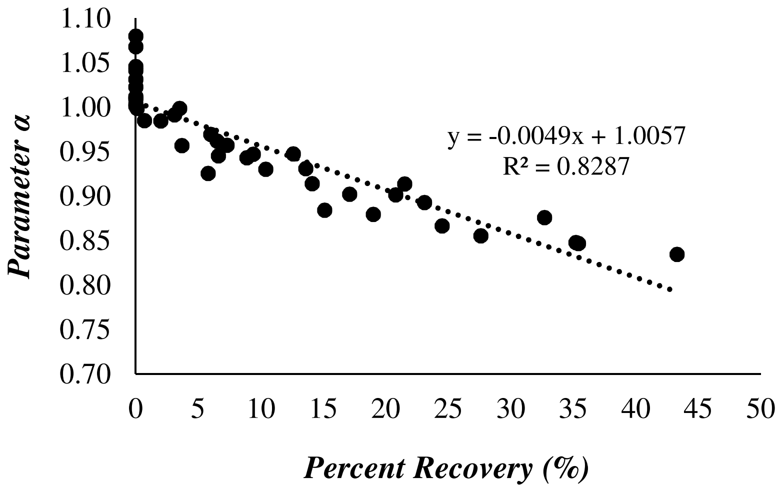

Figure 210 – Degree of correlation between the percent recoveries of the AC+PE and the corresponding α values from the power law models

The rheological modeling of the results of the AC+PE+PPA indicate that there is a limiting test condition in the MSCR protocols (i. e., critical t_F value) after which the patterns of response of the parameters A, B, n and α change significantly. This critical value is equal to 4.0 s and does not depend upon the test temperature. For t_F values higher than 4.0 s, the materials seems to suffer a considerable loss of rutting resistance because either the initial strain or the strain rate tend to increase with increasing creep time. In addition, nonlinearity also becomes more visible ($n > 1.02$) under such loading conditions and the parameter α can easily exceed unity for temperatures of 64°C and higher. The replacement of a portion of the PE content by PPA typically causes reductions in the initial strain of the asphalt binder (lower A values) and has a marginal effect on its strain rate (slight modifications in the B values). Nonlinearity are elastic response are not considerably affected by these changes in the modifier contents and types according to the model parameters, since the α and n values are only a little bit lower for the AC+PE+PPA than for the AC+PE.

Due to the peculiar behavior of the AC+PE+PPA at 8/9 s, the behavior observed for the parameter A with increasing loading time was affected when compared with the AC+PE. In other words, it is not possible to assume that the variations in A with creep time follow a straight line (as noticed for the AC+PE) because the degrees of correlation are quite weak in many cases. On the other hand, the overall correlations for B were influenced by the replacement in the modifier types only in some specific test conditions (i. e., 70 and 76°C, both at 100 Pa). What can be said is that the AC+PE+PPA is more rut resistant than the AC+PE mainly because of the lower initial strains, but the slightly lower strain rates and levels of nonlinear response may have contributed to this better rutting performance as well. Similarly to the previously reported formulations, the parameter α seems to work well in estimating the percent recovery of the AC+PE+PPA because the R^2 values are quite high, especially at 100 Pa. However, this parameter has the disadvantage of showing several values for one single R value (0%).

The ANOVA analysis was conducted in the AC+PE+PPA according to similar procedures that were followed for the other reported asphalt binders. As can be seen in Table 240 (page 414), there are two null *R3200* values when departuring from the creep-recovery times of 1/9 s at the temperature of 52°C. As based on the reasons given in Appendix A, it was decided not to apply the ANOVA technique on these data points. Table 251 provides the rearranged *R100* values of the AC+PE+PPA, whereas Table 252 shows its rearranged $J_{nr}100$ and $J_{nr}3200$ values. It may be important to remind that ANOVA is used in this study as a tool to provide the answers to very important questions: (a) can the effects of temperature and loading time on the R and J_{nr} values of the asphalt binder be considered as statistically different (i. e., too high variances) under a level of significance of 5%?; and (b) based on the rearranged table of data, which is the variable that mostly affects the results of the binder parameters?

Table 251 – Rearranged MSCR testing data of the AC+PE+PPA to be used in the analysis of variance (ANOVA) – percent recovery

stress level of 0.1 kPa (*R100*, %)[a]		stress level of 3.2 kPa (*R3200*, %)[a]	
increasing creep time	increasing temperature	increasing creep time	increasing temperature
43.3	43.3	These calculations were not made due to the lack of enough data points at higher temperatures.	These calculations were not made due to the lack of enough data points at higher temperatures.
35.2	32.7		
27.6	21.5		
19.0	12.6		
N/A[b]	6.6		

[a] the starting point in both cases was the temperature of 52°C.
[b] N/A: Not applicable.

Table 252 – Rearranged MSCR testing data of the AC+PE+PPA to be used in the analysis of variance (ANOVA) – nonrecoverable creep compliance

stress level of 0.1 kPa ($J_{nr}100$, kPa^{-1})[a]		stress level of 3.2 kPa ($J_{nr}3200$, kPa^{-1})[a]	
increasing creep time	increasing temperature	increasing creep time	increasing temperature
0.051	0.051	0.059	0.059
0.101	0.156	0.123	0.188
0.181	0.453	0.228	0.572
0.445	1.202	0.602	1.556
N/A[b]	2.914	N/A[b]	3.717

[a] the starting point in both cases was the temperature of 52°C.
[b] N/A: Not applicable.

Table 253 summarizes the outcomes of ANOVA for the percent recoveries of the AC+PE+PPA. As the data suggest, the *F-value* and the *p-value* give support to the hypothesis that the effects of temperature and loading time on the recoveries of the material are statistically similar when $\alpha = 5\%$. The *F-value* of 0.81 is less than 20% of $F_{critical}$ (about 5.591) and the *p-value* of 0.40 is about 8 times higher than α. According to the organized R values in Table 251, one may infer that temperature has a greater impact on the elastic responses of the AC+PE+PPA because this parameter decreases faster with temperature than with loading time.

Table 253 – Results from the analysis of variance (ANOVA, *p-value* and *F-value*) as based on the percent recoveries of the AC+PE+PPA

null hypothesis H_0	statistical parameters (ANOVA)				recommendation
	$F_{critical}$	*F-value*	α	*p-value*	
equivalency between R values with increasing creep time and temperature, 0.1 kPa	5.5914	0.8100	0.05	0.3980	H_0 is not rejected
equivalency between R values with increasing creep time and temperature, 3.2 kPa	Not calculated due to the lack of enough data points.				

By moving forward to the nonrecoverable creep compliances (Table 254), it can be seen that J_{nr} is much more sensitive to the effects of temperature and loading time than R, regardless of the stress level. This is because the *F-value* increases significantly (almost doubled) and the *p-value* decreases by approximately 45% of its original results for R. However, it was not enough to recommend the rejection of H_0 in any case once the requirements established by $F_{critical}$ and α are still complied. The results show only slight differences from one stress level to the other – no more than 2% – and, as can be inferred from the organized data (Table 252), temperature can increase the nonrecoverable compliances of the AC+PE+PPA at much higher rates than the creep time. Therefore, an increase in the pavement temperature is expected to affect the compliance of the formulation in a greater level than an increase in the creep time.

Table 254 – Results from the analysis of variance (ANOVA, *p-value* and *F-value*) as based on the nonrecoverable compliances of the AC+PE+PPA

null hypothesis H_0	statistical parameters (ANOVA)				recommendation
	$F_{critical}$	*F-value*	α	*p-value*	
equivalency between J_{nr} values with increasing creep time and temperature, 0.1 kPa	5.5914	1.5796	0.05	0.2491	H_0 is not rejected
equivalency between J_{nr} values with increasing creep time and temperature, 3.2 kPa	5.5914	1.5492	0.05	0.2533	H_0 is not rejected

Summary, Concluding Remarks and Rankings of Binders. The use of longer creep times in the MSCR tests was made in this study in an attempt to simulate more severe loading conditions observed in the real asphalt pavements. As discussed earlier, many publications from the literature increased the stress level – rather than the loading time – to represent such conditions in the DSR. However, another serious limitation relies on the apparatuses used in the studies to collect mixture data and correlate them with binder data. It is known that they do not necessarily represent the real world mainly due to the speeds of the wheels and the magnitude of the applied loads. For instance, good correlations between J_{nr} at 25,600 Pa and the mixture data derived from an ALF device from FHWA – single tire load of 45,600 N and average speed of 19 km/h – were found in the papers by D'Angelo (2009) and D'Angelo et al. (2007). As a matter of comparison, D'Angelo et al. (2007) pointed out that reasonable correlations between data derived from field pavements constructed in the state of Mississippi (US) and loaded during the summer of 1996 were found for J_{nr} values at 800 Pa (i. e., a reduction by 3,100% or 32 times in the stress level).

By following quite similar approaches used in the study from D'Angelo et al. (2007), Wasage et al. (2011) found good correlations between J_{nr} at 12,800 Pa and mixture data collected from a wheel tracking test – applied load of 705 N, average contact stress of 0.73 MPa and 52 wheel passes per minute. Much lower loading speeds (about 3 km/h) and relatively high wheel loads (5,000 N) were used in the experimental tests conducted by Laukkanen et al. (2015), but these authors showed very high levels of correlation (about 0.98) between $J_{nr}3200$ and the model parameters *A* and *B* from a conventional power equation typically used in other studies with mixtures (e. g., Witczak et al. (2002)). Hafeez and Kamal (2014) did not change the stress levels in the MSCR tests either, and they observed an R^2 value of 0.96 when the $J_{nr}3200$ values of a PG 76-16 binder – modified with 2% of Elvaloy® by weight – collected at the temperatures of 58, 64, 70 and 76°C were plotted against the rut depth of mixture slabs after 20,000 cycles of loading and unloading at these same temperatures (wheel load of 700 ± 20 N). In summary, it seems that the stress level of 3,200 Pa can do provide good correlations with mixture data depending on the input and output variables of the mixture tests.

As can be seen from the aforementioned comments, the two stress levels reported by D'Angelo et al. (2007) are not compatible and suggest that a very close simulation of the actual pavement and loading conditions in the laboratory – and, as a consequence, the identification of the stress level that better correlates with field pavement rutting data in all cases – still remains as a very challenging task. Field loading conditions are not uniform and the spectrum of load values and speeds vary significantly within a day (DOMINGOS and FAXINA, 2014). Therefore, it is necessary to go further into the discussions and try to find loading times and/or stress levels that can actually represent the conditions observed in the field. Although the approach followed on Superpave® – to decrease J_{nr} in order to account for heavier traffic levels – has many advantages and is somehow practical for routine use, it still needs to be refined and include other variables that are involved in the nonlinear behavior of binders at high temperatures. Perhaps the use of transfer functions and shift factors to make interconversions between laboratory and field data (PEREIRA et al., 2000) could be a step towards the seek for more appropriate solutions, but this needs to be extensively investigated as well.

As an ultimate goal of the present dissertation, the loading time t_F could be added to the current Superpave® specification in an attempt to further understand the role of this creep time on the rheological response of modified asphalt binders, as well as to simulate more critical loading conditions in the pavement. In addition, this concept could be used by researchers and highway agencies to discard binders that are very sensitive to long loading times and become too susceptible to rutting in the pavements. A very recent publication from the author and co-workers (DOMINGOS and FAXINA, 2017) has already highlighted such benefits and showed the differences among the responses of modified asphalt binders in the standardized MSCR tests. Modified power models from Saboo and Kumar (2015) and some traffic speeds derived from theoretical- and field-based equations in the literature (HUANG, 2004; PEREIRA et al., 1998, 2000) were used to see whether they are able to accurately predict the traffic level of the binder. Finally, a statistical analysis of variance (ANOVA) was carried out to investigate the variable that mostly affects the data and whether the differences may be considered as significant or not.

Some main conclusions of this phase of the study can be drawn as follows:

- the application of longer loading times in the MSCR tests leads to decreases in the amount of recovery and increases in the nonrecoverable creep compliance; this means that the binders are more susceptible to rutting and show lower levels of elastic response in such testing conditions; however, the inherent characteristics of each modification type (polymeric, acid-based, crumb rubber and so on) must be considered in the analyses of the laboratory data;
- each modified asphalt binder reacts in a different way when tested at longer creep times and, for the ones with very high levels of elasticity (especially the AC+EVA and the AC+EVA+PPA), the roles of delayed elasticity, steady state and rearrangement/damage of the polymer networks on the results of R and J_{nr} must be carefully investigated; from a practical point of view, this yields increases in some recoveries of the AC+EVA and the AC+EVA+PPA with increasing severity in the laboratory tests;

- the modification of the base binder with plastomers (AC+PE, AC+PE+PPA, AC+EVA and AC+EVA+PPA) typically depicts a boundary testing condition – labeled here as "failure point" – after which there is a considerable loss of rutting resistance in the material; this can be explained by the intrinsic properties of the plastomeric polymers (i. e., they impart very high degrees of stiffness to the binder and the resulting formulation resembles some characteristics of a fragile material, e. g., a critical strain level before failure) and the relatively high polymer contents when compared with those reported in the literature – typically between 3 and 7% by weight (POLACCO et al., 2006, 2015);
- by taking into account a starting point of 52°C and 1/9 s in the MSCR tests and increasing loading time and temperature separately, it can be inferred from ANOVA that the variances within the R and J_{nr} values are not statistically significant in several cases because the limiting requirements for *F-value* and *p-value* – $F_{critical}$ and level of significance α, respectively – were met; the only exception among the studied formulations was the AC+SBS at 100 Pa (the null hypothesis H_0 was rejected) and it is believed that the rearrangement of the SBS polymer particles and the formation of chain entanglements in the formulation during the loading-unloading cycles (POLACCO et al., 2006; ZOOROB et al., 2012) with increasing temperature influenced on the results and differentiated from the ones with increasing creep time;
- temperature was found to be the input variable that mostly affected the percent recoveries and the nonrecoverable compliances of the asphalt binders according to ANOVA, with a few exceptions in the recovery values at 100 Pa such as those of the AC+SBS, the AC+SBS+PPA, the AC+SBR+PPA and the AC+SBR; these exceptions may be attributed to the accumulated damage in the polymeric networks after the application of several loads for longer periods of time;
- the parameter α from the modified power models typically showed good to excellent correlations – R^2 ranging from 0.7 to 0.9 in many cases – with the percent recoveries of the formulations, and lower α values are associated with higher recoveries in the MSCR tests; however, this parameter has the limitation of providing several results in the description of particular recovery values – more specifically, two or more α values can be found in the binder in the cases of null recovery ($R = 0\%$) and very high recoveries ($R > 80\%$);
- the parameter n (which is supposed to describe the degree of nonlinearity in the asphalt binder) does not always provide good correlations with the nonrecoverable compliances, even though these correlations tend to be much better for the data at 3,200 Pa and some formulations (e. g., the AC+PE+PPA, the AC+SBR+PPA and the AC+rubber); it is

hyphotesized that nonlinearity cannot be clearly identified after the application of the loads during 8 s or less or, in other words, much longer creep times and higher strain levels in the binder should be considered to provide better associations between the two parameters; hence, it may be implied that the higher R^2 values for the data at 3,200 Pa than for those at 100 Pa might be associated with these higher strain levels in the samples;

- two different and overall pictures may be formed to describe the variations in the rutting resistances of the asphalt binders with increasing creep time from the point of view of the binder: (a) the formulations with very low susceptibility to rutting and reasonable to high elastic responses in the MSCR test (e. g., AC+Elvaloy+PPA, AC+rubber and AC+EVA) typically show decreases either in the initial accumulated strain (*A* values) or the strain rate (*B* values) and only the level of nonlinearity (*n* values) increases with increasing t_F for a particular pavement temperature; (b) the 50/70 base binder and all the remaining formulations with low to relatively high resistances to rutting (AC+PPA, AC+SBR, AC+SBR+PPA, AC+EVA+PPA, AC+PE, AC+PE+PPA, AC+SBS, AC+SBS+PPA and AC+rubber+PPA), for which there are increases in the strain rate and the level of nonlinearity and decreases in the initial accumulated strain after the increases in the duration of the applied load;
- among these above-mentioned formulations with low to reasonably high rutting resistances, some of them may depict a loss of resistance after a certain test condition in the DSR; in numerical terms, this loss of resistance is represented by a reverse in the behavior of the initial strain and its contribution to the higher rutting potential of the binder – more simply, the parameter *A* starts to increase (rather than to decrease) at longer creep times. This is the case of the two formulations with SBR (AC+SBR and AC+SBR+PPA) and PE (AC+PE and AC+PE+PPA), in which the initial accumulated strains start to increase at the temperature of 64°C for all of them with exception of the AC+PE+PPA (temperature of 76°C); such a behavior may be explained by the accumulation of permanent strains at sufficient levels to exceed the "failure point" (formulations with PE) or cause extensive and irreversible damage in the polymer network (formulations with SBR);
- the traffic speeds provided by the equations from Huang (2004) and Pereira et al. (1998, 2000) show high to excellent correlations ($R^2 > 0.80$) with the $J_{nr}3200$ values of the formulations, but the ability of such equations in predicting the actual traffic levels of these binders – as given by $J_{nr}3200$ and the current Superpave® specification criteria – is seriously questionable: the best predictions for the equations from Huang (2004) and Pereira et al. (1998) were observed at the pavement temperatures of 52 and 58°C with some exceptions and the equation from Pereira et al. (2000) barely showed any correlation with binder data;

- the deficiencies in the predictions of the traffic levels may be explained by (a) the limitations of the equations, especially the empirical-based ones (they are limited to the original mixture data and testing conditions, and cannot be extended to other materials and tests); (b) the ranges of traffic speeds currently used on Superpave®, since there are evidences that some of these speeds for standard traffic were based on the values previously considered in the old version of the specification, i. e., 10 Hz→ 55 mph → ≈ 89 km/h (BAHIA and ANDERSON, 1995; CHEN and TSAI, 1999), and no clear evidences concerning the origin of the other traffic speeds have been found so far; and (c) the diversity of combinations of axles and vehicles may result in several loading times and traffic levels in a real pavement (SARKAR, 2016);
- the use of an additional criterion in the assignment of the most appropriate traffic level to the asphalt binder can identify some critical aspects of the actual resistance of the material to rutting, since a particular formulation with a very small J_{nr} value at 1/9 s may depict a high increase in J_{nr} at longer creep times, and thus be too susceptible to rutting during the passage of slow-moving vehicles in the traffic lane. Some examples of these comments include the AC+PPA, the AC+PE and the AC+EVA at 64°C, the AC+Elvaloy+PPA at 70°C and the AC+rubber+PPA and the AC+SBR at 58°C, for which the traffic level decreased by one grade when moving from the current to the new proposed criteria. By identifying such characteristics of the formulations, one could be more sensible when choosing the most suitable traffic condition for a specific material;
- some modified asphalt binders – especially the AC+rubber, the AC+rubber+PPA, the AC+EVA, the AC+EVA+PPA and the AC+SBS – depicted very high $J_{nr,\ diff}$ values (> 75%) at one or more temperatures and loading times; strictly speaking, they should not be used for paving applications because the stress sensitivity requirement defined by Superpave® is not met, even though their performance in the mixtures were found to be from good to excellent (Chapter 5). This is one more evidence that the current criterion for studying the stress sensitivity of the modified binders needs to be revised due to some characteristics of the modifiers during the MSCR tests (TEYMOURPOUR et al., 2016) and the fact that the parameter $J_{nr,\ diff}$ can depict pretty high variability (ZHOU et al., 2014), among other possible issues that may be raised in the future; and
- the AC+Elvaloy+PPA and the AC+EVA are typically able to hold their classifications as "formulations with high levels of elasticity" at longer loading times, which suggests that their polymeric networks were not considerably damaged during the MSCR tests; however, the

same cannot be said for the AC+EVA+PPA because this material tends to be graded as a "formulation with low level of elasticity" when $t_F \geq 2.0$ s.

As a next step of the analysis of the outcomes of the MSCR tests for the studied binders and modifiers, all of the α and R values were plotted in a same chart in order to establish an overall picture of the relationship between the two parameters. In addition, all the n and J_{nr} values were plotted in a chart to get a general picture of their relationship. A quite similar approach was followed by Saboo and Kumar (2015), and it was made in the present study as well in order to support the positive findings of α observed individually for each material. Since each formulation contains 40 data points collected during all the MSCR tests (5 temperatures × 4 loading times × 2 stress levels), a total of 480 data points (40 × 12 formulations) was grouped into each chart and the levels of linear correlation were determined.

Figure 211 shows the plot of the 480 data points referring to the α and R values and the corresponding correlation between them. The parameter α seems to work well in the estimation of the amount of elastic response in the binders during the creep-recovery cycles because the final correlation is good ($R^2 \approx 0.82$), even though a few outliers for R = 0% (null recovery) and R between 60 and 100% (high to very high recovery) can be observed. In a general context, the α value may be used as a complementary criterion to estimate the level of elasticity in the creep-recovery behavior of the binder. One example is given in the original paper by Saboo and Kumar (2015), in which the authors defined maximum values for α as a function of the traffic level assigned to the binder. This approach resembles the minimum percent recoveries established in the literature for each range of J_{nr} values (ANDERSON, 2011; D'ANGELO, 2008, 2010b), but neither the minimum α values nor the minimum R values are currently found on Superpave®.

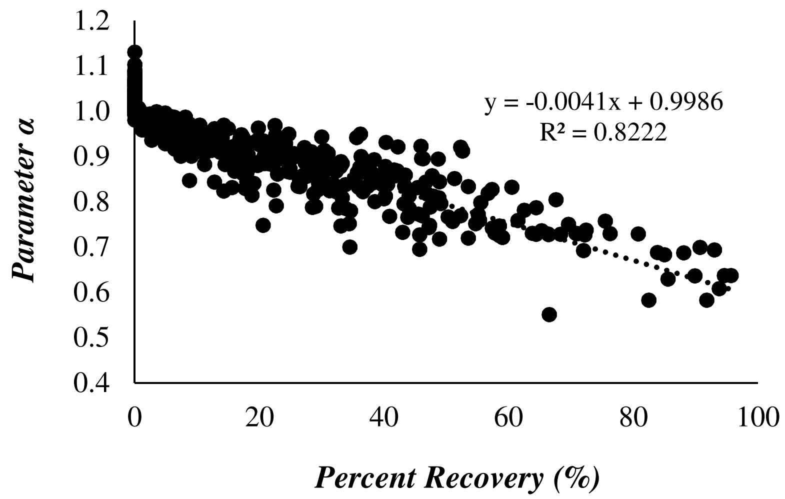

Figure 211 – Degree of correlation between the percent recoveries of all modified asphalt binders and their corresponding α values from the power law models

Figure 212 also depicts 480 data points and the corresponding correlation derived from them, but considering the parameter *n* and the nonrecoverable compliance J_{nr}. There is almost a complete absence of correlation between the two parameters ($R^2 \approx 0.032$) and several outliers within the whole interval of J_{nr} values. The great majority of data points is restricted to the interval between n = 0.95 and n = 1.05, which is where nonlinearity probably does not have much influence on the creep-recovery behavior of the asphalt binders. As pointed out in the literature (DELGADILLO and BAHIA, 2010; DELGADILLO et al., 2012; SANTAGATA et al., 2013, 2015) and shown earlier in this study, the loading times are quite short and do not seem to be enough to reach the nonlinear range of response of the material, even at very high temperatures. This is possibly one of the reasons why *n* is restricted to a narrow interval of results and nonlinearity may not have been clearly reached during the tests.

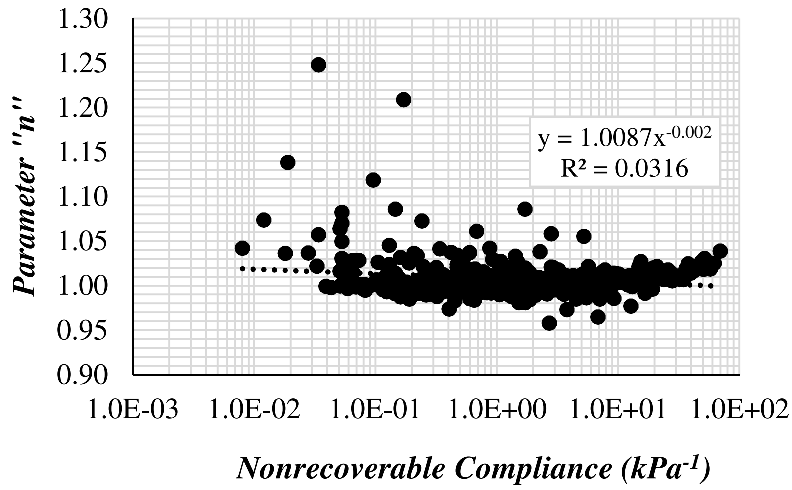

Figure 212 – Degree of correlation between the nonrecoverable compliances of all modified asphalt binders and their corresponding *n* values from the power law models

The next step in the study of the effects of longer creep times on the rheological behavior of the formulations includes the benefits/problems in the replacement of part of the main modifier content (SBS, SBR, EVA, PE or crumb rubber) by PPA. The AC+Elvaloy+PPA and the AC+PPA were directly compared with the 50/70 base material because their corresponding formulations (AC+Elvaloy and air-blown binders, respectively) were not prepared. These comparisons among the results of each formulation were made based on the following criteria: (a) increases and decreases in the *R* and J_{nr} values at all creep times; (b) variations in the $J_{nr,\,diff}$ values at each creep time; and (c) results and variations in the model parameters *A*, *B*, *n* and α in each test condition. To facilitate the understanding and provide the reader with a clear and comprehensive picture of such effects, the data were organized into tables and separated by the main modifier.

50/70 Base Asphalt Binder, AC+PPA and AC+Elvaloy+PPA. Table 255 is a summary of the effects of the addition of PPA and Elvaloy+PPA on the original rheological parameters of the unmodified asphalt binder. In summary, the use of PPA alone imparts higher rutting resistances to the base binder and reasonable levels of elasticity at temperatures no greater than 64°C, but the increased sensitivity of the rheological and model parameters of the AC+PPA to the creep time counteracts the benefits provided by the modification process. The AC+PPA is also overly stress sensitive in some test conditions, which may restrict its use on pavements with very critical loading conditions and PG grades of about 70-xx and 76-xx.

Table 255 – Direct comparisons among the effects of the presence of PPA and the addition of Elvaloy® terpolymer on the rheological properties and parameters of the 50/70 unmodified asphalt binder

rheological or model parameter	brief descriptions of the effects in each formulation	
	AC+PPA	AC+Elvaloy+PPA
percent recovery R	higher R values and rates of decrease in this parameter with loading time and temperature	no null recoveries can be observed and the elastic responses are quite high, regardless of the temperature
nonrecoverable compliance J_{nr}	lower J_{nr} values and higher rates of increase with loading time and temperature	the compliances are very small and the differences between the percentages of increase in J_{nr} at 100 and 3,200 Pa are marginal
percent difference in compliances $J_{nr,\ diff}$	higher $J_{nr,\ diff}$ values and, for some loading times at 70 and 76°C, the limit of 75% is exceeded	the results are slightly higher, but not enough to be ranked as "overly stress sensitive" ($J_{nr,\ diff} < 32\%$)
level of elasticity	this formulation does not show a high level of elasticity	the formlation holds its classification as "high elasticity" in all the testing conditions
model parameters A, B, n and α	decreases in the initial strain and the strain rate and higher elastic responses (lower A, B and α values), but these benefits quite disappear at 70 and 76°C; nonlinearity seems to be more visible only when the test conditions are very severe	much lower results for all the parameters when compared with the base binder (lower initial strains and strain rates and very high elastic responses); the α values never exceed 0.96, but the correlations with R are better at 100 Pa than at 3,200 Pa
variations in the model parameters	the parameters vary at higher rates than for the base binder, especially for A and B	for temperatures up to 64°C, the rutting resistance increases only due to the increased nonlinearity (either A or B decrease with t_F; linear regression trendlines may be used to represent the variations with t_F, despite a few exceptions

With respect to the AC+Elvaloy+PPA, it can be seen that this modification type yields very high elastic responses and a marked decrease in the susceptibility to rutting, together with a degree of stress sensitivity that is in accordance with the Superpave® requirements ($J_{nr,\ diff}$ < 75%). This formulation also contains a high level of elasticity, which is desirable for paving applications and suggests the existence of a strong polymer network acting in the reduction of the amount of permanent strain. The model parameters are also considerably reduced and, despite some exceptions, their variations with t_F may be described by linear trendlines. The rutting resistance of the AC+Elvaloy+PPA at the temperatures of 52, 58 and 64°C mainly decreases with increasing creep time due to the higher contribution of nonlinearity, which is not observed for the 50/70 original binder. Based on this, it can be pointed out that the AC+Elvaloy+PPA is the best formulation among the three binders reported so far (50/70 base binder, AC+PPA and AC+Elvaloy+PPA).

Crumb Rubber-Modified Asphalt Binders. Table 256 summarizes the major differences between the AC+rubber and the AC+rubber+PPA in terms of their MSCR and model parameters studied in the dissertation. The replacement of part of the crumb rubber content by PPA provides benefits to the stress sensitivity of the asphalt binder, since $J_{nr,\ diff}$ complied with the Superpave® requirements for the AC+rubber+PPA but not for the AC+rubber. Conversely, the AC+rubber+PPA is more susceptible to rutting than the AC+rubber because the R values decrease and the J_{nr} values increase when moving from the formulation without PPA to the one with PPA. This suggests that the rubber particles are primarily responsible for the stiffness of the asphalt binder and, due to their nonlinear responses under loading in the DSR, the degree of nonlinearity – as measured by $J_{nr,\ diff}$ – tends to decrease with the use of lower rubber contents.

In terms of the parameters of the power models, one may observe that the higher susceptibility of the AC+rubber+PPA to rutting is mainly based on its higher amounts of permanent strain accumulated in the first loading-unloading cycles (i. e., initial strain). The strain rates are also higher for the AC+rubber+PPA than for the AC+rubber, which further contributes to this decrease in the rut resistance. As a consequence of the reductions in the elastic responses under creep and recovery loading, the parameter α shows higher values for the AC+rubber than for the AC+rubber+PPA; however, the correlations between such parameter and the *R100* and *R3200* values are good for the two formulations. In terms of the variations in the model parameters of the AC+rubber and the AC+rubber+PPA with increasing creep time, it can be said that A typically decreases and either B or α commonly increase with loading time for all of them, but the parameter n shows consistent increases with t_F only for the AC+rubber+PPA.

Table 256 – Direct comparisons among the effects of the presence of PPA and the reduction in the crumb rubber content on the rheological properties and parameters of the AC+rubber+PPA

rheological or model parameter	brief description of the effects when moving from the AC+rubber to the AC+rubber+PPA
percent recovery *R*	the recovery values are lower for the AC+rubber+PPA than for the AC+rubber (decrease in the elastic response), and the rates of decrease in this parameter with creep time are higher for the formulation with PPA than for the one without PPA
nonrecoverable compliance J_{nr}	the J_{nr} values of the AC+rubber+PPA are higher than those of the AC+rubber, and they also increase at faster rates for the AC+rubber+PPA when moving from 2.0 to 4.0 s of loading time
percent difference in compliances $J_{nr,\,diff}$	the AC+rubber is always overly stress sensitive, whereas the $J_{nr,\,diff}$ values of the AC+rubber+PPA never exceed 75%
level of elasticity	none of the formulations show a high level of elasticity, i. e., both are graded as "formulations with poor elasticity"
model parameters A, B, n and α	the AC+rubber+PPA shows higher A and B values than the AC+rubber, but the differences among the results are much greater for the initial strain than for the strain rate; the parameter n is higher for the AC+rubber at 100 Pa, and the α values are higher for the AC+rubber+PPA under all the test conditions
variations in the model parameters	the B values always increase with t_F for the AC+rubber and the AC+rubber+PPA, but the rates of increase tend to be higher for the AC+rubber at 8.0 s of loading time; the A values decrease with t_F for the two formulations, except for a threshold at 4.0 s for the AC+rubber+PPA, in which this parameter increases with t_F; it is not clear that nonlinearity increases with creep time for the AC+rubber, but it seems to constantly increase with t_F for the AC+rubber+PPA

SBS-Modified Asphalt Binders. The comparisons made in Table 257 refer to the formulations prepared with the SBS copolymer, that is, the AC+SBS and the AC+SBS+PPA. Differently from the crumb-rubber modified asphalt binders, the presence of PPA is beneficial to the SBS-modified binders because the recoveries increase and the compliances decrease when moving from the AC+SBS to the AC+SBS+PPA, especially for temperatures and creep times up to 64°C and 4.0 s (respectively). At the same time, the stress sensitivity of the original formulation is reduced and the Superpave® requirements for $J_{nr,\,diff}$ are always met for the AC+SBS+PPA (i. e., $J_{nr,\,diff} < 75\%$). The elastomeric characteristics of the SBS modification type (i. e., asymptote values being reached for *R100* at creep times between 2.0 and 8.0 s) may be observed either for the AC+SBS or the AC+SBS+PPA, even though none of the formulations can be graded as "materials with high elasticity".

Table 257 – Direct comparisons among the effects of the presence of PPA and the reduction in the SBS content on the rheological properties and parameters of the AC+SBS+PPA

rheological or model parameter	brief description of the effects when moving from the AC+SBS to the AC+SBS+PPA
percent recovery R	the combination of PPA with SBS typically increased the R values of the binder for $t_F < 4.0$ s and $T \leq 64°C$, but it also increased the sensitivity of this recovery to the application of such longer creep times; in both cases, these recoveries approximately reach asymptote values at creep times from 2.0 to 4.0 s and temperatures from 58 to 64°C, and they continue to decrease at $t_F = 8.0$ s
nonrecoverable compliance J_{nr}	the J_{nr} values are lower for the AC+SBS+PPA than for the corresponding values for the AC+SBS (i. e., a higher degree of stiffness); at the same time, the percentages of increase in J_{nr} are comparable for the two formulations
percent difference in compliances $J_{nr,\ diff}$	the results are considerably lower for the AC+SBS+PPA than for the corresponding test conditions of the AC+SBS; differently from the AC+SBS, the AC+SBS+PPA is not too stress sensitive at any pavement temperature ($J_{nr,\ diff} < 75\%$)
level of elasticity	neither the AC+SBS nor the AC+SBS+PPA can be graded as "materials with high elasticity" in any test condition
model parameters A, B, n and α	the AC+SBS+PPA shows a higher rutting resistance primarily due to the less accumulated strain in the first few cycles (lower A values); the results for B and n are typically higher for the AC+SBS+PPA than for the AC+SBS for temperatures between 52 and 64°C; the α values tend to be lower for the AC+SBS+PPA than for the AC+SBS within these same temperatures
variations in the model parameters	the variations in B, n and α from one formulation to the other are very small (< 8.0%); on the other hand, the A values can be from 45 to 85% lower for the AC+SBS+PPA than for the AC+SBS

In terms of the model parameters A, B, n and α, it can be seen that the AC+SBS+PPA is more rut resistant mainly due to its lower A values (from 45 to 85% lower than those of the AC+SBS). The variations in the other parameters are very small from one binder to the other (< 8.0%), and the results for B and n are slightly higher for the AC+SBS+PPA than for the AC+SBS at temperatures ranging between 52 and 64°C. On the other hand, the α values are typically lower for the AC+SBS+PPA than for the AC+SBS at these same temperatures. In a general context, the synergy between PPA and the major modifier (in this case, SBS) contributed to the preparation of a more rut resistant, more elastic and less stress sensitive formulation than the original one without PPA in the composition. However, this was not enough to reach the zone of "high elasticity" and maybe the use of other compatibilizing agents (e. g., sulfur) could solve such a problem.

SBR-Modified Asphalt Binders. Table 258 addresses the comparisons between the two formulations with SBR studied here, i. e., one with PPA in the composition (AC+SBR+PPA) and the other without PPA (AC+SBR). In a general context, the change from the formulation without PPA to the one with PPA brings several benefits to the asphalt binder because the elastic response tends to be higher and the degree of stiffness is considerably increased, especially in the amounts of initial accumulated strain. At the same time, the stress sensitivity is reduced and the strain rate is only slightly affected. However one main disadvantage of this change in the modification type is the increase in the sensitivity of the rutting and model parameters to the loading time, especially when the pavement temperature is lower than 64°C.

Table 258 – Direct comparisons among the effects of the presence of PPA and the reduction in the SBR content on the rheological properties and parameters of the AC+SBR+PPA

rheological or model parameter	brief description of the effects when moving from the AC+SBR to the AC+SBR+PPA
percent recovery *R*	the *R* values of the AC+SBR+PPA are higher than those of the AC+SBR only at 52 and 58°C and when $t_F < 4.0$ s (the opposite is seen in the remaining test conditions); the AC+SBR+PPA also has a much higher sensitivity to increases in the loading time when compared with the AC+SBR
nonrecoverable compliance J_{nr}	the J_{nr} values of the AC+SBR+PPA are from 20% to 80% lower than the corresponding values of the AC+SBR – the ratios of J_{nr} for the AC+SBR to the AC+SBR+PPA range from 1.2 to 1.8; however, the compliances of the AC+SBR+PPA depict a high sensitivity to increases in the loading time than those of the AC+SBR
percent difference in compliances $J_{nr,\,diff}$	the $J_{nr,\,diff}$ values typically decrease when moving from the AC+SBR to the AC+SBR+PPA; these reductions in $J_{nr,\,diff}$ range from 4.0 to 48.0% in all cases
level of elasticity	neither the AC+SBR nor the AC+SBR+PPA can be graded as “materials with high elasticity” in any test condition
model parameters *A*, *B*, *n* and *α*	the *n* values are slightly higher for the AC+SBR than for the AC+SBR+PPA, but the results do not differ by more than 3% from one material to the other; small differences (< 4% in modulus) can also be seen among the *α* values of both formulations, and they tend to be lower for the AC+SBR+PPA when the temperature does not exceed 64°C; the *A* values of the AC+SBR are from 25 to 75% higher than those of the AC+SBR+PPA (average of 50%); the *B* values do not differ by more than 3.8% in modulus from one formulation to the other
variations in the model parameters	the initial strain (parameter *A*) plays a less important role in the increase in the susceptibility of the AC+SBR+PPA to rutting at the temperatures of 52 and 58°C when compared with the AC+SBR, but this role increases significantly at temperatures of 64°C and higher

In addition to the aforementioned comments, one may observe that the incorporation of PPA was not enough to rank the AC+SBR+PPA as a binder with "high elasticity", similarly to what happened to the AC+SBS+PPA (Table 257). Also, the great degrees of improvement in the rut resistance of the AC+SBR+PPA can be found in the initial accumulated strain (parameter *A*), even though the strain rates (parameter *B*) also contributed a little bit to such improvement. The level of nonlinearity was not profoundly influenced by PPA, but the *n* values tend to be higher for the AC+SBR than for the AC+SBR+PPA. Based on this, it can be concluded that PPA contributed to the preparation of a stiffer and more elastic formulation, as well as to the decrease in the stress sensitivity during load.

EVA-Modified Asphalt Binders. Table 259 reports the comparisons between the AC+EVA+PPA and the AC+EVA for the parameters collected in the MSCR tests and the rheological models (i. e., modified power law equations). One may see that, in a general context, the reduction in the EVA content and the presence of PPA caused some negative impacts on the MSCR parameters of the AC+EVA+PPA, especially when the temperature is lower than 70°C. These impacts can be summarized as follows: (a) reductions in the percent recovery; (b) increases in the nonrecoverable compliances; and (c) increases in the strain rates during the application of loading-unloading cycles. At the same time, the AC+EVA+PPA retains its classification of "formulation with high elasticity" in less test conditions than the AC+EVA, which indicates that the use of smaller amounts of polymer weakened the polymer network in the formulation. One of the advantages of the modification of the base binder with EVA+PPA is that the $J_{nr,\,diff}$ values are decreased at 52, 58 and 64°C, but an opposite picture is seen at 70 and 76°C.

In summary, there are several disadvantages of the modification of the asphalt binder with EVA+PPA when compared with EVA alone. The main advantage of the AC+EVA+PPA over the AC+EVA is the reduced stress sensitivity, but this is not enough to place the AC+EVA+PPA within the group of formulations with reasonable (and acceptable) stress sensitivity. Nonlinearity does not seem to change significantly from one formulation to the other, since the differences within the *n* values are all lower than 1.0% in modulus. As discussed earlier, it is hypothesized that issues related to the chemical composition of the binder (limitation of the mechanisms of action of the EVA copolymer on the properties of the original material, as caused by the incorporation of PPA) may have limited the degrees of improvement in its original rutting parameters and elastic responses. However, it may be important to remind the reader that the results of the AC+EVA+PPA are still positive and promising, and this was confirmed by its performance in the asphalt mixture (Chapter 5) – i. e., either the AC+EVA or the AC+EVA+PPA did not fail in the FN tests.

Table 259 – Direct comparisons among the effects of the presence of PPA and the reduction in the EVA content on the rheological properties and parameters of the AC+EVA+PPA

rheological or model parameter	brief description of the effects when moving from the AC+EVA to the AC+EVA+PPA
percent recovery *R*	the *R* values of the AC+EVA+PPA at temperatures up to 64°C were decreased by at least 20% when compared with those of the AC+EVA; the percent recoveries are higher for the AC+EVA+PPA only at 70 and 76°C, and the opposite is seen at the remaining temperatures
nonrecoverable compliance J_{nr}	the AC+EVA+PPA is more susceptible to rutting ($J_{nr}3200$ values are higher) than the AC+EVA when the temperature is lower than 64°C; this is especially visible when J_{nr} is no greater than 1.0 kPa^{-1} and, for results higher than this upper limit, the differences among the results tend to be reduced
percent difference in compliances $J_{nr,\ diff}$	similarly to the AC+EVA, the AC+EVA+PPA is overly stress sensitive ($J_{nr,\ diff} > 75\%$) in a general context; the $J_{nr,\ diff}$ values are lower for the AC+EVA+PPA than for the AC+EVA at the temperatures of 52, 58 and 64°C, and the opposite is found at 70 and 76°C
level of elasticity	the AC+EVA retains its level of elasticity in many test conditions, except for 8/9 s (58°C) and 2/9 s (64°C); the AC+EVA+PPA is not able to keep its classification as a formulation with "high elasticity" when $t_F > 1.0$ s and $T > 58$°C
model parameters *A*, *B*, *n* and *α*	the *α* values are greater for the AC+EVA+PPA than for the AC+EVA, with only a few exceptions; the level of nonlinearity (*n*) is smaller for the AC+EVA+PPA than for the AC+EVA once that the polymeric network does not suffer extensive damage and/or is melted at very high temperatures ($T > 64$°C); the *A* values are lower for the AC+EVA+PPA than for the AC+EVA, but the opposite is typically seen for the *B* values; the level of elastic response seems to be lower for the AC+EVA+PPA than for the AC+EVA
variations in the model parameters	the *A* values tend to decrease faster for the AC+EVA+PPA with loading time than for the AC+EVA, and this can be seen at all the test temperatures; the *B* values always increase with creep time for the AC+EVA+PPA and are typically greater for this formulation than for the AC+EVA; the differences between the *n* values are no greater than 1% in modulus at 70 and 76°C because the role of EVA on the response of the asphalt binder is greatly minimized

PE-Modified Asphalt Binders. Table 260 provides the comparisons between the results of the AC+PE+PPA and the AC+PE according to their MSCR testing parameters and model parameters. Differently from the EVA copolymer, the addition of PPA offers major benefits to the PE-modified asphalt binder due to the increased recoveries, decreased compliances and lower stress sensitivity under many test conditions (despite some exceptions at 8/9 s). In other words, the AC+PE+PPA is more resistant to rutting and depicts higher levels of elastic response than the AC+PE, as well as a lower sensitivity to an increase in the stress level during the MSCR tests. In terms of the model parameters, this can be translated into lower accumulated strains in the first few loading-unloading cycles (lower *A* values) and lower strain rates (*B* values) for some testing conditions. The AC+PE+PPA also shows a different pattern of response with increasing loading time – up to a maximum value of 4.0 s – when compared with the AC+PE, i. e., the *A* values decrease and the *B* values become greater with increasing t_F. Both parameters increase for the AC+PE at longer creep times, which suggests a high susceptibility to rutting in more critical loading conditions.

Table 260 – Direct comparisons among the effects of the presence of PPA and the reduction in the PE content on the rheological properties and parameters of the AC+PE+PPA

rheological or model parameter	brief description of the effects when moving from the AC+PE to the AC+PE+PPA
percent recovery *R*	the addition of PPA contributed to the presence of higher recoveries in the AC+PE+PPA when compared with the AC+PE, especially at 3,200 Pa; while the increases at 100 Pa are mainly restricted to 52 and 58°C, the ones at 3,200 Pa cover all the non-null values of the AC+PE
nonrecoverable compliance J_{nr}	the compliances are typically lower for the AC+PE+PPA than for the AC+PE; although J_{nr} seems not to markedly differ from one binder to the other when the values are lower than 0.3 kPa^{-1}, the results are still better for the AC+PE+PPA than for the AC+PE
percent difference in compliances $J_{nr,\,diff}$	the AC+PE+PPA is less stress sensitive than the AC+PE for creep times up to 4.0 s, and the opposite is seen at t_F = 8.0 s; the nonlinear response of the AC+PE+PPA is more pronounced only at very long creep times, which is when the maximum value of 75% is exceeded
level of elasticity	neither the AC+PE nor the AC+PE+PPA can be graded as “materials with high elasticity” in any test condition
model parameters *A*, *B*, *n* and α	the initial strains (*A* values) in the AC+PE+PPA are lower than those of the AC+PE for the same temperature, creep time and stress level; the *B* values are approximately the same for the two formulations in all cases, even though some of the results are slightly lower for the AC+PE+PPA than for the AC+PE; the α values are also lower for the AC+PE+PPA, and the *n* values tend to be a little bit higher for the AC+PE with only a few exceptions
variations in the model parameters	the AC+PE+PPA tends to show a rutting response more commonly found in formulations with a quite high rutting resistance when t_F < 4.0 s: the initial strain (*A* values) decreases, the strain rate (*B* values) increases and nonlinearity (*n* values) shows marginal variations with increasing t_F; this can be interpreted as a great advance in the rutting performance of the AC+PE+PPA when compared with the AC+PE, for which either *A* or *B* increase when t_F becomes higher

Summary of Findings and Correlations with Mixture Data. In conclusion, it can be stated that PPA provides several benefits to the formulations with PE, SBS, SBR and the base asphalt binder, as well as a higher level of workability to the Elvaloy-modified material. These benefits are mainly associated with higher R values and lower J_{nr} values and, in some cases, lower $J_{nr,\ diff}$ values are also observed. The exceptions include the formulations with crumb rubber and EVA, for which opposite phenomena can be seen (i. e., increases in the susceptibility to rutting and lower degrees of elasticity under creep and recovery loading). Although the stress sensitivity is reduced either for the AC+rubber or the AC+EVA and the AC+EVA+PPA still holds its classification as a "binder with high elasticity" in some particular cases, this is not enough to compensate for the deficiencies in the other MSCR testing parameters. It is believed that the lower crumb rubber contents in the AC+rubber+PPA and the chemical issues concerning the EVA copolymer and PPA in the AC+EVA+PPA may explain the limitations of these two formulations (AC+rubber+PPA and AC+EVA+PPA) when compared to their corresponding ones without PPA.

Finally, a complementary analysis was carried out to investigate whether the $J_{nr}3200$ values of the asphalt binders that failed in the mixture tests – not including the AC+PPA due to the explanations given in Chapter 5 – show good or poor correlations with F_N at longer creep times (2/9, 4/9 and 8/9 s). This could be a starting point to see if such creep times may replace the use of very high stress levels in the MSCR tests, as well as to reach conclusions about the suitability of the proportion of 1:10 between the creep times in the mixture and the binder tests (respectively) in correlating the rutting phenomenon in the binder with the one in the mixture. For the reader's convenience, Table 261 groups all the $J_{nr}3200$ values of the asphalt binders at 64°C and 3.2 kPa and the above-cited pairs of creep-recovery times, together with their F_N values.

Table 261 – Nonrecoverable compliances of the selected asphalt binders at 3.2 kPa ($J_{nr}3200$) and 64°C and three pairs of creep-recovery times (2/9, 4/9 and 8/9 s) to be correlated with their corresponding flow number values (F_N)

asphalt binder	F_N (cycles)	$J_{nr}3200$ values (kPa^{-1}) in each test condition		
		2/9 s	4/9 s	8/9 s
base binder (AC)	2,167	6.694	13.153	28.397
AC+Elvaloy+PPA	7,050	0.761	1.520	2.706
AC+rubber+PPA	4,191	2.209	4.883	9.680
AC+SBS	4,991	1.949	4.114	9.202
AC+SBS+PPA	6,110	1.367	2.541	5.521
AC+SBR	3,312	2.318	4.941	10.189
AC+SBR+PPA	5,875	1.434	3.408	7.592

The resulting correlations between $J_{nr}3200$ at longer creep times and the corresponding F_N values of the asphalt binders are provided in Figure 213. By comparing these results with the correlation for the original creep-recovery times of 1/9 s (0.7044, see Figure 36 in page 116), one may conclude that R^2 was improved by 3.2% when the creep time was doubled from 1.0 to 2.0 s (0.7266) and by 8.2% (from 0.7044 to 0.7621) when it was multiplied by four in the MSCR test. Surprisingly, this correlation was decreased by 2.5% (from 0.7621 to 0.7431) when the loading time was doubled from 4.0 to 8.0 s. This is an indication that more severe loading conditions in the MSCR tests (in this case, application of loads for longer periods of time) may be closer to the actual performance of the asphalt mixture in the laboratory tests and the total amount of permanent strain in it. It is suggested that better correlations between binder and mixture data may be obtained not only by increasing the applied stress, but also by keeping the stress level unchanged and increasing the duration of the application of the load in the sample.

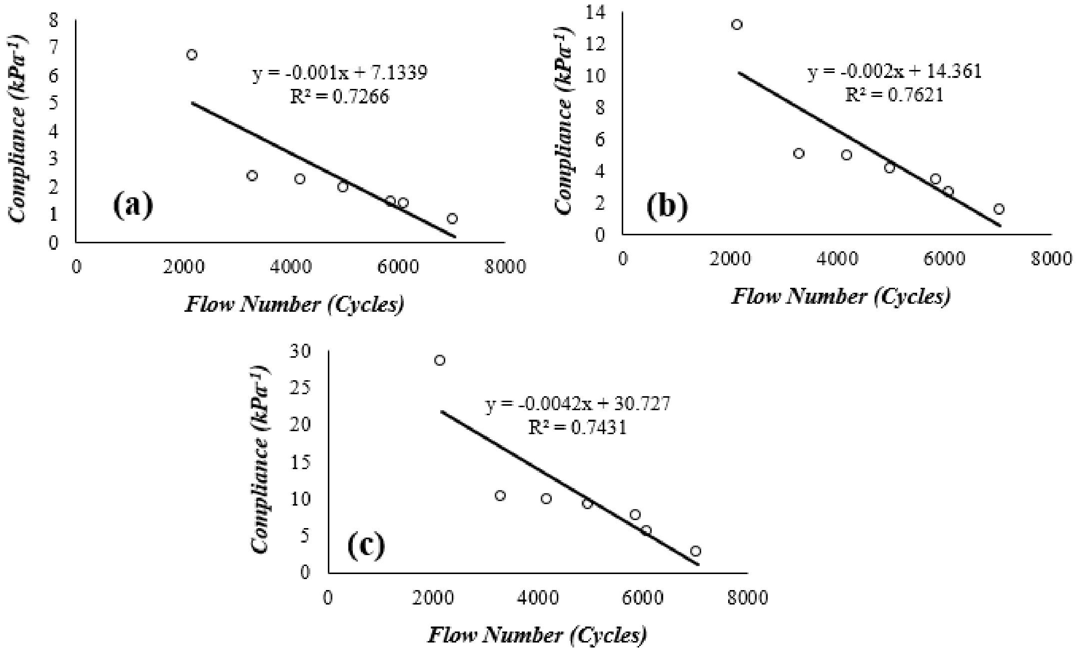

Figure 213 – Levels of correlation between the nonrecoverable compliances of the selected asphalt binders at 64°C and 3.2 kPa and their corresponding flow number values for the creep-recovery times of (a) 2/9 s; (b) 4/9 s; and (c) 8/9 s

As shown earlier, increases in the applied stress have been taken by several researchers as an option to get closer to the actual stresses and strain levels observed in the mixture during creep and recovery. However, this is not a general rule because others also found good correlations for the standardized stress level of 3,200 Pa, refer to Behnood et al. (2016) and Hafeez and Kamal (2014) as examples. Hence, it can be pointed out that one target characteristic of the response of the binder that must be achieved in the rheological tests is the steady state. The MSCR and mixture tests conducted here and in the paper by Behnood et al. (2016) were the standardized ones and, in both cases, the correlations were of about 0.70. Golalipour (2011) and Golalipour et al. (2016) considered the role of steady state on the outcomes of the MSCR tests at 100 and 3,200 Pa, and they observed that the correlations improved when compared with the original protocol (calculations of $J_{nr}100$ and $J_{nr}3200$ based on all the creep-recovery cycles). Thus, it seems that binder data close to the steady state of the material will provide better correlations with the data collected from the accelerated mixture rutting tests.

One interesting aspect of the discussion about the steady state condition of the asphalt binder is that it may not necessarily be associated with the applied stress. This conclusion might be raised by reading the paper from Delgadillo et al. (2006a), where the authors obtained excellent correlations ($R^2 > 0.94$) between mixture data after 5,000 cycles at 46°C and binder data after 100 cycles at 46°C regardless of the stress level (25 or 10,000 Pa). It can be said that a stress level of 25 Pa is very small to reach nonlinearity in several binders, including the modified ones (DELGADILLO et al., 2006b). In addition, the original report from Bahia et al. (2001a) concluded that most binders can reasonably reach steady state after 50 cycles of creep and recovery, even at stress levels no greater than 300 Pa. Based on this, one can imply that the achievement of the steady state condition in the asphalt binder is a mandatory factor in the establishment of better correlations with mixture rutting data sets.

It is not a great surprise at all if one realizes that the excellent correlation between G_V and F_N reported in Chapter 5 (0.9255, Figure 36 in page 116) is due to a more proper consideration of the steady state phenomenon in the results of the binder. As previously described in Chapter 4 (see page 103), only the last two creep-recovery cycles at 100 Pa were used in the determination of the G_V values. As a consequence, the binder is closer to the steady state condition from the point of view of G_V than from $J_{nr}100$ and $J_{nr}3200$ (the last 10 creep-recovery cycles). The increases in the creep times in all cycles may have speeded up the process to achieve steady state by increasing the total accumulated strain in the sample, even for a reduced number of cycles. In other words, the binder more closely approaches steady state at 2/9 s and 4/9 s than at 1/9 s, and this may have contributed to the increase in the R^2 values. It is believed that the slight decrease in R^2 at 8/9 s may be attributed to the increased role of nonlinearity on the rheological response of the asphalt binder, which is rather complicated to be precisely measured and predicted from quite simple mathematical parameters such as J_{nr} (WASAGE et al., 2011).

Rankings of Asphalt Binders. One last part of the investigation about the role of longer creep times on the rheological parameters of the modified asphalt binders in the MSCR tests is associated with their rankings – or relative positions – under each test condition. The use of these rankings is relatively common in the literature (D'ANGELO et al., 2007; LAUKKANEN et al., 2015; MARTINS et al., 2011; TABATABAEE and TEYMOURPOUR, 2010; VERDADE, 2015; WALUBITA et al.; 2013; ZHANG et al., 2015), and they aim at showing the relative degrees of stiffness of each formulation when compared with others. As a consequence, the best and worst formulations according to a predefined binder parameter can be seen and the most appropriate modifiers for each application may be chosen.

Since rutting is the central focus of the present dissertation, the two MSCR parameters mostly associated with this phenomenon were selected: (a) the nonrecoverable creep compliance J_{nr}; and (b) the percent difference in compliances $J_{nr,\ diff}$. The former is directly related to the stiffness of the formulation and is officially used on Superpave® to address and evaluate rutting on binders, whereas the latter provides an idea of the rutting potential of the material under unexpected temperatures and/or loading levels (i. e., an indirect estimation of rutting) and is also officially used in the Superpave® specification. As previously reported, elasticity is not a major factor in the control of the amount of rutting in the asphalt binder when compared with viscosity (ARSHADI, 2013; GOLALIPOUR, 2011). Therefore, it was decided to take into account only the results of the parameters specifically related to viscosity (J_{nr} and $J_{nr,\ diff}$). Another reason why the R values were not evaluated in the rankings is that several binders depict null recoveries at 64, 70 and 76°C, and this could create distortions in the final results. In addition, the base binder was not included in the comparisons because its PG grade (64-xx) is different from the ones of the modified binders (76-xx).

To simplify the notations and interpretations of the outputs of such rankings, each formulation received a unique abbreviation that was used throughout the forthcoming tables. These abbreviations include the letters “A” (for PPA), “B” (for crumb rubber), “EV” (for EVA), “S” (for SBS), “SB” (for SBR), “E” (for Elvaloy®) and “P” (for PE). If PPA is used in the preparation of the formulation, the letter “A” was used together with another abbreviation. For example, the AC+Elvaloy+PPA was hereafter labeled as “EA” – “E” from Elvaloy® and “A” from PPA – in this section. Similarly, the AC+EVA+PPA was hereafter labeled as “EVA” – “EV” from EVA and “A” from PPA – and so on. Obviously, formulations with only one modifier were labeled as a single abbreviation (e. g., “P” for the AC+PE and “S” for the AC+SBS).

Table 262 shows the rankings of the 12 formulations at the temperature of 52°C and based on the $J_{nr}100$ and $J_{nr}3200$ values, together with their corresponding CV’s. The average positions of each material are shown in Figure 214. It can be inferred from the data that the AC+EVA and the AC+PPA are ranked as the most rut resistant materials in a general context (that is, 100 and 3,200 Pa), followed by the AC+EVA+PPA, the AC+PE+PPA, the AC+Elvaloy+PPA, the AC+PE, the AC+SBS+PPA, the AC+rubber, the AC+SBR+PPA, the AC+SBS, the

AC+rubber+PPA, and the AC+SBR. In other words, the plastomeric modification types (i. e., with EVA and PE) show a better rutting performance than the elastomeric modification ones (i. e., SBS and SBR). The AC+Elvaloy+PPA also depicts a quite promising performance, together with the AC+PPA. Overall the results at 100 and 3,200 Pa do not show great variations between them for several binders, with exception of some binders such as the AC+Elvaloy+PPA, the AC+rubber and the AC+EVA+PPA.

Table 262 – Rankings of the modified asphalt binders based on $J_{nr}100$ and $J_{nr}3200$ at the temperature of 52°C – individual and corresponding coeffients of variation (CV, in percentage)

formulation[b]	rankings at 100 Pa[a]					rankings at 3,200 Pa[a]				
	1/9 s	2/9 s	4/9 s	8/9 s	**CV**	1/9 s	2/9 s	4/9 s	8/9 s	**CV**
A	3	2	3	3	**15.7**	2	2	2	2	**0.0**
EA	6	6	5	4	**15.8**	5	5	3	3	**25.0**
B	4	7	6	7	**20.4**	9	9	9	10	**4.7**
BA	10	10	12	11	**7.7**	10	10	12	11	**7.7**
S	11	11	10	10	**4.8**	11	11	10	9	**8.1**
SA	8	8	7	6	**11.4**	7	7	6	6	**7.7**
EV	1	1	1	1	**0.0**	1	1	1	1	**0.0**
EVA	2	3	2	2	**19.2**	3	4	5	4	**17.7**
P	7	5	8	8	**17.5**	6	6	7	7	**7.7**
PA	5	4	4	5	**11.1**	4	3	4	5	**17.7**
SB	12	12	11	12	**3.7**	12	12	11	12	**3.7**
SBA	9	9	9	9	**0.0**	8	8	8	8	**0.0**

[a] each number refers to the relative position of the formulation in a ranking from the less (No. 1) to the most susceptible to rutting (No. 12).
[b] "A" = PPA; "E" = Elvaloy®"; "B" = crumb rubber; "S" = SBS copolymer; "EV" = EVA copolymer; "P" = low-density PE; "SB" = SBR copolymer.

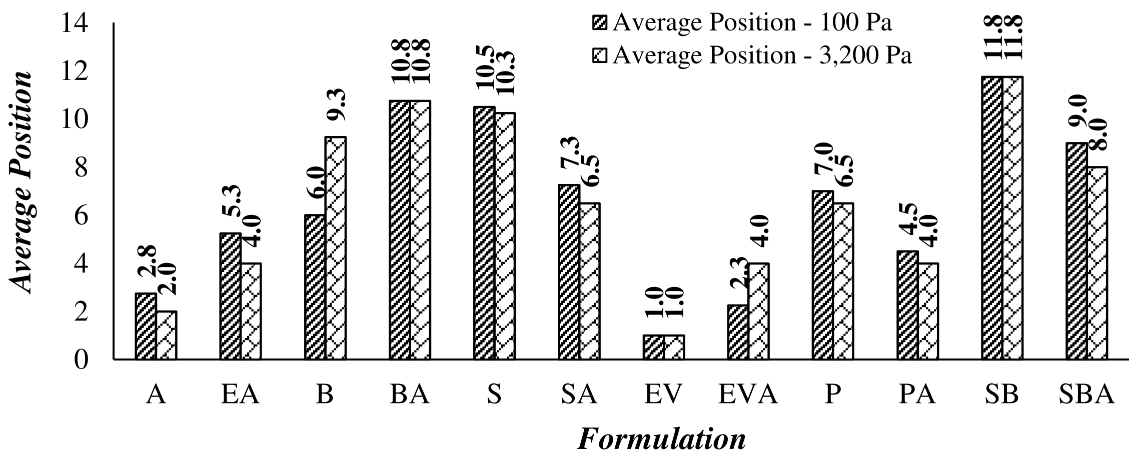

Figure 214 – Average positions of the PG 76-xx formulations at the temperature of 52°C and all the creep-recovery times and stress levels, as based on their J_{nr} values

The great decreases in the average position of the AC+Elvaloy+PPA from 100 to 3,200 Pa (i. e., from 5.3 to 4.0) may be explained by the previously-cited system comprised by asphalt and polymer, which contributes to an increase in the overall elastic response of the material and does not seem to be seriously affected by the application of loads in the MSCR tests. In other words, the other formulations show greater increases in J_{nr} with loading time – especially at 3,200 Pa – and this in turn leads to better positions for the AC+Elvaloy+PPA (lower increases in J_{nr}). With respect to the AC+EVA+PPA, the decreases in the relative positions of the material – from 2.3 to 4.0 – are possibly associated with the accumulation of damage in the polymer network and the high stress sensitivity of the material. This amount of damage does not seem to be very high for the AC+EVA at 52°C, since the position of the binder is always the same (No. 1) regardless of the test condition. Finally, the AC+rubber becomes more susceptible to rutting at 3,200 Pa in a relative context mainly due to its extremely high stress sensitivity, which was not the case of the AC+rubber+PPA (exactly the same average position at 100 and 3,200 Pa).

Table 263 reports the individual rankings and corresponding CV's for all the studied formulations at the temperature of 58°C, whereas Figure 215 shows the average positions of each binder at 100 and 3,200 Pa. Again, the three formulations with the highest resistances to rutting are the AC+EVA, the AC+PPA and the AC+Elvaloy+PPA (in this order) and the ones with the lowest resistances are the AC+SBS, the AC+rubber+PPA and the AC+SBR (also in this order). The other formulations are ranked from the highest to the lowest rut resistance as follows: AC+EVA+PPA, AC+PE+PPA, AC+SBS+PPA, AC+PE, AC+rubber and AC+SBR+PPA. It can also be pointed out that, similarly to the temperature of 52°C, the binders with PPA in the composition typically receive better positions in the rankings than those without PPA except for the AC+rubber+PPA (the poorest resistance, together with the AC+SBR) and the AC+EVA+PPA.

Another remarkable feature of the individual rankings at 100 and 3,200 Pa is that the AC+Elvaloy+PPA shows a considerable degree of improvement in its average position after the increase in the stress level (from 3.8 to 2.0), and the opposite can be said for the AC+EVA+PPA (from 2.0 to 5.3) and the AC+rubber (from 5.8 to 9.0). The AC+PE+PPA and the AC+SBR+PPA may be included in this discussion as well, even though its changes were minor when compared with the other cited binders. The reasons for these variations remain essentially the same, i. e., (a) the asphalt-polymer system in the AC+Elvaloy+PPA contributed to a lower relative rate of increase in J_{nr} with creep time; (b) the levels of damage in the polymer network of the AC+EVA+PPA were sufficiently great to place its rutting resistance at much lower levels; and (c) the stress sensitivity of the AC+rubber was responsible for the drops in the rutting resistance of the formulation at 3,200 Pa when compared with 100 Pa.

Table 263 – Rankings of the modified asphalt binders based on $J_{nr}100$ and $J_{nr}3200$ at the temperature of 58°C – individual and corresponding coeffients of variation (CV, in percentage)

formulation[b]	rankings at 100 Pa[a]					rankings at 3,200 Pa[a]				
	1/9 s	2/9 s	4/9 s	8/9 s	**CV**	1/9 s	2/9 s	4/9 s	8/9 s	**CV**
A	3	3	3	4	**13.3**	2	2	3	2	**19.2**
EA	4	4	4	3	**11.5**	3	3	1	1	**50.0**
B	5	6	5	7	**14.4**	9	9	8	10	**7.9**
BA	11	12	12	12	**3.7**	10	11	12	11	**6.4**
S	10	10	10	8	**9.1**	11	10	10	9	**7.1**
SA	7	9	7	6	**15.0**	7	7	6	4	**20.4**
EV	1	1	1	1	**0.0**	1	1	2	3	**47.4**
EVA	2	2	2	2	**0.0**	5	6	5	5	**8.2**
P	8	5	8	9	**20.0**	6	5	9	8	**22.6**
PA	6	7	6	5	**11.8**	4	4	4	6	**19.2**
SB	12	11	11	11	**3.8**	12	12	11	12	**3.7**
SBA	9	8	9	10	**7.9**	8	8	7	7	**6.7**

[a] each number refers to the relative position of the formulation in a ranking from the less (No. 1) to the most susceptible to rutting (No. 12).
[b] "A" = PPA; "E" = Elvaloy®"; "B" = crumb rubber; "S" = SBS copolymer; "EV" = EVA copolymer; "P" = low-density PE; "SB" = SBR copolymer.

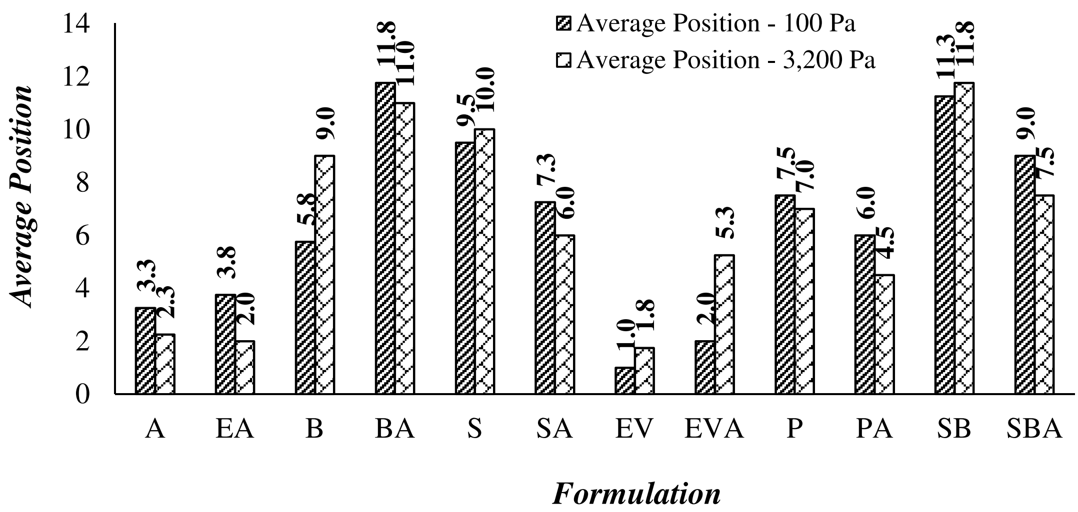

Figure 215 – Average positions of the PG 76-xx formulations at the temperature of 58°C and all the creep-recovery times and stress levels, as based on their J_{nr} values

Although it is not very visible, the polymeric network in the AC+EVA may have been accumulating damage at 3,200 Pa at quite representative levels for creep times longer than 2.0 s. This may explain why the individual position of the material decreases from 1 to 3 when moving from the standardized to the longest loading time (Table 263). At the same time, the AC+Elvaloy+PPA follows the opposite pattern – from 3 to 1 – and occupies the position of the

AC+EVA as the most rut resistant binder within the selected group of materials. It is suggested that the better positions gained by the AC+PE+PPA and the AC+SBR+PPA at 3,200 Pa may be explained by the exchange of their original classifications with other asphalt binders in the rankings, e. g., the AC+SBS and the AC+SBR.

Table 264 provides the rankings and coefficients of variation for all the studied formulations at the temperature of 64°C. The AC+EVA is replaced by the AC+PE+PPA in the list of the three most rut resistant formulations at such pavement temperature, but the AC+Elvaloy+PPA and the AC+PPA still remain as very resistant materials to rutting. The AC+SBS still belongs to the list of less resistant materials together with the AC+SBR and the AC+rubber+PPA. As previously explained, the polymeric networks within the binder phase of the AC+EVA have already started to show damage at 4/9 s and 8/9 s and the temperature of 58°C, and this seems to be aggravated at a much higher pavement temperature (i. e., 64°C). As a consequence, it is hypothesized that the slightly better positions for the AC+EVA+PPA at 100 Pa are due to the presence of PPA in the formulation. The AC+rubber depicts a considerable decrease in its rutting resistance from 100 to 3,200 Pa (from 4.0 to 7.5), and the same can be said for the AC+EVA (from 3.8 to 8.3) and the AC+EVA+PPA (from 5.3 to 8.3).

Table 264 – Rankings of the modified asphalt binders based on $J_{nr}100$ and $J_{nr}3200$ at the temperature of 64°C – individual and corresponding coeffients of variation (CV, in percentage)

formulation[b]	rankings at 100 Pa[a]					rankings at 3,200 Pa[a]				
	1/9 s	2/9 s	4/9 s	8/9 s	**CV**	1/9 s	2/9 s	4/9 s	8/9 s	**CV**
A	2	1	4	2	**48.4**	2	2	2	2	**0.0**
EA	1	3	1	1	**57.7**	1	1	1	1	**0.0**
B	3	5	2	6	**39.5**	8	9	5	8	**20.0**
BA	12	12	12	12	**0.0**	11	11	11	11	**0.0**
S	9	9	10	10	**5.3**	9	10	9	10	**5.3**
SA	4	10	7	7	**30.3**	4	5	4	3	**17.7**
EV	5	2	5	3	**34.6**	7	7	10	9	**15.7**
EVA	10	4	3	4	**52.8**	12	8	8	5	**30.2**
P	6	6	9	9	**20.0**	5	3	7	7	**30.2**
PA	7	7	6	5	**13.3**	3	4	3	4	**14.3**
SB	11	11	11	11	**0.0**	10	12	12	12	**7.5**
SBA	8	8	8	8	**0.0**	6	6	6	6	**0.0**

[a] each number refers to the relative position of the formulation in a ranking from the less (No. 1) to the most susceptible to rutting (No. 12).

[b] "A" = PPA; "E" = Elvaloy®"; "B" = crumb rubber; "S" = SBS copolymer; "EV" = EVA copolymer; "P" = low-density PE; "SB" = SBR copolymer.

In a general context (i. e., by including all the data at 100 and 3,200 Pa), the final list of binders from the less to the most susceptible to rutting is the following: AC+Elvaloy+PPA, AC+PPA, AC+PE+PPA, AC+SBS+PPA, AC+rubber, AC+EVA, AC+PE, AC+EVA+PPA, AC+SBR+PPA, AC+SBS, AC+SBR and AC+rubber+PPA. Again, the formulations with PPA and a polymer in the composition typically provide higher resistances to rutting than those without PPA, similarly to what was reported in previously published studies (e. g., CLYNE et al., 2012; DOMINGOS and FAXINA, 2015a, 2015b; ONOFRE et al., 2013). The drops in the rankings of the AC+EVA and the AC+EVA+PPA from 100 to 3,200 Pa (see Figure 216) are specially associated with the damaging effects of loading time and high stresses and temperatures on their polymer networks. No marked changes in the positions of the AC+Elvaloy+PPA, the AC+rubber+PPA, the AC+SBS, the AC+SBR and the AC+PPA were observed, which may be attributed to their reduced stress sensitivity (relatively low $J_{nr,\ diff}$ values).

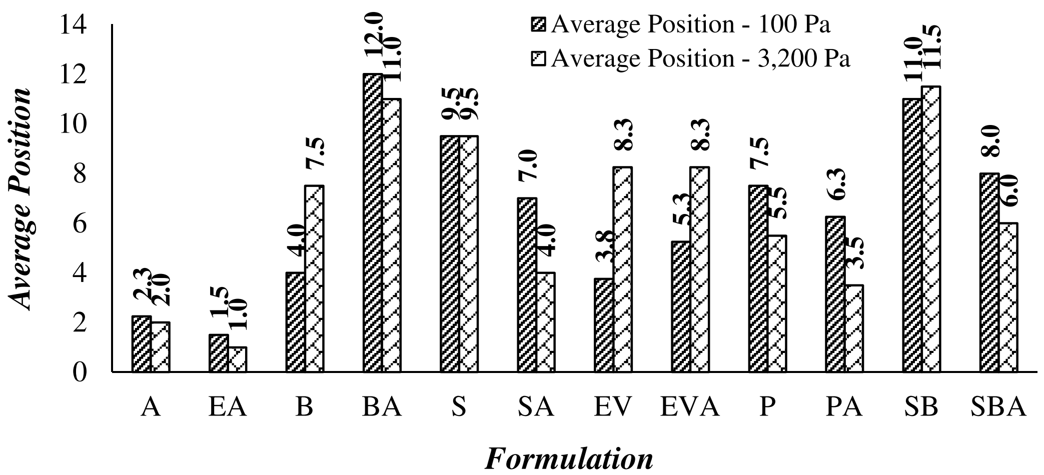

Figure 216 – Average positions of the PG 76-xx formulations at the temperature of 64°C and all the creep-recovery times and stress levels, as based on their J_{nr} values

In addition to the AC+SBS+PPA and the AC+SBR+PPA, the presence of PPA may also have contributed to improve the positions of the AC+PE+PPA at longer creep times when moving from 100 to 3,200 Pa. In other words, the formulations with PPA were able to hold their rutting resistances at longer creep times either by the interaction between PPA and the main modifier – especially Elvaloy®, SBS or SBR – or by modifying the original properties of the binder when used alone in the composition (AC+PPA). One more time, the AC+rubber depicted substantial increases in its average position after the increase in the stress level due to the very high $J_{nr,\ diff}$ values, regardless of the testing condition (Table 107, page 246). It is interesting to note that the rankings of the AC+EVA and the AC+EVA+PPA with increasing t_F are reversed (i. e., the positions of the AC+EVA become worse and those of the AC+EVA+PPA become better at longer creep times), either at 100 or at 3,200 Pa. This is one more evidence of the extent of damage inflicted to the polymer network of the AC+EVA with increasing severity in the MSCR tests, which possibly takes place in the AC+EVA+PPA at lower speeds.

Table 265 shows the positions of the modified asphalt binders at the high pavement temperature of 70°C. The overall ranking of formulations at this temperature is the following (in a descending order of rutting resistance): AC+Elvaloy+PPA, AC+PPA, AC+rubber, AC+PE+PPA, AC+SBS+PPA, AC+PE, AC+SBR+PPA, AC+EVA+PPA, AC+SBS, AC+EVA, AC+SBR and AC+rubber+PPA. By comparing this ranking with those reported for the other temperatures, one may observe that the AC+rubber replaced the AC+PE+PPA and the AC+EVA in the group of the most resistant materials and this same AC+EVA now belongs to the group of less rut resistant materials, together with the AC+SBR and the AC+rubber+PPA. As the comparisons suggest, the AC+EVA suffered a great loss of resistance at 70°C due to reasons that have been discussed earlier in this section. In addition, the tendency of the formulations with PPA in depicting higher resistances to rutting than the corresponding ones without PPA remained unchanged, and the EVA-modified binders may be included in the comparisons as well.

Table 265 – Rankings of the modified asphalt binders based on $J_{nr}100$ and $J_{nr}3200$ at the temperature of 70°C – individual and corresponding coeffients of variation (CV, in percentage)

formulation[b]	rankings at 100 Pa[a]					rankings at 3,200 Pa[a]				
	1/9 s	2/9 s	4/9 s	8/9 s	**CV**	1/9 s	2/9 s	4/9 s	8/9 s	**CV**
A	3	2	3	2	**20.0**	2	2	2	4	**34.6**
EA	1	1	2	1	**34.6**	1	1	1	1	**0.0**
B	2	3	1	4	**44.7**	7	7	5	5	**16.7**
BA	10	12	12	11	**7.4**	10	11	11	10	**4.8**
S	8	9	11	12	**15.8**	8	9	10	11	**11.8**
SA	4	8	6	6	**23.6**	4	5	4	3	**17.7**
EV	12	11	10	10	**7.7**	11	10	9	9	**8.5**
EVA	11	5	4	5	**44.4**	12	8	7	6	**27.6**
P	5	4	8	8	**28.6**	6	3	8	7	**31.2**
PA	7	7	5	3	**30.2**	3	4	3	2	**23.6**
SB	9	10	9	9	**4.7**	9	12	12	12	**11.5**
SBA	6	6	7	7	**7.7**	5	6	6	8	**17.4**

[a] each number refers to the relative position of the formulation in a ranking from the less (No. 1) to the most susceptible to rutting (No. 12).
[b] "A" = PPA; "E" = Elvaloy®"; "B" = crumb rubber; "S" = SBS copolymer; "EV" = EVA copolymer; "P" = low-density PE; "SB" = SBR copolymer.

The average positions of the formulations, as shown in Figure 217, indicate that the variations within the results at 100 and 3,200 Pa are not considerable except for the AC+rubber (from 2.5

to 6.0), the AC+SBS+PPA (from 6.0 to 4.0), the AC+EVA+PPA (from 6.3 to 8.3) and the AC+PE+PPA (from 5.5 to 3.0). The increases in the susceptibility of the AC+rubber and the AC+EVA+PPA to rutting when moving from 100 to 3,200 Pa in the MSCR test were discussed above, and the same reason reported for the AC+EVA+PPA (i. e., damage in the polymer network) may be applied to the AC+SBR as well. The variations in the other mean values may be attributed to a natural interchange among the individual positions of the binders.

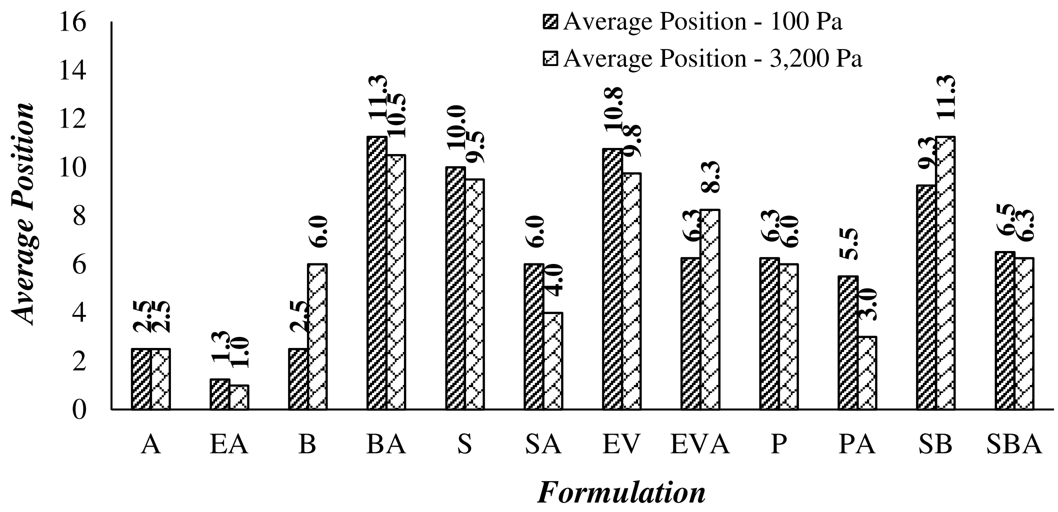

Figure 217 – Average positions of the PG 76-xx formulations at the temperature of 70°C and all the creep-recovery times and stress levels, as based on their J_{nr} values

The data summarized in Table 266 refer to the positions of each formulation at the highest test temperature (76°C) and all creep-recovery times and stress levels. Similarly to the previously studied temperatures, the three most rut resistant binders include the AC+Elvaloy+PPA, the AC+PPA and the AC+rubber (in this order), followed by the AC+PE+PPA. On the other hand, the less rut resistant ones include the AC+EVA, the AC+rubber+PPA, the AC+SBS and the AC+SBR (exactly in this order). The intermediate binders include the following (from the highest to the lowest rutting resistance): AC+SBS+PPA, AC+SBR+PPA, AC+PE and AC+EVA+PPA. In other words, the groups of binders based on their rutting potential – higher or lower – were not markedly changed from the previous temperatures to the current one and the major distinctions among them can be seen in the individual positions of each material within these groups.

It is quite interesting to note that the AC+PPA suffers a massive drop in its relative position when moving from 4.0 to 8.0 s of loading time at 3,200 Pa (from about 2-4 to 12). This is associated with the boost in the $J_{nr}3200$ value of the material by moving from 4/9 s to 8/9 s (Figure 77, page 209), as well as its $J_{nr,\,diff}$ value of almost 300% at 8/9 s (Table 78, page 211). The average positions plotted in Figure 218 closely resemble those obtained at 70°C, especially with respect to the relatively high increases in the positions of the AC+rubber, the AC+EVA+PPA and the AC+SBR when moving from 100 to 3,200 Pa. The key difference between the two figures is the boost in the average position of the AC+PPA from 2.5 to 5.0 with increasing stress level, which is known to be caused by the stress sensitivity and the level of nonlinearity of the material at the creep time of 8.0 s and the temperature of 76°C.

Table 266 – Rankings of the modified asphalt binders based on $J_{nr}100$ and $J_{nr}3200$ at the temperature of 76°C – individual and corresponding coeffients of variation (CV, in percentage)

formulation[b]	rankings at 100 Pa[a]					rankings at 3,200 Pa[a]				
	1/9 s	2/9 s	4/9 s	8/9 s	**CV**	1/9 s	2/9 s	4/9 s	8/9 s	**CV**
A	3	2	3	2	**20.0**	2	2	4	12	**82.5**
EA	1	1	2	1	**34.6**	1	1	1	1	**0.0**
B	2	3	1	4	**44.7**	7	7	3	4	**34.0**
BA	11	11	11	10	**4.0**	9	10	11	8	**11.8**
S	8	12	12	12	**15.7**	10	11	10	10	**4.2**
SA	4	8	6	5	**25.7**	5	6	5	2	**33.3**
EV	12	9	9	9	**13.3**	8	8	7	5	**17.5**
EVA	10	5	5	6	**31.7**	12	9	8	7	**20.8**
P	6	4	8	8	**25.5**	6	3	9	6	**35.4**
PA	7	7	4	3	**34.0**	3	4	2	3	**23.6**
SB	9	10	10	11	**7.1**	11	12	12	11	**4.3**
SBA	5	6	7	7	**13.3**	4	5	6	9	**31.2**

[a] each number refers to the relative position of the formulation in a ranking from the less (No. 1) to the most susceptible to rutting (No. 12).
[b] "A" = PPA; "E" = Elvaloy®"; "B" = crumb rubber; "S" = SBS copolymer; "EV" = EVA copolymer; "P" = low-density PE; "SB" = SBR copolymer.

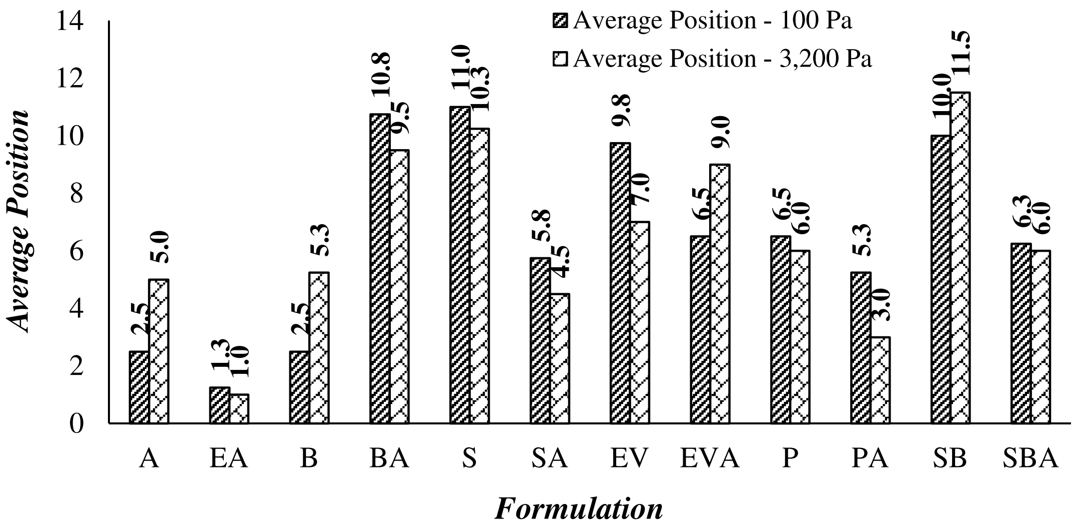

Figure 218 – Average positions of the PG 76-xx formulations at the temperature of 76°C and all the creep-recovery times and stress levels, as based on their J_{nr} values

To show a general picture of the relative resistances of the 12 formulations studied in the present dissertation, Figure 219 was prepared. This figure contains the final average positions for each material, i. e., the mean values of all their individual positions reported from Table 262 to Table 266. As can be seen, the binders with the worst positions in the rankings are those prepared with elastomers and without PPA (AC+SBS and AC+SBR) and the crumb-rubber-modified material with a lower rubber content (AC+rubber+PPA). It also reinforces the opinion that the presence of PPA in these elastomeric-modified binders yields much better positions for them – and thus higher positions in the rankings. In contrast, the AC+PPA and the AC+Elvaloy+PPA are commonly graded as very rut resistant formulations together with the AC+rubber (100 Pa) and the AC+PE+PPA (3,200 Pa) – i. e., one binder modified with a plastomer and PPA and the other containing a higher rubber content. The other materials receive intermediate positions within the groups of binders, as can be inferred from the complete rankings shown below (from the lowest to the highest rutting potential):

- AC+Elvaloy+PPA, AC+PPA, AC+rubber, AC+EVA+PPA, AC+EVA, AC+PE+PPA, AC+SBS+PPA, AC+PE, AC+SBR+PPA, AC+SBS, AC+SBR and AC+rubber+PPA at 100 Pa; and
- AC+Elvaloy+PPA, AC+PPA, AC+PE+PPA, AC+SBS+PPA, AC+EVA, AC+PE, AC+SBR+PPA, AC+EVA+PPA, AC+rubber, AC+SBS, AC+rubber+PPA and AC+SBR at 3,200 Pa.

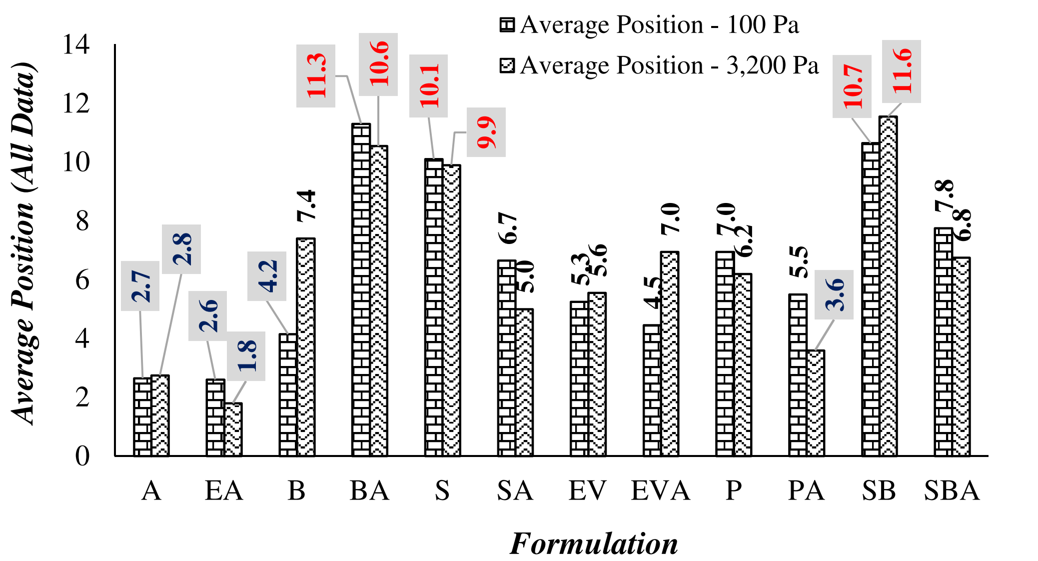

Figure 219 – Average positions of the PG 76-xx formulations at all temperatures, the creep-recovery times and stress levels, as based on the J_{nr} values of these materials (the grey-shaded boxes with texts highlighted in blue and red refer to the binders with the best and worst positions in the rankings, respectively)

With respect to the coefficients of variation, no clear patterns of response between the data at 100 and 3,200 Pa may be found. This can be implied by analyzing the data in Figure 220, according to which the data points do not show any tendency of increase or decrease with increasing stress level, neither it is possible to say that higher stress levels lead to higher CV's in the binder and vice versa. One may thus conclude that the changes in the CV values are not necessarily associated with the stress level, since each formulation will show a particular response and oscillation in the individual positions in the rankings when loaded at higher levels and/or longer creep times in the DSR.

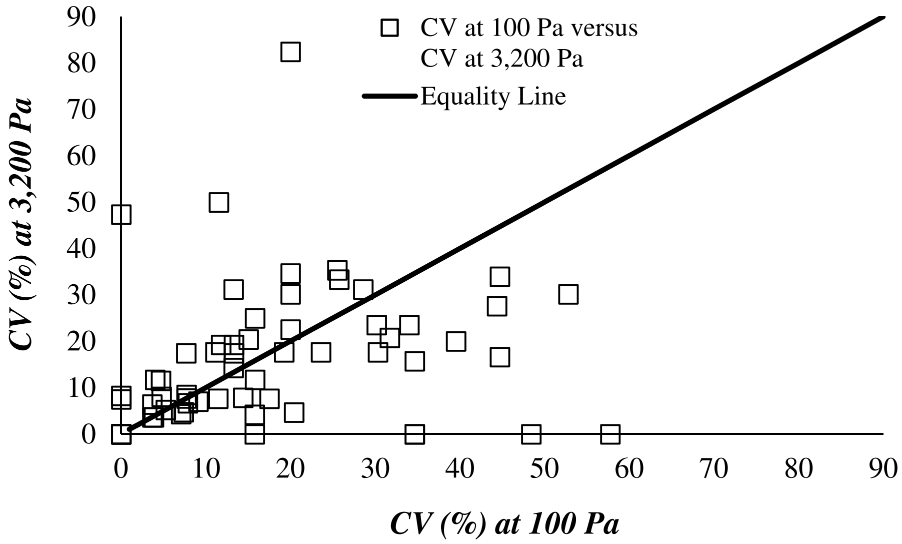

Figure 220 – Plots of the coefficients of variation (CV) at 100 Pa against the corresponding values at 3,200 Pa for all the 12 formulations and the whole ranges of temperatures, loading times and stress levels

Since it is believed that the parameter $J_{nr,\ diff}$ provides an estimation of the rutting potential of the binder for unpredicted loading and temperature conditions in the pavement, the individual and complete rankings of the formulations according to the $J_{nr,\ diff}$ values were also determined. The idea is to identify which binders tend to depict greater susceptibilities to rutting in a general context (i. e., by including all the loading and temperature conditions studied in the present dissertation), as well as those with the lowest susceptibilities. Finally, these rankings were compared with the ones for J_{nr} to highlight the similiarities and differences among them.

Table 267 is a summary of the rankings of the formulations at 52 and 58°C according to the parameter $J_{nr,\ diff}$ and for all the pairs of creep-recovery times. In addition to the best overall rutting performance at all the creep times used in the MSCR tests, the AC+Elvaloy+PPA is also the less stress sensitive material in a relative context (lowest $J_{nr,\ diff}$ values) followed by the AC+SBS+PPA, the AC+SBR+PPA and the AC+PPA. In the opposite extreme of the rankings, the AC+EVA is the most stress sensitive material ($J_{nr,\ diff}$ > 130% in all cases) followed by the AC+rubber, the AC+EVA+PPA and the AC+PE. These comments suggest that, although the AC+EVA, the AC+rubber and the AC+EVA+PPA show quite good rutting performances at several pavement temperatures ($T \leq 64$°C for the two materials with EVA and $T \geq 64$°C for the AC+rubber), their very high susceptibility to rutting under unexpected climate and loading conditions may be an impending factor for the use on some types of pavements.

Table 267 – Rankings of the modified asphalt binders based on $J_{nr,\ diff}$ at the temperatures of 52 and 58°C – individual positions and corresponding mean values

formulation[b]	rankings at 52°C[a]					rankings at 58°C[a]				
	1/9 s	2/9 s	4/9 s	8/9 s	**mean**	1/9 s	2/9 s	4/9 s	8/9 s	**mean**
A	1	2	6	7	**4.0**	1	4	6	5	**4.0**
EA	7	5	1	1	**3.5**	3	2	1	1	**1.8**
B	12	11	11	10	**11.0**	12	11	10	10	**10.8**
BA	8	7	8	8	**7.8**	7	7	5	3	**5.5**
S	5	8	2	4	**4.8**	9	9	7	9	**8.5**
SA	6	1	3	2	**3.0**	8	1	4	2	**3.8**
EV	11	12	12	12	**11.8**	11	12	12	12	**11.8**
EVA	10	10	10	11	**10.3**	10	10	11	11	**10.5**
P	9	9	7	9	**8.5**	6	6	8	6	**6.5**
PA	4	4	5	6	**4.8**	4	3	2	7	**4.0**
SB	3	6	9	3	**5.3**	5	8	9	8	**7.5**
SBA	2	3	4	5	**3.5**	2	5	3	4	**3.5**

[a] each number refers to the relative position of the formulation in a ranking from the less (No. 1) to the most susceptible to rutting (No. 12).
[b] "A" = PPA; "E" = Elvaloy®"; "B" = crumb rubber; "S" = SBS copolymer; "EV" = EVA copolymer; "P" = low-density PE; "SB" = SBR copolymer.

The overall ranking of formulations – from the less to the most sensitive to increases in the applied stress at 52 and 58°C – is given as follows: AC+Elvaloy+PPA, AC+SBS+PPA, AC+SBR+PPA, AC+PPA, AC+PE+PPA, AC+SBR, AC+rubber+PPA, AC+SBS, AC+PE, AC+EVA+PPA, AC+rubber and AC+EVA. It is important to note that $J_{nr,\ diff}$ may be interpreted with caution when applying its upper limit of 75% to some modified binders, especially because these formulations do not necessarily depict a poor rutting performance in the mixture. This is the case of the AC+rubber, the AC+EVA and the AC+EVA+PPA, for which there is a sharp contrast between their substantially high $J_{nr,\ diff}$ values (all greater than 100%) and the excellent performances in the FN tests (absence of failure). Other formulations prepared with these same modifiers also depicted similar trends, either in the binder or the mixture scales (DOMINGOS and FAXINA, 2014; 2016; ONOFRE et al., 2013). Therefore, it seems that $J_{nr,\ diff}$ may be revised to account for these particular characteristics of some highly-modified asphalt binders with results greater than 75% and good performances in the field pavement.

Table 268 provides all the individual positions of the formulations in the rankings according to the $J_{nr,\ diff}$ values at 64 and 70°C, together with their corresponding average positions at each temperature. The considerable increases in the positions of the AC+EVA from 64°C (about 11.8) to 70°C (about 2.5) are intrinsically related to the melting and accumulated damage in the polymeric network of the formulation, as discussed previously. This increase in temperature does not seem to exert a great influence on the stress sensitivity of the AC+EVA+PPA, which remains quite high even after 4.0 and 8.0 s of loading time. With respect to the AC+PPA, its $J_{nr,\ diff}$ values increase significantly from 64 to 70°C (especially at 4/9 and 8/9 s) and this contributes to a worse general classification of the material within the group of studied binders (from about 5.0 to more than 7.0). The AC+Elvaloy+PPA still remains as the binder with the lowest stress sensitivity in a general context, followed by the AC+SBS+PPA, the AC+PE+PPA, the AC+rubber+PPA, the AC+SBR+PPA, the AC+PPA, the AC+PE, the AC+EVA, the AC+SBS, the AC+SBR, the AC+EVA+PPA and the AC+rubber.

Table 268 – Rankings of the modified asphalt binders based on $J_{nr,\ diff}$ at the temperatures of 64 and 70°C – individual positions and corresponding mean values

formulation[b]	rankings at 64°C[a]					rankings at 70°C[a]				
	1/9 s	2/9 s	4/9 s	8/9 s	**mean**	1/9 s	2/9 s	4/9 s	8/9 s	**mean**
A	2	4	8	6	**5.0**	4	6	9	11	**7.5**
EA	1	1	1	1	**1.0**	1	2	2	1	**1.5**
B	12	10	10	10	**10.5**	12	12	12	12	**12.0**
BA	6	7	3	3	**4.8**	7	5	5	4	**5.3**
S	9	9	4	8	**7.5**	11	9	3	5	**7.0**
SA	8	2	5	2	**4.3**	8	1	6	2	**4.3**
EV	11	12	12	12	**11.8**	2	4	1	3	**2.5**
EVA	10	11	11	11	**10.8**	9	11	11	10	**10.3**
P	5	6	7	4	**5.5**	6	8	8	6	**7.0**
PA	3	3	2	7	**3.8**	3	3	4	9	**4.8**
SB	7	8	9	9	**8.3**	10	10	10	8	**9.5**
SBA	4	5	6	5	**5.0**	5	7	7	7	**6.5**

[a] each number refers to the relative position of the formulation in a ranking from the less (No. 1) to the most susceptible to rutting (No. 12).
[b] "A" = PPA; "E" = Elvaloy®"; "B" = crumb rubber; "S" = SBS copolymer; "EV" = EVA copolymer; "P" = low-density PE; "SB" = SBR copolymer.

As can be seen, the AC+EVA is replaced by the AC+SBR in the list of the three most stress sensitive materials (which also includes the AC+rubber and the AC+EVA+PPA). In addition, the formulations with PPA and a polymer (in this case, AC+SBS+PPA, AC+SBR+PPA and AC+PE+PPA) tend to depict lower $J_{nr,\ diff}$ values than the corresponding ones without PPA (AC+SBS, AC+SBR and AC+PE, respectively). This could also be seen at 52 and 58°C (Table 267), and it is suggested that the synergy between PPA and the main modifier and the reduction in the polymer content – polymers are known to depict a nonlinear response at high stresses and strain levels (D'ANGELO et al., 2007) – contributed to such decreases. The weight of each factor in the final results of the formulations essentially depends upon the modifier type, i. e., the compatibility between the SBS and SBR copolymers and the binder may be improved after the addition of PPA and the PE content seems to be the primary reason for the higher $J_{nr,\ diff}$ values in the AC+PE.

The rankings reported in Table 269 refer to the numerical values of $J_{nr,\ diff}$ for each formulation at the highest pavement temperature (76°C), as well as the final ranking according to all the individual positions of the materials. As can be seen, the AC+Elvaloy+PPA is once again graded as the formulation with the lowest stress sensitivity at 76°C, followed by the AC+SBS+PPA, the AC+EVA, the AC+SBS, the AC+rubber+PPA, the AC+PE+PPA, the AC+SBR+PPA, the AC+PE, the AC+PPA, the AC+SBR, the AC+EVA+PPA and the AC+rubber. However, there are some special topics that need to be further discussed with respect to the individual and final rankings of these asphalt binder, as will be provided later.

Table 269 – Rankings of the modified asphalt binders based on $J_{nr,\ diff}$ at the temperature of 76°C (individual positions and corresponding mean values) and average position based on all data from 52 to 76°C

formulation[b]	rankings at 76°C[a]					**average position (all data)**
	1/9 s	2/9 s	4/9 s	8/9 s	mean	
A	4	8	10	12	8.5	**5.8**
EA	1	2	3	1	1.8	**1.9**
B	12	12	12	11	11.8	**11.2**
BA	5	6	6	4	5.3	**5.7**
S	11	5	1	3	5.0	**6.6**
SA	8	1	2	2	3.3	**3.7**
EV	2	4	4	5	3.8	**8.3**
EVA	9	11	11	8	9.8	**10.3**
P	7	9	8	6	7.5	**7.0**
PA	3	3	5	10	5.3	**4.5**
SB	10	10	9	7	9.0	**7.9**
SBA	6	7	7	9	7.3	**5.2**

[a] each number refers to the relative position of the formulation in a ranking from the less (No. 1) to the most susceptible to rutting (No. 12).

[b] "A" = PPA; "E" = Elvaloy®"; "B" = crumb rubber; "S" = SBS copolymer; "EV" = EVA copolymer; "P" = low-density PE; "SB" = SBR copolymer.

The AC+PPA shows a marked increase in $J_{nr, diff}$ with increasing t_F at 76°C, which may be associated with its level of nonlinearity at very high temperatures and for long time durations of the load in the MSCR test. The reductions in the positions of the AC+SBS and the AC+SBS+PPA might be explained by the decreased role of the polymer on the creep-recovery response of the formulation (i. e., great amounts of damage). This could also be seen in the individual positions of the AC+SBR, but with a lesser extent. The trends in the positions of the AC+Elvaloy+PPA do not seem to be significantly affected by the increase in the temperature to 76°C when compared with the data for the temperatures between 52 and 70°C, and the same can be applied to the AC+rubber, the AC+SBS+PPA, the AC+EVA+PPA and the AC+PE.

Figure 221 portrays the comparisons between the final rankings of the formulations according to J_{nr} (Figure 219) and $J_{nr, diff}$ (Table 269). The objective was to see whether a specific binder graded as "very resistant to rutting" according to J_{nr} holds the same classification in the criterion based on $J_{nr, diff}$, either at 100 Pa or at 3,200 Pa. In this figure, ratios higher than one indicate that the relative position of the binder is better (i. e., lower numerical values) for $J_{nr, diff}$ than for J_{nr}, and the opposite is valid for ratios lower than one. In other words, the binders with ratios higher than unity show more promising findings for $J_{nr, diff}$ than for J_{nr}, whereas the binders with ratios lower than unity have a better performance according to J_{nr} than $J_{nr, diff}$. In a general context, the binders with quite high stress sensitivities ranked very poorly in the $J_{nr, diff}$ criterion – e. g., the AC+PPA, the AC+rubber, the AC+EVA and the AC+EVA+PPA – and, as a consequence, their ratios are very small (no greater than 0.7). The opposite may be seen for the AC+rubber+PPA, the AC+SBS, the AC+SBS+PPA, the AC+SBR and the AC+SBR+PPA, for which the rankings based on $J_{nr, diff}$ showed better results than those based on J_{nr}.

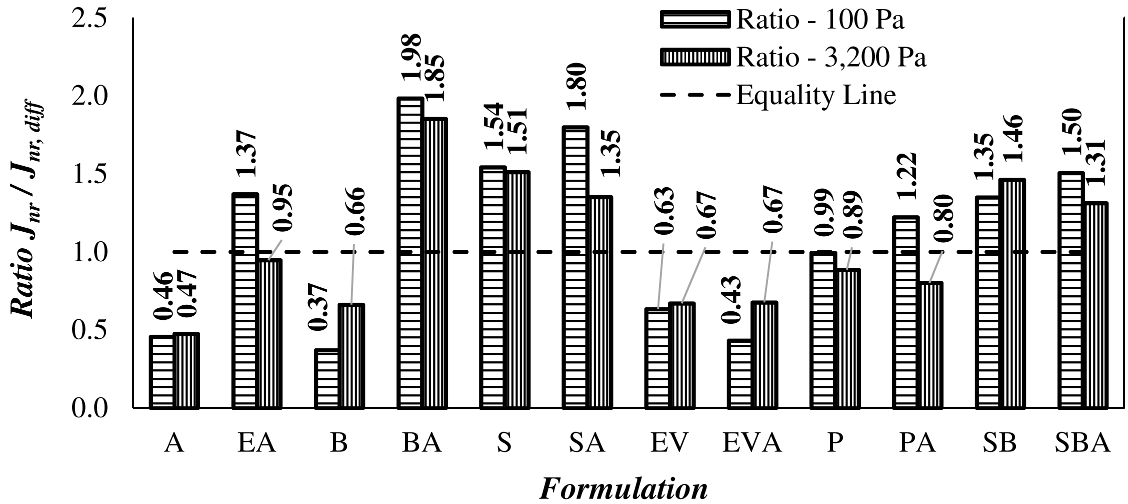

Figure 221 – Ratios of the average positions of the formulations according to J_{nr} to those according to $J_{nr, diff}$ and for the stress levels of 100 and 3,200 Pa

One may imply from the above discussions that the asphalt binders with very small J_{nr} values (that is, a high degree of stiffness and a low susceptibility to rutting) tend to depict a greater stress sensitivity, even though this stress sensitivity is not always in disagreement with the maximum allowed value of 75%. As shown earlier, the AC+PPA and the two formulations with EVA may yield $J_{nr,\ diff}$ values lower than 75% for some testing conditions, especially at the standardized creep-recovery times. On the other hand, the susceptibility to rutting – as based on J_{nr} – is not as promising for the AC+rubber+PPA and the formulations with SBS and SBR as their corresponding results for the stress sensitivity (lower $J_{nr,\ diff}$). This again strengthens the assumption that a specific modified asphalt binder with very high levels of stiffness (small J_{nr} values) does not necessarily show a poor rutting performance when its $J_{nr,\ diff}$ values are greater than 75%. Such a conclusion is reached by comparing the mixture data of the AC+rubber, the AC+EVA and the AC+EVA+PPA with the binder data, as highlighted earlier in the study.

On the basis of the study of the rutting performances and relative positions of the formulations according to the J_{nr} and the $J_{nr,\ diff}$ data at high pavement temperatures from 52 to 76°C, the statements below can be pointed out as conclusions of this section:

- asphalt binders with quite small nonrecoverable compliances (i. e., excellent positions in the rankings of $J_{nr}100$ and $J_{nr}3200$) may depict very good rutting performances, even if their percent differences overcome the maximum limit of 75%; this is the case of the AC+rubber, the AC+EVA and the AC+EVA+PPA, as well as the AC+PE+PPA for some pavement temperatures;
- the evolution of the average position of the AC+EVA with increasing temperature (especially at 64, 70 and 76°C) and loading time reflects the considerable amount of damage in its polymeric network; as a consequence, the last positions in the rankings based on $J_{nr,\ diff}$ when $T \leq 64$°C give place to the first positions at 70 and 76°C and the opposite is seen in the rankings based on J_{nr};
- there is no clear relationship between the coefficients of variation among the rankings of binders according to $J_{nr}100$ and $J_{nr}3200$, which suggests that the CV values are not necessarily linked to the applied stress and each formulation will depict a particular creep-recovery response when loaded in the DSR;
- the formulations with the worst positions in the rankings of J_{nr} are the AC+SBS, the AC+SBR and the AC+rubber+PPA, namely, modifications only with elastomers and with a lower crumb rubber content; this indicates that PPA may further improve the rutting resistances of the elastomeric-modified binders. On the other hand, the AC+PPA and the

AC+Elvaloy+PPA can be ranked as very rut resistant materials in a binder scale together with the AC+rubber (at 100 Pa) and the AC+PE+PPA (3,200 Pa) – that is, binder modifications with a plastomer, higher crumb rubber contents and PPA; and

- by unifying the rankings of $J_{nr}100$ and $J_{nr}3200$ with the one of $J_{nr,\ diff}$ (i. e., by calculating a unique average position for each binder), the following overall ranking of formulations from the less to the most susceptible to rutting can be obtained (see Figure 222): AC+Elvaloy+PPA; AC+PPA; AC+PE+PPA; AC+SBS+PPA; AC+EVA; AC+SBR+PPA; AC+PE; AC+EVA+PPA; AC+rubber; AC+SBS; AC+rubber+PPA and AC+SBR. As it can be seen, the presence of PPA in all the polymer-modified asphalt binders (except for the AC+EVA) helps in preparing a more rut resistant formulation and, to some extent, a lower stress sensitivity as well. This could also be seen in the mixture data (Chapter 5), which gives support to the use of PPA in the degrees of improvement of the rut resistance of some modified materials.

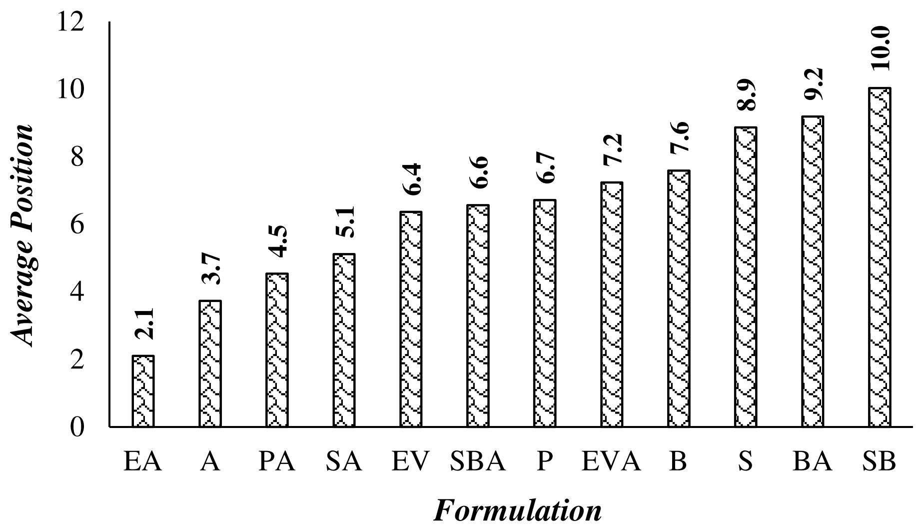

Figure 222 – Final rankings of the studied formulations according to the $J_{nr}100$, $J_{nr}3200$ and $J_{nr,\ diff}$ values from the less (No. 1) to the most susceptible to rutting (No. 12)

6.3.4. The Role of Longer Recovery Times on the Creep-Recovery Responses of Modified Asphalt Binders and Rheological Modeling

As discussed previously, the selection of longer recovery times in the MSCR tests is intended to provide enough time for the material to fully recover the elastic portion of the total strain. This is especially remarkable for the materials that have a high degree of elasticity, which is the case of the AC+Elvaloy+PPA, the AC+EVA and the AC+EVA+PPA (see the previous section). Therefore, it can be said that all of these formulations may be included within the same group – labeled here as "Group A" – to uniform the analysis. The other modified asphalt binders, which do not show a high level of elasticity at any pavement temperature, were included in a group labeled hereafter as "Group B". The 50/70 original binder was not analyzed because its recoveries are null or all lower than 1% at 1/9 s (see Table 63, page 192), and then it is not justifyable to increase the recovery time for a material that does not depict almost any quantity of elastic strain in the standardized loading-unloading conditions.

Table 270 shows the lists of binders that belong to "Group A" and "Group B". Due to the very high recovery values observed for the formulations of the first group (in some cases, approaching 100%), it was decided to utilize the highest recovery time (1/500 s) in their MSCR tests. This was also made to be in accordance with other studies that also considered values greater than 240 s in their creep-recovery tests on binders modified with Elvaloy® terpolymer, EVA and other polymers with a high level of reactivity with the original material (DELGADILLO, 2008; DELGADILLO and BAHIA, 2010; DELGADILLO et al., 2012; SANTAGATA et al., 2013). In turn, the ones of the second group were tested according to the loading-unloading proportion of 1/240 s (i. e., 240 s of unloading time) because their levels of elasticity were not high, even though some formulations such as the AC+rubber may achieve recoveries as higher as 70% at temperatures up to 64°C (see Table 105, page 244). Finally, the raw creep-recovery data were fitted to the modified power model by Saboo and Kumar (2015) and the variations in the parameters A, B and α from one recovery time to the other were investigated.

Table 270 – Separation of the formulations according to the groups "A" and "B" and their corresponding degrees of elasticity

group name	level of elasticity	formulations
"Group A"	high	AC+Elvaloy+PPA, AC+EVA and AC+EVA+PPA
"Group B"	poor	AC+PPA, AC+rubber, AC+rubber+PPA, AC+SBS, AC+SBS+PPA, AC+PE, AC+PE+PPA, AC+SBR and AC+SBR+PPA

Analysis of Data for the Formulations of the Group "A". Table 271 depicts the percent recoveries of the AC+Elvaloy+PPA, the AC+EVA and the AC+EVA+PPA at all the pavement temperatures and stress levels. As can be seen, some asphalt binders show higher recoveries at 3,200 Pa than at 100 Pa ($R3200 > R100$), which is quite surprising. It is also interesting to see that the AC+EVA shows almost full recoveries ($R100 \approx 100\%$) at the temperatures of 52, 58 and 64°C, and that these recoveries drop to null or very small values at 70 and 76°C. The non-null results range from 34 to 83% for the AC+Elvaloy+PPA, from 6 to 100% for the AC+EVA and from 8 to 77% for the AC+EVA+PPA. Some odd cases concerning the identification of higher *R3200* values than *R100* values may be observed in the literature as well, e. g., the AC+Elvaloy+PPA studied in the paper from Domingos and Faxina (2015). However, the differences between the values were not as marginal in this study as they were in the case of the investigation from Domingos and Faxina (2015). Therefore, a more specific and detailed analysis must be carried out to explain such results.

Table 271 – Percent recoveries at 100 Pa (*R100*) and 3,200 Pa (*R3200*) for the AC+Elvaloy+PPA, the AC+EVA and the AC+EVA+PPA at 1/500 s and all the high pavement temperatures

formulation	parameter	results (%) at each pavement temperature				
		52°C	58°C	64°C	70°C	76°C
AC+Elvaloy+PPA	*R100*	78.6	72.9	42.6	49.9	34.3
	R3200	83.0	76.8	68.1	56.9	42.5
AC+EVA	*R100*	100.0	99.9	98.6	85.1	0.0
	R3200	99.8	99.8	97.9	6.6	0.0
AC+EVA+PPA	*R100*	76.3	69.9	82.3	32.3	17.5
	R3200	62.8	54.9	36.2	8.2	0.0

One possible reason given by researchers to explain the increases in recovery is associated with the delayed elastic response of the formulation, since its full recovery is not observed after 9 s of unloading for several modifiers and the remaining elastic response is carried to the next cycle (SOENEN et al., 2013; TEYMOURPOUR et al., 2016). Even though this is a logical reason and has basis in the creep-recovery behavior of asphalt binders, it cannot be fully applied to the present situation because the recovery time of 500 s aims at greatly minimizing the influence of delayed elasticity on the results of the MSCR tests. This could be used as one of the explanations to justify the increases in the recovery values of the AC+Elvaloy+PPA tested by Domingos and Faxina (2015) when moving from 100 to 3,200 Pa, as well as the variations in the *R* values of the AC+EVA and the AC+EVA+PPA at each cycle (see previous section). With respect to the present case, more specific investigations were conducted as shown in the forthcoming paragraphs.

The strains collected in the DSR's are based on the fundamental assumption that the internal variables of the device have a negligible effect on them. In other words, the design projects must be conceived such that the influence of the measurement system on the measured quantities is minimized (MONTEPARA and GIULIANI, 1999). The differences among the results of each branch of DSR and the input criteria for the collection of the strain values also have influence on the reproducibility of the data, as previously highlighted by Montepara and Giuliani (1999) and Soenen et al. (2013), and they may be expressive in some cases. Since the loads at 3,200 Pa are applied after those at 100 Pa in the MSCR tests, another reason for the increased *R3200* values is the hereditary memory effect of the material, which plays a specific role on the strain values for each modification type and may cause the recoveries to be larger in the cycles tested later (SOENEN et al., 2013). In summary, either the variables associated with the DSR or the loading history of the binder may be pointed out as reasons why *R3200* is higher than *R100* for some formulations.

In terms of the variables of the DSR, the most influential ones can be grouped as follows according to the literature: (a) inertia of the upper plate; (b) the control software; (d) the time lag between the transition from the loading to the unloading portion at each cycle and the effective decrease in the stress level from non-null to null and vice versa; (e) the efficiency of the instrument in its structural and logging components; and (f) the control of the testing temperature (JAHFARI and BABAZADEH, 2016; MONTEPARA and GIULIANI, 1999; SOENEN et al., 2013). If one or more of these variables is not adequately addressed, then one may expect that the strain measurements in the binder will reflect their influences and the interpretations of the data must be carefully made. One of the most representative examples of such influences is the observation of negative percent recoveries in some binders and MSCR test conditions, as highlighted by other authors elsewhere (JAHFARI and BABAZADEH, 2016; MOHSENI and AZARI, 2014; SOENEN et al., 2013).

Based on the aforementioned explanations, some individual creep-recovery cycles were provided here to illustrate the effects of the internal variables of the DSR on the strain measurements of the formulations. Figure 223 shows the strain data of two creep-recovery cycles (12^{th} and 13^{th} cycles) for the AC+Elvaloy+PPA at 76°C, whereas Figure 224 shows the raw data for these same cycles and temperatures, but considering the AC+EVA. It is clear that the strains of the AC+Elvaloy+PPA do not follow a uniform pattern of response in the unloading portion of the cycles and, in some cases (e. g., 12^{th} cycle), they depict slight increases after the full recovery is observed. On the other hand, the two curves of the AC+EVA are almost coincident – which is quite logical, since the *R* values are almost 100% – and do not seem to be seriously affected by the internal variables of the DSR. In addition, the two *R* values greatly differ from one cycle to the other for the AC+Elvaloy+PPA (36.2 and 47.0%) and are quite similar for the AC+EVA (from 98.7 to 97.5%).

Based on the explanations given above, it can be said that the variables of the DSR play a more important role on the strain values of the asphalt binder after the full recovery is achieved.

This can also be applied to the case of the negative recoveries mentioned earlier, i. e., any modification in the position of the upper plate (due to its inertia) will lead to increases in the accumulated strain in the binder and changes in the MSCR testing parameters. Since the AC+EVA showed a full recovery only after 500 s of unloading time, it is believed that the effects of these internal variables were minimized due to the continuous recovery process. In other words, the inertia of the upper plate of the DSR may be pointed out as the prevailing factor – among those reported in the literature – to explain the modifications in the strain values of the binder after the achievement of the full recovery within the recovery time. Also, the memory effect mentioned by Soenen et al. (2013) can be taken as the primary reason why the recoveries of the AC+Elvaloy+PPA at 3,200 Pa are higher than those at 100 Pa, since this was not observed for the data of the AC+EVA and the AC+EVA+PPA.

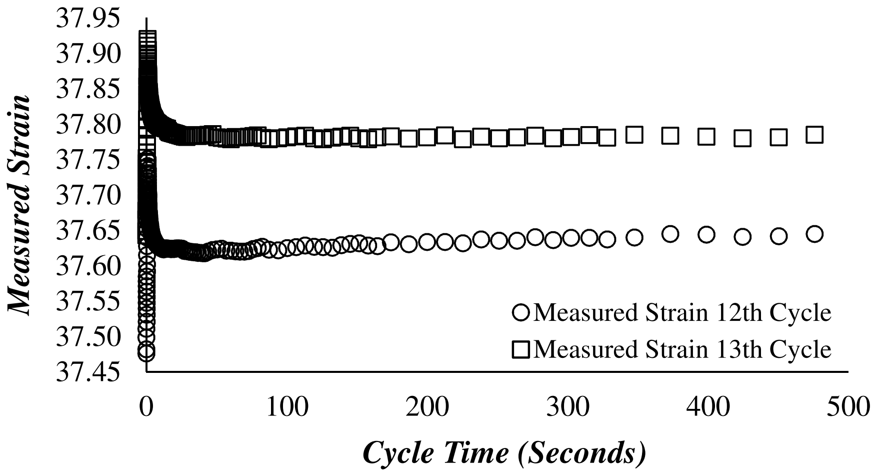

Figure 223 – Raw strain values of the AC+Elvaloy+PPA at the 12th cycle (R = 36.2%) and the 13th cycle (R = 47.0%) at 100 Pa and the temperature of 76°C

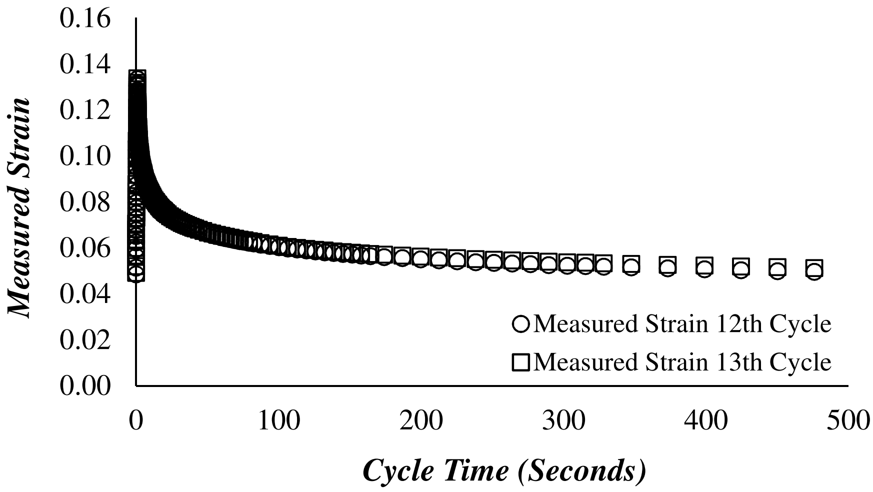

Figure 224 – Raw strain values of the AC+EVA at the 12th cycle (R = 98.7%) and the 13th cycle (R = 97.5%) at 100 Pa and the temperature of 64°C

Table 272 summarizes the nonrecoverable compliances of the AC+Elvaloy+PPA, the AC+EVA and the AC+EVA+PPA at 100 and 3,200 Pa. As a consequence of the higher recoveries of the AC+Elvaloy+PPA at 3,200 Pa than at 100 Pa, the $J_{nr}3200$ values for this material are lower than the corresponding $J_{nr}100$ values for the same temperature (i. e. $J_{nr,\ diff}$ is negative). This is in accordance with the results published by Domingos and Faxina (2015) and the comments made by Soenen et al. (2013) with respect to some laboratory data discussed by them. Again, the roles of the DSR variables – especially the inertia of the upper plate – and the memory effect of the samples may be taken as the primary reasons for such findings. With respect to the very small J_{nr} values for the AC+EVA at 52 and 58°C (less than 0.001 kPa^{-1}), they can be naturally associated with the almost full recoveries of the material. The negative $J_{nr}100$ value at 52°C may be explained by measurement errors – and possibly lack of precision as well – in the DSR, as the residual strain values are practically null in such test conditions.

Table 272 – Nonrecoverable compliances at 100 Pa ($J_{nr}100$) and 3,200 Pa ($J_{nr}3200$) and corresponding percent differences ($J_{nr,\ diff}$) for the AC+Elvaloy+PPA, the AC+EVA and the AC+EVA+PPA at 1/500 s and all temperatures

formulation	parameter	results (kPa^{-1}) at each pavement temperature				
		52°C	58°C	64°C	70°C	76°C
AC+Elvaloy+PPA	$J_{nr}100$	0.045	0.115	0.462	0.734	1.727
	$J_{nr}3200$	0.046	0.098	0.251	0.610	1.420
	$J_{nr,\ diff}$ (%)	-20.1	-14.6	-45.6	-17.0	-17.8
AC+EVA	$J_{nr}100$	-0.0002	0.0002	0.011	0.222	4.051
	$J_{nr}3200$	0.0003	0.0006	0.018	2.374	4.934
	$J_{nr,\ diff}$ (%)	-252.2	201.4	60.2	968.7	21.8
AC+EVA+PPA	$J_{nr}100$	0.033	0.069	0.073	0.714	1.929
	$J_{nr}3200$	0.049	0.103	0.353	1.854	4.589
	$J_{nr,\ diff}$ (%)	48.3	49.1	382.2	159.5	137.9

Even though the $J_{nr,\ diff}$ values of the AC+Elvaloy+PPA are negative, they are in accordance with the Superpave® requirements for paving applications (lower than 75%), and the same can be said for the AC+EVA+PPA at 52 and 58°C ($J_{nr,\ diff} < 50\%$) and the AC+EVA at 64 and 76°C ($J_{nr,\ diff} < 61\%$). Both EVA-modified binders depict substantially high percent differences at several test temperatures, which could also be seen at the creep and recovery times of 1/9 s. In other words, the nonlinear features of the polymer network can be seen even after the increases in the recovery time and the stress level. Finally, the boosts in $J_{nr}100$ and $J_{nr}3200$ by more than two times observed for the AC+EVA and the AC+EVA+PPA after the increase in the temperature from 70 to 76°C may be caused by two factors, namely, melting of the EVA copolymer and strain levels sufficiently higher to exceed the "failure point" described earlier. This does not seem to be the case of the AC+Elvaloy+PPA, for which the J_{nr} values barely overcome 2.0 kPa^{-1} at 76°C regardless of the applied stress.

The comparisons among the results of R and J_{nr} for the studied binders can be made based on the plots shown in Figure 225 and Figure 226 for the percent recoveries and the nonrecoverable compliances, respectively. As can be seen, the recoveries mainly increased and the compliances typically decreased with increasing recovery time (despite a few exceptions), which was quite expected because the binders were allowed to recover more of their delayed elastic response with increasing recovery time. This can be graphically represented by the data points placed above the equality lines in both figures, i. e, ratios of J_{nr} values higher than unity in Figure 226 and recoveries at 1/500 s higher than those at 1/9 s in Figure 225.

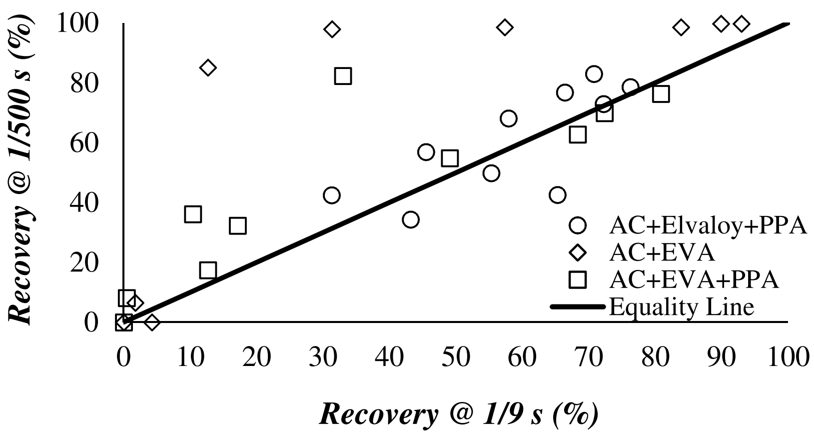

Figure 225 – Comparisons between the percent recoveries of the AC+Elvaloy+PPA, the AC+EVA and the AC+EVA+PPA at 1/9 s and 1/500 s at all pavement temperatures and stress levels

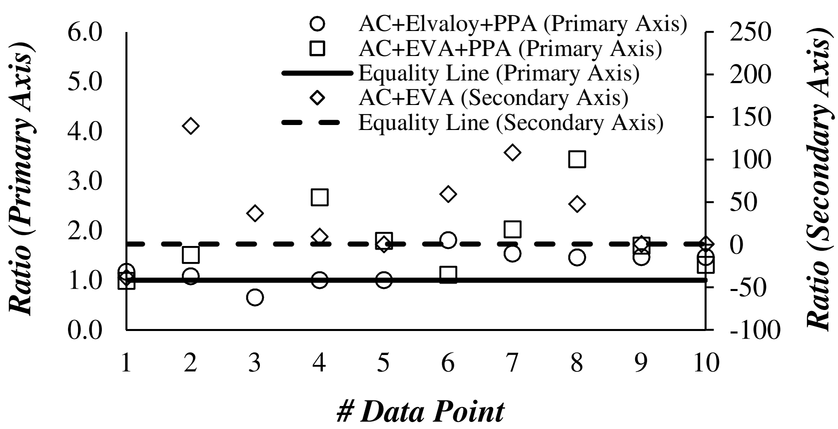

Figure 226 – Ratios of the nonrecoverable compliances of the AC+Elvaloy+PPA, the AC+EVA and the AC+EVA+PPA at 1/9 s to those at 1/500 s for a particular temperature and stress level – each data point corresponds to one temperature (out of five) and one stress level (out of two)

The model parameters *A*, *B* and α were also obtained for the studied binders at 1/500 s and the high pavement temperatures. It is anticipated here that this model was able to fit the data with very good from excellent degrees of correlation, i. e., R^2 values always higher than 0.87 (see an example in Figure 227 for the AC+EVA at 58°C), and also that the *n* values are not shown in the forthcoming tables because they are equal to unity in all cases (0.9995~1.0000). As discussed previously, the α values were able to accurately represent the decreases in *R100* and *R3200* with temperature for all binders and the group of longer creep times (2/9, 4/9 and 8/9 s). This was also investigated in the present section, namely, the α values were plotted against the corresponding percent recoveries of the asphalt binders at 100 and 3,200 Pa and the existence of linear regression trendlines was investigated.

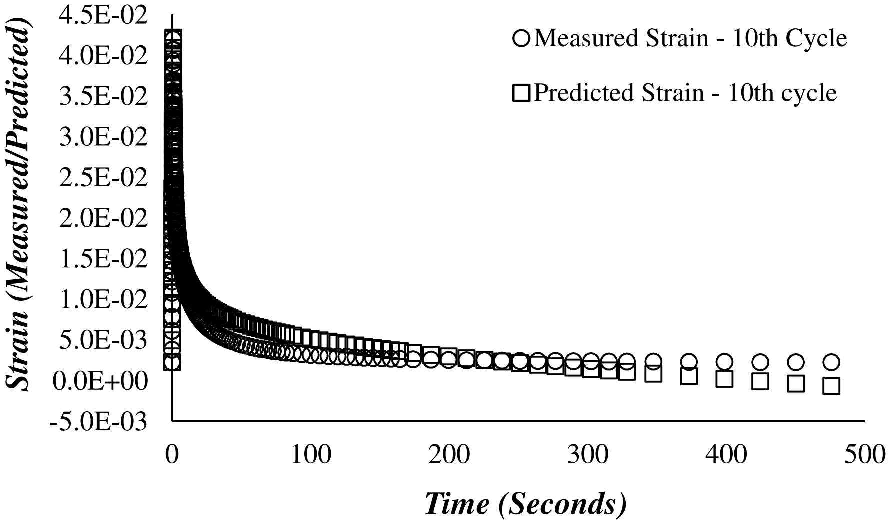

Figure 227 – Fitting of the model from Saboo and Kumar (2015) to the raw strain data of the AC+EVA at the temperature of 58°C and the stress level of 100 Pa

Table 273 summarizes the α values of the AC+Elvaloy+PPA, the AC+EVA and the AC+EVA+PPA under all testing conditions. The results range from about 0.60 at 52°C to almost equal to one at 76°C, which is where the binders typically show null or much smaller recoveries (no greater than 43%). Based on these preliminary analyses, one may imply that α will show a pretty good correlation with the recovery *R* from the MSCR test, as observed earlier for the longer creep times. This question can be partially answered from the general correlation provided in Figure 228, in which a good result ($R^2 \approx 0.74$) is found. In terms of the individual correlations (charts not provided here), a complementary analysis showed that the R^2 values are equal to 0.5916, 0.7655 and 0.9275 for the AC+Elvaloy+PPA, the AC+EVA and the AC+EVA+PPA, respectively.

It is suggested that the correlation for the AC+Elvaloy+PPA is worse than for the other materials because α values very close to each other (around 0.74-0.77) may refer to a variety of recoveries (from 42% to more than 70%). In any case, it appears that α still does a good job with respect to the estimation of the amount of recovery in the asphalt binders subjected to the MSCR tests at 1/500 s. Again, the concentration of data points in the two extreme R values of 100% (around α = 0.60) and 0% (around α = 1.00) has already been observed earlier and may be associated with the limitations of the parameter and the modified power model by itself.

Table 273 – Results of the parameter α from the model by Saboo and Kumar (2015) at 100 and 3,200 Pa and the creep-recovery times of 1/500 s

formulation	stress level (Pa)	results at each pavement temperature				
		52°C	58°C	64°C	70°C	76°C
AC+Elvaloy+PPA	100	0.7166	0.6974	0.7359	0.7770	0.8368
	3,200	0.7140	0.7305	0.7629	0.8089	0.8685
AC+EVA	100	0.5933	0.6251	0.7426	0.9144	0.9815
	3,200	0.6059	0.6314	0.7533	0.9846	0.9996
AC+EVA+PPA	100	0.8246	0.8156	0.8445	0.9498	0.9517
	3,200	0.8298	0.8611	0.9234	0.9921	0.997

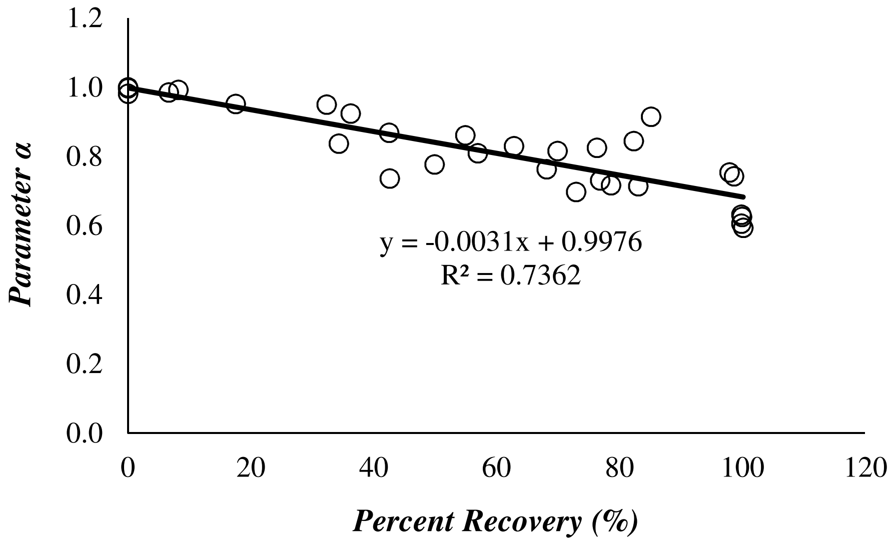

Figure 228 – Degree of correlation between the parameter α from the modified power model and the percent recoveries of the AC+Elvaloy+PPA, the AC+EVA and the AC+EVA+PPA at the creep-recovery times of 1/500 s

The results for the parameters A and B and the three formulations with Elvaloy+PPA, EVA and EVA+PPA are given in Table 274. The data indicate that either A and B increase with temperature and stress level, and also that these increases seem to be greater for the AC+EVA than for the other asphalt binders (especially when moving from 64 to 70 and then 76°C). In other words, the binders become more susceptible to rutting due to the contributions of the initial accumulated strain and the strain rate during the creep-recovery cycles. This is different from what was reported for the AC+Elvaloy+PPA and the AC+EVA at longer creep times and lower pavement temperatures, in which both parameters decreased with increasing temperature up to a critical value (in general, 64°C). Based on such comments, it can be implied that the delayed elasticity performed a critical role on the responses of the materials at a fixed recovery time of 9 s by reducing the amount of permanent strain, either in the first cycles (parameter *A*) or throughout the test (parameter *B*).

Table 274 – Results of the parameters *A* and *B* from the model by Saboo and Kumar (2015) at 100 and 3,200 Pa and the creep-recovery times of 1/500 s

temperature (in °C)	stress (in Pa)	AC+Elvaloy+PPA		AC+EVA		AC+EVA+PPA	
		A	*B*	*A*	*B*	*A*	*B*
52	100	0.0219	0.7168	0.0181	0.5929	0.0153	0.8246
52	3,200	0.7042	0.7141	0.6168	0.6055	0.4339	0.8299
58	100	0.0432	0.6977	0.0411	0.6246	0.0238	0.8156
58	3,200	1.4217	0.7308	1.3493	0.6309	0.7474	0.8612
64	100	0.0820	0.7363	0.0888	0.7421	0.0430	0.8444
64	3,200	2.6157	0.7632	2.9914	0.7530	1.7887	0.9235
70	100	0.1462	0.7775	0.1567	0.9143	0.2037	0.9499
70	3,200	4.6311	0.8091	8.5024	0.9846	8.4310	0.9921
76	100	0.2567	0.8372	0.4052	0.9816	0.2653	0.9518
76	3,200	7.9805	0.8687	16.4320	0.9996	15.5552	0.9970

More specifically, the observation of high recoveries in the AC+Elvaloy+PPA, the AC+EVA and the AC+EVA+PPA at 1/500 s greatly minimizes the effects of delayed elasticity on the creep-recovery responses of the formulations. By doing so, there are much lower levels of elastic response in the material to be carried to the next cycle, and the increases in the level of permanent strain with temperature and applied stress can occur either in the initial cycles or during the test. As the data in Table 274 may indicate, this takes place in both variables and the effects seem to be more concentrated in the parameter *A* (i. e., the increases in strain are more visible in the first creep-cycles than during the test). Finally, examples of limiting test conditions for the use of each formulation in the pavement – as based on a critical value of 1.0 for *A* and *B* and at 3,200 Pa – are probably located at 58°C for the AC+Elvaloy+PPA and the AC+EVA (*A* values around 1.4 and *B* values around 0.70) and 64°C for the AC+EVA+PPA ($A \approx 1.79$ and $B \approx 0.93$). The temperature of 64°C could be used for the AC+Elvaloy+PPA and the AC+EVA as well, but the amount of permanent strain in the first cycles would perhaps be very high ($A \approx 3.0$ for both of them).

Some of the key findings of this part of the investigation that deserve to be mentioned with more emphasis are provided as follows:

- an increase in the unloading time from 9 to 500 s considerably minimized the effects of the delayed elasticity on each creep-recovery cycle of the AC+Elvaloy+PPA, the AC+EVA and the AC+EVA+PPA, and thus full recoveries can be seen for many of them; with exception of a few cases, the recoveries increased and the compliances decreased with such a change in the loading-unloading pattern;
- the AC+EVA depicted recoveries very close or equal to 100% at the lowest temperatures (no greater than 64°C), which could not be seen for the AC+EVA+PPA and the AC+Elvaloy+PPA; this provides an idea of the level of delayed elasticity in the AC+EVA and reinforces the need for much longer unloading times (as longer as 500 s in this case) to have an accurate estimation of the percent recovery and the nonrecoverable compliance of the material under creep-recovery loading;
- some formulations – especially the AC+Elvaloy+PPA – showed higher recoveries at 3,200 Pa than at 100 Pa and, as a consequence, negative $J_{nr, diff}$ values are calculated; the literature suggests the internal variables of the DSR (among which the inertia of the upper plate deserves a careful attention) and the memory effect of the formulation as possible explanations for such findings;
- similarly to the results of the MSCR tests at longer creep times, the parameter α showed good to excellent correlations with the recoveries of the asphalt binders at 100 and 3,200 Pa (R^2 values between 0.75 and 0.93), either in a general or specific context; this gives even more support to the use of α as a complementary indicator of the amount of recovery in the formulation; and
- the considerable reductions in the effect of the delayed elasticity on the response of the asphalt binder at each cycle changed the patterns of variation in A and B with temperature and stress level (and thus the way the binder accumulates strain in the MSCR tests), namely, from decreases to increases in both parameters in the case of the AC+Elvaloy+PPA and the AC+EVA; it is hypothesized that the portion of delayed elasticity not recovered after 9 s of unloading time and carried to the next cycles at 1/9, 2/9, 4/9 and 8/9 s contributed to the decreases in A and B reported earlier.

Analysis of Data for the Formulations of Group "B". Table 275 reports the recovery values for the AC+PPA and all the formulations with crumb rubber (AC+rubber and AC+rubber+PPA) and SBS copolymer (AC+SBS and AC+SBS+PPA). It is worth to mention that the AC+rubber and the AC+SBS depict considerably higher recoveries at 1/240 s than at the original creep-recovery times of 1/9 s (approaching 92-95% in some cases), which suggests that the intrinsic characteristics of the modifiers have a dominant role in the responses of the formulations. As previously noticed in the results at 1/9 s, the use of PPA together with crumb rubber decreased the *R100* and *R3200* values of the AC+rubber+PPA when compared with the AC+rubber, similarly to what was observed for the AC+SBS and the AC+SBS+PPA at longer creep times as well. The results do not exceed 40 and 56% for the AC+SBS+PPA and the AC+rubber+PPA, respectively, and they are typically null at the high PG grade temperature of both materials (76°C).

Table 275 – Percent recoveries at 100 Pa (*R100*) and 3,200 Pa (*R3200*) for the AC+PPA, the AC+rubber, the AC+rubber+PPA, the AC+SBS and the AC+SBS+PPA at 1/240 s and all the high pavement temperatures

formulation	parameter	results (%) at each pavement temperature				
		52°C	58°C	64°C	70°C	76°C
AC+PPA	*R100*	62.7	54.0	40.5	25.4	12.3
	R3200	68.7	55.3	37.2	15.7	0.9
AC+rubber	*R100*	91.7	89.6	82.8	67.3	49.3
	R3200	61.8	41.5	20.7	6.2	0.3
AC+rubber+PPA	*R100*	55.1	48.1	8.1	11.2	2.9
	R3200	45.2	28.1	10.1	0.5	0.0
AC+SBS	*R100*	76.2	92.8	94.4	84.7	45.4
	R3200	55.8	49.6	43.2	32.5	14.4
AC+SBS+PPA	*R100*	34.8	27.6	18.0	9.6	0.0
	R3200	39.6	23.9	9.1	0.2	0.0

The increases in *R100* with temperature for the AC+SBS up to 64°C may be explained by some aspects intrinsically associated with the behavior of elastomers under creep and recovery loading. It may be important to note that some SBR-modified asphalt binders can also depict such increases in the percent recovery with temperature up to a limiting value, see the MSc. Thesis from Domingos (2011) as an example. Firstly, the nonlinear response of polymers tends to be more visible when the degree of stiffness of the binder is reduced, since a stiff binder can act as a reinforcement of the polymer network and "mask" the effects of a poor quality modification in some cases (D'ANGELO, 2010b; SWIERTZ et al., 2017). Based on this and making sure that the strain levels are not very high, one may assume that higher temperatures potentially show a greater role of the behavior of the polymer in the MSCR test when compared with lower ones.

Secondly, it is hypothesized that the aforementioned phenomena of movement of the polystyrene blocks from one region of the formulation to another and rearrangement of the polymeric network also took place during the tests at 1/240 s, even in a limited extent.

It can therefore be concluded that the elastomeric characteristics of the SBS copolymer – including its ability to show rapid recovery when elongated (D'ANGELO et al., 2007) – contributed to a better elastic performance of the AC+SBS under creep and recovery loading and higher temperatures. Since these characteristics could not be seen for the AC+SBS+PPA and PPA is not an elastomer, the recovery results for the AC+SBS+PPA are not too expressive. In terms of the AC+rubber, the substantial increases in recovery at 52 and 58°C can be attributed to a combined effect of the response of the rubber particles and a higher degree of stiffness in the binder. The presence of lower recoveries for the AC+rubber+PPA was expected, once the rubber content is lower for this formulation (11.0% by weight) than the AC+rubber (15.0% by weight).

The plots of the percent recovery values at 1/9 s against the corresponding ones at 1/240 s yield the data points shown in Figure 229. The majority of these data points are located above the equality line, which confirms that the percent recoveries are greater at 1/240 s than at 1/9 s (especially for the AC+PPA, the AC+rubber and the AC+SBS). On the other hand, the results of the AC+rubber+PPA and the AC+SBS+PPA point to a different tendency – i. e., decreases in recovery when moving from 1/9 s to 1/240 s. Since this could be seen for other binders as well (Figure 225, page 477), a more specific investigation is needed to provide explanations for such findings and try to understand the role of the DSR variables on the outcomes of the MSCR tests.

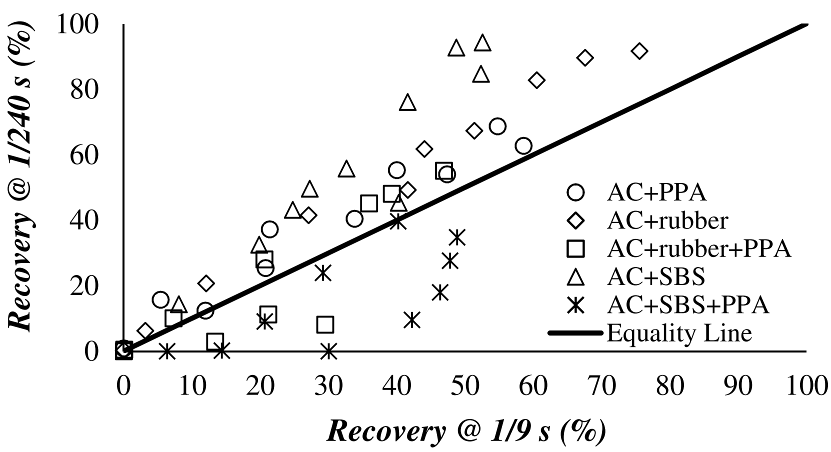

Figure 229 – Comparisons between the percent recoveries of the AC+PPA, the AC+rubber, the AC+rubber+PPA, the AC+SBS and the AC+SBS+PPA at 1/9 s and 1/240 s at all pavement temperatures and stress levels

As pointed out earlier, the inertia of the upper plate of the DSR may influence in the residual strain of the binder when full recovery is achieved. In other words, the strain at the end of the creep-recovery cycle may not be very similar to the one registered right after the observation of the full recovery. The example given in Figure 230 for the AC+SBS+PPA and the AC+rubber+PPA at 70°C precisely indicates that the variables of the device can play a role in the final results of the formulations. In practical terms, this can be interpreted as slight increases in the accumulated strain for the AC+rubber+PPA and oscillations in the strain values for the AC+SBS+PPA. Again, it seems not to be recommended to use recovery times longer than the minimum required ones to observe full recoveries in the binder, since this may highlight the influence of the internal variables of the device on *R* and J_{nr}. It is also possible that the hereditary memory effect, the efficiency of the instrument in its logging components and the control software have a great importance on the measured strains in each formulation, as discussed in the papers by Montepara and Giuliani (1999) and Soenen et al. (2013).

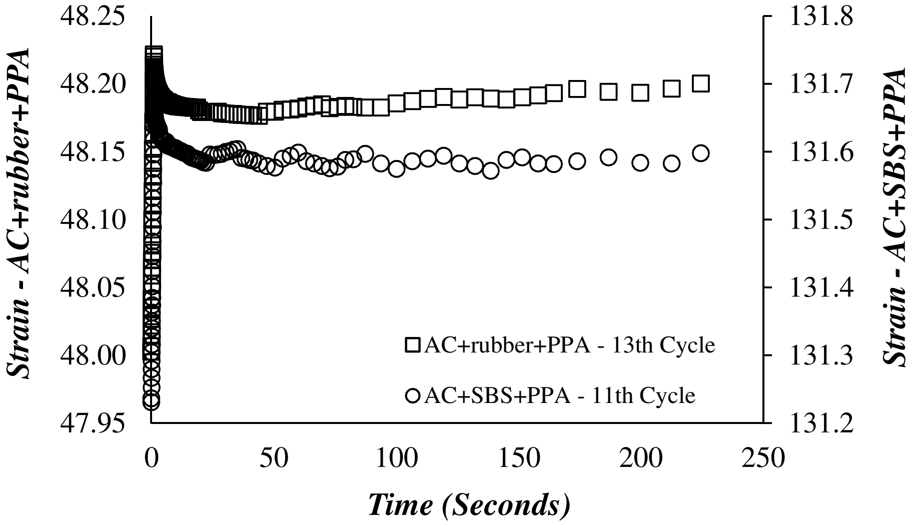

Figure 230 – Raw strain values of the AC+rubber+PPA at the 12th cycle (*R* = 14.5%) and the AC+SBS+PPA at the 11th cycle (*R* = 9.6%) at 100 Pa and the temperature of 70°C

The nonrecoverable compliances of the AC+PPA and the two formulations with crumb rubber (AC+rubber and AC+rubber+PPA) and SBS (AC+SBS and AC+SBS+PPA) can be seen in Table 276. There are some odd cases in which $J_{nr,\ diff}$ is negative (i. e. $J_{nr}3200$ is lower than $J_{nr}100$), but the reasons for such values are similar to those discussed for the materials of the "Group A". The AC+SBS and the AC+rubber are too stress sensitive at several pavement temperatures and, in some cases, the results of $J_{nr,\ diff}$ overcome 400%. This suggests that the accumulation of strain levels at 3,200 Pa is much higher than at 100 Pa, which can be implied from the recovery data as well (Table 275). Similarly to the previously reported data values at longer creep times, the AC+rubber+PPA and the AC+SBS+PPA do not exceed the upper limit of 75% set by Superpave®. The major differences among the results at standardized loading conditions, longer creep times and those at

1/240 s can be seen in the AC+SBS, since this binder barely shows $J_{nr,\ diff}$ values higher than 75% in the former cases and much higher than 75% at 1/240 s.

Table 276 – Nonrecoverable compliances at 100 Pa ($J_{nr}100$) and 3,200 Pa ($J_{nr}3200$) and corresponding percent differences ($J_{nr,\ diff}$) for the AC+PPA, the AC+rubber, the AC+rubber+PPA, the AC+SBS and the AC+SBS+PPA at 1/240 s and all the high pavement temperatures

formulation	parameter	results (kPa^{-1}) at each pavement temperature				
		52°C	58°C	64°C	70°C	76°C
AC+PPA	$J_{nr}100$	0.026	0.072	0.208	0.579	1.516
	$J_{nr}3200$	0.022	0.069	0.221	0.691	2.024
	$J_{nr,\ diff}$ (%)	-17.7	-3.7	6.3	19.3	33.5
AC+rubber	$J_{nr}100$	0.015	0.039	0.134	0.502	1.460
	$J_{nr}3200$	0.069	0.230	0.672	1.690	3.649
	$J_{nr,\ diff}$ (%)	373.9	487.3	402.8	236.4	149.8
AC+rubber+PPA	$J_{nr}100$	0.085	0.224	0.902	1.859	4.117
	$J_{nr}3200$	0.105	0.323	0.952	2.405	5.323
	$J_{nr,\ diff}$ (%)	23.4	43.9	5.6	29.4	29.3
AC+SBS	$J_{nr}100$	0.049	0.034	0.060	0.367	2.855
	$J_{nr}3200$	0.092	0.245	0.648	1.805	4.984
	$J_{nr,\ diff}$ (%)	88.0	618.5	975.5	391.1	74.6
AC+SBS+PPA	$J_{nr}100$	0.081	0.215	0.578	1.479	3.694
	$J_{nr}3200$	0.075	0.229	0.675	1.794	4.179
	$J_{nr,\ diff}$ (%)	-7.4	6.5	16.7	21.3	13.1

As indicated earlier in this section, the capability of the SBS copolymer in recovering higher portions of its delayed elastic strain within 240 s of unloading time further differentiated among the responses of the AC+SBS at 100 and 3,200 Pa. In other words, it can be implied that the considerably higher levels of elastic strain at 100 Pa when compared with the data at 3,200 Pa contributed to the increases in $J_{nr,\ diff}$ at 1/240 s. This can somehow be applied to the AC+rubber as well, since the $J_{nr,\ diff}$ values of this formulation in the other loading-unloading conditions are all between 100 and 200% (Table 107, page 246). Also, it can help in explaining why the percent differences for the AC+EVA may approach 1,000% at some temperatures at 1/240 s and do not overcome 600% in the other testing conditions – comparisons between the $J_{nr,\ diff}$ values reported in Table 197 (page 355) and Table 293 (page 476).

Similarly to the previously studied creep-recovery times, the model parameters A, B, n and α of the modified power equation (SABOO and KUMAR, 2015) were fitted to the raw strain values of the formulations at 1/240 s and the results were compared with each other. This is possible even when the percent recoveries are very high, see an example in Figure 231 for the AC+rubber. The underestimation of the actual strains in the recovery portion of the cycles seems to be the major limitation of the model, especially for very high percent recoveries. This could be seen for some strain values of the AC+EVA as well (Figure 227, page 478), even though R^2 values higher than 0.90 were extremely common under all testing conditions. Again, the *n* values were all around 0.9992-1.0012 (i. e., always approaching unity) and thus they were not reported here for simplification purposes.

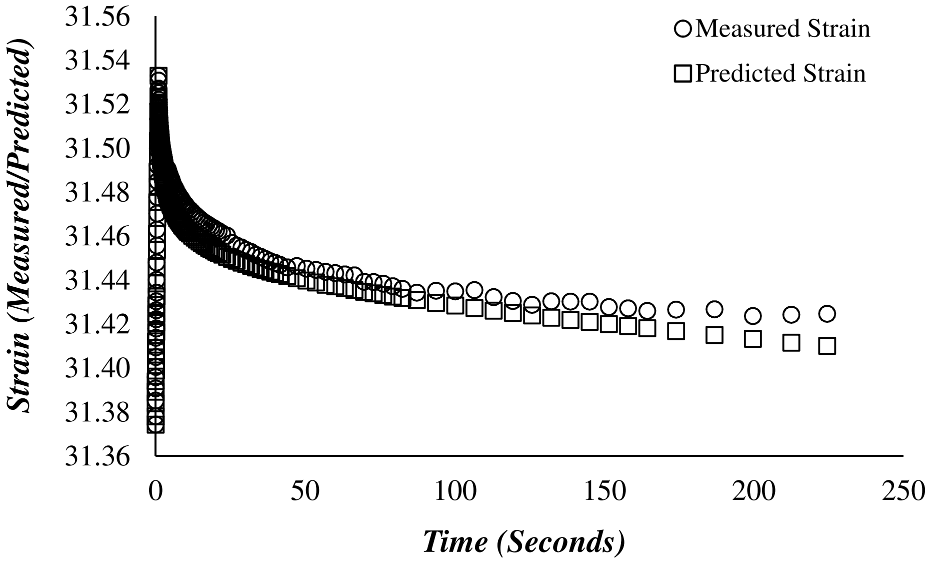

Figure 231 – Fitting of the model from Saboo and Kumar (2015) to the raw strain data of the AC+rubber (11th cycle) at the temperature of 70°C and the stress level of 100 Pa

Table 277 lists the *α* values for each of the formulations with PPA, crumb rubber, rubber+PPA, SBS and SBS+PPA at 1/240 s. Interestingly, the two materials with the highest recoveries (namely, the AC+SBS and the AC+rubber) are not necessarily the ones with the lowest *α* values, especially at temperatures up to 64°C. Also, the increases in *R100* for the AC+SBS at 52, 58 and 64°C is not followed by decreases in *α* at these same temperatures, as initially expected. This put forward the idea that *α* may not work well for all binders with very high recovery values, which could also be seen in the tests at standardized and longer creep times. On the other hand, the presence of results very close or equal to one for small or null recoveries at 76°C was not changed, neither the fact that the *α* values are higher for the AC+rubber+PPA and the AC+SBS+PPA than for the AC+rubber and the AC+SBS, respectively.

In terms of the correlations between the *α* values and the corresponding percent recoveries of all binders, the chart shown in Figure 232 indicates that the overall correlation is reasonable ($R^2 \approx 0.66$). Among the materials included in the analysis, a complementary investigation showed that the individual correlations were excellent for the AC+PPA ($R^2 \approx 0.98$), the AC+rubber ($R^2 \approx 0.97$) and the AC+SBS+PPA ($R^2 \approx 0.98$) and good for the AC+rubber+PPA ($R^2 \approx 0.89$) and the AC+SBS ($R^2 \approx 0.78$). As a consequence, it can be said that the decreased R^2 values may be attributed to the peculiar behavior of the AC+SBS at 100 Pa and the limitations of α for very high recovery values (R ~ 90-100%).

Table 277 – Results of the parameter α from the model by Saboo and Kumar (2015) at 100 and 3,200 Pa and the creep-recovery times of 1/240 s – first group of materials

formulation	stress level (Pa)	results at each pavement temperature				
		52°C	58°C	64°C	70°C	76°C
AC+PPA	100	0.7713	0.7951	0.8539	0.9053	0.9449
	3,200	0.7564	0.8173	0.8891	0.9566	0.9938
AC+rubber	100	0.7787	0.8058	0.8281	0.8478	0.8703
	3,200	0.8331	0.8982	0.9516	0.9826	0.9948
AC+rubber+PPA	100	0.8693	0.8901	0.9296	0.9501	0.9687
	3,200	0.8746	0.9290	0.9732	0.9940	1.0006
AC+SBS	100	0.8823	0.8834	0.8984	0.9056	0.9337
	3,200	0.8914	0.9302	0.9490	0.9542	0.9720
AC+SBS+PPA	100	0.8881	0.9198	0.9520	0.9735	0.9882
	3,200	0.8851	0.9358	0.9748	0.9948	1.0009

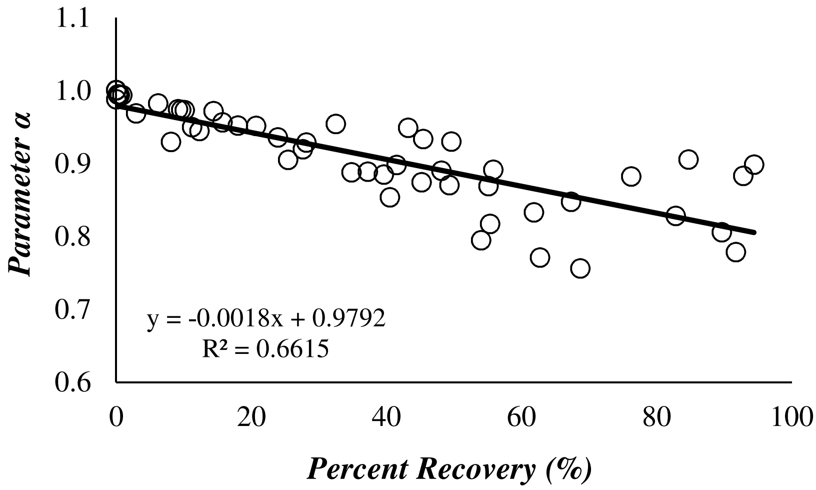

Figure 232 – Degree of correlation between the parameter α from the modified power model and the percent recoveries of the AC+PPA and the formulations with crumb rubber (AC+rubber and AC+rubber+PPA) and SBS (AC+SBS and AC+SBS+PPA) at the creep-recovery times of 1/240 s

The relationships between the nonrecoverable compliance values at 1/9 s to those at 1/240 s for the AC+PPA and the formulations with crumb rubber and SBS are shown in Figure 233.

The data points for the AC+SBS are plotted in the secondary axis due to the observation of much higher rates for this binder (approaching 8.0 or 9.0 in some cases) than for the other materials (no greater than 4.0). As can be seen, the ratios of the compliances of the binders at 1/240 s to those at 1/9 s are commonly greater than 1.0 with only a few exceptions for the AC+SBS+PPA and the AC+rubber+PPA. Again, this suggests that the binders become less prone to rutting at 1/240 s than at 1/9 s and the increases in the amounts of elastic recovery contributed – at least to some extent – to these reduced J_{nr} values.

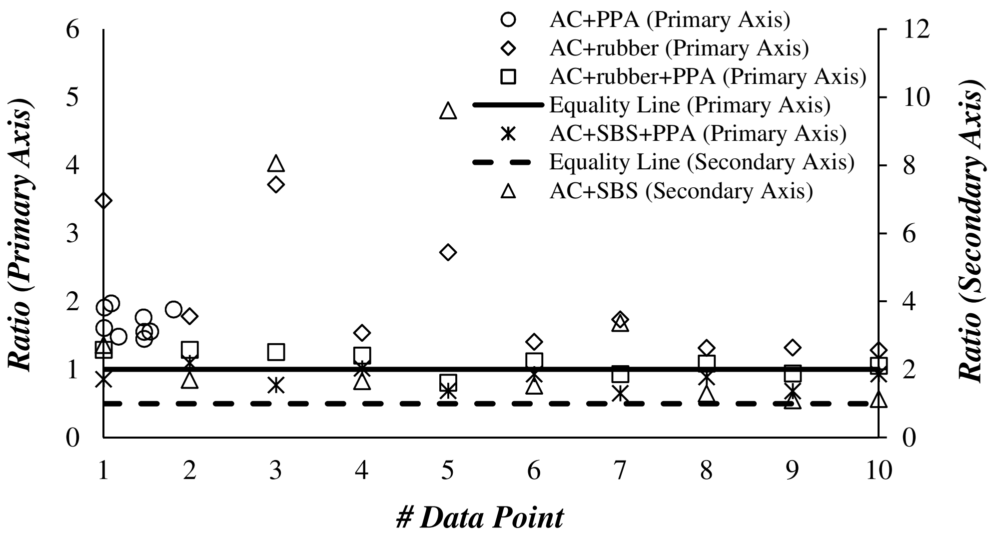

Figure 233 – Ratios of the nonrecoverable compliances of the AC+ PPA, the AC+rubber, the AC+rubber+PPA, the AC+SBS and the AC+SBS+PPA at 1/9 s to those at 1/240 s for a particular temperature and stress level – each data point corresponds to one temperature (out of five) and one stress level (out of two)

Table 278 below provides the *A* and *B* values for the AC+PPA, the AC+rubber and the AC+rubber+PPA at the creep-recovery times of 1/240 s, whereas Table 279 shows these same data for the AC+SBS and the AC+SBS+PPA. The same tendency reported for the asphalt binders at 1/500 s can be seen here, i. e., increases in *A* and *B* with increasing temperature and stress level. This can be seen even for the AC+SBS and the AC+rubber, which showed much greater amounts of recovery after 240 s of unloading time than at 9 s. Such a finding is not exactly similar to what was commonly found for these materials at longer creep times, i. e., decreases in *A* and increases in *B* with variations in the creep time. Again, the minimization of the role of the recovery time on the creep-recovery behavior of the binders is proposed as the major reason why either *A* (initial accumulated strain) or *B* (strain rate) experience increases from one test condition to the other at 1/240 s. Based on the critical value of 1.0 for *A* suggested elsewhere (SARKAR, 2016) and the highest stress level used in the MSCR tests, the temperature of 58°C is proposed as a limiting condition for the use of the AC+rubber, the

AC+rubber+PPA and the AC+SBS (*A* values between 1.0 and 2.0 and *B* values very close to 1.0) and the temperature of 64°C is proposed as the limiting condition for the AC+PPA and the AC+SBS+PPA.

Table 278 – Results of the parameters *A* and *B* from the model by Saboo and Kumar (2015) at 100 and 3,200 Pa and the creep-recovery times of 1/240 s for the AC+PPA, the AC+rubber and the AC+rubber+PPA

temperature (in °C)	stress (in Pa)	AC+PPA		AC+rubber		AC+rubber+PPA	
		A	*B*	*A*	*B*	*A*	*B*
52	100	0.0070	0.7714	0.0181	0.7843	0.0192	0.8737
52	3,200	0.2250	0.7577	0.6031	0.8355	0.6325	0.8783
58	100	0.0153	0.7976	0.0382	0.8070	0.0425	0.8945
58	3,200	0.5095	0.8192	1.3094	0.8997	1.4907	0.9317
64	100	0.0341	0.8564	0.0796	0.8313	0.0980	0.9327
64	3,200	1.1551	0.8903	2.8244	0.9519	3.5664	0.9741
70	100	0.0759	0.9085	0.1564	0.8510	0.2096	0.9563
70	3,200	2.7308	0.9572	6.1161	0.9833	8.1684	0.9944
76	100	0.1710	0.9495	0.2948	0.8728	0.4245	0.9786
76	3,200	6.9493	0.9941	12.6640	0.9952	17.6106	1.0007

Table 279 – Results of the parameters *A* and *B* from the model by Saboo and Kumar (2015) at 100 and 3,200 Pa and the creep-recovery times of 1/240 s for the AC+SBS and the AC+SBS+PPA

temperature (in °C)	stress (in Pa)	AC+SBS		AC+SBS+PPA	
		A	*B*	*A*	*B*
52	100	0.0204	0.8820	0.0122	0.8858
52	3,200	0.6774	0.8913	0.4001	0.8842
58	100	0.0464	0.8824	0.0287	0.9189
58	3,200	1.6228	0.9300	0.9858	0.9356
64	100	0.1068	0.8973	0.0691	0.9522
64	3,200	3.8896	0.9488	2.4877	0.9749
70	100	0.2450	0.9047	0.1624	0.9735
70	3,200	9.2454	0.9541	6.1028	0.9947
76	100	0.5361	0.9335	0.3578	0.9883
76	3,200	20.1585	0.9719	13.8796	1.0010

The following conclusions can be reached with respect to the outcomes of the MSCR tests at longer recovery times (1/240 s) for the AC+PPA, the AC+rubber, the AC+rubber+PPA, the AC+SBS and the AC+SBS+PPA:

- either the AC+SBS or the AC+rubber showed the ability of recovering much higher portions of their total strain at 1/240 s when compared with the original testing condition of 1/9 s (typically between 90 and 95% at temperatures no greater than 64°C), and this indicates that the inherent characteristics of the SBS copolymer and the crumb rubber particles exert a relevant influence on the amount of recovered strain at each creep-recovery cycle;
- the internal variables of the DSR and the memory effect of the formulation may be pointed out as some of the reasons why the AC+SBS+PPA and the AC+rubber+PPA depicted lower recoveries at 1/240 s than at 1/9 s, similarly to what was noticed earlier for the AC+Elvaloy+PPA;
- the parameter α showed a reasonable correlation with the percent recoveries of the materials at 100 and 3,200 Pa (about 0.66) and, since the individual correlations were worse for the AC+SBS than for the other binders, it is believed that the differences within the patterns of response for α and *R100* at the temperatures of 52, 58 and 64°C (i. e., increases in *R100* are not followed by decreases in α) contributed to the reduction in the level of correlation; and
- both parameters *A* and *B* increase with increasing temperature and stress level, which indicates that the minimization of the effects of the delayed elasticity on the outcomes of the MSCR tests (*R* and J_{nr}) contributed to the changes in the patterns of response of the binders when compared with the standardized and longer creep times.

Table 280 summarizes the percent recoveries of the AC+PE, the AC+PE+PPA, the AC+SBR and the AC+SBR+PPA at 1 s of loading time and 240 s of unloading time. The AC+SBR followed a quite similar tendency observed for the AC+SBS, that is, increases in *R100* with temperature until a maximum value of 64°C is achieved. As pointed out earlier, this could be seen in other publications as well (DOMINGOS, 2011) and indicates that the combination of a lower degree of stiffness in the binder due to the presence of higher temperatures with the rubber-like properties of the SBR copolymer (elastomeric modification type) resulted in a substantial increase in this parameter in comparison to the data at 1/9 s. Since the amount of unrecovered strain and the applied stress are higher at 3,200 Pa than at 100 Pa, this leads to greater levels of damage in the polymer and some of its rubber-like characteristics of SBR are minimized. This conclusion can be drawn from the data of the AC+SBS as well, see Table 275 in page 482 for more details.

The different patterns of response for the AC+SBR+PPA when compared with the AC+SBR may be associated with the reduced polymer content in it, since the elastomeric properties of the binder are directy related to the properties of the polymer. The results of the AC+PE may be linked to the very high degree of stiffness of the formulation and, provided that the strain level and the temperature are not very high, the brittle-like characteristics of the material avoid the occurrence of great amounts of unrecovered strain in the sample. This becomes even more clearer when one observes the substantial decreases in recovery when moving from 100 to 3,200 Pa and the lower *R* values of the AC+PE+PPA when compared with the AC+PE, since the low-density PE is the main responsible for the level of stiffness in the binder.

Table 280 – Percent recoveries at 100 Pa (*R100*) and 3,200 Pa (*R3200*) for the AC+PE, the AC+PE+PPA, the AC+SBR and the AC+SBR+PPA at 1/240 s and all the high pavement temperatures

formulation	parameter	results (%) at each pavement temperature				
		52°C	58°C	64°C	70°C	76°C
AC+PE	*R100*	61.6	77.3	65.4	45.8	46.8
	R3200	34.7	24.9	11.8	2.2	0.0
AC+PE+PPA	*R100*	55.8	44.6	30.1	13.7	0.0
	R3200	43.6	27.0	10.6	0.4	0.0
AC+SBR	*R100*	55.9	67.7	68.5	50.0	25.3
	R3200	56.0	49.5	32.4	15.6	2.5
AC+SBR+PPA	*R100*	45.8	36.5	22.7	7.5	5.5
	R3200	52.9	42.2	25.8	8.4	0.0

A plot of the recovery values of the above-cited formulations at 1/240 s against their corresponding values at 1/9 s yields the data points shown in Figure 234. As these data suggest, the recoveries at 1/240 s are higher than the corresponding ones at 1/9 s for the majority of the formulations, with exception of some odd cases for the AC+SBR+PPA and the AC+SBR. Again, the internal variables of the DSR and the memory effect of the modifiers may have played some role on these lower percent recoveries at 1/240 s than at 1/9 s. One representative example of this phenomenon is the chart plotted in Figure 235, in which the accumulated strain increases within the recovery time after the full recovery is observed. This can also affect the loading history of the sample and, as a consequence, the amount of recovered strain in the subsequent creep-recovery cycles. Hence, it is strongly suggested to have the control of the variables associated with the device and avoid (or, at least, minimize) their influence on the binder rutting parameters derived from the MSCR test.

The nonrecoverable compliances of the asphalt binders modified with PE, PE+PPA, SBR and SBR+PPA are given in Table 281. These compliances are much lower for the AC+PE and the AC+PE+PPA when compared with the AC+SBR and the AC+SBR+PPA, which may be explained by the stiffening nature of the low-density PE (a plastomer) when compared with the more elastic nature of the SBR copolymer (an elastomer). As explained above for the percent recovery values, the observation of lower nonrecoverable compliances at 3,200 Pa than at 100 Pa may be associated with the loading history of the formulation and its hereditary memory effect. Interestingly, some binders that were not used to be too stress sensitive at 1/9 s showed much higher $J_{nr,\,diff}$ values at 1/240 s (especially the AC+PE and the AC+SBR), probably because of the marked differences in their percent recoveries at 100 Pa in comparison to the corresponding values at 3,200 Pa. This could not be seen for the AC+PE+PPA and the AC+SBR+PPA, i. e., they still hold their classifications as "not overly stress sensitive materials" at 1/240 s.

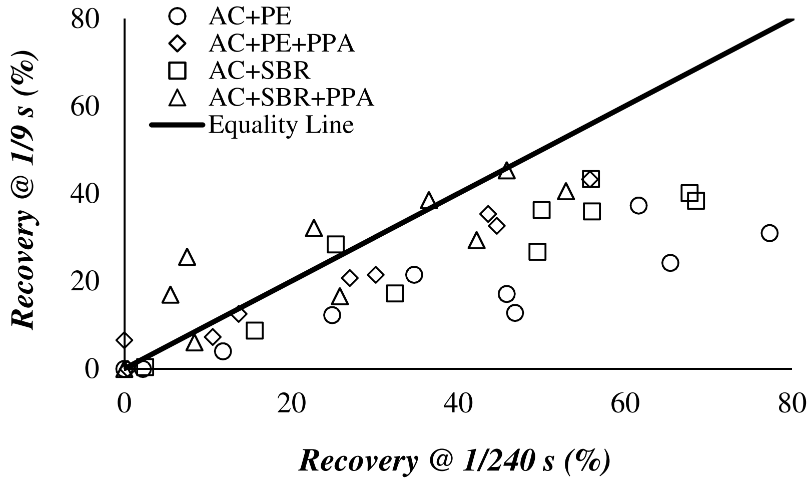

Figure 234 – Comparisons between the percent recoveries of the AC+PE, the AC+PE+PPA, the AC+SBR and the AC+SBR+PPA at 1/9 s and 1/240 s at all pavement temperatures and stress levels

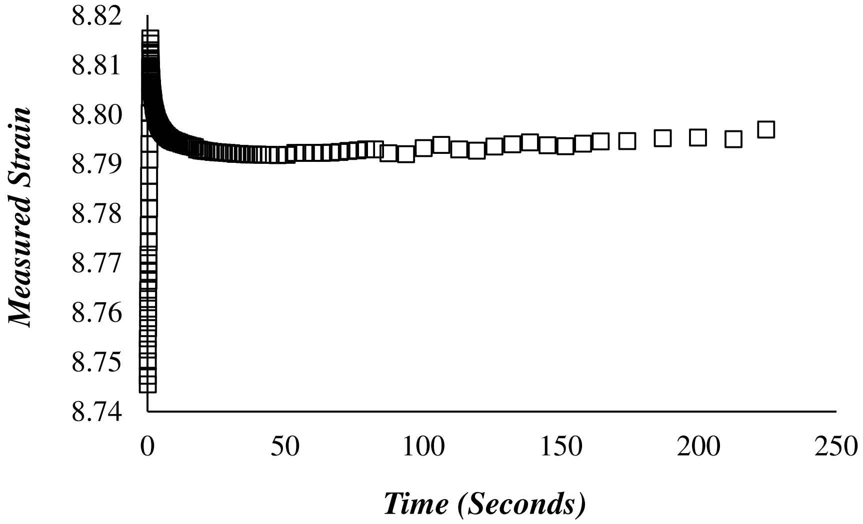

Figure 235 – Raw strain values of the AC+SBR+PPA at the 11th cycle (R = 23.2%), the stress level of 100 Pa and the temperature of 64°C

Table 281 – Nonrecoverable compliances at 100 Pa ($J_{nr}100$) and 3,200 Pa ($J_{nr}3200$) and corresponding percent differences ($J_{nr,\ diff}$) for the AC+PE, the AC+PE+PPA, the AC+SBR and the AC+SBR+PPA at 1/240 s and all the high pavement temperatures

formulation	parameter	results (kPa^{-1}) at each pavement temperature				
		52°C	58°C	64°C	70°C	76°C
AC+PE	$J_{nr}100$	0.037	0.061	0.218	0.736	1.524
	$J_{nr}3200$	0.066	0.204	0.613	1.675	4.173
	$J_{nr,\ diff}$ (%)	79.7	236.9	181.3	127.6	173.8
AC+PE+PPA	$J_{nr}100$	0.038	0.122	0.386	1.135	3.030
	$J_{nr}3200$	0.049	0.166	0.528	1.497	3.815
	$J_{nr,\ diff}$ (%)	28.7	36.3	36.7	31.9	25.9
AC+SBR	$J_{nr}100$	0.105	0.171	0.355	1.135	3.180
	$J_{nr}3200$	0.105	0.277	0.832	2.254	5.374
	$J_{nr,\ diff}$ (%)	0.5	61.9	134.2	98.6	69.0
AC+SBR+PPA	$J_{nr}100$	0.077	0.203	0.544	1.380	2.874
	$J_{nr}3200$	0.066	0.188	0.554	1.565	3.728
	$J_{nr,\ diff}$ (%)	-13.7	-7.2	1.9	13.4	29.7

The ratios of the nonrecoverable compliances of the formulations with PE, PE+PPA, SBR and SBR+PPA at 1/9 s to the corresponding values at 1/240 s can be graphically seen in Figure 236. As these results may indicate, there is a decrease in $J_{nr}100$ and $J_{nr}3200$ by percentages up to 40% when moving from 1/9 s to 1/240 s for several binders. Due to the peculiar characteristic of the AC+SBR+PPA in the percent recovery data, the ratios of J_{nr} values are higher than unity (i. e., J_{nr} is greater at 1/240 s than at 1/9 s) for this material under some testing conditions. The decreases are typically more expressive for the AC+SBR and the AC+PE than for the other formulations, especially at the Data Points #1-6 (temperatures of 52, 58 and 64°C). It is important to remind that such formulations are precisely the ones that depicted very high increases in recovery at the stress level of 100 Pa. The data points approach the equality line in the Data Points #7-10 (temperatures of 70 and 76°C), which is where the delayed elasticity has a considerably lower influence in the creep-recovery behavior of the formulations. This same conclusion can be reached from the data points for the previously reported formulations, see Figure 226 (page 477) and Figure 233 (page 488) for more details.

The α values from the model by Saboo and Kumar (2015) were collected for the formulations with PE, PE+PPA, SBR and SBR+PPA, and their results are summarized in Table 282. Surprisingly, the results of this parameter are all higher than 0.80, even for the binders with percent recoveries greater than 60% at some temperatures such as the AC+PE and the AC+SBR.

This is in indication that the α values do not necessarily need to be much smaller than unity (for instance, 0.60 or 0.70) to reflect the presence of reasonably high percent recoveries. On the other hand, the results are greater for the AC+PE+PPA than for the AC+PE, as based on the *R100* and *R3200* values of both materials. The same can be said for the AC+SBR and the AC+SBR+PPA, namely, the α values are greater for the formulation with PPA than for the one without PPA and the percent recovery data point to this direction as well.

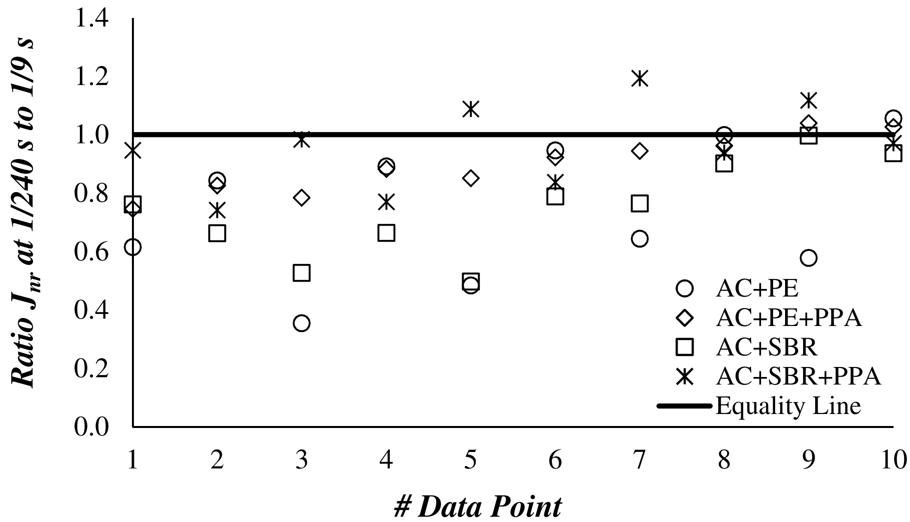

Figure 236 – Ratios of the nonrecoverable compliances of the AC+ PE, the AC+PE+PPA, the AC+SBR and the AC+SBR+PPA at 1/240 s to those at 1/9 s for a particular temperature and stress level – each data point corresponds to one temperature (out of five) and one stress level (out of two)

Table 282 – Results of the parameter α from the model by Saboo and Kumar (2015) at 100 and 3,200 Pa and the creep-recovery times of 1/240 s – second group of materials

formulation	stress level (Pa)	results at each pavement temperature				
		52°C	58°C	64°C	70°C	76°C
AC+PE	100	0.8947	0.9024	0.9151	0.9237	0.9242
	3,200	0.9256	0.9515	0.9761	0.9930	1.0012
AC+PE+PPA	100	0.8747	0.8969	0.9286	0.9566	0.9747
	3,200	0.8811	0.9300	0.9729	0.9943	1.0012
AC+SBR	100	0.8638	0.8597	0.8638	0.8833	0.8944
	3,200	0.8614	0.8886	0.9274	0.9614	0.9871
AC+SBR+PPA	100	0.8586	0.8716	0.8993	0.9255	0.9528
	3,200	0.8525	0.8894	0.9356	0.9762	0.9944

The overall correlation between the α values of the asphalt binders modified with PE, PE+PPA, SBR and SBR+PPA and their corresponding R values can be seen in Figure 237.

Although this correlation was found to be pretty good ($R^2 \approx 0.76$), the data points are quite scattered within the chart area and do not necessarily point to a clear relationship between α and R. This could somehow be seen for the other formulations from "Group B" as well, see Figure 232 (page 487) for further details. In other words, the parameter α does not seem to work perfectly well for all types of loading-unloading proportions found in the literature and used in the present study, even though the individual correlations for the AC+PE ($R^2 \approx 0.92$), the AC+PE+PPA ($R^2 \approx 0.97$), the AC+SBR ($R^2 \approx 0.89$) and the AC+SBR+PPA ($R^2 \approx 0.86$) are quite promising.

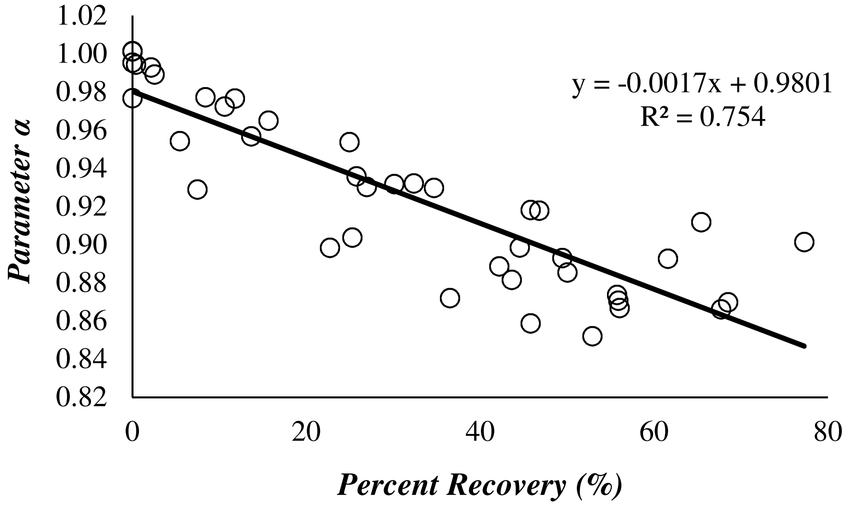

Figure 237 – Degree of correlation between the parameter α from the modified power model and the percent recoveries of the AC+PE, the AC+PE+PPA, the AC+SBR and the AC+SBR+PPA the creep-recovery times of 1/240 s

The remaining parameters of the power model for the AC+PE, the AC+PE+PPA, the AC+SBR and the AC+SBR+PPA (not including the parameter n because the results are all equal to or very close to unity, namely, between 0.9996 and 1.0006) are provided in Table 283. The increases in A and B with stress level and temperature is the dominant feature in the results of all binders, similarly to what was reported earlier for the materials prepared with PPA, crumb rubber and SBS (see Table 278 and Table 279 for the specific results). It can therefore be implied that the minimization of the role of the delayed elasticity on the creep-recovery behavior of the binders contributed to the change in the variations in the initial accumulated strain, that is, from decreases to increases in the A values at higher temperatures and stress levels in some cases (e. g., for the AC+PE+PPA). With respect to the limiting condition for the use of such materials for paving applications, the AC+PE and the AC+PE+PPA would be recommended on pavements with high PG grades up to 64°C and the two formulations with SBR (AC+SBR and AC+SBR+PPA) would not be recommended on pavements with PG grades greater than 58°C (A values between 1.0 and 3.0 in all cases).

Table 283 – Results of the parameters *A* and *B* from the model by Saboo and Kumar (2015) at 100 and 3,200 Pa and the creep-recovery times of 1/240 s for the AC+PE, the AC+PE+PPA, the AC+SBR and the AC+SBR+PPA

T (°C)	stress (Pa)	AC+PE		AC+PE+PPA		AC+SBR		AC+SBR+PPA	
		A	*B*	*A*	*B*	*A*	*B*	*A*	*B*
52	100	0.0097	0.8925	0.0087	0.8737	0.0247	0.8707	0.0147	0.8590
52	3,200	0.3354	0.9298	0.2868	0.8817	0.8123	0.8668	0.4710	0.8522
58	100	0.0255	0.9008	0.0217	0.8985	0.0528	0.8658	0.0318	0.8723
58	3,200	0.9152	0.9537	0.7593	0.9304	1.8683	0.8930	1.0932	0.8887
64	100	0.0620	0.9113	0.0551	0.9319	0.1130	0.8695	0.0697	0.8986
64	3,200	2.3729	0.9767	1.9926	0.9725	4.2026	0.9320	2.5169	0.9359
70	100	0.1388	0.9181	0.1314	0.9569	0.2307	0.8855	0.1490	0.9292
70	3,200	5.8902	0.9928	5.1445	0.9944	9.1455	0.9650	5.8046	0.9774
76	100	0.2978	0.9178	0.3028	0.9769	0.4340	0.9041	0.3014	0.9545
76	3,200	14.0250	1.0012	12.7354	1.0015	18.9667	0.9892	12.7427	0.9953

On the basis of the results reported for the formulations with PE, PE+PPA, SBR and SBR+PPA, the following conclusions can be reached:

- the AC+SBR depicted increases in *R100* with increasing temperature up to a critical value of 64°C, which had already been seen for the AC+SBS at these same temperatures; this suggests that the inherent characteristics of the elastomeric modification type of the binder – among which the "rubber-like" behavior can be mentioned – played a critical role on the creep-recovery response of the AC+SBR;
- the AC+PE also depicted increases in *R100* with temperature up to 64°C, and these increases are associated with the high degree of stiffness of the formulation (i. e., a brittle-like behavior) and possibly the fact that the strain levels are below the "failure point" of the material;
- the AC+SBR+PPA showed decreases in the percent recovery when moving from 1/9 s to 1/240 s at several pavement temperatures, as well as lower percent recoveries at 100 Pa than at 3,200 Pa; this may be caused by the hereditary memory effect of the modifier (s) as pointed out elsewhere in the literature;
- although a general correlation between the α values at 1/240 s and the corresponding percent recoveries of the asphalt binders seemed to be reasonable (about 0.75), the scaterring of the data points suggests that this parameter may not work well for all types of creep-recovery times; on the other hand, the individual correlations were found to be much more promising (no lower than 0.86); and

- either the initial strain or the strain rate (parameters *A* and *B*) increase with increasing stress level and temperature at the creep-recovery times of 1/240 s, and this is one more evidence of the importance of the delayed elasticity on the outcomes of the creep-recovery tests for the studied asphalt binders.

Final Comments on the Creep-Recovery Responses of Asphalt Binders at Longer Creep Times. Finally, the testing of the hypothesis that "the unloading time of 240 s is sufficient to practically eliminate the effects of delayed elasticity on the creep-recovery responses of the asphalt binders from Group B" was verified. According to the literature (ZOOROB et al., 2012), the delayed elasticity plays a role on the creep-recovery response of the binder by decreasing the peak value of each creep-recovery cycle. Due to the fact that the unrecovered portion of the delayed elastic response is carried to the next cycle (TEYMOURPOUR et al., 2016), the percent recoveries of the material typically increase with increasing number of cycles. Such a process is interrupted when steady state is achieved, i. e., the delayed elasticity is fully recovered, the recoveries stabilize and the strains reach an asymptote value at the end of the cycle. This can be made either by increasing the number of cycles – which has been commonly studied in the literature – or by increasing the recovery times at each cycle, which was done in the present study.

Based on these comments and taking into account the criteria mentioned above, an overall and simplified analysis of the creep-recovery data of the formulations at 1/240 s and all testing temperatures was conducted. The conclusions of this section can be inferred from the data summarized in Table 284 below. In this table, "Yes" means that both criteria (strains reaching a plateau and stabilization of the percent recoveries at each cycle, with focus on the data at 100 Pa) were met and "No" means that at least one of these criteria were not satisfied. As can be seen, the AC+SBS and the AC+rubber are two of the materials for which the creep-recovery times of 1/240 s are not mostly adequate for achieving full recovery in the MSCR tests. This is quite logical, since both materials are amongst the ones with the highest recovery values and they were prepared with additives that show elastic properties (rubber particles and elastomers). Also, the temperature of 52°C is the one at which several binders do not seem to provide full recovery at 1/240 s due to their quite high recovery values.

Some examples of the percent recoveries with increasing creep-recovery cycles are given in Figure 238 for the AC+rubber and the AC+PE at 52°C. As can be seen, the results increase significantly for the AC+rubber from the first (about 80%) to the last cycle (more than 90%). The AC+PE also depicts increases in its recovery values (from 50 to about 60%), but the rates are lower than those found in the AC+rubber. This is a clear indication that the delayed elasticity has a relevant role in the outcomes of the MSCR tests for the two materials, even at much longer recovery times (almost 3 times higher than the standardized one). In such a case, it is recommended to further increase the unloading time in an attempt to observe full recoveries in the binders and stabilization in the percent recovery values.

Table 284 – Overall and simplified analysis of the creep-recovery data of the asphalt binders from "Group B" with respect to the criteria for reaching full recovery at each creep-recovery cycle

formulation	compliance with the criteria for showing full recovery at each cycle				
	52°C	58°C	64°C	70°C	76°C
AC+PPA	No	Yes	No	Yes	Yes
AC+rubber	No	No	No	Yes	Yes
AC+rubber+PPA	No	No	Yes	Yes	Yes
AC+SBS	No	No	No	No	No
AC+SBS+PPA	Yes	Yes	Yes	Yes	Yes
AC+PE	No	No	No	No	No
AC+PE+PPA	No	No	No	Yes	Yes
AC+SBR	No	No	No	Yes	Yes
AC+SBR+PPA	No	No	Yes	Yes	Yes

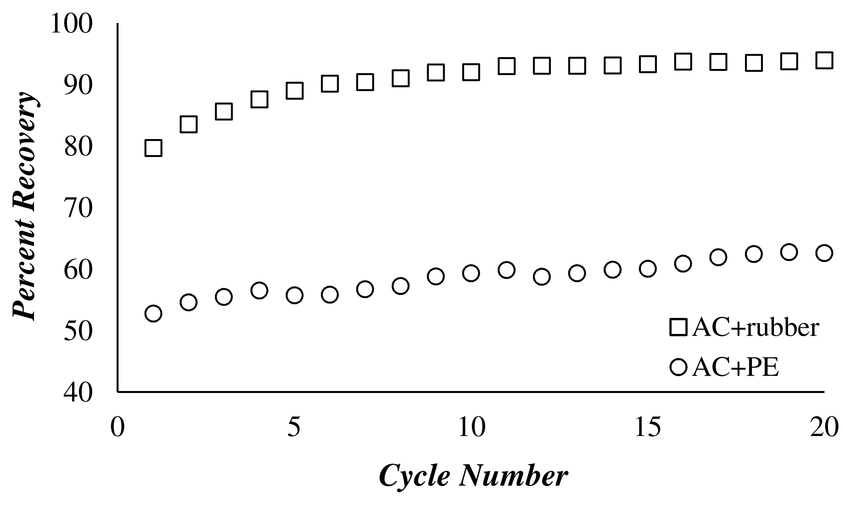

Figure 238 – Variations in the percent recovery of the AC+rubber and the AC+PE for each creep-recovery cycle at 1/240 s, 100 Pa and 52°C

One last example of the role of the delayed elasticity on the creep-recovery cycles of the asphalt binders is given in Figure 239 for the AC+SBS at 70°C and the stress level of 100 Pa. It is clear that the full recovery of the strain values are not achieved within 240 s, which means that much longer recovery times would be required to reach a plateau zone. The same can be said for the creep-recovery data of the AC+rubber+PPA at the temperature of 52°C (see Figure 240), even though the amount of elastic recovery that still needs to be recovered looks much smaller for this binder than for the AC+SBS. These charts and analyses give support to the conclusion that the investigation of the level of elastic response in the binder is essential to estimate its level of delayed elasticity; however, other factors such as the modification type and the temperature are also very important to portray a complete picture of the full recovery in the binder sample.

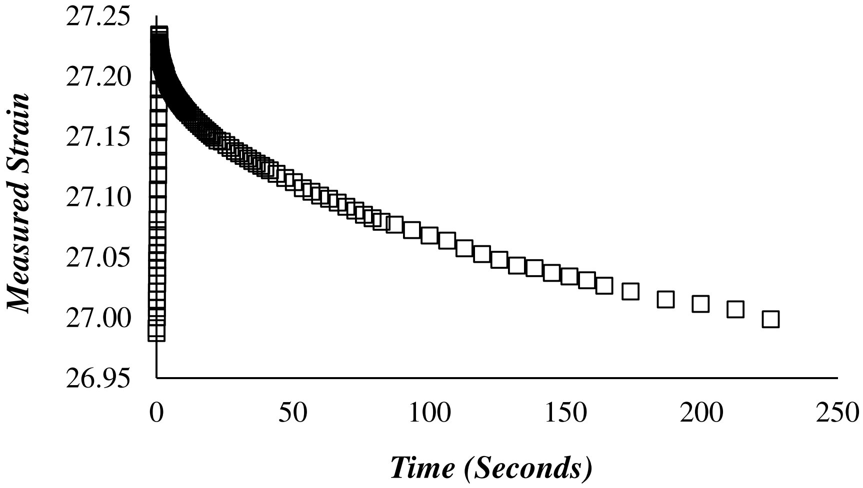

Figure 239 – Raw strain values of the AC+SBS at the 6th cycle (R = 95.2%), stress level of 100 Pa and the temperature of 70°C

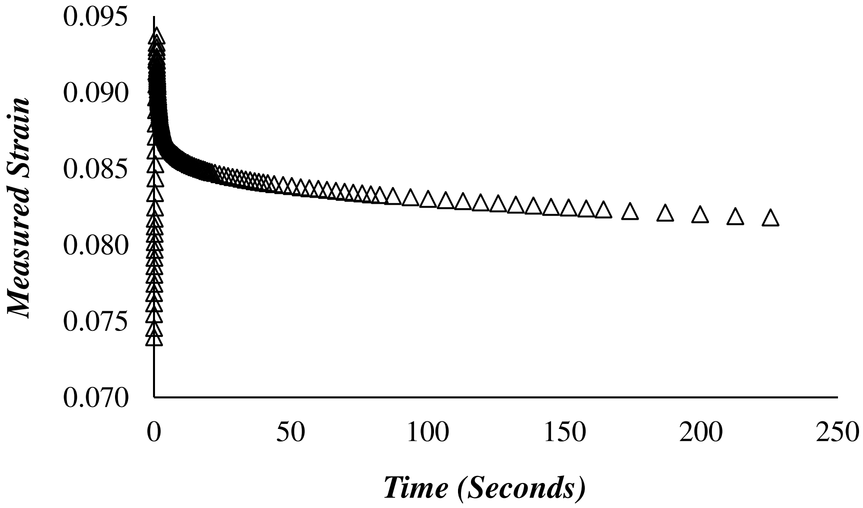

Figure 240 – Raw strain values of the AC+rubber+PPA at the 10th cycle (R = 58.7%), stress level of 100 Pa and the temperature of 52°C

Rankings of the Asphalt Binders at Longer Recovery Times. The forthcoming tables and discussions are intended to rank the asphalt binders as based on their nonrecoverable compliances in the MSCR tests at longer loading times, similarly to what was made for the data at longer creep times. First, the J_{nr} values of the materials were grouped and ranked from the lowest to the highest result (i. e., from the lowest to the highest susceptibility to rutting) at each pavement temperature and comments on the findings were made. The same was done for the $J_{nr,\ diff}$ values, and comparisons between each type of ranking were made. Finally, the average positions of the formulations were determined and compared with the corresponding results at longer creep times in order to identify similarities and differences among them.

Table 285 shows the individual positions of the asphalt binders as based on the nonrecoverable compliance values at 100 and 3,200 Pa. As these data suggest, some materials depict greater variations within their positions with increasing temperature (especially for the AC+Elvaloy+PPA, the AC+rubber, the AC+EVA, the AC+EVA+PPA and the AC+SBR+PPA), whereas others do not. One of the factors that may help in explaining these variations is the degree of nonlinearity of the material, i. e., the rate of increase in J_{nr} with temperature and stress level. Interestingly, all the previously mentioned binders – except for the AC+Elvaloy+PPA – typically show very high stress sensitivity in the MSCR tests, see their average positions in Table 269 as examples. With respect to the AC+Elvaloy+PPA, it is suggested that the changes in the positions of the other asphalt binders (and not its stress sensitivity) are the major reasons why modifications in its rankings could be seen.

Table 285 – Rankings of the modified asphalt binders at longer creep times based on $J_{nr}100$ and $J_{nr}3200$ and for all pavement temperatures

formulation[b]	rankings for $J_{nr}100$[a]					rankings for $J_{nr}3200$[a]				
	52°C	58°C	64°C	70°C	76°C	52°C	58°C	64°C	70°C	76°C
A	3	6	5	4	2	2	2	2	2	2
EA	7	7	9	6	4	3	3	3	1	1
B	2	3	4	3	1	8	9	9	6	3
BA	11	12	12	12	12	11	12	12	12	11
S	8	2	2	2	6	10	10	8	8	10
SA	10	11	11	11	10	9	8	10	7	7
EV	1	1	1	1	11	1	1	1	11	9
EVA	4	5	3	5	5	4	4	4	9	8
P	5	4	6	7	3	6	7	7	5	6
PA	6	8	8	8	8	5	5	5	3	5
SB	12	9	7	9	9	12	11	11	10	12
SBA	9	10	10	10	7	7	6	6	4	4

[a] each number refers to the relative position of the formulation in a ranking from the less (No. 1) to the most susceptible to rutting (No. 12).
[b] "A" = PPA; "E" = Elvaloy®"; "B" = crumb rubber; "S" = SBS copolymer; "EV" = EVA copolymer; "P" = low-density PE; "SB" = SBR copolymer.

By taking into account all of the above-cited individual rankings and calculating their mean values and coefficients of variation, Table 286 is obtained. As can be seen, the AC+PPA (final position of 3.0) and the AC+EVA (3.8) are the formulations with the lowest susceptibility to rutting in a general context, followed by the AC+Elvaloy+PPA (4.4), the AC+rubber (4.8), the AC+EVA+PPA (5.1) and the AC+PE (5.6). On the other hand, the AC+rubber+PPA is the formulation with the highest rutting potential (final position of 11.7), followed by the AC+SBR (10.2), the AC+SBS+PPA (9.4), the AC+SBR+PPA (7.3), the AC+SBS (6.6) and the AC+PE+PPA (6.1). However, it may be important to remind that some materials are ranked completely different in the MSCR tests as a function of the stress level, especially for the AC+Elvaloy+PPA, the AC+rubber, the AC+SBS, the AC+PE+PPA and the AC+SBR+PPA. In a general context, the asphalt binders with PPA in the composition are ranked much better at 3,200 Pa than at 100 Pa. These findings are in aligment with the outcomes obtained for the tests at longer creep times (see Figure 219, page 464, for more details).

Table 286 – Mean values of the rankings of the modified asphalt binders at longer creep times – based on $J_{nr}100$ and $J_{nr}3200$ – and corresponding coefficients of variation (CV)

formulation	CV values (in %)		average positions in the rankings[a]		final ranking
	100 Pa	3,200 Pa	100 Pa	3,200 Pa	
AC+PPA	35.4	0.0	4.0 (3)	2.0 (1)	3.0
AC+Elvaloy+PPA	24.6	44.5	6.6 (6)	2.2 (2)	4.4
AC+rubber	39.2	32.6	2.6 (1)	7.0 (7)	4.8
AC+rubber+PPA	3.4	4.2	11.8 (10)	11.6 (11)	11.7
AC+SBS	63.2	10.6	4.0 (3)	9.2 (9)	6.6
AC+SBS+PPA	4.6	14.2	10.6 (9)	8.2 (8)	9.4
AC+EVA	133.3	96.8	3.0 (2)	4.6 (3)	3.8
AC+EVA+PPA	18.2	38.4	4.4 (4)	5.8 (5)	5.1
AC+PE	28.3	12.1	5.0 (5)	6.2 (6)	5.6
AC+PE+PPA	10.5	17.4	7.6 (7)	4.6 (3)	6.1
AC+SBR	17.4	6.7	9.2 (8)	11.2 (10)	10.2
AC+SBR+PPA	12.7	22.2	9.2 (8)	5.4 (4)	7.3

[a] the numbers in parentheses refer to the position of the binder in the ranking of the mean values (from the lowest to the highest result).

To provide further explanations about the differences within the rankings of the asphalt binders at longer creep and recovery times, one can plot the individual rankings at 100 and 3,200 Pa against each other and analyze the locations of the data points with reference to an equality line. In this case, points close to the equality line indicate that these positions are quite similar and the relative rutting resistance of the binder was not significantly changed when moving from one testing condition to the other. Figure 241 portrays these data points for all the formulations and their corresponding average positions at 100 and 3,200 Pa. As can be observed, the results are scattered for the stress level of 100 Pa and much closer to the equality line for the stress level of 3,200 Pa. Since 3,200 Pa is the stress level officially used on Superpave® to evaluate the susceptibility of the asphalt binders to rutting, it can be said that the differences between the estimations of the rutting resistances of the binders were not markedly affected by modifications in the loading-unloading times (in a relative context).

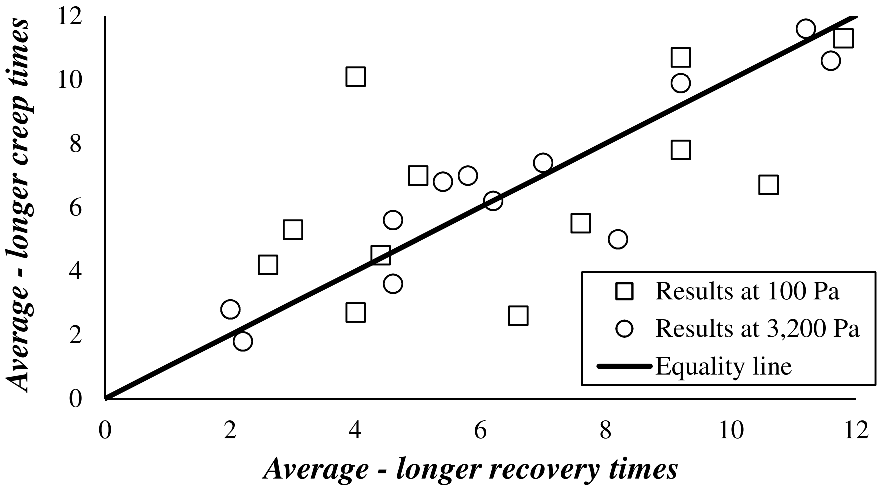

Figure 241 – Plots of the average positions of the 12 formulations in the rankings of $J_{nr}100$ and $J_{nr}3200$ according to the MSCR tests at longer creep and recovery times

One of the reasons for explaining the differences in the rankings at 100 Pa is that, for several binders, they recovered greater portions of the total strain when tested at this stress level and longer recovery times. Depending on the behavior of the material, the DSR internal variables also influenced on the final results as discussed earlier. In such cases, their J_{nr} values experienced considerable variations and their positions changed significantly in the relative rankings. Some examples that give support to this conclusion are the AC+Elvaloy+PPA (positions of 2.6 and 6.6 with increasing creep and recovery times, respectively), the AC+SBS (from 10.1 to 4.0), the AC+SBS+PPA (from 6.7 to 10.6), the AC+EVA (from 5.3 to 3.0) and the AC+PE+PPA (from 5.5 to 7.6). These comments highlight the need for studying the rheological behavior of the modified asphalt binders under testing conditions other than the ones standardized by ASTM and AASHTO, in order to obtain more detailed information on their levels of elastic and delayed elastic responses, stress sensitivity and rutting potential.

Similarly to the J_{nr} values, the parameter $J_{nr,\ diff}$ was also included in the analysis to study the relative levels of stress sensitivity of each material and, in an indirect way, to estimate its rutting potential in unexpected temperature and loading conditions. Table 287 shows a summary of the data together with the corresponding final rankings and coefficients of variation for all of the 12 formulations. As can be observed, the six less stress sensitive materials are the AC+Elvaloy+PPA (average position of 1.2), the AC+SBR+PPA (3.2), the AC+PPA (4.0), the AC+SBS+PPA (4.0), the AC+rubber+PPA (5.2) and the AC+PE+PPA (5.8). On the other hand, the six most stress sensitive binders are the AC+SBS (average position of 11.0), the AC+rubber (11.0), the AC+PE (9.8), the AC+EVA+PPA (9.0), the AC+SBR (7.4) and the AC+EVA (6.4). The CV's typically vary from 5 to 30%, with only a few exceptions.

Table 287 – Rankings of the modified asphalt binders at longer creep times based on $J_{nr,\ diff}$ and for all pavement temperatures, together with the corresponding coefficients of variation (CV)

formulation	individual rankings for $J_{nr,diff}$ [a]					final ranking[b]	CV (%)
	52°C	58°C	64°C	70°C	76°C		
AC+PPA	3	3	4	3	7	4.0	38.7
AC+Elvaloy+PPA	2	1	1	1	1	1.2	33.3
AC+rubber	12	11	11	10	11	11.0	5.7
AC+rubber+PPA	7	6	3	5	5	5.2	25.5
AC+SBS	11	12	12	11	9	11.0	10.0
AC+SBS+PPA	5	4	5	4	2	4.0	27.4
AC+EVA	1	9	7	12	3	6.4	62.2
AC+EVA+PPA	9	7	10	9	10	9.0	12.2
AC+PE	10	10	9	8	12	9.8	13.5
AC+PE+PPA	8	5	6	6	4	5.8	22.9
AC+SBR	6	8	8	7	8	7.4	10.8
AC+SBR+PPA	4	2	2	2	6	3.2	50.0

[a] each number refers to the relative position of the formulation in a ranking from the less (No. 1) to the most susceptible to rutting (No. 12).

[b] this final ranking refers to the average position of the binder at all pavement temperatures.

By comparing the results and rankings of $J_{nr,\ diff}$ for the data at longer recovery times with those at longer creep times (refer to Table 269 for the numerical values), one can observe that two formulations – namely, the AC+SBS and the AC+PE – depicted considerable variations in their stress sensitivity. With respect to the former, it can be said that the rubber-like nature of the SBS copolymer contributed to the occurrence of greater increases in the elastic strain during the unloading phase of the cycles at 100 Pa. With respect to the latter, the stiffening properties of PE and the use of much longer unloading times in the cycles led to decreases in the strain levels during MSCR and, at the same time, the full recovery of the elastic strains. As a consequence, the nonrecoverable compliances at 100 Pa decreased significantly and the $J_{nr,\ diff}$ values increased. The observation of better average positions (i. e., lower stress sensitivity) for the formulations with PPA in the composition when compared with the corresponding ones without PPA is also in alignment with the data at longer creep times.

To illustrate the above discussion on the percent differences in compliances with varying loading-unloading patterns during MSCR, Figure 242 was constructed. As can be observed, approximately half of the data points (five out of 12) are very close to the equality line, whereas the remaining ones show differences between the average positions of the rankings – as based on $J_{nr,\ diff}$ – equal to a factor of about 2.0. This last group of materials includes the AC+PPA (difference between the positions equal to 1.8), the AC+EVA (1.9), the AC+EVA+PPA (1.3), the AC+PE+PPA (1.3) and the AC+SBR+PPA (2.0).The AC+SBS (difference equal to 4.4) and the AC+PE (difference equal to 2.8) are the major outliers within the data set, as mentioned earlier. Therefore, it can be said that the AC+SBS and the AC+PE were the formulations that experienced the greatest increases in $J_{nr,\ diff}$ when moving from the tests with longer creep times to the ones with longer recovery times.

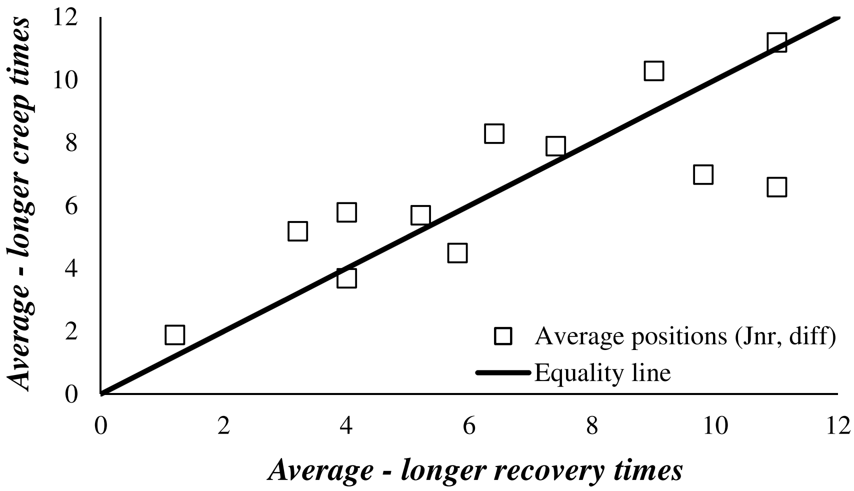

Figure 242 – Plots of the average positions of the 12 formulations in the rankings of $J_{nr,\ diff}$ according to the MSCR tests at longer creep and recovery times

6.3.5. Concluding Remarks on the Use of $J_{nr,\ diff}$ as a Rutting Parameter

Although several papers from the literature have highlighted the benefits of using J_{nr} as a binder rutting parameter (see Chapter 3 of this dissertation for more details), the same cannot be said for $J_{nr,\ diff}$. A very recent publication from Stempihar et al. (2017) emphasized that the parameter $J_{nr,\ diff}$ does not give clear evidences of the rutting performance of the mixture, and thus another parameter or alternative protocols may be needed to solve this issue. To further investigate the relationship between $J_{nr,\ diff}$ and rutting performance either in the binder or the mixture scales, the following correlations were investigated: (a) F_N at 60°C and $J_{nr,\ diff}$ at 64°C and standardized loading-unloading times in the MSCR tests; (b) $J_{nr}3200$ and $J_{nr,\ diff}$ at longer creep times; and (c) $J_{nr}3200$ and $J_{nr,\ diff}$ and longer unloading times.

Figure 243 shows the resulting correlation between F_N at 60°C and $J_{nr,\ diff}$ at 64°C according to the standardized MSCR protocol. It is clear that no correlation exists between the two parameters, which is in agreement with the conclusions drawn by Stempihar et al. (2017). Therefore, the use of $J_{nr,\ diff}$ as a rutting parameter can lead to misleading interpretations about the actual performance of the mixture in the pavement. The same can be said for the correlations between $J_{nr}3200$ and $J_{nr,\ diff}$ at different pairs of creep-recovery times, as depicted in Figure 244 for all the creep times used in the study and the 12 modified materials.

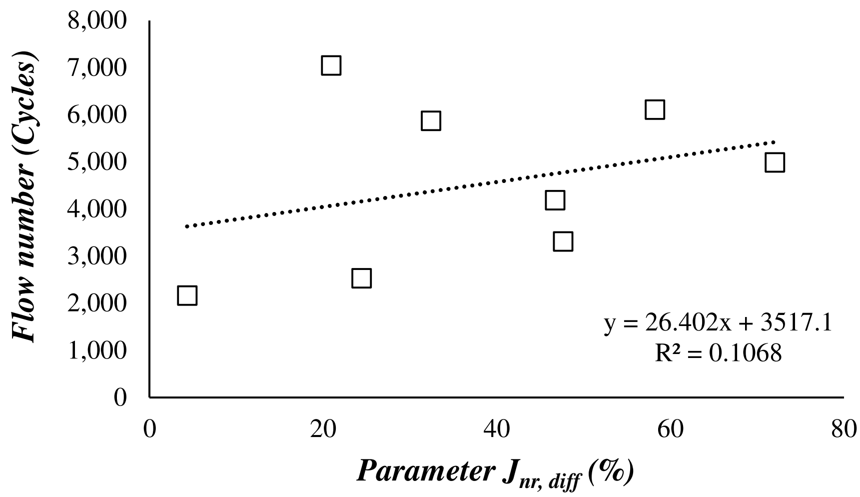

Figure 243 – Resulting correlation between the percent difference in compliances ($J_{nr,\ diff}$) at 64°C and 1/9 s and the flow number values of the asphalt mixtures at 60°C

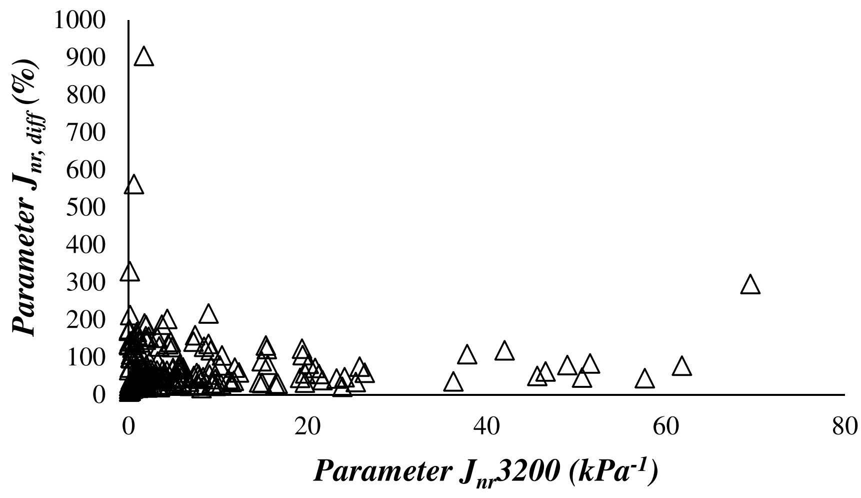

Figure 244 – Plot of the percent differences in compliances ($J_{nr,\ diff}$) against the nonrecoverable compliances at 3,200 Pa ($J_{nr}3200$) for the 12 formulations and all the temperatures (52, 58, 64, 70 and 76°C) and values for the creep times (1/9, 2/9, 4/9 and 8/9 s)

The two earlier figures indicate that there is no clear trendline or pattern of behavior for the percent difference in compliances, i. e., a binder that shows a lower rutting potential (low $J_{nr}3200$ value) does not necessarily depict a small or high value for $J_{nr, diff}$. By considering only the longer recovery times in the analysis (1/240 and 1/500 s), a similar picture is found, see Figure 245. This can also be observed by discussing on the mixture data, especially with respect to the high stress sensitivity of the AC+EVA and the AC+rubber and their excellent rutting performance in the FN tests (refer to Chapter 5 for more specific pieces of information). Again, there are strong evidences that the parameter $J_{nr, diff}$ is not a good indicator of the performance of the binder and the mixture under creep and recovery loading. Hence, other parameters and techniques must be investigated in order to find a parameter that is associated with performance and, at the same time, shows the stress sensitivity of the asphalt binder.

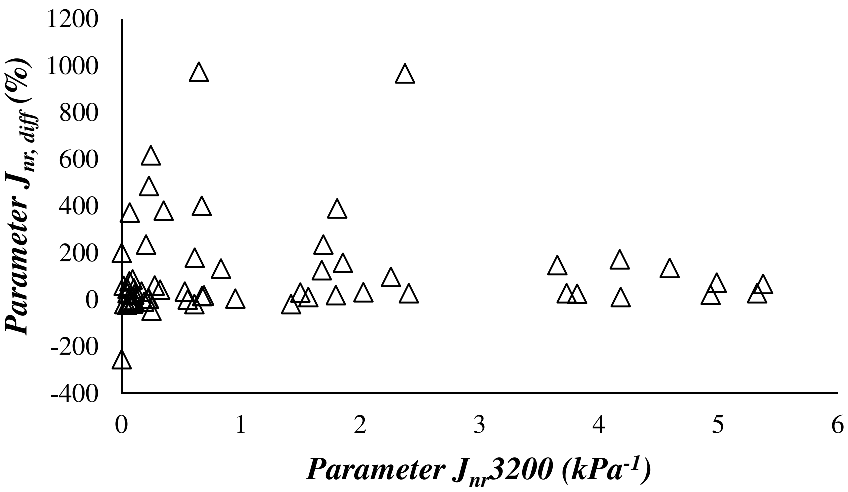

Figure 245 – Plot of the percent differences in compliances ($J_{nr, diff}$) against the nonrecoverable compliances at 3,200 Pa ($J_{nr}3200$) for the 12 formulations and all the temperatures (52, 58, 64, 70 and 76°C) and longer loading times (1/240 s and 1/500 s)

CHAPTER 7: Conclusions and Recommendations

7.1. Preliminary Comments and Leading Questions

Since the release of the first publications and American standards about the multiple stress creep and recovery (MSCR) test approximately in the second half of the 2000's, numerous studies have been carried out worldwide either to find and overcome the deficiencies of its protocols or to give increasing support to its use as a performance-related test. A presentation from Dongré (2016) provides an estimation of the total number of studies about MSCR that have already been published, i. e., little less than 200 documents up to the year of 2016. Nowadays, there seems to be a consensus among researchers that several input variables of the test need to be corrected to better characterize the rutting resistance of modified asphalt binders. The applied stresses, the number of creep-recovery cycles and the methods of calculation of the parameters R (percent recovery) and J_{nr} (nonrecoverable creep compliance) are perhaps the issues that have been mostly covered by the papers and reports in the literature.

Although the loading and unloading times in the repeated creep tests have been discussed in many studies (D'ANGELO et al., 2007; DELGADILLO, 2008; DELGADILLO and BAHIA, 2010; DELGADILLO et al., 2012; DOMINGOS and FAXINA, 2014, 2015a, 2015b, 2016; KATAWARE and SINGH, 2015; MASAD et al., 2009; MERUSI, 2012; MTURI et al., 2012; SANTAGATA et al., 2013, 2015), they show major deficiencies that have not been adequately addressed so far. The use of a limited number of samples, temperatures and/or pairs of creep-recovery times may be cited as examples. The present dissertation specifically gives evidence to these deficiencies. At the same time, it also constitutes an attempt to clarify some points concerning the creep-recovery responses of some modified asphalt binders with the same high PG grades (AC+PPA, AC+Elvaloy+PPA, AC+rubber, AC+rubber+PPA, AC+SBS, AC+SBS+PPA, AC+EVA, AC+EVA+PPA, AC+PE, AC+PE+PPA, AC+SBR and AC+SBR+PPA) and subjected to the MSCR tests at 52, 58, 64, 70 and 76°C and the stress levels of 0.1 and 3.2 kPa.

Some of the questions that drove the conduction of the tests and corresponding analyses can be summarized as follows:

- which are the precise effects of doubling the creep time (from 1/9 s to 2/9 s, 4/9 s and 8/9 s) on the elastic responses, levels of elasticity and susceptibility of the modified asphalt binders to rutting? What about the best and worst formulations in a general context?

- which changes in the amounts of permanent strain and the MSCR parameters can be observed by increasing the recovery time in the laboratory tests to one of the previously selected values (240 or 500 s)? How can this be quantified in terms of the parameters of the rheological models?
- how can the rutting performance of these modified binders in the mixture scale (i. e., flow number tests) be correlated with their corresponding performances in the binder scale? Which binder parameters show the best correlation with the mixture data and why?
- which are the benefits and limitations of the reduction in the main modifier content and the addition of PPA to the binder rutting parameters, stress sensitivity and rheological models? How can these results be correlated with their field performance?
- are the empirical- and theoretical-based equations from Huang (2004) and Pereira et al. (1998, 2000) able to accurately predict the traffic speed and the traffic level of the binder? If not, why?
- which are the roles of delayed elasticity, nonlinearity, modification type and steady state on the amount of recovered strain in the MSCR tests and the variations in the R and J_{nr} values of the formulations?; and
- do the results of the present study offer enough support to the new proposed Superpave® specification criteria for the assignment of the traffic level of the asphalt binder?

To facilitate the localizations in the present chapter of conclusions relative to each of the items mentioned before, the topics were gathered in the following groups: (a) effects of longer creep times on the MSCR testing data and associations with the parameters of the rheoogical models, the groups of AC+modifier/AC+modifier+PPA formulations and the proposed Superpave® criteria for the traffic levels; (b) effects of longer recovery times on the MSCR data and descriptions of their changes in the responses of the asphalt binders from the point of view of the model parameters; (c) mixture rutting tests and correlations between binder data and mixture data; and (d) general aspects of binder modification on the outcomes of the MSCR tests. Finally, some concluding remarks and recommendations for future studies are given at the end of this chapter.

7.2. The Use of Longer Creep Times in the MSCR Tests and Their Effects on the Binder Parameters, Levels of Elasticity and Rheological Models

Three longer creep times – 2.0, 4.0 and 8.0 s – were used in the MSCR tests and their effects on the binder parameters R, J_{nr} and $J_{nr,\ diff}$ (percent difference in compliances) and rheological models were analyzed and contrasted with results from the technical literature. A suggestion of amendment to the current Superpave® criteria for assigning the traffic level to the binder (i. e., based on the J_{nr} values at different creep times and not only the standardized one) was also investigated, and the traffic levels assigned by means of the proposed criteria were compared with those obtained by means of the current criteria. In addition, some of the equations for the calculation the traffic speed and available elsewhere (HUANG, 2004; PEREIRA et al., 1998, 2000) were selected and their estimated traffic levels were compared with those given by the J_{nr} values of the binders. It is important to note that some of the findings and discussions provided here can be found in an early published paper as well (DOMINGOS and FAXINA, 2017). The following conclusions may be drawn with respect to the role of longer creep times on the rheological responses of asphalt binders:

- longer creep times result in lower amounts of recovery at each loading-unloading cycle and higher nonrecoverable creep compliances; in practical terms, the asphalt binders are more susceptible to failure by rutting and show lower levels of elastic response when the load is applied for longer periods of time. However, the specific characteristics of each modification type (polymeric, acid-based, crumb rubber and so on) must be considered while analyzing the laboratory data;
- each formulation behaves in a different way when subjected to longer loading times and, for the binders with very high levels of elasticity (especially the EVA-modified ones), the roles of delayed elasticity, steady state and damage of the polymeric networks on the *R* and J_{nr} values must be carefully investigated; in practical terms, this can lead to increases in some recovery values of the AC+EVA and the AC+EVA+PPA with increasing severity in the tests;
- due to the intrinsic properties of the plastomers (i. e., very high degrees of stiffness and a brittle-like behavior) and the relatively high polymer contents, the use of such modifiers in the modification of the asphalt binder results in a boundary testing condition – labeled here as “failure point” – after which the formulation depicts a considerable loss of rutting resistance; these boundary conditions are typically found at the temperatures of 64 and 70°C and creep times between 1.0 and 4.0 s depending on the modifier and the presence/absence of PPA in the composition;
- the analyses of variance (ANOVA) in the *R* and J_{nr} values suggest that the differences within these values with increasing temperature and loading time – and considering a starting point of 52°C and 1/9 s – are not statistically significant in many cases, since the requirements for *F-value* (no greater than $F_{critical}$) and *p-value* (no lower than α) are all met. The only exception

was the AC+SBS at 100 Pa, for which the null hypothesis H_0 – i. e., equivalency within the variations in R and J_{nr} with increasing temperature and creep time – was rejected probably due to the formation of chain entanglements in the material during loading and unloading;

- the creep time was found to be the variable that mostly influenced on the R and J_{nr} values of the AC+Elvaloy+PPA, the AC+SBS, the AC+SBS+PPA, the AC+SBR and the AC+SBR+PPA according to ANOVA. These cases may be explained by the accumulated damage in the polymer network after the application of cyclic loads for longer periods of time;
- the parameter α derived from the power model by Saboo and Kumar (2015) typically showed intermediate to high degrees of correlation (R^2 values varying from 0.7 to 0.9 in many cases) with the percent recoveries at 100 and 3,200 Pa, and lower α values may be associated with higher recoveries in the MSCR tests. However, this parameter cannot clearly distinguish among the responses of the asphalt binders when the percent recovery is null or very high ($R > 80\%$);
- the parameter n (which is intended to describe the level of nonlinearity in the asphalt binder) does not always depict high degrees of correlation with the J_{nr} values, even though they tend to be much better at 3,200 Pa and for the AC+PE+PPA, the AC+SBR+PPA and the AC+rubber. It is hypothesized that nonlinearity cannot be clearly seen for all binders after only 8.0 s of loading time or, more simply, much longer creep times and higher strain levels are needed to yield better correlations between n and J_{nr}. Based on this, one can imply that the higher R^2 values for the data at 3,200 Pa is somehow associated with these high strain levels in the binder sample;
- two different and general pictures may be developed to describe the variations in the rutting resistances of the binders with increasing creep time t_F, namely, (1) one based on the formulation with very low susceptibility to rutting and at least reasonable elastic responses (the AC+Elvaloy+PPA, the AC+rubber and the AC+EVA); and (2) the other based on the formulations with higher rutting potential (the 50/70 original binder and all the remaining formulations). Decreases either in the initial accumulated strain (A) or the strain rate (B) and increases in the degree of nonlinearity (n) may be seen with increasing t_F for the members of group (1), in which only the level of nonlinearity increases with t_F for a particular pavement temperature. On the other hand, there are increases in n and B and decreases in A after the increases in the duration of the applied load for the members of group (2);
- among the formulations that belong to group (2), some of them may depict a loss of resistance after a specific test condition in the DSR or, in other words, a reverse in the behavior of the

initial strain – from decreases to increases in *A* with creep time – and its contribution to the rutting potential of the binder. This is probably caused by the accumulation of permanent strain at a sufficient level to exceed the "failure point" in the PE-modified binders (AC+PE and AC+PE+PPA) or accumulated damage in such an extent that the polymer network does not further contribute to the rutting performance of the formulation (AC+SBR and AC+SBR+PPA). It can be found at the temperature of 64°C for all the cited binders except for the AC+PE+PPA (temperature of 76°C);

- the traffic speeds given by the equations from Huang (2004) and Pereira et al. (1998, 2000) show high correlations with the compliances at 3,200 Pa, but their ability to predict the actual traffic levels of the materials – as given by the current Superpave® criteria – is questionable: the best predictions may be observed at 52 and 58°C and for the equations from Huang (2004) and Pereira et al. (1998), whereas the one from Pereira et al. (2000) does not show even an intermediate correlation with the binder data;
- the deficiencies in the predictions of the traffic levels may be explained by some specific reasons such as the following: (a) the equations are fairly limited in terms of their original mixture data and testing conditions, and they cannot be extended to other materials and tests; (b) the ranges of traffic speeds currently used on Superpave®, since there seems not to exist clear evidences about the origins of the other traffic speeds; and (c) there is a diversity of combinations of axles and vehicles in an actual pavement, which may result in several loading times and traffic levels (SARKAR, 2016);
- the use of an additional criterion in the assignment of the adequate traffic level to the binder (i. e., a new creep time and its corresponding maximum J_{nr} value) may identify some critical aspects of the actual resistance of the material to rutting, since a particular formulation with a small J_{nr} value at 1/9 s may depict a very high increase in J_{nr} at longer creep times, and thus be prone to rutting during the passage of slow-moving vehicles in the traffic lane. A few examples include the AC+Elvaloy+PPA at 70°C, the AC+rubber+PPA and the AC+SBR at 58°C and the AC+PPA, the AC+PE and the AC+EVA at 64°C: the traffic level decreased by one grade when moving from the current to the new proposed criteria. By identifying such characteristics of the formulations, the highway agencies would have more precise information in hands to choose the most suitable traffic condition for a specific formulation;
- some modification types – especially those with crumb rubber, EVA and SBS – can achieve very high $J_{nr, diff}$ values (> 75%) at one or more temperatures and loading times. From a strict point of view, they should not be used for paving applications because the stress sensitivity

requirement established by Superpave® is not complied, even though their performance in the mixtures ranged from intermediate to high. This is one additional evidence that the current methodology for evaluating the stress sensitivity of the modified binders needs to be revised due to some characteristics of the modifiers during the MSCR tests, as well as the fact that the parameter $J_{nr,\ diff}$ can depict pretty high variability in the laboratory tests;

- the AC+EVA and AC+Elvaloy+PPA are typically able to retain their classifications as "formulations with high levels of elasticity" at longer creep times, which suggests that their polymer networks were not extensively damaged during MSCR; on the other hand, the same cannot be said for the AC+EVA+PPA because this formulation is commonly graded as a "formulation with low level of elasticity" when t_F is higher than 2.0 s;
- the presence of PPA is somehow associated with the benefits found in the parameters of the original binder and the formulations with PE, SBS and SBR, as well as the higher level of workability to the Elvaloy-modified material. In simple terms, these benefits can be described as higher elastic responses (increasing R) and degrees of stiffness (decreasing J_{nr}) and reduced stress sensitivity (decreasing $J_{nr,\ diff}$) in some cases. The exceptions include the formulations with crumb rubber and EVA, for which opposite phenomena are commonly seen (i. e., increases in the susceptibility to rutting and lower degrees of elasticity under creep and recovery loading). It is suggested that the lower rubber contents in the AC+rubber+PPA and the chemical issues concerning the combination of EVA with PPA in the AC+EVA+PPA can reasonably explain the worse rutting performances of these two formulations;
- the correlations between binder data (J_{nr} at 3,200 Pa and 64°C) and mixture data (F_N at 60°C) are improved up to 8.2% with increasing t_F from 1.0 to 2.0 and 4.0 s, and then it decreases by 2.5% when t_F is doubled again from 4.0 to 8.0 s. It is suggested that the target characteristic of the binder response that must be considered in the analysis is the steady state or, in other words, a specific binder that is closer to the steady state will depict better correlations with the corresponding mixture rutting data. This is because the use of longer creep times in the MSCR tests speeds up the process to reach the steady state by increasing the total accumulated strain in the sample, even for a reduced number of cycles when compared with the technical literature. Such a discussion can also be correlated with the increased R^2 values between G_V and F_N when compared with J_{nr} and F_N, since the calculation of G_V takes into account only the last two creep-recovery cycles;

- the evolution of the average position of the AC+EVA with increasing temperature (especially at the ones ranging from 64 to76°C) and loading time in the rankings of J_{nr} and $J_{nr, diff}$ values at the standard and longer creep times (1/9 s, 2/9 s, 4/9 s and 8/9 s) reflects the considerable amount of damage in its polymeric network; in practical terms, the last positions in the rankings based on $J_{nr, diff}$ and for $T \leq 64$°C give place to the first positions at 70 and 76°C, and the opposite trend is seen in the rankings based on J_{nr};
- asphalt binders with small nonrecoverable compliances can depict very good rutting performances; this is the case of the AC+rubber, the AC+EVA, the AC+EVA+PPA and the AC+PE+PPA (this last one should be considered only at 52, 58 and 64°C);
- no clear relationships between the coefficients of variation of the rankings based on J_{nr} at 100 and 3,200 Pa could be found, which indicates that the changes in the rankings are not necessarily linked to the stress level and each formulation will show a particular creep-recovery behavior when loaded in the DSR;
- the formulations with the worst positions in the rankings of J_{nr} are comprised only by elastomers and lower crumb rubber contents (i. e., AC+SBS, AC+SBR and AC+rubber+PPA); this suggests that PPA may further improve the rutting resistances of the elastomeric-modified binders because the positions of the AC+SBS+PPA and the AC+SBR+PPA are close to the first. On the other hand, the AC+PPA and the AC+Elvaloy+PPA are ranked as very rut resistant materials in a binder scale together with the AC+rubber (at 100 Pa) and the AC+PE+PPA (3,200 Pa) – that is, binder modifications with a plastomer, higher crumb rubber contents and PPA;
- by unifying the rankings of J_{nr} at 100 and 3,200 Pa with the one of $J_{nr, diff}$ (i. e., by calculating a unique average position for each binder), the final ranking of formulations from the less to the most susceptible to rutting is the following: AC+Elvaloy+PPA; AC+PPA; AC+PE+PPA; AC+SBS+PPA; AC+EVA; AC+SBR+PPA; AC+PE; AC+EVA+PPA; AC+rubber; AC+SBS; AC+rubber+PPA and AC+SBR. If the parameter $J_{nr, diff}$ is not considered in the calculations, the sequence of binders from the highest to the lowest rutting resistance – as based only on J_{nr} – would be the following: AC+Elvaloy+PPA, AC+PPA, AC+PE+PPA, AC+EVA, AC+EVA+PPA, AC+rubber, AC+SBS+PPA, AC+PE, AC+SBR+PPA, AC+SBS, AC+rubber+PPA and AC+SBR; and
- as it can be seen, the presence of PPA in all the polymer-modified asphalt binders – except for the AC+EVA – helps in reaching a more rut resistant formulation and, to some extent, a lower stress sensitivity as well. This may also be inferred from the mixture rutting data, which

gives support to the use of PPA in the degrees of improvement of the rut resistance of some modified asphalt binders.

7.3. The Use of Longer Recovery Times in the MSCR Tests and their Effects on the Creep-Recovery Behavior of the Asphalt Binders

Two longer recovery times (1/240 s and 1/500 s) were used in the MSCR tests to study the role of delayed elasticity on the elastic responses and the susceptibility of the asphalt binders to rutting. The separation of the formulations by each value of unloading time was made according to the level of elasticity of the material, i. e., formulations with high degrees of elasticity were subjected to the unloading time of 500 s and formulations with low degrees of elasticity were subjected to the unloading time of 240 s. This was made based on the hypothesis that materials graded as materials with "high elasticity" would demand much longer recovery times than those graded as materials with "low elasticity". In this manner, only the AC+Elvaloy+PPA, the AC+EVA and the AC+EVA+PPA were subjected to 500 s of unloading time. For these binders, the following conclusions were obtained:

- an increase in the unloading time from 9 to 500 s greatly reduced the effects of the delayed elasticity on the creep-recovery cycles of the materials, and thus full recoveries could be seen for many of them;
- the AC+EVA depicted recoveries very close or equal to 100% at temperatures no greater than 64°C and for such unloading time, which was not the case of the AC+EVA+PPA and the AC+Elvaloy+PPA;
- some binders – especially the AC+Elvaloy+PPA – showed higher recoveries at 3,200 Pa than at 100 Pa and, due to this fact, negative $J_{nr,\ diff}$ values are obtained; the literature points out that the internal variables of the DSR (especially the inertia of the upper plate) and the hereditary memory effect of the formulation are possible explanations for such findings;
- similarly to the results at longer creep times, the parameter α showed high degrees of correlation with the recoveries at 100 and 3,200 Pa, either in a general or specific context; this suggests that α may be used as a complementary indicator of the amount of elastic recovery in the formulation; and
- the elimination (or considerable reduction) of the effects of the delayed elasticity on the response of the binder at each cycle changed the patterns of variation in the parameters A and B with temperature and stress level, namely, from decreases to increases in both parameters

in the case of the AC+Elvaloy+PPA and the AC+EVA; it is suggested that the portion of the elastic response not recovered after 9 s of unloading time contributed to the decreases in *A* and *B* reported earlier for the longer creep times.

In terms of the results of the asphalt binders that are graded as "materials with low elasticity", the following statements can be made for the AC+PPA, the AC+rubber, the AC+rubber+PPA, the AC+SBS and the AC+SBS+PPA:

- the formulations with SBS and crumb rubber (both without PPA) recovered much higher percentages of their total strain at 1/240 s (approaching 90-95% at temperatures no greater than 64°C) when compared with the original testing condition of 1/9 s, and this indicates that the intrinsic characteristics of these two modifiers have a great role on the amount of recovered strain at each creep-recovery cycle;
- the internal variables of the device and the memory effect of the formulation can be pointed out as some of the reasons why the AC+SBS+PPA and the AC+rubber+PPA showed lower recoveries at 1/240 s than at 1/9 s, similarly to what was observed for the AC+Elvaloy+PPA;
- the parameter α showed only an intermediate degree of correlation (about 0.66) with the recovery data at 100 and 3,200 Pa and for all binders; since the individual correlations were worse for the AC+SBS than for the other binders, it is believed that the differences within the responses for α at 100 Pa and *R100* at the temperatures of 52, 58 and 64°C contributed to such a reduction in the degree of correlation; and
- the parameters *A* and *B* increased with increasing temperature and stress level, which indicates that the minimization of the effects of delayed elasticity on the outcomes of the MSCR tests (*R* and J_{nr}) contributed to the modifications in the types of accumulated strain when compared with the standardized and longer creep times.

With respect to the results of the asphalt binders modified with PE, PE+PPA, SBR and SBR+PPA, the following statements can be made as based on their results at 1/240 s:

- the AC+SBR showed increases in *R100* with temperature up to a critical value of 64°C, similarly to what was observed for the AC+SBS; this indicates that the elastomeric modification type of the binder – among which the "rubber-like" behavior deserves a close attention – has a relevant role on the response of the AC+SBR;
- the AC+PE also showed increases in *R100* with temperature up to 64°C, and these increases are linked to the high degree of stiffness of the material (i. e., a "brittle-like" behavior) and perhaps the fact that the strain levels did not exceed the "failure point" of the material;

- the AC+SBR+PPA showed decreases in *R* when moving from 1/9 to 1/240 s at several pavement temperatures, as well as lower recoveries at 100 Pa than at 3,200 Pa; this may be explained by the hereditary memory effect of the modifier (s) as suggested in the literature;
- although an overall correlation between α at 1/240 s and the corresponding percent recoveries of the binders seemed to be reasonable (close to 0.75), the scaterring of the results around the regression trendline suggests that the parameter may not work well for all creep-recovery times; on the other hand, the individual correlations were much more promising (> 0.86); and
- either the initial strain or the strain rate (*A* and *B* values) increased with increasing stress level and temperature at 1/240 s, and this is one additional evidence of the importance of the delayed elasticity on the results of the creep-recovery tests.

In conclusion, the verification of the preliminary hypothesis that "the use of the unloading time of 240 s for the asphalt binders with low degrees of elasticity is enough to see full recovery in all materials" showed that it may not be perfectly true for all of them. This is because some binders – especially the AC+SBS and the AC+rubber – depicted increases in their percent recoveries at each cycle or the absence of a plateau in the strain curves with the time duration of the cycle, which is an indication that the delayed elasticity is still playing some role on the responses of the binders. If the delayed elasticity does not have such role (e. g., the AC+Elvaloy+PPA and the AC+EVA+PPA at some temperatures at 1/500 s), then the percent recoveries tend to stabilize since the first loading-unloading cycles and, in some cases, they tend to decrease with increasing number of cycles.

7.4. Mixture Rutting Results and Correlations with Binder Data

Two different groups of mixtures could be found in this dissertation based on the flow number (F_N) results at 60°C, namely, one comprised by the samples that did not fail in the tests (AC+rubber, AC+EVA, AC+EVA+PPA, AC+PE and AC+PE+PPA) and another comprised by the materials that failed before 10,000 cycles (50/70 base binder, AC+PPA, AC+Elvaloy+PPA, AC+rubber+PPA, AC+SBS, AC+SBS+PPA, AC+SBR and AC+SBR+PPA). These groups clearly show the inherited characteristics of the modifiers, i. e., the very high degrees of stiffness provided by the plastomers (EVA and PE) and crumb rubber and the lower degree of stiffness given by the elastomers (SBS and SBR) and reactive terpolymers (Elvaloy®). It also confirms that the binder stiffness is the target property when seeking for a mixture with higher resistances to rutting, as previously reported by other authors as well. More specific findings of this section can be pointed out as follows:

- the use of PPA in conjunction with another polymer leads to increases in the F_N values, which can be translated as a reduction in their susceptibility to rutting; the exception is the AC+rubber, for which the lower rubber content in the AC+rubber+PPA could not be compensated by the use of PPA;
- although neither the AC+EVA nor the AC+EVA+PPA failed in the FN tests, the higher amounts of accumulated strain in the formulation with PPA suggest that the replacement of a portion of the EVA content by PPA was not too beneficial to the rutting resistance of the modified asphalt binder;
- the AC+PPA shows F_N values close to the 50/70 base binder (a difference of only 16.9% between these values), even though the high PG grade of the AC+PPA is 12°C higher than the one of the original material; some possible explanations for this surprising finding include the strong dependency of PPA upon the chemical composition of the base binder and the need for the use of PPA at an optimum content to achieve the best binder and mixture rutting performances. More specifically, there is a lack of correspondence between the PG grade of the AC+PPA and its mixture performance It may be important to emphasize that other authors reported similar tendencies for the PPA-modified asphalt binders in the mixture scale;
- the degrees of correlation between the F_N values and the binder rutting parameters were found to be from intermediate to high for J_{nr} ($R^2 \approx 0.71$) and the viscous component of the creep stiffness G_V ($R^2 \approx 0.93$), and the rankings of binders and mixtures from the lowest to the highest rutting potential are practically the same for these two parameters. Despite the intermediate to high correlations obtained for the softening point values ($R^2 \approx 0.47$), the original Superpave® rutting parameter $G^*/\sin\delta$ ($R^2 \approx 0.50$) and the Shenoy's parameter $|G^*|/[1-(1/\tan\delta\sin\delta)]$ ($R^2 \approx 0.76$), these findings cannot be considered as positive because the rankings of asphalt binders and mixtures are completely different;
- the use of power correlations rather than linear ones did not change the overall tendencies observed for the binder parameters, i. e., the R^2 values were high for J_{nr} (almost 0.91) and G_V (almost 0.89) and relatively lower for $G^*/\sin\delta$ (about 0.68), softening point (about 0.60) and $|G^*|/[1-(1/\tan\delta\sin\delta)]$ (about 0.84). What can be pointed out from these findings is that J_{nr} and G_V are among the best binder rutting parameters to estimate the resistance of the formulation to rutting in the mixture at a predefined pavement temperature;

- differently from the mixtures that failed in the FN tests, it is rather difficult to associate the mixture parameters (in this case, the accumulated strain after 10,000 cycles γ_{per}) with the binder parameters J_{nr}, $G^*/sin\delta$, $|G^*|/[1-(1/tan\delta sin\delta)]$, *R&B* (softening point) and G_V because the rankings in the binder and the mixture are very different. This suggests that either the binder or the mixture must be tested up to the same "condition" – that is, the samples must be subjected to loading-unloading cycles up to the moment in which failure or the accumulation of a relevant amount of permanent strain is obtained – before any kind of correlation is investigated;
- the parameter *C* – which is derived from the Francken model – and the flow number index FN_I did not show a good correlation with F_N (the R^2 values were of about 0.56) and their rankings showed great disparities for the studied binders; as a consequence, it can be said that neither *C* nor FN_I are able to replace F_N in the analysis of the rutting behavior of the asphalt mixtures;
- the idea of determining the most appropriate traffic level for the asphalt binder based on their binder and mixture data seems to be an interesting alternative, especially because some formulations that depicted very good results in the binder scale may perform differently in the mixture scale. This was the case of the AC+PPA, to which an intermediate traffic level was assigned because of its poorer mixture performance. According to a new proposed classification based on performance in the binder and the mixture (Table 20, page 128), the formulations with plastomers and elastomers reached approximately the same levels in the categories of rutting resistance (from intermediate to high), and those with PPA in the composition – not including the AC+PPA – typically achieved higher positions in the ranking. The AC+Elvaloy+PPA was the only formulation that reached the highest position in the classification, i. e., "very high" rutting resistance; and
- some possible explanations for the relatively poor mixture performance of the AC+PPA may be given as follows: (a) the binder tests are not able to accurately predict mixture performance for all types of modifiers; (b) binder modification must be analyzed with caution and take into account the inherent characteristics of each additive and its interaction with the base material; and (c) in some cases, the effects of PPA modification on the resistance of the binder to rutting may be more restricted to the binder alone.

7.5. General Aspects of Binder Modification in the MSCR Tests

Typically, asphalt binder modification with one (AC+modifier) or two additives (AC+modifier+PPA) increased the *R* and $J_{nr,\ diff}$ values and decreased the J_{nr} values of the original material. In other words, the binder became more resistant to rutting due to the increased elasticity and degree of stiffness at high pavement temperatures; however, its stress sensitivity also tended to increase and affect the rutting performance when unexpected situations of temperature and loading level are found. The percentages of change in R, J_{nr} and $J_{nr,\,diff}$ were dependent upon the modifier types and contents and the selected test temperature, but some general aspects may be pointed out here.

The use of Elvaloy® in the modification of asphalt binders imparted very high degrees of elasticity to the material, as well as decreased susceptibility to rutting. No marked effects on the stress sensitivity were found, which means that $J_{nr,\,diff}$ would not be a restriction to the use of the AC+Elvaloy+PPA on field pavements (results are all lower than 75%). This high degree of elasticity did not seem to be markedly affected by increasing temperature, stress level and loading time, which is a positive finding. In addition, too long recovery times (as longer as 500 s) were needed to fully capture the amount of recovered strain at each creep-recovery cycle. In other words, the standardized recovery time was inappropriate for a more precise estimation of the actual performance of this formulation in the pavement.

Despite the presence of considerably high stress sensitivities for the asphalt binder after the incorporation of crumb rubber ($J_{nr,\,diff} > 100\%$), the AC+rubber also depicted an intermediate performance either in the binder scale – high R values and low J_{nr} values – or the mixture scale (no failure in the flow number tests). This suggests that the current procedure for investigating the suitability of the AC+rubber to the application of other stress levels must be refined, and it becomes even more critical for crumb rubber-modified materials due to the possible influence of the rubber particles in the measurements with the parallel plates of the DSR. The $J_{nr,\,diff}$ values of the AC+rubber+PPA were in accordance with the Superpave® requirements possibly because of the lower rubber contents (11% by weight), but its rutting resistance (J_{nr}) was much lower when compared with the AC+rubber.

The use of elastomeric polymers (SBS and SBR) on the modification of the asphalt binders also led to a lower susceptibility to rutting, since the R values increase and the J_{nr} values decreased after the modification processes. Stress sensitivity does not seem to be a matter of great concern, since the $J_{nr,\,diff}$ values hardly exceed 75% for both formulations. The fact that neither the SBS- nor the SBR-modified binders are classified as “formulations with high elasticity” may be explained by the lack of enough compatibility between these modifiers and the base material. Although the incorporation of PPA did improve the elastic responses and the stiffening characteristics of the original formulations without PPA (AC+SBS and AC+SBR), it was still not sufficient to achieve a better classification in terms of the levels of elasticity.

The plastomeric modifications of the original binder (i. e., with EVA and PE) provided considerably high degrees of stiffness, that is, very low J_{nr} values. This could also be seen in the mixture data, in that none of the samples prepared with the AC+EVA and the AC+PE failed after 10,000 cycles of creep and recovery. With respect to the amounts of recovered strain and the levels of elastic response in the AC+EVA, the AC+EVA+PPA, the AC+PE and the AC+PE+PPA, the substantially high degree of reactivity of the EVA copolymer with the base binder yields formulations with "high elasticity", even though this classification does not remain unchanged under all the creep-recovery times. The melting of EVA at temperatures higher than 64°C and the accumulation of damage in the sample at each loading-unloading cycle may be cited as the major factors for such decrease in the classifications.

7.6. Concluding Remarks and Suggestions for Future Studies

The MSCR test has still been calling the researchers' attention in the last 2-3 years and, as shown earlier, some of the key topics covered by these recent publications include the steady state, the methodology for calculating R and J_{nr}, the values of the applied loads and the stress sensitivity of some modified asphalt binders. The use of varying loading and unloading times in the same study is perhaps more restricted to the academic publications, probably because the highway agencies do not want to perform a time-consuming test (D'ANGELO et al., 2007). In this manner, a more practical approach was followed in the present dissertation and relatively short creep times (up to 8.0 s) were chosen to assess the feasibility of a more practical, quick-to-run MSCR test. Based on this, a possible refinement on Superpave® was proposed (see Appendix B) to include – at least at a limited extent – the role of nonlinearity on the susceptibility of modified binders to rutting and further improve the choice for the best material (DOMINGOS and FAXINA, 2017).

Since not all the issues about the MSCR test were completely figured out, some recommendations for future studies were offered as follows:

- to draw comparisons between the extents of the steady state phenomena after the application of less creep-recovery cycles with longer creep times and after the application of more creep-recovery cycles with shorter creep-recovery times;
- to develop correlations between the nonrecoverable compliances of the asphalt binders at longer creep times and the mixture data derived from accelerated loading facilities with varying loading speeds;
- to conduct other field-based studies in order to investigate the actual influence of slow-moving vehicles on the amount of rutting in the asphalt pavement – similarly to what was

made by Pereira et al. (1998, 2000) – and compare such data with the results of binders tested in the DSR in more critical loading conditions;

- to study the effect of different aggregate gradations and curves (for instance, limestone aggregates and gap-graded curves) on the correlations between mixture data in the flow number tests and binder data at increasing creep times, since it is known that the aggregate markedly influences on the correlations with binder data (BAHIA et al., 2001a); and
- to investigate the relationship between the newly proposed parameter γ_{diff} (STEMPIHAR et al., 2017) and rutting performance in the binder and the mixture, as based on local formulations, aggregate gradations and climate conditions, and draw further conclusions about the feasibility of the use of $J_{nr,\,diff}$ as a binder parameter and indicator of stress sensitivity.

REFERENCES

ADORJÁNYI, K.; FÜLEKI, P. (2011). Performance evaluation of bitumens at high temperature with multiple stress creep recovery test. **Hungarian Journal of Industrial Chemistry**, Vol. 39, No. 2, pp. 195-199.

______. (2013). Correlation between permanent deformation-related performance parameters of asphalt concrete mixes and binders. **Central European Journal of Engineering**, Vol. 3, No. 3, pp. 534-540. doi: 10.2478/s13531-012-0073-6.

AIREY, G. D. (2002). Rheological evaluation of ethylene vinyl acetate polymer modified bitumens. **Construction and Building Materials**, Vol. 16, No. 8, pp. 473-487. doi: 10.1016/S0950-0618(02)00103-4.

______. (2003). Rheological properties of styrene butadiene styrene polymer modified road bitumens. **Fuel**, Vol. 82, No. 14, pp. 1709-1719. doi: 10.1016/S0016-2361(03)00146-7.

______. (2004). Styrene butadiene styrene polymer modification of road bitumens. **Journal of Materials Science**, Vol. 39, No. 3, pp. 951-959. doi: 10.1023/B:JMSC.0000012927.00747.83.

AFLAKI, S.; HAJIKARIMI, P. (2012). Implementing viscoelastic rheological methods to evaluate low temperature performance of modified asphalt binders. **Construction and Building Materials**, Vol. 36, pp. 110-118. doi: 10.1016/j.conbuildmat.2012.04.076.

AKYILDIZ, F. et al. (1990). On the spring-dashpot representation of linear viscoelastic behaviour. **Rheologica Acta**, Vol. 29, No. 5, pp. 482-484. doi: 10.1007/BF01376800.

AMERI, M. et al. (2014). Evaluation and comparison of flow number calculation methods. **Road Materials and Pavement Design**, Vol. 15, No. 1, pp. 182-206. doi: 10.1080/14680629.2013.868819.

ANDERSON, D. A.; MARASTEANU, M. (2010). **Continuous models for characterizing linear viscoelastic behavior of asphalt binders.** ISAP Workshop on Asphalt Binders and Mastics, Madison, WI. PowerPoint presentation. Retrieved from :https://uwmarc.wisc.edu/files/binders2010/Continuous_Models_for_Characterizing_Linear_Viscoelastic_Behavior_of_Asphalt_Binders_-_Anderson.pdf. Accessed: 15 Ago. 2016.

ANDERSON, D. A. et al. (1992). Rheological properties of polymer modified emulsion residue. In: WARDLAW, K. R.; SHULER, S. (Eds.). **Polymer Modified Asphalt Binders**. Philadelphia: American Society for Testing and Materials, pp. 20-34. ISBN 0-8031-1413-3.

______. (2002). Zero shear viscosity of asphalt binders. **Transportation Research Record**, No. 1810, pp. 54-62. doi: 10.3141/1810-07.

ANDERSON, M. (2007). **Evaluation of DSR creep-recovery testing as a replacement for PG plus tests**. Association of Modified Asphalt Producers Annual Meeting, Boston, MA. PowerPoint presentation.

ANDERSON, M. et al. (2010). MSCR: a better tool for characterizing high temperature performance properties. **Asphalt**, Vol. 25, No. 2, pp. 15-16.18.21-23, ISSN 0004-4954. Retrieved from: <http://asphaltmagazine.com/mscr-a-better-tool-for-characterizing-high-temperature-performance-properties/>. Accessed: 14 Oct. 2015.

ANDERSON, R. M. (2011). **Understanding the MSCR test and its use in the PG asphalt binder specification**. Asphalt Academy Webinars, Lexington, KY. PowerPoint presentation.

APEAGYEI, A. K. (2014). Flow number predictive models from volumetric and binder properties: **Construction and Building Materials**, Vol. 64, pp. 240-245. doi: 10.1016/j.conbuildmat.2014.04.069.

ARSHADI, A. (2013). **Importance of asphalt binder properties on rut resistance of asphalt mixture**. Thesis (Master of Science) – Department of Civil & Environmental Engineering, University of Wisconsin-Madison, Madison.

ASPHALT INSTITUTE. (2010). **Guidance on the use of the MSCR test with the AASHTO M320 specification**. Asphalt Institute Technical Advisory Committee, Executive Offices and Research Center. Lexington, KY. Retrieved from: <http://amap.ctcandassociates.com/wp/wp-content/uploads/Guidance-on-Using-MSCR-with-AASHTO-M320_Final.pdf>. Accessed: 12 Jan. 2016.

______. (2016). **State MSCR implementation status**. Asphalt Institute Specification Database, Lexington, KY. Retrieved from: <http://www.asphaltinstitute.org/specification-databases/state-mscr-implementation-status-database/>. Accessed: 11 Mar. 2016.

AWWAD, M. T.; SHBEEB, L. (2007). The use of polyethylene in hot asphalt mixtures. **American Journal of Applied Sciences**, Vol. 4, No. 6, pp. 390-396.

BAHIA, H. U. (2014). **Performance de asfaltos modificados com polímeros** [Performance of polymer-modified asphalt binders]. DuPont Packaging & Industrial Polymers Inc., Rio de Janeiro. PowerPoint presentation.

BAHIA, H. U.; ANDERSON, D. A. (1995). Strategic highway research program binder rheological parameters: background and comparison with conventional properties. **Transportation Research Record**, No. 1488, pp. 32-39.

BAHIA, H. U. et al. (1997). Applicability of Superpave binder testing protocols to modified binders. **Transportation Research Record**, No. 1586, pp. 16-23. doi: 10.3141/1586-03.

______. (2001a). **Characterization of modified asphalt binders in Superpave mix design**. NCHRP Report 459. National Cooperative Highway Research Program. Washington: Transportation Research Board. ISBN 0-309-06707-3.

______. (2001b). Development of binder specification parameters based on characterization of damage behavior. **Journal of the Association of Asphalt Paving Technologists**, Vol. 70, pp. 442-470.

BALDINO, N. et al. (2012). Low temperature rheology of polyphosphoric acid (PPA) added bitumen. **Construction and Building Materials**, Vol. 36, pp. 592-596. doi: 10.1016/j.conbuildmat.2012.06.011.

BAUMGARDNER, G.; D'ANGELO, J. A. (2012). Evaluation of new dynamic shear rheometer testing geometry for performance testing of crumb rubber-modified binder. **Transportation Research Record**, No. 2293, pp. 73-79. doi: 10.3141/2293-09.

BAUMGAERTEL, M.; WINTER, H. H. (1989). Determination of discrete relaxation and retardation time spectra from dynamic mechanical data. **Rheologica Acta**, Vol. 28, No. 6, pp. 511-519. doi: 10.1007/BF01332922.

BAUMGARDNER, G. L. (2012). Why and how of polyphosphoric acid modification: an industry perspective. **Transportation Research Circular**, No. E-C160, pp. 14-26.

BAUMGARDNER, G. L. et al. (2005). Polyphosphoric acid modified asphalt: proposed mechanisms. **Journal of the Association of Asphalt Paving Technologists**, Vol. 74, pp. 283-305.

BECKER, Y. et al. (2001). Polymer modified asphalt. **Vision Tecnologica**, Vol. 9, No. 1, pp. 39-50. Retrieved from: <http://www.e-asfalto.com/ingles/venezuela.pdf>. Accessed: 10 Dec. 2015.

BEHNOOD, A. et al. (2016). High-temperature properties of asphalt binders: comparison of multiple stress creep recovery and performance grading systems. **Transportation Research Record**, No. 2574, pp. 131-143. doi: 10.3141/2574-15.

BENNERT, T.; MARTIN, J.-V. (2012). Polyphosphoric acid in combination with styrene-butadiene-styrene block copolymer: laboratory mixture evaluation. **Transportation Research Circular**, No. E-C160, pp. 70-85.

BERNUCCI, L. B. et al. (2006). Ligantes asfálticos. In: ______. **Pavimentação Asfáltica: Formação Básica para Engenheiros** [Asphalt Pavements: Basic Knowledge for Engineers]. Rio de Janeiro: Petrobras/ABEDA. Cap. 2, pp. 25-114. In Portuguese.

BHASIN, A. et al. (2005). **Evaluation of selected laboratory procedures and development of databases for HMA.** Texas Department of Transportation, Austin, TX. Report No. FHWA/TX-05/0-4203-3. Retrieved from: <http://d2dtl5nnlpfr0r.cloudfront.net/tti.tamu.edu/documents/0-4203-3.pdf>. Accessed: 27 Jun. 2016.

BILIGIRI, K. P. et al. (2007). Rational modeling of tertiary flow for asphalt mixtures. **Transportation Research Record**, No. 2001, pp. 63-72. doi: 10.3141/2001-08.

BILLITER, T. C. et al. (1996). Investigation of the curing variables of asphalt-rubber binder. **Preprints of Papers – American Chemical Society, Division of Fuel Chemistry,** Vol. 41, No. 4, pp. 1221-1226.

BIRO, S.; FAZEKAS, B. (2005). Asphalt rubber versus other modified bitumens. **Road Materials and Pavement Design**, Vol. 10, No. X, pp. 1-17. Retrieved from: <http://www.ra-foundation.org/wp-content/uploads/2013/02/020-PAP_017.pdf>. Acessed: 10 jun. 2016.

BORGES, R. L. (2014). **Deformação permanente em misturas asfálticas a partir do shift model viscoplástico e ensaios triaxiais de carga repetida** [Rutting in asphalt mixtures based on the viscoplastic shift model and triaxial repeated creep tests]. Dissertação (Mestrado em Engenharia de Transportes) – Departamento de Engenharia de Transportes, Universidade Federal do Ceará, Fortaleza. In Portuguese.

BOULDIN, M. G. et al. (2001). Proposed refinement of Superpave high-temperature specification parameter for performance-graded binders. **Transportation Research Record**, No. 1766, pp. 40-47. doi: 10.3141/1766-06.

BRETAS, R. E. S.; D'ÁVILA, M. A. (2000). **Reologia de polímeros fundidos** [Rheology of molten polymers]. 2. ed. São Carlos: EdUFSCar. 257 p. ISBN 978-85-7600-048-8. In Portuguese.

BROVELLI, C. et al. (2015). Using polymers to improve the rutting resistance of asphalt concrete. **Construction and Building Materials**, Vol. 77, pp. 117-123. doi: 10.1016/j.conbuildmat.2014.12.060.

BRÛLÉ, B. et al. (1994). Relationships among composition, structure, and properties of road asphalts. In: YEN, T. F.; CHILINGARIAN, G. V. (Ed.). **Developments in Petroleum Science**: Asphaltenes and Asphalts, 1. Vol. 40, Part A. Amsterdam: Elsevier Science B. V., Chapter 18, pp. 427-449. doi: 10.1016/S0376-7361(09)70265-1.

BUNCHER, M. (2016). **PPA modification and performance testing**. Asphalt – The Magazine of the Asphalt Institute, Lexington, KY. Retrieved from: <http://asphaltmagazine.com/ppa-modification-and-performance-testing/>. Accessed: 02 May 2016.

BULATOVIĆ, V. O. et al. (2014). Rheological properties of bitumen modified with ethylene butylacrylate glycidylmethacrylate. **Polymer Engineering and Science**, Vol. 54, No. 5, pp. 1056-1065. doi: 10.1002/pen.23649.

BUNCHER, M.; VON QUINTUS, H. L. (2014). **Performance of asphalt mixtures containing polyphosphoric acid.** Technical Report No. 0001946-1, Applied Research Associates. Retrieved from: <http://www.asphaltinstitute.org/wp-content/uploads/public/engineering/pdfs/materials/Final_Report_PPA_Evaluation_9_Sept_2014.pdf>. Accessed: 02 May 2016.

CELAURO, C. et al. (2012). Experimental validation of a fractional model for creep/recovery testing of asphalt mixtures. **Construction and Building Materials**, Vol. 36, pp. 458-466. doi: 10.1016/j.conbuildmat.2012.04.028.

CHEN, J.-S.; TSAI, C.-J. (1999). How good are linear viscoelastic properties of asphalt binder to predict rutting and fatigue cracking? **Journal of Materials Engineering and Performance**, Vol. 8, No. 4, pp. 443-449. doi: 10.1361/105994999770346747.

CHRISTENSEN, R. M. (1982). **Theory of viscoelasticity**. 2nd. ed. New York: Academic Press. 384 p. ISBN 0-486-42880-X.

CORBETT, L. W. (1969). Composition of asphalt based on generic fractionation, using solvent deasphaltening, elution-adsorption chromatography, and densimetric characterization. **Analytical Chemistry**, Vol. 41, No. 4, pp. 576-579. doi: 10.1021/ac60273a004.

CORBETT, L. W.; PETROSSI, U. (1978). Differences in distillation and solvent separated asphalt residua. **Industrial & Engineering Chemistry, Product Research and Development**, Vol. 17, No. 4, pp. 342-346. doi: 10.1021/i360068a011.

CLYNE, T. R. et al. (2012). Field investigation of polyphosphoric acid-modified binders at MnRoad. **Transportation Research Circular**, No. E-C160, pp. 115-130.

CUNHA, M. B. et al. (2007). Revisão da seleção do grau de desempenho (PG) de ligantes asfálticos por estado no Brasil [Revision of the selection of performance-graded (PG) asphalt binders for each state in Brazil]. **Anais do 21º Congresso Nacional de Pesquisa e Ensino em Transportes**, ANPET, Rio de Janeiro. In Portuguese.

D'ANGELO, J. (2008). **Multi-stress creep and recovery test method new specification**. Association of Modified Asphalt Producers Annual Conference, Austin, TX. PowerPoint presentation. Retrieved from: <http://amap.ctcandassociates.com/wp/wp-content/uploads/dangelo-MSCR-2-08E.pdf>. Accessed: 10 Dec. 2015.

______. (2010a). New high-temperature binder specification using multistress creep and recovery. **Transportation Research Circular**, No. E-C147, pp. 1-13. Retrieved from: <http://onlinepubs.trb.org/onlinepubs/circulars/ec147.pdf>. Accessed: 11 Dec. 2015.

______. (2010b). **The multiple stress creep recovery (MSCR) procedure**. US Department of Transportation, Federal Highway Administration, Washington. Technical Brief Number FHWA-HIF-10-XXX. September 2010.

______. (2010c). **Understanding and implementing the multiple stress creep recovery (MSCR) test and specification**. D'Angelo Consulting, Sacramento, CA. PowerPoint presentation.

D'ANGELO, J.; DONGRÉ, R. (2009). Practical use of multiple stress creep and recovery test: characterization of styrene-butadiene-styrene dispersion and other additives in polymer-modified asphalt binders. **Transportation Research Record**, No. 2126, pp. 73-82. doi: 10.3141/2126-09.

D'ANGELO, J. et al. (2007). Revision of the Superpave high temperature binder specification: the multiple stress creep recovery test. **Journal of the Association of Asphalt Paving Technologists**, Vol. 76, pp. 123-162.

D'ANGELO, J. A. (2009). The relationship of the MSCR test to rutting. **Road Materials and Pavement Design**, Vol. 10, Supl. 1, pp. 61-80. doi: 10.1080/14680629.2009.9690236.

D'ANGELO, J. A.; FEE, F. (2000). Superpave binder tests and spec's: how have they performed in the real world. **Journal of the Association of Asphalt Paving Technologists**, Vol. 69, pp. 697-713.

DE VISSCHER, J. et al. (2004). A comparison of the zero shear viscosity from oscillation tests and the repeated creep test. In: EURASPHALT & EUROBITUME CONGRESS, 3, Vienna. **Proceedings…** Vienna: European Asphalt Pavement Association and European Bitumen Association, 2004, v. 2, pp. 1501-1513.

DELGADILLO, R.; BAHIA, H. U. (2010). The relationship between nonlinearity of asphalt binders and asphalt mixture permanent deformation. **Road Materials and Pavement Design**, Vol. 11, No. 3, pp. 653-680. doi: 10.1080/14680629.2010.9690298.

DELGADILLO, R. et al. (2012). A nonlinear constitutive relationship for asphalt binders. **Materials and Structures**, Vol. 45, No. 3, pp. 457-473. doi: 10.1617/s11527-011-9777-y.

______. (2006a). Nonlinearity of repeated creep and recovery binder test and relationship with mixture permanent deformation. **Transportation Research Record**, No. 1962, pp. 3-11. doi: 10.3141/1962-01.

______. (2006b). Why do we need to change $G^*/sin\delta$ and how? **Road Materials and Pavement Design**, Vol. 7, No. 1, pp. 7-27. doi: 10.1080/14680629.2006.9690024.

DESMAZES, C. et al. (2000). A protocol for reliable measurement of zero-shear viscosity in order to evaluate the anti-rutting performance of binders. In: EURASPHALT & EUROBITUME CONGRESS, 2, Barcelona. **Proceedings…** Barcelona: European Asphalt Pavement Association and European Bitumen Association, 2000. Book I, pp. 203-211.

DIVYA, P. S. et al. (2013). Influence of the type of binder and crumb rubber on the creep and recovery of crumb rubber modified bitumen. **Journal of Materials in Civil Engineering**, Vol. 25, No. 4, pp. 438-449. doi: 10.1061/(ASCE)MT.1943-5533.0000608.

DOMINGOS, M. D. I. (2011). **Caracterização do comportamento fluência-recuperação de ligantes asfálticos modificados virgens e envelhecidos** [Characterization of the creep-recovery behavior of unaged and short-term aged modified asphalt binders]. Dissertação (Mestrado em Engenharia de Transportes) – Departamento de Engenharia de Transportes, Escola de Engenharia de São Carlos, Universidade de São Paulo, São Carlos. doi: 10.11606/D.18.2011.tde-12032012-144327. In Portuguese.

DOMINGOS, M. D. I. et al. (2012). Viscosidade rotacional de ligantes asfálticos modificados de mesmo grau de desempenho [Rotational viscosities of modified asphalt binders with the same performance grade]. **Transportes**, Vol. 20, No. 2, pp. 15-22. doi: 10.4237/transportes.v20i2.560. In Portuguese.

DOMINGOS, M. D. I.; FAXINA, A. L. (2014). Multiple stress creep-recovery test of ethylene vinyl acetate and polyphosphoric acid-modified binder. **Journal of Transportation Engineering**, Vol. 140, 04014054. doi: 10.1061/(ASCE)TE.1943-5436.0000707.

______. (2015a). Rheological analysis of asphalt binders modified with Elvaloy® terpolymer and polyphosphoric acid on the multiple stress creep and recovery test. **Materials and Structures**, Vol. 48, No. 5, pp. 1405-1416. doi: 10.1617/s11527-013-0242-y.

______. (2015b). Rheological behaviour of bitumens modified with PE and PPA at different MSCR creep-recovery times. **International Journal of Pavement Engineering**, Vol. 16, No. 9, pp. 771-783. doi: 10.1080/10298436.2014.953503.

______. (2016). Susceptibility of asphalt binders to rutting: literature review. **Journal of Materials in Civil Engineering**, Vol. 28, No. 2, 04015134. doi: 10.1061/(ASCE)MT.1943-5533.0001364.

______. (2017). Towards a further understanding of the role of the creep time in the MSCR test and proposal of a refined traffic level criterion. In: TRANSPORTATION RESEARCH BOARD ANNUAL MEETING, 96, Washington (DC). **Proceedings...** Washington (DC): Transportation Research Board of the National Academies, 2017.

DONGRÉ, R. (2016). **The state of MSCR.** Transportation Research Board 95th Annual Meeting, Washington (DC). AFK20 Meeting, Session 494. PowerPoint presentation. Available from: <http://amonline.trb.org/p16-0218-1.3003177?qr=1>. Accessed 28 Jan. 2017.

DONGRÉ, R.; D'ANGELO, J. (2003). Refinement of Superpave high-temperature binder specification based on pavement performance in the accelerated loading facility. **Transportation Research Record**, No. 1829, pp. 39-46. doi: 10.3141/1829-06.

DONGRÉ, R. et al. (2004). New criterion for Superpave high-temperature binder specification. **Transportation Research Record**, No. 1875, pp. 22-32. doi: 10.3141/1875-04.

DREESSEN, S. et al. (2009). A new performance related test method for rutting prediction: MSCRT. In: LOIZOS, A.; PARTL, M. L.; SCARPAS, T.; AL-QADI, I. L. (Ed.). **Advanced Testing and Characterisation of Bituminous Materials.** Leiden: CRC Press/Balkema. Chapter 7, Vol. II, pp. 971-980. doi: 10.1201/9780203092989.ch93.

DuBOIS, E. et al. (2014). Correlation between multiple stress creep recovery (MSCR) results and polymer modification of binder. **Construction and Building Materials**, Vol. 65, pp. 184-190. doi: 10.1016/j.conbuildmat.2014.04.111.

ELSEIFI, M. A. et al. (2003). Quantitative effect of elastomeric modification on binder performance at intermediate and high temperatures. **Journal of Materials in Civil Engineering**, Vol. 15, No. 1, pp. 32-40. doi: 10.1061/(ASCE)0899-1561(2003)15:1(32).

FAWCETT, A. H.; McNALLY, T. (2001). Studies on blends of acetate and acrylic functional polymers with bitumen. **Macromolecules**, Vol. 286, No. 2, pp. 126-137. doi: 10.1002/1439-2054(20010201)286:2<126::AID-MAME126>3.0.CO;2-X.

FEE, D. et al. (2010). Polyphosphoric acid modification of asphalt. **Transportation Research Record**, No. 2179, pp. 49-57. doi: 10.3141/2179-06.

FEITOSA, J. P. M. (2015). **Avaliação do uso de diferentes tipos de cera de carnaúba como aditivo para misturas mornas** [Study of the use of different types of carnauba wax as additives for warm asphalt mixtures]. Tese (Doutorado em Química) – Departamento de Química Orgânica e Inorgânica, Universidade Federal do Ceará, Fortaleza. In Portuguese.

FONTES, L. P. T. L. et al. (2010). Evaluating permanent deformation in asphalt rubber mixtures. **Construction and Building Materials**, Vol. 24, No. 7, pp. 1193-1200. doi: 10.1016/j.conbuildmat.2009.12.021.

GAHVARI, F. (1997). Effects of thermoplastic block copolymers on rheology of asphalt. **Journal of Materials in Civil Engineering**, Vol. 9, No. 3, pp. 111-116. doi: 10.1061/(ASCE)0899-1561(1997)9:3(111).

GAMA, D. A. et al. (2016). Rheological studies of asphalt modified with elastomeric polymer. **Construction and Building Materials**, Vol. 106, pp. 290-295. doi: 10.1016/j.conbuildmat.2015.12.142.

GHUZLAN, K. A. et al. (2015). Rheological properties of polyethylene-modified asphalt binder. **Athens Journal of Technology and Engineering**, Vol. 2, No. 2, pp. 75-88.

GIAVARINI, C. et al. (1996). Production of stable polypropylene-modified bitumens. **Fuel**, Vol. 75, No. 6, pp. 681-686. doi: 10.1016/0016-2361(95)00312-6.

GIBSON, N. et al. (2012). **Performance testing for Superpave and structural validation**. Federal Highway Administration, McLean, VA. Report No. FHWA-HRT-11-045. Retrieved from:

<http://www.fhwa.dot.gov/publications/research/infrastructure/pavements/11045/11045.pdf>. Accessed: 10 Dec. 2015.

GIERHART, D. (2013). **Multiple stress creep recovery (MSCR): why it should be implemented**. Louisiana Transportation Conference, Baton Rouge, LA. PowerPoint presentation.

GIGANTE, A. C. (2007). **Avaliação da susceptibilidade térmica e do efeito das condições ambientais no enrijecimento de misturas asfálticas densas à luz de seus comportamentos resilientes** [Evaluation of the thermal susceptibility and the effect of environmental conditions in the hardening of dense-graded hot mix asphalt to the light of their resilient behavior]. Dissertação (Mestrado em Engenharia Civil) – Departamento de Engenharia de Transportes, Escola de Engenharia de São Carlos, Universidade de São Paulo, São Carlos. doi: 10.11606/D.18.2007.tde-19032008-135756. In Portuguese.

GOLALIPOUR, A. (2011). **Modification of multiple stress creep and recovery test procedure and usage in specification**. Thesis (Master of Science) – Department of Civil & Environmental Engineering, University of Wisconsin-Madison, Madison.

GOLALIPOUR, A. et al. (2016). Critical considerations toward better implementation of the multiple stress creep and recovery test. **Journal of Materials in Civil Engineering,** 04016295, in press. doi: 10.1061/(ASCE)MT.1943-5533.0001803.

HAFEEZ, I. et al. (2013). To study the viscoelastic behavior of asphalt binders using under multi stress creep recovery test. **Life Science Journal,** Vol. 10, No. 12s, pp. 921-925.

HAFEEZ, I.; KAMAL, M. A. (2014). Creep compliance: a parameter to predict rut performance of asphalt binders and mixtures. **Arabian Journal for Science and Engineering**, Vol. 39, No. 8, pp. 5971-5978. doi: 10.1007/s13369-014-1216-2.

HAGHTALAB, A.; SODEIFIAN, G. (2002). Determination of the discrete relaxation spectrum for polybutadiene and polystyrene by a non-linear regression method. **Iranian Polymer Journal**, Vol. 11, No. 2, pp. 107-113.

HAJIKARIMI, P. et al. (2015). Comparing different rutting specification parameters using high temperature characteristics of rubber-modified asphalt binders. **Road Materials and Pavement Design**, Vol. 16, No. 4, pp. 751-766. doi: 10.1080/14680629.2015.1063533.

HALSTEAD, W. J.; WELBORN, J. Y. (1974). History of the development of asphalt testing apparatus and asphalt specifications. **Proceedings of the Association of Asphalt Paving Technologists**, Vol. 43A, pp. 89-120.

HAND, A. J. et al. (2004). Evaluating field performance: case study including hot mix asphalt performance-related specifications. **Journal of Transportation Engineering**, Vol. 130, No. 2, pp. 251-260. doi: 10.1061/(ASCE)0733-947X(2004)130:2(251).

HARDER, G. A. (2012). **Regional implementation of the MSCR test.** North East Asphalt User/Producer Group Meeting, Philadelphia, PA. PowerPoint presentation. Retrieved from: <http://www.neaupg.uconn.edu/pdf/4%20Regional%20Implementation%20of%20MSCR%20Tes%20-%20Greg%20Harder.pdf>. Accessed: 11 Mar. 2016.

HESP, S. A. M.; SUBRAMANI, S. (2009). Another look at the bending beam rheometer for specification grading of asphalt cements. In: INTERNATIONAL CONFERENCE ON MAINTENANCE AND REHABILITATION OF PAVEMENTS AND TECHNOLOGICAL CONTROL, 6, Turin. **Proceedings…** Turin: International Society for Maintenance and Rehabilitation of Transportation Infrastructure, 2009. 10 p.

HICKS, R. G. et al. (1993). Validation of SHRP binder specification through mix testing. **Journal of the Association of Asphalt Paving Technologists**, Vol. 62, pp. 565-616.

HINTZ, C. (2012). **Understanding mechanisms leading to asphalt binder fatigue**. Dissertation (Doctor of Philosophy) – Department of Civil & Environmental Engineering, University of Wisconsin-Madison, Madison.

HINTZ, C. et al. (2011). Modification and validation of the linear amplitude sweep test for binder fatigue specification. **Transportation Research Record**, No. 2207, pp. 99-106. doi: 10.3141/2207-13.

HUANG, S.-C. et al. (2011). Rheological and chemical properties of hydrated lime and polyphosphoric acid–modified asphalts with long-term aging. **Journal of Materials in Civil Engineering**, Vol. 23, No. 5, pp. 628-637. doi: 10.1061/(ASCE)MT.1943-5533.0000219.

HUANG, Y. H. (2004). **Pavement Analysis and Design**. 2nd ed. Upper Saddle River: Pearson Prentice Hall. ISBN 0-13-142473-4.

ISACSSON, U.; LU, X. (1995). Testing and appraisal of polymer modified road bitumens – state of the art. **Materials and Structures**, Vol. 28, No. 3, pp. 139-159. doi: 10.1007/BF02473221.

JAFARI, M.; BABAZADEH, A. (2016). Evaluation of polyphosphoric acid-modified binders using multiple stress creep and recovery and linear amplitude sweep tests. **Road Materials and Pavement Design**, Vol. 17, No. 4, pp. 859-876. doi: 10.1080/14680629.2015.1132631.

JAFARI, M. et al. (2015). Effects of stress levels on creep and recovery behavior of modified asphalt binders with the same continuous performance grades. **Transportation Research Record**, No. 2505, pp. 15-23. doi: 10.3141/2505-03.

JOHNSON, C. M. (2010). **Estimating asphalt binder fatigue resistance using an accelerated test method**. Dissertation (Doctor of Philosophy) – Department of Civil & Environmental Engineering, University of Wisconsin-Madison, Madison.

JONES, S. D. et al. (1998). Applicability of Superpave to modified asphalts: a mixture study. **Transportation Research Record**, No. 1630, pp. 42-50. doi: 10.3141/1630-06.

KATAWARE, A. V.; SINGH, D. (2015). Rheological performance of asphalt binders under different creep and recovery periods in MSCR test. **International Journal of Pavement Research and Technology**, Vol. 8, No. 6, pp. 410-418.

KHADER, G. A. et al. (2015). A laboratory study on acid modified bituminous mixes in comparison for rutting characteristics. **Civil Engineering and Urban Planning: an International Journal**, Vol. 2, No. 4, pp. 19-33.

KHATRI, A. et al. (2001). Mixing and compaction temperatures for modified binders using the Superpave gyratory compactor. **Journal of the Association of Asphalt Paving Technologists**, Vol. 70, pp. 368-402.

KING, G. et al. (1999). Additives in asphalt. **Journal of the Association of Asphalt Paving Technologists**, Vol. 68, pp. 32-69.

KODRAT, I. et al. (2007). Comparison of polyphosphoric acid–modified asphalt binders with straight and polymer-modified materials. **Transportation Research Record**, No. 1998, pp. 47-55. doi: 10.3141/1998-06.

KOSE, S. et al. (2000). Distribution of strains within hot-mix asphalt binders: applying imaging and finite-element techniques. **Transportation Research Record**, No. 1728, pp. 21-27. doi: 10.3141/1728-04.

KRISHNAN, J.; RAJAGOPAL, K. R. (2005). On the mechanical behavior of asphalt. **Mechanics of Materials**, Vol. 37, No. 11, pp. 1085-1100. doi: 10.1016/j.mechmat.2004.09.005.

LAKES, R. (2009). **Viscoelastic Materials**. New York: Cambridge University Press. ISBN 9780521885683.

LAUKKANEN, O.-V. et al. (2015). Creep-recovery behavior of bituminous binder and its relation to asphalt mixture rutting. **Materials and Structures**, Vol. 48, No. 12, pp. 4039-4053. doi: 10.1617/s11527-014-0464-7.

LEE, S.-J. et al. (2008). Short-term aging characterization of asphalt binders using gel permeation chromatography and selected Superpave binder tests. **Construction and Building Materials**, Vol. 22, No. 11, pp. 2220-2227. doi: 10.1016/j.conbuildmat.2007.08.005.

LEITE, L. F. M. (1999). **Estudos de preparo e caracterização de asfaltos modificados por polímero** [Studies about the preparation and characterization of polymer-modified asphalt binders]. Tese (Doutorado em Ciência e Tecnologia de Polímeros) – Instituto de Macromoléculas Professora Eloisa B. Mano, Universidade Federal do Rio de Janeiro, Rio de Janeiro. In Portuguese.

LEITE, L. F. M.; TONIAL, I. A. (1994). Qualidade dos cimentos asfálticos brasileiros segundo as especificações SHRP [Grading of the Brazilian asphalt cements according to the SHRP specifications]. In: ENCONTRO DE ASFALTO, 12, Rio de Janeiro. **Anais...** Rio de Janeiro: IBP, 1994. pp. 94-119. In Portuguese.

LESUEUR, D. (2009). The colloidal structure of bitumen: consequences on the rheology and on the mechanisms of bitumen modification. **Advances in Colloid and Interface Science**, Vol. 145, No. 1-2, pp. 42-82. doi: 10.1016/j.cis.2008.08.011.

LI, Q. et al. (2014). Evaluating the rutting resistance of asphalt mixtures using an advanced repeated load permanent deformation test under field conditions. **Construction and Building Materials**, Vol. 61, pp. 241-251. doi: 10.1016/j.conbuildmat.2014.02.052.

LI, X. et al. (2015). Analysis of different indices for high- and low-temperature properties of asphalt binder. **Construction and Building Materials**, Vol. 83, pp. 70-76. doi: 10.1016/j.conbuildmat.2015.02.008.

______. (2011). Laboratory evaluation of asphalt binders and mixtures containing polyphosphoric acid. **Transportation Research Record**, No. 2210, pp. 47-56. doi: 10.3141/2210-06.

LIU, S. et al. (2010). Analysis and application of relationships between low-temperature rheological performance parameters of asphalt binders. **Construction and Building Materials**, Vol. 24, No. 4, pp. 471-478. doi: 10.1016/j.conbuildmat.2009.10.015.

LIU, Y.; YOU, Z. (2009). Determining Burger's model parameters of asphalt materials using creep-recovery testing data. In: YOU, Z.; ABBAS, A. R.; WANG, L. (Eds.). **Pavements and Materials**:

Modeling, Testing, and Performance. Reston: American Society of Civil Engineers, pp. 26-36. doi: 10.1061/41008(334)3.

MACOSKO, C. W. (1994). **Rheology: principles, measurements, and applications**. New York: Wiley-VCH. ISBN 0-471-18575-2.

MARASTEANU, M. O. et al. (2005). High-temperature rheological properties of asphalt binders. **Transportation Research Record**, No. 1901, pp. 52-59. doi: 10.3141/1901-07.

MARTINS, A. T. et al. (2011). Fluência e relaxação sob múltiplas tensões (MSCR): avaliação do desempenho de ligantes asfálticos [Multiple stress creep and recovery (MSCR): analysis of asphalt binder performance]. In: CONGRESSO IBERO-LATINOAMERICANO DO ASFALTO, 16, Rio de Janeiro. **Anais…** Rio de Janeiro: Clube de Ideias, Vol. 1, pp. 711-721. In Portuguese.

MASAD, E. et al. (2009). Characterization of asphalt binder resistance to permanent deformation based on nonlinear viscoelastic analysis of multiple stress creep recovery (MSCR) test. **Journal of the Association of Asphalt Paving Technologists**, Vol. 78, pp. 535-566.

MASSON, J.-F. (2008). Brief review of the chemistry of polyphosphoric acid (PPA) and bitumen. **Energy & Fuels**, Vol. 22, No. 5, pp. 2637-2640. doi: 10.1021/ef8005433.

MAURER, D.; D'ANGELO, J. (2012). Department of transportation perspective: a survey on polyphosphoric acid use and issues. **Transportation Research Circular**, No. E-C160, pp. 8-11.

MERUSI, F. (2012). Delayed mechanical response in modified asphalt binders. Characteristics, modeling and engineering implications. **Road Materials and Pavement Design**, Vol. 13, Supl. 1, pp. 321-345. doi: 10.1080/14680629.2012.657096.

MOHAMMAD, L. N. et al. (2006). Permanent deformation analysis of hot-mix asphalt mixtures with simple performance tests and 2002 mechanistic-empirical pavement design software. **Transportation Research Record**, No. 1970, pp. 133-142. doi: 10.3141/1970-16.

MOHSENI, A.; AZARI, H. (2014). High-temperature characterization of highly modifed asphalt binders and mixtures. **Transportation Research Record,** No. 2444, pp. 38-51. doi: 10.3141/2444-05.

MONTEPARA, A.; GIULIANI, F. (1999). Reliability of rheometric measurements in bitumens by means of dynamic shear rheometers. In: EUROBITUME WORKSHOP, Luxembourg, Maggio. **Eurobitume Workshop 1999 – Performance Related Properties for Bituminous Binders:** Workshop Briefing. Brussels: European Bitumen Association, 1999. Retrieved from:

<http://old.unipr.it/arpa/dipcivil/felice_giuliani_files/articoli/Montepara&Giuliani_Eurobit99.PDF>. Accessed: 29 Jan. 2017.

MOREA, F. et al. (2011). The use of asphalt low shear viscosity to predict permanent deformation performance of asphalt concrete. **Materials and Structures**, Vol. 44, No. 7, pp. 1241-1248. doi: 10.1617/s11527-010-9696-3.

______. (2014). Wheel tracking rutting performance estimation based on bitumen low shear viscosity (LSV), loading and temperature conditions. **Materials and Structures**, Vol. 47, No. 4, pp. 683-692. doi: 10.1617/s11527-013-0088-3.

MTURI, G. A. J. et al. (2012). Creep-recovery behaviour of bituminous binders – relevance to permanent deformation of asphalt pavements. In: INTERNATIONAL CONFERENCE ON ROAD AND RAIL INFRASTRUCTURE, 2, Dubrovnik. **Road and Rail Infrastructure II, Proceedings of the Conference CETRA 2012**. Zagreb: University of Zagreb, 2012. ISBN 9789536272501. Chapter 6, pp. 335-341.

NASCIMENTO, L. A. H. (2008). **Nova abordagem da dosagem de misturas asfálticas densas com uso do compactador giratório e foco na deformação permanente** [A new approach on the design of dense-graded mixtures based on the gyratory compactor and focused on rutting]. Dissertação (Mestrado em Engenharia Civil) – Instituto Alberto Luiz Coimbra de Pós-Graduação e Pesquisa de Engenharia, Universidade Federal do Rio de Janeiro, Rio de Janeiro. In Portuguese.

NAVARRO, F. J. et al. (2009). Bitumen modification with reactive and non-reactive (virgin and recycled) polymers: a comparative analysis. **Journal of Industrial and Engineering Chemistry**, Vol. 15, No. 4, pp. 458-464. doi: 10.1016/j.jiec.2009.01.003.

______. (2005). Influence of crumb rubber concentration on the rheological behavior of a crumb rubber modified bitumen. **Energy & Fuels**, Vol. 19, No. 5, pp. 1984-1990. doi: 10.1021/ef049699a.

NEJAD, F. M. et al. (2015). Evaluation of rutting properties of high density polyethylene modified binders. **Materials and Structures**, Vol. 48, No. 10, pp. 3295-3305. doi: 10.1617/s11527-014-0399-z.

ONOFRE, F. C. et al. (2013). Avaliação do efeito de ligantes asfálticos modificados na resistência à deformação permanente de misturas asfálticas densas [Analysis of the effect of modified asphalt binders on the rutting resistance of dense-graded asphalt mixtures]. **Transportes**, Vol. 21, No. 3, pp. 14-21. doi: 10.4237/transportes.v21i3.685. In Portuguese.

ORANGE, G. et al. (2014). Rutting and moisture resistance of asphalt mixtures containing polymer and polyphosphoric acid modified bitumen. **Road Materials and Pavement Design**, Vol. 5, No. 3, pp. 323-354. doi: 10.1080/14680629.2004.9689975.

PAMPLONA, T. F. (2013). **Efeito da adição de ácido polifosfórico em ligantes asfálticos de diferentes fontes** [Effect of polyphosphoric acid on asphalt binders from different crude sources]. Dissertação (Mestrado em Engenharia Civil) – Departamento de Engenharia de Transportes, Escola de Engenharia de São Carlos, Universidade de São Paulo, São Carlos. doi: 10.11606/D.18.2013.tde-29112013-084714. In Portuguese.

PAMPLONA, T. F. et al. (2014). Desenvolvimentos recentes em ensaios de fadiga em ligantes asfálticos [Recent developments in asphalt binder fatigue tests]. **Transportes**, Vol. 22, No. 3, pp. 12-25. doi: 10.14295/transportes.v22i3.682. In Portuguese.

PAPAGIANNAKIS, A. T. et al. (2015). Simulation of asphalt concrete plastic deformation behavior. In: NIKOLAIDES, A. F. (Ed.). **Bituminous Mixtures and Pavements VI**. Leiden: CRC Press/Balkema, pp. 413-419. doi: 10.1201/b18538-60.

PARTAL, P. et al. (1999). Rheological characterisation of synthetic binders and unmodified bitumens. **Fuel**, Vol. 78, No. 1, pp. 1-10. doi: 10.1016/S0016-2361(98)00121-5.

PAVEMENT INTERACTIVE. (2008a). **Loads**. Published online 28 Sept. 2008. Retrieved from: <http://www.pavementinteractive.org/article/loads/>. Accessed: 24 Feb. 2016.

______. (2008b). **Rutting.** Published online 6 May 2008. Retrieved from: <http://www.pavementinteractive.org/article/rutting/>. Accessed: 13 Apr. 2016.

PEREIRA, P. A. A. et al. (2000). Modelling the effect of truck speed on permanent deformation of asphalt mixes. **Road Materials and Pavement Design**, Vol. 1, No. 2, pp. 197-207.

______. (1998). Validation of SHRP A-698 permanent deformation concepts for different truck speeds. In: INTERNATIONAL CONFERENCE ON THE BEARING CAPACITY OF ROADS AND AIRFIELDS. 5, Trondhein. **Proceedings of the Fifth International Conference on the Bearing Capacity of Roads and Airfields**, Trondhein. Vol. I, pp. 339-348.

PETERSEN, J. C. (2009). Asphalt oxidation kinetics and mechanisms of oxidation. In: ______. **A Review of the Fundamentals of Asphalt Oxidation:** Chemical, Physicochemical, Physical Property, and Durability Relationships. Document No. E-C140. Washington: Transportation Research Board. pp. 31-62. ISSN 0097-8515. Retrieved from: <http://onlinepubs.trb.org/onlinepubs/circulars/ec140.pdf>. Acessed: 10 jun. 2016.

PILATI, F. (2008). **Análise dos efeitos da borracha moída de pneu e do resíduo de óleo de xisto sobre algumas propriedades mecânicas de misturas asfálticas densas** [Analysis of the effects of crumb rubber and shale-oil residue on mechanical properties of asphalt mixtures]. Dissertação (Mestrado em Engenharia de Transportes) – Departamento de Engenharia de Transportes, Escola de Engenharia de São Carlos, Universidade de São Paulo, São Carlos. doi: 10.11606/D.18.2008.tde-14062008-202738. In Portuguese.

POLACCO, G. et al. (2015). A review of the fundamentals of polymer-modified asphalts: asphalt/polymer interactions and principles of compatibility. **Advances in Colloid and Interface Science**, Vol. 224, pp. 72-112. doi: 10.1016/j.cis.2015.07.010.

______. (2006). Relation between polymer architecture and nonlinear viscoelastic behavior of modified asphalts. **Current Opinion in Colloid & Interface Science**, Vol. 11, No. 4, pp. 230-245. doi: 10.1016/j.cocis.2006.09.001.

READ, J.; WHITEOAK, D. (2003). **The Shell bitumen handbook**. 5th. ed. London: Thomas Telford Ltd. ISBN 0-7277-3220-X.

REINKE, G. (2010). Use of Hamburg rut test data to validate the use of J_{nr} as a performance parameter for high-temperature permanent deformation. **Transportation Research Circular**, No. E-C147, pp. 14-24.

REINKE, G. et al. (2012). Polyphosphoric acid-modified binders and mixtures: aggregate and binder interactions, rutting, and moisture sensitivity of mixtures. **Transportation Research Circular**, No. E-C160, pp. 86-105.

ROBERTS, F. L. et al. (1996). **Hot mix asphalt materials, mixture design, and construction**. 2nd. ed. Lanham: National Asphalt Pavement Association Research and Education Foundation. 603 p. ISBN-10 0914313010.

RODEZNO, M. C. et al. (2010). Development of a flow number predictive model. **Transportation Research Record**, No. 2181, pp. 79-87. doi: 10.3141/2181-09.

ROWE, G. M. et al. (2002). **Use of the zero shear viscosity as a parameter for the high temperature binder specification parameter**. 3rd International Symposium on Binder Rheology and Pavement Performance, San Antonio, TX. PowerPoint presentation. Retrieved from: <http://www.asphalt-technology.com/pdf_files/rowe(2002)b.pdf>. Accessed: 11 Jan. 2016.

RUAN, Y. et al. (2003). The effect of long-term oxidation on the rheological properties of polymer modified asphalts. **Fuel**, Vol. 82, No. 14, pp. 1763-1773. doi: 10.1016/S0016-2361(03)00144-3.

SABOO, N.; KUMAR, P. (2015). A study on the creep and recovery behavior of asphalt binders. **Construction and Building Materials**, Vol. 96, pp. 632-640. doi: 10.1016/j.conbuildmat.2015.08.078.

______. (2016). Analysis of different test methods for quantifying rutting susceptibility of asphalt binders. **Journal of Materials in Civil Engineering**, 04016024, in press. doi: 10.1061/(ASCE)MT.1943-5533.0001553.

SANTAGATA, E. et al. (2015). A novel procedure for the evaluation of anti-rutting potential of asphalt binders. **International Journal of Pavement Engineering**, Vol. 16, No. 4, pp. 287-296. doi: 10.1080/10298436.2014.942859.

______. (2013). Evaluation of the anti-rutting potential of polymer-modified binders by means of creep-recovery shear tests. **Materials and Structures**, Vol. 46, No. 10, pp. 1673-1682. doi: 10.1617/s11527-012-0006-0.

SARKAR, A. (2016). Combined effect of loading pattern, pulse duration, and stress level on the cyclic creep test of asphalt mixture. **Journal of Materials in Civil Engineering**, 04016185, in press. doi: 10.1061/(ASCE)MT.1943-5533.0001715.

SAUZEAT, C.; DI BENEDETTO, H. (2015). Tridimensional linear viscoelastic behavior of bituminous materials. In: HUANG, S.-C.; DI BENEDETTO, H. (Ed.). **Advances in Asphalt Materials:** Road and Pavement Construction. Cambridge: Elsevier Ltd., pp. 59-96. ISBN 978-0-08-100271-1.

SCHWEYER, H. E. (1974). A pictorial review of asphalt (bitumen) rheology. **Proceedings of the Association of Asphalt Paving Technologists**, Vol. 43A, pp. 121-157.

SEFIDMAZGI, N. R. et al. (2012). Internal structure characterization of asphalt mixtures for rutting performance using imaging analysis. **Road Materials and Pavement Design**, Vol. 13, Supl. 1, pp. 21-37. doi: 10.1080/14680629.2012.657045.

SHALABY, A. (2002). Modelling short-term aging of asphalt binders using the rolling thin film oven test. **Canadian Journal of Civil Engineering**, Vol. 29, No. 1, pp. 135-144. doi: 10.1139/l01-086.

SHELL OIL COMPANY. (1996). Johannes C. van der Werff; Son M. Nguyen. **Process for the Preparation of Phosphoric-Acid-Containing Asphalt/Polymer Mixture and Resulting Asphalt Composition Thereof.** US 5519073, 21 May 1996. Retrieved from:

<https://docs.google.com/viewer?url=patentimages.storage.googleapis.com/pdfs/US5519073.pdf>. Accessed: 23 May 2016.

SHENOY, A. (2001). Refinement of the Superpave specification parameter for performance grading of asphalt. **Journal of Transportation Engineering**, Vol. 127, No. 5, pp. 357-362. doi: 10.1061/(ASCE)0733-947X(2001)127:5(357).

______. (2004a). A comprehensive treatise of the high temperature specification parameter $|G^*|$ / (1-(1/*tanδsinδ*)) for performance grading of asphalts. **Applied Rheology**, Vol. 14, No. 6, pp. 303-314. doi: 10.3933/ApplRheol-14-303.

______. (2004b). High temperature performance grading of asphalts through a specification criterion that could capture field performance. **Journal of Transportation Engineering**, Vol. 130, No. 1, pp. 132-137. doi: 10.1061/(ASCE)0733-947X(2004)130:1(132).

SHERWOOD, J. A. et al. (1998). Correlation of Superpave G*/sinδ with rutting test results from accelerated loading facility. **Transportation Research Record**, No. 1630, pp. 53-61. doi: 10.3141/1630-07.

SIDDIQUI, M. N.; ALI, M. F. (1999). Studies on the aging behavior of the Arabian asphalts. **Fuel**, Vol. 78, No. 9, pp. 1005-1015. doi: 10.1016/S0016-2361(99)00018-6.

SOENEN, H. et al. (2013). The multiple stress creep-recovery test: a detailed analysis of repeatability and reproducibility. **Road Materials and Pavement Design**, Vol. 14, Supl. 1, pp. 2-11. doi: 10.1080/14680629.2013.774742.

STEVENS, R. et al. (2015). Evaluation of multiple stress creep and recovery (MSCR) data for Arizona. **International Journal of Pavement Research and Technology**, Vol. 8, No. 5, pp. 337-345. doi: 10.6135/ijprt.org.tw/2015.8(4).337.

STEMPIHAR, J. et al. (2017). **Alternative interpretation for stress sensitivity in AASHTO T350**. Transportation Research Board 96th Annual Meeting, Washington, DC. PowerPoint Presentation.

STUART, K. D.; MOGAWER, W. S. (1997). Validation of asphalt binder and mixture tests that predict rutting susceptibility using FHWA accelerated loading facility. **Journal of the Association of Asphalt Paving Technologists**, Vol. 66, pp. 109-152.

SWIERTZ, D. et al. (2017). Implementation considerations for the multiple stress creep and recovery test. In: In: TRANSPORTATION RESEARCH BOARD ANNUAL MEETING, 96, Washington (DC). **Proceedings...** Washington (DC): Transportation Research Board of the National Academies, 2017.

SYBILSKI, D. (1996a). Evaluation of validity of conventional test methods in case of polymer-bitumens. **Preprints of Papers – American Chemical Society, Division of Fuel Chemistry**, Vol. 41, No. 4, pp. 1302-1306.

______. (1996b). Zero-shear viscosity of bituminous binder and its relation to bituminous mixture's rutting resistance. **Transportation Research Record**, No. 1535, pp. 15-21. doi: 10.3141/1535-03.

SZEKERES, A. (1999). The wonderful Hooke's law: history, theory and story. **Proceedings of the Estonian Academy of Sciences, Physics and Mathematics**, Vol. 48, No. 3-4, pp. 296-305.

TABATABAEE, N.; TEYMOURPOUR, P. (2010). Effect of modification on rut susceptibility of asphalt binders and mixtures. In: INTERNATIONAL CONFERENCE ON ASPHALT PAVEMENTS, 11, Nagoya. **Proceedings…** Zagreb: HAD, 2010. Retrieved from: <http://data.abacus.hr/h-a-d/radovi_s_kongresa/nagoya_japan_2010/90536.pdf>. Accessed: 24 jun. 2016.

TAM, K. K. (2012). Polyphosphoric acid–modified asphalt cement: Ontario perspective. **Transportation Research Circular**, No. E-C160, pp. 109-114.

TAPKIN, S. et al. (2009). Repeated creep behavior of polypropylene fiber-reinforced bituminous mixtures. **Journal of Transportation Engineering**, Vol. 135, No. 4, pp. 240-249. doi: 10.1061/(asce)0733-947x(2009)135:4(240).

TAREFDER, R. A.; YOUSEFI, S. S. (2015). Rheological examination of aging in polymer-modified asphalt. **Journal of Materials in Civil Engineering**, Vol. 28, No. 2, 04015112. doi: 10.1061/(ASCE)MT.1943-5533.0001370.

TEYMOURPOUR, P. et al. (2016). Effect of parallel plate gap height on repeatability in DSR measurements of crumb-rubber modified binders. **Journal of Materials in Civil Engineering**, 04016047, in press. doi: 10.1061/(ASCE)MT.1943-5533.0001542.

THOMAS, K. P.; TURNER, T. F. (2008). Polyphosphoric-acid modification of asphalt binders. **Road Materials and Pavement Design**, Vol. 9, No. 2, pp. 181-205. doi: 10.1080/14680629.2008.9690113.

VAN DER VEGT, A. K. (2006). Visco-elasticity. In: ______. **From Polymers to Plastics**. Delft: Delft Academic Press, Chapter 6, pp. 115-132. ISBN 978-90-71301-62-9.

VARGAS, M. A. et al. (2013). Asphalt/polyethylene blends: rheological properties, microstructure and viscosity modeling. **Construction and Building Materials**, Vol. 45, pp. 243-250. doi: 10.1016/j.conbuildmat.2013.03.064.

VERDADE, L. L. (2015). **Avaliação do uso de um polietileno de alta densidade e baixo peso molecular oxidado como agente de compatibilização em asfalto modificado com copolímero SBS** [Analysis of the use of an oxidized, high-density polyethylene with low molecular weight as a compatibilizing agent in asphalt binders modified with SBS copolymer]. Dissertação (Mestrado em Engenharia de Transportes) – Departamento de Engenharia de Transportes, Escola de Engenharia de São Carlos, Universidade de São Paulo, São Carlos. doi: 10.11606/D.18.2015.tde-01102015-093027. In Portuguese.

VLACHOVICOVA, Z. et al. (2005). Shear deformation and material properties of polymer-modified asphalt. **Petroleum & Coal**, Vol. 47, No. 3, pp. 38-48.

WALUBITA, L. F. et al. (2012). Hot-mix asphalt permanent deformation evaluated by Hamburg wheel tracking, dynamic modulus, and repeated load tests. **Transportation Research Record**, No. 2296, pp. 46-56. doi: 10.3141/2296-05.

______. (2013). Exploring the flow number (FN) index as a means to characterise the HMA permanent deformation response under FN testing. **Journal of the South African Institution of Civil Engineering**, Vol. 55, pp. 103-112.

WASAGE, T. L. J. et al. (2009). Rutting evaluation of asphalt binders and mixes. In: LOIZOS, A.; PARTL, M. N.; SCARPAS, T.; AL-QADI, I. L. (Ed.). **Advanced Testing and Characterisation of Bituminous Materials**. Leiden: CRC Press/Balkema, Chapter 95, Vol. II, pp. 989-998. doi: 10.1201/9780203092989.ch95.

______. (2011). Rheological analysis of multi-stress creep recovery (MSCR) test. **International Journal of Pavement Engineering**, Vol. 12, No. 6, pp. 561-568. doi: 10.1080/10298436.2011.573557.

WHITE, G. (2016). Grading highly modified binders by multiple stress creep recovery. **Road Materials and Pavement Design**, in press. doi: 10.1080/14680629.2016.1212730.

WIKIPEDIA. (2016). **Viscosity**. Wikipedia, the free encyclopedia. Last modified on July 30, 2016. Available from: <https://en.wikipedia.org/wiki/Viscosity>. Accessed: 04 Aug. 2016.

WITCZAK, M. W. et al. (2002). **Simple performance test for Superpave mix design**. NCHRP Report 465. National Cooperative Highway Research Program. Washington: Transportation Research Board. ISBN 0-309-06715-4.

WOLDEKIDAN, M. F. (2011). **Response modelling of bitumen, bituminous mastic and mortar**. Dissertation (Doctor) – Faculty of Civil Engineering and Geosciences, Delft University of Technology, Delft.

YADOLLAHI, G.; MOLLAHOSSEINI, H. S. (2011). Improving the performance of crumb rubber bitumen by means of poly phosphoric acid (PPA) and Vestenamer additives. **Construction and Building Materials**, Vol. 25, No. 7, pp. 3108-3116. doi: 10.1016/j.conbuildmat.2010.12.038.

YI-QIU, T. et al. (2014). New index used to evaluate the high-temperature and low-temperature performance of asphalt. **Journal of Materials in Civil Engineering**, Vol. 27, No. 8, C4014007. doi: 10.1061/(ASCE)MT.1943-5533.0001201.

YILDIRIM, Y. (2007). Polymer modified asphalt binders. **Construction and Building Materials**, Vol. 21, No. 1, pp. 66-72. doi: 10.1016/j.conbuildmat.2005.07.007.

YILDIRIM, Y. et al. (2000). **Mixing and compaction temperatures for hot mix asphalt concrete**. Research Report No. 1250-5. The University of Texas at Austin, Austin, TX. 100 p.

______. (2006). Evaluation of viscosity values for mixing and compaction temperatures. **Journal of Materials in Civil Engineering**, Vol. 18, No. 4, pp. 545-553. doi: 10.1061/(ASCE)0899-1561(2006)18:4(545).

YUSOFF, N. I. M. et al. (2013). Modelling the rheological properties of bituminous binders using the 2S2P1D model. **Construction and Building Materials**, Vol. 38, pp. 395-406. doi: 10.1016/j.conbuildmat.2012.08.038.

ZAMAN, A. A. et al. (1995). Rheological properties of rubber-modified asphalt. **Journal of Transportation Engineering**, Vol. 121, No. 6, pp. 461-467. doi: 10.1061/(ASCE)0733-947X(1995)121:6(461).

ZHANG, F.; HU, C. (2013). The research for SBS and SBR compound modified asphalts with polyphosphoric acid and sulfur. **Construction and Building Materials**, Vol. 43, pp. 461-468. doi: 10.1016/j.conbuildmat.2013.03.001.

ZHANG, F.; YU, J. (2010). The research for high-performance SBR compound modified asphalt. **Construction and Building Materials**, Vol. 24, No. 3, pp. 410-418. doi: 10.1016/j.conbuildmat.2009.10.003.

ZHANG, J. et al. (2015). Use of the MSCR test to characterize the asphalt binder properties relative to HMA rutting performance – a laboratory study. **Construction and Building Materials**, Vol. 94, pp. 218-227. doi: 10.1016/j.conbuildmat.2015.06.044.

______. (2013). Comparison of flow number, dynamic modulus, and repeated load tests for evaluation of HMA permanent deformation. **Construction and Building Materials**, Vol. 44, pp. 391-398. doi: 10.1016/j.conbuildmat.2013.03.013.

ZHOU, F. et al. (2014). **Laboratory evaluation of asphalt binder rutting, fracture, and adhesion tests.** Technical Report No. FHWA/TX-14/0-6674-1, Texas A&M Transportation Institute, College Station, TX. Retrieved from: <http://tti.tamu.edu/documents/0-6674-1.pdf>. Accessed: 10 Jan 2017.

ZHOU, L. et al. (2012). Atmospheric temperature and vehicle loading affect rutting formation in asphalt concrete pavement. **Journal of Highway and Transportation Research and Development (English Edition)**, Vol. 6, No. 3, pp. 27-32. doi: 10.1061/JHTRCQ.0000103.

ZHU, J. et al. (2014). Polymer modification of bitumen: advances and challenges. **European Polymer Journal**, Vol. 54, pp. 18-38. doi: 10.1016/j.eurpolymj.2014.02.005.

ZOOROB, S. E. et al. (2012). Investigating the multiple stress creep recovery bitumen characterisation test. **Construction and Building Materials**, Vol. 30, pp. 734-745. doi: 10.1016/j.conbuildmat.2011.12.060.

APPENDIX A: Details and Example of the ANOVA Analysis

In this appendix, an example of the statistical analysis of variance (ANOVA) carried out in the present dissertation is demonstrated and described in detail. A brief literature review about the use of such a tool in the studies with asphalt binders is also provided, as well as the major variables involved in the analysis and their corresponding meanings.

A.1. Concepts and Brief Overview of the Use of ANOVA in the Literature

Statistical analyses have been successfully conducted by researchers in order to help them in drawing conclusions and/or further validate their collected data. For example, Sefidmazgi et al. (2012) used ANOVA to determine which factors within a group of four variables – number of aggregate contacts, contact length/area, stress paths within the aggregate skeleton and normal to contact plane orientation – mostly affect the rutting resistance of the asphalt mixture. They concluded that, with exception of the the latter, the influences of all the other variables in such a resistance were statistically significant. More specifically, it is expected that the rutting potential of the mixture is mainly dictated by the remaining three variables. Due to these differences in the relative importances, the authors decided not to choose each variable independtly to be correlated with F_N; rather, they took into account all the variables in the equation of the parameter ISI (internal structure index) and observed that the findings – correlation between ISI and F_N – were pretty good.

While studying the feasibility of different MSCR testing protocols for replacing the standardized one before the release of the AASHTO TP70-13 standard, Golalipour (2011) applied the ANOVA technique to three protocols (10, 30 and 60 creep-recovery cycles at each stress level) to identify at which point the increase in the number of cycles does not decrease the variability among the data significantly, from a statistical point of view. The author concluded that the responses of the binder after 10 and 30 cycles are considerably different, whereas no great differences between such responses after 30 and 60 cycles are observed. In other words, the decreases in the variabilities after 30 cycles of creep-recovery are not considerable anymore according to the ANOVA data, and they do not justify the need for a number of cycles higher than 30. Based on this, he recommended the application of 30 cycles in the MSCR tests to reduce the variability within the cycles and obtain more reliable R and J_{nr} values, and also yield a protocol with a reasonable amount of time to be finished.

Teymourpour et al. (2016) investigated the statistical significance of several variables associated with crumb rubber-modified binders – e. g., date of production of the material (total of five days – May 17, May 21, June 27, July 21 and August 21), number of replicates and gap height in the DSR (two gap heights, namely, 2 and 3 mm) – on the results of the parameter $G^*/sin\delta$. They concluded that either the production day or the gap height are proeminent factors contributing to changes in $G^*/sin\delta$, since the p-value and the F value were far different from the ones collected for the other variables (i. e., p-value much lower than 0.09 and F value much higher than 3.0). According to the authors, this means that taking the binders produced on different days as replicates is not acceptable and their resistances – as measured by $G^*/sin\delta$ – will probably not be lower than a maximum allowed variation. Although the use of the MSCR test decreased such variabilities within the group of production days, the differences among the results were still significant in some cases. As a consequence, the authors recommended the testing of at least two replicates in order to account for these high degrees of variation.

In the development of a new binder fatigue test to replace the original oscillatory shear test procedure, Johnson (2010) employed the ANOVA method to see if a different approach for calculating the energy release rate in the asphalt binder with increasing fatigue damage (as based on the slope of the curve between $log\ G'(\omega)$ and $log\ (\omega)$) could replace a complex interconversion from frequency domain to time domain tests. By considering a level of significance of 95%, the author concluded that the change in the method of calculation will not greatly modify the energy release rate; thus, the former (and simpler) procedure – i. e., based on the slope of the curve formed by $log\ G'(\omega)$ and $log\ \omega$ – could be used instead of the more complex one (mathematical interconversions). This was later implemented in the study together with the proposal of the LAS test as a surrogate to the time sweep and oscillatory shear tests.

More recently, Golalipour et al. (2016) discussed on the statistical significances of two different MSCR protocols (Method A and Method B) under a level of significance of 95%. Method A consists of applying 10 creep-recovery cycles at each of the standardized stress levels of 0.1 and 3.2 kPa. On the other hand, Method B consists of applying 30 creep-recovery cycles at the stress levels of 0.1, 3.2 and 10 kPa. Two null hypotheses were tested by the authors: (a) the mean J_{nr} values of in the first five cycles of both methods are the same; and (b) the mean J_{nr} values of all the cycles in both methods are the same. The results clearly illustrated that both hypotheses should be rejected, that is, the mean values are statistically different and Methods A and B do not yield similar nonrecoverable compliances. This was later used by the authors as arguments to propose changes in the current MSCR test protocols, i. e., to increase the number of cycles from 10 to 30 at each stress level and to calculate the mean R and J_{nr} values based only on the last five individual results (i. e., from cycles 26 to 30). The addition of one more stress level in the protocols (10 kPa) is also proposed by the authors.

These and other studies point out that ANOVA is a simple (but effective) technique in the guidance of researchers during the decision-making processes. As described above, this may be done by selecting simpler methods of calculation or determining the factors that mostly influence on the properties and parameters of the binder and the mixture, for example. Obviously, ANOVA has some limitations that must be known prior to any conclusion reached in the investigation. The limitations can be summarized as follows: (a) the observations are assumed to be independent among them; (b) the residuals are within a normal distribution; and (c) homogeneity of the variances of the data within the groups, also known as *homoscedasticity*. ANOVA may be carried out to evaluate the effects of one or two independent variables on one continuous dependent variable, and these tests are known in the literature as *one-way* or *two-way analysis of variance*, respectively. In general, a minimum of three groups are considered while conducting ANOVA. For two-group cases, either ANOVA or a simple *t-test* may be considered in the studies.

Basically, ANOVA tests a null hypothesis H_0 that samples from different sets of data are derived from populations with the same mean values. If H_0 is not rejected, then one can assume that these sets of data are interpreted as random samples of the same population. If H_0 is rejected and the alternative hypothesis (H_1) is not, one can imply that the groups are strongly affected by changes in the independent variables according to the level of significance α (typically equal to 5%). Either the *F-value* or the *p-value* may be calculated to see if H_0 is not rejected and H_1 is rejected or vice versa. If the *F-value* is higher than the critical value $F_{critical}$ or the *p-value* is lower than the level of significance, then H_0 may be rejected and H_1 is not. In general, the computer method (calculations made on a computer program such as Microsoft Excel or another software) provides the *p-value* and the textbook method (calculations made manually) provides the *F-value*.

The goal of this study is to investigate whether the creep time t_F or the test temperature T has more influence on the MSCR parameters of the asphalt binder (percent recovery R and nonrecoverable compliance J_{nr}). More simply, groups of binder data under two varying testing conditions were compared with each other to see if they come from the same original set of parameters or not. These testing conditions can be described as follows: (a) one fixed pavement temperature and increasing creep times in the MSCR tests; and (b) one fixed pair of creep-recovery times and varying pavement temperatures. The null hypothesis was tested under the level of significance of 5%, which has been used by several researchers such as Golalipour (2011), Golalipour et al. (2016), Johnson (2010) and Teymourpour et al. (2016). The example given in the next section illustrates how the calculations and analyses were made.

A.2. Example of the Application of ANOVA in this Dissertation

Let the data in Table 288 (*R* values collected from some MSCR tests carried out in the AC+Elvaloy+PPA at the temperatures of 52, 58, 64, 70 and 76°C) and Table 289 (J_{nr} values obtained from the same material and the same temperatures) be considered as examples for describing the application of ANOVA to the present dissertation. As pointed out above, the objective is to see whether the two sets of data can be considered as derived from the same group (H_0 is not rejected) or not (H_0 is rejected). In other words, H_0 is not rejected when the increases in the creep time cause approximately the same rates of increase or decrease in the outcomes of the MSCR test (*R* or J_{nr}) when compared with the ones due to increases in the pavement temperature, and thus the mean values do not markedly differ from each other. More simply, the null hypothesis H_0 means that the effects of temperature and creep time on the high-temperature rheological parameters of the asphalt binder are the same from a statistical point of view. As a consequence, the rejection of H_0 means that such effects are not similar and the MSCR parameters of the binder are more sensitive to changes in one of the variables than the other.

To facilitate the understanding of the calculations, the *R* and J_{nr} data were rearranged such that each of the studied variables – creep time and temperature – were isolated. These organized groups of data can be seen in Table 290 (parameter *R*) and Table 291 (parameter J_{nr}).

Table 288 – Examples of *R* values from the AC+Elvaloy+PPA at the temperatures of 64 and 70°C and the creep times of 1/9, 2/9, 4/9 and 8/9 s

temperature and stress level	percent recoveries (*R*) at each pair of creep-recovery times (in %)			
	1/9 s	2/9 s	4/9 s	8/9 s
52°C, 0.1 kPa	76.4	71.2	63.9	53.5
52°C, 3.2 kPa	70.9	64.5	59.0	48.3
58°C, 0.1 kPa	72.2	66.3	57.9	45.1
58°C, 3.2 kPa	66.4	58.6	49.1	34.7
64°C, 0.1 kPa	65.1	57.6	47.4	33.8
64°C, 3.2 kPa	58.0	47.4	33.2	20.8
70°C, 0.1 kPa	55.4	46.4	34.8	22.6
70°C, 3.2 kPa	45.6	33.0	18.9	9.3
76°C, 0.1 kPa	43.4	33.5	22.4	13.0
76°C, 3.2 kPa	31.4	17.6	6.5	1.4

Table 289 – Examples of J_{nr} values from the AC+Elvaloy+PPA at the temperatures of 64 and 70°C and the creep times of 1/9, 2/9, 4/9 and 8/9 s

temperature and stress level	compliances (J_{nr}) at each pair of creep-recovery times (in kPa^{-1})			
	1/9 s	2/9 s	4/9 s	8/9 s
52°C, 0.1 kPa	0.052	0.104	0.198	0.360
52°C, 3.2 kPa	0.065	0.129	0.220	0.387
58°C, 0.1 kPa	0.125	0.247	0.472	0.893
58°C, 3.2 kPa	0.151	0.303	0.560	1.041
64°C, 0.1 kPa	0.305	0.615	1.199	2.238
64°C, 3.2 kPa	0.366	0.755	1.512	2.671
70°C, 0.1 kPa	0.737	1.504	2.994	5.426
70°C, 3.2 kPa	0.894	1.861	3.760	6.654
76°C, 0.1 kPa	1.728	3.567	7.060	12.474
76°C, 3.2 kPa	2.076	4.490	9.274	16.321

Table 290 – Rearranged MSCR testing data of the AC+Elvaloy+PPA to be used in the analysis of variance (ANOVA) – percent recovery *R*

stress level of 0.1 kPa (*R*, %)[a]		stress level of 3.2 kPa (*R*, %)[a]	
increasing creep time	increasing temperature	increasing creep time	increasing temperature
76.4	76.4	70.9	70.9
71.2	72.2	64.5	66.4
63.9	65.1	59.0	58.0
53.5	55.4	48.3	45.6
N/A[b]	43.4	N/A[a]	31.4

[a] The starting point in both cases was the temperature of 52°C.
[b] N/A: Not applicable.

Table 291 – Rearranged MSCR testing data of the AC+Elvaloy+PPA to be used in the analysis of variance (ANOVA) – nonrecoverable compliance J_{nr}

stress level of 0.1 kPa (J_{nr}, kPa^{-1})[a]		stress level of 3.2 kPa (J_{nr}, kPa^{-1})[a]	
increasing creep time	increasing temperature	increasing creep time	increasing temperature
0.052	0.052	0.065	0.065
0.104	0.125	0.129	0.151
0.198	0.305	0.220	0.366
0.360	0.737	0.387	0.894
N/A[b]	1.728	N/A[b]	2.076

[a] The starting point in both cases was the temperature of 52°C.
[b] N/A: Not applicable.

It may be important to note that only the temperature of 52°C was chosen in the study as a starting point to increase the temperature and the creep time in the MSCR tests. Other starting temperatures were not considered due to the need for covering as many temperatures and loading-unloading times as possible. To avoid the risks of drawing misleading conclusions and ensuring that the maximum number of numerical results are analyzed, undamaged samples were selected prior to any change in the variables of the MSCR protocols and groups of data with less than four results were not considered in the analysis.

Table 292 summarizes the statistical parameters collected from ANOVA and based on the percent recoveries of the AC+Elvaloy+PPA. Either the *p-value* or the *F-value* suggest that the null hypothesis cannot be rejected, and this is valid for both stress levels. As explained above, H_0 is not rejected when the *p-value* is higher than α or when the *F-value* is lower than $F_{critical}$. The *p-value* is always higher than 0.50 (at least 10 times higher than α), whereas the *F-value* barely exceeds 0.40 (less than 10% of the parameter $F_{critical}$). In practical terms, one may conclude that both sets of data belong to the same group and the effects of temperature and loading time on the *R* values of the AC+Elvaloy+PPA are similar from a statistical point of view. In other words, the Elvaloy-modified asphalt binder is expected to show quite similar elastic responses in the pavement when the creep time is increased or the pavement temperature becomes higher.

Table 292 – Results from ANOVA (*p-value* and *F-value*) as based on the percent recoveries of the AC+Elvaloy+PPA

null hypothesis H_0	statistical parameters (ANOVA)				recommendation
	$F_{critical}$	*F-value*	α	*p-value*	
equivalency between *R* values with increasing creep time and temperature, 0.1 kPa	5.5914	0.2177	0.05	0.6550	H_0 is not rejected
equivalency between *R* values with increasing creep time and temperature, 3.2 kPa	5.5914	0.4584	0.05	0.5201	H_0 is not rejected

Table 293 also provides the outcomes of ANOVA for the AC+Elvaloy+PPA, but considering the nonrecoverable compliance J_{nr}. Similarly to the percent recovery set of data, the *F-value* and the *p-value* at 0.1 and 3.2 kPa lead to the recommendation of not rejecting the null hypothesis, i. e., the effects of creep time and temperature on the repeated creep responses of the AC+Elvaloy+PPA are similar under a reliability level of 95% (α = 5%). The *p-value* is at least four times higher than α, and the ratio of *F-value* to $F_{critical}$ does not exceed 25% in any case. However, it must be emphasized that the variabilities among the J_{nr} values are higher than the ones obtained for the R values, and this can be inferred from the higher *F-values* and lower *p-values* reported in Table 293 than in Table 292. This means that the rutting susceptibility of the AC+Elvaloy+PPA – as measured by J_{nr} – more clearly differentiates between the two variables involved in the study (creep time and temperature), even though it is not enough to say that the responses are statistically different.

Table 293 – Results from ANOVA (*p-value* and *F-value*) as based on the nonrecoverable compliances of the AC+Elvaloy+PPA

null hypothesis H_0	statistical parameters (ANOVA)				recommendation
	$F_{critical}$	*F-value*	α	*p-value*	
equivalency between J_{nr} values with increasing creep time and temperature, 0.1 kPa	5.5914	1.3411	0.05	0.2848	H_0 is not rejected
equivalency between J_{nr} values with increasing creep time and temperature, 3.2 kPa	5.5914	1.4431	0.05	0.2687	H_0 is not rejected

Overall, based on the results reported in this chapter, it can be said that the repeated creep response of the AC+Elvaloy+PPA at 0.1 and 3.2 kPa is influenced by the creep time and the temperature in a quite similar way, according to a reliability level of 95%. This can be applied either to the percent recovery or the nonrecoverable compliance, even though the degrees of variability (as measured by the *F-value* and the *p-value*) are slightly higher for J_{nr} than for R.

This procedure was followed for all the formulations studied in the dissertation, and it is expected that the conclusions drawn in the analyses will provide researchers and highway agencies with a further understanding about the complex time-temperature dependency of modified asphalt binders. However, it must be noticed that the absence of one or more experimental results (for instance, absence of recovery at 64, 70 and 76°C for a particular asphalt binder) may cause potential problems in the interpretation of the statistical parameters. As a consequence, it was decided not to carry out ANOVA when two or more R values are not found in the MSCR testing data.

APPENDIX B: Refinement in Superpave® Traffic Criteria

This appendix is intended to discuss about a possible refinement on the current Superpave® traffic level criteria, as based on the findings of this dissertation. Preliminary results and analyses have already been published in the paper from Domingos and Faxina (2017), and the reader is referred to this publication for a summary of the present chapter.

The idea of developing refined traffic level criteria for selecting the most appropriate asphalt binder for a specific paving application has emerged from the assumption that, by establishing maximum $J_{nr}3200$ values at longer creep times during MSCR, materials with very high susceptibility to rutting would be avoided. The presence of several slow-moving vehicles on a roadway can accelerate the formation of rutting in the wheelpath and, if the binder is not able to show a minimum level of resistance under such loading conditions, there is a possibility of a premature failure of the pavement by rutting. This becomes even more important when the nonlinear relationship between the increasing J_{nr} values and the decreasing traffic speed (that is, increasing loading time) is observed, e. g., in the publications from Golalipour (2011) and Delgadillo et al. (2012). The study from Domingos and Faxina (2017) and the present dissertation have already highlighted the fact that some modified asphalt binders – e. g., the AC+PPA and the AC+SBS – show different traffic designations, depending on the criteria under consideration.

More specifically, the aforementioned suggesting refinements in Superpave® are derived from the hypothesis that the specification can account for a heavier traffic level not only by decreasing the maximum J_{nr} value, but also by increasing the creep time t_F in the MSCR test. This means that the current and the proposed criteria could be used together in the specification, i. e., two technical approaches would be followed in the definition of the traffic level of the binder at the pavement temperature. Despite the difficulties in finding a unique set of requirements for all types of modified binders and the varying rheological responses of these materials, it is believed that the study of the creep-recovery response of binders at longer loading times is a more practical and rational approach to the wide interval of vehicle speeds on roads and highways. An early draft of these proposed refinements can be seen in Table 294 below, as well as in the paper from Domingos and Faxina (2017). It may be important to emphasize that the present study is a first step towards the development of guidelines for selecting the most appropriate binder for each paving application, and therefore this draft may be thoroughly revised before final acceptance for publication.

Table 294 – Preliminary draft of the revised Superpave® specification for RTFO-aged materials with the creep time as a criterion for choosing the adequate traffic level of the binder

rolling thin-film oven (RTFO) residue, 163°C, 85 min	
64S – "standard" traffic level (S), $J_{nr}3200 \leq 4.0$ kPa^{-1} for creep time = 1.0 s, tested at pavement temperature (°C)	64
64H – "heavy" traffic level (H), $J_{nr}3200 \leq 2.0$ kPa^{-1} for creep time = 1.0 s **and $J_{nr}3200 \leq 4.0$ kPa^{-1} for creep time = 2.0 s**, tested at pavement temperature (°C)	64
64V – "very heavy" traffic level (V), $J_{nr}3200 \leq 1.0$ kPa^{-1} for creep time = 1.0 s **and $J_{nr}3200 \leq 3.5$ kPa^{-1} for creep time = 4.0 s**, tested at pavement temperature (°C)	64
64E – "extremely heavy" traffic level (E), $J_{nr}3200 \leq 0.5$ kPa^{-1} for creep time = 1.0 s **and $J_{nr}3200 \leq 3.5$ kPa^{-1} for creep time = 8.0 s**, tested at pavement temperature (°C)	64

The number of MSCR tests that must be conducted in each traffic level depends on the creep time at which the maximum $J_{nr}3200$ no longer meets the requirements imposed by the method. For instance, a predefined asphalt binder shows $J_{nr}3200$ values equal to 3.976 kPa^{-1} at 1/9 s, 4.152 kPa^{-1} at 2/9 s and 6.309 kPa^{-1} at 4/9 s, all of them at 64°C. According to the intervals provided in Table 294, this binder would be graded as 64S-xx because the maximum $J_{nr}3200$ value at 2/9 s was not met. For this traffic level to be determined, at least two MSCR tests must be carried out in the DSR (i. e., one at 1/9 s and another at 2/9 s).

In another example, a polymer-modified asphalt binder shows nonrecoverable compliances equal to 1.347 kPa^{-1} at 1/9 s, 2.432 kPa^{-1} at 2/9 s, 4.013 kPa^{-1} at 4/9 s and 7.990 kPa^{-1} at 8/9 s, all of the data collected at 64°C. As based on these $J_{nr}3200$ values, the material would be graded as 64V-xx because values higher than 3.5 kPa^{-1} at 8/9 s are observed. Since the very heavy traffic level was the last designation for which the binder complied with the requirements, this material may be graded as 64V-xx in the proposed criteria. However, at least four MSCR tests (one for each of the pairs of creep-recovery times, and not including replicates) are needed for the identification of the correct traffic level in the newly proposed method.

As can be implied from these discussions, one of the major disadvantages of the Superpave® proposed refinement is the higher number of laboratory tests in the DSR when compared with the standardized methods. On the other hand, it is believed that these increases in the number of tests are compensated for the choice of a more appropriate asphalt binder for the traffic level under consideration, and thus economical and technical benefits may be provided to the highway agencies and private companies with respect to pavement construction and/or rehabilitation.

APPENDIX C: History of the Standards about the MSCR Test

This appendix shows a summary of the previous and current versions of the ASTM and AASHTO standards about the MSCR test (ASTM D7405, AASHTO TP70 and AASHTO T350), together with their most important technical details. It aims at helping the readers in gaining more scientific knowledge about the test, as well as to trace the evolution of the protocols and the methods of calculation. This was made by visiting the official websites of the ASTM[34] and AASHTO agencies[35] and the one of the TECHSTREET store[36]. Table 295 depicts the essential characteristics of the ASTM D7405 standard, whereas Table 296 provides the ones of the AASHTO TP70 and the AASHTO T350 standards.

---

[34] AMERICAN SOCIETY FOR TESTING AND MATERIALS. **ASTM D7405:** Standard test method for multiple stress creep and recovery (MSCR) of asphalt binder using a dynamic shear rheometer. West Conshohocken, PA. Available from: <https://www.astm.org/Standards/D7405.htm>.

[35] AMERICAN ASSOCIATION OF STATE HIGHWAY AND TRANSPORTATION OFFICIALS. **AASHTO TP70:** Standard method of test for multiple stress creep recovery (MSCR) test of asphalt binder using a dynamic shear rheometer. Washington, DC. Available from: <https://bookstore.transportation.org/item_details.aspx?ID=2305>. Provisional standard. Current designation AASHTO T350.

[36] **TECHSTREET – Technical Information Superstore**. Managed by Thomson Reuters. Ann Arbor, MI. Available from: <http://www.techstreet.com/>.

Table 295 – Technical details of the MSCR tests according to the current and historical versions of the ASTM D7405 standard

designation	year	test protocol and calculations	parameters	additional details/information
D7405	2015	20 cycles at 100 Pa followed by 10 more cycles at 3,200 Pa. The last 10 cycles at 100 Pa and all the cycles at 3,200 Pa are used in the calculations of the test parameters (*R* and J_{nr})	Percent recovery (*R*), nonrecoverable compliance (J_{nr}) and percent differences in compliances ($J_{nr,\ diff}$) and recoveries (R_{diff})	This is the first time the ASTM standard takes into account 20 creep-recovery cycles at 100 Pa
D7405	2010a	10 cycles at 100 Pa followed by 10 more cycles at 3,200 Pa. All the cycles at 100 and 3,200 Pa are used in the calculations of the test parameters (*R* and J_{nr})	Percent recovery (*R*), nonrecoverable compliance (J_{nr}) and percent difference in compliances ($J_{nr,\ diff}$) and recoveries (R_{diff})	This is the last time the ASTM standard takes into account only 10 cycles at 100 Pa. The table with the maximum variabilities among *R* and J_{nr} is first introduced in this version of the standard
D7405	2010	10 cycles at 100 Pa followed by 10 more cycles at 3,200 Pa. All the cycles at 100 and 3,200 Pa are used in the calculations of the test parameters (*R* and J_{nr})	Percent recovery (*R*), nonrecoverable compliance (J_{nr}) and percent differences in compliances ($J_{nr,\ diff}$) and recoveries (R_{diff})	Not applicable
D7405	2008a	10 cycles at 100 Pa followed by 10 more cycles at 3,200 Pa. All the cycles at 100 and 3,200 Pa are used in the calculations of the test parameters (*R* and J_{nr})	Percent recovery (*R*), nonrecoverable compliance (J_{nr}) and percent differences in compliances ($J_{nr,\ diff}$) and recoveries (R_{diff})	Not applicable
D7405	2008	10 cycles at 100 Pa followed by 10 more cycles at 3,200 Pa. All the cycles at 100 and 3,200 Pa are used in the calculations of the test parameters (*R* and J_{nr})	Percent recovery (*R*), nonrecoverable compliance (J_{nr}) and percent differences in compliances ($J_{nr,\ diff}$) and recoveries (R_{diff})	This is the first time the MSCR test was standardized by ASTM under the fixed designation D7405

Table 296 – Technical details of the MSCR tests according to the current and historical versions of the AASHTO TP70/T350 standards

Designation	Year	Test Protocol and Calculations	Parameters	Additional Details/Information
T350	2014	20 cycles at 100 Pa followed by 10 more cycles at 3,200 Pa. The last 10 cycles at 100 Pa and all the cycles at 3,200 Pa are used in the calculations of the test parameters (R and J_{nr})	Percent recovery (R), nonrecoverable compliance (J_{nr}) and percent difference in compliances ($J_{nr,\ diff}$)	First full standard of the MSCR test. It does not provide the chart for the determination of the level of elasticity of the binder
TP70	2013	20 cycles at 100 Pa followed by 10 more cycles at 3,200 Pa. The last 10 cycles at 100 Pa and all the cycles at 3,200 Pa are used in the calculations of the test parameters (R and J_{nr})	Percent recovery (R), nonrecoverable compliance (J_{nr}) and percent difference in compliances ($J_{nr,\ diff}$)	The last provisional standard of the MSCR test. It provides the chart for the determination of the level of elasticity of the binder
TP70	2012	10 cycles at 100 Pa followed by 10 more cycles at 3,200 Pa. All the cycles at 100 and 3,200 Pa are used in the calculations of the test parameters (R and J_{nr})	Percent recovery (R), nonrecoverable compliance (J_{nr}) and percent differences in compliances ($J_{nr,\ diff}$)	Not applicable
TP70	2010	10 cycles at 100 Pa followed by 10 more cycles at 3,200 Pa. All the cycles at 100 and 3,200 Pa are used in the calculations of the test parameters (R and J_{nr})	Percent recovery (R), nonrecoverable compliance (J_{nr}) and percent difference in compliances ($J_{nr,\ diff}$)	This test protocol is similar to the one found in the corresponding ASTM standard (D7405-10), with exception of the parameter R_{diff}
TP70	2009	10 cycles at 100 Pa followed by 10 more cycles at 3,200 Pa. All the cycles at 100 and 3,200 Pa are used in the calculations of the test parameters (R and J_{nr})	Percent recovery (R), nonrecoverable compliance (J_{nr}) and percent difference in compliances ($J_{nr,\ diff}$)	This is the first time the MSCR test was standardized by AASHTO under the provisional standard TP70. The chart for the determination of the level of elasticity of the binder is also shown here